30th ISOC

سی امین سمینار شیمی آلی ایران

دانشکده شیمی دانشگاه علم و صنعت ایران

۱۷ الی ۱۹ بهمن ماه ۱۴۰۳

محورها:

- ☑ کاتالیزورها (نانوکاتالیزورها، اورگانو کاتالیزورها، آنزیم ها و ...)
- ☑ شیمی دارویی و سیستم های دارورسانی هوشمند
- ☑ نانو شیمی (شیمی سوپرامولکول، ماشین های مولکولی)
- ☑ صنایع شیمیایی (آرایشی و بهداشتی، غذایی، مواد موثره دارویی)
- ☑ شیمی ترکیبات طبیعی (فیتوشیمی، نارکوتیک ها، فرمون ها و ...)
- ☑ شیمی آلی محاسباتی، هوش مصنوعی و یادگیری ماشین
- ☑ سنتزهای آلی (متدولوژی، ترکیبات هتروسیکل، واکنش‌های چند جزئی و ...)
- ☑ توسعه پایدار و انرژی های نو و تجدیدپذیر
- ☑ شیمی نفت، گاز و پتروشیمی و روانکاری
- ☑ شیمی پلیمرها و نانوکامپوزیت های پلیمری
- ☑ شیمی سبز و دوستدار محیط زیست

تاریخ های مهم

ثبت نام و ارسال مقالات:
۳ آذر الی ۲۰ آذر ۱۴۰۳
اعلام نتایج داوری:
۲۲ دی ۱۴۰۳
ارسال فایل ارائه:
۷ بهمن ۱۴۰۳


5 - 7 February 2025

نشانی دبیرخانه: تهران، میدان رسالت،
خیابان هنگام، خیابان دانشگاه، دانشگاه
علم و صنعت ایران، دانشکده شیمی
کد پستی: 16846-13114
تلفن دبیرخانه: 77240579 (21 98+)
09363199250
نمابر: 73227707 (21 98+)
وبگاه:
www.isoc30.iust.ac.ir
پست الکترونیک:
30isoc@iust.ac.ir
@isoc30iust

CIVILICA

ISC


بسم الله الرحمن الرحيم

ن وَ الْقَلَمِ وَ ما یَسْطُرُونَ

"ن، سوگند به قلم و آن چه می نویسند."

سخن دبیر کنفرانس:

خداوند بزرگ و علیم را سپاسگزاریم که توفیق برگزاری سی امین سمینار شیمی آلی ایران را نصیب دانشکده شیمی و گروه شیمی آلی دانشگاه علم و صنعت ایران کرد. قاعدتا برگزاری سی امین سمینار سالانه شیمی آلی، پس از سه دهه تجربه و تلاش ارزشمند همکاران در دیگر دانشگاه‌های کشور وظیفه‌ای خطیر و سترگ بود که خوشبختانه همکاران بزرگوار، دانشجویان گرامی و کارکنان خدوم دانشگاه علم و صنعت ایران برای انجام بهینه آن کمر همت بستند. در همین راستا، به منظور بهره‌گیری از توان علمی، پژوهشی و کارآفرینی دانشگاهیان و صنایع مرتبط با شیمی آلی، شعار کلیدی **"شیمی آلی پلی بین نوآوری، کارآفرینی دانش بنیان و جامعه پویاتر"** برای سی امین سمینار انتخاب شد.

خوشبختانه، با نظر مساعد انجمن شیمی آلی در واگذاری امر برگزاری سمینار به دانشکده شیمی دانشگاه علم و صنعت ایران و تعیین کمیته علمی از سوی دبیران سمینار با توجه به گستره جغرافیایی کشور و وزن علمی همکاران هیات علمی شاغل، مجوز و تأییدیه های لازم از پایگاه استنادی جهان اسلام (ISC) و سیویلیکا (Civilika) در اولین فرصت اخذ شد. همزمان مکاتبات لازم جهت اعلام حمایت معنوی و مالی نهادها و سازمان‌های حاکمیتی و شرکت‌های دولتی و خصوصی انجام و مذاکرات لازم به عمل آمد. در این راستا، معاونت پژوهشی وزارت علوم، تحقیقات و فناوری، مرکز تحقیقات دفاعی کشور با محوریت نیروی راهبردی دریایی ارتش جمهوری اسلامی ایران، بنیاد دانشمند وابسته به بنیاد مستضعفان انقلاب اسلامی، شرکت مصباح انرژی وابسته به مجتمع آب سنگین اراک، شرکت مهامکس و تمادکالا، شرکت تعاونی الیاف سیرنگ یزد، شرکت کیمیا الیکای سپنتا حمایت معنوی و مالی خود را در سطوح الماس، پلاتینیوم، طلایی و نقره ای از سمینار اعلام کردند. همچنین شرکت‌های دارویی امرتات شیمی، مایان گستر دی، رایحه گلبرگ خاطره و عطر مانا با برگزاری غرفه در کنار حامیان اصلی به غنای نمایشگاه جانبی افزودند. به رسم و آداب میزبانی و به تاسی از حدیث نبوی **لا یشکر اللّه من لایشکر النّاس (شکر خدا را بجا نیاورده است آن که از مردم درقبال انعامشان تشکر نکند)** جا دارد از طرف تمامی برگزارکنندگان از حسن نظر و مساعدت مدیران و کارکنان تک تک آنها تشکر و قدردانی نماییم.

در طول سه روز برگزاری سمینار شیمی آلی ایران، بیش از ۴۴۱ نفر از اساتید و متخصصان تراز اول کشور و صنایع مختلف شیمیایی، محققان پسادکترا، دانشجویان دکترای تخصصی و کارشناسی ارشد در دانشگاه علم و صنعت ایران -نگین دانشگاه‌های کشور در امر آموزش، پژوهش و کارآفرینی- حضور یافتند و ضمن ارائه

آخرین دستاوردهای پژوهشی و کارآفرینی خود و همکاران تحقیقاتی به دیگر محققین و دانشجویان، ره توشه‌ای ارزشمند برای مسیر آینده تحقیقاتی خود اندوختند. در همین راستا، شایسته است که مراتب قدردانی و سپاس خود را از مساعدت هیات رئیسه دانشگاه علم و صنعت ایران بویژه جناب آقای دکتر داود یونسیان (ریاست دانشگاه)، جناب آقای دکتر حسین غفوری (ریاست دانشکده شیمی) و همکاران هیات علمی بویژه سرکار خانم دکتر شهرزاد جوانشیر (دبیر اجرائی) و جناب آقای دکتر محمدرضا نعیمی‌جمال (دبیر علمی) و زحمات شبانه‌روزی چند ماهه و از خودگذشتگی بی‌نظیر دانشجویان دکترای تخصصی و کارشناسی ارشد همکار سمینار در بخش علمی و اجرایی به عمل آوریم. امیدواریم که ماحصل این گردهمایی ملی آغازگر فصلی نوین در پیشرفت و ارتباط علمی محققین دانشگاهی و صنعتی شیمی آلی ایران و رشته‌های وابسته در جهت اعتلای نام بلند میهن عزیز اسلامی و رفاه مردم دانش دوست آن باشد. ان شاء الله.

با احترام
محمدقربان دکامین
دبیر سی امین سمینار شیمی آلی ایران
بهمن ۱۴۰۳

سخن دبیر علمی کنفرانس

بسمه تعالی

با استعانت از خداوند متعال، سی‌اُمین کنفرانس شیمی آلی ایران در تاریخ‌های هفدهم الی نوزدهم بهمن ماه ۱۴۰۳ در دانشگاه علم و صنعت ایران، با همیاری و مشارکت گسترده جامعه علمی شیمی آلی کشور، با موفقیت به انجام رسید. در این دوره، شاهد ارائه دستاوردهای پژوهشی ارزشمندی بودیم که بخش اعظم آن‌ها در قالب پوستر و بالغ بر سی مقاله به صورت سخنرانی در معرض دید و تبادل نظر قرار گرفت.

یکی از ویژگی‌های بارز این کنفرانس، توجه ویژه به پژوهشگران جوان کشور بود. فرصتی مغتنم در اختیار این عزیزان قرار گرفت تا نتایج پژوهش‌های خود را در قالب سخنرانی به جامعه علمی ارائه نمایند. در فرآیند انتخاب سخنرانان، تلاش بر این بود تا نمایندگانی از اقصی نقاط ایران، از جنوب تا شمال، از شرق تا غرب، در این رویداد علمی حضور داشته باشند. همچنین، در اقدامی نوآورانه، از یک دانشجوی کارشناسی ارشد از شهر کرمان برای ارائه سخنرانی دعوت به عمل آمد که این مهم، بازخورد بسیار مثبتی را در پی داشت و نشان از پویایی و استعدادهای درخشان موجود در اقصی نقاط کشور دارد.

این کنفرانس، در راستای اهداف خود، بر نکات زیر نیز تأکید داشت:

۱- توزیع موضوعی سخنرانی‌ها: تمرکز بر موضوعات با اهمیت روز کشور و جهان، به منظور همسویی پژوهش‌های علمی با نیازهای جامعه و چالش‌های پیش‌رو.

۲- بخش ویژه جذب و تبدیل کربن دی‌اکسید: اختصاص بخشی مجزا به این موضوع حیاتی، با توجه به اهمیت روزافزون آن در مقابله با تغییرات اقلیمی و حفظ محیط زیست.

۳- انتخاب سخنرانان جوان: بها دادن به نسل جوان و ایجاد بستری مناسب برای ارائه توانمندی‌ها و ایده‌های نوآورانه آن‌ها.

۴- سخنرانی‌های کلیدی در خصوص کاربردهای شیمی در صنعت: ارائه دیدگاه‌هایی جامع و کاربردی در زمینه نقش شیمی در توسعه صنایع مختلف کشور.

همچنین در حاشیه کنفرانس، کارگاه‌های آموزشی متعددی با موضوعات متنوع از جمله آشنایی تئوری و عملی با طیف‌سنجی رامان، مقدمه ای بر شیمی محصولات آرایشی و بهداشتی، کارگاه انگیزشی طراح کسب و کار

خود باشید و کارگاه آشنایی با مبانی فوتوشاپ برگزار گردید که با استقبال شرکت‌کنندگان مواجه شد. بدینوسیله، از مدرسین محترم این دوره‌ها نیز صمیمانه سپاسگزاری می‌نماییم.

اینجانب بر خود لازم می‌دانم از تمامی دست‌اندرکاران و حامیان برگزاری این کنفرانس صمیمانه قدردانی نمایم. از همراهی و مشارکت ارزشمند انجمن شیمی ایران، جامعه علمی شیمی آلی کشور، دانشجویان گرامی دانشگاه علم و صنعت ایران، همکاران محترم در کمیته علمی و اجرایی، کارکنان پرتلاش دانشگاه علم و صنعت ایران، حامیان مالی گرانقدر و تمامی شرکت‌کنندگان عزیز، سپاسگزارم. امید است این کنفرانس، گامی مؤثر در جهت ارتقاء سطح دانش و توسعه علمی کشور عزیزمان در حوزه شیمی آلی باشد.

محمد رضا نعیمی جمال

دبیر علمی سی‌اُمین کنفرانس شیمی آلی ایران

اعضای کمیته علمی

۱) دکتر شهرزاد جوانشیر، دانشگاه علم و صنعت ایران

۲) دکتر محمدرضا نعیمی جمال، دانشگاه علم و صنعت ایران

۳) دکتر محمد قربان دکامین، دانشگاه علم و صنعت ایران

۴) دکتر علی ملکی، دانشگاه علم و صنعت ایران

۵) دکتر صادق رستم نیا، دانشگاه علم و صنعت ایران

۶) دکتر حسین غفوری، دانشگاه علم و صنعت ایران

۷) دکتر احمد شعبانی، دانشگاه شهید بهشتی

۸) دکتر علی اصغر محمدی، پژوهشگاه شیمی و مهندسی شیمی ایران

۹) دکتر علی رمضانی، تحصیلات تکمیلی علوم پایه زنجان

۱۰) دکتر علیرضا کیاست، دانشگاه شهید چمران اهواز

۱۱) دکتر رضا پیمان فر، موسسه انرژی ساوه

۱۲) دکتر علیرضا نجفی چرمهینی، دانشگاه صنعتی اصفهان

۱۳) دکتر علی شیری، دانشگاه فردوسی مشهد

۱۴) دکتر آرش قادری، دانشگاه هرمزگان

۱۵) دکتر عظیم ضیایی حلیمه جانی، دانشگاه صنعتی شریف

۱۶) دکتر بابک کریمی، تحصیلات تکمیلی علوم پایه زنجان

۱۷) دکتر بابک مختاری، دانشگاه شهید چمران اهواز

۱۸) دکتر بابک افتخاری سیس، دانشگاه مراغه

۱۹) دکتر سیده بهاره عظیمی، پژوهشکده محیط زیست و توسعه پایدار

۲۰) دکتر بهزاد زینی زاده، دانشگاه ارومیه

۲۱) دکتر الهه کوثری، دانشگاه امیرکبیر

۲۲) دکتر فرید معین پور، دانشگاه آزاد بندرعباس

۲۳) دکتر فاطمه تمدن، دانشگاه یزد

۲۴) دکتر هادی ادیبی، دانشگاه علوم پزشکی کرمانشاه

۲۵) دکتر حمید بیضایی، دانشگاه زابل

۲۶) دکتر حسن شیبانی، دانشگاه شهید باهنر کرمان

۲۷) دکتر حسین توکل، دانشگاه صنعتی اصفهان

۲۸) دکتر جواد مختاری، دانشگاه آزاد واحد علوم و تحقیقات

۲۹) دکتر کوروش رادمقدم، دانشگاه گیلان

۳۰) دکتر محمود زارعی، دانشگاه قم

۳۱) دکتر علیرضا مدرسی عالم، دانشگاه سیستان و بلوچستان

۳۲) دکتر محمد اسلامی، دانشگاه صنعتی خاتم الانبیا بهبهان

۳۳) دکتر محمد سعید عبایی، پژوهشگاه شیمی و مهندسی شیمی ایران

۳۴) دکتر مصطفی کیامهر، دانشگاه قم

۳۵) دکتر محمدرضا زمانلو، دانشگاه محقق اردبیلی

۳۶) دکتر نادر نوروزی پسیان، دانشگاه ارومیه

۳۷) دکتر رحمان حسین زاده، دانشگاه مازندران

۳۸) دکتر رامین قربانی، دانشگاه بوعلی سینا همدان

۳۹) دکتر رضا نجار، دانشگاه تبریز

دانشجویان کادر علمی

۱) فاطمه رادین کیان

۲) زهرا نظافت

۳) ادیبه محمدی

۴) صفیه حیدرزاده

اعضای کادر اجرایی

مسئول دبیرخانه: علی میری تنها

۱. مریم مهنام پور
۲. علی بدیحی
۳. فرشته فرهادپور
۴. مهدی طاهری
۵. بهنوش محرابی
۶. الناز پیری عالم
۷. مریم جمیلی
۸. امیر محمد شبانی
۹. علی اسمعیلی
۱۰. حمیدرضا عطاردی بیمرغی
۱۱. نیلوفر نشیبی
۱۲. زهرا تولایی
۱۳. نیما دیوانی
۱۴. تهمینه خوشبین فومنی
۱۵. رویا اوزی
۱۶. امیر اسدزاده
۱۷. امیر علی هادیان جزی
۱۸. احمد ملا
۱۹. فرشته پیرو هدایتی
۲۰. نفیسه عزیزی
۲۱. شیدا عابدی بنائی
۲۲. پریا عربی
۲۳. فاطمه سمیعی
۲۴. سارا قاضی پور

۲۵. سپیده حسن زاده بناکار
۲۶. علی نجف زاده
۲۷. خدیجه اسمعیلی
۲۸. مبینا رحمانی
۲۹. محمدرضا پورمحمد
۳۰. نرگس پورغفاری
۳۱. سید میلاد طباطبایی
۳۲. مهسا زهره وند
۳۳. هانیه امیرحسینی
۳٤. لیلا ربیعی
۳۵. مونا رئوف مبینی
۳٦. فرحناز داوودی
۳۷. نگین رستمی
۳۸. سما ترک زبان

سخنرانان

- دکتر محمدرضا نعیمی جمال هیئت علمی دانشگاه علم و صنعت ایران
- دکتر پیمان صالحی معاون پژوهشی وزارت عتف
- دکتر محمد قربان دکامین هیئت علمی دانشگاه علم و صنعت ایران
- دکتر مبلغ اسلامی نماینده شرکت مصباح انرژی
- دکتر مهران رضایی هیئت علمی دانشگاه علم و صنعت ایران
- دکتر احمد شعبانی هیئت علمی دانشگاه شهید بهشتی
- دکتر مجتبی خراسانی هیئت علمی دانشگاه زنجان
- دکتر سعید شفیعی نوید محقق پسا دکتری دانشگاه مازندران
- دکتر سید محمد شاه چراغ نماینده شرکت داروسازی آپرین سما فارمد
- دکتر مژگان حسین نژاد هیئت علمی پژوهشگاه رنگ
- دکتر عظیم ضیایی حلیمه جانی هیئت علمی دانشگاه صنعتی شریف
- دکتر خیبر دشتیان محقق پسا دکتری دانشگاه علم و صنعت ایران
- دکتر میلاد بزاز راستکار آزمایشگاه تحقیقات شیمی دفاعی وزارت دفاع
- دکتر سمیه شهرکی هیئت علمی دانشگاه زابل
- دکتر علی شیری هیئت علمی دانشگاه فردوسی مشهد
- دکتر محمد کریمی نماینده شرکت الیاف سیرنگ یزد
- دکتر ندا سیدی هیئت علمی دانشگاه جیرفت
- دکتر کارن ویلسون هیئت علمی دانشگاه گریفیث استرالیا
- دکتر مسعود حکیم داوود نماینده شرکت کیمیا الیکای سپنتا
- دکتر فاطمه تمدن هیئت علمی دانشگاه یزد
- دکتر علیرضا اویسی هیئت علمی دانشگاه لرستان
- دکتر حمیدرضا کلهر هیئت علمی دانشگاه صنعتی شریف
- دکتر بابک نعمتی هیئت علمی دانشگاه بوعلی سینا همدان
- خانم فاطمه ده یادگاری دانشجوی کارشناسی ارشد دانشگاه شهید باهنر کرمان

- دکتر محمد باقر تیموری هیئت علمی دانشگاه خوارزمی
- آقای سید علی حسینی دانشجوی دکتری دانشگاه تربیت مدرس
- آقای محمد حسین محسنی دانشجوی دکتری دانشگاه علم و صنعت ایران
- دکتر میثم یاریه هیئت علمی دانشگاه بوعلی سینا همدان
- دکتر رضا پیمانفر موسسه آموزش عالی انرژی ساوه
- دکتر حسین توکل هیئت علمی دانشگاه صنعتی اصفهان
- دکتر مرتضی شیری هیئت علمی دانشگاه الزهرا
- دکتر شهرزاد جوانشیر هیئت علمی دانشگاه علم و صنعت ایران

حامیان مالی

۱) نیروی دریایی ارتش جمهوری اسلامی ایران

نیروی دریایی ارتش جمهوری اسلامی ایران

۲) وزارت علوم، تحقیقات و فناوری جمهوری اسلامی ایران

جمهوری اسلامی ایران
وزارت علوم، تحقیقات و فناوری

۳) معاونت علمی و فناوری ریاست جمهوری

ریاست جمهوری
معاونت علمی و فناوری

۴) معاونت علمی، فناوری و اقتصاد دانش بنیان
ستاد توسعه فناوری‌های نانو و میکرو

ریاست جمهوری
معاونت علمی، فناوری و اقتصاد دانش بنیان
ستاد توسعه فناوری‌های نانو و میکرو

۵) CIVILICA

Sponsored and Indexed by
CIVILICA
We Respect the Science

۶) موسسه آموزشی و تحقیقاتی صنایع دفاعی

موسسه آموزشی و تحقیقاتی صنایع دفاعی

۷) موسسه تحقیق و توسعه دانشمند

دانشمند
موسسه تحقیق و توسعه

۸) شرکت تعاونی الیاف سیرنگ یزد

شرکت تعاونی سیرنگ
رنگ ها به ظرافت نخ - ۱۳۷۳

۹) شرکت کیمیا الیکای سپنتا

شرکت کیمیا الیکای سپنتا
KIMIA ELIKA SEPANTA

۱۰) شرکت مصباح انرژی

M E
Mesbah Energy

۱۱) شرکت مهامکس

مهامکس

۱۲) شرکت تماد کالا

تماد کالا
Tamad Kala

چکیده مقالات

Design and synthesis of effective compounds on toll-like receptore 7 (TLR 7)

Nasrin Saberi Harooni[a], Mohammad Reza Naimi-jamal[b], Azar Tahghighi[b], Mohammad Ghorban Dekamin[b]

[1]*Medicinal Chemistry Laboratory, Department of Clinical Research, Pasteur Institute of Iran, Tehran, Iran*

[2]*Department of Chemistry, Iran University of Science and Technology, Tehran, Iran*

Keyword: TLR7, molecular docking, [1,2,4]-triazolo[4,3-a] quinoxaline,

Abestract: A new series of [1,2,4] triazolo [4,3-a] quinoxaline derivatives have been designed, synthesized and biologically evaluated. In addition, molecular docking studies were performed for the new compounds. The binding energies of these ligands were investigated. The interactions of the ligand with the enzyme, including hydrophobic interactions, hydrogen bonds with the amino acids of the enzyme active site, were observed and analyzed using Autodock, DS Visualizer 3. Tools and Ligplot software were used to analyze the results.

Introduction

The intracellular messages of TLR7 are received by pDCs, then these molecules recruit the differentiated protein of myloid 88 through the TIR domain. MyD 88 activates IRAK protein, which accepts interferons, and then with the activation of TLR7, inflammatory cytokines, including interferon type 1, 6, 12 and TNF-α, are released, which regulate and express Genes related to the immune system lead[1-3]. Type 1 IFNs are one of the important products for TLR7/8 activation. TLRs have emerged as key targets in the pursuit of novel adjuvant therapies for vaccines against a wide variety of pathogens. Among a large number of new biologically active compounds synthesized by medicinal chemists, special attention has been paid to polycyclic compounds such as triazolo-quinoxaline due to their wide range of biological activities[4]

Experimental

The synthesis started from the reaction between benzene-1,٢-diamine (١٫٠٠ g), oxalic acid (1.5 g) and 3.00 mL of 10% HCl in 3.00 mL of H_2O, and briefly a mixture of 4-chloro[1,2,4]triazolo[4,3-a]quinoxalineor 4-chloro-1-methyl-[1,2,4]triazolo[4,3-a]quinoxaline (2.00 mmol) and various aliphatic amines (2.3 mmol) was refluxed in ethanol (15 mL) for 4 h. The solvent was then evaporated under reduced pressure. The resulting precipitate was filtered, dried, and crystallized from absolute ethanol ,and the final compound (Figure 1) was synthesized.

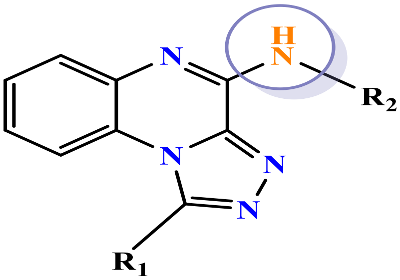

Figure 1: [1,2,4]triazolo[4,3-a]quinoxaline derivatives

Result

In this study, 12 triazole quinoxaline derivatives were investigated. The results of the present study showed that the triazole quinazolinone derivatives studied can inhibit the EGFR enzyme by binding to the active site. Based on the docking results, the inhibitory potential of the studied compounds is different and the strongest binding is related to the following compound

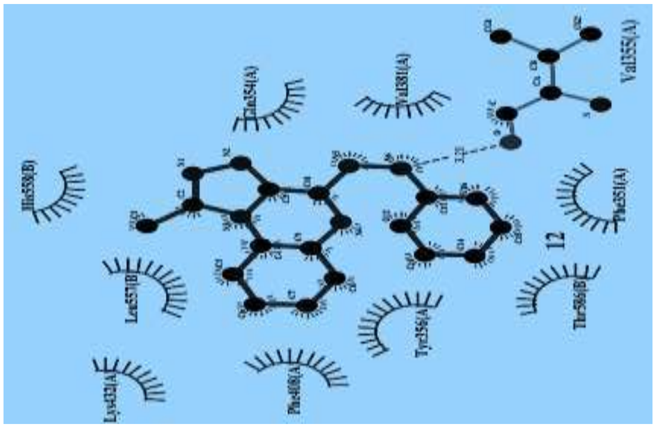

References:

[1] *H. Yu et al., "Toll-Like Receptor 7 Agonists: Chemical Feature Based Pharmacophore Identification and Molecular Docking Studies," 2013.*

[2] *S. Pal et al., "Synthesis and characterization of new potent TLR7 antagonists based on*

analysis of the binding mode using biomolecular simulations," 2021.

[3] *A. Baba et al., "Synthesis and immunostimulatory activity of sugar-conjugated TLR7 ligands," 2020.*

[4] *D. Kaneko et al., "Synthesis of [1, 2, 4] triazolo [4, 3-a] quinoxaline-1, 3, 4-oxadiazole derivatives as potent antiproliferative agents via a hybrid pharmacophore approach," Bioorg. Chem., 104, 104293, 2020.*

The 30th Iranian Seminar of Organic Chemistry
February 7-9, 2025, Iran University of Science and Technology, Tehran, Iran

Synthesis of Quinoxaline Using a Natural Heterogeneous Catalyst

Sepehr Ebadepour, Setareh Habibzadeh*, Masoud Nahali , Afshin sarvary

Noshirvani University of Technology, Babol, Iran

Keyword: Quinoxaline synthesis, natural catalyst, heterogeneous catalyst, green chemistry

Introduction

This study presents a green and efficient method for synthesizing quinoxaline using sheep rib bone as a natural catalyst. This method is not only environmentally friendly but also effectively reduces production costs by decreasing reaction time and increasing yield. Additionally, it demonstrates the potential for employing alternative catalysts that adhere to green chemistry principles.

Methods

For the synthesis of quinoxaline, sheep rib bone was used as a natural heterogeneous catalyst. The rib bone was powdered, washed with distilled water, and dried at 100°C before being used in the reactions. The reactions were conducted at 70°C in the presence of water as a solvent, as this condition yielded the best results.

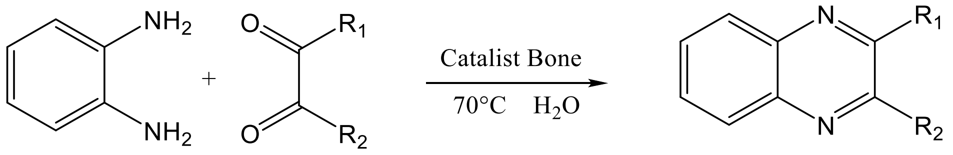

In addition to the sheep rib bone, alternative catalysts, such as DBUT, TNHP, iodine (I_2), and NBS, were tested for comparison. These catalysts were evaluated under similar conditions to determine their effectiveness in terms of reaction time and yield. The optimal catalyst amounts and reaction conditions were recorded for each.

Results

The use of sheep rib bone as a natural catalyst resulted in a high yield of 98% within 40 minutes, highlighting its efficiency and alignment with green chemistry principles. For comparison, other catalysts demonstrated varying levels of effectiveness:

Entry	Catalyst	Yield (%)	Time
1	Sheep rib bone	98	40 min
2	DBUT	92	2 h
3	TNHP	78	2-3 h
4	I_2	76	6-8 h
5	NBS	63	2-4h

This synthesis method supports the principles of green chemistry by using a natural and recyclable catalyst. Additionally, the results indicate that sheep rib bone is more effective than the alternative catalysts in terms of reaction time and yield. These findings demonstrate the suitability of this method for industrial and pharmaceutical applications.

References

1. Zhu, Y., Song, J., et al. (2020). “Transition-metal-free redox condensation for quinoxaline derivatives.” RSC Advances.

2. Kumar, V., et al. (2022). “Eco-friendly approach for quinoxaline synthesis using nanostructured pyrophosphate catalysts.” BMC Chemistry.

3. Zhang, L., et al. (2018). “Recyclable nanocatalysts for the synthesis of quinoxaline derivatives.” Catalysis Today.

Dual-effects of piezocatalysis and photocatalysis on RhB degradation by UiO-66(Zr)@ionic liquid/polyacrylonitrile nanofibers

Shadi Asgari*[1], Ghodsi Mohammadi Ziarani[1], Alireza Badiei[2]

[1]Department of Organic Chemistry, Alzahra University, Tehran, Iran

[2]School of Chemistry, College of Science, University of Tehran, Tehran, Iran

*Email: sh_asgari@alzahra.ac.ir

Abstract

The piezo-photocatalytic technique is deemed an emerging area utilized in environmental remediation. In this study, the piezo-photocatalytic composite nanofibers, UiO-66(Zr)@IL/PAN NFs, were designed to degrade the organic pollutant of Rhodamine B (RhB) under simultaneous ultrasonic (US) and light radiation sources. UiO-66(Zr) was first synthesized via the solvothermal reaction of terephthalic acid and $ZrCl_4$. Then, the ionic liquid (IL) of HMIM$^+$TFSI$^-$ was embedded into the UiO-66(Zr) at various concentrations to provide UiO-66(Zr)@IL-1, UiO-66(Zr)@IL-2, and UiO-66(Zr)@IL-3, which were subsequently embedded into the piezoelectric matrix of polyacrylonitrile (PAN). Finally, the spinning solution of UiO-66(Zr)@IL/PAN was exposed to electrospinning under optimal conditions. The RhB piezo-photodegradation efficiencies were found in the sequences of UiO-66(Zr)@IL/PAN NFs>UiO-66(Zr)/PAN NFs>UiO-***66(Zr)@IL>IL/PAN NFs>pure PAN NFs>UiO-66(Zr)>HMIM$^+$TFSI$^-$, confirming the boosted*** effect of the UiO-66(Zr), HMIM$^+$TFSI$^-$, and PAN NFs in the dye degradation and more efficiency of the fibrous form of catalysts in comparison with their corresponding powders. A boosted effect was observed in the piezo-photodegradation efficiencies of RhB (2.2%-95.4%) in comparison with the individual photodegradation (0.0%-21.3%) and individual piezodegradation efficiencies (2.3%-84.2%). Tauc plots and Mott-Schottky (M-S) results were consistent with the radical trapping experiments that introduced $O_2^{\bullet-}$ and HO$^\bullet$ species as critical in the RhB degradation.

Introduction

Water pollution is indeed a pressing issue that affects ecosystems, human health, and economic development globally [1]. Various techniques have been utilized to resolve the contaminated water-related issues [2]. Amongst, photocatalysis is an economical and environmentally benign phenomenon that can convert light energy into chemical energy and effectively mineralize organic dyes, instead of removing them from the aqueous environments [3]. However, there are certain limitations to the industrial application of photocatalysis, including inefficient use of visible light, rapid recombination of electrons and holes, and limited mobility of the photogenerated electrons and holes from the bulk to the surface of the photocatalyst [4]. Consequently, it is crucial to create new strategies to enhance photocatalytic efficiency to achieve significant advancements in photocatalysis. Piezocatalysis is a new concept of catalysis technology relying on piezoelectric materials agitated by mechanical energy, leading to the temporary polarization and production of piezoelectric potential [5]. Recently, significant efforts have been made to integrate photocatalysis with piezocatalysis, resulting in substantial advancements in the degradation of contaminants [6]. Piezo-photocatalysis is the synergistic effect of piezocatalysis and photocatalysis under mechanical energy and light radiation simultaneously. In this study, we constructed PAN-based IL-loaded UiO-66(Zr) NFs as a piezo-photocatalyst through blending electrospinning and investigated its ability on RhB degradation (Fig. 1).

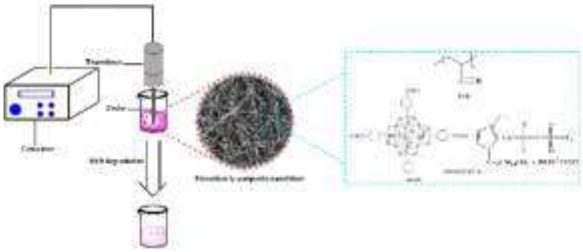

Figure 1. A schematic of the RhB degradation by UiO-66(Zr)@IL/PAN NFs.

Experimental

To fabricate the UiO-*66(Zr)@IL/PAN* NFs, a spinning solution composed of UiO-*66(Zr)@IL-1,* UiO-66(Zr)@IL-*2, or UiO-66(Zr)@IL-3 (1.0 wt%) a*nd PAN (12.0 wt%) was provided in DMF and followed by electrospinning. The optimal electrospinning conditions were selected as the voltage of 17.5 kV, the needle distance to the collector of 15 cm, the needle diameter of 21-gauge, the feeding rate of 0.5 mL/h, and the rotating collector speed of 100 rpm. The electrospun NFs were dried after their peeling off from aluminum foil. The pure PAN NFs (12.0 wt%), UiO-*66(Zr)/PAN NFs (1.0 wt% for UiO-66(Zr)), and IL/PAN NFs (1.0 wt% for IL) were also fabricated* at similar conditions for comparison studies.

Results and Discussion

The degradation efficiencies of RhB are shown in Figure 2. The results indicated that the piezodegradation efficiencies of RhB follow the sequence of UiO-6*6(Zr)@IL/PAN NFs>UiO-66(Zr)/PAN NFs>UiO-66(Zr)@IL>IL/PAN NFs>pure PAN NFs>UiO-66(Zr)>PAN* powder>$HMIM^+TFSI^-$. This confirms the significant impact of UiO-6*6(Zr),* $HMIM^+TFSI^-$*, and* PAN NFs on the RhB piezodegradation, and highlights the enhanced influence of UiO-*66(Zr)@IL/PAN NFs compared to their respective catalytic powders. The incorporation of PAN* NFs with UiO-*66(Zr)@IL inc*reased their piezocatalytic activity. Pure PAN NFs showed higher degradation efficiency of RhB compared to PAN powder, highlighting the significant role of electrospinning in promoting PAN's piezoelectric properties. The photodegradation trend, as illustrated in Figure 2, was detected in the order of UiO-*66(Zr)/PAN NF*s≥UiO-*66(Zr)@IL/PAN* NFs>UiO-6*6(Zr)>UiO-66(Zr)@IL>pure PAN NFs>PAN powder>IL/PAN NFs. PAN indicated* minimal photocatalytic activity, while $HMIM^+TFSI^-$ demonstrated low piezocatalytic activity and no photocatalytic effect. The catalysts under simultaneous US and light sources indicated an improved RhB degradation, confirming the boosted effect of piezocatalysis and photocatalysis.

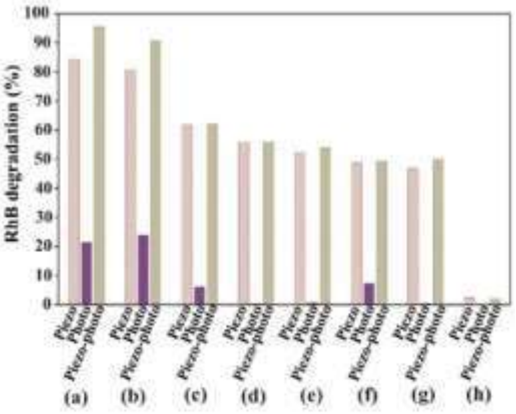

Fig. 2. RhB piezo-/photo/piezo-photodegradation graphs by (a) UiO-*66(Zr)@IL-1/PAN NFs, (b*) UiO-*66(Zr)/PAN NF*s, (c) UiO-*66(Zr)@IL-1, (d) IL/PAN* NFs, (e) pure PAN NFs, (f) UiO-*66(Zr), (g) PAN powder, and (h)* HMIM$^+$TFSI$^-$.

The primary reactive oxygen species (ROS) involved in the degradation of RhB were identified using scavengers of benzoquinone (BQ) to capture $O_2^{\bullet -}$, tertiary butyl alcohol (TBA) for $^{\bullet}OH$, and disodium ethylenediaminetetraacetic acid (Na_2EDTA) to trap h^+. The efficiency of RhB degradation decreased when BQ and TBA scavengers were present, showing that the $O_2^{\bullet -}$ and $^{\bullet}OH$ species play main roles in the degradation of RhB. To further confirm the degradation mechanism, Tauc and M-S plots were recorded. The E_g of +3.31 V and E_{CB} of *-0.34 V were d*etermined from the Tauc plots and M-S plots of UiO-6*6(Zr)@IL-1/PAN NFs, respectivel*y. The E_{CB} of the UiO-*66(Zr)@IL-1*/PAN NFs was found more negative than the $E(O_2/O_2^{\bullet -}) = -0.33$ V, so the photogenerated electrons could create the $O_2^{\bullet -}$ species by reacting with O_2. Additionally, the determined E_{VB} of the NFs (+3.31 V) was found more positive than the $E(H_2O/^{\bullet}OH) = +2.40$ V, confirming the effective role of the $^{\bullet}OH$ species in the RhB degradation.

Conclusion

In conclusion, we presented a PAN-based composite nanofibrous piezo-photocatalyst, UiO-*66(Zr)@IL/PAN NFs, for the US/light*-driven degradation of RhB. A boosted effect was noted in the piezo-photodegradation efficiencies of RhB when compared to the efficiencies of individual photodegradation and piezodegradation processes. The exploration of this novel catalyst and its enhanced photocatalytic performance through piezoelectric effects could stimulate further innovations in environmental management.

References

(1)Jiang, X.; Li, X.; Kong, Y.; Deng, C.; Li, X.; Hu, Q.; Yang, H.; He, C. *Journal of Energy Chemistry* **2023**, *76*, 462-469.

(2)Asgari, S.; Ziarani, G. M.; Badiei, A.; Ajalloueian, F.; Vasseghian, Y. *Environmental Research* **2022**, *215*, 114296.

(3)Choi, H.J.; Kim, D.; Lee, T.J. *Journal of Environmental Science and Health, Part B* **2013**, *48*, 927-934.

(4)He, J.; Kumar, A.; Khan, M.; Lo, I. M. *Science of the Total Environment* **2021**, *758*, 143953.

(5)Li, L.; Ma, Y.; Chen, G.; Wang, J.; Wang, C. *Scripta Materialia* **2022**, *206*, 114234.

(6)Tu, S.; Guo, Y.; Zhang, Y.; Hu, C.; Zhang, T.; Ma, T.; Huang, H. *Advanced Functional Materials* **2020**, *30*, 2005158.

The 30th Iranian Seminar of Organic Chemistry
February 7-9, 2025, Iran University of Science and Technology, Tehran, Iran

Adsorption-assisted photocatalytic degradation of methylene blue by an FcLR-based porous organic polymer

Shadi Asgari*[1], Ghodsi Mohammadi Ziarani[1], Alireza Badiei[2]

[1]Department of Organic Chemistry, Alzahra University, Tehran, Iran

[2]School of Chemistry, College of Science, University of Tehran, Tehran, Iran

**Email: sh_asgari@alzahra.ac.ir*

Abstract

Adsorption-assisted photocatalysis is an effective method for enhancing the removal of pollutants from wastewater. This enhancement can be achieved using a new type of metallocene-based porous organic polymer, called FcLR-P. The synthesis of FcLR-P involves two key steps 1) the creation of a ferrocene-containing metal-organic porous polymer, known as ferrocene-P, through a Friedel-Crafts reaction between dimethoxymethane and ferrocene, and 2) the subsequent reaction of ferrocene-P with phosphonium pentasulfide (P_2S_5). The photodegradation efficiency of methylene blue (MB) using FcLR-P was found to be higher than that of ferrocene-P, indicating a greater photocatalytic activity of FcLR-P, which can be attributed to the presence of FcLR. Conversely, the adsorption efficiency of MB decreased following the reaction of ferrocene-P with P_2S_5. When investigating both photodegradation and adsorption simultaneously (known as adsorption-assisted photocatalysis), a significant increase in dye elimination was observed for both ferrocene-P and FcLR-P.

Introduction

Recent evidence shows that the existence of both adsorption and photocatalysis can lead to an adsorption-assisted photocatalysis phenomenon, which ultimately enhances the overall removal of organic pollutants from water environments [1]. The use of porous organic polymers (POPs) for pollutant removal combines adsorption and photodegradation for the effective elimination of pollutants. Compared with homogeneous and nonporous heterogeneous catalysts, porous and amorphous structures of catalysts, e.g. POPs, facilitate faster and more efficient mass transport of water to the photogenerated charges, making them particularly beneficial for applications in wastewater treatment, hydrogen production, and pollutant degradation [2]. The catalytic application of POPs can be enhanced through metal modification, resulting in the creation of metal-containing or metalated POPs, referred to as metal-organic porous polymers (MOPPs) [3-4]. Research into the use of metallocenes as constructing units for establishing MOPPs is quite rare. The first metallocene, ferrocene, features a unique sandwich-type structure formed by a covalent bond bridge between two cyclopentadienyl (Cp) rings and Fe^{2+} centers [5-7]. Ferrocene can serve as a pore-forming agent for constructing porous networks [8]. Incorporating ferrocenyl units into the structure of POPs can effectively enhance photocatalytic activity for the degradation of organic pollutants [9-10]. Ferrocenyl Lawesson's Reagent (FcLR) is a newly developed ferrocene derivative with high reactivity expected to enhance the photocatalytic activity of MOPPs.

We will develop a new type of ferrocene-based MOPP, called FcLR-P. This product combines the benefits of FcLR units with a porous structure for the adsorption-assisted photocatalytic degradation of cationic and anionic organic dyes.

Experimental

The synthesis procedure of FcLR-P is shown in Figure 1, step by step. Step 1 refers to the Friedel-Crafts reaction. Ferrocene units were crosslinked to produce a porous polymer in 1,2-dichloroethane solvent. In the presence of the Lewis acid of BF_3, the alkylation reaction between the Cp ring and methylene occurred and ferrocene-P with a porous structure was formed. In step *2, the ferrocene parts of the ferrocene-P could react with* P_2S_5 *to generate FcLR-P.*

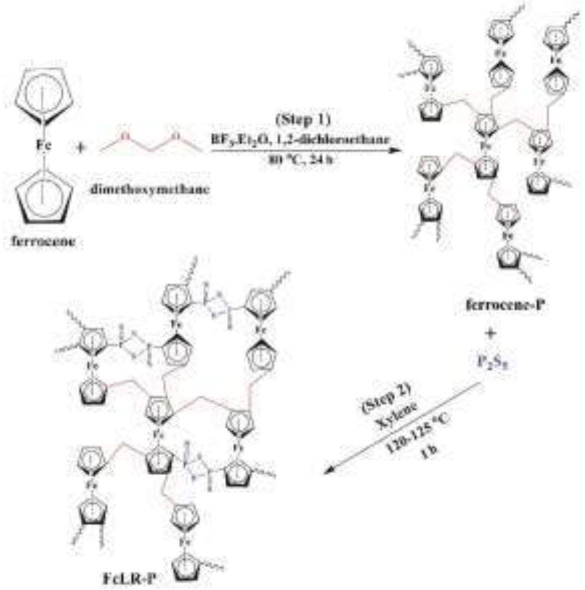

Figure 1. The synthesis procedure FcLR-P by two steps.

Results and Discussion

The photocatalytic activity of ferrocene-P and FcLR-P was evaluated through experiments on the photodegradation of methylene blue (MB). The degradation efficiency of MB with FcLR-P was found to be higher than that with ferrocene-P, which can be attributed to the presence of the FcLR component. In contrast to the catalysts' photodegradation abilities, the adsorption efficiency of the MB dye decreased after the reaction of ferrocene-P with P_2S_5. A significant improvement in the elimination of the MB dye was observed for both ferrocene-P and FcLR-P when the combined effects of degradation and adsorption were analyzed, as shown in Figure 2.

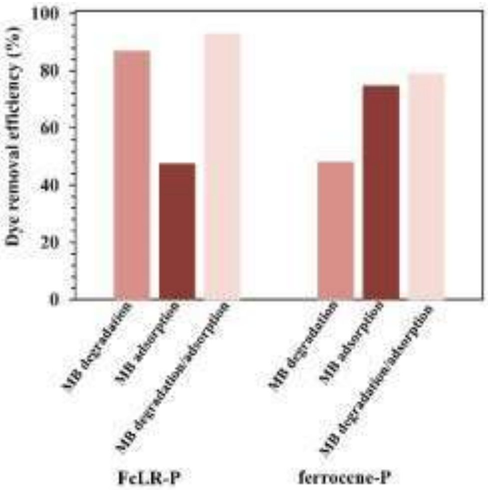

Figure 2. Photodegradation, adsorption, and combined degradation/adsorption efficiencies of MB dye over the ferrocene-P and FcLR-P.

Conclusion

The main objective of this study is to eliminate MB dye by combining two processes: adsorption and photocatalysis. A new type of ferrocene-based porous organic polymer, referred to as FcLR-P, has been developed through two synthetic steps. The first step involves the preparation of ferrocene-P using a one-pot Friedel-Crafts reaction between ferrocene and dimethoxymethane. The second step involves the production of FcLR-P by reacting ferrocene-P with P_2S_5. *FcLR*-P exhibited greater efficiency than ferrocene-P in photodegrading the MB dye, which confirms its enhanced photocatalytic activity. This improvement can be attributed to the combined characteristics of FcLR and the porous polymer. In contrast to the behavior during photodegradation, the adsorption efficiency of the dye decreased for FcLR-P. A boosted dye elimination was observed for ferrocene-P and FcLR-P when investigating adsorption-assisted photocatalysis.

References

(1)Chakraborty, J.; Nath, I.; Verpoort, F. *Chemical Society Reviews* **2022**, *51*, 1124-1138.

(2)Yang, Y.; Lai, Z. F. *Microporous and Mesoporous Materials* **2021**, *316*, 110929.

(3)Boro, B.; Adak, M. K.; Biswas, S.; Sarkar, C.; Nailwal, Y.; Shrotri, A.; Chakraborty, B.; Wong, B. M.; Mondal, J. *Nanoscale* **2022**, *14*, 7621-7633.

(4)Paul, R.; Shit, S. C.; Singh, A.; Wong, R. J.; Dao, D. Q.; Joseph, B.; Liu, W.; Bhattacharya, S.; Mondal, J. *Nanoscale* **2022**, *14*, 1505-1519.

(5)Neuse, E. W. *Nature* **1964**, *204* , 179-180.

(6)Vorotyntsev, M. A.; Vasilyeva, S. V. *Advances in colloid and interface science* **2008**, *139*, 97-149.

(7)Matsuura, Y.; Odani, R.; Tanaka, Y. *Polymer journal* **2008**, *40*, 1185-1190.

(8)Chen, Y.; Cao, X.; Zhu, H.; Liu, Y. *International Journal of Hydrogen Energy* **2012**, *37*, 7629-7637.

(9)Fu, X.; Zhang, Y.; Gu, S.; Zhu, Y.; Yu, G.; Pan, C.; Wang, Z.; Hu, Y. *Chemistry–A European Journal* **2015**, *21*, 13357-13363.

(10)Ma, Q.; Qi, Y.; Li, J.; Wang, W.; Sun, X. *Applied Organometallic Chemistry* **2018**, *32*, e3935.

The 30th Iranian Seminar of Organic Chemistry
February 7-9, 2025, Iran University of Science and Technology, Tehran, Iran

Engineering Co-Al LDH@COF architecture with enhanced photocatalytic properties under visible light irradiation

Ali Banitalebi [a], Ghodsi Mohammadi Ziarani [a,*], Alireza Badiei [b]

[a] *Department of Organic Chemistry, Faculty of Chemistry, Alzahra University, Tehran, Iran*

[b] *School of Chemistry, College of Science, University of Tehran, Tehran, Iran*

[*] *E-mail address: gmohammadi@alzahra.ac.ir*

Abstract

In contemporary times, the accelerated growth of industrial activities and the rising global population have led to significant challenges, including an energy crisis and environmental pollution. Among the various forms of environmental pollutants, organic pollutants represent a critical threat to human health. Consequently, the advancement of green technologies, such as photocatalysis, which utilizes renewable and clean energy resources, has garnered considerable attention for its potential to effectively eliminate organic pollutants. Heterojunction nanostructure construction and morphological engineering are recognized as effective strategies to enhance photocatalytic performance.

Covalent organic frameworks (COFs) are crystalline organic polymers characterized by porous structures formed through covalent bonds between organic monomers. Recent studies have indicated that layered double hydroxides (LDHs) represent a promising candidate for integration with COF, aiming to augment the photocatalytic activity of pure COFs. In this study, we present the fabrication of binary hierarchical hollow structures comprising CoAl-LDH nanoplates deposited on hollow COF (designated as LDH@HCOF), achieved via a templating method followed by a solvothermal process. The resultant composites exhibited superior performance in the photocatalytic degradation of tetracycline (TC) in comparison to pure HCOF and LDH when exposed to visible light illumination.

Keywords: Covalent organic framework; Photocatalysis; Hollow structure; Tetracycline; LDH

1. Introduction

Energy shortages, environmental pollution, and effluent treatment are critical contemporary challenges. There is an urgent need for advanced materials and renewable energy technologies to address these issues. Semiconductor-based photocatalysis provides an eco-friendly method for decomposing organic pollutants under mild conditions, generating byproducts like H_2O and CO_2. Key factors in synthesizing semiconductor materials include: (1) light absorption capacity, (2) specific surface area, and (3) efficient separation and migration of photogenerated electron-hole pairs. Suitable band gap semiconductors can enhance reaction rates during light exposure. Various photocatalysts have been developed, including metal oxides, phosphides, sulfides, and metal-free polymers [1,2].

Covalent organic frameworks (COFs) are porous polymers formed by covalent bonds and exhibit broad absorption spectra and high visible light capture capacity [3]. Despite their potential, pure COFs often show low photocatalytic efficiency due to high recombination rates of charge carriers. Strategies to improve this include doping, morphological regulation, and coupling with other semiconductors. Forming heterostructure materials by integrating COFs with other semiconductors has shown promise in enhancing charge separation efficiency [4]. Metal sulfides, especially Layered Double Hydroxides (LDHs), have emerged as effective photocatalysts due to their favorable properties, including suitable band gaps and stability [5,6]. Morphological innovations like hollow microspheres mimic natural photosynthesis processes, enhancing light absorption and mass transfer, which improve photogenerated charge migration. These hollow structures allow multiple light reflections and provide more active sites, ultimately benefiting solar energy conversion in photochemical reactions [7,8].

Hierarchical hollow heterostructures with two-dimensional nanosheets are valuable for solar energy conversion and chemical storage due to their structural benefits. These materials feature porous networks that enhance transport and reaction dynamics. Hollow scaffolds with cavities can trap light, particularly in multi-shelled designs, while nanosheet-based architectures reduce charge diffusion pathways and increase surface area and active site concentration. This configuration supports better charge separation and photocatalytic performance by decreasing electron-hole recombination and improving analyte capture and photo-redox reaction kinetics [9,10].

We have developed a core-shell structure using HCOF as the scaffold and LDH flakes as the shell for visible-light photocatalysis. Our approach includes enhancing photocatalytic efficiency through distinct morphology that shortens charge diffusion pathways and facilitates light reflections, promoting effective charge carrier separation at the LDH-COF junction. Additionally, the interaction between LDH and COF reduces charge carrier recombination and boosts light absorption. The photocatalytic activity was evaluated using tetracycline degradation under visible light, laying the groundwork for advanced photochemical nanostructures.

2. Method

A monodisperse spherical silica template was synthesized using a modified procedure. First, a solution of 8 mL of aqueous ammonia (32 wt.%) and 10 mL of water was mixed with 180 mL of ethanol and stirred for 20 minutes at 35 °C. Next, 8 mL of tetraethyl orthosilicate (TEOS) was added while stirring vigorously. The mixture stood for 1 hour to form silica spheres, which were then isolated by high-speed centrifugation and washed with ethanol for purity. To modify the silica nanoparticles' surface with amino groups, 1 g of nanoparticles was sonicated in 100 mL of anhydrous toluene for 30 minutes. Then, 1 mL of (3-aminopropyl) triethoxysilane (APTES) and 2 mL of toluene were added, and the mixture was refluxed under nitrogen for 24 hours. Afterward, unbound NH_2 groups were removed through centrifugation and ethanol washes, followed by drying the particles at 70 °C for 24 hours.

2.1. Synthesis of Hollow COF

A seed solution was prepared by dissolving 1,4-phenylenediamine (PDA, 0.052 mmol) and tri-(4-formacylphenoxy)-1,3,5-triazine (TFPTA, 0.018 mmol) in a 5 mL suspension of amine-functionalized SiO_2 nanoparticles in ortho-dichlorobenzene and n-butanol (4:1 ratio). The mixture was stirred for 2 hours, then for an additional hour after adding 10 µL of acetic acid. Next, PDA (0.2 mmol) and TFPTA (0.072 mmol) were sonicated in the seed solution for 15 minutes, followed by the addition of 0.3 mL of acetic acid. The reaction was frozen in liquid nitrogen at 77 K, degassed through three freeze-pump-thaw cycles, sealed under vacuum, and heated at 120 °C for 3 days. The product was isolated by centrifugation and washed with THF, anhydrous ethanol, and acetone before drying in a vacuum oven at 80 °C for 12 hours. The silica framework was dissolved in NH_4HF_2 at 70 °C for 16 hours, with the final product collected by centrifugation, washed with deionized water, and dried under vacuum.

2.2. Synthesis of core-shell LDH@HCOF

The LDH@HCOF architectures were synthesized through the in-situ crystallization of CoAl-LDH nanosheets onto the surface of HCOF. To accomplish this, 120 mg of the synthesized HCOF nanoparticles were initially dispersed in a solution comprising $Al(NO_3)_3 \cdot 9H_2O$ (6 mmol), $Co(NO_3)_2 \cdot 6H_2O$ (16 mmol), NH_4F (25 mmol), urea (40 mmol), and 65 mL of water via ultrasonication for a duration of 20 minutes. The resulting mixture was subsequently transferred to a 100 mL Teflon-lined autoclave and subjected to heating at 100 °C for 14 hours. Following this period, the autoclave was allowed to cool naturally to room temperature, and the core-shell particles were then collected through centrifugation. These particles were washed several times with ethanol and subsequently dried under vacuum at 50 °C overnight.

2.3. Photocatalytic activity evaluation

The photocatalytic activity of the synthesized samples was assessed through the degradation of tetracycline (TC) under simulated solar light generated by a 300 W xenon (Xe) lamp, utilizing a 400 nm cutoff filter. In a standard photodegradation experiment, 100 mg of the photocatalyst was added to 100 mL of a TC aqueous solution at a concentration of 20 ppm. The mixture was stirred in the dark for a duration of 20 minutes to achieve adsorption-desorption equilibrium. Following this, the suspension was subjected to irradiation under the 300 W Xe lamp, while the temperature was maintained at room temperature using a circulating water system. At predetermined intervals, 4 mL of the reaction mixture was extracted and centrifuged to separate the photocatalyst particles. The concentrations of TC were determined using a UV-Vis spectrophotometer (Raleigh UV-1600) at a wavelength of 357 nm.

3. Results and discussion

Powder X-ray diffraction (PXRD) analysis has confirmed that the TFPTA-PDA HCOF exhibits a crystalline structure, characterized by three prominent peaks at 4.70°, 5.43°, and 7.19°, which correspond to reflections from the (110), (200), and (120) facets, respectively (see Figure 1). This finding indicates that the removal of the silica core did not compromise the crystalline integrity of the HCOF. Additionally, the pronounced peak observed at 2.7° (100) suggests a highly ordered structure within the covalent organic framework (COF). Furthermore, the presence of broad diffraction peaks around 20° implies an interlayer π-π stacking distance of less than 3.5 Å, a value that aligns well with typical metrics observed in π-π stacking systems.

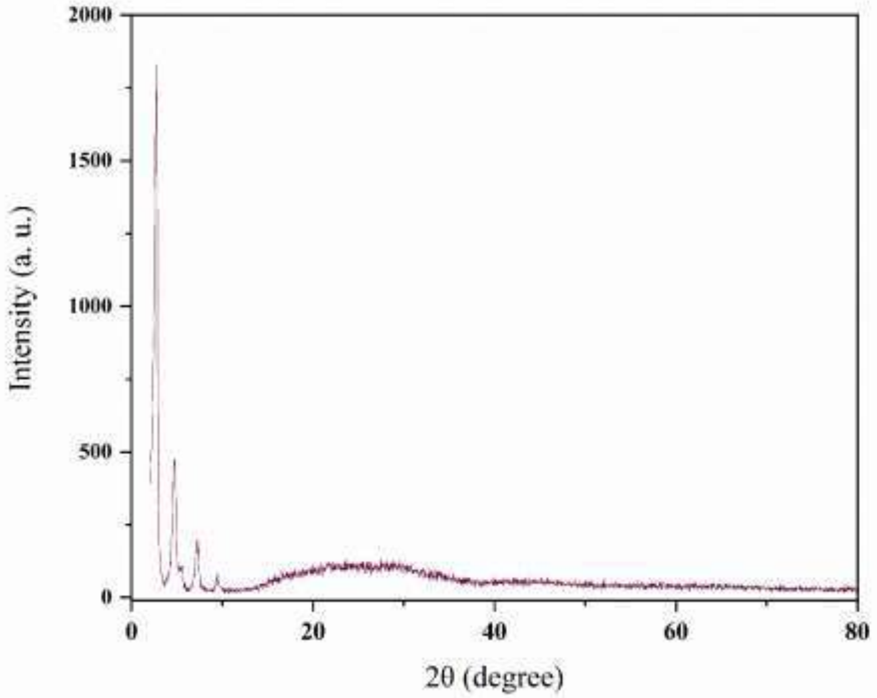

Fig. 1 Powder XRD patterns of HCOF

The structure and morphology of the prepared samples were examined using SEM images. As illustrated in Figure 2, the fabrication process of the LDH@HCOF nanoparticles comprises four primary stages: (i) the synthesis of monodispersed spherical SiO_2 modified with amino groups to serve as starting templates; (ii) the application of uniform shells of amorphous Schiff-base polymer around the silica cores; (iii) the conversion of spherical structures into mesoporous hollow COF through a polymerization reaction followed by the removal of silica; and (iv) the in-situ crystallization of LDH nanoplates on the surface of the HCOF via a hydrothermal process. The silica nanospheres exhibited a high degree of uniformity, with an average diameter of approximately 200 nm (see Fig. 2a). Following the application of the organic building coating, these SiO_2 nanoparticles were entirely encapsulated by Schiff-base shells, resulting in an increased diameter of around 220 nm (see Fig. 2b). Consequently, the thickness of the polymer shell is estimated to be roughly 20 nm. Upon polymerization of the organic buildings and subsequent removal of the silica templates using an NH_4HF_2 aqueous solution, the produced COF@SiO_2 microspheres were transformed into hollow COF spheres. The SEM image presented in Figure 2c reveals that the as-synthesized HCOFs possess a well-defined hollow spherical morphology, with a consistent size of approximately 220 nm. Following the hydrothermal decoration of LDH nanoplates on the surface of the hollow COFs, the resulting LDH@HCOF structures predominantly maintain the spherical morphology of the HCOF, albeit with a distinctly roughened surface (see Fig. 2d).

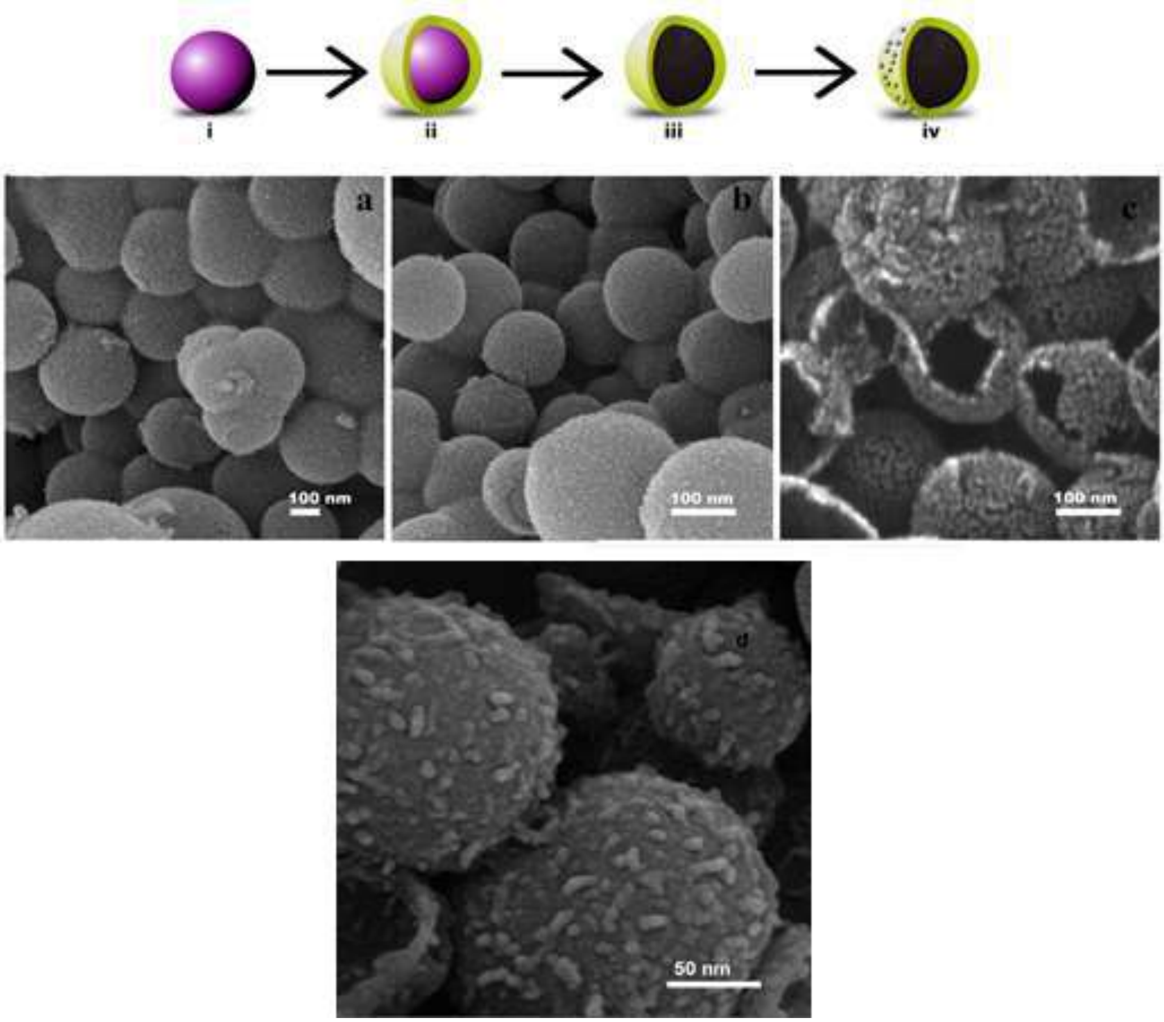

Fig.2 Schematic illustration of the morphological evolution of the prepared nanohybrid catalyst and corresponding FESEM images

Tetracycline (TC) degradation was investigated using as-prepared photocatalysts under visible light irradiation to evaluate their photocatalytic performance. In the absence of a photocatalyst, the photodegradation of TC was insignificant, indicating the photochemical stability of these contaminants. The degradation rates observed for pure LDH and COF after 120 minutes of light irradiation were merely 38% and 45%, respectively. The suboptimal performance of these single-component photocatalysts is likely attributed to the rapid recombination of electrons and holes generated during the photogeneration process. Figure 3 illustrates that the hollow COF (HCOF) sample demonstrates enhanced photocatalytic performance under visible light irradiation compared to pure COF, highlighting the significant influence of its hollow structure. When compared to pure HCOF, the binary composites with a hierarchical structure exhibited superior photocatalytic activities for the photodegradation of TC. Several factors contribute to the enhanced performance of the ternary composite system: firstly, the synergistic interaction between COF and

LDH nanoplates significantly improves the separation of photogenerated electrons and holes, thereby boosting photocatalytic performance; secondly, the increase in specific surface area provides more surface-active sites, facilitating the adsorption and degradation of contaminants; finally, the multiple light reflection effects within the hollow hierarchical structure augment the photocatalyst's ability to capture light, which can be associated with its remarkable photocatalytic capabilities. The data presented in the figure were analyzed utilizing the pseudo-first-order kinetic model to evaluate the degradation reactions of tetracycline (TC): $\ln (C_t/C_0) = -kt$, where t represents the duration of photocatalysis, C_0 denotes the initial concentration of TC, and C_t represents the concentration of TC at time t. The apparent rate constant for TC decomposition is denoted by k. As illustrated in Fig. 3b, the linear correlation between $-\ln (C_t/C_0)$ and illumination time validates the applicability of the model. The fitting results indicate that both pure LDH and COF exhibit relatively low reaction rate constants, as shown in Fig. 3c. Notably, the composite sample demonstrated the highest k value under comparable conditions, which is four times greater than that of pure LDH and COF regarding TC degradation. Consequently, it can be concluded that the LDH@HCOF composite exhibited superior photocatalytic performance compared to all other samples prepared in this study.

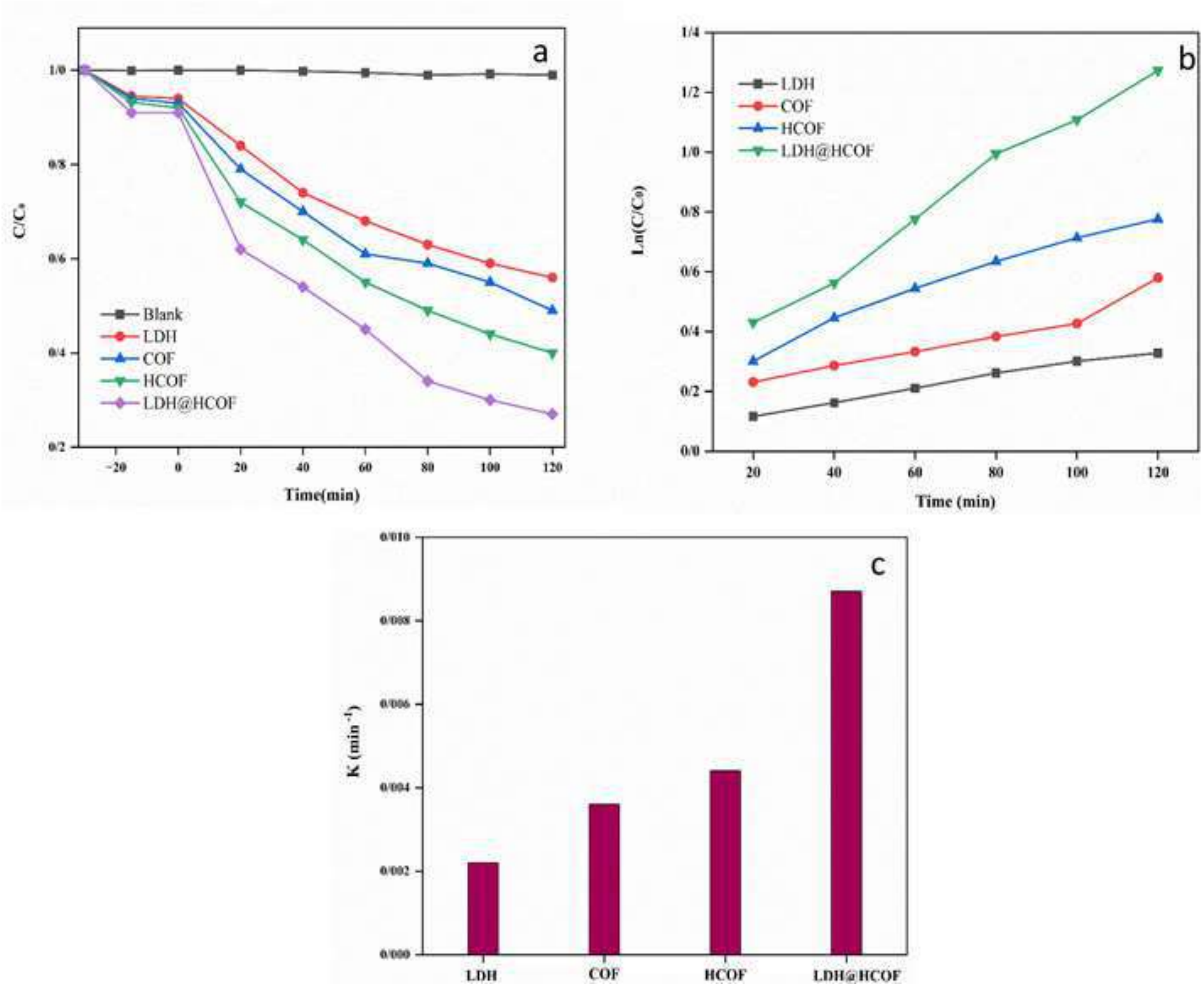

Fig. 3. (a) Photocatalytic degradation efficiency of TC under visible light irradiation over prepared samples, (b and c) kinetic curves and reaction rate constant for TC degradation over the as fabricated photocatalysts.

References

[1] C. Xu, P.R. Anusuyadevi, C. Aymonier, R. Luque, S. Marre, Nanostructured materials for photocatalysis, Chem. Soc. Rev. 48 (2019) 3868–3902.

[2] M.S. Khan, Y. Li, D.-S. Li, J. Qiu, X. Xu, H.Y. Yang, A review of metal-organic framework (MOF) materials as an effective photocatalyst for degradation of organic pollutants, Nanoscale Adv. (2023).

[3] G. Sun, J. Zhang, B. Cheng, H. Yu, J. Yu, J. Xu, Bifunctional CdS/COF S-scheme photocatalyst for enhanced H2 evolution and organic synthesis, Chem. Eng. J. 476 (2023) 146818.

[4] L. Zhang, J. Zhang, H. Yu, J. Yu, Emerging S-scheme photocatalyst, Adv. Mater. 34 (2022) 2107668.

[5] S. Zhang, X. Ou, Q. Xiang, S.A.C. Carabineiro, J. Fan, K. Lv, Research progress in metal sulfides for photocatalysis: From activity to stability, Chemosphere 303 (2022) 135085.

[6] A. Ziarati, A. Badiei, R. Grillo, T. Burgi, 3D yolk@ shell TiO_{2}–x/LDH architecture: tailored structure for visible light CO_2 conversion, ACS Appl. Mater. Interfaces 11 (2019) 5903–5910.

[7] Z. khoshkholgh, S. Sohrabnezhad, Optimizing photocatalytic activity for chromium reduction: the role of MgAl LDH/triazine covalent organic framework/CdS nanocomposite, Emergent Mater. (2024) 1–18.

[8] J. Fu, J. Yu, C. Jiang, B. Cheng, g-C_3N_4-Based heterostructured photocatalysts, Adv. Energy Mater. 8 (2018) 1701503.

[9] P. Zhang, X. Yin, D. Zhang, P. Guo, W. Liu, R. Wang, Z. Zhang, S. Qiu, MOF templated to construct hierarchical $ZnIn_2S_4$-In_2S_3 hollow nanotube for enhancing photocatalytic performance, Chem. Eng. J. 458 (2023) 141394.

[10] M.-C. Tsai, J.-Y. Lee, P.-C. Chen, Y.-W. Chang, Y.-C. Chang, M.-H. Yang, H.-T. Chiu, I.-N. Lin, R.-K. Lee, C.-Y. Lee, Effects of size and shell thickness of TiO_2 hierarchical hollow spheres on photocatalytic behavior: An experimental and theoretical study, Appl. Catal. B Environ. 147 (2014) 499–507.

Cytotoxicity evaluation of *Reseda lutea* extract by BSLA

Mahdi Fatehi Marj*, Abdolrasoul H. Ebrahimabadi

Essential Oils Research Institute, University of Kashan, Kashan, Iran

mahdiifatehimarj@gmail.com

Keywords: *Reseda lutea*, cytotoxicity, anticancer, *Artemia salina*, BSLA

Introduction

Fighting cancer is a big challenge, and scientists are always looking for better ways to treat it. One important method is to use substances having the ability to kill or stop the growth of cancer cells which is called cytotoxicity. *Reseda lutea* L., also known as wild mignonette, is a medicinal plant that has been used for centuries to promote healing. Ancient texts mentioned its use in treating tumors, and modern studies are now providing evidence to support these claims [1]. Recent research has shown that Reseda lutea contains powerful bioactive compounds like flavonoids, isothiocyanates, and phenolic acids. These compounds have antioxidant, anti-inflammatory, and cytotoxic effects [2]. For example, benzyl isothiocyanate and its derivatives have demonstrated strong effects against melanoma and fibroblast cells by stopping their growth and triggering programmed cell death, known as apoptosis [1]. Similarly, flavonol glycosides extracted from the plant have shown enzyme inhibition and cytotoxic effects against lung cancer cells, even at very low concentrations [2]. With the increasing interest in natural products as safer options compared to conventional chemotherapy [3], this study investigates the cytotoxicity of *Reseda lutea* methanolic extract based on brine shrimp lethality bioassay to assess whether this plant could be a source of new compounds for cancer treatment.

Method

The plant was collected in late autumn from Taleghan, Alborz Province, Iran. After collection, the fruits were separated and dried in a dark, air-conditioned space. The dried fruits were finely ground and macerated in methanol on shaker for 24 hours at 50°C and the mixture was filtered to remove any solid residues. The liquid extract was condensed using a rotary evaporator and dried in oven. The dried extract was dispersed in deionized water and subjected to a fractional separation process using n-hexane solvent. This step helped separate the components, allowing phenolic compounds to remain in the aqueous phase. The aqueous phase was carefully decanted and dried to obtain the final extract rich in phenolic content. Saltwater was prepared by dissolving specific salts, including sodium chloride, magnesium chloride, and potassium chloride, in distilled water. The solution was sterilized by heating for 5 minutes, and the pH was adjusted to 9 using sodium carbonate. Brine shrimp eggs were placed in the prepared saltwater and incubated at 30°C under continuous light for 48 hours to hatch into larvae. A stock solution (2 mg/mL) of the plant extract was prepared by dissolving the extract in dimethyl sulfoxide (DMSO), heating slightly at 40°C, and then diluting with saltwater. Different concentrations (10, 100, 300, 500, 700, and 1000 µg/mL) were prepared using serial dilutions. Each concentration was tested in triplicate, and 10 brine shrimp larvae were added to each test tube. The test tubes were incubated at 30°C for 24 hours under light. After this period, the number of dead and alive larvae was counted in each tube. A graph of the percentage of lethality was drawn based on the concentration of the extract to determine the concentration at which 50% of the larvae were killed (LC_{50}) which represents the cytotoxic potential of the extract.

Results and Discussion

The brine shrimp lethality assay was used to evaluate the cytotoxicity of *Reseda lutea* methanolic extract. The results showed a dose-dependent increase in mortality of brine shrimp larvae, indicating the extract's cytotoxic potential. The LC_{50} value was calculated to be 170.69 ± 0.21 µg/mL, suggesting significant cytotoxic activity of the extract. This low LC_{50} value shows the potency of *Reseda lutea* against biological systems, aligning with previous reports of its bioactive compounds such as flavonoids and isothiocyanates exhibiting cytotoxic and apoptotic effects. The observed cytotoxicity can be attributed to the presence of phenolic compounds and benzyl isothiocyanate derivatives in the extract, which have been shown to induce apoptosis and inhibit cancer cell growth. The brine shrimp assay serves as a preliminary indicator of potential anticancer properties, supporting the ethnopharmacological use of this plant in traditional medicine. These findings suggest that Reseda lutea could serve as a promising source of bioactive compounds for further anticancer research. However, additional studies involving specific cancer cell lines, mechanism of action analysis, and in vivo models are required to validate its efficacy and safety.

References

١. Radulović, N. S., Zlatković, D. B., Ilić-Tomić, T., Senerović, L., & Nikodinovic-Runic, J. (2014). Cytotoxic effect of Reseda lutea L.: A case of forgotten remedy. *Journal of ethnopharmacology*, *153*(1), 125-132.

٢. Kiziltaş, H. (2022). Comprehensive evaluation of Reseda lutea L. (Wild Mignonette) and 7 isolated flavonol glycosides: determination of antioxidant activity, anti-Alzheimer, antidiabetic and cytotoxic effects with in vitro and in silico methods. *Turkish Journal of Chemistry*, *46*(4), 1185-1198.

٣. Thuwaini, M. M. (2022). Natural sources as promising future anticancer therapies-A review. *GSC Biological and Pharmaceutical Sciences*, *19*(2), 084-113.

Extraction and evaluation of antioxidants from *Hibiscus sabdariffa*

Mahdi Fatehi Marj*, Abdolrasoul H. Ebrahimabadi

Essential Oils Research Institute, University of Kashan, Kashan, Iran

mahdiifatehimarj@gmail.com

Keywords: *Hibiscus sabdariffa*, antioxidant, phenolic acids, flavonoid, radical scavenging

Introduction

Hibiscus sabdariffa L., known as roselle, is rich in bioactive compounds such as phenolic acids, flavonoids, and anthocyanins. These phytochemicals protect biological systems against oxidative damage, show anti-inflammatory and anti-aging properties [1,2]. Phenolic compounds, including protocatechuic acid, quercetin, and luteolin derivatives, anthocyanins like cyanidin-3-sambubioside and delphinidin-3-sambubioside, are prevalent in *Hibiscus sabdariffa* [3]. These compounds have been reported to significantly contribute to the antioxidant activity measured through assays such as DPPH and ABTS, indicating high radical scavenging efficiency [4]. The antioxidant capacity of roselle has been linked to its role in lowering oxidative stress-related diseases and enhancing cellular detoxification processes [5]. This study investigates the antioxidant properties of the extracts of *Hibiscus sabdariffa* through DPPH, β-carotene-linoleic acid, total phenolic content, and total flavonoid content assays. The findings aim to further clarify the relationship between the characterized phytochemicals and the observed antioxidant activities.

Method

Hibiscus sabdariffa plant was collected, dried, and ground. Extraction was performed using a Soxhlet apparatus with methanol and water as solvents, separately, for 6 hours at approximately 60°C. Extracts were concentrated with a rotary evaporator at 50°C and dried. The antioxidant activity of the extracts was evaluated using the DPPH free radical scavenging method. BHT was used as a standard for comparison. Absorbance was measured at 517 nm, and IC_{50} values were calculated. The ability of the extracts to prevent oxidative degradation of β-carotene in a linoleic acid system was assessed and was monitored at 470 nm. BHT served as the positive control. Total phenolic content was determined using the Folin–Ciocalteu reagent with gallic acid as the standard. Absorbance was measured at 760 nm, and results were expressed as mg gallic acid equivalents (GAE) per gram of extract. Flavonoid content was analyzed using aluminum chloride and sodium acetate reagents, with quercetin as the standard. Absorbance was measured at 415 nm, and results were expressed as mg quercetin equivalents (QE) per gram of extract.

Results and discussion

The extraction yields for methanol and water were 21.6% and 11.14%, respectively. The higher yield in methanol extraction suggests that methanol is more efficient in extracting compounds, especially non-polar and moderately polar compounds. The IC_{50} values for DPPH radical scavenging were 316 ± 17 µg/mL and 512.12 ± 5.77µg/mL for the methanolic and aqueous extract respectively, and BHT showed a lower IC_{50} of 18.26 ± 1.28 µg/mL. The methanolic extract showed 51.76 ± 6.73% inhibition of linoleic acid oxidation, compared to 38.76 ± 5.22% for the aqueous extract. BHT achieved 99 ± 3.11% inhibition. The methanolic extract contained 33.64 ± 6.73 µg GAE/mg and the aqueous extract had 12.54 ± 1.22 µg GAE/mg. Flavonoid content was 16.39 ± 2.28 µg QE/mg and 13.81 ± 3.97 µg QE/mg for the methanolic and the aqueous extract respectively. The results demonstrate that the methanolic extract of *Hibiscus sabdariffa* exhibits higher antioxidant activity compared to the aqueous extract, which can be attributed to its richer phenolic and flavonoid profiles. The higher phenolic and flavonoid content in the methanolic extract likely contributed to its stronger antioxidant performance in both DPPH and β-carotene-linoleic acid assays. The DPPH assay operates based on single electron transfer (SET). In this method, compounds with multiple conjugated rings can donate their electrons to the oxidizing agent, thereby reducing and neutralizing it. An ideal response in this test indicates the presence of polyphenols, which can donate electrons to the oxidizing agent and compensate for the electron deficiency through their electron cloud. However, the β-carotene-linoleic acid assay works based on hydrogen atom transfer (HAT). In this method, compounds containing benzylic or allylic hydrogens can donate these hydrogens to the oxidizing agent, thereby reducing it. So the antioxidant activity of this plant is attributed to both of these reduction mechanisms

References

١. Al-Hashimi, A. G. (2012). Antioxidant and antibacterial activities of Hibiscus sabdariffa L. extracts. *African Journal of Food Science,* 6(21), 506-511.

٢. Widowati, W., Rani, A. P., Hamzah, R. A., Arumwardana, S., Afifah, E., Kusuma, H. S. W., ... & Amalia, A. (2017). Antioxidant and antiaging assays of Hibiscus sabdariffa extract and its compounds. *Natural Product Sciences*, 23(3), 192-200.

٣. Borrás-Linares, I., Fernández-Arroyo, S., Arráez-Roman, D., Palmeros-Suárez, P. A., Del Val-Díaz, R., Andrade-Gonzáles, I., ... & Segura-Carretero, A. (2015). Characterization of phenolic compounds, anthocyanidin, antioxidant and antimicrobial activity of 25 varieties of Mexican Roselle (Hibiscus sabdariffa). *Industrial Crops and Products*, *69*, 385-394.

٤. Zhen, J., Villani, T. S., Guo, Y., Qi, Y., Chin, K., Pan, M. H., ... & Wu, Q. (2016). Phytochemistry, antioxidant capacity, total phenolic content and anti-inflammatory activity of Hibiscus sabdariffa leaves. *Food chemistry*, *190*, 673-680.

٥. Ajiboye, T. O., Salawu, N. A., Yakubu, M. T., Oladiji, A. T., Akanji, M. A., & Okogun, J. I. (2011). Antioxidant and drug detoxification potentials of Hibiscus sabdariffa anthocyanin extract. *Drug and chemical toxicology*, *34*(2), 109-115.

Functionalized Magnetic Graphene Oxide by Trimellitic Anhydride as a Heterogeneous Nanocatalyst for One-Pot Synthesis of Tetrahydrobenzo[b]pyran Derivatives under Green Conditions

Amir Ali Hadiyanjazi*[a], Sepideh Hasanzadeh Banakar[a], Mohammad Ghorban Dekamin[a]

[a] *Pharmaceutical and Heterocyclic Compounds Research Laboratory, Department of Chemistry, Iran University of Science and Technology, Tehran 16846-13114, Iran*

Keyword: Nanocatalyst, Graphen Oxide, magnetic

Abstract

In this study, a novel heterogeneous nanocatalyst based on functionalized magnetic graphene oxide (MGO) with trimellitic anhydride (BTA-APTES-MGO) was successfully synthesized and evaluated for its catalytic efficiency in the one-pot synthesis of tetrahydrobenzo[b]pyran derivatives under environmentally benign, solvent-free conditions. Graphene oxide (GO) was initially prepared using a modified Hummers' method, followed by functionalization with magnetic nanoparticles and aminopropyltriethoxysilane (APTES). The resulting MGO was then treated with trimellitic anhydride (BTA) to create the BTA-APTES-MGO nanocatalyst. The catalyst's structure was characterized by FTIR and 1H^1H NMR, confirming successful functionalization. The catalyst exhibited excellent catalytic activity, reusability, and high selectivity in the synthesis of tetrahydrobenzo[b]pyran derivatives. Furthermore, the magnetic properties of the catalyst allowed for easy separation from the reaction mixture, supporting its potential for sustainable and green chemistry applications. High yields, environmental sustainability, and recyclability make this nanocatalyst a promising alternative for future organic synthesis applications.

Introduction

The increasing demand for sustainable and eco-friendly chemical processes has led to significant interest in green chemistry and the development of multifunctional nanocatalysts. Among the various materials being explored, graphene oxide (GO) has gained widespread attention due to its remarkable properties, including its large surface area, high porosity, and the presence of oxygen-containing functional groups, which make it highly suitable for chemical modification and functionalization.[1] However, GO's direct application in catalysis is hindered by challenges in catalyst recovery and separation from the reaction medium.[2] To overcome these challenges, the integration of GO with magnetic nanoparticles has emerged as an effective approach, allowing for both enhanced catalytic performance and the easy recovery of the catalyst [3].

In the field of heterogeneous catalysis, one-pot multicomponent reactions (MCRs) under green conditions are gaining considerable attention.[4] MCRs are beneficial due to their simplicity, efficiency, and minimal waste generation, making them ideal for sustainable synthesis. One class of compounds that has shown significant biological activity are tetrahydrobenzo[b]pyran derivatives, which have been recognized for their anti-cancer, anti-inflammatory, and antimicrobial properties.[5] As such, the development of efficient, environmentally friendly methods for synthesizing these derivatives is highly valuable.

Previous research has explored the potential of functionalized magnetic nanocatalysts in various organic transformations.[6] For example:**Smith et al.** reported the synthesis of heterocyclic compounds using magnetic nanocatalysts, achieving high catalytic efficiency and easy catalyst separation[7]. **D Wang.** utilized amine-functionalized magnetic graphene oxide to catalyze MCRs, demonstrating high yields and minimal environmental impact.[8]**Chen et al. (2021)** highlighted the importance of chemical modification of graphene oxide for enhancing both the stability and activity of magnetic nanocatalysts.[9]

Building on these studies, the present work aims to design and synthesize a novel functionalized magnetic graphene oxide nanocatalyst (BTA-APTMS-MGO) for the one-pot synthesis of tetrahydrobenzo[b]pyran derivatives under green, solvent-free conditions. This approach not only addresses the environmental concerns associated with conventional methods but also offers a reusable and highly efficient catalytic system, in line with the principles of green chemistry.

Method

Synthesis of Graphene Oxide (GO)

Graphene oxide was synthesized via a modified Hummers' method.[10] Briefly, 1.0 g of graphite powder was mixed with 0.5 g of sodium nitrate ($NaNO_3$) and 23 mL of concentrated sulfuric acid (H_2SO_4) at 0°C under constant stirring. After the addition of 3.0 g of potassium permanganate ($KMnO_4$), the mixture was stirred for 2 hours while keeping the temperature below 4°C. The reaction was then carefully heated to 70°C, and 46 mL of deionized water was slowly added. Following a 30-minute stirring period, 140 mL of distilled water was added, and the reaction was quenched with 10 mL of 30% hydrogen peroxide (H_2O_2). The resulting GO was washed with a 5% HCl solution and distilled water until neutral pH was reached, and then dried in an oven at 60°C.

Preparation of Magnetic Graphene Oxide (MGO)

Magnetic graphene oxide was prepared by adding 0.2 g of GO to 200 mL of distilled water, followed by the addition of 0.97 g of $FeCl_3 \cdot 6H_2O$ and 0.93 g of $FeCl_2 \cdot 4H_2O$. The mixture was stirred for 30 minutes under a nitrogen atmosphere at 50°C. Next, 10 mL of 25% aqueous ammonia solution was slowly added, and the reaction was heated to 80°C for 3 hours. After cooling, the resulting MGO was separated using an external magnet, washed with distilled water to neutralize the pH, and dried in an oven at 60°C.[11]

Functionalization with APTES and BTA

The magnetic graphene oxide (0.3 g) was functionalized with aminopropyltrimethoxysilane (APTMS). The mixture of MGO (0.3 g) and APTMS (3 mL) in 40 mL of ethanol was stirred for 30 minutes and then refluxed for 12 hours at 75°C. The product was washed with ethanol and dried at 60°C.

For further functionalization, 1.0 g of trimellitic anhydride (BTA) was added to 0.112 g of APTMS-functionalized MGO. The mixture was refluxed in a mixture of acetic acid and pyridine (3:2) for 7 hours at 110°C. The resulting BTA-APTMS-MGO was washed with 1 M HCl and hot distilled water, and then dried at 60°C.

Catalytic Application

The catalytic activity of BTA-APTMS-MGO was tested in the one-pot synthesis of tetrahydrobenzo[b]pyran derivatives. A mixture of an aldehyde (114 mg), malononitrile (66 mg), enolizable compound (112 mg), and BTA-APTMS-MGO (10 mg) was added to a test tube under solvent-free conditions. The reaction progress was monitored by thin-layer chromatography (TLC) using a mixture of n-hexane:EtOAc (1:3). After the reaction was complete, the catalyst was removed using a magnet, and the product was isolated. The products were characterized using FTIR, 1H^1H NMR, and melting point analysis.

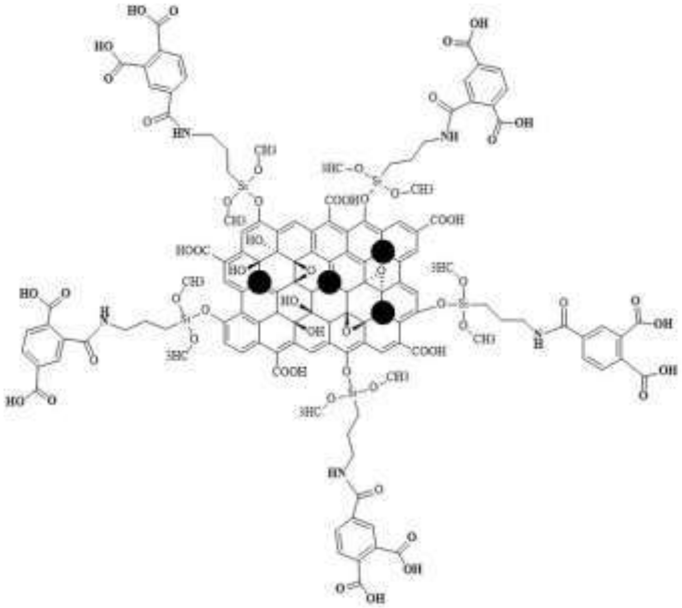

Figure 1: 2D schematic of the TMGO-APT-BTA nanocatalyst, showing the dispersion of magnetic nanoparticles (Fe_3O_4) within the graphene oxide (GO) structure, with attached functional groups.

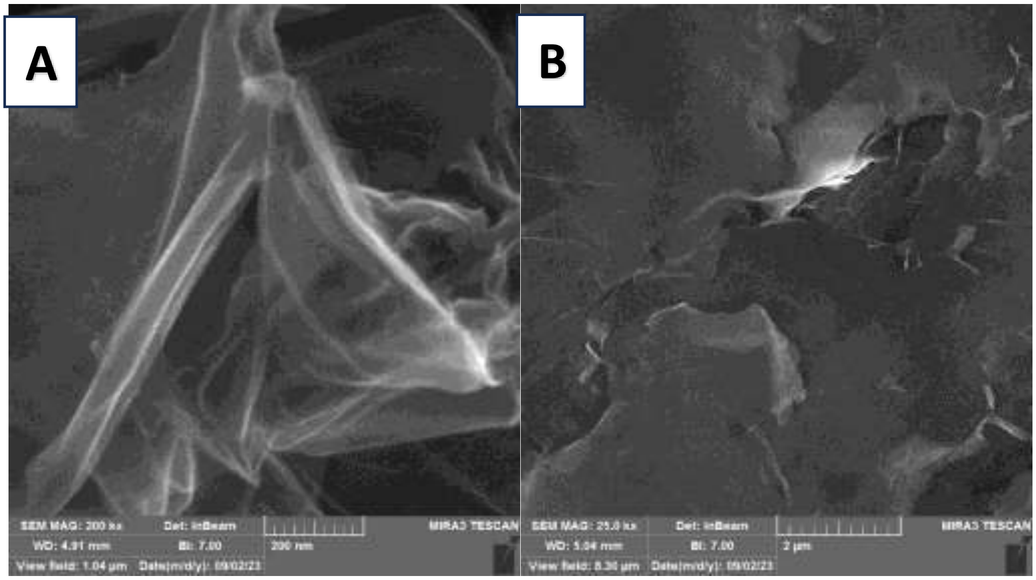

Figure 2: FE-SEM images (A) for GO and (B) for BTA-APTES-MGO.

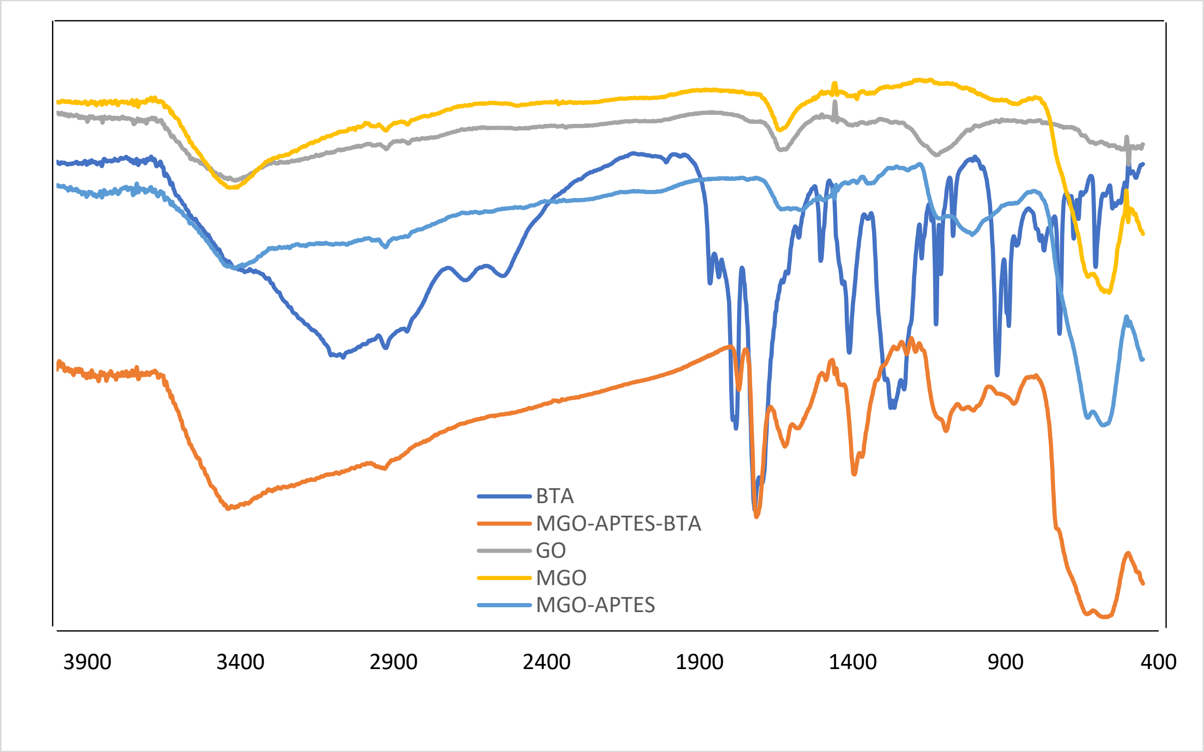

Figur3: FT-IR spectra of BTA,GO, MGO,MGO-APTES, and MGO-APTES-BTA

Table 1 Synthesis of tetraketone derivatives **4a–p** from different aldehydes **2** and enolizable compounds **3a–b** catalyzed by the MGO-APTES-BTA , as a heterogeneous nanocatalyst, under the optimized conditions

Entry	R–CHO 2	Time (min)	Yield (%)	Mp (°C) found
1	4-Chlorobenzaldehyde	20	97	145–146
2	2-Chlorobenzaldehyde	40	90	204–206
3	4-Bromobenzaldehyde	25	94	157
4	4-Formylbenzonitrile	20	96	165–168
5	4-Hydroxybenzaldehyde	40	88	187–188

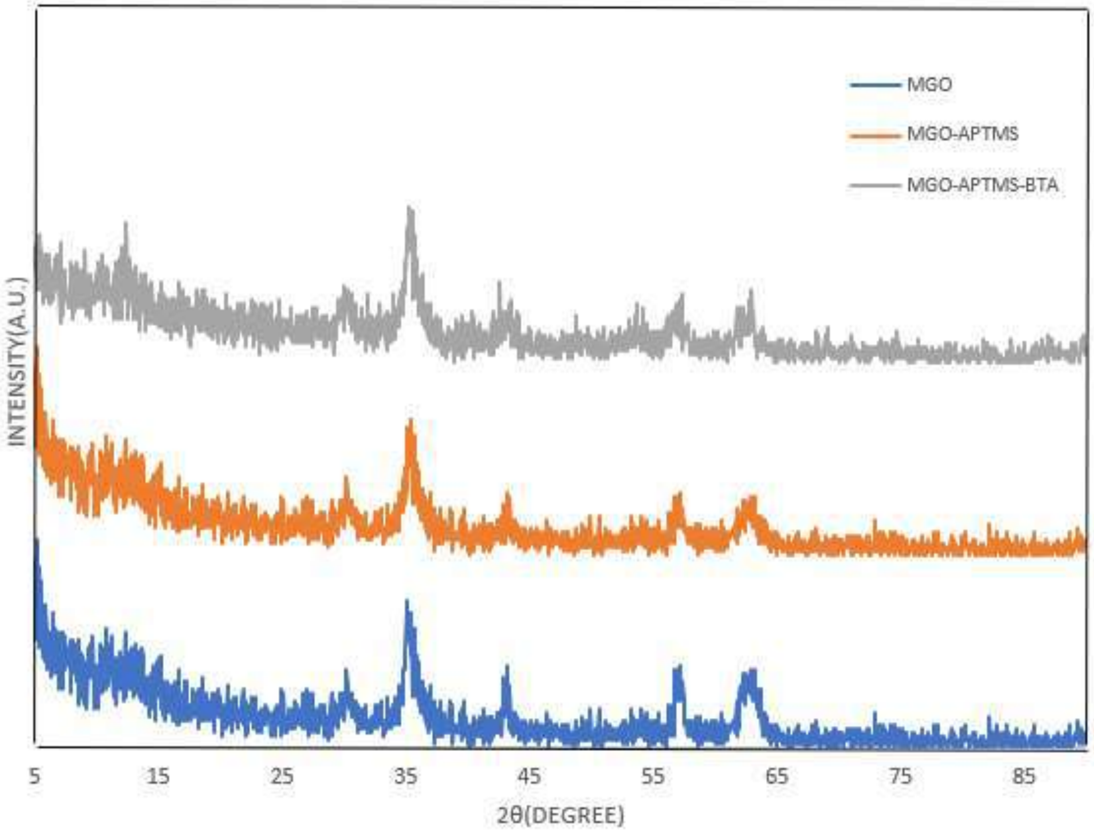

Figure 4: XRD patterns of MGO, MGO-APTMS, and MGO-APTMS-BTA

Results and Discussion

The IR spectrum of the TMGO-APT-BTA composite shows key functional groups: amide C=O stretching (1640-1700 cm^{-1}), amide C-N stretching (1200-1400 cm^{-1}), hydroxyl (O-H stretching) around 3200-3500 cm^{-1}, alkyl (C-H stretching) from APTES (2800-3000 cm^{-1}), Fe-O stretching of magnetic nanoparticles (550-650 cm^{-1}), and siloxane (Si-O stretching) around 1100 cm^{-1}, indicating successful incorporation of amide, siloxane, and magnetic nanoparticles. SEM analysis shows magnetic nanoparticles (10-30 nm) with minimal aggregation before composite formation, while after formation, they are more uniformly dispersed in the graphene oxide, which appears interconnected with the nanoparticles. The surface becomes rougher, likely due to functional groups, suggesting enhanced catalytic potential.

XRD analysis reveals characteristic diffraction peaks for the magnetic nanoparticles at **$2\theta = 30.1°$,** 35.4°, and 43.2°**,** corresponding to the **[220]**, **[311]**, and **[400]** planes of Fe_3O_4, confirming the presence of magnetic nanoparticles in the composite. Additionally, the XRD patterns of MGO-APTMS and MGO-APTMS-BTA show slight broadening and intensity reduction of these peaks, suggesting the successful functionalization of the nanoparticles with APTMS and BTA, as well as the formation of an organic layer around the magnetic core.

The BTA-APTMS-MGO catalyst exhibited high yields (above 90%) in solvent-free synthesis of tetrahydrobenzo[b]pyran derivatives, with easy separation and reuse across five cycles, maintaining its catalytic efficiency, highlighting its suitability for large-scale applications.

Conclusion

the synthesis and characterization of the functionalized magnetic graphene oxide nanocatalyst (BTA-APTMS-MGO) presented in this study demonstrate its remarkable catalytic performance, reusability, and sustainability in the one-pot synthesis of tetrahydrobenzo[b]pyran derivatives under solvent-free conditions. The catalyst’s magnetic properties facilitate easy separation and recovery, ensuring its practical use in eco-friendly and sustainable chemical processes. The incorporation of functional groups such as amide, siloxane, and magnetic nanoparticles enhances its efficiency, as confirmed by IR, SEM, and XRD analyses. The high yields and stability across multiple reaction cycles underline its potential for large-scale applications in organic synthesis. This research not only reinforces the potential of magnetic graphene oxide-based catalysts for advancing green chemistry but also sets the stage for further exploration of its applicability in other complex organic reactions and industrial processes, contributing to more sustainable and environmentally friendly chemical manufacturing.

Refrences

1. Kuila, T., et al., *Chemical functionalization of graphene and its applications.* Progress in Materials Science, 2012. **57**(7): p. 1061-1105.

2. Su, C. and K.P. Loh, *Carbocatalysts: graphene oxide and its derivatives.* Accounts of chemical research, 2013. **46**(10): p. 2275-2285.

3. Rossi, L.M., et al., *Magnetic nanomaterials in catalysis: advanced catalysts for magnetic separation and beyond.* Green Chemistry, 2014. **16**(6): p. 2906-2933.

4. Bosica, G. and R. Abdilla, *Recent advances in multicomponent reactions catalysed under operationally heterogeneous conditions.* Catalysts, 2022. **12**(7): p. 725.

5. Gharghish, S., M.G. Dekamin, and S.H. Banakar, *Functionalized graphene oxide by 4-amino-3-hydroxy-1-naphthalenesulfonic acid as a heterogeneous nanocatalyst for one-pot synthesis of tetraketone and tetrahydrobenzo [b] pyran derivatives under green conditions.* Nanoscale Advances, 2024.

6. Gebre, S.H., *Recent developments of supported and magnetic nanocatalysts for organic transformations: an up-to-date review.* Applied Nanoscience, 2023. **13**(1): p. 15-63.

7. Panda, S.S. and D.W. Hansen, *Microwave-assisted synthesis of five-membered azaheterocyclic systems using nanocatalysts*, in *Nanoparticles in Green Organic Synthesis*. 2023, Elsevier. p. 255-278.

8. Wang, D. and D. Astruc, *Fast-growing field of magnetically recyclable nanocatalysts.* Chemical Reviews, 2014. **114**(14): p. 6949-6985.

9. Yang, W., et al., *Tannic acid/Fe3+ functionalized magnetic graphene oxide nanocomposite with high loading of silver nanoparticles as ultra-efficient catalyst and disinfectant for wastewater treatment.* Chemical Engineering Journal, 2021. **405**: p. 126629.

10. Zaaba, N., et al., *Synthesis of graphene oxide using modified hummers method: solvent influence.* Procedia engineering, 2017. **184**: p. 469-477.

11. He, Y., et al., *Magnetic graphene oxide: synthesis approaches, physicochemical characteristics, and biomedical applications.* TrAC Trends in Analytical Chemistry, 2021. 136: p. 116191.

The 30th Iranian Seminar of Organic Chemistry
February 7-9, 2025, Iran University of Science and Technology, Tehran, Iran

Designing of new dianionic ionic liquids based on Terephthalate dianion and exploring their physicochemical properties by computational method

Mohammad Rizehbandi[1], Behzad Khalili[1]*, Khatereh Ghauri[1]

[a] Department of Chemistry, Faculty of Sciences, University of Guilan, P.O. Box 41335-1914, Rasht, Iran.

[*] *E-mail: b.khalili@guilan.ac.ir&rizehbandi.mohammad@yahoo.com*

In this research, a computational approach based on DFT at M06-2X-GD3/AUG-cc-pVDZ level of theory was used to evaluate the structural, energetic, electronic, and electrochemical properties of new four dianionic ionic liquids (DAILs).

These DAILs are based on dianion Terephthalate $[TP]^{2-}$ and the functionalized cations phenyl methyl imidazolium ($[PMIM]^{+}$), phenyl methyl (1,3,4)- triazolium ($[PMTA1]^{+}$), phenyl methyl (1,3,5)- triazolium ($[PMTA2]^{+}$) and phenyl methyl tetrazolium ($[PMTTA]^{+}$). Electrostatic potential (ESP) maps were also utilized to explore the active sites of the isolated dianion and cations for the formation of $[PMIM]_2[TP]$, $[PMTA1]_2[TP]$, $[PMTA2]_2[TP]$ and $[PMTTA]_2[TP]$ DAILs.

The effect of the type of cation in these DAILs was analyzed by increasing the number of nitrogen atoms and their position in the five-membered ring of the cations. The interaction between the dianion Terephthalate and two cations in any of the DAILs were characterized through an assessment of changes in vibrational frequencies, structures parameters, RDG analysis. Also, the interaction energies, thermodynamic parameters, the properties of electronic and topological of the DAILs were studied. The results show that intermolecular hydrogen bonding in addition to electrostatic interactions plays an important role in the stability of ionic triplets of this group of DAILs and can significantly affect their physical and chemical properties for specific application purposes.

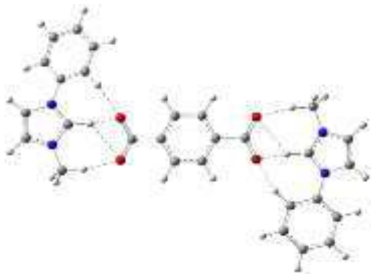

Scheme 1. Fig. 2 Optimized structure of $[PMIM]_2[TP]$ DAILs and some of selected geometric parameters such as bond length C−H(C′−H′), hydrogen bond distances/Å (angles/°).

References

(1)K.S. Egorova, E.G. Gordeev, V.P. Ananikov, Biological activity of ionic liquids and their application in pharmaceutics and medicine, *Chem. Rev*. 117(10) **2017** 7132-89.
(2) R.D. Rogers, K.R. Seddon, Ionic Liquids as Green Solvents: Progress and Prospects; *American Chemical Society*, **2003**.

(3) S.A. Forsyth, J.M. Pringle, D.R. MacFarlane, Ionic Liquids -An Overview. Aust. J. Chem. 57 (2004) 113−119.

(4) J.L. Anderson, R.F. Ding, A. Ellern, D.W. Armstrong, J. Am. *Chem. Soc.* 127 **2005** 593,

(5) A.N. Masri, A.M. Mi, J.M..Leveque, A review on dicationic ionic liquids: *classification and application. Ind. Eng. Manag.* 5 **2016** 197-204.
(6) M. Torkzadeh, M. Moosavi, DFT and COSMO-RS studies on dicationic ionic liquids (DILs) as potential candidates for CO_2 capture: the effects of alkyl side chain length and symmetry in cations, *RSC adv.* 12(54) **2022** 35418-35.

The 30th Iranian Seminar of Organic Chemistry
February 7-9, 2025, Iran University of Science and Technology, Tehran, Iran

Synthesis of Chitosan-Alginate Supported Magnetite Nanoparticles for Smart Drug Delivery Studies

Mahan Hemati[*,1], Manouchehr Mamaghani[1], Asieh Yahyazadeh[1], Iman Rezaei[2]

1. Department of Chemistry, Faculty of Chemistry, University of Guilan, P.O. Box 41335-1914, Rasht, Iran

2. Sobhan Oncology Pharmaceuticals, Rasht, Iran.

* Corresponding author: Mahan Hemati

* Corresponding author email: mahanhemati8696@gmail.com

Abstract

Hydrochlorothiazide is a widely prescribed antihypertensive drug; however, it has significant gastrointestinal side effects. Nanocarriers can enhance the targeted delivery of hydrochlorothiazide to reduce side effects and improve its efficacy. In this study, an iron magnetite nanocarrier was synthesized and evaluated for hydrochlorothiazide's loading and targeted release. The synthesized iron magnetite nanocarrier's morphology, size, and crystalline structure were examined and characterized using FT-IR, SEM, TGA, and XRD techniques. The loading of hydrochlorothiazide onto the nanocarrier was studied using adsorption spectroscopy. Experimental design and optimization of drug release under various pH conditions, times, and amounts of the nanocarrier were investigated. Hydrochlorothiazide was effectively loaded onto the nanocarrier, and its release was pH-dependent. The iron magnetite nanocarrier showed significant potential as a targeted drug delivery system for hydrochlorothiazide. This nanocarrier can help reduce side effects and enhance the efficacy of hypertension treatment.

Introduction: Chitosan-alginate coated magnetic iron oxide nanoparticles offer significant promise for targeted drug delivery due to their ability to be guided by external magnetic fields. These nanoparticles can be precisely directed to a specific location and release their drug payload upon application of an external magnetic field. The chitosan-alginate coating serves as a protective barrier, preventing premature drug release and offering biocompatibility and biodegradability. Additionally, the gel-forming properties of alginate facilitate a controlled drug-release environment [1,2].

Materials and Methods: In this research, magnetic iron oxide nanoparticles were synthesized as a carrier for hydrochlorothiazide and coated with natural polymers chitosan and alginate. To investigate the effect of the environment on drug release, three buffer solutions with different pH values (phosphate pH=7.4, acetate pH=4.5, and hydrochloric acid pH=1.0) were used. By designing an experimental design based on the Response Surface Methodology (RSM) and using the Design-Expert software, the effect of variables such as nanocarrier concentration, pH, and time On drug release was investigated (Figure 1). In this design, Fe_3O_4@Chitosan@Alginate nanoparticles loaded with hydrochlorothiazide were incubated under different pH and time conditions, and then the amount of released drug was measured using UV-Vis spectrophotometry at a single wavelength. The results of data analysis showed that the optimal conditions for maximum drug release were obtained at pH=1, time 30 minutes, and using 50 mg of the nanocarrier. These findings indicate the high potential of the designed nanocarriers for application in targeted drug delivery systems.

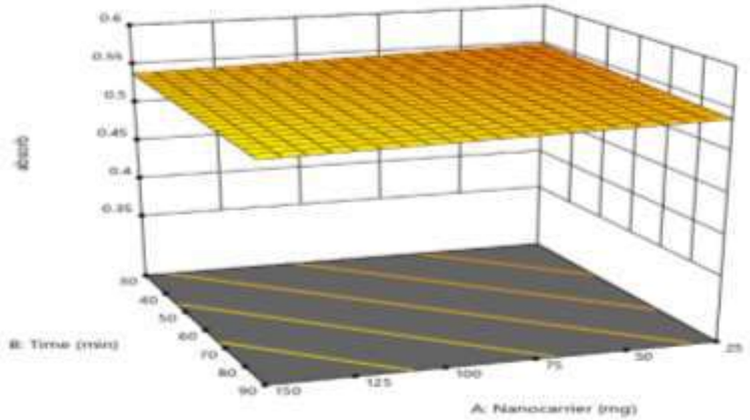

Figure 1: the nanoparticles effectively loaded the drug and that drug release was directly influenced by the pH of the environment.

Results: This research investigated chitosan-alginate-coated magnetic nanoparticles as a novel system for the targeted delivery of hydrochlorothiazide. Results demonstrated that these nanoparticles can effectively load the drug, and the pH of the environment significantly influences the drug release profile. These findings indicate a high potential for designing targeted drug delivery systems that can regulate drug release in various physiological environments.

Discussion and Conclusion: The results of this research demonstrate that the pH of the environment has a significant impact on drug loading onto nanocarriers. An increase in pH led to a change in the rate of drug loading, indicating a key role of pH in altering the surface charge of the nanocarrier and consequently the electrostatic interactions between the drug and the nanocarrier. In contrast, changes in nanocarrier concentration and drug amount had a lesser impact on the loading efficiency. These findings suggest that precise control of the environmental pH is essential to achieve maximum drug loading onto nanocarriers. Additionally, these results can be utilized in the design of targeted drug delivery systems with the ability to regulate drug release in environments with varying pHs, such as tumours. To better understand the exact mechanisms of pH influence on drug loading, further studies on various types of nanocarriers and drugs are recommended. Furthermore, investigating the impact of other factors such as temperature, ionic

strength of the environment, and the presence of other molecules on drug loading can provide a more comprehensive perspective.

Keywords: magnetic iron oxide nanoparticles, chitosan, alginate, smart drug delivery, hydrochlorothiazide

Reference

[1] Han, Y.; et al. (2020). "Ag NPs on Chitosan-Alginate Coated Magnetite for Synthesis of Indazolo [2, 1-b] Phthalazines and Human Iung Protective Effects Against α-Guttiferin." *International Journal of Biological Macromolecules*, Vol. 164, pp. 294–2986.

[2] Khan, I.; Nazir, H.K. (2016). "Alginate Nanoparticles for Drug Delivery: a Comprehensive Review." *International Journal of Pharmaceutics*, Vol. 49۹, pp. ۱–۲۳.


The 30th Iranian Seminar of Organic Chemistry
February 7-9, 2025, Iran University of Science and Technology, Tehran, Iran

Efficient photocatalytic coupling reaction under visible light irradiation

Zahra bazyar [1*], Fatemeh Maraghi [1]

**E-mail: Z.bazyar@bkatu.ac.ir*

[1]Department of Chemistry, Behbahan Khatam Alanbia University of Technology, Behbahan, 63616-63973, I. R. Iran

Abstract: This paper presents a comprehensive investigation into the photocatalytic performance of nanoparticles palladium metal–organic framework (Pd-MOF) in the Suzuki-Miyaura cross-coupling reaction, conducted under visible light irradiation at ambient temperature. Our findings indicate that nanoparticles Pd-MOF serves as an effective photocatalyst when exposed to visible light. The results demonstrate that nanoparticles Pd-MOF exhibits high efficiency and selectivity, with the added advantage of being recyclable and reusable multiple times without significant loss in catalytic activity.

Keywords: Metal–organic framework; Photocatalysis; recycled

Introduction

Palladium-based catalysts are extensively utilized in various reactions within modern organic synthesis, particularly in the formation of carbon-carbon bonds through well-established cross-coupling reactions such as Suzuki-Miyaura, Hiyama, Heck, and Stille reactions. In recent years, there has been a growing interest in harnessing solar energy for chemical transformations, emphasizing the potential of photocatalytic processes [1-3]. These processes offer notable advantages, including operation under ambient conditions, utilization of solar light for chemical reactions, and alignment with sustainable practices through the use of green, renewable energy sources [4, 5].

Our objective is to develop novel heterogeneous catalytic systems that are efficient, easily separable, and compatible with renewable energy sources. Among various types of heterogeneous photocatalysts, noble metals are employed for a range of applications, including innovative organic synthesis, environmental remediation, construction and architecture, energy generation, and biological detection. Noble metals such as gold (Au), silver (Ag), palladium (Pd), and platinum (Pt) exhibit strong visible-light absorption characteristics due to localized surface plasmon resonance (LSPR) effects associated with semiconductor-based photocatalysts [6, 7]. In this study, we explore modified metal–organic framework materials (Pd-MOF) as potential photocatalysts.

Experimental Section

A solution of arylhalids, phenylboronic acid and a base in CH_3CN was prepared, and a catalyst was added to this mixture. The reaction was conducted under an air atmosphere and stirred while being irradiated with visible light from an 11 W LED lamp. Upon completion of the reaction, the catalyst was separated by centrifugation, and the solvent was removed under reduced pressure. The crude product was subsequently purified using column chromatography.

Results and Discussion

We report the synthesis and comprehensive characterization of nanoparticles Pd-MOF. This catalyst was synthesized and fully characterized using techniques including Transmission Electron Microscopy (TEM), Field Emission Scanning Electron Microscopy (FE-SEM), X-ray Diffraction (XRD), Brunauer-Emmett-Teller (BET) surface area analysis, and Inductively Coupled Plasma (ICP) analysis. Initially, the photocatalytic activity of nanoparticles Pd-MOF for the Suzuki cross-coupling reaction between aryl halides and aryl boronic acids (as illustrated in Scheme 1) was evaluated in acetonitrile (CH_3CN) under visible light irradiation (11 W LED lamp bulb, wavelength range of 400–750 nm) at room temperature. Following the optimization of reaction conditions in air at room temperature, the photocatalytic performance of the nanoparticles Pd-MOF catalyst for coupling reactions was investigated using a series of differently substituted aryl halides.

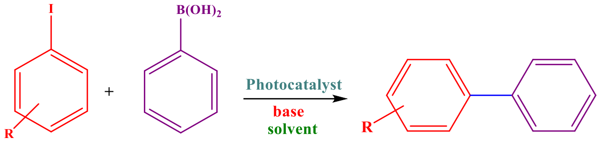

Scheme.1: Carbon-Carbon bond formation.

Conclusions

In conclusion, we have successfully demonstrated the efficacy of a heterogeneous nanoparticles Pd-MOF catalyst for photocatalytic C-C bond coupling reactions under visible light irradiation at ambient temperatures. The photocatalytic activity is influenced by both the wavelength and intensity of the light. The reactions were performed under high irradiation conditions using various wavelengths.

References:

1. Hosseini-Sarvari, M. and Z. Bazyar, *Visible light driven photocatalytic cross-coupling reactions on nano Pd/ZnO photocatalyst at room-temperature.* ChemistrySelect, 2018. 3(6): p. 1898-1907.

2. Till, N.A., et al., *Mechanistic analysis of metallaphotoredox C–N coupling: photocatalysis initiates and perpetuates Ni (I)/Ni (III) coupling activity.* Journal of the American Chemical Society, 2020. **142**(37): p. 15830-15841.

3. Li, X.-H., et al., *Facilitating room-temperature Suzuki coupling reaction with light: Mott-Schottky photocatalyst for CC-coupling.* Scientific Reports, 2013. **3**(1): p. 1743.

4. Bazyar, Z. and M. Hosseini-Sarvari, *On/Off* O_2 *switchable photocatalytic oxidative and protodecarboxylation of carboxylic acids.* The Journal of Organic Chemistry, 2019. 84(21): p. 13503-13515.

5. Ahmad, I., et al., *Review on CdS-derived photocatalysts for solar photocatalytic applications–advances and challenges.* Journal of Industrial and Engineering Chemistry, 2024. 130: p. 105-124.

6. Khan, M.E. and M.H. Cho, *Surface plasmon-based nanomaterials as photocatalyst.* Advanced Nanostructured Materials for Environmental Remediation, 2019: p. 173-187.

7. Vikas, et al., *The role of metals in nanocomposites for UV and visible light-active photocatalysis.* Green Photocatalytic Semiconductors: Recent Advances and Applications, 2022: p. 307-335.

The 30th Iranian Seminar of Organic Chemistry
February 7-9, 2025, Iran University of Science and Technology, Tehran, Iran

Preparation of self-healing hydrogel based on Astragalus sarcocolla /Polyvinyl alcohol

Fatemeh Dehyadegary*[a], Maryam Kalantari [a]

[a] *Department of Chemistry, Faculty of Science, Shahid Bahonar University of Kerman, Kerman, Iran*

Abstract:

Hydrogels are macromolecule network of polymers that can be prepared from natural and synthetic polymers. In this research, the natural material Astragalus sarcocolla (Anzaroot) was used together with the synthetic polymer polyvinyl alcohol (PVA) to make hydrogel, and polyvinyl pyrrolidone (PVP) was added to improve its properties, also borax was used as a crosslinker of these polymers. This hydrogel has high elasticity and self-healing properties.

keywords:

Hydrogel, Self-healing, Astragalus sarcocolla, Polyvinyl alcohol(PVA)

Introduction:

Hydrogels are three-dimensional network of polymers that are connected to each other by crosslinks. Cross-links cause to make pores between polymer chains. The porosity makes hydrogels flexible and gives them the ability to absorb various substances such as water, drugs and biological fluids. This ability leads to use the hydrogels in drug delivery, agriculture, water purification, etc.

Since the first hydrogels were made, polyvinyl alcohol (PVA) has been known as a suitable synthetic polymer for making hydrogels which is made from the radical polymerization of vinyl acetate. The first paper about hydrogel that made with PVA was published by Danno in 1958 [1]. It had been synthesized by using Gamma rays. In the past, scientists considered PVA as a non-degradable material until a study by Chiellini in 2003 [2]. showed that several species of bacteria, fungi, and yeasts use PVA as their only carbon source and thus degrade it. And subsequent studies have shown that PVA is safe even when taken orally.

The hydrogels were made of PVA had limitations that various methods have been proposed to overcome them. Among them, its combination with polyvinyl pyrrolidone (PVP) has shown that various compounds with different properties and applications have been made [3].

Natural polymers can also be used to make hydrogels, although natural polymers are biodegradable and safe, synthetic polymers are used to increase the mechanical stability and improve the properties of hydrogels, so the combination of synthetic and natural polymers creates a product that is biodegradable; They also have good mechanical stability.

Anzaroot, with the scientific name Astragalus sarcocolla, is a gum of a Shrub and is a biologically active compound that has anti-inflammatory properties and is effective in the treatment of joint pain and sciatica, as well as its external use in the treatment of open wounds and their bleeding. It also has anti-fungal and anti-bacterial properties that prevent wound infection [4].

Methods:

1-Preparation of Anzaroot extract:

The yellow Anzaroot gum was ground and 10g of it was added to 100 ml of distilled water for 24 hours to dissolve, then was put in a centrifuge at 5000 rpm for 10 minutes and the extract is ready. It was placed in the laboratory environment for several days to dry and finally it was washed with 70% ethanol for disinfection, then was dried again.

2-preparation of hydrogel:

2-1 Preparation of hydrogel with PVA and borax:

Mixture of water and Anzaroot extract as a natural polymer and PVA as a synthetic polymer are stirred slowly on a stirrer at a temperature of 60°C until they be dissolved, then borax solution is added to it as a crosslinker. And it is stirred quickly. To make this hydrogel, different ratios of PVA/Borax were tested (table1); Although the produced hydrogels are flexible, but they do not have good stability and are sticky (Figure 1).

Table1: different ratios of PVA/Borax

Anzaroot (g)	PVA (g)	Borax (g)	PVA/Borax (w/w)
0.1	0.3	0.06	5:1
0.1	0.3	0.03	10:1

0.1	0.3	0.015	20:1
0.1	0.3	0.012	25:1
0.1	0.3	0.01	30:1
0.2	0.3	0.015	20:1
0.05	0.3	0.015	20:1

Figure1

2-2 Preparation of hydrogel with PVA/PVP and borax:

To increase the mechanical properties of the hydrogel, PVP was added to the solution of Anzaroot and PVA, and after these three types of polymers are mixed at the temperature of 60°C; Borax was added. To preparation suitable hydrogel with good properties, different ratios of PVA/PVP were tested. The produced hydrogel has elasticity and could be film (Figure2).

Figure2

Results and Discussion:

In addition to elasticity, the produced hydrogel have the ability of self-healing. The self-healing property of the prepared hydrogels was evaluated by putting two pieces of each hydrogel close to each other; The images related to this test are presented below.

Figure3: Self-healing of PVA/Borax hydrogel

Figure4: Self-healing of PVA/PVP/Borax hydrogel

References:

[1] Akibumi Danno, Gel Formation of Aqueous Solution of Polyvinyl Alcohol Irradiated by Gamma Rays from Cobalt-60, Journal of the Physical Society of Japan, 1958, Volume 13, Issue 7, Pages 722-727, Released on J-STAGE June 01, 2007, Online ISSN 1347-4073, Print ISSN 0031-9015, https://doi.org/10.1143/JPSJ.13.722,

[2] Emo Chiellini, Andrea Corti, Salvatore D'Antone, Roberto Solaro, Biodegradation of poly (vinyl alcohol) based materials, Progress in Polymer Science, Volume 28, Issue 6, 2003, Pages 963-1014, ISSN 0079-6700, https://doi.org/10.1016/S0079-6700(02)00149-1.

[3] Teodorescu M, Bercea M, Morariu S. Biomaterials of PVA and PVP in medical and pharmaceutical applications: Perspectives and challenges. Biotechnol Adv. 2019 Jan-Feb;37(1):109-131.: https://doi.org/10.1016/j.biotechadv.2018.11.008.

[4] Ayubi-Rad, Mohammadali & Yosefi, Soheila & Hajizadeh, Mohammadreza & Jafari-Naveh, Hamidreza & Hassanipour, Mahsa & Alamchi, Fatemeh & Fadai, Afsaneh & Khorasani, Faridehsadat & Hosseini, Farzanehsadat & Bemani, Mahdieh & Mahmoodi, Mehdi. (2020). Effects of Astragalus fasciculifolius gum on wound healing in streptozotocin-induced diabetic rats. Journal of Herbmed Pharmacology. 9. https://doi.org/10.34172/jhp.2020.41.

A Recyclable Mesalamine-Functionalized on Magnetic Nanoparticles (Mesalamine/GPTMS@SiO_2@Fe_3O_4) for the Knoevenagel Condensation of Aldehydes with Malononitrile

Mahdiyeh Partovi, Sobhan Rezayati, Ali Ramazani*

Department of Chemistry, Faculty of Science, University of Zanjan, Zanjan, Iran

*E-mail:aliramazani@znu.ac.ir

Magnetic nanoparticles play a crucial role as recoverable catalysts in organic reactions, enhancing efficiency and reducing reaction times. Due to their large surface area and easy separation using a magnetic field, these nanoparticles facilitate the production of high-purity products while minimizing chemical waste [1]. In this research, we present the development of mesalaminefunctionalized magnetic nanoparticles (mesalamine/GPTMS@SiO2@Fe3O4) as an effective and magnetically recoverable nanocatalyst. The synthesis of this nanocatalyst was accomplished through a three-step, cost-effective approach, which involves modifying the surface of Fe3O4 nanoparticles with silica and GPTMS to produce GPTMS@SiO2@Fe3O4. The final nanocatalyst was obtained by treating the intermediate with mesalamine, a well-known antioxidant. Various characterization techniques, including FT-IR, SEM, TEM, EDX, XRD, BET, VSM, and TGA, were employed to analyze its structure. The catalytic activity of the synthesized nanocatalyst was tested in the Knoevenagel condensation of several aromatic aldehydes with malononitrile in ethanol at room temperature, yielding good results in a short duration (Scheme 1). This nanocatalyst demonstrated extremely rapid reaction times under mild conditions, impressive recyclability, superior catalytic performance, and an easy work-up process for Knoevenagel condensation. Additionally, it maintained its effectiveness over 6 cycles of reuse with the aid of an external magnet.

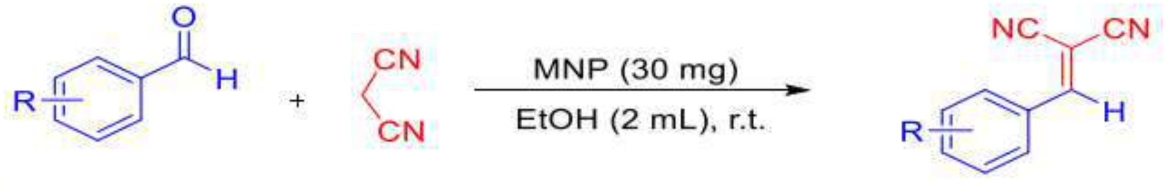

R= *H, 4-Cl, 2,4-Cl, 4-Br, 5-nitrofuran-2-carbaldehyde, 4-OMe, 2-NO_2, 4-F, 4-Me, 4-CN, 4-NO_2*

Scheme 1. Activity of the mesalamine/GPTMS@SiO_2@Fe_3O_4 MNP in the Knoevenagel condensation

References

[1] Partovi, M., Rezayati, S., Ramazani, A., Ahmadi, Y., & Taherkhani, H. (2023). Recyclable mesalamine functionalized magnetic nanoparticles (mesalamine/GPTMS@SiO_2@Fe_3O_4) for tandem Knoevenagel– Michael cyclocondensation.

The 30th Iranian Seminar of Organic Chemistry
February 7-9, 2025, Iran University of Science and Technology, Tehran, Iran

Production of cellulose film using fine pulp through a mild carboxymethylation reaction

Authors: Fatemeh Jaberi1[a], Saeid Khodadoust 2[b], Mohammadhadi Moradian 3*[c] , Theo van de Ven

Recent concerns for the accumulation of non-renewable waste in the environment have encouraged researchers to replace plastic with biodegradable materials. Cellulose is one of the best substitutes. Carboxymethylation of cellulose is as a new method to make biodegradable and recyclable cellulose films, which can replace plastic products. In this research, the possibility of making cellulose films was studied by using the excess fine pulp from Harir Khuzestan Tissue Company. This process includes the carboxymethylation reaction of an alkaline cellulose, making a dope, casting in a 1mm thick mold and then immersion in 10% sulfuric acid bath. Resulting film is then thoroughly washed and dried. Fourier transform infrared spectroscopy showed the formation of carbonyl bonds on cellulose at 1726 cm^{-1} which indicates that the carboxymethylation reaction was successful. Tensile strength, modulus of elasticity and Elongation of the film was 77.15 MPa, 1.72 GPa, and 5.77%, respectively, rendering it suitable for packaging purposes.

Keyword: Fine pulp, Cellulose film, Carboxymethylation.

References:

1.Geyer, R., J.R. Jambeck, and K.L. Law, Production, use, and fate of all plastics ever made. Science advances, 2017. **3**(7): p. e1700782.

2.Tharanathan, R., Biodegradable films and composite coatings: past, present and future. Trends in food science & technology, 2003. **14**(3): p. 71-78.

3. Brocks, J.J., E. Grosjean, and G.A. Logan, *Assessing biomarker syngeneity using branched alkanes with quaternary carbon (BAQCs) and other plastic contaminants.* Geochimica et Cosmochimica Acta, 2008. **72**(3): p. 871-888.

4.Moradian, M., M.S. Islam, and T.G. van de Ven, Insoluble regenerated cellulose films made *from mildly carboxylated dissolving and kraft pulps.* Industrial & Engineering Chemistry Research, 2021. **60**(15): p. 5385-5393.

5.Rahman, M.S., et al., Recent developments of carboxymethyl cellulose. Polymers, 2021. 13(8): p. 1345.

6.Stigsson, V., G. Kloow, and U. Germgård, An historic overview of carboxymethyl cellulose *(CMC) production on an industrial scale.* PaperAsia, 2001. **17**.

7.Klemm, D., et al., Comprehensive cellulose chemistry. Volume 1: Fundamentals and analytical *methods*. 1998: Wiley-VCH Verlag GmbH.

8.Moradian, M., M.N. Alam, and T.G. van de Ven, Influence of carboxyl charge density on *properties of extruded cellulose films.* Industrial & Engineering Chemistry Research, 2021. **60**(38): p. 13756-13763.

9.Li, X., et al., Chemical and enzymatic fiber modification to enhance the mechanical properties *of CMC composite films.* Polymers, 2022. **14**(19): p. 4127.

The 30th Iranian Seminar of Organic Chemistry
February 7-9, 2025, Iran University of Science and Technology, Tehran, Iran

Design of Pd- g-C_3N_4/biochar as an effective nanocatalyst in the Stille C–C coupling reaction

Maryam Nouri 1[a] Maryam Hajjami 2[b]

Department of Organic Chemistry, Faculty of Chemistry and Petroleum Sciences, Bu-Ali Sina University, Postal code 6517838683, Hamedan, Iran. E-mail address, m.hajjami@basu.ac.ir *or* mhajjami@yahoo.com

Keyword: Palladium, Biochar, Stille reaction, Nanocatalyst

Design and synthesis of green and recyclable catalysts in order to improve the efficiency of organic chemistry reactions is a significant challenge. [1] In organic synthesis, the Stille reaction is one of the most general, effective, and selective Pd-catalyzed cross-coupling reactions for the formation of C–C bonds. It is based on organotin compounds using catalytic amounts of Pd complexes under mild reaction conditions normally. The Stille reaction is effective in preparing promising organic molecules and is generally superior for synthesizing complex molecules including natural products. [2] In this study, first, Palladium graphitic carbon nitride Pd-g-C_3N_4/biochar nanosheets with high surface area and chemical stability were synthesized. The synthesis of Biphenyl derivatives was performed, with high yield. The advantages of this reaction include easy catalyst separation and reusability thanks to its recyclable heterogeneous nature, with good to excellent efficiency, and short reaction time. **(Scheme1)**

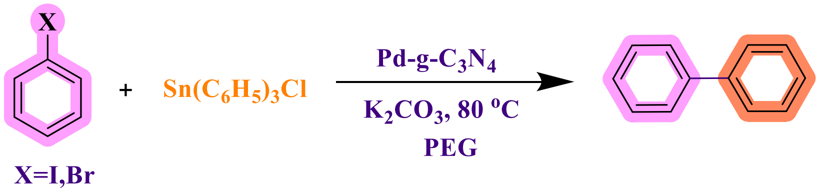

Scheme1: Carbon–carbon coupling reaction of aryl halides with $Sn(C_6H_5)_3Cl$ in the presence of Pd-g-C_3N_4/biochar

Reference:

(1) Moradi, P.; Hajjami, M. RSC Advances **2022**, 12, 13523-13534.

(2) Majhi, S.; K. Jash, S. Synthetic Communications **2023**, 53, 2061-2087.

The 30th Iranian Seminar of Organic Chemistry
February 7-9, 2025, Iran University of Science and Technology, Tehran, Iran

Exploring the Electrocatalytic Efficacy of Iron and Nickel on ZIF-67 for the Oxygen Evolution Reaction

Siamak Pashajavid[a], AliGholi Niaei[a,b], Elnaz Asghari[c], seyed jamaleddin peighambardoust[a]

[a] *Department of Chemical & Petroleum Engineering, University of Tabriz, Tabriz, Iran*
[b] *Department of Physics, Faculty of Science, University of Sakarya, Sakarya, Türkiye*
[c] *Department of Physical Chemistry, Faculty of Chemistry, University of Tabriz, Tabriz, Iran*

Abstract

This study explores the use of iron (Fe) and nickel (Ni) incorporated into ZIF-67 (Zeolitic Imidazolate Framework-67) as electrocatalysts for the Oxygen Evolution Reaction (OER). Using various electrochemical techniques, we evaluate the catalytic performance and kinetics of Fe/Ni-ZIF-67. Characterization methods, including X-ray diffraction (XRD) and scanning electron microscopy (SEM), confirm the successful incorporation of metals and the structural integrity of the material. The results demonstrate that metal doping significantly enhances OER activity compared to pure ZIF-67, with optimal metal ratios resulting in lower overpotentials and improved

current densities. This research highlights the potential of metal-doped MOFs for sustainable energy conversion in electrocatalysis.

Keywords: MOF, electrocatalysts, oxygen evolution reaction, metal-organic framework, OER, water splitting, zeolitic imidazolate framework

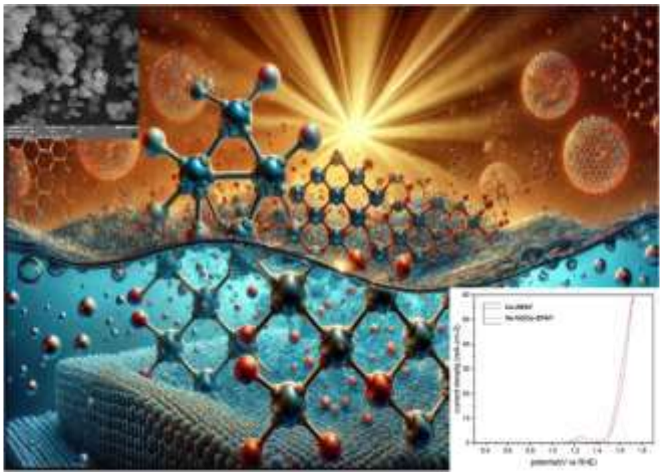

Catalyst synthesis schematic of the Fe-Ni/Co-ZIF67 in OER process

Global energy demand is a critical issue due to climate change and the Paris Agreement. With fossil fuels accounting for about 80% of energy use, cost-effective strategies are needed to ensure energy security and mitigate climate change. Improving electrocatalytic processes is essential, as current efficiencies are limited by slow reaction kinetics. Catalytic coatings can enhance hydrogen production from renewable sources by utilizing affordable electrocatalysts such as metal-organic frameworks (MOFs). These versatile materials, composed of metal nodes and organic linkers, are gaining attention due to recent advancements in chemistry. Evolving from zeolites, MOFs now incorporate metal clusters that improve porosity and stability, with an emphasis on organic ligands and modifications. Zeolitic imidazolate frameworks (ZIFs), a subclass of MOFs, offer excellent thermal and moisture stability. Both MOFs and ZIFs show significant promise for the oxygen evolution reaction (OER) in water splitting, a key process for solar fuel technologies. Integrated systems that combine light-harvesting semiconductors with electrocatalysts hold great potential, although finding effective OER catalysts remains a challenge. Recent advances in rapid screening methods for OER activity in metal oxides are helping to accelerate catalyst synthesis. This work explores the incorporation of iron, cobalt, and nickel ions into the ZIF structure, focusing on the Fe-Ni/Co-ZIF-67 catalyst for OER.

Preparation of Fe-Ni/Co-ZIF67

The Fe-Ni/Co-ZIF-67 compound was synthesized through a two-step process. Initially, two separate solutions were prepared. Solution A contained $Co(NO_3)_2{\cdot}6H_2O$, $Ni(NO_3)_2$, and $FeCl_3{\cdot}6H_2O$, all dissolved in methanol. In parallel, solution B was prepared by dissolving 2-methylimidazole in methanol. Solution B was then gradually added to solution A while continuously stirring the mixture at room temperature for 24 hours, resulting in the formation of a purple precipitate. This precipitate was filtered and washed multiple times with methanol. Finally, the product was dried overnight at 60°C. The preparation of Co-ZIF-67 follows a similar procedure, except the stirring time is 2 hours, followed by 12 hours of rest without stirring.

The microstructure of Fe-Ni/Co-ZIF-67 was analyzed using scanning electron microscopy (SEM). The fracture surfaces of the coatings and the substrate after corrosion were also examined. Phase composition was determined through X-ray diffraction (XRD) with Cu Kα radiation and energy-dispersive X-ray spectroscopy (EDS). Stability, voltage, and current were evaluated using linear sweep voltammetry (LSV) and electrochemical impedance spectroscopy (EIS).

١. Zou, D.; Liu, D.; Zhang, J. From Zeolitic Imidazolate Framework-8 to Metal-Organic Frameworks (MOF s): Representative Substance for the General Study of Pioneering MOF Applications. *Energy & Environmental Materials* **2018**, *1* (4), 209-220.

٢. McCrory, C. C.; Jung, S.; Peters, J. C.; Jaramillo, T. F. Benchmarking heterogeneous electrocatalysts for the oxygen evolution reaction. *Journal of the American Chemical Society* **2013**, *135* (45), 16977-16987.

٣. Turner, J. A. Sustainable hydrogen production. *Science* **2004**, *305* (5686), 972-974.

٤. Lewis, N. S. Toward cost-effective solar energy use. *science* **2007**, *315* (5813), 798-801.

٥. Gray, H. B. Powering the planet with solar fuel. *Nature Chemistry* **2009**, *1* (1), 7-7.

٦. Walter, M. G.; Warren, E. L.; McKone, J. R.; Boettcher, S. W.; Mi, Q.; Santori, E. A.; Lewis, N. S. Solar water splitting cells. *Chemical Reviews* **2010**, *110* (11), 6446-6473.

٧. Vesborg, P. C.; Jaramillo, T. F. Addressing the terawatt challenge: scalability in the supply of chemical elements for renewable energy. *RSC Advances* **2012**, *2* (21), 7933-7947.

The 30th Iranian Seminar of Organic Chemistry
February 7-9, 2025, Iran University of Science and Technology, Tehran, Iran

Investigating the Catalytic Performance of Iron on ZIF-67 as an electrocatalyst in Oxygen Evolution Reaction

Siamak Pashajavid[a], AliGholi Niaei[a،b]

[a] *Department of Chemical & Petroleum Engineering, University of Tabriz, Tabriz, Iran*

[b] *Department of Physics, Faculty of Science, University of Sakarya, Sakarya, Türkiye*

Abstract

Fe/Co-ZIF-67 is a promising iron-based catalyst for the oxygen evolution reaction (OER) in water-splitting applications, integrating iron into a cobalt-based framework to enhance electrochemical performance. Its unique structure facilitates efficient charge transfer and optimizes active sites, resulting in superior catalytic activity compared to traditional catalysts. Notably, it achieves a lower overpotential of 340 mV in NaOH electrolyte. These advantageous properties position

Fe/Co-ZIF-67 as a strong candidate for sustainable hydrogen production, contributing significantly to advancements in renewable energy technologies.

Keywords: electrochemical catalyst, MOF, metal-organic framework, water splitting, OER, oxygen evolution reaction,

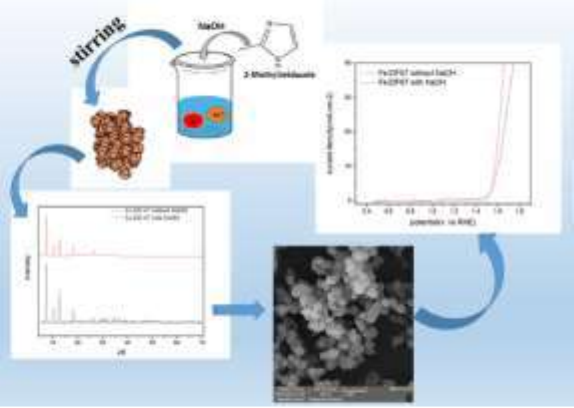

Catalyst synthesis schematic of the Fe/Co-ZIF67 with NaOH

This abstract emphasizes the need to advance sustainable energy technologies to address energy shortages and environmental challenges, with a particular focus on hydrogen as a viable green energy source. Hydrogen can be produced through water splitting, which involves key reactions at the electrodes: the hydrogen evolution reaction (HER) and the oxygen evolution reaction (OER). While these processes are well understood, challenges remain. Metal-organic frameworks (MOFs), particularly zeolitic imidazolate frameworks (ZIFs), are gaining attention for their unique porous structures and customizable properties. Composed of metal ions and imidazolate linkers, ZIFs show significant potential as electrocatalysts for water splitting due to their versatile characteristics. Traditional electrocatalysts, such as IrO_2, RuO_2, and platinum, are effective but suffer from drawbacks, including high cost and toxicity. This study highlights ZIF-67, enhanced with iron, as a promising candidate for improving OER efficiency in water-splitting applications. [1-7]

Preparation of Fe/Co-ZIF67: The synthesis of the Fe/Co-ZIF-67 compound was carried out using a two-step process. First, two distinct solutions were prepared. Solution A consisted of $Co(NO_3)_2 \cdot 6H_2O$ and $FeCl_3 \cdot 6H_2O$ dissolved in methanol. Meanwhile, solution B was prepared by dissolving 2-methylimidazole in methanol (MeOH). Next, solution B was gradually added to solution A while stirring the mixture at room temperature for 24 hours, resulting in the formation of a purple precipitate. The precipitate was then filtered and washed repeatedly with methanol. Finally, the product was dried overnight at 60°C. The preparation of Fe/Co-ZIF-67 in the presence of NaOH follows a similar procedure, with the addition of sodium hydroxide being stirred together with 2-methylimidazole.

The microstructure and morphology of Fe/Co-ZIF-67 were characterized using scanning electron microscopy (SEM, Tescan MIRA3, FESEM, Czech Republic). The fracture surface of the coatings and the substrate surface after corrosion were also examined using SEM. The phase composition of Fe/Co-ZIF-67 was analyzed by X-ray diffraction (XRD, Tongda TD-3700, China) with Cu Kα radiation at a scan rate of 5°/min within the 2θ range of 5°–80°. Stability, voltage, and current were measured using linear sweep voltammetry (LSV, PGSTAT30) and electrochemical impedance spectroscopy (EIS).

١. Sankar, S. S.; Ede, S. R.; Anantharaj, S.; Karthick, K.; Sangeetha, K.; Kundu, S. Electrospun cobalt-ZIF micro-fibers for efficient water oxidation under unique pH conditions. *Catalysis Science & Technology* **2019**, *9* (8), 1847-1856.

٢. Anantharaj, S.; Ede, S.; Karthick, K.; Sankar, S. S.; Sangeetha, K.; Karthik, P.; Kundu, S. Precision and correctness in the evaluation of electrocatalytic water splitting: revisiting activity parameters with a critical assessment. *Energy & Environmental Science* **2018**, *11* (4), 744-771.

٣. Kitagawa, S. Metal–organic frameworks (MOFs). *Chemical Society Reviews* **2014**, *43* (16), 5415-5418.

٤. Maurin, G.; Serre, C.; Cooper, A.; Férey, G. The new age of MOFs and of their porous-related solids. *Chemical Society Reviews* **2017**, *46* (11), 3104-3107.

٥. Chen, X.; Zhao, J.-X.; Wang, J.-W.; Liu, Y.; Wang, L.-C.; Weerasooriya, R.; Wu, Y.-C. Doping ZIF-67 with transition metals results in bimetallic centers for electrochemical detection of Hg (II). *Electrochimica Acta* **2021**, *387*, 138539.

٦. Chen, B.; Yang, Z.; Zhu, Y.; Xia, Y. Zeolitic imidazolate framework materials: recent progress in synthesis and applications. *Journal of Materials Chemistry A* **2014**, *2* (40), 16811-16831.

٧. Moggach, S. A.; Bennett, T. D.; Cheetham, A. K. The effect of pressure on ZIF-8: increasing pore size with pressure and the formation of a high-pressure phase at 1.47 GPa. Angewandte Chemie International Edition 2009, 48 (38), 7087-7089.

Magnetic $BiFeO_3$ nanoparticles: Efficient nanocatalyst for the green one-pot three-component synthesis of highly substituted 3,4-dihydropyrimidine-2(1H) -one/ thione derivatives

Safa Hanifi[a], Mohammad G. Dekamin*[a], Mohammad Eslami[b]

[a]*Pharmaceutical and Heterocyclic Compounds Research Laboratory, Department of Chemistry, Iran University of Science and Technology, Tehran 1684613114, Iran.*

[b]*Department of Chemistry, Behbahan Khatam Alanbia University of Technology, Behbahan 6361663973, Iran.*

Abstract

This research involved the synthesis and characterization of magnetic bismuth ferrite nanoparticles (BFO MNPs) using a straightforward method. The structure and morphology of the nanoparticles were analyzed through FTIR, FESEM, EDS, XRD, and VSM techniques. BFO MNPs were utilized as a heterogeneous Lewis acid catalyst for the synthesis of 3,4-dihydropyrimidin-2(1H)-ones/thiones (DHPMs/DHPMTs). The results demonstrated that BFO MNPs effectively catalyzed the synthesis of various DHPMs with low catalyst loading, high yields, eco-friendly reaction conditions, short reaction times, simple workup, and reusability. The structures of the synthesized compounds were confirmed through ^1H NMR, FTIR, and melting point analyses, highlighting the catalyst's potential for sustainable green chemistry applications.

Key words: Magnetic heterogeneous catalysts; Bismuth ferrite nanoparticles; 3,4-Dihydropyrimidine-2(1*H*)-one/thione; Multi-Component reactions (MCRs) and Green and Sustainable Chemistry.

Introduction

The synthesis of nitrogen-containing 3,4-dihydropyrimidine-2(1H)-one/thione compounds (DHPMs/DHPMTs) is essential due to their diverse biological properties and roles in drug discovery. Despite initial progress, challenges remain, including toxic solvents and expensive catalysts. Recognizing the importance of heterocyclic compounds, researchers are seeking innovative, efficient synthesis methods. In line with green chemistry principles, a novel approach utilizing magnetic bismuth nanoparticles has been investigated to enhance the synthesis process. This method aims to overcome existing challenges and improve overall efficiency.

Preparation of the magnetic bismuth ferrite nanoparticles (BFO MNPs)

The preparation of bismuth ferrite nanoparticles (BFO MNPs) was carried out using the solid-state thermal decomposition method. Initially, a 100 mL round-bottom flask was charged with glycine (8.0 mmol), $Fe(NO_3)_3.9H_2O$ (4.0 mmol), $Bi(NO_3)_3.5H_2O$ (4.0 mmol), and deionized water (40.0 mL). The mixture was heated at 120 °C for one hour. Subsequently, HNO_3 (2.80 mL) was added dropwise to the reaction mixture, which was then heated again at 120 °C, leading to the formation of a brown solid. Finally, the brown solid was placed in an oven at 350 °C for one hour, followed by an additional hour at 550 °C to prepare the bismuth ferrite nanoparticles (BFO MNPs).

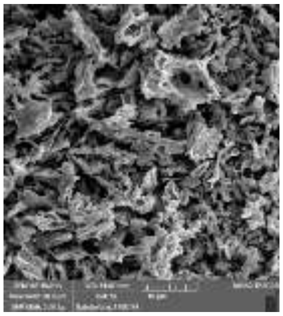

FESEM images of $BiFeO_3$ nanoparticles

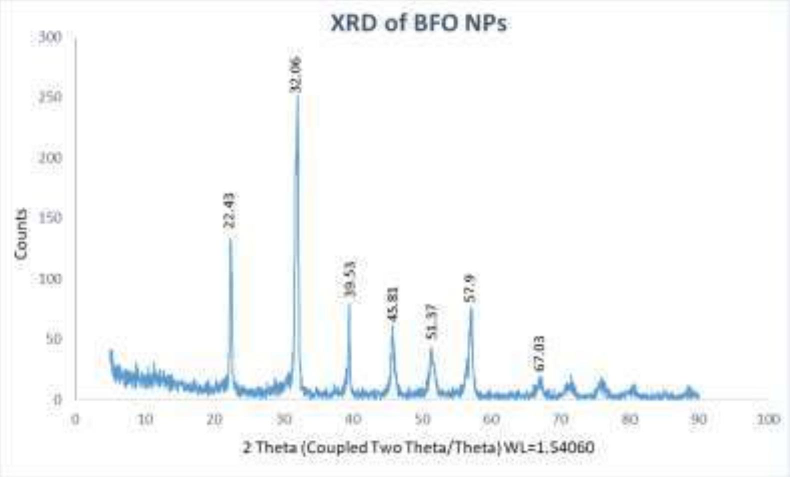

X-Ray diffraction pattern of BFO MNPs.

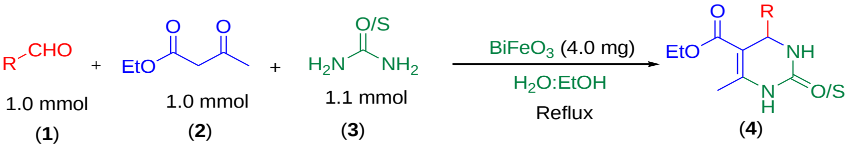

Entry.	**Aldehyde** **(1a-e)**	**ethyl acetoacetate**	**Urea/Thiourea** **(3a-b)**	**Product** **(4a-e)**	**Time** **(min)**	**Yield** [b] **(%)**	**M.p** **(ºC)**
1	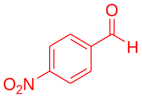 **1a**	**2**	Urea **3a**	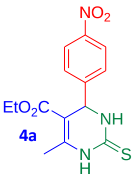	10	96	

							211- 213
2	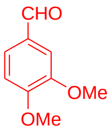 **1b**	**2**	Urea **3a**	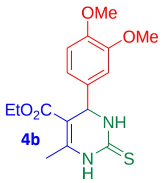	15	92	173- 175
3	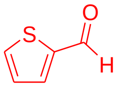 **1c**	**2**	Urea **3a**	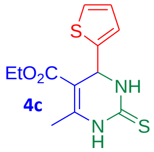	15	93	214- 216
4	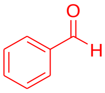 **1d**	**2**	Thiourea **3b**	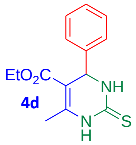	20	98	211- 213

Aromatic aldehydes with electron-withdrawing groups (-NO_2, -Cl, -Br) demonstrate faster product formation compared to those with electron-donating groups (-OMe, -OH, -Me). This is due to their higher carbonyl activity, which facilitates the reaction. In contrast, electron-rich heterocyclic aromatic aldehydes like thiophen-2-carbaldehyde and furfural exhibit longer reaction times because their increased electron density reduces carbonyl activity, hindering electrophilic attack on the carbonyl group. These observations align with the reaction mechanism, where the electrophile's attack on the carbonyl is the rate-determining step. Thus, aldehydes with electron-withdrawing groups promote quicker reactions, while those with electron-donating groups and heterocyclic aldehydes slow them down.

١. Fattahi, B. & Dekamin, M. G. Fe_3O_4/SiO_2 decorated trimesic acid-melamine nanocomposite: a reusable supramolecular organocatalyst for efficient multicomponent synthesis of imidazole derivatives. Sci. Rep. 13, 401. https:// doi. org/ 10. 1038/ s41598- 023 27408-7 (2023).

٢. Eslami, M., Dekamin, M. G. & Mahdavi, E. C (sp^2) –Hal activation for efficient Ullmann-type C–O coupling in water by in situ reduction of supramolecular Cu (II) species stabilized on a modified GO nanosheets support. Surf. Interfaces 104363 (2024).

٣. Moghaddam, F. M., Jarahiyan, A., Eslami, M. & Pourjavadi, A. A novel magnetic polyacrylonotrile-based palladium Core–Shell complex: A highly efficientcatalyst for Synthesis of Diaryl ethers. J. Organometal. Chem. 916, 121266 (2020).

٤. Akbari, A., Dekamin, M. G., Yaghoubi, A. & Naimi-Jamal, M. R. Novel magnetic propylsulfonic acid-anchored isocyanurate-based periodic mesoporous organosilica (Iron oxide@PMO-ICS-$PrSO_3H$) as a highly efficient and reusable nanoreactor for the sustainable synthesis of imidazopyrimidine derivatives. Sci. Rep. 10, 10646. https:// doi. org/ 10. 1038/ s41598- 020- 67592-4 (2020).

The 30th Iranian Seminar of Organic Chemistry
February 7-9, 2025, Iran University of Science and Technology, Tehran, Iran

Preparation of conductive nanocomposite based on nylon 6,6 containing copper and silver nanoparticles

Mohsen Sargordan Fard Arani

Department of Chemistry, Faculty of Science, Yadegar-e-Imam Khomeini (RAH) Shahr-e-

Rey Branch, Islamic Azad University, Tehran, Iran

Abstract:

In this work, nanocomposites comprising copper and silver nanoparticle in nylon 6,6 matrices have been prepared. In this manner, copper and silver nanoparticles prepared by its salt reduced by sodium borohydride at various concentration. Then this nanoparticle solution was mixed with polymer solution and electro spun by electrospinning device. The above nanocomposite has been successfully detected by SEM, EDAX, FT-IR Spectroscopy and indicated that not only nanoparticles and nylon 6,6 nanofiber have created good chemical interaction but also a relatively suitable size and distribution has been yielded in the fibers. The resulted nanocomposite conductivity by four-probe method showed a remarkable conductivity produced by Nano nanoparticles distribution in the tissue of nanocomposites increasing as concentration rises.

Keyword: nanoparticles, conductivity polymer, nylon 6,6, nanofiber.

Introduction:

Nanocomposite material consists out of several phases where at least one, two or three dimensions are in nanometer range. Taking material dimensions down to nanometer level creates phase interfaces which are very important for enhancement of materials properties. The ratio between surface area and volume of reinforced material used during nanocomposites preparation is directly involved in understanding of structure-property relationship. Nanocomposites offer opportunities on completely new scales for solving obstacles ranging from medical, pharmaceutical industry, food packaging, to electronics and energy industry. Nanocomposite can be divided in three classes; metal matrix, ceramic matrix and polymer matrix nanocomposites. One of the methods to produce nanoparticles is the reduction of metal salts [1-3]. The most important method for producing nanofibers is electrospinning due to its high variety and the convenience using the device [4]. Many polymers have been transformed into nanofibers via this method [5]. since the availability of nanoparticles resulted in the improvement of the nanofibers' properties and composite nanofibers' applicability [6,7]. On the other hand, most of the polymers are insulate electrically speaking; however, the conductive metal nanoparticles supply a satisfactory conductivity in the nanocomposites of metal & polymer [8,9].

Method:

To prepare the desired composite, first nylon 66 is dissolved in its solvent formic acid and acetic acid, then silver nitrate and copper nitrate are added to it, and the silver nitrate and copper nitrate in the solution are reduced by the reducing agent sodium borohydride, and finally the obtained solution is converted into fibers by an electrospinning device. To examine the conductivity of the desired fibers at different concentrations of silver and copper, identical solutions of polymer, formic acid and acetic acid are prepared, and different amounts of silver nitrate and copper nitrate are added to them, and for reduction, sodium borohydride is used in proportion to the amount of silver and copper. The produced nanofibers are examined by atomic spectra, UV-VIS, FTIR, SEM and conductivity measurement.

Results and Discussion:

Table (1): Relationship between copper concentration and absorption rate

Concentration(ppm)	Absorbance
BLANK	1.739
500	2.456
1000	2.521
1500	2.573
2000	2.621

Table (2): Relationship between silver concentration and absorption rate

Concentration	Absorbance
BLANK	1.512
500	1.713
1000	1.914
1500	2.124
2000	2.341

To identify the electrospun nanocomposite containing nanoparticles, the following spectrometry and results were obtained:

UV spectroscopy

The table and graph below show that as the concentration of silver and copper in the solution increases, the rate of absorption increases (table 1,2).

As can be seen in the SEM images, the diameter of the fibers is in the nanometer range, the distribution of silver and copper nanoparticles is uniformly distributed to a desirable extent. With closer observation, it is clear that their size is on average between 20-40 nm and increasing the concentration of nanoparticles has not significantly changed their size. However, at higher concentrations, some particles may be joined due to the high concentration of nanoparticles

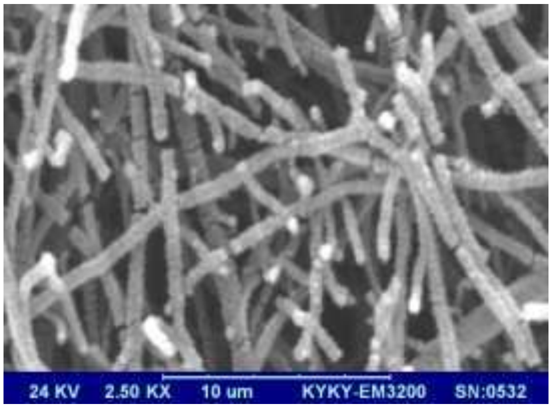

Figure 1: SEM image of a nanocomposite sample with a nanoparticle concentration of 500 PPM.

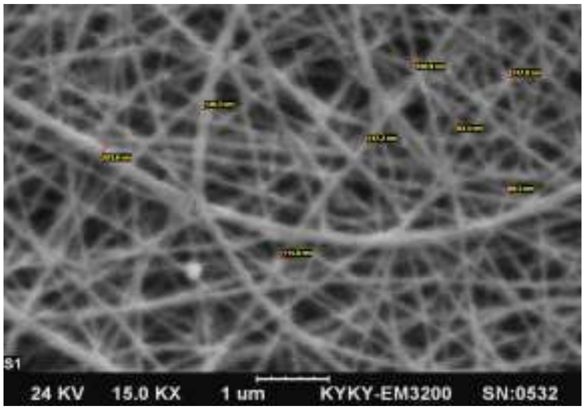

Figure 2: SEM image of electro spun Nano polymer sample without nanoparticles

Also, using energy dispersive X-ray spectroscopy (EDS or EDX), the presence of silver and copper elements in the nanocomposite can be detected.

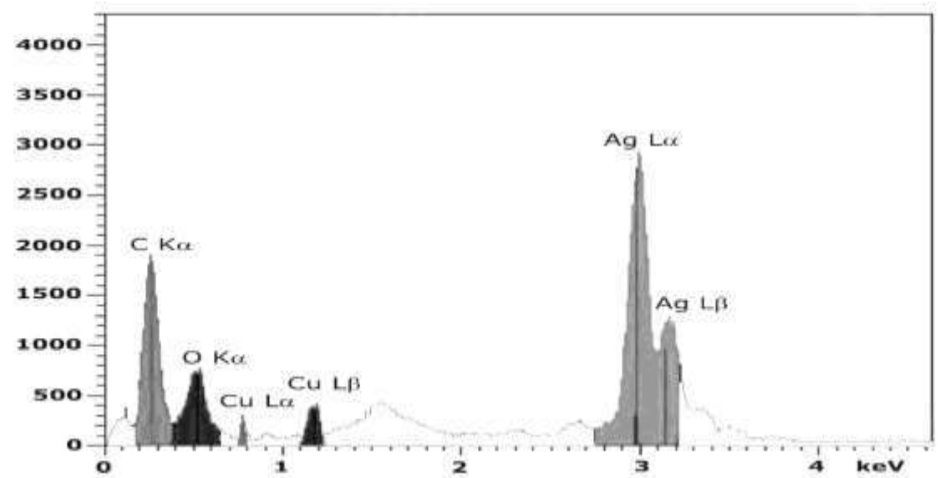

Figure 3: EDX analysis diagram of 500ppm sample

As the solution concentration increased, the intensity of the EDX peaks of silver and copper present in the solution increased.

From the FTIR spectra of the samples, it was concluded that with increasing concentration of the samples, the intensity of the peaks of the functional groups present in the nylon 66 polymer decreased, meaning that elements were involved in these functional groups and limited their mobility and oscillation. So, as a result, Nano elements of copper and silver particles have entered into the nanofibers and interact with the functional groups in the polymer tissue.(fig4&5)

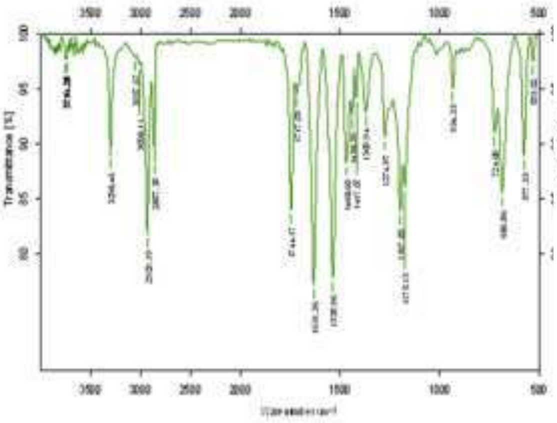

Figure 4: FT-IR spectrum of the nanofiber sample without copper and silver nanoparticles

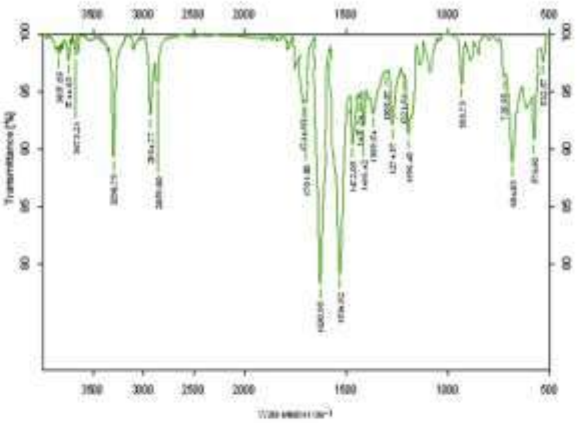

Figure 5: FT-IR spectrum related to the nanocomposite sample of nanofibers containing copper and silver nanoparticles with a concentration of 2000 PPM

The conductivity of composite nanofibers containing nanoparticles was measured through four-point conductometry. In this method, the two ends of the ohmmeter electrode are connected to the two ends of the sample (nanofibers) and its resistance and as a result its conductivity is measured. Figure6

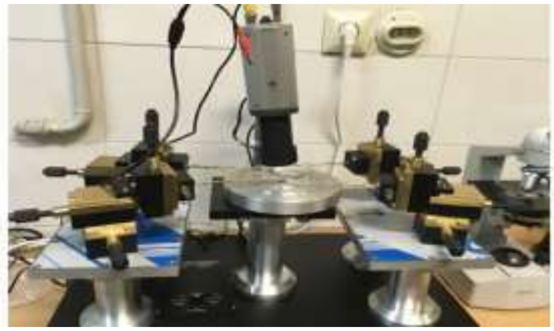

Figure 6: four point probe conduct meter

According to the conductivity results, it was found that while the nano fiber sample is not conductive, but the Nano composite sample containing metal nanoparticles is significantly conductive. Also, with the increase in the concentration of nanoparticles, a significant increase in conductivity is observed. Table 3.

Table (3): Relationship between the concentration of nanoparticles in the polymer and their conductivity

Conductivity	**Concentration of nanoparticle**
٠	Blank
7.3×10^{-7} z/cm	PPM١٠٠٠
3.4×10^{-6} z/cm	PPM٢٠٠٠

Conclusion:

In this work, composite nanofibers based on nylon 66 containing silver and copper particles were prepared. The identification of the resulting nanocomposite was investigated by atomic absorption spectra, UV-Vis spectroscopy, FTIR spectroscopy, and scanning electron microscopy (SEM). Then, conductivity measurements on the resulting nanofibers showed that the nanocomposite has a significant conductivity that increases with increasing concentration of metal nanoparticles.

References

١.C.T. Hsu,C.Wu,C.N.Chuang,S. H.Chen, W-Y. Chiu,K. H. Hsieh,J. Polym. Res., 22. 200 .(٢٠١٥)

٢.M.Sargordan, M.Hoseinkhani, F.Ebrahimi., Research Journal of Pharmaceutical, Biological and Chemical Sciences., 5, 155(2014)

٣ .I.M.Yakutik,G.P. Shevechenko,Surface. Science., 566, 414 (2004)

٤.M.N. Akhtar,A.B.Sulong, A.b. Saniah, C.H. Azhari,M.R.Raza.,Iran.Polym. J., 24, 1025 .(٢٠١٥)

٥.M. Khamforoush,R. Agha-Moalapour, Iran.Polym. J., 25, 875(2016).

6.O.E. Fayemi, A.S.Adekunle,E.E. Ebenso, J.Nanomater.,1,10 (2016).

]٧.D. j. da Silva,M.T. Escote,S. A. Cruz,D.F. Simião,A. Zenatti,M. S. Curvello, Polymer Composite, DOI: 10.1002/pc.24232(2016).

8..V.Kumar,S. Kalia,Swart,H.C.Conducting Polymer Hybrids, C.Tang, N. Nanxi Chen, X.

9.Hu, Conducting Polymer Nanocomposites: Recent Developments and Future Prospects, Springer, England,1-44 (2016).

The 30th Iranian Seminar of Organic Chemistry
February 7-9, 2025, Iran University of Science and Technology, Tehran, Iran

Preparation of nanocomposite based on polystyrene contained copper and investigation of its adsorption properties for removal of colored wastewater

Mohsen Sargordan Arani

Department of Chemistry, Faculty of Science, Yadegar-e-Imam Khomeini (RAH) Shahr-e-Rey Branch, Islamic Azad University, Tehran, Iran

Abstract:

Electrospinning is a versatile and viable technique for generating ultrathin fibers. Remarkable progress has been made in techniques for creating electro-spun and non-electro-spun nanofibers. In this work. to prepare the desired nanocomposite, first polystyrene was dissolved, then silver nitrate was added to the above solution in different concentrations, and these salts were reduced by sodium borohydride reducing agent, and finally the obtained solution containing copper and silver nanoparticles was converted into nanofibers by electrospinning. The above nanocomposite has been systematically identified by atomic absorption spectra, UV-VIS, FTIR, EDX, and SEM. Then, the absorption properties of disperse colored wastewater were investigated, which showed satisfactory and significant results. Also, the whiteness and reflective yellowness properties of the above composite were determined.

Keyword: nanofibers, nanocomposite, wastewater, Electrospinning

Introduction:

Nanofibers were the center of attention for industries and researchers due to their simplicity in manufacture and setup Nanotechnology is one of the fastest growing fields of study and has entered the profession of medicine and other industries as well. Due to the wide variety of applications many researchers hailing from countries all over the world have shown their interest in the technology. With respect to the pharmaceutical industry, nanotechnology made a mark because of its efficacy and reduced adverse event [.1-5] In the method of creation the electrospinning is very common and the basic principle of this method revolves around the static charges that are produced due to stretching of the polymer fiber repel each other which results in the formation of the fibers[6].

Nanotechnology systems ease the water cleaning process because inserting nanomaterials into underground water sources is cheaper and more efficient than pumping for treatment. Among nanomaterials, nanofibers are expected to become effective wastewater treatment materials due to their high specific surface area, high porosity, their ability to be easily functionalized, and superior mechanical performance (stiffness and tensile strength). These compounds are usually produced in the various morphologies and various compounds (synthetic polymers, natural polymers, metal-metal oxide/sulfide/selenide composites, To produce organic-, inorganic-,and polymeric-nanofibers, several techniques have been conducted such as thermally-induced phase separation [7], template synthesis [8], fibrillated bio-component fiber extrusion [9], phase separation [10], electrospinning [11], etc. The electrospinning is a cost-effective, simple, and reproducible process used to fabricate sizable nanofibers in large-scale. The fields of application of nanofibers are too wide and some of them are briefly mentioned here.

The nanofiber membranes prepared by electrospinning exhibited a higher flux with high removal efficiency compared to other membranes due to their higher specific area, high porosity, and fine adjustable pores. In the adsorption process, the Nano fibrous adsorbents indicated a higher adsorption capacity and easier reusability than other adsorbents such as carbons, zeolites [12-]. According to the above mentioned cases, we decided to make polystyrene Nano fibers containing copper particles After determining its structure, measure and determine the absorption property of colored wastewater

Method

To prepare the desired composite, first dissolve sodium borohydride in its solvent (20% DMF) and then add copper nitrate to it and reduce the copper nitrate in the solution by using sodium borohydride reducing agent and then add polystyrene to it. Finally, the obtained solution is converted into fibers by electrospinning machine. Different concentrations of copper are prepared. Solutions of the same polymer and solvent are prepared and different amounts of copper nitrate are added to them and for reduction, sodium borohydride is used in proportion to the amount of copper. The produced nanofibers are examined by reflection spectra, UV-VIS, FT-IR, SEM and

reflection spectrophotometry.

One of the methods for identifying produced nanofibers is scanning electron microscope (SEM) images, which can determine the dimensions of the fibers and nanoparticles

In the infrared spectra taken, the presence of copper nanoparticles in the mixture caused a slight shift in the peaks compared to the control spectrum and a decrease in absorption intensity, which could be a reason for the placement of metal particles within the polymer tissue and the interaction between copper nanoparticles and polystyrene nanofibers.

Figure 1: SEM image of a nanofiber sample without nanoparticles.

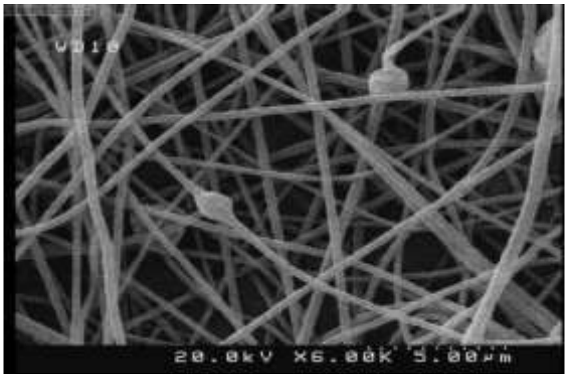

Figure 2: SEM image of a sample of nanofibers containing nanocopper with a concentration of 2000 ppm

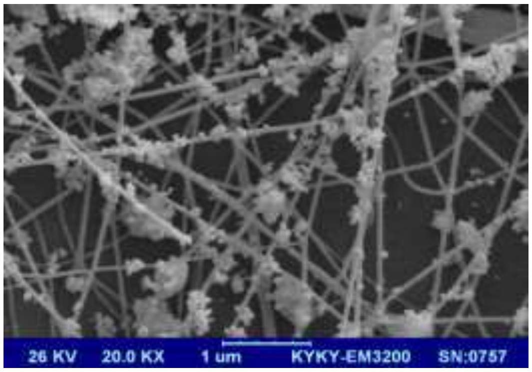

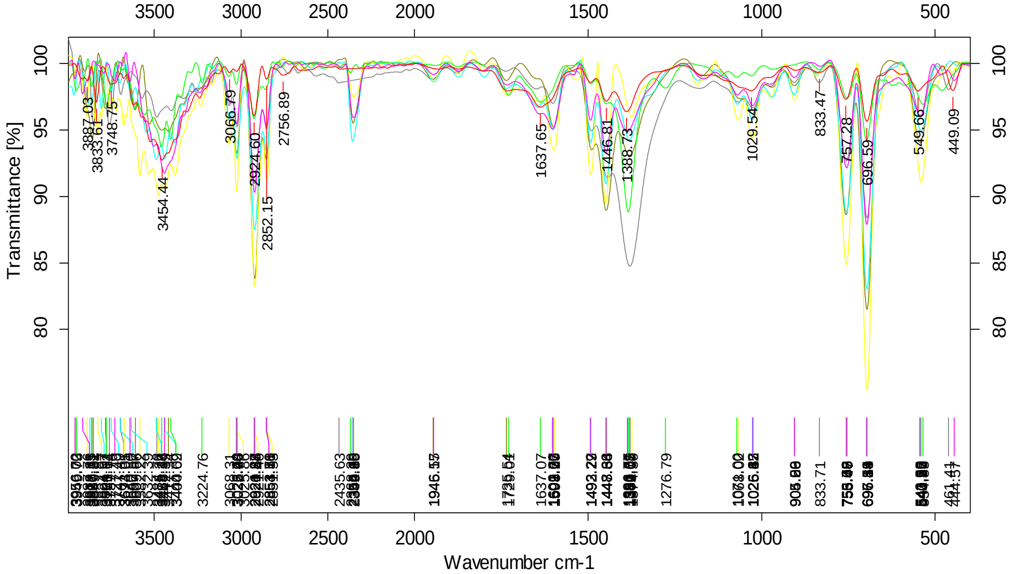

Figure 3: Infrared spectrum of the control sample compared to the sample containing nanoparticles with concentrations of 500, 1000, 1500, and 2000 ppm of nanocopper.

Energy-dispersive X-ray spectroscopy(EDAX) well confirms the presence of copper within the nanocomposite structure.(figure 4, 5)

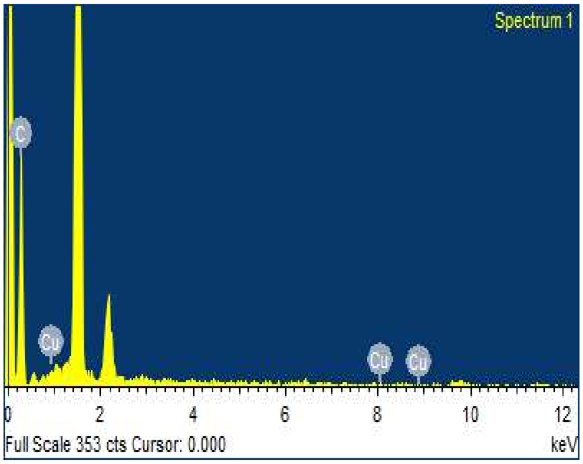

Figure 5: EDAX spectrum of nanocomposite with copper concentration of 1000 ppm

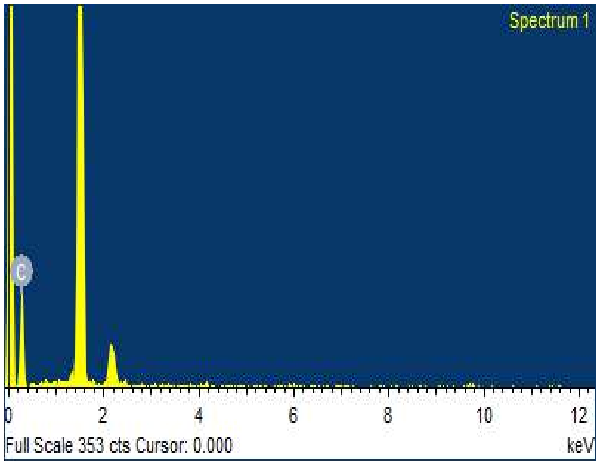

Figure 4: EDX spectrum of the control sample without copper nanoparticles

Wastewater absorption spectrophotometer

In this method, we prepare a 0.01% (weight-volume) solution of disperse dye and distilled water. We put the solution in a stirrer to mix. After it is completely dissolved, we weigh 0.1 of the foil on which the polystyrene and copper nanocomposite has been spun and place it in the above solution. Then, we read its absorption using an absorption spectrophotometer for 10 to 50 minutes. The decrease in the absorption intensity in the solution indicates the absorption of wastewater by the nanocomposite. (figure 6-7):

As can be seen, the nanocomposite containing copper nanoparticles has a much higher wastewater absorption capacity than the control nanocomposite, i.e. without particles. **Fig.6**

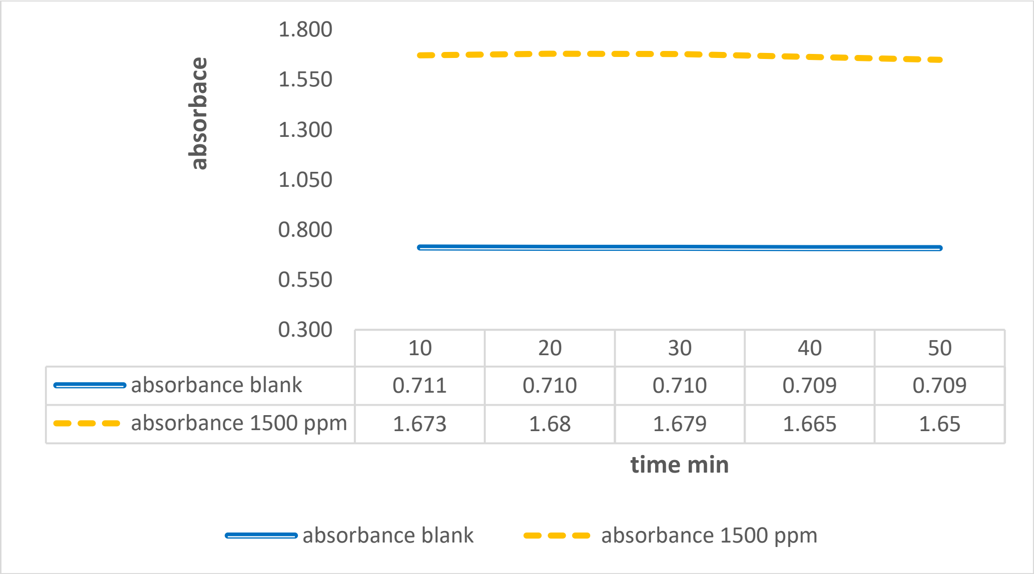

	10	20	30	40	50
absorbance blank	0.711	0.710	0.710	0.709	0.709
absorbance 1500 ppm	1.673	1.68	1.679	1.665	1.65

Fifure 6.Comparison chart of wastewater absorption of polystyrene nanofiber samples without nanoparticles and in the presence of copper nanoparticles with a concentration of 1500 ppm

Also, by examining the uv-vis absorption peaks of the samples, it was found that firstly, the optimal time for maximum absorption is around 30 minutes, and secondly, the amount of absorption increases with the increase in the concentration of nanoparticles (fig. 7)

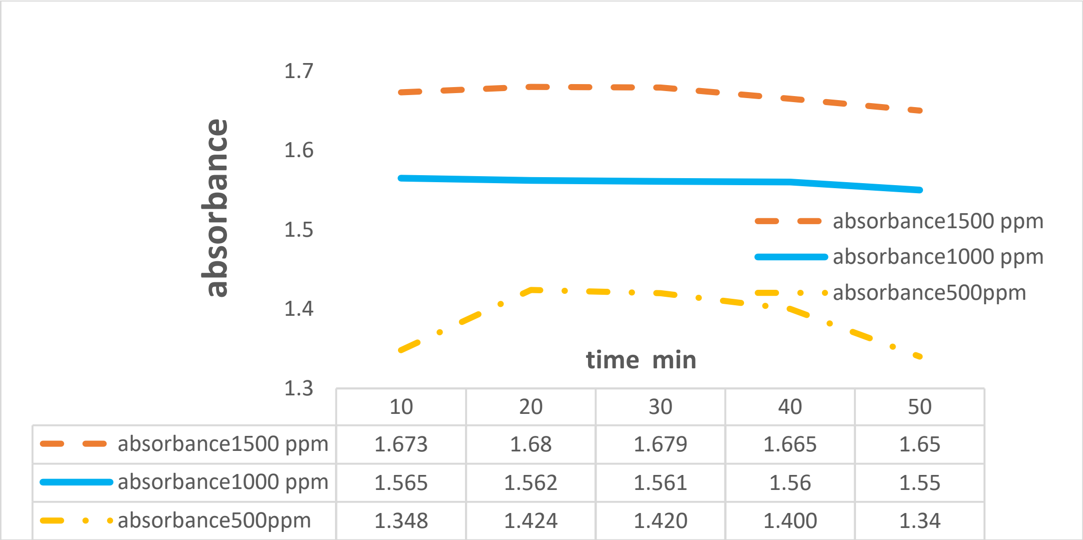

	10	20	30	40	50
absorbance1500 ppm	1.673	1.68	1.679	1.665	1.65
absorbance1000 ppm	1.565	1.562	1.561	1.56	1.55
absorbance500ppm	1.348	1.424	1.420	1.400	1.34

Figure 7: Comparison chart of wastewater absorption of polystyrene nanofiber samples with different concentrations

Result and Conclusion:

In this work, after dissolving polystyrene in a solvent and preparing copper nanoparticles and mixing the two together, this mixture was converted into a nanocomposite of nanofibers containing copper nanoparticles in an electrospinning device. After identifying and determining the structure of the resulting nanocomposite by scanning electron microscopy (SEM), infrared spectroscopy (IR) and energy dispersive X-ray spectroscopy (EDAX), its dispersed dye wastewater absorption properties were investigated, considering that polystyrene itself also has some absorption ability. The investigations and results of the experiment show that the dye wastewater absorption properties increase significantly in the form of nanofibers and in the presence of copper nanoparticles, and this wastewater absorption capacity increases with increasing nanoparticle concentration. Also, the optimal time for maximum absorption is about 30 minutes.

References:

1 .S. E. McNeil, Nanotechnology for the biologist, J. Leukocyte Biol., 2005, 78, 585–594, DOI: 10.1189/jlb.0205074.

2 N. Hasan, M. Imran, P. Kesharwani, K. Khanna,R. Karwasra, N. Sharma, S. Rawat, D. Sharma, F. J. Ahmad, G. K. Jain, A. Bhatnagar and S. Talegaonkar, Int. J. Pharm., 2021, 599, DOI:10.1016/j.ijpharm.2021.120428.

3 A. Sheikh, S. Md and P. Kesharwani,., 2022, 146, 112530, DOI: 10.1016/J.BIOPHA.2021.112530.

4- V. Singh, S. Md, N. A. Alhakamy and P. Kesharwani, Eur. Polym. J., 2022, 162, 110883, DOI: 10.1016/J.EURPOLYMJ.2021.110883.

5 -A. Sheikh, S. Md and P. Kesharwani, J. Controlled Release, 2021, 340, 221242, DOI: 10.1016/J.JCONREL.2021.10.028.

6- H. Wu, W. Pan, D. Lin and H. Li, J. Adv. Ceram., 2012, 1,2–23, DOI: 10.1007/s40145-012-0002-4.

7- A. Khalf et al. . 2017 Mar:112:1-17. doi: 10.1016/j.ejpb.2016.11.010. Epub 2016 Nov 16.(2017)

8- R.S. Barhate et al, Journal of Membrane Science,Volume 296, Issues 1–2, 15 June 2007, Pages 1-8

9- D. Bjorge et al., ,(2009) Desalination,Volume 249, Issue 3, 25 December 2009, Pages 942-948

10. J. Cai et al, . Composites Part A: Applied Science and Manufacturing, Volume 92, January 2017, Pages 10-16,

11. Y. Tian et al Carbohydr. Polym. Volume 83, Issue 2, 10 January 2011, Pages 743-748.

12. Parvaneh Ghaderi-shekhi Abadi , Mohammad Irani , Leila Roshanfekr Rad Journal of the Taiwan Institute of Chemical Engineers, Volume 143, February 2023, 104625.

Magnetic Nb Graphene Oxide Nanocomposite as nanocatalyst for Suzuki-Miyaura Cross-Coupling Reaction

Alireza Gharehkhani [a], Maryam Hajjami* [c]

Department of Organic Chemistry, Faculty of Chemistry and Petroleum Sciences, Bu-Ali Sina University, Postal code 6517838683, Hamedan, Iran. E-mail address, m.hajjami@basu.ac.ir or mhajjami@yahoo.com

Keyword: Graphene oxide, Suzuki-Miyaura, Coupling, Nanocomposite

Abstract

Graphene oxide, which is a two-dimensional aromatic scaffold and oxygen-containing functional groups shows considerable catalytic properties [1,2]. In this research work, an efficient protocol for the design of magnetic nickel graphene oxide [3] functionalized Nb-curcumin nanoparticles (Ni-GO/Cur-Nb) has been developed as a nanocatalyst for the Suzuki-Miyaura (SM) cross-coupling reaction using organic halides and phenyl boronic acid. The synthesized Ni-GO/Cur-Nb nanocatalyst was characterized and showed significant advantages compared to previous methods. The advantages of this method include easy purification, catalyst reusability, green and mild procedure, and high yields in short reaction times.

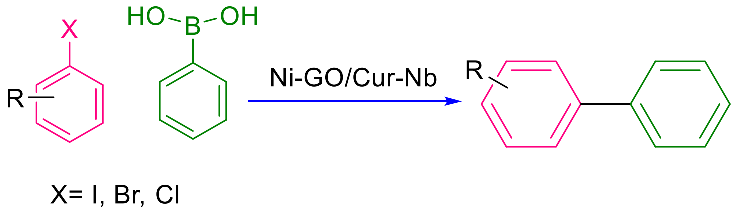

Scheme: General procedure for SM cross-coupling reaction catalyzed by Ni-GO/Cur-Nb

(1) Su, C.; Loh, K. P. Carbocatalysts: graphene oxide and its derivatives. *Accounts of chemical research* **2013**, *46* (10), 2275-2285.
(2) Su, C.; Acik, M.; Takai, K.; Lu, J.; Hao, S.-j.; Zheng, Y.; Wu, P.; Bao, Q.; Enoki, T.; Chabal, Y. J. Probing the catalytic activity of porous graphene oxide and the origin of this behaviour. *Nature communications* **2012**, *3* (1), 1298.
(3) Moradi, P.; Hajjami, M. Magnetization of biochar nanoparticles as a novel support for fabrication of organo nickel as a selective, reusable and magnetic nanocatalyst in organic reactions. *New Journal of Chemistry* **2021**, *45* (6), 2981-2994.

Green synthesis of multi substituted pyrrole derivatives using synthetic novel heterogeneous nano catalyst base on GQDs

Marziyeh Behrouzi[a], Mohadeseh Noei[a], Khadijeh Rabiei*[a]

[a]*Department of Chemistry, Faculty of Science, Qom University of Technology, Qom, Iran*

Abstract

Graphene quantum dots (GQDs) are versatile materials with unique optical and chemical properties that make them suitable for a wide range of applications. Their synthesis can be achieved through various top-down and bottom-up methods, and their properties can be tailored through functionalization and doping to enhance performance in specific applications [1]. Pyrrole and its poly-substituted derivatives are important five-membered heterocyclic compounds which exist in many pharmaceutical and natural product structures [2]. By collecting our previous knowledge on the usage of heterogeneous catalysts and as a part of our continuing interest in the development of green and efficient new synthetic methods in organic reactions, we have reported the synthesis of novel functionalized GQDs with Schiff base Co(II) complexes and survey the catalytic activity of this synthetic catalyst for preparation of pyrrole derivatives. For this purpose, the GQDs was synthesized using citric acid and functionalized Schiff base complex. The structure of the synthetic FGQDs fully characterized using various techniques. Then, the catalytic activity of the synthesized FGQDs catalyst was investigated in a one-pot MCR reaction of acetophenone, nitro methane, aniline and benzaldehyde derivatives for preparation of multi substituted pyrrole derivatives. The synthesis of the desired products was carried out successfully with excellent yields and short reaction times.

Keyword: Pyrrole, Green, FGQDs, Heterogeneous, MCR.

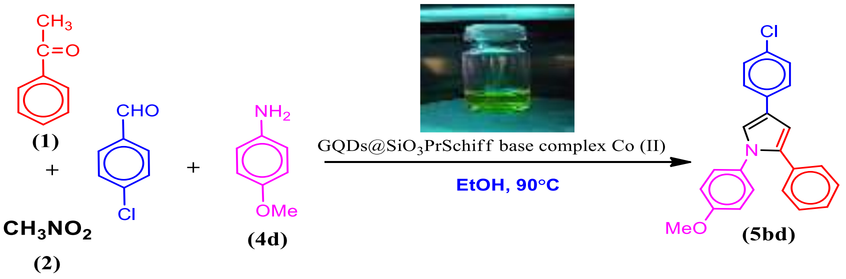

References:

[1] F. F. Habibah, A. L. Ivansyah, S. Ivan, R. Hertadi, *RSC Adv.*, **2023**, **13**, 2949-2962.

[2] Zh. Ma, Z. Ma, D. Zhang, *Molecules*, **2018**, 23, 2666-2677.

Preparation and Characterization of Magnetic Hydrogel Modified with Metal Organic Framework

Authors: Mohammad Mehdi Salehi, Haniyehalsadat Amirhosseini, Leila Choopani, Ali Maleki*.

Catalysts and Organic Synthesis Research Laboratory, Department of Chemistry, Iran University of Science and Technology, Tehran 16846-13114, Iran.

*Corresponding author. E-mail: maleki@iust.ac.ir (A.Maleki) Fax: +98-21-73021584; Tel: +98-21-7322831.

Keyword: Magnetic nanocomposite, Adsorption, MOF, Wastewater Purification, Pharmaceutical contaminant.

The use of antibiotics has significantly increased in recent decades. Consequently, high levels of these contaminants are now present in the environment, making the removal of antibiotics from aquatic environments essential in combating antimicrobial resistance. Various methods including physical, chemical, and biological are employed to treat water. Notably, adsorption stands out as a highly efficient, selective, and versatile technique that effectively removes contaminants, making it beneficial across multiple industries. A novel highly efficient, eco-friendly magnetite nanocomposite (MNC) utilizing xanthan gum (XG) has been developed for the effective removal of ciprofloxacin (CIP) and amoxicillin (AMX) from wastewater. This magnetic nanocomposite is designed for straightforward separation and reuse. The synthesized magnetite nanocomposites were characterized through a range of techniques, including FT-IR, XRD, FESEM, VSM. The effects of pH, adsorbent dose, contact time, and AMX and CIP concentration on the adsorption processes were investigated. The MNC showed a maximum adsorption capacity (Qmax) of 237.56 mg^{-1} for ciprofloxacin (CIP) and 217.37 mg^{-1} for amoxicillin (AMX) using 0.008 g of the adsorbent. Equilibrium data were modelled using Langmuir, Freundlich, among which the Freundlich isotherm model gave the best fit. Furthermore, the adsorption kinetic measurements were accurately captured by the pseudo-second-order (PSO) model. Overall, this study shows that the adsorbent proved to be a viable and promising option for the elimination of antibiotics from water, with high adsorption capacity.

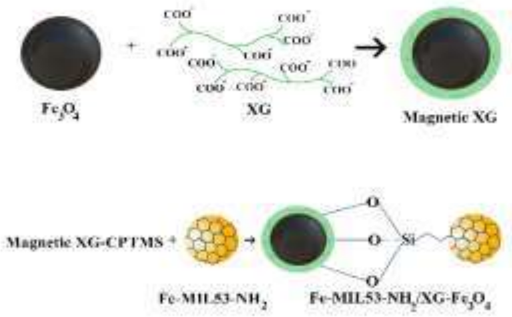

References:

Elella, Mahmoud H. Abu, et al. "Xanthan gum-derived materials for applications in environment and eco-friendly materials: A review." *Journal of Environmental Chemical Engineering* 9.1 (2021): 104702.

Salehi, Mohammad Mehdi, et al. "Performance of magnetic nanocomposite based on Xanthan gum-grafted-poly (acrylamide) crosslinked borax for the effective elimination of amoxicillin from an aquatic environment." *Chemosphere* (2024): 142548.

The 30th Iranian Seminar of Organic Chemistry
February 7-9, 2025, Iran University of Science and Technology, Tehran, Iran

Study on Homo-Cubane (C_9H_{10})^n and Aza-Homo-Cubane (C_8H_9N)^n Molecules and Their Four Reduced States (n=0 and −1 to −4)

Rozhin Fahimi, Avat (Arman) Taherpour*

Department of Organic Chemistry, Faculty of Chemistry, Razi University, P.O.Box: 67149-67346, Kermanshah, Iran

0000-0002-8933-1505

Abstract:

On the basis of the energy storage, importance of chemical energies and the charge transfer, the objective of this research is study on Homo-Cubane and Aza-Homo-Cubane (C_9H_{10} and C_8H_9N; as the energetic with high stress molecules) and their molecular deformation by stepwise reduced states (i.e. $C_9H_{10}{}^n$ and $C_8H_9N^n$; n=0 and −1 to −4). In this study, the molecules of homo-cubane and aza-homo-cubane were optimized to obtain minimize molecular geometry and the electronic structure by the density functional theory (DFT, MO6) using 6-31+G* basis set. Some important properties such as bond order changes, electron densities, frontier orbital (HOMO and LUMO) energies and characters, thermodynamic parameters, natural bond orbital (NBO) populations, computed IR spectrum and structural deformation parameters were calculated and investigated for $C_9H_{10}{}^n$ and $C_8H_9N^n$ (n=0 and −1 to −4). The results of the DFT investigations revealed that this compound exhibit excellent performance in the oxidation process in its reduced form.

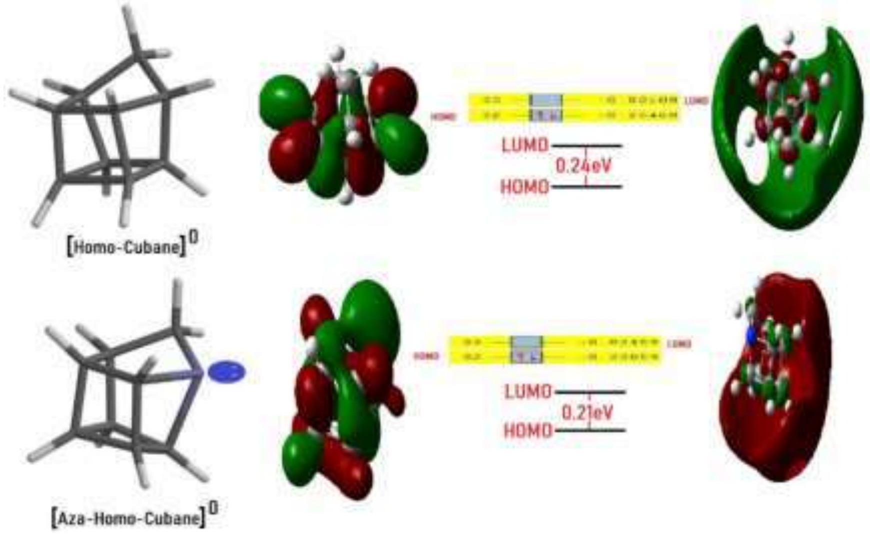

Keywords: Homo-Cubane; Reduction; Molecular deformation; DFT; MO6; Molecular modeling.

References:

[1] M. Naderi-Namivandi, A. A. Taherpour, M. Jamshidi, M. Ghadermazi, Theoretical Study on Cubane Molecule and Its Reduced States ($C_8H_8^n$; n=0 and -1 to -4); A First Principle DFT Study, *J. Iran. Chem. Soci.*, **2021**, 18, 3303–3312.

[2] T. Fahrenhorst-Jones, D. L. Marshall, M. Burns, G. K. Pierens, R. E. Hormann, A. M. Fisher, P. V. Bernhardt, S. J. Blanksby, G. P. Savage, P. E. Eaton, C. M. Williams, 1-Azahomocubane, *Chem. Sci.*, 2023, 14, 2821-2825.

The 30th Iranian Seminar of Organic Chemistry
February 7-9, 2025, Iran University of Science and Technology, Tehran, Iran

Study on Aza-Cubane $(C_7H_7N)^n$ Molecule and Comparing Its Oxidation and Reduction States

Rozhin Fahimi, Avat (Arman) Taherpour*

Department of Organic Chemistry, Faculty of Chemistry, Razi University, P.O.Box: 67149-67346, Kermanshah, Iran

0000-0002-8933-1505

Abstract:
Aza-cubane as a molecule with high chemical energy and its oxidation and reduction states are the objective of this research. In this study on Aza-Cubane (C_7H_7N; as the energetic with high stress structure) and the molecular deformation by stepwise reduced states in the oxidation and reduction states. In this study, aza-cubane were optimized to obtain minimize molecular geometry and the

electronic structure by the density functional theory (DFT, MO6) using 6-31+G* basis set. Some important properties such as bond order changes, electron densities, frontier orbital (HOMO and LUMO) energies and characters, thermodynamic parameters, natural bond orbital (NBO) populations, computed IR spectrum and structural deformation parameters were calculated and investigated for the oxidation and reduction states of C_7H_7N. The results of the DFT investigations revealed the properties and the interesting results of the discussed structure in different oxidation and reduction states.

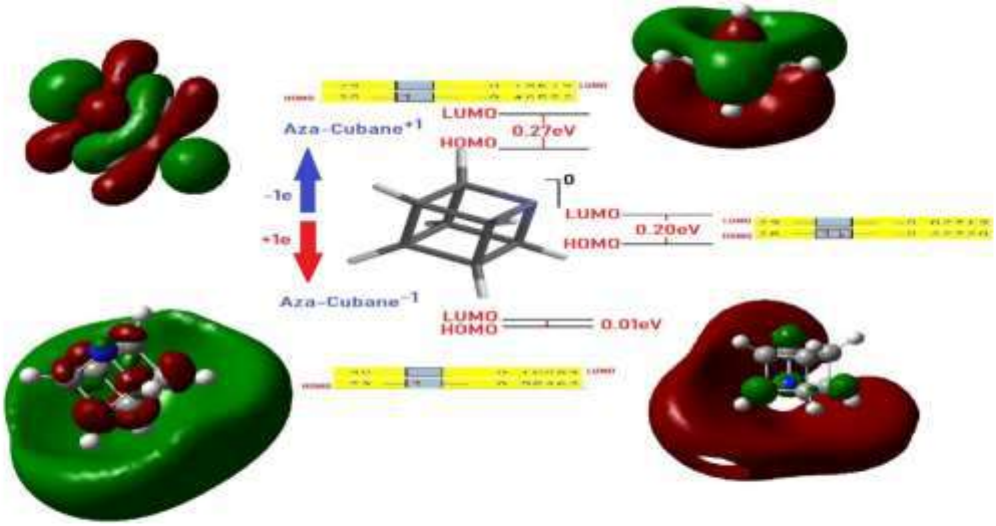

Keywords: Aza-Cubane; Reduction; Molecular deformation; DFT; MO6; Molecular modeling.

References:

[1] M. Naderi-Namivandi, A. A. Taherpour, M. Jamshidi, M. Ghadermazi, Theoretical Study on Cubane Molecule and Its Reduced States ($C_8H_8^n$; n=0 and -1 to -4); A First Principle DFT Study, *J. Iran. Chem. Soci.*, **2021**, 18, 3303–3312.

[2] T. Fahrenhorst-Jones, D. L. Marshall, M. Burns, G. K. Pierens, R. E. Hormann, A. M. Fisher, P. V. Bernhardt, S. J. Blanksby, G. P. Savage, P. E. Eaton, C. M. Williams, 1-Azahomocubane, *Chem. Sci.*, 2023, 14, 2821-2.

The 30th Iranian Seminar of Organic Chemistry
February 7-9, 2025, Iran University of Science and Technology, Tehran, Iran

Theorical study of moleculary imprinted polymers prepared for Allura red

Samaneh Bazaz1[a], Fatemeh Rafiee [b], Mina Ghiasi 3*[c]

[a, b] Department of Organic Chemistry, Factually of Chemistry, Alzahra University, Tehran, Iran.

[c] Department of Physical chemistry and Nano Chemistry, Alzahra University, Tehran, Iran.

Keyword: Molecularly imprinted polymers, Azo dye, Allura red, DFT calculation

Nowadays, the detection of synthetic dyes like Allura Red (**Scheme 1**) is critical due to increasing concerns over food safety and consumer health. the use of molecularly imprinted polymers (MIPs) has gained significant attention for their ability to selectively recognize and bind target molecules, making them valuable for various applications, including food safety and environmental monitoring. This study investigates the development of molecularly imprinted polymers (MIPs) using Allura Red as a template molecule, with methylacrylic acid(MAA) and vinylpyridine(VP) serving as two different functional monomers, **Allura red-MIP$_1$** and **Allura red-MIP$_2$**. Density Functional Theory(DFT) calculations were used to study the structures of each of the pre-polymerized complexes, (Allura red-Complex$_1$ and Allura red-Complex$_2$ refers for Allura red-MIP$_1$ and Allura red-MIP$_2$, respectively). In this study Calculated the complexation energies, solvation energies, The complexation enthalpies and Gibbs free energies of two complexes. Which, as preliminary calculations, shows a more favorable interaction between methacrylic acid and the template structure[1-3].

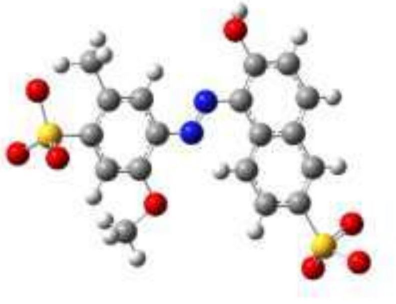

Scheme 1. Allura Red (E129)

References:

1.Ventura-Camargo, B.; Marin-Morales, M., Azo Dyes: Characterization and Toxicity– A Review. *Textiles and Light Industrial Science and Technology* **2013,** *2*.

2.Siddiquee, S.; Shafwanah, A. M. S., 10 - Toxicology and Analytical Methods for the Analysis of Allura Red (E129) in Food and Beverage Products: A Current Perspective. In *Safety Issues in Beverage Production*, Grumezescu, A. M.; Holban, A. M., Eds. Academic Press: 2020; pp 335-357.

3.Bichan, M. J.; Al-Bayati, Y. K.; Al-Abady, F. M.; Awwadi, F. F., Theoretical study of molecularly imprinted polymers prepared for homatropine methylbromide. *Journal of Polymer Research* **2023,** *30* (4), 142.

The 30th Iranian Seminar of Organic Chemistry
February 7-9, 2025, Iran University of Science and Technology, Tehran, Iran

Design, synthesis and application of a magnetic biological catalyst in the preparation of new pyrido[2,3-*b*]indole via CVABO

Seyed Mohammad Gohari Parvar[a], Milad Mohammadi Rasooll[a], Hassan Sepehrmansourie[b], Mohammad Ali Zolfigol*[a]

[a]Department of Organic Chemistry, Faculty of Chemistry and petroleum sciences, Bu-Ali Sina University, Hamedan 6517838683, E-Mail: zolfi@basu.ac.ir & mzolfigol@yahoo.com.
[b]Faculty of Converging Science and Technologies, University of Qom, Qom, Iran, 37185-359.

Keyword: Pyrido[2,3-*b*]indole, Magnetic biological catalyst, CVABO, Heterogeneous catalyst

In recent years, the development of chemical processes and reactions with an approach based on green chemistry has become an important principle for scientists. In the meantime, heterogeneous catalysts have become very important due to their easy separation, reusability, and compatibility with the environment [1]. The functionalization of heterogeneous catalysts with acidic groups leads to the production of an attractive group of catalysts with the ability to increase the speed and reduce the time of many chemical and organic reactions [2]. Integration of solid acid catalysts with magnetic nanoparticles leads to an increase in chemical and thermal stability as well as an increase in the ability to separate the catalyst. This issue is considered an important principle in achieving versatile and more efficient catalytic systems [3]. Therefore, Fe_3O_4@Phosphonic acid was prepared as a magnetic acid catalyst and it was used in the multicomponent reaction to produce pyrido[2,3-*b*]indole **(Scheme 1)**. Recyclability, reuse of catalyst, high reaction speed and high yield of synthesized products are among the attractive features of the above work.

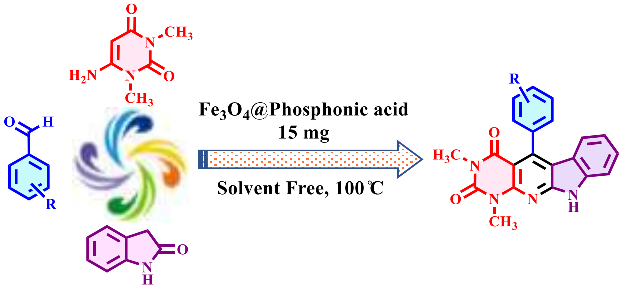

Scheme 1: Preparation of pyrido[2,3-*b*]indole derivatives using Fe_3O_4@Phosphonic acid

References:

[1] Luo, Z., Zhao, G., Pan, H., & Sun, W. (2022). Strong metal–support interaction in heterogeneous catalysts. *Advanced Energy Materials*, *12*(37), 2201395.

[2] Chen, Z., Gong, W., Wang, J., Hou, S., Yang, G., Zhu, C., ... & Cui, Y. (2023). Metallic W/WO2 solid-acid catalyst boosts hydrogen evolution reaction in alkaline electrolyte. *Nature Communications*, *14*(1), 5363.

[3] Danishyar, B., Sepehrmansourie, H., Ahmadi, H., Zarei, M., Zolfigol, M. A., & Hosseinifard, M. (2023). Application of nanomagnetic metal–organic frameworks in the green synthesis of nicotinonitriles via cooperative vinylogous anomeric-based oxidation. *ACS omega*, *8*(21), 18479-18490.

The 30th Iranian Seminar of Organic Chemistry
February 7-9, 2025, Iran University of Science and Technology, Tehran, Iran

[hexadec(Me)$_3$N]$^+$[L-Asc]$^-$:A Novel Bioorganic ionic Liquid to Promote the Ultrasound-Assisted Synthesis of Isoxazoles

Tayebeh Piri[a], Kobra Nikoofar*[a]

Department of Organic Chemistry, Faculty of Chemistry, Alzahra University, Tehran, Iran

Keyword: Ionic liquid, vitamin C, Isoxazoles, ultrasound

Vitamin-based ionic liquids (VILs) are green and nontoxic class of organics that could be synthesized via simple methods. They could play roles as catalysts various kinds of transformations as well as food supplements. Their properties and also toxicity could be affected by their cationic and anionic parts. It proved that in nitrogen -containing cations, toxicity increases with increasing carbon number. In addition, increasing oxygen in the ring, led to lower toxicity in cyclic organic cations. L-ascorbic acid (vitamin C), is an appropriate bioorganic candidate to develop VILs filed. Isoxazoles are class of heterocycles that are applicable in many drugs due to their biological properties such as hypoglycemic, antiviral, antibacterial, analgesic, anti-inflammatory, antidepressant, anti-osteoporotic, anti-Alzheimer's, and even anti-cancer and HIV-inhibiting activities. They are used in the production of penicillin, oxacillin, and cloxacillin. In this research, the ultrasound-assisted synthesis of isoxazoles has been done using novel IL based on vitamin C ([hexadec(Me)$_3$N]$^+$[L-Asc]$^-$), at room temperature with short reaction times.

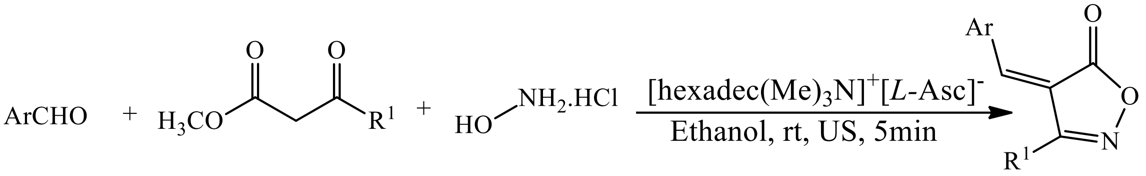

References:

١- Berezianko I.A., Kostjuk S.V. J. Mol. Liq., **2024**, 397.
٢- Niemczak M., Kaczmarek D.K., Klejdysz T., Gwiazdowska D., Marchwińska K., Pernak J. ACS Sustain. Chem. Eng., **2018**, 7, 1072-1084.
٣- Atharifar H., Keivanloo A., Maleki B., Baghayeri M., Alinezhad H. Res. Chem. Intermed., **2023**, 50, 281.
٤- Gulati S, Singh R, Sangwan S. Sci. Rep., **2021**, 11, 23563.

The 30th Iranian Seminar of Organic Chemistry
February 7-9, 2025, Iran University of Science and Technology, Tehran, Iran

A Density Functional Theory Study of Acetylcysteine

Hossein Shirani[a,*], Arefeh Saeidi[b]

[*] *Corresponding author. E-mail: hossein_shirani@iust.ac.ir*

[a] *Department of Chemistry, Iran University of Science and Technology, P.O. Box 16846-13114, Tehran, Iran*

[b] *Department of Microbiology, Faculty of Biological Sciences and Technology, University of Science and Culture, Tehran, Iran*

Introduction: Acetylcysteine, also known as N-acetylcysteine (NAC), not to be confused with N-Acetylcarnosine, which is also abbreviated "NAC," is a medication that is used to treat paracetamol overdose and to loosen thick mucus in individuals with chronic bronchopulmonary disorders like pneumonia and bronchitis. It has been used to treat lactobezoar in infants. It can be taken intravenously, by mouth, or inhaled as a mist [1-2]. Some people use it as a dietary supplement [3-4].

Methods: The study utilized quantum mechanics (QM) calculations conducted through the density functional theory (DFT) method with the GAUSSIAN 09 software at the B3LYP/6-311+G theoretical level. The structure of the Acetylcysteine was designd using GaussView software.

Results: This study conducted calculations for structural parameters like bond lengths, angles, and dihedrals, as well as thermodynamic parameters at the B3LYP/6-311G level of theory and provided the results. The electronic energy of the molecule was determined to be -548930.2 kcal/mole. Additionally, the atomic charge, spin density, and molecular orbital energies were calculated. The highest occupied molecular orbital (HOMO) was found to be -0.25 eV and the lowest unoccupied molecular orbital (LUMO) was -0.03 eV. The dipole moment in Debye was measured as X= 1.52, Y= 0.37, Z= -3.27, with a total of 3.62.

Discussion: Optimization of the drug was performed using the B3LYP/6-311G method. The study focused on Acetylcysteine's electronic characteristics, specifically the energy difference between the HOMO and the LUMO. The HOMO-LUMO gap energy was determined to be -0.28 eV. This provides insights into Acetylcysteine's electronic behavior, which could have applications in various fields.

Keywords: Acetylcysteine, DFT, HOMO and LUMO, Thermodynamic parameters

References:

[1] "Acetylcysteine". The American Society of Health-System Pharmacists. Archived from the original on 23 September 2015. Retrieved 22 August 2015.

[2] The Multifaceted Therapeutic Role of N-Acetylcysteine (NAC) in Disorders Characterized by Oxidative Stress Ganesh Raghu [1], Michael Berk [2], Peter A Campochiaro [3], Hartmut Jaeschke [4], Giancarlo Marenzi [5], Luca Richeldi [6], Fu-Qiang Wen [7], Ferdinando Nicoletti [8], Peter M A Calverley [9] PMID: **33380301** PMCID: PMC8719286 DOI: 10.2174/1570159X19666201230144109

[3] Talbott SM (2012). A Guide to Understanding Dietary Supplements. Routledge. p. 469. ISBN 9781136805707. Archived from the original on 8 September 2017.

[4] "Cysteine". University of Maryland Medical Center. Archived from the original on 1 July 2017. Retrieved 23 June 2017.

A-10-801-1.

The 30th Iranian Seminar of Organic Chemistry
February 7-9, 2025, Iran University of Science and Technology, Tehran, Iran

A Quantum Mechanical Investigation on Deuruxolitinib

Hossein Shirani[a,*], Arefeh Saeidi[b]

[*] *Corresponding author. E-mail: hossein_shirani@iust.ac.ir*

[a]*Department of Chemistry, Iran University of Science and Technology, P.O. Box 16846-13114, Tehran, Iran*

[b]*Department of Microbiology, Faculty of Biological Sciences and Technology, University of Science and Culture, Tehran, Iran*

Introduction: Deuruxolitinib is an orally available small molecule inhibitor of Janus kinases that is used to treat severe alopecia areata. Alopecia areata is an autoimmune disorder that is characterized by hair loss resulting in patches and even complete baldness of the scalp, along with thinning or loss of eyebrows and eyelashes. Inhibitors of JAK kinases have been used to treat several autoimmune diseases including alopecia areata. Deuruxolitinib can cause anemia, lymphopenia, neutropenia, thrombocytopenia, hyperlipidemia, and creatine kinase elevations. Potential severe adverse events may include reactivation of fungal, viral, and opportunistic infections such as tuberculosis, hepatitis B, herpes simplex, and herpes zoster [1-4].

Methods: The study utilized quantum mechanics (QM) calculations conducted through the density functional theory (DFT) method with the GAUSSIAN 09 software at the B3LYP/6-311+G theoretical level. The structure of the Deuruxolitinib was designd using GaussView software.

Results: This study conducted calculations for structural parameters like bond lengths, angles, and dihedrals, as well as thermodynamic parameters at the B3LYP/6-311G level of theory and provided the results. The electronic energy of the molecule was determined to be -619,249.4 kcal/mole. Additionally, the atomic charge, spin density, and molecular orbital energies were calculated. The dipole moment in Debye was measured as X= 3.26, Y= - 0.23, Z= 1.09, with a total of 3.44.

Discussion: Optimization of the drug was performed using the B3LYP/6-311G method. The study focused on dipole moment, Bond Length, Bond angle and atomic charge. This provides insights into Deuruxolitinib's electronic behavior, which could have applications in various fields.

Keywords: Deuruxolitinib, DFT, Dipole moment, Thermodynamic parameters

References:

[1] In: LiverTox: Clinical and Research Information on Drug-Induced Liver Injury [Internet]. Bethesda (MD): National Institute of Diabetes and Digestive and Kidney Diseases; 2012.2024 Nov 7. PMID: **39556685** Bookshelf ID: NBK609110

[2] Brett A King[1], Brittany G Craiglow[2] PMID: **37591562** DOI: 10.1016/j.jaad.2023.05.049

[3] Brett King[1], Maryanne M Senna[2], Natasha A Mesinkovska[3], Charles Lynde[4], Matthew Zirwas[5], Catherine Maari[6], Vimal H Prajapati[7], Sheetal Sapra[8], Pawel Brzewski[9], Lawrence Osman[10], Sameh Hanna[11], Marni C Wiseman[12], Colleen Hamilton[13], James Cassella[13] PMID: **39053611** DOI: 10.1016/j.jaad.2024.06.097

[4] Jeremy Martinez[1][2], Cyriac Manjaly[3], Priya Manjaly[2][4], Sophia Ly[2][5], Guohai Zhou[2]

, John Barbieri [2], Arash Mostaghimi [2] PMID: **37851459** PMCID: PMC10585588 DOI: 10.1001/jamadermatol.2023.3830

Tandem synthesis of highly functionalized spiro-pyrimidines derivatives containing a sulfonyl group

Manijeh Nematpour*

**Department of Chemistry Education, Farhangian University, Tehran, Iran.*

**Email: m.nematpour@cfu.ac.ir*

Mild and efficient methods for the synthesis of pyrimidine-based spirocyclic systems have attracted widespread interest over the years due to their diverse biological activity. The standard protocol for the preparation of pyrimidine-based spirocyclic generally involves nucleophilic addition reactions and cycloaddition reactions.[1, 2] Sulfones are widely used as a key intermediate in the synthesis of organic compounds in many fields, including, polymers, pharmaceuticals, the rubber industry, and agrochemicals.[3] However, although these compounds are of considerable synthetic interest,[4] very few protocols are available for the synthesis of spiro-pyrimidines containing additional sulfonyl groups.

As part of our current studies on the development of new routes to heterocyclic systems,[5-8] we report a novel efficient protocol for the synthesis of sulfonyl-spiro-pyrimidines by a one-pot five component reaction of sodium aryl sulfonate, malononitrile, isatin, trichloroacetonitrile, and various benzylamines in DMF. Compared with conventional methods, this method has considerable advantages such as mild conditions, easier work-up, available starting materials, and purer products with high yields (Scheme 1).

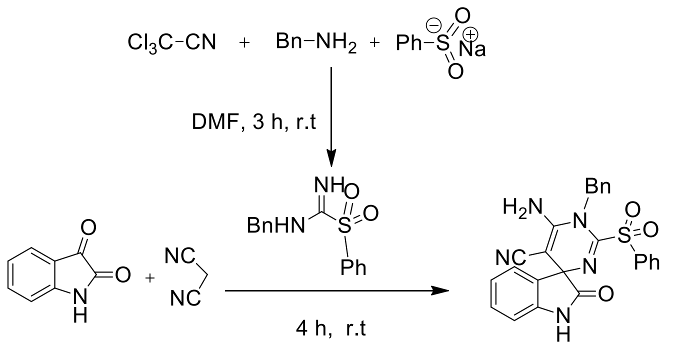

Scheme 1. Synthesis of sulfonyl-spiro-pyrimidines derivatives.

References

١. Field, G. F. *Chem. Commun*. **1969**, 886.
٢. Singh, G. S.; Desta, Z. Y. *Chem. Rev*. **2012**, *112*, 6104.
٣. Prilezhaeva, E. N. *Russ. Chem. Rev*. **2000**, *69*, 367.
٤. Sakya, S. M.; Hou, X. J.; Minich, M. L.; Rast, B.; Shavya, A. M.; De Mello, L.; Cheng, H. Li, J.; Jaynes, B. H.; Mann, D. W.; Petras, C. F.; Seibel, S. B.; Haven, M. L. *Bioorg. Med. Chem. Lett*. **2007**, *17*, 1067.
٥. Yavari, I.; Nematpour, M.; Damghani, T. *Mol. Divers*. **2013**, *17*, 801.
٦. Yavari, I.; Nematpour, M. *Mol. Divers.* **2012**, *16*, 651.
٧. Yavari, I.; Nematpour, M. *Synlett* **2013**, *24*, 165.
٨. Yavari, I.; Nematpour, M.; Sodagar, E. *Synlett* **2013**, *24*, 161.

The 30th Iranian Seminar of Organic Chemistry
February 7-9, 2025, Iran University of Science and Technology, Tehran, Iran

Intramolecular *N*-arylation of hydrazonoyl chlorides *and 2-iodoaniline via* copper-catalyzed

Manijeh Nematpour[1*], Reihane Nouri[2]

*[*1,2] Department of Chemistry Education, Farhangian University, Tehran, Iran.*
E-mail address: M.nematpour@cfu.ac.ir

Benzotriazines are six-membered heterocyclic compounds containing three nitrogen atoms connected to a benzene ring. Among the two existing isomers (1,2,4-benzotriazine and 1,2,3-benzotriazine), the first one has received more attention and extensive research has been conducted on it.[1-4]

The one-pot Cu-catalyzed intramolecular cross-coupling[5-8] reactions of *2-iodoaniline* and hydrazonoyl chlorides for synthesizing benzo [1,2,4] triazine as shown in scheme 1. The advantages of this protocol, such as milder conditions, easier work-up (no column chromatography), availability of starting materials, good efficiency (72-92%), and the absence of the need for ligands, make this approach attractive for the synthesis of these compounds. The ability to achieve good yields of pure products without the need for additional purification steps or reagents is a significant advantage of this synthesis method. Not having to perform additional purification steps not only saves time but also reduces the consumption of resources, making the overall process more efficient and environmentally friendly. This further highlights the practicality and effectiveness of the described protocol.

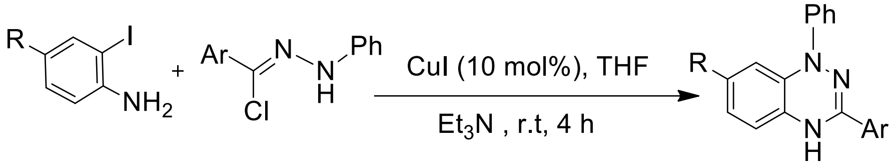

Scheme 1. Synthesis of various benzo [1,2,4] triazine by Cu-catalyzed

References

1. Mohammadi Ziarani, G.; Mostofi, M.; Gholamzadeh, P.; Mohammadi-Khanaposhtani, M.; Yavari, H. *Arkivoc* **2019**, *2019*, 41.

2. Shi, W.; Qiang, H.; Huang, D.; Bi, X.; Huang, W.; Qian, H. *Eur. J. Med. Chem*. **2018**, *158*, 814.

3. Qi, W.; Yadav, P.; Hong, C. R.; Stevenson, R. J.; Hay, M. P.; Anderson, R. F. *Molecules* **2022**, *27*, 812.

4. Bodzioch, A.; Pomikło, D.; Celeda, M.; Pietrzak, A.; Kaszyński, P. *J. Org. Chem.* **2019**, *84*, 6377.

5. Yavari, I.; Nematpour, M.; Damghani, T. *Tetrahedron Lett*. **2014**, *55*, 1323.

6. Yavari, I.; Nematpour, M. *Helv. Chim. Acta*. **2014**, *97*, 1132.

7. Yavari, I.; Nematpour, M. *Mol. Divers*. **2015**, *19*, 703.

8. Nematpour, M.; Abedi, E.; Abedi, E. *Lett. Org. Chem*. **2018**, *15*, 678.

A new route for the synthesis of functionalized sulfonyl-yn-imines *via* copper-catalyzed

Manijeh Nematpour*

Department of Chemistry Education, Farhangian University, Tehran, Iran.

**Email: m.nematpour@cfu.ac.ir*

Keyword: Sulfonyl-yn-imine, Copper-catalyzed, Trichloroacetonitrile, Sodium arylsulfinates

Introduction: Alkynyl imines represent an important class of functionalized alkynes because of their applications in the synthesis of a broad range of biologically important compounds. Alkynyl imines are versatile intermediates, which are used to synthesize different kinds of heterocycles, such as pyrroles, quinolines, pyridines, and others.[1-3] Furthermore, they can also react with conjugated dienes to give bicyclic compounds.[4] Despite their synthetic importance, relatively few methods have been described for the synthesis of alkynyl imines.

Method: Herein, we report a simple procedure for the synthesis of functionalized sulfonyl-yn-imines *via* the Cu catalyzed three-component coupling reaction of trichloroacetonitrile,[5-7] sodium arylsulfinates, and terminal alkynes (Scheme 1).

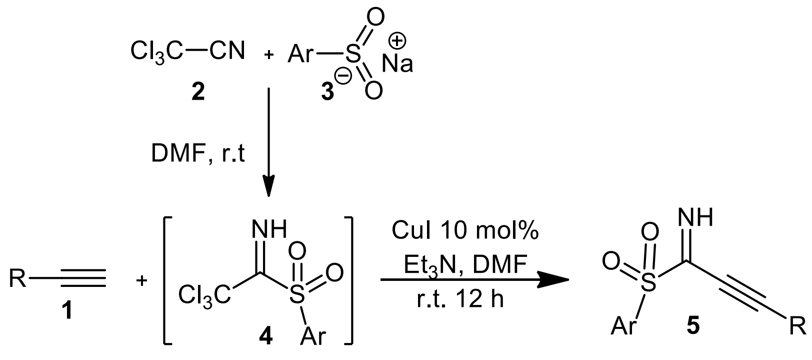

1,3,5	R	Ar	Yield (%) of **5**
a	Ph	Ph	80
b	Ph	*p*-toly	77
c	*n*-Pr	Ph	67
d	*n*-Pr	*p*-toly	61
e	*n*-Bu	Ph	65
f	*n*-Bu	*p*-toly	62

Scheme 1. Synthesis of sulfonyl-yn-imines derivatives.

Results and Discussion: Structures of compounds **5a-f** were assigned by IR, ^{1}H-NMR, ^{13}C-NMR and mass spectral data. The ^{1}H-NMR spectrum of **5a** exhibited 1 *s* for NH (*δ* 5.55), along with characteristic multiplets for the phenyl H-atoms. The ^{13}C-NMR spectrum of **5a** exhibited 11 signals in agreement with the proposed structure. The mass spectrum of **5a** displayed the molecular ion peak at *m*/*z* = 269. The NMR spectra of compounds **5b-f** are similar to those of **5a**, except for the substituents, which showed characteristic signals in the appropriate regions of the spectra.

In conclusion, we have demonstrated that CuI is able to catalyze the formation of functionalized sulfonyl-yn-imines through coupling reaction of trichloroacetonitrile, sodium arylsulfinates, and terminal alkynes. The potential diversity of this type of reaction and available starting materials and catalysts are the main advantages of this methodology.

References

١. Sromek, A. W.; Rheingold, A. L.; Wink, D. J.; Gevorgyan, V. *Synlett* **2006**, *14*, 2325.
٢. Kel'in, A. V.; Sromek, A. W.; Gevorgyan, V. *J. Am. Chem. Soc*. **2001**, *13*, 2074.
٣. Friebolin, W.; Eberbach, W. *Helv. Chim. Acta.* **2001**, *84*, 3822.
٤. Lihar, P. R.; Subhas, M. S.; Roy, S.; Kantam, M. L. *Org. Biomol. Chem.* **2009**, *7*, 85.
٥. Yavari, I.; Nematpour, M.; Damghani, T. *Mol. Divers*. **2013**, *17*, 801.
٦. Yavari, I.; Nematpour, M. *Mol. Divers.* **2012**, *16*, 651.
٧. Yavari, I.; Nematpour, M. *Synlett* **2013**, *24*, 165.

The 30th Iranian Seminar of Organic Chemistry
February 7-9, 2025, Iran University of Science and Technology, Tehran, Iran

One-Step Conversion of Electron-Deficient Aldehydes into the Corresponding Esters in Aqueous Alcohols in the Presence of Potassium cyanid

Mozhgan Entezari,[a] Afshin Sarvary,[a,]* Negin Dehghan,[a] and Mohammad Taghi Nazeri[b]

[a] *Department of Chemistry, Faculty of Science, Babol Noshirvani University of Technology, Shariati Ave., Babol, Iran, Post Code: 47148-71167 (E-mail address: a.sarvary@nit.ac.ir)*
[b] *Department of Organic Chemistry, Shahid Beheshti University, Daneshjou Boulevard, Tehran, 1983969411, Iran*

Keyword: Esterification, Electron-deficient aldehydes, Potassium cyanid, Nucleophilic addition

Ester plays a key role as an intermediate in various chemical, pharmaceutical, and organic synthesis processes. Acids or acid derivatives are synthesized through the oxidation of aldehydes or alcohols, followed by esterification reactions to obtain esters. However, the traditional process is intricate and demands high energy consumption. To address these concerns, the one-step oxidative esterification of aldehydes and alcohols into esters has emerged as a simple, co-friendly and efficient green synthesis method, opening new avenues for cost-effective ester production. Notably, catalysts play crucial role in assisting this reaction [1-2].

The direct conversion of aldehydes into their corresponding esters in the presence of Potassium cyanid in aqueous alcohols is reported (Scheme). In all these reactions, alcohol serves as reactant and also as reaction medium. Almost quantitative yields were obtained with aldehydes containing electron-withdrawing substituents and heterocyclic aldehydes.

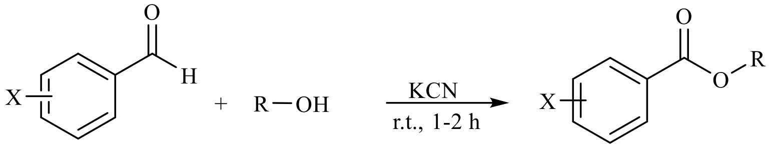

X= NO_2, CO_2R, CN, Br

Scheme: Oxidative esterification of aldehydes promoted by KCN

References:

[1] Y. Zheng, C. Huang, Y. Li, Y. Yang, R. Xu, *Chem. Cat. Chem.* **2024**, *16*, e202300976.

[2] Z. Khan, F. Javed, Z. Shamair, A. Hafeez, T. Fazal, A. Aslam,W. B. Zimmerman, F. Rehman, *J. Ind. Eng. Chem.* **2021**, 103, 80-101.

The 30th Iranian Seminar of Organic Chemistry
February 7-9, 2025, Iran University of Science and Technology, Tehran, Iran

Distinguishing intramolecular from intermolecular hydrogen bonding with ^{1}H NMR

Seyedmohammad Hosseininezhad, Hossein Kaleji, Afshin Sarvary*

Department of Chemistry, Faculty of Science, Babol Noshirvani University of Technology, Shariati Ave., Babol, Iran, Post Code: 47148-71167 (E-mail address: a.sarvary@nit.ac.ir)

Keyword: Hydrogen bonding, Intramolecular, Intermolecular, H NMR

Intermolecular hydrogen bonds are responsible for connecting one molecule with other and keeping them bound together. In opposite to that, when intramolecular hydrogen bonding occur, molecules are less available for interacting with each other and the molecules have a less tendency to stick together. The difference in interaction leads to differences in properties such as stability, solubility, melting point, and also biological properties. Therefore, identifying the type of hydrogen bond in a molecule is important in studying of its physical, chemical, and biological properties.

In this paper, experimental methods for identifying intramolecular from intermolecular hydrogen bonds by using of ^{1}H NMR spectroscopy are presented. The methods include investigating the effect of changes in temperature, solvent, and concentration on chemical shifts of hydrogen involved in hydrogen bond. For example, changes in concentration have no effect on the chemical shift of hydrogen involved in intramolecular hydrogen bonds (benzylidene aminophenol, **A** in the Scheme). While the chemical shift of hydrogen involved in intermolecular hydrogen bonding (phenol, **B** in the Scheme) shifts to a lower field with increasing concentration.

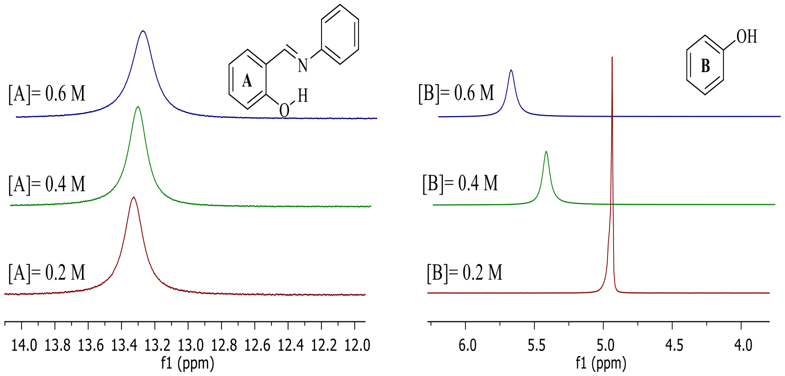

Scheme: Concentration effect on the chemical shifts

References:

[1] S. Scheiner, *Molecules* **2016**, 21, 1426, 1-17.

[2] J. R. Lane, S. D. Schroder, G. C. Saunders, H. G. Kjaergaard, *J. Phys. Chem. A* **2016**, 120, 6371−6378.

The 30th Iranian Seminar of Organic Chemistry
February 7-9, 2025, Iran University of Science and Technology, Tehran, Iran

Catalytic synthesis of nicotinonitriles with zirconium-based MOFs *via* a cooperative vinylogous anomeric based oxidation

Kosar Afsari cheleh, Hossein Ahmadi, Mohammad Ali Zolfigol* and Maryam Hajjami*

Department of Organic Chemistry, Faculty of Chemistry and Petroleum Sciences, Bu-Ali Sina University, Postal code 6517838683, Hamedan, Iran. E-mail: mzolfigol@yahoo.com (M. A. Zolfigol) & mhajjami@yahoo.com (Maryam Hajjami)

Keyword: Anomeric based oxidation, Catalysis, Nicotinonitriles, Zirconium-based MOFs.

Metal-organic frameworks (MOFs) are highly ordered, porous structures that result from the bonding of metal ions with suitable organic ligands. These materials are important for their large surface area, customizable pore sizes, designable and robust chemical stability, making them highly suitable for a variety of applications, including catalysis, molecular adsorption, sensing, and drug delivery. Zirconium-based MOFs (Zr-MOFs) are interesting catalysts due to their exceptional resilience and particularly under extreme conditions. These materials are not only promising for environmental applications such as the removal of pollutants and separation of greenhouse gases, but they also show great potential in the other fields such as biomedicine and materials science. Nicotinonitrile derivatives, which consist of a nitrile (-CN) functional group attached to a pyridine ring, have attracted significant interest due to their broad spectrum of biological activities, such as antibacterial, antifungal, anti-inflammatory, and anticancer effects. Furthermore, they have shown efficacy in treating neurological conditions, including Alzheimer's disease. Herein, we have designed a Zr-MOFs as a valuable catalyst for the preparing Nicotinonitriles. The presented methodology provides an optimized medium that enhances the rate and yield of reactions, while minimizing unwanted byproducts (**Scheme**).

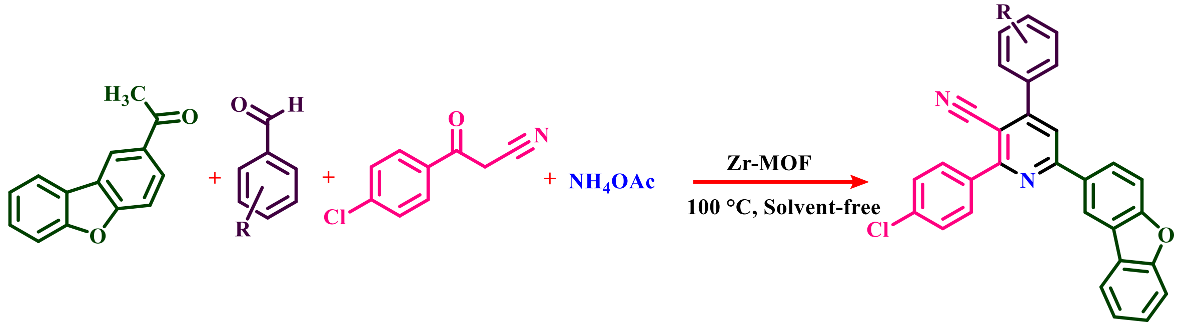

Scheme: Synthesis of nicotinonitrile derivatives catalyzed by Zr-MOFs

References:

١. Navazeni, M., Zolfigol, M. A., Ahmadi, H., Sepehrmansourie, H., Khazaei, A., & Hosseinifard, M. (2024). Design, synthesis and application of a magnetic H-bond catalyst in the preparation of new nicotinonitriles via cooperative vinylogous anomeric-based oxidation. RSC advances, ١٤(٢٣), ١٦٦٠٧-١٦٦١٦.

٢. Bai, Y., Dou, Y., Xie, L. H., Rutledge, W., Li, J. R., & Zhou, H. C. (2016). Zr-based metal–organic frameworks: design, synthesis, structure, and applications. Chemical Society Reviews, ٤٥(٨), ٢٣٢٧-٢٣٦٧.

The 30th Iranian Seminar of Organic Chemistry
February 7-9, 2025, Iran University of Science and Technology, Tehran, Iran

Dispirotripiperazine core anion exchange

Mahya Seydi Sarjobi and Nader Noroozi Pesyan *

Department of Organic Chemistry, Faculty of Chemistry, Urmia University, 57159, Urmia, Iran

Abstract

Herein, a convenient route for the exchanging various anions instead of bromide ions were developed. Two bromide ions of compound 3,12-dicyano-3,6,9,12-tetraazadispiro[5.2.5^9.2^6]hexadecane-6,9-diium dibromide as a starting compound was exchanged with various anions specially with chloride ions. All products' structures were characterized and confirmed by elemental analysis, FT IR, ^{1}H NMR, ^{13}C NMR and Mass spectroscopy techniques.

Keyword: DSTP; Anion exchange; Ion exchange resin

Introduction

Dispirotripiperazines is the class of dispiro compounds, that dispiro system is three six-membered cycles of piperazines or "6-6-6".[1] A unique feature of dispirotripiperazines is the presence of two quaternaries positively charged nitrogen atoms in the structure, which are possibly responsible for electrostatic interactions with negatively charged HSGAGs. Initially, dispirotripiperazines were investigated as antitumor drugs [2]; however, it was found that these compounds also have good antiviral activity.[3] Previously, we have reported an efficient method for the synthesis of dispiritripiperazine core through one-pot reaction of 1,4-diazabicyclo[2.2.2]octane (DABCO) with cyanogen bromide.[4] Sole compound 3,12-dicyano-3,6,9,12-tetraazadispiro[5.2.5^9.2^6]hexadecane-6,9-diium dibromide (**1**) was obtaind with two bromide counter ions. Therefore, in this research, we encouraged to focus our aim on ion exchanging of bromide ions with chloride and other anions.

Results and discussion

This article describes the various ion exchanging on the compound **1** instead of bromide ions (Scheme 1). More recently, we have reported the synthesis of compound **1** in the one-pot reaction of DABCO and BrCN in high yield.[4] Initially, representatively, we performed dropwised silver nitrate ($AgNO_3$) solution into the solution of **1** and the silver bromide (AgBr) precipitated and the solution of 3,12-dicyano-3,6,9,12-tetraazadispiro[5.2.5^9.2^6]hexadecane-6,9-diium dinitrate (**2c**) was obtained.

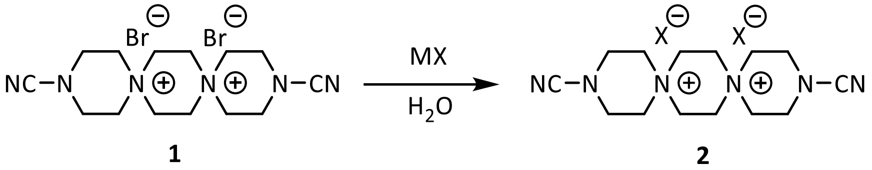

MX: NaCl (**a**), KCl (**b**), $AgNO_3$ (**c**), NaOAc (**d**)

Experimental

In a 50 mL Beacker dissolved 1 mmol DSTP (**1**) in 4 mL distilled water then added dropwise the solution of $AgNO_3$ to precipitate pale yellow AgBr, then filtered off. The mother liquid evaporated and white solid (**2c**) was remained.

References

(1) Egorova, A.; Bogner, E.; Novoselova, E.; Zorn, K. M.; Ekins, S.; Makarov, V. Dispirotripiperazine-core compounds, their biological activity with a focus on broad antiviral property, and perspectives in drug design (mini-review). *Eur. J. Med. Chem.* **2021**, *211*(5), 113014.

(2) Safanova, T. S.; Chernov, V.; Minakova, S.; Dorokhova, M. I.; Levkovskaya, L. G.; Traven, N. I.; Andreayanova, T. A.; Serochkina, L. A.; Mamaeva, I. E. New antitumor agent—spirobromine. *Khim. Farm. Zh.* **1983**, *5*, 626-629.

(3) Schmidtke, M.; Riabova, O.; Dahse, H. M.; Stelzner, A.; Makarov, V. Synthesis, cytotoxicity and antiviral activity of *N*,*N'*-bis-5-nitropyrimidyl derivatives of dispirotripiperazine. *Antivir. Res.* **2002**, *55*, 117-127.

(4) Golmohammadi, M.; Noroozi Pesyan, N.; Şahin, E. A promising direction for the synthesis of dispirotripiperazine (6-6-6 DSTP) core. *Synthesis*, **2024**, *56*, 2742-2746.

Use the outputs of the PV panels mounted on the vehicle under real driving conditions and using different angles

Mohammadreza Mohammadiyan Asiabar

Master's degree, Electrical Engineering, Islamic Azad University, Karaj branch, Karaj, Iran, mohammadrezamohammadiyan28@yahoo.com

Keyword: Electric vehicles, Photovoltaic.

Body Text: Efforts are underway to reduce greenhouse gas emissions worldwide. In 2017, carbon dioxide (CO2) was the most prevalent greenhouse gas. It emitted a total of 1,188 million tons [1]. Of these carbon dioxide emissions, approximately 17.3% were from transportation, such as cars, trains, and domestic aviation. Electric vehicles (EVs) and fuel cell vehicles (FCVs) can help reduce carbon dioxide emissions from vehicles [2]. In this paper, we measured and estimated the outputs of vehicle-mounted PV panels under real driving conditions and different effective shading angles. Public infrastructure can lead to dynamic partial shading across the PV module at high speeds. In addition, effective shading angles close to the sun's elevation can also lead to static partial shading. To improve this three-dimensional radiation model, it is necessary to measure a PV module output, including the partial shading effect, under real driving conditions. In this paper, we measured the output of a vehicle-mounted PV panel under real driving conditions. In addition, the effective shading angle was evaluated and compared with the output performance of a vehicle-mounted PV panel. A typical corporate PV module with an insulating material is mounted on a horizontal car roof along with thermal flux sensors. Photovoltaic module specifications, Mono-Si, peak power 143 W, Peak power is 143 W, maximum power voltage is 16.08 V, maximum power current is 8.92 A, open circuit voltage is 19.73 V, short circuit current is 9.53 A. Fig. 1 shows the GHI as a reference, alongside the I_{roof} and Pm values throughout the experimental period, for (a) a sunny day and (b) an overcast day. The ratio of the integrated direct normal irradiance to the integrated global normal irradiance during the experimental period for the sunny and overcast days were 0.84 and 0.00, respectively. The electronic load measured Pm with MPPA, which was operated by sweeping for maximum power point from the open-circuit voltage to zero every 1 min. As a result, a low Pm was recorded, as shown in the circle in Fig. 1(a). On the sunny day, I_{roof} fluctuated under driving conditions, owing to shade from objects such as buildings and trees. Halation that exceeded the base irradiance was observed. Pm also fluctuated under driving conditions. On the overcast day, however, I_{roof} and Pm showed only gradual changes because of the absence of direct irradiance.

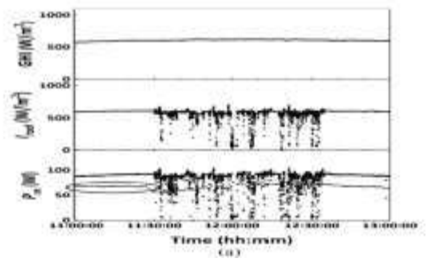

(a)

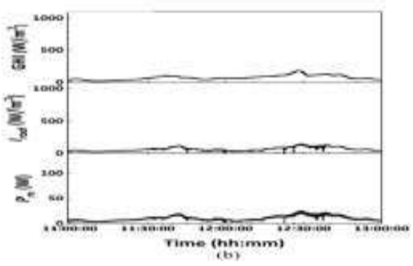

(b)

Fig. 3. global horizontal irradiance (as a reference), I_{roof}, and Pm throughout the experimental period for (a) a sunny day and (b) an overcast day.

References:

[1] “National greenhouse gas inventory report of Japan(2019),” Ministry of the Environment, Japan. Greenhouse Gas Inventory Office Japan (GIO), Center for Global Environmental Research(CGER), NIES.

[2] T. Masuda *et al.*, “Static concentrator photovoltaics for automotive applications,” *Sol. Energy*, vol. 146, pp. 523–531, 2017.

The 30th Iranian Seminar of Organic Chemistry
February 7-9, 2025, Iran University of Science and Technology, Tehran, Iran

Design, synthesis and application of [PVI-CO_2H] as a novel polymeric catalyst for the synthesis of new pyrido[2,3-d]pyrimidines

Mahrokh Farrokh,[a] Hassan Sepehrmansourie,[b] Mohammad Ali Zolfigol [a*]and Maryam Hajjami [a*]

[a] *Department of Organic Chemistry, Faculty of Chemistry and Petroleum Sciences, Bu-Ali Sina University, Hamedan 6517838683, Tel: +988138282807, Fax: +988138380709 Iran.*

[b] *Faculty of Converging Science and Technologies, University of Qom, Qom, Iran, 37185-359.*

Keyword: Heterogeneous catalysts, Polymeric ionic liquids, Pyrido[2,3-d]pyrimidines.

Todays, heterogeneous catalysts are represented a research field for academic and industrial processes, because the reaction takes place on the surface or inside the catalyst, and the advantage of these catalysts over homogeneous catalysts is that they are easily separated at the end of the reaction as well as are more environmentally friendly. Polymers and biopolymers are among the materials that have received much attention in the field of research. Applications of polymers include catalysis, biotechnology, materials science, analytical chemistry, desulfurization of fuels, and energy and environmental applications. An important class of polymers are polymeric ionic liquids, which play a good catalytic role and can be considered as heterogeneous catalysts. Among the cationic and anionic polymeric ionic liquids (PILs), we can mention imidazolium, pyrrolidinium and tetrafluoroborates, hexafluorophosphates.[1] Polymeric ionic liquids (PILs) can be very effective as catalysts due to their nanoporous structure, high surface area and thermal stability [2-3]. In this regard, the aim is to create a new polymeric catalyst based on imidazole. The designed catalyst was used in the synthesis of new pyrido[2,3-d]pyrimidines that have biological components. The structure of the synthesized compounds contains triazole and pyrimidine moieties, whose importance in pharmaceutical compounds has been proven (Scheme 1).

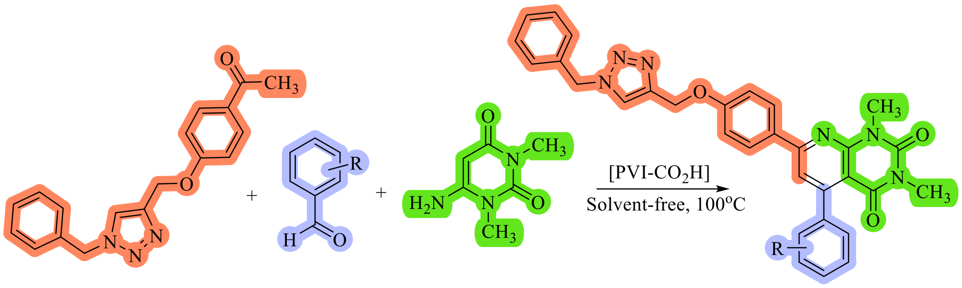

Scheme 1: Synthesis of new pyrido[2,3-d]pyrimidines using [PVI-CO2H] as a novel polymeric catalyst.

References

(1) Kitazawa, Y.; Ueno, K.; Watanabe, M. *The Chemical Record* **2018**, *18*, 391- 409.

(2) Saikia, S.; Gogoi, P.; Dutta, A. K.; Sarma, P.; Borah, R. *Journal of Molecular Catalysis A: Chemical* **2016**, *416*, 63-72.

(3) Soliman, E. A.; Panda, S. S.; Aziz, M. N.; Shalaby, E. M.; Mishriky, N.; Asaad, F. M.; Girgis, A. S. *European Journal of Medicinal Chemistry* **2017**, *138*, 920-931.

The 30th Iranian Seminar of Organic Chemistry
February 7-9, 2025, Iran University of Science and Technology, Tehran, Iran

Preparation of two-component rigid polyurethane foam for packaging applications: investigation of morphological and mechanical properties

Omid Jawhid*[a], Roya Sedghi[b]

[a] *Department of Research and Development, Kara Polymer Arvin Co., P.O. Box 945179-4857 Science and Technology Park of North Khorasan, North Khorasan, Iran*
[b] *Department of Polymer and Materials Chemistry, Faculty of Chemistry and Petroleum Sciences, Shahid Beheshti University, Tehran, Iran*
**E-mail:* O_jawhid@sbu.ac.ir

Rigid polyurethane foams (RPUFs) are highly versatile materials widely employed in packaging applications due to their lightweight, excellent mechanical properties, and superior thermal insulation.[1,2]

This study investigates the development and optimization of RPUFs using a formulation comprising polyether polyol as the primary polyol, an amine-based catalyst to accelerate the reaction kinetics, and propylene glycol as a chain extender to enhance foam rigidity. Water was employed as an eco-friendly chemical blowing agent, promoting the formation of a cellular structure while minimizing environmental impact. A surfactant was included to stabilize the foam during the expansion phase, ensuring uniform cell size and distribution (Scheme 1).

The resulting RPUFs demonstrated a closed-cell structure with consistent density and high compressive strength, which are critical for effective cushioning and shock absorption in packaging applications. Furthermore, the formulation was tailored to achieve a balance between processability, mechanical properties, and sustainability. This research provides a comprehensive framework for producing RPUFs tailored for packaging, contributing to the development of eco-efficient materials in line with industry demands for performance and environmental compliance.

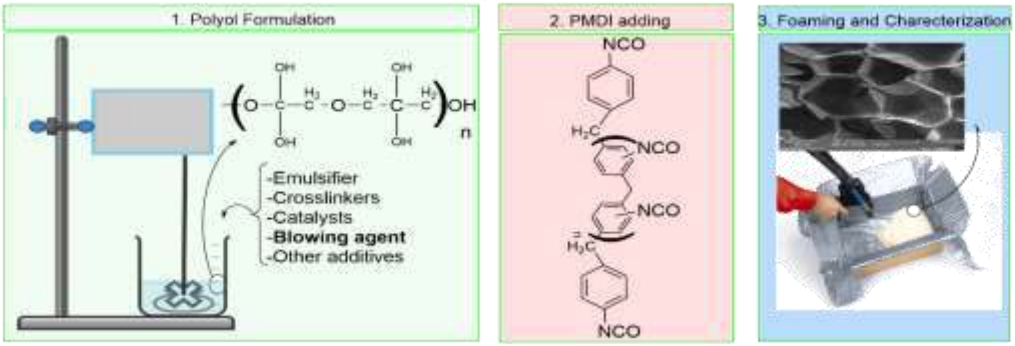

Scheme 1. Polyol formulation, mixing with B component and spraying for RPUF production .

References

(1) Ivdre, A.; Abolins, A.; Volkovs, N.; Vevere, L.; Paze, A.; Makars, R.; Godina, D.; Rizikovs, J.; *Polymers* **2023**, 15, 3124.

(2) Saint, M. F.; Chazeau, L.; Cavaillé, J. Y.; Chabert, E.; *Composites Science and Technology* 2006, 66, 2700-2708.

The 30th Iranian Seminar of Organic Chemistry
February 7-9, 2025, Iran University of Science and Technology, Tehran, Iran

Synthesis of Closed-cell rigid polyurethane foam: investigation of insulating properties

Omid Jawhid*[a], Roya Sedghi[b]

[a] *Department of Research and Development, Kara Polymer Arvin Co., P.O. Box 945179-4857 Science and Technology Park of North Khorasan, North Khorasan, Iran*
[b] *Department of Polymer and Materials Chemistry, Faculty of Chemistry and Petroleum Sciences, Shahid Beheshti University, Tehran, Iran*
**E-mail: O_jawhid@sbu.ac.ir*

Rigid polyurethane foam is a versatile, lightweight material known for its excellent thermal insulation and structural properties.[١] It is widely used in refrigerator insulation to enhance energy efficiency by minimizing heat transfer.[٢] Its low thermal conductivity and adaptability to various shapes make it ideal for modern refrigeration systems.[٣]

This study investigates the insulating properties of closed-cell three-component rigid polyurethane foam (RPUF), focusing on the effects of different components on thermal and mechanical performance. The three-component system includes a blend of polyols, isocyanates, and a specially selected blowing agent to optimize the foam's structure and insulation capabilities (scheme 1). The foam's closed-cell morphology, characterized by a uniform and highly stable structure, contributes to its enhanced thermal insulation performance. The impact of varying the polyol and isocyanate ratios, as well as the type and concentration of the blowing agent, on the foam's density, thermal conductivity, and mechanical properties is systematically explored. Results show that the optimized foam formulation exhibits low thermal conductivity (~0.022 W/m·K) and high compressive strength, making it suitable for high-performance insulation applications. Additionally, the study highlights the influence of the foam's microstructure on its mechanical resilience, with improved durability under varying environmental conditions.

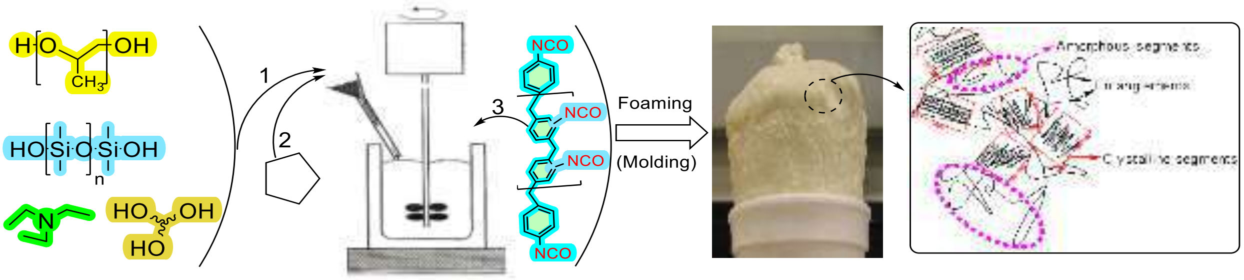

Scheme 1. Schematic of insulating three-component RPUF synthesis and morphological structure of the final product.

References

(1) O. Bello, K.; Yan, N.; *Polymers* **2024**, 16, 2119.
(2) S. Lim, J.; Bejan A.; *Heat Transfer Engineering* 1994, 15, 35-41.
(3) V. Soloveva, O.; A. Solovev, S.; V. Vankov, Yuri.; Z. Shakurova, R.; *Processes* **2022**, *10*(11), 2257.

The 30th Iranian Seminar of Organic Chemistry
February 7-9, 2025, Iran University of Science and Technology, Tehran, Iran

Synthesis of Fe_3O_4@SiO_2@NH_2/TCT-EDA nanocomposite as a reusable catalyst for the preparation of polyhydroquinoline derivatives

Maryam Manafi Moghadam[a*], Ali Ramazani[a,b], Ali Morsali[c] and Sobhan Rezayati[a]

a) *The Organic Chemistry Research Laboratory (OCRL), Department of Chemistry, Faculty of Science, University of Zanjan, Zanjan 45371-38791, Iran*
b) *The Convergent Sciences & Technologies Laboratory (CSTL), Research Institute of Modern Biological Techniques (RIMBT), University of Zanjan, Zanjan 45371-38791, Iran*
c) *Department of Chemistry, Faculty of Sciences, Tarbiat Modares University, P.O. Box 14117-13116, Tehran 14117-13116, Islamic Republic of Iran*

Keyword: Heterogeneous catalyst, Magnetic nanoparticles, Fe_3O_4@SiO_2@NH_2/TCT-EDA

The design, synthesis and development of nanoparticles (NPs) have emerged as an interesting and promising strategy. Among various types of NPs, magnetic nanoparticles e.g. Fe_3O_4 have emerged as powerful tools for the various applications in technology and industry such as drug delivery, treatment of cancer, catalysis, medical therapeutics, magnetic data storage, diagnostics, MRI, and environmental remediation [1]. In this research, we successfully designed and synthesized a new a green and ecofriendly magnetic nanocatalyst through the ethylene diamine immobilized to the core-shell Fe_3O_4 nanomagnetic particles. A variety of analyses such as fourier-transform infrared spectroscopy, energy-dispersive X-ray spectroscopy, scanning electron microscopy, transmission electron microscopy, vibrating sample magnetometry, thermal gravimetric analysis, X-ray diffraction and Brunauer-Emmet-Teller were used to characterize the as-synthesized nanocatalysts. The activity of this as-synthesized nanocatalysts can be successfully used in the grinding synthesis of various aldehydes, malononitrile and dimedone under solvent- and metal-free conditions at room temperature to give polyhydroquinoline derivatives within high purity and excellent yields. Easy fabrication of Fe_3O_4@SiO_2@NH_2/TCT-EDA, waste reduction, effective for large scale synthesis, simple work-up procedure, adherence to the basics of green chemistry, high catalytic efficiency in very small amounts (0.05 g), environmentally friendly and based on natural ingredients are the great advantages of the current method (Scheme 1).

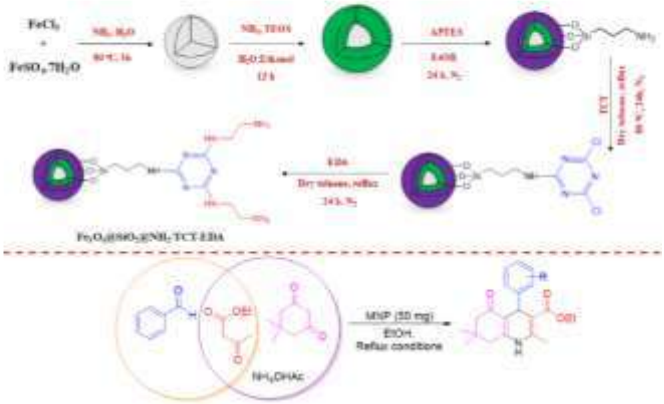

Scheme 1: Synthesis of $Fe_3O_4@SiO_2@NH_2$/TCT-EDA and the one-pot synthesis of polyhydroquinoline derivatives

References:

[1] Rezayati, S., Moghadam, M. M., Naserifar, Z., & Ramazani, A. (2024). Schiff base complex of copper immobilized on core-shell magnetic nanoparticles catalyzed one-pot syntheses of Polyhydroquinoline derivatives under mild conditions supported by a DFT study. Inorganic Chemistry, 63(3), 1652-1673.

The 30th Iranian Seminar of Organic Chemistry
February 7-9, 2025, Iran University of Science and Technology, Tehran, Iran

Design and development of a smart ELISA kit for foot-and-mouth disease (specific for serotype O) based on synthetic immunogenic peptides

Fatemeh Tahoori[a*] (representing author), Mohammad Mehdi Ranjbar[b], Rasool Madani[c], Saeideh Ebrahimi[d]

[a] Department of Human Bacterial Vaccines Production and Research, Razi Vaccine and Serum Research Institute, Agriculture Research, Education and Extension Organization (AREEO), Karaj, Iran
[b] Department of Foot and Mouth Disease Reference Laboratory, Razi Vaccine and Serum Research Institute, Agriculture Research, Education and Extension Organization (AREEO), Karaj, Iran
[c] Department of R&D, Kit and Anti-Body Laboratory, Razi Vaccine and Serum Research Institute, Agriculture Research, Education and Extension Organization (AREEO), Karaj, Iran

[d] *Central branch*, Razi Vaccine and Serum Research Institute, Agriculture Research, Education and Extension Organization (AREEO), Arak, Iran

Keyword: foot-and-mouth disease virus, Peptide, Antibody

Introduction: Foot-and-mouth disease (FMD) is a contagious viral disease which is sometimes fatal. This viral infection is a plague for the livestock industry. The control of the disease depends on vaccination, intensive care of animal transportation, quarantine of infected animals, create regulations on the trade of animals, and sometimes the destruction of infected livestock. Peptides are one of the smart and innovative ways in these areas to detect foot-and-mouth disease virus and focus the immune system's response against specific targets, and on the other hand, to specifically distinguish between types O, A, and ASIA foot-and-mouth disease. Serological methods detect the presence of viral antigens or antibodies in serum or other body fluid samples. Initial foot-and-mouth disease kits are based on polyclonal antibodies against foot-and-mouth disease serotypes and the double-antibody sandwich ELISA (DASELISA) preparation. Currently, various foot-and-mouth disease kits, such as Capture antigen ELISA and Competitive solid phase-ELISA, are commercially available and are available as direct imports to laboratories and research and production centers. These peptides also reduce the costs of kit manufacturing and significantly reduce the time for antigen preparation and subsequent development of the diagnostic method.

Method: After the bioinformatics design stage of foot-and-mouth disease type O-specific immunogenic peptides with neutralizing properties, peptide sequences were synthesized according to the solid-phase peptide synthesis (SPPS) strategy and following the Fmoc protocol on a 2-chlorotrityl chloride resin substrate. At each coupling stage, the amino acid addition was checked with the Kaiser test. After completing the synthesis with the side-chain protections, the sequence was cleaved from the resin using a 1% solution of trifluoroacetic acid. For the removal of side-chain protections, the K reagent was utilized. Specifically, the solid powder obtained from the previous step was introduced into a flask containing the K reagent mixture (20 mL trifluoroacetic acid, 2 mL water, and 0.3 mL triisopropyl silane). The mixture was stirred for 2.5 hours, after which the solvent was evaporated under vacuum until the solution's volume was reduced to 2 mL. Diethyl ether was gradually added to the residual contents. The resulting precipitate was then filtered off and dried.

Using it, we developed a smart indirect ELISA kit at a much more affordable cost than common kits based on complete antigen and antibody. In the next step, these antibodies were purified and then functionally evaluated by ELISA against a peptide derived from foot-and-mouth disease virus as well as intact foot-and-mouth disease serotype O virus.

Results and Discussion: Indirect ELISA tests showed that the peptide was successfully able to bind to antibodies against the virus (average OD ~1.7) and, on the other hand, this peptide did not react with standard sera specific to other types (A and ASIA) (OD lower than Cut-off: 0.3). Also, antibodies produced against the peptide in laboratory animals have neutralizing properties against the virus in the VNT test and have been developed for the Sandwich ELISA kit for the specific search for type O virus in diseased samples of infected animals.

References:

1. Tahoori, F.; Ranjbar, MM., Madani, R., Azimi, SM., Golchinfar, F., Ghanizadeh, A. Investigating the Efficiency of Immunogenicity of Specific Peptides Produced Against FMD Virus.J Vet Res, Volume 79, Number 3, 2024, 167-179.

2. Abd Hatem A, Ahmed Abdul Wahid Al Anbagi N, Al-Alo KZK, Sabah Bustani G. Detection of clinical and subclinical foot and mouth disease virus in cattle in Al-Najaf Province. Arch Razi Inst. 2022;77(3):1185-1189.

3. Wong CL, Yong CY, Ong HK, Ho KL, Tan WS. Advances in the diagnosis of foot-and-mouth disease. Front Vet Sci. 2020;7:477.

4. Ashir Zia1 M, Dobson SJ, Rowlands DJ, Stonehouse NJ, Salahuddin Shah M, Habib M. Development of an ELISA to distinguish between foot-and-mouth disease virus infected and vaccinated animals utilising the viral non-structural protein 3ABC. J Med Microbiol. 2022;71:001516.

5. Blanco, E.; Andreu, D; Sobrino, F. Advantages, challenges and future of peptide vaccines, (2017) pp: 317-331.

The 30th Iranian Seminar of Organic Chemistry
February 7-9, 2025, Iran University of Science and Technology, Tehran, Iran

Beta nucleating additive masterbatch for converting polypropylene random copolymer (PP-R) pipes to polypropylene random copolymer (PP-RCT) pipes

Farhad Moradian Nejad*[a],

Scientific Development Center, Isfahan Azad University, Khorasgan,

*E-mail: polymerazmon@gmail.com

Today, polymers play a significant role in people's daily lives. These materials are widely used in the home appliance, automotive, food, agricultural, and construction industries. One of the polymers used in the construction industry, especially the building plumbing industry, is polypropylene. Polypropylene is available in homopolymer, copolymer, and random copolymer types, which are used in the building plumbing industry. Due to their low thermal resistance, polypropylene random copolymer pipes cannot be used in the building plumbing industry and are only used in the hot and cold drinking water plumbing industry. Due to the advancement of polymer science, a type of polypropylene random copolymer called RCT, which is a type of crystalline random copolymer polymer, has recently been produced that can be used in the building plumbing industry and can be used in utility applications in addition to drinking water piping. This article attempts to discuss and study how to convert polypropylene random copolymer into crystalline polypropylene random copolymer using a beta nucleating additive masterbatch and its application in the building installation industry.

Keywords: polypropylene, masterbatch, random copolymer, crystalline random copolymer

References

[1] Maria C.E, Elena V.S, Alexis N, Simona M, Ivona P, Carmen O. R. Experimental and virtual studies in mechanical applications of PP-RCT pipes with armored materials; material plastic;2019

[2] P. JACOBY, B. H. BERSTED, W. J. KISSEL, and C: E. SMITH. Studies on the β-Crystalline form of Isotactic Polypropylene;1985

[3] *S.* C. TJONG, J. S. SHEN, and R. K. Y. LI. Mechanical Behavior of Injection Molded β-Crystalline Phase Polypropylene; Polymer engineering and sience;1996

[4] Hao Zheng & Fangxinyu Zeng & Zheng fang Chen & Jian Kang & Jinyao Chen & Ya Cao1 & Ming Xiang, Exploring the roles of molecular structure on the β-crystallization of polypropylene random copolymer;2017

[5] Dimitrios G. Papageorgiou, Dimitrios N. Bikiaris, Konstantinos Chrissafis. Effect of crystalline structure of polypropylene random copolymers on mechanical properties and thermal degradation kinetics; Elsevier B.V.;2012

The 30th Iranian Seminar of Organic Chemistry

February 7-9, 2025, Iran University of Science and Technology, Tehran, Iran

Fe_3O_4@Sio_2@Mel@DABCO as a novel catalyst for Knoevenagel Condensation

Behrooz Maleki*, pegah Ebrahimzadeh, Samaneh Sedigh Ashrafi

Department of Organic Chemistry, Faculty of Chemistry, University of Mazandaran, Babolsar, Iran

Corresponding Email: b.maleki@umz.ac.ir

Abstract

This study presents the development and application of a high-performance Fe_3O_4@SiO_2@Mel@DABCO catalyst for the Knoevenagel condensation reaction. The research focuses on the ongoing efforts to heterogenize homogeneous catalysts, which aim to leverage the advantages of both homogeneous and heterogeneous catalysis. A common strategy involves the attachment of catalysts to organic polymer or inorganic solids, facilitating their easy separation and recycling from reaction mixtures. However, these heterogenized catalysts often suffer from reduced reactivity and selectivity compared to their homogeneous counterparts. This work underscores the necessity for exploring innovative methods and strategies to enhance the performance of heterogenized catalysts in organic reactions. A new, highly efficient, and reusable nanocatalyst that incorporates DABCO charge was successfully created on a magnetic silica substrate. This catalyst was characterized using various analytical techniques including XRD, TGA, VSM, FE-SEM, EDX, and FT-IR. Designated as Fe_3O_4@SiO_2@Mel@DABCO, this recoverable catalyst is utilized for the synthesis of benzylidenemalononitrile derivates. Key advantages of this catalyst include the use of a green solvent, high product yields (ranging from 80 % to 98 %) achieved in a short time frame, optimal temperature conditions, straightforward recovery of the reaction medium, and its overall effectiveness.

Keywords: Knoevenagel condensation, Fe_3O_4@SiO_2@Mel@DABCO, Green chemistry

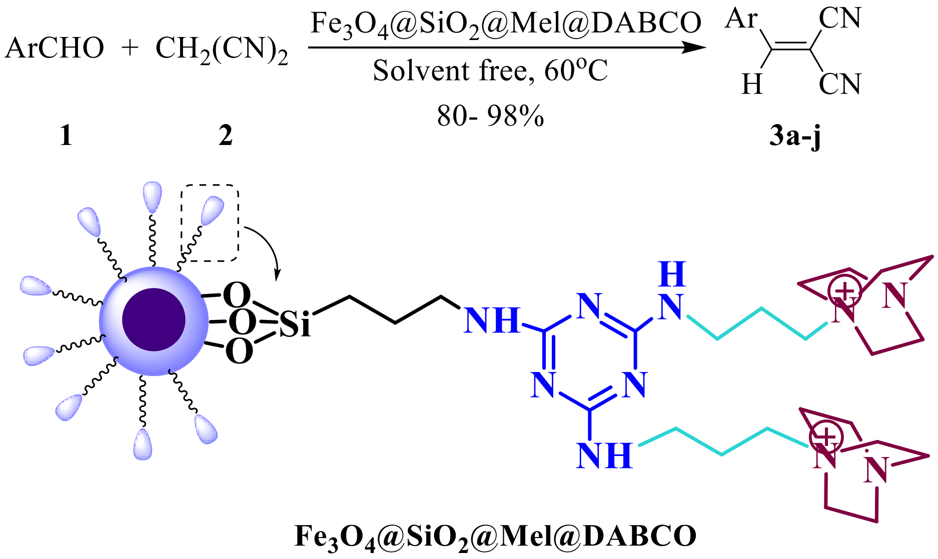

Scheme 1. Synthesis of benzylidene malononitrile derivates catalyzed by Fe_3O_4@SiO_2@Mel@DABCO.

Utilizing Metal Oxide Catalyst in the Sonogashira Reaction

Nastsarn Khajevand Jafari[a], Rahman Hosseinzadeh[a,*], Naser Safari[b]

[a]*Department of Organic Chemistry, Faculty of Chemistry, University of Mazandaran, Babolsar, Iran.*

[b]*Department of Chemistry, Shahid Beheshti University, Tehran, Iran*

Keyword: Metal oxide, Sonogashira reaction, Catalyst

Metal oxide catalysts have emerged as versatile and sustainable alternatives to traditional homogeneous catalysts in organic transformations [1]. These catalysts, including oxides of titanium, copper, zinc, iron, and cerium, offer unique properties such as tunable surface acidity/basicity, redox activity, and thermal stability, enabling efficient catalytic transformations. Perovskites are a specific type of metal oxide with a unique crystal structure, denoted as ABO_3. This structure allows perovskites to have high versatility in catalytic applications due to their ability to accommodate a variety of metal cations in both A and B positions, creating diverse catalytic properties. The Sonogashira reaction is a widely used method for forming carbon-carbon bonds between terminal alkynes and aryl or vinyl halides. Traditionally, the reaction employs palladium (Pd) as a catalyst and copper (Cu) as a co-catalyst [2]. Perovskites can be used as supports for noble metals in catalytic systems, enhancing the stability, dispersion, and activity of active metal species. In this study, Cu supported on perovskite has been explored as alternative catalyst to promote the Sonogashira reaction under milder conditions and in a more environmentally friendly manner (**Scheme**).

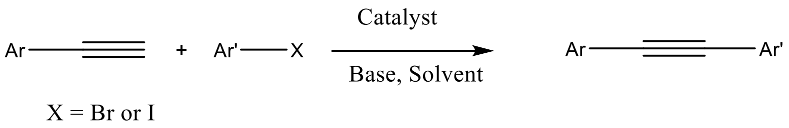

Scheme

References:

1. Sahoo, S., Wickramathilaka, K. Y., Njeri, E., Silva, D., & Suib, S. L. (2024). A review on transition metal oxides in catalysis. Frontiers in Chemistry, 12, 1374878.

2. Arundhathi, K. V., Vaishnavi, P., Aneeja, T., & Anilkumar, G. (2023). Copper-catalyzed Sonogashira reactions: advances and perspectives since 2014. *RSC advances*, *13*(7), 4823-4834.

Ag_2S/ZnO photocatalyst loaded on activated carbon for the removal of organic pollutants from wastewater

Danial Ramin[a], Mohammad Sepehrian[a], Mansoor Anbia*[a]

[a] *Nanoporous Materials Research Laboratory, Department of Chemistry, Iran University of Science and Technology, Tehran, Iran*

**E-mail:* anbia@iust.ac.ir

Abstract:
This study investigates the photocatalytic performance of two catalysts: zinc oxide (ZnO) and ZnO/Ag_2S/activated carbon composite, specifically for the removal of methylene blue. The ZnO/Ag_2S/activated carbon composite was synthesized using a hydrothermal method and characterized via X-ray diffraction (XRD) analysis. Photocatalytic removal tests were conducted utilizing a UV-visible spectrophotometer. The findings reveal that ZnO is capable of removing 51.97% of methylene blue within 60 minutes. In contrast, the ZnO/Ag_2S/activated carbon composite demonstrated remarkable efficacy, achieving a removal rate of 98.8% within just 10 minutes. This research underscores the potential for enhancing photocatalytic performance through the combination of different materials and illustrates that the use of multiple composites can significantly elevate pollutant removal efficiency.

Keywords: Photocatalytic removal, ZnO, ZnO/Ag_2S/Activated Carbon, organic pollutant.

1. Introduction:

Methylene blue (MB) represents a significant organic pollutant utilized across various industries, including dyeing, textiles, and pharmaceuticals. Its distinctive chemical and physical properties render it difficult to eliminate from the environment, categorizing it as a notable environmental concern. Addressing the removal of this pollutant, particularly in aquatic environments, through photocatalytic methods is widely regarded as one of the most effective solutions for contaminated water treatment [1]. Photocatalysts are capable of decomposing pollutants by harnessing light energy to catalyze chemical reactions, with zinc oxide (ZnO) being among the most commonly employed photocatalysts in this domain. Nevertheless, the efficiency of ZnO requires enhancement due to challenges, such as the rapid recombination of charge carriers [2].

To enhance the performance of ZnO, combining it with other materials, such as Ag_2S and activated carbon, can increase its efficiency [3]. This study investigated the photocatalytic performance of two types of catalysts, ZnO and a ZnO/Ag_2S/Activated Carbon composite, for removing methylene blue from aqueous solutions under UV light irradiation.

2. Methode:

The synthesis of the ZnO/Ag_2S/Activated Carbon composite was carried out using a hydrothermal method. Initially, activated carbon and ZnO were combined in 50 mL of distilled water and subjected to stirring for 30 minutes. Subsequently, a silver nitrate solution was introduced, followed by carefully adding sodium thiosulfate solution to the mixture. This resultant solution was transferred to an autoclave, where it was heated to 160°C for a duration of 24 hours. After the heating process, the samples were dried at 80°C for 12 hours and then calcined for 2 hours and 400°C to obtain the ZnO/Ag_2S/Activated Carbon composite. Tests were conducted using a UV-visible spectrophotometer to assess the composite's effectiveness in removing methylene blue pollutants. The experimental procedure employed an initial methylene blue concentration of 10 ppm and a photocatalyst dosage of 20 mg, with exposure to UV light for 60 minutes. Before the UV irradiation, adsorption and desorption equilibrium were established over a 30-minute period to determine the optimal conditions for pollutant removal.

3. Results and discussion:

The experimental results showed that ZnO was able to remove 51.97% of methylene blue within 60 minutes. In contrast, the ZnO/Ag_2S/Activated Carbon composite performed much better, removing 98.8% of methylene blue within 10 minutes. These results indicate the superior ability of the ZnO/Ag_2S/Activated Carbon composite to remove pollutants more quickly than pure ZnO.

The results show that the ZnO/Ag_2S/Activated Carbon composite has higher photocatalytic performance than pure ZnO. This performance improvement is attributed to the specific properties of each component in the composite: ZnO, as the main photocatalyst, is capable of generating active free radicals and degrading pollutants; Ag_2S accelerates photocatalytic reactions by absorbing more UV light and generating active charge carriers; and activated carbon, with its microporous structure, adsorbs pollutants and provides a larger contact surface for photocatalytic reactions. The combination of these three materials synergistically increases the efficiency of the composite and leads to faster pollutant removal.

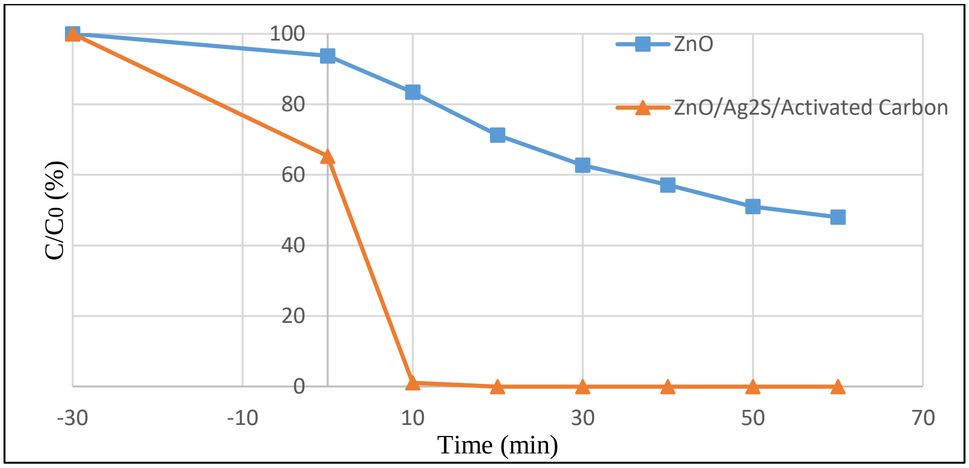

Scheme 1. The percentage of MB degraded after 60 minutes.

References:

[1] Anbia, Mansoor, and Saba Asl Hariri. "Removal of methylene blue from aqueous solution using nanoporous SBA-3." *Desalination* 261.1-2 (2010): 61-66.

[2] Goktas, S., and A. Goktas. "A comparative study on recent progress in efficient ZnO based nanocomposite and heterojunction photocatalysts: A review." *Journal of Alloys and Compounds* 863 (2021): 158734.

[3] Ichipi, Emmanuel O., Shepherd M. Tichapondwa, and Evans MN Chirwa. "Plasmonic effect and bandgap tailoring of Ag/Ag_2S doped on ZnO nanocomposites for enhanced visible-light photocatalysis." *Advanced Powder Technology* 33.6 (2022): 103596.

The 30th Iranian Seminar of Organic Chemistry
February 7-9, 2025, Iran University of Science and Technology, Tehran, Iran

Impact of Pore Structural Characteristics in Metal-Organic Frameworks on Host-Guest Interactions in Drug Delivery

Mobina Mohamadi[a]*, Sina Pirani Ahmad Abad[a]*, Somayeh Tarasi[a], Ali Ramazani[ab]

a) *The Organic Chemistry Research Laboratory (OCRL), Department of Chemistry, Faculty of Science, University of Zanjan, Zanjan 45371-38791, Iran*
b) *The Convergent Sciences & Technologies Laboratory (CSTL), Research Institute of Modern Biological Techniques (RIMBT), University of Zanjan, Zanjan 45371-38791, Iran*

Keywords: Metal-organic frameworks, Curcumin, Drug delivery, Cancer

The pore structure properties of metal-organic frameworks (MOFs) significantly influence the adsorption of target molecules, enhancing MOF efficiency. In this study, we synthesized three MOFs with varying hydrophilicity: TMU-6(RL1), TMU-21(RL2), and TMU-59. We investigated how the hydrophobicity/hydrophilicity of the pores affects drug delivery and sensing capabilities. Characterization was performed using XPS, BET, XRD, IR, and TGA. The drug loading capacity (DLC) and drug encapsulation efficiency (DLE) for TMU-6(RL1), TMU-21(RL2), and TMU-59 were (20%, 70%), (18%, 78%), and (3.6%, 13.6%), respectively. Curcumin release was 74%, 57%, and 8% for TMU-6(RL1), TMU-21(RL2), and TMU-59 after 100 hours in PBS at pH 7.2. The carriers demonstrated high adsorption efficiency and controlled release, with curcumin loading facilitated through mechanisms like $_{\text{Host}}\pi{-}\pi_{\text{Guest}}$ interactions and hydrogen bonds. In vitro anticancer studies indicated that MOFs@Curcumin composites showed greater cytotoxicity against HT-29 cells compared to free curcumin. These results highlight how modifications in hydrophilicity can precisely regulate Host-Guest interactions, drug loading, and release (Scheme1).

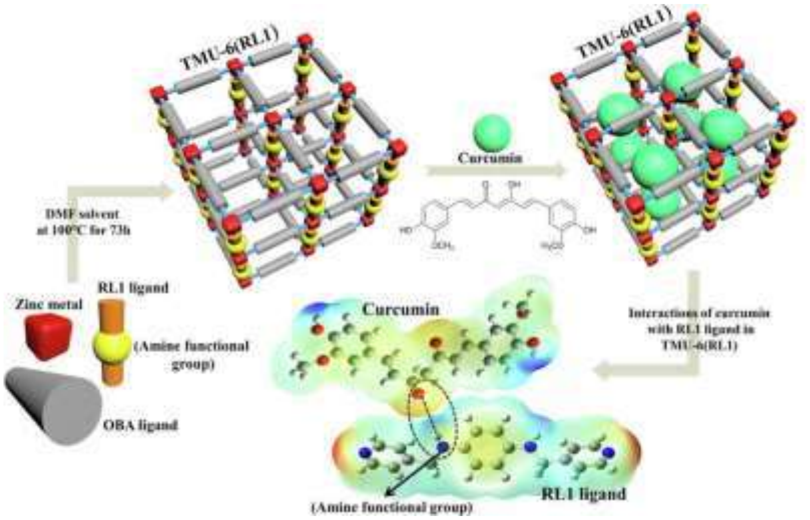

Scheme1: Preparation of MOF and drug loading process

References:

[1] Yan, X.-W.; Tarasi, S.; Wang, S.-J.; Rostamizadeh, K.; Hu, M.-L.; Morsali, A.; Ramazani, A.; Tarasi, R.; Ahmadi, Y. Influence of pore structural properties in metal-organic frameworks on the host-guest interaction in drug delivery. Arabian Journal of Chemistry 2023, 16 (8). DOI: 10.1016/j.arabjc.2023.104887.

[2] Tarasi, S.; Ramazani, A.; Morsali, A.; Hu, M.-L.; Ghafghazi, S.; Tarasi, R.; Ahmadi, Y. Drug Delivery Using Hydrophilic Metal–Organic Frameworks (MOFs): Effect of Structure Properties of MOFs on Biological Behavior of Carriers. Inorganic Chemistry 2022, 61 (33), 13125-13132. DOI: 10.1021/acs.inorgchem.2c01820.

The 30th Iranian Seminar of Organic Chemistry
February 7-9, 2025, Iran University of Science and Technology, Tehran, Iran

Drug Delivery Using Hydrophilic MOFs:
Effect of MOFs Structure Properties on Biological Behavior of Carriers

Mobina Mohamadi[a]*, Sina Pirani Ahmad Abad[a]*, Somayeh Tarasi[a], Ali Ramazani[ab]

c) *The Organic Chemistry Research Laboratory (OCRL), Department of Chemistry, Faculty of Science, University of Zanjan, Zanjan 45371-38791, Iran*
d) *The Convergent Sciences & Technologies Laboratory (CSTL), Research Institute of Modern Biological Techniques (RIMBT), University of Zanjan, Zanjan 45371-38791, Iran*

Keywords: Metal-organic frameworks, Drug Delivery, Nimesulide, Cancer

To investigate how the pore structure of metal–organic frameworks (MOFs) affects drug adsorption and delivery, we created two MOFs, TMU-6(RL1) and TMU-21(RL2), featuring amine-based N-donor pillars with phenyl or naphthyl cores and varying hydrophilic characteristics. We characterized these MOFs using TG, IR, XPS, and PXRD techniques, revealing their high adsorption efficiency, stability, and controlled release. Nimesulide (Nim), an anticancer drug, was adsorbed through multiple mechanisms, including Hostπ–πGuest interactions and hydrogen bonds. Hirshfeld surface analysis indicated that switching from a benzene to a naphthalene core reduced π···π and N···H interactions in TMU-21(RL2) but increased interactions with guest molecules. These findings suggest that altering MOF hydrophobicity/hydrophilicity influences Nim adsorption capabilities. In vitro studies demonstrated that Nim in MOFs@Nim composites exhibited significantly greater cytotoxicity against HeLa and HT-29 cancer cells compared to free Nim. Overall, the biological behavior of the carriers can be fine-tuned by modifying the structural properties of MOFs. (Scheme1).

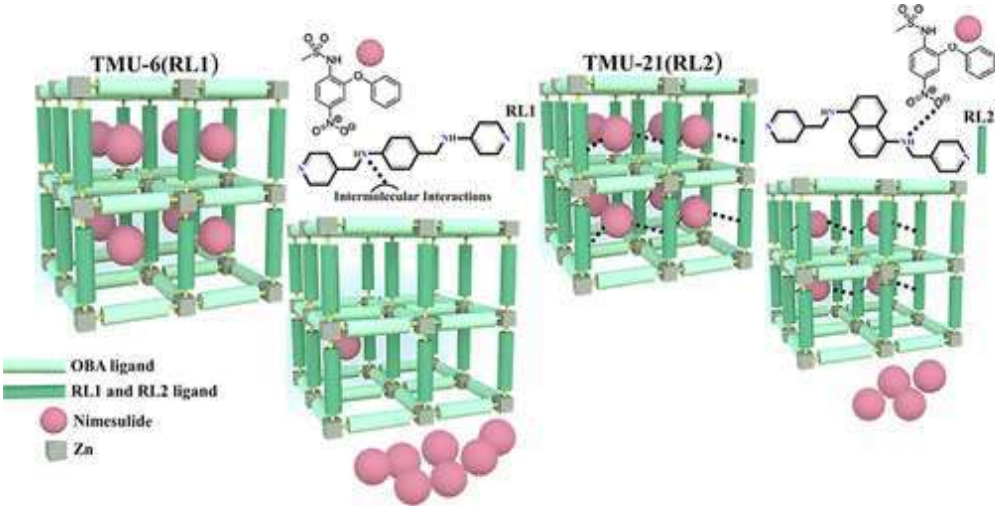

Scheme1: Preparation of MOFs and drug loading process

References:

[3] Tarasi, S.; Ramazani, A.; Morsali, A.; Hu, M.-L.; Ghafghazi, S.; Tarasi, R.; Ahmadi, Y. Drug Delivery Using Hydrophilic Metal–Organic Frameworks (MOFs): Effect of Structure Properties of MOFs on Biological Behavior of Carriers. Inorganic Chemistry 2022, 61 (33), 13125-13132. DOI: 10.1021/acs.inorgchem.2c01820.

[4] Yan, X.-W.; Tarasi, S.; Wang, S.-J.; Rostamizadeh, K.; Hu, M.-L.; Morsali, A.; Ramazani, A.; Tarasi, R.; Ahmadi, Y. Influence of pore structural properties in metal-organic frameworks on the host-guest interaction in drug delivery. Arabian Journal of Chemistry 2023, 16 (8). DOI: 10.1016/j.arabjc.2023.104887.

Examining the Size Effect of Metal−Organic Frameworks in Drug Delivery and Anticancer Activity

Sina Pirani Ahmad Abad[a]*, Mobina Mohamadi[a], Somayeh Tarasi[a] and Ali Ramazani[ab]

a) The Organic Chemistry Research Laboratory (OCRL), Department of Chemistry, Faculty of Science, University of Zanjan, Zanjan 45371-38791, Iran

b) The Convergent Sciences & Technologies Laboratory (CSTL), Research Institute of Modern Biological Techniques (RIMBT), University of Zanjan, Zanjan 45371-38791, Iran

Keyword: Metal-organic framework, Cancer, Drug Delivery, Nimesulide

In this study, we demonstrate that the therapeutic efficacy of a zinc-based metal-organic framework (MOF) is influenced by particle size. The sizes of the MOFs were precisely adjusted to specific ranges (100, 200, and 300 nanometers) by modifying the synthetic conditions. We employed various analytical techniques, including X-ray photoelectron spectroscopy (XPS), Fourier-transform infrared spectroscopy (FT-IR), powder X-ray diffraction (PXRD), and scanning electron microscopy (SEM), to characterize the synthesized structures. The analyses revealed only minor changes in the molecular properties of these structures, regardless of their size, supporting our hypothesis that the identity of MOF nanoparticles is preserved despite size variations. The synthesized carriers undergo structural degradation in response to the weakly acidic environment of tumors, facilitating the release of the Nimesulide drug. Notably, anticancer studies conducted on SKBR3 human breast cancer cells indicated that different sizes of the MOFs resulted in varying degrees of inhibition of cancer cell growth. This research underscores the importance of optimizing the geometry of drug carriers, including their size and shape, to enhance cellular uptake and therapeutic effectiveness. Additionally, theoretical investigations were carried out using B3LYP/6-31G(d,p) methods and density functional theory (DFT) to further explore the drug adsorption mechanisms.

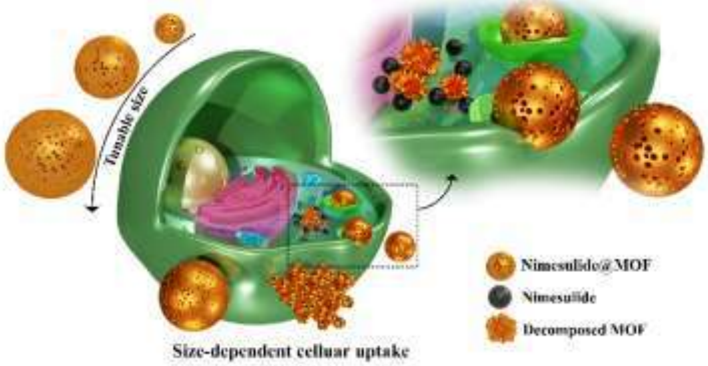

Scheme: The Size Effect of Metal−Organic Frameworks in Drug Delivery and Anticancer Activity

References:

[1] Tarasi, S., Pirani Ahmad Abad, S., Feghhe Miri, O., Danafar, H., Morsali, A., & Ramazani, A. (2024). Investigating the Size Effect of Metal–Organic Frameworks in Drug Delivery and Anticancer Properties. Inorganic Chemistry, 63(40), 19011-19022.

The 30th Iranian Seminar of Organic Chemistry
February 7-9, 2025, Iran University of Science and Technology, Tehran, Iran

Add on Strategy of Modifying Lidocaine With the Adamantane Motif

Ghazal Farayedi 1[a], Adeleh Moshtaghi Zonouz 2*[a]

Department of Chemistry, Faculty of Science, Azerbaijan Shahid Madani University, Tabriz, Iran,

Corresponding author: adelehmz@yahoo.com, Presenter: ghazal.farayedi@gmail.com

Abstract: Lidocaine containing an adamantane moiety was synthesized in two steps. First, 2-chloro-N-(2,6-dimethylphenyl) acetamide was synthesized by nucleophilic acyl substitution reaction of a carboxylic acid and 2,6-dimethylaniline. Then, in the second step, during the nucleophilic reaction with amantadine and 2-chloro-N-(2,6-dimethylphenyl) acetamide, lidocaine containing the adamantane part was synthesized.

Keywords: Diamondoid, Adamantane, Nanodiamond, Lidocaine

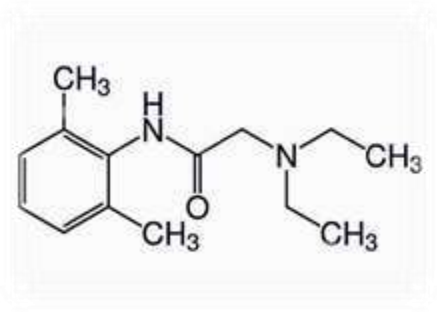

Lidocaine

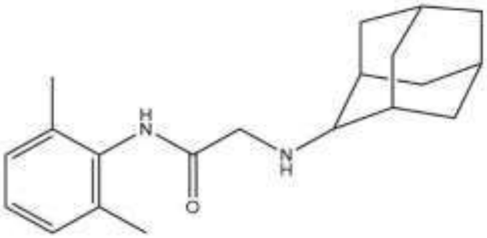

lidocaine containing adamantane part

Introduction

The synthesis of lidocaine derivatives has attracted great interest due to its biological and medicinal activities[1]. Adamantane is a weakly functional hydrocarbon widely used to develop new drug molecules to improve their pharmacokinetic and pharmacodynamic parameters. The compound has an affinity for the lipid bilayer of liposomes, enabling its application in targeted drug delivery and surface recognition of target structures. Adamantane has been used in two ways as a building block to which various functional groups are covalently attached (adamantane-based dendrimers) or as a part of self-aggregating supramolecular systems, where it is incorporated based on its lipophilicity (liposomes) and strong interaction with the host molecule (cyclodextrins). Adamantane represents a suitable structural basis for the development of drug delivery system. Diamondoids are generalizations of the carbon cage molecule known as adamantane (C10H16), the smallest unit cage structure of the diamond crystal lattice. Diamondoids also known as nanodiamonds or condensed adamantanes may include one or more cages (adamantane, diamantane, triamantane, and higher polymantanes) as well as numerous isomeric and structural variants of adamantanes and polymantanes. These diamondoids occur naturally in petroleum deposits and have been extracted and purified into large pure crystals of polymantane molecules having more than a dozen adamantane cages per molecule. These species are of interest as molecular approximations of the diamond cubic framework, terminated with C−H bonds [2]. Lidocaine has a role as a local anesthetic, an anti-arrhythmia drug, an environmental contaminant, a xenobiotic, and a drug allergen. It is a monocarboxylic acid amide, a tertiary amino compound, and a member of benzenes in terms of functionally related to a glycinamide [3]. In many cases, the incorporation of the bulky lipophilic adamantyl moiety into the known drugs has improved their pharmacological properties without increasing toxicity and resulted in many promising drug candidates with an adamantane moiety[4]. Since the combination of adamantane moiety with other pharmacophores on the same scaffold, in most cases, leads to more potent biologically active compounds or drugs, we decided to synthesize novel lidocaine incorporating an adamantane moiety.

Method

Synthesis lidocaine: dimethylaniline (0.25 Mol) in toluene and sodium carbonate (53 g, 0.50 M) at 20-30 °C were added little by little over 30 min to 2-chloroacetyl chloride. The mixture was stirred for one hour at room temperature, diluted with water, and diethylamine was added. The reaction mixture was refluxed for 6-10 hours, and the organic layer was collected and washed three times with water. The organic solvent was removed under vacuum to leave a crude product. After 30 min under stirring the suspension was filtered[5].

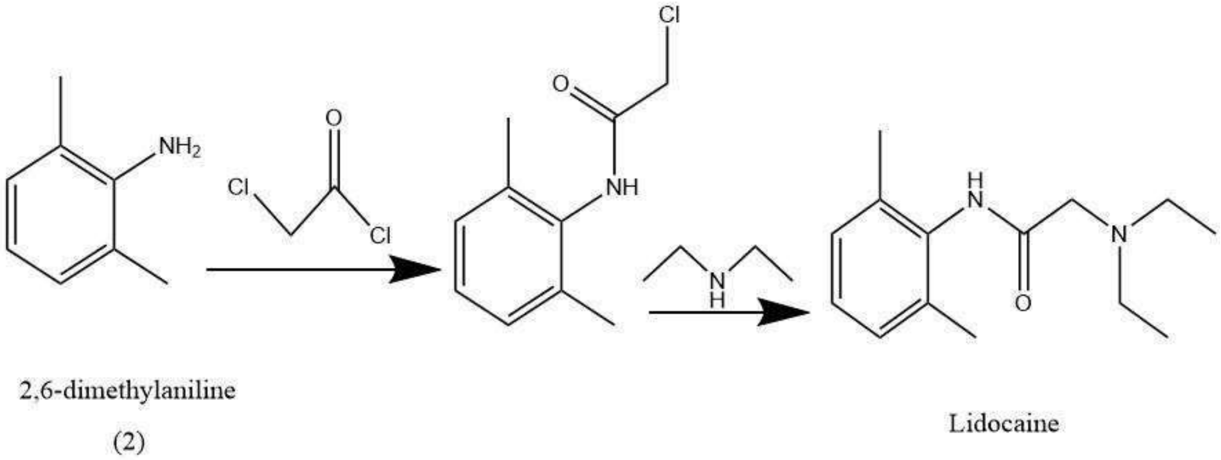

Fig.1: Synthesis of 2-chloro-N-(2,6-dimethylphenyl) acetamide and Synthesis Lidocaine

After obtaining the assurance of lidocaine production, with the same method of lidocaine production, we proceed to make lidocaine with adamantane part. The difference is that instead of using diethylamine, we will use adamantane.

A mixture of 2-chloro-N-(2,6-dimethylphenyl) acetamide (I) (197 mg, 1 mmol) and amantadine (II) (151 mg, 1 mmol) in toluene solvent at reflux temperature (105 °C), completion of the reaction as indicated by TLC (72 h). then the mixture was washed with water and the solvent was separated using a rotary. 2-(((1s,3s)-adamantan-1-yl)amino)-N-(2,6-dimethylphenyl) acetamide (II); mp 189-190 °C; ^{1}H NMR (DMSO-d6, 500 MHz): δ = 1.57 (s, 6H, Ad), 1.84 (s, 6H, Ad), 1.94 (s, 3H, C=C-CH3), 1.95 (s, 3H, Ad), δ = 2.13 (s, 2H, CH3), δ = 3.32 (s, 1H, NH-CH2), δ = 7.05 (d, J= 8 Hz, 3H arom), δ = 9.08 (s, 1H, NH-C=O).

Yield of 2-chloro-N-(2,6-dimethylphenyl) acetamide : 93%, white solid powder, mp:86 °C, IR (KBr): ῡ=3293 (NH), 3283 (NH), 3036 (Ar-H), 2985 (C-H), 1694 (C=O) cm-1

Yield of Lidocaine: 95%, white solid powder, mp: 68 °C, IR (KBr): ʋ̄=3290 (NH), 3275 (NH), 3074 (Ar-H), 2899 (C-H), 1699 (C=O) cm-1.

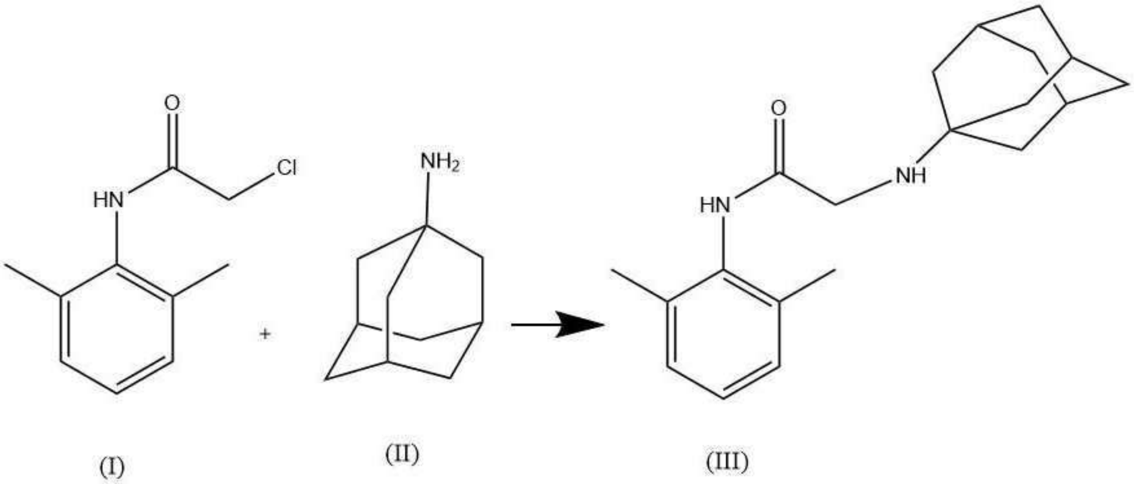

Fig.2: Synthesis of Synthesis of lidocaine containing adamantane part

Results and Discussion

According to the nucleophilic acyl substitution reaction of a carboxylic acid and 2,6-dimethylaniline for conversion of the aromatic amine to the amide was used. Then 2-chloro-N-(2,6-dimethylphenyl) acetamide(I) and amantadine(II) were reacted. The structures of novel compounds were confirmed by ^{1}H and ^{13}C NMR, and IR spectroscopy.

We have developed for the first time a convenient and highly efficient add-on strategy to generate lidocaine incorporating adamantane moiety. To introduce adamantane moiety in the lidocaine skeleton, from amantadine (II) was used in the nucleophilic reaction. We predict the size, rigidity, and approximately spherical shape of adamantane as a lipophilic bullet can influence and modify the physico-chemical features of these lidocaine-based scaffolds.

References:

1. Lee, M., et al., *Journal of Chemical Education*, **2022.** 99(6), 2399-2402.

2. Dragomanova, S. and V. Andonova, *Adamantane-containing drug delivery systems.* Pharmacia, **2023**. 70: 1057-1066.

3. Reyes, V., O. Martínez, and G. Hernández, *National center for biotechnology information.* Plant Breeding. Universidad Autónoma Agraria Antonio Narro, Calzada Antonio Narro, **1923**.

4. Abkar Aras, M. and A. Moshtaghi Zonouz, . *Journal of Sulfur Chemistry*, **2023**. 44(3), 361-376.

5. Costa, J.C., et al., . *Bioorganic & medicinal chemistry letters*, **2008.** 18(3), 1162-1166.

The 30th Iranian Seminar of Organic Chemistry
February 7-9, 2025, Iran University of Science and Technology, Tehran, Iran

An advanced electrochemical sensor designed for the precise determination of methanol, utilizing a PdNPs@SBA-15-PrEn modified electrode

Pouriya Etminan [a], Sadegh Rostamnia*[a]

[a] *Organic and Nano Group (ONG), Department of Chemistry, Iran University of Science and Technology (IUST), Tehran, 16846-13114, Iran*

Keywords: Methanol, PdNPs@SBA-15-PrEn nanocomposite, Electrochemical sensor

Electrochemical sensing is based on the fluctuation of output electrical signals produced by the chemical interactions between electrode-immobilized recognition components and target analyte [1]. To date, numerous techniques have been documented for the quantification of methanol in the literature, including gas chromatography with flame ionization detection (GC-FID), fluorescence, UV-visible spectroscopy, electrochemical approaches, and Fourier-transform infrared spectroscopy (FTIR). Nonetheless, electrochemical methods are considered a promising approach for the quantification of methanol [2]. This study presents a new electrochemical sensor for methanol detection, utilizing palladium nanoparticles supported on Santa Barbara amorphous-15-$PrNHEtNH_2$ (PdNPs@SBA-15-PrEn) as a nanocatalytic substrate. The electro-oxidation efficacy of the proposed sensor was examined by cyclic voltammetry (CV) and amperometry. The findings indicate that the Nafion-PdNPs@SBA-15-PrEn/GCE exhibits potential as an effective and integrated sensor for methanol detection.

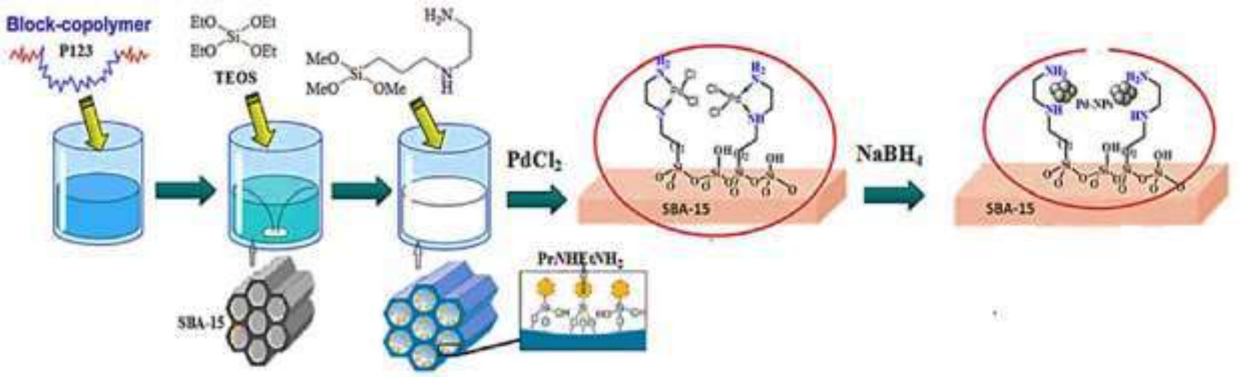

Scheme: Schematic representation of PdNPs@SBA-15-PrEn preparation.

References

[1] Ziyatdinova, G., Kozlova, E., & Budnikov, H. (2018). Selective electrochemical sensor based on the electropolymerized p-coumaric acid for the direct determination of L-cysteine. *Electrochimica Acta*, *270*, 369-377.

[2] Rahman, M. M., Hussein, M. A., Alamry, K. A., Al Shehry, F. M., & Asiri, A. M. (2016). Sensitive methanol sensor based on PMMA-G-CNTs nanocomposites deposited onto glassy carbon electrodes. *Talanta*, *150*, 71-80.

The 30th Iranian Seminar of Organic Chemistry
February 7-9, 2025, Iran University of Science and Technology, Tehran, Iran

Electrochemical detection of indole in plasma utilizing Pd nanoparticles modified metal-organic framework Cr-MIL-101/ionic liquid sensor

Pouriya Etminan [a], Sadegh Rostamnia*[a]

[a] *Organic and Nano Group (ONG), Department of Chemistry, Iran University of Science and Technology (IUST), Tehran, 16846-13114, Iran*

Keywords: Indole, Pd nanoparticles, Metal–organic framework, Ionic liquid (IL)

Due to the chemical structures of several significant medications, bioactive heterocycles, and natural products being derived from the indole framework, current studies on the pharmacological and therapeutic properties of indole-containing compounds have garnered the interest of scientific researchers [1]. A variety of approaches have been employed for the determination of indole. Electroanalytical methods are effective for this purpose owing to their notable characteristics, including quickness, ease of use, cost-effectiveness, and sensitivity [2]. An electrochemical sensor for indole detection was developed using Pd nanoparticles modified Metal-Organic Framework Cr-MIL-101 (Pd@Cr-MOF) and ionic liquid (IL). The electrochemical properties of indole were examined using cyclic voltammetry (CV) and differential pulse voltammetry (DPV) on the surface of the modified electrode. The proposed sensor was effectively utilized for the monitoring of indole in human serum samples, yielding good findings.

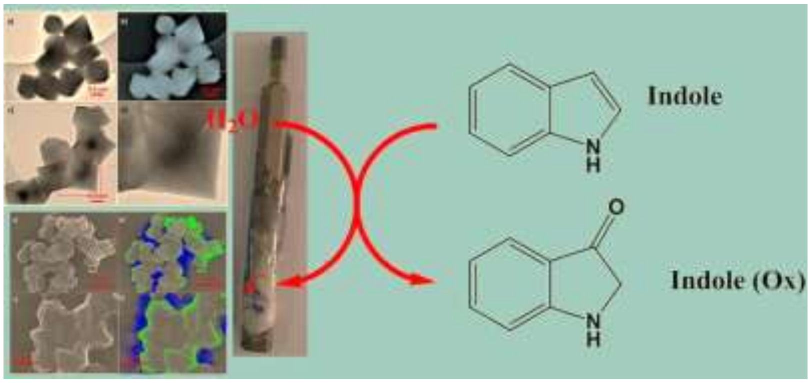

Scheme: Electrochemical behavior of indole at the surface of the electrode

References

[1] Singh, T. P., & Singh, O. M. (2018). Recent progress in biological activities of indole and indole alkaloids. *Mini reviews in medicinal chemistry*, *18*(1), 9-25.

[2] Zhou, Y., Ding, M., Lyu, W., Zhen, Q., Chen, H., Jiang, M., ... & Zhang, X. (2021). A sensitive electrochemical method for indole based on the signal amplification strategy by gold/iron-oxide composite nanoparticles. *Analytica Chimica Acta*, *1142*, 56-64.

The 30th Iranian Seminar of Organic Chemistry
February 7-9, 2025, Iran University of Science and Technology, Tehran, Iran

2- isocyanopyridine and its complexation with organometallic platinum complexes: experimental and biological properties

Fatemeh Masoumi, Niaz Akhavan Rezaie, Mohsen Golbon Haghighi*

Department of Chemistry, Shahid Beheshti University, Evin, Tehran 19839-69411, Iran

Email address: m_Golbon@sbu.ac.ir

Keyword: Isocyanide, organometallic complexes, Molecular Docking

In this study, a series of organometallic complexes based on Pt (II) was synthesized with isocyanide ligand. For the first time, organometallic complexes including [Pt(C^N)(*L*)(2-isocyanopyridine)] (**C1-C4**), which C^N = ppy, bhq and L = *P*-tolyl or isocyanide, were prepared **[1]**. Ligand and all complexes were characterization by ^{1}H-NMR. The structure of new complexes was optimized by gaussian. The interaction between compounds and DNA was studied by molecular docking and lead-like drug properties was investigated at SwissADME website **[2]**. The results showed the isocyanide complexes could interact with DNA through major groove binding and the free binding energies was calculated for all complexes. ADMET comparative results indicated that all complexes are drug likeness.

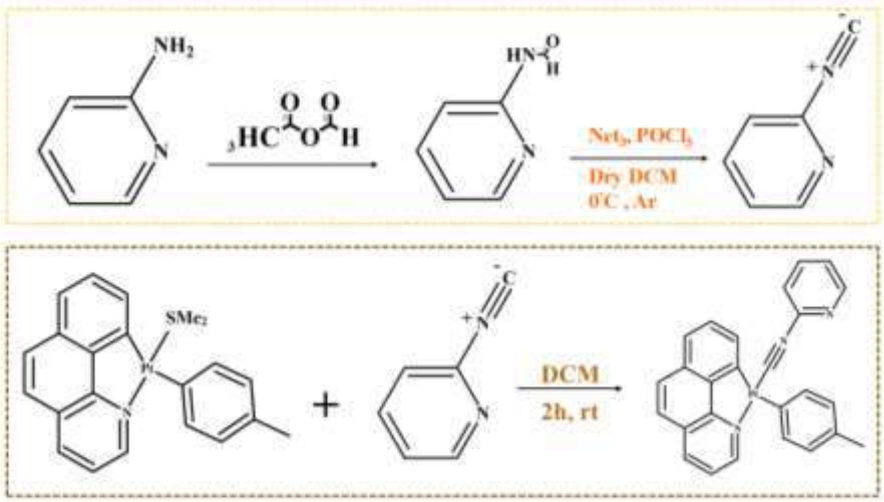

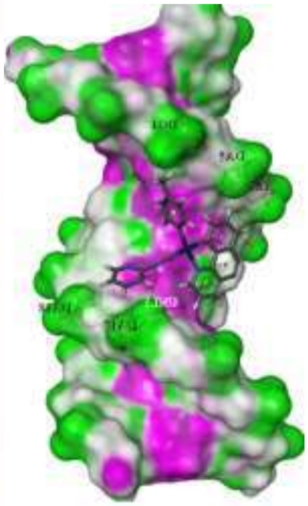

References
[1] Scoch, K., et al., 2018. New Chemistry-A European Journal, 24(52), pp.13788-13791.
[2] Fereidoonnezhad, M., et al., 2018. New Journal of Chemistry, 42(11), pp.8681-8692.

The 30th Iranian Seminar of Organic Chemistry
February 7-9, 2025, Iran University of Science and Technology, Tehran, Iran

Synthesis of Tin(II) 2-ethylhexanoate as a Catalyst

Zohreh Mortezaei [a,b*], Azam Sadeghi [a,b] , Samira Sadeghi [b]

[a] *Department of Chemistry, Faculty of Science, Arak University, Arak 38156-8-8349, Iran*

[b] *Department of Research and Development, Hallal pouyan Co., Arak, Iran*

*E-mail: zeo.sercher@yahoo.com

Keywords: Tin(II) 2-ethylhexanoate, Catalyst, Tin (II) oxide, 2-ethylhexanoic acid

Introduction

Tin(II) 2-ethylhexanoate or stannous octoate ($Sn(Oct)_2$) is a compound of tin. Produced by the reaction of tin(II) oxide and 2-ethylhexanoic acid. It is a clear colourless liquid at room temperature, though it often appears yellow due to impurities, likely resulting from oxidation of Sn(II) to Sn(IV) [1]. The clear yellow liquid is soluble in most organic solvents, but it is practically insoluble in water. It is viscous, combustible and has a variety of applications in the chemical industry. This product sometimes used as a catalyst for ring-opening polymerization, such as in the production of polylactic acid [2]. The aim of this work was synthesis and characterization of tin(II) 2-ethylhexanoate with high purity (**Scheme 1**).

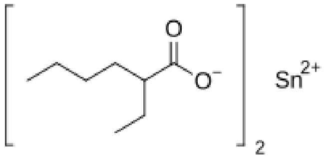

Scheme 1: Tin(II) 2-ethylhexanoate

Experimental

Materials

All the materials such as: tin(II) oxide (SnO), 2-ethylhexanoic acid ($C_8H_{16}O_2$) were purchased from Merck. All samples were characterized using FT-IR (Galaxy series FT-IR 5000 spectrometer), AAS (Atomic absorption spectrometry, Shimadzu AA-7000 Series) and ICP-OES (Inductively Coupled Plasma Optical Emission spectroscopy, PerkinElmer series 4300).

Method

At first, tin(II) oxide was reacted with excess 2-ethylhexanoic acid (molar ration 1: 3-6), while the reaction mixture was heated under different condition (atmospheric, vacuum and nitrogen atmosphere). The water present in the precipitate of tin(II) oxide was removed by distillation and the mixture was heated (3-5 h) under reflux at the desired temperature (115-130 °C). When the reaction was complete, the product was filtered and excess acid was removed by distillation under reduced pressure**.**

Results and Discussion

Tin(II) 2-ethylhexanoate produced by the reaction of tin(II) oxide and 2-ethylhexanoic acid (molar ration 1: 4.5), it is a clear yellow liquid at room temperature.

FT-IR Analysis

The results of FT-IR analysis for tin(II) 2-ethylhexanoate showed that the bands at 1707 and 1262 cm^{-1} were for v(C=O) and v(C-O), respectively. Also, the bands at 2935 and 1461 cm^{-1} that indicated the stretching v(C-H) and the bending v(C-H), respectively. The stretching v(C-H) showed the presence of C-H aromatic group and in range around 2800-3000 cm^{-1} indicated the C-H stretching.

AAS and ICP Analysis

The total percentage of Sn ions was characterized by using AAS and ICP-OES analysis. As a result, suitable reaction conditions were optimized to obtain a product with approximately 28% Sn ion.

References

[1] Kumar Suri, A.; Banerjee, S. (2006). Materials Science and Technology.

[2] Schwach, G.; Coudane, J.; Engel, R.; Vert, M. (1997). Journal of Polymer Science Part A: Polymer Chemistry. 35 (16): 3431–3440.

The 30th Iranian Seminar of Organic Chemistry
February 7-9, 2025, Iran University of Science and Technology, Tehran, Iran

Synthesis, characterization and investigation of photocatalytic performance of carbon based nanostructures

Sadegh Ghadiri Aghcheh kandi, Hakimeh Teymourinia and Ali Ramazani*
Department of Chemistry, Faculty of Science, University of Zanjan, Zanjan 45371-38791, Iran
E-mail: s.ghadiri@znu.ac.ir

Keyword: Carbon nitride, Nanoparticles, Photocatalyst, Hydrothermal

In this study, we successfully developed a C_3N_5/NiAl LDH composite using the hydrothermal method, known for its efficiency in generating nanomaterials with desirable properties. We examined the structural and morphological characteristics of the synthesized nanocomposite using various techniques such as XRD, SEM, TEM, FT-IR, and UV-Vis. Rhodamine B (Rh-B) at a concentration of 10 ppm was used as a model pollutant to evaluate the photocatalytic performance of the composite under visible light irradiation. The results demonstrated that the C_3N_5/NiAl LDH composite exhibited exceptional photocatalytic activity in degrading Rh-B, achieving around 71% degradation within 120 minutes. The enhanced photocatalytic performance can be attributed to factors such as increased specific surface area, reduced band gap, improved charge separation and transfer, and the generation of hydroxyl and superoxide radicals.[1, 2] The findings of this research indicate that the C_3N_5/NiAl LDH composite is an effective photocatalyst for the treatment of organic pollutants in wastewater.

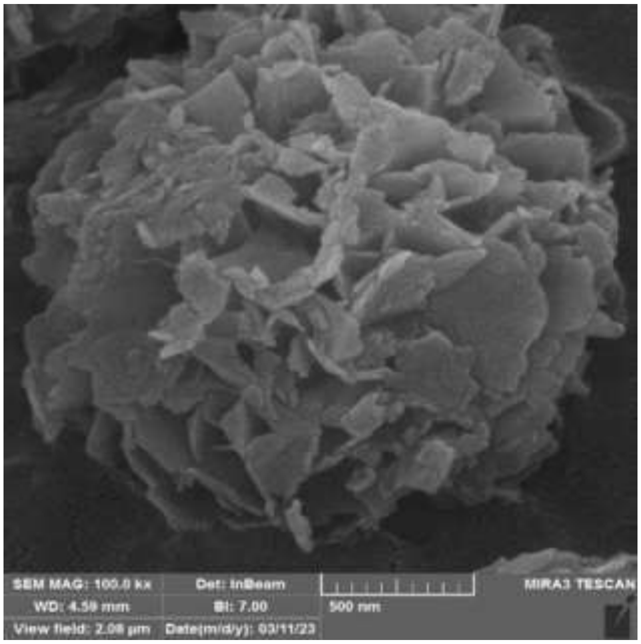

Fig.1: SEM image of C3N5/NiFe LDH

References:

1. Kumar, P., et al., C3N5: A Low Bandgap Semiconductor Containing an Azo-*Linked Carbon Nitride Framework for Photocatalytic, Photovoltaic and Adsorbent Applications.* Journal of the American Chemical Society, 2019. **141**(13): p. 5415-5436.

2. Jo, W.-K., Y.-G. Kim, and S. Tonda, Hierarchical flower-like NiAl-layered double hydroxide *microspheres encapsulated with black Cu-doped TiO2 nanoparticles: Highly efficient visible-*

light-driven composite photocatalysts for environmental remediation. Journal of Hazardous Materials, 2018. **357**: p. 19-29.

Molecular docking and DFT studies of (E)-1-(4-nitrophenyl)-N-[6-[(E)-(4-nitrophenyl) methyleneamino] hexyl] methenimine Schiff base

Parisa Babaei[1], Vahideh Hadigheh Rezvan[1]*, Nastaran Sohrabi Gilani[1] and Somayyeh Rostamzadeh Mansour[1]
[a] Department of Chemistry, Ardabil Branch, Islamic Azad University, Ardabil, Iran
* Corresponding author e-mail:

ABSTRACT

The newly synthesized, characterized, and theoretically investigated Schiff base ligand (E)-1-(4-nitrophenyl)-N-[6-[(E)-(4-nitrophenyl) methyleneamino] hexyl] methenamine. The most important parts of this ligand were di-imines. By employing density functional theory (DFT), researchers could analyze the new compound molecular properties, geometric optimization, vibrational, frontier molecular orbitals, and energy evaluation. In the FT-IR section, we observed N=C stretching vibration at 1500–1700 *cm*$^{-1}$, this vibration mentions the formation of the azomethine group, and the ^{1}H and ^{13}CNMR spectra peak present in 9.15 (s,1H) *ppm* and 161.07 *ppm* respectively, these peaks confirm the Schiff base formation. The HOMO-LUMO and MEP studies were done with the gas phase, NBO calculation represented inter and intra-molecular interactions, and The RDG (non-covalent) interactions were calculated and analyzed inter and intramolecular hydrogen bonding. Lastly, the interaction between the ligand with 1HSG, 6LU7, and 1AJ6 receptors was examined using docking experiments. A docking study of the ligand was done, and docking simulation study results show that ligand(L) has good interaction against 6LU7 protein, and the highest binding energy is – 8.05 *kcal/mol* for synthesized compound and standard.

Keywords: Schiff base, Molecular docking, hexamethylenediamine, DFT, NBO, Mulliken, NMR spectroscopy

1. Introduction

Schiff bases were first discovered more than 150 years ago in 1834 by Hugo Schiff. Condensation products of primary amines with carbonyl compounds are considered a very important class of organic compounds as imines or Schiff bases [1-4]. The Schiff base's broad scope of study has enabled researchers to find ways to combat pathogens. [5-6]. In recent years, Schiff's bases have various properties in the fields of medicine, magnetic properties, catalysis, fluorescence, non-linear optical properties, and medicine, especially in the biological field, in the investigation of antibacterial and antifungal properties. The growing bacterial resistance to commonly used antibiotics is a severe medical problem, therefore researchers are trying to find some way to innovative antimicrobial compounds that may be efficacious against these changed pathogens [7-12]. Therefore, schiff bases have been widely studied due to its wide applications.

Kangah Niameke and her colleagues synthesized this Schiff base in 2017 and investigated its biological properties [13]. Schiff base N, N'(4-nitrophenylmethylene) hexane-1,6-diamine(**L**) was synthesized by hexane-1,6-diamine (1) and 4-nitro benzaldehyde (2), Combination of 1 and 2 were dissolved in ether at room temperature. (Scheme1) The experimentally biological tests have been done on several bacteria, such as Staphylococcus aureus ATCC 25923, Staphylococcus aureus (CIP) 4.83, Pseudomonas aeruginosa (CIP) 103467, E. coli (CIP) 54127AF, and Staphylococcus aureus. that these bacteria are sensitive to penicillin. In vitro antimicrobial activities of this compound were evaluated against both Gram-positive and Gram-negative bacteria and fungal strains. On the other hand, this compound has shown activities on the bacterial strains Staphylococcus aureus (CIP) 4.83 and Staphylococcus aureus sensitive to penicillin. In recent years, researchers have greatly contributed to the experimental process to improve the conclusion process. Based on a series of different research done on Schiff bases that used the DFT [14-19] molecular docking method [20-25], we also tried to use this method to investigate this ligand. Vibrational frequency calculation is essential for theoretical studies of organic molecules and related fields. In addition, the DFT approach is a very important and useful tool to explore the relationship between theoretical and experimental performance. The reactivity descriptors of B3LYP(E, E_{HOMO}, E_{LUMO}, dipole moment, $\Delta\varepsilon$, μ, η, ω) were calculated to predict the stability of newly synthesized compound .which in this part by calculation highest occupied molecular orbital (HOMO)-lowest unoccupied molecular orbital (LUMO) energy with various chemical reactivity parameters, also parameters, Mulliken population analysis, molecular electrostatic potential, natural bond orbital (NBO) has been checked. In addition, Molecular docking is one of the methods used in molecular modeling and is part of structural studies [26-29]. The two-dimensional structure of the desired ligand was drawn by the ChemDraw professional 16.0 program Then to minimize the energy of the molecule from the -dimensional structure of the desired ligand was drawn by ChemDraw professional 16.0 program. [30], and then to minimize the energy of the molecule, HyperChem software and MM+ Field and (PM) Semi-empirical methods were used. The Polak-Ribiere (conjugate gradient) algorithm was used to optimize the molecular structure. Then, the conformer with the lowest energy was selected and transferred to the AutoCAD program for docking studies. Next, the partial charge for the inhibitor molecule was calculated using Gasteiger-Marsili was used to optimize the molecular structure. The crystallographic structure of selected protein receptors was extracted from 75 protein databases (RCSB PDB). At first, using soft Auto dock [31] software, additional ligands and cofactors, and water molecules in the crystal structure Proteins were removed. After removing the unnecessary parts in the docking operation, the protein to The entry title of AutoCAD software was used, until after hydrogen atoms were added to the protein, its overall charge should be determined using Koll man Charge, then non-ionized hydrogens in the atom adjacent carbons are integrated [32-34]

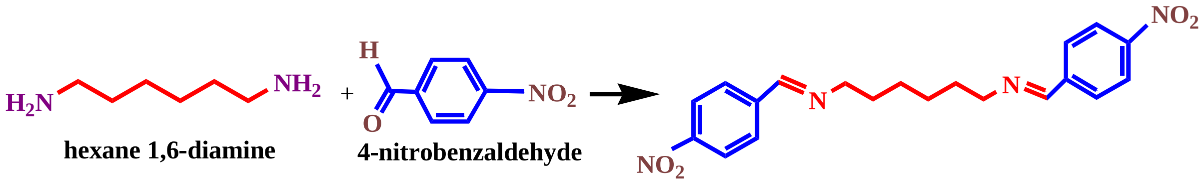

Scheme1. Synthesis reaction of ligand **L**

3. Results & Discussion

3.1. Calculation methods and computational programs

The computational evaluations were performed under the DFT method with basis set of B3LYP/6-311G+(d,p) using Gaussian 09W software and GaussView 6.0.16 visualizer program [35]. The GaussView6 program was used for preprocessing, structure modification, and analyses of structures, Mulliken and NBO charges, frequencies electron affinity were estimated using the energy values of the HOMO and LUMO frontier orbitals, and chemical shifts and computational spectral data and the topological parameter (RDG) were generated using the Gaussian software [36-37]. Based on molecular docking, 3D crystal structures of three target receptors 1HSG, 6LU7, and 1AJ6 with resolutions 2.00 Å, 2.05 Å, and 2.30 Å, respectively, has been obtained from the RCSB Protein Data Bank website (http://www.pdb.org) Three-dimensional structure of the Schiff base ligand (**L**) was drawn in HyperChem 7.0 software, then the ligand (**L**) was optimized using a molecular mechanical force field. . The ultimate conformation was calculated by AM1 as a semi-empirical method, and molecular structure was optimized using the Polak Ribiere conjugate gradient algorithm. Optimized structure was used as inputs for Auto Dock tools to prepare PDBQT file of ligand. Grid box dimensions with a 0.375 Å grid points spacing are given in Table 1. The binding location of the reference ligand was selected as a binding site for finding the best pose of ligand. The molecular docking calculations were performed using the AutoDock 4.2 software package

3.2. Molecular Structure of the *bis*-Schiff Base

The bis-Schiff base (L) is a stable diimine because it lacks imine-enamine tautomerism, which is due to the absence of alpha-hydrogens in this bis-Schiff base. Each imine bond (N=CH) can have two geometrical configurations, resulting in four geometrical isomers (i.e., ZZ, EZ, ZE, and EE) for a bis-Schiff base that contains two imine bonds. Nonetheless, because the same groups are connected to both imine bonds, this bis-Schiff base can only have three geometrical isomers, with the EZ and ZE isomers being the same. All three geometric isomers (the three diastereomers) were optimized via the DFT/B3LYP/6-311G (p, d) method, with their internal energies provided in Table 1. As indicated in Table 1, the EE geometrical isomer exhibits the highest stability. Aryl and alkyl groups introduce steric hindrance, causing the ZZ isomer and the EZ isomer to possess energies that are 7.84 and 6.97 kcal/mol greater than that of the EE isomer, respectively. Consequently, this research emphasizes the characteristics of the EE stereoisomer. The three-dimensional models (created using GussView06 software) of these three configurational isomers are displayed in Figure 1.

Table 1. Calculated energies of three bis-Schiff bases at RB3LYP / 6-311G (d, p) level of theory

bis-Schiff base	**Internal Energy (*au*)**	**ΔE(*au*)**	**ΔE(*kcal/mol*)**
EE	-1295.392	0.0000	0.00
EZ	-1295.3946	0.0111	6.97
ZZ	-1295.3821	0.0125	7.84

1 a.u. of energy = 1 *Hartree* = 627.5095 *kcal/mol*

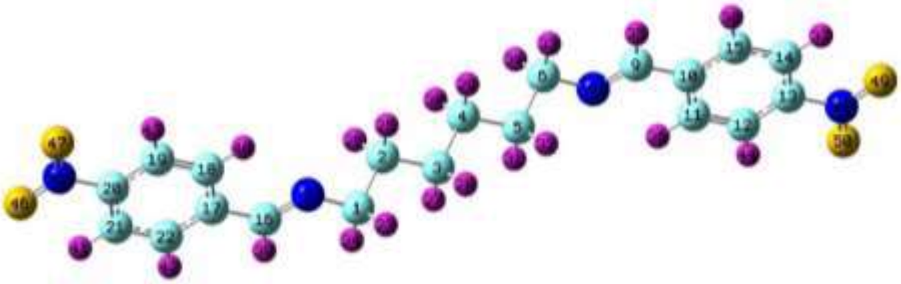

(a) *EE* geometrical isomer

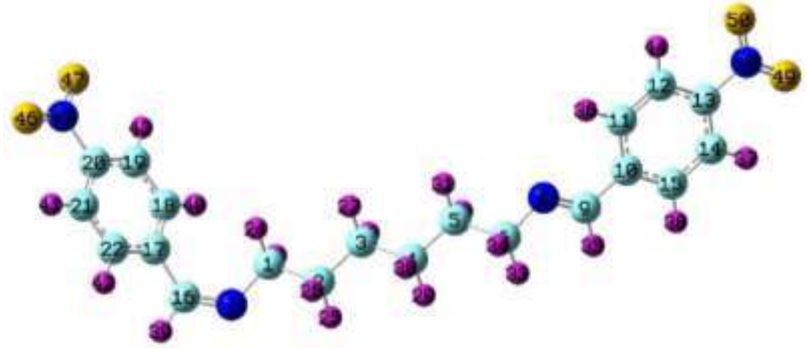

(b) *EZ*-geometrical isomer

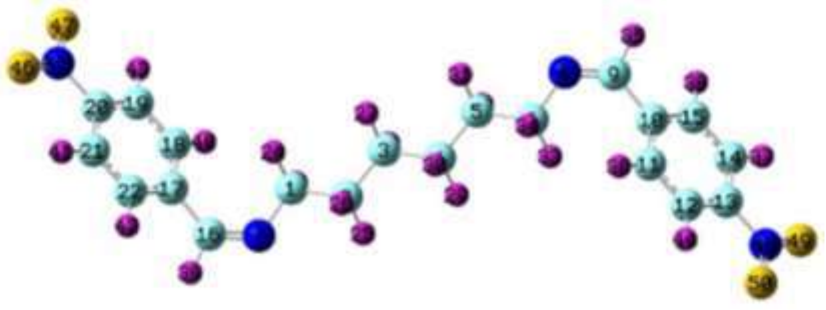

(c) *ZZ*-geometrical isomer

Figure 1. The 3D structures of three geometrical isomers for the *bis*-Schiff base

3.3. Molecular geometry

Energetic optimized geometry, structural parameters, and energy of the Schiff base for three diastereomers were calculated at the DFT/ RB3LYP / 6-311G (d, p) [38,39] level of theory and are listed in **Table 2**. The bond lengths of $r_{C=N}$ and $r_{C\text{-}N}$ in different diastereomers are almost the same. These bond lengths are 1.272 and 1.45 Å, respectively. The dihedral angle Φ_{CCNC} shows an imine bond configuration. The value of 180 belongs to the *E*-geometric isomer and Φ_{CCNC}=zero shows the *Z*- isomer. **Table 2** shows that the dipole moment (*μ,* Debye) for *EE* and *ZZ* isomers are zero because they are symmetrical molecules. According to dipole moment values, the most polar isomer is the *EE*-geometrical isomer. Therefore, we concentrate on researching the *EE*-isomer's characteristics. Figure 1 displays the three-dimensional structures of the three configurational isomers.

Table 2. Some selected molecular structure features (bond lengths (**r**, *Å*), and dihedral Angles (**Φ,** degree)) and dipole moments (***μ***, Debye) obtained for three geometrical isomers of the bis-Schiff base

bis-Schiff base	$\mathbf{r_{C=N}}$	$\mathbf{\Phi_{CCNC}}$	$\mathbf{r_{C\text{-}N}}$	**μ (D)**
EE	1.272	180	1.45	0.00
EZ	*E*: 1.269 *Z*: 1.268	E: 180 Z: 3	E: 1.452 Z: 1.456	6.32
ZZ	1.269	3	1.456	0.00

3.4. Mulliken and NBO atomic charges analysis

Mulliken and NBO analyses are very common and effective population analysis methods. Mulliken atomic charges of the optimized structure were carried out by the B3LYP/6-311G (d, p) method in the gas phase. The calculated electronic charge–density distributions (Mulliken atomic charges) of the ***EE-bis***-Schiff base are tabulated in Table 3. Also, NBO atomic charges are given in Table 4. Results from Mulliken and NBO charge analysis show that all the hydrogen atoms have a net positive charge. The $H_{44,43}$ and $H_{37,41}$ (aromatic CH) atoms have a bigger positive atomic charge than the other hydrogen atoms. This is due to the presence of an electronegative imine and nitro groups. From Table 3, we can observe that most of the carbons have negative charges, apart from C_9, C_{13}, C_{16}, C_{18}, and C_{20} This is due to adjacent electronegative nitrogen atoms. To have an easy look at the charge changes a column chart is illustrated in Figure 2. These data clearly show that the *EE-bis*-Schiff base is reactive toward substitution reactions. The most negative atoms are two nitrogen atoms, as shown in Table 3 and Table 4. It has been found that two nitrogen atoms as donor atoms are suitable sites to coordinate with metal cations. In the following cases, four oxygen atoms have a negative charge The amount of negative charge of oxygen in Mulliken is more than that of NBO.

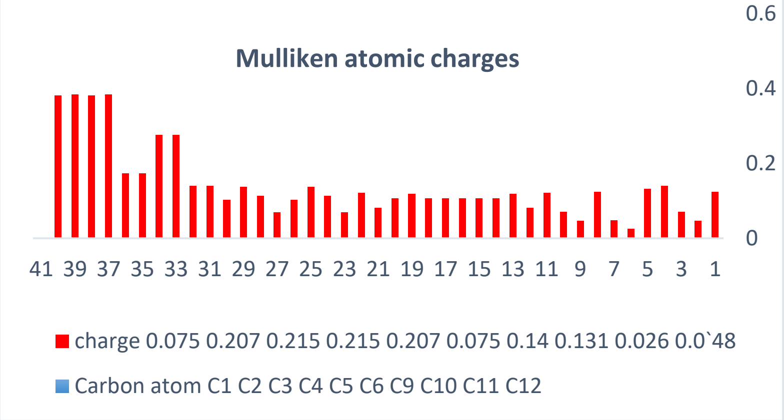

Figure 3. Column chart of Mulliken atomic charges of *EE-bis*-Schiff base

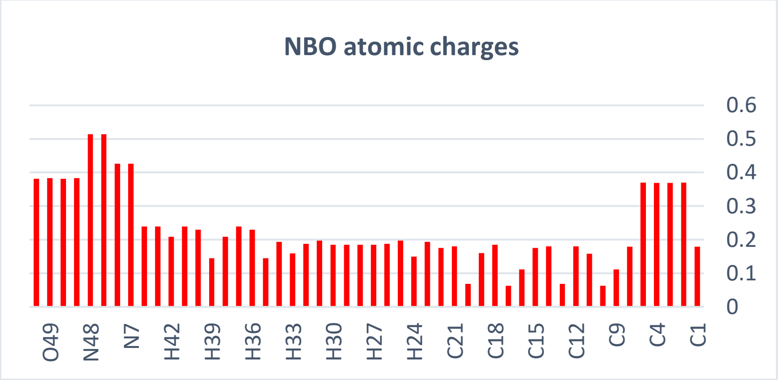

Figure 4. Column chart illustrates NBO atomic charges of *EE-bis*-Schiff base

Table 3. Mulliken atomic charges of *EE-bis*-Schiff

Carbon	**Charge**	**Hydrogen**	**Charg**	**Nitrogen**	**charge**

atom [a]		**atom [b]**	**e**	**atom [c]**	
C1	-0.075	H23	0.121	N7	-0.276
C2	-0.207	H24	0.081	N8	-0.276
C3	-0.215	H25	0.119	N45	0.173
C4	-0.215	H26	0.106	N48	0.173
C5	-0.207	H27	0.107	**Oxygen atom [d]**	**charge**
C6	-0.075	H28	0.107	O46	-0.276
C9	0.140	H29	0.107	O47	-0.266
C10	-0.131	H30	0.107	O49	-0.267
C11	-0.026	H31	0.119	O50	-0.266
C12	-0.048	H32	0.106		
C13	-0.124	H33	0.081		
C14	-0.047	H34	0.121		
C15	-0.071	H35	0.069		
C16	0.140	H36	0.113		
C17	-0.131	H37	0.137		
C18	-0.025	H38	0.102		
C19	-0.048	H39	0.069		
C20	0.124	H40	0.113		
C21	-0.047	H41	0.137		
C22	-0.071	H42	0.102		

a , b , c , d = numbers of atom : Figure1

Table 4. NBO atomic charges of *EE-bis*-Schiff base calculated by DFT/B3LYP method

Carbon atom [a]	**Charge**	**Hydrogen atom [b]**	**Charge**	**Nitrogen atom [c]**	**Charge**
C1	-0.179	H23	0.194	N7	-0.426
C2	-0.370	H24	0.150	N8	-0.426
C3	-0.369	H25	0.197	N45	0.514
C4	-0.369	H26	0.188	N48	0.514
C5	-0.370	H27	0.185	**Oxygen atom [d]**	**Charge**
C6	-0.179	H28	0.185	O46	-0.383
C9	0.112	H29	0.185	O47	-0.381
C10	-0.063	H30	0.185	O49	-0.383
C11	-0.158	H31	0.197	O50	-0.381
C12	-.0.180	H32	0.188		
C13	0.069	H33	0.159		
C14	-0.180	H34	0.194		
C15	-0.175	H35	0.145		
C16	0.112	H36	0.230		
C17	-0.063	H37	0.239		

C18	-0.185	H38	0.209
C19	-0.160	H39	0.145
C20	0.069	H40	0.230
C21	-0.180	H41	0.239
C22	-0.175	H42	0.209
		H43	0.239
		H44	0.239

a , b , c , d = numbers of atom : Figure1

3.5. Optical Properties

The non-linear optical (NLO) activities of **L** are evaluated and presented in Table 5. For NLO purposes, versatile parameters have been computed. NLO activities of a newly synthesized material can be explored through polarizability (α) and first-order hyperpolarizability (β) parameters. The characteristics of NLOs increase with the magnitude of the parameters such as α, and β. B3LYP/6-311G (d, p) method along with the keyword ‘polar’, was employed to calculate polarizability and hyperpolarizabilities.

Electrical polarizability is the relative tendency to distribute charges, such as the electron cloud of a molecule, by an external electrical field. The mean polarizability is defined, as the polarizability anisotropy invariant. The following equation (**1**) describes the mean polarizability (α_{ave}):

$$\alpha_{ave} = (\alpha_{xx} + \alpha_{yy} + \alpha_{zz}) / \text{۳} \qquad \textbf{(1)}$$

The polarizability tensors in the output file of Gaussian09 are in this order: α_{xx}, α_{xy}, α_{yy}, α_{xz}, α_{yz}, and α_{zz}.

Aryl Schiff bases are considered a very remarkable category of organic compounds because of their π-delocalized structure. Thus, the delocalization of the π-electrons defines the classic structures with an optical response due to the large hyperpolarizabilities that result from a push-pull system [40-42]. The non-linear optical response of the *EE-bis*-Schiff base is investigated by the static hyperpolarizability coefficients (β), calculated using the quantum chemistry algorithms (equation **2**).

$$\beta_{total} = [(\beta_x{}^2 + \beta_y{}^2 + \beta_z{}^2)]^{1/2} \qquad (2)$$

$$\beta_x = \beta_{xxx} + \beta_{xyy} + \beta_{xzz} \qquad \beta_y = \beta_{yyy} + \beta_{yzz} + \beta_{yxx} \qquad \beta_z = \beta_{zzz} + \beta_{zyy} + \beta_{zxx}$$

The calculated values of the mean polarizability (α_{ave}) and the first-order hyperpolarizabilities (β_{total}) are listed in Table 5. Urea is one of the prototypical molecules used in the study of the NLO properties of molecular systems. Therefore, it was used frequently for comparative purposes. For the urea molecule, α_{ave} and β_{total} values were calculated at the same theoretical level. These values are 288.82×10^{-24} *esu* and 137.985×10^{-30} *esu*, respectively. The comparison of the optical properties of urea and the bis-Schiff base shows that the optical properties of the synthesized bis-Schiff base are lower than those of urea. The presence of six methylene (CH_2) groups between two aromatic rings prevents electron delocalization and resonance among $N(NO_2)_2$ and C=N groups. This item decreases α_{ave} and β_{total} values for **L**.

Table 5. The computed polarizability, and first hyperpolarizability values of the title compound

Parameter	Value	Parameter	Value
α_{xx}	488.97	β_{xxx}	0.0114815
α_{xy}	17.02	β_{xyy}	0.0018856
α_{xz}	248.81	β_{xzz}	0.0003296
α_{yy}	44.92	β_{yyy}	-0.0001259
α_{yz}	26.74	β_{yxx}	-0.0007933
α_{zz}	152.59	β_{yzz}	-0.0003678
α_{ave} (*a.u.)*	612.09	β_{zzz}	-0.0001978
α_{ave} (*esu)*	288.82×10^{-24}	β_{zxx}	0.0001763
		β_{zyy}	-0.000752
		β_{total} (*a.u.*)	0.0134
		β_{total} (*esu*)	0.13798×10^{-30}

3.6. Infrared Spectrum Analysis

Infrared (IR) spectroscopy is a technique that deals with the IR region of the electromagnetic spectrum. This spectroscopy is used in chemistry for the identification of functional groups to elucidate the structure of a molecule, kinetics of chemical reactions, *etc*. In **Figure 3**, the theoretical (simulated) IR spectrum related to ***EE*** is observable. The bis-Schiff base (***EE***) belongs to the C1 point group and consists of 42 atoms, having 144 normal vibrational modes. The following are some of the critical observed vibrational motions: The stretching, in-plane bending, torsional, and out-of-plane bending vibration modes of this compound are presented in Table 6.

CH vibrations The C-H stretching vibrations of aromatic structures generally occur in the region 3000–3100 cm^{-1}, while the saturated hydrocarbon shows C-H stretching absorption bands in the region 3000–2978 cm^{-1} [43]. ***EE*** has 3 types of C-H bonds: 8 aromatics, 6 CH_2 groups, and two N=C-H bonds. The aromatic stretching bands of this molecule are calculated at 3172, 3204, and 3225 cm^{-1}. For the aliphatic NC-H bonds (N-methyl groups) 2947, the symmetric C-H stretching vibrations are calculated at 3172 cm^{-1} and the unsymmetrical C-H stretching vibrations are at 3225 cm^{-1}. The C-H modes of methylene groups are at 2947 cm^{-1}.

The CH in-plane bending modes are mainly observed as combined with other vibrational modes. For example, the observed bands at 1003, 1005, 1015, 1017, 1027, 1123, 1444, 1522, and 1195 cm^{-1}, including in-plane bending modes, are mixed with other vibrational modes. However, aromatic CH in-plane bending modes of the title compound appear at 1522 cm^{-1}. As a result of these mentioned, we can conclude that the CH in-plane bending vibrations can occur in the region

1000–1600 *cm*$^{-1}$. The CH out-of-plane bending vibrations are observed at the 650–1000 *cm*$^{-1}$ interval. In this connection, the observed bands at 976, 967, 906, 889, 844, 821, and 764 *cm*$^{-1}$ are assigned to the CH out-of-plane bending modes. The aromatic ring C-H in-plane bending vibrations are usually weak and observed in the 1300–998 *cm*$^{-1}$ region (exp. 1286–980 *cm*$^{-1}$), while the C-H out-of-plane bending vibrations lie in the 965–806 *cm*$^{-1}$ region (exp. 980–784 *cm*$^{-1}$).

***CC* vibrations.** The aromatic ring CC stretching vibrations, which are called skeletal vibrations, usually occur in the region 1400–1625 *cm*$^{-1}$ [44]. Nevertheless, these bands can generally be observed as associated with other bands below 1400 *cm*$^{-1}$. As seen from Table 6, the CC stretching modes are available in the region 900–1600 *cm*$^{-1}$ for aromatic rings. The observed bands at 654 *cm*$^{-1}$ can be assigned to the CCC in-plane bending vibrations of aromatic rings in the title compound. Likewise, the CCCC torsional modes are observed at 700,703 *cm*$^{-}$

CN vibrations. The most characteristic band of the Schiff base derivatives is due to N=C stretching vibration in the region 1500–1700 *cm*$^{-1}$ [45]. The azomethine N=C stretching vibration is observed in a strong band in the FT-IR spectrum (Figure 5) at 1639 *cm*$^{-1}$, while the calculated value for this band is predicted at 1712 *cm*$^{-1}$. The N=C stretching mode in our study is in good agreement with similar Schiff base compounds in the literature [46]. All amine compounds exhibit the N-C stretching vibrational in the region 1000–1350 *cm*$^{-1}$. The observed band at 1117 *cm*$^{-1}$ can be assigned to NO_2, while the calculated value for this band is predicted at 1117, 1377 *cm*$^{-1}$.

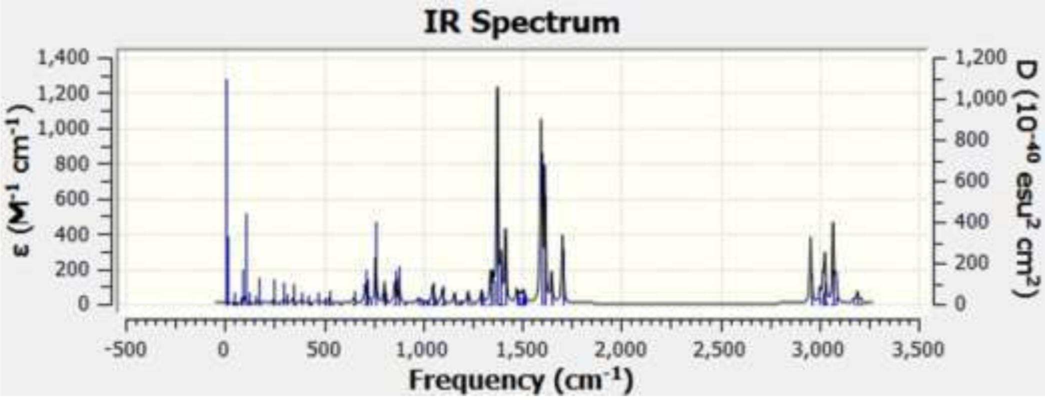

Figure 5. The IR spectrum of Schiff base **L** ligand

Table 6. The calculated and experimental wavenumbers of the *EE*-bis-Schiff base

υ computational	**υexperimental**	**Assignment**
7,12,21,23,32,48,54,59,65,71,74		υ(torsional vibration)
109		υ(skeletal vibration)
123,128		υ(CH2), bending, rocking

134		υ(CH2), bending
148,163,176		υ(N-CH3, CH2, CH=N), bending
189		(CHN-C-N-CH), twisting
236		υ(Ring, CH2), bending
244		υ(CH=N), bending
262,269		υ(N-CH,CH_2), bending, twisting
323,334,342		υ(Skeletal), bending, in plane
378		υ(CH=N-CH2), bending, in plane
404		υ(CH=N-CH2), bending, oop
419		υ(skeletal) bending
422		υ(HCCH(ring), bending, oop, twisting
447	447	υ(CH2), bending, in a plane
482	484	υ(Skeletal), bending, in plane
507,513		υ(Skeletal), bending, oop
530,532		υ (HCCH(ring), bending, oop, wagging
562,567	542	υ (HCCH(ring), bending, oop, wagging, and υ(NMe, CH2),bending, in plane
645		υ(ccc-ring), bending, in plane
700,703,708		υ(cccc-ring), bending, in plane , (CH=N-CH2) bending
738	726	υ(CH2), bending, in plane, rocking
751		υ(HCCH-ring), bending, oop

758,807		υ(CH2) bending, twisting
846,852		υ(HCCH-ring , CH=N-CH2), bending, in plane
854,855,877,878	850	υ(HCCH-ring), bending, oop
882,887		υ(CCC ring, CH=N-CH2), bending, oop, wagging
903		υ(CH2), bending, rocking
976		υ(CH ring, CH=N,CH2), bending, twisting
981		υ(CH ring, CH=N), bending, twisting
992		υ(CH ring), bending, twisting
994		υ(CH ring), bending, twisting
1003		υ(CH2), bending,
1005		υ(CH ring, CH=N), bending, twisting
1015		υ(CH ring), bending, twisting
1017		υ(CH ring, CH=N), bending, twisting
1027		υ(CH2, CH=N), bending,
1030		υ(C-C ring), stretching,
1046		υ(CH=N-C),stretching, unsymmetrical
1049		υ(CH2, CH=N), bending,
1057		υ(CH=N-C), stretching, symmetrical
1062		υ(CH2-CH2 CH2-CH2), stretching, symmetrical
1110		υ(CH=N-C, CH2-CH2), stretching, symmetrical

1117	υ(N-CCH(aromatic), stretching
1123	υ(CH, aromatic), bending, twisting
1171,1190	υ(CH2), bending, twisting
1188,1195	υ(CH2, CH, aromatic), bending, twisting
1239,1240	υ(CH-NCH), bending, twisting,
1244,1255	υ(CH2), Rocking
1297	υ(CH2), twisting
1316	υ (CH,aromatic) bending, twisting
1320	υ(CH2, aliphatic, CH,aromatic), bending
1329,1335	υ(CH2), twisting
1350	υ(CH2, aliphatic, CH=N), bending, oop, wagging,
1353	υ(C-C aromatic), stretching
1357	υ(C-CH aromatic), stretching,(CH=N), bending
1377	υ(N-ring), stretching , υ(CH_2-NCH), bending, twisting
1380	υ(CH2, aliphatic, CH=N), bending, wagging,
1392	υ(CH2, aliphatic, CH=N), bending, wagging
1404	υ(CH2, aliphatic), bending, oop, wagging
1408,1409	υ(CH2, aliphatic, CH=N), bending, in plane, scissoring

1444		υ(CH, aromatic), (CH=N)), bending
1487,1491,1496,1507,1516		υ(CH2, aliphatic), bending, in plane, Rocking
1522	1535	υ(CH, aromatic), bending, in plane
1594		υ(C-C, aromatic), stretching, symmetrical
1640	1643	υ(CH,aromatic)stretching, symmetrical
1650		υ(NO,C-CH)stretching, unsymmetrical
1717,1718		υ(C=N), stretching, symmetrical
2947	2819,2853	υ(NC-H, aliphatic), stretching, unsymmetrical
2978		υ(N=C-H, imine), stretching, unsymmetrical
2997		υ(CH2,aliphatic),stretching, symmetrical
3003,3015		υ(CH2, aliphatic), stretching, unsymmetrical
3018,3019,3029		υ(CH2, aliphatic), stretching, symmetrical
3037		υ(CH2, aliphatic), stretching, unsymmetrical
3064		υ(CH2, aliphatic), stretching, unsymmetrical
3070		υ(CH2, aliphatic), stretching, symmetrical
3204,3172		υ(CH,aromatic),stretching, unsymmetrical
3225		υ(CH, aromatic), stretching, symmetrical

3.7. ^{1}H-NMR and ^{13}CNMR spectra of ligand (L)

The ligand (**EE**) is formed when hexane-1,6-diamine reacts with 4-nitrobenzaldehyde. NMR study ensures the ligand aromatic ring structure, imine (H–C=N), and CH_2 groups. ^{1}HNMR identifies all protons' environments, while ^{13}C characterizes the C-atoms in the ligand structure (Figure 6). In ligand **L**, the aromatic, imine (H–C=N), and CH_2 proton NMR peak appears at δ (9.23, 9.05, and 8.1*)* and δ 9.15 and (1.97- 4.8) *ppm*. The^{1}HNMR study has effectively verified the imine bond formation Table 7, Further, a ^{13}CNMR study in ligand confirmed the C-nature in aromatic-C, C-ET, and C-imine appears a (150.38,146.38,134.10,130.47,127.40) and 161.07 and (69.01,36.58,32.37) *ppm*. In the excremental part, the data are as follows in the ^{1}HNMR data (300 *MHz*, MeOD): 8.50 (s, 2H), 7.98-8.30 (m, 8H), 1.39-3.64 (m, 12H) *ppm*; ^{13}CNMR (75 *MHz*, MeOD): 155.92, 146.44, 139.27, 126.14, 129.06, 160.33, 59.33, 28.12, 24.65*ppm.*

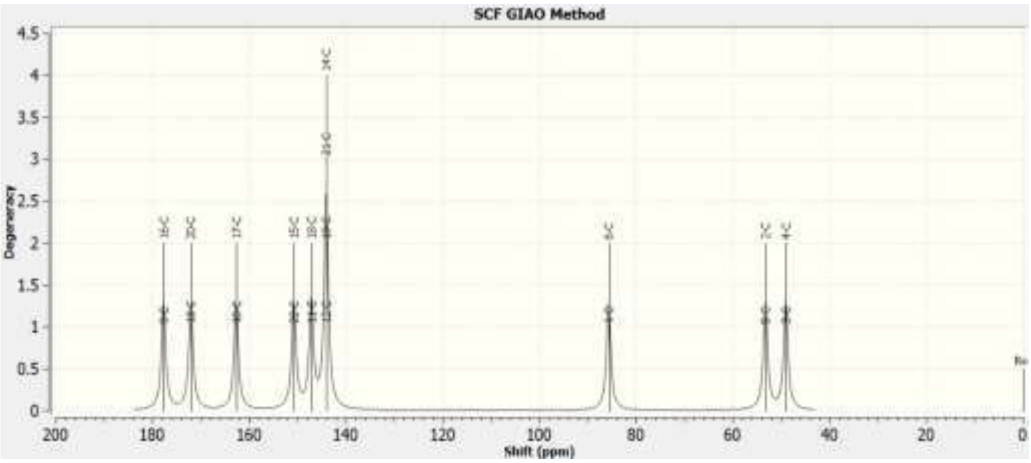

Figure6. 13C.NMR spectrum of Schiff base L ligand

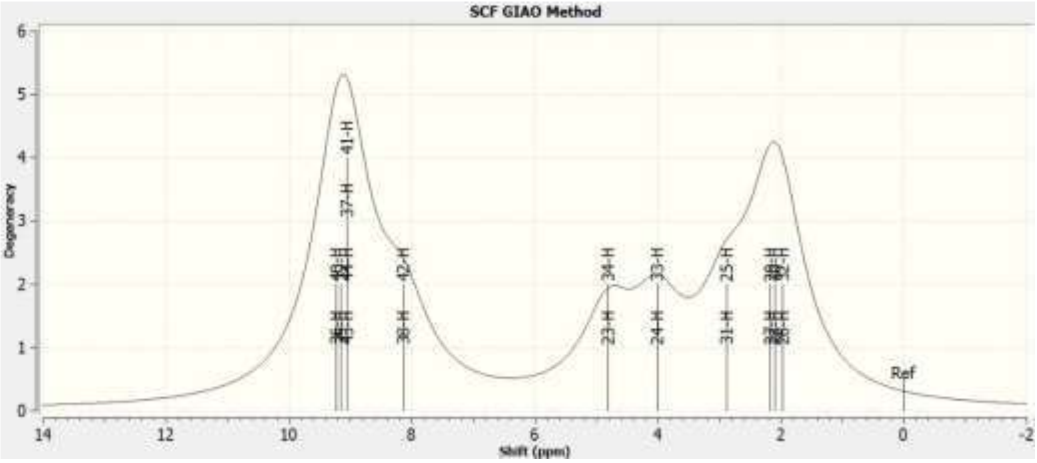

Figure7. ^{1}HNMR spectrum of Schiff base L ligan

Table 7. Characteristics ^{1}H NMR data of the studied compound

Atom	**Computational(*ppm*)**	**Experimental (*ppm*)**
S, 2H -imine	9.15	8.50
m, 8H-aromatice	9.23,9.05,*8.1*	7.98-8.30
m, 12H-CH_2	1.97- 4.8	1.39-3.64

Table 7. Characteristics ^{13}C NMR data of the studied compound

Atom	**Computational(*ppm*)**	**Experimental (*ppm*)**
C-nature	150.38,146.38,134.10,130.47,127.40	155.92, 146.44, 139.27, 126.14, 129.06
C- ET	161.07	160.33
C-imine	69.01,36.58,32.37	59.33, 28.12, 24.65

3.8. Quantum reactivity parameters

Figure 8 shows the HOMO and LUMO orbitals shapes of ***EE*** in the gaseous phase. The HOMO is at -7.451*eV.*, while the LUMO is located at 2.906 *eV.* with a 4.545*eV.* energy gap. The calculated energy gap value revealed the ease of electron excitation from HOMO to LUMO. The HOMO was found to be a predominant molecular orbital, which is consistent with the overall nature of the bidentate ligand with a high degree of nucleophilicity. Also, the HOMO–LUMO energy gap is related to chemical reactivity or kinetic stability.

Using Koopmans's theorem for closed-shell components IP and Electron affinity (EA) can be defined for the compounds. Electron affinity refers to the capability of a ligand to accept precisely one electron from a donor. However, in many kinds of bonding, viz., covalent hydrogen bonding, partial charge transfer takes place. The EA and IP given by the B3LYP method for the title compound are 2.906 *eV* and 1.1361 *eV*, respectively. Chemical hardness (η) is a significant quantity that measures the resistance of a chemical component to the change of its electronic structure, which is defined as the second derivative of energy concerning the number of electrons in a constant external potential. According to Koopmans's theory, the approximate value of chemical hardness is obtained from the relation $\eta=(E_{HOMO}-E_{LUMO})/2$. Lower chemical hardness indicates that the electron density is more easily affected and the molecule is more active. It improves the electron cloud by the electric field towards the acceptor group and causes more intramolecular charge transfer in the molecule. As a result, less chemical hardness means more polarizability and hyperpolarizability. The reactivity descriptors of the reported molecules, namely E_{HOMO}, E_{LUMO}, energy gap (ΔE), chemical hardness (η), electron affinity (*EA*), ionization potential (*IP*), electronegativity (χ), electrophilicity index (ω) and chemical softness (*S*), were estimated by the DFT method. Table 8 gives the global chemical reactivity descriptors for the **EE** ligand.

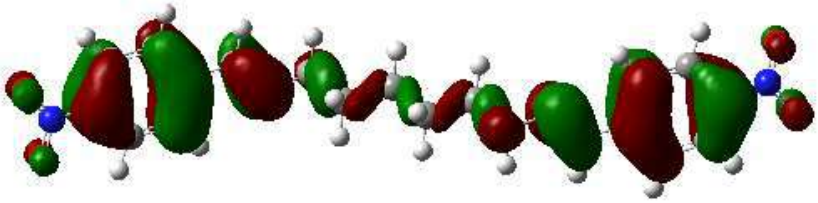

LUMO orbital

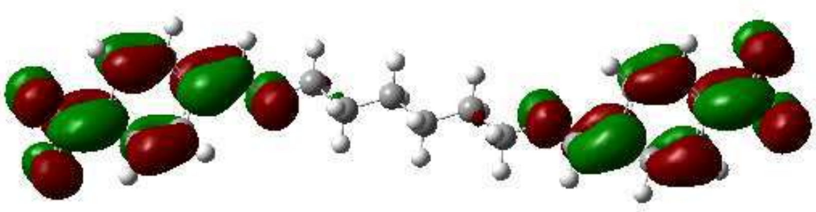

HOMO orbital

Figure 8. HOMO and LUMO orbital

Table 8. The calculated global chemical reactivity descriptors for the **EE** ligand

Parameter (*eV*)	**value**
E_{HOMO}	-7.451
E_{LUMO}	-2.906
ΔE (a.u.)	0.167
$E_{HOMO}–E_{LUMO}$ (ΔE)	4.545
Ionization potential [$I = -E_{HOMO}$]	7.451
Electron affinity [$A = -E_{LUMO}$]	2.906
Chemical hardness [$\eta = (I - A)/2$]	2.2725
Electronegativity [$\chi = -(I + A)/2$]	-2.2725
Softness [$\zeta = 1/2\eta$]	1.1362
Electrophilicity index [$\psi = \chi^2/2\eta$]	1.1361

3.9. Molecular electrostatic potential

Electrostatic potential maps are handy 3D diagrams of molecules that show the three-dimensional charge distribution of the molecule [43]. Charge distribution levels help us a lot in identifying reactive sites and how molecules interact with each other. Electrostatic potential surfaces can be used to understand the chemical reactivity of ligands. In electrostatic potential maps, negative sites with high electron density are colored red. While positive regions with low electron density are blue and green is used for neutral [44]. Figure 9 shows the electrostatic potential map for ligand (**L**). The green color in the ligand (**L**) shows that this part of the molecular structure has no desire to participate in the reaction and is completely neutral regarding reactivity. The highest negative electron density is observed in the place of the imine group (CH=N) of the ligand. The red color of these regions shows that imine groups are suitable sites for attracting electrophilic species. Therefore, the more negative electronegative and positive electrostatic potential sites are more favorable for the attraction of nucleophilic and electrophilic species.

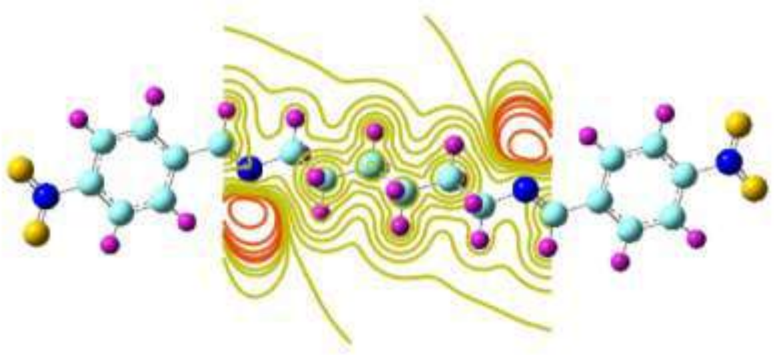

Figure 9. molecular electrostatic potential for **L**

3.11. Reduced Density Gradient (RDG) analysis

RDG analysis is a computational method used in quantum chemistry to analyze the electron density and molecular properties [47-50]. RDG is a technique used to visualize and interpret molecular interactions by examining the electron density and its gradients. The RDG value helps identify regions of significant electron density, which correlate with regions of non-covalent interactions, such as hydrogen bonding, van der Waals interactions, and π-stacking.

In studying Schiff bases, RDG can help identify non-covalent interactions that influence properties like stability, reactivity, and molecular recognition. Analysis may reveal regions of electron donation or acceptance, pertinent to understanding catalytic activity, medicinal chemistry, and materials science or binding affinity in biochemical systems. RDG plots typically show color-coded iso-surfaces or 2D plots that highlight areas of low (blue) and high (red) electron density gradients. This visualization can elucidate interaction hotspots and predict behavior in chemical reactions or interactions with biological targets.

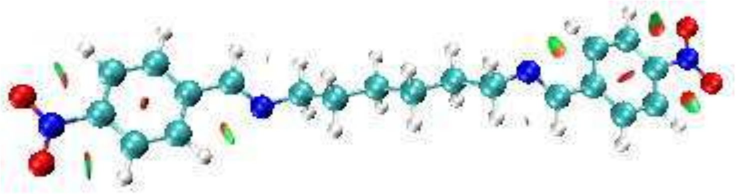

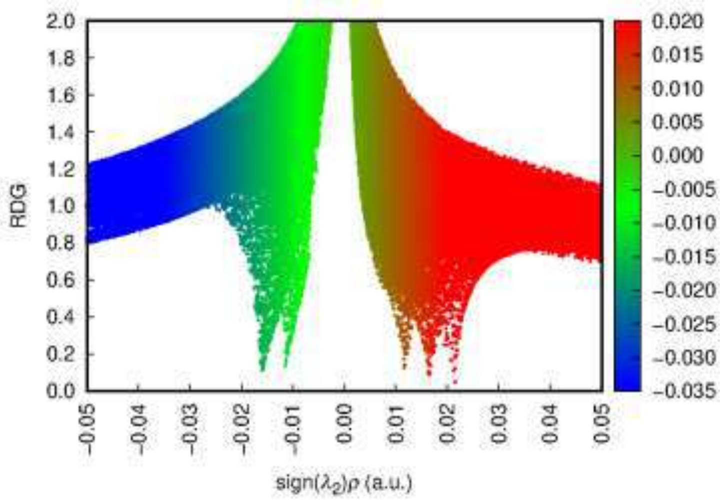

3.10. Molecular docking study

Following the current research, the molecular docking of receptors 1HSG, 6LU7, and 1AJ6 and Doxorubicin has been used as the reference drug with ligand (**L**) (Figure 10) was examined. Table 8 presents the centers and dimensions of the Cartesian grid box of the protein receptors studied for conducting molecular docking with ligand (**L**).

Table 9. Centers and sizes of the Cartesian grid box for the protein receptors under study

Receptor	Center			Size		
	X	Y	Z	X	Y	Z
1AJ6	59.2	5.6	45.0	79.3	29.3	66.7
6LU7	-26.9	12.5	55.6	-3.3	36.1	79.3
1HSG	59.3	6.4	39.3	79.5	30.0	63.0

In Table 9, you can find the data related to the binding free energy and ligand interactions, such as hydrogen and hydrophobic bonds, obtained from molecular docking studies using the AutoDock program. After the docking process, the most favorable conformation with the lowest binding energy was chosen. The lower the energy value, the more the ligand is inclined to occupy the receptor's binding site. According to Table 9**,** the binding energies of the studied ligand (**L$_1$**) with receptors 1HSG, 6LU7, and 1AJ6 are 96.7, 85.0, and 73.7 kilocalories per mole, respectively. It's worth noting that the strongest interaction and binding of the ligand occur at the active site of receptor 6LU7. Qualitative analyses have revealed that specific amino acid residues in the active sites of receptors 1HSG, 6LU7, and 1AJ6, namely, are involved in the formation of hydrogen bonds with nitro groups (Figure 10). The results of molecular docking demonstrated the promising performance and acceptable binding energy of the studied ligand. Given the presence of two nitro groups in the para position of the aromatic ring and the imine moiety, it was anticipated that the studied ligand would act as a potent inhibitor. The docking results of ligand (**L$_1$**) indicated its capability to bind to the active sites of the protein receptors under investigation in this study, exerting some degree of inhibition. Based on the docking results, the inhibitory potential of the studied ligand varies across the protein receptors' active sites, with binding energies ranging from 3.7 to 5.8 *kcal/mol*. The lowest binding energy corresponds to receptor 1AJ6 with an inhibitory constant (K_i) of 6.7 μM, while the highest binding energy is associated with receptor 6LU7 with an inhibitory constant of 25.1 μM.

Table 9. The affinity energy and interaction between ligand (**L**) and amino acids at the Active site of receptors

Receptor	Affinity Energy ($kcal\ mol^{-1}$)	Ki (μM)	Hydrogen interactions (distance: *Å*)	Hydrophobic interactions
1AJ6	-7.03	7.06	ARG192(2.68)-ASP214(1.99)-ASP214(1.92)-ASP214(2.07)-ASP214(1.85)-	TYR184-ALA188-LYS189-PHE216
6LU7	-8.05	1.25	HIS172(2.87)-THR169(2.66)-THR169(2.11)-THR169(2.04)	SER139-GLY138-GLY170-GLU166-PHE140-LEU141-LYS137-VAL171
1HSG	-7.96	1.46	GLY27(2.01)-GLY27(2.05)-ASP30(2.36)-ASP30(1.85)	LEU23-ARG8-GLY49-ILE50-ASP25-ALA28-ASP29-ASP25-GLY27-GLY49-ILE50-ILE84-LEU23-ASP29-VAL32-LEU76-ILE47-CLY48
Doxorubicin	-6.98	7.71	Ala 835 (4.25); Leu 837 (3.38); Tyr 740 (5.59); Glu 842 (5.41); Glu 842 (5.19)	Tyr845, Glu844, His846, Leu846, Gly839, Val741, Glu738,Asn676

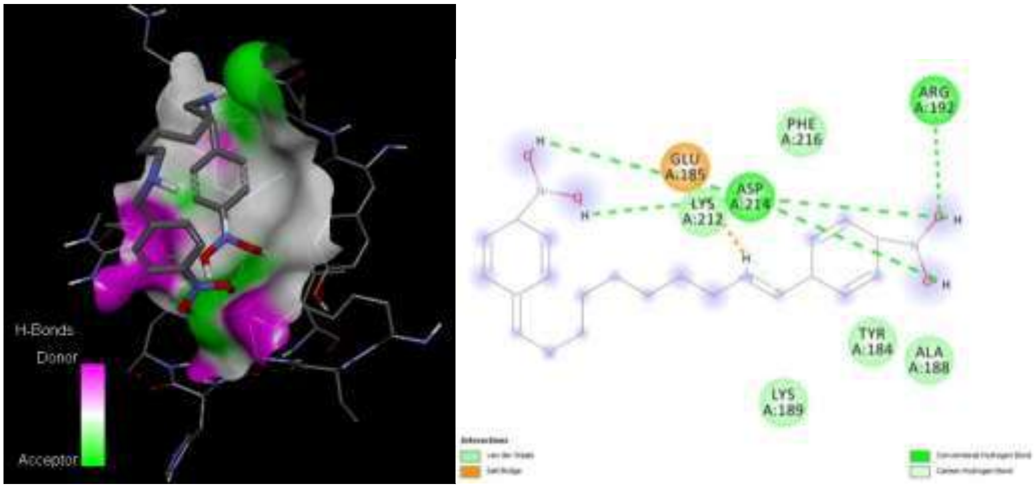
H-Bonds
Donor
Acceptor
ARG A:192
PHE A:216
GLU A:185
ASP A:214
LYS A:212
TYR A:184
ALA A:188
LYS A:189
Interactions

(a) 1AJ6

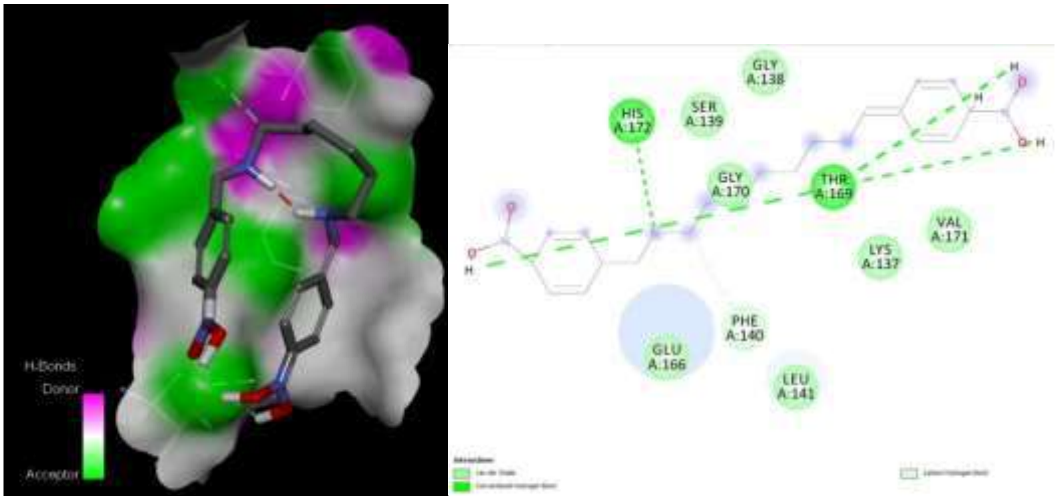
H-Bonds
Donor
Acceptor
GLY A:138
HIS A:172
SER A:139
GLY A:170
THR A:169
VAL A:171
LYS A:137
PHE A:140
GLU A:166
LEU A:141
Interactions

(b) 6LU7

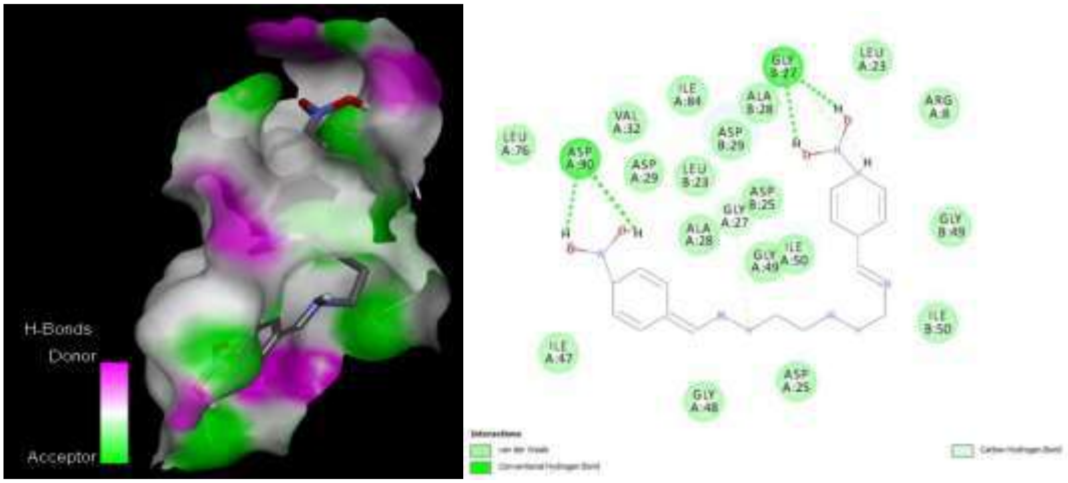

(c) 1HSG

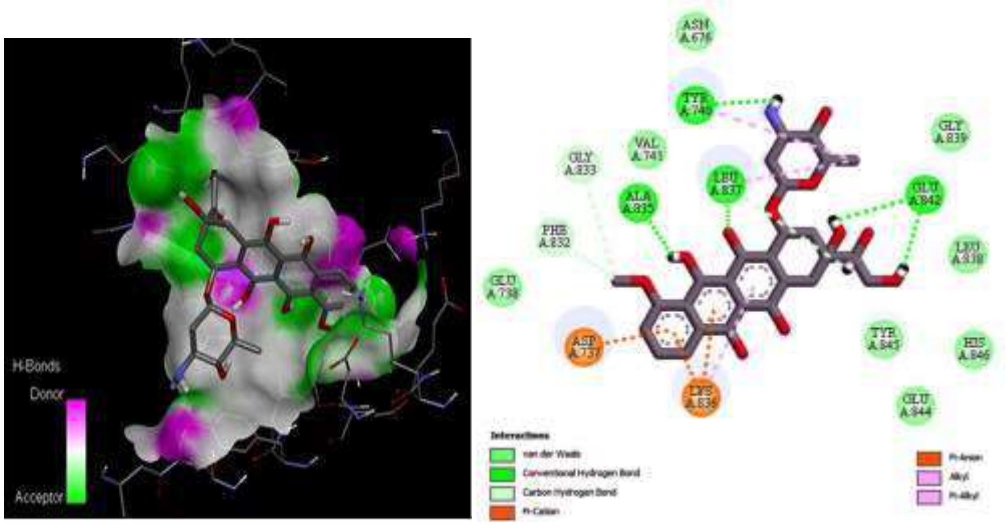

(d) Doxorubicin

Figure 10. Display of two-dimensional and three-dimensional interaction of the ligand (L2) with the active site of receptors: a). 1AJ6, b). 6LU7, and c). 1HSG and d). Doxorubicin

Some of the quantitative assessments of docking results, such as intermolecular energy, van der Waals energy, electrostatic energy, total internal energy, docking energy, binding energy, and inhibition constant (Ki), are listed in Table 10. The findings from the docking simulation reveal the interaction of the studied ligand with the receptor's active site. The derived values of 8.05 *kcal/mol* for binding energy, 11.06 *kcal/mol* for docking energy, and 1.25 μM for the inhibition constant indicate the potential effectiveness of inhibiting this ligand in the activity of receptor 6LU7. In this molecular simulation, the calculated binding energy and docking energy represent a combination of intramolecular energy with free torsional energy and the ligand's internal energy, respectively [45].

Table 10. Results of Molecular Docking Ligand-Receptor *(Kcal/mol)*

Parameters	Receptors		
	1HSG	6LU7	1AJ6
K_i (μM)	+1.46	+1.25	+7.06
Unbound system energy	-0.02	+1.17	+0.86
Torsional Free energy	+4.18	+4.18	+4.18
Final total internal energy	-0.02	+1.17	+0.86
Electrostatic energy	-3.59	-2.72	-2.65
VdW+Hbond+ dissolve energy	-8.55	-9.51	-8.56
Final intermolecular energy	-12.14	-12.23	-11.20
Binding energy	-7.96	-8.05	-7.03
Docked energy	-12.16	-11.06	-10.64

4. Conclusions

Using the DFT method, we investigated a new Schiff base previously synthesized by the classical method. The molecular structure of this compound has been optimized using the DFT/B3LYP method and 6-311G (d, p) basis set. NLO and global reactivity parameters have been calculated to explain the versatile properties of the ligand. The NLO computed α and β parameters suggest that the compounds may have significant optoelectronic applications. the prepared molecule shows potential as an organic NLO material in the field of optoelectronics. The NMR and IR spectrum data from the experimental part are consistent with the DFT data. The calculated bond distances and bond angles showed good agreement with the literature. The IR vibrational frequencies are calculated, and the fundamental bands are assigned and compared with the experimental data. It was found that the relationship between donor/acceptor moieties, the pass length, as well as the energy gap between the highest occupied molecular orbital (HOMO) and the lowest unoccupied molecular orbital (LUMO) strongly influenced the NLO response. Molecular docking was conducted to test the biological potency. Accordingly, results proved the antimicrobial effect of compounds by binding to proteins. This 6LU7 protein interacts most with ligand L and its binding energy is 8.05 kcal/mol. The designed Schiff base ligand can be useful as a suitable candidate for new inhibitory drugs in the future due to its medicinal value with fewer side effects and with suitable hydrophilicity for gastrointestinal absorption and intestinal permeability of the drug.

5. References

[1] MUMIT, Mohammad Abdul, et al. DFT studies on vibrational and electronic spectra, HOMO–LUMO, MEP, HOMA, NBO, and molecular docking analysis of benzyl-3-N-(2,4,5-trimethoxyphenylmethylene) hydrazinecarbodithioate. 2020,1220:128715. https://doi.org/10.1016/j.molstruc.2020.128715

[2] Pillai, R. R., Karrouchi, K., Fettach, S., Armaković, S., Armaković, S.J, Brik, Y, & Faouzi, M. E. A. (2019). Synthesis, spectroscopic characterization, reactive properties by DFT calculations, molecular dynamics simulations and biological evaluation of Schiff bases tethered 1, 2, 4-triazole and pyrazole rings. *Journal of Molecular Structure*, *1177*, 47-54.

[3] REZVAN, Vahideh Hadigheh; AFSANEH, Alireza. Green synthesis of a novel bis-Schiff base derived from 4-N,N-dimethylaminobenzaldehyde and hexamethylenediamine: DFT study. 2024, ١٣٨٧٤٤. https://doi.org/١٠,١٠١٦/j.molstruc.٢٠٢٤,١٣٨٧٤٤

[4] NALINI, R., et al. Synthesis, characterization, DFT analysis, biological evaluation, and molecular docking of Schiff Base derived from Isatin–isoniazid and its metal (II) complexes. 2023, ٤٣,٨: ٧٥٩٧-٧٦١٤. https://doi.org/10.1080/10406638.2022.2138927

[5]Jean-Baptiste, K. N., Guillaume, K. C., Adama, O. Z., Claude, K. A. L., Jacques, D. K., & Nahosse, K. B. A. Z. (2017). Synthesis, Characterization and Biological Evaluation of New Series of Schiff Bases Derived from Hexamethylenediamine as Potential Antibacterial and Antifungal Agents. *Appl. Sci.(ISSN 2455-4499)*, *7*, 69-74. http://dx.doi.org/10.21013/jas.v7.n2.p3

[6] Gomha, S. M., El-Sayed, A. A. A., Alrehaily, A., Elbadawy, H. M., Farag, B., Al-Shahri, A. A., & Zaki, M. E. (2024). Synthesis, molecular docking, in silico study, and evaluation of bis-thiazole-based curcumin derivatives as potential antimicrobial agents. *Results in Chemistry*, *7*, ١٠١٥٠٤. https://doi.org/10.1016/j.rechem.2024.101504

[7] Mondal, S., Mandal, S. M., Mondal, T. K., & Sinha, C. (2017). Spectroscopic characterization, antimicrobial activity, DFT computation and docking studies of sulfonamide Schiff bases. *Journal of Molecular Structure*, *1127*, 557-567. https://doi.org/10.1016/j.molstruc.2016.08.011

[8] Slassi, S., Aarjane, M., & Amine, A. (2022). Synthesis, spectroscopic characterization (FT-IR, NMR, UV-Vis), DFT study, antibacterial and antioxidant in vitro investigations of 4, 6-bis ((E)-1-((3-(1H-imidazol-1-yl) propyl) imino) ethyl) benzene-1, 3-diol. *1255*, 132457. https://doi.org/10.1016/j.molstruc.2022.132457

[9] Sieffert N, Wipff G (2015) Uranyl extraction by N, N-dialkylamide ligands studied using static and dynamic DFT simulations. 44:2623-38. https://doi.org/10.1039/C4DT02443E

[10] Salihović, M., Pazalja, M., Mahmutović-Dizdarević, I., Jerković-Mujkić, A., Suljagić, J., Špirtović-Halilović, S., & Šapčanin, A. (2018). Synthesis, DFT study and antimicrobial activity of Schiff bases derived from benzaldehydes and amino acids. *Rasayan Journal of Chemistry*, *11*(3).http://dx.doi.org/10.31788/RJC.2018.1133077

[11 Salihović, M., Pazalja, M., Mahmutović-Dizdarević, I., Jerković-Mujkić, A., Suljagić, J., Špirtović-Halilović, S., & Šapčanin, A. (2018). Synthesis, DFT study and antimicrobial activity of Schiff bases derived from benzaldehydes and amino acids. *Rasayan Journal of Chemistry*, *11*(3).https://doi.org/10.1016/j.molstruc.2023.137230

[12] Alnoman, M. M., Parveen, S., Alnoman, R. B., Khan, A., Khaleil, M. M., Jaremko, M., & Emwas, A. H. (2024). New Co (II) Schiff base complexes of 3-ethoxy-4-hydroxybenzaldehyde and chlorophenyl ethylamine derivatives as potent antimicrobial agents: Design, synthesis, molecular docking, DFT calculations, and in silico ADME profiles. *Journal of Molecular Structure*, *1307*, 138021.https://doi.org/10.1016/j.molstruc.2024.138021

[13] Jean-Baptiste, K. N., Guillaume, K. C., Adama, O. Z., Claude, K. A. L., Jacques, D. K., & Nahosse, K. B. A. Z. (2017). Synthesis, Characterization and Biological Evaluation of New Series of Schiff Bases Derived from Hexamethylenediamine as Potential Antibacterial and Antifungal Agents. *Appl. Sci.(ISSN 2455-4499)*, *7*, 69-74.https://doi.org/10.21013/jas.v7.n2.p3

[14] Mohapatra, R. K., Sarangi, A. K., Azam, M., & El-Ajaily, M. M. (2019). Kudrat-E-Zahan, M.; Patjoshi, SB; Dash, DC Synthesis, structural investigations, DFT, molecular docking and antifungal studies of transition metal complexes with benzothiazole based Schiff base ligands. *J. Mol. Struct*, *1179*, 65-75. https://doi.org/10.1016/j.molstruc.2018.10.070

[15] Yiğit B, Yiğit M, Taslimi P, Gök Y, Gülçin İ (2018) Schiff bases and their amines: Synthesis and discovery of carbonic anhydrase and acetylcholinesterase enzymes inhibitors. Arch. Pharm. Chem. Life Sci. 351:e1800146. https://doi.org/10.1002/ardp.201800146

[16] MAHMOUD, Walaa; REFAAT, Ahmed M.; MOHAMED, Gehad G. Nano Schiff base, and its metal complexes: synthesis, characterization tools, biological applications, and molecular docking studies. 2020, 63.6: 2157-2176. ١٠,٢١٦٠٨/EJCHEM.٢٠١٩,١٨١٠٩,٢١٠٤

[17] Abedin, M. M., Pal, T. K., Sheikh, M. C., & Alam, M. A. (2024). Investigation on synthesized sulfonamide Schiff base with DFT approaches and in silico pharmacokinetic studies: Topological, NBO, and NLO analyses. *Heliyon*, *10*(14).https://doi.org/10.1016/j.heliyon.2024.e34499

[18] Andiappan K, Sanmugam A, Deivanayagam E, Karuppasamy K, Kim HS, Vikraman D (2018) In vitro Cytotoxicity Activity of Novel Schiff Base Ligand-Lanthanide Complexes.8:3054. https://doi.org/10.1038/s41598-018-21366-1

[19] AVCI, Davut, Novel Schiff base-azide metal complexes: Synthesis, spectral, nonlinear optics, and DFT studies. 2024, 179: 108523. https://doi.org/10.1016/j.mssp.2024.108523

[20] MAJUMDAR, Dhrubajyoti, 8-Aminoquinoline derived two Schiff base platforms: Synthesis, characterization, DFT insights, corrosion inhibitor, molecular docking, and pH-dependent antibacterial study. 2024, 10.15. https://doi.org/10.1016/j.heliyon.2024.e35591

[21] TAHIR, Muhammad Nawaz, Synthesis, Characterizations, Hirshfeld Surface Analysis, DFT, and NLO Study of a Schiff Base Derived from Trifluoromethyl Amine. 2024, 9.2: 2325-2338. DOI: 10.1021/acsomega.3c05199

[21] BABAEI, Parisa, REZVAN, Vahideh Hadigheh. Molecular docking and in vitro biological studies of a Schiff base ligand as anticancer and antibacterial agents. 2024, 7: 101517. https://doi.org/10.1016/j.rechem.2024.101517

[22] Mumit, M. A., Pal, T. K., Alam, M. A., Islam, M. A. A. A. A., Paul, S., & Sheikh, M. C. (2020). DFT studies on vibrational and electronic spectra, HOMO–LUMO, MEP, HOMA, NBO

and molecular docking analysis of benzyl-3-N-(2, 4, 5-trimethoxyphenylmethylene) hydrazinecarbodithioate. *Journal of molecular structure*, *1220*, ١٢٨٧١٥.https://doi.org/10.1016/j.molstruc.2020.128715

[23] SINGHAL, Sugandha; Khanna, Pankaj; Khanna, Leena. Synthesis, DFT studies, molecular docking, antimicrobial screening, and UV fluorescence studies on ct-DNA for novel Schiff bases of 2-(1-aminobenzyl) benzimidazole.2019, 5.10. https://doi.org/10.1016/j.heliyon.2019.e02596

[24] MAHMOUD, Huda K.; ABBAS, Ashraf A.; GOMHA, Sobhi M. Synthesis, antimicrobial evaluation and molecular docking of new functionalized bis (1, 3, 4-thiadiazole) and bis (thiazole) derivatives. *Polycyclic aromatic compounds*, 2021, 41.9: 2029-2041. https://doi.org/10.1080/10406638.2019.1709085

[25] Mahmoud, N. H., Elsayed, G. H., Aboelnaga, A., & Fahim, A. M. (2022). Spectroscopic studies, DFT calculations, cytotoxicity activity, and docking stimulation of novel metal complexes of Schiff base ligand of isonicotinohydrazide derivative. *Applied Organometallic Chemistry*, *36*(7), e6697.https://doi.org/10.1002/aoc.6697

[26] Ganesan, T. S., Elangovan, N., Sirajunnisa, A., Angel, T., Sowrirajan, S., Chandrasekar, S.,& Thomas, R. (2024). Synthesis, quantum mechanical studies, physicochemical properties and molecular docking studies of Schiff base NN-(1, 2-Phenylene) Bis (1-(4-Bromophenyl) Methanimine) from o-phenylenediamine and 4-bromobenzaldehyde. *Polycyclic Aromatic Compounds*, *44*(3), 1971-1990.https://doi.org/10.1080/10406638.2023.2209260

[27] Suhta, A., Saral, S., Çoruh, U., Karakuş, S. E. V. G. İ., & Vazquez-Lopez, E. M. (2024). Synthesis, Single Crystal X-Ray, Hirshfeld Surface Analysis and DFT Calculation Based NBO, HOMO–LUMO, MEP, ECT and Molecular Docking Analysis of N′-[(2, 6-Dichlorophenyl) Methylidene]-2-{[3-(Trifluoromethyl) Phenyl] Amino} Benzohydrazide. *Journal of Structural Chemistry*, *65*(1), 196-215. https://doi.org/10.4103/0975-7406.129170

[28] Evecen, M., Ersanlı, C. C., Doğan, O. E., Bozkurt, İ., & AĞAR, E. Synthesis and analysis (thermodynamic, electronic, NLO, FMO, NBO, MEP, IR, UV properties, Hirshfeld surface analysis and molecular docking) of the novel Schiff base molecule:(Z)-4-bromo-2-((2, 4-dimethoxypheny) limino) methyl)-5-fluorophenol. *Available at SSRN 4976210*. http://dx.doi.org/10.2139/ssrn.4976210

[29] Dawar, N., Devi, J., Kumar, B., & Dubey, A. (2023). Synthesis, characterization, pharmacological screening, molecular docking, DFT, MESP, ADMET studies of transition metal (II) chelates of bidentate schiff base ligand. *Inorganic Chemistry Communications*, *151*, ١١٠٥٦٧.https://doi.org/10.1016/j.inoche.2023.110567

[30] BUNTROCK, Robert E. ChemOffice Ultra 7.0. *Journal of Chemical Information and Computer Sciences*, 2002, 42.6: 1505-1506.

[31] MORRIS, Garrett M., et al. AutoDock4 and AutoDockTools4: Automated docking with selective receptor flexibility. 2009, 30.16: 2785-2791. https://doi.org/10.1002/jcc.21256

[32] ZAYED, Ehab M.; MOHAMED, Gehad. Synthesis, spectroscopic, DFT, and docking studies, the molecular structure of new Schiff base metal complexes. 2022, 65.1: 633-644. 10.21608/EJCHEM.2021.83871.4116

[33] RASHDAN, Huda RM, et al. Synthesis, molecular docking screening, and anti-proliferative potency evaluation of some new imidazo [2, 1-b] thiazole linked thiadiazole conjugates. 2020, 25.21: 4997. DOI 10.1002/jhet.2869

[34] Akbari, Z., Stagno, C., Iraci, N., Efferth, T., Omer, E. A., Piperno, A., & Micale, N. (2024). Biological evaluation, DFT, MEP, HOMO-LUMO analysis and ensemble docking studies of Zn (II) complexes of bidentate and tetradentate Schiff base ligands as antileukemia agents. *Journal of Molecular Structure*, *1301*, 137400.https://doi.org/10.1016/j.molstruc.2023.137400

[35] M. J. Frisch, G.W. Trucks, H.B. Schlegel, G.E. Scuseria, M.A. Robb, J.R. Cheeseman, G. Scalmani, V. Barone, B. Mennucci, G.A. Petersson, H. Nakatsuji, M. Caricato, X. Li, H.P. Hratchian, A.F. Izmaylov, J. Bloino, G. Zheng, J.L. Sonnenberg, M. Hada, M. Ehara, K. Toyota, R. Fukuda, J. Hasegawa, M. Ishida, T. Nakajima, Y. Honda, O. Kitao, H. Nakai, T. Vreven, J.A. Montgomery Jr., J.E. Peralta, F. Ogliaro, M. Bearpark, J.J. Heyd, E. Brothers, K.N. Kudin, V.N. Staroverov, R. Kobayashi, J. Normand, K. Raghavachari, A. Rendell, J.C. Burant, S.S. Iyengar, J. Tomasi, M. Cossi, N. Rega, J.M. Millam, M. Klene, J.E. Knox, J.B. Cross, V. Bakken, C. Adamo, J. Jaramillo, R. Gomperts, R.E. Stratmann, O. Yazyev, A.J. Austin, R. Cammi, C. Pomelli, J.W. Ochterski, R.L. Martin, K. Morokuma, V.G. Zakrzewski, G.A. Voth, P. Salvador, J.J. Dannenberg, S. Dapprich, A.D. Daniels, Ö. Farkas, J.B. Foresman, J.V. Ortiz, J. Cioslowski and D.J. Fox, Gaussian 09, Revision D.01, Gaussian, Inc., Wallingford CT (2009).

[36] Meenukutty, M. S., Mohan, A. P., Vidya, V. G., & Kumar, V. V. (2022). Synthesis, characterization, DFT analysis and docking studies of a novel Schiff base using 5-bromo salicylaldehyde and β-alanine. *Heliyon*, *8*(6). https://doi.org/10.1016/j.heliyon.2022.e09600

[37] Noureldeen, A. F., Aziz, S. W., Shouman, S. A., Mohamed, M. M., Attia, Y. M., Ramadan, R. M., & Elhady, M. M. (2022). Molecular design, spectroscopic, DFT, pharmacological, and molecular docking studies of novel ruthenium (III)–Schiff base complex: An inhibitor of progression in HepG2 cells. *International journal of environmental research and public health*, *19*(20), 13624. https://doi.org/10.3390/ijerph192013624

[38] Ayaz, M., Alam, A., Zainab, Elhenawy, A. A., Ur Rehman, N., Ur Rahman, S., & Ahmad, M. (2024). Designing and Synthesis of Novel Fexofenadine-Derived Hydrazone-Schiff Bases as Potential Urease Inhibitors: In-Vitro, Molecular Docking and DFT Investigations. *Chemistry & Biodiversity*, *21*(8), e202400704.https://doi.org/10.1002/cbdv.202400704

[39] Joseph, J., and Mehta, H. B. (2007) Synthesis, characterization, and thermal analysis of transition metal complexes of polydentate ONO donor Schiff base ligand.*12*, 124-129

[40] HUANG, Sheng-You; ZOU, Xiaoqin. Advances and challenges in protein-ligand docking. 2010, 11.8: 3016-3034. https://doi.org/10.3390/ijms11083016

[41] MUKESH, Bachwani; RAKESH, Kumar. Molecular docking: a review. 2011, 2.6: 1746-5١.

[42] El-Bindary MA, El-Bindary AA (2022) Synthesis, characterization, DNA binding, and biological action of dimedone arylhydrazone chelates. Applied Organometallic Chemistry 36: e6576. https://doi.org/10.1002/aoc.6576

[43] Murray JS, Politzer P (2011) The electrostatic potential: An overview. Wiley Interdiscip. Rev. Comput. Mol. Sci 1: 153–163. https://doi.org/10.1002/wcms.19

[44] DURAI, D. Raja, et al. Local energy decomposition (through methanol), biological activity prediction, solvents interaction (DFT) and molecular docking simulation studies of Schiff base:

synthesis, characterization and fluorescence properties.2023, 6: 101030. https://doi.org/10.1016/j.rechem.2023.101030

[45] Akbari, Z., Stagno, C., Iraci, N., Efferth, T., Omer, E. A., Piperno, A., & Micale, N. (2024). Biological evaluation, DFT, MEP, HOMO-LUMO analysis and ensemble docking studies of Zn (II) complexes of bidentate and tetradentate Schiff base ligands as antileukemia agents. *Journal of Molecular Structure*, *1301*, 137400.https://doi.org/10.1016/j.molstruc.2023.137400

[46] KAVITHA, Natte; ALIVELU, Munagala. Investigation of Structures, QTAIM, RDG, ADMET, and docking properties of SASC compound using experimental and theoretical approach. 2021, 1201: 113287. https://doi.org/10.1016/j.comptc.2021.113287

[47] Eltayeb, N. E., Şen, F., Lasri, J., Hussien, M. A., Elsilk, S. E., Babgi, B. A., & Sert, Y. (2020). Hirshfeld Surface analysis, spectroscopic, biological studies and molecular docking of (4E)-4-((naphthalen-2-yl) methyleneamino)-1, 2-dihydro-2, 3-dimethyl-1-phenylpyrazol-5-one. *Journal of Molecular Structure*, *1202*, 127315. https://doi.org/10.1016/j.molstruc.2019.127315

[48] BOSHAALA, Ahmed, et al. Crystal structure, MEP/DFT/XRD, thione⇔ thiol tautomerization, thermal, docking, and optical/TD-DFT studies of (E)-methyl 2-(1-phenylethylidene)-hydrazinecarbodithioate ligand. 2021, 1238: 130461. https://doi.org/10.1016/j.molstruc.2021.130461

[49] Mumit, M. A., Pal, T. K., Alam, M. A., Islam, M. A. A. A. A., Paul, S., & Sheikh, M. C. (2020). DFT studies on vibrational and electronic spectra, HOMO–LUMO, MEP, HOMA, NBO and molecular docking analysis of benzyl-3-N-(2, 4, 5-trimethoxyphenylmethylene) hydrazinecarbodithioate. *Journal of molecular structure*, *1220*, ١٢٨٧١٥.https://doi.org/10.1016/j.molstruc.2020.128715

[50] Vincy, C. D., Tarika, J. D., Dexlin, X. D., Rathika, A., & Beaula, T. J. (2022). Exploring the antibacterial activity of 1, 2 diaminoethane hexanedionic acid by spectroscopic, electronic, ELF, LOL, RDG analysis and molecular docking studies using DFT method. *Journal of Molecular Structure*, *1247*, 131388.https://doi.org/10.1016/j.molstruc.2021.131388

GRAPHICAL ABSTRACT

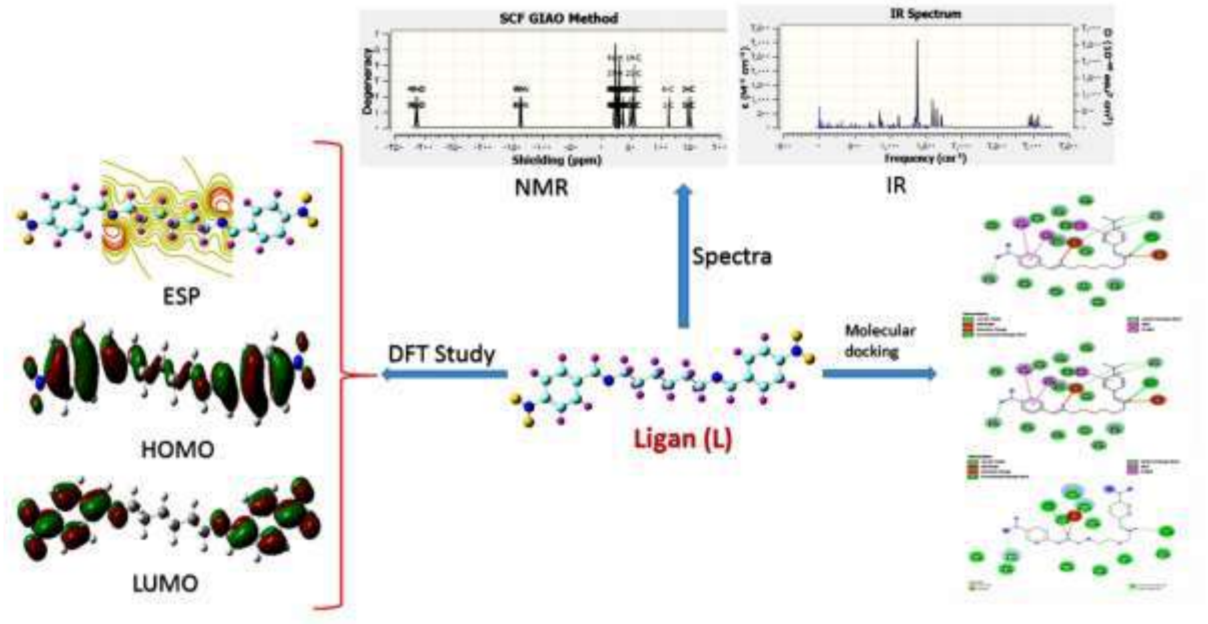

The 30th Iranian Seminar of Organic Chemistry
February 7-9, 2025, Iran University of Science and Technology, Tehran, Iran

Synthesis of amino based Biochar as an effective nanocatalyst in 1,8-Naphthyridine synthesis

Reza Hazbavi 1[a], Maryam Hajjam 2[b]

Department of Organic Chemistry, Faculty of Chemistry and Petroleum Sciences, Bu-Ali Sina University, Postal code 6517838683, Hamedan, Iran. E-mail address, m.hajjami@basu.ac.ir or mhajjami@yahoo.com

Keyword: Biochar, 1,8-Naphthyridine, Nanocatalyst, Multicomponent reaction

Abstract

Multicomponent reactions (MCRs) are referred to one-pot, convergent chemical reactions utilizing more than two starting materials, where final product retains significant portions of all starting materials. This advanced approach has emerged as an efficient, economical, and eco-friendly substitute for conventional sequential multi-step synthesis of various biologically active pharmacophores.[1] In this study, first biochar was produced from air-dried walnut shells.[2] The surface of the nano-substrate was subsequently modified to amine-biochar. After charactisation of

this catalyst, a Knoevenagel–Michael cyclocondensation reaction was conducted using aryl aldehydes, malononitrile, and 2,6-diaminopyridine in the presence of amine-functionalized biochar. This reaction was carried out at room temperature, resulting in excellent yields and very short reaction times.

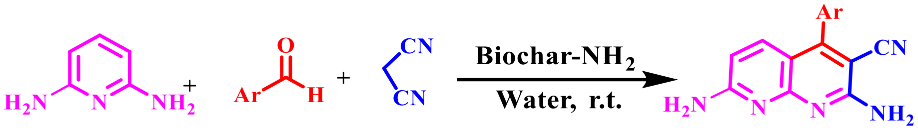

Scheme 1. Three-component reaction of ٢,٦-diaminopyridin, aldehydes and malononitrile in the presence of Biochar-NH_2

References:

1. Rashidi, S.; Gholamian, F., Hajjami, M.. *Journal of nanoparticle research* 2023, 25, 102–120.

2. Moradi, P.; Hajjami, M. *New Journal of Chemistry* 2021, 25, 2981-2994.

Effect of Aluminum Hydroxide Nanoparticles on the Thermal Properties of Polyisocyanurate Foams Based on Soybean Oil

Samaneh Taghvaei Nia[a], Mir Mohammad Alavi Nikje*[a]

[a] *Department of Chemistry, Faculty of Science, Imam Khomeini International University, P.O. Box 34149-1-6818, Qazvin, Iran.*

** Corresponding author: E-mail address: alavi@sci.ikiu.ac.ir*

Keyword: soybean oil (SBO), PIR foam, ATH NPs, thermal resistance, bio-polyol, flame retardant (FR).

Abstract: Rigid polyurethane and polyisocyanurate (PIR) foams are one of the thermal insulation materials that are mainly used in civil engineering as well as in the refrigeration industry. RPUs are formed by exothermic reactions between alcohols with two or more active hydroxyl groups (-OH) per molecule (diols, triols, polyols) and and isocyanates that have more than one reactive isocyanate group (-NCO) per molecule (diisocyanates, polyisocyanates). Polyisocyanurate foams, which are a special type of rigid polyurethane foam, are formed through isocyanate trimerization during RPU formation [1]. The use of vegetable oils in the production of polyurethane and polyisocyanurate (PIR) foams has increased due to environmental concerns surrounding petroleum-based foams [2]. On the other hand, it is important to improve the thermal resistance properties of PIR foams, particularly for applications such as building and industrial insulation [3]. In this study, a bio-polyol was synthesized from soybean oil (SBO) using the direct amidation method. Unlike flame retardants such as tris (chloroisopropyl) phosphate (TCPP), aluminum hydroxide nanoparticles (ATH NPs) is not harmful to the environment and adds to maintaining the biocompatibility of foams. Other additives, incluging catalysts, water, surfactant, and cyclopentane, were also added to the SBO-based polyol to prepare the polyol mixture. PIR foams were produced by adding excess polymeric 4,4′-methylene diphenyl diisocyanate (PMDI) (iso index 3) to the polyol mixture. Different proportions of ATH NPs (0, 5, 10, and 20%) were added to the formulation of foams containing 100% SBO-based polyol. The thermal properties of the resulting foams were evaluated using TGA-DTG analysis. The addition of ATH NPs increased the number of nucleation sites in the foam matrix, resulting in a more regular foam structure. This regular structure is effective in improving both thermal and mechanical properties. The flame retardant properties of ATH NPs are due to the production of water and alumina during thermal decomposition [4]. The onset of decomposition (T_{onset}) increased from 94 ℃ (in reference foam)

to 168 °C (in foam containing 20% ATH NPs). Additionally, the weight loss in samples containing nanoparticles decreased significantly (**Figure 1**).

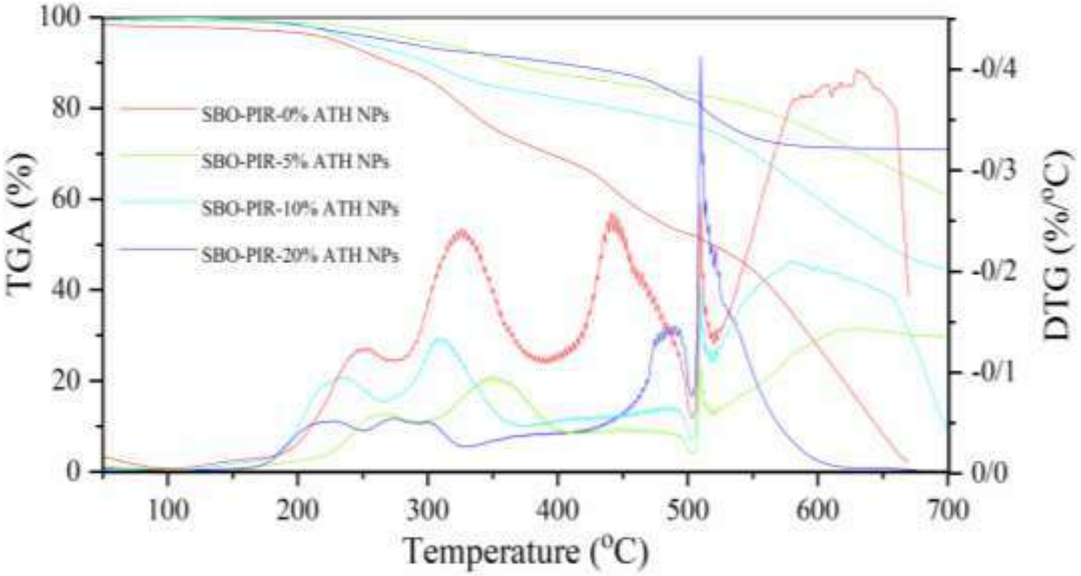

Figure 1: TGA-DTG curves of SBO-based PIR foams containing ATH NPs.

References:

[1] A. Ivdre, A. Abolins, I. Sevastyanova, M. Kirpluks, U. Cabulis, and R. Merijs-Meri, "Rigid Polyurethane Foams with Various Isocyanate Indices Based on Polyols from Rapeseed Oil and Waste PET," *Polymers*, vol. 12, no. 4 , Apr. 2020, doi: 10.3390/polym12040738.

[2] M. Borowicz, J. Paciorek-Sadowska, J. Lubczak, and B. Czupryński, "Biodegradable, Flame-Retardant, and Bio-Based Rigid Polyurethane/Polyisocyanurate Foams for Thermal Insulation Application," *Polymers*, vol. 11, no. 11, p. 1816, Nov. 2019, doi: 10.3390/polym11111816.

[3] M. Kurańska, A. Prociak, U. Cabulis, M. Kirpluks, J. Ryszkowska, and M. Auguścik, "Innovative porous polyurethane-polyisocyanurate foams based on rapeseed oil and modified with expandable graphite," *Ind. Crops Prod.*, vol. 95, p. 316–323, Jan. 2017, doi: 10.1016/j.indcrop.2016.10.039.

[4] T. R. Hull, A. Witkowski, and L. Hollingbery, "Fire retardant action of mineral fillers," *Polym. Degrad. Stab.*, vol. 96, no. 8, p. 1462–1469, Aug. 2011, doi: 10.1016/j.polymdegradstab.2011.05.006.

Preparation of rigid polyurethane-polyisocyanurate foams based on date seed oil modified by nano- Aluminum trihydrate

Samaneh Taghvaei Nia[a], Mir Mohammad Alavi Nikje*[a]

[a] *Department of Chemistry, Faculty of Science, Imam Khomeini International University, P.O. Box 34149-1-6818, Qazvin, Iran.*

** Corresponding author: E-mail address: alavi@sci.ikiu.ac.ir*

Keyword: date seed oil (DSO), PU-PIR foam, nano-ATH, bio-polyol.

Abstract: Approximately 30% of the world's energy is used for heating buildings, making it crucial to improve the thermal insulation properties of buildings. Polyurethane sprays are commonly used to insulate buildings. Improving the thermal properties of polyurethane-polyisocyanurate (PU-PIR) foams is done by adding additives to their formulation [1], [2]. In this study, we aimed to reduce the environmental impact of petroleum-based foams by incorporating date seed oil (DSO) into the foam formulation as a bio-polyol. The DSO was extracted using the Soxhlet method with n-hexane solvent. Bio-polyol was then produced through an amidation process using diethanolamine and sodium methoxide catalyst in a nitrogen atmosphere (**Scheme 1a**). To further improve the properties of the bio-based foams, aluminum trihydrate nanoparticles (nano-ATH) were produced using a mechanical ball mill method added to the polyol mixture. By adding other additives to DSO-based polyol, polyol mixture was prepared. Aromatic isocyanate (pMDI) was then added to the polyol mixture to produce PU-PIR foams. The modified bio-based foams were produced by incorporating the nano-ATH into the foam formulation (**Scheme 1b and 1c**). The mechanism by which nano-ATH acts as a flame retardant is through its thermal decomposition, which produces water and alumina are produced (**Scheme 1d**) [3]. The produced water can partially prevent burning, and on the other hand, the produced alumina acts as a protective layer and prevents the fire from spreading to the lower layers of the foam. Furthermore, increasing the percentage of nano-ATH resulted in a higher foam density, which further improved the mechanical properties, particularly in foams with a high percentage of DSO-based polyol. The results showed that the addition of nano-ATH to the foam matrix significantly improved its thermal and mechanical properties.

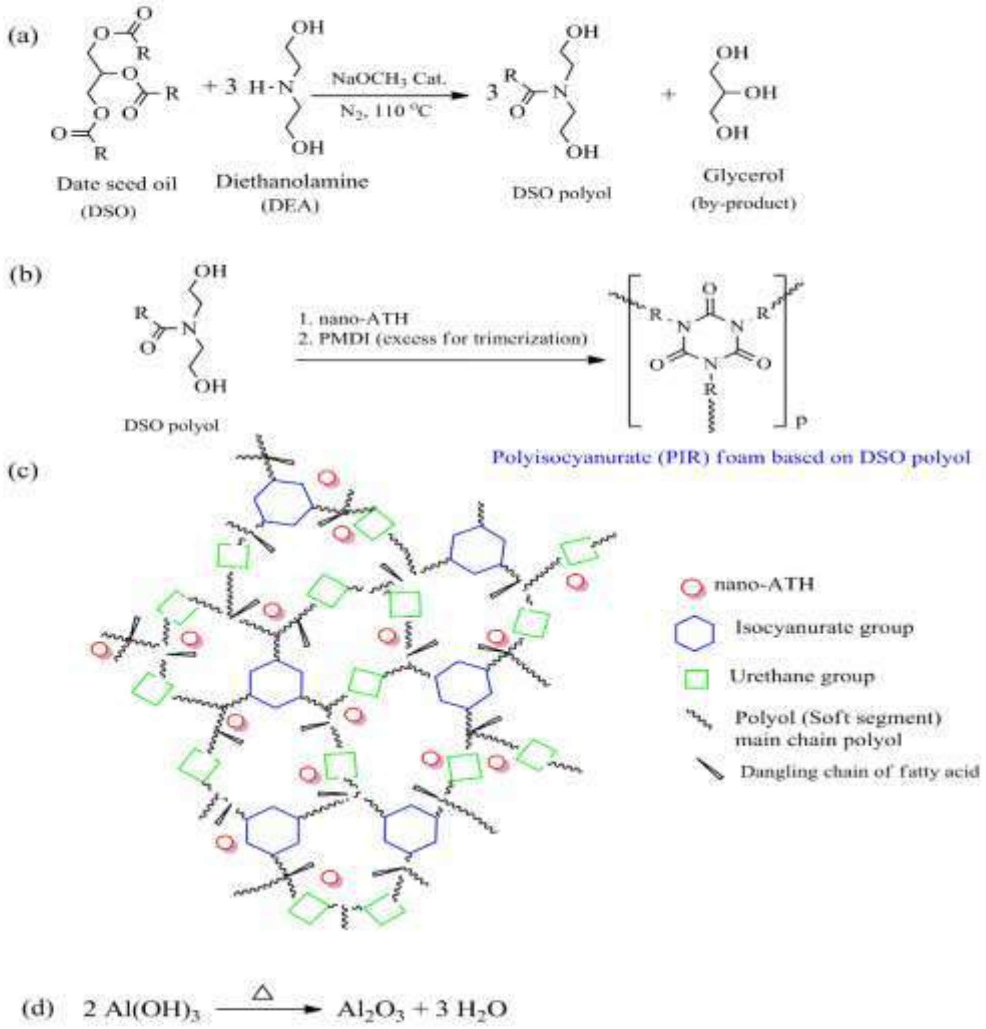

Scheme 1: (a) Bio-polyol synthesis reaction based on DSO by direct amidation using diethanolamine. (b) The process for synthesizing PU-PIR foams involves the use of DSO and the addition of nano-ATH (as a flame retardant additive). (c) The polymer network structure of PU-PIR foam containing DSO nano-ATH. (d) The thermal decomposition reaction of nano-ATH.

References:

[1] S. Reinerte, M. Kirpluks, and U. Cabulis, "Thermal degradation of highly crosslinked rigid PU-PIR foams based on high functionality tall oil polyol," *Polym. Degrad. Stab.*, vol. 167, p. 50–57, Sep. 2019, doi: 10.1016/j.polymdegradstab.2019.06.021.

[2] H. Haridevan, D. A. C. Evans, D. J. Martin, and P. K. Annamalai, "Dispersion engineering of cellulose nanofibres in polyols: for controlled microstructure of high-performance polyurethane foam," *Mater. Adv.*, vol. 5, no. 4, p. 1540–1551, Feb. 2024, doi: 10.1039/D3MA00865G.

[3] T. R. Hull, A. Witkowski, and L. Hollingbery, “Fire retardant action of mineral fillers,” *Polym. Degrad. Stab.*, vol. 96, no. 8, p. 1462–1469, Aug. 2011, doi: 10.1016/j.polymdegradstab.2011.05.006.

The 30th Iranian Seminar of Organic Chemistry
February 7-9, 2025, Iran University of Science and Technology, Tehran, Iran

Microwave-assisted Multi-component and Synthesis of Benzopyrans Employing Triethanolammonium Acetate ([TEAH][OAc]).IL as Green Catalyst

Behjat Pouramiri, *[a]

[a] *Department of Organic Chemistry, Qom University of Technology, Qom, Iran* *b.pouramiri.chem@gmail.com

Keyword: Multi-component synthesis, Benzopyrano, Ionic Liquids, Solvent-free condition

Abstract: A multi-component one-pot green synthesis of diversely functionalized 7-arylbenzopyrano[4,3-b]benzopyran6,8-diones by three-component reaction of 4-hydroxycoumarin, aromatic aldehyde, and dimedone using triethanolammonium acetate ([TEAH][OAc]) under solvent-free condition is reported. The present protocol meets the criteria of green chemistry and the notable advantages of the present method include avoidance of organic solvent in the reaction, high yield of the products, employment of [TEAH][OAc**]** as a green, environmentally-benign, non-toxic, bioorganic and recyclable catalyst, easy isolation of the products without need of column chromatographic purification, mild reaction conditions.

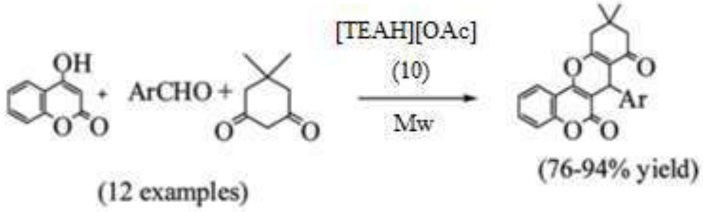

Sheme1. Green synthesis of Benzopyrans Employing Triethanolammonium Acetate ([TEAH][OAc]).IL as Green Catalyst.

Introduction

Benzopyran and its derivatives, fused O-heterocycles, are an important class of scaffold because of their presence in the core of natural products and several synthetic derivatives with diverse bioactivities such as antimicrobial, antidiabetic, antifungal, antitubercular, anticancer, anti-HIV, antihypertensive, and anti-inflammatory activities. Therefore, it grabbed the attention in the field of drug discovery [1-3]. The above stated biological features of benzopyrans drives chemists to discover new and sustainable approaches for its synthesis.

The multicomponent reactions (MCRs) meet the criteria of the green chemistry to a great extent by providing access to complex molecules in one-pot by avoiding extra work-up steps with great atom economy and high bond forming efficiency with reduced waste generation [4,5]. Thus, the MCRs have been utilized extensively in pharmaceutical chemistry 6, natural product synthesis 7, agrochemistry 8, polymer chemistry 9, bioconjugation chemistry 10 and bioactive molecule synthesis 11.

Method,

4-Hydroxycoumarin and dimedone were procured from Merck, Germany . IR spectra were recorded on a Perkin-Elmer FTIR L120-000A. NMR spectra were measured on Brucker DPX-400 (400 MHz).

General Experimental Procedure for the Synthesis of 1a- 12a:

To a mixture of 4-hydroxycoumarin (164mg, 1.01 mmol), aldehyde (1.04 mmol) and dimedone (145mg, 1.04 mmol) in a round-bottomed flask was added triethanolammonium acetate (10 mol%) and the mixture was irradiated under MW for 10 min (TLC monitoring). The reaction mixture was then cooled to room temperature when the product separated out. The precipitated product was washed with water (3x2 mL) and crystallized from ethyl acetate-light petrol to furnish a solid (76-94%). Some selected data:

7-(3,4-Methylenedioxyphenyl)-10,10-dimethyl-6,7,8,9,10,11-hexahydrobenzopyrano[4,3

b]benzopyran-6,8-dione (4a, Table 2) Yield 85%, white solid; mp 220-222 ^{o}C; IR (KBr): 2968, 1723, 1671, 1626, 1502, 1489, 1359, 1189, 1031, 924, 776 cm-1; 1H NMR (400 MHz, CDCl3): δ 7.85 (d, 1H, J = 7.2 Hz), 7.55-7.51 (m, 1H), 7.33 (t, 1H, J = 7.2 Hz), 7.27 (d, 1H, J = 8.4 Hz), 6.87 (d, 1H, J = 1.2 Hz), 6.82 (dd, 1H, J = 8, 1.2 Hz), 6.65 (d, 1H, J = 8 Hz), 5.84 (d, 2H, J = 4 Hz), 4.85 (s, 1H), 2.74-2.63 (m, 2H), 2.35-2.21 (m, 2H), 1.16 (s, 3H), 1.09 (s, 3H); 13C NMR (100 MHz, CDCl3): δ 196.2, 162, 160.6, 153.8, 152.5, 147.5, 146.5, 136.7, 132.3, 124.4, 122.5, 121.9, 116.8, 115.1, 113.6, 109.3, 108.0, 106.7, 100.9, 50.7, 40.7, 33.0, 32.2, 29.2, 27.6; Anal. Calcd. For C25H20O6: C, 72.11; H, 4.84%.

7-(4-Allyloxyphenyl)-10,10-dimethyl-6,7,8,9,10,11-hexahydrobenzopyrano[4,3b]benzopyran-6,8-dione (4b, Table 2) Yield 80%, white solid; mp 166-168 ^{o}C; IR (KBr): 2959, 1721, 1665, 1509, 1363, 1238, 1194, 1031, 762 cm-1; 1H NMR (400 MHz, CDCl3): δ 7.86 (dd, 1H, J = 8, 1.2 Hz), 7.58-7.54 (m, 1H), 7.37-7.31 (m, 2H), 7.28 (d, 2H, J = 8.4 Hz), 6.79 (d, 2H, J = 8.8 Hz), 6.06-5.96 (m, 1H), 5.36 (dd, 1H, J = 17.2, 1.2 Hz), 5.23 (dd, 1H, J = 10.4, 1.2 Hz), 4.91 (s, 1H), 4.46 (dd, 2H, J = 4.4, 1.2 Hz), 2.73-2.62 (m, 2H), 2.34-2.24 (m, 2H), 1.16 (s, 3H), 1.09 (s, 3H); 13C NMR (100 MHz, CDCl3): δ 196.1, 161.8, 160.7, 157.6, 153.8, 152.6, 135.0, 133.4, 132.1, 129.6, 124.3, 122.4, 117.6, 116.9, 115.3, 114.5, 113.7, 106.9, 68.8, 50.7, 40.8, 32.5, 32.3, 29.2, 27.6; Anal. Calcd. For C27H24O5: C, 75.68; H, 5.65%. Found: C, 75.59; H, 5.71%.

Results and Discussion

Initially, we focused on a one-pot, multi-component reaction of dimedon **1** (1.1 mmol), 4-hydroxy coumarin **2** (1 mmol), and benzaldehyde **4** (1 mmol) as the model reaction. To explore suitable conditions, the above mentioned model reaction was conducted in the presence of different amounts of [TEAH][OAc] under various conditions (Table1, entries 1-7).

Table 1. Catalyst screening and reaction condition optimizations for the preparation of benzopyran derivatives[a].

Entry	Catalyst (mol%)	Condition	Time (min)	Yield[b] (%)
1	--------	Solvent-Free (100 °C)	60	trace
2	[TEAH][OAc] (5)	Solvent-Free (r.t)	60	15
3	[TEAH][OAc] (8)	Solvent-Free (40 °C)	40	30
4	[TEAH][OAc] (8)	Mw	10	85
5	[TEAH][OAc] (10)	Mw	10	85
6	[TEAH][OAc] (10)	Solvent-Free (70 °C)	28	75
7	[TEAH][OAc] (25)	Solvent-Free (90 °C)	25	78

[a]Reaction condition: aniline **1** (1.1 mmol), ethyl acetoacetate **2** (1 mmol), nitromethane **3** (1 mmol), and benzaldehyde **4** (1 mmol). [b] Isolated yields.

From these experiments, 10 mol % of [TEAH][OAc] under solvent-free condition at microwave irradiation came out as the optimized conditions for the reaction in terms of yield and time (Table 1, entry 4) for the desired product 7-(3,4-Methylenedioxyphenyl)-10,10-dimethyl-6,7,8,9,10,11-hexahydrobenzopyrano[4,3-b]benzopyran-6,8-dione (4a).

To examine the generality of newly developed protocol, a number of other aniline derivatives and different aromatic aldehydes were utilized using identical reaction conditions. All of reactants underwent the same reaction condition affording the corresponding pyrrole-3-carboxylates in good to excellent yields (78–85%) (Table 2).

Table 2. Synthesis of pyrrole-3-carboxylates using 10 mol % of [TEAH][OAc] under solvent-free condition.

Entry	Aldehyde	Product	Time[a] (min)	Yield[b] (%)	Obs. mp	Lit. mp
1	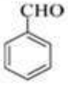	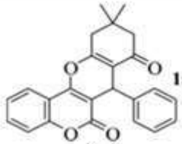 **1a**	10	85	225–227	(lit.[13] 226–227)
2	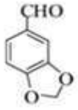	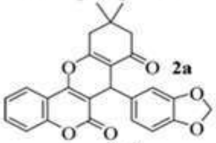 **2a**	12	80	220–222	—
3	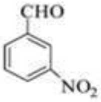	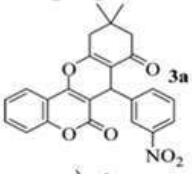 **3a**	8	94	255–257	(lit.[13] 256–257)
4	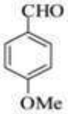	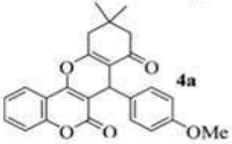 **4a**	15	76	190–192	(lit.[13] 191–192)

Conclusion

In summary, green, facile, and environment friendly approach has been disclosed for synthesis of series of diversely functionalized benzopyran derivatives under microwave. The present protocol offers several advantages such as the utilization of triethanolammonium acetate, as a environment-friendly, inexpensive and green catalyst, recyclability of the catalyst, employment of microwave as green energy source, easy isolation of the products by avoiding column chromatographic purification process, excellent yield of the products and metal-free aspects.

References

١. Lee T.; Gong, Y.-D. Solid-Phase Parallel Synthesis of Drug-Like Artificial 2H-Benzopyran Libraries. Molecules 2012, 17, 5467-5496.

٢. Gracia, A.; Torres-Ruiz, S.; Vila, L.; Villarroel-Vicente, C.; Bernabeu, A.; Eroles, P.; Cabedo N.; Cortes, D. Synthesis of 2-aminopropyl benzopyran derivatives as potential agents against triple-negative breast cancer. RSC Med. Chem. 2023, 14, 2327-2341.

٣. Gupta, S.; Park, S. E.; Mozaffari, S.; El-Aarag, B.; Parang K.; Tiwari, R. K. Design, Synthesis, and Antiproliferative Activity of Benzopyran-4-One-Isoxazole Hybrid Compounds. Molecules 2023, 28, 4220.

٤. Khurana, J. M.; Nand, B.; Saluja, P. DBU: A highly efficient catalyst for one-pot synthesis of substituted 3,4-dihydropyrano[3,2-c]chromenes, dihydropyrano[4,3-b]pyranes, 2-amino-4H-benzo[h]chromenes, and 2-amino-4H benzo[g]chromenes in aqueous medium. Tetrahedron 2010, 66, 5637–5641.

٥. Heravi, M. M.; Sadjadi, S.; Haj, N. M.; Oskooie, H. A.; Bamoharram, F. F. Role of various heteropolyacids in the reaction of 4-hydroxycoumarin, aldehydes, and ethylcyanoacetate. Catal. Commun. 2009, 10, 1643–1646.

٦. Gong, K.; Wang, H.; Luo, J.; Liu, Z.-L. One-pot synthesis of polyfunctionalized pyrans catalyzed by basic ionic liquid in aqueous media. J. Heterocycl. Chem. 2009, 46, 1145–1150.

٧. Khurana, J. M.; Kumar, S. Tetrabutylammonium bromide (TBAB): A neutral and efficient catalyst for the synthesis of biscoumarin and 3,4-dihydropyrano[c]chromene derivatives in water and solvent-free conditions. Tetrahedron Lett. 2009, 50, 4125–4127.

٨. Chen, Z.; Zhu, Q.; Su, W. A novel sulfonic acid–functionalized ionic liquid–catalyzed multicomponent synthesis of 10,11-dihydrochromeno[4,3-b]chromene-6,8(7H,9H)-dione derivatives in water. Tetrahedron Lett. 2011, 52, 2601–2604.

٩. Liang, B.; Kalidindi, S.; Proco, J. A.; Stephenson, C. R. Multicomponent reaction discovery: Three-component synthesis of spirooxindoles. Org. Lett. 2010, 12, 572–575.

١٠. Ganguly, N. C.; Barik, S. K. A facile efficient mild deprotection protocol of 1,3-dithianes and 1,3-dithiolanes with 30% hydrogen peroxide and iodine catalyst in aqueous micellar system. Synthesis 2009, 1393–1399.

١١. Ganguly, N. C.; Roy, S.; Mondal, P.; Saha, R. An efficient one-pot organocatalytic synthesis of 9-(1H-indol-3-yl)-xanthen-4-(9H)-ones under mild aqueous micellar conditions. Tetrahedron Lett. 2012, 53, 7067–7071.

١٢. Pouramiri, B., Daneshi, M., Seyedi, F. and Amirmahani, N., 2021. Triethanolammonium Acetate ([TEAH][OAc]) as a Recyclable Promoter and Medium for Green and Four-component Synthesis of Polyfunctionalized Pyrrole Derivatives. Letters in Organic Chemistry, 18(4), pp.273-280.

Efficient and Multi-component Synthesis of pyrazolo[3,4-*b*]quinolines Benzopyrans Using Triethyl Ammonium Hydrogen Sulfate [Et_3NH][HSO_4] IL as Green Catalyst

Behjat Pouramiri, *[a]

[a] *Department of Organic Chemistry, Qom University of Technology, Qom, Iran*
*b.pouramiri.chem@gmail.com

Keyword: Multi-component synthesis, Pyrazolo[3,4-*b*]quinolones, Ionic Liquids, solvent-free condition

Abstract: A multi-component one-pot green synthesis of diversely pyrazolo quinolones by the three-component reaction of dimedone, 5-amino pyrazolone and aromatic aldehydes in the presence of triethyl ammonium hydrogen sulfate [Et_3NH][HSO_4] IL as catalyst under solvent-free condition has been described. This economical catalyst provides high yields of products, short experimental time and easy workup for green synthesis of pyrazolo[3,4-b]quinolone compounds.

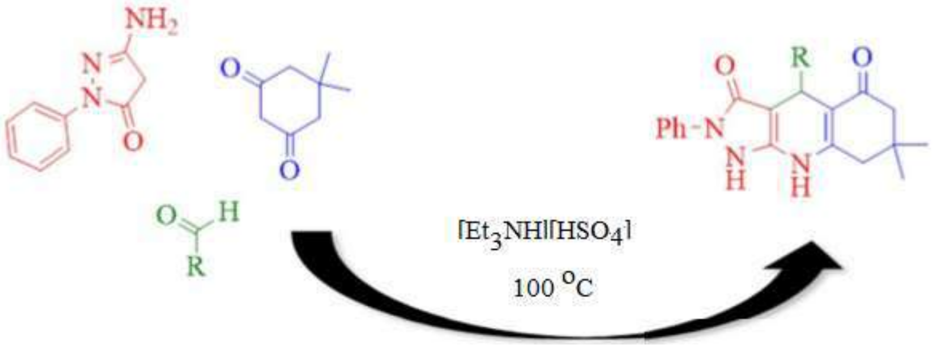

Sheme1. Green synthesis of Synthesis of pyrazolo[3,4-*b*]quinolines Benzopyrans Using Triethyl Ammonium Hydrogen Sulfate [Et_3NH][HSO_4] IL as Green Catalyst

Introduction

Pyrazole skeleton has been widely used in medicinal chemistry and drug design due to their innumerable biological activities such as fungicides, analgesic agents, insecticides, antiviral agents and herbicides [1,2]. Recently, multi-component reactions (MCRs) are considered as unique and powerful tools in organic and medicinal chemistry due to the benefits of atom efficiency and availability of the organic synthesis in one step from three different substrates. Moreover, MCRs provide advantages including synthetic efficiency of drug-like compounds, simplicity and easy workup and minimize waste generation and diversity [3]. Very recently, ionic liquids (ILs) have received great national attention due to their favorable features including non-flammability, reactivity, low vapor pressure, high thermal stability and reusability [1–6]. However, difficult product separation and using large amounts of ILs in biphasic systems that increase toxicological risk are the major challenges of these homogeneous catalysts [7].

Method,

All chemicals were procured from Merck, Germany. IR spectra were recorded on a Perkin-Elmer FTIR L120-000A. NMR spectra were measured on Brucker DPX-400 (400 MHz).

General Experimental Procedure for the synthesis of 1a- 12a:

A solution of 3-amino-1-phenyl-2-pyrazolin-5-one 1 (0.35 g, 2 mmol), dimedone 2 (0.28 g, 2 mmol), aldehyde 3 (0.28 mg, 2 mmol) and [Et_3NH][HSO_4] catalyst (8 mol%) at 100 °C was heated. The progress of the reaction was controlled by TLC (hexane/ethyl acetate, 2:3). After reaction completion, the mixture was cooled to room temperature and then H_2O (5 mL) was added. The solid product was filtered, washed with cold distilled water (2 mL) and was recrystallized from ethanol 96 % to afford the pure products (5a-m).

Some selected data:

7,7-dimethyl-2,4-diphenyl-1,2,4,7,8,9-hexahydro-3H-pyrazolo[3,4-b]quinoline-3,5(6H)-dione (4a): White crystals, mp 230-233 °C. IR spectrum, ν, cm^{-1}: 3205 (NH), 1629, 1595 (C=O), **1542, 1494, 1453. ^{1}H NMR (400 MHz, DMSO-*d₆*): δ (ppm): 11.37 (1H, s, br, NH), 9.93 (1H, s,** br, NH), 7.73 (2H, d, $^3J_{H\text{-}H}$=8Hz, arom), 7.46 (2H, t, $^3J_{H\text{-}H}$=8Hz, arom), 7.31-7.24 (5H, m, arom),

7.13 (1H, t, $^{3}J_{H-H}$=8Hz, arom), 5.17 (1H, s, C_4-H), 2.53-2.47 (2H, m, C_6-H_a ,H_b), 2.24 (1H, d, $^{2}J_{H-H}$=16Hz, C_8-H_a), 2.07 (1H, d, $^{2}J_{H-H}$=16Hz, C_8-H_b), 1.10 (3H, s, methyl), 1.01 (3H, s, methyl). ^{13}C NMR (100 MHz, DMSO-*d6*): δ (ppm): 192.90 (C5), 152.64 (C3), 147.88, 147.53, 146.46, 139.06, 128.77, 127.69, 127.13, 125.32, 124.54, 120.06, 107.78, 90.50, 50.36 (C_6), 40.89 (C_4), 33.01 (C_8), 31.92 (C_7), 28.84 (CH_3), 26.81 (CH_3).

7,7-dimethyl-4-(2-nitrophenyl)-2-phenyl-1,2,4,7,8,9-hexahydro-3H-pyrazolo[3,4-b]quinoline-3,5(6H)-dione (4b): Red crystals, mp 270-271 °C. IR spectrum, ν, cm^{-1}: **3310 (NH), 1685, 1665 (C=O), 1625, 1589, 1437. ^{1}H NMR (400 MHz, DMSO-*d6*): δ (ppm): 11.49 (1H, s,** br, NH), 10.05 (1H, s, br, NH), 8.10 (2H, d, $^{3}J_{H-H}$=8Hz, arom), 7.64 (2H, d, $^{3}J_{H-H}$=8Hz, arom), 7**.48** (1H, d, $^{3}J_{H-H}$=8Hz, arom), 7.39 (2H, t, $^{3}J_{H-H}$=8Hz, arom), 7.17 (2H, d, $^{3}J_{H-H}$=8Hz, arom), 5.20 (**1H,** s, C_4-H), 2.44 (2H, d, $^{2}J_{H-H}$=16Hz, C_6-H_a, H_b), 2.18 (1H, d, $^{2}J_{H-H}$=16Hz, C_8-H_a), 2.00 (1H, d, $^{2}J_{H-H}$=16Hz, C_8-H_b), 1.02 (3H, s, methyl), 0.92 (3H, s, methyl). ^{13}C NMR (100 MHz, DMSO-*d6*)**: δ** (ppm): 192.93 (C5), 154.98 (C3), 153.12, 145.41, 138.86, 128.80, 128.50, 124.72, 124.69, 123.12, **120.1, 120.1, 106.69, 89.12, 50.20 (C_6), 40.81 (C_4), 33.67 (C_8), 31.95 (C_7), 28.69 (CH_3), 26.84** (CH_3).

Results and Discussion

Firstly, the optimization of the reaction condition was checked using 3-amino-1-phenyl-1H-pyrazol-5(4H)-one 1, dimedone 2, and benzaldehyde 3a as the model substrate under various conditions and different amounts of [Et_3NH][HSO_4] IL catalyst in various solvents (Table 1). In order to choose an appropriate solvent, the model substrate was checked in different solvents (Table 1, entries 5,).

Table 1. Catalyst screening and reaction condition optimizations for the preparation of benzopyran derivatives[a].

Entry	Catalyst (mol%)	Condition	Time (min)	Yield[b] (%)
1	--------	Solvent-Free (100 °C)	60	trace
2	[Et_3NH][HSO_4] (5)	EtOH (r.t)	60	35
3	[Et_3NH][HSO_4] (8)	EtOH (78 °C)	40	45
4	[Et_3NH][HSO_4] (8)	CH_3CN	10	20
5	[Et_3NH][HSO_4] (10)	CH_2Cl_2	10	25
6	[Et_3NH][HSO_4] (8)	Solvent-Free (100 °C)	20	91
7	[Et_3NH][HSO_4] (25)	Solvent-Free (90 °C)	25	91

[a]Reaction condition: dimedone, 5-amino pyrazolone and aromatic aldehydes.[b] Isolated yields.

From these experiments, 8 mol % of [Et_3NH][HSO_4] under solvent-free condition at 100 °C came out as the optimized conditions for the reaction in terms of yield and time (Table 1, entry 4) for the desired product 7,7-dimethyl-2,4-diphenyl-1,2,4,7,8,9-hexahydro-3H-pyrazolo[3,4-b]quinoline-3,5(6H)-dione (4a).

Encouraged by these optimized parameters, different substituted pyrazolo[3,4b]quinoline-3,5-dione 4a-n were synthesized using 1:1:1 molar ratio of 3-amino1-aryl-1H-pyrazol-5(4H)-one 1, dimedone 2 and aromatic aldehyde derivatives 3a-n containing electron-withdrawing groups as well as electron-donating in the presence of [Et_3NH][HSO_4] IL catalyst under solvent-free conditions (Table 2).

Table 2. Synthesis of pyrrole-3-carboxylates using 8 mol % of [Et_3NH][HSO_4] under solvent-free condition.

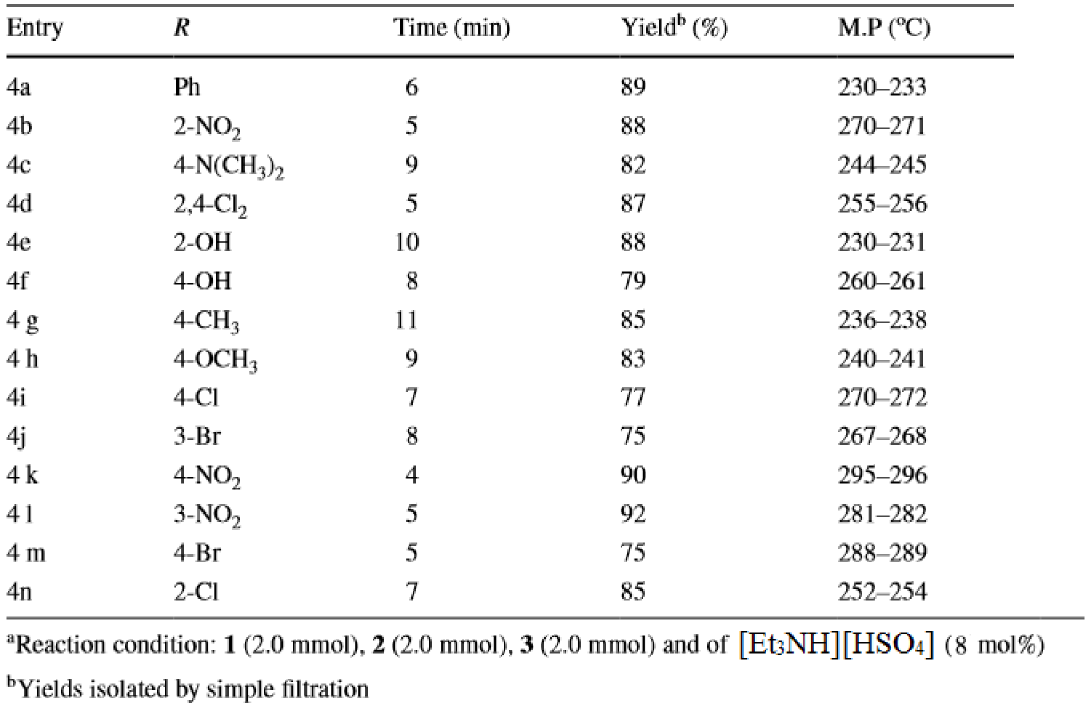

Entry	*R*	Time (min)	Yield^b (%)	M.P (°C)
4a	Ph	6	89	230–233
4b	2-NO_2	5	88	270–271
4c	4-$N(CH_3)_2$	9	82	244–245
4d	2,4-Cl_2	5	87	255–256
4e	2-OH	10	88	230–231
4f	4-OH	8	79	260–261
4 g	4-CH_3	11	85	236–238
4 h	4-OCH_3	9	83	240–241
4i	4-Cl	7	77	270–272
4j	3-Br	8	75	267–268
4 k	4-NO_2	4	90	295–296
4 l	3-NO_2	5	92	281–282
4 m	4-Br	5	75	288–289
4n	2-Cl	7	85	252–254

^{a}Reaction condition: **1** (2.0 mmol), **2** (2.0 mmol), **3** (2.0 mmol) and of [Et_3NH][HSO_4] (8 mol%)

^{b}Yields isolated by simple filtration

Conclusion

The use of [Et_3NH][HSO_4] IL catalyst along with solvent-free condition provides a green method for the synthesis of pyrazolo[3,4-b]quinoline compounds. Furthermore, the simplified experimental setup and the workup, high yields, recyclability of the catalyst, mild conditions and cost effectiveness are the extensive advantages of this procedure.

References:

1. El-Wahab, A.H.A., Al-Fifi, Z.I.A., Bedair, A.H., Ali, F.M., Halawa, A.H. and El-Agrody, A.M., 2011. Synthesis, reactions and biological evaluation of some new naphtho [2, 1-b] furan derivatives bearing a pyrazole nucleus. *Molecules*, *16*(1), pp.307-318.

2. Saad, H.A., Osman, N.A. and Moustafa, A.H., 2011. Synthesis and analgesic activity of some new pyrazoles and triazoles bearing a 6, 8-dibromo-2-methylquinazoline moiety. *Molecules*, *16*(12), pp.10187-10201.

3. Bienaymé, H., Hulme, C., Oddon, G. and Schmitt, P., 2000. Maximizing synthetic efficiency: Multi-component transformations lead the way. *Chemistry–A European Journal*, *6*(18), pp.3321-3329.

4. Vijayaraghavan, R. and MacFarlane, D.R., 2004. Charge transfer polymerization in ionic liquids. *Australian journal of chemistry*, *57*(2), pp.129-133.

5. Chauvin, Y., Mussmann, L. and Olivier, H., 1996. A novel class of versatile solvents for two-phase catalysis: hydrogenation, isomerization, and hydroformylation of alkenes catalyzed by rhodium complexes in liquid 1, 3-dialkylimidazolium salts. *Angewandte Chemie International Edition in English*, *34*(23-24), pp.2698-2700.

6. Klingshirn, M.A., Rogers, R.D. and Shaughnessy, K.H., 2005. Palladium-catalyzed hydroesterification of styrene derivatives in the presence of ionic liquids. *Journal of organometallic chemistry*, *690*(15), pp.3620-3626.

7. Zhao, D., Liao, Y. and Zhang, Z., 2007. Toxicity of ionic liquids. *Clean–soil, air, water*, *35*(1), pp.42-48.

The 30th Iranian Seminar of Organic Chemistry
February 7-9, 2025, Iran University of Science and Technology, Tehran, Iran

Synthesis of Sodium N'-tosylhydrazine-N-dithiocarboxylate to prepare 1-3 dithiol derivatives

Authors: Fateme Sabouri[a]*, Vahid Khakyzadeh[a]

Affiliations: Department of Chemistry, Faculty of basic science, Khajeh Nasir Toosi University of Technology, Tehran, Iran

Keyword: Sodium N’-tosylhydrazine-N-dithiocarboxylate, 1,3-Dithiol derivatives, Heterocyclic compounds, Organic synthesis

Introduction

The synthesis of heterocyclic compounds, particularly those containing sulfur, has attracted considerable attention due to their diverse biological and industrial applications. Among these, 1,3-dithiol derivatives are a class of compounds with notable chemical reactivity and a wide range of applications in medicinal chemistry, material science, and coordination chemistry [1,5]. These compounds often serve as building blocks for pharmaceuticals, ligands in metal complexation, and components in electronic materials. A critical step in the preparation of 1,3-dithiol derivatives involves the synthesis of key intermediates, such as sodium N'-tosylhydrazine-N-dithiocarboxylate. Given that this compound is a versatile reagent in organic synthesis [2,3], the presence of the N-tosyl group increases its stability and reactivity, making it suitable for various chemical transformations [3,4]. In this study, we report the efficient synthesis of sodium N'-tosylhydrazine-N-dithiocarboxylate and demonstrate its application in the preparation of 1,3-dithiol derivatives. This work provides a robust and scalable route for the synthesis of these valuable compounds and paving the way for their utilization in future advanced applications.

Method

The synthesis used a two-neck round-bottom flask equipped with a nitrogen gas inlet and outlet system to ensure an inert atmosphere. The apparatus was flushed with nitrogen gas for 10 minutes before adding reagents to remove any traces of oxygen or moisture. 2 mmol Reactant **1** (4-methylbenzene sulfonyl hydrazide) was dissolved in 4 mL of THF. Then, 1mmol Reactant **2** (carbon disulfide) was slowly added to the solution under continuous stirring. 1mmol Sodium hydroxide (NaOH) was introduced to the mixture to facilitate the reaction, ensuring that the pH was maintained within an optimal range for the formation of the desired product.

The reaction mixture was stirred at room temperature under a nitrogen atmosphere for the required time. The progress of the reaction was monitored using thin-layer chromatography (TLC), ensuring the complete consumption of the starting materials and the formation of the desired product. Upon completion of the reaction, the product was extracted by separating the organic layer and it was sent for NMR to ensure product formation. The solvent (THF) was removed under reduced pressure, and the crude product was subjected to recrystallization for purification.

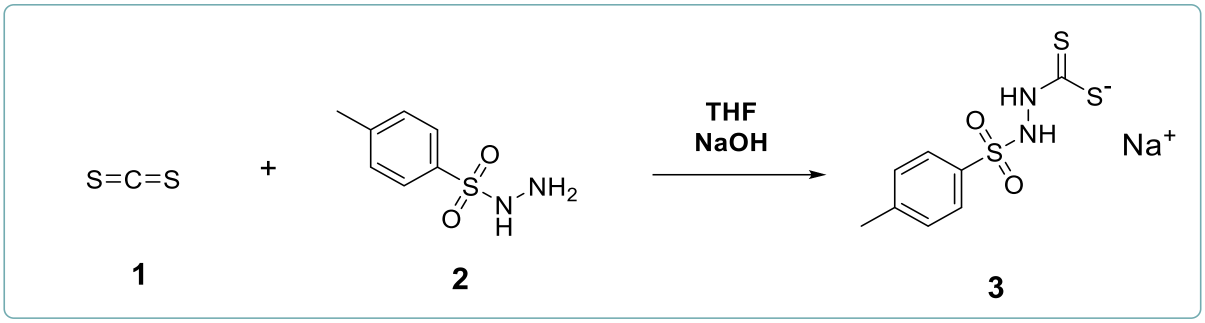

SchemeA: Synthesis of sodium N'-tosylhydrazine-N-dithiocarboxylate.

Next, by adding a-haloketone **4** to the product of the previous step (R_1 and R_2 in first reaction was methyl and next time we use 2-Chlorocyclohexanone), in refluxing acetonitrile, the initial substitution step was followed by spontaneous cyclization to yield compounds **5** and the reaction did not stop at that stage and was followed by elimination of water, yielding the 2-tosylhydrazono-1.3-dithioles. Both the cyclization step and the water elimination are probably acid-catalyzed by the tosylic N-H.

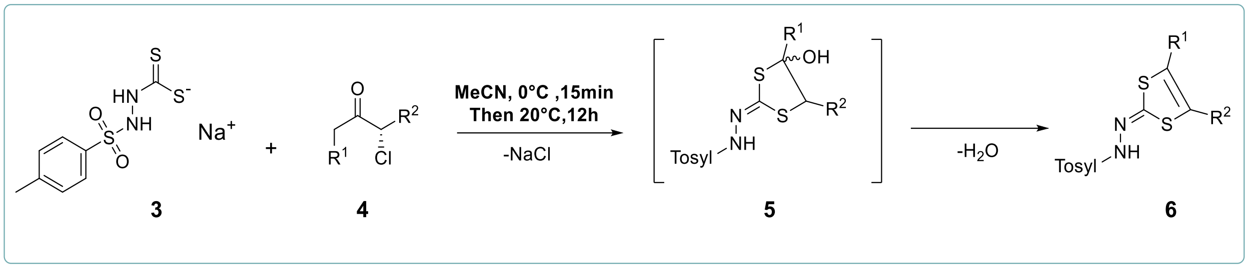

SchemeB: Synthesis of 2-tosylhydrazono-1.3-dithioles.

Results and Discussion

The products were characterized using spectroscopic and analytical methods, including IR and NMR spectroscopy. The IR spectrum exhibited characteristic peaks corresponding to the dithiocarboxylate group. The NMR spectrum revealed the expected chemical shifts for the tosyl group and hydrazine moieties, further validating the structure of the synthesized compound. It was observed that maintaining a dry and oxygen-free environment was critical for the success of the reaction. The presence of excess carbon disulfide could also lead to side reactions, so precise measurements were crucial. Finally, the product, sodium N'-tosylhydrazine-N-dithiocarboxylate, was obtained as a solid with high purity. The presence of the tosyl group enhanced the stability of the intermediate in bis (4-methylbenzene sulfonyl) hydrazide as the starting material proved to be a key factor in the success of this synthesis. The introduced method offers several advantages, including mild reaction conditions, high selectivity, and the use of readily available reagents. Overall, the experimental setup and reaction conditions were optimized to achieve a robust and reproducible protocol, paving the way for future studies and potential scale-up for industrial applications.

References:

[1] Clayden, J., Greeves, N., Warren, S., & Wothers, P. (2012). Organic Chemistry (2nd ed.). Oxford University Press.

[2] Katritzky, A. R., Rees, C. W., & Scriven, E. F. V. (1996). Comprehensive Heterocyclic Chemistry II. Elsevier.

[3] De, A., & Kumar, A. (2019). "Synthesis and Reactivity of Dithiocarboxylate Derivatives." Chemical Reviews, 119(5), 4563–4590.

[4] Trost, B. M., & Fleming, I. (1991). Comprehensive Organic Synthesis: Selectivity, Strategy, and Efficiency in Modern Organic Chemistry. Pergamon Press.

[5] Gaba, R., Singh, S., & Gaba, P. (2021). "Biological Importance of 1,3-Dithiol Derivatives: A Review." Journal of Sulfur Chemistry, 42(2), 198–210.

Circular Economy Method for Recovery of Terephthalic acid from PET Wastes: Effect of Benzalkonium Chloride Phase Transfer Catalyst in Terephthalic Acid Recovery Yield

Mahsa Ataei Ashtiyani and Mir Mohammad Alavi Nikje*

Department of Chemistry, Faculty of Science, Imam Khomeini International University, P.O. Box: 288, Qazvin, Iran email: alavi@sci.ikiu.ac.ir

Keyword: Polyethylene Terephthalate, Terephthalic Acid, Benzalkonium Chloride Catalyst

Introduction:

Poly (ethylene terephthalate), PET is a saturated polyester of terephthalic acid and ethylene glycol. The growing interest in PET recycling is due to the widespread use of packaging made of this polymer mainly as bottles. The pertinent feature of PET, namely, it does not have major side effects on human-beings, is responsible for its wide applications as packaging material for food items [1]. PET does not pose a direct hazard to the environment, but due to its substantial volume fraction in the waste stream and its high resistance to the atmospheric and biological agents, it is seen as a noxious material [2]. Poly (ethylene terephthalate) is synthesized by the polycondensation of terephthalic acid (TPA) and ethylene glycol (EG), or by transesterification of dimethyl terephthalate and EG. Since its development by DuPont in the mid-1940s, it has become one of the most abundant mass-produced thermoplastics. Owing to its excellent mechanical properties, thermal stability, impermeability for liquids and gases, and transparency, it is mostly used for textile fibers, beverage bottles, and food containers. However, as PET is a very stable polymer and resistant to hydrolytic or enzymatic degradation, it has become a major component of plastic waste found in the environment, along with PE, PP, and PS [3]. One of the primary motivations for the research in catalysis is the use of low-cost, earth-abundant materials that can fulfill the scale-up needs of respective technologies [4]. In this study, the use of benzalkonium chloride catalyst in an alkaline medium to improve the efficiency of PET degradation and the effect of monoethylene glycol in the degradation reaction are investigated.

Materials and Methods:

In this study, to degrade polyethylene terephthalate, a combination of 10 grams of water, 30 grams of monoethylene glycol (MEG), 4.2 grams of sodium hydroxide, 0.1 grams of benzalkonium chloride (BNZ), and 10 grams of polyethylene terephthalate was used at 110°C. after defined reaction times, the revored terephthalate nutrolized with hydrochloric acid and terephthalic acid obtained by filtration, washed by distilled water and dried in an oven. In various experiments, the effects of different combinations (presence or absence of monoethylene glycol and benzalkonium chloride) on the degradation reaction efficiency were examined and recovered terephthalic acid identified and data compared by an authentic sample.

Results:

The results obtained from various experiments showed that in the absence of monoethylene glycol and benzalkonium chloride, the degradation reaction of PET wastes dose not processed. On the other hand, and in the presence of monoethylene glycol and without benzalkonium chloride, the reaction efficiency increased on average, but it was still not optimal. In contrast, the best PET degradation efficiency was observed when both monoethylene glycol and benzalkonium chloride were combined. Experimental data summarized in Table 1.

Table 1. summarized data from performed experiments

Reagent	**Reaction time 1 (h)**	**Reaction time 2(h)**	**Reaction time 3 (h)**	**Reaction time 4 (h)**
-----	0	0	0	0
MEG	0.1	0.75	3.28	4.05
MEG/BNZ	0.1	2.57	4.10	4.43

Discussion:

The results indicate that the benzalkonium chloride catalyst has a significant effect on increasing the degradation efficiency of polyethylene terephthalate. This catalyst likely helps accelerate the degradation process of polyethylene terephthalate by activating reactant molecules and reducing activation energy. Additionally, the addition of monoethylene glycol to the reactions increases the degradation efficiency. This may be due to the creation of a favorable environment for breaking the carbon bonds in the polymer structure.

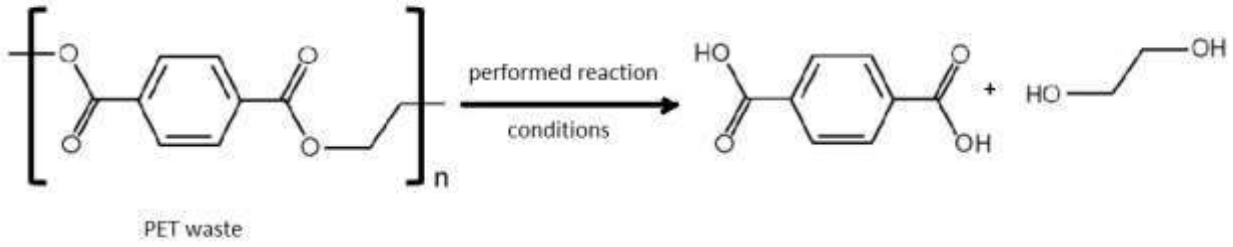

Conclusion:

Based on the obtained results, the combination of monoethylene glycol and benzalkonium chloride in an alkaline medium significantly increases the degradation efficiency of polyethylene terephthalate. This study demonstrates that the use of these catalysts can be considered an effective method for PET degradation and recycling.

References:

[1] J Das and et.al, (2006), Alkaline hydrolysis of poly (ethylene terephthalate) in presence of a phase transfer catalyst.

[2] http”//www.petcore.org.

[3] Kazumi Hiraga and et.al, (2019) Biodegradation of waste PET: A sustainable solution for dealing with plastic pollution

[4] Suraj Gupta and et.al, (2023) A review of cobalt-based catalysts for sustainable energy and environmental applications.

The 30th Iranian Seminar of Organic Chemistry
February 7-9, 2025, Iran University of Science and Technology, Tehran, Iran

Green synthesis of benzimidazoles using a nano cellulose supported on TiCl$_4$ catalyst by an electro-thermal grinding

Authors: Fatemeh Hassan Zadeh Kalali, Abdolhamid Bamoniri*

Corresponding author Email: bamoniri@kashanu.ac.ir

Department of Organic Chemistry, Faculty of Chemistry, University of Kashan, Kashan, Iran

Keywords: Green chemistry, Benzimidazoles, Nano cellulose, Thermal grinding.

Abstract

Heterocyclic compounds play an indispensable role in medicinal chemistry, underpinning the development of numerous pharmaceutical agents. Benzimidazoles, a prominent subclass of heterocyclic compounds, have attracted considerable attention for their wide range of pharmacological activities. These include anticancer, antibacterial, antifungal, antiviral and anti-inflammatory properties.[1] Structurally, benzimidazoles consist of a benzene ring fused with an imidazole ring, a configuration believed to underpin their biological efficacy. Conventional methods for synthesizing benzimidazoles typically involve the reaction of *O*-phenylenediamine derivatives with carboxylic acids or aldehyde derivatives under acidic reflux conditions.[2] While effectively, these processes often rely on hazardous reagents and generate significant environmental waste, the rising emphasis on sustainability and green chemistry has prompted the exploration of eco-friendly methodologies to mitigate these drawbacks. This study focuses on a novel green approach for benzimidazole synthesis using TiCl$_4$/nanocellulose as a heterogeneous catalyst. By supporting TiCl$_4$ on nano cellulose matrix, a catalyst system is created that not only enhances reaction efficiency but also adheres to green chemistry principles by avoiding toxic and hazardous reagents. In the experimental procedure, *O*-phenylenediamine and benzaldehyde derivatives were combined in the presence of the TiCl$_4$/nancellulose. The mixture underwent thermal grinding followed by heating in an oil bath.[3] Reaction progress was monitored using TLC, and the final product was precipitated, washed with ethanol and dried to yield crystalline benzimidazole compounds. The synthesized benzimidazole was characterized using FT-IR and ^{1}H NMR to confirm their structural integrity.

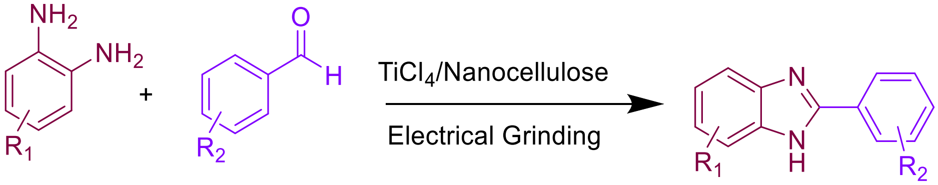

References:

[1] E. Kabir, M. Uzzaman, A review on biological and medicinal impact of heterocyclic compounds, *Results in Chem.*, **2022,** 4,1-11

[2] V.N. Mahire, P.P. Mahulikar, Facile one-pot clean synthesis of benzimidazole motifs: Exploration on bismuth nitrate accelerated subtle catalysis, *Chinese Chem. Lett.*, **2015**, 26,1-9

[3] P. Zhang, C.Liu, Ling Yu, H. Hou, W. Sun, F. Ke, Synthesis of benzimidazole by mortar–pestle grinding method, *Green Chem. Lett. Rev.*, **2021**,14, 612-619

The 30th Iranian Seminar of Organic Chemistry
February 7-9, 2025, Iran University of Science and Technology, Tehran, Iran

A green and efficient synthesis of 1, 2, 4, 5- tetra substituted imidazoles using $SbCl_5$/nano cellulose as catalyst

Authors: Zahra Salehpour Hafshejani , Abdolhamid Bamoniri*

Corresponding author Email: bamoniri@kashanu.ac.ir

Department of Organic Chemistry, Faculty of Chemistry, University of Kashan, Iran

Keywords: Imidazoles, Green synthesis, Nano catalyst, Thermal-electric mortar.

Abstract

Imidazole derivatives, five-membered heterocycles with two nitrogen atoms, have gained considerable interest for their diverse biological activities. They are fundamental components of key biomolecules like histidine and purines. These compounds have been extensively studied for their therapeutic potential against various diseases, including fungal and bacterial infections, cancer and viral infections. The synthesis of imidazole derivatives has been subjected of extensive research, with various synthetic strategies developed over the years.[1] One particularly efficient approach involves a multi-component reaction, combining 1,2-diketones, Aldehydes, ammonium acetate and aromatic amines in the presence of a suitable catalyst. This reaction offers a

straightforward and versatile route to a wide range of imidazole derivatives.[2] In recent years, there has been a growing interest in developing green and sustainable synthetic methodologies. In this context, the use of unconventional energy sources and eco-friendly catalysts has emerged as a promising approach. One method involves using thermal-electric mixing devices, providing a convenient and energy efficient environment for chemical reactions. In this study, we investigated the synthesis of 1, 2, 4, 5-tetrasubstituted imidazoles using a thermal-electric mortar device in the presence of $SbCl_5$ supported on nano silica catalyst.[3] This approach offers several advantages, including short reaction times, high yields and minimal environmental impact. To evaluate the efficiency of this method, we compared it with other methods. The results demonstrated that the thermal-electric mortar method provided superior performance in terms of reaction time, yield and product purity. Furthermore, the use of a heterogeneous catalyst facilitated easy product separation and catalyst recovery, making the process more sustainable. The synthesized imidazole derivatives were characterized using various spectroscopic techniques, including FT-IR and ^{1}H NMR spectroscopy, to confirm their structural integrity.

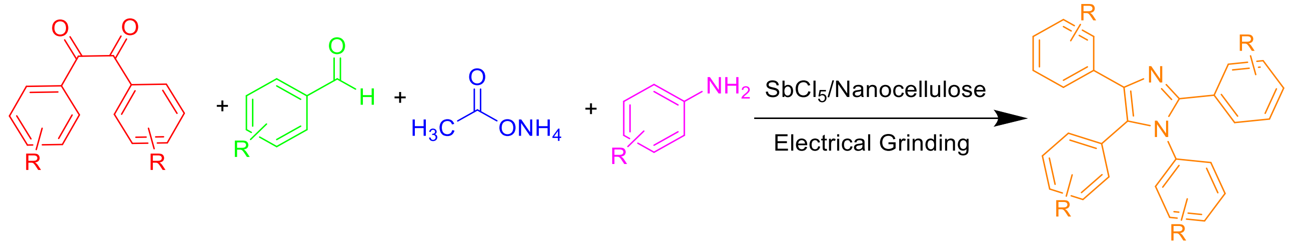

References:

[1] Pandhurnekar, C. P., Pandhurnekar, H. C., Mungole, A. J., Butoliya, S. S. and Yadao, B. G. A review of recent synthetic strategies and biological activities of isoxazole. *J. Heterocycl. Chem.*, **2023**, *60*(4), 537-565.

[2] Abd El-Lateef, H. M., Khalaf, M. M., Shalabi, K. and Abdelhamid, A. A. Multicomponent synthesis and designing of tetrasubstituted imidazole compounds catalyzed via ionic-liquid for acid steel corrosion protection: Experimental exploration and theoretical calculations. *Chinese J. Chem. Eng.*, **2023**, *55*, 304-319.

[3] Duc, D. X. and Lanh, H. T. Microwave-assisted, [Bmim] HSO4-catalyzed synthesis of tetrasubstituted imidazoles via four-component reaction. *Vietnam J. Sci. Technol.*, **2022**, *60*(3), 383-390.

Photocatalytic Degradation of Organic Pollutants Using $FeCl_3$ Catalyst: Synthesis and Application

Sahar Baniyaghoob [1a] ,Ashkan Ahsani Iravan[۲a]

[a]Islamic Azad University Science and Research BranchTehran,Iran

Keywords: Photocatalytic degradation, $FeCl_3$ nanoparticles, organic pollutants, UV light, wastewater treatment.

ABSTRACT

Photocatalytic degradation is a promising green technology for treating wastewater by removing harmful organic pollutants. In this study, we explored the potential of iron chloride ($FeCl_3$) nanoparticles, uniquely designed with nano-sized holes, for photocatalytic degradation of organic pollutants. These nanoparticles, confirmed by scanning electron microscopy (SEM), significantly increase the surface area and reactivity of the nanoparticles, enhancing their ability to break down harmful substances. The nanoparticles were synthesized through a straightforward process by dissolving $FeCl_3$ in deionized water, adding hydrogen peroxide. X-ray diffraction (XRD) confirmed their crystalline structure, and UV-vis spectrophotometry tracked pollutant degradation. The results showed that under UV light, approximately 80% of a model pollutant (methylene blue) was degraded within two hours, with absorption decreasing from 2.731 to 0.603 in that timeframe. Over three hours, the absorption further dropped to 0.037, demonstrating near-complete degradation. The reaction followed pseudo-first-order kinetics with a rate constant of $0.014\ \text{min}^{-1}$. This research highlights the remarkable efficiency of these innovative materials, making them a promising eco-friendly solution for wastewater treatment.

1.Introduction

With the growth of industries and urban areas, the release of harmful organic pollutants into water systems has become a major environmental concern. These pollutants, which include dyes, pesticides, pharmaceuticals, and other chemicals, can pose serious health risks to both humans and wildlife. Conventional wastewater treatment methods, such as biological processes, chemical oxidation, and filtration, often struggle to completely remove these contaminants, especially when they exist in low concentrations or are resistant to breakdown. This challenge has driven the search for more effective, sustainable, and affordable ways to tackle water pollution.

Photocatalysis has emerged as a promising technology for addressing this issue. It involves the use of light-activated materials, known as photocatalysts, to break down pollutants into harmless substances. This process offers an eco-friendly and efficient way to deal with a wide range of organic contaminants. Among the various photocatalysts studied, iron-based materials like ferric chloride ($FeCl_3$) stand out due to their low cost, abundance, and ability to participate in reactions that generate highly reactive species. When exposed to light, $FeCl_3$ can produce hydroxyl radicals (•OH), which are highly effective at degrading complex organic molecules.

Experimental Mechanism

In this experiment, the photocatalytic degradation of methylene blue is carried out using iron(III) chloride-derived catalysts and UV light. The main reaction mechanisms include photo-oxidation processes and attacks by free radicals, especially hydroxyl radicals (•OH), which are highly reactive and help in the breakdown of the dye and other pollutants.

1. Dissolution of Iron(III) Chloride in Water:

When $FeCl_3$ is dissolved in water, it dissociates into iron(III) ions (Fe^{3+}) and chloride ions (Cl^-):

$$FeCl_3 \rightarrow Fe^{3+} + 3Cl^-$$

Addition of Stabilizer (Polyethylene Glycol - PEG)

Polyethylene glycol (PEG) is added to stabilize the nanoparticles during their formation.

PEG molecules form a steric barrier around the growing nanoparticles, preventing their aggregation and ensuring uniform particle size.

3. Formation of Precipitate

Ammonium hydroxide (NH_4OH) is added dropwise to increase the pH to 6–7, initiating the precipitation of ferric hydroxide:

$$Fe^{3+} + 3OH^- \rightarrow Fe(OH)_3$$

This step results in the formation of a gel-like precipitate of hydrated ferric hydroxide, which serves as the precursor for nanoparticles.

4. Aging of the Gel

The gel is allowed to age for 12–24 hours at room temperature. During this time, the structure of the gel stabilizes, and the nanoparticles form through gradual condensation of hydroxide groups.

5. Washing and Purification

The precipitate is washed multiple times with deionized water to remove excess ions (e.g., Cl^-) and other impurities.

Centrifugation at high speeds ensures the separation of purified nanoparticles from the solution.

6. Drying

The purified precipitate is dried at 80°C to remove all water, leaving behind solid nanoparticles.

This drying process retains the nanoparticle integrity without causing significant changes in their structure.

7. Optional Calcination

The dried nanoparticles can be calcined at 300–500°C to improve crystallinity and phase stability. During calcination, any residual organic materials decompose, and ferric hydroxide transforms into crystalline ferric oxide or $FeCl_3$, depending on conditions:

$$Fe(OH)_3 \rightarrow Fe_2O_3 \text{(if calcined)}$$

Summary of Chemical Reactions

١. **Dissolution of $FeCl_3$**:

$$FeCl3 \rightarrow Fe^{3+} + 3Cl^-$$

٢. **Precipitation of Ferric Hydroxide**:

$$Fe^{3+} + 3OH^- \rightarrow Fe(OH)_3$$

٣. **Crystallization and Calcination**:

$$Fe(OH)_3 \rightarrow Fe_2O_3 \text{ (at high temperatures, optional)}$$

Catalyst-free Synthesis of Chromenone Based Bis(indolyl)methane

Saeideh Hasani [a], Morteza Shiri*[a], Benyamin Hosseindoust [a]

[a] *Department of Organic Chemistry, Faculty of Chemistry, Alzahra University, Tehran, Iran*

**E-mail: mshiri@alzahra.ac.ir*

Keyword: Bis(indolyl)methane, Catalyst-free, Indol, Chromenone, Coumarin

Introduction:

Indoles and their derivatives constitute a significant portion of heterocyclic compounds containing nitrogen, playing an essential role in synthetic chemistry, pharmaceuticals, advanced materials, and insecticides.[1]

The foundation of typical BIM structures is the indole unit. Bis(indolyl)methanes and their derivatives are pharmacologically active and are used in the field of pharmaceutical chemistry bis(indolyl)methanes have various biological activities such as antihyperglycemic, anti-inflammatory, antibacterial, anticancer and antileishmaniasis activities, including enzyme inhibition. They play an important role in suppressing many diseases, especially cancer.

The reactivity of the indole ring is highest at carbon atom 3. As a result, 3,3′-BIMs make up the majority of BIMs presented in the literature.[2-4]

Method:

This study describes a simple and efficient approach to the synthesis of bis(indolyl)methane from indole and 4-chloro-3-formylcoumarin under catalyst-free conditions. For this, 4-chloro-3-formylcoumarin 1eq (1 mmol) and indole 2eq (2 mmol) were studied in the toluene (5 mL) at r.t for 4 h, this gratifyingly afforded the bis(indolyl)methane in 73% yield (Scheme 1).

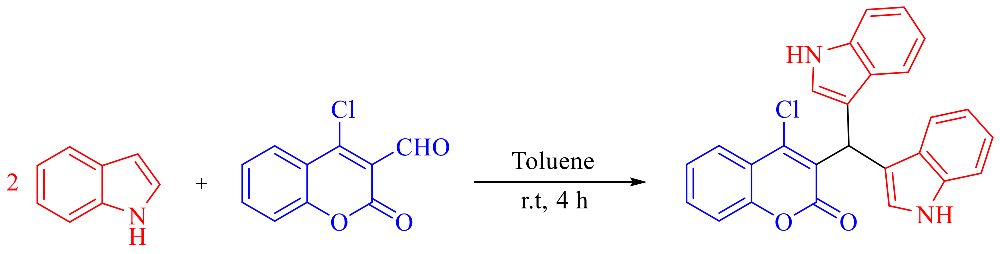

Scheme 1: Synthesis of 4-chloro-3-(di(1H-indol-3-yl)methyl)-2H-chromen-2-one.

Results and Discussion:

A new, environmentally friendly and efficient method for the synthesis of bis(indolyl)methanes (BIMs) under catalyst and solvent-free conditions has been developed. Indoles are condensed with various aromatic aldehydes to produce bis(indolyl)methanes without a catalyst. This approach supports the principles of green chemistry by minimizing the environmental impact and simplifying the reaction process.[5-7]

The direct functionalization of indole offers a more efficient approach to constructing diverse indole scaffolds when contrasted with traditional synthetic methods. As we enter an era of emphasis on green and sustainable chemistry, the use of environmentally friendly solvents such as water demonstrates great potential in the synthesis of valuable indole derivatives. The reaction can be carried out either in a solvent-free environment or in the presence of a mild solvent, both of which provide high yields of the target compound.

References:

(1) Q. Pang, W.-F. Zuo, Y. Zhang, X. Li and B. Han. The *Chemical Record* **2023**, 23, 30.
(2) M. Shiri, M. A. Zolfigol, H. G. Kruger and Z. Tanbakouchian. *Chemical Reviews* **2010**, 110, 2250.
(3) A. Bahuguna, A. Singh, P. Kumar, D. Dhasmana, V. Krishnan and N. Garg. *Computers in Biology and Medicine* **2020**, 116, 103574.
(4) S. Imran, M. Taha and N. Hadiani Ismail. *Current Medicinal Chemistry* **2015**, 22, 4412
(5) M. Shiri. *Chemical Reviews* **2012**, 112, 3508
(6) V. D. Kadu, S. N. Chandrudu, M. G. Hublikar, D. G. Raut and R. B. Bhosale. *RSC Advances* **2020**, 10, 23254
(7) N. Azizi, E. Gholibeghlo and Z. Manocheri. *Scientia Iranica* **2012**, 19, 574

The 30th Iranian Seminar of Organic Chemistry
February 7-9, 2025, Iran University of Science and Technology, Tehran, Iran

Extraction, chemical composition, and anti-microbial properties of Alpha-Pinene from *Pistacia Atlantica* subs. *Kurdica*

Arvin Shajeie[1], Nasrin Kakaei[2], Veria Naseri[2], Abbas Ahmadi[3], Amir Shokoufandeh[4*]

1. Faculty of Health, Qazvin University of Medical Sciences, Qazvin, Iran

2. Department of Research and Development, Jiran Darou Company, Sanandaj, Iran

3. Cellular and Molecular Research Center, Research Institute for Health Development, Kurdistan University of Medical Sciences, Sanandaj, Iran

4. Faculty of Sciences, University of Kurdistan, 6617715175, Sanandaj, Kurdistan, Iran Corresponding author: amir.shokou@gmail.com

Abstract

This study aimed to investigation of using *Pistacia Atlantica subsp. Kurdica* gum essential oil as natural active ingredient for medicinal and health purposes. The gum was collected and subjected to hydro distillation, yielding essential oil with a 20% yield. Gas chromatography-mass spectrometry (GC-MS) and Inductively Coupled Plasma Mass Spectrometry (ICP-MS) are used to determine of chemical and heavy metal composition of essential oil, respectively. Antimicrobial activity was evaluated using the broth microdilution assay against bacterial strains, including *Staphylococcus aureus* and *Streptococcus mutans*. GC-MS analysis identified alpha-pinene as the active pharmaceutical ingredient (>90%), with a retention time of 6.654 minutes and molecular ion peak at m/z 136.0. ICP-MS confirmed minimal heavy metal content, ensuring safety for biological applications. Antimicrobial assays demonstrated significant activity, with MIC values ranging from 0.281 mg/L to 0.624 mg/L across tested strains. Results suggested that the essential oil of *Pistacia Atlantica subsp. Kurdica* gum has the potential to be used in the pharmaceutical industry as a natural active compound.

Introduction

Investigation of chemical products and processes that reduce or eliminate the use and creation of hazardous compounds is the focus of green chemistry, a critical area of contemporary research [1]. It acknowledges the urgent need for environmentally friendly substitutes for conventional, often harmful, industrial processes. The principles of green chemistry promote the utilization of biodegradable resources, such as natural materials derived from plants, as fundamental components in sustainable chemical innovation [2]. These plant-based substances often exhibit unique biological activity and structural characteristics, serving as significant sources of inspiration for creating innovative synthetic pathways and environmentally safe products. By leveraging the vast chemical diversity present in plants, researchers can develop alternative feedstocks and reactions, thereby reducing reliance on finite resources and minimizing waste [3-5].

In pharmaceutical research, the application of chemicals derived from plants is especially significant. Plant-derived compounds are instrumental in the creation of new drug candidates with reduced environmental impact. Incorporating green chemistry principles—such as the use of plant-based chemicals—is pivotal for fostering a more sustainable and ecologically responsible chemical industry [5-7].

Terpenes, a broad class of naturally occurring organic compounds primarily produced by plants, are gaining increasing prominence in green chemistry and the chemical industry [5]. Due to their availability, biodegradability, and often distinctive biological functions, terpenes serve as appealing alternatives to petroleum-derived compounds [8] . Commonly found in essential oils (EOs) and resins, terpenes have diverse applications in solvents, pharmaceuticals, and fragrances [9]. Their inherent biocompatibility, biodegradable nature, and typically lower toxicity profiles compared to synthetic equivalents position them as essential components of sustainable chemical processes. Consequently, heightened interest in terpenes is driving research into their extraction, modification, and utilization in environmentally benign synthetic methods, thus fostering a more ecologically friendly chemical industry[10, 11].

Table 1. Chemical structure of some selected monoterpenes

Monoterpene	Alpha-pinene	Citral		Geraniol	Limonene	
Isomers	-	Citral A	Citral B	-	L-limonene	D-limonene
Structure	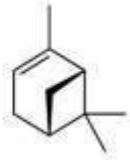	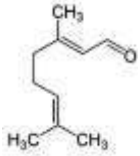	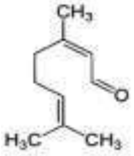	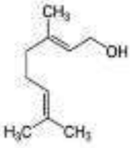	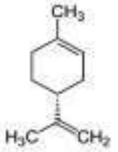	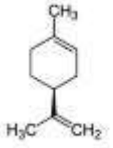

Pistacia atlantica subsp. Kurdica, a member of the Anacardiaceae family, is a primary source of an exudate gum with longstanding use as a treatment for infections. This evergreen shrub or small tree, native to regions spanning the Iranian Plateau to North Africa, comprises three subspecies: mutica, kurdica, and cabulica. The gum derived from this plant has demonstrated robust antibacterial properties, largely attributed to its high content of monoterpene compounds, particularly alpha-pinene (≥90%), which serves as its active constituent [12, 13].

Alpha-pinene, a common monoterpene of *Pistacia atlantica subsp. Kurdica* gum EO, is a volatile, colorless liquid with a characteristic piney odor [14]. Its physical properties include a boiling point of around 155-160°C and a density slightly less than that of water [14]. Chemically, α-pinene is a bicyclic hydrocarbon, exhibiting both electrophilic and radical reactivity, allowing for various chemical transformations. It's often found in pine resin and the essential oils of various coniferous trees, and its extraction typically involves steam distillation. This process utilizes the high vapor pressure of α-pinene to separate it from the plant material. Solvent extraction methods are also sometimes employed, but steam distillation is generally preferred due to its inherent sustainability and lower environmental impact compared to using volatile organic solvents [14, 15].

Alpha-pinene, a monoterpene, finds numerous applications across various industries. In the fragrance industry, its characteristic pine scent makes it a valuable component in perfumes, soaps, and cleaning products. The chemical industry utilizes α-pinene as a precursor for the synthesis of other chemicals, including active ingredients for pharmaceuticals and fine chemicals. Its unique reactivity makes it useful in the production of various resins, and polymers [16]. To our best knowledge, alpha-pinene due to its antimicrobial, anti-inflammatory, and antioxidant properties is a good candidate as active ingredient in the pharmaceutical and health industries. So, the aim of the current study was to investigate the chemical composition and anti-bacterial effect of alpha-pinene from *Pistacia atlantica subsp. Kurdica* gum [17-19].

Materials and methods

Extraction of α-pinene from Pistacia Atlantica Kurdica

The gum of *Pistacia Atlantica subs. kurdica* was collected in the first month of summer in Kurdistan province in Iran. The gum was hydro distilled for 6 hours to obtain a volatile oil in 20% yield based on the fresh weight of the gum. The essential oil was dried with anhydrous sodium sulfate (Sigma-Aldrich, Steinheim, Germany) to remove moisture. The oil was then stored at a low temperature (+4°C) in amber vials to prevent light exposure, ensuring stability until further analysis [20, 21].

Essential Oil Analysis

Gas Chromatography-Mass Spectrometry (GC-MS)

The essential oil composition of *Pistacia atlantica subsp. Kurdica* gum was analyzed using gas chromatography-mass spectrometry (GC-MS) with an Agilent 7890B GC system/5977A MSD. A capillary column (30 m × 0.25 mm, 0.25 µm HP-5 ms) facilitated the separation. Helium was used as the carrier gas at a pressure of 34 psi and a flow rate of 1 mL/min. The temperature program started at 50°C, increasing by 7°C/min to 260°C, then by 5°C/min to 300°C. Mass spectrometry employed electron impact ionization (70 eV) with an ionization source temperature of 230°C. Retention indices were calculated using n-alkanes as references, and essential oil components were identified by comparing mass spectra and retention indices with established GC/MS databases, such as Wiley and NIST.

Heavy Metal Analysis

Heavy metal content was evaluated using Inductively Coupled Plasma Mass Spectrometry (ICP-MS).

Antimicrobial Activity of Alpha-Pinene

The antimicrobial activity of alpha-pinene was evaluated using the broth microdilution assay with resazurin as a metabolic indicator. The minimum inhibitory concentration (MIC) was determined against various bacterial strains (Table 3).

Result and discussion

Quantitative data were obtained via flame ionization detection (FID), which revealed that alpha-pinene dominated the essential oil, constituting over 90% of the volatile organic compounds (VOCs). A retention time (RT) of 6.654 minutes confirmed the alpha-pinene identification. Mass spectrometry yielded a precise molecular ion peak (M+) at m/z 136.0, consistent with the molecular formula $C_{10}H_{16}$. These findings, summarized in Table 1

Table 1. GC-MS Analysis of Pistacia Atlantica subsp. Kurdica Gum Essential Oil

c	Area (Ab*s)	Hit Name	Quality	Mol Weight (amu)	Percent
6.654	2151750723	alpha-Pinene	90	136.125	91.36
6.934	28378631	Camphene	97	136.125	1.20
7.482	15927992	Sabinen	97	136.125	0.68
7.558	90369923	beta-Pinene	97	136.125	3.84
8.712	21568676	D-Limonene	98	136.125	0.92
10.297	29598053	α-Pinene oxide	64	152.12	1.26
10.472	17734747	2,4(10)-Thujadiene	93	134.11	0.75
	2355328745				100.00

The results of heavy metal analysis by ICP, presented in Table 2, confirmed that concentrations of cadmium (Cd), lead (Pb), arsenic (As), and mercury (Hg) were below detectable levels, ensuring the safety and suitability of the essential oil for further biological research.

Table 2. Heavy Metal Analysis

ITEMS	Result (ppm)
Cadmium (Cd)	<0.01
Lead (Pb)	<0.01
Arsenic (As)	<0.01
Mercury (Hg)	<0.01

The assay confirmed significant antimicrobial efficacy, with MIC values ranging from 0.281 mg/L to 0.624 mg/L, depending on the bacterial strain.

Table 3. Antimicrobial Activity Results

Bacterial Strains	**Type of Test**	**Result**	**Reference Test Method**
S. aureus ATCC 25923	Microdilution in broth	0.312 mg/L	CLSI
E. coli ATCC 25922	Microdilution in broth	0.312 mg/L	CLSI
P. aeruginosa ATCC 27853	Microdilution in broth	0.281 mg/L	CLSI
S. mutans ATCC	Microdilution in broth	0.624 mg/L	CLSI

This study highlights the potential of Pistacia atlantica subsp. Kurdica gum as a sustainable resource for green chemistry applications. The high alpha-pinene content (≥90%) underscores its suitability for pharmaceutical and therapeutic use. Comprehensive chemical and antimicrobial analyses validate the gum's efficacy and safety, supporting its role in advancing environmentally benign industrial processes and products.

References

1. Li, C.-J. and P.T. Anastas, *Green Chemistry: present and future.* Chemical Society Reviews, 2012. **41**(4): p. 1413-1414.
2. Zimmerman, J.B., et al., *Designing for a green chemistry future.* Science, 2020. **367**(6476): p. 397-400.
3. Kalidindi, S.B. and B.R. Jagirdar, *Nanocatalysis and prospects of green chemistry.* ChemSusChem, 2012. **5**(1): p. 65-75.
4. Clark, J.H. and D.J. Macquarrie, *Handbook of green chemistry and technology*. 2008: John Wiley & Sons.
5. Tucker, J.L., *Green chemistry, a pharmaceutical perspective.* Organic process research & development, 2006. **10**(2): p. 315-319.
6. Sholikhah, E.N., *Indonesian medicinal plants as sources of secondary metabolites for pharmaceutical industry.* J Med Sci, 2016. **48**(4): p. 226-239.
7. Msingh, R., R. Pramanik, and S. Hazra, *Role of green chemistry in pharmaceutical industry: A review.* J. Univ. Shanghai Sci. Technol, 2021. **23**: p. 291-299.
8. Masyita, A., et al., *Terpenes and terpenoids as main bioactive compounds of essential oils, their roles in human health and potential application as natural food preservatives.* Food chemistry: X, 2022. **13**: p. 100217.
9. Saini, R.K., et al., *Bioactive compounds of citrus fruits: A review of composition and health benefits of carotenoids, flavonoids, limonoids, and terpenes.* Antioxidants, 2022. **11**(2): p. 239.

10. Kim, T., et al., *Therapeutic potential of volatile terpenes and terpenoids from forests for inflammatory diseases.* International journal of molecular sciences, 2020. **21**(6): p. 2187.

11. Weston-Green, K., H. Clunas, and C. Jimenez Naranjo, *A review of the potential use of pinene and linalool as terpene-based medicines for brain health: discovering novel therapeutics in the flavours and fragrances of cannabis.* Frontiers in psychiatry, 2021. **12**: p. 583211.

12. Ahmed, Z.B., et al., *Four Pistacia atlantica subspecies (atlantica, cabulica, kurdica and mutica): A review of their botany, ethnobotany, phytochemistry and pharmacology.* Journal of Ethnopharmacology, 2021. **265**: p. 113329.

13. Majd, F.S., et al., *Efficacy of a standardized herbal product from Pistacia atlantica subsp. Kurdica in type 2 diabetic patients with hyperlipidemia: A triple-blind randomized clinical trial.* Complementary Therapies in Clinical Practice, 2022. **48**: p. 101613.

14. Hasheminya, S.-M. and J. Dehghannya, *Composition, phenolic content, antioxidant and antimicrobial activity of Pistacia atlantica subsp. kurdica hulls' essential oil.* Food Bioscience, 2020. **34**: p. 100510.

15. Dolatyabi, M., G. Adhami, and Y. Maroofi, *Effect of Pistacia atlantica (kurdica) oil extract on promastigotes of Leishmania major.* New Findings in Veterinary Microbiology, 2022. 4(2): p. 92-99.

16. Ebrahimnezhad-Khaljiri, H. and A. Ghadi, *Recent advancement in synthesizing bio-epoxy nanocomposites using lignin, plant oils, saccharides, polyphenols, and natural rubbers: A review.* International Journal of Biological Macromolecules, 2024. **256**: p. 128041.

17. A Kaskoos, R., A. Javed, and S. Uthirapathy, *Chemical composition and cytotoxic activity of Pistacia atlantica var. kurdica fruits.* ARO-The Scientific Journal of Koya University, 2021. 9(2): p. 91-95.

18. Allenspach, M. and C. Steuer, *α-Pinene: A never-ending story.* Phytochemistry, 2021. **190**: p. 112857.

19. Karimkhani, M.M., et al., *Extraction and purification of α-pinene; a comprehensive review.* Critical Reviews in Food Science and Nutrition, 2024. **64**(13): p. 4286-4311.

20. Pogorzelska-Nowicka, E., M. Hanula, and G. Pogorzelski, *Extraction of polyphenols and essential oils from herbs with green extraction methods–An insightful review.* Food Chemistry, 2024: p. 140456.

21. Kant, R. and A. Kumar, *Review on essential oil extraction from aromatic and medicinal plants: Techniques, performance and economic analysis.* Sustainable Chemistry and Pharmacy, 2022. **30**: p. 100829.

Application of alpha-pinene from *Pistacia Atlantica* subs. *Kurdica* in oral care products

Delnia Bahari[1*], Sahereh Esmaeili[1], Veria Naseri[1], Amir shokofandeh[2]

1. *Department of Research and Development, Jiran Darou Company, Sanandaj, Iran*

2. *Faculty of Sciences, University of Kurdistan, 6617715175, Sanandaj, Kurdistan, Iran*

Corresponding author: bahari.delnia@yahoo.com

Keyword: phytochemistry, terpenes, monoterpenes, alpha-pinene, oral care

١. INTRODUCTION

Plants and their derived compounds have been used in medicine and dentistry for centuries. Historically, plant-based products have played a significant role in medical applications. Due to the importance of human health, there is a growing interest in naturally processed oral health care products[1]. Among the natural products that offer medical benefits, terpenes, as a plant active component, play a variety of crucial roles. Common plant sources of terpenes include Pinus ponderosa (*Pinaceae*), spices such as sage, rosemary, caraway, cumin, clove, and thyme, and citrus fruits like lemon, orange, and mandarin[2]. Of the approximately 55,000 known terpene structures, some have potential therapeutic applications. Alpha-pinene (α-pinene) and beta-pinene (β-pinene) are the main components of turpentine, widely used in chemical raw materials, pharmaceutical synthesis, perfumes, cosmetics, and other industries[3].

The essential oils from *Pistacia Atlantica* subs. *Kurdica* gum, which grows in the Zagros Mountains of Iran, were obtained through hydrodistillation using a Clevenger-type apparatus[4]. GC-MS analysis revealed alpha-pinene as the main component with a purity of 93.85%. Alpha-pinene is a bicyclic monoterpene commonly used as a fragrance ingredient in perfumes[5], personal care products[3], household cleaners, and air fresheners. Furthermore, alpha-pinene demonstrates a range of biological activities, including anticancer[6], antibacterial[7], antiviral[8], anti-inflammatory[9], antiparasitic[10], and antioxidant[11] properties. These attributes highlight its potential in oral care products and therapeutic applications. Jiran Darou, a knowledge-based enterprise, has harnessed the benefits of alpha-pinene in advanced oral care formulations, making significant strides in developing innovative and highly effective products.

٢. Experimental Procedure

٢,١. Preparation of Essential Oil

The gum of *Pistacia Atlantica* subs. *kurdica* was collected in the first month of summer in Kurdistan province in Iran. The gum was hydro distilled for 6 hours to obtain a volatile oil in 20% yield based on the fresh weight of the gum. The resulting essential oil was dried with anhydrous sodium sulfate (Sigma-Aldrich, Steinheim, Germany) to remove moisture. The oil was then stored at a low temperature (+4°C) in amber vials to prevent light exposure, ensuring stability until further analysis.

٢،٢. Analysis of Essential Oil Composition

The composition of the essential oil was analyzed using gas chromatograph (Agilent Technologies, USA, 7890B GC System/ 5977A MSD) equipped with a column (30 m×0.25mm ,0.25 Micron HP-5 ms). Helium was employed as the carrier gas with a flow rate of 1 mL/min, and a pressure of 34 psi. Detection was performed using a flame ionization detector (FID). The column temperature program started at 50 °C, increased at a rate of 7 °C/min to 260 °C, and then increased at 5°C/min at to a final temperature of 300 °C. Mass spectrometry analysis was performed with an Agilent 5973 instrument using 70 eV electron impact (EI) ionization. The ionization source temperature was maintained at 230°C. Retention indices were calculated based on the retention times of n-alkanes (obtained from Fluka). Quantitative data were determined by electronic integration of FID peak areas. Identification of the essential oil components was achieved by comparing the mass spectra and retention indices with those in established GC/MS library databases, including Wiley and NIST. This methodology ensured precise and reproducible analysis of the essential oil composition.

3. RESULT AND APPLICATION

3.1. Chemical Analysis

A GC-MS analysis was conducted to determine the chemical components of the essential oil. The major compounds in *Pistacia atlantica Kurdica* gum are alpha-pinene (93.85%) and L-β-pinene (3.45%) as shown in Table 1.

Table 1: The composition of *Pistacia atlantica Subsp. Kurdica* gum essential oil

Peak No.	Compounds	RT (%)	MWt	PERCENT
1	**Alpha-Pinene**	**6.654**	**136.125**	**93.85**
2	**Camphene**	**6.934**	**136.125**	**1.14**
3	**L-β-Pinene**	**7.557**	**136.125**	**3.45**
4	**D-Limonene**	**8.711**	**136.125**	**0.71**
5	**α-Terpinolen**	**10.046**	**136.125**	**0.85**

3.2. Applications in Oral Care Products

Mouthwash

Mouthwashes are essential for oral hygiene, especially for individuals at risk of periodontal diseases. Clinical trials of mouthwashes containing alpha-pinene have shown reductions in plaque formation, gingival inflammation, and microbial load (ref). These formulations offer a natural alternative to synthetic mouthwashes, addressing consumer concerns about chemical additives. In Jiran Darou, five models of natural mouthwashes such as Multi-Action, Mantra (fluoride-free), Sensitive, Complete, and Whitening for adults have been formulated, and scientific research has been conducted on them.

Motallebi et al. (2022) compared a natural mouthwash with chlorhexidine mouthwash in a randomized clinical trial. The plaque and gingival indices between chlorhexidine and alpha-pinene mouthwashes showed no significant difference. However, chlorhexidine mouthwash caused tooth discoloration.

Toothpaste

Incorporating alpha-pinene into toothpaste formulations capitalizes on its antimicrobial and anti-inflammatory properties. Studies suggest that toothpaste containing alpha-pinene can reduce gingival bleeding and plaque scores, particularly when used as part of a comprehensive oral hygiene regimen. Research has been conducted on six models of natural Alpha Dent toothpaste for adults and two models for children. Ebrahimi et al. (2024) studied the comparative effectiveness of natural versus commercial toothpaste on salivary pH and *Streptococcus mutans* count. They resulted natural toothpaste exhibited antimicrobial activity against *S. mutans* and increased the salivary pH (Table 2).

Table 2- comparative evaluation of the salivary pH and *Streptococcus Mutans* colony count between natural and Sensodyne toothpaste

Parameter	Time period	Group	N	Mean ± SD	p-value [a]
Salivary pH	Baseline	Natural	40	6.96±0.47	0.23
		Sensodyne	40	6.79±0.47	
	After brushing	Natural	40	7.06±0.33	0.16
		Sensodyne	40	7.13±0.39	
S. mutans colony count	Baseline	Natural	40	82.22±71.13	0.99
		Sensodyne	40	80.5±62.26	
	After brushing	Natural	40	67.37±54.83	0.35
		Sensodyne	40	57.1±49.12	

[a] Mann–Whitney U test

Ghodsi et al (2022) investigated the effect of two types of anti-hypersensitivity toothpastes (Alpha Dent and Sensodyne) in people with dentin hypersensitivity. As showed, the tooth sensitivity in two groups of Alpha Dent & Sensodyne toothpaste was reduced and oral health and quality of life was improved (Table 3).

Table 3- The mean of sensitivity degree at 24 hours and one month after plaque removal in people with dentin sensitivity in two groups of toothpaste containing alpha-pinene and potassium nitrate

Variable	Frequency	Mean	SD	P-value[a]
Natural toothpaste containing α-pinene				
24 h after dental scaling	**30**	**6.4**	**2.2**	<0.0001
1 month after dental scaling	**30**	**3.3**	**2.3**	
Toothpaste containing potassium nitrate (Sensodyne)				
24 h after dental scaling	**30**	**5.9**	**2.2**	<0.0001
1 month after dental scaling	**30**	**1.33**	**2.1**	

[a] paired t-test

Breath Fresheners

Alpha-pinene's pleasant aroma and antimicrobial properties make it suitable for breath fresheners, such as sprays and chewing gums. These products not only combat halitosis but also address underlying microbial causes, providing therapeutic benefits alongside cosmetic effects[12] .

References:

1. Potocka, W., Assy, Z., Bikker, F. J. & Laine, M. L. Current and potential applications of monoterpenes and their derivatives in oral health care. *Molecules* **28**, 7178 (2023).

2. Cox-Georgian, D., Ramadoss, N., Dona, C. & Basu, C. Therapeutic and medicinal uses of terpenes. *Med. plants from farm to Pharm.* 333–359 (2019).

3. Brahmkshatriya, P. P. & Brahmkshatriya, P. S. Terpenes: Chemistry, biological role, and therapeutic applications. *Nat. Prod. Phytochem. Bot. Metab. alkaloids, phenolics terpenes* 2665–2691 (2013).

4. Sharifi, M. S. Fractionations and analysis of trunk exudates from Pistacia genus in relation to antimicrobial activity. (2006).

5. Naves, Y.-R. Progress in the Synthesis of Perfumes Based on Pinenes. *Russ. Chem. Rev.* **37**, 779 (1968).

6. Han, E.-J. *et al.* Anticancer effects of $α$-pinene in AGS gastric cancer cells. *J. Med. Food* **27**, 330–338 (2024).

7. Borges, M. F. de A., Lacerda, R. de S., Correia, J. P. de A., de Melo, T. R. & Ferreira, S. B. Potential antibacterial action of $α$-Pinene. in *Medical Sciences Forum* vol. 12 11 (2022).

8. Astani, A., Reichling, J. & Schnitzler, P. Comparative study on the antiviral activity of selected monoterpenes derived from essential oils. *Phyther. Res. An Int. J. Devoted to Pharmacol. Toxicol. Eval. Nat. Prod. Deriv.* **24**, 673–679 (2010).

9. Rufino, A. T. *et al.* Anti-inflammatory and chondroprotective activity of (+)-$α$-pinene: structural and enantiomeric selectivity. *J. Nat. Prod.* **77**, 264–269 (2014).

10. TABARI, M. A., ZIZZADORO, C., MOEINI, M., TABATABAEI, S. Z. & YOUSSEFI, M. R. IN VITRO TOXIC EFFECT OF ORDINARY AND MICRO-EMULSIFIED A-PINENE AND B-CARYOPHYLLENE ON HYDATID CYST PROTOSCOLECES. *Bulg. J. Vet. Med.* **27**, (2024).

11. Rahmani, H., Moloudi, M. R., Hashemi, P., Hassanzadeh, K. & Izadpanah, E. Alpha-pinene alleviates motor activity in animal model of Huntington's disease via enhancing antioxidant capacity. *Neurochem. Res.* **48**, 1775–1782 (2023).

12. Pino-Delgado, A., Vado, D., McLeese, D. & Hsieh, S. Volatile Organic Compounds Emitted from Air Fresheners: Plug-Ins at Home and Little Trees in Cars. *J. Student Res.* **10**, (2021).

The 30th Iranian Seminar of Organic Chemistry
February 7-9, 2025, Iran University of Science and Technology, Tehran, Iran

Synthesis of 2,4,5-trisubstitutedimidazoles in the presence of $SbCl_5$ supported on a nanosubstrate under Solvent-free conditions by an electro-thermal grinding

Authors: Zahra Kouheshghiyan , Abdolhamid Bamoniri*

Corresponding author Email: bamoniri@kashanu.ac.ir

Department of Organic Chemistry, Faculty of Chemistry, University of Kashan, Kashan, Iran

Keywords: Heterocyclic compounds, Grinding, Nanocatalyst , Imidazoles , Solvent-free

Abstract

Trisubstituted imidazoles, a versatile class of heterocyclic compounds, have garnered significant attention due to their diverse applications in pharmaceuticals, natural products and material science[1].Traditional methods for their synthesis often rely on multi-step processes involving toxic solvents and catalysts[2].We present a sustainable and efficient approach for synthesizing trisubstituted imidazoles utilizing a solvent-free, one-pot mechanochemical reaction. In this study a list of trisubstituted imidazoles were synthesized through the condensation of 1,2- diketones, benzaldehyde derivatives and ammonium acetate were used in this process of a recyclable heterogeneous catalyst, $SbCl_5$ supported on nanocellulose [3].The reaction was conducted in a thermal electric mortar mill at 60 °C for 15 minutes. This mechanochemical approach offers several advantages, including reduced reaction time, enhanced product yields, and minimized solvent waste. The progress of the reaction was monitored by TLC , and the pure products were isolated through recrystallization. FT-IR and ^1H NMR spectroscopy confirmed the structural characterization of the synthesized imidazoles. Identification of the catalyst was investigated using various characterization techniques, including XRD, EDS, FESEM and TEM.

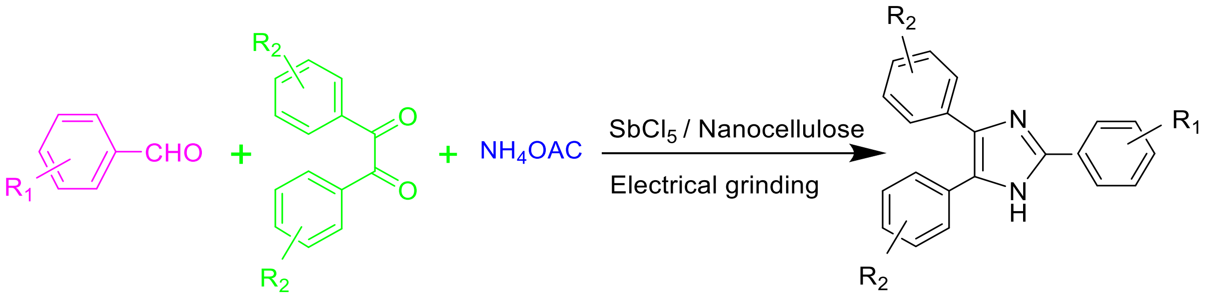

References:

[۱] E. Eidi, M.Z. Kassaee and Z. Nasresfahani, Synthesis of 2, 4, 5-trisubstituted imidazoles over reusable $CoFe_2O_4$ nanoparticles: an efficient and green sonochemical proces, *Appl. Organomet. Chem*., **2016** , 30(7) , 561-565.

[2] J. Sonar, S. Pardeshi , S. Dokhe , R. Pawar , K. Kharat , A. Zine , B. Matsagar , K. Wu and S. Thore , An efficient method for the synthesis of 2, 4, 5-trisubstituted imidazoles using lactic acid as promoter, *Appl. Sci*., **2019** , (1), 1-7.

[3] M . Sakhdari , A. Amoozadeh and E. Kolvari , Magnetic nanoparticle-supported sulfonic acid as a green catalyst for the one-pot synthesis of 2, 4, 5-trisubstituted imidazoles and 1, *2, 4, 5-tetrasubstitut*ed imidazoles under solvent-free conditions , *Heterocycl. Commun.*, **۲۰۲۱**, **۲۷(۱).** ۷۱-۷۸.

One-pot multicomponent synthesis of pyrimidine compounds in the presence of acidic ionic liquid triethyl (butyl-4-sulfonic acid) ammonium hydrogen sulfate

Hossein Sarvari, Nafisehsadat Sheikhan*

*Department of Chemistry, Najafabad branch, Islamic Azad university, Najafabad, Iran. *E-mail; ns_sheikhan@yahoo.com*

Keyword: pyrimidine, One-pot multi-component synthesis, acidic ionic liquid, solvent free

The extensive use of toxic and volatile solvents in the chemical industries leads to serious environmental damage. Therefore, finding suitable replacements for these solvents that are environmentally friendly is urgently needed in the pharmaceutical and chemical sectors. Ionic liquids, due to their very low vapor pressure, have attracted the attention of many scientists as green solvents or catalysts in multi-component one-pot reactions. Speed, diversity, efficiency, and eco-friendliness are some of the key aspects of these reactions. The synthesis of heterocycles containing nitrogen, oxygen, and sulfur, which are structural units in many natural products and active pharmaceutical ingredients, is highly significant using this efficient one-pot multi-component method. The heterocyclic pyrimidine compounds have important biological and pharmaceutical applications [1-3]. So, herein, triethyl (butyl-4-sulfonic acid) ammonium hydrogen sulfate ($[TEBSA]^+[HSO_4]^-$) as an acidic ionic liquid was synthesized, identified by IR and NMR analyses, and then utilized for its catalytic properties in the one-pot three-component synthesis of pyrimidine derivatives from condensation of aldehydes with thiourea or urea and ethyl acetoacetate under solvent-free conditions.

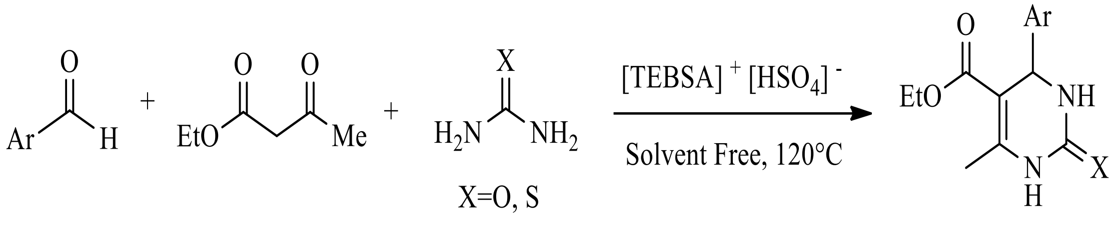

Scheme: Synthesis of dihydropyrimidine derivatives in the presence of acidic ionic liquid

References:

[1] Adhikari, S., Datta, A., Saha, I., Ghosh, K. *Coordination Chemistry Reviews*, 2024, *517*, 2159-2189.

[2] Zolfagharinia, S., Kolvari, E., Koukabi, N. *Catalysis Letters*, 2017,*147*, 1551-1566.

[3] Anjaneyulu, B., Rao, D., GB, A. *Int. J. Eng. Technol. Res*, 2015, *3*(6), 26-37.

Sulfonic acid functionalized graphene oxide as an effective catalyst for one-pot, three-component synthesis of arylidene heterobicyclic pyrimidinones via biginelli-like reaction

Marjan Alizadeh, Nafisehsadat Sheikhan*

*Department of Chemistry, Najafabad branch, Islamic Azad University, Najafabad, Iran.*E-mail; ns_sheikhan@yahoo.com*

Keyword: functionalized graphene oxide, three-component synthesis, pyrimidinone, biginelli-like

Lately, more attention has been paid to the use of Graphene oxide (GO) as solid acids in organic synthesis. graphene oxide (GO) includes high density of hydrophilic organic functional groups including hydroxyl, carboxyl and epoxy functional groups. However, GO and such kind of improved GO is a capable candidate as heterogeneous acid catalyst for organic transformation as well as industrial applications [1]. One-pot multicomponent reactions are known as significant and environmentally benign processes in synthetic chemistry because they decrease the number of steps and reduce energy consumption and waste production. Pyrimidine and its derivatives constitute an important class of natural and synthetic products that have substantial biological and pharmaceutical properties [2]. Specially, functionalized pyrimidines such as fused pyrimidinones with an arylidene part are necessary heterocyclic motifs in antitumor agents. Regarding the importance of arylidene heterobicyclic pyrimidinones and the great need for environmentally benign chemical productions, the development of suitable green synthetic methods for these compounds has attracted considerable interest. So, herein we report a new, convenient, mild, and efficient method for one-pot, three-component synthesis of pyrimidine derivatives from condensation of aldehydes with urea or thiourea and cyclopentanone in the presence sulfonic acid functionalized graphene oxide (GO-SO_3H) as an effective solid acid catalyst. (Scheme).

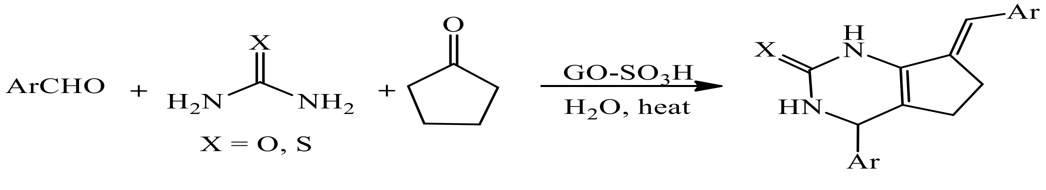

Scheme: synthesis of arylidene heterobicyclic pyrimidinones derivatives by using GO-SO_3H

References:

[1] Hanoon, H.; Kowsari, E.; Abdouss, M.; Zandi, H.; Ghasemi, M. Research on chemical intermediates, 2017, 43, 1751–1766.

[2] Kanevskaya, V.; Bondartsova, A. S.; Fedotova, O. V. *Russian Journal of Organic Chemistry, 2020, 56, 1753–175.*

The 30th Iranian Seminar of Organic Chemistry
February 7-9, 2025, Iran University of Science and Technology, Tehran, Iran

Synthesis and Characterization of Some Novel Antipyrinyl Azopyrazole Sulfonamide Hybrids

Reihane Ghomashi[a,b], Shakila Ghomashi[b], Ahmad Reza Massah*[b]

[a] *Department of Medicinal Chemistry, School of Pharmacy and Pharmaceutical Sciences, Isfahan University of Medical Sciences, Isfahan, Iran*

[b] *Department of Chemistry, Shahreza Branch, Islamic Azad University, P.O. Box 311-86145, Shahreza, Isfahan, Iran*

Keywords: Synthesis, Sulfonamide, Antipyrine, Azopyrazole, Chalcone, Hybridization

In synthetic chemistry, the sulfonamide group is one of the most versatile toolboxes for synthesizing novel organic compounds[1]. Moreover, the hybridization of sulfonamide and heterocycles is the best technique for discovering novel interesting biologically active compounds[2]. In this work, some novel sulfonamide hybrids including antipyrine, azopyrazole, and chalcone group were synthesized using the hybridization technique starting from ampyrone (Scheme 1).

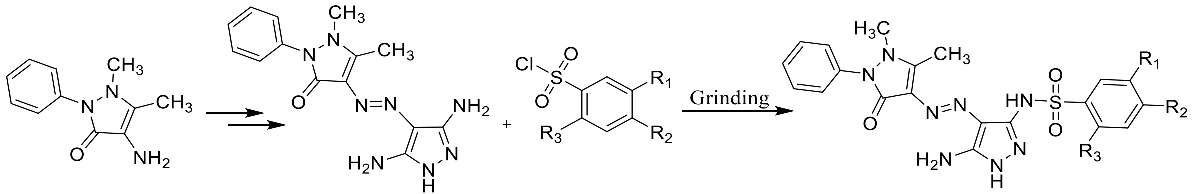

(Ampyrone) **3** **5 (a-c), 7 (a-e)** **8 (a-l)**

R$_1$ = NHCOCH$_3$, COCH$_3$, H,

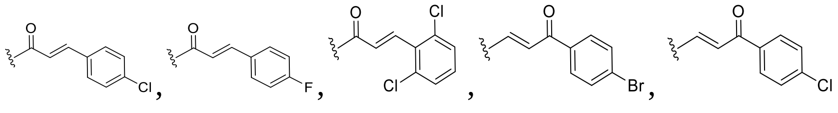

R$_2$ = H, OCH$_3$, NHCOCH$_3$, CH$_3$, NO$_2$

R$_3$ = H, OCH$_3$

Scheme 1. Synthetic route for the preparation of antipyrinyl azopyrazole sulfonamide hybrids

For the synthesis of monosulfonamide hybrids (**8 (a-l)**), the synthesized 3,5-diamino-4-antipyrinyl azopyrazole (**3**), was reacted with various synthesized arylsulfonyl chlorides (**5** (**a-c**), **7** (**a-e**)) by grinding method. Due to the presence of multiple nucleophilic sites in intermediate **3**, the reaction conditions were carefully controlled using solvent-free conditions, room temperature, and equimolar of each of the raw materials in presence of a weak base, sodium bicarbonate, to produce monosulfonamide hybrids. The hybrids were obtained in good to excellent yields (58-91%) after an easy work-up, just by adding water and simple filtration according to the principles of green chemistry. All hybrids were characterized by FTIR, ^{13}C NMR, ^{1}H NMR, and melting point techniques.

References:

١. Mondal, S.; Malakar, S. *Tetrahedron*. **2020**, 76, 131662.
٢. Ghomashi, R.; Ghomashi, S.; Aghaei, H.; Massah, AR. *Curr. Med. Chem.* **2023**, 30, 4181.

The 30th Iranian Seminar of Organic Chemistry
February 7-9, 2025, Iran University of Science and Technology, Tehran, Iran

Application of Cr-MOF metal-organic framework as an efficient and green catalyst in biodiesel production

Arezo Monem, Arash Ghorbani-Choghamarani*

Department of Organic Chemistry, Faculty of Chemistry and Petroleum Science, Bu-Ali Sina University, Hamedan, 6517838683, Iran, a.ghorbani@basu.ac.ir or arashghch58@yahoo.com , arezomonem@yahoo.com

Keywords: Biodiesel, Catalysis, Metal-organic frameworks, Esterification, Oleic acid, palmitic acid, and myristic acid

Metal-organic frameworks (MOFs) are structures made from metal and organic components, used in various applications like gas storage, material separation, pollutant removal, catalysis, and pharmaceuticals [1]. Metal framework catalysts are gaining attention for their effectiveness in chemical processes, particularly in biodiesel production, due to their porous structure and unique properties [2]. Biodiesel is a renewable energy source produced by the transesterification of vegetable oils and animal fats. The use of metal framework catalysts in this process can improve efficiency and lower costs thanks to their high specific surface area, selectivity, and recyclability [3]. These catalysts, with their porous structure, can be specifically designed for transesterification reactions and lead to the production of high-quality biodiesel. Herein, We report an efficient and novel Cr-MOF designed and synthesized through a hydrothermal reaction of chromium(III) nitrate nonahydrate with an organic ligand. The prepared Cr-MOF exhibits efficient and potential performance for the esterification of oleic and palmitic acids, etc. under gentle reaction conditions.

Furthermore, this MOF afforded several benefits, including excellent product yields, stability, easy methodology, easy workup, and greener situations. also, This heterogeneous nanocatalyst MOF could be easily recovered from the reaction mixture by centrifugation (Scheme 1).

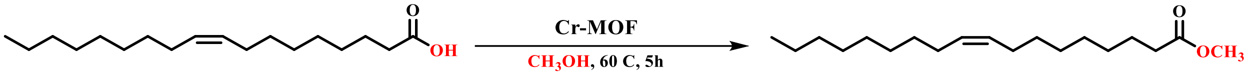

Scheme 1. Esterification of Oleic Acid

References:

١. James, S. L. (2003). Metal-organic frameworks. *Chemical Society Reviews*, *32*(5), 276-288.

٢. Zhou, H. C., Long, J. R., & Yaghi, O. M. (2012). Introduction to metal–organic frameworks. *Chemical reviews*, *112*(2), 673-674.

٣. Jafari, A., Ghorbani-Choghamarani, A., & Aghavandi, H. (2024). Simple Synthesis of Novel Cr-EDTA-MOF: A Green, Reusable, and Versatile Catalyst for the Production of Biodiesel Fuel from Oleic Acid and Palmitic Acid. *ACS omega*, *9*(5), 5255-5264.

The 30th Iranian Seminar of Organic Chemistry
February 7-9, 2025, Iran University of Science and Technology, Tehran, Iran

The Novel Green Catalyst Deep Eutectic Solvent for Preparation of the New Compounds Pyrano[2,3-*d*]Pyrimidines

Arezo Monem, Davood Habibi*

Department of Organic Chemistry, Faculty of Chemistry and Petroleum Science, Bu-Ali Sina University, Hamedan, 6517838683, Iran, Davood.Habibi@gmail.com arezomonem@yahoo.com

Keywords: Green Chemistry, Deep Eutectic Solvent, Catalysis, pyrano[2,3-*d*]pyrimidine, synthesis.

Deep eutectic solvents (DESs) are often cheap and safe and are usually formed by mixing two or three ionic compounds which each component has a high melting point, but when they are combined, the melting point of the prepared DES is lower than that of each component [1]. *N*-heterocyclic compounds are a class of organic compounds that contain at least one nitrogen atom in the heterocyclic ring and often exhibit unique properties and reactivity due to the presence of the nitrogen atom [2]. Nitrogen-containing heterocycles are very important and are found as key elements of numerous drugs, pharmaceuticals, and biologically active molecules. Considering these characteristics, it is not surprising that this group of compounds has been considered very important by chemists and a wide range of methods for their synthesis have been reported [3]. Among them, pyrano[2,3-*d*]pyrimidines are one of the most important skeletons and have shown that they have various pharmacological activities, such as anti-bronchitic, anti-microbial, antitumor, and several methods have been reported for their synthesis (Scheme 1).

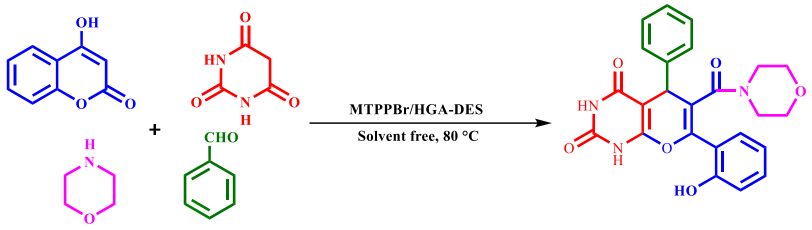

Scheme 1. Synthesis of pyrano[2,3-*d*]pyrimidines derivative

References:

١. Hayyan, M., Hashim, M. A., Hayyan, A., Al-Saadi, M. A., AlNashef, I. M., Mirghani, M. E., & Saheed, O. K. (2013). Are deep eutectic solvents benign or toxic?. *Chemosphere*, *90*(7), 2193-2195.

٢. Rezayati, S., Kalantari, F., Ramazani, A., Sajjadifar, S., Aghahosseini, H., & Rezaei, A. (2021). Magnetic silica-coated picolylamine copper complex [fe3o4@ sio2@ gp/picolylamine-cu (ii)]-catalyzed biginelli annulation reaction. *Inorganic chemistry*, *61*(2), 992-1010.

٣. Tehrani, K. A., D'hooghe, M., & De Kimpe, N. (2003). Novel synthesis of indolizidines and quinolizidines. *Tetrahedron*, *59*(17), 3099-3108.

The 30th Iranian Seminar of Organic Chemistry
February 7-9, 2025, Iran University of Science and Technology, Tehran, Iran

Synthesis and Characterization of Carbon Quantum Dots Based on Carbohydrate based Natural Precursors

Fatemehsadat Jozi[a], Kobra Nikoofar[a*]

Affiliations: Department of Organic Chemistry, Faculty of Chemistry, Alzahra University, Terhan, Iran

*k.nikoofar@alzahra.ac.ir

Keyword: Carbon Quantum Dots, Quantum Dots, CQDs, Hydrothermal Methods, Natural Precursors.

Carbon-based nanomaterials such as carbon quantum dots (CQDs) have attracted special attention due to their distinct structural dimensions as well as their outstanding chemical and physical properties. In general, quantum dots (QDs) are very important due to their features such as ease of synthesis, good solubility in water, high photostability, high photo-responsibility, low cytotoxicity, easy surface functionalization, and good catalytic properties. In this project, novel CQDs synthesized using carbohydrate natural precursors via a modified simple hydrothermal method. The obtained material identified and characterized by FT-IR, DRS, TEM, DLS, VSM, and Raman techniques.

References:

1. Du Z, Shen S-l, Tang Z-h, Yang J-h. Graphene quantum dots-based heterogeneous catalysts. *New Carbon Materials*. 2021, 36(3):449-467.

2. Yadav PK, Chandra S, Kumar V, Kumar D, Hasan SH. Carbon quantum dots: synthesis, structure, properties, and catalytic applications for organic synthesis. *Catalysts*. 2023, ١٣(٢):٤٢٢.

3. Dong Y, Zhou N, Lin X, Lin J, Chi Y, Chen G. Extraction of electrochemiluminescent oxidized carbon quantum dots from activated carbon. *Chemistry of Materials*. 2010, 22(21):5895-5٨٩٩.

The 30th Iranian Seminar of Organic Chemistry
February 7-9, 2025, Iran University of Science and Technology, Tehran, Iran

Bioremediation of organic pollutants by laccase-metal–organic framework composites

Mehdi Aghaee and Mehdi Mogharabi*

Pharmaceutical Sciences Research Center, Hemoglobinopathy Institute, Mazandaran University of Medical Sciences, P.O. Box 48175-861 Sari 4847193698, Iran

Keyword: Bioremediation, Laccase, Metal–organic framework, Organic pollutant

Metal-organic frameworks (MOFs) are intriguing porous crystalline materials made up of metal-containing nodes and organic ligands. In recent decades, researchers across various scientific and industrial sectors have taken an interest in MOFs due to their distinctive properties, including adjustable porosity, a high surface-area-to-volume ratio (generally between 1000 and 10,000 m²/g), diverse structural designs, and relatively high performance [1]. Laccases (EC 1.10.3.2), a type of multicopper-containing phenol oxidase, are highly valued for their remarkable oxidative capabilities and their ability to catalyze the oxidation of a wide array of organic pollutants. This review aims to explore the recent advancements in the developing field of enzyme-MOF composites for wastewater treatment [2].

Scheme: Laccase-MOF composites represent synergistic approach for treatment of organic plutants.

In summary, laccase-MOF composites show exceptional effectiveness as biocatalytic systems for the treatment of industrial wastewater contaminated with phenolic substances. These composites have considerable promise when used with both natural and synthetic mediators, successfully breaking down non-phenolic and complex pharmaceutical pollutants. By immobilizing laccase on MOF-based carriers, an ideal microenvironment is created that maximizes enzyme loading, reusability, and stabilization, while also improving enzyme activity compared to its free form in certain instances. Moreover, the unique properties of laccase-MOF composites produce synergistic effects that boost biodegradation efficiency [3]. Future studies are expected to concentrate on customizing MOF structures to enhance enzyme loading and activity, integrating multi-enzyme systems to replicate complex biological processes, and developing smart MOFs that react to environmental changes to dynamically regulate enzyme activity [4]. Additionally, improvements in the synthesis and functionalization of MOFs may result in composites with better biocompatibility and selectivity, paving the way for scaling up and commercializing enzyme-MOF composites .The convergence of enzyme immobilization and MOF technology promises to create robust, efficient, and sustainable biocatalytic systems, pushing the boundaries of current biotechnological capabilities.

References:

1- Liu, C., Zhang, X., Zhou, Y., Zhu, L., Zhang, C., Yan, X., You, S., Qi, W., Su, R., 2023. A reusable and leakage-proof immobilized laccase@UiO-66-NH2(30) for the efficient biodegradation of rifampicin and lincomycin. Biochem. Eng. J. 194, 108897 https://doi.org/10.1016/j.bej.2023.108897.

2- Nikpour, S., Salehipour, M., Rezaei, S., Mogharabi-Manzari, M., 2024. Design and fabrication of magnetic cross-linked laccase aggregate using superparamagnetic metal-organic frameworks for phenol removal. Biochem. Eng. J. 209, 109385 https://doi.org/10.1016/j.bej.2024.109385.

3- Rezaei, S., Tahmasbi, H., Mogharabi, M., Firuzyar, S., Ameri, A., Khoshayand, M.R., Faramarzi, M.A., 2015. Efficient decolorization and detoxification of reactive orange 7 using laccase isolated from Paraconiothyrium variabile, kinetics and energetics. J. Taiwan Inst. Chem. Eng. 56, 113–121. https://doi.org/10.1016/j.jtice.2015.04.008.

٥- Samal, K., Mahapatra, S., Hibzur Ali, M., 2022. Pharmaceutical wastewater as Emerging Contaminants (EC): Treatment technologies, impact on environment and human health. Energy Nexus 6, 100076. https://doi.org/10.1016/j.nexus.2022.100076

The 30th Iranian Seminar of Organic Chemistry
February 7-9, 2025, Iran University of Science and Technology, Tehran, Iran

Feasibility study of nicotine identification and adsorption by B 12 N 12 nanostructure using computational methods

Authors: Sepehr Barzegar 1[a] (representing author), Aidin Bahrami 2*[c] (corresponding author),

Affiliations: Department of Chemistry, Urmia University, Urmia, Iran

Keyword: Adsorption, Nicotine, $B_{12}N_{12}$, Density functional theory.

Abstract: The first-principle calculations employing density functional theory (DFT) at the M062X/6-311++G** level were utilized to the examine the adsorption tendencies of nicotine molecules on the other surface of pristine $B_{12}N_{12}$ nano-cages. To understand the binding characteristics between the $B_{12}N_{12}$ complex as adsorbent and nicotine, the structural and electronic parameters, including Natural Bond Orbital (NBO) and Atoms in Molecules (AIM) properties were analyzed. The results indicate that nicotine tends to adsorb preferentially via its nitrogen atom, situated on 6-membered BN ring onto the Lewis acid sites of B atoms within the nano-cages. Based on the calculated density of states, the interaction between nicotine and the external wall of $B_{12}N_{12}$ results in significant variations in their conductivities, thereby suggesting its potential suitability as a nicotine sensor. Presence of polar solvent enhances the adsorption of nicotine onto the nano-cage. Furthermore, AIM-based analyses suggested an electrostatic nature for N-B interaction within the Nicotine…$B_{12}N_{12}$ complex. According to the calculated results, the $B_{12}N_{12}$ nano-cage shows promise as an effective absorbent and sensor for detecting nicotine in environmental systems.

Introduction:

Nicotine, a naturally occurring alkaloid found in tobacco plants, possesses both benefits and drawbacks. On the positive side, nicotine has been linked to several cognitive and physiological effects [1]. It acts as a stimulant, increasing alertness, concentration, and cognitive function in some individuals. However, nicotine also carries significant health risks and addictive properties [2]. Nicotine addiction can result in physical dependence, making it challenging for individuals to quit despite the associated health risks [3,4]. Additionally, research is ongoing to explore nicotine's potential in treating neurological disorders such as Parkinson's disease and Alzheimer's disease [5]. Boron nitride nanocages, with their unique structure and properties, have garnered significant attention in the field of nanotechnology. These nanocages, composed of $B_{12}N_{12}$ units, exhibit remarkable stability, high surface area, and excellent thermal and chemical resistance [6]. They hold promise for various applications, including gas storage, drug delivery, catalysis, and nanoelectronics. The aim of this research is to use first-principles computations to analyze how nicotine molecules interact with the external surface of pristine $B_{12}N_{12}$ nano-cages.

By analyzing the interactions between the nicotine molecule and the nano-cage, we can assess whether this particular system would be a suitable adsorbent for a given analyte or class of compounds [7]. Overall, the use of first-principles computations in this study offers a valuable tool for predicting the adsorption behavior of nicotine molecules on $B_{12}N_{12}$ nano-cages. This approach not only saves time and resources but also provides a deeper understanding of the adsorption mechanisms at play, ultimately leading to more effective adsorption processes in the future [8].

Method

The Gaussians package facilitated electronic structure calculations. Geometrical parameters for pristine $B_{12}N_{12}$ were fully optimized using the M062X functional and the 6-311++G** basis set to achieve the most stable complexes [9]. Two types of active sites on the exterior surface of $B_{12}N_{12}$ were investigated, considering all possible orientations for nicotine as a ligand.

The adsorption energy (E_{ad}) of NIC is calculated as:

$$E_{ad} = E_{tot} (B_{12}N_{12}/\text{Nicotine}) - E_{tot} (B_{12}N_{12}) - E_{tot} (\text{Nicotine}) \quad (1)$$

Moreover, solvation effects (water) were examined using the polarized continuum model (PCM). Electron Density of States (DOSs) were generated using Gauss Sum, and the sensitivity of $B_{12}N_{12}$ complexes in terms of the HOMO–LUMO gap (E_g) was compared during the adsorption.

Results and Discussion:

Infrared spectroscopy (IR) (Fig1) is a crucial technique in scientific research that aids in the analysis and identification of materials and chemical compounds. In this study, the structure of $B_{12}N_{12}$ was investigated using M062X/6-311++G** method to do IR spectroscopy. The obtained spectrum, analyzed from the most stable ground state of $B_{12}N_{12}$, indicates the absence of negative frequencies or data, which may suggest the stability of this structure.

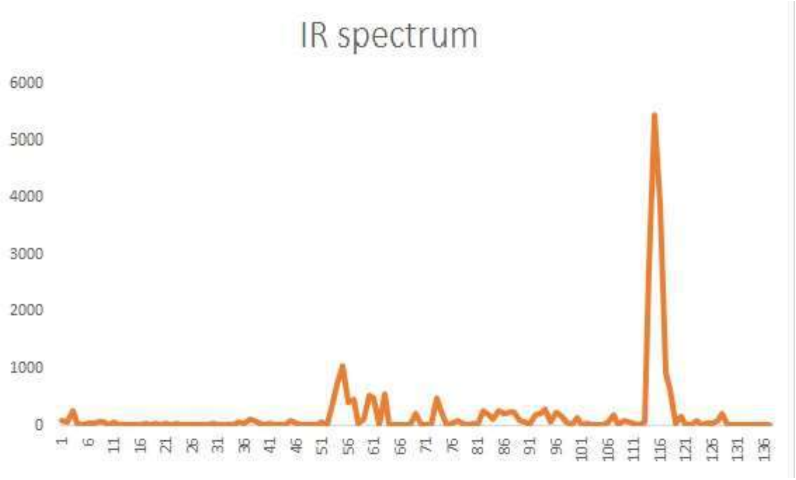

Fig 1: IR spectrum of optimized $B_{12}N_{12}$ nano-cage.

Figure 2 depicts the optimized structure of the $B_{12}N_{12}$ alongside its DOS plot, revealing the nano-cage as an insulator with a HOMO–LUMO gap (E_g) of 9.34 eV.

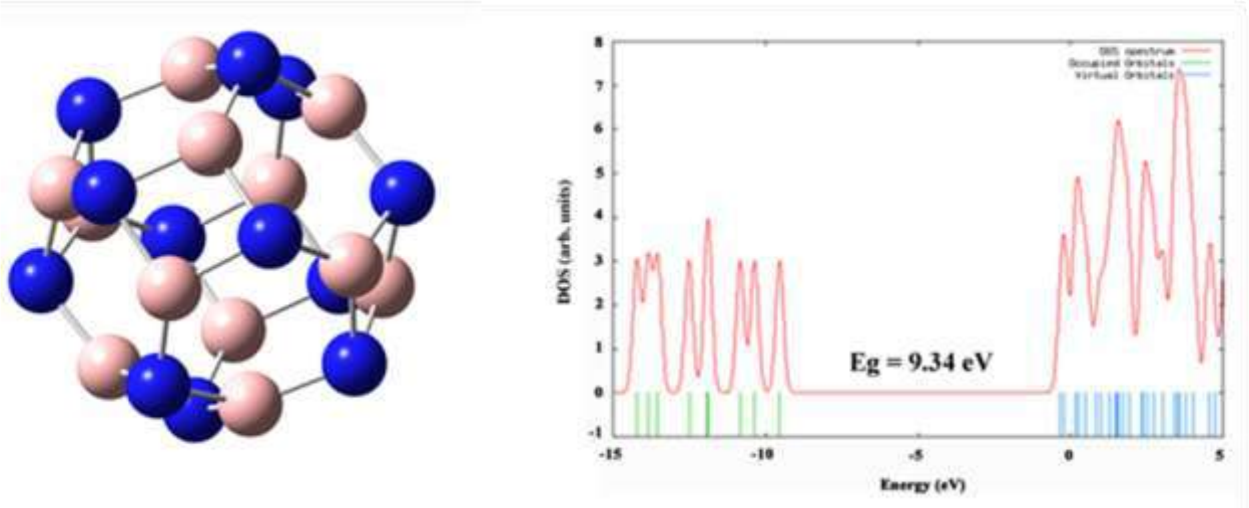

Fig 2: The optimized structure of $B_{12}N_{12}$ and its density of states (DOSs).

Determination of stable configurations for single nicotine adsorbed on the nano-cage was guided by the molecular electrostatic potential (MEP) plot of single nicotine, illustrated in Figure 3. The figure highlights the partial negative charge on the N atom of the hexagon ring of nicotine as a reactive site for Lewis acid interactions with B atoms, allowing nicotine molecules to approach the external surface of the $B_{12}N_{12}$ nano-cage. Additionally, the H atoms of the 5-membered ring of Nicotine exhibit a favorable trend as reactive sites for base acid interactions with N atoms on the external surface of $B_{12}N_{12}$.

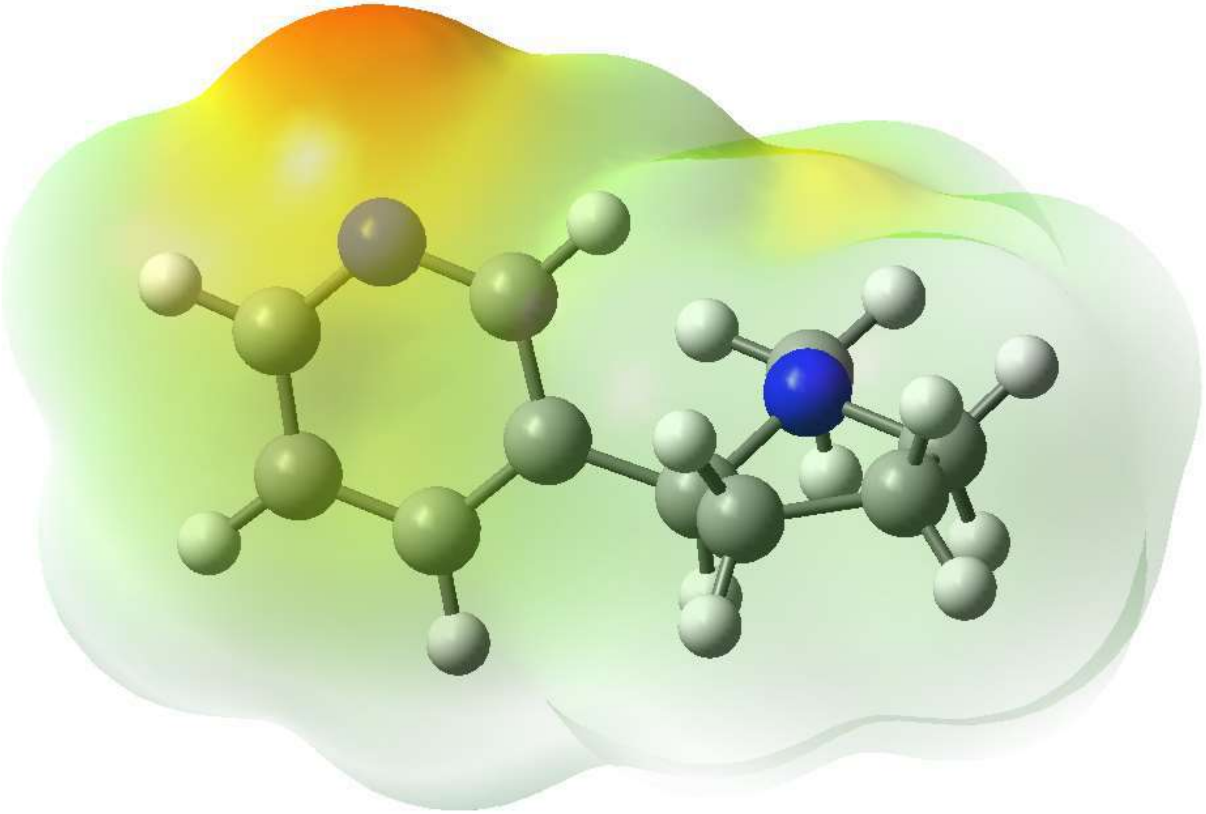

Fig 3: Computed electrostatic potentials on the molecular surfaces of a single Nicotine molecule

Among the five different configurations of nicotine interaction with the nanostructure, one configuration, visible in Figure 4, demonstrates greater stability compared to the others. The reason for the higher stability of this structure lies in the interaction between the nitrogen atom of the hexagonal ring of nicotine and the boron atom of the nanostructure, which stabilizes the overall structure. According to the obtained results, the bond length between the nitrogen atom of the hexagonal ring of nicotine and the boron atom of the nanostructure is calculated to be 1.61 Å, which classifies it as a covalent bond. Furthermore, the adsorption energy of nicotine on the nanostructure, after correcting for basis set superposition error (BSSE), falls within the range of -37 to -38 kcal/mol, further confirming the covalent nature of the formed bond. Therefore, the nitrogen atom of nicotine is identified as the more thermodynamically favorable site for adsorption on the boron atoms of the nano-cage. The results of Natural Bond Orbital (NBO) analysis indicate a charge transfer of 0.065 |e| from the boron atom of the nano-cage to the nitrogen atom of nicotine in the most stable configuration. Additionally, the results show that the electronic properties of the $B_{12}N_{12}$ nano-cage significantly change upon chemisorption of nicotine. Specifically, the energy level of the Highest Occupied Molecular Orbital (HOMO) shifts toward more positive values, while the energy level of the Lowest Unoccupied Molecular Orbital (LUMO) shifts toward more negative values. For instance, the HOMO energy level increases from -9.54 eV in the pure state to -8.39 eV in the nicotine-adsorbed state, as evidenced by the shift of the HOMO toward more positive values in the Density of States (DOS) diagram in Figure 4. On the other hand, the energy level of the Lowest Unoccupied Molecular Orbital (LUMO) decreases from -0.20 eV in the pure state to -1.55 eV in the nicotine-adsorbed state. This decrease can be justified by observing the newly formed electronic states in the Density of States (DOS) diagram in Figure 4, compared to the DOS diagram in Figure 2, which corresponds to the pure state of the nanostructure before nicotine adsorption. The shift of the Highest Occupied Molecular Orbital (HOMO) toward more positive values and the creation of new electronic states within the LUMO region ultimately lead to a reduction in the bandgap to 6.84 eV in Configuration, compared to 9.34 eV in the pure state of the nanostructure, representing a difference of approximately 27%.

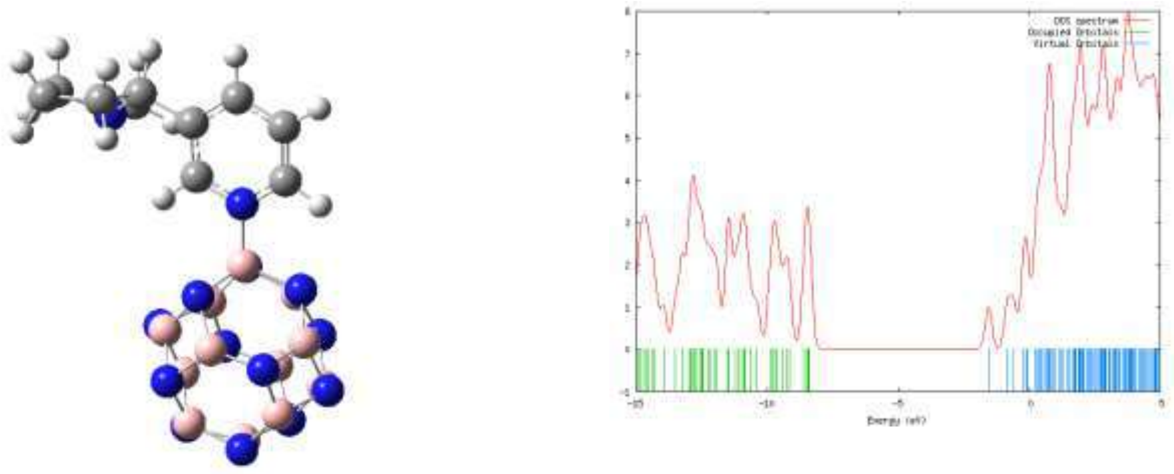

Fig 4: The most stable configuration of nicotine on $B_{12}N_{12}$ and its density of states (DOSs) plot.

This change not only indicates the sensitivity of the electronic properties of the $B_{12}N_{12}$ nano-cage to the presence of nicotine but also suggests that the difference in the bandgap after nicotine adsorption is significant enough to propose the $B_{12}N_{12}$ nanostructure as a potential sensor for nicotine detection. Moreover, since nicotine is often present in aqueous environments in real-world scenarios, the calculations were repeated in the presence of water as a solvent. The results obtained are consistent with those in the gas phase, with the exception that the total energy is more negative by 0.18 eV, indicating greater stability of the final adsorption configuration of nicotine on the $B_{12}N_{12}$ nanostructure. Overall, these findings demonstrate the strong adsorption of nicotine on the $B_{12}N_{12}$ nano-cage and propose the nano-cage as a suitable candidate for nicotine adsorption.

References:

1. Waldum, H.L., et al., *Long-term effects of inhaled nicotine.* Life sciences, 1996. **58**(16): p. 1339-1346.
2. Rezvani, A.H. and E.D. Levin, *Cognitive effects of nicotine.* Biological psychiatry, 2001. 49(3): p. 258-267.
3. Mishra, A., et al., *Harmful effects of nicotine.* Indian Journal of Medical and Paediatric Oncology, 2015. **36**(01): p. 24-31.
4. Heishma, S.J., R.C. Taylor, and J.E. Henningfield, *Nicotine and smoking: a review of effects on human performance.* Experimental and Clinical Psychopharmacology, 1994. 2(4): p. 345.
5. Dwyer, J.B., S.C. McQuown, and F.M. Leslie, *The dynamic effects of nicotine on the developing brain.* Pharmacology & therapeutics, 2009. **122**(2): p. 125-139.
6. Oku, T., et al., *Synthesis, atomic structures and properties of carbon and boron nitride fullerene materials.* Materials Science and Engineering: B, 2000. **74**(1-3): p. 206-217.
7. Ghasemi, A.S., et al., *A study on the effect of 1-butyl-4-methylpyridinium bromide adsorption on the structural and electronic properties of B12N12 nano-cage.* Journal of Molecular Liquids, 2019. **277**: p. 115-122.
8. Soltani, A., et al., *Serine adsorption through different functionalities on the B12N12 and Pt-B12N12 nanocages.* Materials Science and Engineering: C, 2018. **9**2: p. 216-227.
9. Schmidt, M.W., et al., *General atomic and molecular electronic structure system.* Journal of computational chemistry, 1993. **14**(11): p. 1347-1363.

The 30th Iranian Seminar of Organic Chemistry
February 7-9, 2025, Iran University of Science and Technology, Tehran, Iran

Enhanced bioactivity of Artemisia Annua fermented extract: Anti-microbial activity, and Study of Cytotoxicity activity

S. Fouladlou [a], HA. Panahi [a], A. Niazi [a]*, P. Jafari [b], A. Tamadon [a]
[a] Department of Chemistry, Central Tehran Branch, Islamic Azad University ,Tehran, Iran.
[b] Department of Microbiology, Arak Branch, Islamic Azad University ,Arak, Iran.
Email: ali.niazi@gmail.com, ali.niazi@iauctb.ac.ir

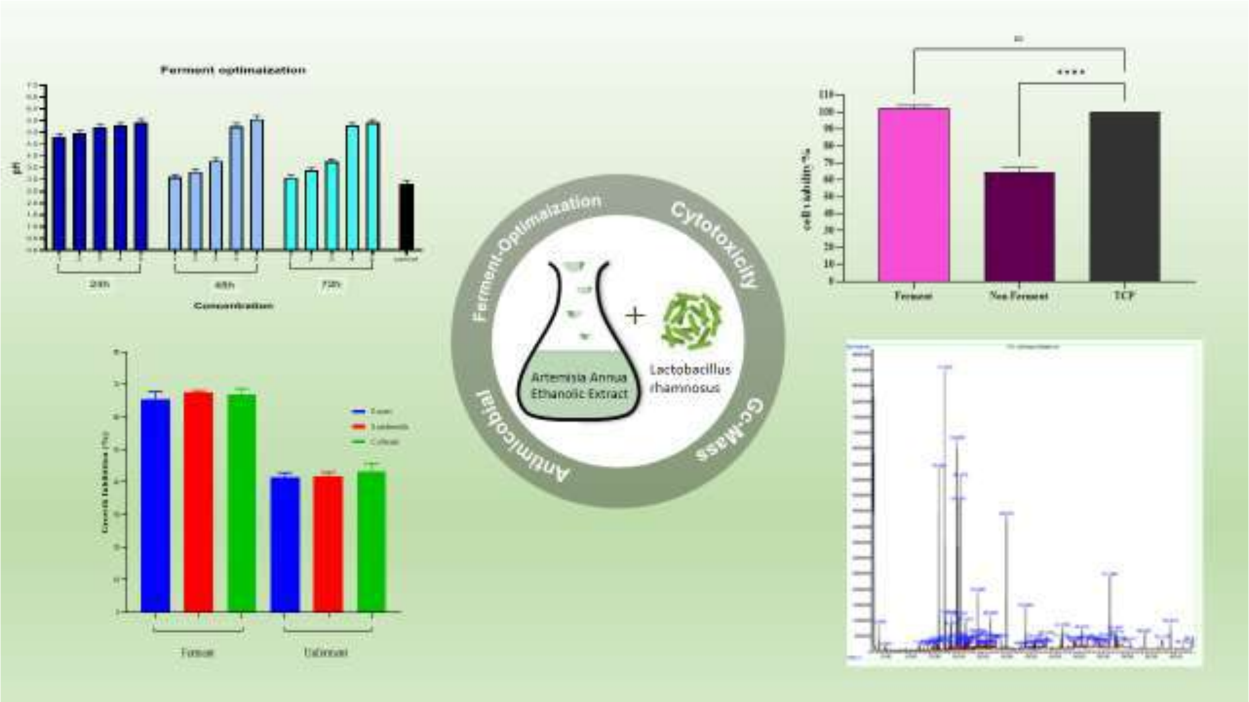

Traditional medicine, including herbal extracts and their active ingredients, is relied upon by over 80% of the global population for their healthcare needs. Additionally, more than 50% of all modern clinical drugs are derived from natural sources. Interestingly, some herbs have demonstrated the ability to resist and inhibit the growth of various bacteria, including those resistant to many types of antibiotics [1].Natural alternatives to synthetic antibacterials and fungicides are gaining prominence as the focus sharpens on green developing protective products [2]. The present study aimed to optimized the fermentation of Artemisia annua extract by the probiotic bacterium Lactobacillus rhamnosus. The objective was to increase the potential for antibacterial and antifungal properties while reducing cytotoxic properties, by identifying the key phytoconstituents. The fermentation process was optimized for the survival and growth of the probiotic bacterium L. rhamnosus. The key parameters, including substrate concentration, fermentation time, and pH, were adjusted to obtain the optimal biofermentative properties. The content of bioactive compounds in the plant extracts was evaluated using gas chromatography-mass spectrometry (GC-MS) analysis [3].Artemisia annua contains a diverse array of secondary metabolites, including monoterpenes (both hydrocarbons and oxygenated compounds), sesquiterpenes, flavonoids, aliphatic compounds, and coumarins. During the fermentation process, the structural degradation of plant cell walls and the hydrolytic activity of bacteria and/or fungi led to an increase in the levels of polyphenols, flavonoids, organic acids, proteins, ceramides, amino acids, biological enzymes, and antioxidants in the fermentation medium . [4] To assess the cytotoxicity of the tested samples, Alamar Blue assay was performed on Human fetal for skin fibroblast (HFF) cells. Cells were treated for 72 hours with 100 µL of each sample and the control group [5]. The results showed a statistically significant increase in fibroblast cells viability with Fermented Extract Artimesia annua (FEAA) treatment at a concentration of 770 µg/mL (102.3 ± 1.74%), while Non-Fermented

Extract Artimesia annua (NFEAA) at a concentration of 770 μg/mL (64.45 ± 3.02%) induced cytotoxic effects on fibroblasts cells . A comparison of the results from both in vitro assays clearly indicates that (FEAA) has a more favorable impact on the viability and metabolic activity of the studied cell lines Additionally, microbiological analyses were performed on various pathogenic skin bacterial and fungal strains, including Staphylococcus epidermidis, Propionibacterium acnes, and Candida albicans, utilizing standardized methods for determining the minimum inhibitory concentration (MIC) and minimum bactericidal/fungicidal concentration (MBC/MFC) at concentrations ranging from 770 to 1.50 μg /mL after 24 hours of incubation using a microplate reader [6] . MIC and MBC values showed that the NFEAA & FEAA were significantly effective at low concentration. The results of the present study indicate that the fermented Artemisia Annua extract exhibited superior biological activity compared to the non-fermented crude extract. These findings suggest the potential for the fermented extract to be utilized as an active ingredient in skincare formulations within the cosmetic industry [7,8]. Numerous studies have reported that the incorporation of these natural compounds into consumer products elicits increased consumer demand and exhibits a favorable environmental impact [9].

Keyword: Artemisia annua , Fermentation process , Medicinal plant , Biotechnology , Antimicrobial Activity, Anti fungal activity, Microorganisms ,Skin cells, biological activity , cytotoxic

[1] Zagórska-Dziok, M.; Ziemlewska, A.; Mokrzyńska, A.; Nizioł-Łukaszewska, Z.; Sowa, I.; Szczepanek, D.; Wójciak, M. Comparative Study of Cytotoxicity and Antioxidant, Anti-Aging and Antibacterial Properties of Unfermented and Fermented Extract of Cornus mas L. Int. J. Mol. Sci. 2023, 24, 13232

[2]Jamshidi N, Mojarrab M, Delnavazi M, Emami A, Bahrami G, et al. Cytotoxic Activity and Phytochemical Analysis of Artemisia biennis Essential Oils at Different Growth Stages. Jundishapur J Nat Pharm Prod. 2024;19(4):e147988.

[3] Tao, Ali, Xuehua Feng, Yajing Sheng, and Zurong Song. "Optimization of the Artemisia polysaccharide fermentation process by Aspergillus niger." Frontiers in Nutrition 9 (2022): 842766.

[4] On, J.-Y.; Kim, S.-H.; Kim,J.-M.; Park, S.; Kim, K.-H.; Lee, C.-H.;Kim, S.-K. Effects of Fermented Artemisia annua L. and Salicornia herbacea L. on Inhibition of Obesity In Vitro and In Mice. Nutrients 2023, 15, 2022.

[5] Park, Y.A.; Lee, S.R.; Lee, J.W.; Koo, H.J.; Jang, S.A.; Yun, S.W.; Kim, H.J.; Woo, J.S.; Park, M.R.; Kang, S.C.; et al. Suppressive effect of fermented Angelica tenuissima root extract against photoaging: Possible involvement of hemeoxygenase-1. J. Microbiol. Biotechnol. 2018, 28, 1391–1400.

[6] Wu L., Chen C., Cheng C., Dai H., Ai Y., Lin C., Chung Y. Evaluation of tyrosinase inhibitory, antioxidant, antimicrobial, and antiaging activities of Magnolia officinalis extracts after Aspergillus niger fermentation. BioMed Res. Int. 2018;2018:5201786. doi: 10.1155/2018/5201786.

[7] Bezerra, K.G.O.; Rufino, R.D.; Luna, J.M.; Sarubbo, L.A. Saponins and microbial biosurfactants: Potential raw materials for the formulation of cosmetics. Biotechnol. Prog. 2018, 34, 1482–1493.

[8] Sharmeen, J.B.; Mahomoodally, F.M.; Zengin, G.; Maggi, F. Essential Oils as Natural Sources of Fragrance Compounds for Cosmetics and Cosmeceuticals. Molecules 2021, 26, 666.

[9] Rybczy´ nska-Tkaczyk, K.;Grenda, A.; Jakubczyk, A.;Kiersnowska, K.; Bik-Małodzi ´ nska,M. Natural Compounds with Antimicrobial Properties in Cosmetics. Pathogens 2023,12, 320.

The 30th Iranian Seminar of Organic Chemistry
February 7-9, 2025, Iran University of Science and Technology, Tehran, Iran

Synthesis, characterization and investigation of electromagnetic wave absorption properties of Graphene oxide/Fe_3O_4/ Polyaniline nanocomposites in frequency ranges of 8-12 GHz

Nafiseh Abazari*[a], Ali Reza Zarei[a], Abbas Abdolmaleki[a]

[a] *Department of Chemistry and Chemical Engineering, Malek Ashtar University of Technology, Tehran, Iran*

**E-mail: nafas7779.a@gmail.com*

Keywords: Electromagnetic waves absorption, Polyaniline (PANI), Nanocomposite, Graphene oxide (GO), Band X.

In recent years, the increase in electromagnetic radiation has raised concerns about environmental hazards.[1] Therefore, coatings and absorbent materials in various sectors such as military and defense industries, electronics, health and treatment, etc. are very important. Various materials have the ability of magnetic loss and dielectric loss together to absorb these waves, which can be carbon fibers, graphene/graphene oxide composites, single-walled and multi-walled carbon nanotubes (CNTs), hybrid composites, ceramic structures, metal organic frameworks (MOFs), iron, cobalt, polymers and etc.[2,3]

Graphene oxide has good mechanical strength and surface area, also magnetite has high magnetic sensitivity and polyaniline has electrical conductivity and tunable properties. Therefore, the intelligent design of this nanocomposite combination of these three components together can show high performance.

In this work, at first the GO/Fe_3O_4/PANI nanocomposites was synthesized. The synthesized composite shows excellent wave-absorbing property with the maximum reflection loss of -30.5 dB in vector network analyzer (VNA). Therefore, this nanocomposite can be recommended for radar absorbing coatings.[4–8]

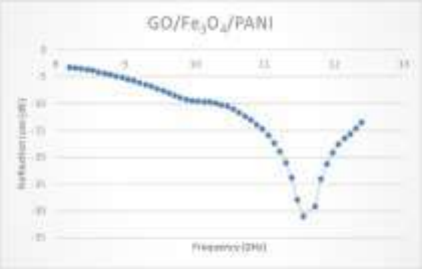

References

(1)Elmahaishi, MF.; Azis, RS.; Ismail, I.; Muhammad, FD. *Journal of Materials Research and Technology* **2022**, *20*, 2188.

(2)Pang, H.; Duan, Y.; Huang, L.; Song, L.; Liu, J.; Zhang, T. *Composites Part B: Engineering* **2021**, *224*, 109173.

(3)Qu, N.; Sun, H.; Sun, Y.; He, M.; Xing, R.; Gu, J. *Nature Communications* **2024**, *15*, 1.

(4)Ebrahimi-Tazangi, F.; Maazallahi, A.; Livreri, P.; Seyed-Yazdi, J. *Journal of Alloys and Compounds* **2024**, *1002*, 175149.

(5)Manna, R.; Srivastava, SK. *ACS Omega* **2021**, *6(13)*, 9164.

(6)Zhao, J.; Lin, J.; Xiao, J ping.; Fan, H. *RSC Advances* **2015**, *5*, 19345.

(7)Chen, T.; Zhu, K.; Che, Y.; Zhang, Y.; Zhang, J.; Li, H. *Journal of Materials Science Materials in Electronic*s **2014**, *25*.

(8)Wang, H.; Shi, P.; Rui, M.; Zhu, A.; Liu, R.; Zhang, C. *Progress in Organic Coatings* **2020**, *139*, 105476.

The 30th Iranian Seminar of Organic Chemistry

February 7-9, 2025, Iran University of Science and Technology, Tehran, Iran

Theoretical study of the racemization of some proline-based dipeptides

Nematollah Arshadi, Iman Eghbaladari.

Affiliations: Department of Chemistry, Faculty of Sciences, University of Zanjan,

Zanjan, Iran

Keyword: Racemization, Dipeptides, Stereoselectivity, DFTcalculations

Introduction: The racemization process in proteins and enzymes causes gene mutations and is a factor in cancer. Since we are faced with several points susceptible to racemization with different pKa in an oligopeptide, we can obtain the point with the highest pKa by obtaining each pKa point through an equation that is an innovation of our project. By applying specific optimal conditions, racemization can be stopped at the desired point and prevent gene mutations and cancer.

Results and Discussion: The optical purity of asymmetric catalysts used in asymmetric synthesis plays an important role in determining the stereoselectivity of the reaction, especially the enantiomeric excess of its product. In this project, we will theoretically study the racemization process of some amino acids individually and in the form of L-proline-based dipeptides and find a linear relationship between the structural or process characteristics calculated for each with the acid constant, or pKa of the alpha carbon proton, or the reported racemization reaction rate constant. To select experimental data in our project, we focused on the acid strength of the alpha carbon during the study of the racemization process. In this project, we are looking for a quantity that is part of the geometric property of the molecule, and let's measure its relationship with the experimental data through calculations. The relationship is that the higher the acid strength of the alpha carbon, the faster the racemization rate and, as a result, the easier hydrogen abstraction occurs. We concluded that the conversion of proline to its D-isomer can reduce the optical purity of this asymmetric catalyst. Observations show that the racemization potential of amino acids bound to L-proline is significantly increased In fact, we are trying to find a relationship between the stereoselectivity of these catalysts and their racemization potential.

Method: In this study, all calculations will be performed with Spartan software using the "density Functional theory" method and at the DFT/M06/6-31++G** theoretical level.

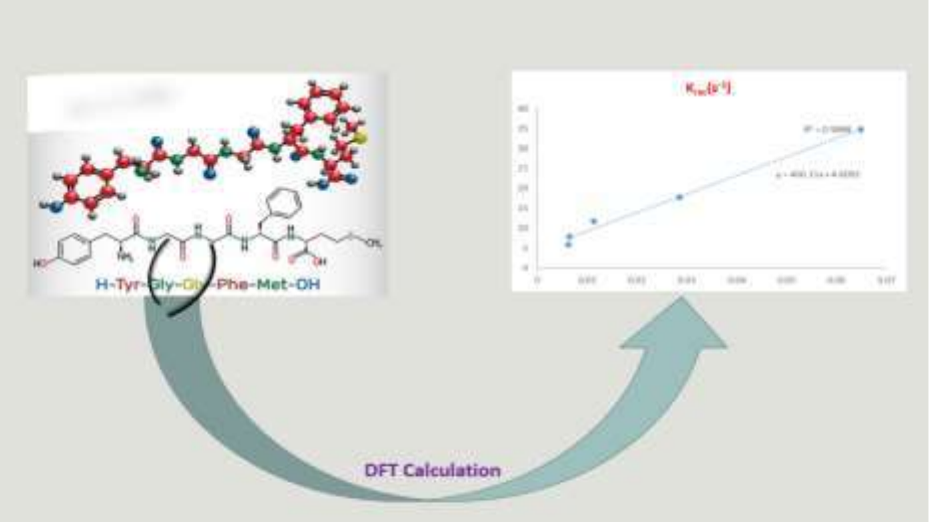

References:

1. Smith G. G, De Sol B. S., ”Racemization of amino acids in dipeptides shows COOH>NH2 for Non-sterically hindered residues”, Science, 1980, 765-767.

2.Triandafillidi I., Bisticha A., Voutyritsa E., Galiatsatou G., Kokotos C. G., “tert-Butyl ester or benzylamide of the dipeptide Pro-Gly as organocatalysts for the asymmetric aldol reaction”, Tetrahedron, 2015, 932-940.

3.Lei M., Shi L., Li G., Chen Sh., Fang W., Ge Z., Cheng T., Li R., “Dipeptide-catalyzed direct asymmetric aldol reactions in the presence of water”, Tetrahedron, 2007, 7892-7898.

4.Krattiger Ph., Kovasy R., Revell J. D., Ivan S., Wennemers J., “Increased Structural Complexity Leads to Higher Activity: Peptides as Efficient and Versatile Catalysts for Asymmetric Aldol Reactions”, Organic Letters, 2005, 1101-1103.

5. Baldasare C. A., Seybold P. G., “Computational Estimation of the Gas-Phase and Aqueous Acidities of Carbon Acids”, The Journal of Physical Chemistry A, 2020, 2152-2159.

The 30th Iranian Seminar of Organic Chemistry
February 7-9, 2025, Iran University of Science and Technology, Tehran, Iran

One-Pot Reaction of 3-Vinylchromones, Aromatic Aldehydes, and Ammonium Acetate: An Efficient Approach for the synthesis 1,6-Dihydropyridine Derivatives

Behnaz Farajpour, Marzie Kakaie, Morteza Shiri*

Department of Organic Chemistry, Faculty of Chemistry, Alzahra University, Vanak, Tehran 1993893973, Iran.

Keyword: Multicomponent reaction, dihydropyridines, 3-vinylchromones, aromatic aldehydes, ammonium acetate.

1,6-dihydropyridines **are mostly known as versatile precursors to complex organic materials** and are frequently employed as building blocks.[1] In this work, we present a novel strategy for the straightforward synthesis of functionalized 1,6-dihydropyridines *via* a three-component reaction of 3-vinylchromones, aromatic aldehydes, and ammonium acetate. A tandem procedure including *in situ* NH aldimine[2] formation/Michael-type addition/opening of the pyrone ring/isomerization/6π-electrocyclization/[1,5]-*H* shift allows rapid access to a series of dihydropyridines bearing an *ortho*-hydroxybenzoyl and a benzoyl scaffold in good yields. Readily available precursors, simple heating conditions, and operational simplicity are some highlighted advantages of this transformation. Notably, the presence of various substituents around the dihydropyridine core could furnish attractive points of postfunctionalization to afford a series of useful compounds that are difficult to prepare with other methods. The structures of the products were characterized by high-resolution mass spectrometry (HRMS) analysis, nuclear magnetic resonance (NMR), and X-ray crystallographic analysis.

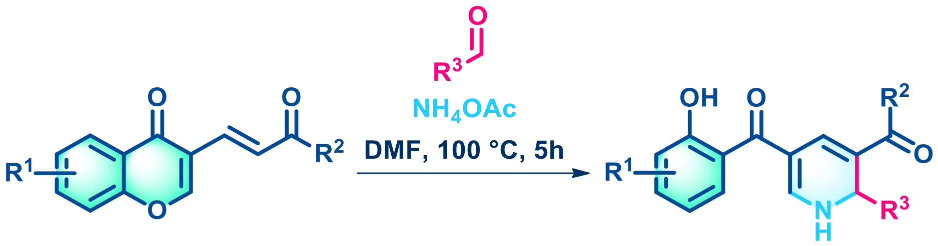

References:

(1) E. M. P. Silva, P. A. M. M. Varandas and A. M. S. Silva, *Synthesis*, 2013, **45**, 3053.

(2) J. Yan, M. Cheng, F. Hu and Y. Hu, *Org. Lett.*, 2012, **14**, 3206.

The 30th Iranian Seminar of Organic Chemistry
February 7-9, 2025, Iran University of Science and Technology, Tehran, Iran

بررسی پتانسیل احیا شدگی غشای اولترافیلتراسیون اصلاح شده با مایع یونی در برابر گرفتگی های بیولوژیکی

آذر اسدی[1*]، سامان علوی نیکو[2]، علی فیوضی[2]

[1*] عضو هیات علمی دانشکده نفت و گاز گچساران، دانشگاه یاسوج، ایران

[2] دانشجوی کارشناسی دانشکده نفت و گاز گچساران، دانشگاه یاسوج، ایران

چکیده

فرآیند های غشایی با داشتن مزایای فراوان مانند کاهش مصرف انرژی به دلیل عدم تغییر فاز، تنوع در شکل، انتقال جرم زیاد و کاربرد برای انواع صنایع بکار گرفته شده اند. با این حال آب گریز بودن غشاء که دلیل عمده گرفتگی غشاء است از جمله معضلات توسعه غشا می باشد. بنابراین افزایش آب دوستی غشاها می تواند تا حد زیادی ازگرفتگی آن جلوگیری کند. در این مقاله میزان مقاومت گرفتگی غشای اولترافیلتراسیون اصلاح شده با مایع یونی مورد بررسی قرار گرفته است. مایعات یونی به دلیل ماهیت آب دوستی بالایی که دارند سطح غشا پلیمری را آب دوست می کنند. جهت بررسی نفوذپذیری (تراوایی) و خاصیت ضد گرفتگی غشاء، آزمایشاتی با استفاده از آب مقطر و دو محلول شیر خشک با غلظت های ۱۰ و ۵۰ گرم بر لیتر به عنوان عامل گرفتگی طراحی شد. در طی آزمایشات میزان فلاکس عبوری در هر مرحله اندازه گیری شد و همچنین پارامتر مهم میزان بازیابی شار (FRR) اندازه گیری شد. طبق نتایج بدست آمده مقدار FRR غشای مورد نظر در برابر محلول شیر خشک ۱۰ گرم بر لیتر و ۵۰ گرم بر لیتر به ترتیب ۸۱% و ۷۰% می باشد که نشان دهنده عملکرد بالای این غشا در برابر پدیده گرفتگی می باشد. همچنین در مرحله نهایی از روش شستشوی معکوس جهت بازیابی غشا بعد از گرفتگی ناشی از محلول ۵۰ گرم بر لیتر استفاده شد که مقدار FRR را از ۷۰% به ۸۰% ارتقا داد.

واژه های کلیدی : شار جریان عبوری- گرفتگی غشاء- تمیز کردن غشاء- آب دوستی- پودر شیر خشک- شست و شوی معکوس[۱]

۱) مقدمه

غشاء (Membrane) به معنای پوسته است که دارای نفوذپذیری انتخابی می باشد و مانند سد عمل میکند که از قرن هجدهم مفهوم غشاء شناخته شده است اما در زمان جنگ در اروپا که ذخایر آب آشامیدنی به خطر افتاد مورد توجه قرار گرفت. امروزه غشا کاربردهای گوناگونی در صنعت دارد از جمله تصفیه آب و فاضلاب که در تامین آب مورد نیاز صنعت و جامعه مورد توجه قرار گرفته است. لازم به ذکر است مهمترین عامل محدود کنندهٔ کاربرد گستردهٔ مشکل پدیده گرفتگی غشاء می باشد. گرفتگی غشاء منجر به کاهش طول عمر مفید غشاء، هزینه های مربوط به تمیز کردن و همچنین کاهش میزان شار می باشد.[۲]

از آنجایی که خاصیت گرفتگی به طور عمده از آب گریز بودن غشاء ناشی می شود؛ [۳] بنابراین افزایش آب دوستی غشاها می تواند تا حد زیادی از گرفتگی غشاء جلوگیری کند.تلاش برای توسعه غشاهای مخلوط که در آنها از نانو ذرات به عنوان مواد افزودنی در غشاهای پلیمری استفاده می شود، به تازگی مورد توجه زیادی قرار گرفته است؛ زیرا وجود نانوذرات در ماتریس غشاء میتواند آب دوستی، مقاومت، پایداری مکانیکی و حرارتی، نفوذپذیری آب و خواص ضد رسوب پلیمر های متکی بر غشاهای نانو کامپوزیتی را بهبود بخشد. از نانوذرات بسیاری به منظور آب دوستی غشاها استفاده شده است که می توان به TiO2 ، Al2O3 ، نانولوله های کربنی، آهن صفر ظرفیتی و پالادیم [۵] اشاره کرد.

جهت احیا غشا از روش های تمیز کردن غشا استفاده می شود که به طور کلی روش های تمیز کردن غشاء به دو طریق انجام می گیرد؛ درجا که در آن غشاء در خود محل، مورد شست و شو قرار می گیرد و یا به صورت غیر درجا که در آن غشاء خارج شده و برای شست و شو فرستاده می شود. تمیز کردن هر کدام از این روش ها، خود توسط چهار روش فیزیکی، شیمیایی، زیستی و ترکیبی از روش شیمیایی- فیزیکی صورت می گیرد. در این مقاله پتانسیل احیا فلاکس عبوری از غشای اولترافیلتراسیون پلی وینیلیدن فلوراید (PVDF) اصلاح شده با مایع یونی مورد بررسی قرار گرفته است. به این منظور از دو محلول شیر خشک با پتانسیل گرفتگی بالا استفاده شد.

۲) مواد و روش ها:

در این تحقیق از غشای اولترافیلتراسیون پلی وینیلیدن فلوراید اصلاح شده با مایع یونی استفاده شده است که در مقاله قبلی همین گروه به چاپ رسیده است و غشای بهینه این مقاله در این تحقیق حاضر استفاده شده است. جهت بررسی عملکرد غشای بهینه در ابتدا از غشاء به مدت ۴۰ دقیقه آب (water1) عبور داده شد و میانگین شار عبوری (flux) با توجه به فرمول زیر محاسبه شد. ابتدا آب (Water 1) را به مدت ۴۰ دقیقه از غشایی با سطح مقطع ۱۹,۶۲۵ سانتی متر مکعب (۰,۰۰۱۹۶۲۵ مترمکعب) عبور داده شد و میانگین شار عبوری (flux) با توجه به فرمول زیر محاسبه شد که در آن V، حجم برحسب لیتر T،زمان برسب ساعت A، سطح مقطع برحسب متر مربع می باشند.

$$\boldsymbol{Flux = \frac{V}{T.A}}$$

سپس پودر شیرخشک با غلظت ۱۰ گرم بر لیتر را به مدت ۷۰ دقیقه از غشاء عبور داده و داده های فلاکس عبوری ثبت شد. پس از ۷۰ دقیقه غشا از ستاپ خارج شد و با آب مقطر شستشو داده شد و به مدت ۱۵ دقیقه در آب مقطر قرار داده شد. در مرحله بعد، مجددا به مدت ۳۰ دقیقه آب مقطر (Water 2)از غشا عبور داده شد و در نهایت با توجه به داده های فلاکس عبوری، میزان احیا فلاکس عبوری FRR با توجه به فرمول زیر محاسبه شد که در آن W1 : آب مقطر اول w2 : آب مقطر دوم می باشند.

---

[۱] Backwash

$$\mathbf{FRR = \frac{w2}{w1} * 100}$$

در ادامه به جهت بررسی دقیق تر پتانسیل غشا در برابر گرفتگی های بیولوژیکی، از محلول شیر خشک با غلظت ۵۰ گرم بر لیتر لستفاده شد که قدرت گرفتگی بسیار بالایی را دارد و تمامی مراحل فوق تکرار شد تا در نهایت FRR غشا در این مرحله نیز محاسبه شود. پس از گرفتگی غشا با محلول ۵۰ گرم بر لیتر از شیر خشک از روش فیزیکی شستشوی غشا جهت احیا آن استفاده شد و FRR غشا بعد از شستشوی معکوس دوباره اندازه گیری شد.

۳) نتایج و بحث:

در پژوهش‌های مربوط به غشاها و عملکرد آن‌ها در فرآیندهای جداسازی، شستشوی مناسب و ارزیابی عملکرد پس از آن از اهمیت ویژه‌ای برخوردار است .در این تحقیق، پتانسیل غشای اولترافیلتراسیون پلی وینیلیدن فلوراید اصلاح شده با مایعات یونی مورد بررسی قرار گرفت. به این منظور در مراحل مختلف آب مقطر و محلول شیر خشک با غلظت‌های ۱۰ و ۵۰ گرم بر لیتر از غشای مورد نظر عبور داده شد که داده‌های بدست آمده را در شکل ۱ ملاحظه می‌کنید. همانطور که در نمودار رسم شده دیده می‌شود فلاکس عبوری غشا بعد از گذراندن شیر خشک با غلظت ۱۰ گرم بر لیتر کاهش پیدا کرده است بطوریکه فلاکس عبوری بعد از ۷۰ دقیقه از ۱۵ به ۳ کیلوگرم بر متر مربع در ساعت رسیده است. قابل توجه است که بعد از عبور دادن آب مقطر دوم فلاکس عبوری تا حد زیادی احیا شده است. جهت بررسی دقیق تر میزان احیا شدگی غشا دز طی تست گرفتگی انجام شده، پارامتر FRR محاسبه شد که نتایج آن در جدول ۱ ارائه شده است. طبق داده های بدست آمده مقدار FRR در این مرحله ۸۱% می باشد که حاکی از پتانسیل بالای این غشا در برابر گرفتگی های شدید می باشد.

همانطور که می دانیم شیر خشک، به ویژه در غلظت‌های مختلف، یکی از موارد حائز اهمیت در مطالعات علمی مربوط به پتانسیل‌های صنعتی و آزمایشگاهی به شمار می‌آید. طبق شواهد موجود، شیر خشک با غلظت ۱۰ گرم بر لیتر، دارای قدرت گرفتگی چشمگیری است که می‌تواند اثرات قابل ملاحظه‌ای بر فرآیندهای غشایی داشته باشد. در این راستا، به منظور بررسی عمیق‌تر پتانسیل ضد گرفتگی این غشا، محلول شیر خشک با غلظت ۵۰ گرم بر لیتر به عنوان یک نمونه آزمایشی انتخاب شد.. در ادامه به منظور کنکاش بیشتر در خصوص پتانسیل ضد گرفتگی این غشا، محلول شیر خشک با غلظت ۵۰ گرم بر لیتر مورد آزمایش قرار گرفت که در واقع قدرت گرفتگی محلول ۵ برابر شد. در نهایت، پس از گذشت ۲۵۰ دقیقه از عبور محلول شیر خشک با غلظت بالا، مقدار فلاکس عبوری به نزدیکی صفر رسید که نشان‌دهنده اثرات منفی غلظت‌های بالا بر عملکرد غشا و افزایش قابلیت گرفتگی است. این یافته‌ها اهمیت توجه به غلظت‌های مختلف و تأثیر آن‌ها بر کارایی فرآیندهای جداسازی را به وضوح نمایان می‌سازد .

در مرحله بعد غشای مورد نظر با آب مقطر شستشو داده شد و بعد از آن فلاکس آب مقطر عبوری دوباره اندازه گیری شد که این بار هم میزان عبور آب قابل ملاحظه بود. مقدار FRR اندازه گیری شده نیز این موضوع را اثبات کرده است بطوریکه مقدار FRR ۷۰% گزارش شده است که حاکی از توانایی این غشا در مقابله با عوامل گرفتگی و حفظ کارایی در طول زمان است. این مقدار FRR نشان‌دهنده پتانسیل قابل توجه غشا در فراهم کردن جریان پایدار و مؤثر آب تصفیه شده است.

همچنین روش شستشوی معکوس به عنوان یکی از روش های موثر و رایج در احیای غشاها به شمار می‌آید. در این تحقیق، به منظور ارزیابی قابلیت احیای مجدد غشا پس از گرفتگی، از این روش استفاده گردید. فرایند شستشوی معکوس به مدت ۵۰ دقیقه انجام شد و نتایج حاصله نشان دهنده افزایش قابل توجه میزان آب مقطر عبوری از غشا نسبت به حالت پس از گرفتگی بود. این تغییرات در نمودار به وضوح قابل مشاهده است. علاوه بر این، میزان FRR از ۷۰% به ۸۰% افزایش یافته است. این افزایش درصد، گویای کارایی و قابلیت استفاده مجدد از غشا پس از بروز گرفتگی‌های شدید می‌باشد. این نتایج نشان می‌دهد که روش شستشوی معکوس می‌تواند به عنوان یک راهکار موثر برای احیای غشای مورد نظر مورد استفاده قرار گیرد که از لحاظ اقتصادی مقرون به صرفه می باشد و از لحاظ زیست محیطی روشی بی ضرر خواهد بود چون از مواد شیمیایی استفاده نمی شود. به طور کلی، نتایج به‌دست‌آمده مؤید این نکته است که غشای مورد مطالعه، گزینه‌ای مناسب برای کاربردهای صنعتی و زیست‌محیطی به شمار می‌آید و می‌تواند به بهبود فرآیندهای تصفیه کمک شایانی نماید.

نتیجه گیری:

بطور کلی میتوان نتیجه گرفت که غشای اولترافیلتراسیون پلی وینیلیدن فلوراید اصلاح شده با مایعات یونی، عملکرد مناسبی جهت فیلتراسیون شیر خشک با غلظت های بالا (که قدرت گرفتگی بالایی دارد) نشان می دهد. آزمایش‌ها نشان دادند که غلظت‌های بالای محلول شیر خشک، باعث کاهش شدت جریان عبوری (فلاکس) و افزایش لزجت و گرفتگی نهایی غشا

می‌شود. با این حال، شستشوی مجدد با آب مقطر و استفاده از روش شستشوی معکوس می‌تواند کارایی غشا را به طور قابل توجهی بهبود بخشد بطوریکه مقدار FRR از ۷۰٪ پس از فیلتراسیون محلول شیر خشک با غلظت ۵۰ گرم بر لیتر به ۸۰٪ پس از شستشوی معکوس رسید.

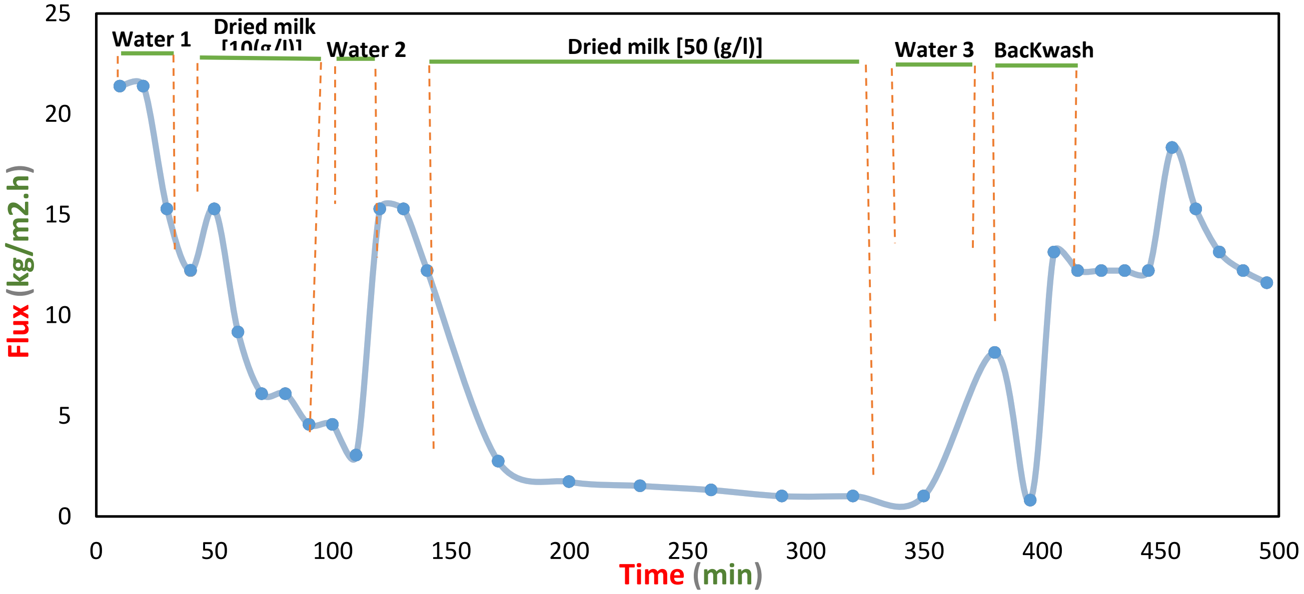

شکل ۱: نمودار فلاکس عبوری از غشا در مراحل مختلف

جدول ۱: داده های FRR در مراحل مختلف

ردیف	شرایط	FRR, %
۱	پس از افزودن پودر شیر ۱۰ گرم بر لیتر (g/l)	81.1594
۲	پس از افزودن پودر شیر ۵۰ گرم بر لیتر (g/l)	70.6087
۳	پس از Backwash	80.3478

منابع:

[1] Mulder, M. H. V., (1996) "Basic principles of membrane technology", Kluwer academic publishers, Dordrecht, netherland, second edition, 428- 475.

[2] برزین، جلال، اسماعیلی، مجید، (۱۳۸۸)، گرفتگی غشاء و روش های احیاء آن، " پژوهشگاه پلیمر و پتروشیمی ایران."

[3] Rana D., Matsura T., Surface modifications for antifouling membranes. Chemical reviews; 110:2448- 2471(2010)

[4] Poecelli, Nicandro, Judd, Simon, (2010), " Chemical cleaning of potable water membranes: A review" , separation and Purfication Technology (71) 137 – 143.

[5] Chen D., Feng H., Li J., Graphene oxide: preparation, functionalization. Chemical reviews; 112:6027–6053 (2012)

The 30th Iranian Seminar of Organic Chemistry
February 7-9, 2025, Iran University of Science and Technology, Tehran, Iran

"Innovative MOF-303/LDH Frameworks with Dual-Pyrazol Functionalities for Metal Separation and Recycling"

Seyed Mohsen Eisari[a] and Ali Morsali[a*]

Department of Chemistry, Faculty of Basic Sciences, Tarbiat Modares University, Tehran, Iran.
Email: morsali_a@yahoo.com

Keywords: Metal-organic framework, Dual-pyrazol sites, Adsorption and separation, Metal recovery, Layered Double Hydroxides

Introduction

Layered Double Hydroxides (LDHs) and Metal-Organic Frameworks (MOFs) have emerged as advanced materials with significant potential for the efficient removal of heavy metals from wastewater. Among the common metals, copper (Cu), nickel (Ni), and cobalt (Co) are especially valuable, with widespread industrial uses, and are often found together in wastewaters from steel-making and electroplating industries [1]. Consequently, the separation and recovery of these metals from aqueous solutions has become a major focus of research. Over the past few decades, a variety of water-phase separation techniques for metals have been developed, including adsorption, metal replacement, precipitation, ion exchange, electrochemical methods, and biological approaches. Among these, adsorption is considered one of the most effective methods due to its high efficiency, low cost, and ease of operation. The development of adsorbents with excellent selectivity and large adsorption capacities is critical for the effective separation and recovery of metal ions [2].

The integration of LDHs and MOFs into hybrid composites takes advantage of their complementary properties, offering an innovative and efficient approach to water and wastewater treatment [3]. LDHs are known for their unique layered structure, positive charge, and outstanding anion exchange capacity, which make them highly effective for the adsorption of heavy metals. On the other hand, MOFs, characterized by their high surface area, tunable porosity, and structural flexibility, have gained significant attention as potential adsorbents in environmental applications. When combined into a composite material, LDHs and MOFs enhance each other's performance, particularly in metal ion removal [4]. In these composites, LDHs serve as a structural backbone, providing stability to MOFs in aqueous environments, while MOFs contribute to increased surface area and adsorption capacity. These composites have shown remarkable ability to remove heavy metals such as cadmium, lead, mercury, and nickel, primarily through mechanisms like surface adsorption, ion exchange, and chemical reactions.

LDH@MOF composites have shown superior performance compared to the individual components, offering advantages such as improved chemical stability, enhanced adsorption efficiency, and the ability to selectively target specific heavy metals. Furthermore, these materials are economically and environmentally advantageous, thanks to their reusability and low production costs. The flexibility in designing these composites also allows for customization, making them suitable for a wide range of applications. In conclusion, LDH@MOF composites represent a cutting-edge solution for sustainable water management and the effective remediation of heavy metal pollution.

Method

MOF-303 was synthesized through a solvothermal reaction using aluminum chloride hexahydrate ($AlCl_3·6H_2O$) and 3,5-pyrazoledicarboxylic acid (H_2PDC), following a previously reported procedure [5]. The synthesis of Ni-Ti LDH was carried out by the co-precipitation method in an aqueous medium, involving the reaction between nickel nitrate or chloride salts and titanium salts, using a strong base like NaOH or Na_2CO_3 as the precipitating agent [6]. The synthesized LDH was then dispersed in the MOF reaction solution, which contained aluminum chloride hexahydrate as the metal precursor and 3,5-pyrazoledicarboxylic acid as the organic ligand. The mixture was stirred for several hours or heated at elevated temperatures (80–120°C) in a hydrothermal reactor. During this process, the MOF grew uniformly on the surface of the LDH.

Results and Discussion

The material under investigation, LDH@MOF composites, was tested for the selective adsorption of Cu^{2+} ions from binary metal systems, such as Cu^{2+}/Ni^{2+} and Cu^{2+}/Co^{2+}. The LDH@MOF composite exhibited a high adsorption capacity of 330 mg/g for Cu^{2+} ions. It also demonstrated exceptional selectivity in separating Cu^{2+} from other metal ions, with separation factors of 6076 for Cu^{2+}/Ni^{2+} and 2662 for Cu^{2+}/Co^{2+}. The adsorption mechanism of these composites is primarily attributed to the dual-pyrazol sites in MOF-303, which play a key role in selectively binding and removing Cu^{2+} ions. These sites are organized in a manner that enhances the framework's ability to separate metal ions from complex mixtures, improving both selectivity and efficiency.

This study highlights the potential of LDH@MOF composites as a promising material for the separation and recovery of high-value metals like copper from wastewater, particularly in binary metal systems. The research underscores the importance of the dual-pyrazol sites in improving the separation of metal ions, which is crucial for recovering valuable metals from industrial wastewaters. In addition, the study emphasizes the role of MOFs in environmental sustainability, demonstrating their potential in the recovery and reuse of valuable metal ions, and offering a solution for more efficient and eco-friendly metal resource recovery.

References:

[1] R. Panda, M.K. Jha, D.D. Pathak, R. Gupta, Recovery of Ag, Cu, Ni and Fe from the nitrate leach liquor of waste ICs, Miner. Eng. 158 (2020), 106584.

[2] F. Werlinger, R.S. Rojas, Evaluation of novel imino-phenol ligands in divalent metal ion extraction/recovery processes from leaching solutions, Sep. Purif. Technol. 252 (2020), 117451.

[3] S. Yang, L.i. Peng, O.A. Syzgantseva, O. Trukhina, I. Kochetygov, A. Justin, D. T. Sun, H. Abedini, M.A. Syzgantseva, E. Oveisi, G. Lu, W.L. Queen, Preparation of highly porous metal–organic framework beads for metal extraction from liquid streams, J. Am. Chem. Soc. 142 (31) (2020) 13415–13425.

[4] F. Fathieh, M.J. Kalmutzki, E.A. Kapustin, P.J. Waller, J. Yang, O.M. Yaghi, Practical water production from desert air, Sci. Adv. 4 (6) (2018) eaat3198,https://doi.org/10.1126/sciadv.aat3198.

[5] P. Roy Chowdhury, K. G. Bhattacharyya, Retracted Article: Ni/Ti layered double hydroxide: synthesis, characterization and application as a photocatalyst for visible light degradation of aqueous methylene blue, Dalton Trans., 2015,44, 6809-6824.

The 30th Iranian Seminar of Organic Chemistry
February 7-9, 2025, Iran University of Science and Technology, Tehran, Iran

Analysis and investigation of the advanced oxidation process of malachite green dye using photocatalysts under UV-Vis light irradiation

Nastaran Parsafard* and Homa Moodi
Department of Applied Chemistry, Faculty of Basic Sciences and Engineering, Kosar University of Bojnord, Bojnord, Iran
** Email:* n-parsafard@kub.ac.ir

Keyword: Photodegradation, Photocatalyst, Malachite Green, UV-Vis Radiation.

Malachite green (MG) is one of the cationic dyes that has been banned in many parts of the world due to its azo groups and toxic aromatic compounds. Therefore, extensive research is underway to remove it from wastewater by various methods, including photocatalysis. In this study, three types of catalysts, Sn-TiO_2/CaO, La@M_xO_y/TiO_2 (M = V, Cr, Mn, Fe), and La@SnO_2–CaO, were used for MG degradation. The results showed that doping transition metals in these catalysts improved their photocatalytic properties. The direct relationship between time and pH in the Sn-TiO_2/CaO and La@M_xO_y/TiO_2 catalysts are quite clear [1-3]. These catalysts had increasing performance at all three pHs (Figure 1), but the photodegradation percentage (PDE%) was always higher for Sn-TiO_2/CaO. This is while the relationship between pH and time is less evident in La@SnO_2–CaO. This issue occurred for two reasons; first, due to the non-uniform dispersion of lanthanum on the catalytic support and second, due to the very small pore volume of the La@M_xO_y/TiO_2 and La@SnO_2–CaO catalysts, which despite the high surface area, the small pore volume prevents high dye adsorption into the pores and requires more time for the photocatalytic process of this catalyst. Tin and titanium doping and the process of nucleation and growth of nanoparticles in the

Sn-TiO_2/CaO catalyst clearly state that the uniform distribution of particle size has a significant effect on its performance in removing malachite green dye.

Figure 1: The effect of pH on the PDE of MG in the ranged from 5–35 min.

References:

١. Parsafard, N., Abedi, R., & Moodi, H. (2024). RSC Advances, 14(28), 19984-19995.

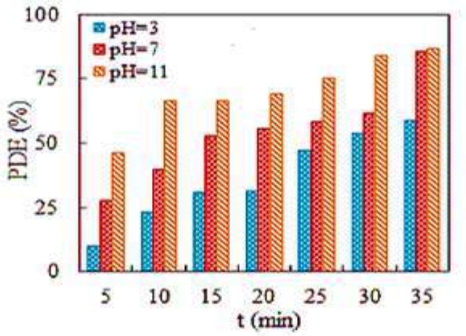

٢. Parsafard, N., & Shoorgashti, Z. (2024). Applied Water Science, 14(10), 220.
٣. Parsafard, N., & Aghajari, G. (2024). BMC Chemistry, 18(1), 221.

The 30th Iranian Seminar of Organic Chemistry
February 7-9, 2025, Iran University of Science and Technology, Tehran, Iran

Comparative study of Pt/MCM-48 based catalysts in the n-heptane isomerization process

Nastaran Parsafard* and Homa Moodi
Department of Applied Chemistry, Faculty of Basic Sciences and Engineering, Kosar University of Bojnord, Bojnord, Iran
** Email :n-parsafard@kub.ac.ir*

Keywords: Pt/MCM-48 catalysts, n-heptane isomerization, catalyst, catalytic performance.

Gasoline is one of the most important fossil fuels used in transportation and internal combustion engines. It is derived from a mixture of hydrocarbons and features properties such as rapid evaporation and high energy density, but its use generates pollutants like carbon dioxide, posing environmental challenges. New regulations aimed at reducing benzene levels in gasoline have been implemented to improve air quality. However, these changes lower the octane number, potentially causing engine knocking. To address this issue, catalytic isomerization of linear alkanes such as *n*-heptane into branched isomers, using acidic catalysts, helps increase the octane number and

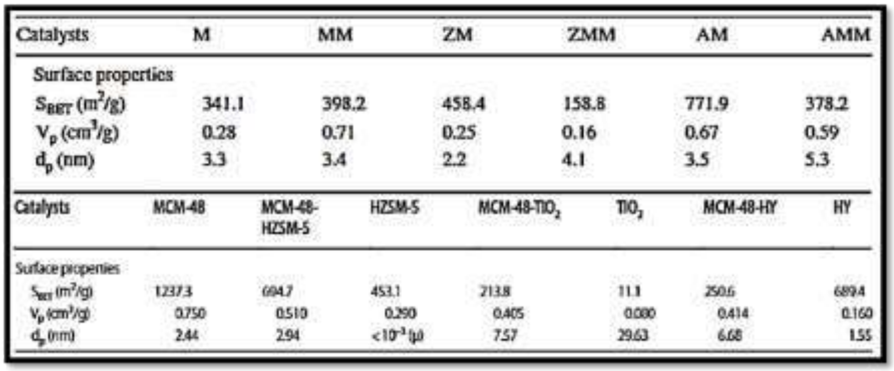

Catalysts	M	MM	ZM	ZMM	AM	AMM
Surface properties						
S_{BET} (m^2/g)	341.1	398.2	458.4	158.8	771.9	378.2
V_p (cm^3/g)	0.28	0.71	0.25	0.16	0.67	0.59
d_p (nm)	3.3	3.4	2.2	4.1	3.5	5.3

Catalysts	MCM-48	MCM-48-HZSM-5	HZSM-5	MCM-48-TiO_2	TiO_2	MCM-48-HY	HY
Surface properties							
S_{BET} (m^2/g)	1237.3	694.7	453.1	213.8	11.1	250.6	689.4
V_p (cm^3/g)	0.750	0.510	0.290	0.405	0.080	0.414	0.160
d_p (nm)	2.44	2.94	$<10^{-3}$ (μ)	7.57	29.63	6.68	1.55

enhance fuel performance [1].This study presents a comparative analysis of platinum catalysts supported with different supports, including MCM-48, HZSM-5, HY, mordenite, and composites modified with zirconium, aluminum, and titanium [2, 3]. This study evaluates the structural characteristics, acidity distribution, catalytic performance, and stability during n-heptane isomerization. The results show that composite catalysts such as Pt/Al-MCM-48-Mordenite and Pt/MCM-48-HZSM-5 have outstanding performance in n-heptane isomerization and have been able to produce branched isomers with high octane numbers. These catalysts have been effective in producing high-quality fuels and reducing environmental pollutants by reducing the formation of by-products such as coke and aromatics. This research shows that the combination of zeolites and precious metals can have a significant impact on improving industrial processes and achieving cleaner fuels. The Pt/Al-MCM-48-Mordenite catalyst showed very good performance, especially at low temperature (200°C). The conversion rate of 78.8% and the selectivity of 81.9% for the multi-branched isomers indicate the extraordinary ability of this catalyst to produce high-quality products. This is while the Pt/MCM-48-HZSM-5 catalyst had a maximum selectivity of 37.8% under the best conditions. The major difference in the performance of these two catalysts is attributed to the more optimized structure of Pt/Al-MCM-48-Mordenite, which is associated with increased porosity and a uniform distribution of acidic sites. The larger pore diameter (5.3 nm) in Pt/Al-MCM-48-Mordenite allows for more efficient diffusion of multi-branched isomers (Table 1). This feature prevents the accumulation of products in the pores and reduces the possibility of their cracking. In addition, the high specific surface area of 771.9 m2/g in this catalyst provides a larger surface area for catalytic reactions, while this value was lower in Pt/MCM-48-HZSM-5. Another important feature of this catalyst is its optimized acidic properties. The total number of acidic sites (552.9 μmol NH_3) and the appropriate ratio of strong to weak acids (S/W=1.4) accelerated the isomerization reaction and reduced the by-products. In contrast, the second catalyst had fewer acidic sites, which limited its ability to produce multi-branched isomers.

The high resistance of Pt/Al-MCM-48-Mordenite to coke formation is another key point. In long-term tests, coke formation in this catalyst was much lower than that of Pt/MCM-48-HZSM-5 due to the better balance between acidity and porosity. This feature increases the stability of the catalyst and allows its long-term use in industrial processes. Finally, the high octane number (RON) of 96.5 for Pt/Al-MCM-48-Mordenite indicates the production of high-quality isomers that are more resistant to knock. This number is significantly higher than the octane number of 58. For the Pt/MCM-48-HZSM-5 catalyst, indicating the superiority of Pt/Al-MCM-48-Mordenite for application in the production of quality fuels.

Table 1: Physicochemical properties of the Pt-synthesized catalysts

References:

1. Simon, D., & Taylor, B., (2009). Journal of Catalysis, 262(1), 127-133.
2. Ghaderi, Z., Peyrovi, M. H., & Parsafard, N., (2021). BMC Chemistry, 15(1), 61.
3. Ghaderi, Z., Peyrovi, M. H., & Parsafard, N., (2023). Journal of Porous Materials, 30(5), 1789-1795.

The 30th Iranian Seminar of Organic Chemistry
February 7-9, 2025, Iran University of Science and Technology, Tehran, Iran

Design and synthesis of efficient and reusable Biochar-g-C_3N_4/PEI@SO_3H as nanocatalyst in biodiesel production

Maryam Hajjami*, Zahra Siahpour

Department of Organic Chemistry, Faculty of Chemistry and Petroleum Sciences, Bu-Ali Sina University, Postal code 6517838683, Hamedan, Iran. E-mail address, m.hajjami@basu.ac.ir or mhajjami@yahoo.com

Keyword: Biochar, Biodiesel, Nanocatalyst, g-C_3N_4

Abstract

Biodiesel is acknowledged as a more sustainable alternative to fossil fuel products. Transesterification, as well as esterification, is a common chemical reaction for the preparation of biodiesel [1,2]. Biochar, an inexpensive carbon-rich material derived from the thermochemical decomposition of biomass, showcases unique characteristics that make it valuable in various scientific applications. This work first presents the method and design for synthesizing g-C_3N_4/biochar composite (Biochar-Based Graphitic Carbon Nitride) as support catalysts [3]. The surface of g-C_3N_4/biochar composites was modified and characterized using FT-IR, XRD, SEM, EDS, TGA, and BET techniques. The applications of this nano catalyst in biodiesel production are thoroughly discussed. The structure of biodiesel synthesized in this work was confirmed using validated techniques such as NMR and FT-IR techniques. This green catalyst offers easy isolation and recyclability due to its heterogeneity, along with good to excellent efficiency and a short reaction time. Its reusability was tested over five cycles, showing no significant loss in catalytic activity or efficiency.

Scheme: Synthesis of biodiesel in the presence of g-C_3N_4/biochar composite

References

1- Corma, A., Iborra, S. & Velty, A. Chemical routes for the transformation of biomass into chemicals. Chem. Rev. 107, 2411–2502 (2007).

2- Gomes, R., Bhanja, P. & Bhaumik, A. Sulfonated porous organic polymer as a highly efficient catalyst for the synthesis of biodiesel at room temperature. J. Mol. Catal. A: Chem. 411, 110–116 (2016).

3- Elkhalifa, S. Al-Ansari, T. Mackey, H. R. & McKay, G. Food waste to biochars through pyrolysis: A review. Resour. Conserv. Recy., 144, 310−320 (2019).

The 30th Iranian Seminar of Organic Chemistry
February 7-9, 2025, Iran University of Science and Technology, Tehran, Iran

Synthesis of Polyelectrolyte based on Chitosan and Urea as Coagulant in Wastewater Treatment

Mina Moghanni Khosroshahi[a], Sedigheh Ehsanimehr, Peyman Najafi Moghadam*

[a]*Department of Organic Chemistry, Faculty of Chemistry, Urmia University, Urmia, Iran*

Keywords: Coagulant, Polyelectrolyte, Chitosan, Urea

Introduction:

Coagulation and flocculation processes are widely employed in industrial wastewater treatment to remove colloidal particles, dyes, heavy metals, and organic compounds.(Badawi et al., 2023) Polyelectrolytes are versatile materials that can enhance water treatment processes either directly, by serving as treatment agents, or indirectly, by acting as additives to improve the efficiency of existing systems.(Chen et al., 2024) It has garnered significant attention in wastewater treatment due to its ability to remove a wide range of pollutants. Chitosan's unique structure, comprising amino ($–NH_2$) and hydroxyl (–OH) groups, makes it an excellent adsorbent for both anionic and cationic contaminants. These functional groups act as active sites for pollutant adsorption, enabling the effective removal of impurities from aqueous solutions. However, chitosan's practical application faces challenges, such as limited selectivity, weak mechanical properties, and low solubility in acidic conditions. Therefore, various strategies have been explored to modify the physicochemical properties of chitosan to address these limitations and enhance its performance.(Bhatt et al., 2023)

Method:

For the synthesis of polyelectrolyte, a solution of different molar ratios of chitosan and urea in deionized water was prepared and refluxed at 90°C for 24 h (**Table 1**). After the reaction was completed, the pH of the final solution was adjusted to 3 using HCl and the solution was gradually heated to concentrate. The reaction product was obtained as a thick gel, which was separated and washed with methanol. The obtained gel was dried in an oven at 60°C and powdered. It was analyzed using spectroscopic and performance evaluation methods. The overall reaction was shown in **scheme 1.**

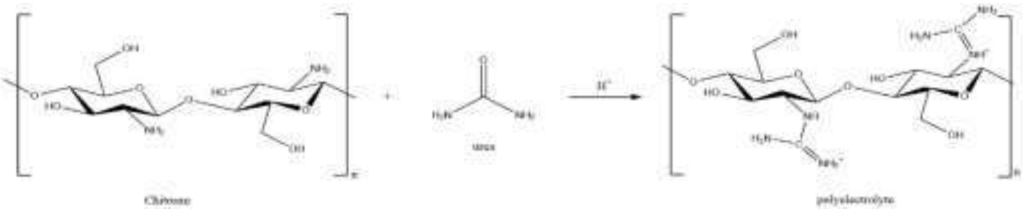

Scheme 1. Schematic representation of polyelectrolyte synthesis

Table 1. The synthesized samples compassion

Samples	Chitosan	Urea	Ratio W/W	Yield%
Sample 1	1 g	0.5 g	2:1	٤٦,٠٦
Sample 2	1 g	1 g	1:1	٦٥,١
Sample 3	1 g	2 g	1:2	٤٢,٩
Sample 4	1 g	0.25 g	4:1	٦٨,١٦

Results and Discussion:

The procedure for synthesis of polyelectrolyte was simple and quantitative and the synthesized polyelectrolytes were characterized through instrumental analyses and evaluated for their performance as coagulant. Key experiments included determining filtration time (TTF), turbidity (FTU), total suspended solids (TSS), and sludge cake moisture percentage were carried out. The coagulation tests for synthesized polyelectrolytes were done at a concentration of 0.01 wt% of polyelectrolyte in suspension of clay (1% w/w) as the turbidity agent. Results showed that varying the urea to chitosan ratios significantly influenced on coagulation speed and coagulation quality (**figure 1**). The optimal performance was observed in the sample 2 achieving maximum clarity and rapid coagulation. Further analysis indicated that the ratio of urea to chitosan plays a crucial role in improving the efficiency of the coagulation process. The sample with an equal ratio of urea and chitosan demonstrated superior results, including the highest solution clarity and the fastest coagulation rate, highlighting its potential for effective water treatment. The findings of this study suggest that chitosan-urea-based polyelectrolytes can serve as effective coagulants for municipal wastewater treatment.

Figure 1. The images of samples after coagulation

References:

Badawi, A. K., Salama, R. S., & Mostafa, M. M. M. (2023). Natural-based coagulants/flocculants as sustainable market-valued products for industrial wastewater treatment: a review of recent developments. *RSC advances*, *13*(28), 19335-19355.

Bhatt, P., Joshi, S., Bayram, G. M. U., Khati, P., & Simsek, H. (2023). Developments and application of chitosan-based adsorbents for wastewater treatments. *Environmental Research*, *226*, 115530.

Chen, M., Xu, R., Wu, Y., Xiong, J., Keleş, S. Z., & Hankins, N. P. (2024). Application of polyelectrolytes for contaminant removal and recovery during water and wastewater treatment: A critical review. *Journal of Water Process Engineering*, *64*, 105528.

The 30th Iranian Seminar of Organic Chemistry

February 7-9, 2025, Iran University of Science and Technology, Tehran, Iran

Synthesis of 1,2,3-triazole drivatives using a functionalized Cobalt-based metal-organic-framework catalyst

Mahtab Amirian [a], Ramin Ghorbani Vaghei[ab], Sedigheh Alavinia[a]

[a]*Department of Organic Chemistry, Faculty of Chemistry and Petroleum Sciences, Bu-Ali Sina University, Hamedan 6517838683, Iran*

[b]*Department of Organic Chemistry, Faculty of Chemistry, University of Guilan, Rasht, Iran*

Keyword: Triazole, Synthesis, Cobalt, Metal-Organic-Framework, Aldehyde, Sodium azid

1,2,3-Triazoles have always constituted an important class of heterocyclic organic frameworks due to the immense pharmacological activities associated with them. [1] Metal-organic frameworks (MOFs) have shown potential applications due to their high porous hybrid structure. [2] In this project, a new structure of Co-MOF was synthesized through functionalization with pyrimidine-triazine as an effective catalyst in the synthesis of different triazole derivatives. Three-component reactions of aldehydes, nitroalkanes, and sodium azide for the synthesis of NH-1,2,3-triazoles have been developed. The reaction provides a safe and efficient approach for the synthesis of various NH-1,2,3-triazoles in good to excellent yields. [3]

Scheme

References:

١. Bhuyan, P., Bhorali, P., Islam, I., Bhuyan, A. J., & Saikia, L. (2018). Magnetically recoverable copper ferrite catalyzed cascade synthesis of 4-Aryl-1H-1, 2, 3-triazoles under microwave irradiation. *Tetrahedron Letters*, *59*(16), 1587-1591

٢. Sargazi, G., Afzali, D., Ghafainazari, A. *et al.* (2014). Rapid Synthesis of Cobalt Metal Organic Framework. *J Inorg Organomet Polym* 24, 786–790

٣. Hui, R., Zhao, M., Chen, M., Ren, Z., & Guan, Z. (2017). One-Pot Synthesis of 4-Aryl-NH-1, 2, 3-Triazoles through Three-Component Reaction of Aldehydes, Nitroalkanes and NaN3. *Chinese Journal of Chemistry*, *35*(12), 1808-1812

The 30th Iranian Seminar of Organic Chemistry
February 7-9, 2025, Iran University of Science and Technology, Tehran, Iran

Preparation of natural deep eutectic solvents (NADES) based on sugar and their application in the synthesis of hetrocyclic compounds such as pyrimidinones

Authors: Sedigheh Ayazi Jannatabadi[a], Rahman Hosseinzadeh[b]*, Behrooz Maleki[c]*

Affiliations: Department of Organic Chemistry, Faculty of Chemistry, University of Mazandaran, Babolsar, Iran[a,b,c]

Keyword: Natural deep eutectic solvent, Dihydropyrimidinone, Polyhydroquinoline, Multicomponent reactions, Heterocyclic chemistry

Abstract:

Natural deep eutectic solvents (NADESs) have emerged as a novel class of solvents with properties reminiscent of ionic liquids while offering additional advantages in terms of cost, environmental impact, and synthesis. This article focuses on the applications of NADESs of mannose:urea and glucose:dimethylurea as inexpensive, accessible, and reusable catalysts in the synthesis of dihydropyrimidinone and polyhydroquinoline derivatives. The results demonstrate significant yields for both dihydropyrimidinones (47-99%) and polyhydroquinolines (90-97%) reactions using mannose:urea and glucose:dimethylurea as catalysts. The advantages of NADESs as catalysts include their simple and reproducible preparation, low cost, environmentally benign nature, long-term durability, and tunable properties. This NADESs can also be recovered and reused for four times without a significant loss of activity.

Scheme:

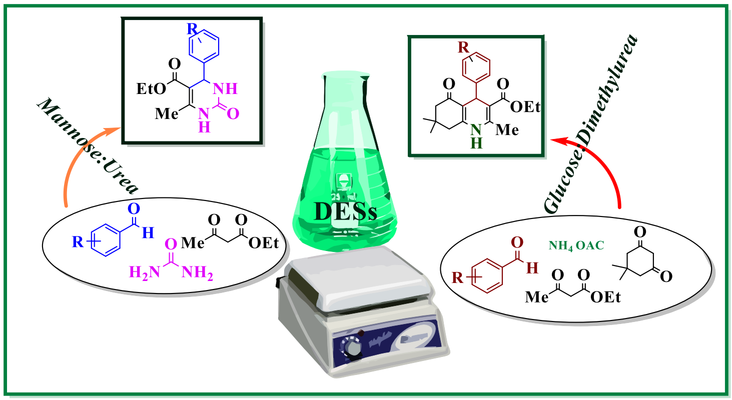

References:

[1] C. Falcini, G. de Gonzalo, Deep eutectic solvents as catalysts in the synthesis of active pharmaceutical ingredients and precursors, Catalysts. 120, 14(2024). https://doi.org/10.3390/catal14020120.

[2] A.K. El-Deen, K. Shimizu, Deep eutectic solvents as promising green solvents in dispersive liquid–liquid microextraction based on solidification of floating organic droplet: recent applications, challenges and future perspectives, Molecules. 7406, 26(2021). https://doi.org/10.3390/molecules26237406.

[3] T. Swebocki, A. Barras, A. Abderrahmani, K. Haddadi, R. Boukherroub, Deep eutectic solvents comprising organic acids and their application in (Bio)medicine, Int. J. Mol. Sci. 8492, 24(2023). https://doi.org/10.3390/ijms24108492.

Synthesis of Polyhydroquinolines catalyzed by Ni(II) and Cu(II) complexes

Masoud Bigdeloo[a], Maryam Manafi Moghadam[a], Sobhan Rezayati[a] and Ali Ramazani*[a,b]

[a] *Department of Chemistry, Faculty of Science, University of Zanjan, Zanjan 45371-38791, Iran*
[b]*Department of Biotechnology, Research Institute of Modern Biological Techniques (RIMBT), University of Zanjan, Zanjan 45371-38791, Iran, E-mail:* aliramazani@gmail.com

Keyword: Polyhydroquinolines (PHQs), Homogenous Catalysts, Ni(II)Salen, Cu(II)Salen, Heterocyclic compounds

Homogeneous catalysts have considerable advantages over heterogeneous ones due to their solubility in the reaction medium, which improves substrate accessibility to catalytic sites and increases their efficacy in chemical processes [1]. Multicomponent reactions have become effective methods for the synthesis of heterocyclic molecules. Polyhydroquinolines are particularly significant due to their varied biological and therapeutic applications, encompassing anti-inflammatory, antibacterial, wound-healing, and antioxidant characteristics [2]. For this purpose, we have synthesized two novel Ni(II) and Cu(II) Salen Schiff-base complexes from salicylaldehyde and ethylenediamine in ethanol at ambient temperature. These catalysts have remarkable efficacy in the Polyhydroquinolines reaction, which entails a four-component one-pot synthesis that integrates substituted aromatic or aliphatic aldehydes, ethyl acetoacetate, dimedone, and ammonium acetate in ethanol under reflux conditions (Figure 1).

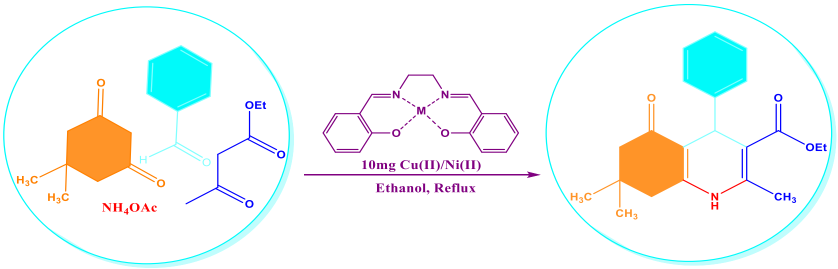

Figure 2 One-pot synthesis of PHQs

References:

1. Shiri, L., L. Heidari, and M. Kazemi, *Magnetic Fe3O4 nanoparticles supported imine/Thiophene-nickel (II) complex: A new and highly active heterogeneous catalyst for the*

synthesis of polyhydroquinolines and 2, 3-dihydroquinazoline-4(1H)-ones. Applied Organometallic Chemistry, 2018. **32**(1): p. e3943.

2. Amiri-Zirtol, L., et al., *Preparation of a new reusable magnetic organocatalyst to synthesis of polyhydroquinoline derivatives as cytotoxic Agents: Synthesis and biological evaluation.* Journal of Saudi Chemical Society, 2024. **28**(6): p. 101922.

The 30th Iranian Seminar of Organic Chemistry
February 7-9, 2025, Iran University of Science and Technology, Tehran, Iran

Green synthesis of TiO_2 nanoparticles (NPs) by pomegranate waste applied in home and office dental bleaching gels

Fatemeh Mohajer[1,*] **and Fakhrisadat Hosseini[1,*]**

[1]*Department of Biotechnology, Faculty of Biological Sciences, Alzahra University, Tehran, Iran.*
f.mohajer@alzahra.ac.ir

Keyword: Green synthesis, nanoparticles (NPs), pomegranate waste, dental bleaching gels.

Introduction

NPs have exceptional biological properties, unlike whitening agents, and have been used in diverse applications in prosthetic dentistry, implants, restorative dentistry, periodontology, and oral cancer treatments. NPs display antibacterial, antifungal, and antiviral possessions.[1] Nevertheless, few studies have used NPs for tooth whitening because NPs might irreversibly damage teeth through invasive whitening. Though, through the green synthesis of nanoparticles without reducing agents we could save sources and produce nanoparticles with better properties.[2].[3-4]

In terms of environmentally friendly and green chemistry synthesis, pomegranate waste applied to provide applicable product in health arena, which could be more efficient in comparison with other reported work.[5-6] First, it is better to examine the structure of the tooth and consider the mechanism of the bleaching process from the perspective of dental physiology **(Scheme 1).** The tooth is made up of various parts. 1. The crown of the tooth (the part above the gum) 2. The root of the tooth (the part below the gum). The outer part of the crown of the tooth is covered with enamel, which is very similar to bone in terms of hardness and mineral content, although unlike bone, it is brittle and fragile. Tooth enamel is mainly made of hydroxyapatite. The color of enamel can range from light yellow to grayish white depending on personal hygiene. Beneath the enamel is dentin, which is less strong than enamel and, unlike it, is a living tissue and is sensitive to irritation. The color of dentin is light yellow and has a tubule-like structure. Dentin protects the pulp of the tooth**.** [7]

Scheme 1. Dental anatomy[8]

The mechanism of action of hydrogen peroxide in tooth bleaching is considered oxidation, although the process is not well understood. 20 It is felt that oxidants remove some of the unbound organic material from the tooth to a colorless state without dissolving the enamel matrix. There are concerns that continued long-term treatment may lead to dissolution of the enamel matrix . (Scheme2) [۹].

[۱۰] Scheme 2. Bleaching process

Method

To prepare aqueous leaf extract, the pomegranate waste was collected from Saveh, Iran India. The fresh waste was washed with tap water to remove the dust particles on their surface and homogenized using mortar and pestle. The homogenized solution was prepared by adding 200 ml of sterile distilled water. The homogenized content was boiled at 60°C for 10 min using microwave irradiation. The mixer was allowed to cool and filtered through Whatman No.1 filter paper. The filtered extract was used for nanoparticle synthesis.[11]

For the green synthesis of TiO_2 nanoparticles, 25 ml of filtered extract was added to 5 mM of 225 ml of $TiO(OH)_4$. The mixture was then incubated for 12 h. The appearance of color change chiefly established the making of TiO_2NPs. The reaction mixture was then centrifuged at room temperature. The supernatant was cast-off and settled pellets were dissolved in appropriate volume of sterile distilled water. The nanoparticle pellet was dried and used for characterization. [11]

Various analyses such as examining the structure of nanoparticles by scanning electron microscope spectroscopy (FE-SEM), Raman spectroscopy, scanning electron microscope (SEM), transmission electron microscope (TEM), and..., and biological tests such as toxicity testing Cellular, antimicrobial activity, and specific product tests will be done based on existing standards.

The synthesis nanomaterials and diatom were added to the three brand gels and evaluated according to the following formula.

3 types of bleaching were bought and our type was added and compared the teeth whiting process (Table 1).

Table 1. types of bleaching

No.	Types
1	Pulpdent

2	Smileactive
3	Colgate
4	(1-3) +Diatom+TiO_2

Results and Discussion

To prepare aqueous leaf extract, the pomegranate waste was collected from Saveh, Iran India. The fresh waste was washed with tap water to remove the dust particles on their surface and homogenized using mortar and pestle. The homogenized solution was prepared by adding 200 ml of sterile distilled water. The homogenized content was boiled at 60°C for 10 min using microwave irradiation. The mixer was allowed to cool and filtered through Whatman No.1 filter paper. The filtered extract was used for nanoparticle synthesis.[11]

For the green synthesis of TiO_2 nanoparticles, 25 ml of filtered extract was added to 5 mM of 225 ml of $TiO(OH)_4$. The mixture was then incubated for 12 h. The appearance of color change chiefly established the making of TiO_2NPs. The reaction mixture was then centrifuged at room temperature. The supernatant was cast-off and settled pellets were dissolved in appropriate volume of sterile distilled water. The nanoparticle pellet was dried and used for characterization. [11]

The TiO_2 nanoparticles were synthesis in the presence of the pomegranate waste, which was applied in bleaching gel. Then, the whiting process was evaluated based on the following formulation and it was proved that the presence of TiO_2 nanoparticles and diatom could be highly important in terms of whiting. [12]

The synthesis nanomaterials were added to the three brand gels and evaluated according to the following formular and it was proved that the presence of the TiO_2 and diatom could be highly important to be added in formulation to increase the teeth whiteness.

$$\Delta E=\left[(\Delta L^*)^2+(\Delta a^*)^2+(\Delta b^*)^2\right]^{1/2}$$

References

1. Foong, L. K.; Foroughi, M. M.; Mirhosseini, A. F.; Safaei, M.; Jahani, S.; Mostafavi, M.; Ebrahimpoor, N.; Sharifi, M.; Varma, R. S.; Khatami, M., Applications of nano-materials in diverse dentistry regimes. *Rsc Advances* **2020,** *10* (26), 15430-15460.
2. Kim, D.-H.; Bae, J.; Heo, J. H.; Park, C. H.; Kim, E. B.; Lee, J. H., Nanoparticles as next-generation tooth-whitening agents: Progress and perspectives. *ACS nano* **2022,** *16* (7), 10042-10065.
3. Ziental, D.; Czarczynska-Goslinska, B.; Mlynarczyk, D. T.; Glowacka-Sobotta, A.; Stanisz, B.; Goslinski, T.; Sobotta, L., Titanium dioxide nanoparticles: prospects and applications in medicine. *Nanomaterials* **2020,** *10* (2), 387.
4. Yamashita, C.; Moraes, I. C. F.; Ferreira, A. G.; Branco, C. C. Z.; Branco, I. G., Multi-response optimization of alginate bleaching technology extracted from brown seaweeds by an eco-friendly agent. *Carbohydrate polymers* **2021,** *251*, 116992.

5. Abuzeid, H. M.; Julien, C. M.; Zhu, L.; Hashem, A. M., Green synthesis of nanoparticles and their energy storage, environmental, and biomedical applications. *Crystals* **2023,** *13* (11), 1576.

6. Paul, A.; Radhakrishnan, M., Pomegranate seed oil in food industry: Extraction, characterization, and applications. *Trends in Food Science & Technology* **2020,** *105,* 273-283.

7. Mellanby, M., The Structure of Human Teeth. **1927**.

8. https://teachmeanatomy.info/head/other/child-adult-dentition/.

9. Haywood V, B., History, safety, and effectiveness of current bleaching techniques and applications of the nightguard vital bleaching technique. *Quintessence Int* **1992,** *23,* 471-488.

10. Yang, S.; Sui, B.; Liu, X.; Sun, J.; Wang, J., A novel tooth bleaching gel based on peroxymonosulfate/polyphosphates advanced oxidation process: Effective whitening avoiding pulp damage and sensitivity. *Chemical Engineering Journal* **2022,** *429,* 132525.

11. Ganesan, S.; Babu, I. G.; Mahendran, D.; Arulselvi, P. I.; Elangovan, N.; Geetha, N.; Venkatachalam, P., Green engineering of titanium dioxide nanoparticles using Ageratina altissima (L.) King & HE Robines. medicinal plant aqueous leaf extracts for enhanced photocatalytic activity. *Ann. Phytomed* **2016,** *5* (2), 69-75.

12. Kishi, A.; Otsuki, M.; Sadr, A.; Ikeda, M.; Tagami, J., Effect of light units on tooth bleaching with visible-light activating titanium dioxide photocatalyst. *Dental materials journal* **2011,** *30* (5), 723-729.

The 30th Iranian Seminar of Organic Chemistry
February 7-9, 2025, Iran University of Science and Technology, Tehran, Iran

Synthesis and characterization of polyazomethine containing porphyrin units

Raziyeh Akbarzadeh*

*Assistant Professor, Department of Chemistry, Faculty of Basic Science, Behbahan Khatam Alanbia University of Technology, Behbahan, Iran. *E-mail: r.akbarzadeh@bkatu.ac.ir*

Keyword: Porphyrin, polymer, polyazomethine, ^{1}H-NMR

Porphyrin molecules have been intensively studied because they present a variety of desirable features such as rigid planar geometry, small HOMO-LUMO energy gap, intense electronic absorption and emission and high stability. Porphyrins can be incorporated to polymers via conjugated bonds [1]. Kinds of porphyrin molecules and their polymers, that possess large planar π-conjugated structure and good thermal and photochemical stability, have attracted attention as

useful materials for organic electronics and photonics devices. Applications of porphyrin-based polymers for diverse functions such as preparation of epoxy oligomer, field-effect transistors (OFETs), solar cells, light-emitting diodes (OLEDs),and charge storage have been reported [2].
In this study, firstly, the 5,15-bis(4-formylphenyl)–10,20-diphenylporphyrin have been prepared by a three-step procedure. Then an π-conjugated polyazomethine was synthesized by polycondensation of this monomer and complex of β-cyclodextrin/ 1,4-phenylenediamine (Scheme 1). Appearance of cyclodextrin in π-conjugation polymers can be used to increase solubility of polymers and protects the imine bonds that thus enables gaining suitable stabilities [3].The structure and purity of monomers and as-prepared polymer were characterized by ^{1}H-NMR, UV-Vis and FT-IR spectra.

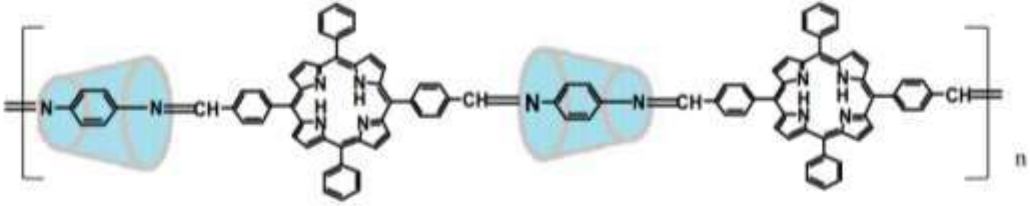

Scheme 1. π-conjugated polyazomethine containing porphyrin units

References

[1] Babu Bodedla, G.; Zhu, X.; Wong W.Y. Recent progress in the development of self-assembled porphyrin derivatives for photocatalytic hydrogen evolution. EnergyChem. 2024, In Press, Journal Pre-proof.
[2] Park, S.E.; Yoon, H.Ch.; Jong, E.J.; Kim, K.M.; Kwon J.S.; Development and validation of polymer-based porphyrin-incorporated reference materials for calibration of quantitative light-induced fluorescence device. Photodiagnosis and Photodynamic Therapy 2024, *50*, 104391.
[3] Zhou, W.; Zhao, X.; Chen, Y.; Liu, Y. Construction and heterogeneous photooxidization reactivity of a cyclodextrin/porphyrin polyrotaxane network. Organic Chemistry Frontiers, 2019, 6(1) 10-14.

The 30th Iranian Seminar of Organic Chemistry
February 7-9, 2025, Iran University of Science and Technology, Tehran, Iran

Study of removal of Methyl orange by Oxidized Multiwalled carbon nanotube

Raziyeh Akbarzadeh*

*Assistant Professor, Department of Chemistry, Faculty of Basic Science, Behbahan Khatam Alanbia University of Technology, Behbahan, Iran. *E-mail: r.akbarzadeh@bkatu.ac.ir*

Keyword: Multiwalled carbon nanotube, Methyl orange, Removal, pH, Isotherm

The Oxidized Multiwalled carbon nanotube is effective adsorbent for the removal of Methyl orange (scheme 1) aqueous solutions. Equilibrium and kinetic fitting of the experimental data were carried out to value and study the adsorption of Methyl orange from aqueous solutions onto this new adsorbent concentration range 50–200 mg/L at pH 3. The equilibrium data have been analyzed using Langmuir, Freundlich and Tempkin isotherms and the characteristic parameters for each isotherm and related correlation coefficients have been determined. The Langmuir isotherm was demonstrated to provide the best correlation for the adsorption of Methyl orange onto Oxidized Multiwalled carbon nanotube. The adsorbed amounts of Methyl orange increased with increase in contact time and reached the equilibrium after 22 min for Oxidized Multiwalled carbon nanotube. The kinetics of adsorption of Methyl orange onto Oxidized Multiwalled carbon nanotube was studied by using pseudo first- and second-order equations, the Elovich equation and the intraparticle diffusion equation. The data showed that the second-order equation was the more appropriate one, although intraparticle diffusion is the rate-limiting factor.

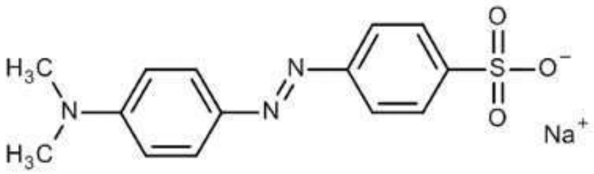

Scheme 1. Methyl orange structure

References:

[1] Rania A, M.; Ghazali N.M.; Kassem L.M.; Elgazzar, E.; Mostafa W.A.; Synthesis of MnCoO/CNT nanoflakes for the photocatalytic degradation of methyl orange dye and the evaluation of their activity against Culex pipiens larvae in the purification of fresh water. RSC Advances, 2022, *12*(45) 29048-29062.

[2] Ahmad, A.; Razali M.H.; Mamat, M.; Mehamod F.S.B.; Mat Amin K.A, Adsorption of methyl orange by synthesized and functionalized-CNTs with 3-aminopropyltriethoxysilane loaded TiO_2 nanocomposites. Chemosphere, 2017, *168,* 474-482.

[3] Thakkar, H.; Bhatt, M.; Thakore, S.; Barbituric acid derived covalent organic framework and its CNT composite as high-performance adsorbents for organic dye removal. Journal of Environmental Chemical Engineering, 2023, 11, 109890

The 30th Iranian Seminar of Organic Chemistry
February 7-9, 2025, Iran University of Science and Technology, Tehran, Iran

Modified chromium (III) oxalato complex anchored magnetic nanoparticles as catalysts for synthesis of various heterocyclic derivatives

Ghobad Mansouri[1,*a]

[a]*Department of Chemistry, Payame Noor Universtiy (PNU), PO Box 19395-4697, Tehran, Iran.*

Keyword: Cr(III) complex, Nanocatalyst, Heterocyclic.

Cr(III) complexs are an inert, highly stable and coordinatively saturated complexes, that are of great interest because of its different applications such as catalytic uses for reactions like polymerization of ethylene[1], and oxidation of alcohols to aldehydes and ketones[2,3]. In this study, the synthesis and characterization of a new magnetic nanocatalyst based on a Cr (III) oxalate complex were investigated. This nanocatalyst was synthesized by immobilizing the chromium complex on the surface of magnetic nanoparticles, and to enhance its stability and catalytic efficiency, an oxalate ligand was used. After the synthesis of the nanocatalyst, its characterization was carried out using various techniques such as FT-IR, XRD, SEM, EDS, TEM, BET, TGA and VSM. The results of these analyses indicate the successful formation of the nanocatalyst with nanometric particle size and appropriate magnetic properties. Subsequently, the catalytic activity of the synthesized nanocatalyst was evaluated in the synthesis of polyhydroquinoline compounds (schem1). The results show that this nanocatalyst exhibits high catalytic activity in the synthesis of various heterocyclic derivatives and can be used as a green and efficient catalyst in organic compound synthesis. The advantages of this nanocatalyst are easy separation from the reaction medium due to its magnetic properties, high stability, and the ability to be recovered and reused.

schem1.

References:

1. Xu L, Trudell M.L, Tetrahedron Lett. 44 (2003) 2553.
2. Boorboor Azimi. E, Badiei, A, Mohammadi Ziarani. G, *Transition Met Chem.* 34 (2009) 637.
3. Maurya. M.R, Titinchi. S. J.J, Chand. S, *J. Molec. Catal. A Chem*. 214 (2004) 257.

The 30th Iranian Seminar of Organic Chemistry
February 7-9, 2025, Iran University of Science and Technology, Tehran, Iran

The fabrication of Pd(II) Complex on Fe$_3$O$_4$@UiO-66-NH$_2$ as an Efficient Nano catalyst for Suzuki coupling reactions

Ghobad Mansouri[1,*a]

[a]*Department of Chemistry, Payame Noor Universtiy (PNU), PO Box 19395-4697, Tehran, Iran.*

Keyword: MOFs, Pd(II) complex, Nano catalyst.

Metal–organic frameworks (MOFs), also called porous coordination polymers or porous coordination networks, are constructed from rigid multipodal organic linkers and inorganic nodes coordination bonds. It is well-known that a wide variety of MOF applications results from their unique properties, such as high amount of transition metals, adjustable and permanent porosity, ultrahigh surface area, active-site uniformity, and ability of post-synthetic modification[1-3].

In this study, a novel magnetic hybrid catalyst based on a metal-organic framework (MOF) has been designed and synthesized. The MOF catalyst was constructed using magnetic nanoparticles and UiO-66-NH_2, resulting in the composite **Fe_3O_4@UiO-66-NH_2,** which was further modified with acetylacetonate (acac$^-$) to introduce active amine groups. This modification enhances the anchoring of palladium onto the support, leading to a significant improvement in the catalyst's performance. The catalyst structure was characterized using various techniques to confirm its composition and properties. Furthermore, the catalyst exhibited excellent to good yields in Suzuki coupling reactions. The magnetic properties of the MOF-based catalyst facilitate its easy separation from the reaction mixture, allowing for efficient reuse in subsequent reactions.

References:

1. Zhao, S.-N., Wang, G., Poelman, D. & Van Der Voort, P. *Molecules.* 23 (2018) 2947.
2. **Mansouri. G, Abdizad. M, Abbasi. A.R, Rezayati. Sobhan.** J. App. Organomet. Chem. 36 (2022) e6866.
3. G.-J. Ma, H-C, Xin. W-L, Li. X-B, Jin. F-Z, Wang. J-S, Liu. M-Y, Dong. Y-B, Chen. *Inorg. Chem.* 56 (2017) 654.

The 30th Iranian Seminar of Organic Chemistry
February 7-9, 2025, Iran University of Science and Technology, Tehran, Iran

Studies on the synthesis of Atracurium Besilate

Babak Kaboudin [1a], Fahimeh Aghaei [2a], Masoumeh Sohrabi [3a]

a) Organic Chemistry Laboratory, Department of Chemistry, Institute for Advanced Studies in Basic Sciences (IASBS), Gava Zang, Zanjan 45137-66731, Iran, kaboudin@iasbs.ac.ir and fahimeh.aghaei@iasbs.ac.ir

Keyword: Atracurium Besilate, Neuromuscular blocking drugs, Tetrahydropapaverine

Introduction

Neuromuscular blocking agents are structurally similar to acetylcholine and contain at least one positively charged quaternary ammonium group. They are classified into two main groups based on their mechanism of action at the neuromuscular junction: **Depolarizing Neuromuscular Blocking Drugs** and **Non-Depolarizing Neuromuscular Blocking Drugs** [1]. Atracurium besilate is a non-depolarizing neuromuscular blocking agent commonly used in anesthesia to induce muscle relaxation during surgery. It works by inhibiting the action of acetylcholine at nicotinic receptors. This agent is an intermediate-acting bisquaternary ammonium compound and is metabolized by two pathways: **hofmann degradation** and **ester hydrolysis** [2].

Method

Synthesis of Tetrahydropapaverine

In a 25 mL round-bottom flask, which contained 5 mL of solvent, was added 1 mmol of acid and 1mmol of amine. It was stirred for 10 min at 25 °C. Next, after stirring the reaction mixture, 0.5 mmol of the coupling reagent was added to the reaction container. The mixture was stirred at 25 °C for 24h. After the completion of the reaction, material obtained was purified by column chromatography on silica gel to provide the Amide as a white solid. The amide was then treated with $POCl_3$ in a 25 mL flask which contained 5ml of solvent at room temperature for 24h to provide a cyclic imine. The last step of the synthesis was reduction of imine with $NaBH_4$ to provide the tetrahydropapaverine in 70% yield [3].

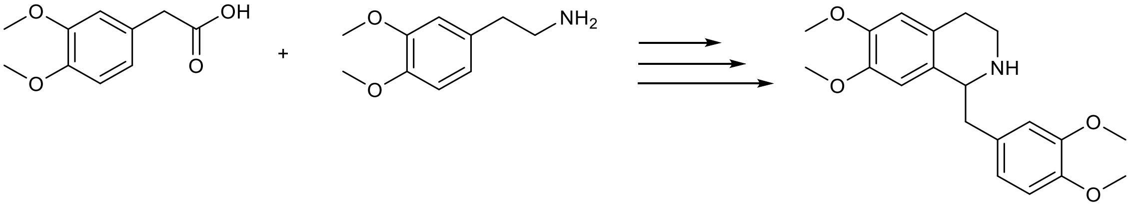

Synthesis of 1,5-Pentanediol diacrylate

To a stirred solution of 1 mmol of 1,5-pentanediol and 1 mmol of triethylamine in 5 mL of toluene as the solvent at room temperature, were added 4 mmol of acryloyl chloride. The mixture was stirred at room temperature for 24h. After the completion of the reaction, material obtained was purified by column chromatography on silica gel to provide the 1,5-pentanediol diacrylate as a yellow liquid product in 90% yield.

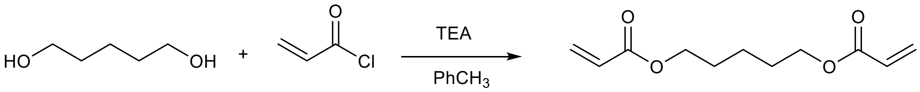

Results and Discussion

As part of our ongoing reseach on the synthesis of atracurium besilate, the Michael addition of tetrahydropapaverine with 1,5-pentanediol diacrylate will be carried out to yield atracurium. Atracurium besilate will then be prepared from atracurium by reacting it with benzenesulphonic methyl acid ester.

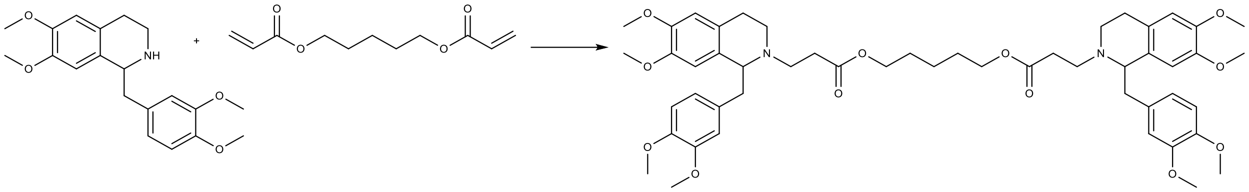

References

[1] Farooq, Khorat, and Jennifer M. Hunter. "Neuromuscular blocking agents and reversal agents." *Anaesthesia & intensive care medicine* 18.6 (2017): 279-284.

[2] Tuba, Zoltan, Sandor Maho, and E. Vizi. "Synthesis and structure-activity relationships of neuromuscular blocking agents." *Current medicinal chemistry* 9.16 (2002): 1507-1536.

[3] Li, Yu, et al. "Design and synthesis of tetrahydroisoquinoline derivatives as potential multidrug resistance reversal agents in cancer." *Bioorganic & medicinal chemistry letters* 18.12 (2008): 3652-3655.

The 30th Iranian Seminar of Organic Chemistry
February 7-9, 2025, Iran University of Science and Technology, Tehran, Iran

Chitosan coated magnetic nanoparticles for controlled release of doxorubicin

Fatemeh Sajadian[a], Zahra Asadi[a*]

a) Department of Chemistry, College of Science, Shiraz University, Shiraz, Iran, email of corresponding author: zasadi@shirazu.ac.ir, email of presenter: fatemehsajadian1375@gmail.com

Keyword: Iron oxide nanoparticles, Chitosan, Doxorubicin, Targeted drug delivery, pH sensitivity

Introduction

Although the chemotherapy is a common method for the treating of cancer cells, it has some disadvantages such as side effects for normal cells, insufficient dosages for the killing of cancer cells and nonspecific delivery of chemotherapeutic agents [1]. Recently, drug carriers based on nanoparticles have attracted much attention in the biomedical applications due to its efficient loading, controlled release and targeted delivery of drugs [2]. Among these nanoparticles, the use of magnetic nanoparticles (MNPs) in development of drug delivery systems for controlled release of drugs has received an increasing attention [3]. Among the different kinds of MNPs, iron oxide (Fe_3O_4), with its ideal biocompatibility, tunable surface modification and superparamagnetic properties, has attracted the most interest in biomedical applications [4].

Chitosan (CS), a natural compound and a deacetylated derivative of chitin, is a positively charged polymer carrier. The cell adhesion and potential uptake of chitosan particles are also most favorable due to their attraction to negatively charged cell membranes, an attractive feature for the treatment of solid tumors [5]. The chitosan along with nanoparticles has been utilized as a stabilizing agent due to its excellent mechanical strength, biocompatibility, non-toxicity, susceptibility to chemical modifications, cost-effectiveness [6].

Method

Synthesis of CS-Fe_3O_4: chitosan (0.05 g) was dissolved in 15 mL of 1% acetic acid and the pH was adjusted to 5 by 10 M NaOH. Under the nitrogen gas flow and by vigorously stirring at 50 °C, the iron salts (0.67 g of $FeCl_2.4H_2O$ and 1.70 g of $FeCl_3.6H_2O$) were dissolved in 15 mL of chitosan solution. Then 15 mL of aqueous ammonia solution (25%) was added slowly to produce smaller sized nanoparticles. The resulting solution was stirred for an additional 45 min. The colloidal chitosan coated Fe_3O_4 nanoparticles were washed with deionized water and separated by magnetic decantation for several times.

Loading and release study: in the loading procedure, 20 mg of CS-Fe_3O_4 was added in 20 ml of DOX•HCl solution (0.1 mg/ml, pH=7.4) and stirred at room temperature for 72 h. At appropriate time intervals, drug loaded CS-Fe_3O_4 was separated from the supernatant with the help of permanent magnet. The next step is to measure the amount of drug in the supernatant using a UV-vis spectrophotometer at 480 nm, referencing a standard calibration curve of absorbance against concentration. The release studies were carried out at pH 5.4 and 7.4 (at 37°C) for 48 h. 20 mg of drug loaded nanoparticles were added to 24 mL of deionized water under a constant slow magnetic stirring of 100 rpm. At specific time intervals, 2 mL of the sample was taken out and substituted with an equal volume of deionized water in order to release the drug into a constant volume. These samples were then determined for DOX content at 480 nm by UV-Vis spectrophotometer. The concentration of DOX was calculated by using the standard curve.

Results and Discussion

In this work, CS-Fe_3O_4 nanoparticles were synthesized by coating chitosan onto the surface of iron oxide nanoparticles by in situ coating method (Scheme 1) and their structural and morphological properties were determined by different analytical techniques. The anticancer drug doxorubicin (DOX) was used to illustrate the nanocarriers' ability to deliver the drug in a controlled fashion, and drug loading efficiency and release behavior of the nanoparticles were studied. This nanocarrier provided a high drug loading efficiency (83.8%) and exhibited pH sensitivity. The cumulative release at 37 °C and pH values of 5.4 and 7.4 was 62.4 and 57.3%, respectively. So that, the amount of DOX released from the CS-Fe_3O_4 nanoparticles was much higher at lower pH levels, which indicated that CS-Fe_3O_4/ DOX can be used efficiently in treatment of cancerous cells.

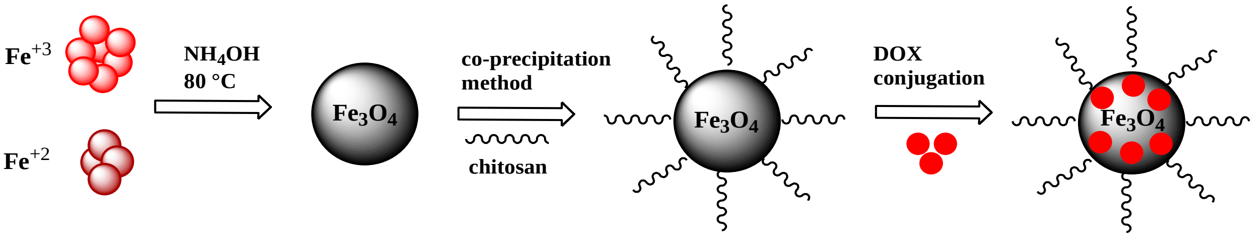

Scheme 1: Illustration of the modification mechanism of Fe_3O_4 with chitosan, followed by DOX loading.

References:

1. Zhang, W., et al., *Synergistic effect of chemo-photothermal therapy using PEGylated graphene oxide.* 2011. **32**(33): p. 8555-8561.
2. Hashemi, H. and H.J.U.S. Namazi, *Sonochemically synthesized blue fluorescent functionalized graphene oxide as a drug delivery system.* 2018. **42**: p. 124-133.
3. Kariminia, S., et al., *Analytical characteristics and application of novel chitosan coated magnetic nanoparticles as an efficient drug delivery system for ciprofloxacin. Enhanced drug release kinetics by low-frequency ultrasounds.* 2016. **129**: p. 450-457.
4. Hu, Y., et al., *Construction of iron oxide nanoparticle-based hybrid platforms for tumor imaging and therapy.* 2018. **47**(5): p. 1874-1900.
5. Javid, A., et al., *Chitosan-coated superparamagnetic iron oxide nanoparticles for doxorubicin delivery: synthesis and anticancer effect against human ovarian cancer cells.* 2013. 82(3): p. 296-306.
6. Moradi, S., et al., *Effect of clinoptilolite on structure and drug release behavior of chitosan/thyme oil γ-Cyclodextrin inclusion compound hydrogels.* 2021. **138**(6): p. 49822.

The 30th Iranian Seminar of Organic Chemistry
February 7-9, 2025, Iran University of Science and Technology, Tehran, Iran

Synthesis of carboxymethyl-β-cyclodextrin conjugated magnetic nanoparticle for ciprofloxacin delivery

Fatemeh Sajadian[a], Zahra Asadi[a*]

a) Department of Chemistry, College of Science, Shiraz University, Shiraz, Iran, email of corresponding author: zasadi@shirazu.ac.ir, email of presenter: fatemehsajadian1375@gmail.com

Keyword: Magnetic nanoparticles, Carboxymethyl-β-cyclodextrin, Ciprofloxacin, Release study

Introduction

Ciprofloxacin (CIP) is a potent broad-spectrum antibiotic of quinolones. Several drug delivery systems (DDS), such as polymeric gels, particulate carriers, and lipids, have been used as drug delivery matrices. Therefore, it is of great importance to solve the problems of CIP's poor systemic distribution, short half-life, low oral bioavailability, and poor hydrophilicity while designing carriers [1]. As proven, biodegradable and bioabsorbable polymers provide a magical option for many novel DDS. For instance, CD derivatives are one of the natural polymers for polymeric drug delivery carriers [2]. β-CD has a versatile potential with its suitable geometry for forming inclusion complexes with innumerable drugs [3].

Magnetic separability plays an important role in expanding the medical applications of magnetic nanoparticles (MNPs), which usually contain a magnetic component, such as the oxides of iron, nickel and cobalt. Among magnetic metal oxides, Fe_3O_4 presents a higher extent of biocompatibility and stability [4]. That is why it has been represented as an appropriate candidate for extensive medical applications, including improving the function of effective substances in the treatment of various diseases such as Alzheimer's disease and HIV [5].

Method

Synthesis of carboxymethyl-β-CD: briefly, appropriate amounts of β-CD (2.0 g) and NaOH (1.8 g) were dissolved in 7.4 mL of deionized water. Then, 5.4 mL of monochloroacetic acid (16.3%) was added to the reaction medium. The reaction mixture was allowed to stir for 5 h (at 50 ˚C). Afterward, the solution was cooled to room temperature, and the pH of the reaction medium was adjusted to the range of 6-7 by adding a concentrated solution of HCl drop by drop. The neutral solution obtained was poured into methanol to collect the residues. The resulting white precipitate product was filtered and dried at 25 ˚C for a whole day.

Synthesis of carboxymethyl-β-CD modified Fe_3O_4 nanoparticles (CMCD-Fe_3O_4): Briefly, 0.8 g of $FeCl_2 \cdot 4H_2O$, 2.3 g $FeCl_3 \cdot 6H_2O$ and 1.5 g CM-β-CD were dissolved in 40 mL of deionized water with vigorous stirring at a speed of 1200 rpm. 5 mL of NH_4OH (25%) was added after the solution was heated to 90 ˚C. The reaction was continued for 1 h at 90 ˚C under constant stirring and nitrogen environment. The resulting nanoparticles were then washed with deionized water and dried. Loading and release study: in the loading procedure, 100 mg of CMCD-Fe_3O_4 was added in 25 mL of drug solution (0.2 mg/ml, pH=7.4) and stirred at room temperature for 48 h. At appropriate time intervals, drug loaded CMCD-Fe_3O_4 was separated from the supernatant with the help of permanent magnet. The next step is to measure the amount of drug in the supernatant using a UV-vis spectrophotometer at 272 nm, referencing a standard calibration curve of absorbance against concentration. In the release study, 20 mg of drug loaded nanoparticles were filled into a dialysis bag, and then it was immersed into 50 mL of phosphate buffer saline (PBS) of pH 5.4 and 7.4. The pH-sensitive release of CIP was carried out at 37 °C for 72 h with continuous stirring. To quantify the amount of CIP released from the CMCD-Fe_3O_4, 2mL of the PBS was taken out for the UV analysis at λ_{max}=270 nm and an equal volume of fresh PBS was added to the solution for replenishment.

Results and Discussion

In this work, CM-β-CD modified Fe_3O_4 nanoparticles were synthesized by simple one-step co-precipitation where iron precursors (Fe^{2+} and Fe^{3+}) and CM-β-CD were mixed together in the reaction medium (Scheme 1). The binding of CM-β-CD on the magnetic surface was confirmed by different analytical techniques. As an antibiotic drug model, CIP was loaded onto the CMCD-Fe_3O_4 nanoparticles. The drug loading efficiency was reached at 98.2% for 48 h. The pH responsiveness of the nanocarrier was investigated using two different pH levels over a time period of 3 days. The cumulative release at 37 °C and pH values of 5.4 and 7.4 was 89.8 and 73.5%, respectively. So that, the amount of CIP released from the CMCD-Fe_3O_4 nanoparticles was much higher at lower pH levels.

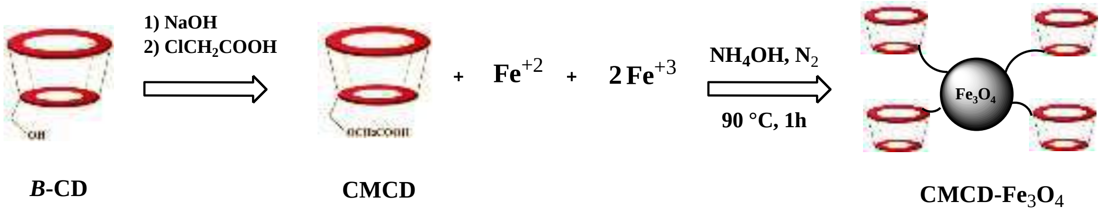

Scheme 1: An illustration for the carboxymethylation and binding of cyclodextrin onto Fe_3O_4 nanoparticles.

References:

1. Wu, S., et al., *Functionalized phosphorylated cellulose microspheres: Design, characterization and ciprofloxacin loading and releasing properties.* 2021. **254**: p. 117421.
2. Taheri-Ledari, R., et al., *An effective antimicrobial complex of nanoscale β-cyclodextrin and ciprofloxacin conjugated to a cell adhesive dipeptide.* 2022. **12**(54): p. 35383-35395.
3. Stella, V.J. and R.A.J.I.J.o.P. Rajewski, *Sulfobutylether-β-cyclodextrin.* 2020. **583**: p. 119396.
4. Karimi Ghezeli, Z., M. Hekmati, and H.J.A.O.C. Veisi, *Synthesis of Imatinib-loaded chitosan-modified magnetic nanoparticles as an anti-cancer agent for pH responsive targeted drug delivery.* 2019. **33**(4): p. e4833.
5. Amiri, H., et al., *Alzheimer's disease: pathophysiology and applications of magnetic nanoparticles as MRI theranostic agents.* 2013. **4**(11): p. 1417-1429.

Synthesis and characterization of a new biscrown compound formed from diamide crown ligands

Amir Ghanaat Gharamaleki[1], Samad Bavili Tabrizi[1]*, Gholamhossein Shahverdizadeh [1]

[1] Department of Chemistry, Tabriz Branch, Islamic Azad University, Tabriz, IRAN

*Corresponding Authors: 1: sbavili@iaut.ac.ir

Abstract

Diamide macrocycles are valuable intermediates for the synthesis of aza crown compounds as well as more complex ligands such as various cryptands and cryptohemispherands. Their versatility in many fields, such as chemistry, biochemistry, biophysics, biology, agriculture, industry, medicine, molecular diagnosis, sensors, and phase transfer catalysts, has captured the interest of many. In the first step, 2,4-dimethylphenol was converted to the oxythiobis [4,6-dimethylphenyl] (1) by reacting with thionyl chloride. Then, oxythiobis [4,6-dimethyl phenoxy methyl acetate] (2) was obtained from the reaction of oxythiobis [4,6-dimethylphenyl] (1) with methyl chloroacetate. The reaction of oxythiobis [4,6-dimethyl phenoxy methyl acetate] (2), with a diethylenetriamine, produced the tri-aza dibenzo sulfoxide macrocyclic diamides (3). Bis [tri-aza dibenzo sulfoxide macrocyclic diamides] (4) was prepared from the reaction of tri-aza dibenzo sulfoxide macrocyclic diamides (3) with a suitable active compound such as diacid or dichloride. The structures of all synthesized compounds were characterized by ^{1}H NMR, ^{13}C NMR, FT-IR, and mass spectra.

Keywords: Macrocycle, Biscrown, Crown ether, Dimer

Introduction

The area of supramolecular research has become one of the fast-growing fields in organic chemistry in recent times [1, 2]. Supramolecular systems typically consist of intricate and uncommon organic compounds, prompting researchers to conduct studies on their synthesis.

Furthermore, predicting the properties of compounds in supramolecular systems and creating specific methods for their self-assembly is significant in supramolecular chemistry [3-8]. In the field of supramolecular chemistry, macrocycles reign as the most commonly utilized category of host compounds [9]. The development of host-guest chemistry has seen remarkable breakthroughs over the past few years, mainly due to the inception of crown ethers by Pedersen in 1967 [10, 11]. The chemistry of synthetic macrocycles has evolved significantly in the past 50 years with the discovery of crown ethers [10]. This development has led to the creation of highly selective and structure-specific supramolecular complexes that have been utilized for various purposes, including the creation of optically active sensors and mobile ion carriers [12-15]. Crown ethers, with their simplicity, are one of the most captivating groups of compounds in the realm of supramolecular chemistry [16-18]. Crown ethers possess a structural arrangement consisting of a hydrophobic ring that envelops a hydrophilic cavity, thus enabling them to form complexes with metal ions [19]. Crown ethers also have potential in the development of novel therapeutics. DNA intercalates and echinomycin D are examples of crown ethers with antitumor activity [20, 21]. Over the last twenty years, considerable focus has been on the chemistry of biscrown ethers due to their captivating structures and superior capability to form complexes with various cations. Many different kinds of biscrown ethers have been successfully synthesized and documented [22-27]. The production of cyclic diamides has received significant attention across different classes of supramolecular chemistry because of their different uses, such as chemistry, biology, molecular recognition, medicine, industry, and agriculture [9, 28]. Macrocyclic diamides play an essential role in synthesizing aza crown compounds and complex ligands, including cryptands and cryptohemispherands [29-31]. Researchers have extensively studied macrocyclic diamides and their corresponding aza crown compounds due to their wide range of applications in fields such as biology, microanalysis, enzyme mimics, medicine, and industry [32]. The particular interest in aza and diaza crown ethers is because of the introduction of various substituents on the nitrogen atoms of aza and diaza crown ethers that give rise to modified biological properties of them [33, 34]. Macrocycles have excellent characteristics due to having O, S, and N atoms and can bond with various ions and molecules. The synthesis of macrocycles with high efficiency in technology and industries such as medicine and pharmaceuticals has been considered. Also, biscrown ethers have more linking and complexing capabilities than crown ethers. Therefore, their preparation and molecular design are essential. The purpose of this research work is the synthesis of a new biscrown diamide macrocycles compound. Diamide macrocycles are essential intermediates in preparing of azacrown ethers, cryptands, biscrowns, cryptohemispherands, and other similar compounds, with many applications.

Materials and methods

Syntheses of oxythiobis[4,6-dimethylphenyl[(1)

The synthesis of oxythiobis(4,6-dimethylphenyl) as a precursor for the preparation of oxythiobis [2,4-dimethyl phenoxy methyl acetate] derivative was reported by Bavili and Chandrasekaran et al [35, 36].

(25 g, 0.187 mol) anhydrous aluminum chloride and 200 mL dry dichloromethane were stirred in the ice bath. Then, 16 mL of 2,4-dimethylphenol was added to the solution and stirred for 30 min. Then, a solution of 8 mL thionyl chloride in 50 mL of dry dichloromethane was added dropwise for 1 h. After that, the solution was stirred for 15 h in the ice bath, and the product obtained a white precipitate. Later, the precipitate was filtered with a Buchner funnel and washed with 35 mL of chloroform and 5 mL of a 10% HCl solution to ensure the removal of aluminum oxide-containing

impurities. After separating the organic phase from the aqueous phase, ethanol was used to crystalize and purify the product. The product had a melting point of 192-196 ℃ and a reaction yield of 65% (Scheme 1).

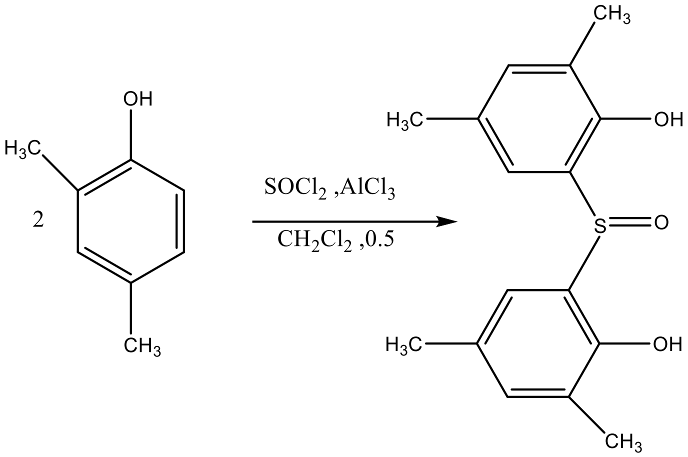

Scheme 1 Synthesis and structure of oxythiobis [4,6-dimethylphenyl] (1)

IR (KBr): 3400, 3200, 3040, 3010, 2920, 2558, 1900, 1880, 1762, 1760, 1580, 1500, 1480, 1400, 1360, 1280, 1230, 1140, 1060, 940, 880, 820, 760 cm^{-1}. ^{1}H NMR (400 MHz, $CDCl_3$) δ: 2.23 (s, 6H), 2.26 (s, 6H) , 6.73 (s, 2H), 6.92 (b, 2H) , 7.05 (s, 2H) ppm.

Synthesis of oxythiobis [4,6-dimethyl phenoxy methyl acetate] (2)

(8 g, 0.0017 mol) oxythiobis [4,6-dimethylphenyl] (1), 5.86 mL methyl chloroacetate, and (7.46 g, 0.0034 mol) potassium carbonate were mixed in 100 mL acetonitrile and refluxed for 18 hours at 82 °C. The mixture was filtered and organic layer evaporated and the obtained yellow viscous product was dried. The product was crystallized and purified in methanol and the oxythiobis [4,6-dimethyl phenoxy methyl acetate] (2) was obtained as a white cotton solid with a yield of 98%. The melting point of the compound is 98-100 °C and Rf = 0.3 in ethyl acetate/petroleum ether (3:1) solvent system [37].

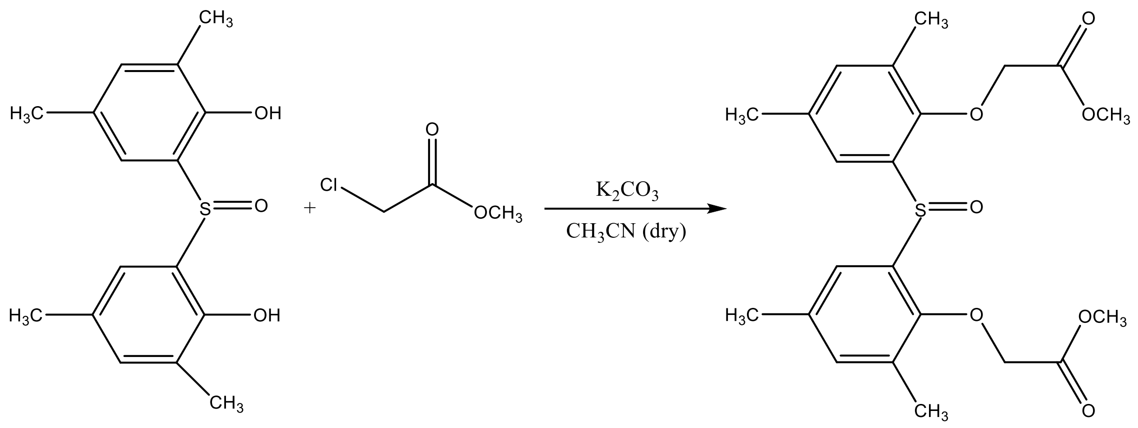

Scheme 2 Synthesis of oxythiobis [4,6-dimethyl phenoxy methyl acetate] (2)

IR(KBr): 2980, 2920, 1760, 1730, 1480, 1440, 1300, 1280, 1250, 1150, 1080, 990, 800 cm^{-1}

^{1}H NMR (400 MHz,$CDCl_3$) δ: 2.23 (s, 6H), 2.26 (s, 6H), 3.79 (s, 6H), 4.65 (s, 4H)، 6.72 (s, 2H), ٧،٠٢ (s ,٢H) ppm. ^{١٣}C NMR (400 MHz, $CDCl_3$) δ: 168.27, 153.58, 132.61-132.51, 129.7, 122.19, 112.29, 67.88, 49.33, 39.25, 22.51, 21.53 ppm.

Synthesis of tri-aza dibenzo sulfoxide macrocyclic diamides (3)

(2 g, .0046 mol) of oxythiobis [4,6-dimethyl phenoxy methyl acetate] (2) and 49 mL of diethylenetriamine in the presence of 25 mL dry methanol refluxed for 18 hours. After cooling, a white precipitate formed. The precipitate was separated from the solvent and several times washed with water. The solvent was evaporated and the solid residue was recrystallized in 20 mL of dichloromethane. The organic phase was washed with 20 mL of HCl (10%) and 20 mL of H_2O. The solvent evaporated and the residue was recrystallized in methanol and the glassy-needled crystals were obtained with a yield of 70%. The melting point of macrocycle diamide was 218-220 °C and Rf = 0.2 in the ethyl acetate/methanol (1:2) solvent system.

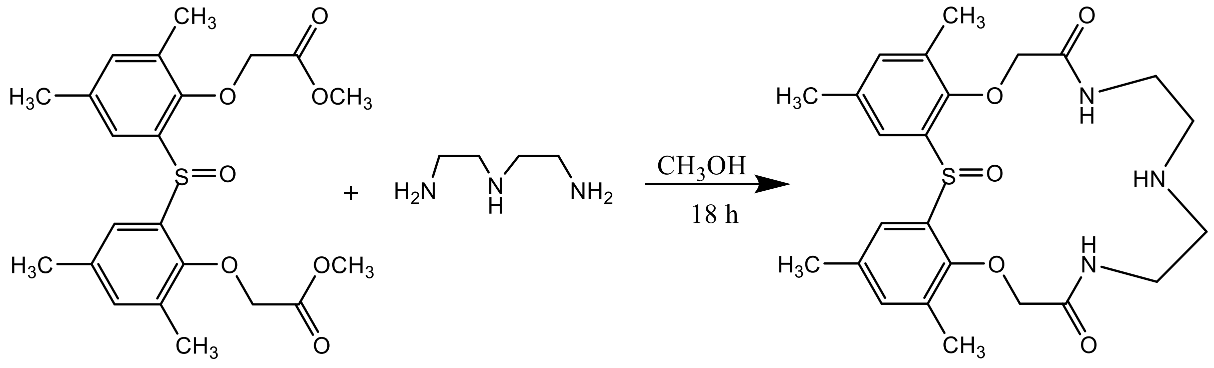

Scheme. 3 Synthesis of tri-aza dibenzo sulfoxide macrocyclic diamides (3)

IR (KBr, cm^{-1}): 3420, 3360, 3040, 2940, 2880, 1680, 1570, 1490, 1280, 1250, 1210, 1080, 1050, ٨٣٠, ٨٠٠, ٧٧٠, ٦٨٠, ٥٩٠, ٥٦٠, ٤٣٨ cm$^{-١}$. ^{١}H NMR (٤٠٠ MHz, $CDCl_3$) δ: 2.21-2.31 (s, 6H), 2.73-2.76 (t, 4H, J= 4Hz), 3.33-3.37 (m: disturbed ddd, 4H), 4.55 (s, 4H), 6.92 (s, 2H), 7.04 (s, 2H), ٧،٤٨ (s, ٢H) ppm.^{١٣}C NMR (400 MHz, $CDCl_3$) δ: 168.27, 153.58, 132.61, 132.51, 129.7, 122.19, 112.29, 67.88, 49.33, 39.25, 22.51, 21.53 ppm. MS (EI): m/z 445 (M)$^+$, 446 (M+1)+, 447 (M+2)$^+$, 402, 376, 371, 332, 319, 273, 257, 244, 206, 196, 194, 180, 167, 137, 124, 121, 107, 101, 100, 72, 65, 59, 46.

Synthesis of bis (tri-aza dibenzo sulfoxide macrocyclic diamides) (4)

(0.033 g, 0.28 mmol) of heptanedioyl dichloride, (0.24 g, 0.56 mmol) tri-aza dibenzo sulfoxide macrocyclic diamides (3), and 0.08 mL triethylamine was mixed in 25 mL dry dichloromethane and refluxed for 24 hours. Then the reaction mixture was filtered and the organic phase was washed with 20 mL of 10% NaOH solution and 20 mL of H_2O and dried with Na_2SO_4. The solvent was removed by rotary evaporation and a white solid compound was obtained. The solid compound was crystallized in n-hexane/chloroform, with a yield of 60%. The melting point was 260-263 °C and Rf = 0.44.

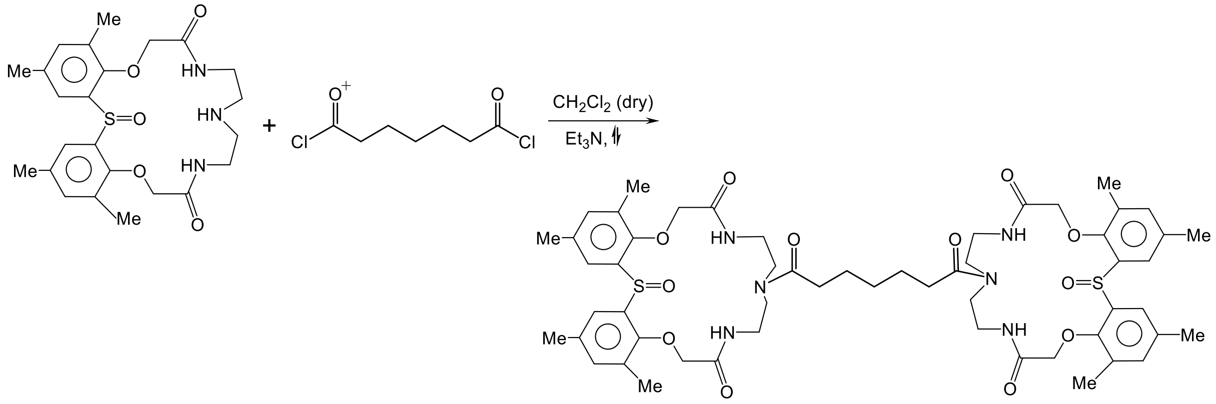

Scheme 4 Synthesis of bis(tri-aza dibenzo sulfoxide macrocyclic diamides) (4)

IR (KBr, cm^{-1}): 3440, 3410, 3027, 2936, 2868, 1681, 1636, 1533, 1496, 1437, 1362, 1292, 1254, 1081, 811 cm^{-1}. ^{1}H NMR (400 MHz, $CDCl_3$) δ: 1.23-1.29 (m: disturbed ddd, 3H), 2.13-2.37 (m, 16H), 3.27-3.69 (m: disturbed ddd, 8H), 4.41-4.67 (s, 2H), 6.75-6.78 (s, 1H) , 6.95-6.97 (s, 1H), ٧,٣٨-٧,٤٤ (s, ١H) ppm. ^{١٣}C NMR (400 MHz, $CDCl_3$) δ: 174.42, 168.85, 168.74, 154.56, 152.09, 136.83, 132.57, 132.28, 131.53, 130.44, 128.55, 124.31, 120.26, 113.23, 112.53, 68.27, 67.9, 49.64, 49.03, 39.11, 38.41, 32.97, 26.62, 24.82, 21.42, 21.36, 20.69, 20.52 ppm. MS (EI) m/z (%): 543 (M)$^+$, 544 (M+1)$^+$, 545 (M+2)$^+$, 473, 369, 304, 288, 284, 272, 270, 241, 217, 184, 154, 146, 136, 122, 106.

Results and discussion

Fig. 1 [A] shows the FT-IR spectrum of the compound (1). A broad and strong absorption band in the region of 3200–3400 cm^{-1} is related to the O-H stretching vibration with hydrogen bonding, an absorption band related to the C-H ring in the 3040 cm^{-1}, and an aliphatic C-H shows an absorption band in the 2920 cm^{-1}. Two absorption bands in the region of 1230–1280 cm^{-1} correspond to the C-O vibration, and two absorption bands with the same intensity in the 1360–1400 cm^{-1} correspond to the bending vibration of methyl, and the stretching absorption band of the C=C ring in the 1500–

1580 cm^{-1}. In the 760–880 cm^{-1} region, there are weak bands related to aromatic ring substitutions, indicating the formation of the desired sulfoxide. The FT-IR spectrum of compound (2) is shown in Fig. 1 [B]. The disappearance of the broad phenolic OH absorption band in the region of 3200–3400 cm^{-1} and the appearance of the strong carbonyl ester absorption band at 1730–1760 cm^{-1} and the strong ether C–O absorption band at 1300 cm^{-1} indicate the formation of the desired dimethyl ester.

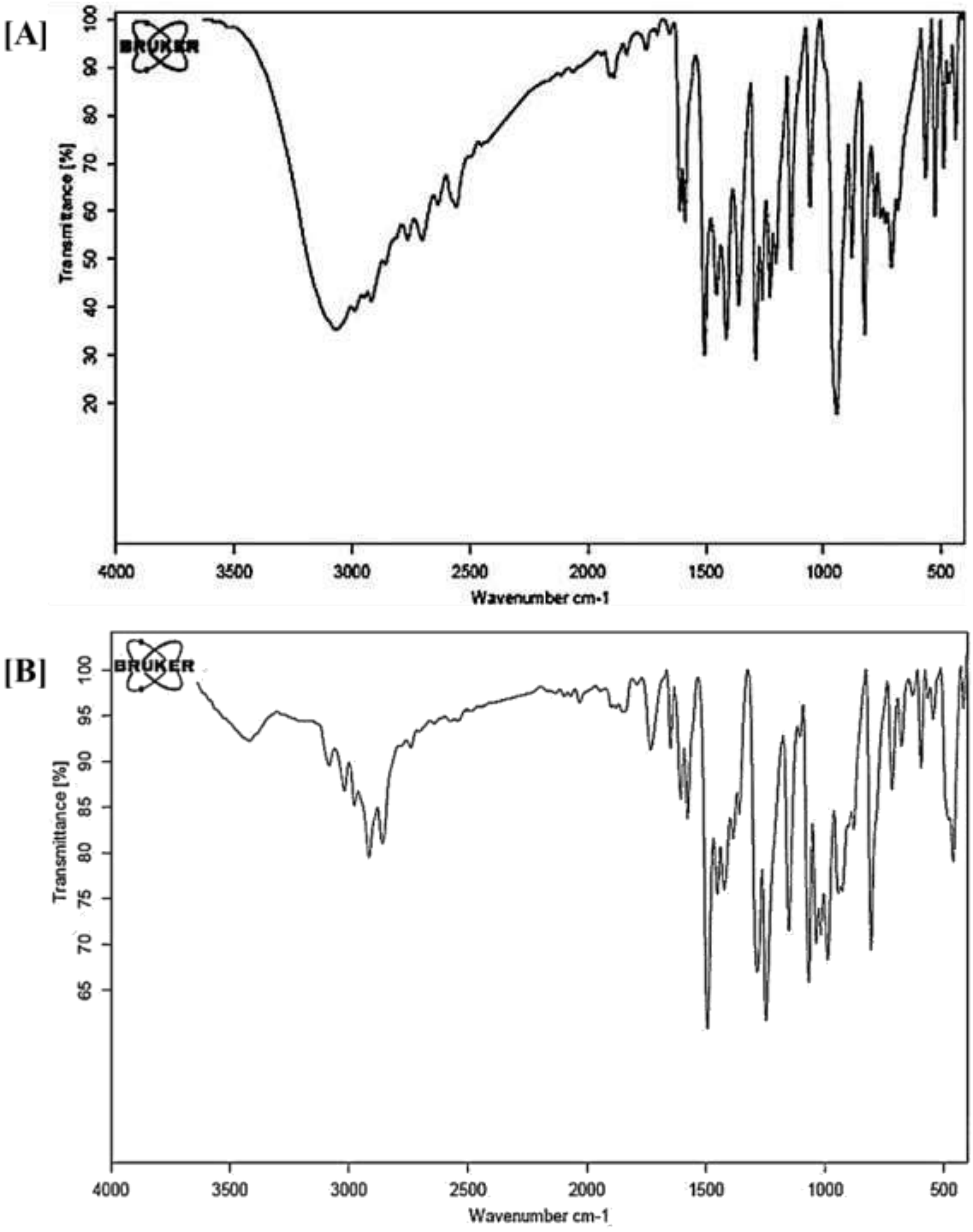

Fig. 3 FT-IR spectrum of compound (1) [A] and compound (2) [B]

Fig. 2 shows the FT-IR spectrum of compound (3). The C=O absorption band is observed at 1680 cm^{-1}. The sharp and strong absorption band at 3420 is related to NH amide. Absorption bands at

3040, 2880, 1680, 1570–1490, 1210–1250–1280, and 830 cm^{-1} are related to aromatic CH stretching, aliphatic CH stretching, carbonyl amide group stretching vibration, aromatic C=C stretching vibration, phenolic C-O stretching vibration, and aromatic C-H bending vibration, respectively. The absorption band at 1080 indicates the S=O bond.

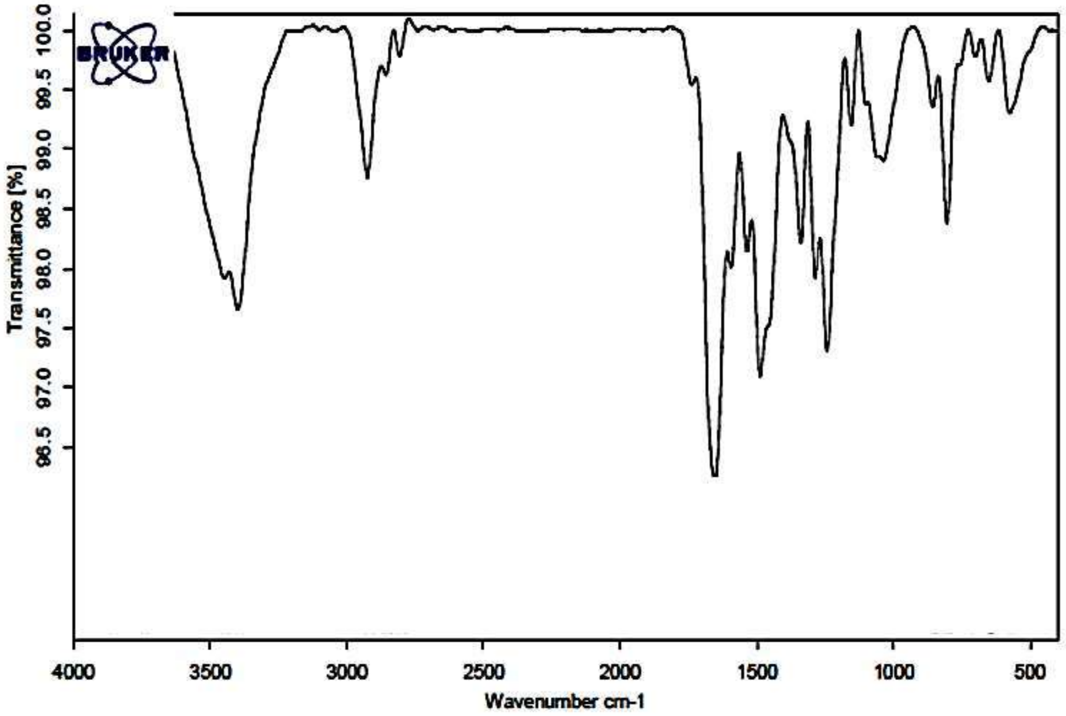

Fig. 4 FT-IR spectrum of compound (3)

Fig. 3 shows the FT-IR spectrum of compound (4). Sharp and strong absorption bands at 3440 and 3410, 2936-3027, 2868, 1636-1681, 1533, 1437-1496, 1254-1292, and 811 cm^{-1} indicate the amide N-H stretching vibration, aromatic C-H stretching, aliphatic C-H stretching, carbonyl amide stretching vibration, N-H bending vibration, aromatic C=C stretching vibration, phenolic C-O stretching vibration, and aromatic C-H bending vibration, respectively.

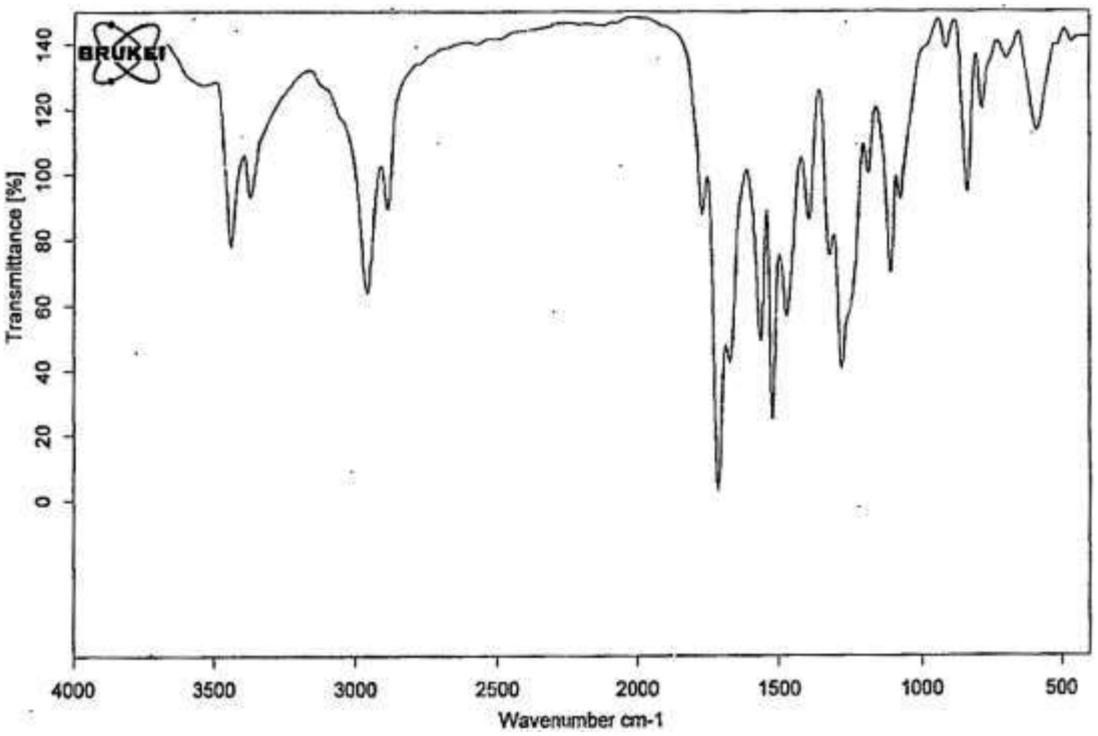

Fig. 5 FT-IR spectrum of compound (4)

The ^{1}H NMR spectrum of compound (1) is shown in Fig 4. The absorption bands of aromatic protons including Hc and Hd have appeared at 6.92 and 7.05 ppm (singlet). The absorption band in the 6.73 ppm is related to the (OH proton). The absorption bands of aliphatic protons, including Ha and Hb, are seen in the region of 2.23 and 2.26 ppm, respectively.

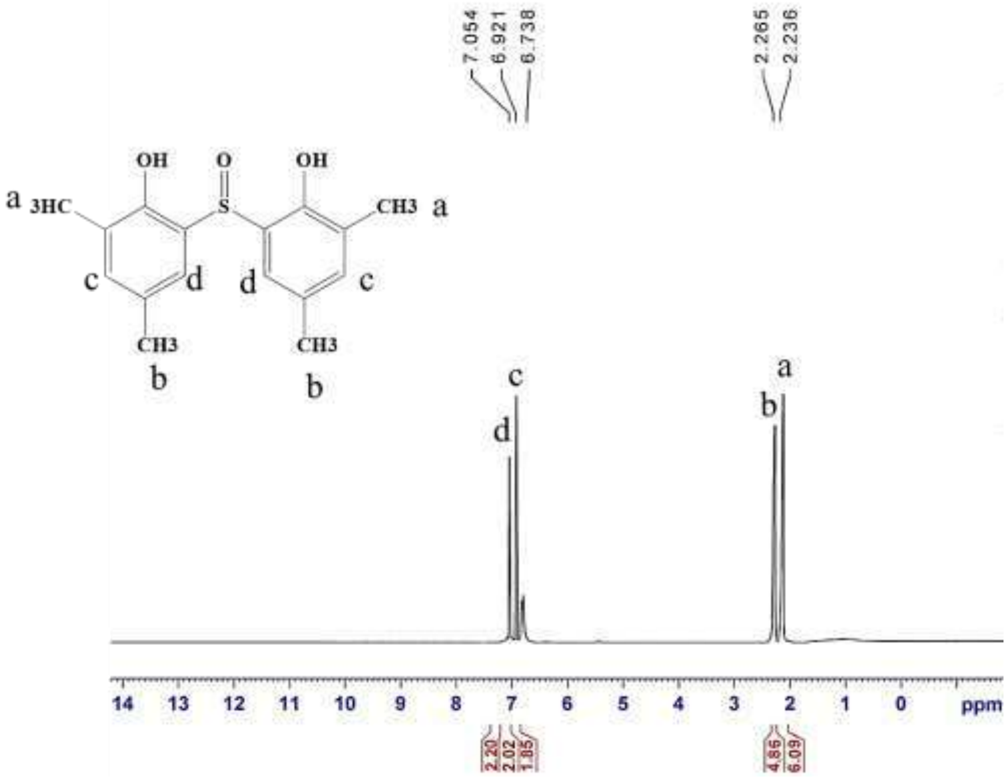

Fig. 6 ^{1}H-NMR spectra of compound (1)

The ^{1}H NMR spectra of compound (2) are shown in Fig. 5 [A]. The peaks that have appeared at 6.72-7.02 ppm are related to (He and Hf) aromatic ring protons. Also, the aliphatic protons (Ha and Hb) appeared at 2.23 and 2.26 ppm, and protons related to methyl acetate (Hc and Hd) were observed at 3.79 and 4.65 ppm. The ^{13}C NMR spectra of compound (2) are shown in Fig. 5 [B]. The absorption band of Ck carbonyl ester can be seen in the region of 168.72. The absorption band of aromatic carbons is seen in the region of 112.29-153.58. Cd, Cc, Ca, and Cb have appeared in 72.12, 67.88, 22.58, and 21.57, respectively. Therefore, the presence of 11 absorption bands corresponding to 11 types of carbons in the ^{13}C NMR spectrum confirms the synthesis of compound oxythiobis [4,6-dimethyl phenoxy methyl acetate]. The melting point of compound (2) is 100 °C, which confirms the formation of ester.

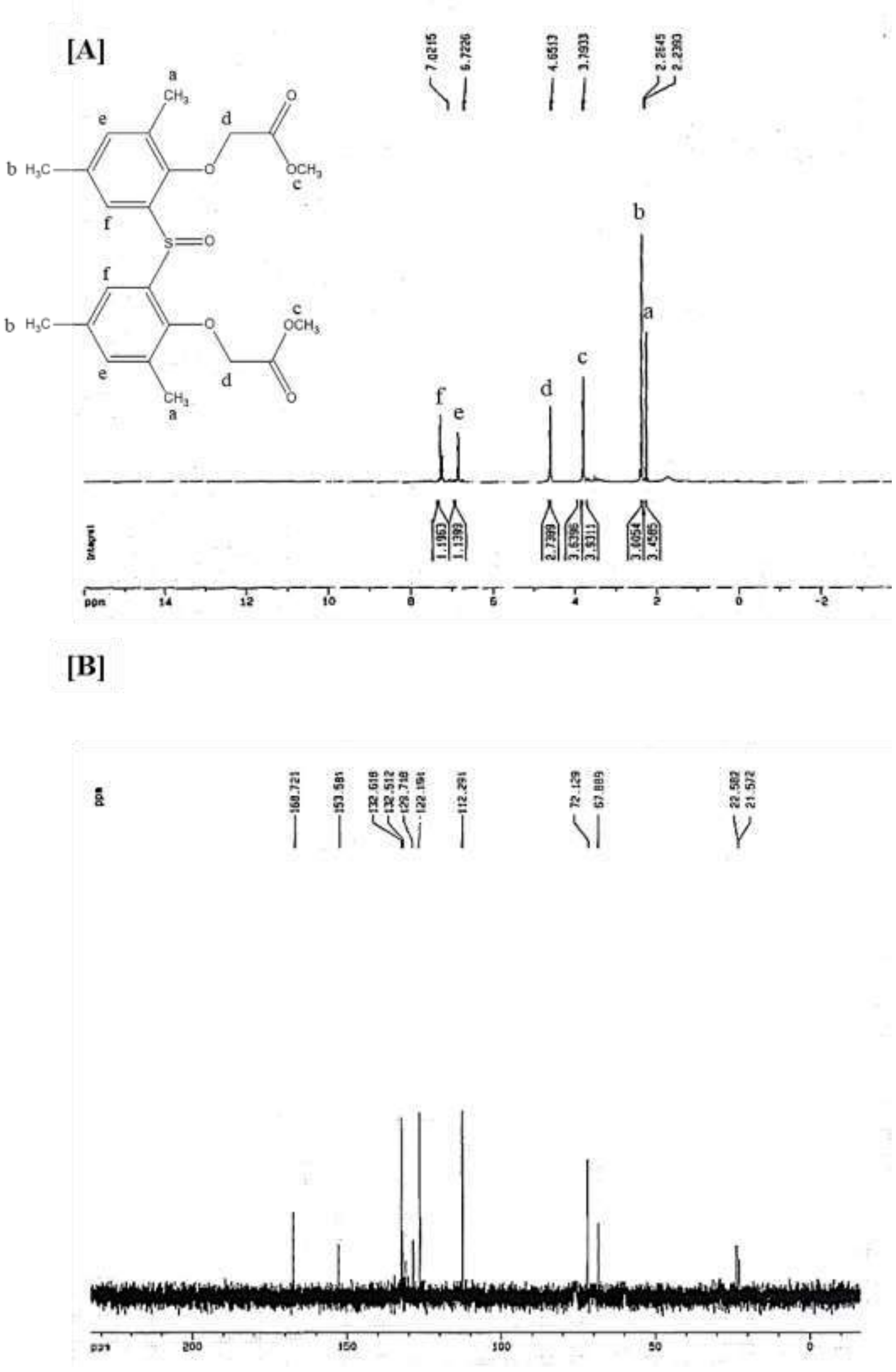

Fig. 7 [A] ^{1}H-NMR spectra and [B] ^{13}C NMR spectrum of compound (2)

Fig. 6 shows the ^{1}H NMR and ^{13}C NMR spectrum of compound (3). In Fig. 6 [A], the absorption bands of aromatic protons and amide including He, Hf, and Hj are seen in the region of 6.92, 7.04, and 7.48 ppm. The absorption bands of methyl and aliphatic protons including Ha, Hb, Hc, and Hd have appeared in the region of 2.21-2.31, 2.73-2.76, 3.33-3.37, and 4.55 ppm. In Fig. 6 [B], the absorption bands of Cm (C=O) in the region of 168.27 ppm, Ck in the region of 153.58, the absorption band of C_i in the region of 132.61 ppm, Cf in the region of 132.51 ppm, the absorption band of Cj in the region of 129.78 ppm, Ch in 122.19 ppm, Cg in 112.29 ppm, Ce in 67.88 ppm, Cd in 49.33 ppm, Cc in 39.25 ppm, Ca in 22.51 ppm, and Cb in the region of 21.53 ppm are seen.

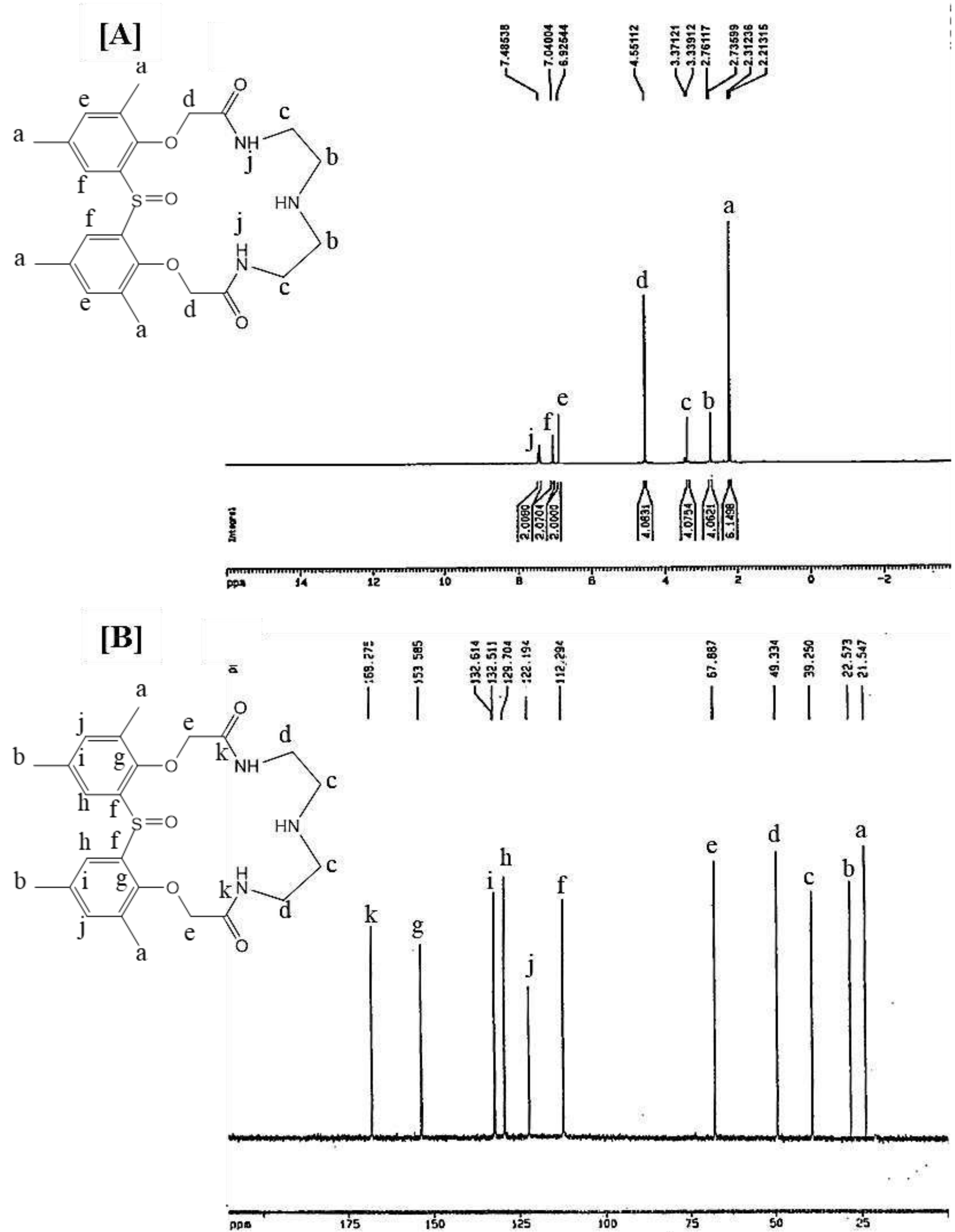

Fig. 8 [A] ^{1}H-NMR spectra and [B] ^{13}C NMR spectrum of compound (3)

A mass spectrum was obtained by electron impact (EI) at 70 eV. Peaks were detected at m/z (%): 429 (M)$^+$, 430 (M+1)$^+$, 431 (M+2)$^+$, 386, 360, 355, 316, 303, 257, 241, 228, 190, 180, 178, 164, 151, 121, 108, 105, 91, 85, 84, 56, 49, 43, 30.

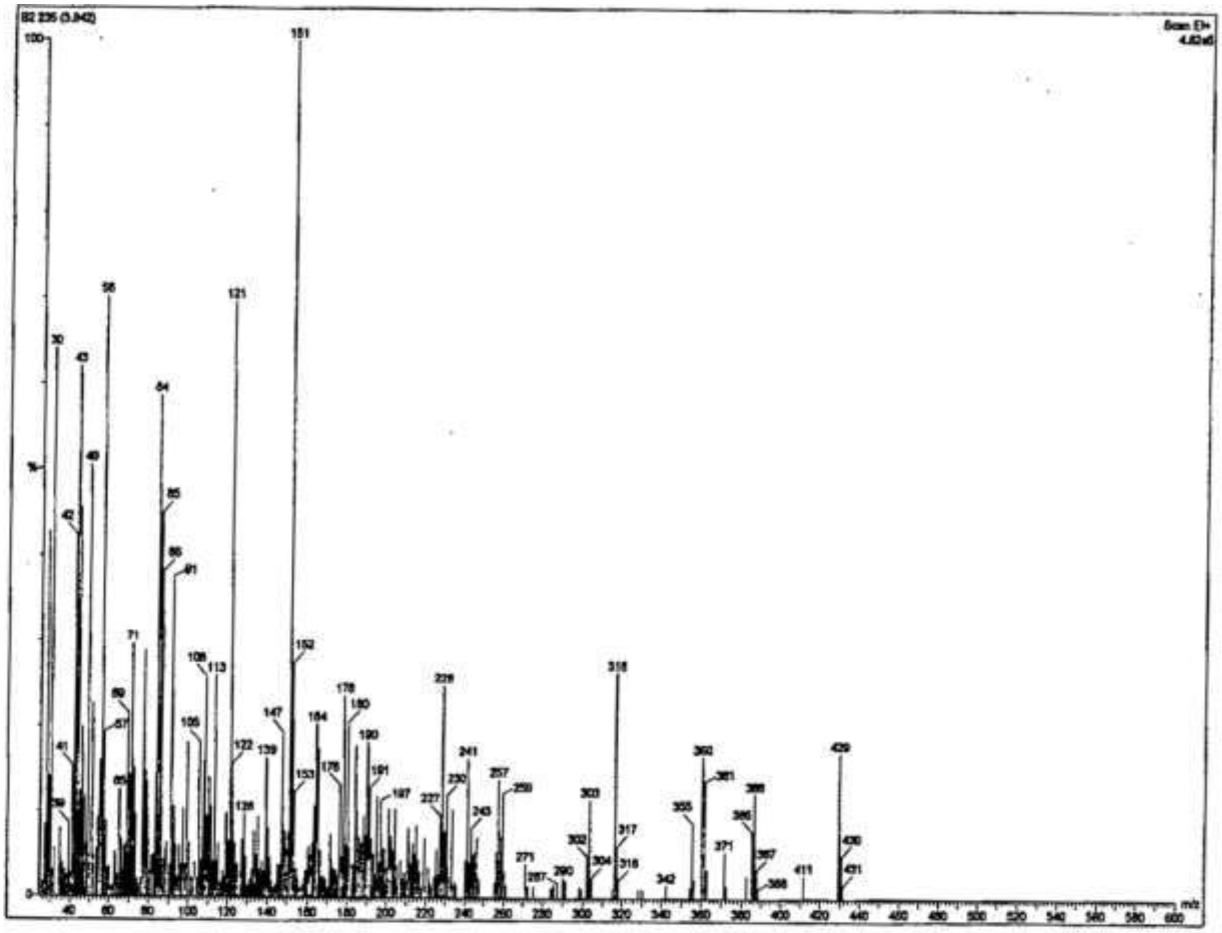

Fig.9 Mass spectrometry analysis of compound (3)

Fig. 8 shows the ^{1}H NMR and ^{13}C NMR spectra of compound (4). In Fig. 8 [A], the absorption bands of aromatic protons, including Hf and He in the region of 7.44-7.38 and 6.97–6.75 ppm. The aliphatic protons including Hd, Hc, Hd, and Ha appeared in regions of 4.67-4.41, 3.69-3.27, 2.37-2.13. and 1.29-1.23, respectively. In Fig. 8 [B], the absorption bands of Cp and Co are seen at

174.42 ppm and 168.85–168.74 ppm. Aromatic carbon atoms are seen at 154.56–112.53 ppm. The absorption band of Cf in the region of 67.90–68.27 ppm, the absorption band of Ce in the region of 49.03–49.64 ppm, the absorption band of C_d in the region of 38.41–39.11 ppm, the absorption band of Cc at 32.97 ppm, and the absorption bands of C_a and Cb at 24.82 and 26.62 ppm have appeared, respectively.

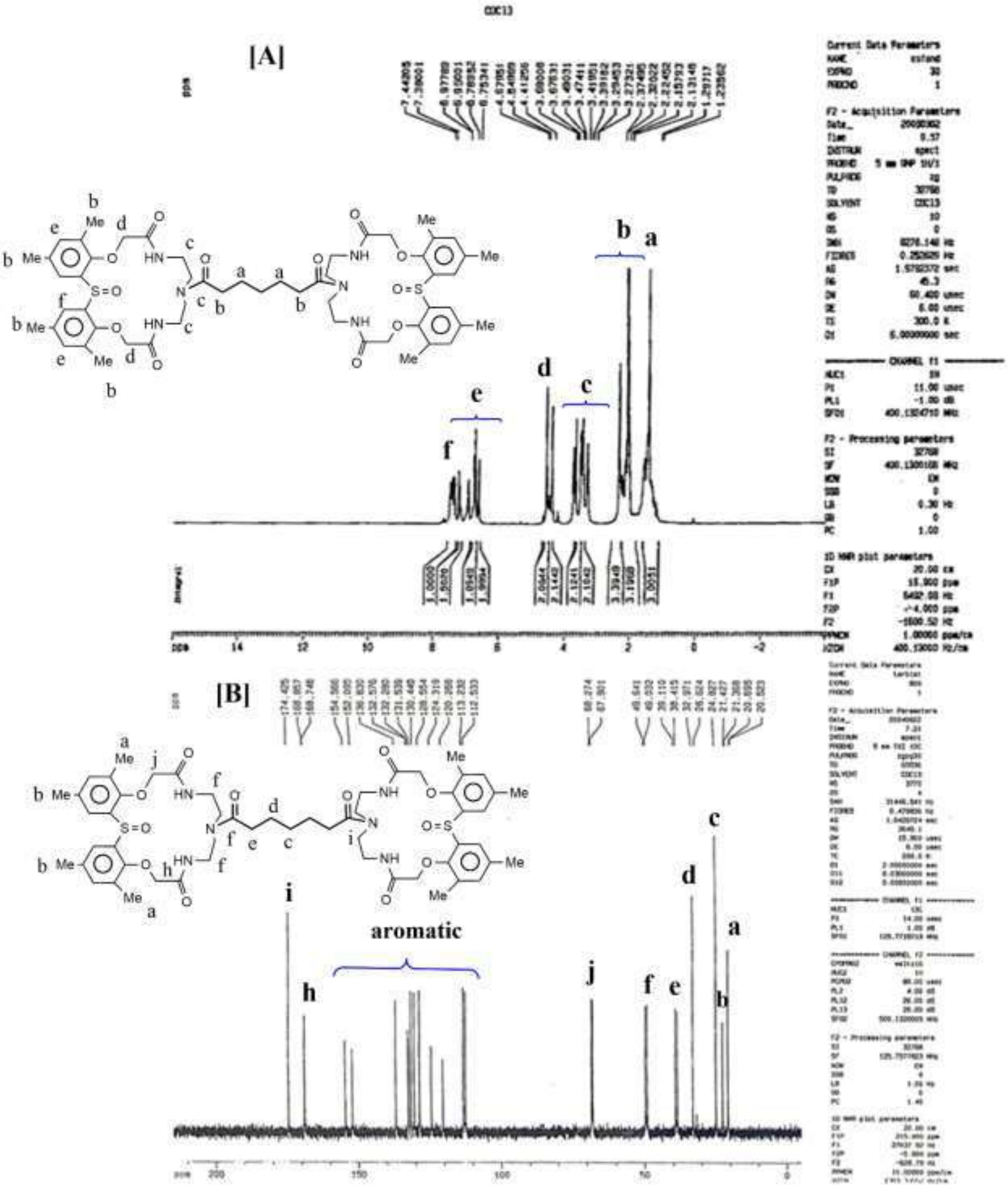

Fig. 10 [A] ^{1}H-NMR spectra and [B] ^{13}C NMR spectrum of compound (4)

A mass spectrum was obtained by electron impact (EI) at 70 eV. Peaks were detected at m/z (%): 543 $(M)^+$, 544 $(M+1)^+$, 545 $(M+2)^+$, 473, 369, 304, 288, 284, 272, 270, 241, 217, 184, 154, 146, 136, 122, 106.

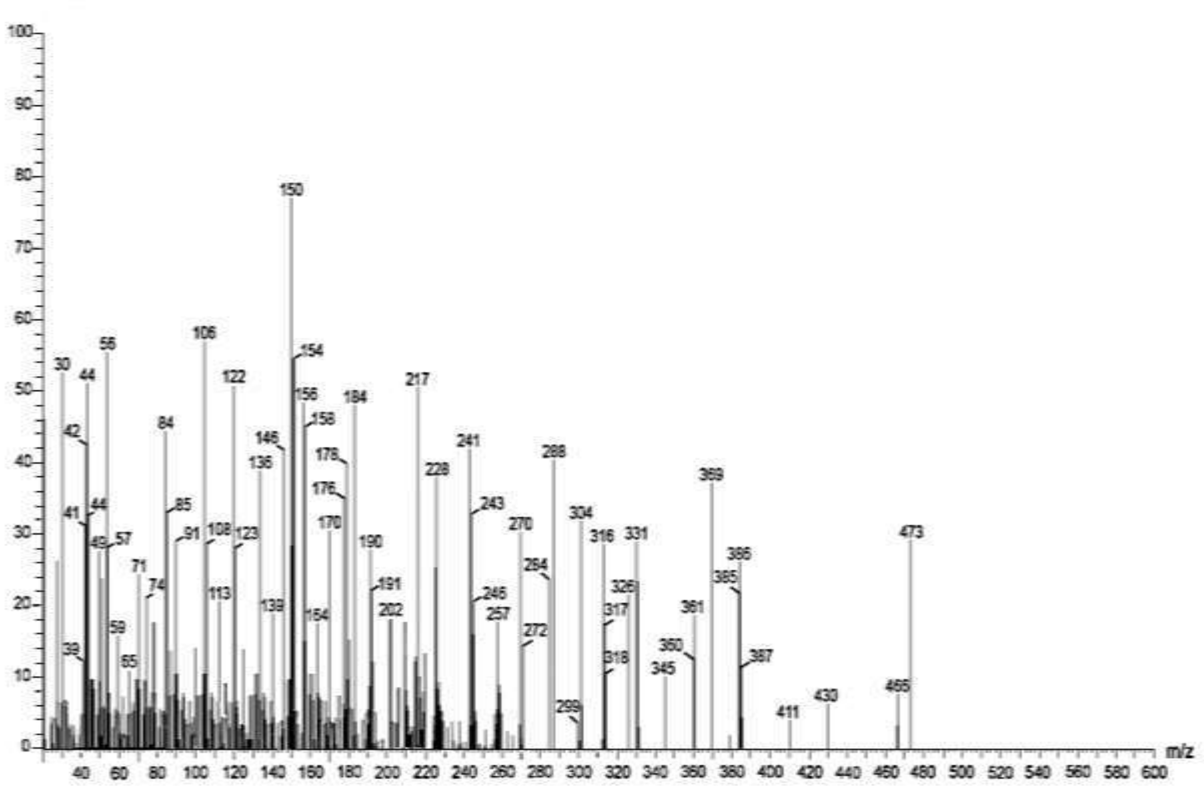

Fig. 11 Mass spectrometry analysis of compound (4)

Conclusions

In this research, the synthetic method of preparing the biscrown compound from the primary diester has been carried out. The diester method is simple, convenient, and suitable for preparing diamide crowns. This research showed that by using simple chemical reactions, it is possible to synthesize new coronands, such as biscrown compounds, based on diamide crown compounds. The compounds resulting from this process were characterized using different chemical analyses, which showed appropriate chemical characteristics. Due to their reactivity and unique properties, these compounds can be used for various applications, especially in medicine, chemicals, and carriers. This research has helped to increase knowledge in the synthesis of biscrown compounds based on diamide crown compounds.

References

1. Steed, J. W. and Atwood, J. L.: *Supramolecular Chemistry.* Wiley, Oxford(2022)

2. Nuriev, V. *et al.: Synthesis, structure, spectral properties, and electrochemistry of bis* (crownether) containing 1, 3-distyrylbenzenes. Russ. J. Org. Chem. vol. 53, pp. 1726-1737 (2017)

3. Schalley, C.A. ed.: Analytical methods in supramolecular chemistry. (2012)

4. Loehr, H.G. and Voegtle, F.:Chromo-and fluoroionophores. A new class of dye reagents. Acc. Chem. Res. 18(3), pp.65-72 (1985)

5. Ushakov, E.N., Alfimov, M.V. and Gromov, S.P.: Design principles for optical molecular sensors and photocontrolled receptors based on crown ethers. Russ. Chem. Rev. 77(1), p.39 (2008)

6. Gromov, S.P.: Molecular meccano for light-sensitive and light-emitting nanosized systems based on unsaturated and macrocyclic compounds. Russ. Chem. Bull. 57, pp.1325-1350 (2008)

7. Fedorova, O. A. *et al.: Supramolecular assemblies of photochromic benzodithia-18-*crown-*6* ethers in crystals, solutions, and monolayers. New J Chem. vol. 26, no. 5, pp. 543-553 (2002)

8. Ushakov, E. N. and Gromov, S. P.: Supramolecular methods for controlling intermolecular photocycloaddition reactions of unsaturated compounds in solutions. Russ. Chem. Rev. vol. 84, no. 8, p. 787 (2015)

9. Gloe, K.: *Macrocyclic Chemistry.* Springer, (2005)

10. Pedersen, C. J. Cyclic polyethers and their complexes with metal salts. J. Am. Chem. Soc. vol. 89, no. 26, pp. 7017-7036 (1967)

11. Huang, Z. B. and Chang, S. H.: Synthesis and complexation behavior studies of novel bis-crown ethers. J. Incl. Phenom. Macrocycl. Chem. vol. 55, pp. 341-346 (2006)

12. Móczár, I. and Huszthy, P.: Optically active crown ether-based fluorescent sensor molecules: A mini-review. Chirality. vol. 31, no. 2, pp. 97-109 (2019)

13. Li, J. Yim, D. Jang, W. D. and Yoon, J.: Recent progress in the design and applications of fluorescence probes containing crown ethers. Chem Soc Rev vol. 46, no. 9, pp. 2437-2458 (2017)

14. Yu, L. Li, F.-z. Wu, J.-y. Xie, J.-q. and Li, S.: Development of the aza-crown ether metal complexes as artificial hydrolase. J. Inorg. Biochem. vol. 154, pp. 89-102 (2016)

15. Otis, F. Auger, M. and Voyer, N.: Exploiting peptide nanostructures to construct functional artificial ion channels. Acc. Chem. Res. vol. 46, no. 12, pp. 2934-2943 (2013)

16. Balzani, V. and Credi, A.: Molecular machine, in *McGraw*-Hill Encyclopedia of Science and Technology, 11th Edition. vol. 11: McGraw-Hill, pp. 349-354 (2012)

17. Raymo, F. M. and Stoddart, J. F.: Interlocked macromolecules. Chem. Rev. *vol*. 99, no. 7, pp. 1643-1664 (1999)

18. Salorinne, K. and Nissinen, M.: Novel tetramethoxy resorcinarene bis-crown ethers.Org. Lett. vol. 8, no. 24, pp. 5473-5476 (2006)

19. Basok, S. S. and *et al.: Synthesis, biological evaluation, and molecular modeling of aza*-crown ethers. Mol. vol. 26, no. 8, p. 2225 (2021)

20. Karawajew, L. and *et al.*: Role of crown-like side chains in the biological activity of substituted-phenoxazone drugs. Anti-cancer Drug Design. vol. 15, no. 5, pp. 331-338 (2000)

21. Fukuda, R. Takenaka, S. and Takagi, M.: Metal ion assisted DNA-intercalation of crown ether-linked acridine derivatives. J. Chem. Soc., Chem. Commun. no. 15, pp. 1028-1030 (1990)

22. Marcotte, N. Rodrigues, F. Lavabre, D. and Fery-Forgues, S.: Biscrown fluoroionophores: has the dye conformation an influence upon the formation of sandwich complexes in the ketocyanine series. New J Chem. vol. 28, no. 2, pp. 295-301 (2004)

23. Kondo, S.-i. Kinjo, T. and Yano, Y.: Barium ion sensing by a 2, 2′-binaphthalene derivative bearing two monoaza-15-crown-5 ethers. TETL. vol. 46, no. 18, pp. 3183-3186 (2005)

24. Nakamura, Yokono, M. H. Tomita, K.-i. Ouchi, M. Miki, M. and Dohno, R.: Substitution effect, absorption, and fluorescence behaviors of 11, 12-benzo-1, 7, 10, 13-tetraoxa-4-aza-cyclopentadec-11-ene (benzoaza-15-crown-5) derivatives upon cation complexation in solvent extraction. J. Org. Chem. vol. 67, no. 10, pp. 3533-3536 (2002)

25. Sousa, C. Gameiro, P. Freire, C. and de Castro, B.: Nickel (II) and copper (II) Schiff base complexes bearing benzo-15-crown-5 functionalities as probes for spectroscopic recognition of lanthanide ions. Polyhedron. vol. 23, no. 8, pp. 1401-1408 (2004)

26. Taraszewska, J. Zięba, K.and Korybut-Daszkiewicz, B.: Crown ethers appended copper tetraazamacrocyclic complexes as receptors for cationic guests. Electrochim. Acta. vol. 49, no. 16, pp. 2675-2681 (2004)

27. Bourguignon, J. and *et al.:* Chiral ditopic receptors. Application to palladium-catalyzed allylic alkylation. Tetrahedron. vol. 59, no. 48, pp. 9583-9589 (2003)

28. Dietrich, B. Viout, P. Lehn, J.-M. and Douglas, W. E.: Macrocyclic chemistry: aspects of organic and inorganic supramolecular chemistry. (No Title), (1993)

29. Elwahy, A. H.: New trends in the chemistry of condensed heteromacrocycles Part A: Condensed azacrown ethers and azathiacrown ethers.J. Heterocycl. Chem. vol. 40, no. 1, pp. 1-23 (2003)

30. Huczyński, A. Ratajczak-Sitarz, M. Katrusiak, A. and Brzezinski, B.: Cyclic oxaalkyl diamide of o-phthalic acid as a new macrocyclic ligand for complexation of Li+ cation. J. Mol. Struct. vol. 930, no. 1-3, pp. 26-31 (2009)

31. Krakowiak, K. E. Bradshaw, J. S. and Zamecka-Krakowiak, D. J.: Synthesis of aza-crown ethers. Chem. Rev. vol. 89, no. 4, pp. 929-972 (1989)

32. Bradshaw, J. S. Krakowiak, K. E. and Izatt, R. M.: Preparation of diamino ethers and polyamines. Tetrahedron. vol. 48, no. 22, pp. 4475-4515 (1992)

33. Adamovich, S. and *et al.:* New quaternary ammonium salts and metal complexes of organylheteroacetic acids with diaza-18-crown-6 ether. Russ. J. Gen. Chem. vol. 80, pp. 1007-1010 (2010)

34. Marjanović, M. and *et al*.: Antitumor potential of crown ethers: structure− activity relationships, cell cycle disturbances, and cell death studies of a series of ionophores. J. Med. Chem. vol. 50, no. 5, pp. 1007-1018 (2007)

35. Shockravi, A. Alizadeh, R. Aghabozorg, H. Moghimi, A. Rostami, E. and Bavili, S.: Synthesis and crystal structure determination of 2, 2′-sulfinyl-bis (4-methyl phenol) and 2, 2′-thio-bis (4-methyl phenol). Phosphorus, Sulfur, and Silicon. vol. 178, no. 12, pp. 2519-2527 (2003)

36. Chandrasekaran, A., Day, R.O. and Holmes, R.R.: Structural influence of a sulfinyl group in eight-membered rings of diorganosilanes. Organomet. 15(14), pp.3182-3188 (1996)

37. Shockravi, A. Bavili T, S. Rostami, E. Yousefi, A. Dehjurian, A. and Tohidi, R.: Synthesis of new dibenzosulfide and dibenzosulfoxide macrocyclic compounds. J. Incl. Phenom. Macrocycl. Chem. vol. 49, pp. 163-166 (2004)

The 30th Iranian Seminar of Organic Chemistry
February 7-9, 2025, Iran University of Science and Technology, Tehran, Iran

Synthesis and Investigation of an Organic Dyes for Dye-sensitized Solar Cells

M. Hosseinnezhad*[1] and K. Gharanjig [1]

1) Department of Organic Colorants, Institute for Color Science and Technology, Tehran, Iran. Fax: +98 21 22947537; Tel: +98 21 22941132; E-mail: hosseinnezhad-mo@icrc.ac.ir

Keyword: Dye-sensitized solar cells, Synthesis, Efficiency, Thioindigo, Indoline.

The organic molecules with D–π–A structures have attracted increasing attention since they can serve as electro active and photoactive materials in molecular electronics, such as biochemical fluorescent technology, NLO materials, electro generated chemiluminescence, OLEDs, and solar cells [1]. In this work, new metal free dye (Figure 1) is reported and its optical, electrochemical, photovoltaic properties and structural relationships are investigated in detail. The absorption spectrum of dye in CH_3CN has three distinct absorption bands at around 395 nm. The absorption peaks at around 496 nm correspond to an intramolecular charge transfer between the phenothiazine-based donor and the cyanoacrylic acid [2], providing efficient charge-separation at the excited state. The wavelength of maximum absorption (λ_{max}) of dye adsorbed on a TiO_2 film is 509 nm. Upon dye adsorption on to a TiO_2 surface, the wavelength of maximum absorption is bathochromically shifted by 13 as compared to the corresponding spectra in solution, implying that dye adsorbed on to TiO_2 surface contain partial J-type aggregates [3]. The DSSCs were prepared and compared to investigate the relationships between the sensitizing behaviour of dye molecule and its structures. The efficiency (η) of the DSSCs is 7.69% (Figure 1).

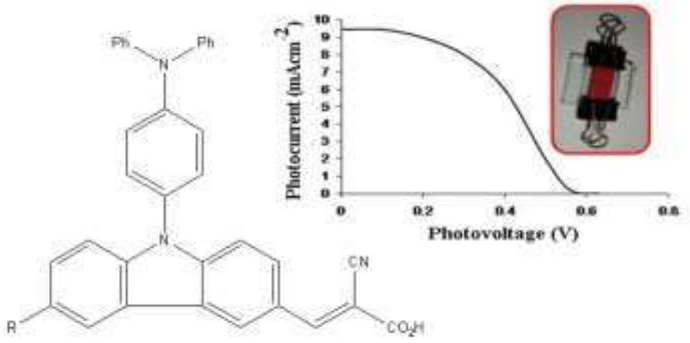

Figure 1. Chemical structure of Photosensitizer and J-V diagram of DSSCs; R= thioindigo.

References

[1] M. Hosseinnezhad, S. Nasiri, V. Nutalapati, and K. Gharanjig, *Optical Materials,* 2024, **150**, 115273.
[3] S. S. Park, Y. S. Choi and J. H. Kim, *Energy and Fuels*, 2022, **41**, 3732.
[4] M. Hosseinnezhad, M. Ghahari, G. Mobarhan, S. Rouhani and M. Fathi, *Optical Materials*, 2024, **139**, 113775.

The 30th Iranian Seminar of Organic Chemistry
February 7-9, 2025, Iran University of Science and Technology, Tehran, Iran

Study of the effect of conjugated bridge on the efficiency of organic photosensitizers used in dye-sensitized solar cells

M. Hosseinnezhad*[1] and K. Gharanjig [1]

1) Department of Organic Colorants, Institute for Color Science and Technology, Tehran, Iran.
Fax: +98 21 22947537; Tel: +98 21 22941132; E-mail: hosseinnezhad-mo@icrc.ac.ir

Keyword: Photosensitizers, Efficiency, Dye-sensitized solar cells, Synthesis, Conjugated bridge.

World energy resources, including households, industry and technology, are rising with population growth. Solar radiation is one of the energy sources with the characteristics mentioned above. One of the emerging technologies for the generation of energy from solar radiation is dye-sensitized solar cells (DSSCs) [1]. 1 Sensitizers are the main components of this technology, which are responsible for producing electrons based on the light received from the sun. Organic compounds are a good option for preparing new and highly efficient photosensitizers, and the conjugated bridge for connecting functional groups plays an important role in the maximum and shape of the absorption band of organic dyes [2]. To prepare sensitizers, electron-withdrawing and electron-donating groups are connected to each other through a conjugated bridge. The presence of at least one effective electron-withdrawing node is essential for bonding to the semiconductor surface [3]. Thiophene rings were used as conjugated bridges. The number of thiophene rings was evaluated to compare the effect of conjugated bond length on the maximum absorption and efficiency of DSSCs. The chemical structure of the dye is shown in the figure1. The maximum absorption of synthesized dyes 1-4 is 493, 507, 519, and 532 nm, respectively. The efficiency of the DSSCs prepared based on the synthesized dye, 1-4, is about 7.78, 7.92, 8.12, and 8.32%, respectively.

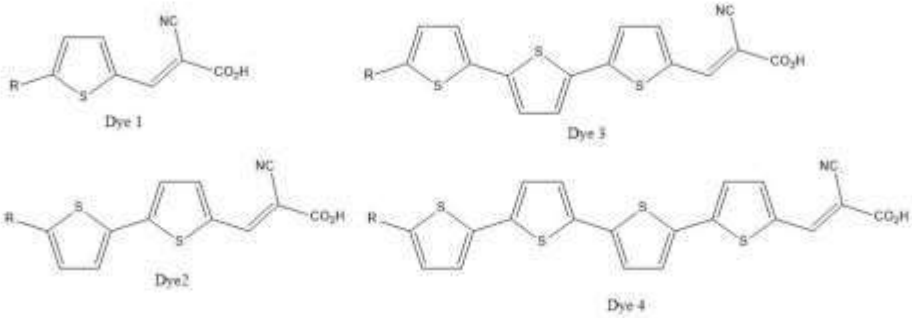

Figure 1. Chemical Structure of Photosensitizers; R=thioindigo.

References

[1] M. Hosseinnezhad, S. Nasiri, V. Nutalapati, and K. Gharanjig, *Optical Materials*, 2024, **150**, 115273.
[2] S. S. Park, Y. S. Choi and J. H. Kim, *Energy and Fuels*, 2022, **41**, 3732.
[3] M. Hosseinnezhad, M. Ghahari, G. Mobarhan, S. Rouhani and M. Fathi, *Optical Materials*, 2024, **139**, 113775.

Natural compound quantification using enzymatic biosensor

Seyed Hojjat Tayefi[a], Mitra Ghodrati[b], Mehdi Mogharabi-Manzari*[a], Ebrahim Fooladi*[b]

[a] *Pharmaceutical Sciences Research Center, Hemoglobinopathy Institute, Mazandaran University of Medical Sciences, Sari, Iran*

[b] *Department of Food Safety and Quality Control, Research Institute of Food Science and Technology (RIFST)*

Keywords: Biosensor, Enzyme, Laccase, Dephostatin, Graphene

Dephostatin is known as a natural protein-tyrosine phosphatase inhibitor that contains a nitrosamine moiety that is often mutagenic and carcinogenic. Therefore, development of approaches for detection and quantification of this natural compound is crucial (1). Compared to conventional methods for measuring analytes and controlling biochemical processes, biosensors offer advantages such as reusability, rapid response times, and high specificity (2). Laccase, an enzyme from the oxidoreductase family, is particularly effective in catalyzing reactions involving ortho- and para-diphenols, with its effectiveness varying based on the producing organism (3). Unlike many enzymes that target specific substrates, laccase can oxidize a wide range of substances, including diphenols, polyphenols, diamines, methoxyphenols, aromatic amines, and ascorbate. Additionally, protein tyrosine phosphatases are enzymes that remove phosphate groups from protein residues (4).

The electrochemical properties of the electrodes were evaluated through cyclic voltammetry (CV) and electrochemical impedance spectroscopy (EIS). Key parameters such as oxidation potential, pH, temperature, and concentration were optimized. The current response for each sample was measured at an oxidation potential of 0.45 V relative to the Ag/AgCl electrode. Calibration curves were established, and measurements were taken by interpolating the amperometric signals from dephostatin solutions. Dephostatin standards were then added to a diluted Nescafe sample (phosphate buffer, 0.05 M, pH 6.5) without any pretreatment, and recovery rates were subsequently calculated.

By immobilizing graphene oxide and laccase onto the electrode surface, the modified electrode demonstrated enhanced cathodic and anodic currents when compared to the unmodified electrode in a $K_4Fe(CN)_6/K_3Fe(CN)_6$ solution. The incorporation of graphene nanoparticles on the electrode surface facilitated an improved electron transfer rate, resulting in an increase of 20 µA. The electrode's response was linear over a concentration range of 10 to 900 nM, with a detection limit established at 6 nM.

Given the critical roles of protein tyrosine phosphatases in cell signaling pathways and disease progression, there is growing interest in using dephostatin as an inhibitor. Consequently, developing a precise and rapid method for measuring dephostatin is essential within the pharmaceutical industry. The biosensor developed for this purpose incorporates laccase enzyme and graphene nanoparticles stabilized with a chitosan nanocomposite, enabling accurate dephostatin measurements.

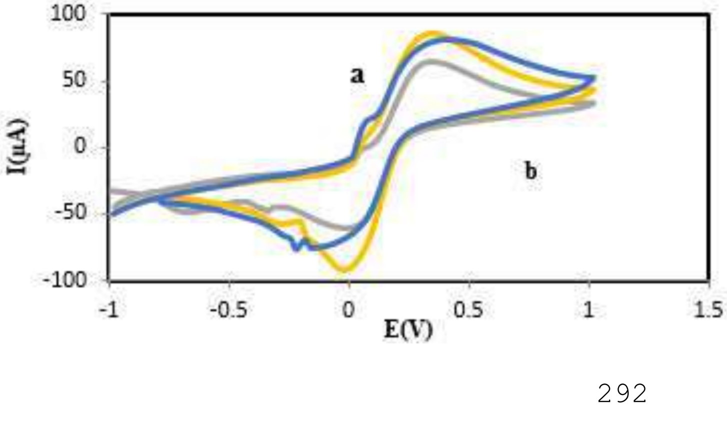

Scheme: cyclic voltammetry of the prepared biosensor in $K_4Fe(CN)_6/K_3Fe(CN)_6$ solution.

References:

1. Davis J, Huw Vaughan D, Cardosi MF. Elements of biosensor construction. Enzyme Microb Technol. 1995 Dec;17(12):1030–5.

2. Goode J, Rushworth J, Millner P. Biosensor regeneration: a review of common techniques and outcomes. Langmuir. 2015;31(23):6267–76.

3. Mayer A. Laccase: new functions for an old enzyme. Phytochemistry. 2002 Jul;60(6):551–65.

4. Khatami SH, Vakili O, Movahedpour A, Ghesmati Z, Ghasemi H, Taheri-Anganeh M. Laccase: Various types and applications. Biotechnol Appl Biochem. 2022 Dec;69(6):2658–72.

The 30th Iranian Seminar of Organic Chemistry
February 7-9, 2025, Iran University of Science and Technology, Tehran, Iran

Phytochemical Analysis and Antioxidant Activity of Lichen *Melanelixia glabra*

Atieh Salehnejad*[a], Mahdi Moridi Farimani [b], Mohammad Sohrabi [c]

[a] *Department of Phytochemistry, Medicinal Plants and Drugs Research Institute, Shahid Beheshti University, Tehran, Iran*

[b] *Iranian Research Organization for science and technology (IROST), Tehran, Iran*

Abstract: This study investigates the antioxidant properties of the lichen *M. glabra*, known for its medicinal potential due to bioactive compounds. Using Thin Layer Chromatography (TLC) and various solvent systems, we identified key metabolites, including lecanoric acid. Results showed that while the methanol extract had higher extraction efficiency, the acetone extract exhibited superior antioxidant activity, highlighting the potential of *M. glabra* in natural pharmaceuticals.

Keywords: Lichen, *Melanelixia glabra*, Phenol, Flavonoid, Antioxidant activity.

Introduction:

Lichens are fascinating symbiotic entities formed through the collaboration of a fungus and one or more photosynthetic organisms. Certain lichens are referred to as medicinal due to their rich array of bioactive compounds. They are known to produce a wide range of secondary metabolites, many of which are distinctive and present promising opportunities for the discovery of new classes of antioxidant agents. The unique and often underexplored metabolites of lichens contribute to their resilience in extreme environments. Given the limited efficacy of many synthetic pharmaceuticals, there is a growing interest in researching natural bioactive compounds. In this study, we focused on *M. glabra*, a lichen of ecological and potential medicinal value, to evaluate its antioxidant properties [1,2].

Material and Method:

Lichen samples of *M. glabra* were carefully gathered from the lush forests of Gilan. To explore the secondary metabolites present, the Thin Layer Chromatography (TLC) technique was employed. The species *P. acetabulum* served as an internal control to accurately determine the R_f values of the compounds analyzed. In this study, three distinct solvent systems were utilized as the mobile phase: System A: Toluene, 1,4-Dioxane, and Acetic Acid in a ratio of 180:60:8 (v/v/v), System B: n-Hexane, Diethyl Ether, and Formic Acid in a ratio of 130:1000:20 (v/v/v), System C: Toluene and Acetic Acid in a ratio of 200:30 (v/v). A 10% sulfuric acid solution was utilized as a reagent to facilitate the detection process. Furthermore, a spot test method was incorporated as a supplementary technique to identify metabolites, employing reagents such as KOH, NaOCl, and PPD. Spotting tests were conducted under a stereomicroscope to enhance the visibility of color changes. To assess antioxidant activity, acetone and methanol extracts of *M. glabra* were obtained through the maceration method, and the extraction efficiency for both solvents was calculated. The phenolic content was quantified using the Folin–Ciocalteu colorimetric method, with gallic acid serving as the standard reference. The total flavonoid content was determined following the modified Dowd method, employing rutin to establish a standard curve. Finally, the antioxidant properties of the extracts were evaluated by measuring their capacity to inhibit DPPH free radicals, and the IC_{50} values were compared to assess their effectiveness.

Results and Discussion:

The findings revealed that the methanol extract demonstrated superior extraction efficiency. Through Thin Layer Chromatography (TLC) and spot tests, lecanoric acid was identified among the extracted substances. Interestingly, the amounts of phenolic and flavonoid compounds obtained from acetone extraction were higher than those from the methanol extract, despite the latter's greater efficiency. Additionally, the DPPH free radical inhibition assay showed that at all tested concentrations, the acetone extract exhibited a stronger inhibitory activity compared to the methanol extracts.

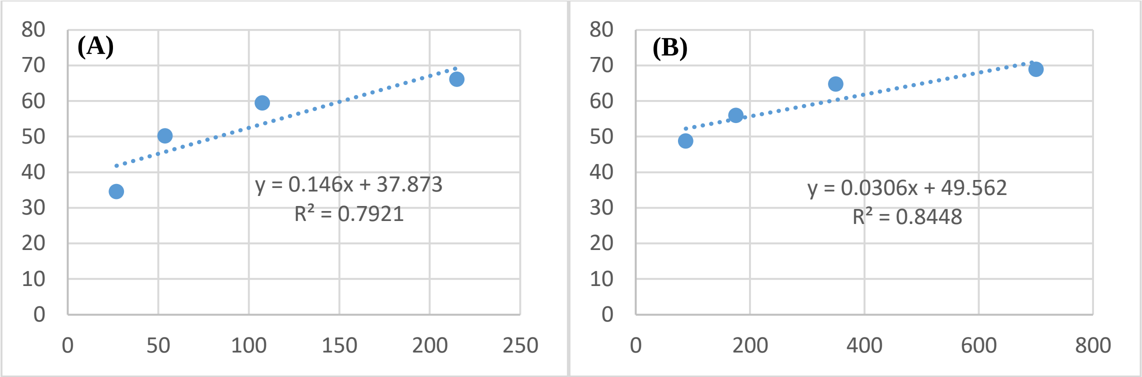

Fig: % inhibition vs concentration for a) Methanol and b) Acetone extracts

Table: Comparison of extracts

Extracts	Efficiency	Total phenol (mg/gr)	Total Flavonoid (mg/gr)	IC50
Acetone	2.03	231.202±6.50	22.25±1.25	13.86
Methanol	3.72	99.84±1.95	11.83±1.91	83.06

References:

١. Kumar, A., & Sharma, S. (2022). "Antioxidant potential of lichen metabolites: A review." *Journal of Ethnopharmacology*, 283, 114628. DOI: 10.1016/j.jep.2021.114628.

٢. González, M. C., & Valdés, J. (2023). "Exploring the bioactive compounds of lichens: Implications for drug discovery." *Phytochemistry Reviews*, 22(1), 1-24. DOI: 10.1007/s11101-022-09958-4.

The 30th Iranian Seminar of Organic Chemistry
February 7-9, 2025, Iran University of Science and Technology, Tehran, Iran

Synthesis and application of Fe-based metal-organic frameworks (Fe-MOFs) with CuO in the Click reaction for the preparation of triazole derivatives

Milad Mohammadi Rasooll[a], Hassan Sepehrmansourie[b], Mohammad Ali Zolfigol[*a]

[a]Department of Organic Chemistry, Faculty of Chemistry and petroleum sciences, Bu-Ali Sina University, Hamedan 6517838683, E-Mail: zolfi@basu.ac.ir & mzolfigol@yahoo.com.

[b]Faculty of Converging Science and Technologies, University of Qom, Qom, Iran, 37185-359.

Keyword: Click Reaction, Fe-MOF@CuO, Metal Organic Frameworks, Triazol derivatives

Material engineering has attracted a lot of scientific attention among scientists in recent years. Meanwhile, metal-organic frameworks (MOFs) are a promising class of engineered materials. The ability to design and target synthesis, attractive porous architecture and flexibility are among the characteristics of these crystal structures, which are obtained by connecting organic ligands to metal clusters. The attractive nature and properties of MOFs have caused these crystalline porous materials to have potential applications in sensors, drug delivery, gas absorption, catalysts, and photocatalysts [1]. Nowadays, green and low-cost synthesis of organic compounds has become an attractive challenge. Therefore, an attractive approach in this field is the synthesis of organic and pharmaceutical compounds with the help of MOFs catalyst, which provide a suitable platform for chemical reactions. Expanding the potential capabilities of MOFs in Click reactions and especially the synthesis of triazole compounds is a very attractive scientific approach [2]. Therefore, in this report, Fe-MOF@CuO, which is a MOF modified with CuO, was designed and its capability in the preparation of triazole derivatives was measured. Triazole compounds are very important because of their medicinal and biological properties, such as antibacterial, antifungal, etc. [3]. This was a strong motivation for us in this research **(Scheme 1)**.

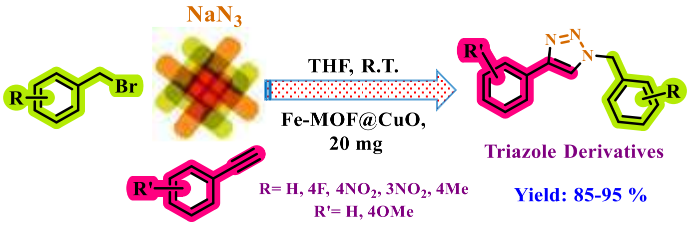

Scheme 1: Preparation of triazole derivatives using Fe-MOF@CuO

References:

[1] Li, C., Ji, Y., Wang, Y., Liu, C., Chen, Z., Tang, J., ... & Xia, C. (2023). Applications of metal-organic frameworks and their derivatives in electrochemical CO2 reduction. Nano-Micro Letters, 15(1), 113.

[2] Li, P. Z., Wang, X. J., & Zhao, Y. (2019). Click chemistry as a versatile reaction for construction and modification of metal-organic frameworks. *Coordination Chemistry Reviews*, *380*, 484-518.

[3] Guan, Q., Xing, S., Wang, L., Zhu, J., Guo, C., Xu, C., ... & Sun, H. (2024). Triazoles in Medicinal Chemistry: Physicochemical Properties, Bioisosterism, and Application. *Journal of Medicinal Chemistry*, *67*(10), 7788-7824.

Preparation, characterization and application of Ionic Liquid Metal Organic Frameworks as an efficient catalyst for the solvent-free synthesis of macromolecules

Milad Mohammadi Rasooll[a], Hassan Sepehrmansourie[b], Mohammad Ali Zolfigol*[a]

[a]Department of Organic Chemistry, Faculty of Chemistry and petroleum sciences, Bu-Ali Sina University, Hamedan 6517838683, E-Mail: zolfi@basu.ac.ir & mzolfigol@yahoo.com.
[b]Faculty of Converging Science and Technologies, University of Qom, Qom, Iran, 37185-359.

Keyword: Heterogeneous catalysts, Ionic liquid, Macromolecules, Metal Organic Frameworks

In recent years, the synthesis of metal-organic frameworks (MOFs) as a new generation of nanoreactors has expanded significantly. MOFs are crystalline structures with tunable pores, the attractive scientific properties of this class of porous materials have attracted much scientific attention. Nowadays, MOFs have wide applications in various fields such as catalysts, photocatalysts, energy storage, gas absorption and sensors [1]. Catalytic applications of MOFs have created an interesting research motive due to the high porosity, high surface area, chemical and thermal stability of these compounds. In this context, the placement of ionic liquids that have low volatility, high thermal stability, low vapor pressure and are environmentally friendly in the pores of MOFs has caused interesting physical and chemical properties in MOFs [2]. With these attractive features in mind, we have developed the highly motivated [Zr-UiO-66-imidazole]Br, a Catalyst Ionic Liquid Metal Organic Frameworks (ILMOFs). The catalytic application of the above ILMOFs was measured in the preparation of a wide range of macromolecule compounds which mainly have significant biological properties such as anti-cancer, anti-tumor, and anti-bacterial properties **(Scheme 1)** [3].

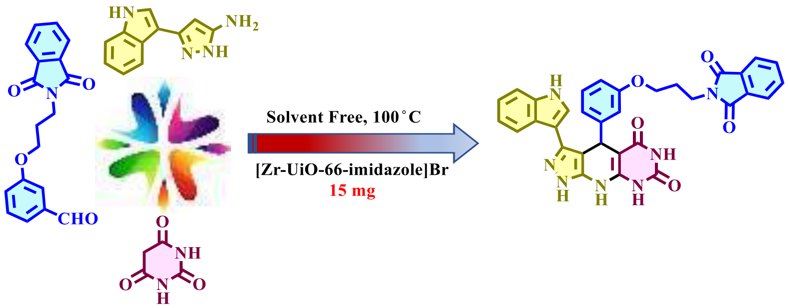

Scheme 1: Preparation of macromolecule derivatives using [Zr-UiO-66-imidazole]Br

References:

[1] Yang, F., Du, M., Yin, K., Qiu, Z., Zhao, J., Liu, C., ... & Pang, H. (2022). Applications of metal-organic frameworks in water treatment: a review. Small, 18(11), 2105715.

[2] Kinik, F. P., Uzun, A., & Keskin, S. (2017). Ionic liquid/metal–organic framework composites: from synthesis to applications. ChemSusChem, 10(14), 2842-2863.

[3] Dhara, A. K., & Nayak, A. K. (2022). Biological macromolecules: sources, properties, and functions. In *Biological macromolecules* (pp. 3-22). Academic Press.

The 30th Iranian Seminar of Organic Chemistry
February 7-9, 2025, Iran University of Science and Technology, Tehran, Iran

Synthesis of 2-(pyrrolidin-2-ylidene)-1*H*-indene-1,3-diones *via* 1,3-dipolar cycloaddition of azomethine ylides with chalcones

Seyed Alireza Hadian, Issa Yavari*

Department of Chemistry, Tarbiat Modares University, PO Box 14115-175, Tehran, Iran
yavarisa@modares.ac.ir

Keyword: Diastereoselective synthesis, Huisgen reaction, Ninhydrin, Chalcones, Pyrrolidine-2-ylidene

Pyrrolidine-2-ylidenes, a specific category of *N*-heterocycles, are commonly found in abundant biologically active natural compounds.[1] Natural products containing pyrrolidine-2-ylidenes, such as azinomycins are characterized by their significant antitumor properties.[2] While simple pyrrolidine derivatives are commercially accessible, synthesizing pyrrolidine-2-ylidenes often requires significant synthetic effort. A notable strategy involves [3+2] dipolar cycloadditions of azomethine ylides, which enable the direct construction of the five-membered ring.[3] Herein, a diastereoselective synthesis of pyrrolidin-2-ylidene derivatives through the Huisgen reaction of H-bond-assisted azomethine ylides with chalcones is described. This reaction forms three stereogenic centers with remarkable diastereoselectivity. The practical applicability of this approach was further illustrated through a gram-scale experiment. The final product's structure was confirmed *via* single-crystal X-ray analysis, affirming the successful synthesis of the target compounds. Various features of this protocol will be presented and discussed.

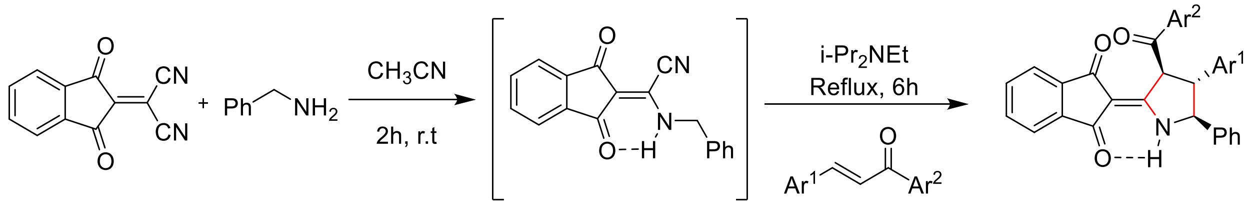

References:

1. Petri, G. L.; Raimondi, M. V.; Spanò, V.; Holl, R.; Barraja, P.; Montalbano, A. *Top. Curr. Chem.* **2021**, 379, 34.
2. Bräse, S.; Gläser, F.; Kramer, C. S.; Lindner, S.; Linsenmeier, A. M.; Masters, K. S.; Meister, A. C.; Ruff, B. M.; Zhong, S. *Prog. Chem. Org. Nat. Prod.* **2013**, *97*, 1-300.
3. M. Breugst, M.; Reissig, H.-U. *Angew. Chem., Int. Ed.* **2020**, *59*, 12293-12307.

The 30th Iranian Seminar of Organic Chemistry
February 7-9, 2025, Iran University of Science and Technology, Tehran, Iran

Synthesis and Catalytic Application of Magnetic Copper Nanoparticles $Fe_3O_4@SiO_2@$Schiff Base-Cu(II) in the Biginelli Reaction

Authors: Elham Abbasi 1[a], Fatemeh Ajormal 2[b], Nader Noshiran Zadeh 3*[c], Rahman Bikas 4[*d]

Keyword: Synthesis, Biginelli, Nanoparticles, Catalytic

Biginelli reactions are a valuable tool in organic synthesis, specifically for the creation of dihydropyrimidinones (DHPMs) [1]. These heterocyclic compounds are essential building blocks for various pharmaceutical and medicinal compounds [2]. Traditionally, Biginelli reactions often require harsh conditions, such as high temperatures and long reaction times [3]. Magnetic nanoparticle catalysts have emerged as a promising solution to address these limitations. These tiny particles, often composed of magnetic materials like iron oxide, exhibit unique catalytic properties due to their large surface area and magnetic susceptibility. When employed as catalysts in Biginelli reactions, magnetic nanoparticles can significantly enhance reaction rates, improve product yields, and allow for milder reaction conditions [4]. Additionally, their magnetic properties facilitate easy separation from the reaction mixture using an external magnetic field, making them environmentally friendly and cost-effective [5]. This study, we is reported the synthesis of magnetic copper nanoparticles and their application as an efficient and reusable catalyst for synthesis of dihydropyrimidinone by Biginelli reaction. The nanoparticles were characterized using various techniques, including X-ray diffraction (XRD), Fourier Transform Infrared Spectrometer (FT-IR). The catalytic activity of the synthesized nanoparticles was evaluated in the Biginelli reaction under 70 °C, and 30-150 min conditions, and the results showed high yields of the desired products. The catalyst could be easily recovered using an external magnet and reused for 5 cycles without significant loss of activity.

Scheme: center

References:

[1] Khasimbi S, Ali F, Manda K, Sharma A, Chauhan G, Wakode S. Dihydropyrimidinones scaffold as a promising nucleus for synthetic profile and various therapeutic targets: A Review. Current Organic Synthesis. 2021 May 1;18(3):270-93.

[2] Neupane NP, Wu YS, Verma A. Introduction of dihydropyrimidinones: a medicinal chemistry perspective. InDihydropyrimidinones as Potent Anticancer Agents 2023 Jan 1 (pp. 1-15). Elsevier.

[3] Costa dos Santos PH, Guimar Souza VL, Carvalho Santos AC, Esteves H, Modolo LV, de Fma N. Synthesis of Biginelli Compounds using Microwave-Assisted Methods. Current Microwave Chemistry. 2023 Sep 1;10(2):70-87.

[4] Bhatt BR, Dixit BC, Kataria VB, Dixit RB, Saiyad S. Recent Advances in Biginelli Reaction using Nanoparticles, Zeolites and Metal Compounds as Catalyst: A Concise Review. Letters in Organic Chemistry. 2024 Oct 1;21(10):821-46.

[5] Sanap D, Avhad L, Ahire S, Mirzaei M, Kumar D, Ghotekar S, Gaikwad ND. Insights into the promising heterogeneous catalysis of eco-friendly synthesized spinel $CuFe_2O_4$ nanoparticles for Biginelli reaction. Research on Chemical Intermediates. 2024 Jun 16:1-25.

The 30th Iranian Seminar of Organic Chemistry
February 7-9, 2025, Iran University of Science and Technology, Tehran, Iran

Green Synthesis of Tetrazoles catalysed by Magnetic Nanoparticles Supported Zinc(II) complex (Fe_3O_4 @SiO_2 -Schiff Base-$Zn(OAc)_2$)

Authors: Elham Abbasi 1[a], Fatemeh Ajormal 2[b], Nader Noshiran Zadeh 3*[c], Rahman Bikas 4*[d]

Keyword: Green Synthesis, Tetrazoles, Nanoparticles, Catalyst

Tetrazoles, a class of heterocyclic compounds, have garnered considerable attention in recent years due to their fascinating properties and versatile applications [1]. Structurally, tetrazoles are five-membered rings consisting of four nitrogen atoms and one carbon atom [2]. This unique composition lends tetrazoles exceptional chemical stability and high nitrogen content, making them attractive for various applications. Tetrazoles have also been recognized for their bioactive potential, with several compounds showing promising activity against various diseases [3].

Furthermore, tetrazoles have been extensively explored as building blocks in organic synthesis and functional materials [2]. Their synthetic versatility has been demonstrated through the development of diverse methodologies for their preparation, modification, and incorporation into complex molecular structures [4]. In addition, their electronic properties have been exploited in the design of new materials for optoelectronics, sensing, and energy storage applications [5].

In conclusion, tetrazoles have proven to be a remarkable class of heterocyclic compounds with far-reaching implications in both chemical and materials science. Their intriguing properties and versatile synthetic routes continue to inspire researchers to explore new avenues for their application and discovery.

In this work, we present the synthesis of tetrazoles using Magnetic nanoparticles supported zinc (II) complex (Fe_3O_4@SiO_2-schiff base-$Zn(OAc)_2$) as efficient catalysts. The (Fe_3O_4@SiO_2-schiff base-$Zn(OAc)_2$) were prepared via a co-precipitation method and characterized using various techniques(XRD-FT-IR, map). The catalytic performance of the nanoparticle was evaluated in the synthesis of tetrazoles. The results demonstrated that the nanoparticle exhibited excellent catalytic activity, and recyclability (five cycle). The magnetic properties of the catalyst allowed for easy separation and recovery, making them a environmentally friendly catalyst for the synthesis of valuable tetrazole derivatives.

Scheme: Preparation of tetrazole catalyzed by Fe_3O_4 @SiO_2 -Schiff Base-$Zn(OAc)_2$

References:

[1] Kaushik N, Kumar N, Kumar A, Singh UK. Tetrazoles: Synthesis and biological activity. Immunology, Endocrine & Metabolic Agents in Medicinal Chemistry (Formerly Current Medicinal Chemistry-Immunology, Endocrine and Metabolic Agents). 2018 1;18(1):3-21.

[2] Neochoritis CG, Zhao T, Domling A. Tetrazoles via multicomponent reactions. Chemical reviews. 2019 1;119(3):1970-2042.

[3] Uppadhayay RK, Kumar A, Teotia J, Singh A. Multifaceted chemistry of tetrazole. Synthesis, uses, and pharmaceutical applications. Russian Journal of organic chemistry. 2022;58(12):1801-11.

[4] Nasrollahzadeh M, Nezafat Z, Bidgoli NS, Shafiei N. Use of tetrazoles in catalysis and energetic applications: Recent developments. Molecular Catalysis. 2021 1;513:111788.

[5] Gharbi S, Zrida H, Hriz K, Chemek M, Wazzan N, Majdoub M. Synthesis of new Tetrazole based-semiconducting polymers for optoelectronic application: Study of the effect of anthracene group on photophysical properties. Journal of Molecular Structure. 2022 15;1250:131760.

The 30th Iranian Seminar of Organic Chemistry
February 7-9, 2025, Iran University of Science and Technology, Tehran, Iran

The Synthesis of Organic Polymers in Advanced Photocatalytic System Under Visible Light

Amir Farkhondeh [a], Foad Kazemi*[a] and Mostafa Gholizadeh [b]

[a] Department of Chemistry, Institute for Advanced Studies in Basic Sciences (IASBS), Zanjan, Iran.
[b] Department of Chemistry, Faculty of Science, Ferdowsi University of Mashhad, Mashhad, Iran.

Introduction:

In recent years, reports show that the use of β-cyclodextrin on the surface of titanium dioxide and the formation of the TiO_2-β-CD structure will lead to an increase in photocatalyst activity.[1] Photopolymerization of free radical is of high commercial importance. Ritter and his colleagues revealed that the first type photoinitiator complex 2-hydroxy-1-phenyl-1-propanone with methylated beta-cyclodextrin causes the formation of a water-soluble host-guest complex. Also, this cyclodextrin complex shows a more effective start for organic monomer polymerization compared to a single photoinitiator.[2] Investigations show that by changing the physical properties of water through magnetization, it can be used as a media solvent in organic reactions. [3] Magnetized water has been passed through a static magnetic field with a certain strength and as a result its physical properties has changed.[4]

Results and Discussion

In this work, photocatalytic polymerization of organic monomers using TiO_2-β-CD, 400nm LED and magnetized water were selected as the model reaction. The reduction of refractive index in magnetized water compared to deionized water makes the water environment transparent when light hits the photocatalyst, and causes more photons to be absorbed and electron transfer to be better, thus increasing the reaction speed. Therefore, the effect of magnetized water and its utilization is reasonable and justified (Scheme).

(Scheme): Synthesis of organic polymers by TiO_2-β-CD as photoinitiator under visible light in magnetized water

Conclusion:

In the present work, by changing the physical properties of water through magnetization, it was used as a green solvent in photocatalytic polymerization. Therefore, in this system and through an efficient method, photocatalytic polymerization of organic monomers using TiO_2-β-CD photocatalyst has been reported as a photoinitiator under visible light.

References:

[1] I. Arora, H. Chawla, A. Chandra, S. Sagadevan and S. Garg, *Inorg. Chem. Commun*. **2022**, 143, 109700.
[2] F. Kazemi, Z. Mohamadnia, B. Kaboudin, Z. Karimi, *J. Appl. Polym. Sci*. **2016**, 133, 19.
[3] M. Bakherad, A. Keivanloo, A. Hossein Amin and A. Farkhondeh, J. Mex. Chem. **2019**, 63, 199-207.
[4] Gholizadeh. M, United States patent US, 10,507,450," process of Chemical Reaction in Magnetized Sovents" **2019**, 12,17.

The 30th Iranian Seminar of Organic Chemistry
February 7-9, 2025, Iran University of Science and Technology, Tehran, Iran

Eosin Y Impregnated Basil Seed Hydrogel: A Metal and Reducing Agent-Free Photocatalyst for p-Nitrophenol Reduction

Shadi Mirzaali Ghanbari[a], Armin Sanei [a], Eskandar Kolvari [a]*, Nadia Koukabi [a], Kheibar Dashtian[b,]*

a Department of Chemistry, Semnan University, P.O. Box 35131-19111, Semnan, Iran

[b] *Department of Chemistry, Iran University of Science and Technology, Tehran, 16846-13114, Iran*

Corresponding author, E-mail addresses: kolvari@semnan.ac.ir (E. Kolvari), kdasht68@gmail.com (K. Dashtian)

Keyword: Photoreduction of p-nitrophenol, eosin Y, Electron Transfer, Visible light irradiation, Metal-Free photoreduction.

The development of biomaterials-based catalysts for photo-induced transformation reactions of organic compounds holds significant promise as a sustainable solution for addressing environmental and resource challenges. The cleanliness, affordability, moderate reaction conditions, ease of handling, sustainability, and, most importantly, the environmental friendliness of visible light as an energy source are what make visible light-induced organic reactions appealing and increase their potential for real-world use [1].Organic photoredox catalysts have been employed in many useful chemical reactions and have developed into effective instruments for activating organic molecules in visible light . In organic synthesis, eosin Y (EY) is frequently employed as a photoredox catalyst. In organic photochemistry, it has been used as an economical and sustainable visible light absorption photocatalyst[2] .Notwithstanding all of the benefits discussed, photoredox dyes frequently experience stability problems in reaction media because of their delicate chromophores, which are readily harmed by various reaction circumstances .For dyes to be used effectively in photoredox catalysis, an efficient stabilizing method is therefore necessary [3]. 3D water-swollen networks made of artificial or naturally occurring polymers are called hydrogels. They are becoming more widely acknowledged as a promising platform for carrying out chemical reactions and bear a striking resemblance to microreactors[4]. In order to overcome this difficulty, hybrid materials that combine photoredox dyes with other hydrogels exhibit promise. Furthermore, these disadvantages can be addressed by the method of creating a covalent link between the photoredox dye and anchoring material, such as hydrogels based on polysaccharides. In addition, reduction reactions of nitroaromatic compounds in a water environment with EY catalyst are typically carried out in the presence of chemical reducing agents (such as $NaBH_4$ or triethanolamine as strong H-donor compounds) and metal/metal-oxide nanoparticles[5]. In the current study, Eosin powder was added to the substrate at room temperature and dried in an oven. p-NP was efficiently transformed into p-AP using an environment-friendly and sustainable photoredox EY-BS catalyst under metal-free conditions and without chemical-reducing agents (Scheme1). The novel photoredox EY-BS catalyst, which contains covalently immobilized eosin Y (EY) dye on Basil seed (BS), exhibited long-term stability and a high photoreduction rate. The findings showed that the BS substrate significantly contributes to catalyst stability in the reaction environment through the rapid regeneration process of oxidized eosin-Y. In the optimal condition, the 96.7% conversion rate of p-NP into p-AP was obtained within 45 min under white LED illumination. We also pointed out BS hydrogel's leading roles as an efficient reducing agent and hydrogen-donor molecule through the SET reaction mechanism. The light absorption characterization analysis of EY-BS shows that utilizing the light-trapping structure of porous hydrogel led to radiant photon management and increased light absorption and harvesting in a wide spectrum. Such a light-trapping behavior makes the EY-BS an intelligent material that may be valuable to apply to photo-mediated organic transformations. The catalyst was extensively characterized using FT-IR, XRD, TGA, TEM, FE-SEM, and EDS. The synthesized EY-BS presents several advantages, including environmental sustainability, cost-effectiveness, and high chemical stability.

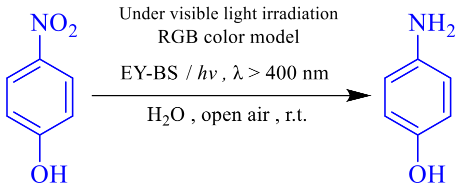

Scheme1

1. Xiong, W., et al., *Ni-Catalyzed Deoxygenative Cross-Coupling of Alcohols with Aryl Chlorides via an Organic Photoredox Process.* ACS Catalysis, 2024. **14**(18): p. 14089-14097.
2. Wu, J.-H. and F. Zhang, *Rapid aerobic visible-light-driven photo-reduction of nitrobenzene.* Science of the total environment, 2020. **710**: p. 136322.
3. Blázquez-Moraleja, A., et al., *Covalent or ionic bonding of Eosin Y to silica: New visible-light photocatalysts for redox wastewater remediation.* Journal of Environmental Chemical Engineering, 2023. **11**(5): p. 111024.
4. Fatima, R. and B. Almeida, *Methods to achieve tissue-mimetic physicochemical properties in hydrogels for regenerative medicine and tissue engineering.* Journal of Materials Chemistry B, 2024.
5. Zhang, Z., et al., *Pd nanoparticles embedded in nanolignin (Pd@ LNP) as a water dispersible catalytic nanoreactor for Cr (VI), 4-nitrophenol reduction and CC coupling reactions.* International Journal of Biological Macromolecules, 2024. **254**: p. 127695.

Investigation of Cobalt Oxide and Graphene-Like Carbon Composite on Carbon Felt for High-Performance Pseudocapacitive Negative Electrodes

Shadi Mirzaali Ghanbari[a], Armin Sanei [a], Eskandar Kolvari [a]*, Nadia Koukabi [a], Kheibar Dashtian[b,]*

a Department of Chemistry, Semnan University, P.O. Box 35131-19111, Semnan, Iran

[b] *Department of Chemistry, Iran University of Science and Technology, Tehran, 16846-13114, Iran*

Corresponding author, E-mail addresses: kolvari@semnan.ac.ir (E. Kolvari), kdasht68@gmail.com (K. Dashtian)

Keyword: Supercapacitor, Pseudo-capacitive, Negative electrode, Carbon felt, Cobalt oxide, Reduced graphene oxide

Pseudocapacitors are appropriate for applications needing a high power density because they have higher energy densities than conventional capacitors and store energy through quick faradaic redox processes. The performance of pseudocapacitive supercapacitors is examined in this paper, with particular attention paid to a negative electrode made of carbon felt that contains active elements such as graphene-like carbon and cobalt oxide. With a specific capacitance of 218 A/g, this electrode showed promise for effective energy storage[1, 2]. Because of their high surface area and conductivity, graphene-like carbon and cobalt oxide, when mixed with carbon felt as a negative electrode substrate, improve capacitive performance.[3]

Hierarchical porous carbon, especially graphene, is widely used to anchor and stabilize mixed metal oxide nano-heterojunctions due to its exceptional properties, such as a large specific surface area, high conductivity, and numerous surface defects. With a charge mobility of approximately 200,000 $cm^2 V^{-1} s^{-1}$, graphene also exhibits chemical inertness, biocompatibility, thermal stability, and electron mediating capabilities, making it an ideal support material for functional components. However, manufacturing processes involving metal oxides often struggle with controlling textural characteristics, hindering the achievement of high graphitization and porosity in graphene. This highlights the need for simple, secure, affordable, and environmentally friendly synthesis methods for these compounds. One promising approach is using biomass as a carbon source to create a hierarchical porous graphene-like carbon (GLC) network suitable for metal oxide loading. Basil seeds (Ocimum basilicum L.), rich in mucilage, provide an inexpensive green precursor for GLC production through pyrolysis. The carboxylic acid and hydroxyl groups in basil seeds enhance metal ion insertion, improving catalyst dispersity, preventing aggregation, and reducing charge recombination due to graphene's carrier capabilities. Moreover, the hierarchical porous carbon network facilitates charge transfer between nanograins, enhancing electron transmission by serving as a charge carrier. [4]

Cobalt oxide and other transition metal oxides are well-known for their pseudocapacitive qualities, which enable them to produce large energy densities via reversible redox processes.[5] In line with the performance of other cutting-edge pseudocapacitive materials, the study's specific capacitance of 218 A/g shows a notable improvement above conventional materials. The electrochemical performance of pseudocapacitors is greatly influenced by the electrolyte selection, in this case potassium hydroxide. It has an impact on the electrode materials' overall stability and ion transport . Long-term applications require cycling stability and rate performance, which can be enhanced by electrolytes with bigger cations, according to studies.[6]

For applications such as hybrid electric vehicles, pseudocapacitors provide a compromise between high power and moderate energy densities, bridging the gap between batteries and capacitors.[3] [5] The nanocatalyst was extensively characterized using FT-IR, XRD, TGA, XPS, HR-TEM, FE-SEM, and EDS. The synthesized Co_3O_4/GLC presents several advantages, including environmental sustainability, cost-effectiveness, and high electrochemical stability.

1. Sanei, A., et al., *Unveiling magnetite metal-organic frameworks for asymmetric pseudo-supercapacitor with high energy density and magnetocapacitance.* Journal of Energy Storage, 2024. **100**: p. 113759.
2. Mao, X., et al., *Surface Reconstruction of Co3O4/rGO heterointerface enabling high-performance asymmetric supercapacitors.* Journal of Energy Storage, 2024. **102**: p. 114128.
3. Reenu, et al., *Electrode materials for supercapacitors: A comprehensive review of advancements and performance.* Journal of Energy Storage, 2024. **84**: p. 110698.
4. Nalkyashree, Z.K., et al., *Synergistic atom co-sharing and S-scheme heterojunction: constructing Cu/CuO/Cu 2 O with ultrathin graphene-like carbon derived from basil seeds*

for enhanced photo-oxidation of benzyl alcohols to aldehydes. Nanoscale Advances, 2024. 6(21): p. 5348-5360.

5. Joseph, A. and T. Thomas, *Pseudocapacitance: An Introduction*, in *Pseudocapacitors: Fundamentals to High Performance Energy Storage Devices*, R.K. Gupta, Editor. 2024, Springer Nature Switzerland: Cham. p. 1-17.
6. Jiang, Y., et al., *Effects of Electrolyte Salts on the Electrochemical Performance of Aromatic Polyaroxydiazole Anodes for Pseudocapacitors.* ACS Applied Energy Materials, 2024. 7(23): p. 11161-11171.

The 30th Iranian Seminar of Organic Chemistry
February 7-9, 2025, Iran University of Science and Technology, Tehran, Iran

Investigation of catalytic properties of metal-organic framework (MIL-53(Fe)) in the preparation of some heterocyclic compounds (Bispyrazolyl methanes

Samira Bujarian-movahed[a], Majid Rezaeivala[a,*], Ahmadreza Mousavi-zare[a]

[a]*Faculty of Chemical Engineering and Basic Sciences, Hamedan University of Technology, Hamedan,65155, Iran (email:mrezaeivala@hut.ac.ir)*

Keyword: Metal-organic framework(MOF), MIL-53(Fe), Bispyrazolylmethane, Green chemistry

Investigating the catalytic properties of the MIL-53(Fe) metal framework in the synthesis of bis(3-metyl-1-phenyl-1H-pyrazol-5-ol)s [1]. Bispyrazolyl methane derivatives used through the three-component one-pot condensation reaction of phenylhydrazine,acetoacetate and aromatic aldehydes. This reaction is used in neutral and solvent-free environments and it is catalyzed by green chemistry. This method has several advantages, including non-toxic materials, high yield, short reaction time, and clean operation. Pyrazoles have attracted particular attention due to the diverse biological activities associated with this heterocyclic system, and some have been shown to be cytotoxic to several human cell lines. Several drugs currently on the market have this heterocycle as the key structural motif, and some have been approved for the treatment of different types of cancer [2].

MIL-53(Fe) is synthesized and fully investigated by XRD, MAPPING, EDAX, SEM, FT-IR, VSM, TGA and AFM. Bis(3-metyl-1-phenyl-1H-pyrazol-5-ol)s are checked by ^{1}HNMR, ^{13}CNMR, FT-IR, MASS, Investigation of Anticancer and anti corrosion activity

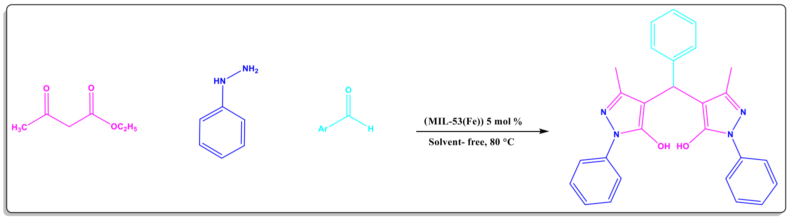

Scheme. Synthesis of Bispyrazolylmethanes derivatives in the presence of MIL-53(Fe)

References:

[1]. Zhou, J., Han, X., Ke, T., van Baten, J. M., Bao, Z., Zhang, Z., ... & Yang, Q. (2024). Engineering pore limiting diameter of metal–organic frameworks for benchmark separation of mono-and di-branched hexane isomers. Chemical Engineering Journal, 488, 150833. https://doi.org/10.1016/j.cej.2024.150833

[2]. Hojati, S. F., Amiri, A., Mohamadi, S., & Soleimanian, S. (2023). MOF-199 as an Efficient Metal Organic Framework Catalyst for the Synthesis of Spiro [Indoline-3, 4′-Pyrano [2, 3-c] Pyrazole] Derivatives. Polycyclic Aromatic Compounds, 43(9), 8134-8146. https2144915://doi.org/10.1080/10406638.2022.

The 30th Iranian Seminar of Organic Chemistry
February 7-9, 2025, Iran University of Science and Technology, Tehran, Iran

Investigating the anticancer properties of some Bispyrazolyl methane derivatives catalyzed by Metal-Organic Framework (MIL(53)Fe)

Samira Bujarian-movahed[a], Majid Rezaeivala[a,*], Ahmadreza Mousavi-zare[a]

[a]*Faculty of Chemical Engineering and Basic Sciences, Hamedan University of Technology, Hamedan,65155, Iran (email:mrezaeivala@hut.ac.ir)*

Keyword: :Bispyrazolyl methane, MIL(53)Fe, MTT, Cytotoxic, cell line, Anti cancer .

Due to the anticancer properties of some pyrazolyl, in this work have been demonstrated to 14 compound of pyrazolyl derivatives to were synthesized in the presence of MIL-53(Fe), to be cytotoxic on several human cell lines namely, glioblastoma (U-87), breast (MCF-7), cervical (HeLa), colon (HT-29), prostate (DU-145), and normal mouse adipose fibroblast cell line (L-929). MTT assay using to evaluate cell viability for 48 h [1, 2].

Cell lines was purchased (ATCC, Manassas, VA, USA). Line (L-929) was purchased from the (ECACC, Salisbury, UK). DMEM (Gibco) . The media were supplemented with a 1% penicillin and streptomycin mixture (100 U/mL penicillin, and 100 µg/ml streptomycin) (Gibco 15140-122) and mixed with 10% heat-inactivated fetal bovine serum (Capricorn FHS-HI-12B). Cells were passaged at 70–80% confluence, about twice a week by trypsinization (Multicell 325-542-C1). DMSO and cisplatin (Sigma-Aldrich).

conclusion: [a] Non-cancer cells.[b]The data are presented as IC_{50} values represents the mean ± S.E.M, µM, obtained by five replicates experiments (n=5), as measured by the MTT assay after 48 h of incubation. Cisplatin was used as positive control. SI = IC_{50} of a compound in a normal cell line/IC_{50} of the same compound in the cancer cell line. A favorable SI > 1.0 indicates a drug with efficacy against tumor cells greater than the toxicity against normal cells.

The selectivity index (SI) was calculated to evaluate the toxicity of the compounds studied against normal cells and to predict their therapeutic potential. High SI values result from large differences between the cytotoxicity against cancer and normal cells. From the tested compounds with **BPM-3** and **BPM-13** have showed SI >1.0. Complex **BPM-3** (SI>17.7) and **BPM-13** (SI>3.12) have highest selectivity index for DU-145 and MCF-7 cancer cells, respectively.

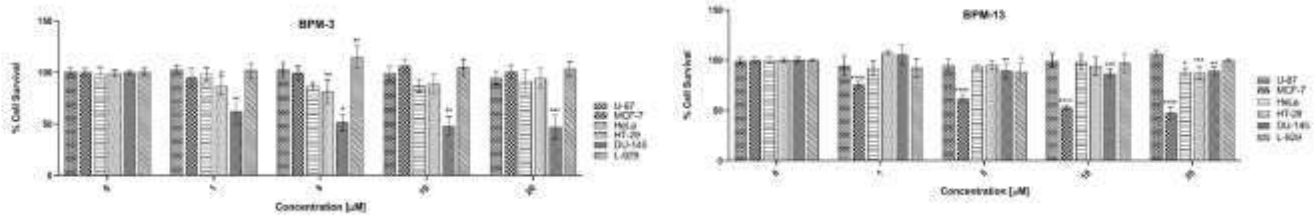

Scheme. Two examples of cell lines (**BPM-3** and **BPM-13**)

	IC$_{50}$ (μM)^{b}					
	Cell Line					
	U-87	**MCF-7**	**HeLa**	**HT-29**	**DU-145**	**L-929^{a}**
BPM 1	>20	>20	>20	>20	>20	>20
BPM 2	>20	>20	>20	>20	>20	>20
BPM 3	>20	>20	>20	>20	1.13 ± 1.40 SI^{c} > 17.7	>20
BPM 4	>20	>20	>20	>20	>20	>20
BPM 5	>20	>20	>20	>20	>20	>20
BPM 6	>20	>20	>20	>20	>20	>20
BPM 7	>20	>20	>20	>20	>20	>20
BPM 8	>20	>20	>20	>20	>20	>20
BPM 9	>20	>20	>20	>20	>20	>20
BPM 10	>20	>20	>20	>20	>20	>20
BPM 11	>20	>20	>20	>20	>20	>20
BPM 12	>20	>20	>20	>20	>20	>20
BPM 13	>20	6.40 ± 0.17 SI^{c} > 3.12	>20	>20	>20	>20
BPM 14	>20	>20	>20	>20	>20	>20
Cisplatin	>20	>20	>20	>20>20	>20	>20

Scheme. Cytotoxic activity of synhesized compounds (**BPM 1-14**) and cisplatin against human cancer cells and L-929 non-cancer cells *in vitro* IC$_{50}$ (μM)

References:

[1]. Mani, P., Murugan, R., Kasi, V., & Namasivayam, S. (2024). Crystal structure, DFT investigation, molecular docking, antioxidant and thrombolytic investigation of thioxo pyrimidine-5-carboxylate. Polycyclic Aromatic Compounds, 44(2), 1095-1108. https://doi.org/10.1080/10406638.2023.2186443

[2]. T Mosmann. Rapid colorimetric assay for cellular growth and survival: application to proliferation and cytotoxicity assays. J Immunol Methods. 1983 Dec 16;65(1-2):55-63. doi: 10.1016/0022-1759(83)90303-4.

The 30th Iranian Seminar of Organic Chemistry
February 7-9, 2025, Iran University of Science and Technology, Tehran, Iran

Preparation of basic ceramic nanocatalyst based on eggshell waste using ultrasonic waves and its application in the synthesis of some DHPMs compounds

Asadollah Farhadi

Department of Basic Sciences, Petroleum University of Technology, Ahvaz, Iran, 61981-44471

farhadichem@put.ac.ir

Abstract: In this research, ceramic nanocatalyst based on eggshell (ES) was prepared from food waste using ultrasonic wave method. Ultrasonic bath waves were used to prepare nanoparticles of this catalyst. This catalyst was characterized by FESEM, EDX and zeta potential spectrum. Finally, some 3,4-DHPMs were synthesize by this catalyst.

Keywords: Eggshell, Catalyst, FESEM, EDX, Zeta potential, 3,4-DHPMs

---

۱. Introduction

Used the chemical compounds as catalyst lead to generation the toxicity problem and environmental issues. So, it is very necessary to using the green reactants in chemical reaction. There have been reviews on use of egg shell (ES) waste focusing on synthesis of syngas, dimethyl carbonate, and waste water. Also, the synthesis of Schiff bases compounds and biodiesel production from green waste and nonedible cooking oil waste in particular by using ES was investigated [1,2] So, in this project used the egg shell as base catalyst for synthesis of some heterocyclic compounds.

۲. Experiment Section

۲,۱. Materials and Equipments

Catalyst was prepared from recycled egg shells. Compounds were purchased from Sigma-Aldrich chemical company. The entire materials were used without any further purification.

Melting points were determined on a Melting point meter M3000 apparatus and were uncorrected. FT-IR spectrum was recorded from KBr discs on a Bruker ALPHA FTIR spectrometer. ^{1}HNMR spectrum was recorded using a Bruker Ascend 300 ^{1}HNMR machine. Morphological analysis of the particle was obtained by Field Emission Scanning Electron Microscope (FESEM TESCAN MIRA2) apparatus which was equipped with an X-ray unit at an accelerator voltage of 20 kW. Zeta spectrum was recorded using Malvern Instruments apparatus.

۲,۲. Preparation of ES catalyst

At first step, the outer shell of the egg was separated, then the thin white layer that was attached to the inner wall of the shell was removed. The remaining shell was ground into finer powder particles by grinding. To separate the organic compounds, present in the resulting powder, 5 grams of the powder was mixed with 50 mL of ethanol and refluxed for 1 hour. Then the powder was mixed with water, and was placed in an ultrasonic bath for 5 hours. Finally, the resulting mixture was filtered and placed in an oven at 100°C for 5 hours. The structure of ES was characterized by FESEM, EDX and Zeta potential spectrums.

٢,٣. Synthesis of some 3,4-dihydropydrimidin-2(1*H*)-ones (DHPMs) using ES as catalyst

According data of optimization conditions for synthesis of for 2**a** compound are obtained, for synthesis of DHPMs is used 10 mmol of aldehydes, 10 mmol of EAA, 12 mmol of urea and 0.1 g of ES as catalyst in ethanol as solvent under reflux conditions. (Scheme 1)

$$\underset{1\ \mathbf{a\text{-}o}}{\mathrm{ArCHO}} + \mathrm{EAA} + \mathrm{Urea} \xrightarrow[\mathrm{EtOH/\ reflux}]{\mathrm{ES}} \underset{2\ \mathbf{a\text{-}o}}{\mathrm{3,4\text{-}DHPMs}}$$

X: H (a), 4-MeO (b), 3-MeO (c), 2-MeO (d), 4-Cl (e), 3-Cl (f), 2-Cl (g), 4-NO_2 (h), 3-NO_2 (i), 4-Me (j), 3-Me (k), 2-Me(l), 4-Br (m), 3-Br (n), 2-Br (o)

Scheme 1: Synthesis of various 3,4-DHPMs by used ES as catalyst.

٣. Results and Discussion

According to data that obtained from FESEM, the particles size of catalyst is below 80 nm. Also, the morphology of ES catalyst prepared is similar to structure reported in pervious paper. [3]. EDX data obtained, confirm the exist of Ca and Mg compounds in this catalyst. Too, according to zeta potential data, the potential of ES in water as solvent is 1.1 V and the average particle size is 2231 nm. The zeta potential show that the surface charge of ES is positive. As well, for confirm the basic property of ES catalyst, pH of water solution of its was recorded. pH of mixture that contain 1 g of ES catalyst in 20 mL of distilled water at 25 ºC after 2 h was 11.

Conclusion

In this work, an extremely simple, convenient and efficient protocol for the synthesis of some DHPMs by using ES as catalyst was reported, because:

1. It does less harm to the environment; 2- It is economically more efficient; 3- Compared to some chemical catalysts use, this method has better reaction efficiency and time the reaction is less.

References:

[1] Patil, S., Jadhav, S. D., Shinde, S. K. *Org. Chem. Int.* (2012) *2012*, 1–5.

[2] Aleman-Ramirez, J.L., Okoye, P. U., Torres-Arellano, S., Paraguay-Delgado, F., Mejía-López, M., Moreira, J., Sebastian, P.J. *Fuel.* (2022) *324*, 124601.

[3] Awais, A., Jini. D., Aravind. M., Parvathiraja. C., Rabia. A., Kiyani. M.Z., Alothman. A. *Arab. J. Chem.* (2020) *13*, 8717–8722.

Investigated the production of methanol from CO_2 by used Zeta potential spectra and DFT method

Asadollah Farhadi

Department of Basic Sciences, Petroleum University of Technology, Ahvaz, Iran, 61981-44471

farhadichem@put.ac.ir

Abstract: Currently, demand for using the fossil fuels such as petroleum oil and coal energy are growing swiftly with global economic growth. These fuels are major environmental threats due to the release of CO_2 into the atmosphere. So, used the technology for reducing greenhouse gases is one of the novel methods today. One a way method for reduction this gas, used the various catalysts for conversion it to methanol. In this work, the zeta potential spectra were used for investigation of this reaction. Data obtained from zeta potential shown that Al_2O_3 is the best nano catalyst for production methanol.

Keywords: CO_2, Methanol, Zeta Potential, Al_2O_3, DFT

---

٤. Introduction

In recent years, many industrial fields used fossil fuels, which contribute to greenhouse gas (GHG) emissions, especially carbon dioxide (CO_2). this parameter was led to increase the global temperature [1,2]. Compared with the GHG level in 2010, CO_2 reduction of 41–72% by 2050 and 78–118% by 2100 is necessary to preserve the temperature change below 2 ◦C relative to preindustrial levels. [3] In this case, converting CO_2 into valuable products through several processes is one of the promising strategies for reducing its emission. For instance, electrocatalytic and photocatalytic CO_2 reduction is subjected as a potential process for future. Several important chemical products could be obtained from this process, e.g., methane, alkanes, carbon monoxide, olefins, and alcohol [4]. Therefore, methanol production from CO_2 benefits from environmental and economic points of view. Generally, a catalyst is needed to transform the CO_2 into a methanol product because CO_2 is a highly stable molecule. Some of these catalysts are Cu, Zn, Cr, V_2O_5 and others compounds [5]

٥. Experiment Section

٥,١. Materials and Equipment

Compounds were purchased from Sigma-Aldrich chemical company. The entire materials were used without any further purification. Zeta spectrum was recorded using Malvern Instruments apparatus. Density functional theory was done by Gaussian software.

٢,٣. Synthesis of Methanol from CO_2

Recently, producing methanol from CO_2 is a promising pathway because this method is benefitting environmental point of view. Generation of methanol from greenhouse gas leads to reduce impact environmental and help to resolving climate change. CuO, ZnO and Al_2O_3 as catalysts for synthesis of methanol were used [6]. Used of zeta potential spectra helps to investigation the mechanism of this reaction. So, in this work, zeta potential of CuO, ZrO_2, Fe_2O_3 and Al_2O_3 nano catalysts in water media was done. Data obtained of these catalysts are reported in Table 1.

Table 1: Zeta potial of some nano catalyst in water media in range -200 to +200 (eV).

catalyst	CuO	ZrO_2	Fe_2O_3	Al_2O_3
Zeta potential (eV)	+105	+80.3	+56.9	+123

۳. Results and Discussion

Data reported in Table 1, shown that the Al_2O_3 has the more zeta potential data, for this reason this compound is the best catalysts for conversion of CO_2 to methanol. According to data reported in Table 1, the best mechanism was proposed for conversion of CO_2 to methanol.

Conclusion

The results reported based on the potential spectrum of colloidal suspensions of some catalysts used in methanol synthesis show that the charge on the surface of these catalysts is positive, which is why these catalysts play a significant role in the conversion of greenhouse gases to methanol. Also, the use of mixed catalysts increases the surface charge, which is one of the reasons for increasing the rate of methanol production under milder conditions.

References:

[1] Pana, S., Chen, G., Rena, W., Dangala, S.R.S., Bangera, K., Yanga, J., Taoa, B., Tian, H. *International J. Digital Earth.* (2018) 11, 558–582.

[2] Kabir, M., Habiba, U., Khan, W., Shah, A., Rahim, S., Rios-Escalante, P.R. D., Farooqi, Z.-U.-R., Ali, L., Shafiq, M. *J. King Saud University - Science.* (2023) 35, 102693.

[3] Azhari, N.J., Erika, D., Mardiana, S., Ilmi, T., Gunawan, M.L., Makertihartha, I.G.B.N., Kadja, G. T.M. *Results in Engineering.* (2022) 16, 100711

[4] Lawes, N., Gow, I. E., Smith, L. R. et al, *Faraday Discuss.* (2023) 242, 193-211

[5] فرهادی، مجله علمی *پژوهشی گاز*، (۲۰۲۲) ۱۷، ۲۷-۱۸.

[6] Prapatsorn, B., Aroonsri, N. *Front. Energy Rese.* (2019) 7, 1-10.

Synthesis and characterization of new Rotaxanes from related crown compounds

Abdullah Najdhashemi[1]*, Samad Bavili Tabrizi[1]*, Mirzaagha Babazadeh[1]

1 Department of Chemistry, Faculty of Science, Tabriz Branch, Islamic Azad University, Tabriz, I.R. IRAN

*Corresponding Authors: 1:stu.anhashemi@iaut.ac.ir, 2:stbavili@gmail.com

Abstract

Physical manipulation can be carried out on molecules and cells through the utilization of nanomachines which are machines with nano dimensions. There are different types of nanomachines .Among them, rotaxanes stand out as the most well-known. The term of rotaxane originates from the combination of the Latin words wheel and axis. The application of nanomachines is identifying and measuring the concentration of toxic substances in the environment, targeted drug delivery and cancer diagnosis .The objective of this study is to synthesize and identify several new nanomachines in the form of rotaxanes (internally locked molecules) with nanopharmaceutical properties from the corresponding crown compounds. In the first step, 2,2-dimethylphenol was converted into bisphenol compound (1) in reaction with thionyl chloride. Bisphenol compound (1) was converted into methyl diester compound (2) in reaction with methyl chloroacetate. The methyl diester compound (2) reacts with the appropriate diamine to form the diamide macrocycle compound (3). Rod (4) is prepared from the reaction of diethylene glycol ditosylate, 4,4-bipyridine and a bulk phenol such as 4-tert-butylphenol in DMF. Each of the rings in the presence of the prepared rod leads to the corresponding rotaxane compound (5). Chemical structure of the obtained compounds were established by ^{1}HNMR, ^{13}CNMR, FT-IR and SEM spectroscopic methods.

Keywords: Nano machine, Drug delivery, Cancer diagnosis, Rotaxane, Interlocked compounds

١. Introduction

In recent times, there has been a significant advancement in the realm of supramolecular chemistry [1]. This progress has led to its widespread use in various fields owing to its ability to employ precise, directional, adjustable, and reversible molecular recognition motifs [2-6]. One area of particular interest is the development of molecular machines using mechanically interlocked molecules (MIMs) [7]. These MIMs involve the assembly of multiple components that are mechanicaly connected [8, 9]. For instance, rotaxanes and pseudorotaxanes are examples of such MIMs which are formed through the utilization of macrocyclic molecules including crown ethers, cyclodextrin, cucurbituril, and calixarene. These macrocyclic molecules have proven to be extremely valuable in diverse areas such as supramolecular gels, fluorescence studies, and biological applications [9-14].

The manipulation of molecular motion on a molecular scale presents an extraordinary challenge for contemporary nanotechnology. As a result, there has been a rapid advancement in the development of mechanically interlocked molecules that possess the ability to effectively react to external stimuli [15-21]. Amongst these compounds, rotaxanes have garnered considerable attention due to their remarkable potential as molecular switches and machines [22, 23]. The composition of rotaxanes entails the mechanical interlocking of a macrocycle (a molecular wheel) onto a thread-like molecular axle with the aid of bulky stoppers. Additionally, rotaxanes incorporate two or more recognition sites, known as stations, which enable the macrocycle to seamlessly traverse between them along the thread [24, 25].

The components of the molecular machines are continuously in random motion due to thermal fluctuations, unlike their macroscopic counterparts . Consequently, when energy is provided to these molecular systems, often in the form of chemical [26, 27], electrochemical [28, 29], or photochemical input [30, 31], it disrupts their equilibrium for a short time and influence the macrocycles movement in a specific direction [32-35]. The activation of light as an energy source has advantages since it does not produce any byproducts and can directly convert solar energy into mechanical work. Additionally, when researchers combine this light-induced molecular motion with optical monitoring using time-resolved laser spectroscopy techniques that are able to track changes over time very precisely, they gain a superior ability to analyze intricate kinetics [25].

The linkage of molecules through non-covalent, mechanical bonds allows for the development of unique physical and chemical qualities in these supramolecular systems that are hard to attain or perhaps impossible through conventional synthetic methodologies [36, 37]. With the use of external stimuli, scientists have made headlines by successfully controlling the shape and dynamic motion of mechanically interlocked molecules, leading to advancements in artificial molecular machine development [38]. Functional supramolecular compounds have exhibited versatility through their application in various areas including logic gates or molecular switches for electronic devices [39], controlled drug release [40], and catalytic activity [41, 42]. rotaxanes can be particularly useful in advanced drug delivery mechanisms that rely on enzyme-mediated separation and subsequent activation of prodrugs within tumor cells [43-45].

۲. MTERIALS AND METHODS

۱،۲. Synthesis of 2,2´-bis[(2-(4-methyl 1-hydroxy)phenyl)] sulfoxide (1):

To perform this reaction, we used the method reported by Bavili et al. Based on this method, 200 ml of dry dichloromethane (25 g, 0.187 mol) and aluminum chloride were stirred in an ice bath environment. Then 16 ml (2 mol) of 2,4-dimethylphenol was gradually added and stirred for half an hour. After stirring for half an hour, a mixture of 8 ml of thionyl chloride solution and 50 ml of dry dichloromethane was added dropwise to the solution. The mixture was stirred in an ice bath for 15 h until a white precipitate formed. After that, the precipitate was filtered using a Buchner funnel and then washed with 35 mL of chloroform and 5 mL of 10% HCl solution to remove aluminum oxide. After that, distilled water is added to neutralize the pH of the solution. After washing and separating the organic phase from the aqueous phase, the precipitate was crystallized and purified in ethanol. The melting point of the product was 192-196 ℃ and the reaction yield was 65%. The reaction carried out is shown in diagram (1) [46].

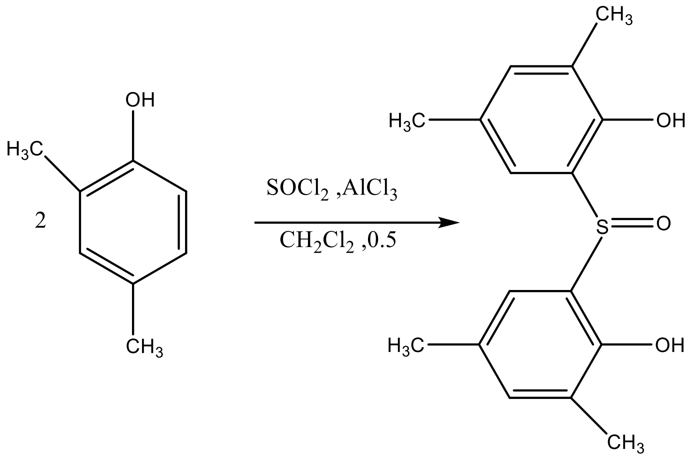

Scheme 5: synthesized compounds structure of dihydroxy crown is well-formed.

IR (KBr): 3450, 3310, 1889, 1762, 1668, 1642, 1450, 1226, 1052 cm^{-1}

^1H NMR (400 MHz, $CDCl_3$) δ: 2.23 (s, 6H), 2.26 (s, 6H) , 6.73 (s, 2H), 6.84 (b, 2H) , 7.05 (s, 2H) ppm

۲,۲. Synthesis of Sulfoxo-2,'2-bis[(2,4-dimethyl) phenoxy) methylacetate] (2):

To carry out this reaction, a mixture of bisphenol (1) (8 g, 0.0017 mol), methyl chloroacetate (5.86 mL, 0.0034 mol), potassium carbonate (7.46 g, 0.0034 mol), and potassium iodide (0.23 mol, 0.23 mol) was added. 0.) was prepared. Then 100 ml of acetonitrile was added and the resulting mixture was refluxed for 18 hours. The mixture was filtered using a Buchner funnel and purified using methanol. The obtained pure compound shows a melting point in the range of 98-100 °C and its Rf value was determined to be 0.3 in the ethyl acetate/petroleum ether (3:1) solvent system. It is also essential to maintain the system temperature below 5°C during the initial 8-hour period [47].

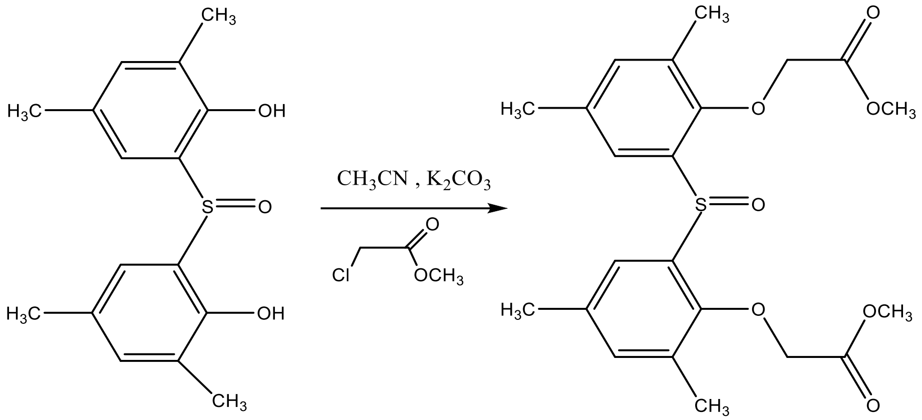

Scheme 6: Sulfoxo 2,'2-bis[(2,4-dimethyl methoxy) methylacetate].

IR(KBr): 2915, 2858, 1740, 1720, 1600, 1577, 1200, 1069 cm^{-1}

^{1}H NMR (400 MHz,$CDCl_3$) δ: 2.23 (s, 6H), 2.26 (s, 6H), 3.82 (s, 6H), 4.56 (s, 4H)، 6.81(s, 2H), 7/02 (s ,2H) ppm

۳٫۲. Synthesis of diamide macrocycles

I.Synthesis of 1,7-dioxo-4-sulfoxo-11-methyl-2,3-5,6-di(2′,4′-dimethyl)benzo-10,13-diaza-14-crown-5 (3a):

Diasteremethyl (2) (0.0046 mol, 2 g) and 1,2-diaminopropane (0.39 mL) were added to 25 mL of methanol and refluxed for 18 h. Triethylamine or pyridine was used to increase the reaction yield. The solvent was removed by rotary and a white precipitate remained. Then the precipitate was crystallized in methanol, which led to the formation of white cotton crystals. The reaction yield is 75% and Rf = 0.1-0.2 in the ethyl acetate/methanol (1:2) solvent system.

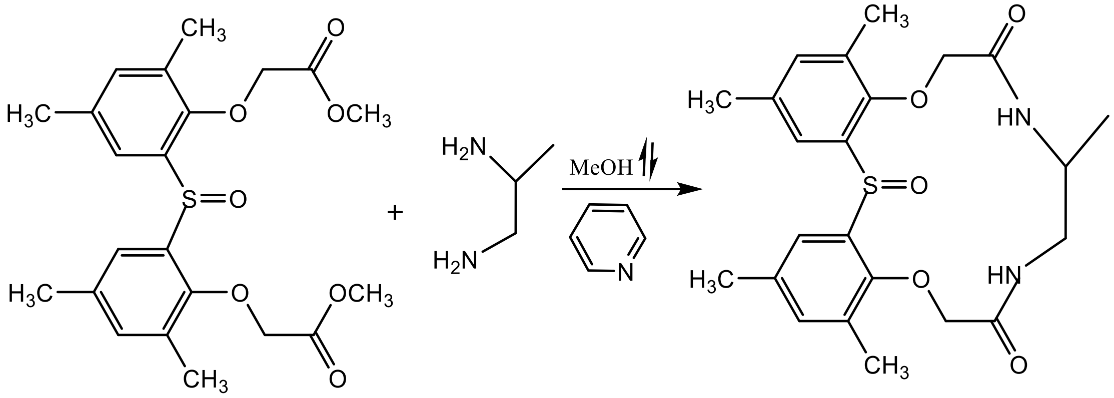

Scheme 7: Synthesis of crown diamide macrocycle (3a).

IR(KBr, cm^{-1}): 3449, 3010, 2921, 1696, 1671, 1494, 1251, 1212, 1072, 894 cm^{-1}
^{١}H NMR (٥٠٠ MHz,CDCl$_{٣}$) δ: ١٫٠٧ (s, ٣H), ٢٫٢ (s, ٦H), ٢٫٢٥ (s, ٦H) ،٣٫٣٢- 3.33 (m, 1H), 4.29-4.31 (d, 2H, J= 8 Hz), 4.83 (s, 4H), 6.91 (s, 2H), 7.29 (s, 2H), 7.38 (s, 2H) ppm.
^{13}C (500 MHz,CDCl$_3$) δ: 168.50, 154.06, 134.03, 131.83, 129.08, 126.66, 113.53, 68.19, 39.86, 38.51, 22.94 , 21.9, 19.47 ppm.

II. Synthesis of 1, 7-dioxa-9, 30-dixo-10, 13, 16, 19-tetraaza-4-sulfoxo-2, 3, 5, 6-di(2, 4-dimethyl)benzo- 21- Crown-7 (3b):

Diasteremethyl (2) (0.0046 mol, 2 g) and triethylene tetraamine (0.68 ml) were added to 20 mL of methanol and refluxed for 18 h. The solvent was removed by rotary and a white viscous precipitate remained. Then the precipitate was crystallized in methanol, which led to the formation of white cotton crystals. The reaction yield is 75% and Rf value ranged from 0.0 to 1.2 in the ethyl acetate/methanol (1:2) solvent system.

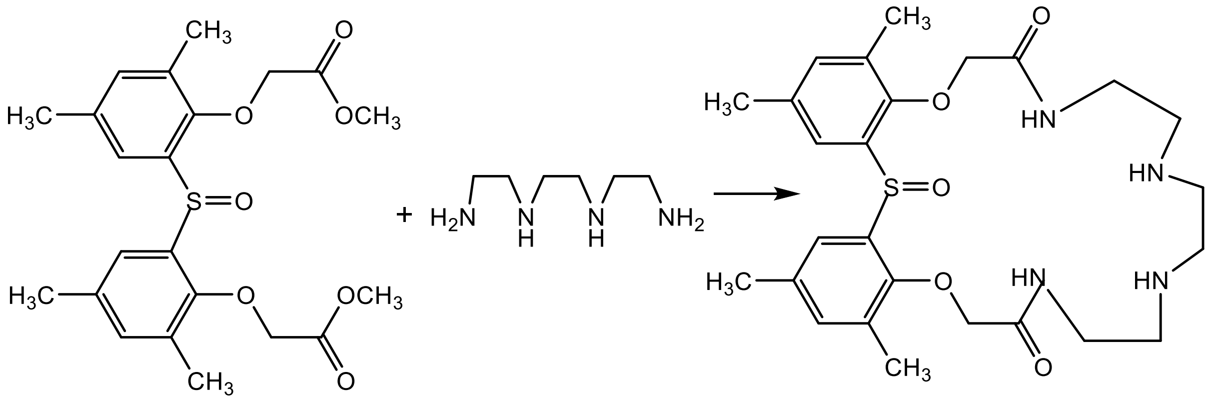

Scheme 8: Crown diamide macrocycle (3b).

IR(KBr, cm^{-1}): 3420, 3398, 3040, 2850, 1680,1570, 1490, 1368, 1350, 1074, 830 cm^{-1}
^{1}H NMR (400 MHz,CDCl$_3$)δ: 2.22 (s, 6H) 2.24 (s, 6H), 2.73- 2.76 (t, 4H, J= 9 Hz), 2.89- 2.92 (t, 4H, J= 12 Hz), 3.33 - 3.37 (m, 4H) , 4.65 (b, 2H), 6.92 (s, 2H), 7.04 (s, 2H), 7.38 (s, 2H) ppm.

^{13}C NMR(400 MHz,$CDCl_3$) δ: 168.27, 153.58, 132.61, 132.51, 129.7, 122.19, 112.29, 67.88, ٤٩,٣٣, ٤٢,٤٣, ٣٩,٢٥, ٢٠,٩, ٢٠,٨ ppm.

٤,٢. Synthesis of N-((4-tertbutyl methoxy) ethoxy) ethyl) 4,4′-bipyridinium axel (4):

Synthesis of axle has 2 steps. In the first step, 2 mol, (1 g) diethylene glycol ditosylate and 2 mol, (0.881 g) 4-tertiobutylphenol and 0.372 g of potassium carbonate were refluxed in 20 ml of acetonitrile for 18 hours. Then the solvent was removed by rotary. The contents of the flask were extracted with 20 ml of chloroform. A white solid product was obtained and was crystallized in ethanol solvent.

In the next step, 0.615 g of the material obtained from the first step and 0.2 g (1 mol) 4,4′-bipyridinium were refluxed in 20 ml of DMF solvent for 18 hours. Then the solvent was evaporated by rotary. Recrystallization of the product in ethanol resulted in cottony white crystals.

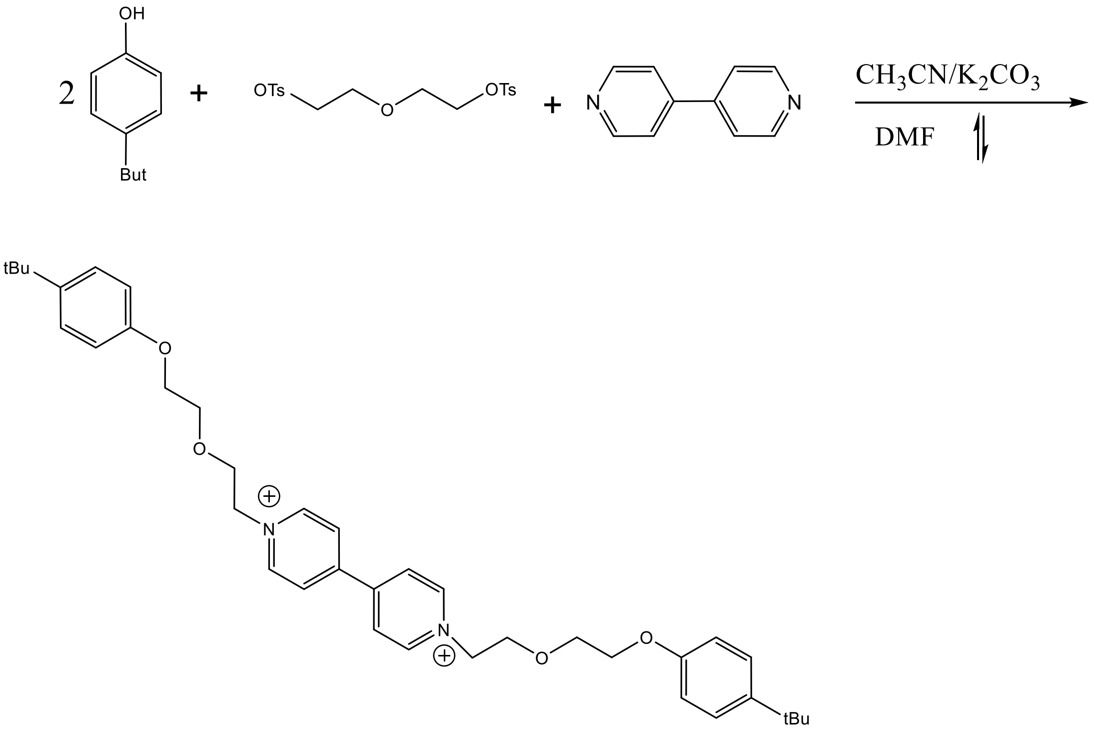

Scheme 9: synthesis of axle.

IR (KBr, cm^{-1}): 3432, 3380,3047, 2957, 1506, 1360, 1215, 1121, 1011, 815 cm^{-1}

^{1}H NMR (500 MHz,CDCl$_3$) δ: 1.3 (s, 9H), 3.71- 3.74 (m, 2H), 3.95- 3.97 (m, 2H), 4.10- 4.12 (m, 2H), 4.46- 4.48 (m, 2H), 6.74- 6.76 (d, 2H, J= 10 Hz), 7.25- 7.27 (d, 2H, J= 9 Hz), 8.86- 8.89 (d, 2H, J= 15.5 Hz), 9.30-9.32 (d, 2H, J= 10.5 Hz) ppm.

^{13}C NMR (500 MHz,CDCl$_3$) δ: 157.15, 151.66, 146.37, 145.90, 126.91, 124.28, 114.72, 69.29, 68.82, 68.32, 56.05, 34.43.ppm.

۵,۲. Synthesis of rotaxane nanomachines

I. Binding between axle and 1,7-dioxo-4-sulfoxo-11-methyl-2,3-5,6-di(2,4-dimethyl)benzo-10,13-diaza-14- wheel with Crown-5 (5a):

Axle and wheel (3a) with a molar ratio of 1:1 was refluxed in methanol solvent for 12 hours in the presence of templating metal. Then the solvent was removed by rotary and the material obtained was washed with hydrogenated water and distilled water. The obtained product crystallized in ethanol and resulted in cotton-white crystals.

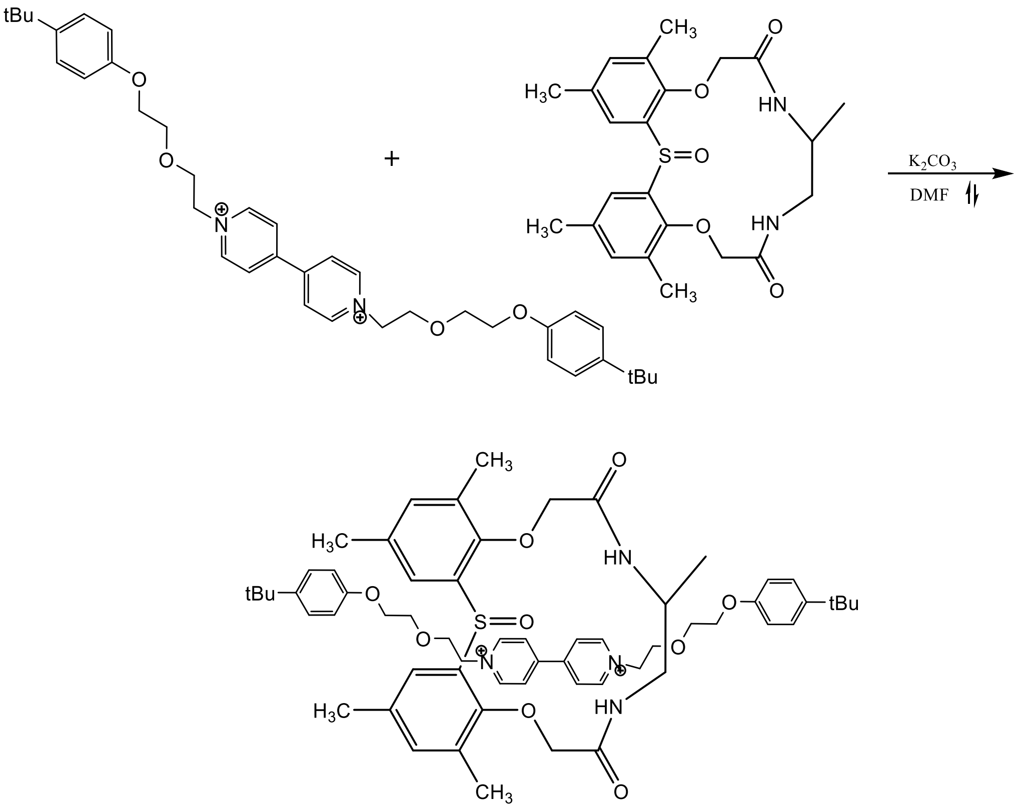

Scheme 10: Rotaxane (5a)

IR(KBr, cm^{-1}): 3449, 3432, 3380, 3047, 3010, 2957, 2921, 1696, 1671, 1506, 1494, 1360, 1251, 1215, 1212, 1121, 1072, 1011, 894, 815 cm^{-1}

^1H NMR (500 MHz,$CDCl_3$) δ: 1.07 (s, 3H), 1.3 (s, 9H), 2.2 (s, 6H), 2.25 (s, 6H), 3.32-3.33 (d, 2H, J= 5 Hz), 3.71- 3.74 (m, 2H), 3.95-3.97 (m, 2H), 4.10- 4.12 (m, 2H), 4.29- 4.31 (d, 2H, J= 7.5 Hz), 4.46- 4.48 (m, 2H), 4.83 (s, 4H), 6.74- 6.76 (d, 2H, J= 10 Hz), 6.91 (s, 2H), 7.25- 7.27 (d, 2H, J= 15.5 Hz), 7.29 (s, 2H), 7.38 (s, 2H), 8.86- 8.89 (d, 2H, J= 15.5 Hz), 9.30-9.32 (d, 2H, J= 10.5 Hz) ppm.

^{13}C NMR (500 MHz,$CDCl_3$) δ: 168.50, 157.15, 154.06, 151.66, 146.37, 145.90, 134.03, 131.83, 129.08, 126.91,126.66, 124.28, 114.72, 113.53, 69.29, 68.82, 68.32, 68.19, 56.05, 39.86, 38.51, 34.43, 22.94, 21.9 19.47 ppm.

II. Binding between axle and 1, 7-dioxa-9, 30-dixo-10, 13, 16, 19-tetraaza-4-sulfoxo-2, 3, 5, 6-di(2, 4-dimethyl)benzo-21-wheel with Crown -7 (5b):

Axle and wheel (3b) with a molar ratio of 1:1 was refluxed in methanol solvent for 12 hours in the presence of templating metal. Then the solvent was removed by rotary and the material obtained was washed with hydrogenated water and distilled water. The obtained product crystallized in ethanol and resulted in cotton-white crystals.

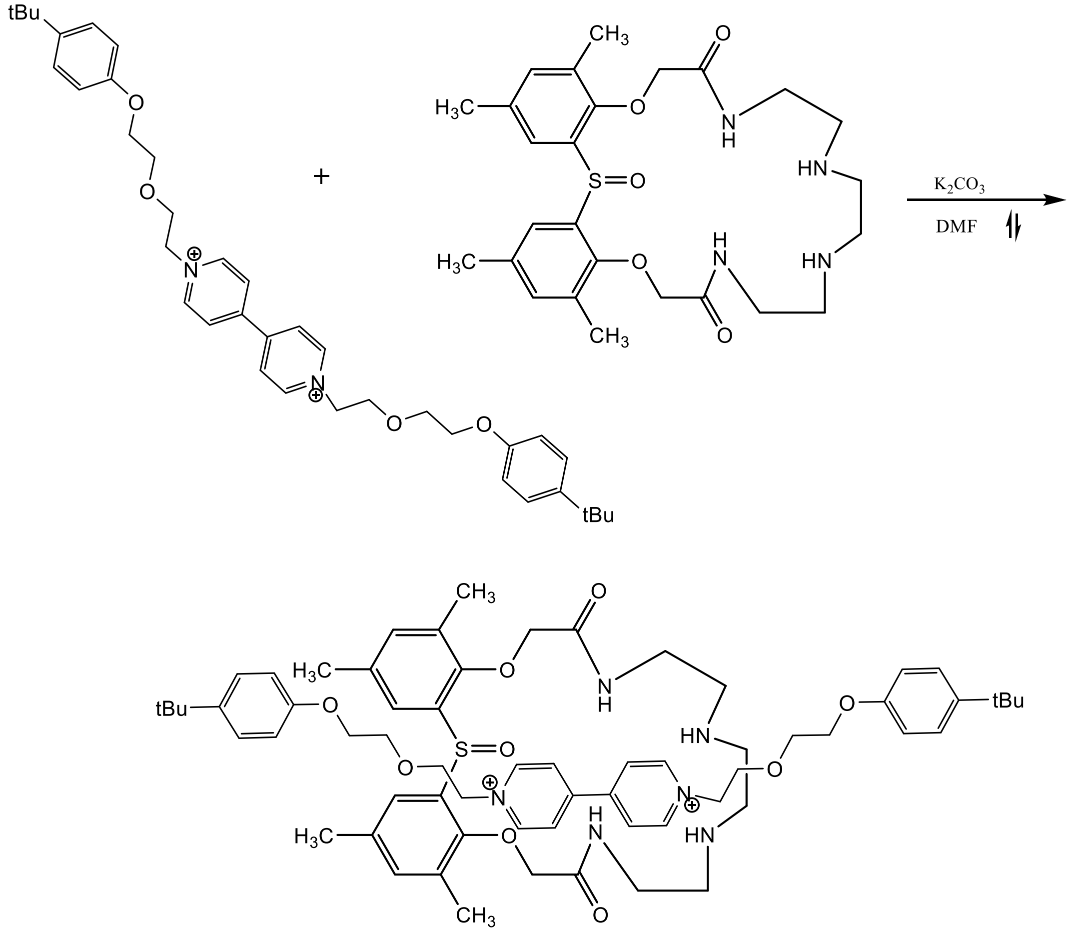

Scheme 11: Rotaxane (5b)

IR(KBr, cm^{-1}): 3432, 3420, 3380, 3047, 3040, 2957, 2850, 1680, 1570, 1506, 1490, 1368, 1360, 1350, 1215, 1121, 1074, 1011, 830, 815 cm^{-1}

^{1}H NMR (500 MHz,$CDCl_3$) δ: 1.3 (s, 9H), 2.25 (s, 6H), 2.31 (s, 6H), 2.73-2.76 (m, 4H), 2.89-2.92 (m, 4H), 3.33- 3.37 (m, 4H), 3.71-3.74 (m, 2H), 3.95- 3.97 (m, 2H), 4.10- 4.12 (m, 2H), 4.46- 4.48 (m, 2H), 4.55 (s, 4H), 6.74- 6.76 (d, 2H, J= 9 Hz), 6.92 (s, 2H), 7.04 (s, 2H), 7.25- 7.27 (d, 2H, J= 9 Hz), 7.43 (s, 2H), 8.86- 8.89 (d, 2H, J= 15.5 Hz), 9.30-9.32 (d, 2H, J= 10.5 Hz) ppm.

^{13}C NMR (500 MHz,$CDCl_3$) δ: 168.27, 157.15, 153.58, 151.66, 146.37, 145.90, 132.61, 132.51, 129.7, 126.91, 124.28, 122.19, 114.72, 112.29, 69.29, 68.82, 68.32, 67.88, 56.05, 49.33, 42.43, 39.25, 34.43, 31.17, 20.9, 20.8 ppm.

٣. RESULTS AND DISCUSSION

In the Fig.1 [A] IR spectrum of compound (1) showed a broad and strong absorption band in the region of 3310 cm^{-1} corresponds to O-H stretching vibration with hydrogen bond and two absorption bands with the same intensity at 1450 cm^{-1} corresponding to methyl bending vibration, a broad absorption band at 3450 cm^{-1} corresponded to O-H Phenolic, the absorption band at 1052 cm^{-1} indicated the S=O bond. The absorption band in the region of 1226 cm^{-1} corresponded to phenolic C-O, the stretching absorption band of C=C of ring in the region of 1668-1642 cm^{-1}, and in the region of 1889-1762 cm^{-1} there were weak bands related to aromatic ring substituents, which indicated the formation of the desired sulfoxide. In the Fig.1 [B] IR spectrum of compound (2) indicated the intensity decrease of the broad absorption band of phenolic O-H in the region of 3200-3400 cm^{-1}. The strong absorption band at 1720-1740 cm^{-1} and the absorption band at 1069 cm^{-1} corresponded to carbonyl ester and S=O. The absorption band at 1577-1600 ,2858 and 2915 cm^{-1} corresponded to C=C of the aromatic ring, C-H aromatic and aliphatic stretching, respectively. The presence of a strong absorption band for C-O ether at 1200 cm^{-1} indicated the formation of the desired methyl diester compound. In the Fig.1 [C] IR spectra of compound (3a), the absorption band at 894, 1074, 1671, 2921, 3010 and 3449 cm^{-1} indicated the bending vibration of aromatic C-H, S=O bond, C=O, aliphatic and aromatic C-H, and Stretching N-H ,respectively. The absorption bands observed at 1251-1212 cm^{-1} indicated the ether bond. The presence of absorption band at 1696-1494 cm^{-1} is for aromatic C=C bond. In the Fig.1 [D] IR spectra of compound (3b) the absorption band of the aromatic C-H bending vibration, S=O bond, C=O, C-H aliphatic and aromatic stretching, and N-H (amide) at 830, 1074, 1680, 2850, 3040 and 3398 cm^{-1} is observed, respectively. The absorption band at 1490-1570 cm^{-1} corresponded to aromatic C=C bond and bands at 1368 and 1250 cm^{-1} corresponded to the C-O stretching vibration. The stretching N-H absorption band is observed at 3420 cm^{-1}. 1- 3b

[A]

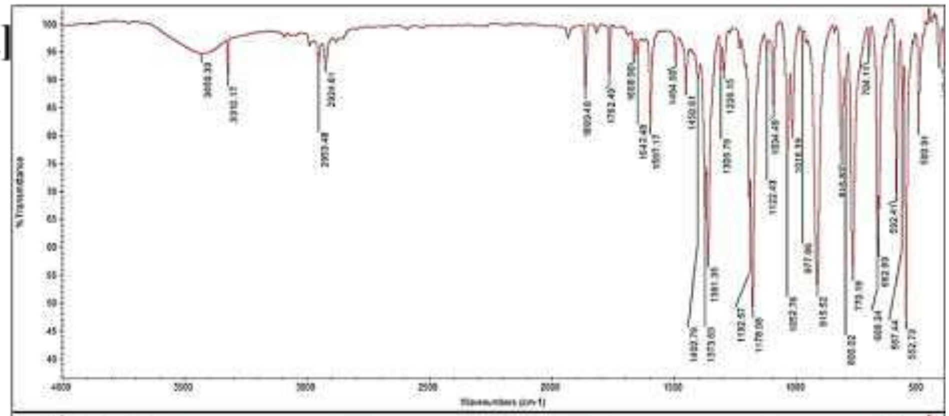

% Transmittance
100
95
90
85
80
75
70
65
60
55
50
45
40
4000
3500
3000
2500
2000
1500
1000
500
Wavenumbers (cm-1)
3458.33
3310.17
2953.48
2924.61
1869.46
1762.40
1658.96
1542.48
1597.17
1494.66
1450.61
1492.79
1373.65
1361.35
1309.79
1239.15
1192.57
1176.06
1122.43
1034.48
1052.76
1016.19
977.96
915.52
816.83
800.02
773.18
704.11
608.34
652.93
592.41
567.44
552.73
589.91

[B]

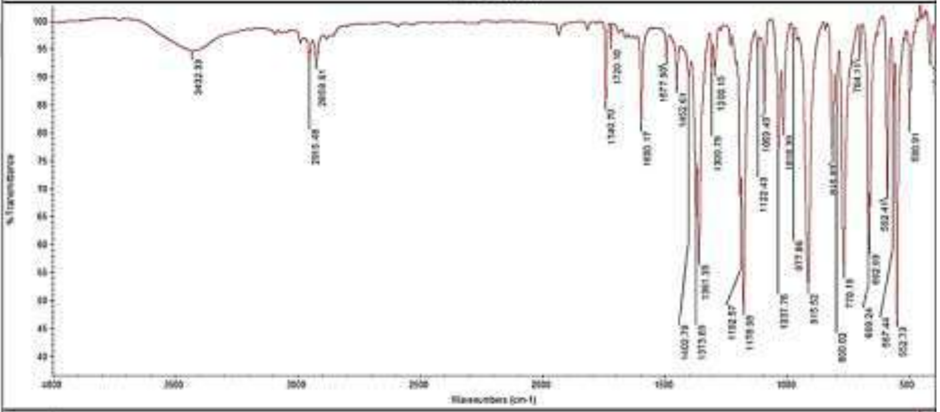

% Transmittance
100
95
90
85
80
75
70
65
60
55
50
45
40
4000
3500
3000
2500
2000
1500
1000
500
Wavenumbers (cm-1)
3432.33
2915.48
2859.61
1740.70
1720.10
1600.17
1677.50
1452.61
1402.79
1373.65
1361.35
1300.79
1238.15
1192.57
1176.06
1122.43
1063.43
1037.76
1016.39
977.86
915.52
816.83
800.02
770.18
704.11
669.24
652.93
592.41
567.44
552.73
590.91

[C]

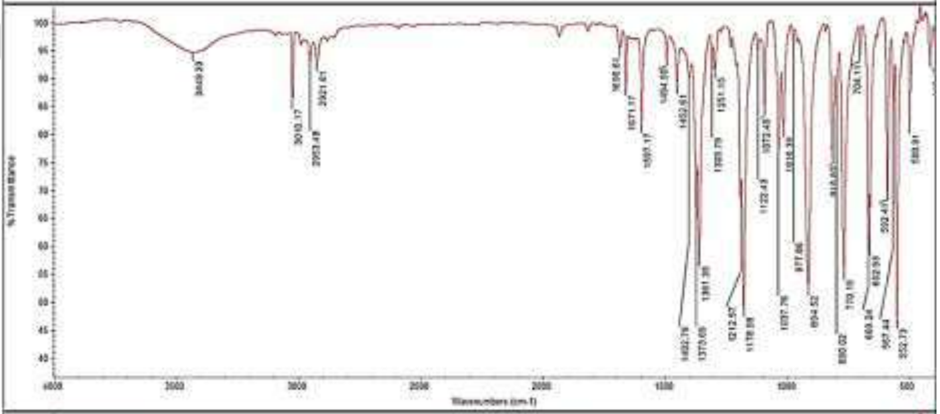

% Transmittance
100
95
90
85
80
75
70
65
60
55
50
45
40
4000
3500
3000
2500
2000
1500
1000
500
Wavenumbers (cm-1)
3449.33
3010.17
2953.48
2921.61
1698.61
1671.17
1597.17
1464.66
1452.61
1402.79
1373.65
1361.35
1303.79
1251.15
1212.57
1176.06
1122.43
1072.48
1037.76
1016.39
977.86
894.52
816.83
800.02
770.18
704.11
669.24
652.93
592.41
567.44
552.73
589.91

[D]

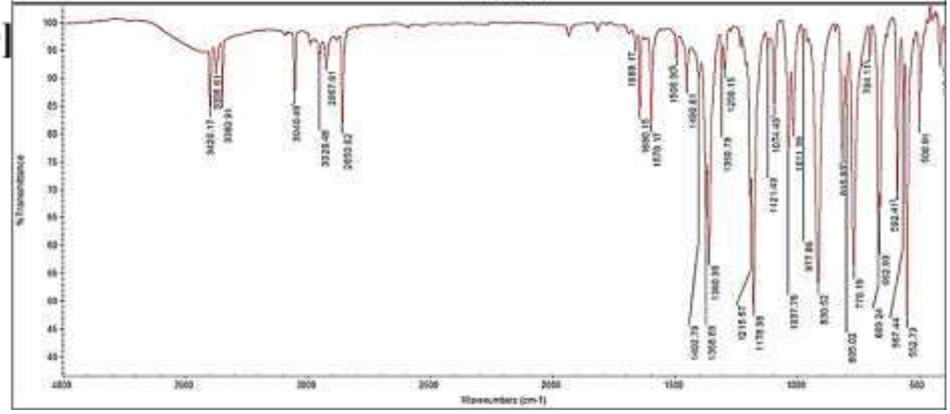

% Transmittance
100
95
90
85
80
75
70
65
60
55
50
45
40
4000
3500
3000
2500
2000
1500
1000
500
Wavenumbers (cm-1)
3428.17
3356.61
3363.91
3040.45
2925.48
2867.61
2850.62
1689.17
1690.15
1676.17
1509.66
1460.61
1402.79
1368.65
1360.35
1308.79
1258.15
1216.57
1176.06
1121.43
1074.48
1011.39
1037.76
977.86
930.52
816.83
805.02
770.18
704.11
669.24
652.93
592.41
567.44
552.73
588.91

Figure 12: IR spectrum of compound (1) [A], compound (2) [B], compound (3a) [C], compound (3b) [D]

In the Fig.2 IR spectra of compound (4) the stretching vibrations related to the N-H bond in the region of 13380 cm^{-1} and the bending N-H bond in the region of 1506 cm^{-1} were seen with strong absorption. The out-of-plane C-H bond, ether bonds in C-O (aromatic) Ar-O-C, C-O-C, C-N, and aliphatic and aromatic C-H bond was seen in the region of 815, 1011, 1121, 1215, 1360, 2957, 3047 cm^{-1}, respectively. The peak observed at 3432 cm^{-1} indicated Ar-H.

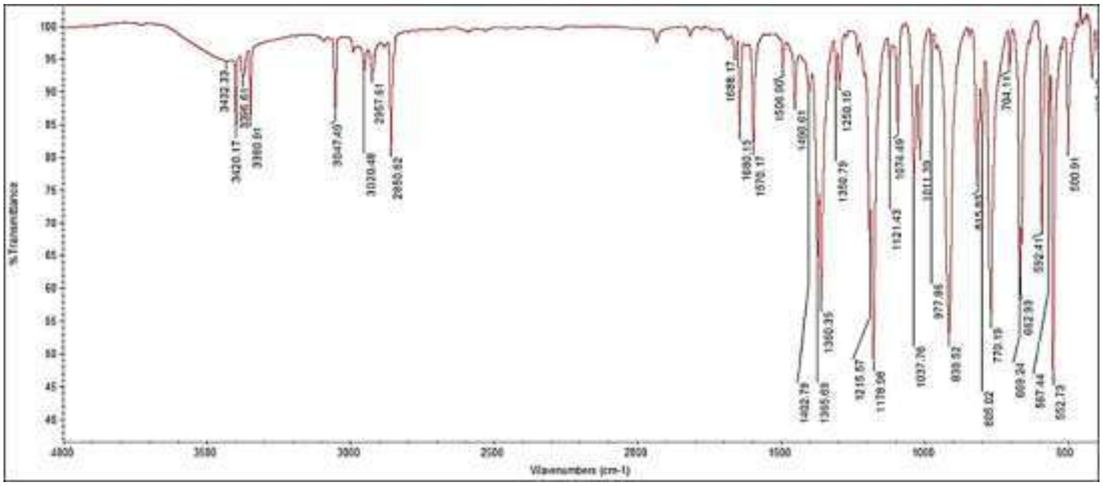

Figure 13: IR spectrum of compound (4)

In the Fig.3 [A] IR spectrum of rotaxane (5a), the absorption band at 1074 cm^{-1} indicatesd the S=O bond. The absorption band observed at 3449-3380 cm^{-1} is related to the stretching vibration of N-H bond and strong absorption at 1506 cm^{-1} corresponded to the bending vibration of N-H bond. The aliphatic C-H bond in the region of 2921-2957 cm^{-1} shows a weak absorption and aromatic C-H bond in 3010-3047 cm^{-1} region. The absorption band of out-of-plane C-H bond in 815 cm^{-1} were observed. The absorption band at 1696-1494 cm^{-1} for the aromatic C=C bond. The absorption band observed at 894, 1011, 1121, 1212, 1215 , 1251, 1360, 1671 and 3432 cm^{-1} indicated the aromatic C-H bending vibration, ether bonds in C-O (aromatic), Ar-O-C ,C-O-C , C-N ,C=O of carbonyl group and Ar-H, respectively. In the Fig.3 [B] IR spectrum of rotaxane (5b), the absorption band at 1074 cm^{-1} indicatesd the S=O bond. The absorption band observed at 3420-3380 cm^{-1} is related to the stretching vibration of N-H bond and strong absorption at 1506 cm^{-1} corresponded to the bending vibration of N-H bond. The aliphatic C-H bond in the region of 2850-2957 cm^{-1} shows a weak absorption and aromatic C-H bond in 3040-3047 cm^{-1} region. The absorption band of out-of-plane C-H bond in 815 cm^{-1} were observed. The absorption band at 1570-1490 cm^{-1} for the aromatic C=C bond. The absorption band observed at 830, 1011, 1121, 1215 , 1250 , 1368, 1680 and 3432 cm^{-1} indicated the aromatic C-H bending vibration, ether bonds in C-O (aromatic), Ar-O-C, C-O-C, C=O of carbonyl group and Ar-H, respectively. The absorption band of C-N observed at 1360 cm^{-1}.

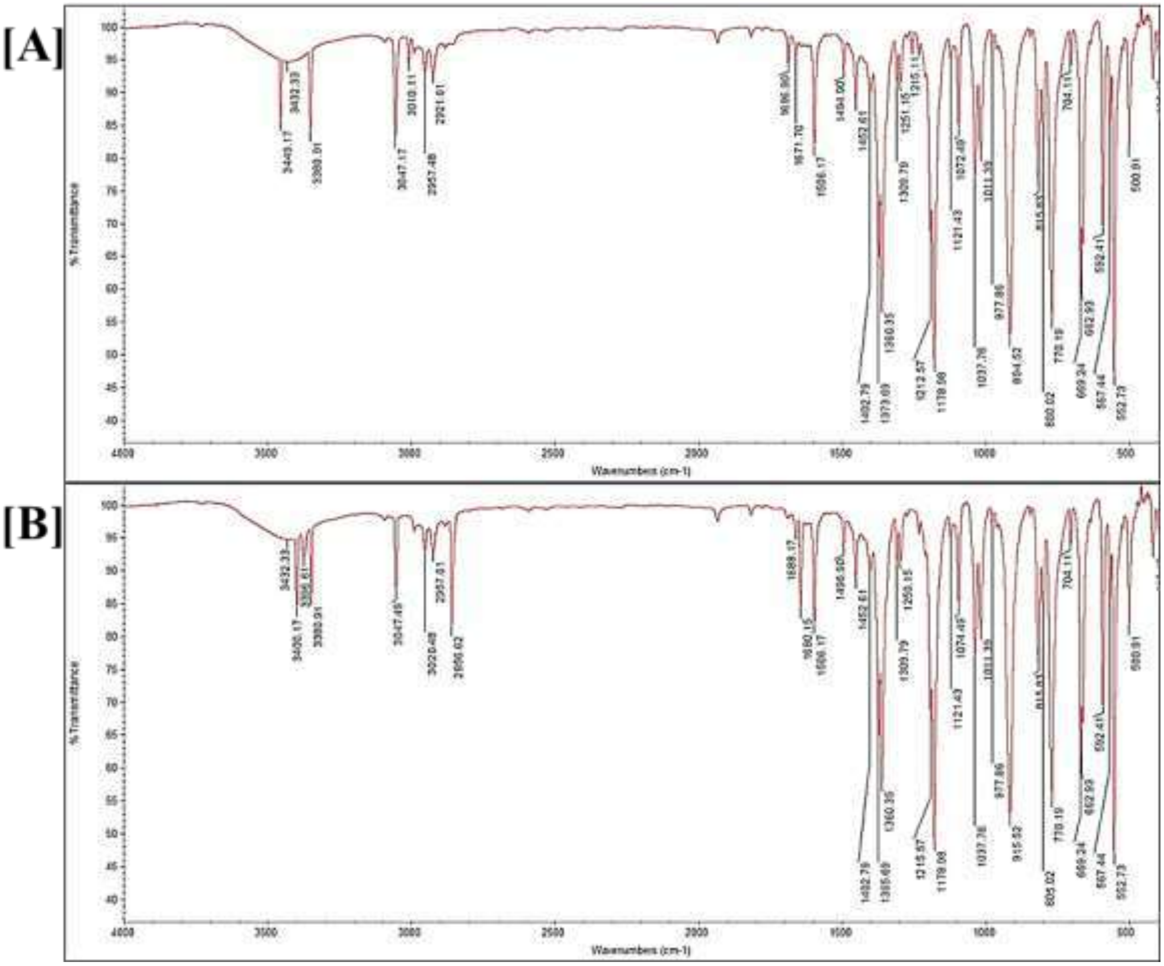

Figure 14: IR spectrum of [A] Rotaxane (5a), [B] Rotaxane (5b)

In the Fig.4 ^{1}H NMR spectrum of compound (1) were found to be in good agreement with the suggested structure. The signals of aromatic protons due to H_c and H_d protons indicated singlet peaks appeared at 6.73 and 7.05 ppm and H_e proton (OH) indicated a broad peak at 6.84 ppm. The signals of aliphatic protons due to H_a and H_b protons indicated singlet peaks at 2.23 and 2.26 ppm.

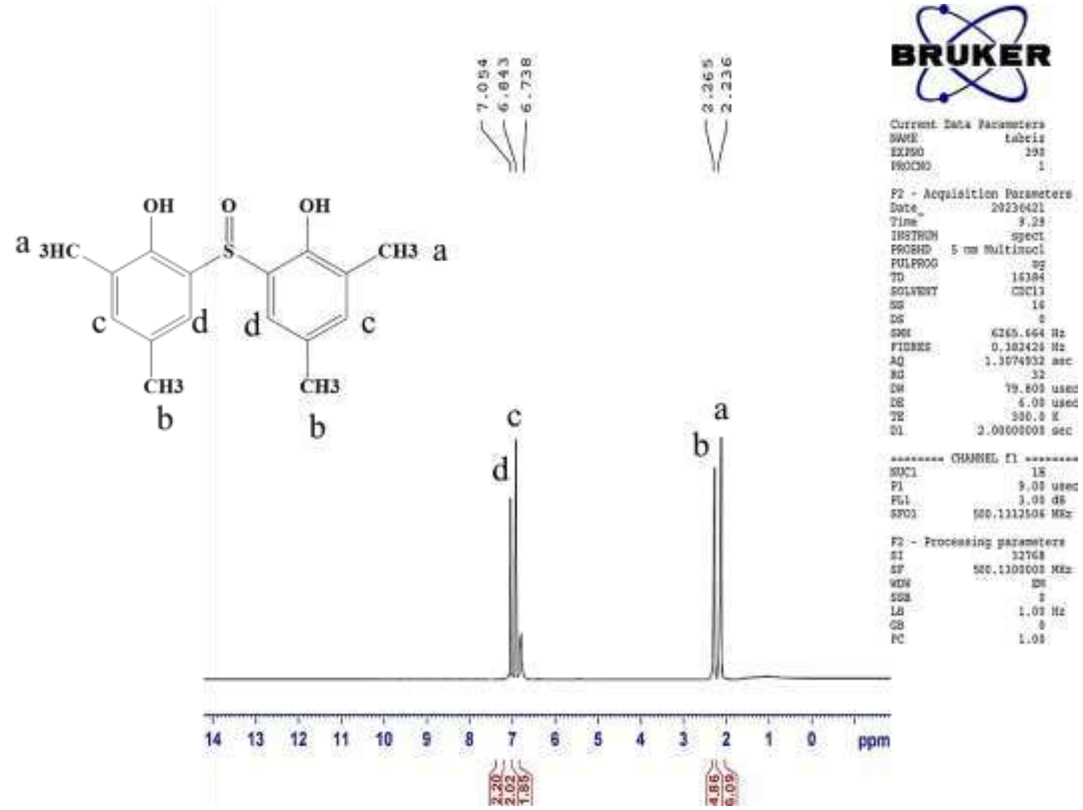

Figure 15: ^{1}H-NMR spectra of compound (1)

^{1}H NMR spectra of compound (2) showed in Fig.5 [A]. The signals of aromatic protons indicated singlet peaks at 6.81 and 7.02 ppm related to H_e and H_f. The signals of aliphatic protons due to H_a, H_b, H_d and H_c indicated singlet peaks at 2.23, 2.26, 4.56 and 3.82 ppm. Fig.5 [B] shows ^{13}C NMR spectra of compound (2). Signals of various carbon atoms indicated C_k signal at 168.21 ppm, C_g at 152.73 ppm, C_i at 132.21 ppm, C_j at 131.92 ppm, C_h at 128.57 ppm, C_f at 126.35 ppm, C_e at 113.29 ppm, C_d at 70.62 ppm, C_c at 68.26 ppm, C_b at 20.41 ppm, C_a at 19.5 ppm.

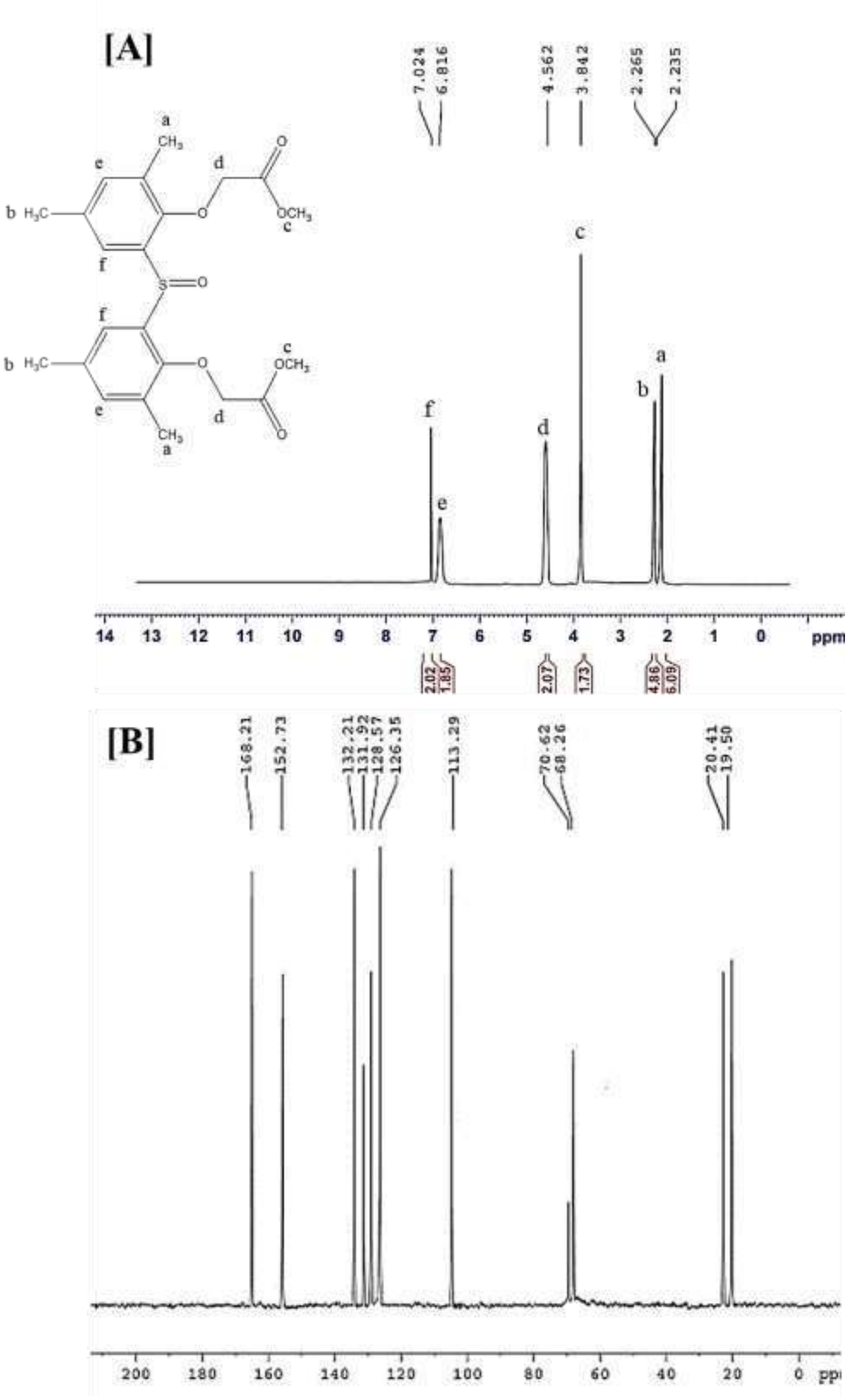

Figure 16: [A] ^{1}H-NMR spectra and [B] ^{13}C NMR spectrum of compound (2)

The Fig.6 [A] showed ^{1}H NMR spectra of compound (3a). The signals of aromatic protons due to H_g and H_f indicated singlet peaks in the region of 6.91 and 7.29 ppm. The signal of amide proton showed a singlet peak in the region of 7.38 ppm related to H_h. The signals of aliphatic protons indicated a singlet peak in the region of 1.0 7, 2.2 and 2.25 ppm related methyl protons H_a,H_e and $H_{e'}$. H_c protons indicated multipet (ddd) peaks in the region of 3.32-3.33 ppm. H_b protons indicated doublet peaks at 4.29-4.31 ppm. H_d protons showed a singlet peak at 4.83 ppm. Fig.6 [B] shows ^{13}C NMR spectra of compound (3a). Signals of various carbon atoms indicated C_l (C=O) signal at 168.50 ppm, C_f at 154.06 ppm, C_i at 134.03 ppm, C_g at 131.83 ppm, C_h at 129.08 ppm, C_j at 129.66 ppm, C_k at 113.53 ppm, C_d at 68.19 ppm, C_c at 39.86 ppm, C_b at 38.51 ppm, $C_{e'}$ at 22.94 ppm, C_e at 21.9 ppm and C_a at 19.47 ppm.

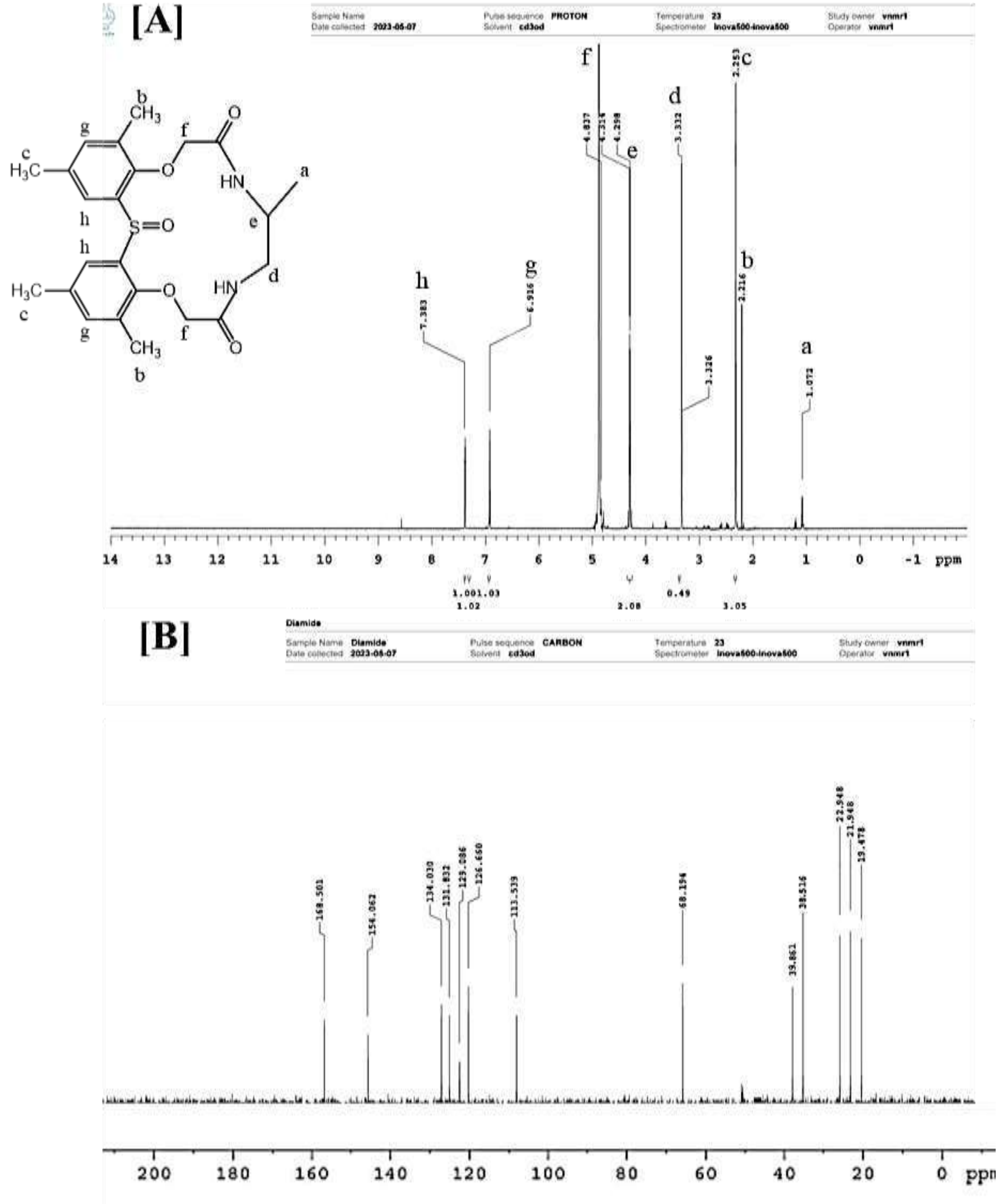

Figure 17: [A] ^{1}H-NMR spectra for compound (3a), [B] ^{13}C NMR spectrum of compound (3a)

A mass spectrum was obtained by electron impact (EI) at 70 eV. Peaks were detected at m/z (%): 430 (M^+), 431 $(M+1)^+$, 432 $(M+2)^+$, 345, 331, 326, 316, 304, 288, 272, 184, 170, 158, 122, 106, 74, 59, 44.

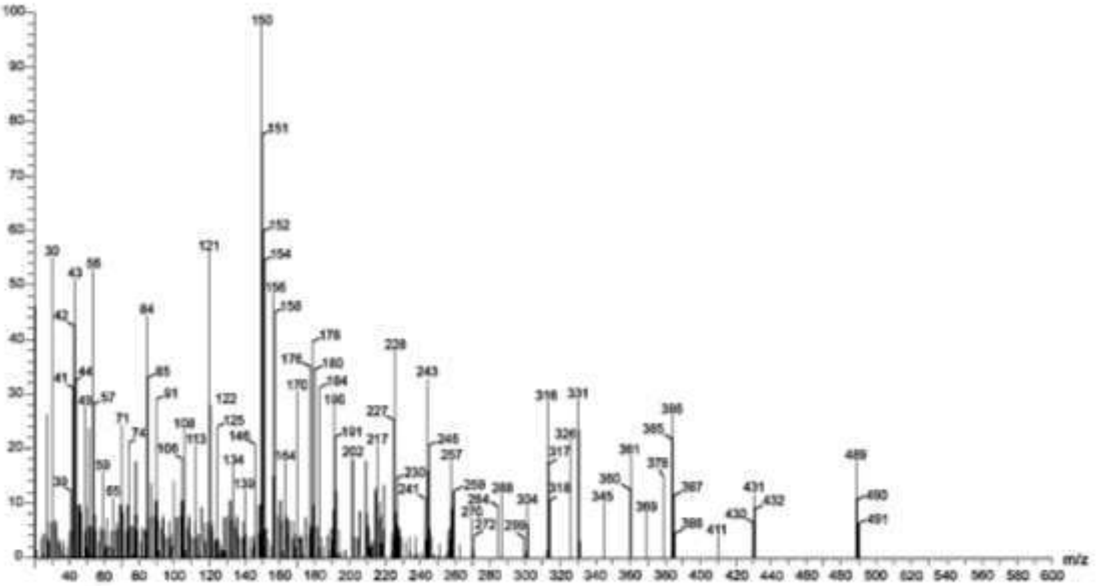

Figure 18: Mass spectrometry analysis of compound (3a)

Fig.8 [A] shows ^{1}H NMR spectrum of compound (3b). The signals of aromatic protons due to H_f and H_g indicated singlet peaks at 6.92 and 7.04 ppm. The signal of amide proton due to H_h showed a broad peak at 7.48 ppm. The signals of aliphatic protons due to methyl protons H_e and $H_{e'}$ indicated singlet peaks at 2.25-2.31 ppm. H_a, H_b and H_c showed multipet (ddd) peaks in the region of 2.73-2.76 ppm, 2.89-2.92 ppm and 3.30-3.37 ppm and H_d indicated a singlet peak at 4.62 ppm. Fig.8 [B] shows ^{13}C NMR spectra of compound (3b). Signals of various carbon atoms indicated C=O signal at 168.27, C_j at 153.5 ppm, C_g (aromatic carbon atoms) at 132.6 ppm, C_e at 132.5 ppm, C_i at 129.7 ppm, C_h at 122.19 , C_f at 112.3 ppm, C_d at 67.88 ppm, C_a at 49.3 ppm, C_b at 42.7 ppm, C_c at 39.25 ppm , C_l and $C_{l'}$ at 20.8 and 20.9 ppm.

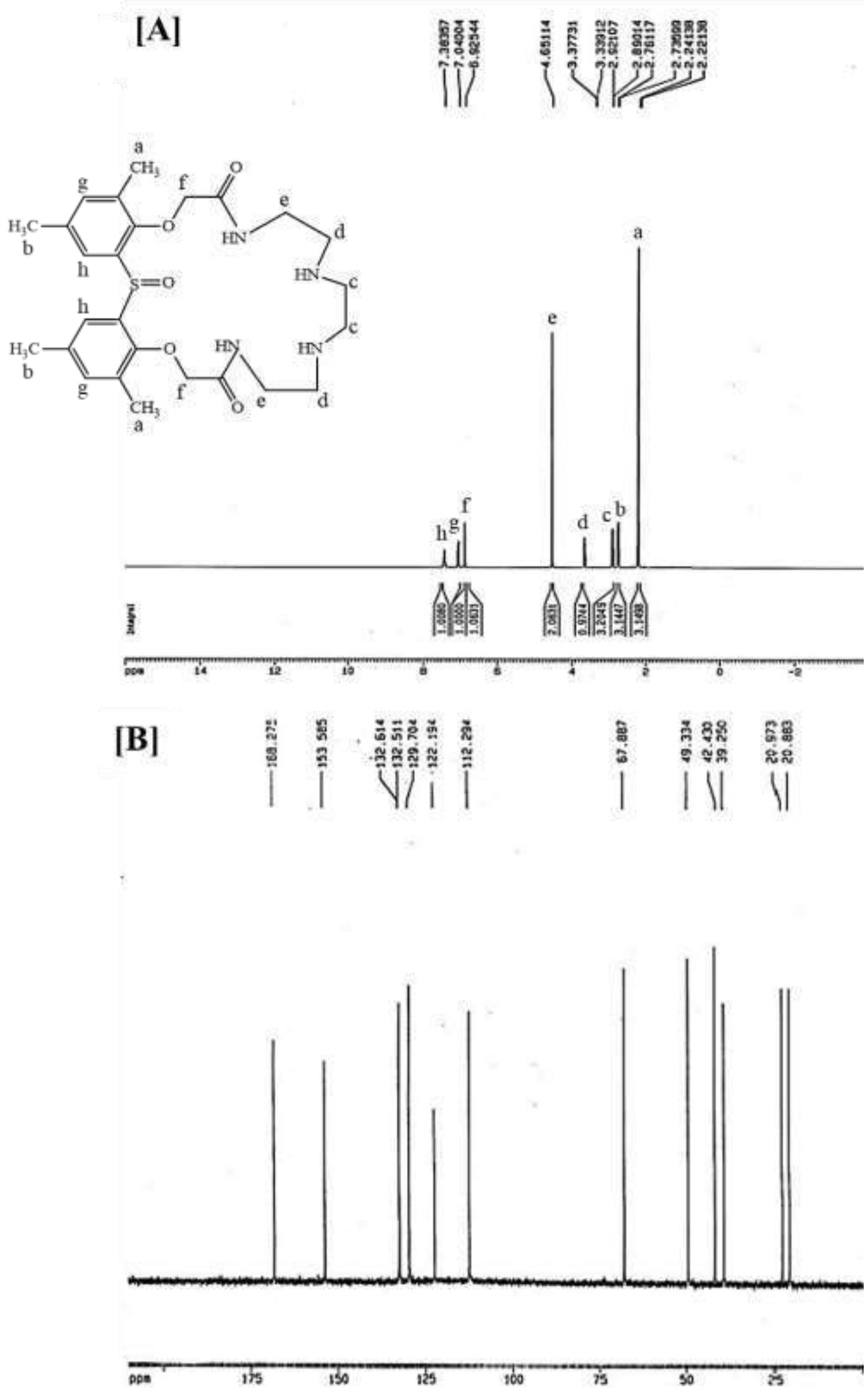

Figure 19: [A] ^{1}H-NMR spectra for compound (3b) and [B] ^{13}C NMR spectrum of compound (3b)

A mass spectrum was obtained by electron impact (EI) at 70 eV. Peaks were detected at m/z (%): 473 (M^+), 474 $(M+1)^+$, 475 $(M+2)^+$, 369, 304, 288, 284, 272, 270. 241, 217, 184, 154, 146, 122, 106.

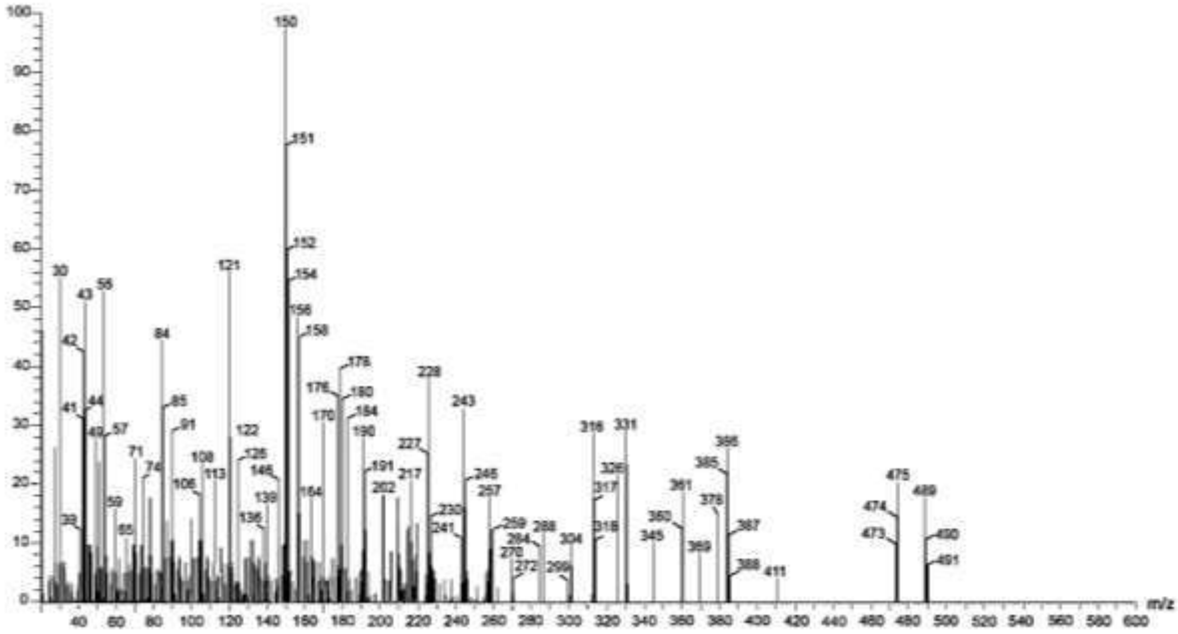

Figure 20: Mass spectrometry analysis of compound (3b)

^{1}H NMR spectrum of compound (4) has been shown in the Fig.10 [A]. The signals of aromatic protons due to H_f indicated doublet peaks (due to coupling with H_e) in the region of 6.74-6.76 ppm. H_e signals in the region of 7.25-7.27 ppm showed doublet peaks (due to coupling with H_f). H_h signal at 8.86-8.89 ppm showed doublet peaks (due to coupling with H_g). H_g showed doublet peak at 9.30-9.32 ppm (due to coupling with H_h). The signals of aliphatic protons due to H_i showed a singlet peak at 1.3 ppm. The signals of H_b and H_c showed multipet peaks (ddd) at 3.71-3.74 and 3.95-3.97 ppm, respectively. The signals of H_a and H_d indicated multipet peaks (ddd)at 4.10-4.12 ppm and 4.46-4.48. Fig.10 [B] shows ^{13}C NMR spectra of compound (3b). Signals of various carbon atoms indicated C_g signal at 157.15 ppm, C_k at 151.66 ppm, C_h at 146.37 ppm, C_i at 145.90 ppm, C_e at 126.91 ppm, C_j at 124.28 ppm, C_f at 114.72 ppm, C_a at 69.29 ppm, C_b at 68.82 ppm, C_c at 68.32 ppm, C_d at 56.05 ppm, C_m at 34.43 ppm.

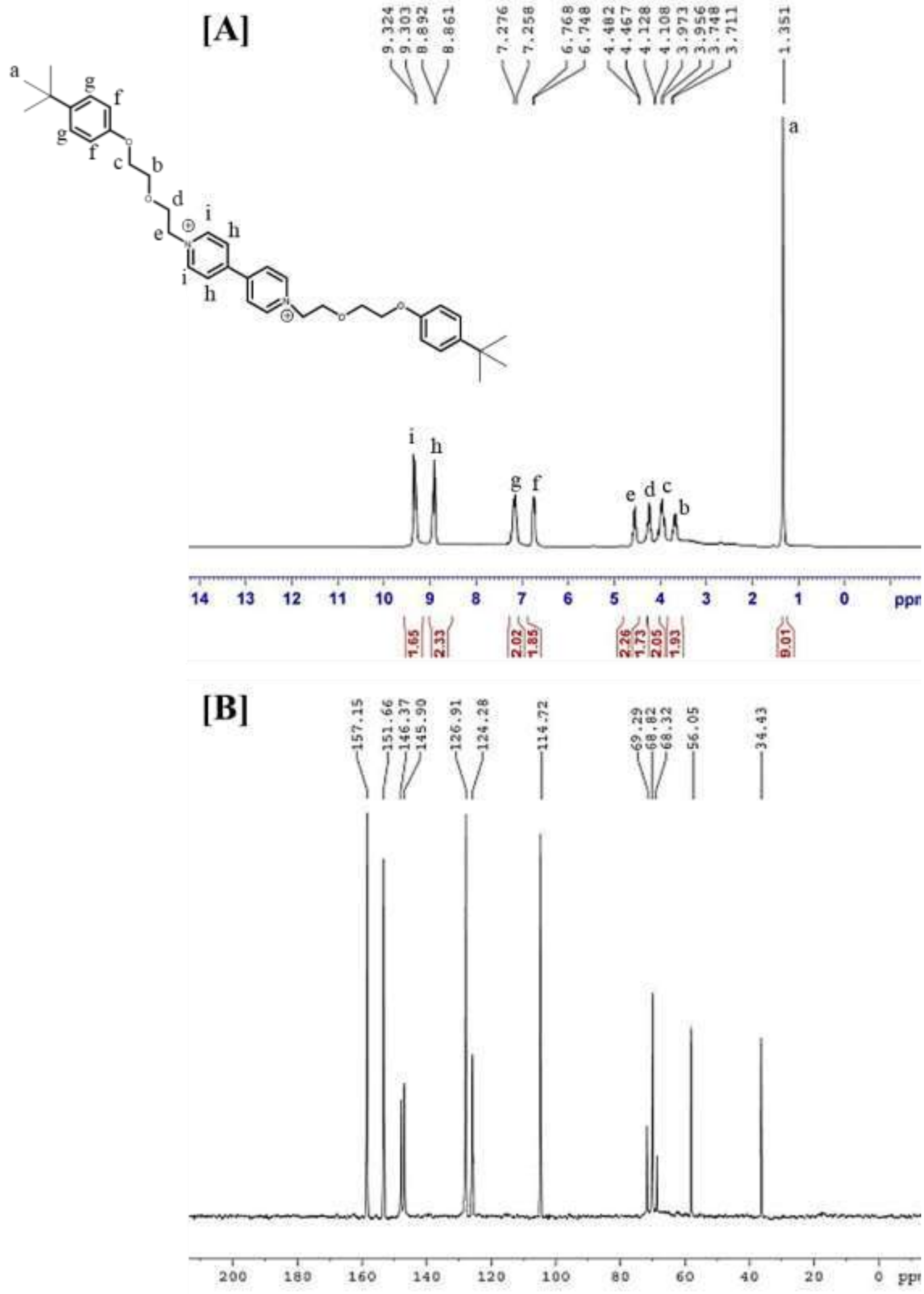

Figure 21: [A] ^{1}H-NMR spectra and [B] ^{13}C NMR spectrum of compound (4)

A mass spectrum was obtained by electron impact (EI) at 70 eV. Peaks were detected at m/z (%): 598 (M^+), 599 $(M+1)^+$, 600 $(M+2)^+$, 466, 378, 299, 246, 243, 202, 156, 150, 134, 125.

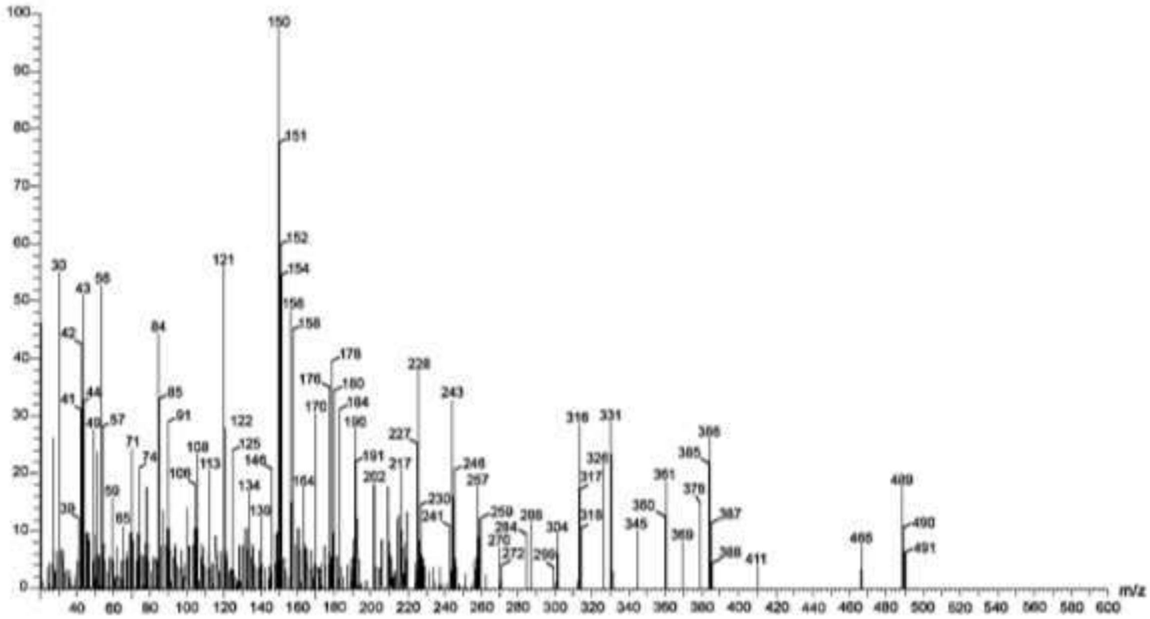

Figure 22: Mass spectrometry analysis of compound (4)

^{1}H NMR spectrum of rotaxane (5a) has been shown in the Fig.12 [A]. The signals of aromatic protons due to H_g and H_f showed singlet peaks at 6.91 and 7.29 ppm. The signals of H_k indicated doublet peak (due to coupling with H_j) at 6.74-6.76 ppm, H_j showed doublet peak (due to coupling with H_k) at 7.25-7.27 ppm, H_q showed doublet peak (due to coupling with H_p) at 8.86-8.89 ppm and H_p showed doublet peak (due to coupling with H_q) at 9.30-9.32 ppm. The signal of amide proton due to H_h indicated a singlet peak in the region of 7.38 ppm. The signals of aliphatic protons due to methyl protons H_a, H_i, H_e and $H_{e'}$ showed singlet peaks at 1.07, 1.3, 2.2 and 2,25 ppm. H_c imdicated a multipet peak (ddd) in the region of 3.32-3.33 ppm. H_m and H_n showed multipet peaks (ddd) in the region of 3.71-3.74 and 3.95-3.97, respectively. H_l and H_o indicated multipet peaks (ddd) in the region of 4.10-4.12 and 4.46-4.48 ppm, respectively. H_b showed a doublet peak in the region of 4.29-4.30 ppm and H_d showed a singlet peak in the region of 4.83 ppm. Fig.12 [B] shows ^{13}C NMR spectra of rotaxane (5a). Signals of various carbon atoms indicated C_l (C=O) signal at 168.50 ppm, C_q at 157.15 ppm, C_f at 154.06 ppm, C_x at 151.66 ppm, C_p at 146.37 ppm, C_v at 145.90 ppm, C_i at 134.03 ppm, C_g at 131.83 ppm, C_h at 129.08 ppm, C_o at 126.91 ppm, C_j at 126.66 ppm, C_w at 124.28 ppm, C_n at 114.72 ppm, C_k at 113.53 ppm, C_r at 69.29 ppm, C_s at 68.82 ppm,

C_t at 68.32 ppm, C_d at 68.19 ppm, C_c at 39.86 ppm, C_b at 38.51 ppm, C_m at ppm 34.43, C_e at 21.9 ppm, C_a at 19.47 ppm.

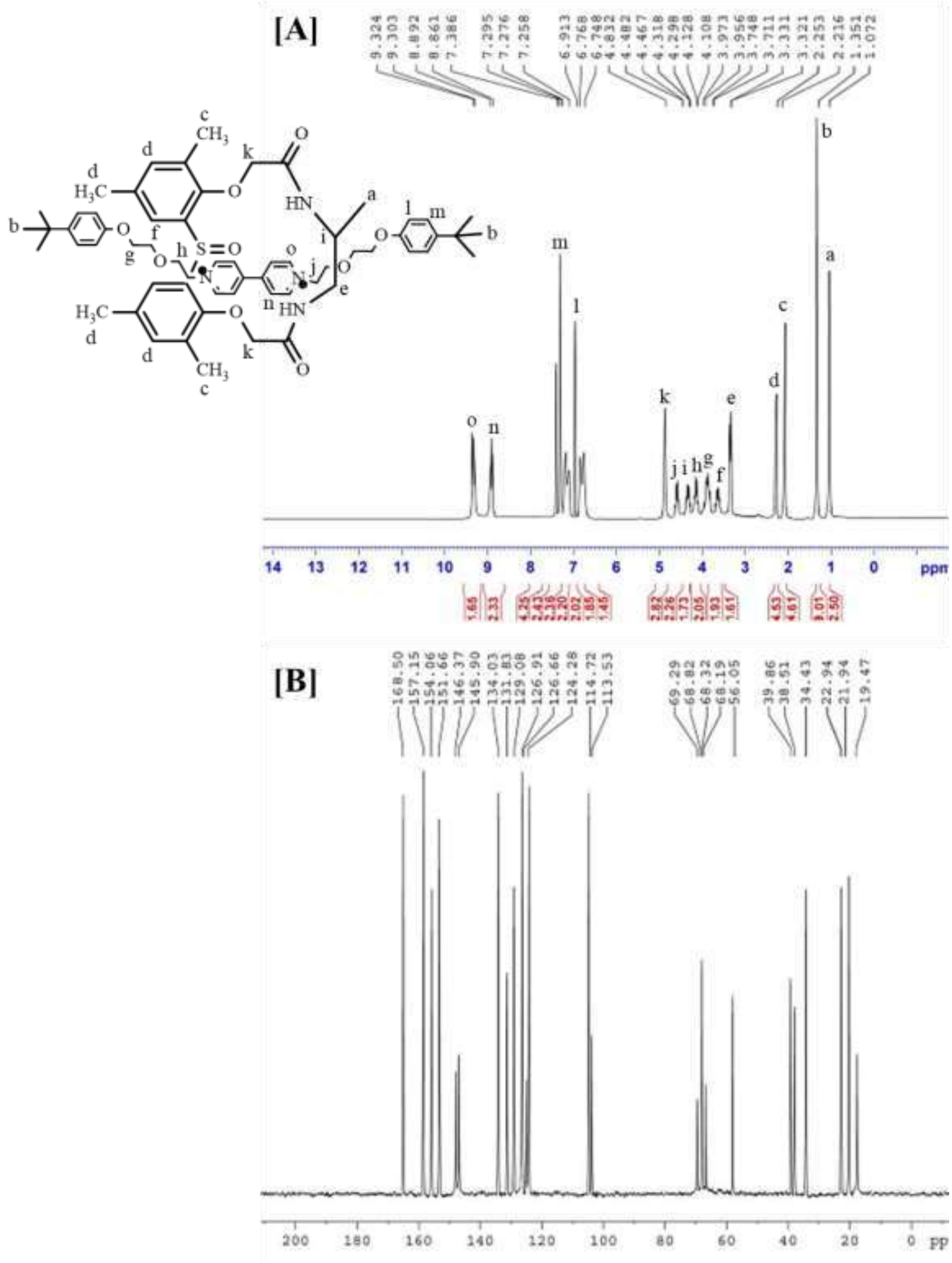

Figure 23: [A] ^{1}H-NMR spectra for Rotaxane (5a), [B] ^{13}C NMR spectrum of Rotaxane (5a)

A mass spectrum was obtained by electron impact (EI) at 70 eV. Peaks were detected at m/z (%): 598 (M^+), 599 $(M+1)^+$, 600 $(M+2)^+$, 466, 430, 378, 345, 331, 326, 316, 304, 299, 288, 272, 246, 243, 202, 184, 170, 158, 156, 150, 134, 125, 122, 106, 74, 59, 44.

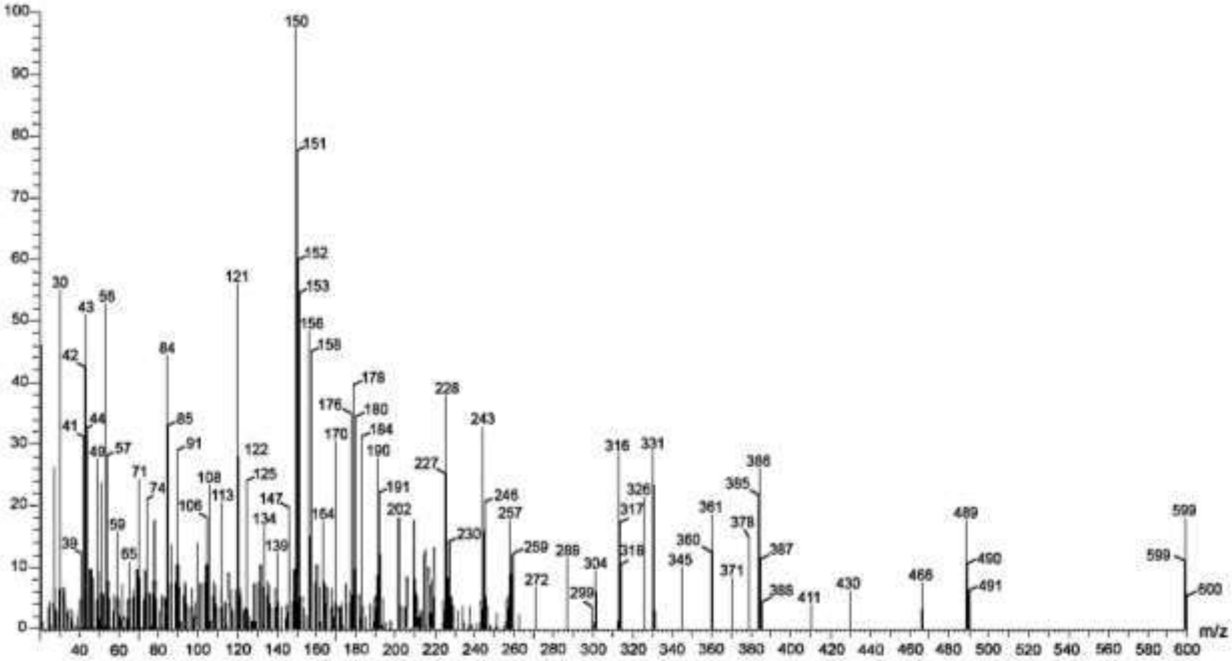

Figure 24: Mass spectrometry analysis of compound (5a)

^{1}H NMR spectrum of rotaxane (5b) has been shown in the Fig.14 [A]. The signals of aromatic protons due to H_f and H_g indicated singlet peaks in the region of 6.92 and 7.04 ppm. H_k showed a doublet peak (due to coupling with H_j) in the region of 6.74-6,76 ppm, H_j showed a doublet peak (due to coupling with H_k) in the region of 7.25-7.27 ppm, H_q showed a doublet peak (due to coupling with H_p) in the region of 8.86-8.89 ppm and H_p showed a doublet peak (due to coupling with H_q) in the region of 9.30-9.32 ppm. The signal of amide proton due to H_h showed a singlet peak at 7.48 ppm. The signals of aliphatic protons due to H_i, H_e and $H_{e'}$ showed singlet peaks at 1.3, 2.2 and 2.3 ppm, respectively. H_a, H_b and H_c showed multipet peaks (ddd) in the region of 2.73-2.76, 2.89- 2.92 and 3.33-3.37 ppm, respectively. H_d showed a singlet peak at 4.62 ppm. H_m, H_n, H_l and H_o showed multipet peaks (ddd) in the region of 3.71-3.74, 3.95-3.97, 4.10-4.12 and 4.46-4.48 ppm, respectively. Fig.14 [B] shows ^{13}C NMR spectra of rotaxane (5b). Signals of various carbon atoms indicated C_l (C=O) signal at 160.50 ppm, C_q at 157.15 ppm, C_f at 154.06 ppm, C_x at 151.66 ppm, C_p at 146.37 ppm, C_v at 145.90 ppm, C_i at 134.03 ppm, C_g at 131.83 ppm, C_h at 129.08 ppm, C_o at 126.91 ppm, C_j at 126.660 ppm, C_w at 124.28 ppm, C_n at 113.72 ppm, C_k at 113.53 ppm, C_r at 69.29 ppm, C_s at 68.82 ppm, C_t at 68.32 ppm, C_d at 68.19 ppm, C_o at 56.05 ppm, C_c at 39.86 ppm, C_b at ppm 38.51, C_m at 34.43 ppm, C_e at 22.9 ppm, C_a at 19.47 ppm [48-50].

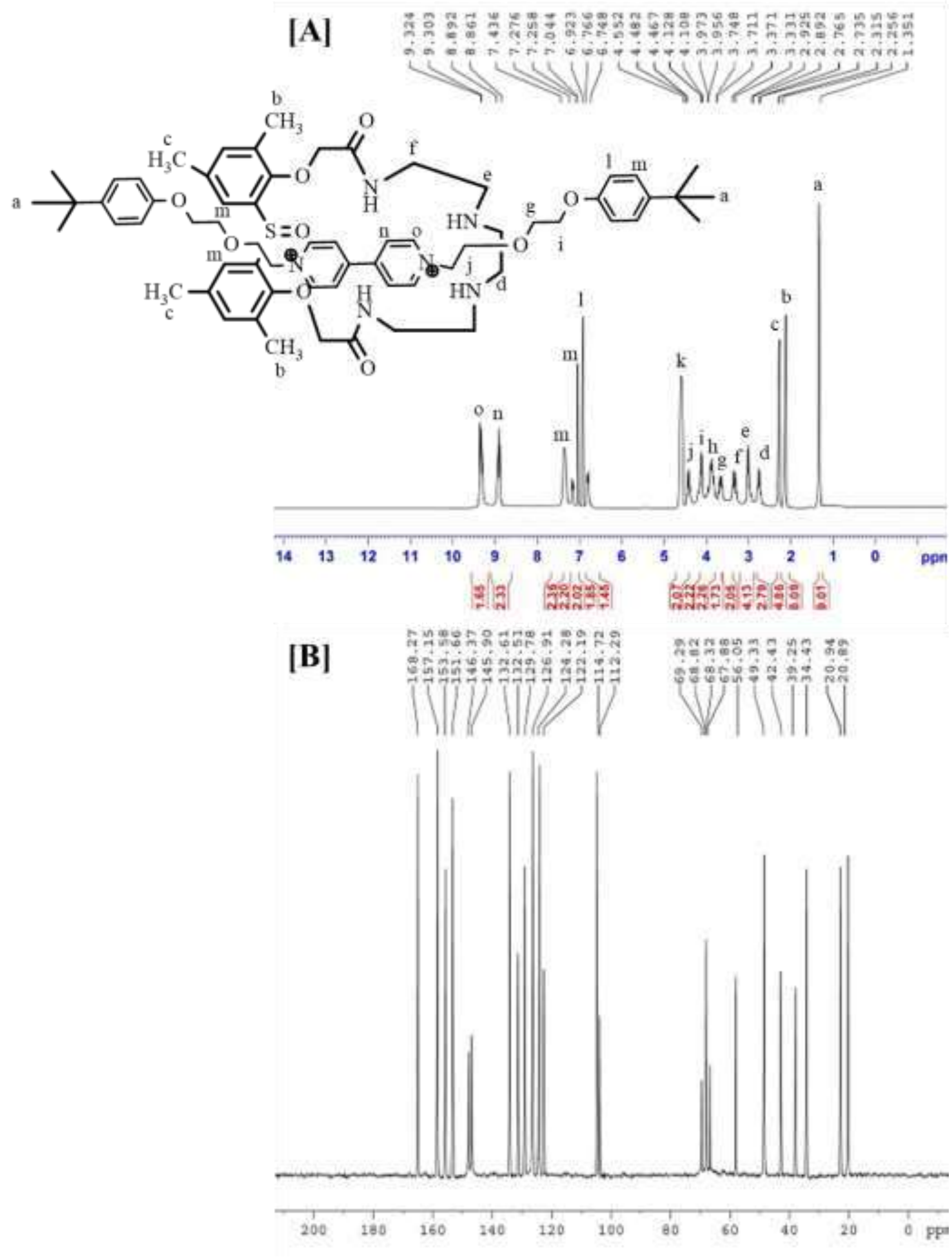

Figure 25: [A] ^{1}H-NMR spectra for Rotaxane (5b) and [B] ^{13}C NMR spectrum of Rotaxane (5b)

A mass spectrum was obtained by electron impact (EI) at 70 eV. Peaks were detected at m/z (%): 598 (M^{+}), 599 $(M+1)^{+}$, 600 $(M+2)^{+}$, 473, 466, 378, 369, 304, 299, 288, 284, 272, 270, 246, 243, 241, 217, 202, 184, 156, 154, 150, 146, 134, 125, 122, 106.

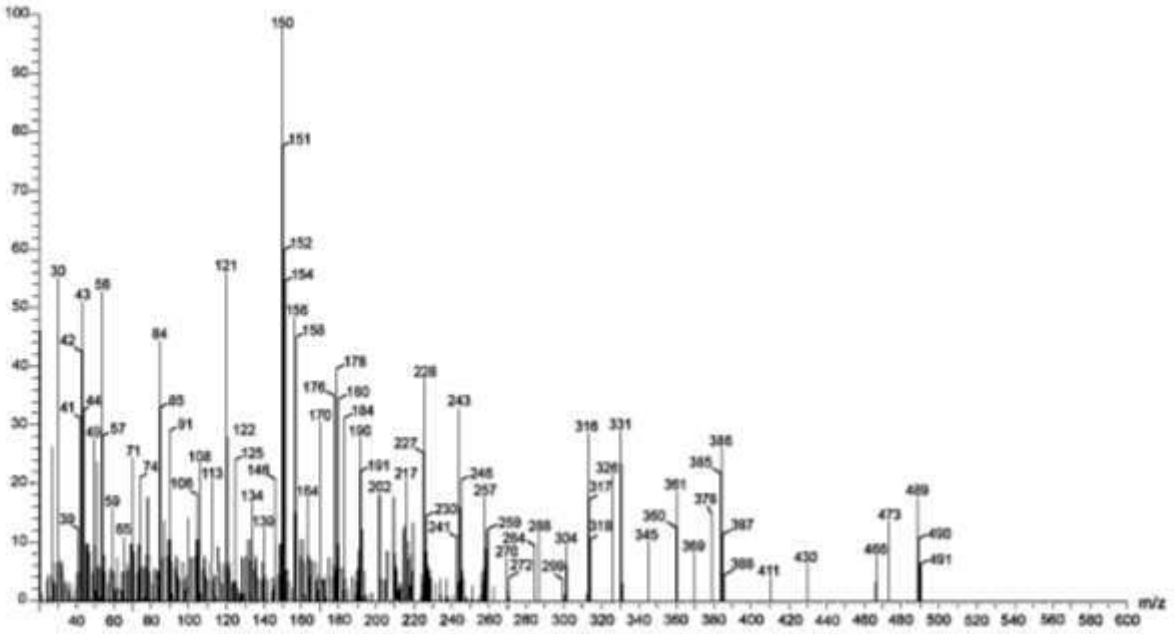

Figure 26: Mass spectrometry analysis of compound (5b)

Surface morphology

The morphologies of the compound 3a were investigated through scanning electron microscopy (SEM) experiments. According to Fig 16, the images demonstrate the formation of randomly dispersed rectangle-like structures with diameter ranging from 26 to 98 nm. The main advantage of this synthesis technique is its capability to generate particles in nano-scale dimensions without depending on traditional methods typically used for nanostructure synthesis [51].

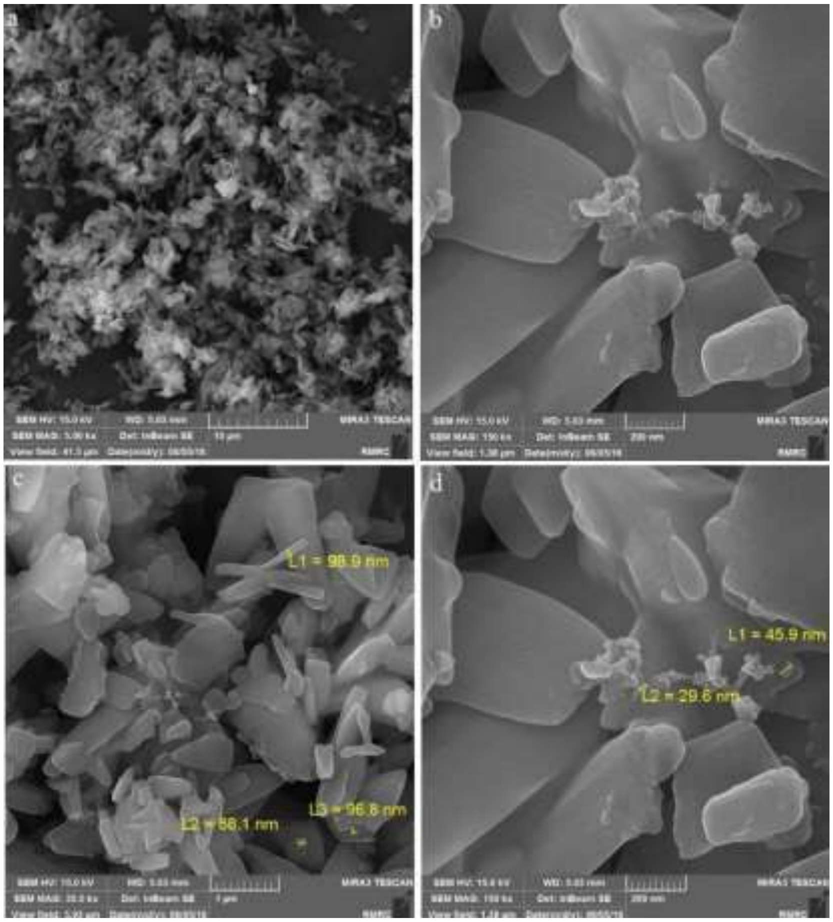

Figure 27: 1,7-dioxo-4-sulfoxo-11-methyl-2,3-5,6-di (2´,4´-dimethyl)benzo-10,13-diaza-14-crown-5 (3a)

۱. Conclusions

The method employed in this research facilitated the efficient and simple preparation of the diester utilized in macrocycle synthesis under mild conditions. The preparation of diamide macrocycles becomes significantly simpler and more efficient by the diester method, which not only provides high efficiency but also enables large-scale mass synthesis. The prepared chiral diamide crown macrocycle is a new ligand that has biological properties and the ability to bind to all kinds of molecules. This macrocycle was used as a component of rotaxane, which is one kind of nanomachines with new pharmaceutical applications.

Refrences

[1] J. W. Steed and J. L. Atwood, *Supramolecular chemistry*. John Wiley & Sons, 2022.

[2] L. You, D. Zha, and E. V. Anslyn, "Recent advances in supramolecular analytical chemistry using optical sensing," *Chemical reviews,* vol. 115, no. 15, pp. 7840-7892, 2015.

[3] T. L. Mako, J. M. Racicot, and M. Levine, "Supramolecular luminescent sensors," *Chemical reviews,* vol. 119, no. 1, pp. 322-477, 2018.

[4] X. Ma and Y. Zhao, "Biomedical applications of supramolecular systems based on host–guest interactions," *Chemical reviews,* vol. 115, no. 15, pp. 7794-7839, 2015.

[5] L. Yang, X. Tan, Z. Wang, and X. Zhang, "Supramolecular polymers: historical development, preparation, characterization, and functions," *Chemical reviews,* vol. 115, no. 15, pp. 7196-7239, 2015.

[6] G. Yu, K. Jie, and F. Huang, "Supramolecular amphiphiles based on host–guest molecular recognition motifs," *Chemical reviews,* vol. 115, no. 15, pp. 7240-7303, 2015.

[7] J. E. Lewis, M. Galli, and S. M. Goldup, "Properties and emerging applications of mechanically interlocked ligands," *Chemical Communications,* vol. 53, no. 2, pp. 298-312, 2017.

[8] X. Hou, C. Ke, and J. F. Stoddart, "Cooperative capture synthesis: yet another playground for copper-free click chemistry," *Chemical Society Reviews,* vol. 45, no. 14, pp. 3766-3780, 2016.

[9] A. Vedernikov *et al.*, "Synthesis, structure and complexation of biscrown-containing 1, 4-distyrylbenzenes," *Russian Chemical Bulletin,* vol. 65, pp. 2686-2703, 2016.

[10] S. P. Gromov *et al.*, "Synthesis, structure, and properties of supramolecular photoswitches based on ammonioalkyl derivatives of crown ether styryl dyes," *The Journal of Organic Chemistry,* vol. 79, no. 23, pp. 11416-11430, 2014.

[11] Y. Akae, H. Sogawa, and T. Takata, "Cyclodextrin‐Based [3] Rotaxane‐Crosslinked Fluorescent Polymer: Synthesis and De‐Crosslinking Using Size Complementarity," *Angewandte Chemie,* vol. 130, no. 45, pp. 15048-15052, 2018.

[12] Y. Akae, M. Sakurai, and T. Takata, "Alcohol Moiety-Tethering Acylazides as Versatile Isocyanate Precursors for Polymerization Initiators and Monomers," *Macromolecules,* vol. 54, no. 18, pp. 8488-8494, 2021.

[13] Y. Akae, K. Iijima, M. Tanaka, T. Tarao, and T. Takata, "Main chain-type polyrotaxanes derived from cyclodextrin-based pseudo [3] rotaxane diamine and macromolecular diisocyanate: synthesis, modification, and characterization," *Macromolecules,* vol. 53, no. 6, pp. 2169-2176, 2020.

[14] W. Niu, Z. Li, F. Liang, H. Zhang, and X. Liu, "Ultrastable, Superrobust, and Recyclable Supramolecular Polymer Networks," *Angewandte Chemie,* p. e202318434, 2024.

[15] M. Xue, Y. Yang, X. Chi, X. Yan, and F. Huang, "Development of pseudorotaxanes and rotaxanes: from synthesis to stimuli-responsive motions to applications," *Chemical Reviews,* vol. 115, no. 15, pp. 7398-7501, 2015.

[16] S. Erbas-Cakmak, D. A. Leigh, C. T. McTernan, and A. L. Nussbaumer, "Artificial molecular machines," *Chemical reviews,* vol. 115, no. 18, pp. 10081-10206, 2015.

[17] B. Colasson, A. Credi, and G. Ragazzon, "Light-driven molecular machines based on ruthenium (II) polypyridine complexes: Strategies and recent advances," *Coordination Chemistry Reviews,* vol. 325, pp. 125-134, 2016.

[18] S. Kassem, T. van Leeuwen, A. S. Lubbe, M. R. Wilson, B. L. Feringa, and D. A. Leigh, "Artificial molecular motors," *Chemical Society Reviews,* vol. 46, no. 9, pp. 2592-2621, 2017.

[19] M. Baroncini, L. Casimiro, C. De Vet, J. Groppi, S. Silvi, and A. Credi, "Making and operating molecular machines: a multidisciplinary challenge," *ChemistryOpen,* vol. 7, no. 2, pp. 169-179, 2018.

[20] L. Zhang, V. Marcos, and D. A. Leigh, "Molecular machines with bio-inspired mechanisms," *Proceedings of the National Academy of Sciences,* vol. 115, no. 38, pp. 9397-9404, 2018.

[21] M. Baroncini, S. Silvi, and A. Credi, "Photo-and redox-driven artificial molecular motors," *Chemical reviews,* vol. 120, no. 1, pp. 200-268, 2019.

[22] H. Li, X. Li, Y. Wu, H. Ågren, and D.-H. Qu, "A musclelike [2](2) rotaxane: synthesis, performance, and molecular dynamics simulations," *The Journal of Organic Chemistry,* vol. 79, no. 15, pp. 6996-7004, 2014.

[23] P. Waelès, B. Riss-Yaw, and F. Coutrot, "Synthesis of a pH-Sensitive Hetero [4] Rotaxane Molecular Machine that Combines [c2] Daisy and [2] Rotaxane Arrangements," *Chemistry–A European Journal,* vol. 22, no. 20, pp. 6837-6845, 2016.

[24] P. Waelès, K. Fournel-Marotte, and F. Coutrot, "Distinguishing Two Ammonium and Triazolium Sites of Interaction in a Three-Station [2] Rotaxane Molecular Shuttle," *Chemistry–A European Journal,* vol. 23, no. 48, pp. 11529-11539, 2017.

[25] T. Kumpulainen, M. R. Panman, B. H. Bakker, M. Hilbers, S. Woutersen, and A. M. Brouwer, "Accelerating the shuttling in hydrogen-bonded rotaxanes: active role of the axle and the end station," *Journal of the American Chemical Society,* vol. 141, no. 48, pp. 19118-19129, 2019.

[26] G. Ragazzon, A. Credi, and B. Colasson, "Thermodynamic insights on a bistable acid–base switchable molecular shuttle with strongly shifted co-conformational equilibria," *Chemistry–A European Journal,* vol. 23, no. 9, pp. 2149-2156, 2017.

[27] W. Zhou, Y. Wu, B.-Q. Zhai, Q.-C. Wang, and D.-H. Qu, "An anthracene-containing bistable [2] rotaxane featuring color and fluorescence changes," *RSC advances,* vol. 4, no. 10, pp. 5148-5151, 2014.

[28] C. J. Bruns *et al.*, "Redox switchable daisy chain rotaxanes driven by radical–radical interactions," *Journal of the American Chemical Society,* vol. 136, no. 12, pp. 4714-4723, 2014.

[29] T. Yasuda *et al.*, "A redox-switchable [2] rotaxane in a liquid-crystalline state," *Chemical communications,* vol. 46, no. 8, pp. 1224-1226, 2010.

[30] D. A. Leigh, V. Marcos, T. Nalbantoglu, I. J. Vitorica-Yrezabal, F. T. Yasar, and X. Zhu, "Pyridyl-acyl hydrazone rotaxanes and molecular shuttles," *Journal of the American Chemical Society,* vol. 139, no. 20, pp. 7104-7109, 2017.

[31] J.-J. Yu *et al.*, "Pumping a ring-sliding molecular motion by a light-powered molecular motor," *The Journal of Organic Chemistry,* vol. 84, no. 9, pp. 5790-5802, 2019.

[32] C. Pezzato, C. Cheng, J. F. Stoddart, and R. D. Astumian, "Mastering the non-equilibrium assembly and operation of molecular machines," *Chemical Society Reviews,* vol. 46, no. 18, pp. 5491-5507, 2017.

[33] Y. Akae, H. Sogawa, and T. Takata, "Synthesis of a structure-definite α-cyclodextrin-based macromolecular [3] rotaxane using a size-complementary method," *Angewandte Chemie,* vol. 130, no. 36, pp. 11916-11920, 2018.

[34] Y. Akae, Y. Koyama, S. Kuwata, and T. Takata, "Cyclodextrin-Based Size-Complementary [3] Rotaxanes: Selective Synthesis and Specific Dissociation," *Chemistry–A European Journal,* vol. 20, no. 51, pp. 17132-17136, 2014.

[35] Y. Akae, H. Okamura, Y. Koyama, T. Arai, and T. Takata, "Selective synthesis of a [3] rotaxane consisting of size-complementary components and its stepwise deslippage," *Organic letters,* vol. 14, no. 9, pp. 2226-2229, 2012.

[36] C. J. Bruns and J. F. Stoddart, "The nature of the mechanical bond: from molecules to machines," 2016.

[37] E. A. Neal and S. M. Goldup, "Competitive formation of homocircuit [3] rotaxanes in synthetically useful yields in the bipyridine-mediated active template CuAAC reaction," *Chemical Science,* vol. 6, no. 4, pp. 2398-2404, 2015.

[38] D. Leigh, V. Marcos, and M. Wilson, "ACS Catal., 2014, 4, 4490–4497;(b) S. Erbas-Cakmak, DA Leigh, CT McTernan and AL Nussbaumer," *Chem. Rev,* vol. 115, pp. 10081-10206, 2015.

[39] S. F. van Dongen, S. Cantekin, J. A. Elemans, A. E. Rowan, and R. J. Nolte, "Functional interlocked systems," *Chemical Society Reviews,* vol. 43, no. 1, pp. 99-122, 2014.

[40] F. d'Orchymont and J. P. Holland, "Supramolecular Rotaxane-Based Multi-Modal Probes for Cancer Biomarker Imaging," *Angewandte Chemie,* vol. 134, no. 29, p. e202204072, 2022.

[41] J. Lewis *et al.*, "High yielding synthesis of 2, 2′-bipyridine macrocycles, versatile intermediates in the synthesis of rotaxanes," *Chemical Science,* vol. 7, no. 5, pp. 3154-3161, 2016.

[42] A. W. Heard and S. M. Goldup, "Synthesis of a mechanically planar chiral rotaxane ligand for enantioselective catalysis," *Chem,* vol. 6, no. 4, pp. 994-1006, 2020.

[43] R. Barat *et al.*, "A mechanically interlocked molecular system programmed for the delivery of an anticancer drug, Chem," ed: Sci, 2015.

[44] B. R. L. T. Tranoy-Opalinski, "I. Renoux B. Péraudeau E. Clarhaut J. Poinot P. Fernandes AE Aucagne V. Leigh DA Papot S," *Chem. Sci,* vol. 6, pp. 2608-2613, 2015.

[45] A. Fernandes, A. Viterisi, V. Aucagne, D. A. Leigh, and S. Papot, "Second generation specific-enzyme-activated rotaxane propeptides," *Chemical Communications,* vol. 48, no. 15, pp. 2083-2085, 2012.

[46] A. Shockravi, R. Alizadeh, H. Aghabozorg, A. Moghimi, E. Rostami, and S. Bavili, "Synthesis and crystal structure determination of 2, 2′-sulfinyl-bis (4-methyl phenol) and 2, 2′-thio-bis (4-methyl phenol)," *Phosphorus, Sulfur, and Silicon,* vol. 178, no. 12, pp. 2519-2527, 2003.

[47] A. Shockravi, S. Bavili T, E. Rostami, A. Yousefi, A. Dehjurian, and R. Tohidi, "Synthesis of new dibenzosulfide and dibenzosulfoxide macrocyclic compounds," *Journal of inclusion phenomena and macrocyclic chemistry,* vol. 49, pp. 163-166, 2004.

[48] Y. Akae *et al.*, "Structural Analysis and Inclusion Mechanism of Native and Permethylated α-Cyclodextrin-Based Rotaxanes Containing Alkylene Axles," *Chemistry–A European Journal,* vol. 22, no. 15, pp. 5335-5341, 2016.

[49] Y. Akae, H. Sogawa, and T. Takata, "Effective synthesis and modification of α-cyclodextrin-based [3] rotaxanes enabling versatile molecular design," *European Journal of Organic Chemistry,* vol. 2019, no. 22, pp. 3605-3613, 2019.

[50] Y. Akae and T. Takata, "O-Acylative Vinylation of Cyclodextrin-Based [3] Rotaxane Towards Rotaxane Crosslinkers," *European Journal of Organic Chemistry,* vol. 26, no. 12, p. e202300009, 2023.

[51] Y. Akae and P. Theato, "Aggregation Behavior of Cyclodextrin-Based [3] Rotaxanes," *Chemistry–A European Journal,* vol. 29, no. 50, p. e202301582, 2023.

The 30th Iranian Seminar of Organic Chemistry
February 7-9, 2025, Iran University of Science and Technology, Tehran, Iran

Phytochemical Evaluation of *Daphne stapfii* Root Extracts

Peyman Piran Kashani*[a], Mahdi Moridi Farimani[a]

[a] *Department of Phytochemistry, Medicinal Plants and Drugs Research Institute, Shahid Beheshti University, Tehran, Iran*

Abstract

This study investigates the phytochemical properties of *Daphne stapfii*, focusing on its total phenol and flavonoid content, alongside antioxidant potential using the DPPH assay. Results demonstrate a significant presence of phenolic and flavonoid compounds, which contribute to its potent antioxidant activity. These findings highlight the therapeutic potential of *Daphne stapfii* and provide a foundation for further research on its bioactive properties.

Keywords: *Daphne stapfii*, phytochemical evaluation, DPPH assay, phenol, flavonoid

Introduction

Plants from the genus *Daphne* have been renowned for their pharmacological benefits, largely attributed to their rich phytochemical content, including phenolics, flavonoids, and terpenes [1]. *Daphne stapfii*, endemic to certain regions, has received little scientific attention despite its traditional medicinal uses [2]. This study aims to quantify its total phenol and flavonoid contents and evaluate its antioxidant activity using the DPPH method.

Materials and Methods

Plant material was collected from Jiroft, dried, and ground into fine powder. Methanolic, ethyl acetate, and hexane extracts were prepared through maceration. Total phenolic content (TPC) was determined using the Folin-Ciocalteu method, and total flavonoid content (TFC) was assessed via the aluminum chloride method. Antioxidant activity was evaluated using the DPPH radical scavenging assay, with results expressed as IC_{50} values.

Results and Discussion

The best TPC of *D. stapfii* extract was methanolic extract and quantified at 191.0909 mg GAE/g, indicating a high concentration of phenolics. TFC analysis revealed 68.5 mg RUT/g, confirming the presence of substantial flavonoid content in ethyl acetate extract. Antioxidant activity, measured via DPPH assay, showed an IC50 value of 263.58 µg/mL in methanolic extract, demonstrating strong radical scavenging potential. The high levels of phenolics and flavonoids correlate with significant antioxidant activity, aligning with prior studies on similar species. These findings underscore the plant’s potential as a source of natural antioxidants and its applicability in the development of health-promoting agents. The results are summarized in Table 1.

Extracts	**Total phenol (mg/gr)**	**Total Flavonoid (mg/gr)**	**DPPH IC$_{50}$ (µg/mL)**
Methanol	191.0909±0.69	14.75±0.72	263.58
Ethyl Acetate	113.1313±15.12	68.5±0.72	_
Hexane	32.72727±2.32	32.12±1.44	_

Table1: the result of (TPC), (TFC) and DPPH assay

Conclusion

This study establishes *Daphne stapfii* as a rich source of phenolic and flavonoid compounds with notable antioxidant activity in methanolic extract. Further investigations into its bioactive constituents and mechanisms are recommended to explore its therapeutic potential.

References

[1] Mohamadi N, Sharififar F, Koohpayeh A, Daneshpajouh M. Traditional and Ethnobotanical uses of medicinal plants by ancient populations in Khabr and Rouchon of Iran. Journal of Applied Pharmaceutical Science. 2015 Nov 27;5(11):101-7.

[2] Nikahd M, Aghaei M, Ali Z, Sajjadi SE, Khan IA, Ghanadian M. Phytochemical analysis of Daphne pontica L. stems with their pro-apoptotic properties against DU-145 and LNCaP prostate cancer cells. DARU Journal of Pharmaceutical Sciences. 2022 Jun;30(1):85-101.

The 30th Iranian Seminar of Organic Chemistry
February 7-9, 2025, Iran University of Science and Technology, Tehran, Iran

Synthesis and application of novel nano magnetic catalyst based melamine in the synthesis of pyrazolo[3,4-*b*]pyridines

Fatemeh Fallahi Fard,[a] Mahrokh Farrokh,[a] Hassan Sepehrmansourie,[b] and Mohammad Ali Zolfigol [a*]

a Department of Organic Chemistry, Faculty of Chemistry and Petroleum Sciences, Bu-Ali Sina University, Hamedan 6517838683, Tel: +988138282807, Fax: +988138380709 Iran.

b Faculty of Converging Science and Technologies, University of Qom, Qom, Iran, 37185-359.

Keyword: Magnetic catalyst, Pyrazolo[3,4-*b*]pyridines.

In recent years, the design and application of biological-based catalysts in organic synthesis and functional groups transformation have attracted intensive attention in the science and industry because of their unique properties, such as biodegradable ability, efficiency, reusability, reactivity, stability, selectivity, and easy separation of the catalyst.[1] In continuation of our investigation for developing biological based catalysts, we wish to introduce a novel nano magnetic catalyst with phosphorus acid tags. Magnetic catalysts have been used for the synthesis of a good range of pharmaceutical and chemical compounds, due to their easy removal and convenient separation. The reported catalysts can be easily isolated from the reaction mixture with an external magnetic field.[2] Magnetic catalysts are usually made of magnetic nanoparticles such as iron oxide nanoparticles (Fe_3O_4) or other magnetic nanoparticles to which various catalytic materials such as precious metals or organic compounds are attached.[3] Fe_3O_4@MHMHPA as new catalyst containing phosphorus acid tags will be used in the synthesis of new pyrazolo[3,4-b]pyridines to determine the importance of its synthesis. Synthesized pyrazolo[3,4-*b*]pyridines can be suitable candidates for medical and environmental uses due to the presence of biological nuclei.

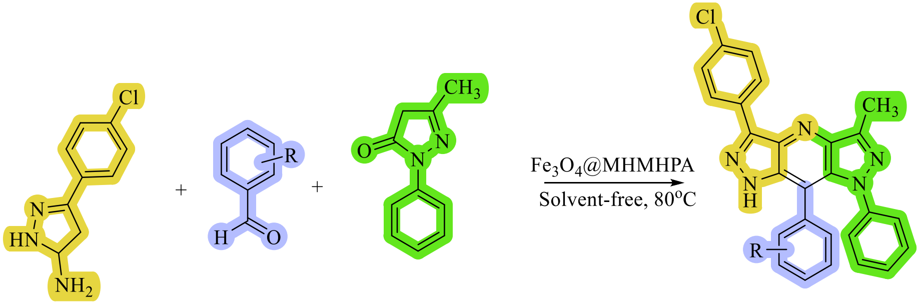

Scheme 1: Synthesis of new pyrazolo[3,4-*b*] pyridines using Fe_3O_4@MHMHPA as a magnetic catalyst.

References:

(1) Akiyama, R.; Kobayashi, S. *Chemical reviews*, 2009, *109*, 594-642.
(2) Huang, H.; Wen, G.; Liang, A.; Jiang, Z. *Journal of Food Composition and Analysis*, 2024, *136*, ١٠٦٧٤٩.

(3) Sharma, S.; Sharma, H.; Sharma, R. *Chemistry of Inorganic Materials*, 2024, *2*, 100035.

The 30th Iranian Seminar of Organic Chemistry
February 7-9, 2025, Iran University of Science and Technology, Tehran, Iran

Synthesis of Cellulose-Based Nanocomposites with Amine-Functionalized Graphene Oxide and Iron/Zinc Oxide Nanoparticles and Application in the removal of cationic dyes

Fatemeh Janati*, Yusof Dadashzadeh

Department of Chemistry, payam noor University, Tehran, Iran

Keyword: Nanocomposite, Graphene Oxide, Iron Oxid, Zinc Oxide, Nanoparticles

Introduction

Water pollution, particularly from heavy metals, presents a major environmental challenge worldwide. Contaminants such as lead, cadmium, mercury, and arsenic are not only harmful to aquatic life but also pose significant health risks to humans through the food chain and direct water consumption [1]. Cellulose serves as an excellent matrix for the development of nanocomposites [2]. The incorporation of functionalized graphene oxide (GO) into cellulose can significantly enhance the surface area and adsorption capacity due to the high surface-to-volume ratio of graphene, making it a valuable addition for heavy metal adsorption [3]. Amine-functionalized graphene oxide (AFGO) specifically offers additional advantages due to the presence of amine groups that can further increase metal ion binding through chelation, enhancing the overall removal efficiency of the composite.. Iron oxide nanoparticles are particularly effective for magnetic separation and can catalyze redox reactions, thus playing a dual role in both adsorption and degradation of pollutants [4]. Zinc oxide nanoparticles are known for their photocatalytic activity, which can facilitate the degradation of organic pollutants when activated by UV light, thereby providing an additional mechanism for water purification. This study aims to synthesize a novel cellulose-based nanocomposite that integrates amine-functionalized graphene oxide, iron oxide, and zinc oxide nanoparticles to enhance the removal efficiency of heavy metals from contaminated water.

Experimental Synthesis Method of Catalyst

Graphene oxide synthesized from graphite through the Hummers' method [5].To functionalize GO with amine groups, disperse GO in ethanol, and add APTES while stirring at room temperature for 24 hours. Prepare iron oxide nanoparticles by dissolving iron(III) sulfate (FeSo$_4$) in deionized water and adjusting the pH to around 12 using sodium hydroxide. Create zinc oxide nanoparticles by dissolving 0.1 M zinc sulfate in deionized water, then add an equimolar amount of sodium hydroxide to the solution under constant stirring. Gradually add the synthesized AFGO, Fe_3O_4, and ZnO nanoparticles to the cellulose solution while stirring. Maintain the stirring for 4–6 hours to ensure uniform dispersion of the nanoparticles in the cellulose matrix.[6,7]

Result and Discussion

ZnO is a semiconductor with a wide band gap (approximately 3.2 eV), which allows it to absorb UV light. When ZnO is irradiated with UV light, electrons in the valence band can be excited to the conduction band, generating electron-hole pairs. The generated electron-hole pairs play a crucial role in the photocatalytic process. The holes (positive charge carriers) can oxidize water or hydroxide ions (OH^-) to form hydroxyl radicals ($\bullet OH$), while the electrons can reduce oxygen to form superoxide radicals ($\bullet O_2^-$) (Zhao et al., 2020). These ROS are highly reactive and can degrade organic contaminants effectively The synthesis of cellulose-based nanocomposites incorporating amine-functionalized graphene oxide (AFGO), iron oxide nanoparticles (Fe_3O_4), and zinc oxide nanoparticles (ZnO) presents a promising approach for enhancing water pollution remediation, particularly in the removal of heavy metals and organic contaminants from wastewater. Zinc oxide nanoparticles incorporated into the composite provide an additional layer of functionality through photocatalytic activity. Under UV light, ZnO can generate reactive oxygen species (ROS) that assist in the degradation of organic pollutants and enhance the overall efficiency of the composite [8].This dual function of adsorption and catalytic degradation establishes the composite as a multifunctional material for wastewater treatment.

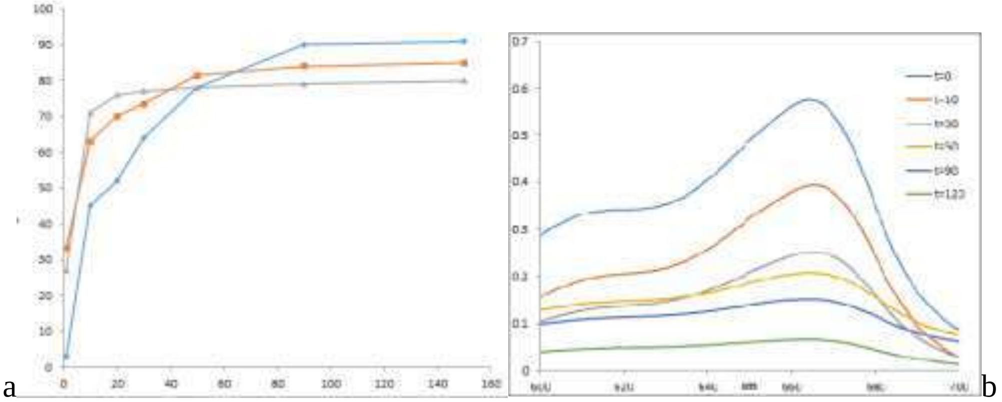

a) Photocatalytic results in the presence of UV light. b) Color removal of MB under UV lamp at different times

References

[1]. Tju Hendry, Ardiansyah Taufik, and Rosari Saleh1725, 020027 (2016)

[2] R. Tiwari, S. C. Ameta, M. K. Sharma, Effect of photocatalytic treatment on quality parameters of Phodamine B, J. Environ. Res. and Devlop 6 (2011) 82-85.

[3] P. D. Cozzoli, E. Fanizza, R. Comparelli, M. L. Curri, A. Agostiano, D. Laub, J. Phys. Chem. B 108, 96239630 (2004) .(

[4] T. L. Thompson, J. T. Yates Jr., Chem. Rev. 106, 4428-4453 (2006).

[5] Hummers, W. S., Offeman, R. E. (1958). Preparation of Graphitic Oxide. Journal of the American Chemical Society 80(6), 1339

[6] Sagadevan, S., et al. (2018) Materials Science in Semiconductor Processing, 82, 30-38

[7] Khan, Y., et al. (2021). Environmental Science and Pollution Research, 28(18), 23077-23090

[8] Zhao, Y., et al. (2020). Photocatalytic degradation of organic pollutants by ZnO based nanocomposites: Design, synthesis, and environmental applications. Applied Catalysis B: Environmental, 264, 118530

The 30th Iranian Seminar of Organic Chemistry
February 7-9, 2025, Iran University of Science and Technology, Tehran, Iran

Water Decontamination through Photocatalysis Utilizing Coupled Graphene Oxid and ZnO Green Synthesized

Fatemeh Janati* ,Yusof Dadashzadeh

Department of Chemistry, payam noor University, Tehran, Iran

Keyword: Photocatalysis, Graphene Oxid , ZnO ,Green synthesized

Introduction

In recent years with the rapidly growing industries and population, water pollution has emerged as major challenge for scientific community that demands an intense and real-world solution. According to the United Nation World Water Development report, around 748 million people around the world do not have provision for pure drinking water and water demand for industrial manufacturing will increase by 400% by 2050 [1]. Approx. 3.2 million children die every year due to unsafe drinking water and poor sanitation conditions in developing countries [2]. Graphene (G) based nanomaterials received a lot of attention in the field of photocatalytic waste water treatment. It has been extensively explored and utilized for the alteration of semiconductor photocatalysts due to its exceptional properties i.e. high specific surface area, high electron conductivity and high thermal stability. On the other hand, zinc oxide (ZnO) as a photocatalyst possesses excellent qualities as strong oxidation ability, good photocatalytic property, chemical stability, biocompatibility, non-toxicity, high photosensitivity, piezoelectric and pyroelectric properties. But inherited with some limitations such as absorption in Ultraviolet (UV) region, photocorrosion etc. as a consequence of modification due to demand of visible light active photocatalysis. Hybrid of ZnO with graphene based nanocomposites is an alternative for the degradation of organic and inorganic contaminants present in water.[3]

Experimental Synthesis Method of Catalyst

Begin by oxidizing graphite powder to produce graphene oxide using the Hummers' method [4], as follows -Mix concentrated sulfuric acid (H_2SO_4) with graphite powder and add potassium permanganate ($KMnO_4$) .(Stir the mixture at low temperatures, then add deionized water and hydrogen peroxide to quench the reaction. Wash the product with hydrochloric acid to remove impurities and obtain GO. In a typical synthesis, zinc nitrate (0.1 M) was dissolved in 50 ml of double deionized water with 10 min slight constant magnetic stirring. Reducing agent as well as capping agent of leaf extract was used in precursor solution and heated at 60 °C to 90 °C and colour changed from clear white to yellow colour paste confirming ZnO NPs formation. Then obtained paste was moved into ceramic crucible for 2hr calcination at 400 °C in muffle furnace (Fig. 1). 4 mg of GO was dissolved in a mixture of distilled H2O (20 ml) and ethanol (10 ml) via utrasonication (1 h) and 0.1 mol of ZnO was added into attained GO colloidal dispersion followed by 2 h stirring to form homogeneous suspension. The resultant suspension was then employed in a 50 ml Teflon-sealed autoclave at 200 ◦C for 6 h to reduce GO and ZnO deposition on graphene sheet.[5]

Fig. 1. Schematic depiction of green synthesized ZnO NPs.

Result and Discussion

The ZnO@GO nanocomposite attained 98.5% maximum degradation efficacy in a neutral solution under UV-light irradiation for 15 min than pure ZnO (degradation efficacy is 49% after 60 min of irradiation). The photodegradation efficiency of ZnO nanoparticles was explored for the degradation of MB (methylene blue) under solar light irradiation and the observed degradation efficacy observed was 49% even after 60 min (degradation efficacy was found 12% after 15 min of irradiation) displayed in Fig. 2(c, d). The degradation efficacy (%) of MB only (absence of catalyst-Blank) was about 6.5% even after 180 min which was 1.5% after 15 min irradiation. Thus the results exposed that prepared ZnO@GO nanocomposite is an efficient photocatalyst for effective photocatalytic degradation of MB.

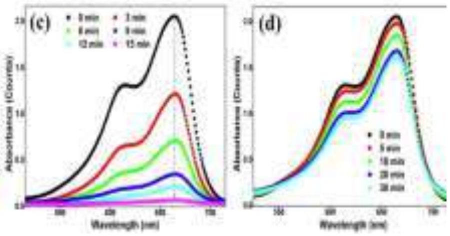

Fig. 2. Schematic representation of ZnO, GO and ZnO@GO composite

References

[1] P. Raizada, P. Singh, A. Kumar, B. Pare, S.B. Jonnalagadda, Zero valent ironbrick grain nanocomposite for enhanced solar-Fenton removal of malachite green, Sep. Purif. Technol. 133 (2014) 429–437.
[2] K. Micheal, A. Ayeshamariam, R. Boddula, P. Arunachalam, M.S. AlSalhi, J. Theerthagiri, S. Prasad, J. Madhavan, A.M. Al-Mayouf, Assembled composite of hematite iron oxide on sponge-like BiOCl with enhanced photocatalytic activity, Mater. Sci. Energy Technol. 2 (2019) 104–111.
[3] A. Sudhaik, P. Raizada, P. Shandilya, P. Singh, Magnetically recoverable graphitic carbon nitride and NiFe2O4 based magnetic photocatalyst for degradation of oxytetracycline antibiotic in simulated wastewater under solar light, J. Environ. Chem. Eng. 6 (2018) 3874–3883.
[4] W.S. Hummers Jr, R.E. Offeman, Preparation of graphitic oxide, J. Am. Chem. Soc. 80 (1958) 1339–1349.
[5] M.Yilmaz, N.Mengelizadeh, M.khodadadi Saloot, S.shahbaksh, D.Balarak, Materials Science in Semiconductor Processing. 144 (2022) 106593,

---

The 30th Iranian Seminar of Organic Chemistry
February 7-9, 2025, Iran University of Science and Technology, Tehran, Iran

The synthesis, spectroscopic characterization, and DFT calculations of the novel charge-transfer complex of 2-aminopyrazine Schiff base with 4-nitrobenzoic acid

Abolfazl Zakavat Moghanlu[a], Gholamreza Ebrahimzadeh-Rajaei*[b]

[a] *Young Researchers and Elite Club, Ardabil Branch, Islamic Azad University, Ardabil, Iran*

[b] *Department of chemistry, Ardabil branch, Islamic Azad University, Ardabil, Iran*

[*] *E-mail: gh_rajaei@iau.ac.ir*

Abstract:

The novel charge-transfer (CT) solid complex of pyrazine Schiff base, derived from 2-aminopyrazine (2-AMP) and 4-nitrobenzoic acid (4-NBA)) as an aromatic nitro compounds have been synthesized and characterized experimentally. The aim of the study is to estimate the reaction nature of bonding between 2-AMP and 4-NBA, and some spectroscopic parameters. CT complexe was formed in a molar ratio of 1 : 1 with good indications for the existence of charge-transfer in its molecular structure. In addition, theoretical studies were done on donors and acceptors, elucidating their structures and active sites where the charge-transfer occurs. The experimental work was done in methanol. The calculations of geometries and energies were performed using the density functional theory with Becke's three-parameter exchange functional method. The Lee–Yang–Parr correlation functional approach (B3LYP/DFT) combined with the 6-31G(d,p) basis set has been consecutively carried out in solution using methanol as a solvent to compliment measured results, and to justify CT within donors and acceptors. In addition, the nature and structure of the reaction product of CT complex in both solution and gas phase can be determined using the spectroscopic techniques like 13C-NMR, FTIR, 1H-NMR, and UV–Vis electronic absorption. DFT calculations were in good agreement with the experimental data and provided further evidence of the CT complex formation. The molecular stability, N-H…O bond strength and intramolecular CT have been investigated applying natural bond orbital (NBO) analysis.

Keyword:, DFT, Schiff base, 4-nitrobenzoic acid, 2-aminopyrazine, Charge-transfer complex

Introduction:

Schiff bases, named after Hugo Schiff, formed by a condensation reaction of a primary amine with an aldehyde or ketone were reported in the 19th century[1]. Charge transfer (CT) complexes are formed between electron donors with sufficiently low ionization potentials and electron acceptors with sufficiently high electron affinities. The transfer of an electron from a donor to an acceptor is readily possible in a CT-complex [2]. The HOMO–LUMO energies explain that the charge transfer occurs within the molecule [3]. The energy eigenvalues of these orbitals are generally used to define various reactivity descriptors such as ionization, electron affinity, hardness, softness, chemical potential, and so on [4].

Method:

All materials were obtained from Merck Company. All calculations were performed using the B3LYP approach with the 6-31G(d,p) basis set. The hyperconjugative interactions, molecular stability, bond strength and intramolecular CT have been investigated applying natural bond orbital (NBO) analysis. The mean polarizability, total static dipole moment, anisotropy of polarizability, and mean first-order hyperpolarizability have also been attained [5].

Results and discussion:

The calculated HOMO/LUMO energy levels of new charge-transfer complex are –4.92/–2.06 eV, respectively. The reaction between 2-AMP and 4-NBA to form the CT complex is shown in Scheme 1.

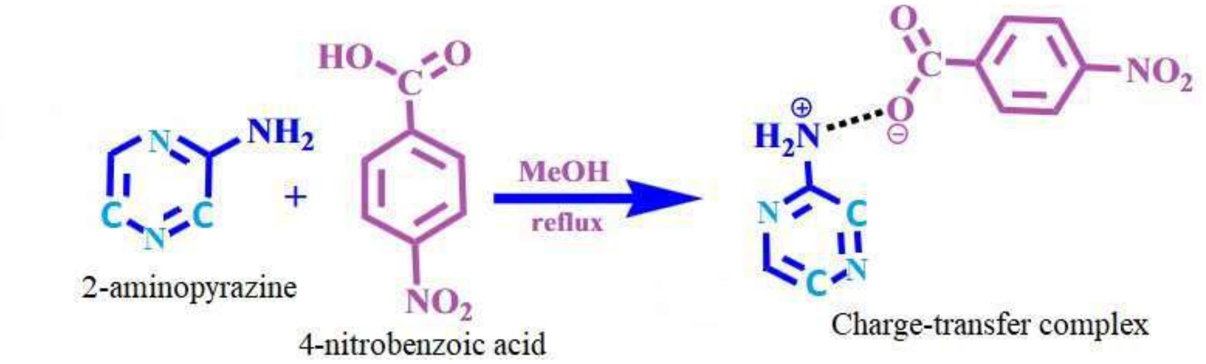

Scheme 1: The structure of CT complex derived from 2-AMP and 4-NBA

The main relationship between donor and acceptor molecules is through the π–π* interaction. The vibrational wavenumbers were also determined using B3LYP/6-31G(d,p), and the results match with the experiment. Also, the DFT calculations provide reasonable explanations for electronic structure and absorption spectra of new CT complex. The obtained values show that CT complexes are accomplished candidates to non-linear optical (NLO) materials.

References:

[1] Y. M. Issa, S.A. Abdel-Latif, A. L. El-Ansary, H. B. Hassib, *New Journal of Chemistry*, **2021**, 45(3), 1482-1499.

[2] V. Murugesan, M. Saravanabhavan, M. Sekar, *Spectrochimica Acta Part A: Molecular and Biomolecular Spectroscopy*, **2015**, 147, 99-106.

[3] N. Azizi Bala Beigloo, V. Hadigheh Rezvan, G. Ebrahimzadeh-Rajaei, Ali Shamel, *Journal of Molecular Structures*, **2024**, 1322, 140469.

[4] P. Devi, P. Rani, J. Kataria, *Journal of the Taiwan Institute of Chemical Engineers*, **2024**, 159, *105468.*

[5] N. Singh, A. Ahmad, *Journal of Molecular Structures*, **2014**, 1074, 408-415.

Evaluation of the Extract Yield and Anthocyanins Content of *Crataegus monogyna L.* Using Different Solvents

Parisa Koutahi[1], Saeed Mollaei [2]*

Affiliations: Department of Chemistry, Faculty of Sciences, Azarbaijan Shahid Madani University, Tabriz, Iran

Keyword: Anthocyanin, *Crataegus monogyna*, Extract, Yield.

1. Introduction

In recent years, due to the significant role of secondary phytochemicals and their traditional and pharma ceutical application, the development of green extraction methods has improved substantial attention. These methods aim to minimize solvent using up wile optimizing process efficiency. Among these, ultrasound assisted extraction has emerged as an innovative and efficient approach for isolating bioactive compounds (1,2).

Hawthorn (*Crataegus monogyna* L.), a species from the Rosaceae family, is an important representative of the plant community. Its fruits are found in various colors, such as red, yellow, or black-purple. The fruits of Crataegus monogyna are highly valued for their high levels of secondary metabolites, which have several medicinal activities and properties, including anti-anxiety and anti-depressant effects, cardioprotective effects, blood lipid-lowering effects, and anti-inflammatory properties. These benefits are attributed to the presence of key polyphenols such as quercetin, chlorogenic acid, and epicatechin (3,4). The natural compounds of hawthorn, such as anthocyanins, exhibit strong antioxidant activity and low cytotoxicity. The extraction of these natural compounds, which contribute to cancer prevention and treatment as well as pharmaceutical drugs, is of significant importance (5). Anthocyanins are recognized as the most abundant pigments among flavonoids, with over 540 types of these compounds identified from various plant sources. Artificial colorants are commonly used in the food industry; however, due to their harmful effects such as carcinogenicity and allergenicity, their use is being limited. Therefore, the extraction of anthocyanins from natural sources has gained significant importance. These compounds, with their antioxidant properties and appealing colors, serve as suitable alternatives to harmful synthetic colorants (7). recently, according to scientific studies, ultrasonic extraction, by facilitating mass transfer from inside plant cells to the solvent (via the cavitation phenomenon), significantly increases the efficiency of the extraction process and is recognized as a widely applied advanced technique (8).

The selection of suitable solvents for extracting natural chemical compounds from plants depends on various factors, such as the solubility of the target compound, the physical and chemical properties of the plant sample, and the used extraction method. These processes have long played a crucial role in environmental chemistry, with a focus on optimizing extraction efficiency while minimizing solvent usage (9,10). Recently, there has been significant attention on the use of safer solvents and more efficient techniques such as ultrasound-assisted extraction. These advancements aim to reduce environmental impacts while enabling the extraction of high-quality compounds with high yields.

The aim of this study is to evaluate the extraction yield of active compounds from hawthorn fruit using different solvents and ultrasonic-assisted extraction method. Additionally, the anthocyanin contents present in hawthorn fruit and their antioxidant properties are investigated to better understand their potential applications in disease prevention and treatment.

2. Material and Methods

2.1. Plant collection

The plant material of Crataegus monogyna L. were collected from Marand, East Azerbaijan Province, Iran in September 2023. They were dried at room temperature, without any direct sunlight.

2.2. Extraction method

About 1 gr of plant was mixed with different solvents (water, ethanol, ethyl acetate, and diethyl ether), and then the extraction was done using an ultrasonic apparatus at various times (10, 30, and 50 minutes) at room temperature the extraction yield was calculated below equation.

$$Yield(\%) = (\frac{(Weight\ of\ Dried\ Extract)}{(Weight\ of\ Raw\ Material)}) \times \text{١٠٠}$$

2.3. Determination of anthocyanins content

The total anthocyanin content was determined using the pH differential method. This method is based on the reversible color change of anthocyanins in response to pH. The technique measures the colored oxonium form of anthocyanins at pH 1.0 and the colorless hemiketal form at pH 4.5. For the analysis, the extracts were diluted with buffers at pH 1.0 and pH 4.5 until the absorbance at 520 nm fell within the range of 0.2–1.4, which was used to determine the dilution factor (Df). Absorbance measurements were conducted at two wavelengths, 520 nm (to quantify the anthocyanin content) and 700 nm (to correct for haze).

The total anthocyanin content was calculated using the following equation:

$$A = (A_{\text{٥٢٠}} - A_{\text{٧٠٠}})_{pH=\text{١}} - (A_{\text{٥٢٠}} - A_{\text{٧٠٠}})_{pH=\text{٤.٥}}$$

$$Concentration = {A \times M_W \times DF \times \text{١٠}^{\text{٣}}}/{\varepsilon}$$

In this equation, M_W is the molecular weight of cyanidin-3-glucoside (449.2 g/mol), DF is the dilution factor, ε is the molar extinction coefficient for cyanidin-3-glucoside (26900 L/mol·cm).

Results were expressed as milligrams of cyanidin-3-glucoside equivalents per 100 grams of dry weight (mg CGE/100 g DW). This method provides accurate and reproducible quantification of anthocyanins in plant materials (9,10).

3. Results and Discussion

The quantity and quality of active pharmaceutical compounds in medicinal plants are highly influenced by different extraction conditions. Therefore, to optimize the extract, it is essential to precisely evaluate and adjust extraction parameters.

The extraction of anthocyanins from plant cells, similar to phenolic compounds, is significantly influenced by key factors such as particle size, solvent-to-sample mass ratio, and extraction time. Reducing particle size enhances surface area and solvent penetration, thereby substantially improving extraction efficiency. Additionally, the extraction time must be carefully optimized to ensure the effective release of target compounds. The solvent-to-sample mass ratio should also be appropriately adjusted to provide sufficient solvent for complete dissolution of the desired compounds while avoiding unnecessary solvent use. Proper selection and adjustment of these parameters play a crucial role in maximizing the recovery and purity of anthocyanins (12).

this extraction of bioactive compounds using ultrasound is facilitated by thermal, mechanical, and cavitation effects. The thermal effect is directly dependent on the type of solvent and results from the conversion of ultrasonic energy into heat. The mechanical effect is characterized by the vibration of particles in the medium, induced by ultrasonic mechanical waves. In contrast, the cavitation phenomenon occurs due to the collapse of microscopic bubbles in the medium (13).

3.1. The yield and anthocyanin content extracted by water

The yield and anthocyanin content extracted by water solvent under various conditions were investigated. The results indicated that the highest yield was obtained at a solvent-to-plant ratio of 1:15 g/mL and an extraction time of 50 minutes. On the other hand, the highest anthocyanin content was observed at a solvent-to-plant ratio of 1:5 g/mL and an extraction time of 50 minutes (Figure 1).

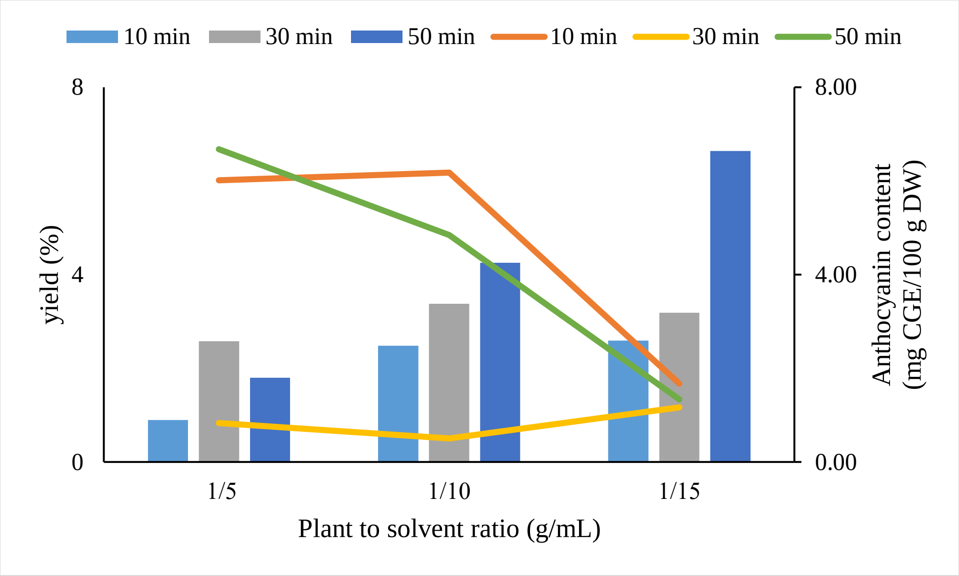

Figure 1. Extraction yield and anthocyanin content of hawthorn using water as a solvent under different conditions

3.2. The yield and anthocyanin content extracted by ethanol

The yield and anthocyanin content extracted by ethanol solvent under various conditions were investigated. The results indicated that the highest yield was obtained at a solvent-to-plant ratio of 1:10 g/mL and an extraction time of 50 minutes. On the other hand, the highest anthocyanin content was observed at a solvent-to-plant ratio of 1:5 g/mL and an extraction time of 10 minutes (Figure 2).

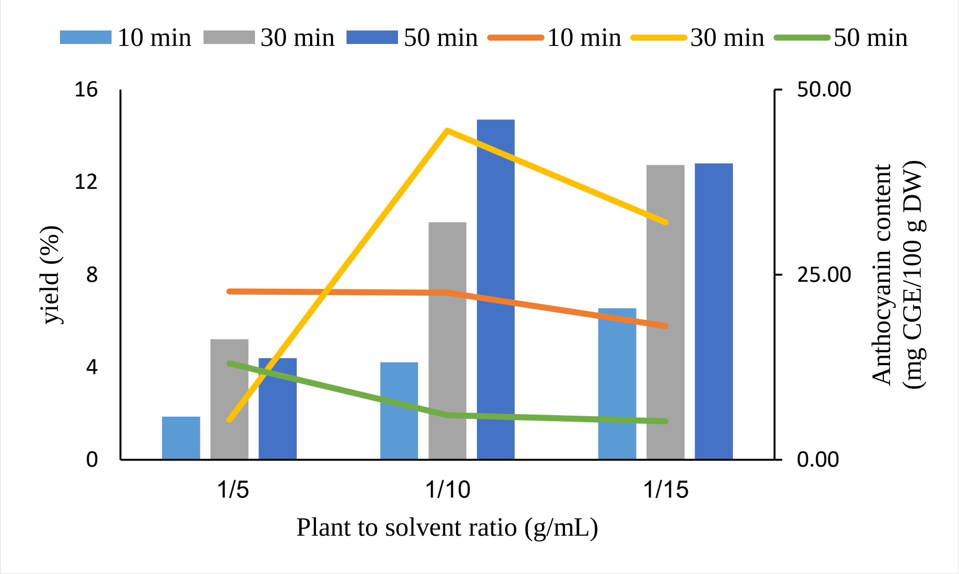

Figure 2. Extraction yield and anthocyanin content of hawthorn using ethanol as a solvent under different conditions

3.3. The yield and anthocyanin content extracted by diethyl ether

The yield and anthocyanin content extracted by diethyl ether solvent under various conditions were investigated. The results indicated that both the highest yield and the highest anthocyanin content were obtained at a solvent-to-plant ratio of 1:15 g/mL and an extraction time of 50 minutes (Figure 3).

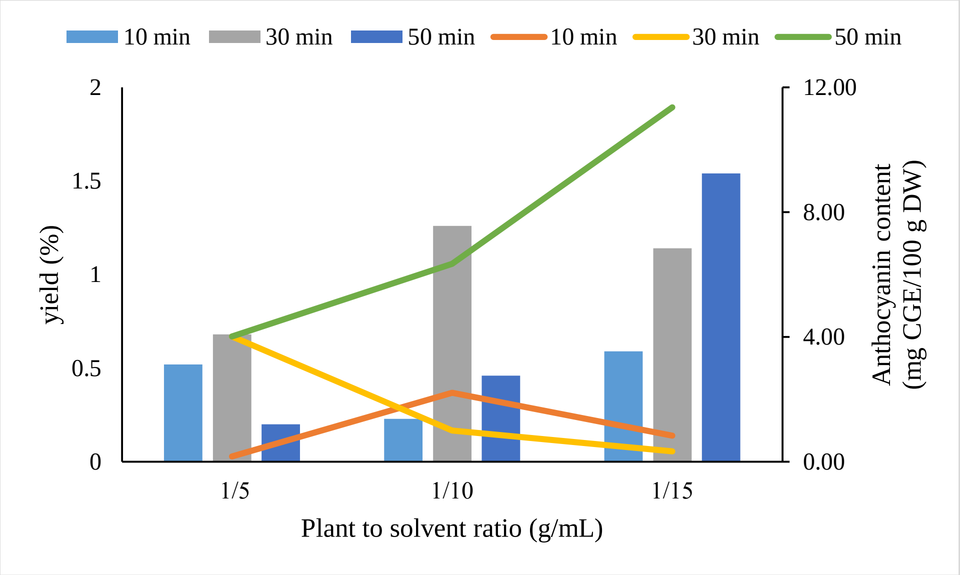

Figure 3. Extraction yield and anthocyanin content of hawthorn using diethyl ether as a solvent under different conditions

3.4. The yield and anthocyanin content extracted by ethyl acetate

The yield and anthocyanin content extracted by ethyl acetate solvent under various conditions were investigated, with the highest yield obtained at a solvent-to-plant ratio of 1:10 g/mL and the highest anthocyanin content observed at a ratio of 1:15 g/mL, both after an extraction time of 50 minutes (Figure 4).

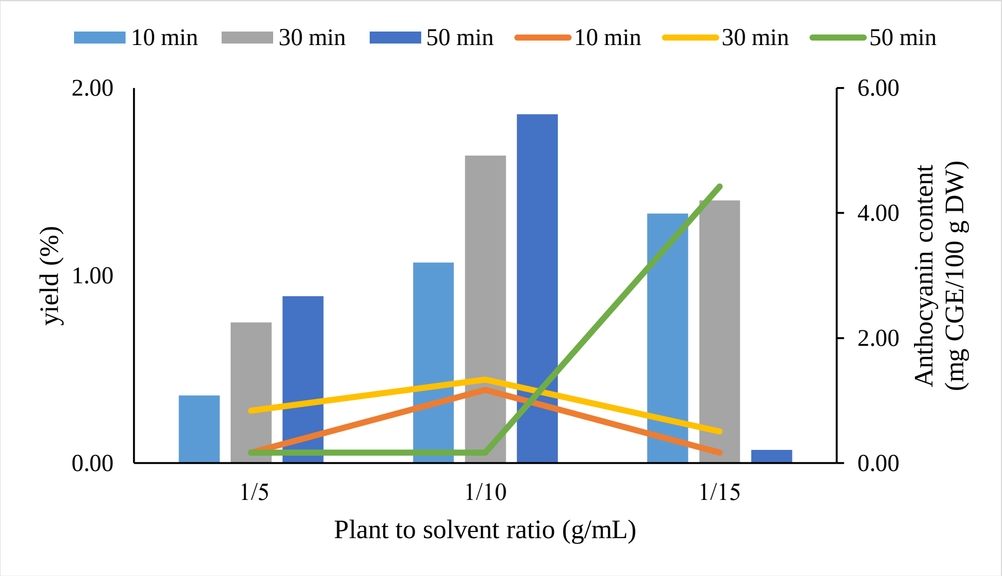

Figure 4. Extraction yield and anthocyanin content of hawthorn using ethyl acetate as a solvent under different conditions

In summary, the highest extraction yield was achieved using ethanol as the solvent, with a plant-to-solvent ratio of 1:10 g/mL and an ultrasonic extraction time of 50 minutes. Also, the highest anthocyanin content was obtained with ethanol solvent at a plant-to-solvent ratio of 1:10 and an extraction time of 30 minutes. These findings underscore the significant role of solvent-to-plant ratio and extraction time in optimizing both yield and anthocyanin content, which is essential for improving the extraction process of this valuable compound from plants.

References

[1] G. Paun, E. Neagu, C. Albu, A. Alecu, A.-M. Seciu-Grama, and G. L. Radu, "Antioxidant and Antidiabetic Activity of Cornus mas L. and Crataegus monogyna Fruit Extracts," *Molecules,* vol. 29, no. 15, p. 3595, 2024.

[2] N. Bencheikh *et al.*, "Ethnobotanical, phytochemical, toxicological, and pharmacological properties of Ziziphus lotus (L.) lam.: a comprehensive review," *Pharmaceuticals,* vol. 16, no. 4, p. 575, 2023.

[3] K. Kotsou *et al.*, "Enhancing the Nutritional Profile of Crataegus monogyna Fruits by Optimizing the Extraction Conditions," *Horticulturae,* vol. 10, no. 6, p. 564, 2024.

[4] M. Belkhir *et al.*, "Comparative analysis of Tunisian wild Crataegus azarolus (yellow azarole) and Crataegus monogyna (red azarole) leaf, fruit, and traditionally derived syrup: Phenolic profiles and antioxidant and antimicrobial activities of the aqueous-acetone extracts," *Journal of agricultural and food chemistry,* vol. 61, no. 40, pp. 9594-9601, 2013.

[5] Z. Wang *et al.*, "Hawthorn Proanthocyanidin Extract Inhibits Colorectal Carcinoma Metastasis by Targeting the Epithelial-Mesenchymal Transition Process and Wnt/β-Catenin Signaling Pathway," *Foods,* vol. 13, no. 8, p. 1171, 2024.

[6] M. Kharazi, M. Moghimi, M. Hashemi, and N. Noshirvani, "Investigating the effect of different physical and chemical parameters on the quality and stability of blackberry-enriched anthocyanin pigments," *Journal of Food Research,* vol. 33, no. 3, pp. 1-21, 2023.

[7] M. Kharazi and J. Saien, "Mechanism responsible altering in interfacial tension and emulsification of the crude oil-water system with nano Gemini surface active ionic liquids, salts and pH," *Journal of Petroleum Science and Engineering,* vol. 219, p. 111090, 2022.

[8] N. Surmanidze *et al.*, "Optimization of the method of ultrasonic extraction of lycopene with a green extract from the fruit of Elaeagnus umbellata, common in Western Georgia," *Food Science & Nutrition,* vol. 12, no. 5, pp. 3593-3601, 2024.

[9] D. A. Jinoni, M. A. Z. Benjamin, A. A. Mus, L. P. W. Goh, N. A. Rusdi, and M. A. Awang, "Phaleria macrocarpa (Scheff.) Boerl.(Mahkota Dewa) seed essential oils: Extraction yield, volatile components, antibacterial, and antioxidant activities based on different solvents using Soxhlet extraction," *Kuwait Journal of Science,* vol. 51, no. 2, p. 100173, 2024.

[10] H. Pashazadeh, A. A. Redha, J. B. Johnson, I. Koca, and M. F. Ertugay, "Microwave drying of black rosehip (Rosa pimpinellifolia L.) fruit: optimization for enhanced anthocyanin content and analysis of physicochemical properties and bioaccessibility," *Journal of Food Composition and Analysis,* vol. 132, p. 106316, 2024.

[11] D. Čulum, A. Čopra-Janićijević, and D. Vidic, "The investigation of selected bioactive compounds and antioxidant properties of Crataegus monogyna L," *Natural Product Research,* pp. 1-5, 2024.

[12] S. Silva, E. Costa, C. Calhau, R. Morais, and M. Pintado, "Anthocyanin extraction from plant tissues: A review," *Critical reviews in food science and nutrition,* vol. 57, no. 14, pp. 3072-3083, 2017.

[13] M. Lianza and F. Antognoni, "Green Method Comparison and Optimization of Anthocyanin Recovery from "Sangiovese" Grape Pomace: A Critical Evaluation of the Design of Experiments Approach," *Molecules,* vol. 29, no. 11, p. 2679, 2024.

The 30th Iranian Seminar of Organic Chemistry
February 7-9, 2025, Iran University of Science and Technology, Tehran, Iran

Preparation, Characterization, and Properties of New Polyurethanes Containing Silyl Ether and Sulfone Groups with Improved Thermal stability

Shahram Mehdipour-Ataei*[a], Negin Rezaei[b]

[a] Iran Polymer and Petrochemical Institute, P.O. Box 14965/115, Tehran, Iran

[b] Department of Chemistry, Science and Research Branch, Islamic Azad University, Tehran, Iran

Keyword: Polyurethane, sulfone, silyl ether, thermal stability

Introduction

Polyurethanes (PUs) are a group of valuable materials with wide range of applications that can typically be prepared by polyaddition of diols with diisocyanates. Wide range applications of this polymer have been observed in various industries. A major deficiency of polyurethanes is their low heat-resistance. Above 80 °C their usual physical-mechanical properties diminish and above 200 °C their thermal degradation occurs. To improve heat-resistance of polyurethanes different challenges have been made over decades. Incorporation of some thermally stable functional groups into the backbone of PUs is an important strategy in this way [1,2].

In the present work novel polyurethanes containing silyl ether and sulfone groups with desirable properties including improved thermal stability and good solubility were prepared. This was achieved by preparation of new urethane-diols comprising silyl ether units (as monomers) via reaction of diphenylsilanediol with methylene diphenyl diisocyanate (MDI) and also toluene diisocyanate (TDI) in the first step. Polycondensation reactions of these monomers with 4,4′-dichlorodiphenyl sulfone (DCDPS) in the second step resulted in preparation of related polyurethanes.

Experimental

Materials

Synthesis of urethane diol monomers (Si-MDI and Si-TDI)

Into a two-necked round-bottomed flask equipped with a magnetic stirrer, condenser, and N_2 inlet tube, 0.645 g (2.5 mmol) of MDI was placed and 5 mL of dry dimethylacetamide (DMAc) were added. It was stirred for a few minutes and then 2 drops of DBTDL was added into it and the mixture was stirred by gradual heating of the solution to 110 °C. Then, 1.1385 g (5 mmol) of diphenylsilanediol was dissolved in 13 mL of dry DMAc and added to the flask content at the same temperature. After 4 hr heating, the flask was cooled and its content poured into water. The mixture was stirred and then the precipitate was collected by vacuum filtration and vacuum dried.

The same procedure was executed for preparation of Si-TDI monomer using TDI instead of MDI.

Polymer synthesis (Si-MDI-DCDPS and Si-TDI-DCDPS)

Into a two-necked round-bottomed flask (100 mL) equipped with a magnetic stirrer, Dean-stark trap, condenser, thermometer, N_2 gas inlet, and oil bath was placed 1.3924 g (2.0 mmol) of Si-MDI diol, 0.5860 g (2.0 mmol) of 4,4′-dichlorodiphenyl sulfone (DCDPS), and 0.5724 g (4.1 mmol) of K_2CO_3. After that, 16 mL of dry DMAc and 8 mL of dry toluene were added to the flask and the reaction mixture was heated at 110 °C for 2 hr and 140 °C for about 6 hr. After cooling the mixture, it was poured into 300 mL of distilled water (non-solvent) and stirred overnight until the polymer was completely precipitated (Scheme 1).

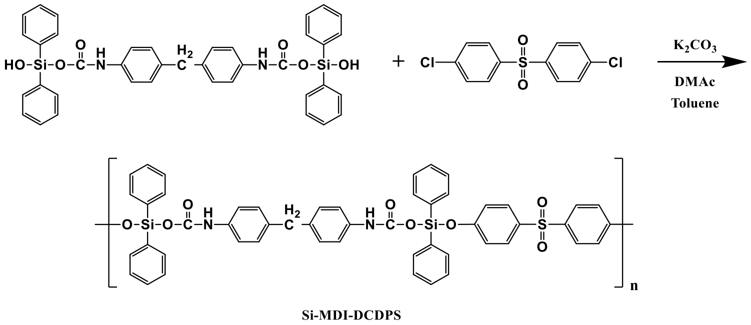

Scheme 1: Preparation of Si-MDI-DCDPS polymer

Results and discussion

The monomers and polymers were characterized using FT-IR, H-NMR, and elemental analysis.

Polymer films were prepared by dissolving the dried polymers in DMAc (20 %w/v) under stirring at ambient temperature. The homogeneous solutions were filtered and cast on a clean glass plate.

Thermal and mechanical properties of the polymers were investigated and the results were collected in Table 1.

Table 1. Data of thermal analysis and mechanical properties

Polymer	T_g(°C)	T_0(°C)	T_{10}(°C)	C.Y.at 600°C (%)	Tensile strength (MPa)	Elongation (%)
Si-MDI-DCDPS	165	275	315	21.5	79.6 ± 2.3	12.4 ± 1.3
Si-TDI-DCDPS	143	255	293	18.7	75.3 ± 3.1	10.2 ± 1.2

Thermal analyses showed increased glass transition and enhanced heat-resistance in comparison to conventional polyurethanes without silyl ether units and sulfone group [3,4]. Good solubility of the prepared polymers originated from their flexible ether, polar sulfone groups, and presence of bulky aromatic groups in the polymers. Therefore, introduction of silyl ether and sulfone groups in companion with bulky units into the backbone of polymers led to preparation of a new class of polyurethanes with high thermal stability and good solubility.

References:

1.Oprea, S., Potolinca, V.O. Soft Mater. 2023, 21 (2), 149-160.
2.Dankert, F., Hänisch, C.V. Eur. J. Inorg. Chem. 2021, 29, 2907-2927.
3.Lobanovskaya, E.S., Mokeev, M.V., Zuev, V.V. Polym. Adv. Technol. 2023, 35 (1), e6249
4.Lin, C.L., Lin, W.L., Rwei, S.P. J. Polym. Res. 2023,30, 54.

The 30th Iranian Seminar of Organic Chemistry
February 7-9, 2025, Iran University of Science and Technology, Tehran, Iran

Enhancing Thermal Properties of Polyurethane by Introduction of Silicon and Ester Units

Shahram Mehdipour-Ataei*[a]

[a] Iran Polymer and Petrochemical Institute, P.O. Box 14965/115, Tehran, Iran

Keyword: Silicon, ester, urethane, thermal stability

Introduction

By improving modern technology in today’s life, the product of polyurethanes needs to grow. Owing to numerous requirements, ranging from chemical characteristics to physical properties, and to novel uses and sustainability, the chemistry and technology of polyurethane are quickly responding to and adopting such changes and requirements. Despite wide-spread applications and

massive market for polyurethane products, definite subjects such as low thermal stability and high flammability, limit their usage in valuable applications that need more scientific attention [1].
This study was devoted to improving thermal stability of polyurethanes by introducing silicone and ester units. For this purpose, a new silicone- and ester-containing diol was synthesized through reaction of diphenylsilanediol with terephthaloyl chloride. After characterization of the diol, it was polycondensed with methylene diphenyl diisocyanate (MDI) and also toluene diisocyanate (TDI) to produce related polyurethanes named as M-SEP and T-SEP, respectively.

Experimental

Materials

Synthesis of diol monomers

Into two-necked, round-bottomed flask equipped with a magnetic stirrer, nitrogen gas inlet tube, condenser, and dropping funnel was charged with 1.14 g (5 mmol) of the diphenylsilanediol and ١٥ mL of ١،٢-dichlorobenzene. The mixture was stirred and 0.10 g of triethylamine hydrochloride was added to it. Next, 0.50 g (2.44 mmol) of terephthaloyl chloride was dissolved in 10 mL of 1,2-dichlorobenzene and added to the flask gently through dropping funnel. The mixture was heated gradually to 120 °C and remained at that temperature for about 12 hr. The mixture was cooled and product was precipitated by pouring the flask content into hexane.

Polymer synthesis

About 1.29 g (5 mmol) of MDI was placed into a dry 100 mL, round-bottomed flask equipped with a magnetic stirrer, condenser, and N_2 inlet tube, then 10 mL of dry dimethylacetamide (DMAc) were added to it. The solution was stirred for a couple of minutes and 2 drops of DBTDL was added into it and the mixture was stirred by slow heating of the solution to 110 °C. Then, 2.81 g (5 mmol) of prepared diol was dissolved dry DMAc and added to the flask content. After 4 hr heating, the flask was cooled and its content poured into water. The mixture was stirred for 1 hr at room temperature and then the precipitate was collected by vacuum filtration. (Scheme 1).

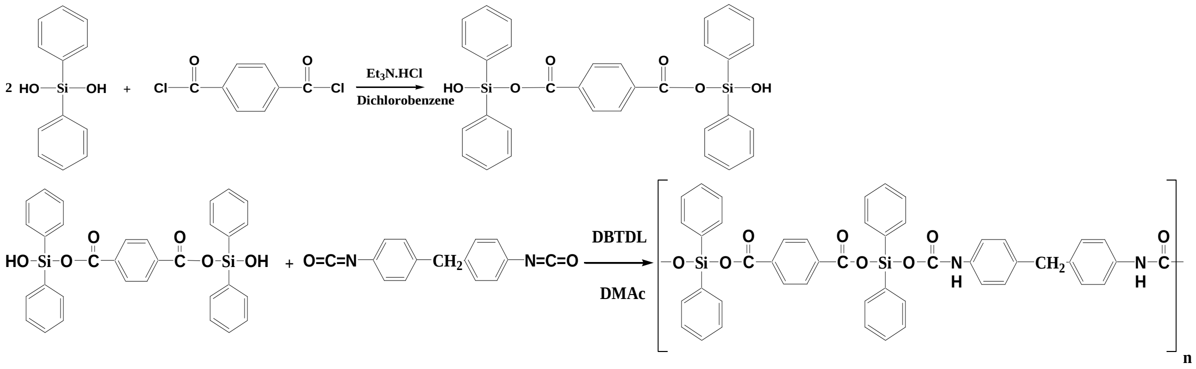

Scheme 1: Preparation of monomer and M-SEP polymer

Results and discussion

After characterization of monomer and polymers by common spectroscopic methods, polymer films were prepared by solution casting method. The Tg of M-SEP and T-SEP of the polymers were 153 °C and 132 °C, respectively. Thermal properties of the polymers were investigated and TGA curve of polymers was shown in Figure 1.

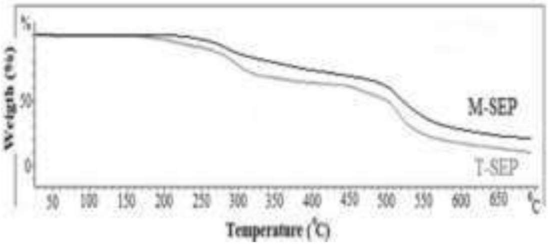

Figure 1. TGA curves of polymers

In order to find information about the flame retardancy of the prepared polyurethanes, the values of limiting oxygen index (LOI) were obtained using the Van Krevelen equation. The result showed that these polyurethanes had suitable flame-retardant properties with LOI of over 25 [2,3].

Tensile strength and elongation at break of the polymer films were in the range of 73.2-81.3 MPa and 10.9-13.2% for M-SEP and T-SEP, respectively (Table 1).

Table 1. Thermal and mechanical analysis data

Polymer	T_g (°C)	T_{IDT} (°C)	T_{10} (°C)	Char yield at 600 °C (%)	Tensile strength (MPa)	Elongation at break (%)	LOI
M-SEP	153	225	292	29.1	81.3 ± 3.3	13.2 ± 1.5	29.14
T-SEP	132	205	265	18.8	73.2 ± 3.8	10.9 ± 1.3	25.02

In sum, thermal stability and flame retardancy that are the main deficiencies of polyurethanes in various industries, were overcome by preparation of polyurethanes through incorporation of silicon and ester units and phenylation of backbone.

References:

١. Swati, J., Sonalee, D., Kingshuk, D. 2023, J. Coat. Tech. Res. 21, 137-172.
٢. Gopinath, S., Adarsh, N.N., Radhakrishnan Nair, P., Mathew, S. 2023, Plast. Technol. Eng. 62, 563-581.
٣. Lin, C.L., Lin, W.L., Rwei, S.P. J. Polym. Res. 2023, 30, 54.

The 30th Iranian Seminar of Organic Chemistry
February 7-9, 2025, Iran University of Science and Technology, Tehran, Iran

Synthesis and characterization of Novel Poly(keto ether amide)s for Application as Ultra-Filtration Membrane

Shahram Mehdipour-Ataei*[a], Maryam Jalili Marand[a]

[a] Iran Polymer and Petrochemical Institute, P.O. Box 14965/115, Tehran, Iran

Keyword: Amide, ether, ketone, ultra-filtration

Introduction

Aromatic polyamides are an important class of high performance polymers. These groups of polymers show excellent thermal stability, mechanical properties, chemical and oxidative resistance. Despite their remarkable properties, all these aromatic polymers generally have restricted solubility arising from the presence of rigid aromatic structures in the polymer chain and also strong hydrogen bonds between the amide groups. Therefore, one of the important challenges in the field of thermally stable polymers is increasing the solubility of them while maintaining other appropriate properties [1].

Main aim of this article was preparation of new types of polyamides with high thermal stability and improved solubility. This was achieved by synthesis of a novel diamine containing flexible ether bonds and polar ketone group. The diamine was synthesized via reaction of 4-aminophenol with 4,4’-difluorobenzophenone. Then the diamine was polycondensed with terephthaloyl chloride (TPC) and isophthaloyl chloride (IPC) to attain related poly(keto ether amide)s.

Experimental

Materials

Synthesis of diamine

Into a three-necked, round-bottomed flask equipped with a Dean-stark trap, a condenser, a nitrogen inlet tube, a thermometer, an oil bath, and a magnetic stirrer were placed 0.02 mol of 4-aminophenol, 0.01 mol of 4,4’-difluorobenzophenone, 25 mL of dry NMP, and 15 mL of dry toluene. Then 0.02 mol of K_2CO_3 was added to the mixture and the reaction mixture was heated to 140 °C for 6 h with continuous stirring. The reaction temperature was raised to 160 °C by removing more toluene, and maintained at the same temperature for 20 h. The mixture was cooled and poured into water. Then it was isolated by filtration and dried in a vacuum oven.

Polymer synthesis

A two-necked flask equipped with a magnetic stirrer, a nitrogen gas inlet tube, and a calcium chloride drying tube was charged with 1 mmol of diamine and 10 mL of dry NMP. The mixture was stirred at room temperature for 1 h. The solution was cooled to -5 °C, then 1 mL of triethylamine was added. After 5 min, 1 mmol of diacid chloride (TPC or IPC) was added and the mixture was stirred at room temperature for 6 h. Polymer was precipitated by pouring the content into water. It was filtered then washed with hot water and methanol several times.

Results and discussion

All materials were characterized using FT-IR, ^{1}H-NMR, and elemental analysis techniques. FT-IR spectra of the polyamides were shown in Figure 1.

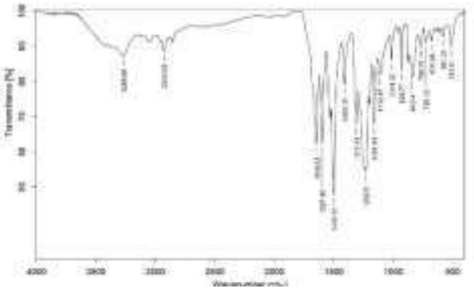

a

b

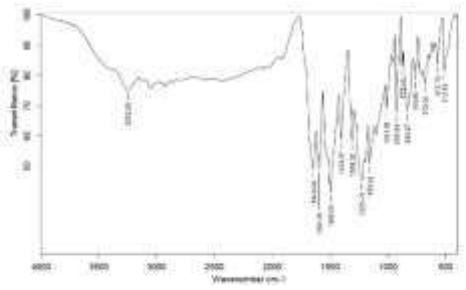

Figure 1. FT-IR spectrum of a) TPC-based, and b) IPC-based polyamides

Inherent viscosity of polymers measured at a concentration of 0.5 g.dL^{-1} in NMP at 30 ^{o}C was in the range of 0.68-0.73 dL.g^{-1}. Inherent viscosity is a criterion for assessment of molecular weights, and these polyamides had moderate-high molecular weights compared to other polyamides [2].

Low water uptake values (ranging from 1.5 to 2.0%) were observed for the polyamide samples in comparison to the common commercial polyamides (for instance polyamide 6 shows 2.75% water uptake at room temperature and 50% humidity). Such favorable low water uptake might be related to a decrease in the content of polarizing amide functional groups originated from lengthy diamine moieties that could function as spacer units in the polymer chains and hence decrease backbone polarizability to some extent. According to the thermogravimetric analysis, the initial decomposition temperature (T_o) of polyamides was about 295-338 ^{o}C. The temperature for 10% gravimetric loss (T_{10}) which is an important criterion for assessment of thermal stability was in the range of 390-440 ^{o}C. The solubility of the polymers in polar aprotic solvents including NMP, DMAc, DMF, and DMSO was in the range of 2.2-2.7 g.dL^{-1}. This improved solubility could be attributed to the presence of polar ketone and flexible ether units in the backbone.

The performance of polyamide asymmetric membranes [3] was evaluated by measuring their pure water flux over a duration of 120 minutes, at operating pressures of 5, 10, and 15 bar that was in the range of 25-300, 550-600, and 700-800 L.m^{-2}.h^{-1}, respectively.

The rejection values of various salt solutions ($MgSO_4$, $MgCl_2$) were measured (94-97%). TPC-based membranes exhibited superior salt rejection. This phenomenon could be related to the zeta potential of these membranes. TPC-based membranes showed higher negative surface charge due to its symmetric aromatic structure. This enhanced negative charge caused an increase in rejection values. The repulsive electrostatic interactions between the anions and the negatively charged membrane surface hindered the passage of salt ions. The rejection order of the salts was as follows: $MgSO_4$ >$MgCl_2$.

References:

1. D.B. Stojanović, M. Zrilić, R. Jančić-Heinemann, I. Živković, A. Kojović, Polym. Adv. Technol. 2013; 24, 772.
2. M. Cai, M. Chen, Y. Yu, C. Song, Polym. Adv. Technol. 2013; 24, 466.
3. V. Freger, G.Y. Ramon. Prog. Polym. Sci. 2021, 122, 101451.

The 30th Iranian Seminar of Organic Chemistry

February 7-9, 2025, Iran University of Science and Technology, Tehran, Iran

Comparison of $MnFe_2O_4/TiO_2/g\text{-}C_3N_4$ and $MnFe_2O_4/TiO_2/GO$ nanohybrids for arsenic removal from aqueous environment

Hossein Sadeghpour[a], Zohreh Boroumand[b], Seyedeh Bahareh Azimi*[c](corresponding author)

[a]*School of Mining, College of Engineering, University of Tehran, Iran*

[b]*Head of NanoBioEarth department, Applied research center of geological survey*

[c]*Assistant Professor, Research Group of Environmental Assessment and Risk, Research Center for Environment and Sustainable Development (RCESD), Department of Environment, Tehran, Iran*

Abstract

In this research, we investigated the effectiveness of two types of spinel ferrite nanoparticles, MnFe2O4/TiO2/GO and MnFe2O4/TiO2/g-C3N4, for the removal of arsenic from groundwater. The magnetic adsorbents were thoroughly characterized using various analytical techniques, including X-ray diffraction (XRD), field emission scanning electron microscopy (FE-SEM), energy-dispersive X-ray spectroscopy (EDS). We examined the influence of several factors on the adsorption process, such as pH, contact time, initial arsenic concentration, and temperature. Both MnFe2O4/TiO2/GO and MnFe2O4/TiO2/g-C3N4 were employed to effectively reduce arsenic concentration. The results showed a significant decrease in arsenic levels, from an initial concentration of 17.8 mg/L to 197 µg/L and 177 µg/L, respectively, for MnFe2O4/TiO2/GO and MnFe2O4/TiO2/g-C3N4, which corresponds to removal efficiencies of 98.89% and 99.01%

Key words: nanoparticles, arsenic, adsorption, water, reusability

References:

Abdel-Wahed, M.S. *et al.* (2020) ‘Core double-shell MnFe2O4@rGO@TiO2 superparamagnetic photocatalyst for wastewater treatment under solar light’, *Chemical Engineering Journal*, 382, p. 122936. doi:10.1016/J.CEJ.2019.122936.

Sahu, N., Singh, J. and Koduru, J.R. (2021) ‘Removal of arsenic from aqueous solution by novel iron and iron–zirconium modified activated carbon derived from chemical carbonization of Tectona grandis sawdust: Isotherm, kinetic, thermodynamic and breakthrough curve modelling’, *Environmental Research*, 200, p. 111431. doi:10.1016/J.ENVRES.2021.111431.

Wang, X. *et al.* (2021) ‘High-efficient removal of arsenite by coagulation with titanium xerogel coagulant’, *Separation and Purification Technology*, 258(P2), p. 118047. doi:10.1016/j.seppur.2020.118047.

The preparation of Putrescine-Dextran copolymer and evaluating its protective activity against Dnase

Kianoosh Karami[1], Seyed Sepehr Uroomiye[2,3], Seyedeh Bahareh Azimi[4*] (corresponding author)

[1]*Department of Biology, Payame Noor University (PNU), Tehran, Iran*

[2]*Medicinal Plants and Natural Products Research Center, Hamadan University of Medical Sciences, Hamadan, Iran*

[3]*Department of Pharmacology and Toxicology, Faculty, School of Pharmacy, Hamadan University of Medical Sciences, Hamadan, Iran*

[4]*Assistant Professor, Research Group of Environmental Assessment and Risk, Research Center for Environment and Sustainable Development (RCESD), Department of Environment, Tehran, Iran*

Abstract

Gene therapy vectors come in viral and non-viral forms. While viral vectors excel at cell invasion, non-viral vectors offer advantages like low immunogenicity, cheaper production, and scalability. Among non-viral carriers (Liposomes, Cationic polymers, Exosomes, Dendrimers), cationic polymers effectively transport DNA through electrostatic interactions. Natural polymers like the aminated Dextran can be modified for nucleic acid delivery. (1-11)

Dextran dialdehyde was produced using 2 mmol sodium periodate and 1g Dextran (9000-11000 Da) in water for 6h. After dialysis and lyophilization, amination was performed using 11 mmol Putrescine and 15 mmol Sodium Cyanoborohydride for 24h. The product was analyzed using NMR spectroscopy, retardation assay, DNase protection test, and MTT cytotoxicity assay.(6, 7)

NMR confirmed successful synthesis with aldehyde peaks at 9.86 and 9.96 ppm, and Putrescine methylene peaks at 1.54, 1.66, 1.78, and 1.81 ppm. HEK-293 cells showed minimal toxicity. Retardation assay demonstrated strong plasmid interaction, and DNase testing showed plasmid protection.

The Dextran dialdehyde-Putrescine copolymer successfully demonstrated nucleic acid interaction and protection against nucleases while remaining biologically inert.Key words: nanoparticles, arsenic, adsorption, water, reusability

Key Words: Copolymer, Dextran , Putrescine, Malprade method, Gene Delivery, Plasmid

References:

1. Ramamoorth M, Narvekar A. Non viral vectors in gene therapy-an overview. Journal of clinical and diagnostic research: JCDR. 2015;9(1):GE01.
2. Lundstrom K. Viral vectors in gene therapy. Diseases. 2018;6(2):42.

3. Duan L, Xu L, Xu X, Qin Z, Zhou X, Xiao Y, et al. Exosome-mediated delivery of gene vectors for gene therapy. Nanoscale. 2021;13(3):1387-97.

٤. Hosseinkhani H, Azzam T, Tabata Y, Domb A. Dextran–spermine polycation: an efficient nonviral vector for in vitro and in vivo gene transfection. Gene therapy. 2004;11(2):194-203.

٥. Zink M, Hotzel K, Schubert US, Heinze T, Fischer D. Amino Acid–Substituted Dextran-Based Non-Viral Vectors for Gene Delivery. Macromolecular Bioscience. ٢٠١٩;١٩(٨):١٩٠٠٠٨٥.

6. Nonsuwan P, Matsugami A, Hayashi F, Hyon S-H, Matsumura K. Controlling the degradation of an oxidized dextran-based hydrogel independent of the mechanical properties. Carbohydrate polymers. 2019;204:131-41.

7. Maia J, Carvalho RA, Coelho JF, Simões PN, Gil MH. Insight on the periodate oxidation of dextran and its structural vicissitudes. Polymer. 2011;52(2):258-65.

8. Wang Y, Bruggeman KF, Franks S, Gautam V, Hodgetts SI, Harvey AR, et al. Is viral vector gene delivery more effective using biomaterials? Advanced Healthcare Materials. 2021;10(1):2001238.

9. Chen F, Huang G, Huang H. Preparation and application of dextran and its derivatives as carriers. International journal of biological macromolecules. 2020;145:827-34.

10. Gong H, Li W, Sun J, Jia L, Guan Q, Guo Y, Wang Y. A review on plant polysaccharide based on drug delivery system for construction and application, with emphasis on traditional Chinese medicine polysaccharide. International journal of biological macromolecules. 2022;211:711-28.

11. Li Y, Wang R, Bai H, Yang J. Polysaccharides: A carrier for gene therapy. Current Drug Delivery. 2023;20(1):31-40.

The 30th Iranian Seminar of Organic Chemistry
February 7-9, 2025, Iran University of Science and Technology, Tehran, Iran

تدوین نقشه راه و برنامه اقدام راهبردی مدیریت پسماند کشور

سیده بهاره عظیمی*[1]، پیام جوهرچی[2]

1[illegible]

2[illegible]

خلاصه

امروزه تغییر سبک زندگی تمایل روز افزون شهروندان به مصرف مصرف گرایی، تنوع محصولات و کالاهای تجاری و به دنبال آن تحولات پدید آمده در میزان و کیفیت مواد مصرفی، مناطق مختلف شهری و روستایی را با بحران بسیار جدی به نام

تولید بیش از اندازه و غیر منطقی انواع و اقسام مواد زائد یا به عبارتی پسماندها روبرو ساخته است[۱]. افزایش روزافزون تعداد صنایع و کسب‌وکارها، همراه با افزایش شهرنشینی و رشد جمعیت جهانی، منجر به افزایش چشمگیر حجم پسماندها در کشورهای توسعه‌یافته و در حال توسعه شده است. بنابراین، مدیریت مؤثر پسماندها در تمام سطوح جامعه برای مقابله با این مشکل رو به رشد ضروری است [۲].

مشکل اصلی ناشی از تولید بیش از اندازه و غیر منطقی پسماندها که در سالهای اخیر به یکی از مهمترین معضلات زیست محیطی برای تمامی مناطق شهری و روستایی ایران تبدیل شده است تلنبار شدن مواد زائد در زمینهای اطراف شهرها و روستاها رودخانه ها، جنگل ها و حتی در مزارع است که منجر به آلودگی خاک، هوا، آبهای سطحی و زیرزمینی و اکوسیستم های خشکی - آبی گردیده است. در این میان علاوه بر محیط طبیعی محیط انسانی و حتی حیات خود انسانها و جانوران هم تحت تأثیر و تهدید قرار گرفته است [۱].

مدیریت پسماند در کشورهای توسعه‌یافته و در حال توسعه متفاوت است. رویکردهای متنوعی در مناطق مختلف، شامل مناطق شهری و روستایی، و بخش‌های مسکونی و صنعتی به کار گرفته می‌شود. فرآیندهای صنعتی به طور قابل توجهی در تولید انواع پسماندهای گازی، مایع و جامد مشارکت دارند [۳].

با وجود اینکه ایران به لحاظ سرانه تولید پسماند در جایگاه پایین تری نسبت به دیگر کشورهای جهان و حتی کشورهای همسایه میباشد ولی برعکس با مشکلات زیست محیطی شدیدتری مواجه می باشد. از آنجایی که ایران کشوری رو به صنعتی شدن افزایش شهرنشینی و در آینده بهبود شرایط اقتصادی می باشد، انتظار می رود که میزان تولید پسماند در سالهای آینده افزایش چشمگیری داشته باشد چرا که ارتباط مستقیمی بین میزان شهرنشینی و درآمد با میزان تولید پسماند وجود دارد. مدیریت پسماند به عنوان یک چالش اساسی در ایران، نیازمند رویکردهای نوین و استراتژیک است. با توجه به افزایش جمعیت و تغییرات سبک زندگی، تولید پسماند در کشور به شدت افزایش یافته و این امر تهدیدی جدی برای محیط زیست و سلامت عمومی محسوب می‌شود.

لذا بایستی پیش بینی های لازم برای بهبود ساختار مدیریت پسماند در کشور از ابعاد مختلف زیر ساختی، اقتصادی، قانونی و فرهنگی اتخاذ شود.

کلمات کلیدی؛ پسماند، نقشه راه، محیط زیست

۱-بند چ ماده ۲۲ قانون برنامه توسعه هفتم

سازمان حفاظت محیط زیست مکلف است با همکاری وزارتخانه های کشور، صنعت، معدن و تجارت، نیرو، نفت، جهادکشاورزی و بهداشت، درمان و آموزش پزشکی برنامه ملی راهبردی مدیریت پسماندها را با رویکرد اصلاح الگوی تولید و مصرف، کاهش حداکثری تولید پسماندها، تفکیک از مبدأ و پیاده سازی نظام اقتصاد چرخشی در چرخه مدیریت پسماندها در پایان سال اول برنامه تهیه کند و به تصویب هیأت وزیران برساند. دستگاه های ذیربط مکلفند در طول سالهای اجرای برنامه به گونه‌ای عمل نمایند که برنامه ملی راهبردی مدیریت پسماندها در کلانشهرها و شهرهای استانهای شمالی به صورت کامل اجرائی گردد.

۱-۱- مشکلات وضع موجود

مهمترین مشکلات مدیریت پسماند در کشور و نیز تهدیدهای آن در نمودارهای شکل ۱- و شکل ۲- آورده شده است. رتبه بندی این عوامل بر اساس نظرات متخصصان حوزه پسماند و نیز کارشناسان نهادهای اجرایی و نظارتی صورت گرفته است.

۱-۲- تبعات ادامه وضع موجود

مهمترین نتایج ادامه وضع موجود را به صورت زیر می توان جمع بندی کرد.

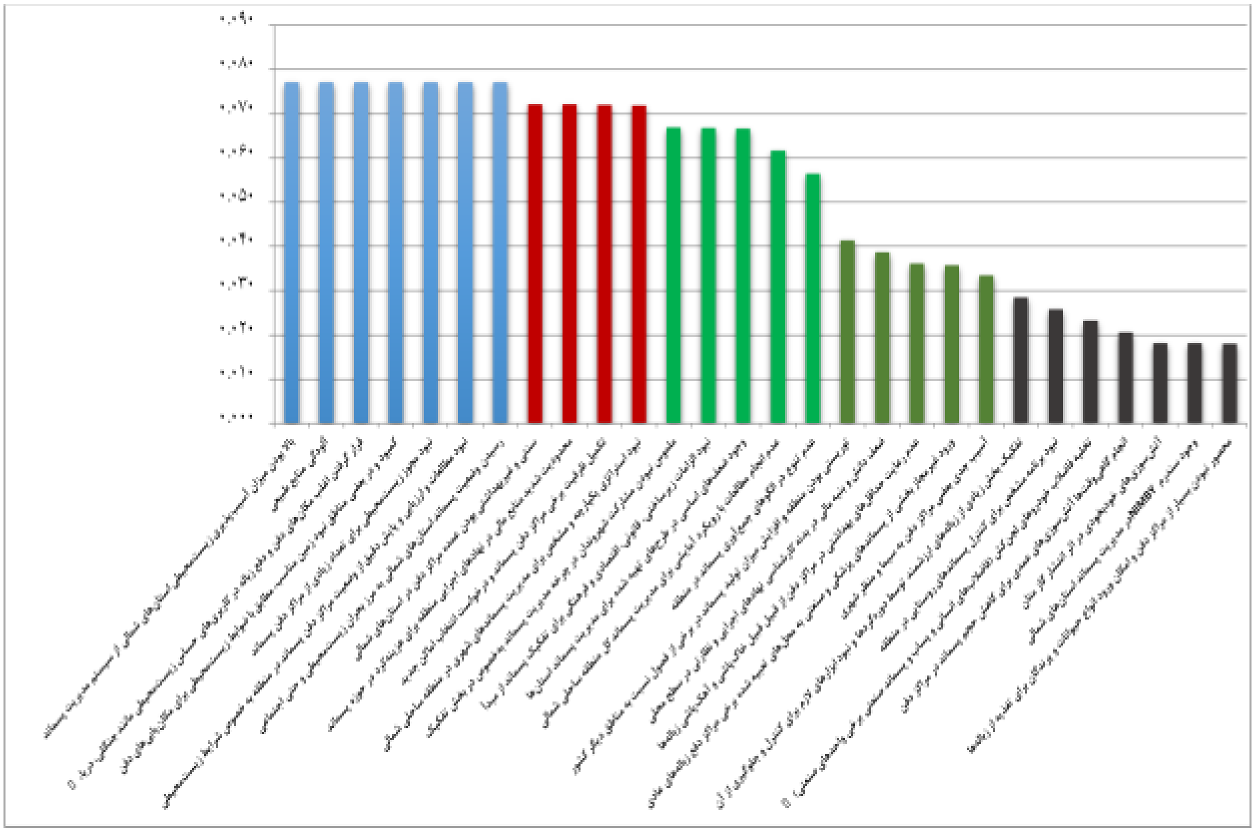

شکل۱- رتبه‌بندي‌نقاط‌ضعف‌مدیریت‌پسماند

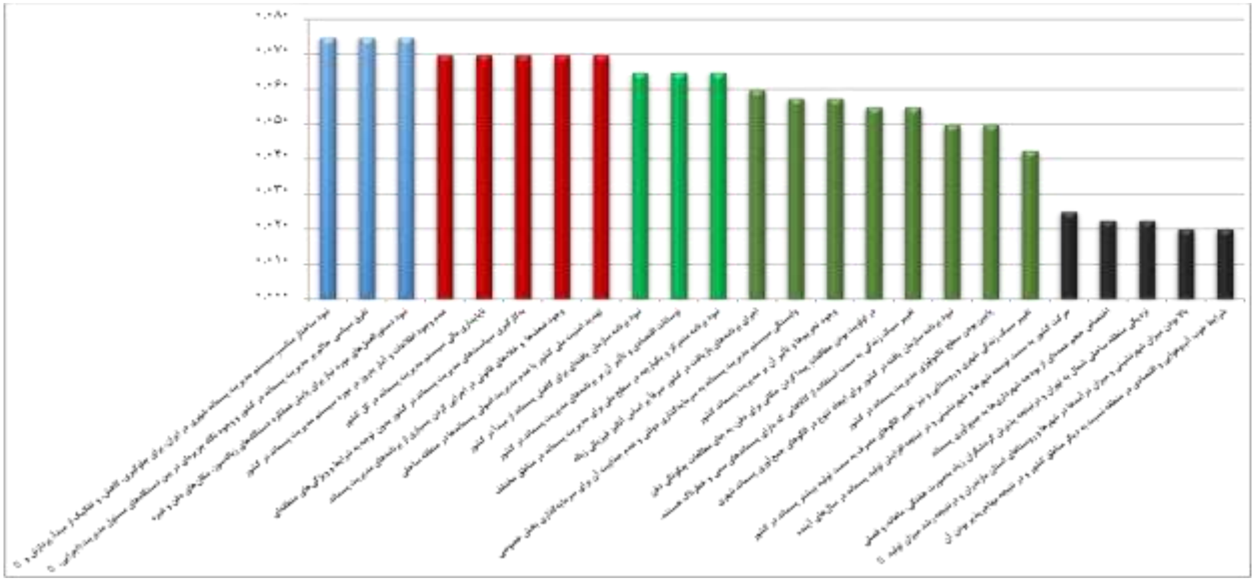

شکل۲- رتبه بندی تهدیدهای مدیریت پسماند

☐ مدیریت نادرست پسماندها دفن غیر اصولی عدم تفکیک عدم بازیافت مناسب و غیره، سالانه حدود ۸۷۰ هزار میلیارد ریال خسارت زیست محیطی به کشور وارد میکند این خسارت ها ناشی از اشغال زمین برای دفن آلودگی آبهای زیرزمینی ناشی از نفوذ شیرابه تولید گازهای گلخانه ای، عدم استفاده مناسب از منابع قابل بازیافت آلودگی آبهای سطحی آلودگی خاک، منظر شهری و روستایی و غیره می باشد.

□ تهدید امنیت ملی در صورت ادامه مشکلات زیست محیطی امروزه از تهدیدات زیست محیطی به عنوان یکی از تهدیدات نوین امنیت ملی یاد میشود نگرانی فزاینده در مورد آینده بشر و تأثیر منفی تخریب محیط زیست بر زندگی انسان باعث شده که مشکلات زیست محیطی اهمیتی روز افزون در سیاست ملی و بین المللی پیدا کند. منطق اساسی امنیت زیست محیطی بر این انگاره است که در چشم انداز جهانی، نوع بشر به گونه ای گذران زندگی میکند که از حد تحمل کره زمین خارج است. امنیت زیست محیطی دو مسئله مجزا را بیان میکند تخریب عوامل زیست محیطی و نیز تأثیر تخریب محیط زیست بر سلامتی جوامع انسان که هر دوی اینها میتواند به مثابه عاملی در ایجاد بی ثباتی و نزاع نقش آفرینی کند. با توجه به اینکه الگوی مصرف در کشور در سالهای اخیر به تبع تحولات جهانی به شدت تغییر پیدا کرده است ظهور انواع پسماندهای جدید که مواد خطرناک و سمی زیادی دارند افزایش جمعیت شهری و شهرنشینی و به تبع آن افزایش میزان تولید پسماند نبود زیر ساخت های مناسب مدیریت پسماند در کشور مکانهای دفن بهداشتی سیستمهای پردازش و بازیافت استاندارد و غیره) و عوامل مشابه دیگر، عدم مدیریت صحیح پسماندهای شهری هم به طور مستقیم منجر به تخریب محیط زیست می شود و هم بر سلامتی جوامع اطراف تأثیر منفی دارد که ممکن است با ایجاد بی ثباتی و نزاع به عنوان عامل نوین تهدید کننده امنیت ملی عمل کند.

□ تشدید چالش آب به عنوان یکی از مهمترین چالشهای جهانی در حال حاضر سرانه منابع آب تجدید شونده جهان ۷۶۰۰ متر مکعب در سال بوده و ایران با سرانه ۱۶۲۵ متر مکعب در آستانه ورود به تنش آبی و بحران میباشد. در تقسیمات اقلیمی حدود ۸۵ درصد کشور در منطقه فراخشک نیمه خشک و بیابانی قرار دارد. منابع سالانه آب سطحی و زیرزمینی کشور ۱۳۰ میلیارد متر مکعب می باشد که حدود ۱۰۰ میلیارد متر مکعب آن سالانه استحصال میگردد از این میزان حدود ۹۳ درصد سهم مصارف بخش کشاورزی متوسط جهانی آن ۷۰ درصد است و ۶ درصد در بخش شرب و ۱ درصد در بخش صنعت مصرف می گردد. مدیریت پسماند در کشور به خودی خود چالش زیست محیطی مهمی است. با این وجود در یک نگاه یکپارچه مدیریت نادرست پسماندها، منابع آبی را هم به شدت تهدید میکند. با تلنبار کردن زباله ها در مکانهای دفع و دفن غیر بهداشتی و کنترل نشده به فاصله نه چندان زیاد شیرا به این زباله ها وارد رودخانه ها و از آنجا وارد زمین ها و محصولات کشاورزی و دریا می‌شود و زندگی و سلامت تمام کسانی که از این محصولات استفاده می کنند و یا در تماس هستند را تحت تأثیر قرار می‌دهد. برای نمونه بنا بر آمار آب و فاضلاب مازندران بیش از ۹۰ درصد آب مازندران از سفره های زیر زمینی تأمین میشود و این سفره ها از آب باران و رودخانه تغذیه می شوند و سطح آنها نیز در مقایسه با کل کشور بسیار بالا می باشد.

□ شکل گیری بحرانهای اجتماعی در منطقه در صورت ادامه مشکلات موجود به تهدیدات امنیتی پسماند بایستی از دو بعد نگاه کرد اول ماهیت خود پسماند که میتواند منجر به انواع مشکلات زیست محیطی، سلامتی روانی و اجتماعی شود و دوم تأثیر مستقیم آنها بر منابع آب زیرزمینی و سطحی که خود آب امروزه از مهمترین چالشهای کشور و جهان میباشد. پسماند اگر اصولی مدیریت نشود، علاوه بر مشکلات زیست محیطی محیط زیست انسانی را حتی در کوتاه مدت هم با مشکل مواجه خواهد کرد. شیوع این مشکلات در قالب انواع بیماری بو، تغییر کیفیت خاک، آب، خشک شدن جنگل ها و غیره منجر به شکل گیری بار روانی بر شهروندان و ساکنان منطقه خواهد شد که خود این بار روانی می تواند منجر به بحران اجتماعی در شکل های مختلف شود.

□ جمع بندی روند موجود به عنوان جمع بندی روند موجود ادامه هر کدام از مشکلات و تهدیدهایی که از جانب مدیریت پسماند در منطقه وجود دارد منجر به تشدید آنها شده و این مشکلات با توجه به شرایط حساس زیست محیطی منجر به شکل گیری انواع بحرانهای زیست محیطی و اجتماعی امنیتی و غیره خواهد شد.

۲- وضعیت مطلوب

۲-۱- مأموریت جمعی

گام اول در وضعیت مطلوب تعریف یک مأموریت فراسازمانی برای مدیریت پسماند است. با تدوین این مأموریت نگاه جزیره ای هر دستگاه به منطقه باید حذف شود و یکپارچه سازی استراتژی ها صورت بگیرد.

۲-۲- چشم انداز مدیریت پسماند کشور

با توجه به آسیب شناسی صورت گرفته از چالشهای مدیریت پسماند در ایران و شناسایی عوامل مؤثر داخلی و خارجی و نیز در راستای مأموریت جمعی چشم انداز مدیریت پسماند به صورت شکل زیر تدوین و مورد اجماع قرار گرفته است. چشم انداز تدوینی شامل چهار محور اساسی کارآیی اقتصادی مشارکت مردمی پایداری زیست محیطی و پایداری اجتماعی می‌باشد (شکل۳).

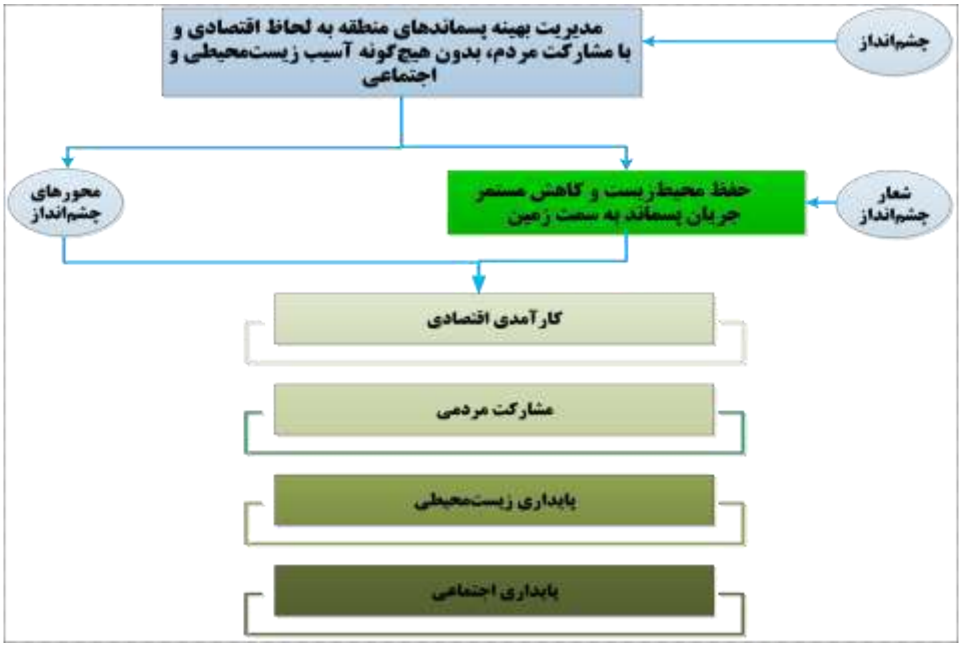

شکل۳- چشم‌انداز نقشه‌راه مدیریت پسماند

۳- نقشه راه وضعیت مطلوب و اقدامات مورد نیاز

جهت تدوین نقشه راه مدیریت پسماند در کشور اقدام به سناریوسازی شده است. بر اساس بررسی های صورت گرفته مطالعه ادبیات جهانی برگزاری کارگاه هم اندیشی مطالعه اسناد بالادست و غیره) ۶ سناریو تدوین و با توجه به ۱۷ شاخص در ۵ بعد اقتصادی، اجتماعی- فرهنگی زیست محیطی، سیاسی - مدیریتی و فنی - اجرایی مورد ارزیابی قرار گرفته است. در نهایت بعد از ارزیابی و مشخص شدن سناریوهای برتر از ترکیب ۳ سناریویی که بیشترین امتیاز را آورده بودند، سناریوی برتر برای کشور تدوین شده است. سناریوی برتر برای مدیریت پسماند کشور در شکل ٤ آورده شده است.

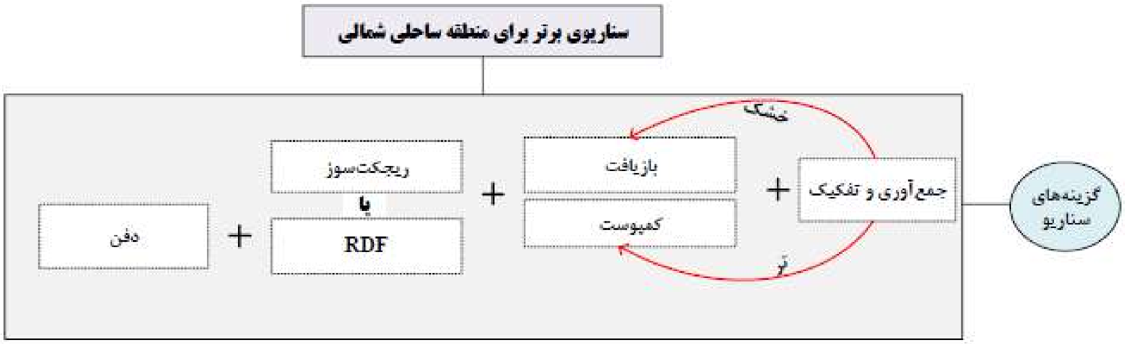

شکل٤- شکل سناریوی برتر برای مدیریت پسماند

بعد از تدوین سناریوی برتر و با توجه به این سناریو برای هر منطقه برنامه ریزی شامل ۱۴ منطقه)، برنامه عملیاتی مختص آن منطقه تدوین شده است. لازم به توضیح است که در برنامه عملیاتی هر منطقه اصل نگاه سیستمی و یکپارچه به منطقه

اصل توسعه تدریجی و نیز پروژه های نیمه تمام و موجود هر منطقه مورد توجه بوده است. در نهایت با توجه به برنامه عملیاتی هر منطقه موازنه جرمی پسماند برای هر منطقه به همراه برآورد هزینه ها به تفکیک سال برنامه نوع فرایند و با توجه به موزانه جرمی) صورت گرفته است.

سناریوی نهایی منطقه ساحلی شامل جمع آوری و تفکیک بازیافت پسماند خشک، کمپوست پسماند تر و استفاده ترکیبی از RDF و زباله سوز در مناطق مختلف بسته به شرایط جغرافیایی طبیعی اقتصادی پسماندی و غیره حاکم بر آن منطقه میباشد در خصوص این سناریو و اجرایی کردن آن موارد زیر بایستی یادآوری شود:

۱- منظور از جمع آوری، جمع آوری مکانیزه و پوشش حرفه ای جمع آوری پسماند است. هر پسماندی که تولید میشود باید بلافاصله و با بهترین شرایط زیست محیطی جمع شود.

۲-رویکرد به تفکیک در این سناریو رویکردی تدریجی است و از کمترین میزان درصد در سال ۱۴۰۳ شروع شده و به ۲۵ درصد در سال ۱۴۰۷ خواهد رسید.

۳-بر اساس طرح های بالادستی ، مطالعات جهانی و مطالعات داخلی صورت گرفته ایجاد کارخانه کمپوست در مناطقی که میزان تولید پسماند آنها کمتر از ۱۰۰ تن در روز باشد به صرفه اقتصادی نبوده و پیشنهاد نمی شود.

٤- بر اساس طرح های بالادستی مطالعات جهانی و مطالعات داخلی صورت گرفته ایجاد واحد زباله سوز و بیوگاز در مکانهایی که تولید پسماند آنها کمتر از ۴۰۰ تن در روز است دارای توجیه فنی و اقتصادی نبوده و پیشنهاد نمی شود.

۵- سناریوی برتر هر منطقه با توجه به وجود تاسیسات مدیریت پسماند نیمه تمام پتانسیل های موجود در منطقه و میزان پسماند تولیدی قابل تغییر میباشد.

٦- برنامه های مورد نظر به نحوی پیشنهاد شده است که هیچ پسماندی به صورت خام و پردازش نشده دفن نگردد و دفن بهداشتی تنها برای پسماند ریجکت سایر تاسیسات صورت می گیرد.

۷- در صورت وجود سرمایه گذار بخش خصوصی با آورده بیشتر از ۷۰ درصد و فراهم آمدن شرایط برای اجرای سناریوهای جایگزین برخی سناریوهای آلترناتیو با اولویت مناطق اعلامی توسط وزارت کشور و تایید سازمان حفاظت محیط زیست مناطق قابل اجرا خواهد بود.

منابع:

محمدزاده، محمد، ۱٤۰۰، بررسی چالش ها و راهبردهای زیست محیطی پسماند [۱]

[2] Sen Gupta, Y., Mukherjee, S., Dutta, R., & Bhattacharya, S. (2022). A blockchain-based approach using smart contracts to develop a smart waste management system. *International Journal of Environmental Science and Technology*, 1-24.

[3] Boostani, F., Golzary, A., Huisingh, D., & Skitmore, M. (2024). Mapping the Future: Unveiling Global Trends in Smart Waste Management Research. *Results in Engineering*, 103485.

The 30th Iranian Seminar of Organic Chemistry
February 7-9, 2025, Iran University of Science and Technology, Tehran, Iran

An effective method for the synthesis of new bis(indole)methane analogs using PVPP-*p*-TSA

Masoud Mokhtary[a]*, Majid Kia[a], Mahsa Bakrani[b]

Department of Chemistry, Rasht Branch, Islamic Azad University, Rasht, Iran
Department of Biology, Rasht Branch, Islamic Azad University, Rasht, Iran

Keyword: *Bis(indole)methane*, *Formylarylsulfonates*, *PVPP-p-TSA*

Bis(indole)methanes have been considered an important pharmaceuticals due to their diverse biological properties [1-3]. In this research, an effective method for the synthesis of new derivatives of bis(indole)methane using polyvinylpolypyrrolidone supported *p*-toluene sulfonic acid (PVPP-*p*-TSA) as an efficient catalyst was presented. This reaction has various advantages, including high yield, reusability of the catalyst, short reaction time, and simple procedure, making this method an attractive and efficient option in the field of bis(indole)methane construction.

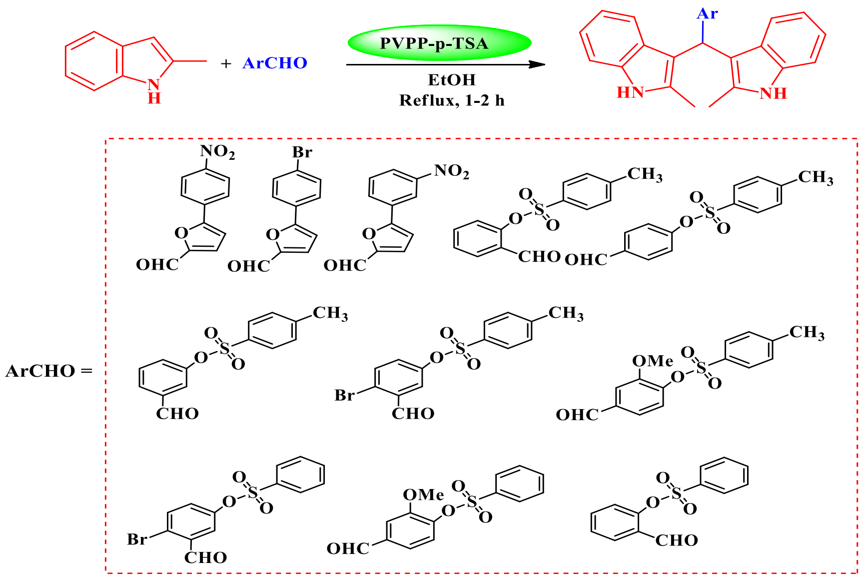

References:

[1] J.H. Lee, J. Lee, *FEMS Microbiol. Rev.* 2010, *34*, 426–444.
[2] J.R. Weng, C.H. Tsai, S.K. Kulp, D. Wang, C.H. Lin, H.C. Yang, Y. Ma, A. Sargeant, C.F. Chiu, M.H. Tsai, C.S. Chen, *Cancer Res.* 2007, *67*, 7815-7824.
[3] V. Jamsheena, G. Shilpa, J. Saranya, N.A. Harry, R.S. Lankalapalli, S. Priya, Chem. Biol. Interactions, 2016, *247*, 11-21.

The 30th Iranian Seminar of Organic Chemistry
February 7-9, 2025, Iran University of Science and Technology, Tehran, Iran

Topical Drug Delivery of Nystatin-Loaded Hydrogel-Lipid Mucoadhesive Composite for Targeted Treatment of Candida Albicans Buccal Ulcers

Seyedeh Fatemeh Hajimirzaei, Sarvenaz Pakian, Mohammad Reza Nabid*

Department of Polymer and Materials Chemistry, Faculty of Chemistry & Petroleum Sciences, Shahid Beheshti University, Tehran, Iran

Keyword: Mucoadhesive composite, Liposome, Hydrogel, Buccal ulcers, Nystatin

Abstract

Buccal candidiasis, a fungal infection primarily caused by *Candida albicans*, presents a significant challenge in oral health, particularly in immunocompromised patients. This study introduces a targeted therapeutic system using a mucoadhesive hydrogel-lipid composite loaded with nystatin for localized treatment. The hydrogel, synthesized from hyaluronic acid modified with cysteamine and dopamine, exhibits enhanced mucoadhesion and controlled drug release. Liposomes encapsulating nystatin were prepared via microfluidics and incorporated into the hydrogel matrix. Characterization tests, including SEM, TEM, DLS, and Zeta potential, Rheological properties, confirmed the properties of the composite. Drug release profiles and antifungal assays demonstrated the efficacy of the system, suggesting its potential for targeted oral candidiasis treatment.

Introduction

Buccal candidiasis is a common fungal infection that affects the mucosal membranes, often leading to pain and discomfort[1]. Conventional treatments, including systemic antifungal drugs, are associated with side effects and suboptimal drug concentrations at the infection site. Hence, topical drug delivery systems have gained interest as an alternative approach[2]. Hyaluronic acid, a naturally occurring biopolymer, has been extensively used in drug delivery systems due to its biocompatibility and mucoadhesive properties[3]. In this study, we developed a mucoadhesive hydrogel-lipid composite incorporating nystatin for the targeted treatment of oral candidiasis. The composite system leverages the advantages of liposomes for controlled release and hyaluronic acid based- hydrogels for prolonged retention at the site of infection.

Method

١. **Liposome Preparation:** Phosphatidylcholine (PC) was extracted from soybean and egg yolk using solvent-based methods. Liposomes based-PC were fabricated using a microfluidic device, ensuring uniform size and efficient nystatin encapsulation.

٢. **Hydrogel Synthesis:** Hyaluronic acid was chemically modified with cysteamine and dopamine to enhance mucoadhesion. The hydrogel was crosslinked using BDDE (1,4-butanediol diglycidyl ether), optimizing its rheological properties.

٣. **Composite Formation:** The prepared liposomes were incorporated into the hydrogel matrix. The resulting composite was characterized for mucoadhesion, swelling behavior, and drug release properties.

Result and Discussion

The mucoadhesive hydrogel-lipid composite demonstrated excellent properties for topical drug delivery. The strong mucoadhesion, confirmed through rheological tests, ensures prolonged retention at the infection site, significantly enhancing targeted delivery. Controlled drug release profiles, measured through in vitro studies, showed a sustained and efficient release of nystatin, These results underline the composite's potential to improve the efficacy of oral candidiasis treatment by reducing systemic side effects and increasing patient compliance. The dual functionality of mucoadhesion and controlled release provides a promising strategy for precise and effective localized drug delivery.

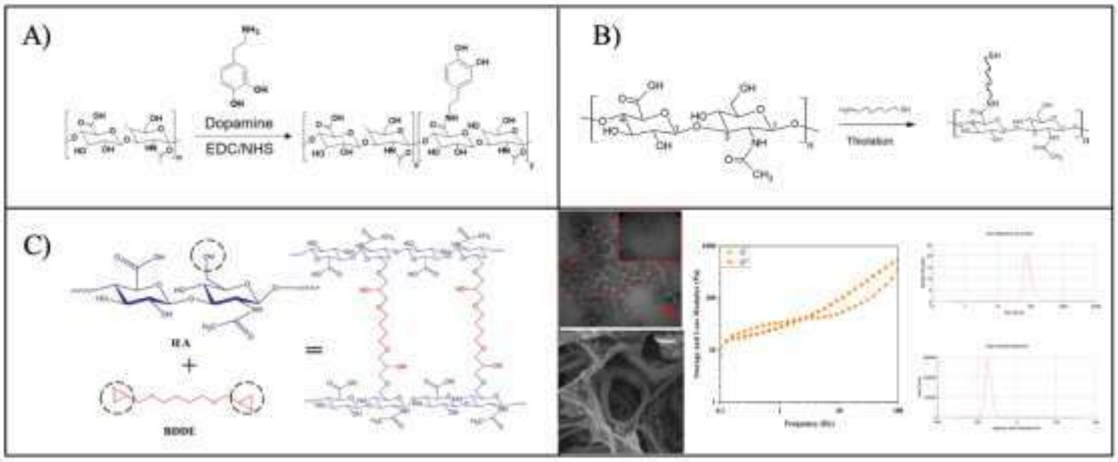

Figure: Synthesis and chemical structures of reaction A) Hyaluronic acid-Dopamine B) Hyaluronic acid-Cysteamine C) Hyaluronic acid-BDDE

References

1. Bhattacharya, S., Sae-Tia, S. & Fries, B. C. Candidiasis and Mechanisms of Antifungal Resistance. *Antibiotics* **9**, 312 (2020).

2. Desai, D. D. *et al.* Nanotechnology-Based Mucoadhesive and Mucus-Penetrating Drug-Delivery Systems for Transbuccal Drug Delivery. *Nanomedicine* **18**, 1495–1514 (2023).

3. Diaz-Salmeron, R. *et al.* Mucoadhesive Poloxamer-Based Hydrogels for the Release of HP-β-CD-Complexed Dexamethasone in the Treatment of Buccal Diseases. *Pharmaceutics* **13**, 117 (2021).

The 30th Iranian Seminar of Organic Chemistry
February 7-9, 2025, Iran University of Science and Technology, Tehran, Iran

Preparation of Four-Component Janus Particles and Fibers

F. Gholami*, S. Ghasemirad, M. H. Hassankhani, M. H. N. Famili

Keywords: Nanoparticles, Particle, Fiber, Electrospray, Electrospinning, Polyaniline

Introduction

Anisotropic particles, such as Janus particles, have recently attracted significant attention in various applications such as drug delivery, catalysts, and molecular imaging [1]. The electrohydrodynamic method, consisting of electrospinning and electrospraying of polymer solutions, is a direct technique for producing micro and nanoparticles and fibers by applying an electric voltage to polymer solutions. Electrospinning and electrospraying differ in the polymer solution density, applied voltage, and collection method [2]. Studies have been conducted on usage of nanoparticles in production of Janus particles [3]. Herein, Janus particles and fibers have been successfully produced using two polymers and two nanoparticles and analyzed.

Experimental

Polyethersulfone (PESU, with a molecular weight of 75 kg mol^{-1}) was acquired from BASF Co. (Germany). Dimethylformamide (DMF) and ethyl acetate (EAc) were obtained from Merck Co. (Germany). Polyaniline (PANI) was purchased from Mahan Sanat Iranian Co. (Iran). Copper (Cu, 25 nm) and titanium dioxide (TiO_2, 30 nm) were obtained from US-Nano (USA). Two 14-gauge needles with an inner diameter of 1.753 mm were used together. The distance between the needle and the collector was 10 cm. The collector plate was made of aluminum. A syringe pump with a flow rate of 0.15 ml/h was used for electrospinning and electrospraying of polymer solutions. To prepare Janus particles and fibers, first in solutions (A) 5 wt. % and 25 wt. % PESU and PANI were prepared in a 2:1 ratio in DMF and EAc in a 4:1 ratio, respectively, by mixing each on a hot-plate stirrer at 900rpm. After that, 10 wt. % polyethersulfone and polyaniline, copper nanoparticles were added to the solution. In preparing solutions (A) for Janus particles and fibers, first a polyethersulfone solution was prepared in DMF solvent and then 10 wt. % polyethersulfone, titanium dioxide nanoparticles were added to the solution. Solution A was sonicated for 15 min, while solution B was stirred for 2 hours at room temperature at 900 rpm. Finally, Janus particles and fibers were produced by applying a high voltage to two nozzles placed side by side. The morphology of the resulting particles and fibers was examined using field emission scanning electron microscopy (FESEM), and the Janus nature was confirmed using energy-dispersive X-ray spectroscopy (EDX).

Results and Discussion

After determining the flow rate, the voltage was increased to 16 and 18 kV, respectively, which led to the formation of two-component Taylor cones at the nozzle exit and the induction of stable jets aligned next to each other by the electric field. In the electrospinning and electrospraying process, the solvent evaporation and solidification of the product occurred rapidly. As shown in In Figure 1, the average fiber diameter is 205±100 nm and the average particle diameter is divided into two categories: large particles, 600±200 nm, and small particles, 215±55 nm.

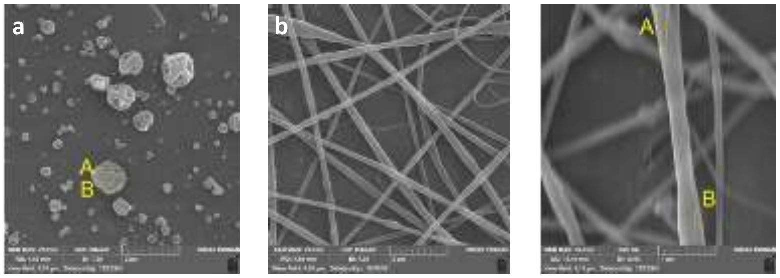

Figure 1. FESEM images: (a) Particle and (b and c) Fiber

EDX was performed on specific regions of the produced particles and fibers, which are determined in Figure 1 with alphabets A and B. Table 1 shows the elemental analysis of the two regions on the particle and fiber along with the elemental composition. The results revealed that region A contained a significant amount of titanium dioxide nanoparticles and a small amount of copper nanoparticles. In contrast, region B contained only copper nanoparticles, which confirmed the formation of Janus particles and fibers. These findings indicated that despite the preservation of the two-phase nature in the Janus particles and fibers, some degree of mixing between the two phases occurred.

Table 1. EDX results of Janus particle and fiber

Morphology	Part	Element (wt. %)			
		Sulfur	**Nitrogen**	**Copper**	**Titanium**
Particle	**A**	59.18	10.05	0.64	30.13
	B	64.27	30.70	5.03	0
Fiber	**A**	74.51	14.44	0.45	10.60
	B	66.01	30.21	3.78	0

References

[1] Bhaskar, S., Pollock, K. M., Yoshida, M., and Lahann, J., “Towards designer microparticles: Simultaneous control of anisotropy, shape and size”, Small, 6, 404–411 (2010).

[2] Park, T.-H. and Lahann, J., “Janus particles with distinct compartments via electrohydrodynamic co-jetting”, in: Jian, S. and Granick, S. (Eds.), Janus particle synthesis, self-assembly and applications”, The Royal Society of Chemistry, pp. 54–73 (2012).

[3] Hwang, S., Roh, K. H., D. Lim, W., Wang, G., Uher, C., and Lahann, J., “Anisotropic hybrid particles based on electrohydrodynamic co-jetting of nanoparticle suspensions”, Physical Chemistry Chemical Physics, 12, 11894–11899 (2010).

The 30th Iranian Seminar of Organic Chemistry
February 7-9, 2025, Iran University of Science and Technology, Tehran, Iran

Synthesis of Tilmanocept as a tracer for lymphatic mapping

Seyyed Mohammad Shahcheragh*[a], Maryam Khoshdoun[a], Sara Roustaei[a], Azim Ziyaei Halimehjani[b], Mehdi Akhlaghi[c], Arsalan Pashapour[a]

a: Aprin Sama Pharmed Company
b: Department of Chemistry, Sharif University of Technology
c: Research Center for Nuclear Medicine, Shariati Hospital, Tehran University of Medical Sciences,

Keyword: tilmanocepot, breast cancer, Sentinel lymph node

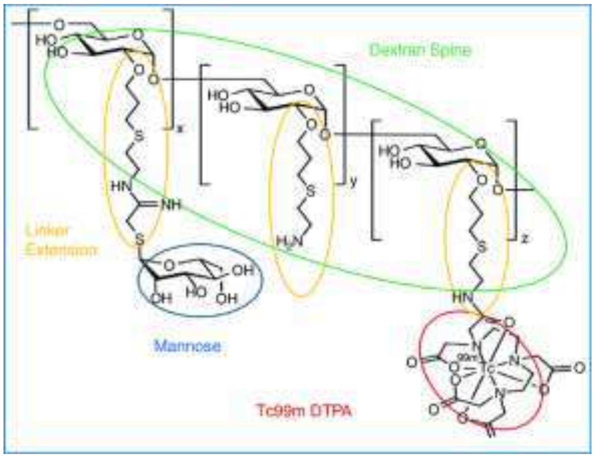

Scheme 1: Structure of Tilmanocept

The first node to receive lymphatic drainage straight from the primary tumor site is the sentinel lymph node (SLN). The detection of SLN is considered valuable prognostic information for certain types of cancers, specifically, melanoma, breast, lung, and colon. Tilmanocept is a synthetic molecular radiopharmaceutical that was designed to reduce the limitations of currently used agents for SLN identification. Improving lymphatic uptake and high retention in the sentinel node can be achieved by optimal size and binding properties, ultimately enabling an enhancement in the precision of cancer staging in conditions that employ SLNM.

Tilmanocept is the generic name for DTPA mannosyl dextran. It is a macromolecule consist of a dextran backbone and multiple subunits of DTPA and mannose.

Method: The molecule has an average size of 7 nm, enabling swift entry into lymphatic channels and quick clearance of the injection site. Synthesis commenced with a 2-step method that binds a high density of amino-terminated leashes to a dextran backbone. Allyl-bromide was reacted with dextran to yield allyl-dextran. After diafiltration with water and lyophilization, allyl-dextran was reacted with aminoethanethiol and ammonium persulfate. The resulting amino-conjugated dextran was dialyzed and lyophilized. The mixed anhydride method was used to attach DTPA; after dialysis, filtration, and lyophilization, 2-imino-2-methoxyethyl-1-D-mannose was used to attach the receptor substrate.

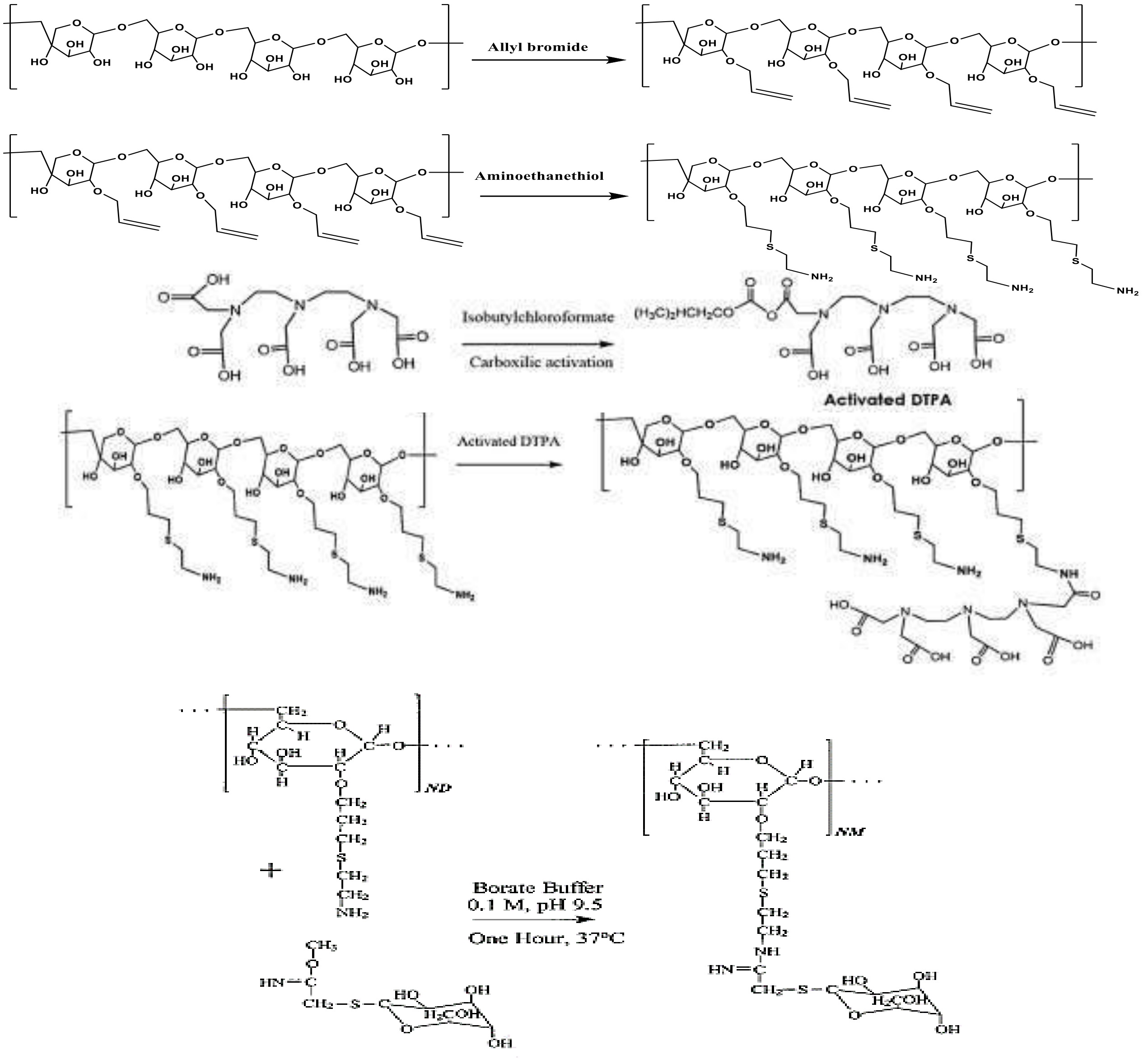

Scheme 2: synthesis of tilmanocept

Results: DTPA-mannosyl-dextran had a molecular weight of 35,800 g/mol and a molecular diameter of 7.1 nm. The final amine, mannose, and DTPA densities were 23, 55, and 8 mol per dextran.

References:

1. Azad, A. K., Rajaram, M. V., Metz, W. L., Cope, F. O., Blue, M. S., Vera, D. R., & Schlesinger, L. S. (2015). γ-Tilmanocept, a new radiopharmaceutical tracer for cancer sentinel lymph nodes, binds to the mannose receptor (CD206). *The Journal of Immunology*, *195*(5), 2019-2029.

2. Rovera, G., de Koster, E. J., Rufini, V., Zollino, M., Zagaria, L., Giammarile, F., ... & Collarino, A. (2023). 99mTc-Tilmanocept performance for sentinel node mapping in breast cancer, melanoma, and head and neck cancer: a systematic review and meta-analysis from a European expert panel. *European Journal of Nuclear Medicine and Molecular Imaging, 50*(11), 3375-3389.

3. Wallace, A. M., Han, L. K., Povoski, S. P., Deck, K., Schneebaum, S., Hall, N. C., ... & Vera, D. R. (2013). Comparative evaluation of [99m Tc] tilmanocept for sentinel lymph node mapping in breast cancer patients: results of two phase 3 trials. Annals of surgical oncology, 20, 2590-2599.

The 30th Iranian Seminar of Organic Chemistry
February 7-9, 2025, Iran University of Science and Technology, Tehran, Iran

Bi_2NiTiO_6: A Novel Titanium-Based Double Perovskite for Sustainable and Efficient Energy Storage Solutions.

Hadis Akbari[a],Masood Hamadanian[a,b*]

[a] *Institute of Nano Science and Nano Technology, University of Kashan, Islamic Republic of Iran.*
[b] *Department of Physical Chemistry, Faculty of Chemistry, University of Kashan, Islamic Republic of Iran*

Abstract

In this study, Bi_2NiTiO_6 nanoparticles were successfully synthesized using a co-precipitation method, and their electrochemical performance was assessed in a symmetric two-electrode system with a 2 M KOH electrolyte. The galvanostatic charge-discharge (GCD) experiments revealed an impressive specific capacitance of 253.6 F/g at a current density of 0.5 A/g. Additionally, cyclic voltammetry (CV) studies indicated a specific capacitance of 281.2 F/g at a scan rate of 10 mV/s. These findings highlight the significant potential of titanium-based double perovskite oxides as advanced supercapacitor electrodes, paving the way for future advancements in energy storage technology.

Keywords: Copercipitation, electrochemical performance, Specific capacitance, Supercapacitor Electrode

١. Introduction

The global energy crisis highlights the urgent need for renewable and sustainable energy sources, making efficient storage solutions essential [1]. Electrochemical energy storage technologies, especially supercapacitors, offer promising options due to their high power density, rapid charge-discharge capabilities, and extended cycle life. However, challenges such as low energy density and stability pose obstacles to their broader adoption [2,3]. To overcome these limitations and enhance storage performance, developing advanced electrode materials, including carbon compounds, transition metal oxides, and conductive polymers, is crucial. Perovskite oxides, particularly single (ABO_3) and double ($A_2BB'O_6$) perovskites, are highly esteemed for their diverse range of properties. These materials exhibit a significant presence of oxygen vacancies, adaptability to multiple valences, cost-effectiveness, and ease of synthesis [4]. A-site cations play a crucial role in enhancing thermodynamic stability, while B-site cations are instrumental in promoting electrochemical activity. Notably, double perovskites stand out for their exceptional ionic and electronic conductivity, minimized lattice distortion, and enhanced cyclic stability, making them promising candidates for advanced applications in supercapacitors and energy storage systems [5,6]. Bi_2NiTiO_6, a double perovskite oxide, is a multiferroic material with notable ferroelectric and magnetic properties, rendering it invaluable for fundamental and technological research. Synthesized by Zhou et al. in 2013 under high-temperature (1273 K) and high-pressure (5 GPa) conditions, the structural stability of this material was confirmed through X-ray diffraction, which identified two high-temperature phase transitions resulting from the displacement of bismuth ions [7]. These findings highlight the material's potential for advanced applications, particularly in studying multiferroic materials. In this research, Bi_2NiTiO_6 double perovskite nanoparticles were synthesized for the first time using a novel chemical method. The electrochemical performance of these nanoparticles was evaluated in a three-electrode system with a 2 M KOH solution as the electrolyte. The results demonstrated that the fabricated electrodes exhibited exceptional electrochemical properties, emphasizing their potential for energy storage applications.

۲. Methods

۲،۱. Preparation of Bi_2NiTiO_6 nanoparticles

Bi_2NiTiO_6 nanostructures were synthesized via the co-precipitation method using $Bi_5O(OH)_9(NO_3)_4$, $Ni(NO_3)_2{\cdot}6H_2O$, and TTIP in a 2:1:1 molar ratio [8]. TTIP was hydrolyzed in acetic acid and ethanol, while Bi and Ni precursors were dissolved in water with PVP as a surfactant. After combining the solutions and inducing precipitation with NH_4OH, the product was dried at 80 °C and annealed at 700 °C, yielding a homogeneous green powder suitable for advanced applications.

۳. Result and discussion

۳،۱. Characterization

The X-ray diffraction pattern of the Bi_2NiTiO_6 (BNT) sample, shown in Figure 1 (a), perfectly agrees with the X-ray diffraction pattern of the BNT sample prepared in 2013 [7]. Both samples exhibit an orthorhombic crystal structure with the space group Pn21a.

۳،۲. Electrochemical Study

All electrochemical tests of the prepared materials were conducted using a three-electrode system. In this setup, nickel foam coated with active materials served as the working electrode, an Ag/AgCl electrode acted as the reference electrode, and a Pt electrode was used as the counter electrode. The electrolyte employed was a 2 M potassium hydroxide solution. Cyclic voltammetry tests were performed within a potential range of 0 to 0.5 V, while galvanostatic charge-discharge curves were obtained at current densities ranging from 0.5 to 10 A/g. Additionally, electrochemical impedance spectroscopy (EIS) was utilized to investigate the electrical conductivity behavior of the prepared materials within a frequency range of 100 kHz to 0.01 Hz, with a scan amplitude of 0.01 V. Figure 1 (b) illustrates the charge-discharge curve of the BNT sample at current densities ranging from 0.5 to 10 A/g. The longest charge-discharge time occurs at a current density of 0.5 A/g. The specific capacity of the BNT electrode was calculated using Equation 1, derived from the charge-discharge curves [9].

$$SC = \frac{I\Delta t}{m\Delta v} \qquad (1)$$

In this equation , I represent the current density (A/g) , while Δt denotes the difference between charge and discharge times (s), m signifies the mass of the active material on the Ni Foam, and Δv represents the potential window. At a current density of 0.5 A/g, the specific capacity was measured at 253.68 F/g, which decreased to 106.6 F/g as the current density increased. Figure 1(c) depicts the effect of scan rates on the electrochemical performance of the BNT sample. The specific capacitance for this sample was calculated using Equation 3 [10].

$$SC = \frac{\int I dv}{ms\Delta v} \qquad (3)$$

The values obtained at scan rates of 10, 20, 30, 40, and 50 mV/s were 281.2, 237.4, 215.33, 207.6, and 203.85 F/g, respectively. Electrochemical impedance spectroscopy (EIS) was performed to investigate charge transfer resistance and electrical conductivity behavior of the BNT sample. Figure 1(d) depicts the Nyquist plot corresponding to the BNT sample. The small diameter of the semicircle in the high-frequency region indicates negligible charge transfer resistance and excellent electrical conductivity of the prepared material. The solution resistance (Rs) for the fabricated electrode, derived from the intersection of the Nyquist plot with the real axis, was determined to be 1.05 Ω.

4. Conclusion

In this study, BNT nanoparticles were synthesized via the co-precipitation method and evaluated for supercapacitor applications. The electrochemical performance was tested using a symmetric two-electrode setup with 2 M KOH as the electrolyte. The nanoparticles showed specific capacitances of 253.6 F/g at 0.5 A/g and 281.2 F/g at a scan rate of 10 mV/s. These results demonstrate the promising potential of BNT, a titanium-based double perovskite oxide, for efficient energy storage in supercapacitors, especially in neutral electrolytes.

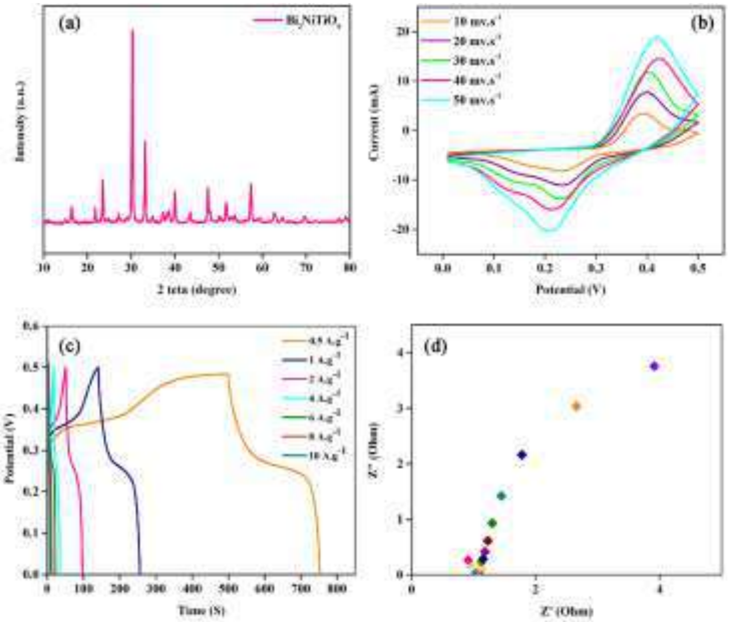

Fig.1. (a) the XRD pattern, (b) the effect of scan rate on the electrochemical performance, (C) the GCD Plot at different current densities, (d) EIS Spectra of Bi_2NiTiO_6 as synthesized nanoparticles.

References:

1. Balasingam, S.K., et al., *Freeze-dried MoS 2 sponge electrodes for enhanced electrochemical energy storage.* Dalton Transactions, 2017. **46**(7): p. 2122-2128.
2. Nandagudi, A., et al., *Hydrothermal synthesis of transition metal oxides, transition metal oxide/carbonaceous material nanocomposites for supercapacitor applications.* Materials Today Sustainability, 2022. **19**: p. 100214.
3. Dissanayake, K. and D. Kularatna-Abeywardana, *A review of supercapacitors: Materials, technology, challenges, and renewable energy applications.* Journal of Energy Storage, 2024. 96: p. 112563.
4. Monama, G.R., et al., *Progress on perovskite materials for energy application.* Results in Chemistry, 2022. **4**: p. 100321.
5. Mohan, M., N.P. Shetti, and T.M. Aminabhavi, *Perovskites: A new generation electrode materials for storage applications.* Journal of Power Sources, 2023. **574**: p. 233166.
6. Cao, Y., et al., *Recent advances in perovskite oxides as electrode materials for supercapacitors.* Chemical Communications, 2021. **57**(19): p. 2343-2355.
7. Zhu, J., et al., *Temperature and pressure effects of multiferroic Bi2NiTiO6 compound.* Journal of Applied Physics, 2013. **113**(14).
8. Vu, T., et al., *Influence of temperature on near-infrared luminescence, energy transfer mechanism and the temperature sensing ability of* La_2MgTiO_6*:* Nd^{3+} *double perovskites.* Sensors and Actuators A: Physical, 2021. **317**: p. 112453.

9. Nagpal, D., et al., *Low temperature synthesis of $BiNi_{0.6}Mn_{0.4}O_3$ nanostructures via citric acid and ethylene glycol assisted hydrothermal process for energy storage applications.* Nano Express, 2023. **4**(4): p. 045005.

10. Shereef, A., et al., Synthesis, magnetic properties, and electrochemical evaluation of La_2NiMnO_6 double perovskite as electrode materials for supercapacitor applications. Ceramics International, 2024. 50(9): p. 15756-15766.

The 30th Iranian Seminar of Organic Chemistry
February 7-9, 2025, Iran University of Science and Technology, Tehran, Iran

Silver-Doped La_2ZnTiO_6 Nanoparticles with Dual Incorporation Strategies: Synthesis and Electrochemical Assessment for Advanced Supercapacitor.

Hadis Akbari[a], Masood Hamadanian[a,b*]

[a] Institute of Nano Science and Nano Technology, University of Kashan, Islamic Republic of Iran.

[b] Department of Physical Chemistry, Faculty of Chemistry, University of Kashan, Islamic Republic of Iran

Abstract

This study successfully synthesized silver-doped La_2ZnTiO_6 (LZT) double perovskite nanoparticles through sol-gel and photochemical methods. Silver was integrated both into the crystal structure and on the surface of the nanoparticles. The electrochemical performance of these synthesized materials was evaluated using a three-electrode system. The pristine LZT nanoparticles exhibited a specific capacitance of 230.4 F/g, as determined by galvanostatic charge-discharge (GCD) curves. Remarkably, doping the structure with 10% silver enhanced the specific capacitance to 593 F/g. These findings highlight the potential of Ag-doped LZT nanoparticles as promising electrode materials for supercapacitor applications, ultimately contributing to advancements in high-performance energy storage solutions.

Keywords: Ag-doped La_2ZnTiO_6, Solgel, Photochemical, Specific Capacitance, Supercapacitor

1. Introduction

Renewable energy sources are essential for mitigating greenhouse gas emissions and ensuring long-term energy sustainability; however, their output is subject to fluctuations that present challenges [1]. Supercapacitors are pivotal in stabilizing these systems due to their rapid charge-discharge rates, high power density, and extended lifespan [2]. Supercapacitors can be categorized into three primary types based on their charge storage mechanisms: electric double-layer capacitors (EDLCs), which accumulate charge through non-faradic electrostatic interactions; pseudo-capacitors, which depend on faradic redox reactions; and hybrid supercapacitors, which integrate the benefits of both EDLCs and pseudo-capacitors to enhance charge storage performance [3]. Double perovskite metal oxides ($M_2NN'O_6$), which incorporate rare earth elements (M) and transition metals (N, N'), are promising candidates for use as supercapacitor electrodes due to their impressive conductivity, stability, and structural versatility. However, their low energy density poses challenges for practical applications. To enhance their electrochemical performance, strategies such as metal ion doping and the formation of binary composites with two-dimensional materials are essential [4,5]. Combining these materials with gold, copper, silver nanoparticles, and nickel oxide nanowires has shown significant potential in supercapacitor applications. Notably, Poudel et al. successfully used hydrothermal to deposit silver nanoparticles onto a WO_3/MoS_2 nanorod structure, achieving a remarkable specific capacitance of 637.77 F/g. This performance is primarily attributed to the excellent electrical conductivity of the silver nanoparticles, which enhances charge transfer between the electrode and electrolyte [6]. In this study, we synthesized silver-doped perovskite oxide LZT nanoparticles, both at the surface and within the structure, utilizing sol-gel and photochemical methods for the first time. We assessed the influence of silver doping on the electrochemical performance of these synthesized nanoparticles within a three-electrode system. With 10% silver doping incorporated into the structure, the resulting electrodes demonstrated a specific capacitance of 593 F/g, indicating their strong potential for energy storage applications.

2. Methods

2.1. preparation of Ag- LZT Nanoparticles (within & on the structure)

To synthesize silver-doped LZT perovskite within its structure using the sol-gel method, a solution containing lanthanum nitrate, zinc nitrate, and silver nitrate was combined with a hydrolyzed TTIP solution in ethanol and acetic acid. This final mixture was maintained at 90°C for 12 hours and calcined at 550°C and 1050°C [7] for surface doping using a photochemical process; LZT and silver nitrate were processed under a nitrogen atmosphere, followed by exposure to UV light with continuous stirring for 12 hours. The resulting precipitates were then dried at 90°C [8].

3. Result & Discussion

3.1. characterization

We utilized XRD, FT-IR, SEM, and BET analyses to characterize the synthesized nanostructures. Figures 1(a) and 1(b) display the XRD patterns of the synthesized materials. The XRD pattern for pure LZT aligns with reference card No. 17-2755, confirming the successful formation of the perovskite structure. The patterns of the silver-doped samples correspond to the primary perovskite phase without any impurities. However, a secondary silver oxide phase was observed in the surface-doped samples, indicating a potential reduction in electrochemical performance due to oxidation and environmental exposure [9].

3.2. Electrochemical analysis

The electrochemical performance of the synthesized nanoparticles was investigated using a three-electrode system comprising an Ag/AgCl electrode as the reference, nickel foam coated with active material as the working electrode, and platinum as the counter electrode. The experiments were conducted in a 2 M KOH electrolyte using cyclic voltammetry (CV) and galvanostatic charge-discharge (GCD) techniques. Figure 1 (c) displays the CV curves of pure LZT and silver-doped LZT samples (with different doping levels both on the surface and within the structure) within a potential window of 0–0.5 V at a scan rate of 50 mV/s. The specific capacitance of each sample was calculated using Equation 1, yielding values of 64.64, 132.48, 155.48, 65.64, and 53.6 F/g for pure LZT and LZT doped with 5% and 10% silver (both internally and externally), respectively [10].

$$SC = \frac{\int Idv}{ms\Delta v} \qquad (1)$$

Among these, the highest specific capacitance (155.48 F/g) and surface area were observed for LZT doped with 10% silver internally. Figure 1D shows the GCD curves of the samples measured at current densities of 4 A/g within the same potential window. The specific capacitance was also derived from these curves according to equation 2 , with LZT doped with 10% silver internally exhibiting the highest charge-discharge time and specific capacitance of 593 F/g, significantly higher than that of the pure LZT perovskite, which was 230.4 F/g [11].

$$Sc = \frac{I\Delta t}{m\Delta v} \qquad (2)$$

The superior electrochemical performance of silver-doped LZT nanoparticles with internal silver doping is attributed to the presence of metallic silver nanoparticles. Due to their excellent electrical conductivity, these nanoparticles interact effectively with the porous LZT perovskite structure, facilitating charge transfer between the electrode and electrolyte, thereby enhancing electrochemical performance. In contrast, for surface-doped silver samples, forming a secondary silver oxide phase reduces electrical conductivity and adversely affects electrochemical performance, resulting in lower capacitance values.

4. Conclusion

In conclusion, this study successfully demonstrated the synthesis of silver-doped LZT nanoparticles, employing sol-gel and photochemical methods to achieve doping both within and on the surface of the perovskite structure. Comprehensive characterization confirmed the successful formation of the perovskite phase and highlighted the impact of doping on structural and electrochemical properties. The electrochemical analysis revealed that internal doping with 10% silver significantly enhanced the specific capacitance, reaching an impressive 593 F/g, attributed to the high electrical conductivity of metallic silver nanoparticles and their effective integration with the porous LZT structure. In contrast, surface doping reduced performance due to forming a secondary silver oxide phase. These findings underscore the potential of internally silver-doped LZT nanoparticles as promising candidates for advanced energy storage applications.

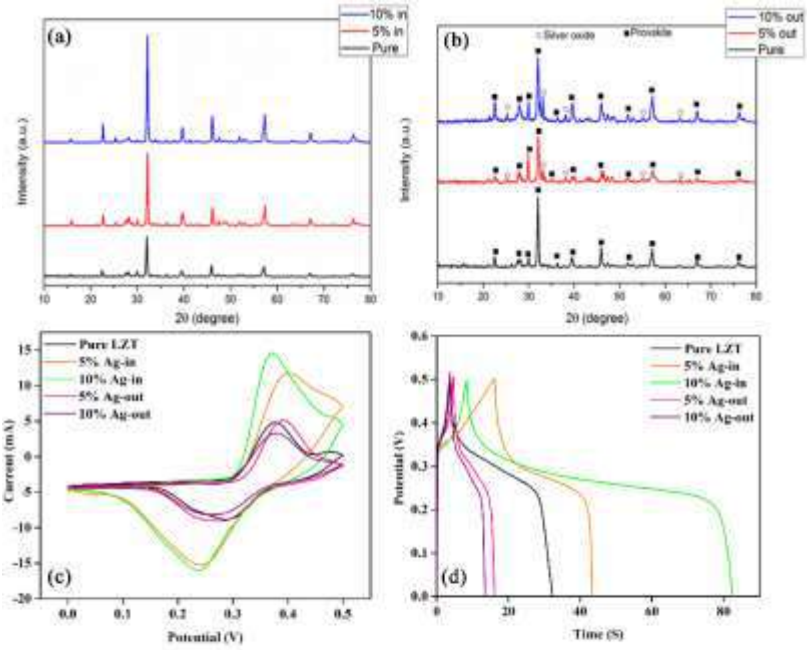

References:

1. Davidson, D. J. (2019). Exnovating for a renewable energy transition. *Nature Energy*, *4*(4), 254-256.

2. Ramachandran, T., Sana, S. S., Kumar, K. D., Kumar, Y. A., Hegazy, H. H., & Kim, S. C. (2023). Asymmetric supercapacitors: Unlocking the energy storage revolution. *Journal of Energy Storage*, *73*, 109096.

3. Dissanayake, K., & Kularatna-Abeywardana, D. (2024). A review of supercapacitors: Materials, technology, challenges, and renewable energy applications. *Journal of Energy Storage*, *96*, 112563.

4. Qian, Y., Ruan, Q., Xue, M., & Chen, L. (2024). Emerging perovskite materials for supercapacitors: Structure, synthesis, modification, advanced characterization, theoretical calculation and electrochemical performance. *Journal of Energy Chemistry*, *89*, 41-70.

5. Cao, Y., Liang, J., Li, X., Yue, L., Liu, Q., Lu, S., ... & Sun, X. (2021). Recent advances in perovskite oxides as electrode materials for supercapacitors. *Chemical Communications*, *57*(19), 2343-2355.

6. Poudel, M. B., Karki, H. P., & Kim, H. J. (2020). Silver nanoparticles decorated molybdenum sulfide/tungstate oxide nanorods as high performance supercapacitor electrode. *Journal of Energy Storage*, *32*, 101693.

7. Liao, J., Kong, L., Wang, Q., Li, J., Peng, G., Sun, Y., & Wen, H. (2018). Sol-gel preparation and near-infrared emission properties of Yb^{3+} sensitized by Mn^{4+} in double-perovskite La_2ZnTiO_6. *Optical Materials*, *84*, 82-88.

8. Rafiee-Pour, H. A., Hamadanian, M., & Koushali, S. K. (2016). Nanocrystalline TiO_2 films containing sulfur and gold: Synthesis, characterization and application to immobilize and direct electrochemistry of cytochrome c. *Applied Surface Science*, *363*, 604-612.

9. Liao, J., Wang, M., Han, Z., Huang, J., Gong, G., Fu, J., & Wen, H. R. (2021). Luminescence properties and energy transfer mechanism of La_2ZnTiO_6: Mn^{4+}/Er^{3+} far-red/green dual-emitting phosphors for plant lighting. *Journal of Solid State Chemistry*, *303*, 122470.

10. Sundriyal, S., Sharma, M., Kaur, A., Mishra, S., & Deep, A. (2018). Improved electrochemical performance of rGO/TiO_2 nanosheet composite based electrode for supercapacitor applications. *Journal of Materials Science: Materials in Electronics*, *29*, 12754-12764.

11. Shereef, A., Kunjumon, J., Jose, A. K., Tomy, M., Akram, W., Jebin, R. P., ... & Sajan, D. (2024). Synthesis, magnetic properties, and electrochemical evaluation of La_2NiMnO_6 double perovskite as electrode materials for supercapacitor applications. *Ceramics International*, *50*(9), 15756-15766.

The 30th Iranian Seminar of Organic Chemistry
February 7-9, 2025, Iran University of Science and Technology, Tehran, Iran

Synthesis of 2-(1*H*-indol-1-yl)-N-(1-methyl-1*H*-benzo[d]imidazole-2-yl) acetamide

Mahmoud Nassiri

Department of Marine Chemistry, Faculty of Marine Science, Chabahar Maritime University, Chabahar, Iran. P. O. Box 99717-56499, Corresponding author: tel / fax: +98-545-2220020. E-mail: mdnassiri@cmu.ac.ir

Keyword: Three-component reaction; Benzimidazole; Indole; Chloroacetyl chloride

Introduction

Among the various N-containing heterocyclic compounds, benzimidazole and its derivatives are common building blocks usually found in biologically active and therapeutically useful products [1]. Benzimidazoles can easily interact with the biopolymers of the living systems, which are responsible for their numerous biological activities and functions. In particular, benzimidazole derivatives exhibit antimicrobial, antiviral, anticancer, anti-inflammatory and antioxidant [2, 3]. They are also acclaimed for their widespread applications as enzyme inhibitors, drugs, dyes and polymers [4]. Indole is a kind of heterocyclic compound, which is composed benzene and pyrrole ring and has rich biological activities. Indoles are found almost universally throughout the body in biologically active products, and when substituted, they have the ability to bind to multiple receptors or coordinate with several other molecules. Many drugs have been synthesized using indole structures with various substituents that elicit anticancer, antihypertensive, antidepressant, and anti-inflammatory properties [5-7]. This article details the outcomes of my innovative simple and efficient multicomponent reactions of benzimidazole (**1**), chloroacetyl chloride (**2**) and indoles (**4**) for the preparation of 2-(1*H*-indol-1-yl)-N-(1-methyl-1*H*-benzo[d]imidazole-2-yl) acetamide **5** (See Scheme 1).

Method

A mixture of 1-methyl-1*H*-benzimidazole-2-amine (**1**) (1 mmol) and triethylamine (1eq) was stirred in THF (20 mL) at 0-5 °C. then, chloroacetyl chloride (**2**) (1 mmol) was added dropwise to the reaction mixture under the same conditions and stirring was continued for 4 hours. After 4 hours, the solvent was removed under reduce pressure. The product **3** was washed with water to remove triethylamine hydrochloride and crystallized from ethanol. Next, a mixture of 2-chloro-*N*-(1-methyl-1*H*-benzimidazol-2-yl) acetamide **3** (2 mmol) and indole (**4**) (2 mmol) in acetone was stirred at room temperature for 6 hours in the presence of triethylamine. After 6 hours the product **5** was filtered, the residue was washed with water and crystallized from ethanol.

Results and discussion

A simple and efficient approach for the synthesis of 2-(1*H*-indol-1-yl)-N-(1-methyl-1*H*-benzo[d]imidazole-2-yl) acetamide **5** is reported from benzimidazole (**1**), chloroacetyl chloride (**2**) and indole derivatives (**4**) in tetrahydrofuran and acetone under mild and catalyst-free conditions. Although the mechanistic details of the reaction are not known, but the preparation of compounds **3** and **5** are outlined in Scheme 1. In this study, the target compounds, containing both benzimidazole and indole moieties were successfully synthesized using a convenient and efficient catalyst-free approach. The reaction exhibited advantages such as simple purification, short research time, easy work up and readily accessible starting materials.

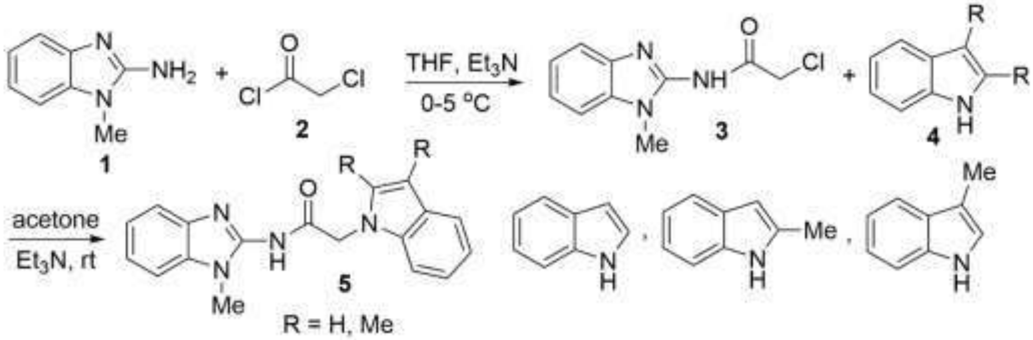

Scheme 1: The synthetic route for the preparation of compounds **5**

References

1. Altintop MD, Mohsen UA, Ozkay Y, Demirel R and Kaplancikli ZA. *Turk. J. Pharm. Sci* 2015; 12; 29-38.
2. Tzani MA, Gabriel C and Lykakis IN. *Nanomaterials* 2020; 10; 2405-2421.
3. Ansari KF and Lai C. *Eur. J. Med Chem* 2009; 44; 4028-4033.
4. Zhang P, Liu C, Yu L, Hou H, Sun W and Ke F. *Green. Chem. Lett. Rev* 2021; 14; 612-619.
5. Fenner K, Reynolds G and Basu S. *Spectrochimi. Act. Part. A* 2020; 239; 118473-118478.
6. Garg V, Maurya RK, Thanikachalam PV, Bansal G and Monga V. *Eur. J. Med. Chem* 2019; 180; 562-568.
7. Gautam BK, Jindal A, Dhar AK and Mahesh R. *Pharmacol. Biochem. Behav* 2013; 109; 91-96.

The 30th Iranian Seminar of Organic Chemistry
February 7-9, 2025, Iran University of Science and Technology, Tehran, Iran

Synthesis of 2-(1*H*-indol-1-yl)-N-(pyridin-2-yl) acetamide

Mahmoud Nassiri

Department of Marine Chemistry, Faculty of Marine Science, Chabahar Maritime University, Chabahar, Iran. P. O. Box 99717-56499, Corresponding author: tel / fax: +98-545-2220020. E-mail: mdnassiri@cmu.ac.ir

Keyword: Three-component reaction; pyridine-2-amine; Indole; Chloroacetyl chloride

Introduction

Pyridine and its derivatives are a volatile liquid of disagreeable odor, colorless, organic produced from coal tar or by chemical synthesis. Pyridine and its derivatives have high solubility in water and non-polar solvents. The World Health Organization (WHO) has listed them as priority pollutants because of their strong carcinogenic and teratogenic risks after long-term exposure. A large amount of pyridine and its derivatives have been emitted in modern industrial pro duction, so it is particularly important to detect them quickly and sensitively [1, 2]. Diversified biological activities and electronic properties make pyridine ring as unique structural motif. Due to its uniqueness pyridine core has found numerous applications in pharmaceutical science, agriculture, material science, catalysis and organometallic chemistry [3-5]. Indole core is a privileged structure found in biologically active natural products and are known as an important class heterocyclic compounds and bioactive intermediate in pharmacutical industry. Many drugs have been synthesized using indole structures with various substituents that elicit anticancer, antihypertensive, antidepressant, and anti-inflammatory properties [6, 7]. This article details the outcomes of my innovative simple and efficient multicomponent reactions of benzimidazole (**1**), chloroacetyl chloride (**2**) and indoles (**4**) for the preparation of 2-(1*H*-indol-1-yl)-N-(1-methyl-1*H*-benzo[*d*]imidazole-2-yl) acetamide **5** (See Scheme 1).

Method

A mixture of pyridine-2-amine (**1**) (1 mmol) and triethylamine (1 mmol) was stirred in dichloromethane (20 mL) at ambient temperature. then, chloroacetyl chloride (**2**) (1 mmol) was added dropwise to the reaction mixture under the same conditions and stirring was continued for 3 hours. After 3 hours, the solvent was removed under reduce pressure. The product **3** was washed with water to remove triethylamine hydrochloride and crystallized from ethyl acetate. Next, a mixture of 2-chloro-*N*-(pyridin-2-yl) acetamide **3** (2 mmol) and indole (**4**) (1 mmol) in dichloromethane was stirred at ambient temperature for 5 hours in the presence of triethylamine. After 5 hours the product **5** was filtered, the residue was washed with water and crystallized from ethyl acetate.

Results and discussion

A Convenient and efficient procedure for the preparation of 2-(1*H*-indol-1-yl)-N-(pyridin-2-yl) acetamide **5** is reported from pyridine-2-amine (**1**), chloroacetyl chloride (**2**) and indole derivatives (**4**) in dichloromethane under mild and catalyst-free conditions. Although the mechanistic details of the reaction are not known, but the synthesis of compounds **3** and **5** are outlined in Scheme 1. In this work, the target compounds, containing both pyridine and indole moieties were successfully synthesized using a convenient and efficient catalyst-free approach. The reaction exhibited advantages such as simple purification, short research time, easy work up and readily accessible starting materials.

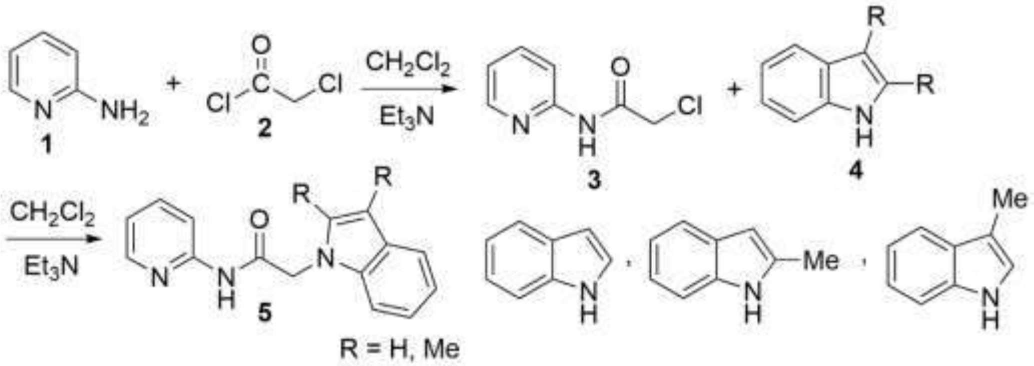

Scheme 1: The synthetic route for the preparation of compounds **5**

References

1. Liu Q, Zhao C, Shao X, Wang W and Ji X. *Dye. Pigment* 2021; 185; 108902-108907.
2. Lataye DH, Mishra IM and Mall ID. *Ind. Eng. Chem. Res* 2006; 45; 3934-3943.
3. Akram M, Adeel M, Khalid M, Tahir MN, Aliabad HAR, Ullah MA, Iqbal J and Braga AAC. *J. Mol. Struct* 2020; 1213; 128131-128145.
4. Reimann S, Ehlers P, Parpart S, Surkus A, Spannenberg A and Longer P. *Tetrahedron* 2015; 71; 5371-5384.
5. Srinivasarao S, Nandikolla A, Nizalapur S, Yu TT, Pulya S, Ghosh B, Murugesan S, Kumar N and Sekhar KVGC. *RSC Adv* 2019; 9; 29273-29292.
6. Aghazadeh M. *Arkivoc* 2019; vi; 141-148.
7. Gautam BK, Jindal A, Dhar AK and Mahesh R. *Pharmacol. Biochem. Behav* 2013; 109; 91-96.

The 30th Iranian Seminar of Organic Chemistry
February 7-9, 2025, Iran University of Science and Technology, Tehran, Iran

Synthesis of 2-((1*H*-benzo[*d*]imidazole-2-yl) thio)-N-(benzo[*d*]thiazol-2-yl) acetamide

Mahmoud Nassiri

Department of Marine Chemistry, Faculty of Marine Science, Chabahar Maritime University, Chabahar, Iran. P. O. Box 99717-56499, Corresponding author: tel / fax: +98-545-2220020. E-mail: mdnassiri@cmu.ac.ir

Keyword: Three-component reaction; 2-Amino-benzothiazole; 2-Mercaptobenzimidazole; Chloroacetyl chloride

Introduction

Used heterocyclic compounds are very important compounds partially because of their pharmacological properties which include wide applications in medicinal chemistry. Benzothiazole is a class of heterocyclic compounds having sulfur and nitrogen hetero atoms. The analogs of benzothiazole and its derivatives have an important role particularly in medicinal, synthetic, and pharmaceutical chemistry due to their biological and pharmacological activities. Especially in the last few years, some benzothiazoles have found application in bioorganic and medicinal chemistry and in the development of clinical drugs such as pramipexole, lubeluzole, probenazole, ethoxazolamide, zopolrestat and bentaluron. Benzothiazoles rarely occur in various marine or terrestrial natural compounds, which have useful biological activities. They form part of the structure of firefly luciferin and are also known as aroma constituents of tea leaves and cranberries or flavor compounds produced by the fungi *Aspergillus clavatus* and *Polyporus frondosus* [1-4]. Benzimidazole is a heterocyclic aromatic organic compound. It is an important pharmacophore and a privileged structure in medicinal chemistry. This compound is bicyclic in nature which consists of the fusion of benzene and imidazole. Benzimidazole moiety is supposed to be an advantageous component because many drugs contain this nucleus as important constituent such as; astemizole (antihistaminic), telmisartan (antihypertensive), omeprazole (antiulcer), albendazole and mebendazole (anthelmintic) and pimobendan (ionodilator) [5-7]. This article details the outcomes of my innovative simple and efficient multicomponent reactions of 2-amino-benzothiazole (**1**), chloroacetyl chloride (**2**) and 2-mercaptobenzimidazole (**4**) for the preparation of 2-((1*H*-benzo[*d*]imidazole-2-yl)thio)-N-(benzo[*d*]thiazol-2-yl) acetamide **5** (see Scheme 1).

Method

A mixture of 2-amino-benzothiazole (**1)** (1 mmol) and triethylamine (1eq) was stirred in acetone (20 mL) at ambient temperature. then, chloroacetyl chloride (**2**) (1 mmol) was added dropwise to the reaction mixture under the same conditions and stirring was continued for 1 hours. After 1 hours, the solvent was removed. The product **3** was washed with water to remove triethylamine hydrochloride and crystallized from ethanol. Next, a mixture of N-(benzo[*d*]thiazol-2-yl)-2-chloroacetamide **3** (1 mmol) and 2-mercaptobenzimidazole (**4**) (1 mmol) in acetone was stirred under reflux conditions for 4-5 hours in the presence of potassium carbonate. After 4-5 hours the product **5** was filtered, the residue was washed with water and crystallized from ethanol.

Results and discussion

A new and efficient method for the synthesis of 2-(1*H*-indol-1-yl)-N-(1-methyl-1*H*-benzo[*d*]imidazole-2-yl) acetamide **5** is reported from 2-amino-benzothiazole (**1**), chloroacetyl chloride (**2**) and 2-mercaptobenzimidazole (**4**) in acetone under mild and catalyst-free conditions. Although the mechanistic details of the reaction are not known, but the preparation of compounds **3** and **5** are outlined in Scheme 1. In this study, the target compounds, containing both benzothiazole and benzimidazole moieties were successfully synthesized using a convenient and efficient catalyst-free approach. The reaction exhibited advantages such as simple purification, short research time, easy work up and readily accessible starting materials.

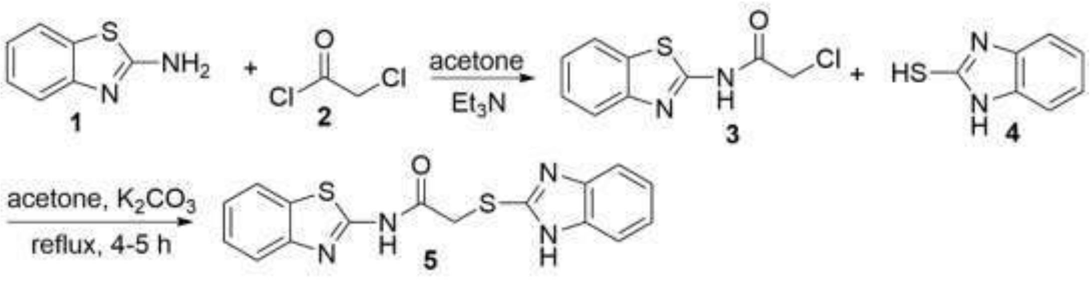

Scheme 1: The synthetic route for the preparation of compounds **5**

References

1. Uremis N, Uremis MM, Tolun FI, Ceylan M, Doganer A and Kurt AH. *Antican. Res* 2017; 37; 6381-6389.
2. Chadegani F, Darviche F and Balalaie S. *Int. J. Org. Chem* 2012; 2; 31-37.
3. Keri RS, Patil MR, Patil SA and Budagumpi S. *Eur. J. Med. Chem* 2015; 89; 207-251.
4. Tahlan S, Ramasamy K, Lim SM, Shah SAA, Mani V and Narasimhan B. *BMC Chem* 2019; 13; 1-16.
5. Altintop MD, Mohsen UA, Ozkay Y, Demirel R and Kaplancikli ZA. *Tur. J. Pharm. Sci* 2015; 12; 29-38.
6. Chawla A, Kaur G and Sharma AK. *Int. J. Pharm. Phytopharmacol. Res* 2012; 3; 148-159.
7. Sharma J, Soni PK, Bansal R and Halve AK. *Cur. Org. Chem* 2018; 22; 2276-2295.

The 30th Iranian Seminar of Organic Chemistry
February 7-9, 2025, Iran University of Science and Technology, Tehran, Iran

An effective method for the synthesis of new polysubstituted imidazole analogs using nano-SiO_2 in DES ($ChCl/NH_4OAc$)

Masoud Mokhtary[a]*, Majid Kia[a], Hediyeh Heydary[a]

Department of Chemistry, Rasht Branch, Islamic Azad University, Rasht, Iran

Keyword: *Nano-SiO_2, benzyl or 9,10-phenanthrene quinine, DES*

Benzimidazoles are very useful intermediates used in the synthesis of pharmaceutical and biological compounds [1-2].This research presents an effective method for synthesizing new polysubstituted imidazole derivatives. The method involves a three-component reaction using a compound of 1,2-diketones (such as acenaphthene quinone, benzyl, or 9,10-phenanthrene quinone), synthetic aldehydes with a nano-SiO_2 catalyst in $ChCl/NH_4OAc$ at 120 °C. Some advantages of this method include high performance, high yield, and wide applicability in producing various imidazoles with different compositions. The research demonstrates that this method can be an effective approach for producing polysubstituted imidazoles with desired properties.

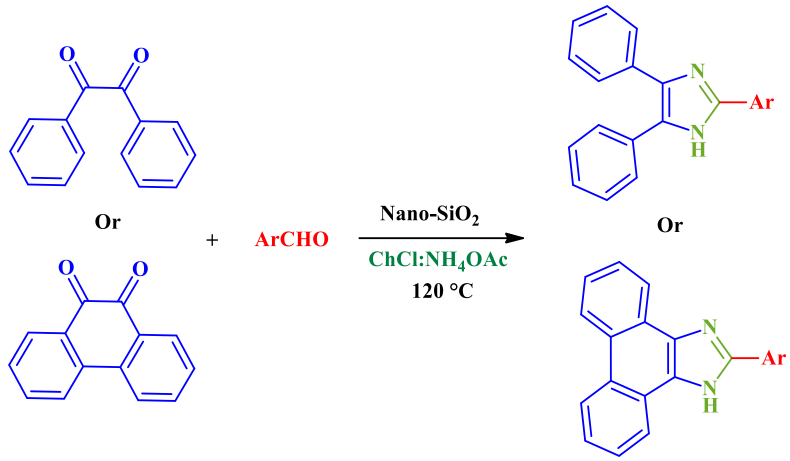

References:

[1] Ma, H. Q., Wang, Y., Li, J. P., Wang, J., *Heterocycles*, 2007, *71*, 135.

Mohammad, B.G., Hussien, M.A., Abdel-Alim, A.A., Hashem, M., *Arch. Pharm. Res.*, 2006, *29*, 26.

The 30th Iranian Seminar of Organic Chemistry
February 7-9, 2025, Iran University of Science and Technology, Tehran, Iran

Synthesis of natural mulch, quick sand stabilizer (qss)

Authors: Sepideh Norouzi 1[a], Zahra Moradi 2[b] (representing author), Masoud Hakimdavod 3*[c] (corresponding author)

1[a] The research and development unit of the oil and gas materials and processes research center of Kimia Elika Sepenta, Isfahan, Iran

2[b] The research and development unit of the oil and gas materials and processes research center of Kimia Elika Sepenta, Isfahan, Iran

3*[C] The research and development unit of the oil and gas materials and processes research center of Kimia Elika Sepenta, Isfahan, Iran

*Corresponding Author's E-mail: m.kimia@gmail.com

Presenter's E-mail: noroozisepideh۴۸@gmail.com

Abstract

In order to de-desert and stabilize quicksand, oil and petroleum products can be used in large areas and at a lower cost, but it has many environmental effects. Therefore, it is recommended to use

environmental compounds and polymers to reduce the harmful environmental effects. Carboxymethyl cellulose is an organic polymer synthesized from a natural polysaccharide, which is non-toxic, renewable and biocompatible. CMC was first discovered in Germany and then spread in America and then in other western countries and is widely used in both industrial and food grades. Based on this, the extraction of carboxymethyl cellulose from textile waste is presented in this research. The production process of recycled carboxymethyl cellulose includes two stages of alkalization (converting cellulose to alkaline cellulose in a concentrated sodium hydroxide environment) and etherification (reaction of alkaline cellulose with monochloroacetic acid in alcoholic environments such as isopropyl alcohol, methanol or ethanol). Considering that the side product of the reaction is NaCl salt, for purification, the obtained product is washed with alcohol. This product is a hydrophilic colloid with remarkable thickening properties, which can be used with additives such as Eremurus, gum and clay to stabilize loose sand and prevent the spread of deserts.

Keyword: wastes, carboxymethyl cellulose, desertification, stabilization of quicksand.

Scheme: center

References:

١.Bamboo-derived carboxy methyl cellulose for liquid film as renewable and biodegradable agriculture mulching /١٠,١٠١٦/j.ijbiomac.٢٠٢١,٠٩,١٥٢.

2.Efficient Stabilization of Soil, Sand, and Clay by a Polymer Network of Biomass-Derived Chitosan and Carboxymethyl Cellulose/ 10.1016/j.jece.2021.107084.

3.Wind erosion control using carboxymethyl cellulose: From sand bombardment performance to microfabric analysis/ 10.1016/j.aeolia.2021.100696.

4.Persian Gum: A Comprehensive Review on its Physicochemical and Functional Properties.

5.Chemical composition and some physical properties of a water-soluble gum in taro (Colocasia esculenta).
6.Wind erosion control using carboxymethyl cellulose: From sand bombardment performance to microfabric analysis.
7.Optimization of Reaction condition for synthesis of CMC from oil palm Fronds.
8.Recent Developments of Carboxymethyl Cellulose.
9.Synthesis of carboxymethyl cellulose from waste of cotton ginning industry.
10.Carboxymethyl cellulose fiber as a fast binding and biodegradable adsorbent of heavy metals.
11.Synthesis and swelling behaviors of carboxy methyl cellulose-based superabsorbent resin hybridized with graphene oxide.
12.The effect of CMC and arabic gum stabilizer combination on the characteristics of soursop velva (Annona muricata L .)
13.Solubilisation of Persian gum: Chemical modification using acrylamide.
14.A Comparison Between the Hot and Cold Water Soluble Fractions of Two Locust Bean Gum Samples.
15.Improvement of water solubility and humidity stability of tapioca starch film by incorporating various gums.

16.Preparation of amorphous solid dispersions by rotary evaporation and KinetiSol Dispersing: approaches to enhance solubility of a poorly water-soluble gum extract.
17.Water-soluble polymers in agriculture: xanthan gum as eco-friendly alternative to synthetics.
18.Chemical composition and some physical properties of a water-soluble gum in taro (Colocation esculent.

The 30th Iranian Seminar of Organic Chemistry
February 7-9, 2025, Iran University of Science and Technology, Tehran, Iran

Photo formylation of amines with ethers

Reyhaneh Shahsavari[a] , Moosa Ramdar[a] , Foad Kazemi[a,*]

[a] *Department of Chemistry, Institute for Advanced Studies in Basic Sciences (IASBS), Gava Zang, 49195-1159 Zanjan, Iran*

Keywords: Formylation, Amines, Photocatalysis, Ethers, LED irradiation

Abstract

This study explores the use of ethers such as dioxane, diglyme and THF as alternative formylation agents under photocatalytic conditions, involving: TiO_2 , sunlight irradiation and in another experiment uses 400 nm LED irradiation. the work emphasizes the trapping and utilization of formic acid, a significant intermediate formed during photodegradation by demonstrating the conversion of these intermediates into valuable chemical products.

Introduction

Photocatalytic synthesis offers a promising solution to environmental pollution and the global energy crisis by effectively converting solar energy into chemical energy. A key focus in this field is the development of eco-friendly photocatalytic materials with high activity. Among these, TiO_2 stands out as a versatile catalyst for various oxidative, reductive and radical reactions. Notably, TiO_2 facilitates sunlight-induced radical reactions of ethers with heterocyclic bases and three-component coupling reactions involving ethers, aldehydes, and amines under UV light. The Formylation of amines is a significant process in organic chemistry, as it is essential for producing materials like heterocycles, pharmaceuticals, and agrochemicals [1-3].

Method

A notable discovery is that photocatalytic degradation of ethers such as dioxane and THF produces formic formic acid as an intermediate, which can potentially be used as in situ formylation agent for amines. using ethers as both solvents and formylating agents offers several advantages: they are inexpensive, readily available, and environmentally friendly. Photocatalytic reactions were carried out irradiated by sun light under magnetic stirring. (scheme1) The reaction was carried out in the presence of TiO_2 in dioxane and aromatic amine and give formamide product [4-6].

Results and Discussion

Based on the evidence, the photocatalytic degradation of ethers appears to generate formic acid as an intermediate, which holds potential as a formylating agent for amines. this insight opens new possibilities for designing sustainable formylation reaction.in this study, aniline was selected as a representative aromatic substrate, sunlight as a natural energy source, and titania as the catalyst to evaluate the efficiency of this approach in an aerobic oxidation model system.

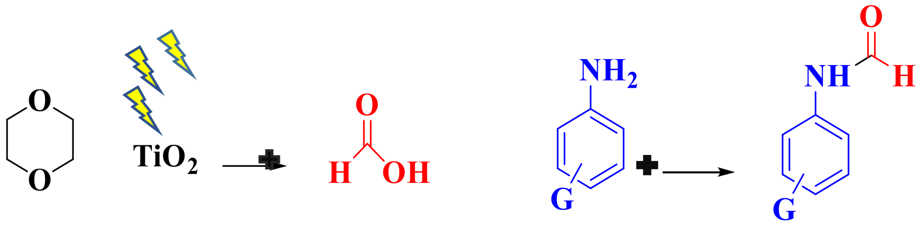

Scheme1. Formamide formation by dioxane solvent and arylamines with formic acid and TiO_2 under sunlight irradiation.

References:

[1] T. Caronna, C. Gambarotti, L. Palmisano, C. Punta, F. Recupero, Sunlight-induced reactions of some heterocyclic bases with ethers in the presence of TiO_2: a green route for the synthesis of heterocyclic aldehydes, J. Photochem. Photobiol. A: Chemistry 171 (2005) 237–242.

[2] B. Alcaide, P. Almendros, C. Aragoncillo, β-Lactams: versatile building blocks for the stereoselective synthesis of non-β-lactam products, Chem. Rev. 107 (2007) 4437–4492.

[3] M. Nasrollahzadeh, N. Motahharifar, M. Sajjadi, A. Moradzadeh Aghbolagh, M. Shokouhimehr, R.S. Varma, Recent advances in N-formylation of amines and nitroarenes using efficient (nano) catalysts in eco-friendly media, Green Chem. 21 (2019) 5144–5167

[4] N. Li, X. Lang, W. Ma, H. Ji, C. Chen, J. Zhao, Selective aerobic oxidation of amines to imines by TiO_2 photocatalysis in water, Chem. Commun. 49 (2013) 5034–5036.

[5] L. Zhang, Y. Deng, F. Shi, Light promoted aqueous phase amine synthesis via three component coupling reactions, Tetrahedron Lett. 54 (2013) 5217–5219

[6] S. Higashimoto, N. Kitao, N. Yoshida, T. Sakura, M. Azuma, H. Ohue, Y. Sakata, Selective photocatalytic oxidation of benzyl alcohol and its derivatives into corresponding aldehydes by

molecular oxygen on titanium dioxide under visible light irradiation, J. Catalysis 266 (2009) 279–285.

The 30th Iranian Seminar of Organic Chemistry
February 7-9, 2025, Iran University of Science and Technology, Tehran, Iran

Effect of sovlent in chemoselectivity reaction of 4-chloro-3-formylcoumarin and aromatic amines

Babak Kaboudin[1a], Mojtaba Ghashghaeea[2a]

a) Organic Chemistry Laboratory, Department of Chemistry, Institute for Advanced Studies in Basic Sciences (IASBS), Gava Zang, Zanjan 45137-66731, Iran, kaboudin@iasbs.ac.ir and mojtabaghashghaee@iasbs.ac.ir

Keyword: Synthesis, Coumarin, Organophosphorus, Hetrocycles

Introduction

Aminophosphonates are one of the most extensively studied organophosphorus compounds in interdisciplinary scientific fields due to their biological and physical characteristics, as well as their synthetic intermediate usage.These compounds have a wide range of applications in industrial, agricultural, and medicinal chemistry fields. Recently, the use of aminophosphonate derivatives embedded in heterocyclic frameworks has demonstrated intriguing biological and physical properties.[1]

Coumarins with natural and synthetic origin are important compounds that have various pharmacological and biological activities. In addition to the coumarins' medicinal properties, a number of fluorescent coumarin-fused heterocyclic skeletons made of π-conjugated fraction are utilized as molecular sources in chemical sensors, optical brighteners, lasers, light-emitting diodes, and biomedical imaging markers.[2]

As part of our ongoing research to develop the synthesis and applications of novel organophosphonic esters, we describe the effect of solvent on the chemoselectivity reaction of 4-chloro-3-formylcoumarin and aromatic amines.

Method

In a 10 mL oven-dried round-bottom flask, which contained 2 mL of solvent, was added 1 mmol of 4-chloro-2-oxo-2*H* -chromene-3-carbaldehyde. It was stirred for 10 min at 25 °C. To this, 2 mmol of dialkyl phosphite (or diphenyl phosphine oxide) was added. Next, after stirring the reaction mixture, 1 mmol of the corresponding amine was added to the reaction container. It was then stirred in an oil bath at 70 °C for 8−12 h. After the completion of the reaction, crude material obtained was purified by column chromatography on silica gel.

Results and Discussion

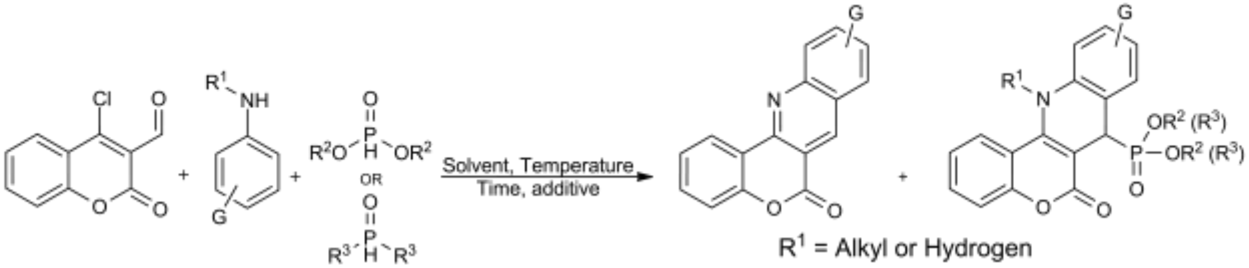

Scheme1: General procedure for the synthesis

Entry	Additive (eq)	Solvent	T (°C)	Time (h)	Diethyl Phosphite (eq)	Yield % 5 + 4
1	---	Dioxane	70	8	1.5	15 + 72
2	---	MeCN	70	8	1.5	20 + 76
3	---	DMF	70	8	1.5	Trace + > 90
4	---	DMSO	70	8	1.5	Trace + > 90
5	---	DMF	70	8	0	Trace + > 90
6	ZnCl2 (0.2)	Dioxane	70	8	1.5	22 + 65
7	ZnCl2 (0.2)	MeCN	70	8	1.5	30 + 62
8	ZnCl2 (0.2)	DMF	70	8	1.5	Trace + > 90
9	ZnCl2 (0.2)	DMSO	70	8	1.5	Trace + > 90
10	ZnCl2 (0.2)	DMF	70	8	1.5	Trace + > 90

11	$ZnCl_2$ (1)	MeCN	70	12	1.5	51 + 30
12	$ZnCl_2$ (3)	MeCN	70	12	1.5	65 + 27

Table 1: Optimum tabl for 2-methylaniline

References

[1] a) Demkowicz, S.; Rachon, J.; Dasko, M.; Kozak, W. Selected organophosphorus compounds with biological activity. Applications in medicine. RSC Adv. 2016, 6, 7101−7112. b) Sevrain, C. M.; Berchel, M.; Couthon, H.; Jaffres, P.-A. Phosphonic acid: preparation and applications. Beilstein J. Org. Chem. 2017, 13, 2186−2213. c) Kaboudin, B.; Daliri, P.; Faghih, S.; Esfandiari, H. Hydroxy- and Amino-Phosphonates and -Bisphosphonates: Synthetic Methods and Their Biological Applications. Front. Chem. 2022, 10, 890696.

[2] Kaboudin, B., Ghashghaee, M., Fukaya, H., & Yanai, H. Stereoselective synthesis of vinylphosphonates through aromatic aza-Claisen rearrangement of α-aminophosphonates. Chem. Comm., 2023, 59, 7076-7079.

The 30th Iranian Seminar of Organic Chemistry
February 7-9, 2025, Iran University of Science and Technology, Tehran, Iran

Synthesis of new ethyl cyanoacetate analogs catalyzed by nano-SiO_2 in deep eutectic solvent

Masoud Mokhtary[a]*, Majid Kia[a], Aynaz Lotfinezhad[b]

[a]*Department of Chemistry, Rasht Branch, Islamic Azad University, Rasht, Iran*

[b]*Department of Medical Engineering, Rasht Branch, Islamic Azad University, Rasht, Iran*

Keyword: *Deep eutectic solvent*; *Knoevenagel condensation; Formylarylsulfonates; Nano-SiO_2*

Ethyl 2-cyano-3-phenyl acrylates are considered important organic compounds with various applications in pharmaceutical and chemical industries. The synthesis of these compounds through the Knoevenagel reaction is an efficient and common method for their production. The unique properties of these compounds make them valuable intermediates in the synthesis of more complex compounds and active substances in various industries [1,2]. In this research, we present an effective method for synthesizing new derivatives of ethyl using nano-SiO_2 as a catalyst in choline chloride-urea deep eutectic solvent. The unique characteristics of nanosilica, such as high yield and simplicity of the process, make this method an attractive option for synthesizing Knoevenagel ethyl cyanoacetate analogs with high yields.

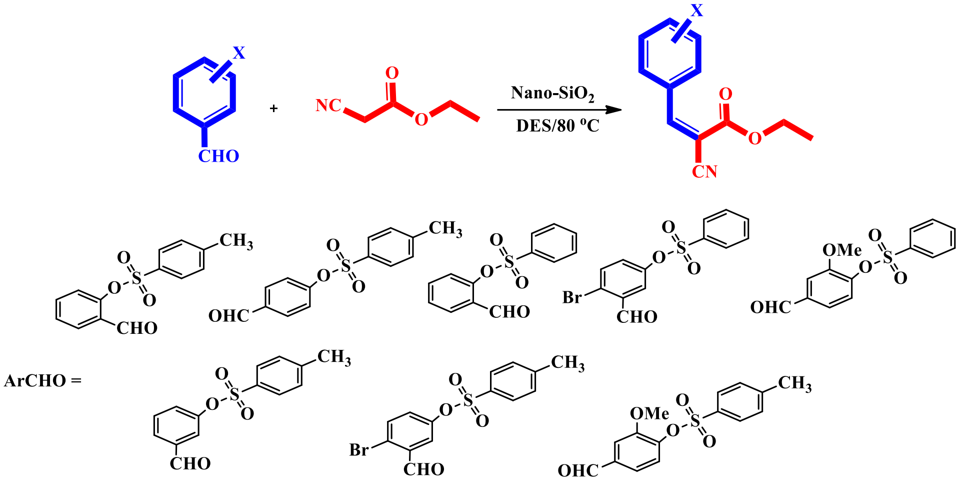

References:

[1] Knezevic, S., Ghafoor, A., Mehri, S., Barazi, A., Dziura, M., Trant, J. F., Dieni, C. A., (2021), PharmaNutrition 17: 100273.

[2] Uddin, K. M., Sakib, M., Siraji, S., Uddin, R., Rahman, S., Alodhayb, A., Alibrahim, K. A., Kumer, A., Matin, M. M., Bhuiyan, M. M. H., (2023), ACS Omega, 8: 25817- 2583.

The 30th Iranian Seminar of Organic Chemistry
February 7-9, 2025, Iran University of Science and Technology, Tehran, Iran

An efficient and convenient protocol for the Synthesis of 1'H-spiro[indoline-3,2'quinazoline]-2,4'(3H)-diones

Elmira Askari*[a], Alireza Alborzi[b]

Department of Chemistry, Shiraz Branch, Islamic Azad University, Shiraz, Iran

Keywords: Multicomponent reaction, Spirooxindole, Quinazoline, Isatin, Isatoic anhydride, Amines, Ammonium iron(III) sulfate

INTRODUCTION

Nitrogen-containing heterocycles are some of the most important structural elements found in pharmaceuticals[1]. Quinazoline derivatives are nitrogen-containing heterocyclic compounds that are the current research focus for pharmaceutical chemists due to their diverse and significant biological activity [2]. Quinazolines were found to have anti-SARS-CoV-2 [3], anti-tumor[4], anti-viral[5], anti-bacterial[6], anti-oxidant[7], and anti-cancer[8] activities.

Herein, we report a simple approach for the synthesis of 1'H-spiro[indoline-3,2'quinazoline]-2,4'(3H)-diones using ammonium iron(III) sulfate, an inexpensive heterogeneous acid catalyst (Scheme 1).

Scheme1 synthesis of 1'H-spiro[indoline-3,2'quinazoline]-2,4'(3H)-diones

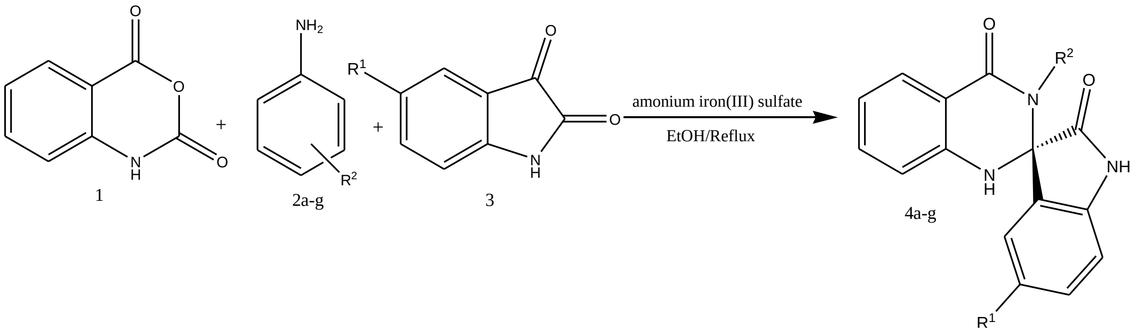

Method

A mixture of isatoic anhydride 1, isatin 3, primary amines 2a-g, ammonium iron(III) sulfate, and EtOH in a 25 ml flask was stirred at reflux. After the completion of the reaction (monitored by TLC), distilled water was added, then the resulting solid product was filtered and dried. The crude product was recrystallized and dried to provide powder compounds of 4a-g.

RESULTS AND DISCUSSION

In summary, we have developed a novel, simple, and efficient protocol for the synthesis of 1'H-spiro[indoline-3,2'quinazoline]-2,4'(3H)-diones using easily available ammonium iron(III) sulfate as a catalyst. This method offers several advantages: (a) inexpensive ammonium iron(III) sulfate as the catalyst; (b) environment-friendly ethanol as the solvent; (c) high reaction yields; (d) short time duration.

Spectral data of selected compound

1'H-spiro[indoline-3,2'quinazoline]-2,4'(3H)-dione(4a)

Cream powder; mp 261–263 °C dec; IR (KBr) (ν_{max}, cm^{-1}): 3491 (NH), 3227(NH), 2964, 1725 (C=O), 1642 (C=O), 1614, 1526; ^{1}H NMR (300 MHz, DMSO-d_6): : δ_H 6.60 (d, 1H, J=8.0, ArH), 6.68 (t, 1H, J=7.4, ArH), 6.84 (d, 1H, J=7.7, ArH), 7.05 (t, 1H, J=7.4, ArH), 7.22 (t, 1H, J=7.2, ArH), 7.28 (s, 1H, NH), 7.33 (t, 1H, J=7.8, ArH), 7.47 (d, 1H, J=7.3, ArH), 7.59 (d, 1H, J=7.4, ArH), 8.36 (s, 1H, NH), 10.30 (s, 1H, NH); ^{13}C NMR (75 MHz, DMSO-d6): δ_C 71.41, 110.53, 114.31, 114.76, 117.61, 122.73, 125.81, 127.30, 129.89, 131.26, 133.75, 142.58, 147.28, 164.40, 176.47; MS (EI, 70 eV) (*m*/z, %): 265 (M$^+$, 25), 263 (50), 237 (100), 119 (95), 92 (60), 63 (35), 50 (30), 39 (40). Anal. Calcd for C15H11N3O2: C, 67.92; H, 4.18; N, 15.84. Found: C, 67.80; H, 4.11; N, 15.73.

References:

١. Vitaku, E., D.T. Smith, and J.T. Njardarson, *Analysis of the structural diversity, substitution patterns, and frequency of nitrogen heterocycles among US FDA approved pharmaceuticals: miniperspective.* Journal of medicinal chemistry, 2014. **57**(24): p. 10257-10274.
٢. Karan, R., et al., Recent advances on quinazoline derivatives: A potential bioactive scaffold in medicinal chemistry. ChemEngineering, 2021. 5(4): p. 73.
٣. Reza, R., et al., *Inhibitory efficiency of quinazoline derivatives against SARS-CoV*-2: *virtual screening and molecular dynamics study*. Proceedings of the Indian National Science Academy, 2024: p. 1-13
٤. Ewes, W.A., et al., *Synthesis, biological evaluation and molecular modeling study of [1, 2,* 4]-T*riazolo [4, 3-c] quinazolines: New class of EGFR-TK inhibitors.* Bioorganic & medicinal chemistry, 2020. **28**(7): p. 115373.
٥. Wang, M., et al., *Design, synthesis and anti-influenza A virus activity of novel 2, 4-disubstituted quinazoline derivatives.* Bioorganic & Medicinal Chemistry Letters, 2020. **30**(11): p. 127143
٦. Misra, A., et al., Bacterial cell leakage potential of newly synthesized quinazoline derivatives of 1, 5-benzodiazepines analogue. Journal of Heterocyclic Chemistry, 2020. 57(4): p. 1545-1558.
٧. Al-Salahi, R., et al., Antioxidant activities and molecular docking of 2-thioxobenzo [g] quinazoline derivatives. Pharmacological Reports, 2019. 71: p. 695-700.
٨. Ataollahi, E., et al., Novel quinazolinone derivatives as anticancer agents: Design, synthesis, biological evaluation and computational studies. Journal of Molecular Structure, 2024. 1295: p. 136622.

The 30th Iranian Seminar of Organic Chemistry
February 7-9, 2025, Iran University of Science and Technology, Tehran, Iran

One-pot, Multicomponent Synthesis of 3,4-Dihydropyrimidin-2(1H)-one Derivatives using MgCuO$_2$@SiO$_2$@La$_2$O$_3$ as Catalyst

Fatemeh Bahramifar, Nayyer Afsharpour, Abbas Nikoo*, Sahar Khandani, Zahra Nikkhah

Department of Organic Chemistry, Faculty of chemistry, Urmia University, Urmia, Iran

Keyword: Heterogeneous catalyst, One-pot synthesis, Biginelli reaction

Introduction: Metal oxides are a class of inorganic materials that have diverse applications as catalysts. Metal oxides contain various types of anionic and cationic defects and vacancies that play an important role in catalytic phenomena. This surface unsaturation is usually compensated by reaction with water, which leads to the formation of surface hydroxyl groups and consequently acid-base and redox properties. Single or complex metal oxides based on first-row transition metals exhibit a wide range of non-stoichiometric properties, such as the case of A_xBO_3 perovskites that exhibit cationic defects at A or B sites. These non-stoichiometries and vacancies strongly affect the catalytic properties due to the presence of defects or changes in the redox and electrical properties of the solids. Metal oxide catalysts have gained importance in most refining and petrochemical processes, in the synthesis of certain chemicals, in pharmaceutical fields, and especially recently in improving environmental issues [1,2]. More than a hundred years ago, the Italian chemist Pietro Biginelli first performed the three-component condensation reaction of arylaldehyde, ethyl acetoacetate, and urea using HCl as a catalyst in ethanol solvent. The result of this reaction was the synthesis of 3,4-dihydropyrimidine-2(1H)-one derivatives [3]. With the discovery of the pharmacological properties and biological effects of dihydropyrimidones, the one-pot three-component synthesis of this class of compounds has attracted attention, so that in recent years, many studies have been conducted on the pharmacological and biological properties of dihydropyrimidones. By changing each of the reactants urea, alkyl acetoacetate, and arylaldehyde, numerous compounds of 3,4-dihydropyrimidones derivatives can be synthesized. The Biginelli reaction is a one-step method for the synthesis of 3,4-dihydropyrimidine-2(1H)-ones. These compounds have broad biological applications as anticancer, antihypertensive, antiviral, antibacterial, antioxidant, and anti-inflammatory [4].

Method: A mixture of ethyl acetoacetate (2.5 mmol, 325 mg), benzaldehyde derivatives (2.5 mmol), urea (3.75 mmol, 225 mg) and $MgCuO_2@SiO_2@La_2O_3$ nanocatalyst in 20 mL of distilled water as a green solvent was heated at 100 °C. After the reaction time, as monitored by TLC (ether/n-hexane 4:1), the reaction temperature was reduced to 25 °C and 25 mL of distilled water was added to the reaction mixture. The 3,4-dihydropyrimidine-2(1H)-ones were extracted with 30 mL of ether three times and the organic phase was dried over Na_2SO_4. Using rotary evaporation, ether was separated from the products. The 3,4-dihydropyrimidine-2(1H)-ones were purified and identified using ethanol. The $MgCuO_2@SiO_2@La_2O_3$ was separated by filtration for reuse in subsequent reactions and washed several times with water, ethanol and ethyl acetate, and finally was dried at 80°C for 2 hours.

Results and Discussion: Initially, the progress of the reaction without catalyst was investigated at room temperature and reflux conditions. At room temperature, no product was produced after stirring for 90 minutes, and under reflux conditions, little product was produced after stirring for 90 minutes. In the present study, $MgCuO_2@SiO_2@La_2O_3$ nanoparticles were used as catalysts to carry out the Biginelli reaction. The reaction was carried out at room temperature and water as a green solvent in the presence of $MgCuO2@SiO_2@La_2O_3$ nanocatalyst, which showed no progress in product formation. Then, in the presence of different amounts of catalyst under reflux conditions and the same time, the reaction efficiency was calculated. The results showed that the best performance was obtained using 20 wt% of the catalyst relative to ethyl acetoacetate. It is possible to separate and purify the $MgCuO_2@SiO_2@La_2O_3$ nanocatalyst. The $MgCuO_2@SiO_2@La_2O_3$ nanocatalyst was separated by filtration. The $MgCuO_2@SiO_2@La_2O_3$ nanocatalyst was reused after washing with water, ethanol and ethyl acetate and then drying at 80°C for 2 h. This process was performed five times and showed that all reactions were carried out in the desired yield. The $MgCuO_2@SiO_2@La_2O_3$ nanocatalyst showed excellent stability and activity during 5 consecutive reaction cycles. The reaction efficiency indicates that the $MgCuO_2@SiO_2@La_2O_3$ nanocatalyst maintains its activity and durability during recycling.

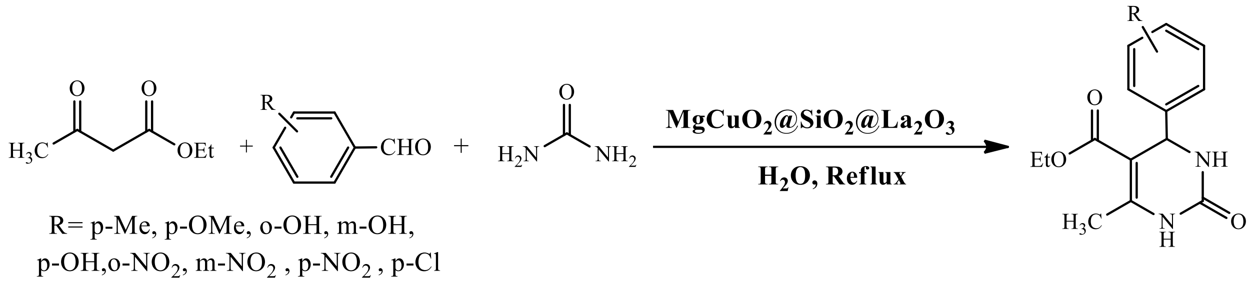

Scheme: Synthesis of 3,4-Dihydropyrimidin-2(1H)-ones using $MgCuO_2@SiO_2@La_2O_3$

References:

1. Védrine, J. C. (**2019**). Metal oxides in heterogeneous oxidation catalysis: State of the art and challenges for a more sustainable world. ChemSusChem, *12(3),* 577-588.
2. Rana, S., & Jonnalagadda, S. B. (**2017**). A facile synthesis of Cu–Ni bimetallic nanoparticle supported organo functionalized graphene oxide as a catalyst for selective hydrogenation of p-nitrophenol and cinnamaldehyde. RSC Advances, *7(5),* 2869-2879.
3. Biginelli, C. P. (**1893**). Aldehyde-urea derivatives of aceto-and oxaloacetic acids. Gazz. chim. ital, *23(1),* 360-413.
4. Kumarasamy, D., Roy, B. G., Rocha-Pereira, J., Neyts, J., Nanjappan, S., Maity, S., & Naesens, L. (**2017**). Synthesis and in vitro antiviral evaluation of 4-substituted 3, 4-dihydropyrimidinones. Bioorganic & Medicinal Chemistry Letters, *27(2),* 139-142.

The 30th Iranian Seminar of Organic Chemistry
February 7-9, 2025, Iran University of Science and Technology, Tehran, Iran

A Simple and efficient protocol for the synthesis of 3,4-Dihydropyrimidones catalyzed by $CuAl_2O_4@Fe_2O_3$

Sahar Khandani, Zahra Nikkhah, Fatemeh Bahramifar, Nayyer Afsharpour, Abbas Nikoo*

Department of Organic Chemistry, Faculty of chemistry, Urmia University, Urmia, Iran

Keyword: Chalcone, Nanocatalyst, Synthesis

Introduction: Nowadays, the synthesis of various nanocatalysts has become a topic of interest for researchers in the field of nanochemistry. Design and fabrication of a new catalyst for organic reactions is required to increase efficiency, improve reaction conditions and reduce environmental impacts. Synthesized nanocatalysts are metal nanooxides, which can be increased in surface area to volume ratio depending on the synthesis method. The role of mixed metal nanooxides in organic reactions for the synthesis of important chemicals in industries and the production of pharmaceutical compounds with high efficiency, selectivity and reusability has been accepted. Metal oxides are key components for catalysis of a variety of chemical reactions. Therefore, the importance of metal oxides in the field of catalysis is vast. Until now, the main interest in heterogeneous catalysts has focused on the kinetics of reactions and their mechanisms have received less attention. Now, it is the catalyst itself, and in particular its surface, that is in the spotlight. In investigating the performance of a catalyst and its surface, two specific factors have been considered. One is the geometric factor, which chemical adsorption and catalysis experiments on different facets of single crystals have helped to determine. The second factor is the role of electrons in the catalytic process, and the science of metal oxide surfaces has attracted much attention in recent years. The emergence of several advanced techniques for probing surfaces has led to a new understanding of their surface properties and structure, which has helped researchers in the field of catalysis to tune the properties of oxide materials for suitable applications [1-3].

Method: A mixture of chalcones (2.5 mmol), urea or thiourea (3.75 mmol) and $CuAl_2O_4@Fe_2O_3$ nanocatalyst in 20 mL of ethanol was heated at 80 °C. After the reaction time, as monitored by TLC (EtOAc/n-hexane 2:5), the reaction temperature was reduced to 25 °C and 25 mL of distilled water was added to the reaction mixture. The 3,4-Dihydropyrimidones were extracted with 30 mL of ethyl acetate three times and the organic phase was dried over Na_2SO_4. Using rotary evaporation, ethyl acetate was separated from the products. The 3,4-Dihydropyrimidones were purified and identified using ethanol. The $CuAl_2O_4@Fe_2O_3$ was separated by filtration for reuse in subsequent reactions and washed several times with water, ethanol and ethyl acetate, and finally was dried at 120°C for 2 hours.

Results and Discussion: The results of images and spectra showed that the synthesized nanocatalysts have small particle size distribution, homogeneous morphology and acceptable and desirable surface. The $CuAl_2O_4@Fe_2O_3$ nanocatalyst, which was synthesized for the first time, was used as a recyclable catalyst in the synthesis of 3,4-Dihydropyrimidones derivatives. The notable points of this new protocol are the reaction in the presence of the economy and cheapness of the methods and materials used, environmental compatibility, high efficiency, reduced reaction time, easy recovery and reuse of the nanocatalyst, all of which are in line with green chemistry.

The good results obtained from the optimization with benzaldehyde encouraged us to continue working on other aldehydes, including those with electron-donating and electron-withdrawing groups. All reactions were carried out in the presence of $CuAl_2O_4@Fe_2O_3$ nanocatalyst using 20 Wt% catalyst relative to ethyl acetoacetate in ethanol at 80°C. The experimental results showed that the yield and rate of the reaction changed with the change of the functional groups on benzaldehyde, such that electron-withdrawing functional groups led to an increase in the yield and rate of the reaction. However, electron-donating functional groups caused a decrease. Electron-withdrawing groups improve and increase the efficiency of the reaction, which is due to the activation of the carbonyl aldehyde group to react with ethyl acetoacetate, while electron-donating groups reduce the activity of the carbonyl aldehyde group, which leads to a decrease in the rate and efficiency. In general, 45–140 min are required to complete all the reactions. The synthesis of 3,4-Dihydropyrimidone derivatives was achieved in 80–95% yield.

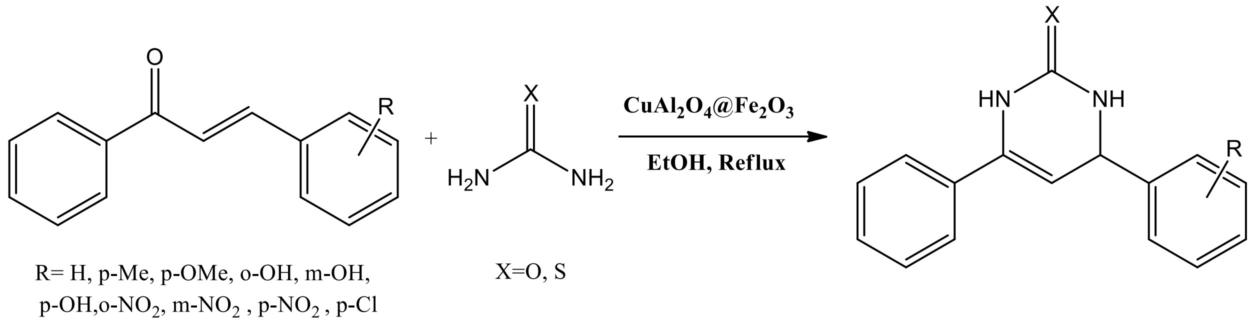

Scheme: Synthesis of 3,4-Dihydropyrimidones by $CuAl_2O_4@Fe_2O_3$

References:

1. Lindström, B., & Pettersson, L. J. (**2003**). A brief history of catalysis. Cattech, *7(4),* 130-138.

2. He, Y., Yin, Z., Wang, Z., Wang, H., Xiong, W., Song, B., & Zeng, G. (**2022**). Recent progress on mixed transition metal nanomaterials based on metal–organic frameworks for energy-related applications. Journal of Materials Chemistry A, *10(18),* 9788-9820.

3. Bhaskaruni, S. V., Maddila, S., Gangu, K. K., & Jonnalagadda, S. B. (**2020**). A review on multi-component green synthesis of N-containing heterocycles using mixed oxides as heterogeneous catalysts. Arabian Journal of Chemistry, *13(1),* 1142-1178.

The 30th Iranian Seminar of Organic Chemistry
February 7-9, 2025, Iran University of Science and Technology, Tehran, Iran

$MgCuO_2@Fe_2O_3$: Synthesis, Characterization and Heterogeneous Catalyst for the One-pot Synthesis of 3,4-Dihydropyrimidin-2(1H)-thiones in Water

Nayyer Afsharpour, Abbas Nikoo*, Fatemeh Bahramifar, Zahra Nikkhah, Sahar Khandani

Department of Organic Chemistry, Faculty of chemistry, Urmia University, Urmia, Iran

Keyword: Metal oxide, Nanocatalyst, Green chemistry, 3,4-Dihydropyrimidin-2(1H)-thione

Introduction: Metal oxides have special properties such as acidity or basicity and redox behavior (in the presence of transition metal ions) that lead to specific catalytic properties. They are also substrates for single or multi-metallic catalysts. Metal oxides may be used as supports for active phases such as silica, alumina, silica-alumina, mesoporous oxides and MOFs and affect the catalytic properties due to synergistic interactions, electronic or thermal conductivity [1]. Metal oxide-based catalysts are mainly used in refining and petrochemical processes. Many of them are being replaced by homogeneous catalysts to reduce the environmental factor E-factor. At the beginning of green chemistry in the early 1990s, the E-factor was developed to assess the environmental impact of chemical processes. Hence, great efforts are needed to improve the E-factor in all industrial processes, and this has led to extensive research. Most catalysts used in industrial applications contain an oxide as the active phase or substrate [2]. Considering the biological importance of dihydropyrimidone compounds, we decided to continue our research work in this direction to develop new improved methods for the Biginelli reaction [3]. The 3,4-dihydropyrimidin-2(1H)-thiones were confirmed by specific physical data and the $MgCuO_2@Fe_2O_3$ nanocatalyst with XRD, EDX, BET, FTIR, FESEM and Mapping.

Method: Synthesis of $MgCuO_2@Fe_2O_3$ core-shell nanoparticles was prepared by impregnating $MgCuO_2$ nanoparticles with a secondary metal precursor. In other words, the oxide nanoparticles used as the core and the nitrate precursor used in the shell formed the final nanoparticle. Another important point in this regard was the molar ratio of nanoparticles to the precursor used, which should be 1:1. After the end of this process, the obtained solid was calcined at 500 °C.

In a typical procedure, 5.7 mmol of thiourea, 5 mmol of ethyl acetoacetate and 5 mmol of aldehyde derivatives with a 15 Wt% of $MgCuO_2@Fe_2O_3$ nanocatalyst were poured into 50 mL of distilled water and a round bottom flask equipped with a condenser, and the desired mixture was stirred well under reflux conditions using a magnetic stirrer. The progress of the reaction was monitored using thin layer chromatography. In this chromatography method, the stationary phase was an aluminum plate impregnated with silica gel and the mobile phase was a 6:4 mixtures of hexane and ethyl acetate. After the reaction was completed, the prepared 3,4-dihydropyrimidin-2(1H)-thione was extracted using ethyl acetate and the residue of the reaction vessel was dried at 80°C after filtration to be used for subsequent times and to investigate the recovery of the catalyst.

Results and Discussion: The reaction of benzaldehyde derivatives with electron-withdrawing and electron-donating functional groups with thiourea and ethyl acetoacetate was investigated to prepare 3,4-dihydropyrimidin-2(1H)-thiones. All reactions were carried out in the presence of $MgCuO_2@Fe_2O_3$ using a catalytic amount of 15 Wt% in water at 100 °C and a time of 45-90 min. The synthesis of 4,3-dihydropyrimidine-2(H1)-one/thione was achieved with a yield of 72-93%. According to experimental data, electron-withdrawing functional groups are effective in the activity of benzaldehyde and increase the reaction efficiency. Steric repulsion can reduce the reaction rate and efficiency. It should be noted that increasing the amount of catalyst increases the reaction efficiency, but increasing the amount of catalyst excessively leads to clumping of particles together and a decrease in catalyst performance.

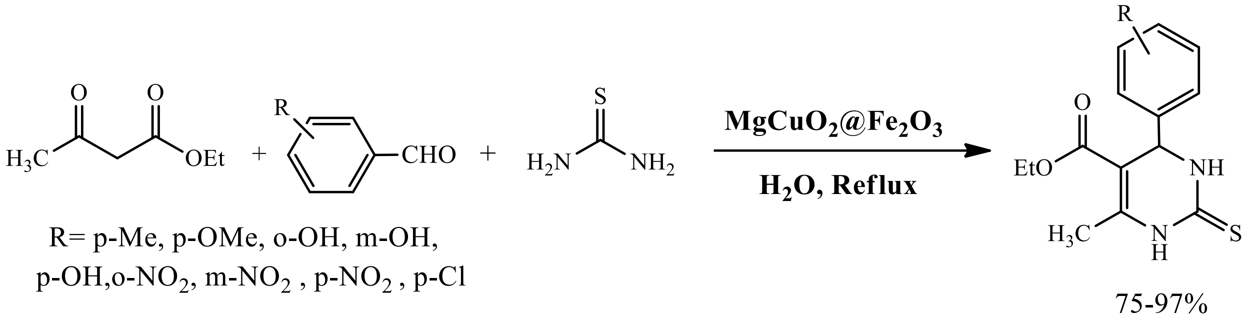

Scheme: Synthesis of 3,4-Dihydropyrimidin-2(1H)-thiones by $MgCuO_2@Fe_2O_3$ NPs

References:

1. Karami, C., Mohammadi, H., Ghodrati, K., Ahmadian, H., Jamshidi, F., Nouri, M., & Haghnazarie, N. (**2015**). Cobalt manganese oxide nano catalysts as a recyclable catalyst for the synthesis of 3,4-dihydropyrimidin-2(1H)-ones-thiones. Synthesis and Reactivity in Inorganic, Metal-Organic, and Nano-Metal Chemistry, *45(2),* 271-276.

2. Eshghi, H., Javid, A., Khojastehnezhad, A., Moeinpour, F., Bamoharram, F. F., Bakavoli, M., & Mirzaei, M. (**2015**). Preyssler heteropolyacid supported on silica coated NiFe2O4 nanoparticles for the catalytic synthesis of bis (dihydropyrimidinone) benzene and 3,4-dihydropyrimidin-2(1H)-ones. Chinese Journal of Catalysis, *36(3),* 299-307.

3. Azizi, M., Maleki, A., & Bodaghi, A. (**2022**). Green synthesis of Poly (ethylene oxide)-coated sulfonated copper ferrite nanoparticles and highly efficient application in the synthesis of dihydropyrimidine derivatives. Nanochemistry Research, *7(2),* 68-78.

The new NADES as a versatile catalyst for the synthesis of pyrimidines

Zahra Jahanyan, Davood Habibi*,Arezo Monem, Elnaz Chegeni

Department of Organic Chemistry, Faculty of Chemistry and Petroleum Science, Bu-Ali Sina University, Hamedan, 6517838683, Iran, Davood.Habibi@gmail.com
Zahrajahaniyan99519@gmail.com, arezomonem@yahoo.com

Keywords: Green Chemistry, Deep Eutectic Solvent, Catalysis, pyrimidine, synthesis.

Deep eutectic solvents (DESs) are solvents that moreover to having the properties of green solvents due to properties such as easy synthesis, low melting point, stability towards moisture and air, low vapor pressure, and high thermal stability can be used as an alternative to ionic liquids (IL)[1]. DESes are be made of mixture a hydrogen-bond acceptors (HBA) and hydrogen-bond donors (HBD). Generally, a DES is a type of solvent composed of a mixing two or more components under simple operation of that forms an eutectic with a much lower melting point than either of the individual components[2]. deep eutectic solvent was prepared with a mixture of amino acids and acid used as a novel catalyst for the green synthesis. The eutectic point phase diagram showed that one mole of amino acids to two moles of acid is the best mole ratio for the synthesis of the new DES. Then, NADES was characterized by the FT-IR, TGA/DTA, densitometer, eutectic points, and ^{1}H NMR techniques, and used as a novel catalyst for green synthesis[3].

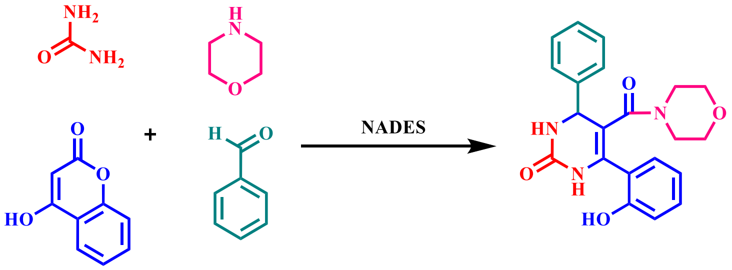

Scheme 1. Synthesis of 3,4-dihydropyrimidines derivative

References:

٤. **Zhang, Q., Vigier, K. D. O., Royer, S., & Jérôme, F. (2012). Deep eutectic solvents: syntheses, properties and applications. *Chemical Society Reviews, 41*(21), 7108-7146.**

٥. Maugeri, Z., & de María, P. D. (2012). Novel choline-chloride-based deep-eutectic-solvents with renewable hydrogen bond donors: levulinic acid and sugar-based polyols. *Rsc Advances*, *2*(2), 421-425.

٦. Monem, A., Habibi, D., & Goudarzi, H. (2024). The Novel Catalyst (Hypogallic Acid-Based Deep Eutectic Solvent) for Preparation of the New Compounds (Pyrano [2, 3-d] Pyrimidines). *Polycyclic Aromatic Compounds*, *44*(7), 4531-4544.

A Quantum Mechanical Investigation on furosemide

Hossein Shirani[a,*] and Nazanin Zahra Shahmir[b]

[*] *Corresponding author. E-mail: hossein_shirani@iust.ac.ir*

[a] *Department of Chemistry, Iran University of Science and Technology, P.O. Box 16846-13114, Tehran, Iran*
[b] *Department of Chemical Engineering, Technical and Engineering Faculty, Islamic Azad University, Central Tehran Branch, Tehran, Iran*

Introduction: furosemide is a prescription medicine that treats congestion caused by fluid build-up in a person with heart failure. furosemide should be replaced with oral diuretics as directed by healthcare provider. Follow the instructions provided by your physician when taking furosemide.

Figure1: Optimized structure of furosemide at the B3lyp/6-311g level of theory

Methods: The study utilized quantum mechanics (QM) calculations conducted through the density functional theory (DFT) method with the GAUSSIAN 09 software(1). The structure of the furosemide drug was first optimized through gradient procedures at both restricted Hartree-Fock (HF) and hybrid density functional B3LYP levels of theory using the 6-311G basis set. Examination of the results revealed that the optimized structure achieved in this research was situated at the minimum point on the potential energy surface, displaying no negative modes.

Results: This study conducted calculations for structural parameters like bond lengths, angles, and dihedrals, as well as thermodynamic parameters at the B3LYP/6-311G level of theory and provided the results. The electronic energy of the molecule was determined to be -1134338.606 kcal/mole. Additionally, the mulliken atomic charge, spin density, and molecular orbital energies were calculated. The highest occupied molecular orbital (HOMO) was found to be -0.25296 eV and the lowest unoccupied molecular orbital (LUMO) was -0.09510 eV. The dipole moment in Debye was measured as X=-11.1037, Y=-3.1885, Z=-2.6970, with a total of 11.8631.

Discussion: Optimization of the drug was performed using the B3LYP/6-**311G method. T**he study focused on furosemide's electronic characteristics, specifically the energy difference between the HOMO and the LUMO. The HOMO-LUMO gap energy was determined to be **0.15786 eV. This provides insights into** furosemide**'s electronic behavior, which could have** applications in various fields.(2,3)

Keywords: furosemide; DFT; B3LYP/6-311G, HOMO-LUMO gap

References:

1) Gaussian 09, Revision B.o1, M. J. Frisch et al., Gaussian, Inc., Wallingford CT, 2009

2) DrugBank furosemide: Wishart, D. S., Knox, C., Guo, A. C., Cheng, D., Shrivastava, S., Tzur, D., ... & Liu, P. (2018). DrugBank 5.0: a major update to the DrugBank database. Nucleic acids research, 46(D1), D1074-D1082.

3) WHO - Essential Medicines: World Health Organization (WHO). Essential medicines list

---

The 30th Iranian Seminar of Organic Chemistry
February 7-9, 2025, Iran University of Science and Technology, Tehran, Iran

Palladium nanoparticles supported on polydopamine-modified TiO_2 microparticles: An efficient nanocatalyst for Suzuki-Miyaura coupling

Mozhgan Pirhayati*

Department of Applied Chemistry, Faculty of Science, Malayer University, Malayer, Iran

mozhgan.pirhayati@malayeru.ac.ir

Keywords: Pd nanoparticles, Polydopamine, TiO_2, Suzuki-Miyaura coupling

Abstract

The present study describes the development of a novel nanocomposite, consisting of palladium nanoparticles (Pd NPs) immobilized on the surface of polydopamine (PDA)-modified TiO_2 microparticles (TiO_2/PDA-Pd NPs). The physical and chemical characteristics of the synthesized TiO_2/PDA-Pd nanocomposite were analyzed using different techniques, such as FT-IR, FE-SEM, EDX, TEM, XPS, and ICP-OES. This TiO_2/PDA-Pd NPs nanocomposite was then investigated

for its catalytic application in the Suzuki-Miyaura coupling reaction, yielding biphenyl products with good efficiency. Furthermore, the nanocatalyst exhibited exceptional catalytic performance, maintaining its high activity after seven reaction cycles, highlighting its potential for use as a sustainable and recyclable catalyst.

1. Introduction

In the past decade, nanoscale materials have gained attention for their catalytic potential and unique chemical properties [1], also serving as support for immobilizing homogeneous catalysts, combining the benefits of both homogeneous and heterogeneous catalysis [2]. Palladium (Pd) is valued for its excellent catalytic performance and stability. Polydopamine (PDA) is used to modify noble metal nanoparticle catalysts, with functional groups that anchor and reduce metal ions to nanoparticles, stabilizing them [3-4]. In this study, TiO_2 nanoparticles were functionalized with PDA, and Pd nanoparticles were deposited to form a TiO_2/PDA-Pd NPs composite. The composite was characterized by FT-IR, FESEM-EDX, TEM, XPS, and ICP, and tested in the Suzuki-Miyaura reaction for synthesizing biaryl compounds.

2. Result and discussion

2.1. Characterization

Figure 1 displays the FE-SEM images of the TiO_2/PDA-Pd NPs nanocomposite. As shown in Figure 1a, the TiO_2 microparticles consist of nearly uniform sub-microspheres, each with an approximate diameter of 200 nm. In Figure 1b, it is evident that the Pd nanoparticles are evenly dispersed throughout the PDA coating on the TiO_2 microparticles, with a nearly uniform morphology, and the Pd nanoparticles have diameters ranging from 80 nm to 90 nm.

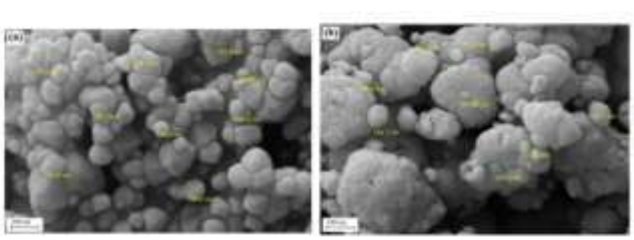

Fig. 1. (a) FESEM image of TiO_2 micro (b) FESEM image of TiO_2@PDA/Pd NPs

2.2. Catalytic performance of TiO_2@PDA/Pd NPs in the Suzuki-Miyaura coupling reactions

After thoroughly characterizing the synthesized TiO_2@PDA/Pd NPs catalyst, its catalytic performance was assessed in the Suzuki-Miyaura coupling reaction. Various haloarenes were reacted with phenylboronic acid, resulting in a diverse array of C-C coupled biaryl products**.**

3. Conclusion

The current study introduced the novel synthesis of palladium nanoparticles (Pd NPs) supported over the surface of polydopamine (PDA)-functionalized TiO_2 microparticles (TiO_2/PDA-Pd NPs). The as-prepared TiO_2/PDA-Pd nanocomposite was characterized using various advanced techniques and applied as an efficient nanocatalyst in the Suzuki-Miyaura coupling reaction.

References

[1] X. Huang, J. Hu, H. Zhu, J. Chen, Y. Liu, Z. Mao, J. Lee, H. Chen, Biosensors and Bioelectronics. 191 (2021).

[2] Z. Chen, E. Vorobyeva, S. Mitchell, E. Fako, M.A. Ortuño, N. López, S.M. Collins, P.A. Midgley, S. Richard, G. Vilé, J. Pérez-Ramírez, Nature Nanotechnology. 13 (2018) 702–707.

[3] Y. Ni, G. Tong, J. Wang, H. Li, F. Chen, C. Yu, Y. Zhou, *RSC Advances*. 2016, **6**, 40698-40705.

[4] G. Su, C. Yang, J.J. Zhu, *Langmuir*. 2015, **31**, 817-823.

The 30th Iranian Seminar of Organic Chemistry
February 7-9, 2025, Iran University of Science and Technology, Tehran, Iran

Theoretical study of the Remdesivir adsorption on the boron nitride nanocluster by density functional theory method

Masoumeh Shahi, Shahin Ahmadi, Parvin Fekri

Department of Organic Chemistry, Faculty of Pharmaceutical Chemistry, Tehran Medical Sciences, Islamic Azad University, Tehran, Iran

Abstract

In this research, the nonbonding interaction of Remdesivir antiviral drug and the boronnitride nanocluster($B_{12}N_{12}$) was investigated by the DFT method at the B3LYP/6-31G (d) level of theory. The adsorption energy of Remdesivir on $B_{12}N_{12}$ at 298 K and 1 atm pressure, in the gas phase and water solvent, was calculated to be -24.488 and -23.756 kcal/mol, respectively. The calculations of thermodynamic functions and the energy values indicate that Remdesivir is less reactive and more stable with the presence of B12N12. A non-bonded interaction between Remdesivir and $B_{12}N_{12}$ results in lower Enthalpy and Gibbs energies. It is highly hoped this study could provide theoretical guidance for choosing suitable carriers to deliver the Remdesivir drug, and further expand the application of B_nN_n nanocages in drug delivery.

Keyword: Remdesivir, Boron Nitride Nanocluster, DFT, Adsorption, Drug Delivery

Introduction

The COVID-19 pandemic was met with rapid, unprecedented global collaboration and action. Even still, the public health, societal, and economic impact may be felt for years to come. The risk of another pandemic occurring in the next few decades is ever-present and potentially increasing due to trends such as urbanization and climate change. While it is difficult to predict the next pandemic pathogen threat, making reasonable assumptions today and evaluating prior efforts to plan for and respond to disease outbreaks and pandemics may enable a more proactive, effective response in the future [1].Different drugs were investigated for control of COVID-19 infection. Clinical researches show that Remdesivir (RDV, GS-5734) drug, which has been known as a promising antiviral drug against some RNA viruses, can be as an important drug in prophylactic and therapeutic efficacy of patients with COVID-19 illness. Remdesivir is a prodrug of a nucleoside analogue that hinders viral RNA polymerases because it is intracellularly metabolized to an analogue of adenosine triphosphate. The clinical and antiviral effectiveness of Remdesivir in COVID-19 illness remains to be recognized [2-7]. In order to improve therapeutic efficiency of Remdesivir drug, the use of nano medicine and design of drug delivery vehicles based on nanomaterials, which may increase efficiency of absorption of drugs, is important [8,9]. The boosting of nanotechnology renders nanomaterials a promising and popular candidate for controllable drug delivery systems. Nanomaterials can not only improve the solubility of poorly water-soluble drugs and prolong the half-life of drugs, but also release the drug in a controlled or environmentally responsive manner to regulate the biological distribution of drugs and thus minimize side effects [10, 11]. In recent decades, various nanomaterials have been developed and adopted as drug delivery vehicles, especially these low-dimensional nanomaterials based on carbon and boron nitride (BN), such as fullerenes, graphene derivatives, boron nitride nanocages and so on [11, 12]. Among them, BN nanocages with different sizes have been repeatedly studied for varied applications (e.g., drug delivery and biosensors) due to their superior biocompatibility, remarkable stability as well as excellent physical and chemical properties [13-24]. For example, the potential applications of $B_{12}N_{12}$ for serine [18], penicillamine [19], cladribine [20],ciclopirox [17] and flucytosine [24] were computationally investigated. Recently, the use of boronnitride nanoparticles drug delivery systems for antiviral drugs like Favipiravir has also been considered, for example Mehade Hasan et al. proposed the computational quantum mechanical investigation of the functionalized boron nitride nanocage as the smart carriers for favipiravir drug delivery [13]. Nevertheless, the adsorption behaviors of Remdesivir onto the BN nanocages remains unknown. Therefore, in this study, we used boron nitride nanocluster ($B_{12}N_{12}$) as a drug carrier for Remdesivir and investigated non-bonded interaction of Remdesivir with BN($B_{12}N_{12}$) using density functional theory (DFT) calculations.

Method

This process was carried out in Gaussian 09W software using DFT with the B3LYP method and 6-31G(d) basis set. It was performed with gaseous and solvent phase, 298.15 degrees Kelvin and 1 atm. Remdesivir adsorption energy on $B_{12}N_{12}$ was computed according to the following formula:

$$E_{ad} = E_{RDV/BN} - (E_{RDV} + E_{BN})$$

The energy of ($E_{RDV/BN}$) represents the total energy of the RDV- $B_{12}N_{12}$ complex, including both the compound RDV and the compound BN. The energy of (E_{RDV}) and (E_{BN}) represents the total energy of their respective compounds.

Results and Discussion

The geometric structures of $B_{12}N_{12}$, RDV drug were reoptimized by using B3LYP functional in conjunction with the 6-31G(d) basis set (Figure. 1).

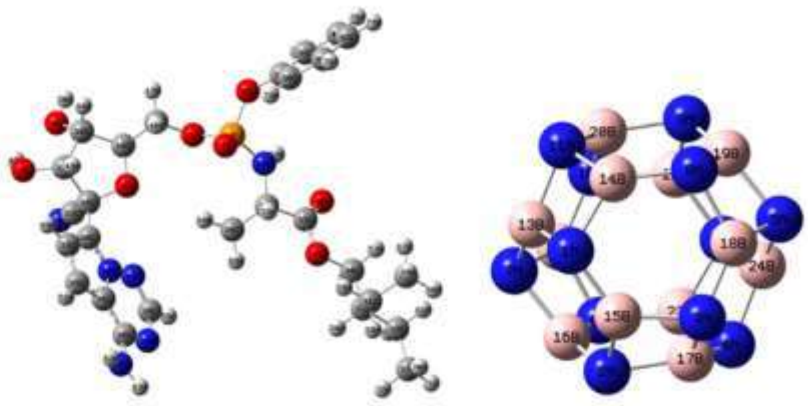

A:Remdesivir(C27H35N6O8P)   B:Boron nitride nanocluster(B12N12)

Figure 1. Optimized structures of the compound Remdesivir and Boron nitride nanocluster ($B_{12}N_{12}$) using the B3LYP/6-31G* level of theory

In order to load the RDV onto the boron nitride nanocluster($B_{12}N_{12}$), RDV was placed in different directions of the $B_{12}N_{12}$. We have considered four interactions between the RDV with the $B_{12}N_{12}$. The four optimized states (I–IV) were calculated at the HF/STO-3G basic set (Fig. 2).

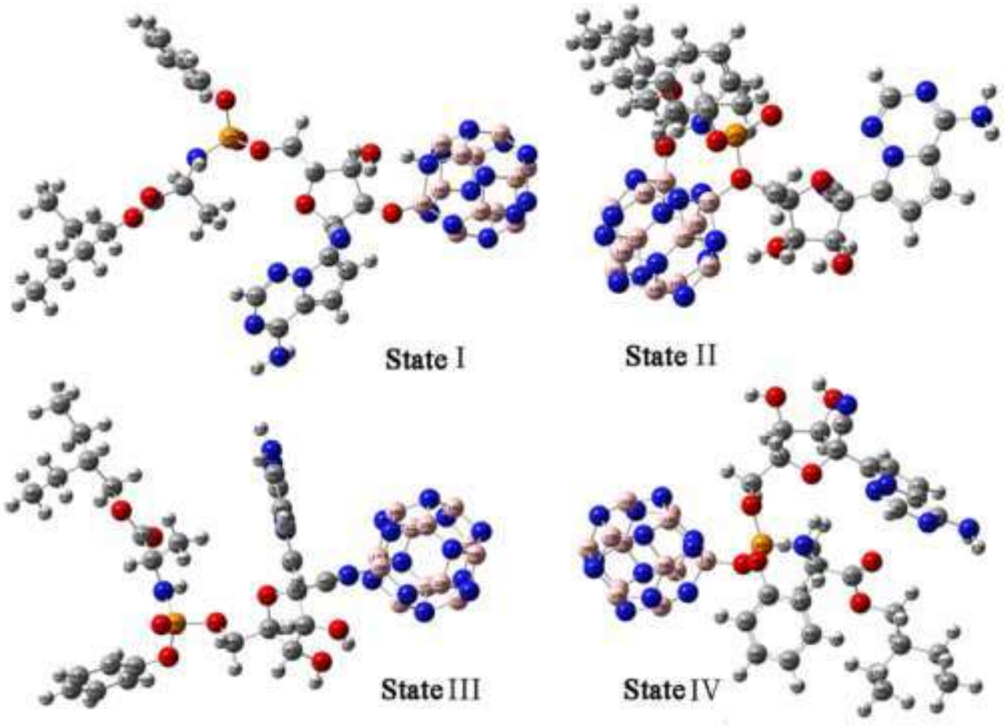

Figure 2. Four interaction states of the compound Remdesivir with $B_{12}N_{12}$ with the optimized at HF/STO-3G level of theory

The calculated values of electronic energy (E) for the four states I-IV were calculated: − 2,019,961.218, − 2,019,958.494, − 2,019,918.522, − 2,019,973.593 kcal/mol, respectively. The IV conformation turns to be the lowest by energy, and its energy was chosen as the reference energy.

The most stable RDV-$B_{12}N_{12}$ complex(state IV) was optimized with the 6-31G(d) basis set (Fig. 3) and the adsorption energy (E adsorption) of RDV on $B_{12}N_{12}$ was calculated in the gas and solvent (water) phases at B3LYP/6-31G* level. The values of electronic energies of $B_{12}N_{12}$, RDV and RDV-$B_{12}N_{12}$ complex and the adsorption energy (E adsorption) of RDV on $B_{12}N_{12}$ were reported in Table 1.

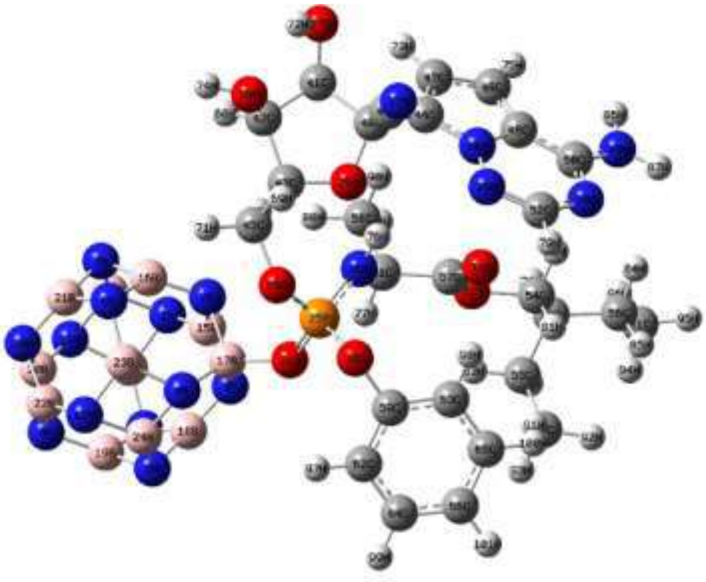

Figure 3. Optimized structure of RDV-$B_{12}N_{12}$ at B3LYP/6-31G* level

Table1. The values of electronic energies of $B_{12}N_{12}$, RDV and RDV-$B_{12}N_{12}$ complex and the adsorption energy (E adsorption) of RDV on $B_{12}N_{12}$ at B3LYP/6-31G* level

SCF done energy (kcal/mol)			Adsorption Energy (kcal/mol)	SCF done energy(kcal/mol)			Adsorption Energy (kcal/mol)
Eel (BN/RDV)	Eel (RDV)	Eel (BN)	$E_{adsorption}$	Eel (BN/RDV)	Eel (RDV)	Eel (BN)	$E_{adsorption}$
In the gas phase				In the solvent phase			
-2056850.84	-1456835.93	-599990.42	-24.488	-2056876.82	-1456859.02	-599994.0507	-23.756

According to Table 1, the adsorption energy (E adsorption) of RDV on $B_{12}N_{12}$ has an exothermic nature due to its negative adsorption energy in the gas (-24.488 kcal/mol) and solvent (-23.756 kcal/mol) phases.

The thermodynamic parameters optimized at the B3LYP/6-31G* level of theory for $B_{12}N_{12}$, RDV and RDV-$B_{12}N_{12}$ complex in the gas and solvent phases. These parameters include the thermal energies (T), the thermal enthalpies (H), and the thermal free energies (G) (Table 2). As can be seen from the data of Table 2, the negative electron energy, enthalpies, and Gibbs energies of RDV-$B_{12}N_{12}$ complex make it stable vibrational states.

Table 2. The thermodynamic parameters of Remdesivir, $B_{12}N_{12}$ and RDV-$B_{12}N_{12}$ complex at B3LYP/6-31G* level of theory calculated in kcal/mol

Thermodynamic parameters (Kcal/mol)	In the gas phase			In the solvent phase		
	(BN/RDV)	(BN)	(RDV)	(BN/RDV)	(BN)	(RDV)
T	-2056344.622	-599903.548	-1456419.151	-2056371.659	-599907.235	-1456442.621
H	-2056344.030	-599902.955	-1456418.559	-2056371.066	-599906.643	-1456442.028
G	-2056438.015	-599931.737	-1456498.908	-2056465.572	-599935.489	-1456521.987

Table 3 shows the thermochemical parameters for interaction of the compound Remdesivir with $B_{12}N_{12}$ (state IV) optimized using B3LYP/6-31G* method in the gas and solvent phase. According to Table 3, all of the calculated parameters are negative and show an exothermic process in the adsorption of RDV on the $B_{12}N_{12}$ surface for more stable configurations. A non-bonded interaction between Remdesivir and $B_{12}N_{12}$ results in lower Enthalpy and Gibbs energies. The energy values indicate that Remdesivir is less reactive and more stable with the presence of $B_{12}N_{12}$.

Table3. Thermodynamic functions for the adsorption process of RDVon $B_{12}N_{12}$ at B3LYP/6-31G* level.

Thermodynamic parameters for the adsorption process (Kcal/mol)	In the gas phase	In the solvent phase
ΔET_{ad}= T ($B_{12}N_{12}$/RDV) – [T($B_{12}N_{12}$) + T(RDV)]	-21.923	-21.803
ΔH_{ad}= H ($B_{12}N_{12}$/RDV) – [H($B_{12}N_{12}$) + H(RDV)]	-22.516	-22.395

$\Delta G_{ad} = G\ (B_{12}N_{12}/RDV) - [G(B_{12}N_{12}) + G(RDV)]$	-7.37	-8.096

Conclusion

In this work, the nonbonding interaction of Remdesivir antiviral drug and the boronnitride nanocluster($B_{12}N_{12}$) was investigated by the DFT method at the B3LYP/6-31G (d) level of theory. The adsorption energy of the Remdesivir on the $B_{12}N_{12}$, in the gas and solvent (water)phase, was calculated -24.488 kcal/mol and -23.756 kcal/mol, respectively, indicating that the adsorption of Remdesivir on the $B_{12}N_{12}$ is exothermic and that it is feasible at ambient temperature. The calculations of thermodynamic functions and the energy values indicate that Remdesivir is less reactive and more stable with the presence of $B_{12}N_{12}$ and again denoting that $B_{12}N_{12}$ nanocluster is suitable for the adsorption of RDV drug and it can be an effective guide for experimental trials.

References:

١- Williams BA, Jones CH, Welch V, True JM. Outlook of pandemic preparedness in a post-COVID-19 world. npj Vaccines [Internet]. 2023 Nov 20;8(1):1–12. Available from: https://www.nature.com/articles/s41541-023-00773-0

٢- Wit E de, Feldmann F, Cronin J, Jordan R, Okumura A, Thomas T, et al. Prophylactic and therapeutic remdesivir (GS-5734) treatment in the rhesus macaque model of MERS-CoV infection. Proceedings of the National Academy of Sciences [Internet]. 2020 Feb 13; Available from: https://www.pnas.org/content/early/2020/02/12/1922083117

٣- Sheahan TP, Sims AC, Leist SR, Schäfer A, Won J, Brown AJ, et al. Comparative therapeutic efficacy of remdesivir and combination lopinavir, ritonavir, and interferon beta against MERS-CoV. Nature Communications. 2020 Jan 10;11(1).

٤- Mulangu S, Dodd LE, Davey RT, Tshiani Mbaya O, Proschan M, Mukadi D, et al. A randomized, controlled trial of Ebola virus disease therapeutics. New England Journal of Medicine. 2019 Dec 12;381(24):2293–303.

٥- Zhou F, Yu T, Du R, Fan G, Liu Y, Liu Z, et al. Clinical course and risk factors for mortality of adult inpatients with COVID-19 in Wuhan, China: a retrospective cohort study. The Lancet. 2020 Mar;395(10229):1054–62.

٦- Sheahan TP, Sims AC, Leist SR, Schäfer A, Won J, Brown AJ, et al. Comparative therapeutic efficacy of remdesivir and combination lopinavir, ritonavir, and interferon beta against MERS-CoV. Nature Communications. 2020 Jan 10;11(1).

٧- Warren TK, Jordan R, Lo MK, Ray AS, Mackman RL, Soloveva V, et al. Therapeutic efficacy of the small molecule GS-5734 against Ebola virus in rhesus monkeys. Nature. 2016 Mar;531(7594):381–5.

٨- Bagheri Novir S, Aram MR. Quantum mechanical simulation of Chloroquine drug interaction with C60 fullerene for treatment of COVID-19. Chemical Physics Letters. 2020 Oct;757:137869.

٩- Parlak C, Alver Ö. A density functional theory investigation on amantadine drug interaction with pristine and B, Al, Si, Ga, Ge doped C60 fullerenes. Chemical Physics Letters. 2017 Jun;678:85–90.

١٠-Zhang L, Gu F, Chan J, Wang A, Langer R, Farokhzad O. Nanoparticles in Medicine: Therapeutic Applications and Developments. Clinical Pharmacology & Therapeutics. 2007 Oct 24;83(5):761–9.

١١-Rahman H, Hossain MdR, Ferdous T. The recent advancement of low-dimensional nanostructured materials for drug delivery and drug sensing application: A brief review. Journal of Molecular Liquids. 2020 Dec;320:114427.

١٢-Angizi S, Ahmad A, Hasanzadeh Azar M, Shayeganfar F, Manning MI, Hatamie M, et al. A comprehensive review on planar boron nitride nanomaterials: From 2D nanosheets towards 0D quantum dots. Progress in Materials Science. 2022 Feb 1;124:100884–4.

١٣-Md. Mehade Hasan, Ashish Chandra Das, Md. Rakib Hossain, Md. Kamal Hossain, Md. Abul Hossain, Neher B, et al. The computational quantum mechanical investigation of the functionalized boron nitride nanocage as the smart carriers for favipiravir drug delivery: a DFT and QTAIM analysis. Journal of Biomolecular Structure and Dynamics. 2021 Oct 1;40(23):13190–206.

١٤-Zhou Z, Liu X, Li P. B24N24 nanocage as an electronic sensor for metronidazole drug: density functional theory studies. Journal of Molecular Modeling. 2022 May 1;28(5).

١٥-Zhang L, Cheng X, Li XH, Chen JH, Sun WM. A DFT study on the adsorption behavior of antiviral Favipiravir drug on B N (n = 12, 16, 20, and 24) nanocages: The size effect. Journal of Molecular Liquids. 2022 Aug 1;360:119388–8.

١٦-Luo Y, Wang K, Mu J, Cai Y, Zhu W. Exploring the adsorption behavior of pyrazinamide on the surface of X12Y12(X = B, Al; Y = N, P) nanocages: A in-silico study. Journal of Molecular Liquids. 2023 Jan 6;372:121211–1.

١٧-Kaviani S, Shahab S, Sheikhi M, Potkin VI, Zhou H. A DFT study of Se-decorated B12N12 nanocluster as a possible drug delivery system for ciclopirox. Computational and Theoretical Chemistry. 2021 Jul 1;1201:113246–6.

١٨-Soltani A, Taghartapeh MR, Erfani-Moghadam V, Javan MB, Heidari F, Aghaei M, et al. Serine adsorption through different functionalities on the B12N12 and Pt-B12N12 nanocages. Materials Science and Engineering C. 2018 Jun 27;92:216–27.

١٩-Cao Y, Khan A, Balakheyli H, Lup ANK, Ramezani Taghartapeh M, Mirzaei H, et al. Penicillamine functionalized B12N12 and B12CaN12 nanocages act as potential inhibitors of proinflammatory cytokines: A combined DFT analysis, ADMET and molecular docking study. Arabian Journal of Chemistry [Internet]. 2021 Jul 1;14(7):103200. Available from: https://www.sciencedirect.com/science/article/pii/S187853522100215X

٢٠-Hosseinzadeh E, Foroumadi A, Firoozpour L. A DFT study on the transition metal doped BN and AlN nanocages as a drug delivery vehicle for the cladribine drug. Journal of Molecular Liquids. 2023 Mar 1;374:121262–2.

٢١-Flores Bautista MC, Cortés-Arriagada D, Shakerzadeh E, Chigo Anota E. Acetylsalicylic acid interaction with Boron nitride nanostructures – A density functional analysis. Journal of Molecular Liquids. 2022 Jun;355:118980.

٢٢- Gholami A, Shakerzadeh E, Chigo Anota E, Flores Bautista M. A theoretical perspective on the adsorption performance of pristine and Metal-encapsulated B36N36 fullerenes toward the hydroxyurea and nitrosourea anticancer drugs. Inorganic Chemistry Communications [Internet]. 2023 Feb 1 [cited 2023 Dec 13];148:110326. Available from: https://www.sciencedirect.com/science/article/pii/S1387700322011340

٢٣- Gholami A, Shakerzadeh E, Chigo Anota E. Exploring the potential use of pristine and metal-encapsulated B36N36 fullerenes in delivery of β-lapachone anticancer drug: DFT approach. Polyhedron. 2023 Mar 1;232:116295–5.

٢٤- Yao X, Mu J, Zheng Y, Wu J, Zhu W, Wang K. Tailoring the adsorption behaviors of flucytosine on BnNn (n = 12, 16, 20, and 24) nanocage scaffolds: A computational insight on drug delivery applications. Colloids and Surfaces A Physicochemical and Engineering Aspects. 2023 Dec 1;678:132481–1.

The 30th Iranian Seminar of Organic Chemistry
February 7-9, 2025, Iran University of Science and Technology, Tehran, Iran

Fabrication of Microwave-Assisted Multi-Component Nanocomposites Using Copper, Iron Carbonyl, Carbon Nanofibers, Graphite Nanoflakes, and Polypyrrole

Authors: Ali azimi[1*], Seyed Hossien Hosseini[2], Golnaz Ghanoun[3]

[1] *Department of Chemistry, Science and Research Branch, Islamic Azad University, Tehran, Iran*

[2] *Nika Pooyesh Industrial Research Institute, NBP Economic Group, Tehran, Iran*

[3] *Department of Chemistry, Science and Research Branch, Islamic Azad University, Tehran, Iran*

Abstract- Nanocomposites comprising Cu, Carbonyl Iron (CI), Carbon Nanofiber (CNF), Graphite Nanoflake (GNF), Polypyrrole (PPy), and [(Cu-CI-CNF-GNF)$_{0.5}$-PAA]-PPy$_{0.5}$ were synthesized through various methods, including in-situ polymerization on core-shell structured nanoparticles (NPs). This study presents a detailed process for polyacrylic acid (PAA) coating of NPs in an aqueous solution, followed by PPy coating via template polymerization. The morphology, magnetic properties, and electrical conductivity of the nanocomposites were characterized using scanning electron microscopy (SEM), vibrating sample magnetometer (VSM), and the four-probe method, respectively. Microwave absorption performance was evaluated using the arch method with a network analyzer. The synthesized PPy nanocomposites demonstrated excellent multi-band microwave absorption in the 2–18 GHz range. Furthermore, nanocomposites with 50% w/w composition and lightweight exhibited effective absorption properties within the 2–3 GHz and 5–

14 GHz frequency ranges, making them suitable for applications such as cellphone, radio frequency, and radar shielding.

Keywords: nanocomposites, polypyrrole (ppy), microwave absorption, carbon nanofiber (cnf), electrical conductivity

١. Introduction

In the last decade, various microwave (MW) absorption materials have been widely investigated for electromagnetic interference to protect human health and electronic equipment from electromagnetic pollution which is caused by the wide applications of high-power electronic devices and communication technology [1,2]. High absorption, wide frequency band and low density are a pursuing in the design of microwave absorption materials. Some current researches of electromagnetic absorption are focused on the range from 2-18 GHz [3,4]. Polypyrrole (PPy) and polyaniline (PANI), the most extensively studied conducting polymers, have attracted great interest in the construction of electromagnetic absorbers for its low weight, high electrical conductivity and suitable Physical chemistry properties [5,6]. For instance, MWCNT/$Ba_{0.2}Sr_{0.2}La_{0.6}MnO_3$ nanocomposite based PANI was synthesized by core-shell structure which exhibit Ku band absorption property [7]. Increased absorption of electromagnetic waves based on nanoparticles and carbon nanostructures has also received much attention [8]. The multiband microwave absorption films epoxy-based multilayered coating containing carbon nanotube (CNT), silicon carbide (SiC), and carbonyl iron (CI) particles were prepared by Mahdavi and his coworkers [9]. In addition to absorbing electromagnetic waves, polypyrrole and epoxy nanocomposites also increase enhanced flame retardancy in the presence of nano magnetite [10]. On the other hand, nanocomposites with shell core structure have been extensively developed and have several applications [11,12]. The conductive and magnetic nanocomposites with core-shell and different nanostructures were used for electromagnetic absorption application [13,14]. The preceding works, we have synthesized magnetic and conductive nanofiber-nanocomposites based polythiophene which exhibit excellent MW absorption in the X-band range [15]. Therefore, we fabricated double core-shell structure polyaniline nanocomposites which exhibit both good MW absorption and thermal infrared performance [16-18]. The graphite nanoflake (GNF) and carbon nanofiber (CNF) as a new kind of absorbers have attracted much attention for their unique physical, chemical and mechanical properties, such as their light weight, flexibility, high specific surface and excellent electronic conductivity [15,19]. In this work, we attempted to add Cu and CI nanoparticles into the CNF, GNF and PPy composite to synthesize a new nanocomposite with five components, $[(Cu\text{-}CI\text{-}GNF)_{0.5}\text{- }PPA]\text{-}PPy_{0.5}$. A green chemical method was applied to prepare by in-situ polymerization on the surface of all components after were coated by PAA. This paper is a revised and expanded microwave absorption properties in the frequency of 2-18 GHz.

٢. Experimental Materials

Natural flake graphite with an average size of 500 µm was used for preparing the expanded graphite nanoflakes. Concentrated sulfuric acid and concentrated nitric acid were used as chemical intercalate and oxidizers. Pyrrole monomer (analytical grade, Merck) distilled twice under reduced pressure and stored blew 0 °C. The liquid carbonyl iron was commercially from Aldrich. Carbon nanofiber was purchased size of 10 to20 nm industrial. Dodecylbenzene sulfuric acid (DBSA, 90%) and polyacrylic acid (PAA) were purchased from the Aldrich. All the other chemical reagents were purchased from Merck without further purification.

٣. Preparation of Green Cu Nanoparticles

For biological synthesis of copper nanoparticles, Nag champa (Artabotrys odoratissimus, Family: Annonaceae), leaves were collected and dried for 4 days at room temperature. The plant leaf broth solution was prepared by taking 25 g of thoroughly washed and finely cut leaves in a 1 L beaker with 500 mL of sterile distilled water and then boiling the mixture for 5 min before finally decanting it. It was stored at 4 °C and used within a week. Typically, 30 mL of leaf broth was added to 170 mL of 1 $mmolL^{-1}$ aqueous $CuSO_4.5H_2O$ solution for the reduction of copper ions. The effects of temperature on synthesis rate and particle size of the prepared copper nanoparticles were studied by carrying out the reaction in a water bath at 95 °C with reflux. The copper nanoparticle solution thus obtained was purified by repeated centrifugation at 15,000 rpm for 20 min followed by re-dispersion of the pellet in deionized water.

٤. Preparation of Green Cu Nanoparticles

A mixture of concentrated sulfuric acid and nitric acid (3:1, v/v) was mixed with graphite flake at room temperature. The reaction mixture was stirred continuously for 12 h. The acid treated natural graphite was washed with water until neutralized and was then dried at 60 °C to remove any remaining water. The dried flakes were heat-treated at 1050 °C for 15s to obtain expanded graphite. Expanded graphite was immersed in a 70% of aqueous alcohol solution in an ultrasonic bath. The mixture was sonicated for 12 h, and then was filtered and dried to produce GNF.

4.1. Coating of NPs with PAA (NPs-PAA)

0.5 g NPs and 50 mL PAA (5% w/v) were added into 250 mL flask and the mixture were ultrasonicated for 15 min. The mixture was stirred vigorously at 25 °C for 24 h. The mixture was filtered and then washed with acetic acid (2% v/v) and acetone. After vacuum drying the filtrate, NPs-PAA was achieved.

4.2. Preparation of PPy Nanocomposite, [(Cu-CI-CNF-GNF)0.5-PAA]-$PPy_{0.5}$

The PPy nanocomposite as core-shell nanocomposite was prepared with template polymerization by in-situ polymerization in the presence of DBSA as the surfactant and dopant and $Fe(NO_3).9H$ O as the oxidant. The 0.5 g DBSA dissolved in morphologies of samples. The magnetic measurements carried out at room temperature using a Termo company 7400 model (USA), vibrating sample magnetometer (VSM) with maximum magnetic of 10 KOe. The XRD patterns of the samples were collected on a Philips-PW 1800 with Cu Kα radiation (λ=1.54184 Å) in the 2θ= 4-900 with steps of 0.020, scanning operated at 40 kV and 30 mA (Netherland). The electrical conductivity of compressed pellet of samples and nanocomposites were calculated using a standard four-probe set-up connected to a Keithly system comprising a voltmeter and constant high-current source, made in IRAN. Microwave absorption properties of nanocomposites were measured using microwave vector network analyzer (Agilent technologies Inc.8722-USA) in the 2-18 GHz range at room temperature.

٥. Results and Discussion

٥٫١. FTIR Study

Figure.1 shows FTIR spectrum of [(Cu-CI-CNF-GNF)$_{0.5}$-PAA]-PPy$_{0.5}$ nanocomposites. We synthesized GNF by acid treatment and thermal shock. We expect see hydroxyl and carboxyl functional group on GNF. So, the band at 3439 cm-1 can be attributed to3 2 distilled water with vigorous stirring for about 20 min. The 0.287 g NPs-PAA were added to the DBSA solution under stirring condition for approximately 1 h .Then 1 mL (0.015 mol) of freshly distilled pyrrole as monomer added to the suspension and stirred for 30 min. The NPs-PAA were dispersed well in the mixture of PPy/ DBSA under ultrasonication for 2 h. 12.12 g (0.03 mol) $Fe(NO_3)_3.9H_2O$ as initiator dissolved in 30 mL deionized water and added drop wise to stirred reaction mixture. Polymerization was allowed to proceed for 6 h. The nanocomposite was obtained by filtering was washing the suspension with deionized water and acetone, respectively. The obtained dark powder contains [(Cu-CI-CNF-GNF)$_{0.5}$-PAA]-PPy$_{0.5}$ and dried under vacuum for 24 h.

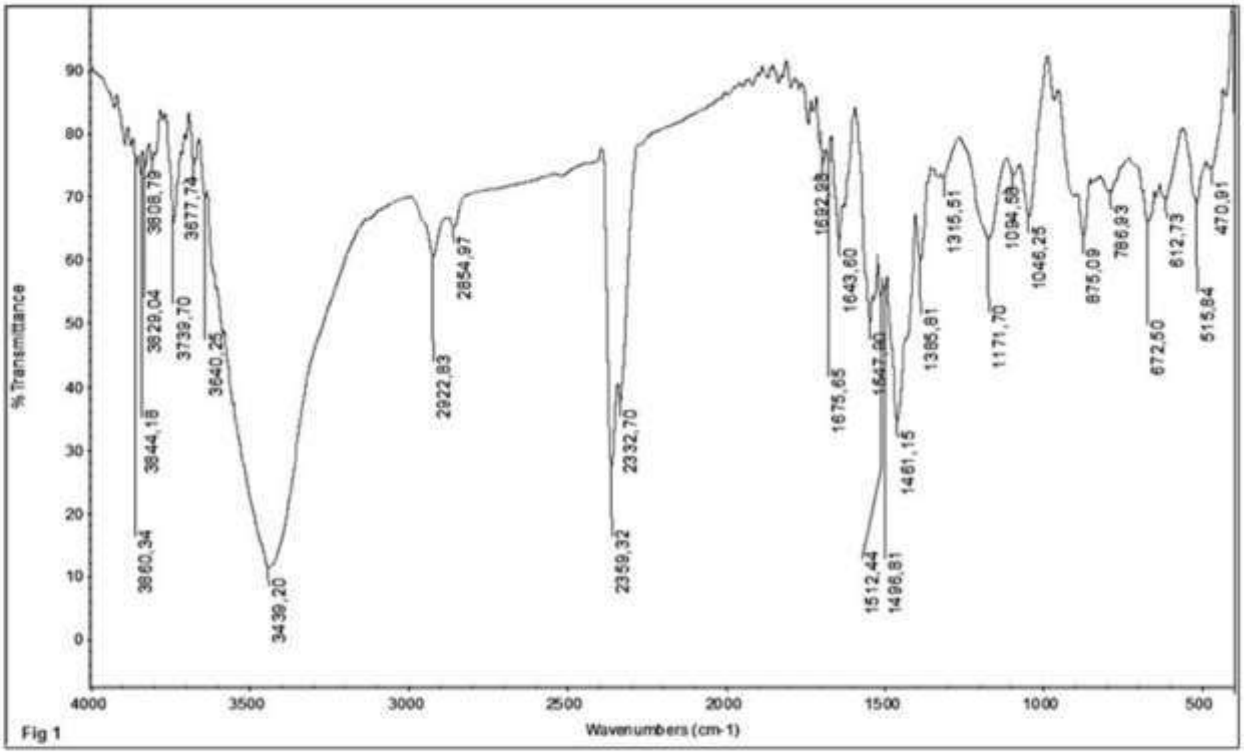

Figure 1. FTIR spectrum of [(Cu-CI-CNF-GNF)$_{0.5}$-PAA]-PPy$_{0.5}$

٥٫٢. Characterization

The ultrasonic experiment was carried out by an ultrasonic disperser (Hielsche, UP4005, Germany). Field emission scanning electron microscopy (FESEM) was performed by TESCAN MIRA to observe surface O-H stretching (st.) vibrations of alcoholic functional group presented on the GNF, PAA and DBSA. And attributed to N-H st. vibrations of PPy, The peak at 2922 and 2845 cm^{-1} are attributed to aliphatic C-H st. vibrations of PAA and DBSA. The peaks at 2359, 2332 cm^{-1} and 1675, 1643 cm^{-1} are related to C=O st. vibration of CI, PAA and DBSA, respectively. The different angles of Fe-C=O have been obtained for CI, so we observed to higher frequency for C=O. The specific peaks around 1537 and 1461 cm-1 are attributed with vibrational modes of quinonic and aromatic type ring for PPy. The peaks at 1385,1461 cm^{-1} are attributed to C=C st. vibration of CNF and GNF that 1461 cm^{-1} cover to aromatic mode with PPy. The peaks at 1171 and 1046 cm^{-1} are attributed to C-N and C-C st. vibration mode for PPy and CNF, GNF, respectively. The peaks at 779, 665 and 601, 517 cm^{-1} are attributed to Cu-O and Fe-O st. vibration for Cu and CI NPs.

٥,٣. XRD Patterns Study

Figure 2 shows XRD pattern for GNF that the peak at 2θ=26 related to carbon of GNF. The XRD patterns of molecular structures of CI-PAA-PPy, Cu-PAA-PPy and CNF-PAA-PPy in Figure 3 (a-c), were showed, respectively. The results show the diffraction peaks of NPs structures were not destroyed after the chemical polymerization of PPy as shell. We see all patterns of core NPs and shell polymers well. According to Figure 3 (a-c) characteristic peaks at 2θ=16-25, 2θ=17-25, 42, 44, 48, 50,72.38 and 2θ=16-23 with base peaks at 2θ=22.33, 72.38 and 24.83 for the CI-PAA-PPy, Cu-PAA-PPy and CNF-PAA-PPy were observed that correspond to JCPDS files no. 4073-004-98, 1646-002-98 and 2719-008-98, respectively. Figure 2 shows XRD pattern for GNF that the peak at 2θ=26 related to GNF. The XRD patterns showed molecular structures of CI-PAA-PPy, Cu-PAA-PPy and CNF-PAA-PPy in Figure 3 (a-c), respectively. The results show the diffraction peaks of NPs structures were not destroyed after the chemical polymerization of PPy as shell. We see all patterns of core NPs and shell polymers well, too.

According to Figure 3 (a-c) characteristic peaks at 2θ=16-25, 2θ=17-25, 42, 44, 48, 50,72.38 and

2θ=16-23 with base peaks at 2θ=22.33, 72.38 and 24.83 were observed for the CI-PAA-PPy, Cu-PAA-PPy and CNF-PAA-PPy that correspond to JCPDS files no. 4073-004-98, 1646-002-98 and 2719-008-98, respectively. These results and the relative width of the peaks indicate that the nanocomposite containing NPs-PAA-PPy are semi-crystalline and amorphous. According to these results and peaks observed in XRD patterns, we can ensure the existence of NPs. The average crystallite size can be calculated by the Debye-scherrer formula: $D= 0.89\ \lambda/\beta \cos\theta$ where λ is the wavelength of Cu Kα radiation and the value of K depends on several factors, including the Miller index of reflection plane and the shape of the crystal.

If the shape is unknown, K is often assigned as a value of 0.89, D is average crystallite size, θ is the Bragg's angle, and β is the full width at half-maximum of the diffraction peaks. Therefore, from the width of the peaks observed in the XRD patterns, the average crystallite sizes of GNF, CI, Cu and CNF are calculated to 70, 21.5, 20.3 and 19.8 nm, respectively.

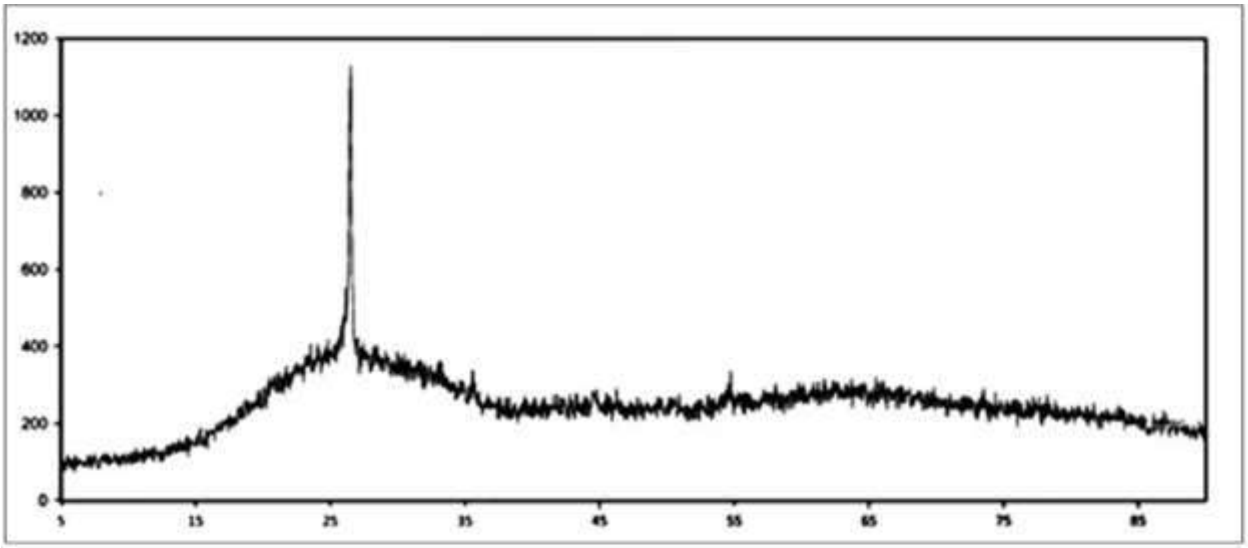

Figure 2. XRD pattern for GNF that the peak at 2θ

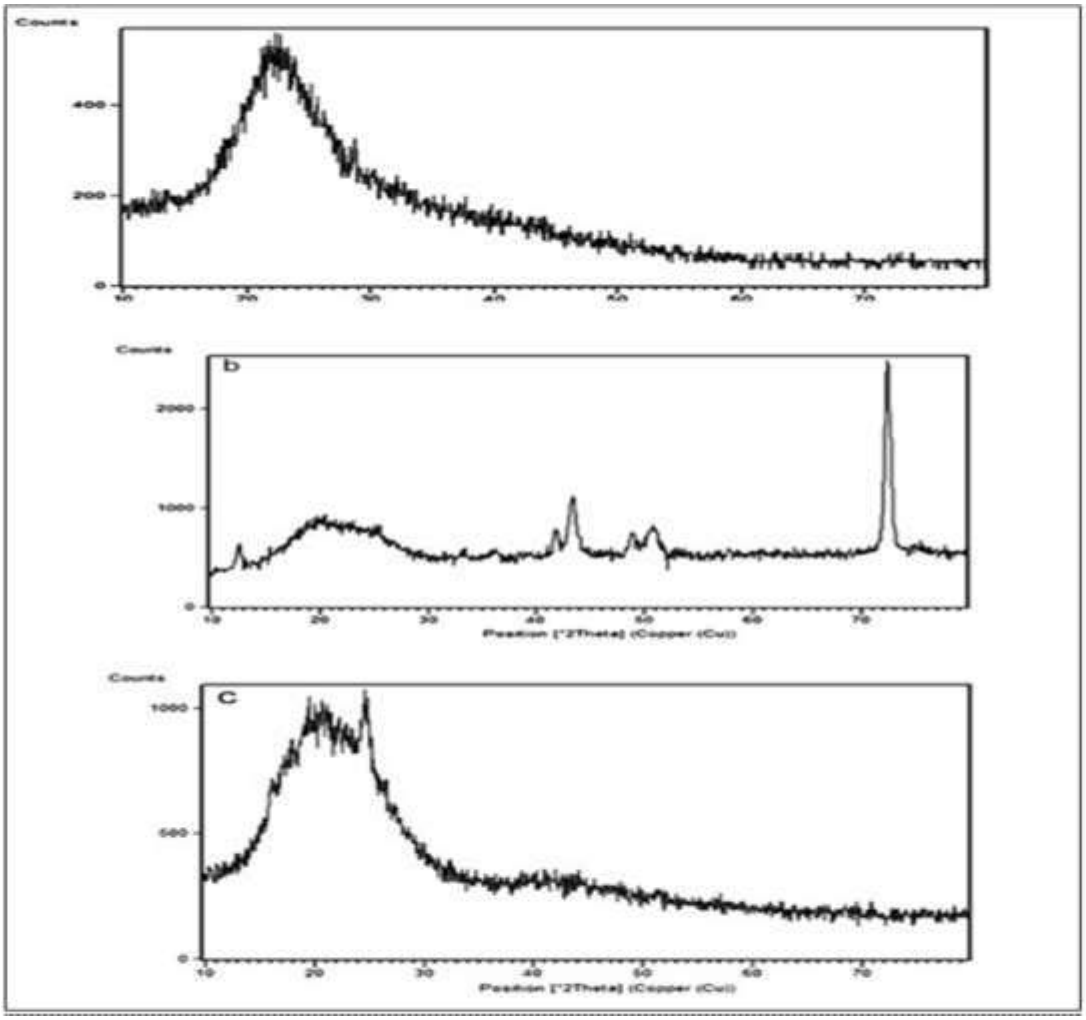

Figure 3. XRD of a) CI-PAA-PPy , b) Cu-PAA-PPy and c) CNF-PAA-PPy

٥,٤. SEM Images Study

Figure 4 (a-d) shows FESEM images of Cu, CI NPs and Cu-PAA-PPy, CI-PAA-PPy nanocomposites. The diameters of samples are about 30, 59, 40 and 65 nm, respectively. Figure 5 (a-b) shows the FESEM image of the CNF and CNF-PAA-PPy. Images analysis calculation results showed that the average diameters of CNF and its nanocomposite are 18 and 55 nm, respectively. Figure 6 (a,b) shows the FESEM images of the GNF and GNF-PAA-PPy nanocomposite. We adopted ultrasonic irradiation technique to break down the expanded graphite and then obtained GNF. The average distribution of all NPs, both pure and in the composite substrate, is very good and well dispersed. This will have a direct effect on their absorption properties. Image analysis calculation results showed that the average sheet diameter is approximately 5μ m, and average thickness of nanoflake is about 80 nm. In Figure 6 b, we can see that PPy was coated on the most of GNF. All NPs are completely coated by PPy. The thickness of PPy as shell in all nanocomposites are about 10-20 nm. The surfaces of SEM images of nanocomposites were shown uniformity with some hollow and sponge structures. This structure, which is porous and has composite cavities, helps to reduce the energy of microwaves. By observing the shapes of nanofibers and nanoflakes and their composites, it is clear that the nanofibers in the composite are completely blurred, while the nanosheets have almost retained their shape in the composite.

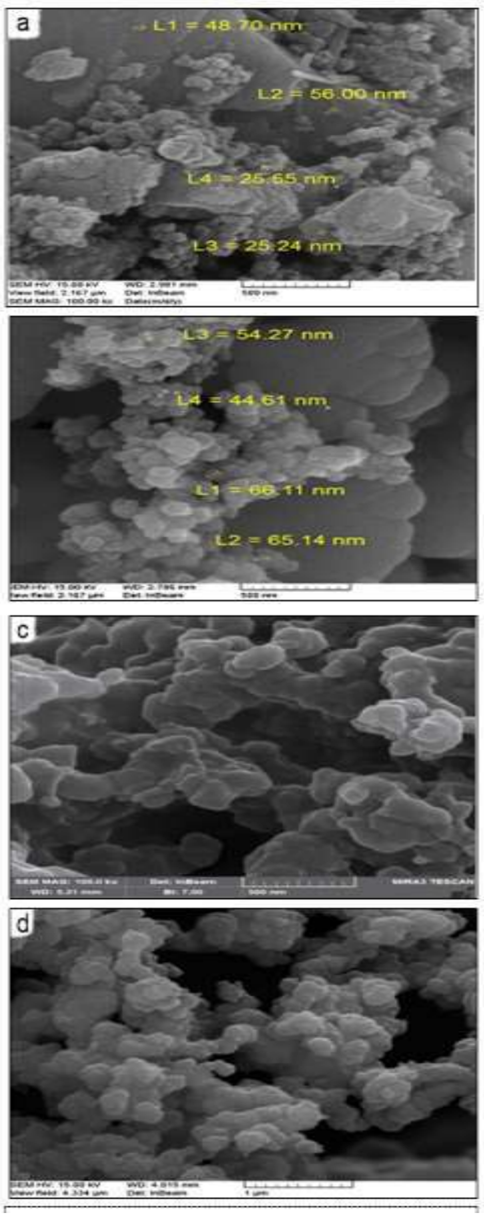

Figure 4. FESEM images of a) Cu b) CI NPs and c) Cu-PAA-PPy d) CI-PAA-PPy nano composite

٥,٥. Vibrating Sample Magnetometer (VSM) Study

The magnetization curves versus the magnetic field of CI NPs and CI-PAA-PPy nanocomposite are shown in Figure 7 (a,b). The samples are ferromagnetic behavior and applied fields are 20 and 30 kOe for CI NPs and CI-PAA-PPy respectively. The magnetic parameters such as saturation magnetization (Ms), coercivity (Hc) and remnant magnetization (Mr) are measured by the hysteretic loops. As shown in Figure 7 (a,b), the value of Ms decreased from 225.87 to 51.164 emu/g and the value of Mr increased from 1.882 to15.452 emu/g for CI to nanocomposite. On the other hands, Hc was increased from 16.558 to 151.53 Oe, too. VSM curve of nanocomposite showed semi hard magnetization behavior that can be used to magnetic memories and microwave absorber.

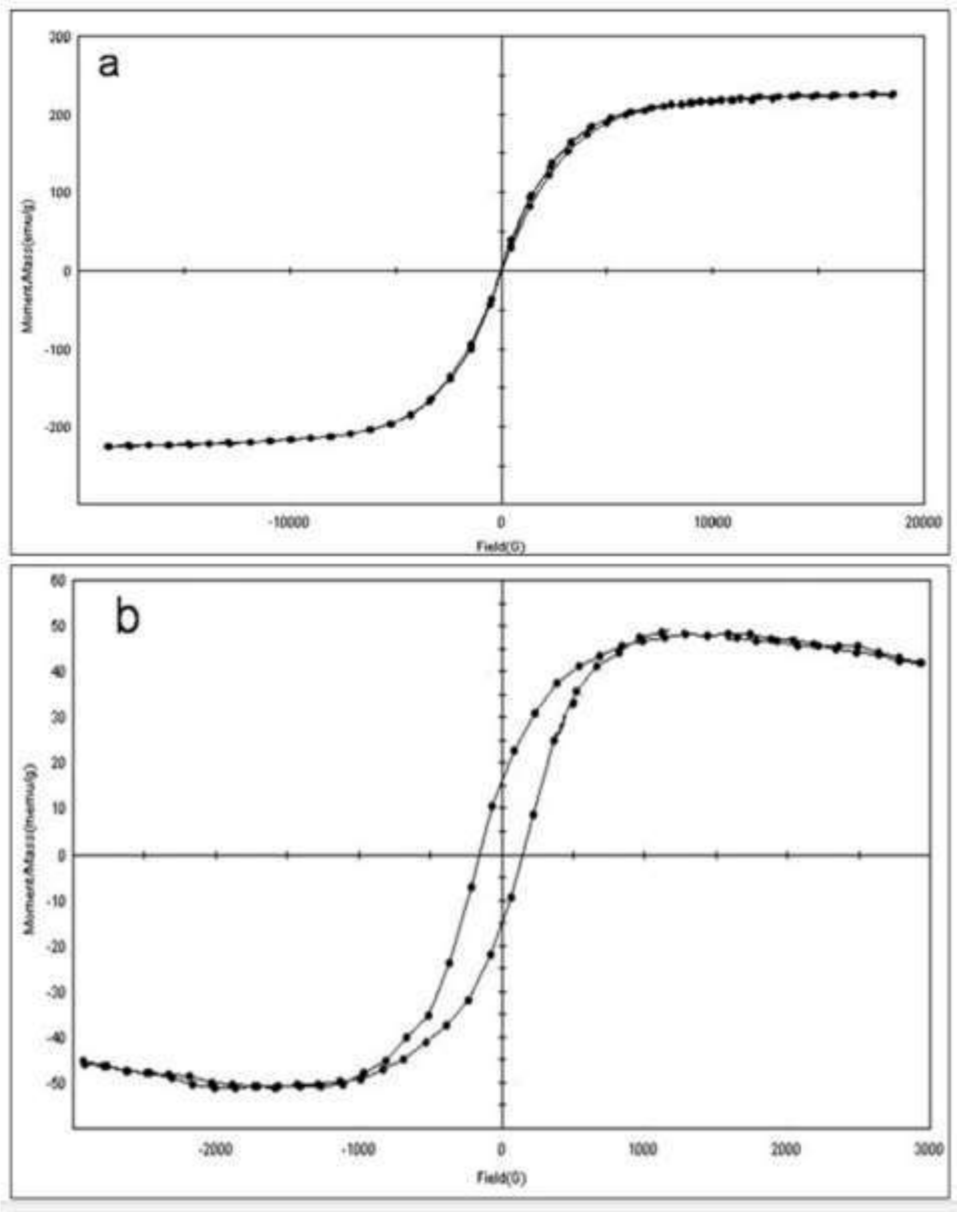

Figure 7. Vibrating sample magnetometer (VSM) field of a) CI NPs and b) CI-PAA-PPy nanocomposite

٥,٦. Electrical Conductivity Study

Electrically conductivity of NPs and their nanocomposites were measured by four probe method and were summarized in Table 1. The conductivity of PPy after polymerization by Fe(III) as initiator and DBSA as dopant is 0.044 S/cm. The conductivity of Cu that prepared by chemically method is higher than green method. This is due to completely of reduction in chemical method. On the other hands, conductivity of CNF is higher than GNF that is related to high molecular weight and crystallity of GNF. When mass content of Cu, CNF and GNF as core and PPy as shell were incorporated in composites, conductivities are increased. But incorporation of CI NPs, conductivity is decreased.

Table 1. The electrical conductivity of samples

Sample	Conductivity (S/cm)	Sample	Conductivity (S/cm)
Cu (chemical)	245	Cu-PAA-PPy	133
Cu (green)	170	CI-PAA-PPy	0.083
GNF	20	GNF-PAA-PPy	0.88
CNF	264	CNF-PAA-PPy	320
PPy (doped)	0.044	[(Cu-CI-CNF-GNF)$_{0.5}$-PAA] - PPy$_{0.5}$	280
PPy (undoped)	1.4×10^{-6}		

٥،٧. Microwave Absorbing Study

The microwave absorbing properties of nanocomposites with the coating thickness of 1 mm investigated by using vector network analyzers in the frequency range of 2-18 GHz, that this range is contained S, H, C, X and Ku bands.

The results for PPy, Cu-PAA-PPy, CI-PAA-PPy and [(Cu-CI-CNF-GNF)-PAA] PPy nanocomposite are for CNF-PAA-PPy, 9.14 and 16.5 GHz for GNF-PAA-PPy with minimum reflection loss in -17.5, -10, -17, -19, -31, -27, -18, -27.5 and -25 dB, respectively. The absorption bandwidth under -10 dB are 3.2, 3.5, 8.4, 12.9, 13 and 15.5 GHz ranging from 2 to 18 GHz for PPy, Cu-PAA-PPy, CI-PAA-PPy, CNF-PAA-PPy, GNF-PAA-PPy and [(Cu-CI-CNF-GNF)$_{0.5}$-PAA]-PPy$_{0.5}$.

٦. Conclusion

The absorption properties of electromagnetic waves are primarily influenced by two factors: conduction and magnetic characteristics. In the selected samples, carbonyl iron (CI) provides strong magnetic properties, while other nanoparticles exhibit excellent electrical conductivity. Moreover, the final polymer (PPy) enhances electrical conductivity. This project aimed to engineer these materials in a systematic manner to maximize microwave absorption across different frequency ranges. Green copper powder and graphite nanoflakes (GNF) were synthesized, while CI and carbon nanofibers (CNF) were acquired commercially. A polyacrylic acid (PAA) coating was applied to the nanoparticles, followed by the in-situ template polymerization of PPy to produce nanocomposites. Microwave absorption data for PPy, CNF-PAA-PPy, GNF-PAA-PPy, and [(Cu-CI-CNF-GNF)$_{0.5}$-PAA]-PPy$_{0.5}$ are shown in Figures 8 and 9. Key absorption peaks were observed at 9.5 GHz for PPy, 3 and 9 GHz for Cu-PAA-PPy, and 9.5 GHz for CI-PAA-PPy. Samples with core-shell structures exhibited dual peaks at 8.5 and 11 GHz. The absorption properties were further analyzed over the 2–18 GHz frequency range (S, H, C, X, and Ku bands). The optimal absorption ranges were identified as 2–4 GHz and 5–14 GHz, achieving reflection loss (RL) values of -12.5 dB and -33 dB at a thickness of 1 mm. The absorption performance improved with an increased core-to-PPy weight ratio and enhanced electrical conductivity. These results confirm the potential of these nanocomposites as efficient multiband microwave absorbers, suitable for diverse applications in civil and military electromagnetic shielding.

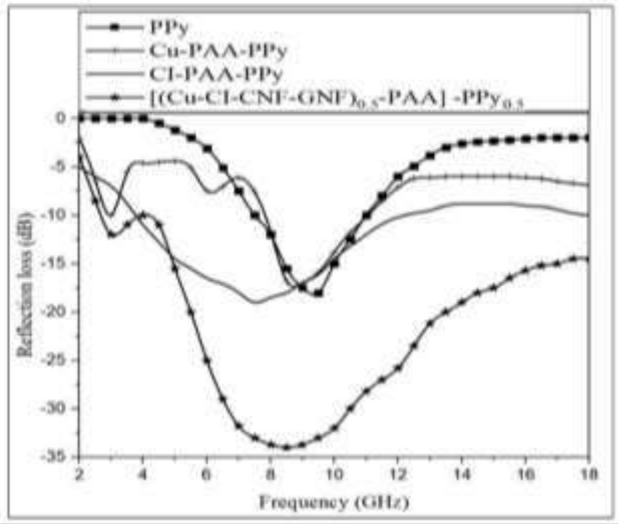

Figure 8. Microwave absorbing results for PPy, Cu-PAA-PPy, CI-PAA-PPy, and [(Cu-CI-CNF-GNF)$_{0.5}$-PAA] -PPy$_{0.5}$ nanocomposite

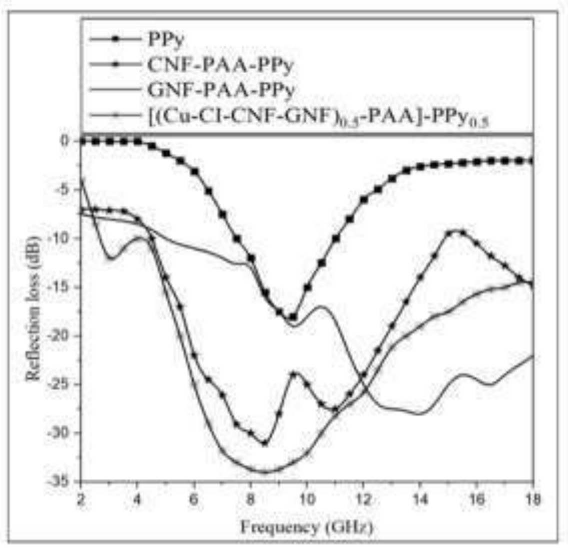

Figure 9. Microwave absorbing results for PPy, CNF-PAA-PPy , GNF-PAA-PPy, and [(Cu-CI-CNF-GNF)$_{0.5}$-PAA]-PPy$_{0.5}$

References

[1] V. Shukla, “Review of electromagnetic interference shielding materials fabricated by iron ingredients,” *Nanoscale Adv*, vol. 1, no. 5, pp. 1640–1671, 2019.

[2] D. Jiang *et al.*, “Electromagnetic interference shielding polymers and nanocomposites-a review,” *Polymer Reviews*, vol. 59, no. 2, pp. 280–337, 2019.

[3] Y. Duan *et al.*, “Enhanced electromagnetic microwave absorption property of peapod-like MnO@ carbon nanowires,” *ACS Appl Mater Interfaces*, vol. 10, no. 46, pp. 40078–40087, 2018.

[4] J. Li, W. Lu, J. Suhr, H. Chen, J. Q. Xiao, and T.-W. Chou, “Superb electromagnetic wave-absorbing composites based on large-scale graphene and carbon nanotube films,” *Sci Rep*, vol. 7, no. 1, p. 2349, 2017.

[5] C. Xu *et al.*, “Hollow polypyrrole nanofiber-based self-assembled aerogel: large-scale fabrication and outstanding performance in electromagnetic pollution management,” *Ind Eng Chem Res*, vol. 59, no. 16, pp. 7604–7610, 2020.

[6] S. H. Hosseini, M. Tarakameh, and S. S. Hosseini, “Preparation of thermal neutron absorber based B4C/TiO2/polyaniline nanocomposite,” *International Journal of Physical Sciences*, vol. 15, no. 2, pp. 49–59, 2020.

[7] S. H. Hosseini, R. Paymanfar, T. Afshari, and S. S. Hosseini, “Preparation of MWCNT/Ba0. 2Sr0. 2La0. 6MnO3/PANI nanocomposites and investigation of its electromagnetic properties in KU-band,” *International Journal of Physical Sciences*, vol. 15, no. 4, pp. 171–181, 2020.

[8] B. Zhao *et al.*, “Enhanced electromagnetic wave absorbing nickel (Oxide)-Carbon nanocomposites,” *Ceram Int*, vol. 45, no. 18, pp. 24474–24486, 2019.

[9] F. Ghanbari, S. Moradi Dehaghi, and H. Mahdavi, “Epoxy-based multilayered coating containing carbon nanotube (CNT), silicon carbide (SiC), and carbonyl iron (CI) particles: as efficient microwave absorbing materials,” *J Coat Technol Res*, vol. 17, no. 3, pp. 815–826, 2020.

[10] J. Guo *et al.*, “Polypyrrole-interface-functionalized nano-magnetite epoxy nanocomposites as electromagnetic wave absorbers with enhanced flame retardancy,” *J Mater Chem C Mater*, vol. 5, no. 22, pp. 5334–5344, 2017.

[11] N. Shah *et al.*, “Preparation and characterization of agar based magnetic nanocomposite for potential biomedical applications,” *Curr Pharm Des*, vol. 25, no. 34, pp. 3672–3680, 2019.

[12] I. Meazzini *et al.*, “Synthesis and characterisation of biocompatible organic–inorganic core–shell nanocomposite particles based on ureasils,” *J Mater Chem B*, vol. 8, no. 22, pp. 4908–4916, 2020.

[13] S. H. Hosseini, P. Zamani, and S. Y. Mousavi, “Thermal infrared and microwave absorbing properties of SrTiO3/SrFe12O19/polyaniline nanocomposites,” *J Alloys Compd*, vol. 644, pp. 423–429, 2015.

[14] H. Liu, G. Cui, L. Li, Z. Zhang, X. Lv, and X. Wang, “Polypyrrole chains decorated on CoS spheres: a core-shell like heterostructure for high-performance microwave absorption,” *Nanomaterials*, vol. 10, no. 1, p. 166, 2020.

[15] S. H. Hosseini, A. Alamian, and S. M. Mousavi, “Preparation of magnetic and conductive graphite nanoflakes/SrFe 12 O 19/polythiophene nanofiber-nanocomposites and its radar absorbing application,” *Fibers and Polymers*, vol. 17, pp. 593–599, 2016.

[16] S. H. Hosseini and P. Zamani, “Preparation of thermal infrared and microwave absorber using SrTiO3/BaFe12O19/polyaniline nanocomposites,” *J Magn Magn Mater*, vol. 397, pp. 205–212, 2016.

[17] M. Boujar Dolabi, A. Azimi, and S. Hossein Hosseini, “Preparation of thermal infrared and microwave absorber using WO3/MnFe3O4/polyaniline nanocomposites,” *Materials Research Innovations*, vol. 24, no. 6, pp. 326–334, 2020.

[18] S. Hossein Hosseini, A. Azimi, and M. B. Dolabi, “Study of UV-Visible and near infrared absorption CsXWO3/polypyrrole nanocomposite,” *Materials Research Innovations*, vol. 24, no. 6, pp. 335–340, 2020.

[19] H. Cai, Q. Wei, H. Xiao, H. Liu, and J. Wang, “Preparation and microwave absorption properties of petal CoO/CNFs composites,” *Journal of Materials Science: Materials in Electronics*, vol. 31, pp. 7606–7615, 2020.

The 30th Iranian Seminar of Organic Chemistry
February 7-9, 2025, Iran University of Science and Technology, Tehran, Iran

Microwave Absorption Properties of MoO_3/Polypyrrole Nanocomposites in the Ku-band

Authors: Ali azimi[1*], Golnaz Ghanoun[1]

[1] *Department of Chemistry, Science and Research Branch, Islamic Azad University, Tehran, Iran*

Abstract- Composites of MoO_3/polypyrrole (PPy) were synthesized using various methods through in-situ polymerization, resulting in a core-shell structure. This paper outlines a method for coating nanoparticles with polyacrylic acid (PAA) in an aqueous solution, followed by a PPy coating applied using template polymerization on NPs-PAA. The enhancement mechanism is attributed to suitable interactions and improved electromagnetic compatibility between these materials. The microwave characterization of the nanocomposite was evaluated through arch tests using a network analyzer. The PPy nanocomposites demonstrated excellent Ku-band microwave absorption properties in the 12–18 GHz range. Optimal absorption was observed at 12 GHz for

PPy and 14.5 GHz for MoO_3-PAA-PPy, with minimum reflection loss (RL) values of -19 dB at a thickness of 2 mm. Additionally, nanocomposites with 50% w/w demonstrated lightweight properties and effective microwave absorption.

Keywords: composite, Microwave, Polyacrylic acid, Polypyrrole, MoO_3

١. Introduction

The rapid advancement of electronic information technology has resulted in a significant increase in electromagnetic wave (EMW) emissions. These emissions pose risks to human health, interfere with sensitive equipment, and compromise military security. Consequently, the development of high-performance EMW-absorbing materials has become critical for advancing societal and technological progress [1-٤].

Over the past few decades, various types of EMW absorbers have been explored, with carbon-based materials emerging as a predominant class due to their lightweight nature, favorable electrical properties, and wide range of structural tunability [5-٧]. In parallel, conducting polymers have gained significant attention as EMW absorbers, offering advantages such as facile synthesis, tunable electrical properties, and environmental stability, which make them attractive candidates for practical applications [8-١٣]. Despite the promise of these materials, single-component absorbers often suffer from poor impedance matching and limited energy dissipation mechanisms, resulting in suboptimal absorption efficiency.

To overcome these limitations, researchers have turned to binary or multi-component nanocomposites that integrate the strengths of individual materials, creating synergistic effects and enabling multiple energy-loss mechanisms for enhanced EMW absorption [14,15]. Advances in interface engineering and structural design have been particularly instrumental in improving energy dissipation, as heterogeneous interfaces promote charge transfer, enhance interfacial polarization, and improve overall absorption performance. Additionally, the incorporation of conductive materials further boosts the electrical conductivity of these composites, enabling greater conductive losses [16]. Optimization strategies such as morphology control, elemental doping [17,18], and oxygen vacancy engineering [19,20] have expanded the design possibilities for high-performance EMW absorbers. Among these approaches, oxygen vacancy engineering has proven especially effective, as it introduces defects that facilitate charge carrier mobility and increase polarization loss. For instance, Dong et al. demonstrated that SnO_2−x/N-rGO composites, composed of SnO_2 hollow nanospheres with oxygen vacancies and conductive graphene, exhibit remarkable EMW absorption performance due to the synergistic effects of their components [21].

Conducting polymers, particularly PPy, have garnered significant interest for their lightweight nature, ease of synthesis, and tunable electrical properties. PPy stands out for its superior environmental stability, higher conductivity, and enhanced mechanical flexibility compared to other conducting polymers, making it a highly promising candidate for EMW absorption applications. Recent developments in core-shell architectures and other complex nanostructures have further expanded the potential of PPy-based and other polymer-based nanocomposites for achieving high-efficiency EMW absorption [22-٢٤].

In this study, we report the synthesis of MoO_3 nanoparticle composites via in-situ polymerization on PAA-coated surfaces. The microwave absorption properties of these composites were systematically analyzed within the frequency range of 12–18 GHz, with a focus on optimizing their structural design and interface properties to enhance EMW absorption.

٢. Experimental

٢,١. Synthesis of o-MoO_3

o-MoO_3 synthesis follows a previously described method. Initially, 1 gram of commercial MoO_3 and 0.5 grams of $NaBH_4$ were combined in a mortar and ground for 20 minutes. Subsequently, the mixture was stirred in cold water for 2 hours to remove any residual $NaBH_4$. The solid product was then filtered, rinsed with water and methanol, and dried under vacuum at 60 °C overnight. The resulting gray material was designated as o-MoO_3.

٢,٢. Coating of NPs with PAA (NPs-PAA)

To prepare the NPs-PAA composite, 0.5 grams of nanoparticles (NPs) were mixed with 50 ml of 5% w/v PAA in a 250 mL flask. This mixture was subjected to ultrasonication for 15 minutes and then stirred continuously at 25 °C for 24 hours. Following this, the mixture was filtered and washed with 2% v/v acetic acid and acetone. After drying the filtered material under vacuum, the NPs-PAA composite was obtained.

٢,٣. Synthesis of PPy

PPy was synthesized as a core-shell nanocomposite using in situ template polymerization in the presence of dodecyl benzene sulfonic acid (DBSA) as the surfactant. Approximately 0.5 g of DBSA was dissolved in distilled water and stirred vigorously for about 20 minutes. Then, 0.287 g of NPs-PAA were added to the DBSA solution and stirred for nearly 1 hour. Following this, 1 mL (0.015 mol) of freshly distilled pyrrole, serving as the monomer, was added to the suspension and stirred for 30 minutes. The NPs-PAA were efficiently dispersed in the PPy/DBSA mixture under ultrasonication for 2 hours. 12.12 g (0.03 mol) of $Fe(NO_3)_3.9H_2O$, used as the initiator, was dissolved in 30 mL of deionized water and slowly added to the actively stirring reaction mixture. Polymerization was allowed to proceed for 6 hours. The nanocomposite was isolated by filtration and then washed with deionized water and acetone. The resulting dark powder was dried under vacuum for 24 hours.

٣. Results and discussion

3.1. Microwave absorbing study

The microwave absorbing properties of nanocomposites with a 1 mm thick coating were examined using vector network analyzers over the 12-18 GHz frequency range, which corresponds to the Ku band. This study is crucial for developing advanced materials for electromagnetic interference shielding and radar stealth technologies, where effective absorption in the Ku band is particularly important. PPy exhibited significant microwave absorption characteristics, making it a promising candidate for applications in electromagnetic interference shielding. The absorption peak at 12-18

GHz and the substantial absorption bandwidth indicate PPy's potential effectiveness in various practical scenarios within the Ku band frequency range.

3.2. Microwave absorption properties

To evaluate the EMW absorption performance of MoO_3-PAA-PPy composites, the reflection loss (RL) curves for various samples have been computed and are presented. Using the principles of transmission line theory, the RL values across the tested frequency range can be derived as follows:

$$RL = \text{٢٠١}\square \left|\frac{Z_{in} - Z_{\text{٠}}}{Z_{in} + Z_{\text{٠}}}\right|$$

$$Z_{in} = Z_{\text{٠}} \sqrt{\frac{\mu_r}{\varepsilon_r}}\, tanh\left(j\frac{\text{٢}\square\square\square}{c}\sqrt{\mu_r \varepsilon_r}\right)$$

In this context, Z_{in} and Z_0 represent the impedance values of the absorber and air, respectively. Meanwhile, μ_r, ε_r, d, f, and cc denote the complex permeability, complex permittivity, absorber thickness, frequency, and the speed of light. The frequency range where the RL value falls below −10 dB is defined as the effective absorption bandwidth (EAB) of the absorber, as it indicates that over 90% of the electromagnetic waves are absorbed in this range. As illustrated pristine MoO_3 does not exhibit a clear EAB within the tested frequency range, suggesting that its intrinsic structural properties are not well-suited for EMW absorption.

The microwave absorbing properties of nanocomposites with the coating thickness of 2 mm investigated by using vector network analyzers in the frequency range of 8-12 GHz, that this range is contained Ku band. The results for PPy, MoO_3-PAA-PPy The best microwave absorption were obtained in 12 GHz for PPy, 14.5 GHz for MoO_3-PAA-PPy, with minimum reflection loss in -19 dB, respectively the absorption band with under -10 dB from 12 to 18 GHz for PPy, MoO_3-PAA-PPy.

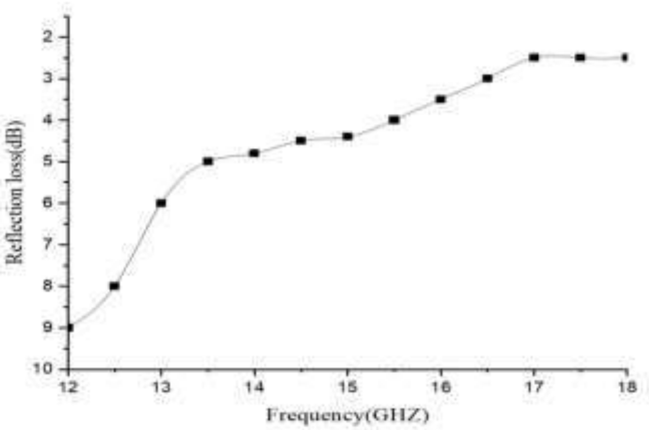

Figure 1. Microwave absorbing results for PPy

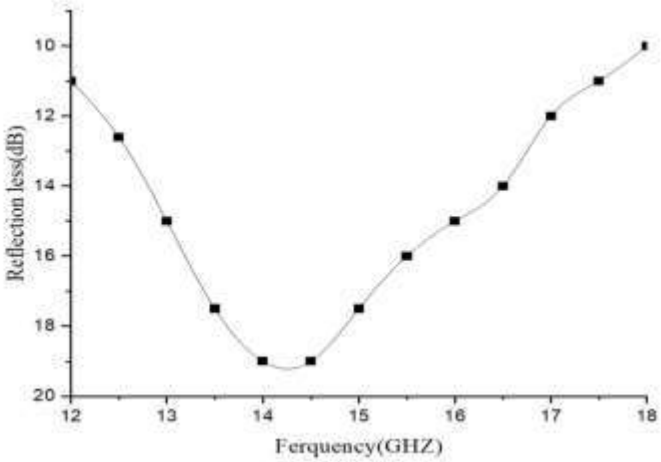

Figure 2. Microwave absorbing results for o-MoO_3-PAA-PPy

٤. Conclusion

We synthesized MoO_3 powder and developed a method to coat it with PAA. Subsequently, a PPy coating was applied using template polymerization through an in-situ process. Finally, we prepared nanocomposites, either individually or as a complex with a core-shell structure. We then investigated their microwave absorption properties in the 12-18 GHz range, corresponding to the Ku band. Our findings demonstrate significant absorption characteristics, highlighting the potential of these composites for applications in electromagnetic interference (EMI) shielding and radar stealth technologies, particularly within Ku band frequencies.

References

[1] S. Gupta and N.-H. Tai, “Carbon materials and their composites for electromagnetic interference shielding effectiveness in X-band,” *Carbon N Y*, vol. 152, pp. 159–187, 2019.

[2] M. Qin, L. Zhang, and H. Wu, “Dielectric loss mechanism in electromagnetic wave absorbing materials,” *Advanced Science*, vol. 9, no. 10, p. 2105553, 2022.

[3] G. Redlarski *et al.*, “The influence of electromagnetic pollution on living organisms: historical trends and forecasting changes,” *Biomed Res Int*, vol. 2015, no. 1, p. 234098, 2015.

[4] S. Cheng *et al.*, “Carbon nanofilm stabilized twisty V2O3 nanorods with enhanced multiple polarization behavior for electromagnetic wave absorption application,” *J Mater Sci Technol*, vol. 119, pp. 37–44, 2022.

[5] Q. Li, Z. Zhang, L. Qi, Q. Liao, Z. Kang, and Y. Zhang, “Toward the application of high frequency electromagnetic wave absorption by carbon nanostructures,” *Advanced Science*, vol. 6, no. 8, p. 1801057, 2019.

[6] P. Liu *et al.*, “Carbon nanocages with N-doped carbon inner shell and Co/N-doped carbon outer shell as electromagnetic wave absorption materials,” *Chemical Engineering Journal*, vol. 381, p. 122653, 2020.

[7] L. Wu *et al.*, “Metal/nitrogen co-doped hollow carbon nanorods derived from self-assembly organic nanostructure for wide bandwidth electromagnetic wave absorption,” *Compos B Eng*, vol. 228, p. 109424, 2022.

[8] M. Boujar Dolabi, A. Azimi, and S. Hossein Hosseini, “Preparation of thermal infrared and microwave absorber using WO3/MnFe3O4/polyaniline nanocomposites,” *Materials Research Innovations*, vol. 24, no. 6, pp. 326–334, 2020.

[9] S. Hossein Hosseini, A. Azimi, and M. B. Dolabi, “Study of UV-Visible and near infrared absorption CsXWO3/polypyrrole nanocomposite,” *Materials Research Innovations*, vol. 24, no. 6, pp. 335–340, 2020.

[10] S. H. Hosseini, A. Azimi, and S. S. Hosseini, “Preparation of Microwave Multi-Adsorbent Nanocomposites Based on Copper, Iron Carbonyl, Carbon Nanofiber, Graphite Nanoflake and Polypyrrole,” *J. Adv. Nanotechnol*, vol. 1, pp. 42–55, 2020.

[11] H. Sh and Azimi A, “Preparation of Modern Nanocomposites of Polyaniline Multi-Adsorbents for X-Ku Bands and UV-Visible-Near IR Regions Based On Carbon Nanofiber, Carbonyl Iron, Cu, WO 3 and Cs 0.3 WO 2.7,” *Pubtexto Publishers | www.pubtexto.com 1 Int J Nanomater Mol Nanotechnol Open Access International Journal of Nanomaterials & Molecular Nanotechnology*, vol. 3, 2021, doi: 10.36266/IJNMN/121.

[12] A. Azimi and S. H. Hosseini, “Preparation absorption microwave X-band based carbonyl iron/polypyrrole nanocomposite”.

[13] A. Azimia and S. H. Hosseinib, “Study of microwave absorption based Copper/polypyrrole nanocomposite”.

[14] T. Hou *et al.*, “Preparation of two-dimensional titanium carbide (Ti3C2Tx) and NiCo2O4 composites to achieve excellent microwave absorption properties,” *Compos B Eng*, vol. 180, p. 107577, 2020.

[15] X. Yan *et al.*, “Balancing interface polarization strategy for enhancing electromagnetic wave absorption of carbon materials,” *Chemical Engineering Journal*, vol. 391, p. 123538, 2020.

[16] Z. Wu *et al.*, “Facile preparation of core–shell Fe3O4@ Polypyrrole composites with superior electromagnetic wave absorption properties,” *The Journal of Physical Chemistry C*, vol. 121, no. 29, pp. 15784–15792, 2017.

[17] L. Mai, B. Hu, Y. Qi, Y. Dai, and W. Chen, “Improved cycling performance of directly lithiated MoO3 nanobelts,” *Int J Electrochem Sci*, vol. 3, no. 2, pp. 216–222, 2008.

[18] K. Paipitak, W. Techitdheera, S. Porntheeraphat, and W. Pecharapa, “Influence of Ti and Zn dopants on structural properties and electrochromic performance of sol-gel derived WO3 thin films,” *Energy Procedia*, vol. 34, pp. 689–696, 2013.

[19] S. Cheng *et al.*, “Modulating surficial oxygen vacancy of the VO 2 nanostructure to boost its electromagnetic absorption performance,” *J Mater Chem C Mater*, vol. 9, no. 29, pp. 9158–9168, 2021.

[20] M. Al-Hashem, S. Akbar, and P. Morris, “Role of oxygen vacancies in nanostructured metal-oxide gas sensors: a review,” *Sens Actuators B Chem*, vol. 301, p. 126845, 2019.

[21] N. Wu *et al.*, “Hollow SnO 2 nanospheres with oxygen vacancies entrapped by a N-doped graphene network as robust anode materials for lithium-ion batteries,” *Nanoscale*, vol. 10, no. 24, pp. 11460–11466, 2018.

[22] A. Azimia and S. H. Hosseinib, “Study of microwave absorption based Copper/polypyrrole nanocomposite”.

[23] M. Sedlačík, V. Pavlínek, P. Sáha, P. Švrčinová, P. Filip, and J. Stejskal, “Rheological properties of magnetorheological suspensions based on core–shell structured polyaniline-coated carbonyl iron particles,” *Smart Mater Struct*, vol. 19, no. 11, p. 115008, 2010.

[24] S. H. Hosseini, A. Asadnia, and M. Moloudi, “Preparation and electromagnetic wave absorption hard–soft Ba ferrite/polypyrrole core–shell nanocomposites,” *Materials Research Innovations*, vol. 19, no. 2, pp. 107–112, 2015.

The 30th Iranian Seminar of Organic Chemistry
February 7-9, 2025, Iran University of Science and Technology, Tehran, Iran

$MgCuO_2$: A Simple and Efficient Mixed Metal Oxide Nanocatalyst for the Synthesis of Unsymmetrical 1,4-Dihydropyridine

Imran Jadidi, Seyyed Mohiyeddin Seyyed Rahmani, Abbas Nikoo*, Amir Mohammad Qazi Khani

Department of Organic Chemistry, Faculty of chemistry, Urmia University, Urmia, Iran

Keyword: Mixed metal oxide, Sol-Gel, Auto-combustion, 1,4-Dihydropyridine

Introduction: Mixed metal oxide nanoparticles are known as heterogeneous catalysts in a variety of organic reactions. In general, nanoparticles are considered more reactive because they offer a higher surface area. The surface area of the catalyst increases dramatically with size reduction to nanoscale levels, which is responsible for higher catalytic activity and has the potential to improve the efficiency, selectivity, and yield of catalytic processes. The use of transition metal nanoparticles in catalysis is of great importance because they provide surface activation of the metal and catalyst at the nanoscale, thereby bringing selectivity and efficiency to heterogeneous catalysis. The use of mixed metal oxides plays an important role in organic reactions due to their ease of control, reduced corrosion problems, cost-effectiveness, and because most of them are reusable and recyclable. Multicomponent one-pot reactions (MCRs) have emerged as a powerful method for the synthesis of organic compounds. The development of multicomponent reactions (MCRs) is currently an integral part of numerous research efforts worldwide. In such reactions, three or more reactants are simultaneously combined in a single reaction vessel and successive chemical reactions are carried out to form new products. The synthesized products contain fractions of all the starting materials, providing rapid access to new organic molecules [1,2]. In fact, the products are produced in a single reaction step, and the diversity can be easily increased by changing each component. Due to the rapidity of the reaction, the reduction in the number of synthesis steps, and the consequent increase in the efficiency of these types of reactions, they are often referred to as green, and thus contribute to the development of synthetic methods. Unlike multi-step reactions, multi-component reactions (MCRs) can synthesize complex molecules in a single-pot process with lower cost and time, greater selectivity, and higher yields. From an environmental and economic perspective, MCRs are recognized as a valuable tool for the preparation of structurally well-defined pharmaceutical compounds. This approach is also desirable from a green chemistry perspective due to the reduction in the number of synthesis steps and the consequent increase in efficiency and speed. The MCR approach using heterogeneous catalysts is the most effective option in organic synthesis [3].

Method: In this research project, 20 mol% of $MgCuO_2$ nanocatalyst was used during the experiment compared to ethyl acetoacetate. 2.5 mmol of various chalcone and 3.75 mmol of ammonium acetate were stirred with 2.5 mmol of ethyl acetoacetate in 20 mL EtOH at 80°C in the presence of $MgCuO_2$ nanocatalyst to produce Unsymmetrical 1,4-Dihydropyridine derivatives with excellent yields. The progress of the reaction was regularly monitored by TLC plates and monitored by UV light (254 nm). After the reaction was completed, the Unsymmetrical 1,4-Dihydropyridine derivatives were extracted with ethyl acetate.

Results and Discussion: In this work, an efficient method for the synthesis of Unsymmetrical 1,4-dihydropyridine derivatives using recyclable $MgCuO_2$ nanocatalyst in ethanol solvent is reported for the first time. Urea was used as fuel for the synthesis of the $MgCuO_2$ nanocatalyst. The $MgCuO_2$ nanocatalyst was characterized by XRD, BET, FT-IR, FESEM and EDS techniques. In this study, the catalytic role of MgO and CuO was compared with $MgCuO_2$ nanocatalyst.

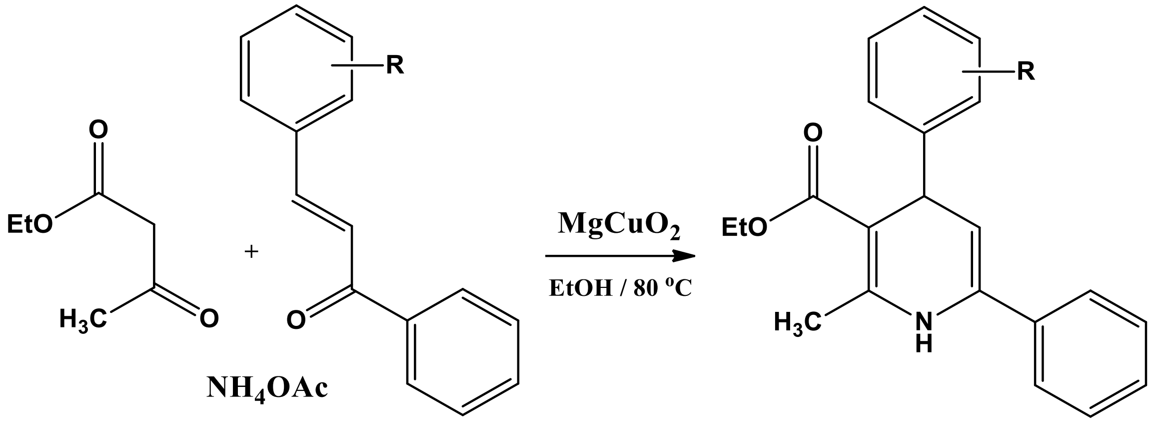

R= H, p-Me, p-OMe, o-OH, m-OH,
p-OH,o-NO$_2$, m-NO$_2$, p-NO$_2$, p-Cl

Scheme: Synthesis of unsymmetrical 1,4-Dihydropyridines by MgCuO$_2$ nanocatalyst

References:

1. Rodrigues, M. O., Eberlin, M. N., & Neto, B. A. (**2021**). How and why to investigate multicomponent reactions mechanisms? A critical review. The Chemical Record, *21(10),* 2762-2781.

2. Habibi, N., Wang, Y., Arandiyan, H., & Rezaei, M. (**2017**). Low-temperature synthesis of mesoporous nanocrystalline magnesium aluminate (MgAl$_2$O$_4$) spinel with high surface area using a novel modified sol-gel method. Advanced Powder Technology, *28(4),* 1249-1257.

3. Tan, J., & Chen, J. (**2022**). Multicomponent reactions. In Comprehensive Aryne Synthetic Chemistry (pp. 125-221). Elsevier.

Hantzsch Reaction on $CuAl_2O_4@SiO_2@ZnO$ Nanocatalyst: Excellent Reactivity Combined with Facile Catalyst Recovery and Recyclability

Amir Mohammad Qazi Khani, Seyyed Mohiyeddin Seyyed Rahmani, Abbas Nikoo*, Imran Jadidi

Department of Organic Chemistry, Faculty of chemistry, Urmia University, Urmia, Iran

Keyword: Homogeneous catalysts, Heterogeneous catalysts, Hantzsch reaction

Introduction: In general, catalysts are divided into three categories, which include homogeneous catalysts, heterogeneous catalysts, and biocatalysts. The practical application of homogeneous catalysts is limited due to the difficulties of separating the catalyst from the product after the reaction is completed [1]. In heterogeneous catalysis, the starting materials and the catalytic material are in different phases, and as a result, the separation of the products and the catalyst is easier. The main drawback of traditional heterogeneous catalyst systems compared to their homogeneous counterparts is the reduction of the contact surface area available to the reactant molecules, thereby limiting their catalytic activities and leading to a high consumption of expensive catalytic materials [2]. One possible way to solve this problem is to increase the surface-to-volume (S/V) ratio by reducing the size of the catalytically active material. High surface-to-volume (S/V) ratios can be achieved by synthesizing specifically engineered catalysts at the nanoscale. Key goals pursued with nanocatalysts include selectivity close to 100%, very high activity, excellent yields, all of which are traditionally associated with homogeneous catalysts, as well as enhanced product separation and catalyst recovery. Recovery of used catalysts would be beneficial in two respects. On the one hand, catalytic nanomaterials, especially metals such as platinum, gold, and silver, are very expensive. On the other hand, unrecovered catalysts are a major source of unwanted impurities, e.g., in pharmaceutical products. Efficient separation of the catalyst from the reaction mixture can help to more easily meet regulatory standards for impurities. Some experts consider nanocatalysts to be “semi-heterogeneous” catalysts [3].

Given that one of the main goals of medicinal chemistry and organic chemistry is the design and synthesis of biologically active molecules, the 1,4-dihydropyridine ring is one of the most attractive heterocyclic frameworks found in many generic drugs. Among the most important pharmaceutical products, for example, nifedipine, nicardipine, felodipine and amlodipine are on the World Health Organization (WHO) list of essential medicines and contain the 1,4-dihydropyridine ring [4].

Method: In a one-pot four-component reaction, taking into account the time required for each reaction, a mixture of aryl aldehyde (2.5 mmol), ammonium acetate 289.06 mg (3.75 mmol), ethyl acetoacetate 650.7 mg (5 mmol) and $CuAl_2O_4@SiO_2@ZnO$ nanocatalyst in water was placed in a round-bottomed flask under reflux conditions at 80 °C and the mixture was stirred with a magnetic stirrer until the reaction was complete. The reaction progress was regularly monitored with ethyl acetate/petroleum ether TLC plates at a ratio of 1:3. After the reaction was complete and a yellow precipitate formed, the temperature was reduced to 25 °C. The 1,4-dihydropyridine derivatives were extracted with 25 mL of ethyl acetate three times and the organic layer was dried with Na_2SO_4 (5 g). Ethyl acetate was separated from the product by rotary evaporation and 1,4-dihydropyridine derivatives were obtained with a yield of 78-97%. The 1,4-dihydropyridine derivatives were eluted with ethanol for purification and identification. The $CuAl_2O_4@SiO_2@ZnO$ nanocatalyst was separated by filtration for reuse in subsequent reactions, washed several times with water, ethanol and ethyl acetate, and finally the $CuAl_2O_4@SiO_2@ZnO$ nanocatalyst was dried in vacuum at 80 °C for 2 hours.

Results and Discussion: The Hansch reaction is a four-component reaction used to prepare 1,4-dihydropyridine derivatives, and the synthetic products offer very useful pharmaceutical properties. Therefore, the development of new nanocatalysts for the Hantzsch reaction has attracted much research studies. The reaction involves aldehyde, ammonium acetate and ethyl acetoacetate in a suitable solvent. In this paper, an efficient method for the synthesis of 1,4-dihydropyridine derivatives using a recyclable $CuAl_2O_4@SiO_2@ZnO$ nanocatalyst in water solvent is reported for the first time. Urea was used as a fuel for the synthesis of the $CuAl_2O_4@SiO_2@ZnO$ nanocatalyst and was characterized by XRD, FT-IR, EDS, mapping and BET techniques.

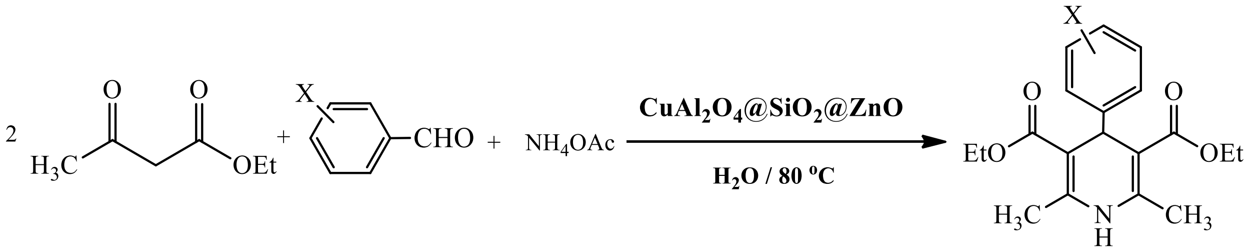

Scheme: Synthesis of 1,4-DHP derivatives by $CuAl_2O_4@SiO_2@ZnO$ nanocatalyst.

References: Times New Roman, Font size: 11, Align left, Arabic numeral

1. Behr, A., & Neubert, P. (**2012**). Applied homogeneous catalysis. John Wiley & Sons.

2. Jacoby, M. (**2009**). Perfecting solid-catalyst synthesis. Chemical & Engineering News, *87(17),* 37-38.

3. Campelo, J. M., Luna, D., Luque, R., Marinas, J. M., & Romero, A. A. (**2009**). Sustainable preparation of supported metal nanoparticles and their applications in catalysis. ChemSusChem: Chemistry & Sustainability Energy & Materials, *2(1),* 18-45.

4. World Health Organization. (**2021**). WHO model list of essential medicines-22nd list, 2021. Tech. Doc, 2021.

The 30th Iranian Seminar of Organic Chemistry
February 7-9, 2025, Iran University of Science and Technology, Tehran, Iran

A Simple, Green and One-Pot Four-Component Synthesis of 1,4-Dihydropyridine with Barbituric Acid by $CuAl_2O_4$

Seyyed Mohiyeddin Seyyed Rahmani, Abbas Nikoo*, Amir Mohammad Qazi Khani, Imran Jadidi

Department of Organic Chemistry, Faculty of chemistry, Urmia University, Urmia, Iran

Keyword: Xerogel, Mixed metal oxide, Multicomponent reaction

Introduction: 1,4-Dihydropyridines (DHPs) are important pharmaceutical compounds and are synthesized through a one-pot, multicomponent reaction. 1,4-Dihydropyridines are prepared through the cyclization reaction of a β-keto ester, an aldehyde, with an ammonia source [1]. The long reaction time and low product yields are among the drawbacks of this reaction. Over the past decades, various catalysts have been synthesized to optimize these reactions [2]. However, cost-effectiveness, high efficiency, ease of access to raw materials for catalyst synthesis, recyclability, and environmental compatibility are important parameters that are not all combined in a single catalyst. However, the effort to maximize these parameters prompted us to synthesize a suitable nanocatalyst. Mixed metal oxide nanoparticles are one of the most widely used materials as nanocatalysts that have overcome many disadvantages in catalytic systems [3,4]. Not only can they be easily separated from the reaction mixture, but they can also be reused for multiple reactions without losing their catalytic properties.

Method: First, a solution of metal nitrate salts, which acts as an oxidant, is prepared together with a water solvent and an organic compound (urea) which acts as a reducer or fuel. In the colloidal stage, nanoparticles are formed. After initial heating in an oven, the water in the solution is gradually removed and becomes concentrated. After most of the water is removed, a gel with a metallic structure and containing metal ligand polymers is produced. By completely drying the gel, the water is completely removed, which is known as a xerogel when heated. With a further increase in temperature, the complexing agent or fuel in the oven begins to burn. Energy is released from the exothermic reaction of metal nitrate and fuel, and this released heat is so high that it can raise the system to a high temperature, and the result of this ignition is the release of CO_2, N_2 and H_2O gases. In this way, a foam-shaped powder with a high volume that fills the entire container is obtained and nanoparticles are synthesized. One of the most important steps in this method is the calcination process, in which the metal hydroxide is converted to metal oxide, and the calcination step affects the final properties of the nanoparticles, such as morphology, particle size, purity, and magnetic properties.

Results and Discussion: In the first step, the reaction was investigated without the presence of catalyst under reflux conditions and after stirring for 60 minutes, a small amount of product was produced. In the next step, the reaction was carried out under reflux conditions and in the presence of $CuAl_2O_4$ nanocatalyst, which showed a much better result. In the next step, the reaction was carried out with 10, 20 and 30 mol% of the nanocatalyst. The efficiency of each of these amounts was 75, 90 and 89%, respectively. The best efficiency was achieved with 20 mol% relative to ethyl acetoacetate of the $CuAl_2O_4$ nanocatalyst at 100 ^oC in water solvent. The use of more catalyst did not facilitate the efficiency and reaction time, and in fact, there was no change in efficiency with increasing the amount of catalyst. Based on the experiments, it was determined that the addition of 20 mol% relative to ethyl acetoacetate of $CuAl_2O_4$ nanocatalyst leads to the best result. Due to the hydrophobicity of the catalyst and organic reactants, the presence of water does not pose a problem and the product is produced in 90% yield.

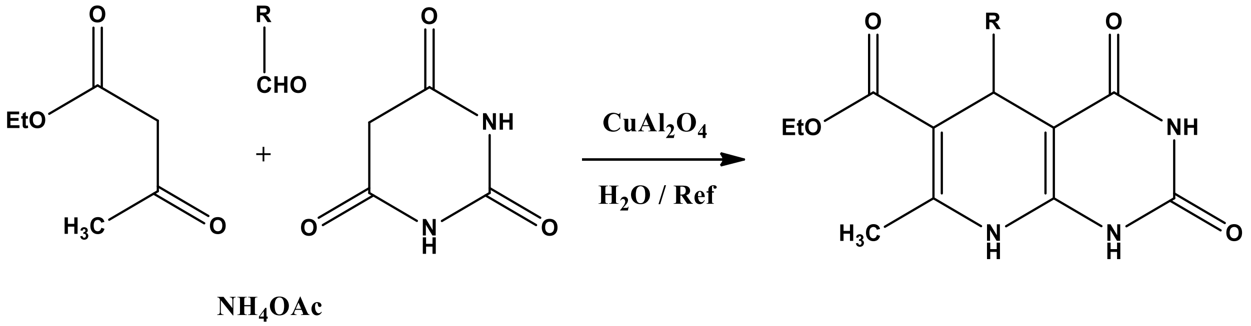

Scheme: Synthesis of 1,4-DHP derivatives by $CuAl_2O_4$ nanocatalyst.

References:

1. Sellitepe, H., Dogan, İ., Eroglu, G. A. M. Z. E., Barut, B. U. R. A. K., & Özel, A. (**2019**). Synthesis, characterization and investigation of cholinesterase enzyme inhibition and antioxidant activities of some 4-aryl-1,4-dihydropyridine derivatives. Journal of Research in Pharmacy, *23(4)*.

2. Khaled, A., Stiti, M. Z., Habila, T., Ferkhi, M., Pirotte, B., Pireaux, J. J., & Khelili, S. (**2022**). Synthesis and characterization of $La_{1-x}Sr_xMn_{1-y}Zn_yO_3$ perovskites as an efficient and recoverable catalyst for the Hantzsch reaction. Journal of Chemical Sciences, *134(3),* 86.

3. Naik, T. R., & Shivashankar, S. A. (**2016**). Heterogeneous bimetallic $ZnFe_2O_4$ nanopowder catalyzed synthesis of Hantzsch 1,4-dihydropyridines in water. Tetrahedron Letters, *57(36),* 4046-4049.

4. Zargarzadeh, R., Akbari Dilmaghani, K., & Nikoo, A. (**2021**). One-pot synthesis of 1,4-dihydropyridine derivatives using the $Fe_2ZnAl_2O_7$ catalyzed Hantzsch three-component reaction. Journal of the Chinese Chemical Society, *68(7),* 1310-1316.

Green Synthesis of Ally Dithiocarbamates Using Allenes

Arman Nazari Samarin, Azim Ziyaei Halimehjani
Department of Chemistry, Sharif University of Technology, Tehran, Iran.

Nucleophilic reaction, allenes, Dithiocarbamate, Green chemistry

In the last four decades, allenes have been recognized as one of the most important and versatile structures in organic synthesis. Allenes are used to prepare both natural and unnatural compounds [1]. A subgroup of allenes includes compounds where the terminal carbon is attached to a heteroatom such as nitrogen, oxygen, or sulfur [2]. Attention and reports regarding the functionalization and use of allenes are increasing due to their reactivity, selectivity, and unique availability. The electron-donating effect of the heteroatom in allenes increase their electrophilic and nucleophilic character in comparison to simple allenes. This is due to the resonance with the lone electron pair of heteroatom in the allylic position [3].

We are interested to report the synthesis of various allyl dithiocarbamates via a one-pot three-component reaction of amines, CS_2 and heteroatom-coupled allenes under green conditions. Various catalyst such as heteropoly acids, acidic organic salts, and ionic liquids were screened in green organic solvents to achieve the excellent yield. Diversities of heteroatom-coupled allenes and various primary and secondary amines were used in this protocol to afford the corresponding allyl dithiocarbamates in high to excellent yields.

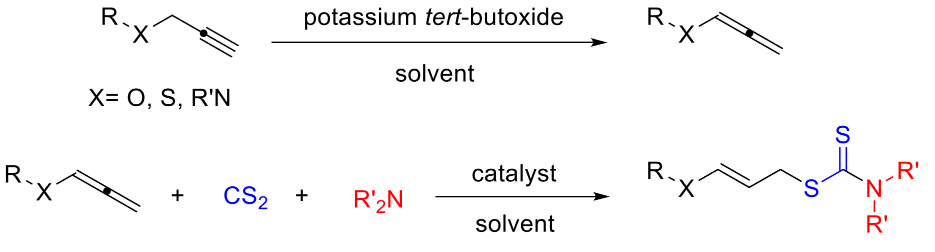

20 examples
80-100% isolated yields

References

1) T. Lu, Z. Lu, Z.-X. Ma, Y. Zhang, R. P. Hsung, *Chem. Rev.* **2013**, *113*, 4862–4904.

2) L. Wei, H. Xiong, R. P. Hsung, *Acc. Chem. Res*. **2003**, *36*, 773–782.

3) X. Li, Y. Liu, N. Ding, X. Tan, Z. Zhao, *RSC Adv*., **2020**,*10*, 36818-36827.

The 30th Iranian Seminar of Organic Chemistry
February 7-9, 2025, Iran University of Science and Technology, Tehran, Iran

Ag nanoparticles immobilized on mesoporous SBA-15 functionalized with ionic liquid-triethylammonium chloride as efficient catalysts for reducing 4-nitrophenol."

Mozhgan Pirhayati*[a], Hamidreza Torki[a]

[a]*Department of Applied Chemistry, Faculty of Science, Malayer University, Malayer, Iran*

mozhgan.pirhayati@malayeru.ac.ir

Keywords: Mesoporous SBA-15 silica, Ag nanoparticles, 4-nitrophenol

Abstract

A simple and efficient method was used to successfully synthesize novel silver (Ag) nanoparticles immobilized on triethanolamine-functionalized mesoporous silica SBA-15 [SBA-15/IL/Ag]. Its catalytic performance was evaluated in the reduction of 4-nitrophenol to 4-aminophenol in the presence of $NaBH_4$. The structural properties of the synthesized nanocatalyst were characterized using Fourier-transform infrared spectroscopy (FT-IR), X-ray powder diffraction (XRD), Field Emission Scanning Electron Microscopy (FE-SEM), Transmission Electron Microscopy (TEM), and N_2 adsorption/desorption isotherms (BET). The catalytic activity of the material during the reduction process was quantitatively monitored using Ultraviolet-Visible (UV-Vis) spectroscopy, which resulted in excellent yields within a short reaction time in aqueous media at room temperature, using a very low catalyst load. A kinetics study was also carried out, which yielded a good rate constant. Moreover, the synthesized nanocatalyst was easily recoverable from the reaction mixture and could be reused multiple times without significant activity loss.

1. Introduction

The rapid industrial growth and urbanization in recent years have increased environmental pollution, especially water contamination by hazardous organic pollutants like 4-nitrophenol (4-NP), which threaten both the environment and human health. Catalytic reduction of 4-NP to 4-aminophenol (4-AP) using NaBH4 is an effective, cost-efficient method for pollutant removal. Mesoporous materials like SBA-15, with high surface area and stability, are widely used in catalysis, particularly for pollutant reduction [1]. SBA-15's hexagonal pore structure and surface-functionalization ability make it an excellent catalyst support [2].

This study used functionalized SBA-15 mesoporous silica to support silver nanoparticles (AgNPs) as a catalyst. The catalyst (SBA-15/IL/Ag) was prepared by immobilizing AgNPs on chloropropyl-modified SBA-15, functionalized with triethanolamine, which stabilized the AgNPs. The catalyst showed high activity and stability, confirmed by the reduction of 4-nitrophenol to 4-aminophenol.

2. Result and discussion

2.1. Characterization

The specific surface area, mesoporous volume, and average pore diameter of SBA-15 and SBA-15/IL/Ag were determined using the BET method. After modification, a significant decrease in these properties was observed, indicating successful grafting of the ligand and formation of the final catalyst. According to the IUPAC classification, both samples (Fig. 1) show type-IV isotherms, with a hysteresis loop characteristic of mesoporous materials.

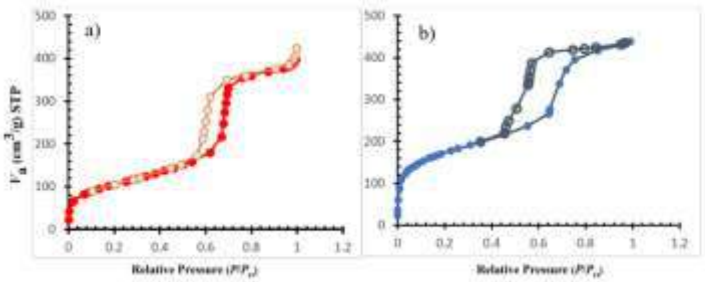

Fig. 1. The N_2 adsorption/desorption isotherm for a) SBA-15, and b) final catalyst

۲.۲. Catalytic activity of SBA-15/IL/Ag for reduction of 4-NP

The catalytic reduction of 4-Nitrophenol (4-NP) to 4-Aminophenol (4-AP) was studied using $NaBH_4$ as a hydrogen donor and SBA-15/IL/Ag as the nanocatalyst. As the reaction progressed, the solution color changed from yellow to colorless at room temperature, allowing real-time reaction monitoring via UV-Vis spectroscopy at short intervals.

3. Conclusion

This study presents an efficient, environmentally friendly method for reducing 4-nitrophenol in water using SBA-15/IL/Ag as a catalyst. The catalyst showed excellent activity, high yield, and stability over five cycles. It is easy to separate, making the process simple and effective.

References

١) Mahmoudi, F., Saravanakumar, K., Maheskumar, V., Njaramba, L. K., Yoon, Y., & Park, C. M. (2022). Application of perovskite oxides and their composites for degrading organic pollutants from wastewater using advanced oxidation processes: Review of the recent progress. Journal of Hazardous Materials, 436, Article 129074.

٢) Fan, P., Zhang, X., Deng, H., & Guan, X. (2021). Enhanced reduction of p-nitrophenol by zerovalent iron modified with carbon quantum dots. Applied Catalysis B: Environmental, 285, Article 119829.

The 30th Iranian Seminar of Organic Chemistry
February 7-9, 2025, Iran University of Science and Technology, Tehran, Iran

Familiarity with the Application of Artificial Intelligence in Predicting Chemical Reactions

Hamidreza Torki[a*]

[a]*Department of Applied Chemistry, Faculty of Science, Malayer University, Malayer, Iran*

hamidreza.toorkiii@gmail.com

Keywords: Chemistry Education, Artificial Intelligence, Chemical Simulations, Educational Chatbots, Artificial Intelligence Platforms

Abstract

Nowadays, Artificial Intelligence (AI) plays a significant role as an advanced tool in enhancing educational processes in the fields of chemistry and organic material science. This technology simplifies and makes learning complex concepts more interactive by offering innovative methods such as chemical reaction simulations, molecular modeling, and material property predictions. AI-based tools like educational chatbots, adaptive platforms, and computational chemistry software provide personalized learning experiences and facilitate solving chemical problems. This article explores the application of AI in predicting chemical reactions, including organic reaction

predictions, material structure modeling, and optimizing learning processes. Additionally, it analyzes the benefits and challenges of using this technology in basic science education.

Introduction

With the advancement of technology, Artificial Intelligence (AI) has gained a significant position as a transformative tool in the field of chemistry. One of the prominent applications of AI is in predicting chemical reactions, made possible by advanced platforms such as **IBM RXN for Chemistry.** This platform utilizes deep learning models and intelligent algorithms to predict reaction products, design synthesis pathways, and optimize reaction conditions. By leveraging this technology, researchers and students can reduce laboratory time and costs while accelerating the discovery of new materials. This article explores the application of this tool in chemistry education and research and analyzes its importance in advancing scientific and industrial processes.

Tool Explanation

One of the most prominent platforms that uses neural networks to predict chemical reactions is **IBM RXN for Chemistry**. This free tool leverages deep learning to provide advanced capabilities for modeling and analyzing chemical reactions. Key features of this platform include: **Prediction of Chemical Reactions**: IBM RXN can simulate chemical reactions and propose possible reaction pathways using molecular structures entered in SMILES format. Its neural network models, such as Transformer Models, utilize vast and accurate chemical data to predict the final products of reactions. **Retro-synthesis Design**: One of the standout features of IBM RXN is retro-synthesis. Users can input a specific product, and the tool suggests the raw materials and potential pathways for synthesizing it. This process directly uses deep learning to identify optimal synthesis routes.**Simulation and Optimization of Reaction Conditions**: The tool is capable of predicting optimal reaction conditions, including solvents, temperature, and catalysts. Neural networks, by analyzing data from similar reactions, propose conditions that yield the highest efficiency and the least amount of by-products.**Ease of Use**: This platform is free and web-based, requiring no programming knowledge or complex computations. Its simple interface allows students, researchers, and industry professionals to easily input reactions and view results.

Applications

Pharmaceutical Industry: Prediction of synthesis pathways for new pharmaceutical compounds. **Advanced Organic Chemistry**: Identification of optimal routes for the production of complex organic compounds. **Chemistry Education**: Interactive learning on how to synthesize materials and predict reactions. **Scientific Research**: Accelerating the discovery of new materials and modeling chemical reactions.

Level of AI Integration

IBM RXN follows some of the most advanced AI technologies, particularly in the fields of machine learning and natural language processing. Its primary goal is to simplify complex chemical tasks that traditionally require a high level of expertise and knowledge. However, this tool still requires the knowledge and judgment of chemists, as results generated by AI models may sometimes require further review.

Conclusion

The **IBM RXN for Chemistry** tool, with its integration of artificial intelligence and deep learning, has revolutionized reaction prediction and synthesis pathway design. This platform not only reduces time and costs but also delivers unparalleled accuracy and speed in chemistry education and research. Its widespread adoption can open new horizons in science and industry, paving the way for innovation.

References

١. IBM. (2021). "IBM RXN for Chemistry: AI-powered predictions of chemical reactions." *IBM Research*.
٢. Schwaller, P., et al. (2019). "Molecular Transformer: A Model for Uncertainty-Calibrated Chemical Reaction Prediction." *ACS Central Science, 5*(9), 1572–1583.

The 30th Iranian Seminar of Organic Chemistry
February 7-9, 2025, Iran University of Science and Technology, Tehran, Iran

Isolation and Characterization of Unique Meroterpenoids from Gum Ammoniacum

Maryam Kharatha[a], Nunziatina De Tommasi[b], Mahdi Moridi Farimani*[a]

[a]*Department of Phytochemistry, Medicinal Plants and Drug Research Institute, Shahid Beheshti University, G. C., Evin, Tehran, Iran.*

[b]*Department of Pharmacy, University of Salerno, 84084 Fisciano (SA), Italy.*

Keyword: Gum ammoniacum, Isolation, sesquiterpene 2,4-chromandione, NMR.

Introduction

Meroterpenoids are a group of terpenoid-containing hybrid natural products with unique structural architectures and impressive pharmacological properties. Meroterpenoids can be classified based on their nonterpenoid moiety into polyketide-terpenoids, shikimate-terpenoids, and alkaloid-terpenoids. These compounds are synthesized by a wide range of organisms, including bacteria, fungi, algae, plants, animals, and marine organisms. Notably, meroterpenoids derived from chromane/chromene can be condensed with hemi-, mono-, sesqui-, and diterpenoid units; their presence has been observed in various organisms, such as tunicates (*Botryllus*), brown macroalgae (*Sargassum, Cystoseira*), and Rhododendron (*Ericaceae*), Sarcandra (*Chloranthaceae*), and Mimosa (*Fabaceae*) plant species [1]. Previous phytochemical studies of gum ammoniacum identified unique meroterpenoids derived from chromane [2,3], prompting us to further explore the plant's extract.

Method

Two kilograms of resin were ground and extracted three times by maceration with ten liters of ethyl acetate. The extract was concentrated under reduced pressure at 45° C to 860 grams and separated on a silica gel column using a gradient solvent system of *n*-hexane-ethyl acetate (95:5 to 0:100), followed by an increasing concentration of MeOH (up to 40%) in ethyl acetate. Based on TLC analysis, fractions with similar compositions were combined, resulting in 18 main fractions (A1-A18). The third fraction (A3) was processed through a silica gel column using a gradient of n-hexane-chloroform (50:50 to 0:100), followed by an increasing concentration of MeOH (up to 5%), resulting in 20 subfractions (B1-B20). Subfractions B3, B5, and B7 were individually analyzed using reversed-phase high-performance liquid chromatography with isocratic MeOH-H_2O (70:30) as the solvent, resulting in the isolation of fifteen pure sesquiterpene 2,4-chromandiones from gum ammoniacum.

Results and Discussion

A phytochemical study of the ethyl acetate extract of gum ammoniacum using reversed-phase high-performance liquid chromatography led to the isolation of fifteen sesquiterpene 2,4-chromandiones, including four primary structures and their stereoisomers. Among them, compounds **1-13** were reported as new compounds. Identification was achieved through NMR (1D-NMR, 2D-COSY, HSQC, HMBC, NOESY, and ROESY) and HRMS analysis. Their unique structures present significant opportunities for further exploration in the realm of chemical research and application.

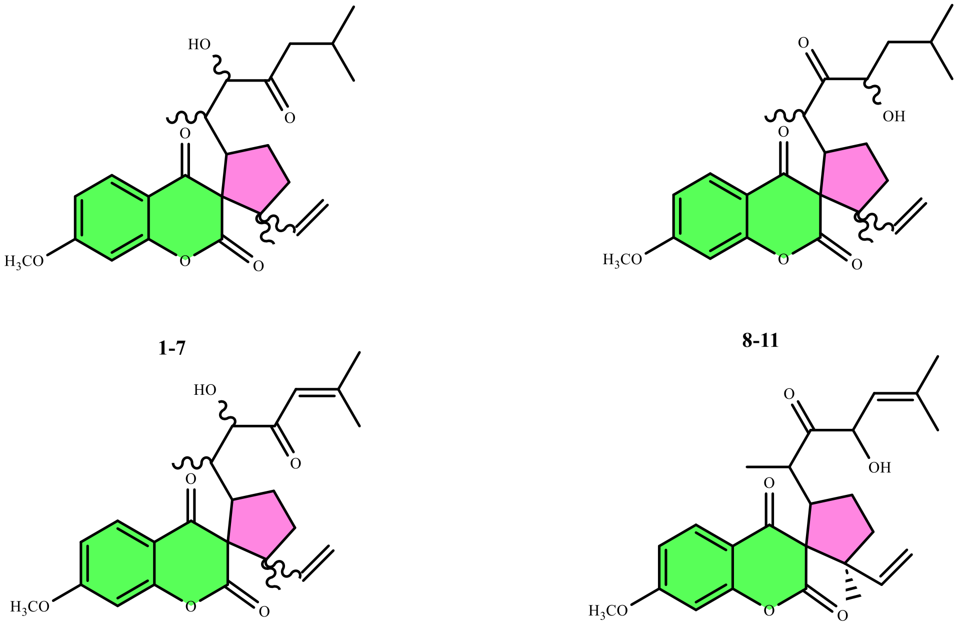

1-7

8-11

12-14

15

Figure 1: Isolated compounds from gum ammoniacum

References:

[١] Krstić, Gordana, et al. "Anticancer Meroterpenoids from *Centrapalus pauciflorus* leaves: Chromone-and 2, 4-Chromadione-Monoterpene Derivatives." ACS omega 8.34 (2023): 31389-31398.

[٢] Appendino, Giovanni, et al. "Ammodoremin, an epimeric mixture of prenylated chromandiones from Ammoniacum." *Helvetica Chimica Acta* 7٤,٣ (١٩٩١): ٤٩٥-٥٠٠.

[٣] Adhami, Hamid-Reza, et al. "Compounds from gum ammoniacum with acetylcholinesterase inhibitory activity." Scientia pharmaceutica 81.3 (2013): 793-806.

Synthesis of 2-Amino-1,3,4-Thiadiazole Derivatives Using Nano $NiCuAl_2O_5$ as a Reusable Catalyst

Afsaneh Valinezhad Asl, Abbas Nikoo*

Department of Organic Chemistry, Faculty of chemistry, Urmia University, Urmia, Iran

Keyword: Citric acid, Calcination, 1,3,4-Thiadiazole, Anticancer

Introduction: Since the mid-1950s, metal oxides have been shown to effectively catalyze a wide range of chemical reactions. These catalysts include simple oxides such as silica, alumina, silica-alumina, hydrotalcites, layered clays, zeolites, titania, zirconia, zinc oxide, and copper oxide, porous and mesoporous metal oxides such as MOFs, and complex oxides such as polyoxometalates (POMs) [1]. The performance of metal oxide catalysts depends on their nature, size, shape and surface area, and the relationships between them are influential in determining catalytic activity and selectivity. In recent years, mixed metal oxides have been widely studied as active phases and as substrates. The presence of two or more metal cations in mixed oxides provides an opportunity to control, design the morphology and properties of the materials and they are considered as substitutes for simple metal oxides [2]. In general, mixed oxides are crystalline, but their nature depends on the calcination temperature because at moderate calcination, some phases may remain amorphous. Considering their diverse properties and compositions, the advantages of crystalline mixed oxides are many [3]. The reason for the better catalytic activity of mixed metal oxides is related to the increase in active acidic or basic sites and their increased surface area, which reduces the reaction time and increases the reaction efficiency or conversion of reactants. The synthesis of 2-amino-1,3,4-thiadiazole and its derivatives is of particular importance due to the high anticancer activity of these compounds. 2-amino-1,3,4-thiadiazole and its derivatives are used in the production of polymers, dyes, herbicides, and insecticides [4].

Method: First, monoaqueous citric acid was dissolved in deionized distilled water. Then, 25% ammonia solution was added dropwise to sharply increase the pH and form an ammonium citrate solution. Then, $Cu(NO_3)_2\cdot 3H_2O$, $Ni(NO_3)_2\cdot 6H_2O$, and $Al(NO_3)_3\cdot 9H_2O$ were each dissolved separately in deionized distilled water. After preparing the solutions, each of the metal nitrate solutions was added to the monoaqueous citric acid solution, which was being mixed by a magnetic stirrer, at an interval of 10 minutes, and the stirring process was carried out at room temperature for 3 hours. Mixing with stirring led to the formation of colloidal particles or sol. The resulting mixture was transferred into an oven and allowed to form a gel, which is a polymeric material, at a temperature of 120°C for 24 hours. Gel formation and drying occurred simultaneously in the oven. Gel formation under heating conditions is known as xerogel. In this way, the hydroxyl groups were placed as bridges between the metals. The resulting material was thoroughly ground in a mortar and turned into powder. The resulting powder was transferred to an oven for calcination at a temperature of 600, 700, and 800 °C for one hour.

Results and Discussion: First, a solution of metal nitrate salts, which acts as an oxidant, is prepared with a suitable solvent of water and monohydrate citric acid, which acts as a fuel. It is worth noting that ammonia is added to the solution to increase the pH and ammonium citrate is formed in the colloidal phase. After initial heating in an oven for 24 hours, the water in the solution is gradually removed and thickened. The resulting xerogel has connections between metal centers and oxygen in the form of oxygen-containing bridges, and metal-ligand polymers are produced. With a further increase in temperature, the complexing agent or fuel begins to burn in the oven. Energy is released from the exothermic reaction of metal nitrate and fuel, and the result of this ignition is the release of CO_2, NO_2 and H_2O gases. In this way, a foam-shaped powder with a high volume that fills the entire container is obtained. In the calcination step, the metal hydroxide is converted to metal oxide, and this step affects the final properties of the nanoparticles, such as morphology, particle size, and purity.

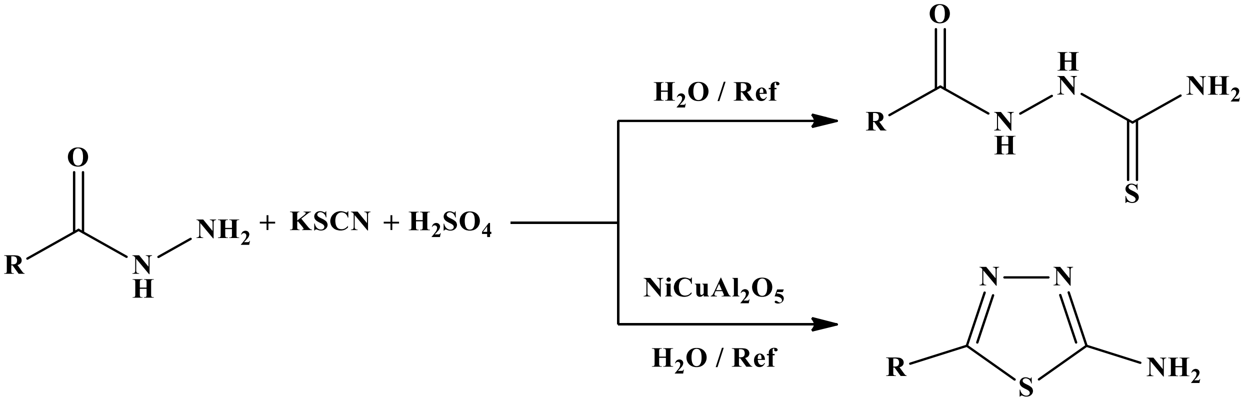

Scheme: Synthesis of 2-amino-1,3,4-thiadiazoles by $NiCuAl_2O_5$ nanocatalyst.

References:

1. Védrine, J. C. (**2019**). Metal oxides in heterogeneous oxidation catalysis: State of the art and challenges for a more sustainable world. ChemSusChem, *12(3),* 577-588.

2. Isahak, W. N. R. W., & Al-Amiery, A. (**2024**). Catalysts driving efficiency and innovation in thermal reactions: A comprehensive review. Green Technologies and Sustainability, 100078.

3. Wachs, I. E., & Routray, K. (**2012**). Catalysis science of bulk mixed oxides. ACS Catalysis, *2(6),* 1235-1246.

4. Stecoza, C. E., Nitulescu, G. M., Draghici, C., Caproiu, M. T., Hanganu, A., Olaru, O. T., Mihai, D. P., Bostan, M., & Mihaila, M. (**2023**). Synthesis of 1,3,4-Thiadiazole Derivatives and Their Anticancer Evaluation. Int J Mol Sci. *24(24),* 17476.

Effect of Solvent and $CuAl_2O_4$@NiO Nanocatalyst on Synthesis of 2-Amino-1,3,4-Thiadiazole Derivatives

Afsaneh Valinezhad Asl, Abbas Nikoo*

Department of Organic Chemistry, Faculty of chemistry, Urmia University, Urmia, Iran

Keyword: X-ray Diffraction, Scanning electron microscopy, Brunauer-Emmett-Teller, Porosity

Introduction: Most corrosion inhibitors are organic molecules. Heterocyclic compounds containing nitrogen, sulfur, and conjugated double bonds perform best. Some 2-amino-1,3,4-thiadiazole derivatives, including 2-amino-5-methyl-1,3,4-thiadiazole, 2-amino-5-ethyl-1,3,4-thiadiazole, 2-amino-5-n-propyl-1,3,4-thiadiazole, and 2-amino-5-t-buthyl-1,3,4-thiadiazole have been introduced as corrosion inhibitors [1-3]. Compounds containing heterocyclic rings play an important role among organic compounds with pharmacological activity. 2-Amino-1,3,4-thiadiazole are nitrogen and sulfur containing heterocyclic compounds that have wide applications as biologically active molecules and as useful intermediates in medicinal chemistry. 2-Amino-1,3,4-thiadiazoles have been extensively studied due to their wide range of pharmacological activities. 2-Amino-1,3,4-thiadiazole derivatives can be considered as intermediates for the synthesis of drugs [4,5]. In the present study, 2-amino-1,3,4-thiadiazoles were synthesized by the reaction of thiosemicarbazide and benzoic acid derivatives in water solvent and in the presence of $CuAl_2O_4$@NiO nanocatalyst. The chemical structure of the synthesized compounds was confirmed using FT-IR, ^{1}H NMR, and ^{13}C NMR.

Method: A mixture of thiosemicarbazide (9.11 g, 0.1 mol), benzoic acid derivatives (0.1 mol) and $CuAl_2O_4$@NiO nanocatalyst in 20 ml of distilled water was heated at 100 °C. After the reaction time, as monitored by TLC (ethyl acetate/n-hexane 3:5), the reaction temperature was reduced to 25 °C. The 2-amino-1,3,4-thiadiazole derivatives were extracted with 30 ml of ethyl acetate three times and the organic phase was dried over Na_2SO_4. The ethyl acetate was separated from the product using rotary evaporation and the 2-amino-1,3,4-thiadiazole derivatives were obtained in 74-90% yield. The 2-amino-1,3,4-thiadiazole derivatives were purified using ethanol. The $CuAl_2O_4$@NiO nanocatalyst was separated by centrifugation for reuse in subsequent reactions and washed several times with water, ethanol and ethyl acetate. Finally, the $CuAl_2O_4$@NiO nanocatalyst was dried at 120 °C for 2 hours.

Results and Discussion: XRD technique was used to identify the crystal structure, determine the phase type and size of the nanocatalyst particles. According to the XRD pattern, it was determined that the $CuAl_2O_4$@NiO nanocatalyst is crystalline. The data were analyzed in the range of 10^o to 80^o with a scan rate of 0.5 per second. Considering that urea was used as a fuel, stabilizer and reducer in the synthesis of $CuAl_2O_4$@NiO nanocatalyst, it had a significant effect on the size. The size distribution, surface morphology and shape of the $CuAl_2O_4$@NiO nanocatalyst were investigated by scanning electron microscopy (FESEM), which revealed the nanostructure of the $CuAl_2O_4$@NiO catalyst. The BET technique was used to determine the porosity of the $CuAl_2O_4$@NiO nanocatalyst and to calculate its surface area. N_2 adsorption and desorption isotherms were used to measure the size distribution, specific surface area, and pore volume of $CuAl_2O_4$@NiO nanocatalyst in K77. The pore size distribution and pore volume were calculated using the BJH method. The surface area was calculated using the BET equation. Before the BET experiment, the $CuAl_2O_4$@NiO nanocatalyst was degassed in vacuum at 120 °C for 4 h to remove the adsorbed moisture. The type (IV) adsorption isotherm in the range (2p/p_0 0.990) confirmed the nature of the mesoporous sample. The hysteresis loop formed was of the H3 type and the pore shape was of the lamellar type.

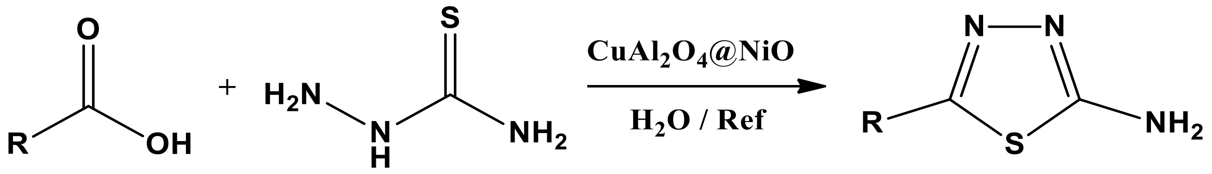

Scheme: Synthesis of 2-amino-1,3,4-thiadiazoles by $CuAl_2O_4$@NiO.

References:

1. Sherif, E. M., & Park, S. M. (**2006**). 2-Amino-5-ethyl-1,3,4-thiadiazole as a corrosion inhibitor for copper in 3.0% NaCl solutions. Corrosion science, *48(12),* 4065-4079.

2. Khan, S., & Quraishi, M. A. (**2010**). Synergistic effect of potassium iodide on inhibitive performance of thiadiazoles during corrosion of mild steel in 20% sulfuric acid. Arabian Journal for Science and Engineering, *35(1),* 71-81.

3. JOSEPH, R., & Rajendran, N. (**2011**). Corrosion inhibition effect of substituted thiadiazoles on Brass [J]. International Journal of Electrochemical Science, *6(2),* 348-366.

4. Upadhyay, P. K., & Mishra, P. (**2017**). Synthesis, antimicrobial and anticancer activities of 5-(4-substituted phenyl)-1,3,4-thiadiazole-2-amines. Rasayan J Chem, *10(1),* 254-262.

5. Berkelhammer, G., & Asato, G. (**1968**). 2-Amino-5-(1-methyl-5-nitro-2-imidazolyl)-1,3,4-thiadiazole: a new antimicrobial agent. Science, *162(3858),* 1146-1146.

An Efficient Method for the Synthesis of 2-Amino-1,3,4-Thiadiazole Derivatives Using CuO Loaded on $NiAl_2O_4$ as Catalyst

Afsaneh Valinezhad Asl, Abbas Nikoo*

Department of Organic Chemistry, Faculty of chemistry, Urmia University, Urmia, Iran

Keyword: Core-shell nanoparticles, Dynamic light scattering, Oxidative cyclization

Introduction: Catalytic processes play an important role in the advancement of chemical and industrial reactions and these processes are widely recognized as the heart of some chemical reactions. It should be noted that the application of catalysts has now expanded from an academic research laboratory to an industrial unit [1,2]. In addition, catalysts are very important in chemistry and, most importantly, the synthesis of organic materials because these compounds can potentially accelerate the process and produce products effectively and sustainably [3]. The development of new, bio-stable and non-toxic catalytic materials for the synthesis of natural compounds, drugs and bioactive molecules is not possible without the use of some catalysts [4]. A good catalyst will guarantee the performance of a reaction with the lowest energy. In recent years, catalysts and catalytic processes have attracted much attention to themselves so that they can be used to prepare and produce useful materials in the pharmaceutical industry. Thus, it can be said that catalysts have become an integral part of medicinal chemistry in recent years and have been one of the most strategic technologies in this field in the current century [5]. In other words, the new era in organic chemistry has been driven towards a direction in which creative approaches are carried out with a focus on green chemistry and sustainable catalysts. 1,3,4-Thiadiazole structures, which are five-membered heterocycles, have a wide range of biological activities. In this study, the synthesis of 1,3,4-thiadiazole derivatives is described by oxidative cyclization.

Method: Synthesis of $NiAl_2O_4$@CuO core-shell nanoparticles was prepared by impregnating $NiAl_2O_4$ nanoparticles with a secondary metal precursor. In other words, the $NiAl_2O_4$ nanoparticles used as the core and the nitrate precursor used in the shell formed the final nanoparticle. Another important point in this regard was the molar ratio of nanoparticles to the precursor used, which should be 1:1. After the end of this process, the obtained solid was calcined at 500 °C.

Results and Discussion: Bimetallic nanoparticles with heterogeneous composition in terms of the type of metals present in the clusters can play an important role in many fields of materials science due to their orbital properties and size-dependent characteristics. These nanoparticles can be the reason for these characteristics due to their unique electronic and magnetic properties resulting from the combination of two metals or their oxides in a matrix. These nanostructures can be composed of metal oxides in different ratios and include core-shell nanoparticles. Various methods have been proposed for the synthesis of these nanomaterials, including bottom-up and top-down methods. The conventional methods for the synthesis of core-shell structures include the sol-gel method and co-precipitation. The orbital properties of these particles of these structures have led to these materials having wide applications in catalytic chemistry. A better investigation of the size of nanoparticles was also carried out using the dynamic light scattering (DLS) method. The particle size obtained in the dynamic light scattering method was slightly larger than the sizes obtained from the electron microscope. This can be related to the principle that in the dynamic light scattering method the particle size can be represented hydrodynamically.

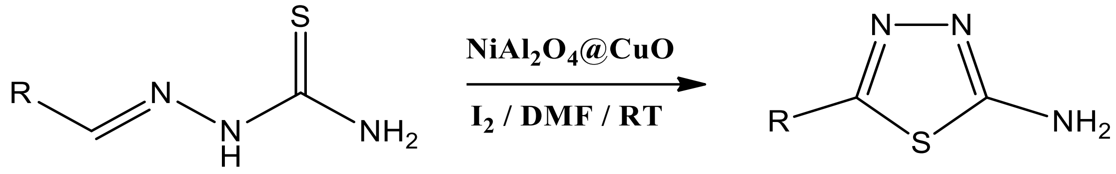

Scheme: Synthesis of 2-amino-1,3,4-thiadiazoles using $NiAl_2O_4$@CuO.

References:

1. Pu, Q., Kazemi, M., & Mohammadi, M. (**2020**). Application of transition metals in sulfoxidation reactions. Mini-Reviews in Organic Chemistry, *17(4),* 423-449.

2.Chen, L., Noory Fajer, A., Yessimbekov, Z., Kazemi, M., & Mohammadi, M. (**2019**). Diaryl sulfides synthesis: copper catalysts in C–S bond formation. Journal of Sulfur Chemistry, *40(4),* 451-468.

3. Chen, Z., Nasr, S. M., Kazemi, M., & Mohammadi, M. (**2020**). A mini-review: achievements in the thiolysis of epoxides. Mini-Reviews in Organic Chemistry, *17(4),* 352-362.

4. Heravi, M. M., Ghanbarian, M., Ghalavand, N., & Nazari, N. (**2018**). Current applications of the sonogashira reaction in the synthesis of heterocyclic compounds: An update. Current Organic Chemistry, *22(14),* 1420-1457.

5. Sultana, S., Borah, G., & Gogoi, P. K. (**2019**). Ru (III) Schiff-base complex anchored on nanosilica as an efficient and retrievable catalyst for hydration of nitriles. Applied Organometallic Chemistry, *33(1),* e4595.

The 30th Iranian Seminar of Organic Chemistry
February 7-9, 2025, Iran University of Science and Technology, Tehran, Iran

Synthesis and application of Fe_3O_4@Chitosan@CPTMS@Asparagine-Ag nanocatalyst in Hantzsch Reaction

Afagh Ranjbar Alvar, Fatemeh Kiani Bashir, Araz Taravati, Ahmad Poursattar Marjani* *a.poursattar@urmia.ac.ir

Department of Organic Chemistry, Faculty of Chemistry, Urmia University, Urmia, Iran

Keyword: Magnetic Nanocatalyst, Core-shell structure, Hantzsch reaction

This study focused on developing a core-shell structured heterogeneous nanocatalyst, Fe_3O_4@Chitosan@CPTMS@Asparagine-Ag. It highlighted several essential features, including stability, magnetic properties, easy separation, and recyclability. The catalyst enhances product yield, reduces reaction time, and allows for straightforward separation using a magnet, facilitating subsequent washing and reuse without reducing its catalytic efficiency. Additionally, it shows promise in promoting environmentally friendly synthesis reactions, such as the production of Hantzsch compounds. The modification began with treating Fe_3O_4 as a magnetic core, applying Chitosan coating, then functionalization with 3-chloropropyltrimethoxysilane (CPTMS) and asparagine, and finally incorporating silver metal. Silver is renowned for its excellent catalytic properties, making it a preferred choice for environmental and industrial applications, further enhancing the magnetic nanocatalyst's overall performance [1, 2].

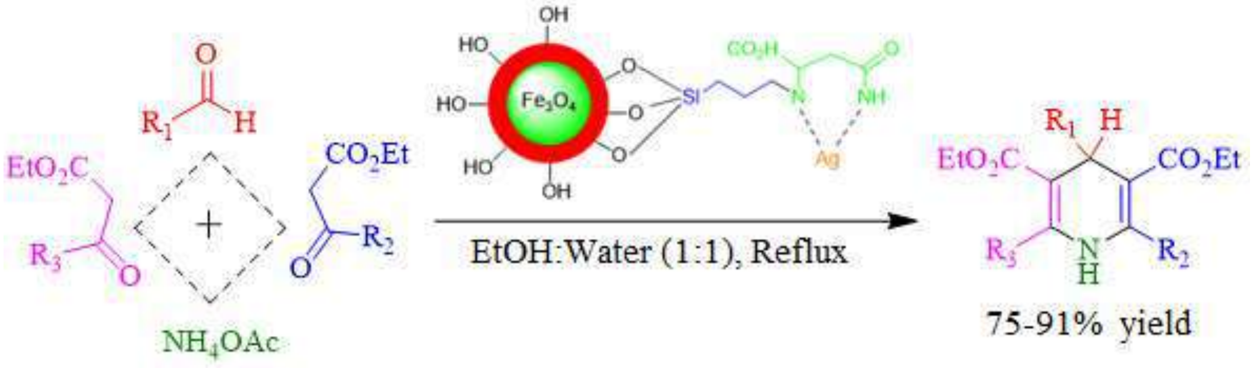

References:

1. Liu, S., et al., *Preparation, surface functionalization and application of Fe_3O_4 magnetic nanoparticles.* Advances in Colloid and Interface Science, 2020. **281**: p. 102165.

2. Ghaffarzadeh, M., *Synthesis and characterization of a novel heterogenized six-coordinate aspergillomarasmine A-nickel(II) complex and its applications as an efficient nanomagnetic catalyst for hantzsch reaction.* Journal of Molecular Structure, 2024. **1295**: p. 136635.

Synthesis and characterization of two-dimensional metal-organic frameworks and their photocatalytic application in advanced oxidation process

Authors: Zahra Shrifzadeh[a], Elaheh Saleh[b] (representing author) , Sayed Ali Akbar Razavi, Ali.Morsali*[c] (corresponding author)

Affiliations: Department of Chemistry, Faculty of Sciences, Tarbiat Modares University, P.O. Box 14117-13116, Tehran, Islamic Republic of Iran

Keyword: Two-dimensional Metal-organic framework (MOF), Advanced oxidation process, sulfate radicals, degradation of organic pollutants

Introduction

2D MOFs have been used for photocatalytic reactions such as decomposition of water, catalysis of oxidation-reduction reactions exposed to light, oxidation and selective degradation of antibiotics, water decontamination. The catalytic performance is attributed to metal nodes and flexible ligands and large aspect ratio, which provides a high diversity and density of active sites during the photocatalytic process.

Herein; the PMS (peroxymonosulfate)activation is catalyzed by NiZrCu-BDC 2D MOF structure which is synthesized via a simple ultrasonic route at room temperature. The attained 2D MOF is utilized in catalytic degradation of organic pollutants like 2,4-dichlorophenol(DCP).

Method

In a 100 mL beaker, 124.6 mg of terephthalic acid, 32 mL of DMF, and 2 mL of ethanol were combined and dissolved. Next, 116.3 mg of $Ni(NO_3)_2·6H_2O$, 35 mg of $ZrCl_4$, and 48.3 mg of $Cu(NO_3)_2·3H_2O$ were added, and the mixture was sonicated. Then, 0.8 mL of TEA was introduced, and the mixture was stirred. The beaker was sonicated continuously for 8 hours. Finally, the product was washed five times with ethanol and dried in an oven at 60 °C.

Results and Discussion

Scheme 1 presents the powder X-ray diffraction (XRD) patterns for NiZrCu-BDC and Cu-BDC. The XRD pattern of NiZrCu-BDC closely matches the simulated pattern for Ni-BDC, suggesting that the two-dimensional Ni-BDC is well crystallized. The primary diffraction peaks for all three catalysts are observed around 8.9°, corresponding to the characteristic (200) facet.

Scheme 2 illustrates the Fourier transform infrared (FTIR) spectra for Cu-BDC, NiZr-BDC, and NiZrCu-BDC. The peak at 3610 cm^{-1} is attributed to the terephthalic acid linkers coordinating to metal ions.

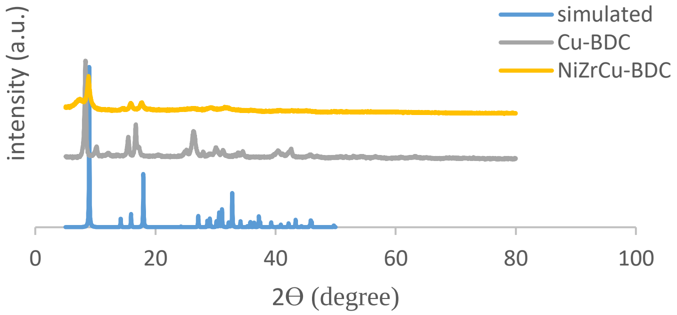

Scheme 1. Comparison XRD patterns of as-synthesized 2D-MOFs.

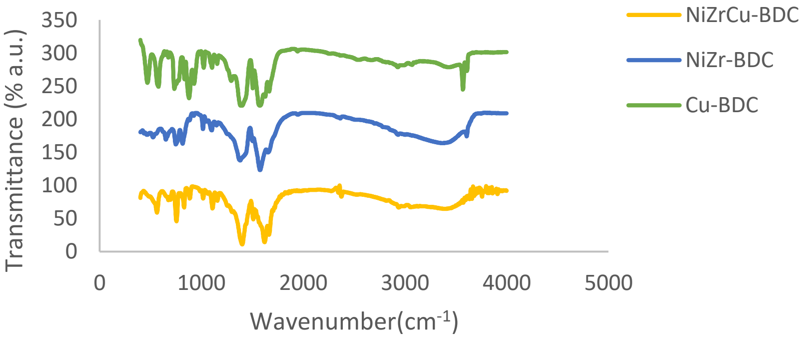

Scheme 2. Comparison FTIR spectrum of as-synthesized 2D-MOFs

Our study showed that the trimetallic MOF nanosheets (NiZrCu-BDC) perform better than the monometallic MOFs (Cu-BDC) in activating PMS for the effective oxidation of organic compounds in water. The activation of PMS takes place with the reaction between PMS and metal ions attended in the MOF structure, coupled with continuous redox cyclic reactions, which led to the generation of reactive oxygen species, primarily $^{1}O_2$ and $O_2^{\bullet-}$.

References:

[1] Xue, Y., Zhao, G., Yang, R., Chu, F., Chen, J., Wang, L., & Huang, X. (2021). 2D metal–organic framework-based materials for electrocatalytic, photocatalytic and thermocatalytic applications. *Nanoscale*, *13*(7), 3911-3936.

[2] Dhakshinamoorthy, A., Asiri, A. M., & Garcia, H. (2019). 2D metal–organic frameworks as multifunctional materials in heterogeneous catalysis and electro/photocatalysis. *Advanced Materials*, *31*(41), 1900617.

[3] Hu, M., Liu, J., Song, S., Wang, W., Yao, J., Gong, Y., ... & Li, Z. (2022). Ultra-thin two-dimensional trimetallic metal–organic framework for photocatalytic reduction of CO2. *ACS Catalysis*, *12*(5), 3238-3248.

[4] Wang, Q., Lu, J., Jiang, Y., Yang, S., Yang, Y., & Wang, Z. (2022). FeCo bimetallic metal organic framework nanosheets as peroxymonosulfate activator for selective oxidation of organic pollutants. *Chemical Engineering Journal*, *443*, 136483.

The 30th Iranian Seminar of Organic Chemistry
February 7-9, 2025, Iran University of Science and Technology, Tehran, Iran

Efficient niobium-ionic liquid based heterogeneous nanocatalyst for selective oxidation of sulfides to sulfoxides

Hamed Gholami, Maryam Hajjami*

Department of Organic Chemistry, Faculty of Chemistry and Petroleum Sciences, Bu-Ali Sina University, Postal code 6517838683, Hamedan, Iran. hamedgholamichemistry@gmail.com, m.hajjami@basu.ac.ir & mhajjami@yahoo.com

Keyword: Niobium, Oxidation of sulfides, Nanocatalyst, Biochar

Since the oxygenated products are useful as platform commodities and specialty chemicals, liquid-phase selective oxidation of organic substrates is an important reaction [1]. Sulfoxides and sulfones are useful organosulfur compounds as synthetic intermediates for natural products and biologically important molecules [2], ligands used for asymmetric catalysis [3], and oxygen atom donors [4]. Niobium compounds and materials are shown to be useful as promoters and supports of catalysts and as unique solid acid catalysts, selective oxidation catalysts and photosensitive catalysts. In this study, first biochar was formed out of biomass in high temperature. Afterwards, the surface of biochar was modified with ionic-liquid and $NbCl_4$ to obtain niobium catalyst. The ideal oxidation reaction was performed in absence of solvents and room temperature (25°C), with high yield. As result Methylphenylsulfoxide, Ethylphenylsulfoxide, Benzylphenylsulfoxide, Dibutylsulfoxide, and Diphenylsulfoxide were synthesized with the help of catalyst.

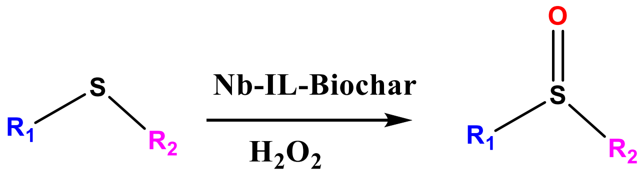

Scheme: Oxidation of sulfides in the presence of niobium-IL-Biochar nanocatalyst.

The advantages of this work include easy catalyst preparation, separation and reusability, selective and highly efficient reactions with short reaction time.

References:

[1] Kamata, K.; Sugahara, K.; Kato, Y.; Muratsugu, S.; Kumagai, Y.; Oba, F.; and Hara, M. Heterogeneously Catalyzed Aerobic Oxidation of Sulfides with a $BaRuO_3$ Nanoperovskite.ACS Appl. Mater. Interfaces. 2018, 10 (28), 23792-23801.

[۲] Carreño, M. C. Applications of Sulfoxides to Asymmetric Synthesis of Biologically Active Compounds. Chem. Rev. 1995, 95,1717−1760.

[3] Trost, B. M.; Rao, M. Development of Chiral Sulfoxide Ligands for Asymmetric Catalysis. Angew. Chem., Int. Ed. 2015, 54, 5026−5043.

[4] Otocka, S.; Kwiatkowska, M.; Madalinska, L.; Kielbasinski, P. Chiral Organosulfur Ligands/Catalysts with a Stereogenic Sulfur Atom: Applications in Asymmetric Synthesis. Chem. Rev. 2017, 117, 4147−4181.

The 30th Iranian Seminar of Organic Chemistry
February 7-9, 2025, Iran University of Science and Technology, Tehran, Iran

A green one-pot Biginelli synthesis of 3,4-dihydropyrimidin-2-(1H)-ones catalyzed by sulfated zirconia nanostructures under solvent-free condition

Parisa Khosravi , Atisa yazdanipour , Majid ghashang

Islamic Azad University of Central Tehran Branch

Keywords: Green chemistry , Multicomponent reactions, Catalysts, sulfated zirconia, NiO/ZrO2-SO4, 3,4-dihydropyrimidin-2(1H)-ones

Introduction: Green Chemistry seeks to reevaluate and innovate chemical products and synthesis methodologies to mitigate detrimental effects on human health, animal welfare, and ecological systems. Since its introduction in the 1990s by Paul Anastas and John Warner, progress has been made in addressing the dangers of toxic chemicals and promoting sustainable practices. Examples include safer insulating foams and reduced fossil fuel use. Nevertheless, there remains a substantial necessity for the implementation of more sustainable methodologies in both chemical manufacturing and agricultural practices to mitigate ecological degradation(Kadam & Bhangale, ۲۰۲٤). One way to achieve green chemistry goals is to use of nanocatalysts in the synthesis of multicomponent reactions(Zolfagharinia et al., 2020).Sulfated nanocatalysts have many applications in medical field, pollution control, energy storage and as catalysts in important reactions(Lowe et al.,2022). Zirconium oxide (Zirconia) can be transformed into an acidic catalyst by adding sulfate ions. The performance of these catalysts can be enhanced with noble metals like platinum and nickel , which also alter their surface properties. Key factors influencing sulfated zirconia catalyst performance include calcination temperature and sulfur concentration(Hsu et al.,2009).

As part of our initiative toward green synthesis and ongoing research into utilizing eco-friendly, recyclable, and efficient heterogeneous catalysts for the Biginelli reaction, we aim to present NiO/ZrO2-SO4 as catalyst for the synthesis of 3,4-dihydropyrimidin-2(1H)-ones. These compounds are produced via the reaction of various aromatic aldehydes (1a-m), urea (2), and ethyl acetoacetate (3).

---- solvent free 80 °C NiO/ZrO2-SO4 ----------->

Preparation of NiO/ZrO2-SO4 nanocatalyst: Initially, 40 mmol of sulfuric acid was mixed with 2 cc of oleaster extract. Then, nickel acetate and zirconium chloride were added to the solution, and the mixture was stirred for one hour until a yellow, gelatinous mixture formed. The mixture was filtered and dried at 80°C. Finally, the dried precipitate was calcined at 500°C for 4 hours.

General procedure for preparation of 3,4-dihydropyrimidin-2-(1H)-ones: In a reaction vessel, urea (1 mmol), ethyl acetoacetate (1 mmol), and aromatic aldehyde (1 mmol) were introduced in the presence of the NiO/ZrO2-SO4 nanostructured catalyst (0.1 mmol) while employing magnetic stirring at a temperature of 80 °C for an appropriate duration. The advancement of the reaction was monitored utilizing thin layer chromatography (TLC). Upon the completion of the reaction, the resulting mixture was subjected to washing with hot ethanol and subsequently centrifuged multiple times, with the hot ethanolic solution being transferred to a beaker after each centrifugation. The crude product was amassed within the beaker, recrystallized using ethanol, and subsequently washed with cold ethanol before being dried.

Results and Discussion:

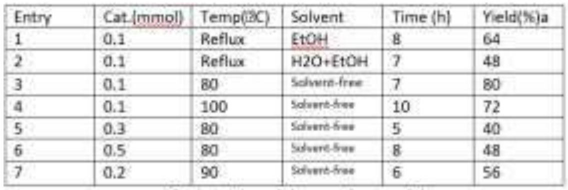

Entry	Cat.(mmol)	Temp(°C)	Solvent	Time (h)	Yield(%)a
1	0.1	Reflux	EtOH	8	64
2	0.1	Reflux	H2O+EtOH	7	48
3	0.1	80	Solvent-free	7	80
4	0.1	100	Solvent-free	10	72
5	0.3	80	Solvent-free	5	40
6	0.5	80	Solvent-free	8	48
7	0.2	90	Solvent-free	6	56

Optimization of the reaction conditions

As outlined in Table, the reaction of benzaldehyde, ethyl acetoacetate, and urea was tested using various solvents, catalyst quantities, and temperatures with NiO/ZrO2-SO4 nanostructures as catalysts. When performed with different solvents and under reflux at varying temperatures, the reactions resulted in slow progress, low yields, and the formation of side products. However, conducting the reaction under solvent-free conditions at 80 °C yielded the best results, with no side products and significant improvements in both yield and reaction time. Finally, evaluating catalyst quantities of 5, 10, 20, and 30 mol% identified 10 mol% (0.1 mmol) as the optimal amount. The experiment is ongoing, and the final results will be announced at the time of the presentation.

References:

1. Kadam, S. S., & Bhangale, C. J. (2024). A Review on Challenges and Impact of Green Chemistry on Environment. Journal of Pharmaceutical Research International, 36(7), 39–50.
2. Zolfagharinia, S., Kolvari, E., Koukabi, N., & Hosseini, M. M. (2020). Core-shell zirconia-coated magnetic nanoparticles offering a strong option to prepare a novel and magnetized heteropolyacid based heterogeneous nanocatalyst for three- and four-component reactions. Arabian Journal of Chemistry, 13(1), 227–241.
3. Lowe, B., Gardy, J., & Hassanpour, A. The Role of Sulfated Materials for Biodiesel Production from Cheap Raw Materials. Catalysts .(2022). 12(2), 223.
4. Hsu, Y. S., Wang, Y. L., & Ko, A. N. Effect of sulfation of zirconia on catalytic performance in the dehydration of aliphatic alcohols. Journal of the Chinese Chemical Society .(2009). 56(2), 314-322.

The 30th Iranian Seminar of Organic Chemistry

February 7-9, 2025, Iran University of Science and Technology, Tehran, Iran

Design, synthesis and molecular modeling studies of new 1-alkyl-2-aryl-tetrahydroindole derivatives as selective cyclooxygenase 2 inhibitors

Mohadeseh Karimi[1], Tannaz Zebardast[2], Salimeh Amidi[3], Elmira Meghrazi Ahadi[4]

1-Department of Pharmaceutical Chemistry, Faculty of Pharmaceutical Chemistry, Tehran Medical Sciences, Islamic Azad University, Tehran, Iran

2-Department of Pharmaceutical Chemistry, Faculty of Pharmacy and Pharmaceutical Sciences, Tehran Medical Sciences, Islamic Azad University, Tehran, Iran

3-Department of Medicinal Chemistry, School of Pharmacy, Shahid Beheshti University of Medical Sciences, Tehran, Iran

4-Department of Medicinal Chemistry, Faculty of Pharmacy, Tehran University of Medical Sciences, Tehran 1417614411, Iran

Corresponding author: Tannaz Zebardast

Corresponding Author Email: T.zebardast@iautmu.ac.ir

Keywords: Synthesis, design, selective cyclooxygenase 2 inhibitors, tetrahydroindole, molecular modeling

Introduction: Inflammation is a natural defense response of the body against many types of internal and external stimuli. Prolonged inflammation is often associated with the pathogenesis and progression of cancer, arthritis, autoimmunity, cardiovascular problems, and neurological disorders. Cyclooxygenase enzymes are key inflammatory markers because they catalyze the production of prostaglandins. Nonsteroidal anti-inflammatory drugs (NSAIDs) act by inhibiting the activity of cyclooxygenase enzymes, namely the COX-2 and COX-1 isoenzymes, in a selective and nonselective manner. Diaryl heterocyclic Compounds are a common and important scaffold in many specific COX-2 inhibitors because of their greater selectivity for this enzyme. They have better enzyme and safety profiles, which is why they have been studied in different central ring pharmacophore formats. In this study, based on the structure-activity relationship of selective cyclooxygenase-2 inhibitors, new 1-alkyl-2-aryl-tetrahydroindole derivatives were designed and synthesized as selective cyclooxygenase 2 inhibitors.

Method: Target derivatives were synthesized in two steps. In the first step, methyl sulfonyl phenacyl bromide, dimedone and potassium carbonate were mixed together at room temperature in a small amount of dry chloroform. After the completion of the reaction, the resulting precipitates were filtered, dissolved in water and then acidified. Finally, the precipitates were crystallized with ethanol. In the second step, the amine derivatives were added to the intermediate obtained from the previous step in a mixture of water and ethanol and the solution was refluxed. After the completion of the reaction the resulting precipitates were filtered and crystallized with methanol-acetone.

Result and Discussion: A series of novel 1-alkyl-2-aryl-tetrahydroindole derivatives were synthesized in good yields and the structure of the compounds was confirmed by FT-IR, ^{1}HNMR and MASS spectroscopy. In this study new derivative of 1-alkyl-2-aryl-tetrahydroindole was synthesized in two steps according to the structure activity relationship of selective COX-2 inhibitors. Molecular structure of the synthesized compounds was confirmed by FT-IR, ^{1}HNMR and MASS spectroscopy.

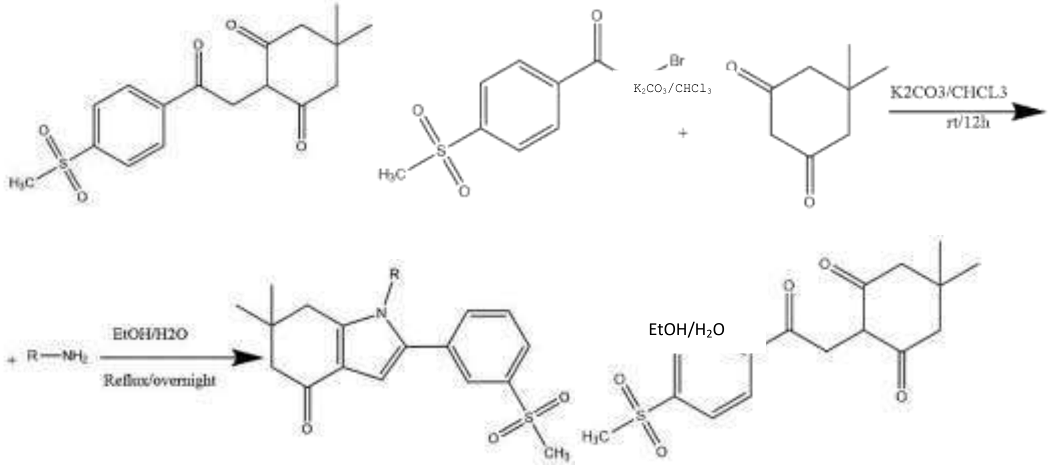

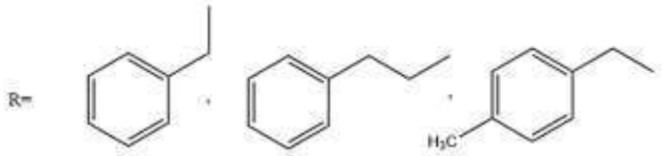

1- N.K. Kaushik, N. Kaushik, P. Attri, N. Kumar, C.H. Kim, A.K. Verma, E.H. Choi, *Molecules.* 18, 6620 (2013).

2- R. Dhani, A. Avinash, S.K. Salenaagina, M.V.S. Teja, P. Masthanaiah, P.R. Rathnam, V.C. Silpa, *J. Chem. Pharm. Res.* 519 (2011).

The 30th Iranian Seminar of Organic Chemistry
February 7-9, 2025, Iran University of Science and Technology, Tehran, Iran

Design, synthesis and Docking studies of new diaryl tetrahydroindol derivatives as selective cyclooxygenase-2 inhibitors

Zohreh Ahmadi[1],Tannaz Zebardast[2],Salimeh Amidi[3],Elmira Meghrazi Ahadi[4]

1.Department of Pharmaceutical Chemistry, Faculty of Pharmaceutical Chemistry,Tehran Medical Sciences.Islamic Azad Univercity,Tehran,Iran

2.Department of Pharmaceutical Chemistry,Faculty of Pharmacy and Pharmaceutical Sciences, Tehran Medical Sciences, Islamic Azad University,Tehran,Iran

3.Department of Medicinal Chemistry,School of Pharmacy,Shahid Beheshti University of Medical Sciences,Tehran,Iran

4.Department of Medicinal Chemistry,Faculty of Pharmacy,Tehran University of Medical Sciences ,Tehran1417614411 ,Iran

Corresponding author:Tannaz Zebardast

Corresponding author Email:T.zebardast@iautmu.ac.ir

Faculty of Pharmaceutical Chemistry,Tehran Medical

Keywords:Synthesis,Design,Selective cyclooxygenase 2 inhibitors,Tetrahydroindole

Introduction**:**The non-steroidal-anti-inflammatory drugs(NSAIDs) that act via inhibition of the cyclooxygenase(COX) enzyme,are widely used as anti-inflammatory agents.However the gastrointestinal toxicities associate with wide-spread use of NSAIDs proved to be a major problem during long therapy,they are due to the inhibition of gastroprotective PGs synthesized through the COX-1 pathway. Thus selective inhibition of COX-2 over COX-1is useful for the treatment of inflammation.In this study novel diaryl tetrahydroindole derivatives were designed and synthesized according to the structure activity relationship of selective COX-2 inhibitor.

Method:In the first step methylsulfonyl phenacyl bromide and dimedone were stirred in dry chloroform in the presence of K_2CO_3 as a catalyst at room temperature. After completion of the reaction the resulting precipitates were filtered and dissolved in water,then acidified and finally the resulting product was filtered and crystallized with ethanol .In the second step,aniline derivatives were added to the resulting product from the previous step in a mixture of water and ethanol.The solution was refluxed for 48 hours.After that the precipitates were filtered and crystallized with acetone-methanol.

Result and Discussion: In this study,new diaryl tetrahydroindole derivatives were designed,synthesized and purified.The structure of the synthesized compounds was confirmed by FT-IR,^{1}HNMR and mass spectroscopy.The COX-2 inhibitory activity of the target compunds is under investigation.

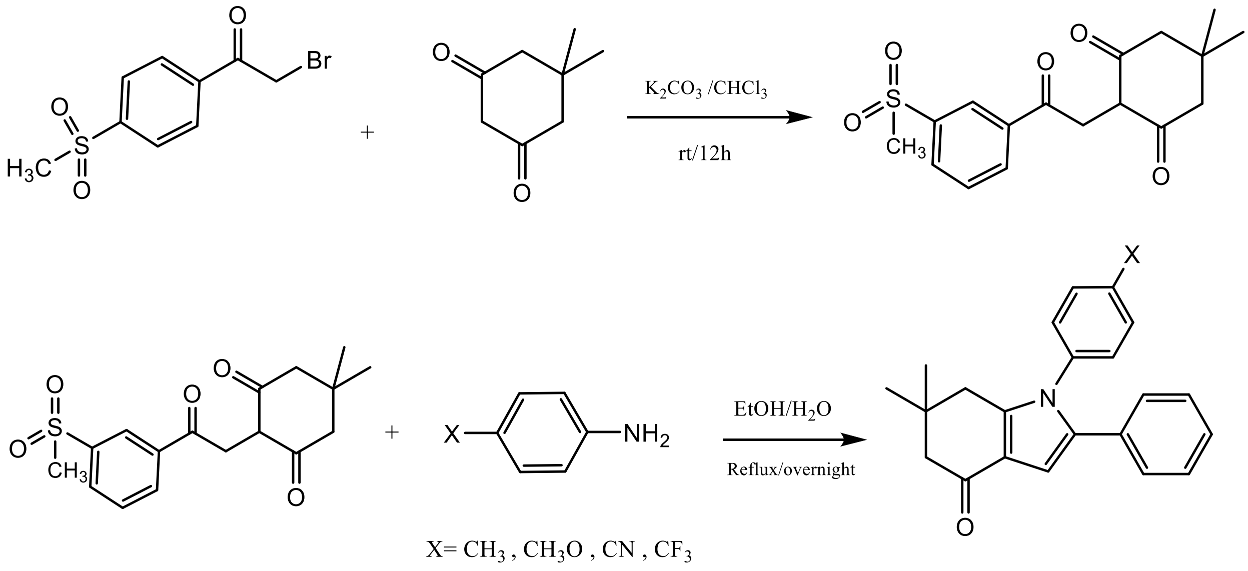

X= CH_3 , CH_3O , CN , CF_3

References:

1-Abdelall.E.K (2020).synthesis and biological evalutions of novel isoxazoles and furoxan derivative as anti inflammatory agents.Bioorg chem.94103441

2-Mohamed.LK&Ismael.A(2017).Design & synthesis of novel oxazolone&triazinone derivatives and their biological evaluation as COX-2 inhibitors.Bioorg chem.72308-314

The 30th Iranian Seminar of Organic Chemistry
February 7-9, 2025, Iran University of Science and Technology, Tehran, Iran

Prussian carbon obtained from for Grape waste-Derived the destruction of oxytetracycline in a flow reactor

Fateme Mohammadi[a], Nadia Koukabi[*a], Eskandar Kolvari[*a], Kheibar Dashtian[*b]

[a] *Department of Chemistry, Semnan University, 35131-19111 Semnan, Iran*

[b] *Department of Chemistry, Iran University of Science and Technology, Tehran 16846- 13114, Iran*

[*] *E-mail: n.koukabi@semnan.ac.ir, kolvari@semnan.ac.ir, kdasht68@gmail.com*

Keyword: Advanced oxidation processes, Biomass, Grape waste-Derived, Oxytetracycline

Body Text: Oxytetracycline (OTC) is a widely used antibiotic for treating infections in both humans and animals, yet it remains in wastewater, creating health hazards for people and ecosystems. Researchers are exploring different treatment approaches for Oxytetracycline residues. Conventional techniques such as adsorption and biochemical processes are expensive and ineffective, possibly leading to secondary pollution. Advanced oxidation processes (AOPs), especially semiconductor photocatalytic degradation, have surfaced as effective solutions because of their high efficiency and minimal toxicity[1] . Global attention has turned to environmental issues, especially regarding micropollutants that threaten ecosystems and human health. Advanced oxidation processes (AOPs) efficiently tackle these pollutants by employing generated radicals to break them down into CO2 [2]. Biochar, a valuable carbon-rich product, is created through the pyrolysis of various biomass precursors such as corn stalks, rice husks, Grape waste-Derived and coconut shell. It showcases excellent characteristics, including a large surface area, high porosity, stability, and retention of nutrients and water, making it valuable for multiple applications [3],[4]. Converting organic waste into biochar benefits both environmental remediation and sustainable waste management. Often produced as a green alternative to activated carbon for wastewater decontamination, biochar production relies on pyrolysis, a method favored for its ability to preserve carbon and recover energy. The efficiency of biochar production depends on the characteristics of the organic waste and specific pyrolysis conditions, categorized into slow, fast, and flash pyrolysis based on temperature and processing duration, yielding biochar, bio-oil, and gas, respectively [5 ,6].

10g Grape waste-Derived underwent hydrothermal carbonization at 200°C with 10 g of water for 12 hours in autoclave. The solid product was filtered, washed with 100 ml of water and dried at 100◦C for 24 h. Samples were ground with KOH (KOH / sample = 2 by weight) and heated at 5°C/min to 800°C under N2 for 1 hour. They were then washed with 10 wt% HCl and boiling distilled water until conductivity was below 2 μS-1 Finally, they were dried at 100°C for 24 hours[7].

Scheme 1 : EDX spectrum of Grape waste-Derived

The EDX analysis shows thats Grape waste-Derived consist of organic materials with a high percentage of carbon and oxygen.

1. Qin, H., et al., *Ce-Fe bimetallic oxide derived from Prussian blue precursors presents enhanced photodegradation ability for tetracycline under visible light: Its controlled morphology and mechanism studies.* Journal of Environmental Chemical Engineering, 2021. 9(6): p. 106739.
2. Wang, F.-X., et al., *Prussian blue analogue nanospheres immobilized on self-floating biochar for micropollutant degradation via photo-Fenton process.* Chemical Engineering Journal, 2024. **487**: p. 150506.

3. Francoeur, M., et al., *Removal of antibiotics by adsorption and catalytic ozonation using magnetic activated carbons prepared from Sargassum sp.* Journal of Water Process Engineering, 2023. **53**: p. 103602.
4. Manjunath, S., R.S. Baghel, and M. Kumar, *Antagonistic and synergistic analysis of antibiotic adsorption on Prosopis juliflora activated carbon in multicomponent systems.* Chemical Engineering Journal, 2020. **381**: p. 122713.
5. Nazari, G., H. Abolghasemi, and M. Esmaieli, *Batch adsorption of cephalexin antibiotic from aqueous solution by walnut shell-based activated carbon.* Journal of the Taiwan Institute of Chemical Engineers, 2016. **58**: p. 357-365.
6. Yaashikaa, P., et al., *A critical review on the biochar production techniques, characterization, stability and applications for circular bioeconomy.* Biotechnology reports, 2020. **28**: p. e00570.
7. Guardia, L., et al., *Winery wastes as precursors of sustainable porous carbons for environmental applications.* Journal of Cleaner Production, 2018. **193**: p. 614-624.

The 30th Iranian Seminar of Organic Chemistry
February 7-9, 2025, Iran University of Science and Technology, Tehran, Iran

Synthesis of a novel nickel-supported heterogeneous magnetic nanocatalyst for sulfide oxidation

Fatemeh Mohammadi, Arash Ghorbani-Choghamarani*, Arezo Monem

Department of Organic Chemistry, Faculty of Chemistry and Petroleum Science, Bu-Ali Sina University, Hamedan, 6517838683, Iran, a.ghorbani@basu.ac.ir or arashghch58@yahoo.com, f.mohammadii1379@gmail.com, arezomonem@yahoo.com,

Keywords: Heterogeneous Catalysis, Sulfoxides, Tin Ferrite, magnetic nanoparticles

Sulfoxides are one of the most important functional groups in organic chemistry and are found in many pharmaceuticals and natural products. Sulfoxides are usually obtained from the oxidation of the corresponding sulfides [1]. The use of magnetic nanocatalysts is a rapidly growing area for developing sustainable and green processes. Magnetic separation not only eliminates the need for filtering or centrifuging the catalyst after the reaction is completed but also provides practical methods for recovering these catalysts [2,3].

In this project, the magnetic Tin Ferrite nanocatalyst, after achieving optimal conditions, showed good performance in sulfide oxidation reactions. The resulting catalyst was investigated using various analyses such as IR, XRD, SEM, EDS, ICP, and TGA. After the synthesis of each compound, the synthesized structures were identified and confirmed using instrumental analysis methods such as IR and NMR, as well as melting point measurements. (Scheme 1).

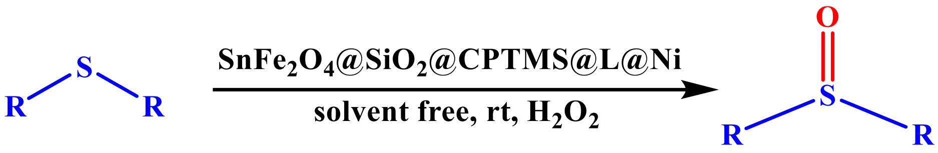

Scheme 1. Oxidation of sulfides to sulfoxides

References:

١- Skolia, E., Gkizis, P. L., & Kokotos, C. G. **2022**. *Aerobic photocatalysis: oxidation of sulfides to sulfoxides*. ChemPlusChem., Vol. 874: e202200008.

٢- Roy, A., Elzaki, A., Tirth, V., Kajoak, S., Osman, H., Algahtani, A.,… and Bilal, M. **2021**. *Biological synthesis of nanocatalysts and their applications*. Catalysts., Vol. 11:12, 1494.

٣- Chen, M. N., Mo, L. P., Cui, Z. S., and Zhang, Z. H. **2019**. *Magnetic nanocatalysts: Synthesis and application in multicomponent reactions*. Curr. Opin. Green Sustain. Chem., Vol. 15:27-37.

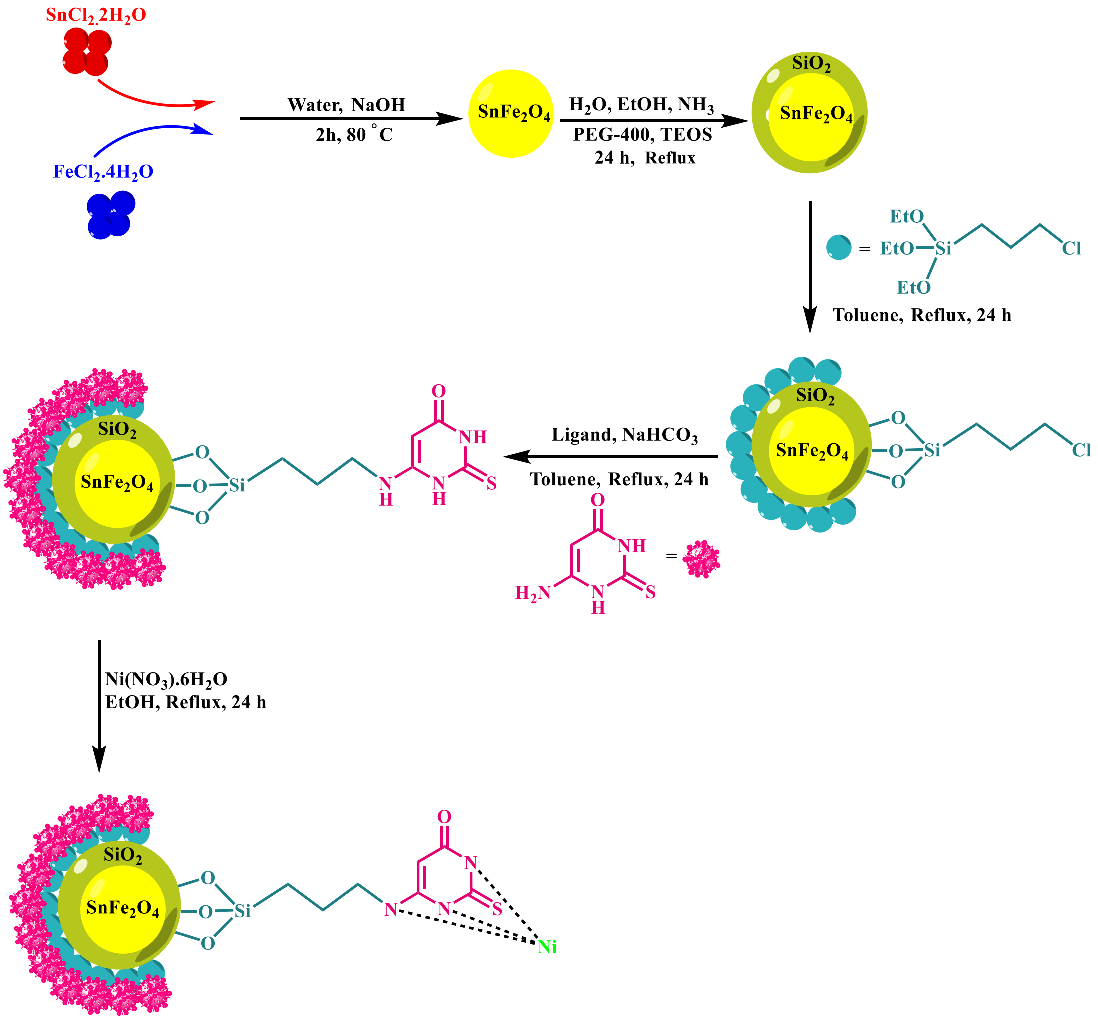

The 30th Iranian Seminar of Organic Chemistry
February 7-9, 2025, Iran University of Science and Technology, Tehran, Iran

Preparation of Fe/g-C_3N_4 nanophotocatalyst and its application in degradation of oxytetracycline

Authors: [a] Zeinab Rabiei kerahrodi, *[a]Nadiya koukabi, [a] Eskandar Kolvari, [b] Kheibar Dashtian

[a] *Department of Chemistry, Semnan University, 35131-19111 Semnan, Iran*

[b] *Department of Chemistry, Iran University of Science and Technology, Tehran 16846- 13114, Iran*

* *E-mail:* n.koukabi@semnan.ac.ir

Keyword: Oxytetracycline, Hemoglobin, Single Atom Catalyst, Graphitic Carbon Nitride

Oxytetracycline (OTC), a prevalent antibiotic in both medical and agricultural domains, presents considerable threats as an organic contaminant in aquatic environments, raising alarms regarding antibiotic resistance and public health risks, while its resistance to conventional wastewater treatment underscores the critical necessity for innovative and sustainable remediation strategies[1]. Advanced oxidation processes (AOPs) and reactive oxygen species (ROS) such as hydroxyl radicals ($OH^•$), sulfate radicals ($SO_4^•$), and superoxide radicals ($O_2^•$) are highly efficient at breaking down organic compounds in wastewater, demonstrating significant promise in recent studies. The sulfate radical ($SO_4^•$) is primarily produced by activating peroxymonosulfate (PMS) and peroxydisulfate (PDS) using ultraviolet (UV) irradiation[2]. Single atom catalysts (SACs) are a type of catalyst in which single catalytically active metal atoms are attached to the substrate and interact with the reactants. Normally, the valence of the metal at the surface of the substrate should be zero, but the zero valence metal atom is unstable. For this reason, the metal atom is placed on the substrate through ionic or covalent interaction with surface atoms or through ligands to remain fixed. It should be noted that in this type of catalysts, metal ions have a positive charge and the substrate has a negative charge. Due to the strong bond between the single metal atom and the supporting substrate, charge transfer and separation is facilitated in these compound particles[3].

In this research, considering the significant potential of single atom catalysts in photocatalytic processes, a single atom catalyst based on iron and graphitic carbon nitride (Fe/g-C_3N_4) was designed. The designed Fe/g-C_3N_4 catalyst has the ability to coordinate with Fe(II) and Fe(III) due to the presence of six electron pairs of nitrogen in the heptazine and triazine rings. This catalyst has been used to activate PDS for the degradation of OTC antibiotics (Scheme1). XRD, EDS, FT-IR and UV Spectroscopy were employed to characterize and elucidate the properties of the catalyst, facilitating its identification and providing insights into its structural and compositional attributes[4, 5].

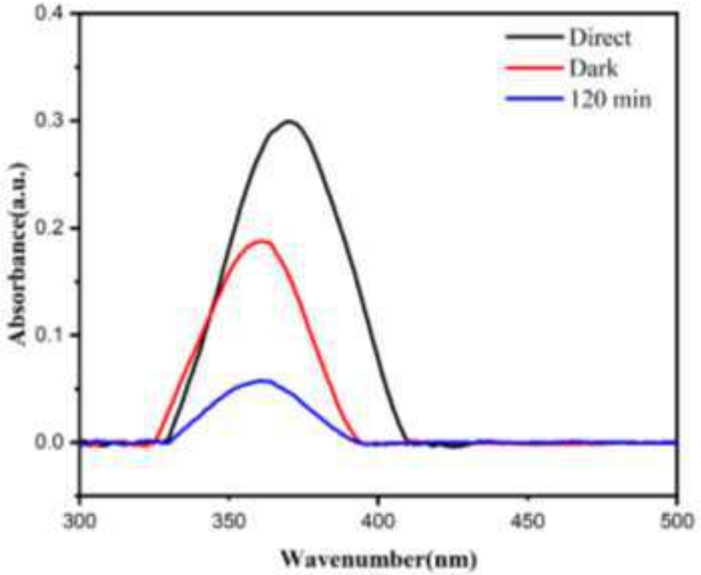

Scheme1. UV results from OTC degradation using the prepared photocatalyst during 120 min of reaction

1. Paghaleh, E.S., et al., Green synthesis of stable $CuFe_2O_4$/CuO-rGO heterostructure photocatalyst using basil seeds as chemo-reactors for improved oxytetracycline degradation. Journal of Environmental Chemical Engineering, 2023. 11(5): p. 110676.
2. Deng, Y. and R. Zhao, Advanced oxidation processes (AOPs) in wastewater treatment. Current Pollution Reports, 2015. 1: p. 167-176.
3. Lei, G., et al., Isolated iron sites embedded in graphitic carbon nitride (g-C_3N_4) for efficient oxidative desulfurization. Applied Catalysis B: Environmental, 2020. 267: p. 118663.
4. Cao, H., et al., Different roles of Fe atoms and nanoparticles on g-C_3N_4 in regulating the reductive activation of ozone under visible light. Applied Catalysis B: Environmental, 2021. 296: p. 120362.
5. Chen, L., et al., Well-dispersed iron and nitrogen co-doped hollow carbon microsphere anchoring by g-C_3N_4 for efficient peroxymonosulfate activation. Chemosphere, 2021. 280: p. 130911.

The 30th Iranian Seminar of Organic Chemistry
February 7-9, 2025, Iran University of Science and Technology, Tehran, Iran

Synthesis and Pyrolysis of Cu/Ni-Based MOF for Heavy Metal Ion Adsorption

Authors: Paria Soleimani Abhari, Behnam Habibi and Ali Morsali *

Affiliations: Department of Chemistry, Faculty of Sciences, Tarbiat Modares University, P.O. Box 14115-175, Tehran, Iran.

Keyword: Cu/Ni-Based MOF, Heavy Metal Ion Adsorption, MOF Pyrolysis, Porous Adsorbent Materials

Introduction

The increasing contamination of water by heavy metal ions highlights the urgent need for efficient and sustainable remediation strategies due to their toxicity, persistence, and bioaccumulative[2-3] nature[1]. In this study, a bimetallic Cu/Ni-based metal-organic framework (MOF) was synthesized using benzene tricarboxylic acid as the organic ligand under solvothermal conditions. The synthesized MOF was subsequently pyrolyzed at 500°C under an inert nitrogen atmosphere to enhance its structural stability, thermal resistance, and surface properties. Characterization techniques, including XRD, FTIR, and SEM confirmed the successful conversion of the MOF into a porous carbonaceous composite with well-dispersed Cu and Ni active sites. These features significantly increased the active site availability, making it highly suitable for adsorption. Adsorption experiments demonstrated high removal efficiencies for heavy metal ions in aqueous solutions, with the performance attributed to the synergistic effects of the bimetallic centers, enhanced porosity, and functionalized carbon matrix applications.

Scheme1: Schematic representation of the synthesis and pyrolysis process for Cu/Ni-based MOF

References:

1. Luo, J., Wang, J., and Zhang, H. Environmental Science: Nano, 2020. DOI: 10.1039/C9EN01042A.

2. Khan, N. A., Hasan, Z., and Jhung, S. H. Journal of Hazardous Materials, 2013. DOI: 10.1016/j.jhazmat.2013.01.036.

3. Li, X., and Yu, J. RSC Advances, 2021. DOI: 10.1039/D3RA08815D.

Efficient Removal of Arsenic Ions from Water Using Amino Acid Functionalized Zr-MOF-808 with Mixed Linkers

Authors: Zahra Sharifzadeh[a], Zahra Davoudi[a], Sayed Ali Akbar Razavi[a] and Ali Morsali*[a]

Affiliations: Faculty of Basic Sciences Tarbiat Modares University, Tehran, Iran.

Email: Morsali_a@modares.ac.ir

Keyword: MOFs, amino acid, mixed linker, Heavy metal ion removal

The removal of heavy metal ions from water is crucial due to their harmful environmental and health impacts. Among various materials, Metal-Organic Frameworks (MOFs) have gained attention for their high surface area, tunable structures, and functional properties. [1] Functional MOFs, especially those incorporating amino acids, offer enhanced adsorption capabilities for specific ions. [2] This study explores the potential of a mixed linker Zr-MOF 808 for the effective removal of arsenic (As) ions from contaminated water. [3]

The Zr-MOF 808 was synthesized using a mixed linker approach, incorporating benzene tricarboxylic acid and histidine amino acid-based linker. Characterization techniques, including XRD, FT-IR, BET and TGA were used to confirm the structure of the MOF. The arsenic ion removal process was evaluated under varying conditions of pH, contact time, and concentration, using batch adsorption experiments via ICP.

The mixed linker Zr-MOF 808 exhibited superior performance in arsenic removal, with a high removal efficiency and selectivity over other common metal ions up to 85%. The material demonstrated remarkable stability and recyclability, maintaining high performance even after multiple reuse cycles.

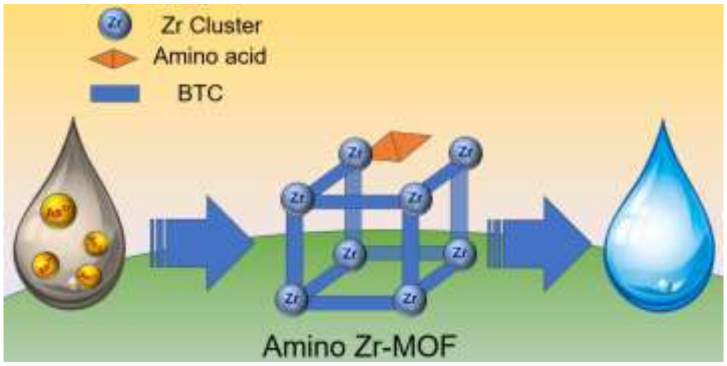

Scheme1: Heavy metal removal via mixed linker Zr-MOF

References:

1. Furukawa, H., et. al, J. Am. Chem. Soc., (2014), 136, 11, 4369.

2. Abdollahi, N. et. al, J. Hazard. Mater., (2020), 387, 121667.

3. Sharifzadeh, Z., et. al, ACS Appl. Mater. Interfaces, (2024) (just accepted).

The 30th Iranian Seminar of Organic Chemistry
February 7-9, 2025, Iran University of Science and Technology, Tehran, Iran

Synthesis and Characterization of Novel Sulfur Ligands for the Modification of Metal-Organic Framework Applications

Sara kheiroddin [a], Ali morsali*[b]
[a] *Department of Chemistry, Faculty of Sciences, Tarbiat Modares University, Tehran, Islamic Republic of Iran. Email: s.kheiroddin@modares.ac.ir.*
[b] *Department of Chemistry, Faculty of Sciences, Tarbiat Modares University, Tehran, Islamic Republic of Iran. Tel: (+98) 21-82884416; Email: morsali_a@modares.ac.ir.*

Keyword: Sulfur based linkers, Metal-Organic framework.

Introduction:

Metal-organic frameworks (MOFs) are innovative porous materials formed by metal ions or clusters linked with organic ligands. They exhibit remarkable structural diversity and high surface areas, making them valuable for various applications. Among the diverse types of MOFs, those incorporating sulfur-based ligands have gained attention due to enhanced stability and reactivity. Sulfur integration within the organic linkers modifies the frameworks' physicochemical properties, increasing their catalytic activity and broadening their potential applications, including in environmental remediation, gas storage, catalysis, energy storage, and biomedicine.[1, 2]

A notable example is HKUST-1, or Copper Benzene-1,3,5-tricarboxylate, recognized for its significant surface area and durability. Recent modifications to HKUST-1 with sulfur-containing ligands have further improved its properties, enhancing its catalytic efficiency and adsorption capabilities. This article investigates the synthesis and structural attributes of sulfur-modified HKUST-1, emphasizing its superior catalytic performance, gas adsorption, and potential in water purification and biomedical applications. The insights gained aim to leverage these advancements to tackle contemporary challenges and foster innovation across varied fields.[3-5]

Method:

Synthesis of Ligands SH-1 and SH-2: The synthesis of the sulfur-containing ligands SH-1 and SH-2 was conducted as follows: In a 100 mL round-bottom flask, 1 mmol of thiosemicarbazide (Merck, 97% purity) was dissolved in hot methanol at 80°C. Subsequently, 3 mmol of either 4-pyridine carboxaldehyde (Merck) for SH-1 or 4-methylpyridine carboxaldehyde (Merck) for SH-2 was added to the flask. The reaction mixture was refluxed at this temperature for 6 hours, during which a light yellow precipitate formed. This precipitate was collected by filtration and washed thoroughly with methanol to remove any unreacted starting materials. The purity and structural confirmation of the synthesized ligands were assessed using 1H NMR spectroscopy and infrared (IR) spectroscopy.

Preparation of HKUST-1: The synthesis of HKUST-1 was carried out following established protocols[4] with modifications for a post-synthetic ligand exchange. Initially, 300 mg of HKUST-1 was treated with 1 mL of 0.1 M HCl. Subsequently, a solution containing either SH-1 or SH-2, dissolved in 10 mL of distilled water, was added to the HKUST-1. The mixture was left to react for three days, allowing for the incorporation of the ligands into the metal-organic framework. Post-reaction, the modified HKUST-1 (referred to as HS-1 and HS-2) was thoroughly washed with distilled water and methanol to eliminate any unbound ligands. Finally, the materials were dried in a preheated oven at 80°C for 24 hours to ensure complete removal of solvents.

Result and discussion:

The synthesis of two novel sulfur linkers, designated as SH-1 and SH-2, was confirmed using ^{1}HNMR and IR spectroscopy. The ^{1}H NMR spectrum, recorded in DMSO, displayed chemical shifts at 12 ppm (1H), 10 ppm (1H), and peaks between 6-8 ppm (6H) and at 1 ppm (6H). Infrared spectroscopy revealed characteristic absorption bands at 800 cm^{-1} and around 1800 cm^{-1}, indicative of C=S functional groups. The modification of HKUST was conducted via the post-synthesis modification (PSM) approach, and the results were corroborated using ^{1}HNMR, IR spectroscopy, and thermal gravimetric analysis (TGA). The powdered X-ray diffraction (PXRD) patterns of HS-1 and HS-2 exhibited a remarkable similarity to the simulated PXRD pattern of the synthesized HKUST, confirming that the crystal structure and packing of the HKUST framework remain stable after the incorporation of the second linker. The TGA analysis of HS-1 and HS-2 identified four distinct weight-loss steps. The first step was attributed to the release of encapsulated solvents, such as methanol and water, from the pores. The second step corresponded to the loss of the introduced linkers (SH-1 and SH-2), while the third step involved the degradation of the BTC linker, and the final step was linked to the metal cluster decomposition. Utilizing sulfur linkers in the HKUST metal-organic framework significantly enhanced the adsorption capacity for heavy metals, including Hg^{2+} and Pb^{2+}. This increase in adsorption efficacy was demonstrated through UV-Vis spectrophotometric analysis conducted over time intervals of 1, 3, and 5 hours.

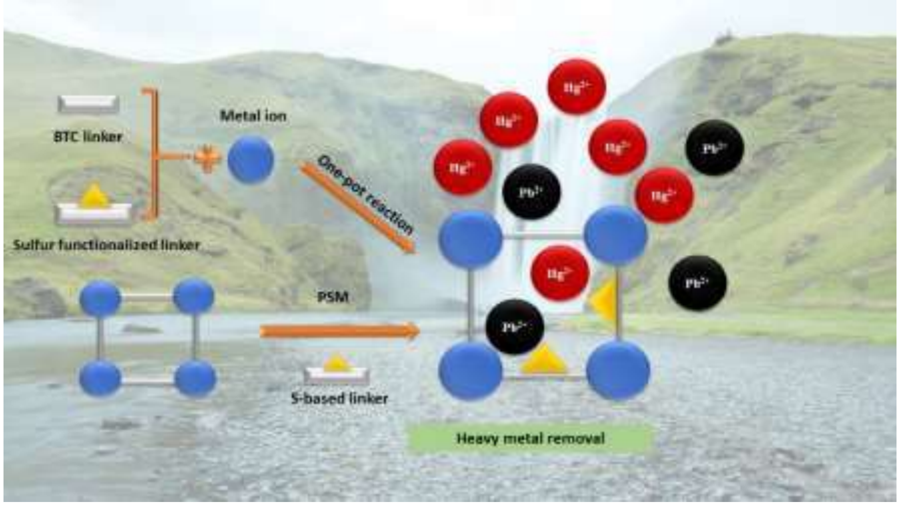

References:

١. Morales, E. M. C.; Méndez-Rojas, M. A.; Torres-Martínez, L. M.; Garay-Rodríguez, L. F.; López, I.; Uflyand, I. E.; Kharisov, B. I., Ultrafast synthesis of HKUST-1 nanoparticles by solvothermal method: Properties and possible applications. *Polyhedron* **2021,** *210*, 115517.

٢. Vishnyakov, A.; Ravikovitch, P.; Neimark, A.; Bülow, M.; Wang, Q. M., Nanopore Structure and Sorption Properties of Cu−BTC Metal−Organic Framework. *Nano Letters (2003 AiChE Annual Meeting)* **2003,** *3*, 713-718.

٣. Chen, Y.; Mu, X.; Lester, E.; Wu, T., High efficiency synthesis of HKUST-1 under mild conditions with high BET surface area and CO2 uptake capacity. *Progress in Natural Science: Materials International* **2018,** *28* (5), 584-589.

٤. Abou-Elyazed, A. S.; Ftooh, A. I.; Sun, Y.; Ashry, A. G.; Shaban, A. K. F.; El-Nahas, A. M.; Yousif, A. M., Solvent-Free Synthesis of HKUST-1 with Abundant Defect Sites and Its Catalytic Performance in the Esterification Reaction of Oleic Acid. *ACS Omega* **2024,** *9* (36), 37662-37671.

٥. Yuan, B.; Yin, X.-Q.; Liu, X.-Q.; Li, X.-Y.; Sun, L.-B., Enhanced Hydrothermal Stability and Catalytic Performance of HKUST-1 by Incorporating Carboxyl-Functionalized Attapulgite. *ACS Applied Materials & Interfaces* **2016,** *8* (25), 16457-16464.

The 30th Iranian Seminar of Organic Chemistry
February 7-9, 2025, Iran University of Science and Technology, Tehran, Iran

Synthesis and Characterization of a Novel and Efficient Magnetic Catalyst for Biodiesel Production

Fatemeh Salehi, Arash Ghorbani-Choghamarani*, Arezo Monem

Department of Organic Chemistry, Faculty of Chemistry and Petroleum Science, Bu-Ali Sina University, Hamedan, 6517838683, Iran, a.ghorbani@basu.ac.ir or arashghch58@yahoo.com , salehi99f@gmail.com , arezomonem@yahoo.com

Keyword: Biodiesel, Heterogeneous Catalysis, Magnetic nanoparticles, Esterification, Oleic acid, palmitic acid, and myristic acid

Due to global concerns about energy demand and environmental problems caused by fossil fuels, researchers are looking for clean and renewable biofuels. Biodiesel is known as one of the most important of these fuels, which has attracted much attention due to its biodegradability and ability to reduce greenhouse gas emissions. This fuel is produced through the transesterification reaction of vegetable oils or animal fats with alcohol and is usually carried out in the presence of acid, base, or enzyme catalysts [1]. Magnetic heterogeneous catalysts have many advantages over homogeneous catalysts. These nanoparticles are well dispersed in solution in the absence of an external magnetic field and provide a large surface area for the access of reactant molecules. Also, the easy separation of these catalysts is another advantage [2]. In this regard, a new and environmentally friendly magnetic nanocatalyst ($SrFe_2O_4$) was synthesized and characterized by various techniques. High activity under mild conditions and simple recovery from the reaction are suitable features of this magnetic heterogeneous catalyst (Scheme 1), The yield of methyl ester products with a catalyst amount of 0.03 in various derivatives is between 77 and 86 percent.

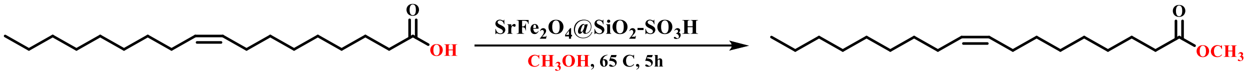

Scheme 1. Esterification of Oleic Acid

References:

1. Ghorbani-Choghamarani, A., Taherinia, Z., & Tyula, Y. A. (2022). Efficient biodiesel production from oleic and palmitic acid using a novel molybdenum metal–organic framework as efficient and reusable catalyst. Scientific Reports, 12(1), 10338.

2- Khanmohammadi-Sarabi, F., Ghorbani-Choghamarani, A., Aghavandi, H., & Zolfigol, M. A. (2023). l-Methionine-Zr complex supported on magnetic ZnFe 2 O 4 as a novel, green, and efficient heterogeneous magnetic nanocatalyst for the synthesis of 1 H-tetrazole and polyhydroquinoline derivatives. New Journal of Chemistry, 47(9), 4252-4266.

The 30th Iranian Seminar of Organic Chemistry
February 7-9, 2025, Iran University of Science and Technology, Tehran, Iran

Synthesis and characterization of a magnetic catalyst based on tin ferrite and its application in cross-coupling reactions

Hadis Jalili, Arash Ghorbani-Choghamarani*, Arezo Monem

Department of Organic Chemistry, Faculty of Chemistry and Petroleum Science, Bu-Ali Sina University, Hamedan, 6517838683, Iran, a.ghorbani@basu.ac.ir or arashghch58@yahoo.com, hadisjalili1377@gmail.com, arezomonem@yahoo.com

Keywords: Heterogeneous Catalysis, magnetic nanoparticles, $SnFe_2O_4$, Suzuki reaction

In recent years, magnetic nanocatalysts have become increasingly important and are recognized as an excellent option for catalyst immobilization. These magnetic nanocatalysts have various applications, including serving as adsorbents for dyes and pollutants in wastewater, acting as drug carriers, and being used as catalysts in various organic reactions [1]. In this project, we focused on the magnetic nanocatalyst $SnFe_2O_4$ and its application in cross-coupling reactions. Cross-coupling reactions, such as the Suzuki and Stille reactions, are considered fundamental methods in modern synthetic organic chemistry. These reactions have a wide range of applications in both academic and industrial fields, particularly in the production of drugs, pesticides, chemicals, polymers, liquid crystal materials, and advanced materials [2,3]. This project aims to address the challenges associated with the synthesis of biphenyl compounds through cross-coupling reactions, such as long reaction times, low yields, and the necessity of organic solvents for catalyst separation. By utilizing the proposed catalyst, we hope to overcome these issues. Heterogeneous palladium nanocatalysts immobilized on tin ferrite magnetic nanoparticles were characterized by various techniques such as FT-IR, TGA-DSC, EDX, ICP-OES, Elemental Mapping, SEM, TEM, and VSM. (Scheme 1).

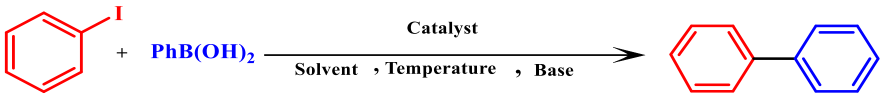

Scheme: Suzuki reaction

References:

١. Khanmohammadi-Sarabi, F., Ghorbani-Choghamarani, A., Aghavandi, H., & Zolfigol, M. A. (2022). ZnFe2O4@ SiO2-ascorbic acid: Green, magnetic, and versatile catalyst for the synthesis of chromeno [2, 3-d] pyrimidine-8-amine and quinazoline derivatives. *Applied Organometallic Chemistry*, *36*(8), e6768.

٢. Ghorbani-Choghamarani, A., Tahmasbi, B., & Moradi, P. (2016). Palladium–S-propyl-2-aminobenzothioate immobilized on Fe3O4 magnetic nanoparticles as catalyst for Suzuki and Heck reactions in water or poly (ethylene glycol). *Applied Organometallic Chemistry*, *30*(6), 422-430.

٣. Hajipour, A. R., & Rafiee, F. (2015). Dimeric ortho-palladated complex of 2, 3-dimethoxybenzaldehyde oxime catalyzed Suzuki–Miyaura cross-coupling reaction under microwave irradiation. *Journal of the Iranian Chemical Society*, *12*, 1177-1181.

Preparation and application of Deep Eutectic Solvents based on valine as a new and capable catalyst in the synthesis of *N*-heterocycles

Nastaran Dehnokhalaji, Davood Habibi *, Arezo Monem, Afagh Ranjbaran

Department of Organic Chemistry, Faculty of Chemistry and Petroleum Science, Bu-Ali Sina University, Hamedan, Iran, nastaran.dehnokhalaji78@gmail.com, davood.habibi@gmail.com, arezomonem@yahoo.com, afaghranjbaran@gmail.com

Keywords: Natural Deep Eutectic Solvents, Homogeneous Catalysis, multicomponent reactions

Deep eutectic solvents consist of a hydrogen bond donor (HBD) and a hydrogen bond acceptor (HBA) component that can be used as catalysts in reactions. The use of deep eutectic solvents as acid catalysts has several advantages, including non-toxicity, catalytic activity similar to or higher than that of the acid itself, and the possibility of recovery and reuse without significant loss of activity. If both components of the DES are from natural sources, they are called Natural Deep Eutectic Solvents (NADES). NADES are mainly formed by natural molecules such as amino acids, primary metabolites such as sugars, or organic acids through the complexation of HBA and HBD [1-2]. In this project, a cheap, simple, and non-toxic method for the synthesis of benzo[4,5]thiazolo[3,2-a]-pyrimidin derivatives was considered using a NADES catalyst. The structure and properties of the NADES catalyst were investigated by FT-IR, TGA/DTA, condensation, eutectic point, and ^{1}HNMR. Among the advantages presented by this study, we mention the reaction in solvent-free conditions (reduction of pollution), short reaction time, high productivity, easy recycling and separation of the catalyst, as well as high selectivity (Scheme 1).

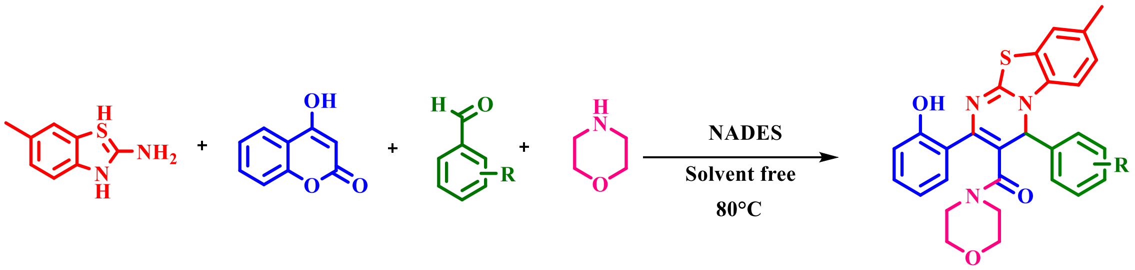

Scheme 1. Synthesis of derivatives of benzo[4,5]thiazolo[3,2-a]-pyrimidin

References:

١- Liu, Y., Friesen, J. B., McAlpine, J. B., Lankin, D. C., Chen, S. N., & Pauli, G. F. (2018). Natural deep eutectic solvents: properties, applications, and perspectives. Journal of natural products, 81(3), 679-690.
٢- Procentese, A., Johnson, E., Orr, V., Campanile, A. G., Wood, J. A., Marzocchella, A., & Rehmann, L. (2015). Deep eutectic solvent pretreatment and subsequent saccharification of corncob. Bioresource technology, 192, 31-36.

The 30th Iranian Seminar of Organic Chemistry
February 7-9, 2025, Iran University of Science and Technology, Tehran, Iran

Porous Carbon Derived From Solid Waste Of Sesame For The Degradation Of Pollutants In Aquatic Environments.

Mina Sadat Hosseini Geshnigani [a], Nadiya Koukabi[*a], Eskandar Kolvari*[a], Kheibar Dashtian[*b]

[a] *Department of Chemistry, Semnan University, 35131-19111 Semnan, Iran*

[b] *Department of Chemistry, Iran University of Science and Technology, Tehran 16846- 13114, Iran*

[*] *E-mail:* n.koukabi@semnan.ac.ir, kolvari@semnan.ac.ir, kdasht68@gmail.com

Keyword: Activated carbon, Biomass, Photocatalyst, Wastewater Treatment

The degradation of pharmaceutical pollutants, such as oxytetracycline hydrochloride (OTC), in aqueous environments has become a pressing environmental concern. OTC, a frequently used antibiotic, can persist in water bodies, posing risks to aquatic life and human health[1].Among various techniques,utilizing porous carbon materials derived from biomass for drug degradation has garnered significant attention due to their extensive surface area, customizable pore structure, and eco-friendly attributes[2]. Biomass,being a renewable and plentiful resource, presents a promising starting point for the creation of functional carbon materials. Converting agricultural waste into useful products addresses waste management issues while also promoting the circular economy[3]. In recent times, different biomass sources have been investigated for the generation of activated carbon, such as tea waste, wood, sesame residue and agricultural byproducts[4]. Sesame (Sesamum indicum) is a primary oil crop widely cultivated in various regions, resulting in substantial quantities of residual biomass in the form of leaves and stems. Currently, these by-products are often discarded or incinerated, which not only contributes significantly to environmental pollution but also represents a considerable waste of valuable resources. Notably, the discarded sesame biomass is rich in cellulose, hemicellulose, and lignin. Consequently, utilizing sesame straw to develop high-performance biomass-based adsorbents for the removal of antibiotics from water presents a significant opportunity. Such an approach would provide an economical and effective raw material for water purification efforts. The preparation of porous carbon from biomass generally entails carbonization and then activation. The chemical activation process that follows, frequently using potassium hydroxide (KOH), improves the porosity and surface area of the carbon material[5]. Recent studies have demonstrated that biomass-derived porous carbons exhibit significant adsorption and catalytic properties, making them suitable for wastewater treatment application [6].

In this method, pre-carbonization is conducted in conjunction with activation using potassium hydroxide (KOH). The powdered sesame residue is subjected to direct flame exposure, after which the resultant carbonized material is collected. Following this, the carbonized material undergoes activation with KOH. The mixture is then heated within a horizontal tube under a nitrogen atmosphere to facilitate the activation process. Finally, the activated material is immersed in 1 M hydrochloric acid (HCl), washed with distilled water to remove potassium species, and subsequently dried in an oven to yield the final activated carbon product[7].

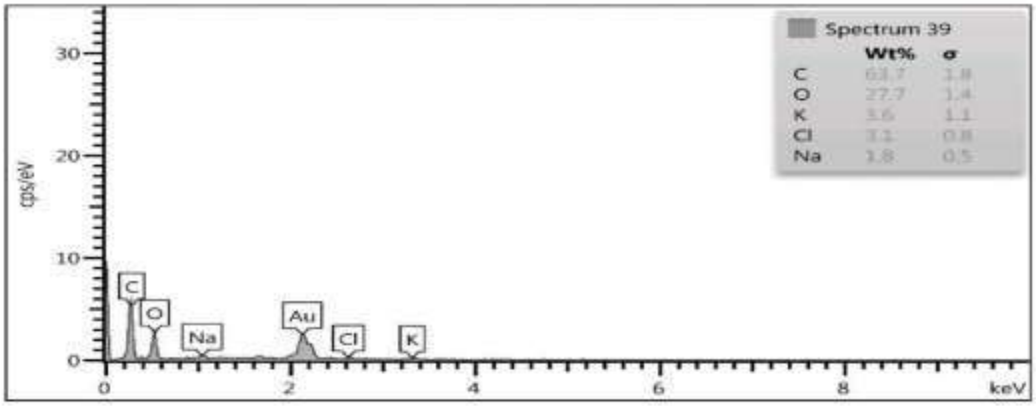

Scheme 1 : EDX spectrum of Sesame residue -Derived

The EDX analysis shows thats Sesame residue -Derived consist of organic materials with a high percentage of carbon and oxygen.

References:

1. Ding, H., et al., *Biomass porous carbon as the active site to enhance photodegradation of oxytetracycline on mesoporous g-C3N4.* RSC Advances, 2022. **12**(3): p. 1840-1849.
2. He, H., et al., *Functional carbon from nature: biomass-derived carbon materials and the recent progress of their applications.* Advanced science, 2023. **10**(16): p. 2205557.
3. Villora-Picó, J.J., et al., *Renewable Carbonaceous Materials from Biomass in Catalytic Processes: A Review.* Materials, 2024. **17**(3): p. 565.
4. Qu, X., et al., *A Simple Route to Produce Highly Efficient Porous Carbons Recycled from Tea Waste for High-Performance Symmetric Supercapacitor Electrodes.* Molecules, 2022. 27(3): p. 791.
5. Zhang, Y., L. Cheng, and Y. Ji, *A novel amorphous porous biochar for adsorption of antibiotics: Adsorption mechanism analysis via experiment coupled with theoretical calculations.* Chemical Engineering Research and Design, 2022. **186**: p. 362-373.
6. Son, B.T., N.V. Long, and N.T.N. Hang, *The development of biomass-derived carbon-based photocatalysts for the visible-light-driven photodegradation of pollutants: a comprehensive review.* RSC advances, 2021. **11**(49): p. 30574-30596.
7. Qu, X., et al., *Effect of different pretreatment methods on sesame husk-based activated carbon for supercapacitors with aqueous and organic electrolytes.* Journal of Materials Science: Materials in Electronics, 2019. **30**: p. 7873-7882.

The 30th Iranian Seminar of Organic Chemistry
February 7-9, 2025, Iran University of Science and Technology, Tehran, Iran

Sulfonated Fe_3O_4 magnetic nanoparticles as recoverable catalyst for efficient synthesis of various pyrazole derivatives

Seyed Mohammad Taghi Mousavi, Akbar Mobaraki*, Mahdi Pirasteh, Azizollah Habibi*

1) Department of Organic and Polymer Chemistry, Faculty of Chemistry, Kharazmi University, Tehran, 49 Mofateh St., Tehran, IRAN, P. O. Box 15719-14911. 2) Department of Organic and Polymer Chemistry Faculty of Chemistry, Kharazmi University, Daneshgah Square, Shahid Beheshti Street, Karaj, IRAN P. Code 31979-37551, E-mails: akbar.mobaraki@khu.ac.ir and habibi@khu.ac.ir

Keyword: Fe_3O_4 magnetic nanoparticles, pyrazole, reusability

Incorporating a polymer coating onto Fe_3O_4 magnetic nanoparticles significantly enhances their surface characteristics for application in catalytic systems.[1] In this study, a novel core-shell solid acid featuring a magnetic core and a sulfonated polymeric shell, Mag-$BuSO_3H$, has been effectively designed, characterized, and synthesized. The Mag-$BuSO_3H$ solid acid exhibits good to excellent catalytic performance for the synthesis of various pyrazole derivatives in ethanol at room temperature as showed below. The synthesized solid acid can be easily separated from the reaction medium using a permanent magnet, allowing for its recovery and reuse. The innovative structure of the Mag-$BuSO_3H$ solid acid may also be utilized to develop other green and reusable catalytic systems.

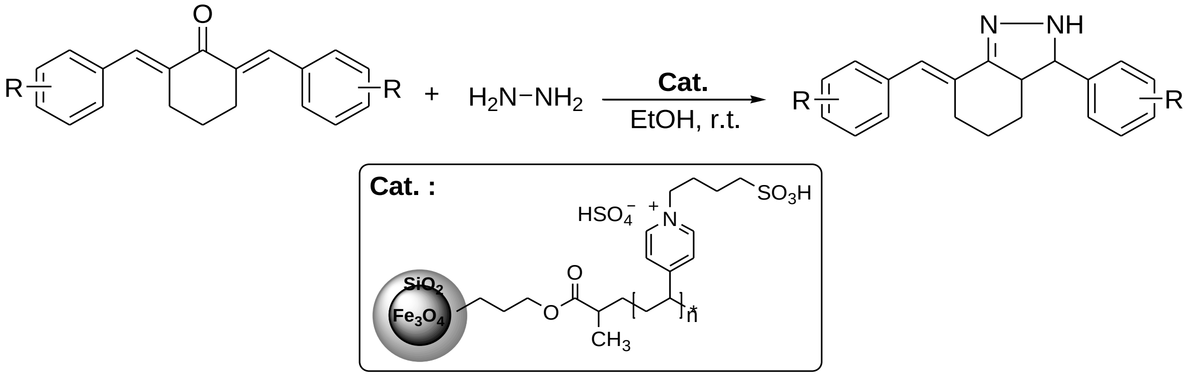

References

[1] Wang X., Wang L., Sun B., Chu X., Xing X., Liu Sh., Tang E. *J. Appl. Polym. Sci.* **2020**, e49992.

[2] Yu J, Wang Y, Sun L, Xu Z, Du Y, Sun H, Li W, Luo S, Ma C, Liu S. *ACS omega*. **2021** ;6(11):7896-909.

The 30th Iranian Seminar of Organic Chemistry
February 7-9, 2025, Iran University of Science and Technology, Tehran, Iran

Design and Investigation of a Porphyrin Dye-sensitized Solar Cell

Authors: Fatemeh Sepehrpoor, Zohreh Ahmadiyeh, Rahmatollah Rahimi, Mohammad-Reza Zamani-Meymian, Karim Khanmohammadi, Mohammad-Sadegh Asgari

Corresponding authors: Zohreahmadiyeh77@gmail.com, Rahimi_Rah@iust.ac.ir

Abstract-In this study, a dye-sensitized solar cell (DSSC) was designed based on porphyrin dye and ZnO nanomaterial. The porphyrin dye was analyzed using UV/Vis and FTIR spectroscopy, which indicated the successful synthesis of porphyrin dye. A crystalline layer of ZnO was deposited on the surface of fluorine-doped tin oxide (FTO) transparent conductive oxide (TCO) substrate and the obtained results show that the porphyrin dye can be used as a sensitizer in the fabricated dye-sensitized solar cell due to appropriate anchoring functional groups, donor and acceptor in its molecular structure.

Keywords: dye, porphyrin, solar cell, zinc oxide

1. Introduction

The industrialization of advanced countries, imposes the demand for fossil fuels to be replaced with renewable energy sources, and need for their application in societies is increasing, rapidly. The photovoltaic cells as an electronic component that converts sunlight photons to electricity directly, work based on the photovoltaic effect which in their third generation, dye-sensitized solar cells (DSSCs), have attracted considerable attention due to their cheap manufacturing processing[1]. The operation of the solar cell begins with the absorption of light and continues with the separation of the opposite charge carriers and the flow of the carriers in the external circuit[2]. Organic and organometallic sensitizers provide cheaper and easier synthesizing opportunities. For these dyes with main advantages such as high molar extinction coefficients, simple modeling, and easy synthesis, easily adjustable adsorption energies, the ability to integrate into thin solid-state electrolyte cells, and low cost. A large number of organic sensitizers have been studied for DSSCs, the most promising of which are coumarins, porphyrins, and indoline dyes. Among them, the molecular structure of a porphyrin dye consists of four meso and eight beta positions, which can serve to function as one or more linkers containing carboxylic acids that play as anchors to the surface[3]. Applying ZnO nanoparticles as less toxic n-type semiconductor materials as substrates for dye sensitization, and wide band gaps have been at the core of interests of fabrication DSSCs [4]. In this work, the DSSCs were fabricated following instructions as:1) Photoanode, which consists of a semiconductor such as TiO_2 or ZnO placed on a conductive glass substrate. 2) porphyrin dye as a sensitizer 3) Iodide/triiodide electrolyte, 4) A counter electrode like platinum-coated FTO sheets[5].

2. Experimental

2.1.Preparation of [5,10,15,20-Tetrakis(4-carboxyphenyl)porphyrinato]-Fe(III) Chloride

The obtained ester (0.75 g) was stirred in THF (25 mL) and MeOH (25 mL) mixed solvent, to which a solution of KOH (2.63 g, 46.95 mmol) in H2O (25 mL) was introduced. This mixture was refluxed for 12 h. After cooling down to room temperature, THF and MeOH were evaporated. A solution of TCPP 0.854 g (1.0 mmol) and FeCl2·4H2O (2.5 g, 12.8 mmol) in 100 mL of DMF was refluxed for 6 h. After the mixture was cooled to room temperature, 150 mL of H2O was added. The resultant precipitate was filtered and washed with 50 mL of H2O for two times. The obtained solid was dissolved in CHCl3, followed by washing three times with 1 M HCl and twice with water. The organic layer was dried and evaporated to afford quantitative dark brown crystals[6].

2.2. Preparation of ZnO

Dissolve 3.7 grams of zinc acetate dihydrate in 350 ml of distilled water and stir for 10 minutes. Add 2.8 g of hexamine and 0.09 g of sodium citrate to the solution and stir for 1 h. Place the solution in a water bath at 90°C for 6 hours until a white precipitate of zinc oxide nanoparticles is formed. Wash the sediments five times with ethanol and dry them in an oven at 60°C for 12 h[7].

3. Results and discussion

3.1. Energy Conversion Efficiency

The overall solar conversion efficiency (η) represents the amount of incident radiation the device can convert into electrical power. Equation (1) reports the most commonly known expression of the overall conversion efficiency for Dye-sensitized solar cells: (1)$\eta=(J_{sc}.V_{oc}.FF)/Pin$ where J_{sc} is the photocurrent produced per unit area (mA cm^{-1}) under illumination, at shortcircuit conditions, while V_{oc} is the potential difference between the quasi-Fermi level of the semiconductor and the redox couple at open-circuit conditions. FF, the fill factor, expresses the relative area between an imaginary rectangle representing the maximum power obtainable from the cell in ideal conditions, and the one drawn to get the maximum area inside the real J-V curve. According to Figure 1 and the mentioned formula, the energy conversion efficiency of the solar cell is equal to 0.095%.

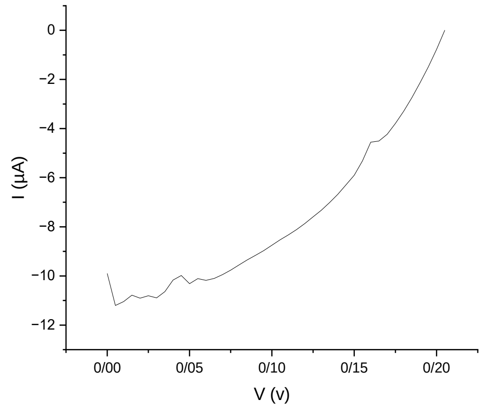

Fig. 1: I–V curve of the Fe-TMCPP Porphyrin-based DSSC

3.2.UV/Vis spectroscopy

The UV-Vis spectrum of Fe-TMCPP (Figure. 2) demonstrates significant peak shifts compared to the metal-free porphyrin, reflecting changes in the electronic structure upon metalation. The variations in peak intensity and the emergence of new features (as highlighted in Figure 2) indicate enhanced electronic transitions and altered molecular symmetry due to Fe(III) coordination.

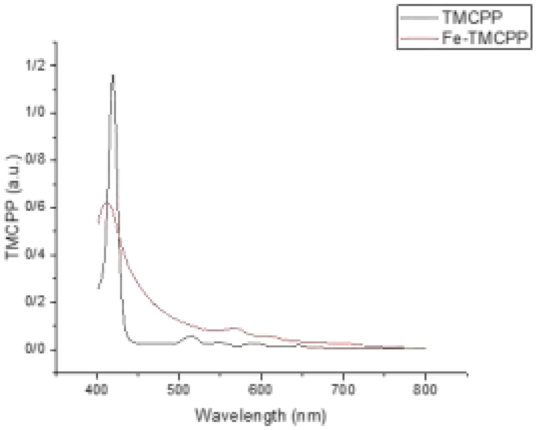

Figure. 2: UV-Vis absorption spectra of TMCPP (black line) and Fe-TMCPP (red line). The comparison illustrates the spectral differences.

3.3.FT-IR spectrum

The FT-IR spectrum of Fe-TMCPP (Figure. 3) is expected to exhibit shifts in porphyrin core vibrations (C=C and C=N at 1500–1600 cm^{-1}) and broadening of carboxylic acid O–H and C=O bands (2500–3300 cm^{-1} and 1700–1750 cm^{-1}). Metal-ligand interactions (Fe–N) likely appear below 600 cm^{-1} (see Figure 3), confirming the successful incorporation of Fe(III).

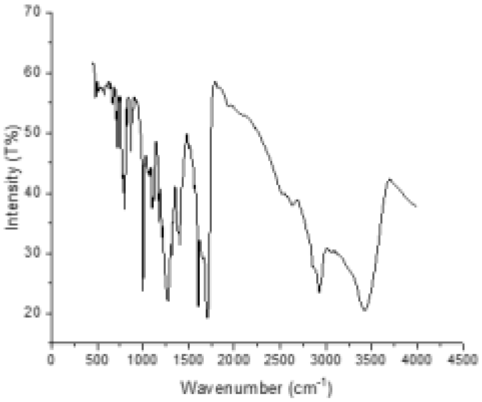

Figure. 3: FT-IR spectrum of Fe-TMCPP

Conclusion

This paper investigates the use of Fe-TMCPP porphyrin as DSSC and the results show that these porphyrin dyes can be used as a sensitizer with appropriate photovoltaic parameters such as short-circuit current, open-circuit voltage, and power conversion efficiency.

References:

[1]. Zeng, K., et al., Molecular engineering strategies for fabricating efficient porphyrin-based dye-sensitized solar cells. Energy & Environmental Science, 2020. 13(6): p. 1617-1657.

[2]. Bagher, A.M., M.M.A. Vahid, and M. Mohsen, Types of solar cells and application. American [3].

[3]. Li, L.-L. and E.W.-G. Diau, Porphyrin-sensitized solar cells. Chemical society reviews, 2013. 42(1): p. 291-304.

[4]. Huang, J., Z. Yin, and Q. Zheng, Applications of ZnO in organic and hybrid solar cells. Energy & Environmental Science, 2011. 4(10): p. 3861-3877.

[5]. Birel, Ö., S. Nadeem, and H. Duman, Porphyrin-based dye-sensitized solar cells (DSSCs): a review. Journal of fluorescence, 2017. 27: p. 1075-108.

[6]. Feng, D., Gu, Z. Y., Li, J. R., Jiang, H. L., Wei, Z., & Zhou, H. C. (2012). Zirconium-metalloporphyrin PCN-222: mesoporous metal–organic frameworks with ultrahigh stability as biomimetic catalysts. Angewandte Chemie-International Edition, 51(41), 10307.

[7]. Noor, S., Sajjad, S., Leghari, S. A. K., Shaheen, S., & Iqbal, A. (2018). ZnO/TiO2 nanocomposite photoanode as an effective UV-vis responsive dye sensitized solar cell. Materials Research Express, 5(9), 095905.

The 30th Iranian Seminar of Organic Chemistry
February 7-9, 2025, Iran University of Science and Technology, Tehran, Iran

A new adsorbent for Uranium removal from water samples using a high energy method

Omid Sarafraz[a], Abdolhamid Bamoniri[a*], Bi Bi Fatemeh Mirjalili[b], Reza Hafezi Moghaddam[c]

a) Department of Organic Chemistry, Faculty of Chemistry, University of Kashan, Kashan, Iran

b) Department of Organic Chemistry, College of Science, Yazd University, Yazd, Iran

c) Central Iran Research Complex, Iran Radiation Application Development Company, Atomic Energy Organization of Iran, Tehran, Iran.

Keywords: Hydrogel, Composite polymers, Electron beam iiradiation, Removal of pollutants

Abstract

A biocompatible hybrid hydrogel adsorbent was prepared by chemically grafting aspartic acid (AA) with pectin (Pc) and hybridizing it with polyacrylic acid (PAAc) using a high-energy electron irradiation method[1-3]. The chemical structure of the hybrid hydrogel was evaluated through FTIR, SEM, EDX, TGA and XRD. The ability of hydrogels to recover uranium from aqueous solutions was investigated. The results of this work introduced a new efficient adsorbent with biocompatibility and biodegradability properties for the practical applications of removing uranium from aqueous wastes.

Introduction

There are various techniques to remove various organic and inorganic pollutants from water resources such as surface adsorption, membrane filtration, flocculation/coagulation, biological processes, electrolysis, photochemical degradation, chemical precipitation and oxidation processes. Among the mentioned methods, the surface adsorption method is a suitable and more effective method than other methods due to its low cost, simple operator and higher selectivity. Considering the ability to absorb heavy metals by the synthetic polymer polyacrylic acid (PAAc), in this study, it was tried to use this synthetic polymer to prepare a hybrid hydrogel with a semi-IPN structure. In the present study, grafting of this amino acid with pectin was used in order to increase the capacity of uranium adsorption. In the next step, by hybridizing it with PAAc, a new hybrid hydrogel was synthesized with the help of electron irradiation method and its ability to remove uranium from aqueous environments was used.

Results and discussions

The use of biopolymers such as pectin to prepare hydrogel absorbents increases their biodegradability and biocompatibility properties, and due to their abundance and availability, cheap hydrogel absorbents can be prepared with them. Pc is one of the biopolymers of anionic polysaccharides, which has many acidic, ester and alcoholic functional groups. Therefore, it can easily react with various chemical reagents. the preparation of hydrogel based on pure biopolymer using high-energy electron irradiation method leads to breaking of polymer chains and failure to form hydrogel macromolecule structure. One of the ways to solve this problem is to hybridize biopolymer with synthetic polymers. Considering the high adsorption capacity of heavy metals by PAAc synthetic polymer, in this study, it was tried to use this polymer to prepare hybrid hydrogel. Therefore, AA-grafted pectin (Pc-AA) was mixed with PAAc and subjected to electron irradiation, and a new hydrogel with a porous structure was obtained to remove uranium (VI) ions from aqueous samples. This process is shown schematically in (Fig. 1). To confirm the successful grafting of AA with Pc and also the formation of Pc-AA/PAAc hydrogel, FTIR spectra of hybrid hydrogel components were prepared (Fig. 2).

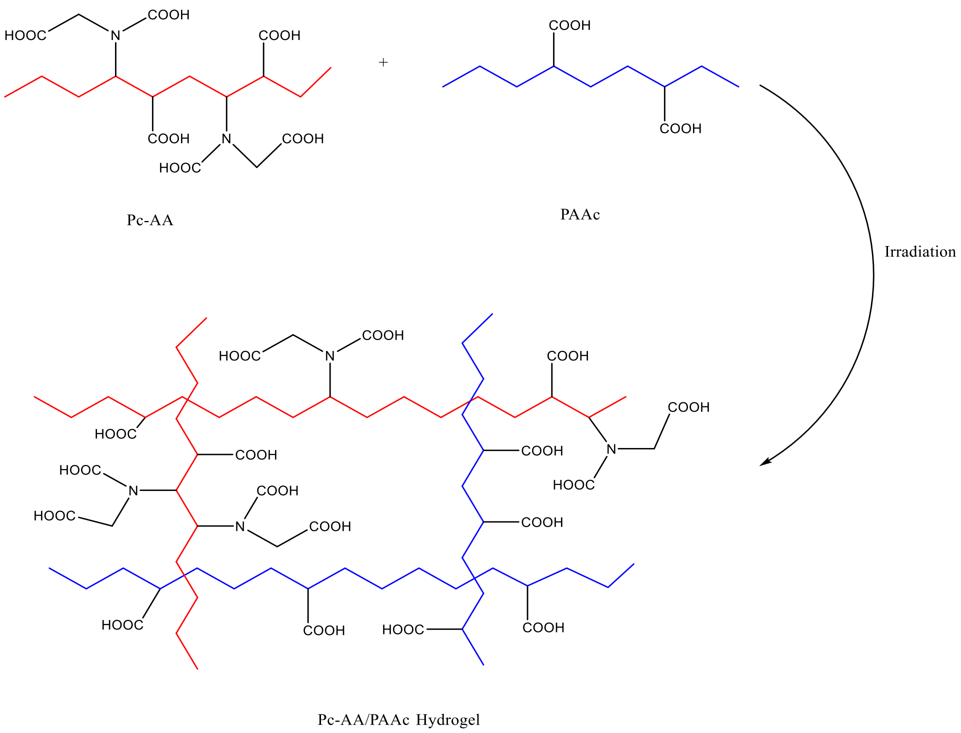

Fig. 1. Formation of hybrid hydrogel by irradiation method.

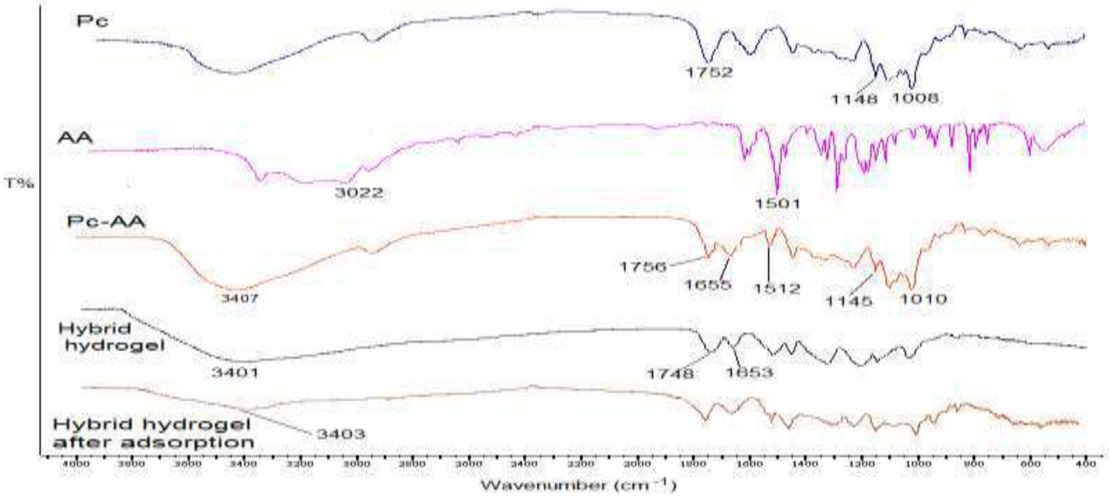

Fig. 2. FT-IR spectra of Pc, AA, Pc-AA, Pc-AA/PAAc hybrid hydrogel, and hybrid hydrogel after uranium adsorption.

References

[1] U. S. K. Madduma Bandarage, S. V. Madihally, Synthetic hydrogels: Synthesis, novel trends, and applications, *J. Appl. Polym. Sci*., **2021**, 138, 503756.

[2] M. Zhou, S. Wang, M. Qiu, B. Hu, G. Wang, Y. Lu, Recent advances in the removal of U(VI) by magnetic metal oxides, *J. Mol. Liq*., **2023**, 385, 122295.

[3] Y. Tian, Y. Wang, C. Wang, G. Zhu, L. Liu, F. Ma, H. Dong, W. Zhang, Highly efficient adsorbent for removing uranium (VI) from water based on a novel phosphate esterification hyper-cross-linked polymer, *J. Mol. Liq*., **2023**, 386, 122431.

The 30th Iranian Seminar of Organic Chemistry
February 7-9, 2025, Iran University of Science and Technology, Tehran, Iran

A novel and efficient Heterogeneous bimetallic Mn–Co Catalyst for Three-Component Coupling Synthesis of Propargylamines

Mansoore shahabi*[a], Mohammad ali nasseri[a], Seyyedeh Ameneh Alavi G [a]

[a] *Department of Chemistry, College of Sciences, University of Birjand, Birjand, Iran*

Abstract

Fe_3O_4@SiO_2@Cyt-Mn/Co as a novel heterogeneous bimetallic nanocatalyst was successfully synthesized and characterized by different techniques. It was catalyzed the three-component coupling synthesis of propargylamines with high yields in short reaction times and solvent-free conditions.

Keyword: Heterogeneous, bimetallic, Propargylamines

Introduction

Recently, the heterogeneous catalysts in the form of magnetic nanoparticles (MNPs) have attracted considerable attentions due to their unique properties such as ease of availability, high accessible surface area and excellent thermal stability [1-2]. In addition, these magnetic nanoparticles strongly response to magnetic field and efficiently recover from the reaction mixture by an external magnet. Among the numerous heterogeneous catalysts are currently known, bimetallic composites are of particular importance. Bimetallic catalysts can perform multi-step reactions in one-pot to obtain the target product with high efficiency, high selectivity, low reaction time and elimination of intermediate purification/separation step. In this regard, various bimetallic systems reported for a variety of organic reactions such as multi component, cross coupling, and domino one-pot reactions [3-7]. Recently, some heterogeneous nanoparticles have been reported as the efficient catalytic systems for the A_3-coupling reactions of aldehydes, amines, and terminal alkynes [8-11]. Propargylamines are key intermediates for the synthesis of many biologically active nitrogen molecules such as β-lactams and therapeutic drugs [11-1٣]. Moreover, some propargylamines are known to be neurodegenerative protecting groups. Rasagiline and Deprenyl are used in the treatment of dementia diseases such as the Parkinson [14-15].

Experimental

A mixture comprising aldehyde derivatives (1 mmol), secondary amines (1.5 mmol), and phenylacetylene (1.2 mmol) and Fe_3O_4@SiO_2@Cyt-Mn/Co catalyst (10 mg) under solvent-free condition was stirred vigorously at 100 ◦C (Scheme 1). As soon as the reaction was complete (monitored by TLC), the resultant mixture was diluted with EtOAc. The catalyst was easily removed using an external magnet, washed with ethanol, and dried in the oven (70 ˚C) for 12 h to use in the next run. The pure products were procured using silica gel column chromatography (hexane: EtOAc, 8:2).

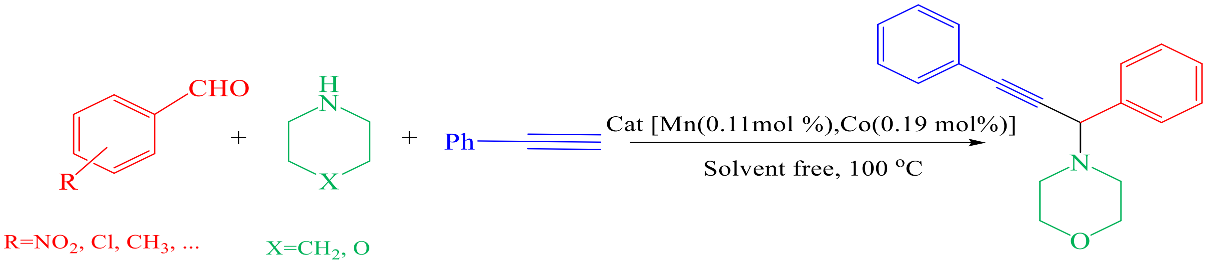

Scheme 1. The A3-coupling reaction of aldehyde, amine, and terminal alkyne.

Results and Discussion

Regarding to the advantages of bimetallic magnetic nanocomposite and their high efficiency in the synthesis of organic compounds, we synthesized a novel magnetically manganese-cobalt cytosine complex as a recoverable bimetallic magnetic nanocatalyst for the efficient A_3 coupling reactions in short reaction time (Scheme 2). The prepared catalyst was well characterized by different methods (Scheme 3). The vibrating sample magnetometer (VSM) analysis showed the behavior of magnetic bimetallic nanoparticles was sufficient to complete the separation from the mixture under an externally applied magnetic field which indicates the magnetic nature of the synthesized catalyst. The presence of the desired bands of FT-IR analysis confirmed the successful synthesis of the nanocatalyst.

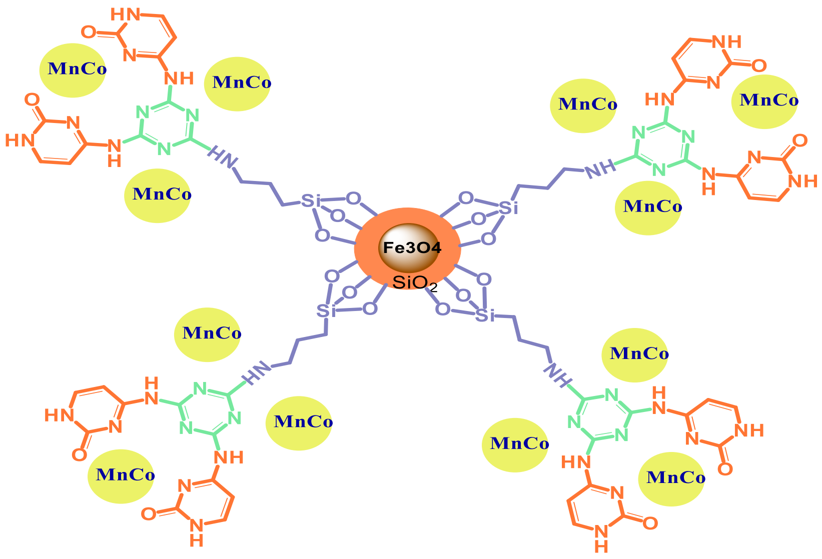

Scheme 3. Structure of $Fe_3O_4@SiO_2@Cyt\text{-}Mn/Co$ bimetallic nanocatalyst

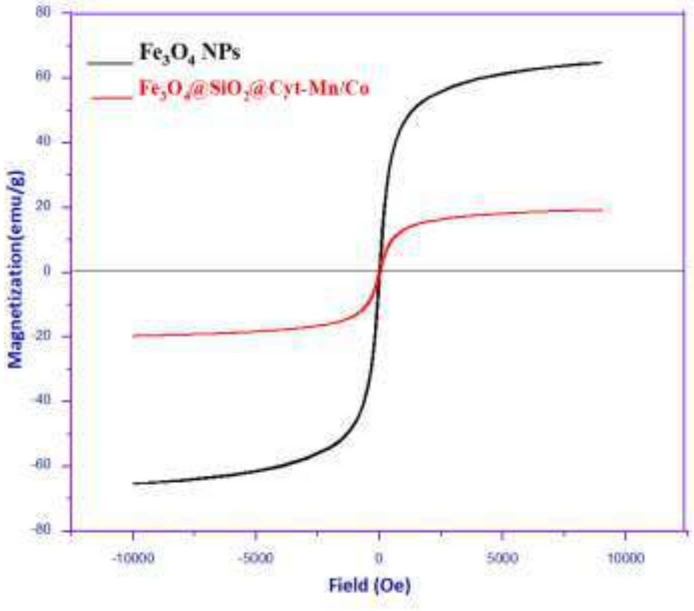

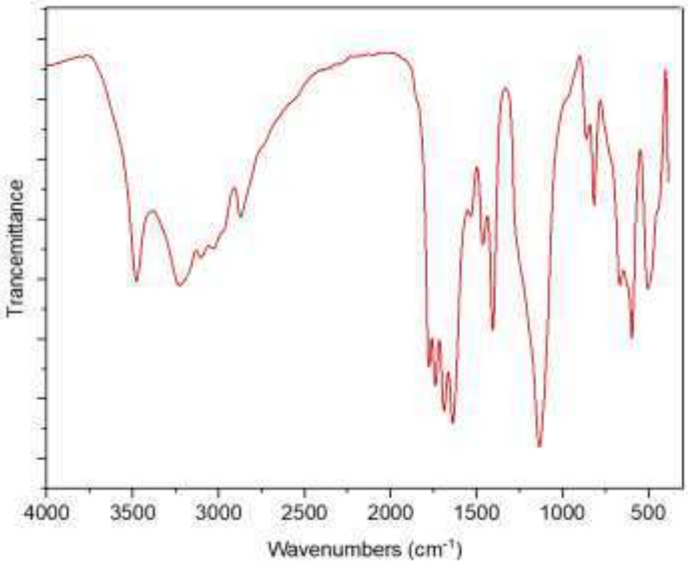

Scheme 3. VSM (left) and FTIR (right) of the Fe_3O_4@SiO_2@Cyt-Mn/Co bimetallic nanocatalyst.

References:

[1] Rezaeifard, A., Jafarpour, M., Farrokhi, A., Parvin, S., & Feizpour, F. (2016). Enhanced aqueous oxidation activity and durability of simple manganese (III) salen complex axially anchored to maghemite nanoparticles. *Rsc Advances*, *6*(69), 64640-64650.

[2] Hemmat, K., Nasseri, M. A., & Allahresani, A. (2019). CoFe2O4@ SiO2@ Co (III) salen complex: a magnetically recyclable heterogeneous catalyst for the synthesis of quinoline derivatives in water. *ChemistrySelect*, *4*(14), 4339-4346.

[3] Nemygina, N. A., Nikoshvili, L. Z., Tiamina, I. Y., Bykov, A. V., Smirnov, I. S., LaGrange, T., ... & Kiwi-Minsker, L. (2018). Au Core–Pd shell bimetallic nanoparticles immobilized within hyper-cross-linked polystyrene for mechanistic study of Suzuki cross-coupling: homogeneous or heterogeneous catalysis?. *Organic Process Research & Development*, *22*(12), 1606-1613.

[4] Chen, Y. Z., Zhou, Y. X., Wang, H., Lu, J., Uchida, T., Xu, Q., ... & Jiang, H. L. (2015). Multifunctional PdAg@ MIL-101 for one-pot cascade reactions: combination of host–guest cooperation and bimetallic synergy in catalysis. *ACS Catalysis*, *5*(4), 2062-2069.

[5] Katkar, S. V., & Jayaram, R. V. (2014). Cu–Ni bimetallic reusable catalyst for synthesis of propargylamines via multicomponent coupling reaction under solvent-free conditions. *RSC advances*, *4*(89), 47958-47964.

[6] Hou, Y. L., Sun, R. W. Y., Zhou, X. P., Wang, J. H., & Li, D. (2014). A copper (I)/copper (II)–salen coordination polymer as a bimetallic catalyst for three-component Strecker reactions and degradation of organic dyes. *Chemical Communications*, *50*(18), 2295-2297.

[7] Feng, F., Ye, J., Cheng, Z., Xu, X., Zhang, Q., Ma, L., ... & Li, X. (2016). Cu–Pd/γ-Al 2 O 3 catalyzed the coupling of multi-step reactions: direct synthesis of benzimidazole derivatives. *RSC advances*, *6*(76), 72750-72755.

[8] Kalbasi, R. J., & Khojastegi, A. (2018). Fabrication of Bimetallic Ag-Co Nanoparticle Deposited on Hierarchical ZSM-5 as a Selective Catalyst for Synthesis of Propargylamine in Water via Multicomponent A3 Coupling. *ChemistrySelect*, *3*(44), 12666-12675.

[9] Loni, M., Yazdani, H., & Bazgir, A. (2018). Gold nanoparticles-decorated dithiocarbamate nanocomposite: an efficient heterogeneous catalyst for the green A 3-coupling synthesis of propargylamines. *Catalysis Letters*, *148*, 3467-3476.

[10] Gholinejad, M., Bonyasi, R., Najera, C., Saadati, F., Bahrami, M., & Dasvarz, N. (2018). Gold nanoparticles supported on imidazole-modified bentonite: environmentally benign heterogeneous catalyst for the three-component synthesis of propargylamines in water. *ChemPlusChem*, *83*(5), 431-438.

[11] Gholinejad, M., Bonyasi, R., Najera, C., Saadati, F., Bahrami, M., & Dasvarz, N. (2018). Gold nanoparticles supported on imidazole-modified bentonite: environmentally benign

heterogeneous catalyst for the three-component synthesis of propargylamines in water. *ChemPlusChem*, *83*(5), 431-438.

[12] Bolea, I., Gella, A., & Unzeta, M. (2013). Propargylamine-derived multitarget-directed ligands: fighting Alzheimer’s disease with monoamine oxidase inhibitors. *Journal of neural transmission*, *120*, 893-902.

[13] Youdim, M. B., Kupershmidt, L., Amit, T., & Weinreb, O. (2014). Promises of novel multi-target neuroprotective and neurorestorative drugs for Parkinson's disease. *Parkinsonism & related disorders*, *20*, S132-S136.

[14] Chen, J. J., & Swope, D. M. (2005). Clinical pharmacology of rasagiline: a novel, second-generation propargylamine for the treatment of Parkinson disease. *The journal of clinical pharmacology*, *45*(8), 878-894.

[15] Bar-Am, O., Weinreb, O., Amit, T., & Youdim, M. B. (2005). Regulation of Bcl-2 family proteins, neurotrophic factors, and APP processing in the neurorescue activity of propargylamine. *The FASEB journal*, *19*(13), 1899-1901.

The 30th Iranian Seminar of Organic Chemistry
February 7-9, 2025, Iran University of Science and Technology, Tehran, Iran

One-pot synthesis of geminal dichlorides from alcohols and silyl ethers using *N*-chlorosuccinimide and chlorodiphenylphosphine

Farzaneh Kalatehseifary [a], Ghasem Aghapour *[a], Esmail Rezaei-Seresht[b]

[a] *School of Chemistry, Damghan University, Damghan 36716-41167, Iran*
[b] *Department of Chemistry, School of Sciences, Hakim Sabzevari University, Sabzevar, Iran.* **E-mail: gh_aghapour@du.ac.ir*

Keyword: Alcohol, Silyl ether, *gem*-Dichloride, *N*-Chlorosuccinimide, Chlorodiphenylphosphine

Geminal dihalides constitute a very important group in organic chemistry. These compounds have very interesting properties and applications in the fields of medicine, industry and also organic synthesis. In this connection, many important drugs containing antifungal, antibacterial or enzyme inhibitory properties have this functional group in their structures [1-2]. However, far fewer methods have been introduced for the synthesis of these valuable compounds from alcohols and especially from protected alcohols compared to aldehydes [3]. With these descriptions in this work, a one-pot, oxidative and efficient way is described for the conversion of both benzylic alcohols

and silyl ethers as protected alcohols containing electron withdrawing or donating groups in different positions of aromatic ring to *gem*-dichlorides using *N*-chlorosuccinimide (NCS) and chlorodiphenylphosphine ($ClPPh_2$) (Scheme 1). These conversions can be operated in the presence of different other functional groups such as nonbenzylic alcohol, epoxide, acetal, carboxylic ester and amid, ketone, and phenol with excellent chemoselectivity. Operation in a one-pot manner and in the neutral media, simple work up, applicability for both alcohols and protected alcohols, and excellent chemoselectivity can be considered as main advantages of the present work.

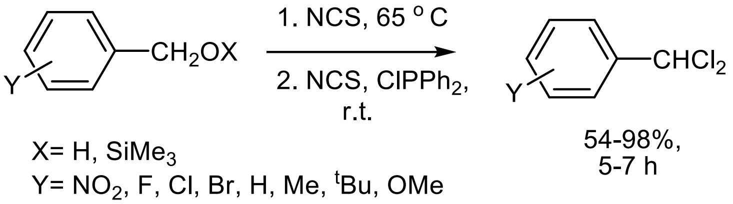

Scheme 1: Conversion of alcohols and silyl ethers to *gem*-dichlorides using NCS and $ClPPh_2$.

References:

[1] Wang, Y. B.; Chen, F.; Li, M.; Bu, Q.; Du, Z.; et al. *Green Chem*. **2023**, *25*, 1191.
[2] Li, Y.; Mou, T.; Lu, L.; Jiang, X. *Chem. Commun*. **2019**, *55*, 14299.
[3] Xiao, X.; Yao, X.; Yu, J.; Tang, T.; Xiao, C.; et al. *J. Fluorine Chem*. **2020**, *240*, 109649.

The 30th Iranian Seminar of Organic Chemistry
February 7-9, 2025, Iran University of Science and Technology, Tehran, Iran

Synthesis of a novel and efficient arginine-based NADES for the synthesis of Pyrano[2,3-d]-pyrimidine

Afagh Ranjbaran, Davood Habibi *, Arezo Monem, Nastaran Dehnokhalaji

Department of Organic Chemistry, Faculty of Chemistry and Petroleum Science, Bu-Ali Sina University, Hamedan, Iran, afaghranjbaran@gmail.com, davood.habibi@gmail.com, arezomonem@yahoo.com, nastaran.dehnokhalaji78@gmail.com

Keyword: Natural Deep Eutectic Solvents, Catalysis, multicomponent reactions

Deep eutectic solvents (DESs) are usually mixtures of two solid or liquid components that have low melting points so that they turn into liquids at room temperature. The compounds that make up these DESs include amino acids, organic acids, sugars, and quaternary ammonium and phosphonium salts. Today, chemists are looking for ways to prepare safer and more environmentally friendly compounds, which are called green compounds. Deep eutectic solvents are used in the preparation of organic compounds for the purpose of solvents and catalysts due to their capacities and capabilities.DESs are widely used due to their easy recovery and high potential for dissolving non-polar and polar compounds. these solvents have special properties that make them a reliable and safe alternative to ionic liquids and distinct organic solvents [1-3]. In this study, a new natural deep eutectic solvent (DES) based on arginine was prepared. The eutectic point phase diagram showed that the 1:1 ratio was the best molar ratio for the synthesis of this new DES. Then, NADES was characterized by FT-IR, TGA/DTA, densitometry, eutectic points, and 1 HNMR techniques and was shown to be a novel catalyst for the green synthesis of Pyrano[2,3-d]-pyrimidine derivatives via a one-pot condensation reaction of 4-hydroxycoumarin, barbituric acid and benzaldehydes at 80 °C under solvent-free conditions (Scheme 1).

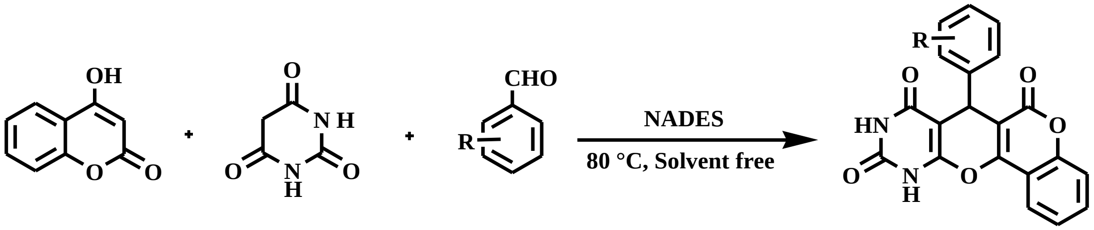

Scheme 1. Synthesis of derivatives of Pyrano[2,3-d]-pyrimidine

References:

١- Procentese, A., Johnson, E., Orr, V., Campanile, A. G., Wood, J. A., Marzocchella, A., & Rehmann, L. (2015). Deep eutectic solvent pretreatment and subsequent saccharification of corncob. Bioresource technology, 192, 31-36.

٢- Hayyan, M., Hashim, M. A., Hayyan, A., Al-Saadi, M. A., AlNashef, I. M., Mirghani, M. E., & Saheed, O. K. (2013). Are deep eutectic solvents benign or toxic?. Chemosphere, 90(7), 2193-2195.

٣- Liu, Y., Friesen, J. B., McAlpine, J. B., Lankin, D. C., Chen, S. N., & Pauli, G. F. (2018). Natural deep eutectic solvents: properties, applications, and perspectives. Journal of natural products, 81(3), 679-690.

Traditional and Modern methods of Aspirin production: challenges and opportunities

Authors: Alireza senardack

Introduction

Aspirin (acetylsalicylic acid) is one of the most widely consumed pharmaceuticals globally, playing a crucial role in alleviating pain, reducing inflammation, and preventing cardiovascular diseases. As global demand for aspirin increases, the methods of its production have come under continuous scrutiny and improvement. Traditional aspirin production methods, which have been in use for decades, are simple and cost-effective but come with numerous environmental and economic drawbacks. Modern methods, aimed at improving efficiency and reducing negative environmental impacts, have emerged. These include the use of biotechnology, green catalysts, and advanced technologies such as microwave and ultrasound methods, which not only offer higher efficiency but also have significantly less environmental impact.

Traditional Aspirin Production Methods and Their Drawback

Traditional Methods Traditional aspirin production methods primarily rely on a simple chemical reaction between salicylic acid and acetic anhydride, catalyzed by strong acids such as sulfuric or phosphoric acid. The primary reaction is as follows: This process is simple and economical on an industrial scale but has significant negative consequences. Drawbacks 1. Environmental Effects - Chemical Waste Generation: The primary byproduct of this process is acetic acid, which, if not managed properly, can pollute water and soil. - Acidic Waste Disposal: The strong acidic catalysts, when discharged in waste streams, pose severe risks to the ecological balance of surrounding areas. 2. Lower Product Quality Traditional methods often result in lower product purity due to inadequate control of reaction parameters, leading to higher purification costs in subsequent stages. 3. Reduced Global Market Competitiveness - Traditional methods, compared to modern green methods adopted in advanced countries, yield products of lower quality and efficiency. - High environmental costs reduce the competitiveness of products in international markets.

Advantages of Traditional Methods

Despite the challenges and environmental concerns, traditional methods remain widely used in many countries, including Iran, due to certain advantages: 1. Easy Access to Raw Materials - Salicylic acid and acetic anhydride are readily available and cost-effective. 2. Simple Equipment and Lower Costs - The process does not require advanced equipment or complex technologies, keeping initial production costs relatively low. 3. Meeting Domestic Market Needs - Due to its simplicity and capacity for mass production, the traditional method has successfully met the domestic market demand in Iran and other developing countries at affordable prices.

Modern Aspirin Production Methods

Higher Efficiency and Reduced Environmental Impact Modern aspirin production methods are designed to maximize reaction efficiency while minimizing waste generation. The use of advanced technologies and environmentally friendly approaches has enabled the production of aspirin with higher quality and reduced environmental impact. 1. Biosynthesis This method uses enzymes or microorganisms to produce aspirin. Biosynthesis is considered a green method because it operates under milder conditions and does not require hazardous chemicals. Advantages: - Reduced chemical waste. - Higher product purity. Challenges: - High costs of enzymes and biotechnological equipment. - Complexity in scaling up for industrial production. 2. Use of Green Catalysts Replacing traditional acidic catalysts with environmentally friendly materials, such as organic acids or nanocatalysts, reduces environmental impact. Advantages: - Decreased production of acidic waste. - Faster reactions with higher yields. 3. Advanced Techniques: Microwave and Ultrasound These methods use microwave energy or sound waves to accelerate reactions. Advantages: - Reduced reaction time. - Savings in energy and raw materials.4. European Approach to Aspirin Production European countries have achieved greater success in aspirin synthesis through the adoption of advanced technologies. Their approach emphasizes: - Renewable Energy Use: Incorporating renewable energy sources in production processes. - Emission Control: Strict regulations on greenhouse gas emissions. - Advanced Catalysts: Use of innovative catalysts for cleaner and more efficient reactions. These strategies have allowed European manufacturers to produce aspirin with minimal environmental impact and maximum efficiency.

Conslusion

Given the critical role of aspirin in the pharmaceutical industry and the need to reduce environmental impacts, replacing traditional methods with modern technologies is essential. Advanced methods such as biosynthesis, green catalysts, and cutting-edge techniques like microwave and ultrasound have demonstrated higher efficiency and reduced environmental harm. European countries serve as a successful example of integrating science and industry for sustainable production. It is imperative for Iran to invest in research, development, and technology transfer to improve its aspirin production processes and align with global standards.

Reference:

CDC.WHO.GlaxoSmithklinne.sanofi.شرکت داروسازی دانا   شرکت داروسازی تهران حکیم.١

The 30th Iranian Seminar of Organic Chemistry
February 7-9, 2025, Iran University of Science and Technology, Tehran, Iran

Design of Deep Eutectic Solvent for Synthesis of Cyclic Carbonates from CO_2 and epoxide

S. Kafash, A. Abdolmaleki *.

Department of Chemistry, College of Sciences, Shiraz University, abdolmaleki@shirazu.ac.ir.

Department of Chemistry, College of Sciences, Shiraz University, smnkafash@gmail.com.

Abstract

The present research work reports the pyridinium-based deep eutectic solvents were easily synthesized and characterized by FT-IR and NMR techniques. Pyridinium salts and aromatic compounds containing active hydrogens were used as hydrogen bond acceptors (HBA) and donors (HBD), respectively, for the efficient cycloaddition of Carbon dioxide (CO_2) with styrene oxide without metal cocatalysts.

Keywords: Cyclic carbonate, Epoxides, Deep eutectic solvents.

۱. Introduction

Carbon dioxide (CO_2) has attracted much attention as a greenhouse gas and its use as a starting material in the synthesis of valuable chemicals[1]. Cyclic carbonates produced from CO_2 have wide applications in organic synthesis and polymer production[2]. In recent years, efforts have been made to synthesize these carbonates using a variety of innovative catalytic methods, including homogeneous and heterogeneous catalysts. However, many of these catalysts have limitations such as high cost and hard reaction conditions .In response to these challenges, the development of deep eutectic solvents (DESs) has been proposed as an environmentally friendly and low-cost alternative[3]. DESs are made of specific combinations of hydrogen bond acceptors (HBA) and donors (HBD) and have distinct physical and chemical properties that can aid in the activation and conversion of CO_2. These efforts represent significant advances in the design of high-performance catalytic systems for the conversion of CO_2 into useful chemicals.

۲. Experimental

Phenol was chosen as an aromatic compound with active hydrogens as HBD for DES. 4-Dimethylaminopyridinium with a four-carbon chain length was used as HBAs for the synthesis of pyridinium-based DES (scheme 1). In a 25 mL flask, these two materials were mixed together in equal proportions and stirring at room temperature until a homogeneous liquid was formed.

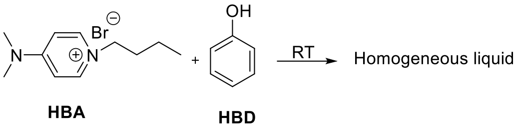

Scheme (1): Synthesis procedures of DES.

٣. Results

The FT-IR spectra of the pure ionic liquid, the absorption peak appearing at 3057 cm^{-1} belongs to the C-H stretching peak which is broadened and shifted to a higher wavenumber region, 3044 cm^{-1}, after the formation of DES. With the formation of DES, the OH stretching vibration was shifted to a higher wavenumber region, 3290 cm^{-1}. The broadening of the peaks indicated that the O-H is involved in a more extensive hydrogen bonding network. In ^{1}H-NMR spectrum of DES, the hydroxyl group in phenol peaks at 9 ppm, but the chemical shift of the hydroxyl hydrogen in DES at 7.24 ppm indicates the formation of new hydrogen bonds. The formation of intermolecular hydrogen bonds generally leads to a change in the hydrogen field in ^{1}H-NMR. The ^{13}C-NMR indicate that the compound was properly synthesized. These results are consistent with the IR spectrum.

٤. Conclusion

Finally, the deep eutectic solvent was used as a solvent and catalyst in the conversion of carbon dioxide into valuable cyclic carbonate compounds under mild conditions. The results confirm the great efficiency of the deep eutectic solvent in the synthesis of cyclic carbonate from carbon dioxide.

References:

١. Liu, X., et al., Solvent-free self-assembly synthesis of N-doped ordered mesoporous carbons as effective and bifunctional materials for CO_2 capture and oxygen reduction reaction. Chemical Engineering Journal, 2022. 427: p. 130878.

٢. Kamphuis, A.J., F .Picchioni, and P.P. Pescarmona, CO $_2$-fixation into cyclic and polymeric carbonates: principles and applications. Green chemistry, 2019. 21(3): p. 406-٤٤٨.

٣. Norouzi, F. and A. Abdolmaleki, High-performance and selective catalyst for the chemical fixation of CO_2 into cyclic carbonates based on pyridinium-based deep eutectic solvent. Journal of Environmental Chemical Engineering, 2024. 12(2): p. 111984.

The 30th Iranian Seminar of Organic Chemistry
February 7-9, 2025, Iran University of Science and Technology, Tehran, Iran

Deep Eutectic Solvent as catalysts and solvent for synthesis of cyclic carbonates

S. Kafash, A. Abdolmaleki *.

Department of Chemistry, College of Sciences, Shiraz University, abdolmaleki@shirazu.ac.ir.

Department of Chemistry, College of Sciences, Shiraz University, smnkafash@gmail.com.

Abstract

The present research work reports the synthesis of a deep eutectic solvent (DES) based on the pyridinium ionic liquid [C_4DMAPy]Br. Full characterization of DES was then performed using ^{1}H-NMR, ^{13}C-NMR, FTIR. DES was then used in the synthesis of cyclic carbonates from carbon dioxide and epoxide. The results confirm the excellent efficiency of DES in the synthesis of cyclic carbonates.

Keyword: Deep Eutectic Solvents, CO_2 Fixation, Cycloaddition reaction.

۵. Introduction

The increasing use of fossil fuels and the subsequent CO_2 pollution are causing health and environmental hazards, so chemists are looking for ways to reduce this pollution and convert CO_2 into valuable materials and carbonates[1]. Carbonates are used in lithium batteries, as solvents, and in the synthesis of polyurethanes. Efforts have mainly focused on the synthesis of carbonates from CO_2 and epoxides under mild conditions using green solvents and efficient catalysts[2]. Green solvents such as ionic liquids (ILs) and deep eutectic solvents (DESs) are used as catalysts and solvents in these processes. DESs have been proposed as superior alternatives to ILs due to their unique physical and chemical properties, lower toxicity, and greater flexibility[3]. This research focuses on the design and synthesis of DESs using ethylene glycol (EG) as hydrogen bond donor (HBD) and 1-butyl-4-(dimethylamino)pyridinium bromide ([C_4DMAPy]Br) as hydrogen bond acceptor (HBA). These novel DESs are expected to improve the CO_2 adsorption reaction by accelerating the reaction.

۶. Experimental

The deep eutectic solvent was synthesized according to the Scheme 1. The synthesis process of DES were carried out in a 25 mL round-bottom flask. [C_4DMAPy]Br was mixed with EG. It was stirrig magnetically at room temperature until a homogeneous liquid was observed. This DES was characterized by IR and NMR. Finally, it was used to synthesize the cyclic carbonate.

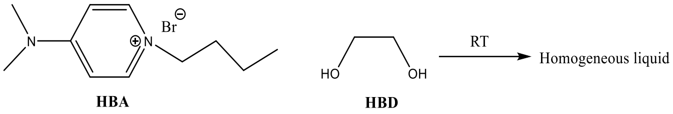

Scheme (1): Synthesis procedures of DES.

3. Results

The synthesized DES was characterized by ^{1}H-NMR, ^{13}C-NMR and FT-IR. In FT-IR spectrum we see that the peak at 1077 cm^{-1} represents the ethylene glycol structure and the peak at 3325 cm^{-1} represents the OH group, both of which are shifted relative to the original structure. So, hydrogen bonding causes a decrease in the peak wavenumber. In ^{1}H-NMR spectrum, the peaks appearing at 3.55 ppm and 4.49 ppm represent the ethylene glycol group. Appear in the original structure at 3.8 ppm and 4.58 ppm. In both the ^{13}C-NMR and ^{1}H-NM spectra, the peaks of the synthesized compound are shifted relative to the parent structures, indicating the formation of hydrogen bonds, confirming the correct synthesis of DES.

4. Conclusion

deep eutectic solvent was synthesized under solvent-free conditions and used in the synthesis of cyclic carbonate from carbon dioxide and epoxide. These processes are also very suitable from an economic point of view and can help improve the economic conditions of the country.

Refrence:

1. Pan, D., et al., Recent advances in solar-driven photothermal nanostructured materials for CO_2 reduction: A review. Journal of Environmental Chemical Engineering, 2023. 11(4): p. 110324.

2. Liu, J., et al., Metal-free imidazolium hydrogen carbonate ionic liquids as bifunctional catalysts for the one-pot synthesis of cyclic carbonates from olefins and CO_2. Green Chemistry, 2019. 21(14): p. 3834-3838.

3. Płotka-Wasylka, J., et al., Deep eutectic solvents vs ionic liquids: Similarities and differences. Microchemical Journal, 2020. 159: p. 105539.

Quantum dot synthesis of Hydro-alcoholic Extract *Thymus Vulgaris* plant

Fatemeh Rahmani [a],Zahra Khajavi [a], Behnam Mahdavi*[a], Jafar Vatandoost [b]

[a] Department of Chemistry, Faculty of Science, Hakim Sabzevari University, Sabzevar, Iran

[b] Department of Biology, Faculty of Science, Hakim Sabzevari University, Sabzevar, Iran

Corresponding Author E-mail: b.mahdavi@hsu.ac.ir

Introduction:

Quantum dots, a class of nanomaterials, offer significant potential across pharmaceutical and chemical applications. Numerous applications utilizing plant-synthesized carbon quantum dots have been documented. These compounds find utility in drug delivery systems and biosensor development. These points have achieved widespread adoption and recognition due to their superior biocompatibility and low toxicity profile. [1][2] *Thymus vulgaris*, a widely used medicinal plant, contains compounds such as thymol, carvacrol, and para-cymol. [3] This research employed *T. vulgaris* as the raw material for quantum dot synthesis via a hydrothermal method.

Materials and work methods:

A 0.05-gr quantity of *T. vulgaris* hydroalcoholic extract powder was dissolved in 10 milliliters of 70% ethanol. The mixture underwent a 12-hour, 160°C thermal treatment within a PTF-lined autoclave for the synthesis of CQDTV. Carbon quantum dot synthesis was also performed in the presence of iron ions CQDTVFe. Under identical conditions, 5 ml of iron (III) nitrate solution was added for this experiment. Following completion of the photoluminescence reaction, both resultant products underwent UV irradiation across the wavelength of 360 nm. Subsequently, UV-Vis spectral analysis of each product was performed using a spectrophotometer.

Results:

Figure 1 (1a and b) present the UV-Vis spectra of CQDTVFe and CQDTV. The CQDTVFe reveals that the observed peaks at 465 nm and 230 nm correspond to π-π* and n-π* transitions of C=C and C=O bonds, respectively. Furthermore, the CQDTV sample exhibited absorption peaks at 283 nm and 430 nm, consistent with π-π* and n-π* transitions of C=C and C-N bonds, respectively.

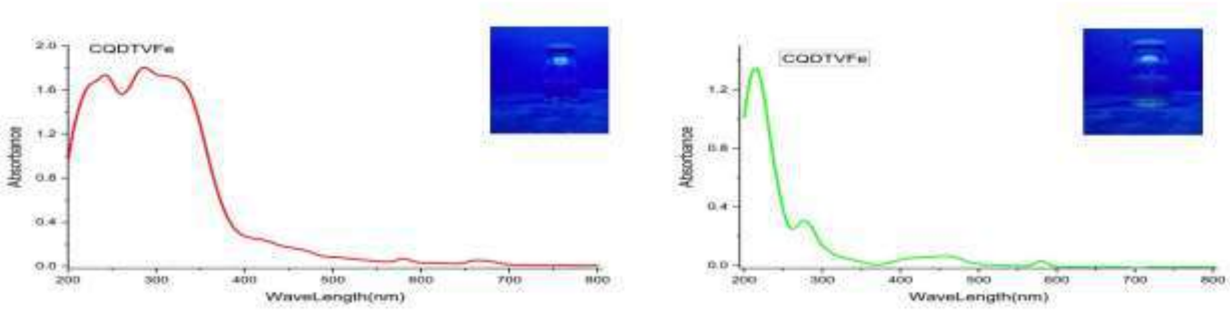

Figure 1. The fluorescence and UV-VIS spectra CQDA, CQDB

Conclusion:

Research findings indicate the potential utility of quantum dots (QDs) as biosensors for different applications such as water pollutant detection and treatment; however, further investigation is recommended.

Keyword:

Thymus vulgaris, hydrothermal method, nanomaterial, Quantum dots.

References:

1] Khajavi Z, Ghasedi A, Mahdavi B, Koushki E. On the role of UV-generated ROS in the desorption of cephalexin from CQDs-based drug-loadable platform. Journal of Photochemistry and Photobiology A: Chemistry. 2023 Aug 1;442:114813.

2] Paulo S, Stoica G, Cambarau W, Martinez-Ferrero E, Palomares E. Carbon quantum dots as new hole transport material for perovskite solar cells. Synthetic Metals. 2016 Dec 1;222:17-22.

3] Prasanth Reddy V, Ravi Vital K, Varsha PV, Satyam S. Review on Thymus vulgaris traditional uses and pharmacological properties. Med Aromat Plants. 2014;3(164):2167-0412.

Total flavonoids content of Hydro-alcoholic extract of *Thymus Vulgaris*

Fatemeh Rahmani [a], Behnam Mahdavi*[a], Jafar Vatandoost [b], Haniye Haroonzadeh Arani [b]

Corresponding Author E-mail : b.mahdavi@hsu.ac.ir

[a] Department of Chemistry, Faculty of Science, Hakim Sabzevari University, Sabzevar, Iran

[b] Department of Biology, Faculty of Science, Hakim Sabzevari University, Sabzevar, Iran

Keyword: Keywords: Flavonoid; Rutin; *Thymus Vulgaris.*

Introduction:

Medicinal plants contain various secondary metabolite, which are dependent on different factors of plant growth conditions (1). *Thymus Vulgaris* grows in the dry slopes of different Mediterranean areas. The plant has several medicinal uses due to the presence of various active compounds. So far, anti-flatulent, sedative, and antispasmodic properties have been reported for the plant (2). Flavonoids are useful antioxidants that have received much attention due to their beneficial effects in fighting diseases. In this research, we intend to investigate the amount of flavonoids in the hydroalcoholic extract of *T. vulgaris*. (3)

Experimental Section:

The aerial parts of *T. vulgaris* was extracted by maceration in 70% ethanol solvent for 72 h at room temperature. After this period, the extract was passed through filter paper and dried at room temperature. A colorimetric method using $AlCl_3$ was run to measure the TFC of *T. vulgaris* extract at different concentrations. A standard curve of rutin was used to calculate the TFC amount of extracts. The results were expressed as mg of rutin per gram of dry extract (RE/g extract).(4)

Results and Discussion:

According to Figure 1, the maximum amount of TFC was obtained for extract at concentration of 1000 ppm with the amount of 51.90±3.10. RE/g extract. Furthermore,

The results show a concentration depending for the TFC of the plant extract. The presence of flavonoids in *T. vulgaris* may be responsible **for a wide spectrum of biological activity such as radical scavenging activity.**

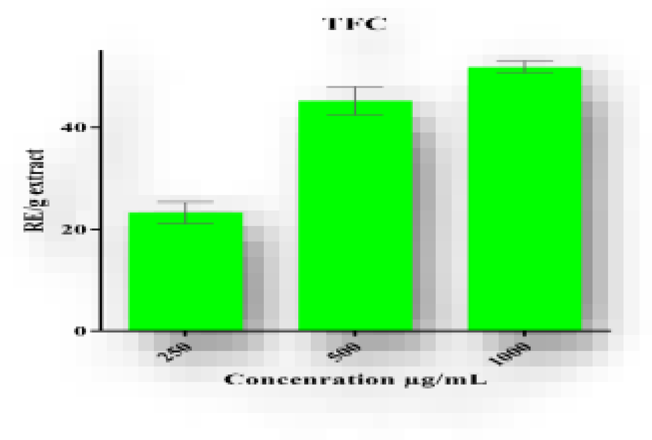

Fig.1: Total flavonoids content *Thymus vulgaris* extract at different concentration.

Conclusions:

The obtained results, revealed the presence of flavonoids in *T. vulgaris* extract with an acceptable amount. The compounds are known as a main secondary metabolite with various medical uses such as **coronary heart disease prevention hepatoprotective, anti-inflammatory, and anticancer activity.**

Reference**:**

1. Seyedi FS, Nafchi MG, Reezi SJH. Effects of light spectra on morphological characteristics, primary and specialized metabolites of Thymus vulgaris L. 2024;10(1).

2. DARDONA Z, AMANE M, DARDONA A, BOUSSAA S. The anti-parasitic activity of Thymus vulgaris (Thyme): A literature review. 2024.

3. Mokhtari R, Kazemi Fard M, Rezaei M, Moftakharzadeh SA, Mohseni AJJoFQ. Antioxidant, Antimicrobial Activities, and Characterization of Phenolic Compounds of Thyme (Thymus vulgaris L.), Sage (Salvia officinalis L.), and Thyme–Sage Mixture Extracts. 2023;2023:1-9.

4. HOSSEINPOOR MAZ, Mahdavi B, REZAEI SE. Contents of aerial parts of Salvia leriifolia Benth. 2016.

Effect of ethyl acetate extracts of *Medicago Sativa* leaf on blood coagulation

Fatemeh Rahmani [a], Behnam Mahdavi*[a], Jafar Vatandoost [b]

[a] Department of Chemistry, Faculty of Science, Hakim Sabzevari University, Sabzevar, Iran

[b] Department of Biology, Faculty of Science, Hakim Sabzevari University, Sabzevar, Iran

Corresponding Author E-mail: b.mahdavi@hsu.ac.ir

Keyword: Traditional medicine, coagulation, *Medicago Sativa*, extraction

Introduction:
Medicago Sativa contains various secondary compounds and many of these compounds are effective in primary and secondary hemostasis of blood coagulation(1). This plant, having compounds such as flavonoids, tannins, alkaloids, can be effective in blood coagulation. The aim of this study is to investigate the effect of ethyl acetate extract on the blood coagulation process(2).

Materials and work methods:

Medicago sativa was extracted by maceration in 70% ethanol solvent for 72 h at room temperature. The extract was concentrated by a rotary device and dried in an oven. First, a 1000 ppm solution was prepared and solutions (500, 250, 50, 25 ppm) were made from this solution. The effect of different concentrations (500, 250, 50, 25 ppm) of the extract using prothrombin time (PT) and The activated partial thromboplastin time (APTT) test was evaluated(3).

Result:

Ethyl acetate extract had a significant effect on APTT and PT coagulation time. Ethyl acetate extract increased APTT at a concentration of 50, 250, 500 ppm and also increased PT at a concentration of 50, 250, 500 ppm. It seems that the compounds of ethyl acetate extract are effective on the coagulation factors of the internal and external pathways of blood coagulation.

Conclusion:
According to the results of APTT and PT tests, ethyl acetate extract has anticoagulant effect and can be used to treat cardiovascular diseases.

References:

[1] Krakowska A, Rafińska K, Walczak J, Kowalkowski T, Buszewski BJJoAI. Comparison of various extraction techniques of Medicago sativa: yield, antioxidant activity, and content of phytochemical constituents. 2017;100(6):1681-93.Times New Roman, Font size: 11, Align left, Arabic numeral.

[2] Vahidipour HR, Cheniany M, Lahouti M, Ganjeali A, Moghaddam Matin MJIJoAB, Research B. The Correlation of Some Secondary Metabolites of Alfalfa (Medicago sativa L.) with Plant Organ and Harvest Time. 2024;12.

[3] Vatandoost J, Mashkani ZS, Hajjar T, Mahdavi BJHMJ. The Coagulant Effect of the Medicago sativa L. Hydroalcoholic Extract: An in vivo Study on Mice. 2022;7(2):45-52.

The 30th Iranian Seminar of Organic Chemistry
February 7-9, 2025, Iran University of Science and Technology, Tehran, Iran

Laccase Activity in Reline Deep Eutectic Solvent: A Molecular Dynamics Study

Rafe Naijian, Mehdi Mogharabi*

Pharmaceutical Sciences Research Center, Mazandaran University of Medical Sciences, P.O. Box 48175-861 Sari 4847193698, Iran

Keyword: Laccase, Deep Eutectic Solvents, Molecular Dynamics, GROMACS, OPLS-AA

Laccases are multicopper oxidase enzymes known for their ability to catalyze a wide range of reactions. They can oxidize various substrates, producing water as the sole byproduct. This characteristic makes laccases an excellent choice for applications in green chemistry. Their versatility allows them to be used in diverse industrial fields, including food processing, chemical manufacturing, and pharmaceuticals (1). While Laccase has numerous industrial applications, but its inactivity in organic solvents limits its use. While stable in water and aqueous solvents, laccase denatures in the presence of high amounts of organic solvents, which are often necessary for dissolving certain substrates in industry. This inactivity restricts its broader application in industrial processes (2).

Deep eutectic solvents (DES) have emerged as a promising solution due to their low vapor pressure, environmental friendliness, and ability to dissolve a wide range of chemicals including organic compounds, which, as mentioned before, can act as substrates for laccases (3). Recent studies have shown that DESs offer a conducive environment for enzymes, preserving their stability and functionality. Therefore, DESs can function as suitable solvents, offering an environment that maintains the structure and activity of laccases while simultaneously dissolving their substrates with varying polarities (4). *In light of the increasing significance of in-silico studies, this research aims to examine the functionality and stability of laccase derived from Trametes versicolor in the presence of reline deep eutectic solvent and compare that with water, ethanol, and n-hexane. This study employs molecular dynamics simulations using GROMACS 2024.3 with OPLS-AA as a force field to investigate the activity of laccase in various solvents, including water, ethanol, n-hexane, and choline chloride-urea. Comparative analysis of protein activity in these solvents highlights the potential of deep eutectic solvents in maintaining enzyme activity.*

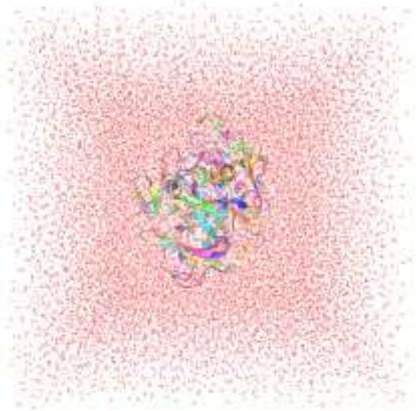

Figure: Simulation of laccase enzyme in water within a cubic box containing 23376 water molecules, conducted using the OPLS-AA force field at 300 K.

Promising results indicate that choline chloride-urea can maintain laccase activity, paving the way for efficient industrial use by preserving activity and dissolving substrates. Experimental validation is needed to confirm *in-silico* findings. Future researches should explore enzyme interactions and industrial conditions to optimize the use of deep eutectic solvents.

References:

1. Mate DM, Alcalde M. Laccase: a multi-purpose biocatalyst at the forefront of biotechnology. Microb Biotechnol. 2017 Nov;10(6):1457–67.

2. Wu MH, Lin MC, Lee CC, Yu SM, Wang AHJ, Ho THD. Enhancement of laccase activity by pre-incubation with organic solvents. Sci Rep. 2019 Jul 5;9(1):9754.

3. Vicente FA, Tkalec N, Likozar B. Responsive deep eutectic solvents: mechanisms, applications and their role in sustainable chemistry. Chem Commun. 2025;10.1039.D4CC05157B.

4. Mannu A, Blangetti M, Baldino S, Prandi C. Promising Technological and Industrial Applications of Deep Eutectic Systems. Mater Basel Switz. 2021 May 12;14(10):2494.

The 30th Iranian Seminar of Organic Chemistry
February 7-9, 2025, Iran University of Science and Technology, Tehran, Iran

An efficient and feasible pathway for three-component synthesis of spiro-2-amino-3-cyano-4*H*-pyran derivatives in the presence of Quinoline-based catalyst

Mahdiye Ghasemi [a], Narges Seyedi [a], Farhad Shirini [a]*, Bahman Sharifzadeh [b]

[a] *Department of Organic Chemistry, Faculty of Chemistry, University of Guilan, Rasht, 41335-19141, Iran*
[b] *Department of Engineering Science, Faculty of Technology and Engineering, East of Guilan, University of Guilan, Rudsar-Vajargah, 44891-63157, Iran*
* *Corresponding author: E-mail: shirini@guilan.ac.ir, fshirini@gmail.com*

Keywords: Quinoline, Molten salts, Spiro-4*H*-pyrans, One-pot three-component reaction, Homogeneous catalyst

The compatibility of molten salts with a diverse array of reactions, substrates, and conditions highlights their versatility in facilitating catalytic transformations across various branches of chemistry. Among these, ionic liquids (ILs) are recognized as a distinctive subgroup of classical molten salts. They are defined as liquid compounds possessing both ionic and covalent characteristics within their crystalline structures. This classification more effectively differentiates ionic liquids from molten salts than their melting points alone [1]. In this context, we present an efficient methodology for synthesizing spiro-4*H*-pyran derivatives—compounds of significant biological and pharmaceutical importance—*via* a one-pot, three-component reaction. This approach employs active carbonyl compounds (such as isatins or acenaphthoquinone), malononitrile, and a range of C-H activated acidic substrates. A novel quinoline-based molten salt catalyst was introduced to accelerate the synthesis of the target molecules [2] (Scheme 1). Previously, this catalyst has been utilized as a reactant and anti-corrosion agent. However, the present study investigates its efficacy as a catalytic agent for the first time. The quinoline-based catalyst demonstrated exceptional catalytic performance, functioning as an efficient molten salt that promotes the desired transformations with remarkable effectiveness. This method offers several advantages, including environmentally friendly and straightforward catalyst synthesis, high efficiency, reduced reaction times, operational simplicity without the need for acidic or basic catalysts, ease of product isolation without column chromatography, reliance on commercially available starting materials, and excellent catalyst recyclability over multiple cycles. Additionally, the antibacterial properties of this catalyst, along with its primary component, quinoline, were assessed using the agar well diffusion method. The *in vitro* activity was evaluated against Escherichia coli (Gram-negative) and Staphylococcus aureus (Gram-positive), providing further insights into its multifaceted applications.

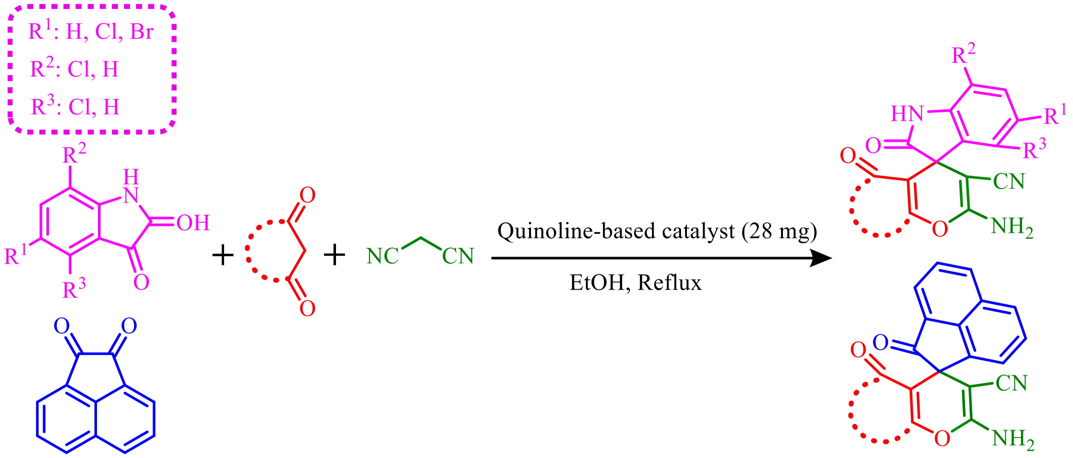

Scheme 1. Synthesis of spiro-2-amino-3-cyano-4*H*-pyran derivatives using quinoline-based catalyst.

References:

[1] J. Dupont, R.F. de Souza, P.A.Z. Suarez, Chem. Rev. 102 (2002) 3667–3692.

[2] D. Kumar, P. Sharma, K. Nepali, G. Mahajan, M.J. Mintoo, A. Singh, G. Singh, D.M. Mondhe, G. Singh, S.K. Jain, G.K. Gupta, F. Ntie-Kang, Heliyon 4 (2018) e00661-e00686.

The 30th Iranian Seminar of Organic Chemistry
February 7-9, 2025, Iran University of Science and Technology, Tehran, Iran

Green Synthesis of Copper Ferrite Magnetic Nanoparticles Using Pomegranate Seed Extract for 4-Nitrophenol Reduction

Authors: Jeyran Shams Beiranvand, Saeid Taghavi Fardood*

Department of Chemistry, Faculty of Science, Ilam University, Ilam, Iran

E-mail: s.taghavi@ilam.ac.ir

Keyword: Green Synthesis, Copper Ferrite, 4-Nitrophenol Reduction

Over the past few years, industries have rapidly developed around the manufacture of insecticides, pesticides, fungicides, herbicides, and paints, which are major contributors to the accumulation of toxic pollutants in the environment. Aromatic nitro compounds, such as 4-nitrophenol and nitrobenzene, are widely used in various industries. However, these compounds are highly toxic pollutants that pose serious risks to both the environment and human health. Conversely, 4-aminophenol (4-AP), a reduction product of 4-nitrophenol (4-NP), is extensively utilized in industry as an intermediate for manufacturing corrosion inhibitors, analgesic medications, anticorrosion lubricants, and other materials. Nitrophenol has numerous adverse effects on the human body, including headaches, respiratory tract irritation, cyanosis, and eye and skin conditions, whereas 4-AP is significantly less harmful to humans and the environment [1,2].

In this study, magnetic copper ferrite nanoparticles were synthesized as an effective and recyclable catalyst using a green method. Characterization of the synthesized materials included XRD, FTIR, BET, FESEM, TEM, EDS, and VSM analyses. The catalyst effectively reduced 4-nitrophenol to 4-aminophenol under optimized conditions. Notably, the magnetic nanoparticles were easily separated using an external magnet, and the catalyst retained its stable and high catalytic performance even after five consecutive cycles under the same conditions.

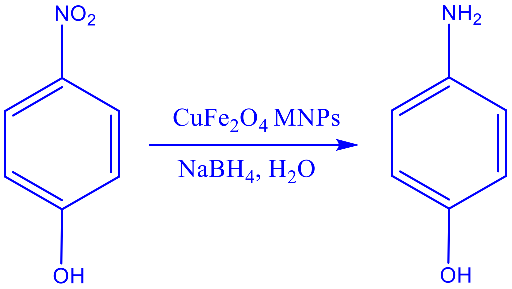

Scheme: Reduction of 4-nitrophenol using $CuFe_2O_4$ MNPs.

References

[1]. Dey, C., De, D., Nandi, M., Goswami, M.M.: *Mater. Chem. Phys.*, 2020, **242**, 122237.

[2]. Palanivel, D., Venugopal, A., Ranganathan, S., Cingaram, R., Sundramurthy, K.N.: *J. Indian Chem. Soc.*, 2024, **101**, 101337.

Green Synthesis of $Cu_{0.5}Cd_{0.5}FeCrO_4$ Magnetic Nanoparticles using Oak Fruit Peel and Their Photocatalytic Activity in Dye Degradation

Authors: Jeyran Shams Beiranvand, Shirin Havasipour, Saeid Taghavi Fardood*, Ali Naghipour*

Department of Chemistry, Faculty of Science, Ilam University, Ilam, Iran

E-mail: s.taghavi@ilam.ac.ir

Keyword: Green Synthesis, Magnetic Nanoparticles, Photocatalysis

The textile industry has expanded rapidly in recent decades due to human demand. Dye pollutants in the environment can adversely affect aquatic flora and microorganisms. Congo red is an aromatic, direct heterocyclic diazo compound. The dye is primarily utilized for paper, textiles, printing, and leather. Congo red is a carcinogenic substance that is harmful to humans. Fish, shrimp, aquatic organisms, and algae are endangered by Congored dye in water. Water bodies containing organic dyes such as Congo red are eutrophic and exhibit light limitation. A minimal concentration of Congo red can significantly diminish light intensity, impairing the photosynthetic efficiency of aquatic organisms. The stable benzene and naphthalene rings of Congo red are resistant to aerobic biodegradation. The structure of this compound is resistant to light, heat, and oxygen. The removal of Congo red dye pollution from wastewater is challenging, necessitating effective solutions [1]. Various methods, including adsorption, photocatalysis, and biodegradation, have been proposed to remove this toxic dye. Among them, photocatalysis is preferred due to its safety, cost-effectiveness, efficiency, and environmental friendliness [2,3].

In this study, $Cu_{0.5}Cd_{0.5}FeCrO_4$ magnetic nanoparticles were synthesized using a green approach. The sample was thoroughly characterized by various analytical techniques, including FTIR, BET, XRD, FESEM, TEM, UV-Vis DRS, and VSM. Additionally, the photocatalytic performance of the nanoparticles was evaluated for the degradation of Congo red dye under visible light irradiation. The efficiency of the photocatalytic process was investigated by varying factors such as initial dye concentration, photocatalyst dosage, and irradiation time. The results highlighted the exceptional capability of $Cu_{0.5}Cd_{0.5}FeCrO_4$ MNPs to efficiently degrade Congo red dye. This approach offers several advantages, including low cost, simplicity, reduced processing time, environmental sustainability, and scalability, making it a promising candidate for large-scale applications.

References

[1] N.T.T. Nguyen, L.M. Nguyen, T.T.T. Nguyen, N.H. Nguyen, D.H. Nguyen, D.T.C. Nguyen and T.V. Tran, *J. Environ. Manage.*, **2023**, *326*, 116746.

[2] M.T. Kiani, A. Ramazani, S. Rahmani and S. Taghavi Fardood, *Int. J. Environ. Anal. Chem.*, 2022, 1.

[3] S. Taghavi Fardood, F. Moradnia, S. Ganjkhanlu, L. Ouni, A. Ramazani and M. Sillanpää, *Inorg. Chem. Commun.*, **2024**, *167*, 112719.

The 30th Iranian Seminar of Organic Chemistry
February 7-9, 2025, Iran University of Science and Technology, Tehran, Iran

Synthesis and characterization of CuI based on magnetic 2,2'-biimidazole functionalized nano cellulose as a novel catalyst for synthesis of 1-aryl 1,2,3-triazoles in DES

Selin Yeghyazarian Tabrizi, Arefe Salamatmanesh, Samane Ansari and Akbar Heydari*

Department of Chemistry, Faculty of Basic Science of Tarbiat Modares University

Keywords: 1-aryl 1,2,3-triazoles, copper(I) catalyst, deep eutectic solvent

1 | INTRODUCTION

1,2,3-Triazoles are nitrogen containing heterocyclic compounds that find extensive use in various fields, especially in medicinal chemistry and materials science. They are prominent in drug discovery due to their biological activities, including antiviral, antimicrobial, and anticancer properties. These compounds function as essential scaffolds in the formulation of numerous pharmaceuticals, including Rufinamide and Cefatrizine, and play a crucial role in the innovation of novel bioactive agents aimed at combating diseases such as tuberculosis.[1,2]Triazoles are also utilized in agriculture as fungicides, contributing to crop protection.[3]The synthesis of 1,2,3-triazoles can be achieved through various methods, including: Huisgen 1,3-dipolar cycloaddition,[4] metal-free methods,[5]one-pot reactions[6]and Diazo-transfer reactions.[7] Herein we report one-pot three-component reaction of aryl halides, sodium azide, and dimedone using choline chloride:Glycerol deep eutectic mixture as a green and recoverable solvent and CuI based on magnetic 2,2'-biimidazole functionalized nano cellulose as a catalyst. Glyceline is a deep eutectic solvent (DES) formed from choline chloride and glycerol, respectively in a 1:2 molar ratio. It has garnered interest due to its unique properties and potential applications.

2 | EXPERIMENTAL SECTION

2.1 | General procedure for the synthesis of 1-aryl 1,2,3-triazoles

A mixture of aryl halides (1 mmol), dimedone (1 mmol), sodium azide (1.2 mmol), base (2 mmol) and catalyst (**30** mg) was stirred at **120**℃ in choline chloride:Glycerol (2 ml, 1:2) for the appropriate time until the reaction was completed as monitored by TLC.

2.2 | Preparation of DESs

In order to synthesize DES, a certain molar ratio (2: 1) of HBD (glycerol) and HBA (choline chloride) was mixed and then heated at **80**℃ under continuous stirring until a homogeneous and transparent liquid was formed.

3 | RESULTS AND DISCUSSION

3.1 | Catalyst preparation

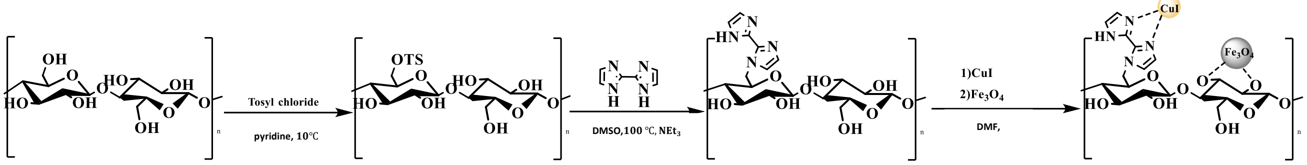

3.2 | Catalyst characterization

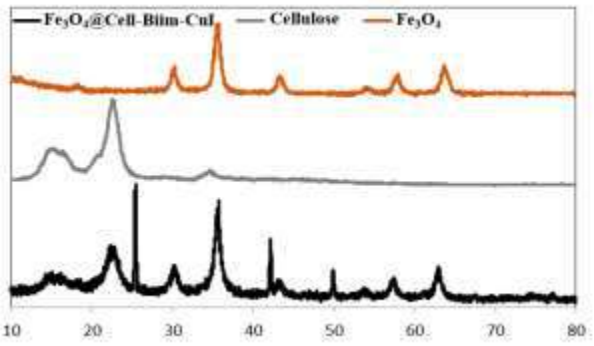

XRD pattern of catalyst

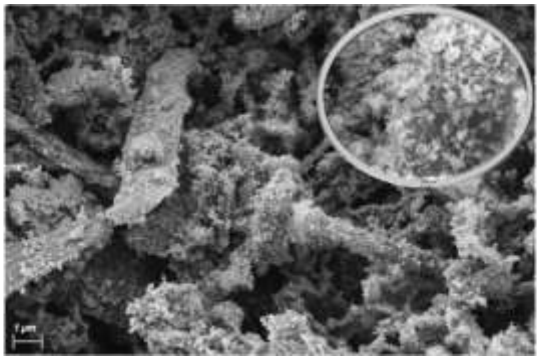

SEM analysis of the

Scheme:

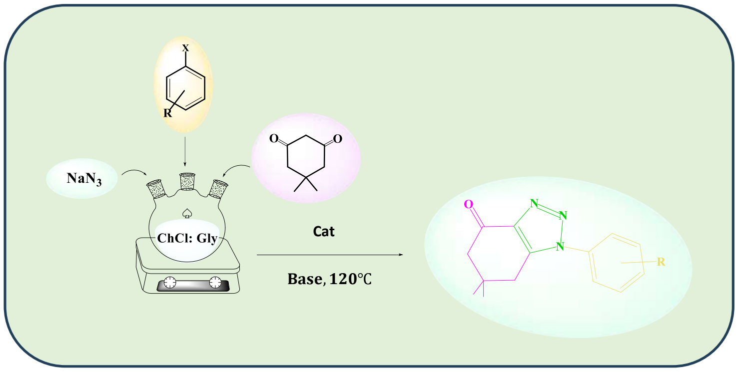

REFERENCES:

[1] S. Raic-Malic and A. Mescic, Curr. Med.Chem. ٢٠١٥, ٢٢, ١٤٦٢-١٤٩٩.

[2] J. Dai, S. Tian, X. Yang and Z. Liu, Front. Chem.٢٠٢٢, ١٠, ٨٩١٤٨٤.

[3] A. Rammohan, B. C. Venkatesh, N. M. Basha, G. V. Zyryanov and M. Nageswararao, Chem. biol. drug des.٢٠٢٣, ١٠١, ١١٨١ – ١٢٠٣.

[4] G. Cheng, X. Zeng, J. Shen, X. Wang and X. Cui, Angew. Chem. Int. Ed.٢٠١٣, ٥٢.

[5] H. B. Jalani, A. Ç. Karagöz and S. B. Tsogoeva, Synthesis ٢٠١٧, ٤٩, ٢٩ – ٤١.

[٦] B. Kaboudin, Y. Abedi and T. Yokomatsu, Org. Biomol. Chem.٢٠١٢, ١٠, ٤٥٤٣ – ٤٥٤٨.

[7] J. O. F. Melo, C. L. Donnici, R. Augusti, M. T. Paz Lopes and A. Grigorievitch Mikhailovskii, Heterocycl Comm ٢٠٠٣,٩,٢٣٥ – ٢٣٨.

The 30th Iranian Seminar of Organic Chemistry
February 7-9, 2025, Iran University of Science and Technology, Tehran, Iran

Deep eutectic solvent-immobilized magnetic nanoparticles as a capable catalyst for the green synthesis of triazolopyrimidines

Amin Benrashid *[a], Davood Habibi [b]

*Department of Organic Chemistry, Faculty of Chemistry and Petroleum Sciences, Bu-Ali Sina University, Hamedan 6527838683, Iran. * E-mail: aminbenrashid1@gmail.com*

Keywords: 1,2,4-Triazolo[4,3-*a*]pyrimidines, catalysis, magnetic DES, immobilization, green synthesis

One of the principles of green chemistry is the use of catalysts to prevent and eliminate hazardous chemicals. Recently, remarkable developments have been made in the field of green catalysis, the design of safer chemicals, and green solvents. In this paper, novel magnetic choline chloride-based deep eutectic solvent immobilized on Fe_3O_4 magnetic nanoparticles (Fe_3O_4@SiO_2@THAM @ChCl = D) was obtained from the sequential synthesis of Fe_3O_4 (A), Fe_3O_4@SiO_2 (B), and Fe_3O_4@SiO_2@THAM (C), and characterized with various techniques such as Fourier transform-infrared spectroscopy (FT-IR), energy-dispersive X-ray spectroscopy (EDX), elemental mapping, vibrating sample magnetometer (VSM), field emission scanning electron microscopy (FE-SEM), transmission electron microscopy (TEM), thermo-gravimetric-differential thermal analysis (TGA-DTA) and X-ray diffraction analysis (XRD). TEM images confirm that the nanoparticles are core-shell. Then, the novel D was used as a capable heterogeneous catalyst for the one-pot three-component condensation reaction of 3-amino-1,2,4-triazole, aromatic aldehydes, and malononitrile for the synthesis of 1,2,4-triazolo[4,3-*a*]pyrimidines under solvent-free conditions with high yields and short reaction times. Some advantages of using this catalyst are the novelty, easy separation from the reaction medium, reusability, high thermal stability, excellent yield, and short reaction times.

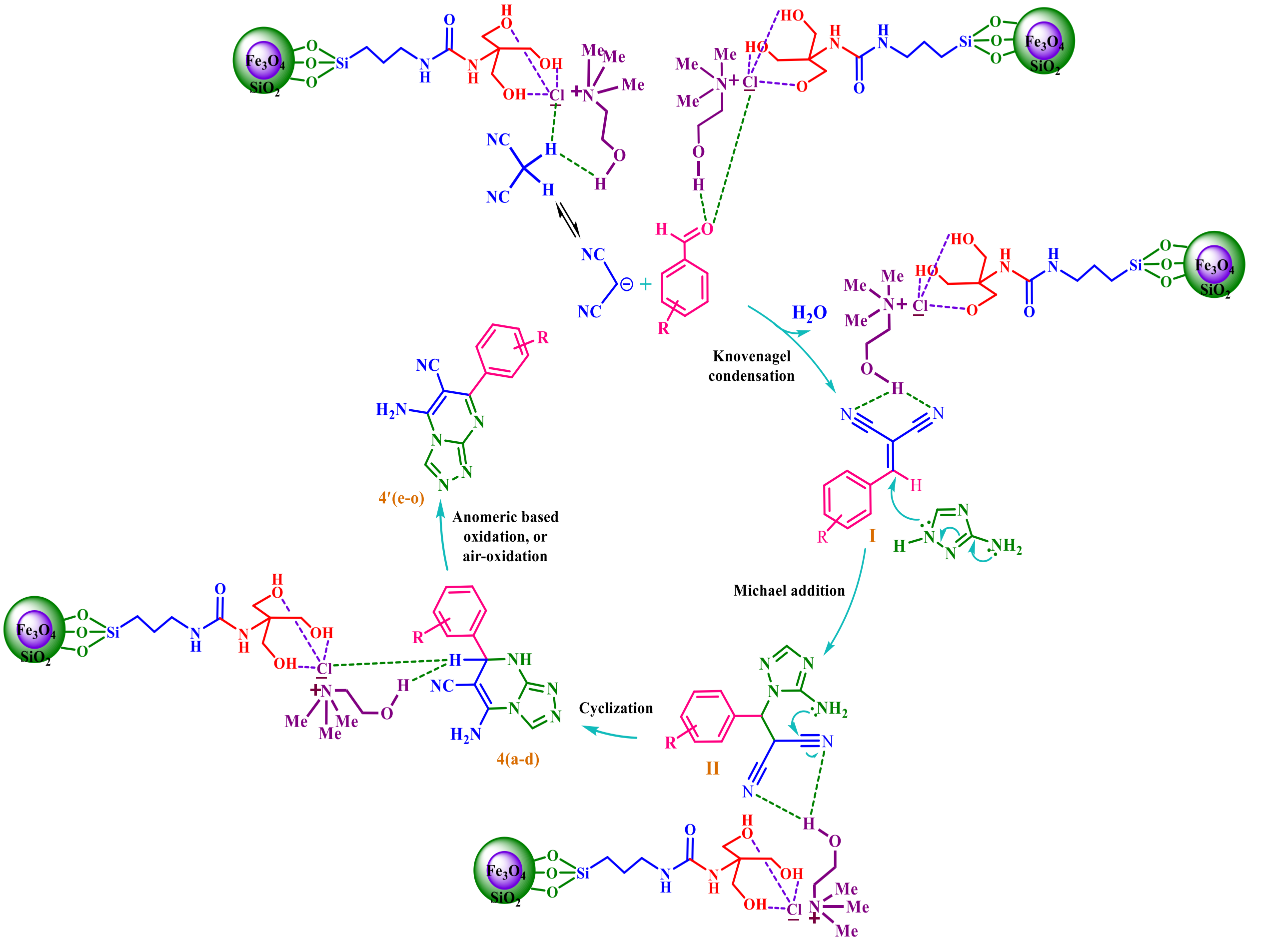

Scheme: D-catalyzed three-component condensation reaction to prepare 4(a-d), and 4′(e-o)

[1] S. Sadjadi, Magnetic (poly) ionic liquids: A promising platform for green chemistry. J. Mol. Liq. 323 (2021) 114994.

[2] M. Beiranvand, D. Habibi, Design, preparation and application of the semi carbazide-pyridoyl-sulfonic acid-based nanocatalyst for the synthesis of pyranopyrazoles, Sci. Rep. 12 (2022), 14347.

[3] M.R. Anizadeh, M.A. Zolfigol, M. Torabi, M. Yarie, B. Notash, Urea-dithiocarbamic acid-functionalized magnetic nanoparticles modified with Ch-Cl: Catalytic application for the synthesis of novel hybrid pyridones via cooperative geminal-vinylogous anomeric-based oxidation. J. Mol. Liq. 364 (2022) 120016.

[4] N, Zarei, M.A. Zolfigol, M. Torabi, M. Yarie, Synthesis of new hybrid pyridines catalyzed by $Fe_3O_4@SiO_2$@urea-riched ligand/Ch-Cl. Sci. Rep. 13 (2023) 9486.

The 30th Iranian Seminar of Organic Chemistry
February 7-9, 2025, Iran University of Science and Technology, Tehran, Iran

The role of amine-based organocatalysts in aldol reactions

Authors: Mohammad Asgharian[a]

[a] BS, Department of Chemistry, Faculty of Converging Sciences and Technologies, Islamic Azad University, Science and Research Branch, Tehran, Iran.

Keywords: Organocatalysis, Aldol Reaction, Amines, Catalytic Efficiency, Green Chemistry.

ABSTRACT

The role of amine-based organocatalysts in aldol reactions has emerged as a significant area of research in organic chemistry, particularly in the context of asymmetric synthesis. Aldol reactions, which involve the nucleophilic addition of ketone enolates to aldehydes, are pivotal for constructing carbon-carbon bonds and creating chiral molecules. The introduction of amine-based organocatalysts, especially secondary amines like proline, has revolutionized this process by enhancing stereoselectivity and reactivity under mild conditions, making these reactions more accessible and environmentally friendly than traditional metal-based catalysts.[1][2]

The notable contributions of chemists such as David W.C. MacMillan and Benjamin List in the early 2000s have established amine-based organocatalysts as powerful tools in synthetic organic chemistry, showcasing their effectiveness in promoting highly enantioselective aldol reactions. These catalysts facilitate reaction mechanisms, including enamine and iminium catalysis, that stabilize transition states and intermediate species, thereby optimizing product formation and selectivity.[1][3] Additionally, the shift towards solvent-free protocols and green chemistry principles has further highlighted the advantages of these catalysts, underscoring their role in minimizing waste and employing safer reaction conditions.[2]

Despite their advantages, the use of amine-based organocatalysts is not without challenges. Issues such as the reversible nature of aldolization steps can lead to low yields, and enantioselectivity may be significantly influenced by catalyst loading and reaction conditions. The need for specific solvents and additives also complicates optimizing these reactions, presenting barriers to achieving desired outcomes in certain contexts.[2][4]

Ongoing research continues to address these limitations while exploring novel catalytic systems and methodologies to enhance the efficiency and applicability of amine-based organocatalysts in aldol reactions. As the field progresses, amine-based organocatalysts are poised to play an increasingly integral role in the total synthesis of complex natural products and pharmaceuticals, aligning with sustainable practices in chemical synthesis. Innovations in catalyst design and mechanistic understanding are expected to further expand the utility of these organocatalysts, driving future developments in asymmetric synthesis and contributing to the broader goals of green chemistry.[1][3]

References:

[1] Mestres, Ramon. "A green look at the aldol reaction." *Green Chemistry* 6, no. 12 (2004): 583-603.

[2] Verma, Ajay K., Braj Nandan Kishor, and Om Prakash. "Recent Advancement and Novel Application of Organocatalyzed Aldol Condensation Reactions: A Comprehensive Review." *Mini-Reviews in Organic Chemistry* 19, no. 6 (2022): 779-795.

[3] D'Amato, Assunta, Maria Voccia, Filippo Bruno, Sara D'Aniello, Lucia Caporaso, Francesco De Riccardis, Irene Izzo, Giorgio Della Sala, and Mina Mazzeo. "Bis-thiourea and macrocyclic polyamines as binary organocatalysts for the ROP of lactide." *Catalysis Science & Technology* (2024).

[4] Oliveira, Vanessa da Gama, Mariana Filomena do Carmo Cardoso, and Luana da Silva Magalhães Forezi. "Organocatalysis: A brief overview on its evolution and applications." *Catalysts* 8, no. 12 (2018): 605.

[5] Lee, Hyo-Jun, Natarajan Arumugam, Abdulrahman I. Almansour, Raju Suresh Kumar, and Keiji Maruoka. "Design of New Amino Tf-Amide Organocatalysts: Environmentally Benign Approach to Asymmetric Aldol Synthesis." *Synlett* 30, no. 04 (2019): 401-404.

[6] Agarwal, Jyoti, and Rama Krishna Peddinti. "Glucosamine-based primary amines as organocatalysts for the asymmetric aldol reaction." *The Journal of Organic Chemistry* 76, no. 9 (2011): 3502-3505.

[7] Reddy, Ummareddy Venkata Subba, Bheemreddy Anusha, Zubeda Begum, Chigusa Seki, Yuko Okuyama, Michio Tokiwa, Suguru Tokiwa, Mitsuhiro Takeshita, and Hiroto Nakano. "Catalytic Efficiency of Primary α-Amino Amides as Multifunctional Organocatalysts in Recent Asymmetric Organic Transformations." *Catalysts* 12, no. 12 (2022): 1674.

[8] Nakashima, Yuta, Kenta Rakumitsu, and Hayato Ishikawa. "Recent Advances in the Total Synthesis of Alkaloids Using Chiral Secondary Amine Organocatalysts." *Organic & Biomolecular Chemistry* (2024).

Design, synthesis and application of ferrocene-based covalent organic framework as a heterogeneous catalyst at the preparation of tetrazole derivatives

Authors: Zahra Alishahi[a], Mohammad Ali Zolfigol*[a], Morteza Torabi[a]

[a]*Department of Organic Chemistry, Faculty of Chemistry and Petroleum Sciences, Bu-Ali Sina University, Hamedan, Iran. 6517838683, Tel: +988138282807, Fax: +988138380709 Iran.*

Corresponding Author E-mail: mzolfigol@yahoo.com

Keyword: Catalyst; ferrocene; COF; Tetrazole

Introduction

Covalent organic frameworks **(**COFs) as a new generation of porous materials, are assembled by covalent linkers which have strong building blocks [1,2]. In recent years, COFs due to having diverse properties such as excellent thermal and physical stability, large surface areas, designable and post modification ability, are various application chemistry and organic synthetic methodologies [3]. Tetrazoles and their nitrile-linked derivatives are known as one of the most important families of *N*-heterocycle compounds, have a decisive role in most of sciences. These chemicals have been used in diverse fields such as medicinal chemistry, sensors, energetic materials, and agriculture [4,5]. In this work, we synthesized a ferrocene-based covalent organic framework as highly active catalyst. After full characterization of the mentioned catalyst, it was used for the preparation of nitrile-linked tetrazole derivatives.

Method

In current study, the ferrocene-linked COF was synthesized on the surface of carbon nanotube and was applied as robust catalyst for the preparation of nitrile-linked tetrazoles by using starting materials such as aryl aldehydes, malononitrile, sodium azide and EtOH as solvent under reflux condition (Scheme 1).

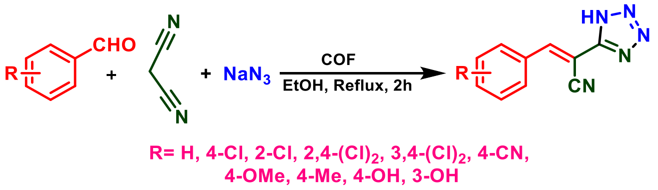

R= H, 4-Cl, 2-Cl, 2,4-$(Cl)_2$, 3,4-$(Cl)_2$, 4-CN, 4-OMe, 4-Me, 4-OH, 3-OH

Scheme 1: Schematic preparation of nitrile linked tetrazoles by synthesized COF as catalyst

Results and Discussion

In this study, a novel ferrocene-based COF was designed, synthesized and constructed via a simple and green synthetic route. After that, the ferrocene-based COF was functionalized with copper acetate and its structure approved by using several techniques including FT-IR, SEM, TEM, BET, TGA and XRD analysis.

According to the SEM and TEM results, the catalyst has tube-type core-shell morphology (Figure 1). XRD patterns of COF1 and COF1@Cu(OAc)$_2$ were illustrated in figure 2. In the XRD motifs of these materials, the diagnostic peaks at 26.2, 30.3, 35.5 and 43.4◦ correspond to crystalline structure of COF and the distinctive peak of Cu(OAc)$_2$ is clearly observed at 6.85◦.

In another study, we delve into the generality of catalytic activity of synthesized COF in the preparation of nitrile-linked tetrazole derivatives. A variety of aromatic aldehyde derivatives with electron-withdrawing and electron-donating nature were used and all of the products have high yield and short reaction times.

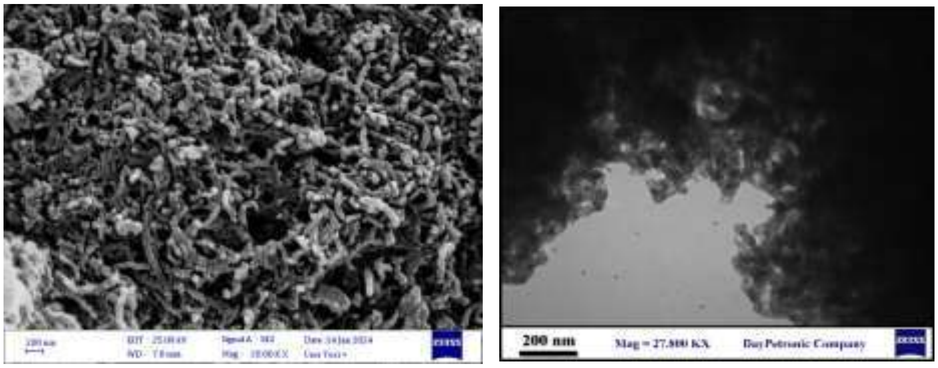

Fig.1: SEM and TEM images of synthesized COF

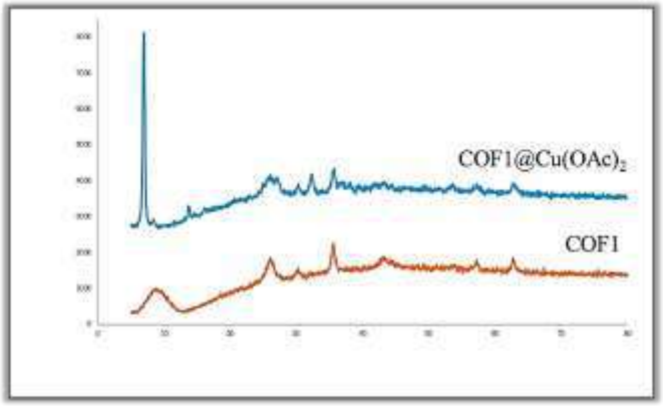

Fig.2: XRD patterns of COF1 and COF1@Cu(OAc)$_2$

References

[1] Daliran, S., Oveisi, A. R., Peng, Y., López-Magano, A., Khajeh, M., Mas-Ballesté, R., ... & Garcia, H. (2022). Chemical Society Reviews, 51(18), 7810-7882.

[2] Sarkar, C., Shit, S. C., Das, N., & Mondal, J. (2021). Chemical Communications, 57(69), 8550-8567.

[3] Kazemnejadi, M., Mahmoudi, B., Sharafi, Z., Nasseri, M. A., Allahresani, A., & Esmaeilpour, M. (2020). Applied Organometallic Chemistry, 34(2), e5273.

[4] Chen, W., Chen, P., Zhang, G., Xing, G., Feng, Y., Yang, Y. W., & Chen, L. (2021). Chemical Society Reviews, 50(20), 11684-11714.

[5] Nanda, A., Kaur, N., Kaur, M., Husain, F. M., Han, H., Bhowmik, P. K., & Sohal, H. S. (2024). Molecules, 29(18), 4339.

The 30th Iranian Seminar of Organic Chemistry
February 7-9, 2025, Iran University of Science and Technology, Tehran, Iran

Copper nanoparticle-decorated reduced graphene oxide as a highly effective catalyst for ullmann-type *n*-arylation reactions

Fahimeh Bayat[a], Sodeh Sadjadi*[a]

Radiation Application Research School, Nuclear Science and Technology Research Institute, P.O. Box 11365-3486, Tehran, Iran

Keyword: Copper nanoparticles, Reduced graphene oxide, Ullmann C−N coupling

Ullmann-type aryl amination has been widely utilized in both academic and industrial research due to its promising applications in the development of pharmaceuticals, polymers, and functional materials (1). In contrast to the Pd-catalyzed approach, which depends on air- and moisture-sensitive conditions, the Cu-catalyzed coupling reaction proceeds under milder conditions. Among the various copper-based catalysts, ligand-free heterogeneous zero-valent copper nanoparticles (Cu NPs) continue to attract considerable and growing attention from researchers, owing to their advantages, including high specific surface area and size- and shape-tunable catalytic properties (2). Herein, a simple electrochemical method for the preparation of a composite of reduced graphene oxide (rGO) decorated with Cu NPs is presented, along with an evaluation of its catalytic performance in Ullmann C−N coupling reactions. The efficient and recyclable Cu-rGO catalyst is used to synthesize N-arylated compounds through Ullmann coupling under ligand-free conditions at relatively mild temperatures.

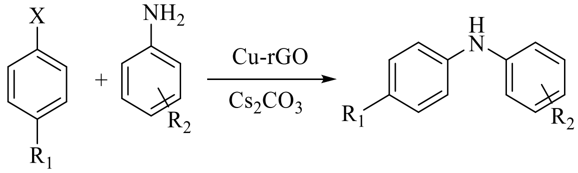

x= Cl, Br, I
R_1= H, OMe, NO_2 R_2= H, Me, OMe, NO_2, Cl

References:

(1) Devambatla, R. K. V.; Namjoshi, O. A. Choudhary, S.; Hamel, E.; Shaffer, C. V.; Rohena, C. C.; Mooberry, S. L.; Gangjee, A., Design, Synthesis, and Preclinical Evaluation of 4-Substituted-5-methyl-furo[2,3-d]pyrimidines as Microtubule Targeting Agents That Are Effective against Multidrug Resistant Cancer Cells. *J. Med. Chem.* **2016,** *59* (12), 5752-5765.

(2) Ma, D.; Cai, Q.; Zhang, H. Mild Method for Ullmann Coupling Reaction of Amines and Aryl Halides. *Org. Lett.* **2003,** *5* (14), 2453-2455.

The 30th Iranian Seminar of Organic Chemistry
February 7-9, 2025, Iran University of Science and Technology, Tehran, Iran

Synthesis of a novel magnetic porous organic polymer as an efficient hybrid nanocomposite for removal of heavy metal ions

Mohammad Ali Bodaghifard*[a,b], Fatemeh Mozaffari[a]

[a] *Department of Chemistry, Faculty of Science, Arak University, Arak 384817758, Iran*

[b] *Institute of Nanosciences and Nanotechnology, Arak University, Arak 384817758, Iran*

**E-mail: mbodaghi2007@yahoo.com; m-bodaghifard@araku.ac.ir*

Keyword: Heavy metal ions; Magnetic nanoparticles; Nanocomposite; Porous organic polymer.

The rapid industrialization and human activities in catchments have posed notable global challenges in removing of heavy metal contaminants from wastewater. Numerous industries, such as paint, battery manufacturing, mining, textile, steel, alloy, and electrical equipment manufacturing, generate industrial wastewater that often contains elevated levels of heavy metal ions such as lead (Pb), cobalt (Co), cadmium (Cd), copper (Cu), chromium (Cr), arsenic (As), and mercury (Hg) [1, 2]

Porous organic polymers (POPs) are a crucial type of organic porous materials that have shown significant promise as adsorbents [3, 4]. In continuation of our research on covalent organic frameworks and porous organic polymers [5-7], hearin, a Phloroglucinol-based magnetic porous organic polymer (Ph-MPOP) was successfully created through a catalyst-free Schiff's base condensation process involving 4,4-oxydianiline and a novel trisaldehyde in the presence of magnetic nanoparticles ($Fe_3O_4@SiO_2$) in dimethylformamide (DMF) under solvothermal conditions (Scheme 1). The structural properties of Ph-MPOP were characterized using different spectroscopic techniques.

The prepared porous organic polymer (Ph-MPOP) demonstrated strong binding capabilities and high efficiency in adsorbing Pb(II) and Cd(II) metal ions from aqueous solutions with removal efficencies of 97% and 95%, respectively. The heavy metal ions were adsorbed through coordination with nitrogens and oxygens of the nanostructure, as well as electrostatic interactions. The adsorption process followed the Freundlich isotherm with a high correlation coefficient (R^2 = ٠.٩٧, ٠،٩٦) and a pseudo-second-order kinetic model. Results from batch adsorption experiments revealed that porous organic polymer (Ph-MPOP) is highly effective in removing heavy metal ions with maximum adsorption capacities of 351 mg/g for Pb(II) and 343 mg/g for Cd(II). The recycled hybrid nanostructure was dried and subjected to various adsorption-desorption tests, revealing a desorption efficiency of 97%.

In conclusion, the newly synthesized magnetic adsorbent shows great promise in effectively removing heavy metal ions from water and wastewater.

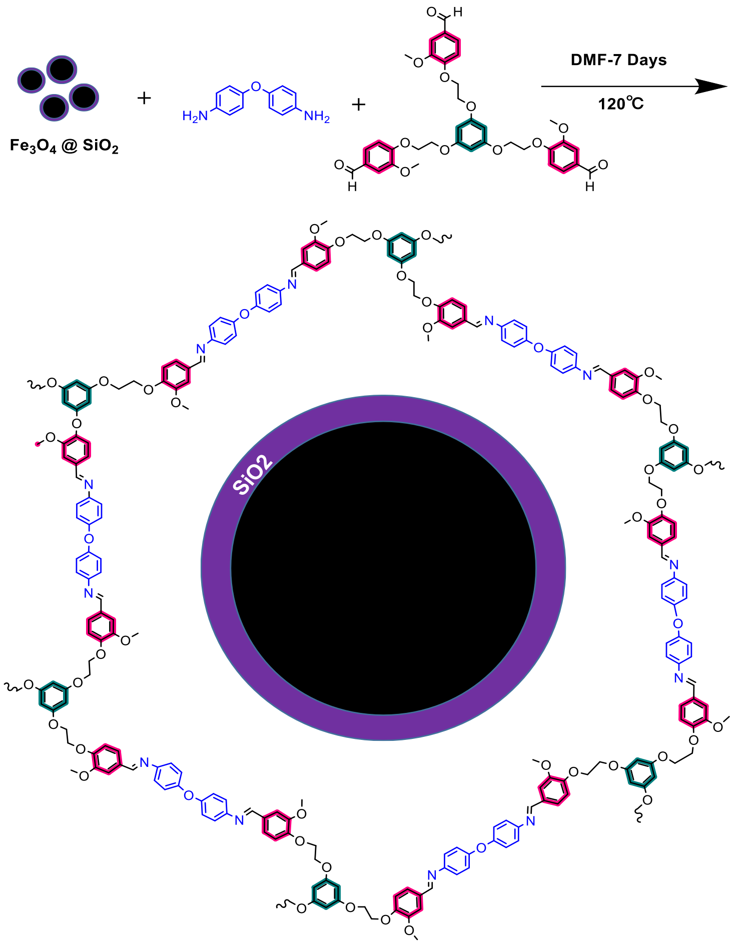

Scheme 1. Synthesis of Phloroglucinol-based magnetic porous organic polymer (Ph-MPOP) as an efficient adsorbent for heavy metal ions

References

(1) Futalan, C.M. and Wan, M.-W., Fixed-bed adsorption of lead from aqueous solution using chitosan-coated bentonite, *International Journal of environmental research and public health* **2022**, *19 (5)*, 2597.

(2) Abd Elnabi, M.K., et al., Toxicity of heavy metals and recent advances in their removal: a review. *Toxics* **2023**, *11 (7)*, 580.
(3) Chongdar, S.; Bhattacharjee, S.; Bhanja, P.; Bhaumik, A., Porous organic–inorganic hybrid materials for catalysis, energy and environmental applications, *Chem. Commun.*, **2022**, *58*, 3429-3460.
(4) Arameshian, S.; Dinari, M.; Rezaei, R., Green synthesis of novel nitrogen-rich covalent organic polymer for efficient removal of methylene blue from aqueous solutions, *J. Polym. Res.*, **2024**, *31*, 97.
(5) Faraki, Z.; Bodaghifard, M.A., Synthesis and characterization of a highly functionalized cationic porous organic polymer as an efficient adsorbent for removal of hazardous nitrate and chromate ions, *Results in Chemistry* **2022**, *4*, 100657.
(6) Faraki, Z.; Bodaghifard, M.A., A triazine-based cationic covalent organic framework as a robust adsorbent for removal of methyl orange, *Polycyclic Aromatic Compounds* **2023**, *43 (7)*, 5940-5957.
(7) Faraki, Z.; Bodaghifard, M.A., Design and synthesis of nitrogen-rich imine-based porous organic polymer as an efficient adsorbent for CO2 capture, *Journal of Materials Science* **2023**, *58 (36)*, 14587-14596.

The 30th Iranian Seminar of Organic Chemistry
February 7-9, 2025, Iran University of Science and Technology, Tehran, Iran

Synthesis and Characterization of Cross-Linked Polyacrylamide-Based Catalyst for Efficient Click Reaction

Ali Rahmatpour[1]*, Abolfazl Jahani[1]

[1]Polymer Chemistry Research Laboratory, Faculty of Chemistry and Petroleum Science, Shahid Beheshti University, *Corresponding author: E-mail: a_rahmatpour@sbu.ac.ir

Keyword: Cross-linked polyacrylamide, copper(I) iodide, click reaction

Cross-linked polymers, with their stable three-dimensional structure, offer high mechanical strength, thermal and chemical stability, making them ideal for applications in water purification, energy storage and drug delivery [1]. These polymers also serve as a support for the immobilization of metals and catalysts. Acrylamide-based polymers are increasingly used due to their accessibility and versatility [2]. In this study, cross-linked polyacrylamide (CPAM) was synthesized using acrylamide and N,N'-methylenebisacrylamide (MBA). CPAM was modified with propylene diamine to form CPAM_{PD}, then reacted with isatoic anhydride to form a bidentate ligand that coordinates with copper(I) iodide. FT-IR, UV-Vis, DRS, ICP-OES, SEM-EDS and XRD confirmed the catalyst structure. Immobilization of copper(I) was confirmed by FT-IR peaks at around 620 cm^{-1} and 755 cm^{-1}, and ICP analysis showed that 9.3% of copper(I) was immobilized.The results showed that the synthesized catalyst efficiently performed the click reaction heterogeneously in 45 min with 0.7 mol% catalyst and was recyclable.

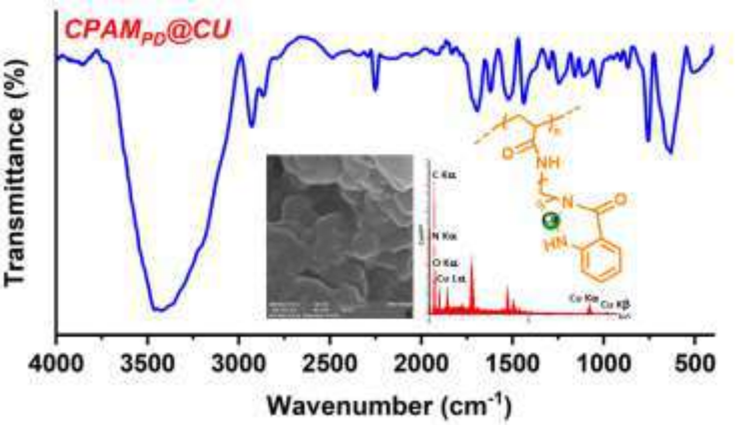

Scheme 1: Structural and Analytical Characterization of the Final Catalyst: FT-IR, FE-SEM, and EDS Analysis

References:

(1) Thang, N. H.; Chien,T.B; Cuong, D. X. *Gels* **2023**, *9*, 523.

(2) Radhakrishnan, A.; Panicker, U. G. *Polymer Bulletin* **2024**, 1-49.

The 30th Iranian Seminar of Organic Chemistry
February 7-9, 2025, Iran University of Science and Technology, Tehran, Iran

Improvement of carboxymethyl cellulose/β-cyclodextrin polymer by functionalization with carboxamide as a new efficient ampicillin bio-carrier for oral bacterial infection treatment

Mohammad Hossein Alizadeh[a], Malihe Pooresmaeil[a], Hassan Namazi[a,b*]

[a]*Polymer Research Laboratory, Department of Organic and Biochemistry, Faculty of Chemistry, University of Tabriz, Tabriz, Iran.*
[b]*Research Center for Pharmaceutical Nanotechnology, Biomedicine Institute, Tabriz University of Medical Science, Tabriz, Iran.*

---

[*] Corresponding author: P.O. Box 51666, Tel: +98 4133393121, Fax: +98 4133340191, Email:namazi@tabrizu.ac.ir, ORCID: http://orcid.org/0000-0002-1977-4677.

Keywords: Carboxymethyl cellulose; Functionalizaed carboxamide; Polymer hybrids; Ampicillin; drug delivery.

Introduction

In the last years, several attempts have been made to design and prepare new hydrogels with high performance and low cost which can be used as pharmaceutical carriers. In multicomponent reactions (MCRs), most reactants are extracted from nature, are very cheap, and are available materials. Also, the combination of the MCRs with hydrogels makes them superior in drug delivery properties. This work has tried to use carboxymethyl cellulose/β-cyclodextrin as an acidic component of the Ugi MCR to obtain a better drug carrier system versus carboxymethyl cellulose/β-cyclodextrin [1, 2].

Method

Ugi multicomponent reaction was performed on CMC@β-CD in the one-pot method to obtain the CMC@β-CD@FCA with cyclohexyl isocyanide, 4-methoxy benzaldehyde, and ethylenediamine and then used ampicillin as an antibiotic drug to load on the desired carrier for oral bacterial infection treatment [3].

Results and discuss

The in vitro drug loading test displayed the enhancement of the ampicillin (AMP) loading efficiency from 64.22 % to 92.44 % which is a sign of more possible interactions between CMC@β-CD@FCA with AMP than CMC@β-CD.

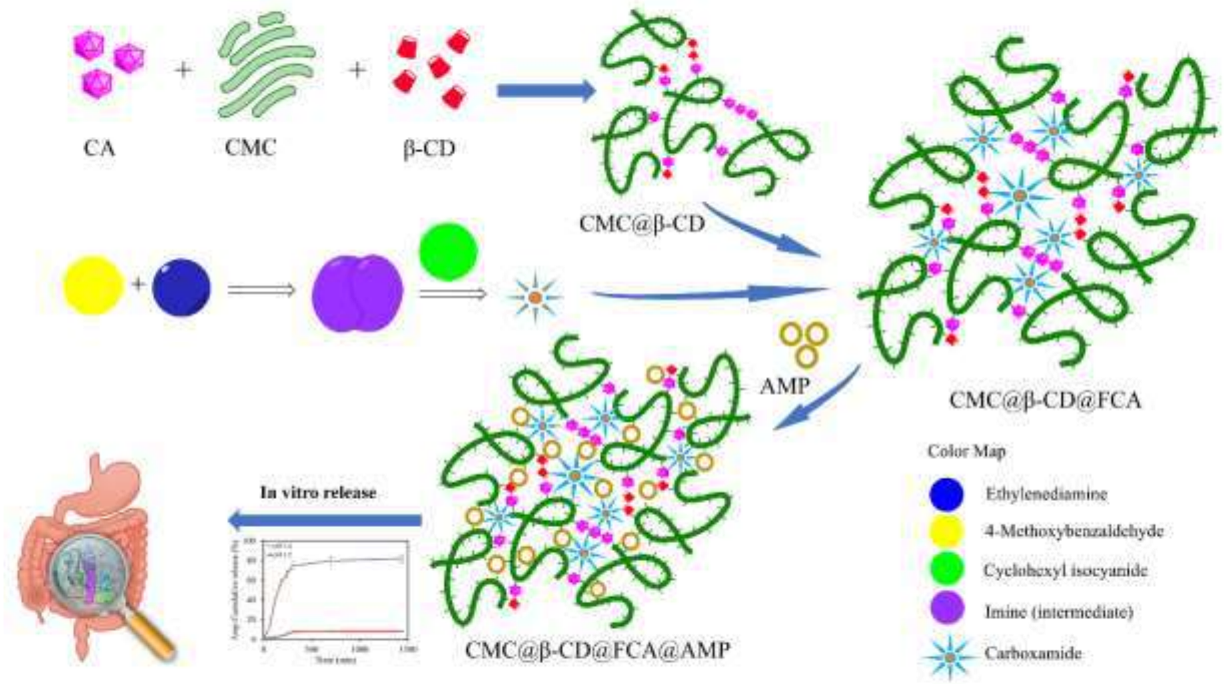

Scheme: Graphical abstract of the CMC@β-CD@FCA action for oral bacterial infection treatment.

References:

[1] V.S. Ghorpade, A.V. Yadav, R.J. Dias, Citric acid crosslinked β-cyclodextrin/carboxymethylcellulose hydrogel films for controlled delivery of poorly soluble drugs, Carbohydrate Polymers 164 (2017) 339-348.

[2] S. Javanbakht, A. Shaabani, Carboxymethyl cellulose-based oral delivery systems, International journal of biological macromolecules 133 (2019) 21-29.

[3] S. Javanbakht, M.T. Nazeri, A. Shaabani, M. Ghorbani, Green one-pot synthesis of multicomponent-crosslinked carboxymethyl cellulose as a safe carrier for the gentamicin oral delivery, International Journal of Biological Macromolecules 164 (2020) 2873-2880.

Phytochemical Profiling and Identification of Secondary Metabolites from *Asarum europaeum* L.

Authors: Mahdieh Kurepaz-Mahmoodabadi [a], Mina Saeedi [a,b], Elham Fani [c], Azadeh Manayi [a], Mahnaz Khanavi [b,c*]

[a]*Medicinal Plants Research Center, Faculty of Pharmacy, Tehran University of Medical Sciences, Tehran, Iran.*
[b]*Persian Medicine and Pharmacy Research Center, Tehran University of Medical Sciences, Tehran, Iran.*
[c]*Department of Pharmacognosy, Faculty of Pharmacy, Tehran University of Medical Sciences, Tehran, Iran.*

Keyword: *Asarum*, neohesperidin, phthalate

Introduction: *Asarum europaeum* L. belongs to the family Aristolochiaceae, known as Asarum or European wild ginger. This plant has been used traditionally to treat many diseases, and it is famously known to improve memory. Therefore, phytochemical study of the ethyl acetate fraction of methanol extract of *A. europaeum* rhizomes was investigated to identify compounds that have not been previously reported for this plant. Methods: Purification of compounds was done following column chromatography of the ethyl acetate fraction with increasing polarity solvents. The structure of isolated compounds was determined by the comparison of the NMR spectrum data with the literature values. Results and Discussion: Three compounds were isolated and identified: bis(2-ethylhexyl) terephthalate (**1**), 4-(3-glucopyranosyloxy-4-hydroxyphenyl)-(*E*)-3-buten-2-one (**2**), and neohesperidin (2R) (**3**). To extend the notion of drug discovery development, this study described the isolation and identification of the structure of secondary metabolites that are yet to be determined for *A. europaeum*.

References:

[1] Akhlaq S, Ara SA, Fazil M, Ahmad B, Akram U, Haque M, Khan AA. Ethno pharmacology, phytochemical analysis, safety profile, prophylactic aspects, and therapeutic potential of *Asarum europaeum* L. in Unani medicine: an evidence-based appraisal. *Phytomed Plus.* 2022; 2(2): 1-11.
[2] Azam Khan H. The greatest elixir (Exir Azam). Tehran: Research Institute for Islamic and Complementary Medicine, 2009.
[3] Saeedi M, Vahedi-Mazdabadi Y, Rastegari A, Soleimani M, Eftekhari M, Akbarzadeh T, Khanavi M. Evaluation of *Asarum europaeum* L. rhizome for the biological activities related to Alzheimer's disease. *Res J Pharmacogn.* 2020; 7(3): 25-33.

Evaluation of the biological activity of fermented and unfermented extracts of bay Laurus nobilis for skin applications

P. Ansari [a], A. Niazi [a], A. Yazdanipour [a], P. Jafari [b]*

[a] *Department of Chemistry, Central Tehran Branch, Islamic Azad University, Tehran, Iran.*

[b] *Department of Microbiology, Arak Branch, Islamic Azad University, Arak, Iran.*

**Email: ali.niazi@gmail.com, ali.niazi@iauctb.ac.ir*

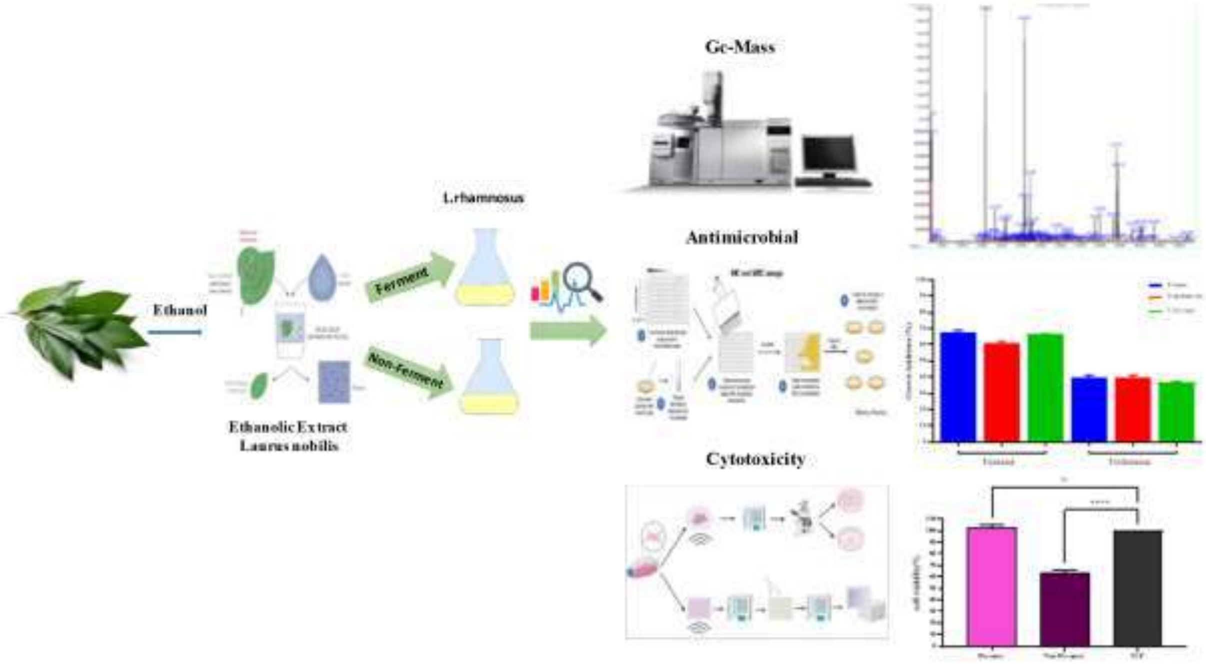

Biotechnology is recognized as a more efficient and safer alternative to synthetic chemicals due to its ability to produce bioactive compounds. The cosmetics and personal care industry places significant emphasis on high-bioactivity compounds and their availability for treating and preventing skin diseases. In this context, plant extracts and bioferments have garnered considerable attention as valuable sources of phytochemicals. In this study, we compared the antimicrobial activity (MIC, MBC) and cell viability (MTT) of non-fermented ethanolic extracts of Laurus nobilis (NFELN) and fermented ethanolic extracts of Laurus nobilis (FELN) under controlled laboratory conditions. The fermentation process utilized the probiotic bacterium Lactobacillus rhamnosus A6-5 as the inoculum. The extracts' bioactive compounds' content was assessed using gas chromatography-mass spectrometry (GC-MS). The Alamar Blue assay was performed on human fetal skin fibroblast (HFF) cells to evaluate cytotoxicity in the tested samples. Cells were treated with 100 µL of each sample and the control group for 72 hours. The results indicated a significant increase in fibroblast cell viability when treated with FELN at a an 810 µg/mL

concentration, yielding a viability percentage of 102.8 ± 2.27%. In contrast, NFELN at the same concentration (810 µg/mL) induced cytotoxic effects on HFF, resulting in a viability of 63.52 ± 2.49%. A comparison of the results from both assays demonstrates that FELN exerts a more beneficial effect on the viability and activity of the examined cells. Additionally, microbiological analyses were conducted on various pathogenic skin strains, including Staphylococcus epidermidis, Propionibacterium acnes, and Candida albicans, employing methods to determine the minimum inhibitory concentration (MIC) and minimum bactericidal concentration (MBC). The MIC and MBC of FELN and NFELN were assessed at concentrations ranging from 810 µL to 1.58 µL after a 24-hour incubation using microplate reader. The results of the present study indicate that the fermented extract of Laurus nobilis (FELN) exhibits significant antimicrobial efficacy, particularly at low concentrations, demonstrating superior biological activity when compared to the non-fermented crude extract. These findings suggest that the fermented extract could be utilized as an active ingredient in skincare formulations within the cosmetic industry. Numerous studies have reported that incorporating such natural compounds into consumer products not only increases consumer demand but also demonstrates a favorable environmental impact.

Keyword: Laurus Nobilis, Fermentation process, Medicinal plant, Biotechnology, Antimicrobial Activity, Antifungal activity, Microorganisms (S. epidermidis, P. acnes, and C. albicans), Skin cells, biological activity, cytotoxic

References:

١. Al-Abdullah, A. A. A. R., Jasim, E. Q., & Muhammad-Ali, M. A. (2023). Antibacterial Efficacy and Molecular Docking of Leaf Extract of Laurus nobilis L Against some Isolated Pathogenic UTI Bacteria. *IOP Conference Series: Earth and Environmental Science*, *1215*. https://doi.org/10.1088/1755-1315/1215/1/012057

٢. Karami, P., Zandi, M., & Ganjloo, A. (2022). Evaluation of key parameters during ohmic-assisted hydro-distillation of essential oil from aerial part of yarrow (Achillea millefolium L.). Journal of Applied Research on Medicinal and Aromatic Plants, 31. https://doi.org/10.1016/j.jarmap.2022.100425

٣. Balouiri, M., Sadiki, M., & Ibnsouda, S. K. (2016). Methods for in vitro evaluating antimicrobial activity: A review. In Journal of Pharmaceutical Analysis (Vol. 6, pp. 71–79). Xi'an Jiaotong University. https://doi.org/10.1016/j.jpha.2015.11.005

٤. Beyene, R., Geremew, T., & Dekebo, A. (2024). Antibacterial and antioxidant properties and phytochemical screening of Laurus nobilis L. extract from Ethiopia. International Journal of Secondary Metabolite, 11, 494–506. https://doi.org/10.21448/ijsm.1375324

٥. Masiá, C., Geppel, A., Jensen, P. E., & Buldo, P. (2021). Effect of lactobacillus rhamnosus on physicochemical properties of fermented plant-based raw materials†. Foods, 10. https://doi.org/10.3390/foods10030573

٦. Bontzolis, C. D., Dimitrellou, D., Plioni, I., Kandylis, P., Soupioni, M., Koutinas, A. A., & Kanellaki, M. (2024). Effect of solvents on aniseed aerial plant extraction using soxhlet and ultrasound methods, regarding antimicrobial activity and total phenolic content. Food Chemistry Advances, 4. https://doi.org/10.1016/j.focha.2024.100609

٧. Rodríguez-Melcón, C., Alonso-Calleja, C., García-Fernández, C., Carballo, J., & Capita, R. (2022). Minimum Inhibitory Concentration (MIC) and Minimum Bactericidal Concentration (MBC) for Twelve Antimicrobials (Biocides and Antibiotics) in Eight Strains of Listeria monocytogenes. Biology, 11. https://doi.org/10.3390/biology11010046

٨. Parvekar, P., Palaskar, J., Metgud, S., Maria, R., & Dutta, S. (2020). The minimum inhibitory concentration (MIC) and minimum bactericidal concentration (MBC) of silver nanoparticles against Staphylococcus aureus. Biomaterial Investigations in Dentistry, 7, 105–109. https://doi.org/10.1080/26415275.2020.1796674

٩. Park, Y. A., Lee, S. R., Lee, J. W., Koo, H. J., Jang, S. A., Yun, S. W., Kim, H. J., Woo, J. S., Park, M. R., Kang, S. C., Kim, Y. K., & Sohn, E. H. (2018). Suppressive effect of fermented Angelica tenuissima root extract against photoaging: Possible involvement of hemeoxygenase-1. Journal of Microbiology and Biotechnology, 28, 1391–1400. https://doi.org/10.4014/jmb.1805.05065

١٠. Sun, Q., Fang, J., Wang, Z., Song, Z., Geng, J., Wang, D., Wang, C., & Li, M. (2022). Two Laminaria japonica Fermentation Broths Alleviate Oxidative Stress and Inflammatory Response Caused by UVB Damage: Photoprotective and Reparative Effects. Marine Drugs, 20. https://doi.org/10.3390/md20100650

١١. Lorenz, P., Zilkowski, I., Mailänder, L. K., Klaiber, I., Nicolay, S., Garcia-Käufer, M., Zimmermann-Klemd, A. M., Turek, C., Stintzing, F. C., Kammerer, D. R., & Gründemann, C. (2023). Comparison of Aqueous and Lactobacterial-Fermented Mercurialis perennis L. (Dog's Mercury) Extracts with Respect to Their Immunostimulating Activity. Fermentation, 9. https://doi.org/10.3390/fermentation9020190

١٢. Mousavi, S. A., Nateghi, L., Javanmard Dakheli, M., Ramezan, Y., & Piravi-Vanak, Z. (2022). Maceration and ultrasound-assisted methods used for extraction of phenolic compounds and antioxidant activity from Ferulago angulata. Journal of Food Processing and Preservation, 46. https://doi.org/10.1111/jfpp.16356

١٣. Mishra, D., & Patnaik, S. (2020). GC-MS analysed phyto-chemicals and antibacterial activity of Withania somnifera (L.) dunal extract in the context of treatment to liver cirrhosis. Biomedical and Pharmacology Journal, 13, 71–78. https://doi.org/10.13005/bpj/1862

The 30th Iranian Seminar of Organic Chemistry
February 7-9, 2025, Iran University of Science and Technology, Tehran, Iran

Reduced Graphene Oxide Photocatalyst heterogeneous with Visible-Light for selective oxidation of alcohols to aldehydes

Zahra Kohansal Nalkyashree, [a], Mohammad Mahdi Roozbahani[a], Nadiya Koukabi[*a], Eskandar Kolvari*[a], Kheibar Dashtian[*b]

[a] *Department of Chemistry, Semnan University, 35131-19111 Semnan, Iran*

[b] *Department of Chemistry, Iran University of Science and Technology, Tehran 16846- 13114, Iran*

[*] *E-mail:* n.koukabi@semnan.ac.ir, kolvari@semnan.ac.ir, kdasht68@gmail.com

Keywords: Basil seed, Photocatalysis, Alcohol oxidation, Graphene-like carbon, Microwave Irradiation

The oxidation of alcohols to aldehydes is a very important process in organic reactions[1]. Benzaldehyde is a valuable industrial compound which was employed mainly as a precursor for the manufacture of diverse key chemicals in the pharmaceutical and food industries.In industry, the traditional method of preparing aldehydes by alcohol oxidation usually requires high reaction temperature and high valence metal salts as oxidants, which is a high energy consumption method and will inevitably produce environmental pollutants containing metal ions with high valence[2]. Compared to other classical methods, using multiphase photocatalysis requires milder conditions, and the main problem with these reactions is to find effective factors and optimize them to have appropriate selectivity. The selective synthesis of benzaldehyde from benzyl alcohol by visible light is a promising green synthesis method The use of photocatalysts in the presence of visible light energy for chemical transformation is an active area of research today[3]. Nature is a vast resource pool with an abundance of natural biomass. Natural biomass can meet the demand for green chemistry, cut costs, and maximize resource usage. In this respect, the use of natural substances in the production of catalysts has seen significant growth among researchers; natural materials such as fibroin , starch , chitosan , cellulose , and basil seeds could appear effectively in this field[4].

In this research, graphene-like carbon (GLC) incorporated with Ag-Cu_2O was effectively produced by activating basil seeds with sodium hydroxide via a two-step microwave-assisted method that involved reactions with silver and copper metal salts. The resulting photocatalyst was applied in the alcohol oxidation reactionreaction (Scheme 1), showing excellent performance in optimized conditions. An extensive characterization of the nanocatalyst was performed using a range of analytical methods, including FT-IR, XRD, TGA, XPS, HR-TEM, FE-SEM, AAS, and EDS. The prepared Ag-Cu_2O/GLC presents multiple advantages, including environmental sustainability, affordability, and high catalytic efficiency.

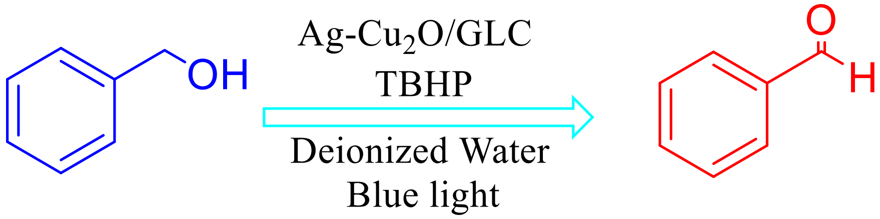

Scheme 1: oxidation of alcohols to aldehydes Photocatalyst by Ag-Cu_2O/GLC

References:

1. Sudrajat, H., et al., *Atomistic understanding of enhanced selectivity in photocatalytic oxidation of benzyl alcohol to benzaldehyde using graphitic carbon nitride loaded with single copper atoms.* Nanoscale, 2024. **16**(31): p. 14813-14830.

2. Nalkyashree, Z.K., et al., *Synergistic atom co-sharing and S-scheme heterojunction: constructing Cu/CuO/Cu 2 O with ultrathin graphene-like carbon derived from basil seeds for enhanced photo-oxidation of benzyl alcohols to aldehydes.* Nanoscale Advances, 2024. **6**(21): p. 5348-5360.

3. Kumar, A., et al., *Microwave chemistry, recent advancements, and eco-friendly microwave-assisted synthesis of nanoarchitectures and their applications: a review.* Materials Today Nano, 2020. **11**: p. 100076.

4. Kheirabadi, Z.A., M. Rabbani, and M.S. Foroushani, *Green Fabrication of Nonenzymatic Glucose Sensor Using Multi-Walled Carbon Nanotubes Decorated with Copper (II) Oxide Nanoparticles for Tear Fluid Analysis.* Applied Biochemistry and Biotechnology, 2022. **194**(8): p. 3689-3705.

The 30th Iranian Seminar of Organic Chemistry
February 7-9, 2025, Iran University of Science and Technology, Tehran, Iran

Synthesis of tetrahydrobenzo[*b*]pyran using functionalized TiO_2 as the reaction catalyst

Zahra Dargahi, Zahra Basiri Rad, Hadiseh Shafitali, Behnam Mahdavi *, Seyedeh Fatemeh Hojati

Department of Chemistry, Faculty of Science, Hakim Sabzevari University, Sabzevar, Iran

Email: b.mahdavi@hsu.ac.ir

Keyword: Tetrahydrobenzo[b]pyran, functionalized TiO2

Introduction

Piperazine is a cyclic diamine with two amino groups (NH) positioned in a hexagonal ring. TiO_2 thin films is drastically increasing due to their various and promising applications, such as photocatalysis, catalysts and optical filters, production of pigments, cosmetics [1]. The functionalized TiO_2 materials are classified as a new type of catalysts to synthesis wide variety of compounds. Tetrahydrobenzo[b]pyrans are known as heterocyclic compounds with diverse medicinal applications. These compounds possess anti-cancer, anti-microbial, and anti-coagulant properties, and are effective in the treatment of diseases such as Alzheimer's and Parkinson's[۲]. In the present study, Tetrahydrobenzo[b]pyran was synthesized using functionalized TiO2. For this propose, Piperazine as a cyclic diamine was used for functionalizes of TiO_2 as a new catalyst (TiO_2@Pip).

Method

Preparation of TiO_2@Pip**:** A 10 mL of aqueous solution piprazine (0.12 M) was added to a 10 mL of dispersed TiO_2 in water. The mixture was stirred for 30 min at RT. Next, the mixture was heated in an autoclave for 12 h at 120 °C. After that, the yield was centrifuged and washed with water.

General procedure for the synthesis of Tetrahydrobenzo[b]Pyran: A mixture of benzaldehyde (1 mmol), malononitrile (1 mmol), dimedone (1 mmol), and 0.05 gr of TiO_2@Pip was refluxed at 90°C. The reaction process was monitored by TLC to complete.Scheme1)

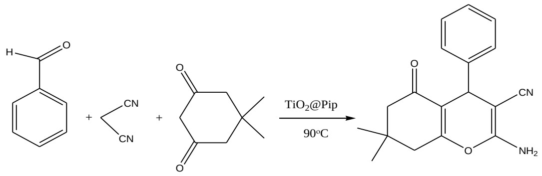

Scheme1. The synthesis procedure of Tetrahydrobenzo[b]pyran

Discussion

TiO_2@Pip and tetrahydrobenzo[b]pyran were characterized using FT-IR spectroscopy (see Figure 1 a,b,c,d). For TiO_2@Pip, a band at 667belongs to Ti – O [۱]. The bands of TiO_2@Pip were observed at 2967 cm^{-1} and 2886 cm^{-1}, which correspond to the asymmetric and symmetric stretching vibrations of -CH-, respectively. The bending vibrations of N-H and C-N were observed at 1527 and 1459 cm^{-1}, respectively. Furthermore, the characteristic peak at 3400 cm^{-1} for belongs to the stretching vibration of N-H [3]. All of these results indicated that piperazine was conjugated to the surface of Titanium dioxide.

Characterization of tetrahydrobenzo[b]pyran: The stretching bands at 3500 and 3300 cm^{-1} belong to N-H. The band of stretching aromatic hydrogens were observed at 3150 cm^{-1}. The band at 2921 cm^{-1} belongs to stretching vibrations of -CH-. The stretching vibrations of C-O, C=C, and C=N were observed at 1250, 1475, and 2250 cm^{-1}, respectively. In addition, the bending peaks of CH_2 and CH_3 were appeared at 1465, 1375 and 1450 cm$^{-1.}$ Finally, the bending band of aromatic C-H was appearance at 900 and 960 cm^{-1}. All the results indicated that the successfully synthesis of Tetrahydrobenzo[b]pyran.

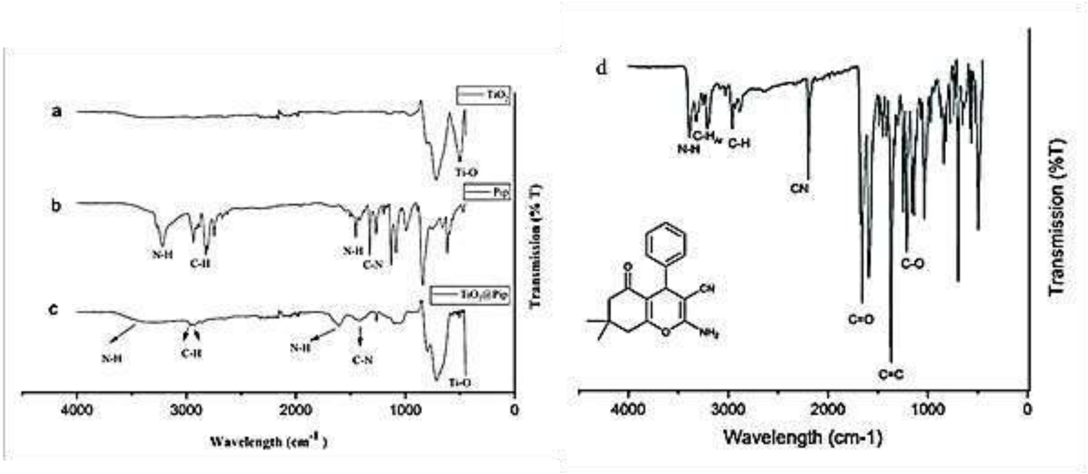

Fig1. a (TiO$_2$), b (Piperazine), c (TiO$_2$@Pip), d (tetrahydrobenzo[*b*]pyran)

References

[1]. Al-Oubidy, Esraa A., and Firas J. Kadhim. "Photocatalytic activity of anatase titanium dioxide nanostructures prepared by reactive magnetron sputtering technique." *Optical and Quantum Electronics* 51.1 (2019): 23

[2]. . Hojati, Seyedeh Fatemeh, et al. "Polypyrrole/Fe3O4/CNT as a recyclable and highly efficient catalyst for one-pot three-component synthesis of pyran derivatives." *Applied Organometallic Chemistry* 32.4 (2018): e4235.

[3]. Subashini, K., and S. Periandy. "Spectroscopic (FT-IR, FT-Raman, UV, NMR, NLO) investigation and molecular docking study of 1-(4-Methylbenzyl) piperazine." *Journal of Molecular Structure* 1134 (2017): 157-170.

The 30th Iranian Seminar of Organic Chemistry
February 7-9, 2025, Iran University of Science and Technology, Tehran, Iran

A green natural catalyst in the preparation of tetrahydrobenzo[*b*]pyrans

Seyedeh Fatemeh Hojati*, Zahra Borghebani، Zahra Dargahi, Arezo Mehmandoust، ElaheSadat Hoseini Tabatabai

Department of chemistry, Hakim Sabzevari university, Sabzevar, Iran, Email: *sf.hojati@hsu.ac.ir*

Keyword: multi-component reactions, one-pot synthesis, tetrahydrobenzo[*b*]pyran

Introduction

During the past years, the use of recyclable heterogeneous catalyst (a solid catalyst that is dispersed on a supporting material to increase surface area and provide stability) has received significant importance in organic chemistry [1].

The pistachio hard shell is an agricultural waste and would be an excellent biosource for preparing solid acids because of its high adsorption ability, low cost, and easy sustainability [2].

Much like other agricultural lignocellulose biomass, such as coconut shell, sawdust, peanut shell pistachio hard shell is composed mainly of lignin, cellulose and hemicelluloses. Consequently, the main active sites of pistachio shell are a wide variety of hydroxyl groups that can be used for the preparation of solid acid catalysts [3].

Multi-component reactions (MCRs) have significant role in organic chemistry, because of some merits like selectivity, synthetic convergence, high atom economy, simplicity, short reaction time, facility of workup, synthetic efficiency and high yield of products. An efficient way for the synthesis of heterocyclic compounds is using multi-component reactions, which have great value in design of biologically new active compounds. Tetrahydrobenzo[*b*]pyrans as one of the significant group of oxygen-containing heterocycle compounds are highly considered due to their medicinal and biological properties such as spasmolytic, antitumor, antibacterial, anti HIV, insulin-sensitizing activity and hypotensive antiviral [4].

Experimental

A mixture of aromatic aldehyde (1 mmol), malononitrile (1 mmol) and dimedone (1 mmol) was prepared and 0.01 gr of Hard Shell of Pistachio (HSP) was added to the mixture and heated at 80 °C in Ethanol. The progress of the reaction was monitored by TLC (eluent: EtOAc/ *n*-hexane, 1:1) (Scheme1).

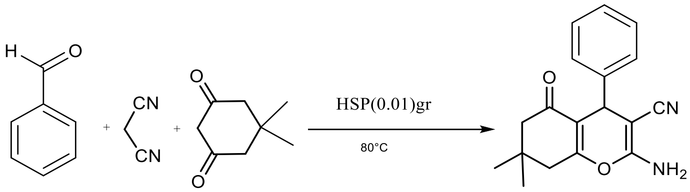

Scheme 1. The preparation of benzopyrans using Hard Shell of Pistachio (HSP)

results & discussion

The results obtained from the energy dispersive X-ray spectroscopy of pistachio shell show that it consists of 62.5% carbon and 37.2% oxygen, along with trace amounts of other elements present in its structure (Fig1).

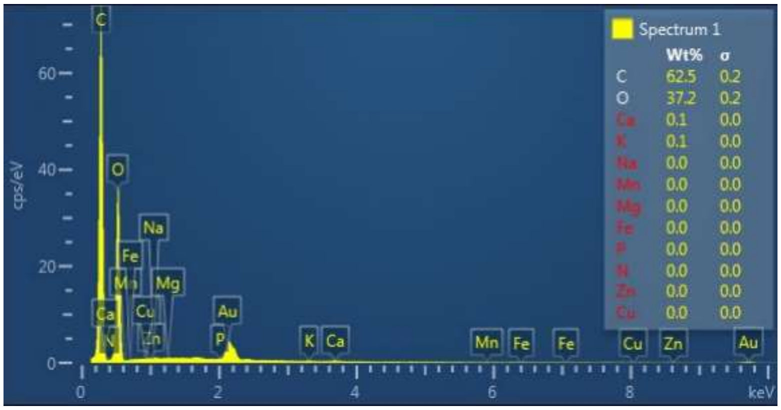

Fig1. "X-ray Powder Diffraction Spectroscopy Analysis of Hard Shell of Pistachio."

References:

[1] Arzehgar Z, Aydi A, Mirzaei Heydari M. Silver functionalized on hydroxyapatite-core-shell magnetic γ-Fe_2O_3: an enviromentaly and readily recyclable nanatalyst for the one-pot synthesis of 14H-dibenzo [a, j] xanthenes derivatives. Asian J. Green Chem. 2018;2:281-98.

[2] Taghizadeh A, Rad-Moghadam K. Green fabrication of Cu/pistachio shell nanocomposite using Pistacia Vera L. hull: An efficient catalyst for expedient reduction of 4-nitrophenol and organic dyes. Journal of Cleaner Production. 2018 Oct 10;198:1105-19.

[3] Kamali-Gharamaleki M, Sadeghi B, Rouhani M, Mirjafary Z. Nano-pistachio hull-OSO_3 H: synthesis, characterization and application as an effective and novel nanocatalyst for one-pot synthesis of dihydropyrano [3, 2-b] chromene dione derivatives. Reaction Kinetics, Mechanisms and Catalysis. 2021 Feb;132:251-60.

[4] Mehravar M, Mirjalili BB, Babaei E, Bamoniri A. Nano-SiO_2/DBN: an efficacious and reusable catalyst for one-pot synthesis of tetrahydrobenzo [*b*] pyran derivatives. BMC chemistry. 2021 May 21;15(1):34.

The 30th Iranian Seminar of Organic Chemistry

February 7-9, 2025, Iran University of Science and Technology, Tehran, Iran

Investigation of the catalytic activity of zeolite beta in the preparation of spiro-indoline-pyranopyrazole compounds

Arezou Mehmandoust, Seyedeh Fatemeh Hojatia*, Zahra Borghebani, Sarah Soleimani, Zahra Dargahi

Department of chemistry, Hakim Sabzevari university, Sabzevar, Iran, Email: sf.hojati@hsu.ac.ir

Keyword: Zeolite beta, One-pot synthesis, spiropyrazoles

Introduction

Zeolites are crystalline microporous materials formed by corner-sharing TO_4 (T = Si or Al) tetrahedra, which have the periodic one-to-three dimensional frameworks, unique porous structure, and fine thermal and chemical stability. They have found widespread applications in many industrial fields such as catalysis, adsorption, separation, and ion exchange [1].

Heterocyclic compounds containing the 4H-pyran ring have played important roles in synthetic and medicinal chemistry, and polyfunctionalized 4H-pyran groups have attracted the attentions of many researchers involved in drug discovery process. The main interest in the 4H-pyran group is due to its biological and pharmacological characteristics. Pyrano[2,3-c]pyrazoles are heterocyles with significant activities, such as anti-tumor, analgesic, anticancer and anti-inflammatory properties. In addition, these compounds are important precursors for promising drugs in the field of medicinal chemistry. They also serve as potential inhibitors of human Chk1 kinase. Spiro compounds containing pyrans have also been proven to have a wide range of biological activities, as hypertensive and potential novel analgesic agents [2].

Experimental

Ethyl acetate (1 mmol) and hydrazine hydrate (2 mmol) were poured into the flask, and one ml of water solvent and 0.003 gr of zeolite beta catalyst were added to the reaction mixture and stirred for 10 minutes at room temperature. Then malononitrile (1 mmol) and isatin (1 mmol) were added. After completion of the reaction as monitored by TLC

(eluent: EtOAc/ n-hexane, 1:1).(Scheme1)

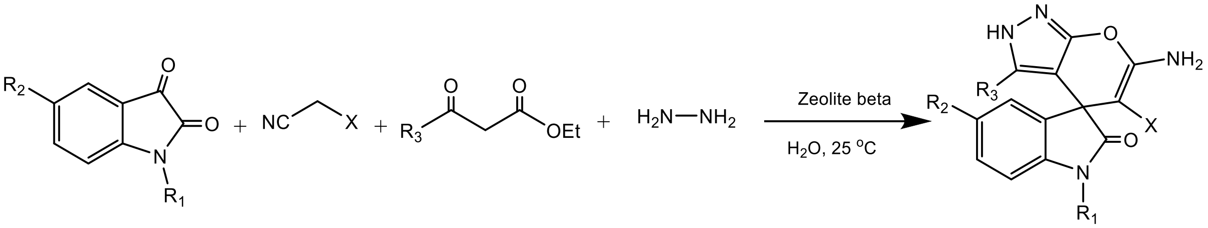

Scheme 1. The preparation of spiropyrazoles using Zeolite beta

results & discussion

The XRD diffraction pattern of zeolite beta is observed as two characteristic peaks at 2ɵ= 20-25 and 2ɵ=8, indicating the crystalline structure of the synthesized zeolite beta.(Scheme 2)

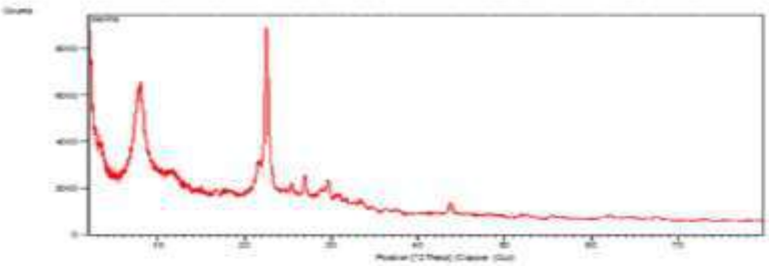

Scheme 2. XRD diagram of zeolite beta

References

[1] Lu T, Yan W, Xu R. Chiral zeolite beta: structure, synthesis, and application. Inorganic Chemistry Frontiers. 2019;6(8):1938-51.

[2] Mamaghani M, Hossein Nia R, Shirini F, Tabatabaeian K, Rassa M. An efficient and eco-friendly synthesis and evaluation of antibactrial activity of pyrano [2, 3-c] pyrazole derivatives. Medicinal Chemistry Research. 2015 May;24:1916-26.

The 30th Iranian Seminar of Organic Chemistry
February 7-9, 2025, Iran University of Science and Technology, Tehran, Iran

A green and efficient synthesis of alkyl 2-((5-hydroxy-1*H*-pyrazole-4-carbonothioyl)thio)acetates *via* a one-pot, solvent-free reaction

Seyedeh Reyhaneh Samaei* and Farough Nasiri

Department of Applied Chemistry, University of Mohaghegh Ardabili, P.O. Box 56199-11367, Ardabil, Iran, E-mail:r.samaei@uma.ac.ir

Keyword: Pyrazolones; carbon disulfide; green chemistry; solvent-free reactions; one-pot reactions

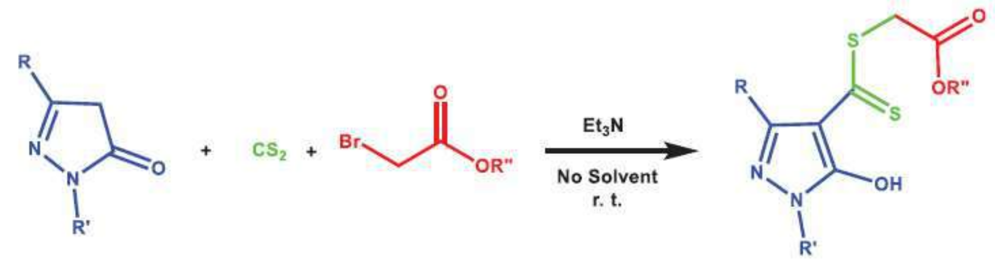

4a-4f
R: Me, Ph, Pr; **R'**: Ph, H

5a, 5b
R": Me, Et

3a-3g
(62%-97%)

Scheme: Solvent-free synthesis of alkyl 2-((5-hydroxy-1H-pyrazole-4-carbonothioyl)thio)acetates 3a-3g.

Introduction: Pyrazoles, a versatile class of heterocyclic compounds, have captured significant attention due to their broad spectrum of properties and applications [1,2]. These compounds exhibit various pharmacological activities, including analgesic, antiinflammatory,antimicrobial, herbicidal, and pesticidal effects [3,4]. Additionally, they have shown promise in addressing cognitive disorders such as Alzheimer's disease [5].

Results and discussion: Alkyl 2-((5-hydroxy-1H-pyrazole-4-carbonothioyl)thio)acetates 3 were synthesized in a two-step process from pyrazolone derivatives 4, carbon disulfide, and alkyl bromoacetate derivatives 5. The reaction was initiated by adding a base to a mixture of compound 4 and carbon disulfide in a sealed test tube. TLC analysis was used to monitor the consumption of the starting material, 4. Once 4 was completely consumed, alkyl bromoacetate 5 was added, and the reaction quickly proceeded to completion, as confirmed by TLC (step 2). The crude product was purified by washing with water followed by recrystallization from diethyl ether.

References:

1. Ansari A, Ali A, Asif M. Biologically active pyrazole derivatives. New J Chem. 2017;41:16–41.

2. Alsolimani AK, Ali TE,Assiri MA, et al.Novel coumarin-pyrazole-thiazoles hybrids: synthesis,anticancer activity, molecular docking and in silico ADMET prediction studies. Chemistry Select. 2024;9:e202401738.

3. Hassanin NM, Ali TE, Assiri MA, et al. Novel carbazolyl–thiazolyl–chromone and carbazolyl–thiazolyl–pyrazole hybrids: synthesis, cytotoxicity evaluation and molecular docking studies. RSC Adv. 2024;14:17245–17260.

4. Orabi EA. Tautomerismand antioxidant activity of some 4-acylpyrazolone-based schiff bases:a theoretical study. RSC Adv. 2018;8:30842–30850.

5. Wang BL, Li QN, Zhan YZ, et al. The synthesis and biological activitiesof [5-(4-substituted phenylsulfinyl/sulfonyl)-1,3-dimethyl-1H-pyrazol-4-Yl]-arylmethanones. Phosphorus Sulfur Silicon. 2014;189:483–491.

Tungstic Acid-functionalized Silica-coated Glucose as a Novel Solid Acid Catalyst for the Synthesis of 4-Substituted-1,5-benzodiazepines

Farzaneh Tayebi, Fatemeh Ahmadzadeh and Mahnaz Farahi*

*Department of Chemistry, Yasouj University, P. O. Box 353, Yasouj 75918-7**4831, Iran***

Keyword: glucose, tungstic acid, 4-substituted-***1,5***-benzodiazepines, aromatic aldehydes, o-phenylenediamine

Abstract: In this study, Glu.@SiO_2@$(CH_2)_3OWO_3H$ as a green, benign and recyclable nanocatalyst was prepared via anchoring of tungstic acid onto 3-chloropropyl-grafted SiO_2-coated glucose nanoparticles. Glu.@SiO_2@$(CH_2)_3OWO_3H$ was characterized via FE-SEM, XRD, FT-IR and EDX analysis. This catalyst was used to achieve a high-efficiency, low-cost and eco-friendly approach for synthesizing 4-substituted-**1,5-**benzodiazepines by the multi-component reaction of aromatic aldehydes, *o*-phenylenediamine and dimedone. The presence of tungstic acid group on glucose-entrapped SiO_2 possessed both Lewis and Brønsted acidity, which is responsible for the high catalyst activity. The results revealed that this catalyst showed high catalytic activity in the presented protocol and can be reused at least six times without any change in its catalytic activity.

Introduction

Homogeneous transition metal catalysts often exhibit excellent performance in organic transformations, but show drawbacks regarding recovery and recyclability.[24,25] From both industrial and environmental points of view, immobilization of transition metal on solid supports, such as mesoporous silica or polymers to produce reusable catalysts have many benefits.[26] Heterogeneous catalysts compared to their homogeneous counterparts have some inherent advantages such as milder experimental conditions, an easier set-up and work-up. mixture by filtration or centrifugation and reused for more turns. The heterogeneous catalytic systems not only decrease the production of waste, but also show high activity and good selectivity.[27-31]

2.1. Methods and materials

All chemicals and reagents were purchased from Fluka and Merck companies. The reaction progress was monitored by using TLC on silica gel polygram SIL G/UV254 plates. Reported melting points were determined by an elecrtothermal KSB1N apparatus. NMR spectra was recorded in DMSO solvent using a Bruker advanced DMX-400 MHz spectrometer. IR spectra were obtained with a JASCO FT-IR/680 instrument spectrometer using KBr pellets. Energy dispersive spectroscopy (EDX) was obtained using TESCAN vega model instrument. X-ray powder diffraction (XRD) pattern was obtained using a Panalytical X-Pert diffractometer. The morphology of the particles was investigated by field emission scanning electron microscopy (FE-SEM) of Zeiss sigma VP.

١،٢. Procedure for the synthesis of glucose-silica coated nanoparticles (Glu.@SiO_2)

Firstly, glucose (6 g) was dissolved in deionized water (6 mL). Then, tetraethyl orthosilicate (TEOS) (18 mL) was added dropwise to the solution, and kept stirred for 3 h at room-temperature. Subsequently, sulfuric acid (4 mL) was added dropwise to the mixture and stirred for 2 h. Finally, the product was washed three times with distilled water and dried at 100 °C for 24 h.[49]

٢. Results and discussion

The preparation of Glu.@SiO_2@$(CH_2)_3OWO_3H$ has been carried out according to the steps shown in Scheme 1. Initially, the surface of glucose was modified with a coating layer of SiO_2 using TEOS. To obtain the desired catalyst, Glu.@SiO_2 nanoparticles were treated with 3-chloropropyltrimethoxysilane followed by the reaction with H_2WO_4. Identification and characterization of physicochemical properties of this new catalyst was performed via various analyzes methods such as FT-IR, XRD, FE-SEM and EDX technique.

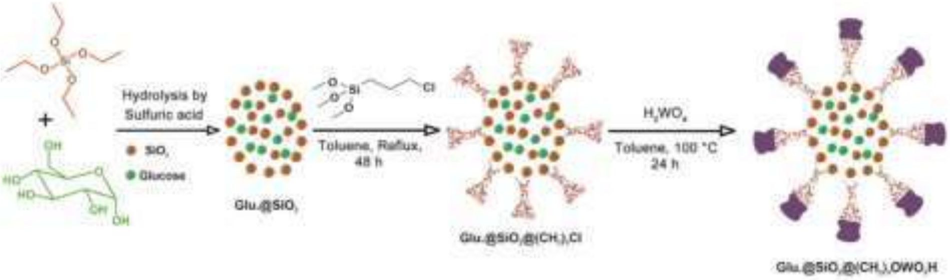

Scheme 1. Preparation of Glu.@SiO_2@$(CH_2)_3OWO_3H$ (**1**).

References

24 J. Liu, A. Plog, P. Groszewicz, L. Zhao, Y. Xu, H. Breitzke, A. Stark, R. Hoffmann, T. Gutmann and K. Zhang, Design of a heterogeneous catalyst based on cellulose nanocrystals for cyclopropanation: Synthesis and solid-state NMR characterization, *Chem. Eur. J.*, 2015, 21, 12414-12420.

25 M. H. Valkenberg and W. F. Holderich, Preparation and use of hybrid organic-inorganic catalysts, *Catal. Rev.*, 2002, **44**, 321-374.

26 L. Z. Fekri, M. Nikpassand, S. Pourmirzajani and B. Aghazadeh, Synthesis and characterization of amino glucose-functionalized silica-coated $NiFe_2O_4$ nanoparticles: a heterogeneous, new and magnetically separable catalyst for the solvent-free synthesis of pyrano [3,2-*c*] chromen-5 (4*H*)-ones, *RSC Adv.*, 2018, **8**, 22313-22320.

27 B. Karami, M. Farahi, N. Farmani and H. Mohamadi Tanuraghaj, Novel synthesis of coumarin-containing secondary benzamide derivatives using tungstate sulfuric acid, *New J. Chem.*, 2016, **40**, 1715-1719.

28 N. Ahmad and Z. Siddiqui, Sulphated silica tungstic acid as a highly efficient and recyclable solid acid catalyst for the synthesis of tetrahydropyrimidines and dihydropyrimidines, *J. Mol. Catal. A: Chem.*, 2014, **387**, 45-56.

29 S. Sharma, P. Parikh and R. Jasra, Reconstructed Mg/Al hydrotalcite as a solid base catalyst for synthesis of jasminaldehyde, *Appl. Catal. A*, 2010, **386**, 34-42.

30 E. Kolvari, N. Koukabi and M. Hosseini, Perlite: A cheap natural support for immobilization of sulfonic acid as a heterogeneous solid acid catalyst for the heterocyclic multicomponent reaction, *J. Mol. Catal. A: Chem.*, 2015, **397**, 68-75.

31 S. Ghodke and U. Chudasama, Solvent free synthesis of coumarins using environment friendly solid acid catalysts, *Appl. Catal. A*, 2013, **453**, 219-226.

The 30th Iranian Seminar of Organic Chemistry
February 7-9, 2025, Iran University of Science and Technology, Tehran, Iran

heterogeneous nanocatalysts based on metal-organic/polymer frameworks for the synthesis of 2-arylpyrroloacridines

Samireh Rasoolabadi [a], Ramin Ghorbani -Vaghei *[a,b] , Seigheh Alavinia[c]

[a] *Department of Organic Chemistry, Faculty of Chemistry and Petroleum Sciences, Bu-Ali Sina University, Hamedan 6517838683, Iran*

[b] *Department of Organic Chemistry, Faculty of Chemistry, University of Guilan, Rasht, Iran*

Keyword: Heterocycles, Heterogeneous, Nanocatalysts, Metal-organic/polymer frameworks

Introduction:

Synthesis of heterocycles has always been a topic of great interest owing to the pharmacological, agricultural, and industrial significance of most heterocyclic structures. Among an immense variety of N-heterocyclic compounds, acridine moieties are notable for their antitumor, antiparasitic, antifungal, antibacterial, and anthelmintic properties. During our research efforts to develop efficient methods for synthesizing heterocycles and preparing nanocatalysts, we would like to report the highly stable and recyclable synthesis and application of heterogeneous nanocatalysts based on metal-organic/polymer frameworks for the synthesis of 2-arylpyrroloacridines. We have developed a novel, efficient and clean route for the synthesis of a new class of pyrroloacridines via an unexpected three-component reaction between dimedone, various anilines and isatin on a new catalyst. The products were successfully synthesized under the reaction conditions.

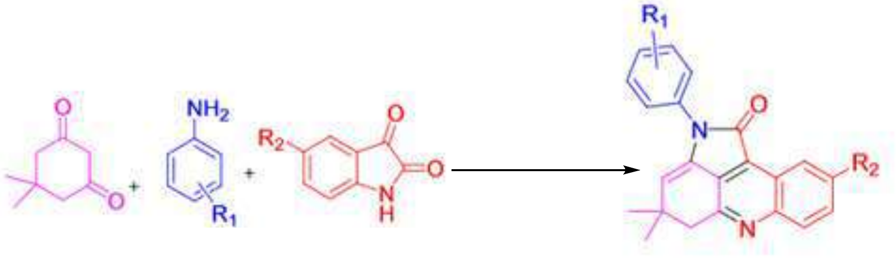

References:

١. Gao, X., Liyang Tang, Lehao Huang, Zu-Sheng Huang, Yunfei Ma,. and Ge Wu., **2019.** *Oxidative aminoarylselenation of maleimides via copper-catalyzed four-component cross-coupling*. Organic letters,.Vol. 21: 745-748.

٢. Yang, Z.H., Hong-Ru Tan,a Yu-Long An, Yu-Wei Zhao, Hao-Peng Lin,. and Sheng-Yin Zhao., **2018.** *Three-Component Coupling Reactions of Maleimides, Thiols, and Amines: One-Step Construction of 3, 4-Heteroatom-functionalized Maleimides by Copper-Catalyzed C (sp2)− H Thioamination*. Advanced Synthesis & Catalysis,. Vol. 360: 173-179.

٣. Yang, Z.H., Yu-Long An, Ying Chen, Zhi-Yu Shao,. and Sheng-Yin Zhao., **2016.** *Copper (I) Iodide-Catalyzed Sulfenylation of Maleimides and Related 3-Indolylmaleimides with Thiols*. Advanced Synthesis & Catalysis,.Vol. 358: 3869-3875.
٤. Kefayati, H., F. Narchin,. and K. Rad-Moghadam, **2012.** *An unexpected multicomponent reaction leading to 2-arylpyrrolo [2, 3, 4-kl] acridin-1 (2H)-ones*. Tetrahedron Letters,.Vol. 5: 4573-4575.

The 30th Iranian Seminar of Organic Chemistry
February 7-9, 2025, Iran University of Science and Technology, Tehran, Iran

A Quantum Mechanical Investigation on Dextroamphetamine

Hossein Shirani[a,*] and Sahar Badrloo[b]

[*] *Corresponding author. E-mail: hossein_shirani@iust.ac.ir*

[a] *Department of Chemistry, Iran University of Science and Technology, P.O. Box 16846-13114, Tehran, Iran*
[b] *Department of Biotechnology, Faculty of Biological Sciences and Technology, University of Science and Culture, Tehran, Iran*

Introduction: Dextroamphetamine is a prescription medication primarily used to treat attention deficit hyperactivity disorder (ADHD) and narcolepsy. It works by increasing the levels of certain chemicals in the brain that help with focus, attention, and impulse control. Dextroamphetamine should be taken as directed by your healthcare provider, who may adjust the dosage based on your specific needs and response to the medication. Follow your physician's instructions carefully when taking dextroamphetamine to ensure its effectiveness and minimize potential side effects.

Methods: At the outset, the molecular composition of Dextroamphetamine was meticulously crafted using GaussView software, followed by detailed quantum mechanical computations at the B3LYP/6–311G theoretical level with the aid of Gaussian09 software.

Results: Computational modeling of the medication Dextroamphetamine was conducted using GaussView software at the B3LYP/6-311G theoretical method, with the presentation of structural data.The thermodynamic properties for the molecular structure of Dextroamphetamine have been determined at the B3LYP/6-311G level. The calculated electronic energy value is -405.5293961 kcal/mol.Tables 1 and 2 showcase the structural parameters of Dextroamphetamine, while Tables 4 and 5 display the calculated dipole moments (Debye) values and HOMO-LUMO energy, obtained using the B3LYP/6-311G method.

Table 1. Calculated Bond Length Values for Dextroamphetamine Molecule using B3LYP/6-311G Computational Method.

C1-C2	C1-C6	C8-N1	C4-C5	C3-C4	C1-C7
1.40326	1.40518	1.47243	1.39801	1.39679	1.51430

Table 2. Calculated Bond Angles Values for Dextroamphetamine Molecule using B3LYP/6-311G Computational.

Table 3. Calculated Dihedral Angle Values for Dextroamphetamine Molecule using B3LYP/6-311G Computational.

C1-C7-C8-C9	C7-C8-C9-N1	C1-C2-C3-C4	C2-C4-C5-C6	C1-C2-C6-C7	C6-C7-C8-N1
-65.28261	-119.60674	0.01305	-0.00742	179.53555	146.38403

C1-C2-C3	C8-C9-N1	C1-C6-C7	C8-C6-C1	C1-C2-C5	C1-C7-C9
121.02863	34.78580	120.67621	48.45584	61.01557	97.72075

Table 4. Calculated Dipole Moments Values for Dextroamphetamine Molecule using B3LYP/6-311G Computational.

μx	μy	μz	μtot
-0.3110	-0.9387	-0.7918	1.2669

Table 6. Calculated HOMO-LUMO Energy Gap Values for Dextroamphetamine Molecule using B3LYP/6-311G Computational.

EHOMO	HLG	ELUMO
-0.22322	0.21567	-0.00755

Discussion: The optimization of Dextroamphetamine was conducted using the B3LYP/6-**311G** method, focusing on its electronic properties. provides important insights into the drug's stability, reactivity, and electronic behavior. These findings are valuable for enhancing its pharmacological potential and applications.

Keywords: Dextroamphetamine; DFT; B3LYP/6-311G, HOMO-LUMO gap, Electronic energy, Dihedral Angle, Bond Angles, Bond Length, Dipole Moments

References:

1) Gaussian 09, Revision B.o1, M. J. Frisch et al., Gaussian, Inc., Wallingford CT, 2009

2) Griffith, J. D., Cavanaugh, J., Held, J., & Oates, J. A. (1972). Dextroamphetamine: Evaluation of psychomimetic properties in man. *Archives of General Psychiatry*, *26*(2), 97-100.

3) Mattay, V. S., Callicott, J. H., Bertolino, A., Heaton, I., Frank, J. A., Coppola, R., ... & Weinberger, D. R. (2000). Effects of dextroamphetamine on cognitive performance and cortical activation. *Neuroimage*, *12*(3), 268-275.

The 30th Iranian Seminar of Organic Chemistry
February 7-9, 2025, Iran University of Science and Technology, Tehran, Iran

Efficient adsorptive removal of tetracycline drug from contaminated water by magnetic ZIF-8 metal-organic framework/alginate hydrogel beads

Mohammad Amini[a], Soheyla Karimi[a], Hassan Namazi*[a, b]
[a]*Polymer Research Laboratory, Department of Organic and Biochemistry, Faculty of Chemistry, University of Tabriz, Tabriz, Iran.* *moh.amini1999@gmail.com*

[b]*Research Center for Pharmaceutical Nanotechnology (RCPN), Biomedicine Institute, Tabriz University of Medical Science, Tabriz, Iran. Corresponding author: H. Namazi; E-mail: namazi@tabrizu.ac.ir*

Abstract

Currently, the presence of drugs from contaminated water is worrisome due to their high toxicity, which necessitates their critical removal by developing highly efficient adsorbents. Hence, in this study, alginate *hydrogel beads* of magnetic ZIF-8 metal-organic frameworks (ZIF-8@Fe_3O_4-SA) were prepared for the first time and then utilized as a new absorption *system* for the removal of tetracycline drug (TC) from aqueous solutions by batch adsorption manner (Scheme 1). The effects of *different* experimental factors, such as *adsorbent dosage*, contact time, pH, and drug concentration for the removal of TC drug. Based on the study, the ZIF-8@Fe_3O_4-SA *hydrogel beads* could be considered a sustainable, simple, economical, environmentally friendly absorption *system* for the removal of pharmaceutical contaminants from water.

Keyword: *Hydrogel beads*, Metal-organic frameworks, Absorption *system*, Tetracycline.

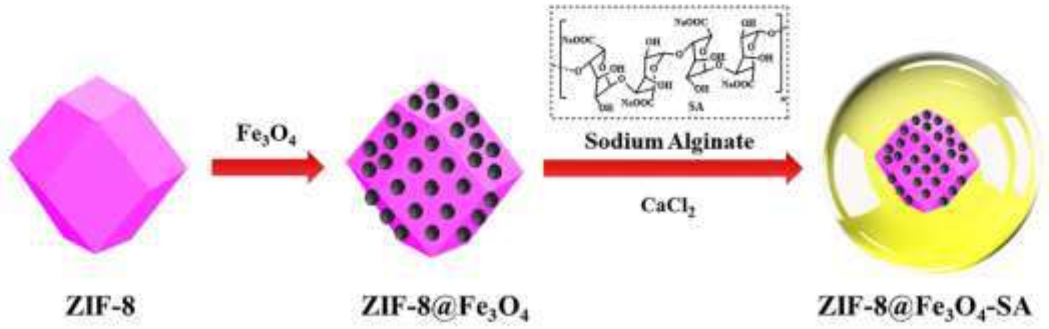

Scheme 1: Schematic illustration of the synthesis of ZIF-8@Fe_3O_4-SA *hydrogel beads.*

Introduction

Nowadays, contamination of water sources by various organic and inorganic pollutants (pharmaceuticals, industrial additives, organic dyes, etc.) is considered to be one of the serious pandemic problems worldwide [1, 2]. Among the various contaminants, antibiotic drugs as a type of contaminant have garnered significant attention due to their large-scale production, diverse uses, and frequent detection in surface water [3, 4]. Therefore, it is crucial to efficiently remove antibiotic drugs from the water before entering the natural environment. In the present study, we report the preparation and characterization of ZIF-8@Fe_3O_4-SA *hydrogel beads* as a new and effective adsorbent for the removal of TC antibiotic from aqueous solutions by the batch method. The effects of different parameters on the adsorption process were evaluated. The obtained results showed that the designed ZIF-8@Fe_3O_4-SA *hydrogel beads* could be potentially used as a new adsorbent for the removal of water environmental pollutants.

Method

Preparation of ZIF-8@Fe_3O_4-SA hydrogel beads

For the preparation of the ZIF-8@Fe_3O_4-SA *hydrogel beads*, 0.02 g of as-prepared ZIF-8@Fe_3O_4 was uniformly dispersed for 15 min in 5 mL deionized water. Then, a 2% w/v SA *solution* was prepared and slowly added to the above suspension and stirred at room temperature. After 2 h, the homogeneous solution was added *drop by drop* to 2% w/v solution of $CaCl_2$ (2% w/v) under continuous stirring using a syringe. Finally, the ZIF-8@Fe_3O_4-SA *hydrogel beads* were isolated easily by a magnet, washed continuously with distilled water, and dried at room temperature.

Results and Discussion

The effect of adsorbent dose (10-60 mg) indicated that increasing the mass of the *hydrogel beads* led to an increase in the removal efficiency of TC drug from 27.05% to 75.06%, due to the presence of more vacant adsorption sites and greater surface area of the *hydrogel beads*. Therefore, economically, 30 mg of *hydrogel beads* were selected as the optimum dosage for further adsorption studies. In addition, the maximum adsorption of TC onto *hydrogel beads* was achieved at pH 5. The adsorption capacity of TC increased gradually with an increase in the concentration of drugs from 10 mg/L to 50 mg/L. Also, at high initial concentrations, the lower removal efficiencies are probably due to the saturation of the adsorptive surface sites. Therefore, 30 mg/L was determined as the optimal initial concentration for further investigation. Also, the removal efficiency of TC was enhanced gradually by an increase in the contact time (0-90 min). As a result, 25 min was considered as the optimum contact time for further studies. Based obtained results, the prepared *hydrogel beads* could be considered as simple, economical, environmentally friendly adsorbent with high adsorption capacity for drug contaminants removal from water.

References:

1. Deng, Y.-y., et al., Journal of Cleaner Production, 2023. 394: p. 136271.
2. Karimi, S. and H. Namazi, Chemosphere, 2024: p. 141397.
3. Vinayagam, V., et al., Chemosphere, 2022: p. 134597.
4. Karimi, S. and H. Namazi, International Journal of Biological Macromolecules, 2022.

Chitosan/layered double hydroxide/copper metal organic framework-based cross-linked citric acid as a novel adsorbent **for the removal of penicilin drug**

Mohammad Amini[a], Soheyla Karimi[a], Hassan Namazi*[a, b]

[a]*Polymer Research Laboratory, Department of Organic and Biochemistry, Faculty of Chemistry, University of Tabriz, Tabriz, Iran.* moh.amini1999@gmail.com

[b]*Research Center for Pharmaceutical Nanotechnology (RCPN), Biomedicine Institute, Tabriz University of Medical Science, Tabriz, Iran. Corresponding author: H. Namazi; E-mail:* namazi@tabrizu.ac.ir

Abstract

The excessive release of antibiotic pharmaceuticals endanger the ecological environment as well as human health. Hence, it is of profound significance to develop effective removing strategies by developing highly efficient adsorbents. Hence, in this work, layered double hydroxide supported copper metal organic framework were coated with chitosan biopolymer in the presence of citric acid to prepare Cu MOF-LDH@CS were prepared and then utilized as a new absorption *system* for the removal of penicilin drug (PC) from aqueous solutions by batch adsorption method (Scheme 1). The effects of *different* experimental factors, such as *adsorbent dosage*, contact time, pH, and drug concentration for the removal of PC drug. Based on the study, the Cu MOF-LDH@CS could be considered an environmentally friendly absorption *system* for the removal of pharmaceutical contaminants from water.

Keyword: Chitosan, Metal-organic frameworks, Absorption *system*, Tetracycline.

Scheme 1: Schematic illustration of the synthesis of Cu MOF-LDH@CS.

Introduction

With increasing in world population as well as the improvement of living standards, the use of antibiotics pharmaceuticals has increased [1]. The presence of these drugs in the wastewater of pharmaceutical industries, hospitals, livestock and municipal wastewater, and ultimately their penetration into groundwater and drinking water has been one of the most important environmental challenges [2]. Therefore, it is crucial to efficiently remove antibiotics from the water before entering the natural environment. In this study, Cu MOF-LDH@CS absorption *system* were prepared. Then, their performances for the adsorption and removal of penicilin drug (PC) from aqueous solutions were investigated by study from the effects parameters such as contact time, adsorbent dosage, and solution pH. The obtained results showed that the designed Cu MOF-LDH@CS could be potentially used as a new adsorbent for the removal of water environmental pollutants.

Method

Preparation of Cu MOF-LDH@CS

The Al-Zn LDH nanocomposite was prepared by the co-precipitation method in the alkaline medium [3]. In this work, the Cu MOF-LDH composite was synthesized by an in-situ growth method in hydrothermal conditions [4]. For preparation *Cu MOF-LDH@CS*, the CS solutions (%1) were obtained by adding 0.1 g of CS powder into 100 mL of 1 wt% of acetic acid solution at 40 ◦C for 2 h. Then, 20 mL of the sonicated *Cu MOF-LDH* solution was added to the prepared CS solutions under vigorous stirring. Then, 0.8 g of citric acid was dissolved in 5 mL of distilled water and added into above solutions. The pH of the prepared solutions was then adjusted to 4.5 using NaOH (0.1 M), and these solutions were stirred (200 rpm) for another 2 h at 70 °C. The Cu MOF-LDH@CS were washed with excess distilled water followed by the freezedrying process.

Results and Discussion

The results of the effect of adsorbent dose indicated that increasing the mass of the Cu MOF-LDH@CS from 5 to 40 mg led to an increase in the removal efficiency of PC drug from 31.45% to 81.06%, due to the presence of more vacant adsorption sites and greater surface area of the *hydrogel beads*. Therefore, economically, 25 mg of Cu MOF-LDH@CS were selected as the optimum dosage for further adsorption studies. The effect of the initial concentration of PC drug (5-25 mg/L) showed that the adsorption capacity of PC increased gradually with an increase in the concentration of drugs. Also, at high initial concentrations, the lower removal efficiencies are probably due to the saturation of the adsorptive surface sites. Therefore, 15 mg/L was determined as the optimal initial concentration for further investigation. Also, the removal efficiency of PC was enhanced gradually by an increase in the contact time (0-120 min). As a result, 40 min was considered as the optimum contact time for further studies. Based obtained results, the prepared Cu MOF-LDH@CS could be considered as environmentally friendly adsorbent with high adsorption capacity for drug contaminants removal from water.

References:

1. Ahamad, T., et al., *F*. International journal of biological macromolecules, 2019. 134: p. 180-188.

2. de Araujo, C.M.B., et al., Environmental Research, 2023. 216: p. 114425.

3. Karimi, S. and H. Namazi, Journal of Polymers and the Environment, 2024: p. 1-16.

4. Karimi, S., H. Rasuli, and R. Mohammadi, International Journal of Biological Macromolecules, 2023: p. 123538.

Facile preparation of a pH-sensitive nanocarrier based on magnetic MIL 100 MOFs-chitosan crosslinked κ-carrageenan for controlled release of curcumin

Mohammad Amini[a], Soheyla Karimi[a], Hassan Namazi*[a, b]
[a]*Polymer Research Laboratory, Department of Organic and Biochemistry, Faculty of Chemistry, University of Tabriz, Tabriz, Iran.* *moh.amini1999@gmail.com*
[b]*Research Center for Pharmaceutical Nanotechnology (RCPN), Biomedicine Institute, Tabriz University of Medical Science, Tabriz, Iran. Corresponding author: H. Namazi; E-mail: namazi@tabrizu.ac.ir*

Abstract

In this study, we design a pH-controlled carrier based on magnetic copper metal-organic framework-chitosan crosslinked κ-carrageenan hydrogel nanoparticles (Fe_3O_4-MIL 100 MOF-CUR-CS@CAR) for targeted release from curcumin (CUR) to breast cancer cells (Scheme 1). The encapsulation efficiency and drug loading capacity of the CUR were obtained to be 86.1% and 8.6%, respectively. These *in vitro* release results confirmed the controlled release and pH-response behavior of hydrogel nanoparticles. On these findings, the present study suggests the potential of the prepared Fe_3O_4-MIL 100 MOF-CUR-CS@CAR hydrogel nanoparticles as a pH-controlled drug delivery system for cancer treatment.

Keyword: Chitosan, Metal-organic frameworks, κ-carrageenan, Curcumin.

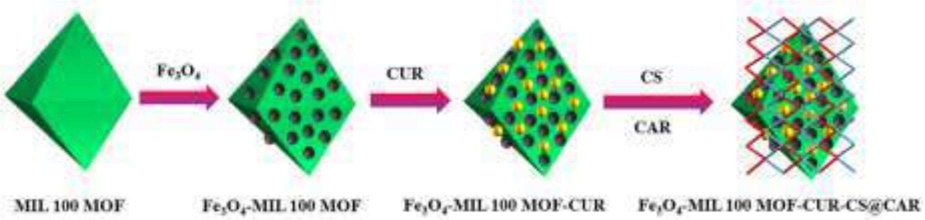

Scheme 1: Schematic illustration of the synthesis of Fe_3O_4-MIL 100 MOF-CUR-CS@CAR.

Introduction

Recently, various drug delivery systems composed of various materials such as graphene oxide, Metal-organic frameworks, magnetic Fe_3O_4, starch, κ-carrageenan, alginate, and Chitosan, have been widely investigated for anticancer drug delivery to cancer cells [1]. Amongst, metal-organic frameworks (MOFs) as drug delivery systems have been receiving increasing attention due to their unique properties such as high surface area, effective biodegradability, minimal toxicity to cells, high drug loading capacity, long-term controlled release, good biocompatibility, and tunable surface functionalities. However, drug delivery applications of MOFs are limited due to their tendency to aggregate [2, 3]. Therefore, modification of MOFs with biopolymers not only improves their drug loading capacity, and biocompatibility but also increases the stability of MOFs [21, 22]. Therefore, in this study, Fe_3O_4-MIL 100 MOF-CUR-CS@CAR hydrogel nanoparticles were prepared for targeted CUR delivery within breast cancer cells.

Method

CUR loading in the Fe_3O_4-MIL 100 MOF

In this work, the *Fe_3O_4-MIL 100 MOF* was synthesized by an in-situ growth method in hydrothermal conditions. Then, 50 mg of the prepared *Fe_3O_4-MIL 100 MOF* was dispersed in 5 mg of CUR (2 mg/mL) for 10 min in ethanol. Then, the suspensions at dark were shaken at room temperature for 72 h. Finally, by collecting and measuring the supernatant solution at 428 nm with a UV-Vis spectrophotometer.

Preparation of Fe_3O_4-MIL 100 MOF-CUR-chitosan crosslinked with κ-carrageenan (Fe_3O_4-MIL 100 MOF-CUR-CS@CAR*)*

For the preparation of Fe_3O_4-MIL 100 MOF-CUR-CS@CAR, 0.5 g of CAR was dissolved separately in 50 mL of deionized water. On the other hand, 0.5 g of CS was dissolved in 100 mL of acetic acid solution (1% w) to obtain a CS solution (0.5% w/v). Next, 0.18 g of Fe_3O_4-MIL 100 MOF-CUR was dispersed for 10 min in 5 mL of deionized water and then was added dropwise to the CS solution. Finally, CAR solution was added dropwise to Fe_3O_4-MIL 100 MOF-CUR and CS mixture under vigorous stirring. The final pH of the mixture was around 6 to prepare crosslinked hydrogel nanoparticles. The produced hydrogel nanoparticles were isolated using an external magnet and washed multiple times with distilled water and then dried using a freeze-dryer.

In vitro CUR release from Fe_3O_4-MIL 100 MOF-CUR-CS@CAR

To release CUR, 20 mg of hydrogel nanoparticles were mixed with 10 mL of PBS solution (pH 7.4 and 5.5) and the resulting suspension was kept for 72 h on a shaker incubator with a temperature of 37°C. The hydrogel nanoparticles were separated with an external magnet and after removing the 5 mL of supernatant solution, 5 mL of fresh buffer was added to each treatment. The amount of drug released was estimated by UV-Vis spectroscopy.

Results and Discussion

The CUR loading on Fe_3O_4-MIL 100 MOF showed an encapsulation efficiency of 85.3% and a drug loading capacity of 8.5%.The release of CUR from the Fe_3O_4-MIL 100 MOF-CUR-CS@CAR showed that the CUR release in pH 5.5 is accelerated in compared to pH 7.4, which suggest a pH-dependent release behavior from Fe_3O_4-MIL 100 MOF-CUR-CS@CAR. The obtained result suggests that hydrogel nanoparticles can be a potential system in cancer treatment.

References:

1. Moghadam, M.R., S. Karimi, and H. Namazi, Food Bioscience, 2024: p. 103578.
2. Karimi, S. and H. Namazi, International Journal of Pharmaceutics, 2023: p. 122675.
3. Karimi, S., V. Zeyni, and H. Namazi, Diamond and Related Materials, 2023: p. 110502.

The 30th Iranian Seminar of Organic Chemistry
February 7-9, 2025, Iran University of Science and Technology, Tehran, Iran

Synthesis and extraction of the pharmacopeial Epimer impurity of the active pharmaceutical ingredient Spironolactone from industrial liquor

Authors: Maryam JahangirVazifeh[a], Farhad Shirini[b], Bahman Sharifzadeh[c]

Department of Chemistry, Faculty of Science, University of Guilan, Rasht, Iran,

[a]JahangirVazifeh.r.d@gmail.com; [b]shirini@guilan.ac.ir; [c]sharifzadeh@guilan.ac.ir

Keyword: Impurity, Pharmacopoeia, Epimer, Active Pharmaceutical Ingredient, Spironolactone, Extraction

In pharmaceutical industry, pharmacopeial standards are defined in the form of monographs to analyze active pharmaceutical ingredients (APIs) and determine their purity (BP pharmacopeia and USP pharmacopeia).

One of the analyses performed is the impurity test, and in most cases, HPLC (High-Performance Liquid Chromatography) is used for this purpose. Structure of some impurities are known, limits is defined for them, and during HPLC test, these impurities need to be injected into the device as References and should be identified in Final API. Many of these impurities are synthesized by regulatory organizations (BP and USP) and sold to other countries at high costs, which creates significant annual expenses for the pharmaceutical industry.

Spironolactone is an active pharmaceutical ingredient (API) which after undergoing a specific formulation process, is transformed into a pharmaceutical product (spironolactone tablet).

One of known impurities in pharmacopeia for spironolactone is its epimer which its price of 30 mg is 800$.

Spironolactone

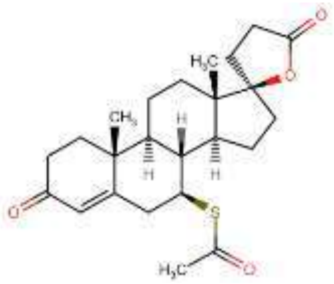

Epimer

We have developed a method for extracting the epimer impurity of Spironolactone from the liquor produced in the industrial process (Behdasht Kar Company).[۲]

Efforts to analyze the HPLC spectra of several industrial batches and investigate the cause of the increased epimer impurity in the company's products, along with reviewing scientific literature on the synthesis of this impurity, led to the discovery of a method for synthesizing and recovering this impurity from the main production liquor.

This approach ensures that, alongside the synthesis of the epimer impurity, the main active ingredient, spironolactone, which also has significant economic value, is synthesized, making the method economically viable thus preventing waste of raw materials.

Method of synthesis and separation

Reaction of Canrenone with an excess amount of Thioacetic acid, under solvent-free conditions and indirect heating with steam during 6 hours, leads the reaction to formation of the Epimer impurity.

The progress of the reaction was monitored using TLC. Upon observing no change in the TLC appearance, tetrahydrofuran and ethyl acetate were added to the mixture. Saturated sodium bicarbonate solution was then gradually added, resulting in the cessation of bubbling and neutralization. After phase separation and dehydration of the organic phase using magnesium sulfate, the solvent was distilled. After drying, fluffy brown-orange precipitate was obtained.

HPLC analysis revealed that approximately 46% of the compound was the main product, spironolactone (alpha form), while about 45% was Epimer impurity.

During the purification of the product in methanol, spironolactone is separated, and the recovery of the impurity from the separated liquor is carried out through distillation, re-crystallization, and thin-layer chromatography. After obtaining the epimer with over 80% purity, in subsequent steps, the separation of the epimer from the liquor is achieved through seeding, under very precise and controlled conditions.

---

[۲] https://www.bk-api.com/; Info@behdashtkar.com

References:

[1]. Peter G., Allen R.; *J. Org. Chem*., **1989**, 54, 5180 – 5182.
[2]. Tweit R., Colton F.; *J. Org. Chem*., **1962**, *27(9)*,3325
[3]. Van Herck A.M., Landfester K.; *Adv Polym Sci*., **2010**, *233*, 1-18.
[4]. Liu X., Guan Y.; *Langmuir*., **2004**, *20*, 10278 – 10282.

The 30th Iranian Seminar of Organic Chemistry
February 7-9, 2025, Iran University of Science and Technology, Tehran, Iran

A New and Practical Approach for Synthesizing 1,2,4-Oxadiazole-5-Thiones

Babak Kaboudin 1[a*], Saman Soleymanie 2[a], Ali Sabzalipour 3[a],

Department of Chemistry, Institute for Advanced Studies in Basic Sciences (IASBS), Gava Zang, Iran

Keyword: Oxadiazole, Synthesis, Benzothioamide

Heterocyclic compounds, particularly five-membered rings such as 1,2,4-oxadiazoles, have garnered significant attention due to their wide range of biological activities, including antiinflammatory, antimicrobial, anticonvulsant, and antihypertensive properties. Among these, 5-thione derivatives of 1,2,4-oxadiazoles hold promise as intermediates for synthesizing biologically important compounds. However, despite extensive research on oxadiazole derivatives, the synthesis of 5-thione derivatives has been relatively underexplored. This study presents a novel and efficient method for synthesizing 1,2,4-oxadiazole-5-thiones using carbon disulfide (CS_2) as a cost-effective and practical C=S donor under super basic conditions. The proposed methodology is scalable, economically viable, and yields products with high efficiency, offering a valuable contribution to the development of heterocyclic compounds for pharmaceutical applications.

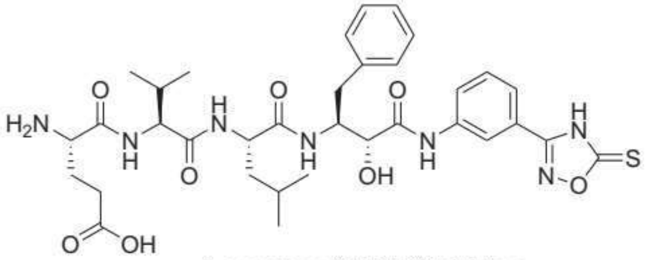

β-secretase (BACE1) inhibitors

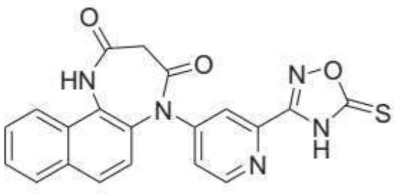

Neuroprotective Activity

The proposed method involves reacting amidoximes with carbon disulfide (CS_2) under super basic conditions (KOH/DMSO) at 40°C. This reaction efficiently yields 1,2,4-oxadiazole-5-thiones with good to excellent yields. The method is notable for its simplicity, scalability, and the use of CS_2 as a cost-effective C=S donor. Additionally, it offers straightforward purification processes and demonstrates compatibility with various substrates, making it highly practical for pharmaceutical and industrial applications.

In the "Results and Discussion" section, we investigated the synthesis of 1,2,4-oxadiazole-5-thiones through the reaction of amidoximes with carbon disulfide (CS_2) under super basic conditions (KOH/DMSO) at 40°C. Our results demonstrated that KOH is the most effective base, leading to high yields of the desired products, particularly when excess CS_2 was used. The method proved versatile, efficiently converting a range of amidoximes, including those with electronwithdrawing groups and halogen substituents, into 5-thione derivatives. However, amidoximes with methoxy or bulky groups exhibited reduced yields. Additionally, we successfully synthesized a benzothioamide derivative from p-cyanobenzamidoxime and CS_2, further illustrating the method's broad applicability. The proposed mechanism involves the formation of an intermediate via O-C=S bond formation, followed by the elimination of H2S, resulting in the final 1,2,4- oxadiazole-5-thione products.

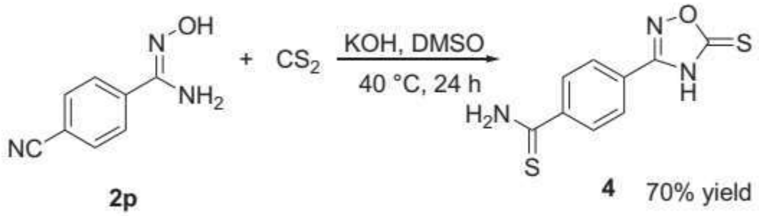

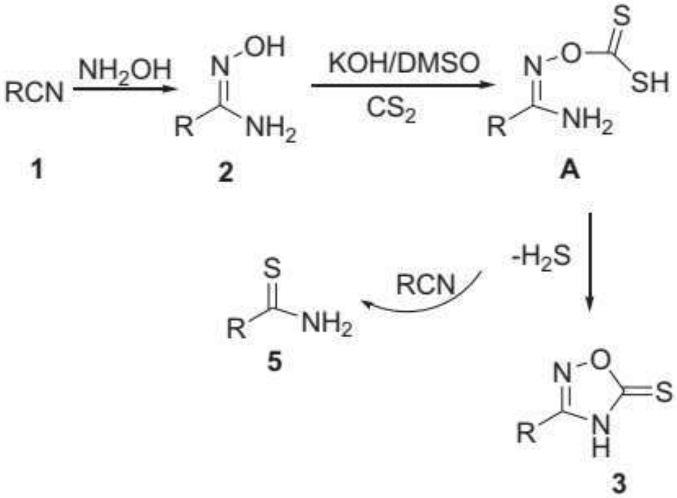

References:

[1] B. Kaboudin, F. Saadati, J. Heterocyclic Chem. 2005, 42, 699.

[2] B. Kaboudin, E. Hajmohammadi, M. Sohrabi, F. Kazemi, J. Iran. Chem. Soc. 2024, 21, 561.

[3] B. Kaboudin, D. Elhamifar, Synthesis 2006, 2006, 224.

The 30th Iranian Seminar of Organic Chemistry
February 7-9, 2025, Iran University of Science and Technology, Tehran, Iran

Synthesis of Dihydrothiophenes via a Three-Component Reaction of Aromatic Amines, 3-Formyl-2-Mercaptoquinoline, and Nitroepoxide

Mohammad Sohrabi*, Sahar Harati Beiranvand, Ahmad Takallou, Azizollah Habibi

Department of Organic and Polymer Chemistry, Faculty of Chemistry, Kharazmi University, Tehran, 49 Mofateh St., Tehran, IRAN, P. O. Box 15719-14911y

**E-mail:* mohammadso3227@gmail.com, habibi@khu.ac.ir

Keywords: dihydrothiophene, 3-formyl-2-mercaptoquinoline, aromatic amines, nitroepoxide

Quinoline and dihydrothiophene structures are well-known for their significant medicinal and biological properties. Inspired by these attributes, we aimed to synthesize novel derivatives of these biologically important compounds using a new and innovative method.[1-3] This study focuses on a three-component reaction involving 3-formyl-2-mercaptoquinoline, nitroepoxide, and aniline to produce dihydrothiophene and quinoline rings (Scheme 1). Key advantages of this reaction include excellent yields, the absence of a catalyst, the ability to synthesize a variety of dihydrothiophene derivatives, and a straightforward procedure that proceeds efficiently within a short timeframe.

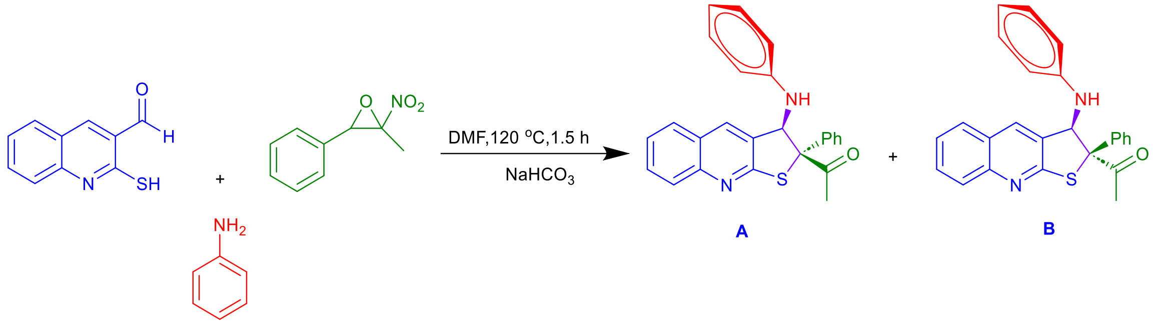

Scheme 1. Synthesis of dihydrothiophene rings from 3-formyl-2-mercaptoquinoline, aromatic amines, and nitroepoxide.

References

(1) Jadhav, C. K.; Nipate, A. S.; Chate, A. V.; Dofe, V. S.; Sangshetti, J. N.; Khedkar, V. M.; Gill, C. H.. *ACS omega* **2020**, *5* (45), 29055-29067.

(2) Scott, D. A.; Balliet, C. L.; Cook, D. J.; Davies, A. M.; Gero, T. W.; Omer, C. A.; Poondru, S.; Theoclitou, M.-E.; Tyurin, B.; Zinda, M. J. **2009**, *19* (3), 697-700.

(3) Singh, B.; Chetia, D.; Puri, S.; Srivastava, K.; Prakash, A.. *Medicinal Chemistry Research* 2011, 20, 1523-1529.

The 30th Iranian Seminar of Organic Chemistry
February 7-9, 2025, Iran University of Science and Technology, Tehran, Iran

Synthesis of *N*-(9,10-Dioxo-9,10-dihydroanthracen-1-yl)-9,10-dioxo-9,10-dihydroanthracene-1-sulfonamide derivatives

Fereshteh Albouyeh[a], Ghasem Aghapour*[a]

[a] *School of Chemistry, Damghan University, Damghan 36716-41167 Iran*

**E-mail: gh_aghapour@du.ac.ir*

Keyword: Anthraquinone-1-sulfonamide, Anthraquinone-1-sulfonyl chloride, 1-Amino anthraquinone.

Sulfonamides and anthraquinones (AQs) are two important groups in organic chemistry. This importance stemmed from their valuable and attractive properties in different fields especially in medicine such as antibacterial, antifungal, antiulcer, antidiabetic, antiparasitic, enzyme inhibitory, anticancer, antiviral, antioxidant, analgesic, antiinflammatory and so on [1-2]. Despite this great importance, the reports concerning the synthesis of chemical structures containing both these moieties are rare in the literature [3]. In this work, the synthesis of anthraquinone-1-sulfonamides having an additional anthraquinone derivative on nitrogen atom is described. For this purpose, first anthraquinone-1-sulfonyl chloride (AQ-1-SO_2Cl) was prepared from the reaction of sodium anthraquinone-1-sulfonate with phosphorus (V) oxychloride. Then the synthesized AQ-1-SO_2Cl was treated with a basic solution of different primary and secondary 1-aminoanthraquinones (AQ-1-NHR) in DMF *via* a nucleophilic substitution reaction affording the desired anthraquinone-1-sulfonamides. A model reaction is shown in Scheme 1. Some these 1-aminoanthraquinones themselves were synthesized *via* the reductive Claisen rearrangement of the related 1-(*N*-allylamino)anthraquinones reported in the literature [4]. Some of these anthraquinone-1-sulfonamides have even more potent antibacterial properties than chloramphenicol.

Scheme 1: synthesis of anthraquinone-1-sulfonamides having an additional anthraquinone core.

References:

[1] Pareek, A.; Rani, P.; Kishore, D. *Int. J. Pharma Bio Sci.* **2013**, *4*, 812.

[2] Wang, J.; Qin, X.; Chen, Z.; Ju, Z.; He, W.; Tan, Y.; Zhou, X.; Tu, Z.; Lu, F.; Liu, Y. *Phytochem. Lett.* **2016**, *15*, 13.

[3] Ramadan, A.; Khoudari, K. *Int. J. Acad. Sci. Res.* **2020**, *8*, 24.

[4] Albooyeh, F.; Aghapour, G. ***Turk. J. Chem*. 2023, *47*, 514.**

The 30th Iranian Seminar of Organic Chemistry
February 7-9, 2025, Iran University of Science and Technology, Tehran, Iran

2-Hydroxy Ethyl Methacrylate grafted to Chitosan as an efficient heterogeneous catalyst for the one-pot synthesis of Imidazole derivatives

Yosra Mostafapour Kandelous, Niloufar Nashibi and Mohammad G. Dekamin*

Pharmaceutical and Heterocyclic Compounds Research Laboratory, Department of Chemistry, Iran University of Science and Technology, Tehran 1684613114 , Iran; yosramostafapour190979@gmail.com ; n.nashibi@gmail.com ; mdekamin@iust.ac.ir

** Corresponding author: mdekamin@iust.ac.ir ; Iran University of Science and Technology, Tehran 16846-13114, Iran*

Keyword: Heterogeneous catalyst, Multicomponent reaction, Chitosan, Imidazole derivatives

Abstract:

Recent developments have highlighted the significance of chitosan in heterogeneous catalytic processes. in this research, we synthesized 2-Hydroxy Ethyl methacrylate grafted to Chitosan as a heterogeneous catalyst for multicomponent reactions (MCRs). 2-Hydroxy Ethyl methacrylate (HEMA) is recognized as a multifunctional monomer, hydrophilic and biocompatibe with diverse applications across various domains. the synthesized catalyst underwent characterization using Fourier transform infrared (FTIR) spectroscopy, field emission scanning electron microscopy (FESEM), energy dispersive X-ray spectroscopy (EDS), elemental mapping, and X-ray diffraction analysis (XRD). this catalyst effectively promoted the synthesis of Imidazole derivatives as a one-pot multicomponent reaction with high product yields and reduced reaction times. additionally, the heterogeneous catalyst showcased exceptional reusability, retaining its catalytic performance for a minimum of six cycles without significant efficiency loss.

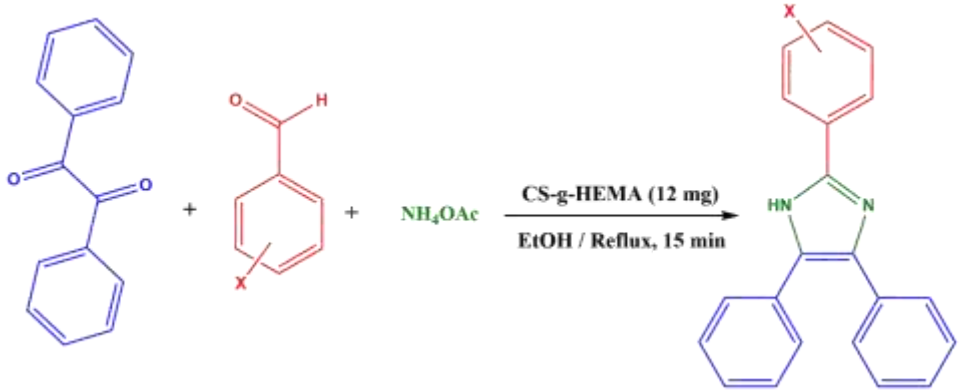

Scheme 1. Schematic reaction of synthesis of imidazole derivatives via one-pot three component reaction

Conclusion:

In this paper, we studied the new CS-g-HEMA catalyst was utilized in the multicomponent reaction for the synthesis of imidazole derivatives. the nanocatalyst has advantages such as easy separation, good recovery, low-cost, high product yield and maintenance of the catalytic activity up to several cycles. also, the low need for catalyst and solvent and on the other hands, are use of solvent non-toxic are other benefits of this catalyst in reactions.

Acknowledgments: Acknowledgments: We are grateful for the financial support from The Research Council of Iran University of Science and Technology (IUST), Tehran, Iran (Grant No 160/24293).

Reference: (Some references we used in the article)

1. Dos Santos, J.A., et al., *Multicomponent Reactions Applied to Total Synthesis of Biologically Active Molecules: A Short Review.* Current Topics in Medicinal Chemistry, 2023. 23(11): p. 990-1003.
2. Graziano, G., et al., *Multicomponent reaction-assisted drug discovery: A time-and cost-effective green approach speeding up identification and optimization of anticancer drugs.* International Journal of Molecular Sciences, 2023. **24**(7): p. 6581.
3. Cores, Á., et al., *Multicomponent reactions for the synthesis of active pharmaceutical ingredients.* Pharmaceuticals, 2022. **15**(8): p. 1009.
4. Das, P., et al., *Heteropolyaromatic Covalent Organic Frameworks via One-Pot Multicomponent Reactions.* Journal of the American Chemical Society, 2024.
5. Bosica, G. and R. Abdilla, *Recent advances in multicomponent reactions catalysed under operationally heterogeneous conditions.* Catalysts, 2022. **12**(7): p. 725.
6. Akbarzadeh, A. and M.G. Dekamin, *A facile and environmentally benign polyethylene glycol 600-mediated method for the synthesis of densely functionalized 2-aminothiophene derivatives under ultrasonication.* Green Chemistry Letters and Reviews, 2017. **10**(4): p. 315-323.
7. Akbari, A., et al., *Novel magnetic propylsulfonic acid-anchored isocyanurate-based periodic mesoporous organosilica (Iron oxide@ PMO-ICS-PrSO3H) as a highly efficient and reusable nanoreactor for the sustainable synthesis of imidazopyrimidine derivatives.* Scientific Reports, 2020. **10**(1): p. 10646.
8. Karami, S., et al., *DABA MNPs: A new and efficient magnetic bifunctional nanocatalyst for the green synthesis of biologically active pyrano [2, 3-c] pyrazole and benzylpyrazolyl coumarin derivatives.* New Journal of Chemistry, 2020. **44**(33): p. 13952-13961.
9. Dekamin, M.G. and S.Z. Peyman, *Phthalimide-N-oxyl salts: efficient organocatalysts for facile synthesis of (Z)-3-methyl-*4*-(arylmethylene)-isoxazole-5 (4 H)-one derivatives in water.* Monatshefte für Chemie-Chemical Monthly, 2016. **147**: p. 445-450.
10. Dekamin, M.G., M. Azimoshan, and L. Ramezani, *Chitosan: a highly efficient renewable and recoverable bio-polymer catalyst for the expeditious synthesis of α-amino nitriles and imines under mild conditions.* Green Chemistry, 2013. **15**(3): p. 811-820.

Bovine serum albumin immobilized on the magnetic triazine-functionalized chitosan as an efficient nanocatalyst in the synthesis of 1,4-dihydropyridines and 3,4-dihydropyrimidinones

M. Amere,[a] Fatemeh Rafiee ,*[b]

[a, b] Department of Organic Chemistry, Factually of Chemistry, Alzahra University, Tehran, Iran.

Keyword: Chitosan, Bovine serum albumin, Multi-component reaction, Magnetic catalyst

There is considerable research on the expansion of biocatalysts in organic reactions is due to their high catalytic efficiency, selectivity, mild and environmentally friendly reaction conditions, simple operational procedures and low energy requirements [1-2]. Among the reported biocatalysts, commercially available and inexpensive bovine serum albumin (BSA) as most abundant protein of mammalian blood plasma has been used as an active and efficient catalyst or co-catalyst in various organic transformations [3]. In this research work, chitosan biopolymer was functionalized with 2,4,6-trichloro-1,3,5-triazine to produce new arms for further modification with BSA protein. The magnetization of biosupport was done through treatment of Fe_3O_4 nanoparticle with chitosan biopolymer that functionalized with chlorinated derivative of 1,3,5-triazine. BSA-immobilized on the magnetic chitosan support (Fe_3O_4@CSC-BSA (Scheme 1)) was applied as an efficient magnetic heterogeneous catalyst in the synthesis of dihydropyridine derivatives through Hantzsch reaction and dihydropyrimidinones by Biginelli reaction.

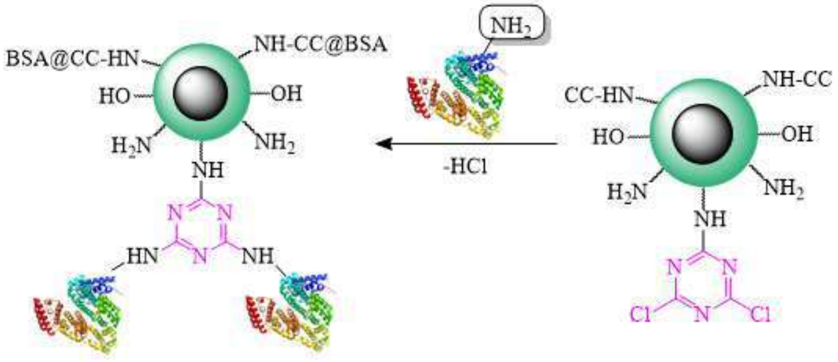

Scheme 1.

References:

1. Jumbam, N.D.; Masamba, W. Bio-catalysis in multicomponent reactions, *Molecules*, **2020**, 25, 5935.

2. Albanese, D.C.; Gaggero, N. Albumin as a promiscuous biocatalyst in organic synthesis, *RSC advances*, **2015**, 5, 10588-10598.
3. Sharma, U.K.; Sharama, N.; Kumar, R.; Sinha, A.K. Biocatalysts for multicomponent Biginelli reaction: Bovine serum albumin triggered wasted-free synthesis of 3,4-dihydropyrimidin-2-(1 H)-ones, *Amino Acids*, **2013**, 44, 1031.

The 30th Iranian Seminar of Organic Chemistry
February 7-9, 2025, Iran University of Science and Technology, Tehran, Iran

Application of metal-organic framework (UiO66-NH$_2$) as an efficient catalyst in the synthesis of 2-amino-3-cyano-pyridine derivatives

Elahe Ahmadi [a], Fatemeh Rafiee [b]*

[a, b] Department of Organic Chemistry, Factually of Chemistry, Alzahra University, Tehran, Iran.

Keyword: 2-Amino-3-cyanopyridines, Multi component reaction, Metal-organic frameworks

Nitrogen-containing compounds are of great importance in medicinal chemistry and related sciences due to their unique chemical and biological properties. Among these compounds, 2-amino-3-cyanopyridine has many biological properties.[1] In this context, various metallic catalysts have been introduced as efficient catalytic system for the synthesis of this evaluable compounds[2]. Metal-organic frameworks (MOFs) have porous structures consisting of metals and organic ligands. Due to their large surface area and special chemical properties, these structures have the ability to facilitate and optimize chemical reactions[3]. In this project, the metal-organic framework UiO66-NH$_2$ was used as a recyclable catalyst for the synthesis of 2-amino-3-cyanopyridine derivatives (**Scheme** 1). This reaction is a four-component reaction between aromatic aldehyde, acetophenone, malononitrile and ammonium acetate. High efficiency and selectivity, ability for easy separation and recovery from the reaction mixture, reusability, low energy consumption, high yield and short reaction time are some of the advantages of the synthesized catalyst.

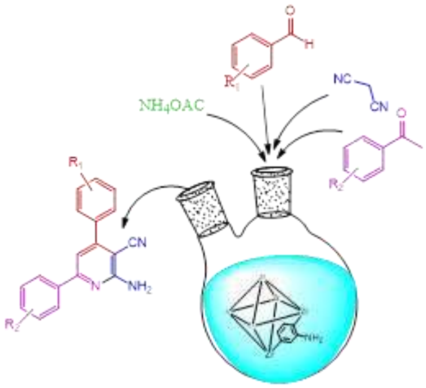

Scheme 1. Preparation of 2-amino-3-cyanopyridine catalyzed by UiO66-NH_2

References:

١. Mamedov, I.; Naghiyev, F.; Maharramov, A.; Uwangue, O.; Farewell, A.; Sunnerhagen, P.; Erdelyi, M., Antibacterial activity of 2-amino-3-cyanopyridine derivatives. *Mendeleev Communications* **2020**, *30*(4), 498-499.
٢. Motahari, S.; Khazaei, A., Preparation and characterization of Co (II) supported on modified magnetic Fe_3O_4 nanoparticles and its application as catalyst for the synthesis of 2-amino-3-cyanopyridines. *Polycyclic Aromatic Compounds* **2023**, *43*(1), 945-٩٥٦.
٣. Chen, M.; Tu, Y.; Wu, S., Preparation of UiO-66-NH_2@ PDA under water system for chemical warfare agents degradation. *Materials* **2021**, 14(9), 2419.

The 30th Iranian Seminar of Organic Chemistry
February 7-9, 2025, Iran University of Science and Technology, Tehran, Iran

Theoretical investigation of the potential energy surface and some chemical-physical descriptors of diethyl ether

Zeinab SaeediPour *[a], S.H. Reza Shojaei [b]

[a] *Department of Physics, Sahand University of Technology, Tabriz*

[b] *Department of Physics, Sahand University of Technology, Tabriz*

Keyword: Diethyl ether, Potential Energy Surface, Dipole Moment, Homo-Lumo gap.

Introduction: Diethyl ether (CH3CH2OCH2CH3) is a well-known anesthetic drug and also a dipolar protic solvent widely used in organic synthesis. Additionally, diethyl ether is potentially an interstellar molecule [1]. Despite its pharmacological importance, limited studies have focused on the conformers of this molecule and its potential energy surface (PES). The aim of this research is to present a new PES map of DEE through dihedral angle scans. Furthermore, a comprehensive study has been conducted on the stable conformers, transition states, HOMO-LUMO gap, and variations in the electric dipole moment.

Method: All calculations were performed using the Gaussian 09 software at two levels of theory: Hartree-Fock and Density Functional Theory [2] (B3LYP), with the aug-cc-pVDZ basis set [3-5]. In this study, the angles D1 (corresponding to the C-C-O-C rotation) and D2 (corresponding to the C-O-C-C rotation) were scanned in 10-degree steps over a range of 0 to 360 degrees, resulting in the generating of 1369 independent structures. These structures were subjected to single-point calculations at the same level of theory used in the PES scan to obtain the values for μ (Dipole Moment) and $\Delta E = E_{LUMO} - E_{HOMO}$.

Results and Discussion: The molecular energy variation, electric dipole moment and $E_{LUMO} - E_{HOMO}$ as a function of the dihedral angles D1 and D2 at two levels, HF/aug-cc-pVDZ and B3LYP/aug-cc-pVDZ , is shown in Figure 1.

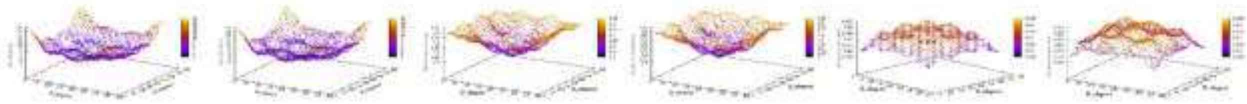

Figure 28: From the left, respectively, the Potential Energy Surface at the B3LYP and HF levels, the Electric Dipole Moment at the B3LYP and HF levels, the Homo-Lumo gap at the B3LYP and HF levels of the DEE.

Both computational levels produced similar PES, which differs only in the range of energy values covered. To fully calculate the energy of the conformers, each of these structures was completely optimized. This analysis confirms that, after relaxing the selected structures, 4 ground-state conformers and 6 transition-state structures were identified. To check the consistency of our results, the reader is referred to the article by Kuze et al. [6]. The structure of the diethyl ether molecule and the ground-state conformers of the molecule are shown in Figure 2.

Figure 29: From the left, respectively, the structure of the DEE and the angles D1 and D2 ; The ground state conformers of DEE: TG, GG, GG' and TT.

Overall, the DFT and HF calculations yield identical results, with only minor structural differences observed in the location of the minimums on the PES, originating from the level of theory applied. Additionally, in both cases, the conformers are nearly isoenergetic. The widely used parameter $\Delta E = E_{LUMO} - E_{HOMO}$, which reflects the chemical reactivity and molecular stability, does not appear to have a direct correlation with the PES. However, our results indicate that careful consideration is required when using this parameter to evaluate the kinetic stability of a molecule, as DFT results may strongly depend on the specific method employed. In these plots, a larger HOMO-LUMO gap indicates greater molecular stability, whereas lower values correspond to molecules in a transition state or an unstable condition. As expected, any change in geometry may alter the centers of molecular charge symmetry, leading to a change in the molecule's electric dipole moment. The dipole moment is commonly used to explain certain physical and chemical properties of molecules. The greater the dipole variations, the stronger the band intensity in the IR spectrum. Additionally, in that state, the molecular interaction is stronger than in other states. In the ground-state conformers, the instantaneous dipole moment and potential energy are low.

References:

[1] I. Medvedev *et al.*, "The millimeter-and submillimeter-wave spectrum of the trans–gauche conformer of diethyl ether," *Journal of Molecular Spectroscopy,* vol. 228, no. 2, pp. 314-328, 2004.

[2] W. Kohn, A. D. Becke, and R. G. Parr, "Density functional theory of electronic structure," *The journal of physical chemistry,* vol. 100, no. 31, pp. 12974-12980, 1996.

[3] T. H. Dunning Jr, "Gaussian basis sets for use in correlated molecular calculations. I. The atoms boron through neon and hydrogen," *The Journal of chemical physics,* vol. 90, no. 2, pp. 1007-1023, 1989.

[4] R. A. Kendall, T. H. Dunning Jr, and R. J. Harrison, "Electron affinities of the first-row atoms revisited. Systematic basis sets and wave functions," *The Journal of chemical physics,* vol. 96, no. 9, pp. 6796-6806, 1992.

[5] D. E. Woon and T. H. Dunning Jr, "Gaussian basis sets for use in correlated molecular calculations. III. The atoms aluminum through argon," *The Journal of chemical physics,* vol. 98, no. 2, pp. 1358-1371, 1993.

[6] N. Kuze, N. Kuroki, H. Takeuchi, T. Egawa, and S. Konaka, "Structural and conformational analysis of diethyl ether by molecular orbital constrained electron diffraction combined with microwave spectroscopic data," *Journal of molecular structure,* vol. 301, pp. 81-94, 1993.

The 30th Iranian Seminar of Organic Chemistry
February 7-9, 2025, Iran University of Science and Technology, Tehran, Iran

Synthesis, spectroscopic studies and DFT calculations of some new 3-(di-substituted phenyl azo)-4-hydroxybenzo[*h*]quinolin-2(1*H*)-ones

Asieh Yahyazadeh[*], E.O. Moradi Rufchahi [b], Alireza Khabazkar fumani[a]

[*]*Department of Chemistry, University of Guilan, P.O. Box 41335-1914, Rasht, I.R. Iran.*
[b]*Department of Chemistry, Faculty of Science, Lahijan Branch, Islamic Azad University, Lahijan, Iran*
[a]*Department of Chemistry, University of Guilan, P.O. Box 41335-1914, Rasht, I.R. Iran*

Abstract

Diazo coupling products with cyclic enol-type coupling components are a fascinating group of compounds. They are especially useful for studying azo-hydrazone tautomerization because they can exist in a number of different tautomeric and isomeric forms in both solution and solid state [1-5].

The present study examined the impact of electron-donating and electron-withdrawing groups (in the azo coupling component) on the physical and chemical properties of three novel azo derivatives of 4-hydroxybenzo[*h*]quinolin-2(1*H*)-one. Mass spectroscopy, ^{1}H NMR, ^{13}C NMR, and FT-IR were used to characterize final structures of the compounds. DFT quantum chemical calculations were carried out on the optimized structures of the products and compared with experimental data in order to gather more information about the structure of compounds. The optimized compounds' frontier orbital energy gap, which includes HOMO-LUMO and HOMO-1-LUMO+1, was also examined in this study. Furthermore, the characteristics, uses, and solubility of the produced dyes in six solvents—DMF, DMSO, CH_3CN, chloroform, ethanol, and acetic acid—were examined using UV-visible spectroscopy.

Keywords: 4-hydroxybenzo[h]quinolin-2(1H)-one, azo dyes, solvatochromism, NMR, DFT

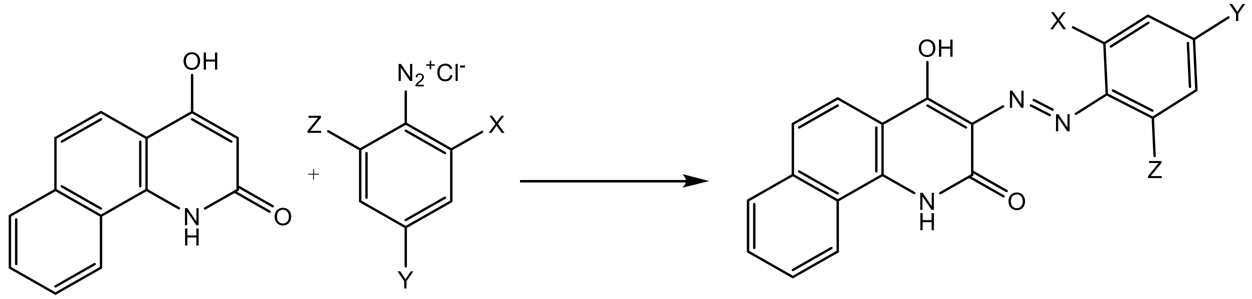

(**1**): X=Y=CH_3 , Z=H (**2**): X=Z=CH_3, Y=H, (**3**): X=Z=Cl, Y=H

References:

[1] F. Karcı and N. Ertan, *Dyes Pigm.* **64**, 243 (2005).
[2] N. Noroozi Pesyan and H. Rashidnejad, *Magn. Reson. Chem.* **54**, 358 (2016).
[3] E.O. Moradi Rufchahi and A. Ghanadzadeh Gilani, *Dyes Pigm.* **96**, 632 (2012).
[4] E.O. Moradi Rufchahi and A. Ghanadzadeh Gilani, *Color. Technol.* **135**, 391 (2019).
[5 F. Ashouri Mirsadeghi, E. M. Rufchahi and S. Zarrabi, *J. Mol. Struct.* **1268**, 133726 (2022).

Preparation and Characterization of Efficient $NiFe_2O_4$@Chitosan Nanocatalyst for the Green Synthesis of Pyrimidine-Based Spiro Heterocycles

Maryam Mousavi-Ebadi[a], Javad Safaei-Ghomi[a]*

[a]*Department of Organic Chemistry, Faculty of Chemistry, University of Kashan, Kashan, 51167, I. R. Iran*

**Corresponding author, Tel: +98 31 55912385; E-mail: safaei@kashanu.ac.ir*

Keyword: Magnetic chitosan, Nano catalyst, multi-component reaction, Spiro heterocycles

Introduction

Magnetite nanoparticles are commonly utilized as solid supports in core-shell catalysts due to their unique electrical and magnetic properties. However, challenges such as surface contamination and particle aggregation necessitate surface modifications [1]. Polysaccharides like chitosan are frequently employed to modify these surfaces, enhancing properties such as solubility, stability, and catalytic activity. The surface of chitosan can be altered through physical loading or covalent grafting of active groups [2, 3]. Pyrimidines are significant heterocyclic compounds with diverse biological activities, making them crucial in drug design and valuable in pharmaceuticals and agriculture [4]. Spiro heterocycles are typically synthesized using multicomponent reactions. Although various catalytic systems have been developed for the synthesis of pyrimidine-based spiro heterocycles, many face challenges such as high costs, recovery difficulties, or limited reactivity [5-7]. This study aims to address these issues by utilizing $NiFe_2O_4$@chitosan as a heterogeneous catalyst for the synthesis of spiro heterocycles based on pyrimidine derivatives through multicomponent reactions.

Scheme 1: Graphic abstract of the synthesis pyrimidine-based spiro heterocycles by $NiFe_2O_4$@Chitosan catalyst

Experimental

Preparation of $NiFe_2O_4$@Chitosan

To prepare $NiFe_2O_4$@Chitosan, chitosan was dispersed in ethanol, and the medium was made alkaline with triethylamine. $NiFe_2O_4$ was then added to the mixture. Subsequently, the mixture was sonicated for one hour and stirred vigorously at 80°C for one hour. The magnetic precipitate was collected using an external magnet, and the obtained solid was dried at 80°C after washing with ethanol.

Synthesis of Indene-2,2'-pyrrolidine-4',5"-pyrimidine]-1,2",3,4",6"(1"H,3"H)-pentaone derivatives using the provided catalyst

First, aldehyde derivatives, barbituric acid, glycine, and ninhydrin were dissolved in hot ethanol, followed by the addition of the catalyst. After a few minutes of reflux, a precipitate formed, which was purified by washing with ethanol.

Results and Discussion

The EDX data indicate the percentage of the expected elements in the structural phase of NiFe2O4 and magnetic chitosan favorably (Fig. 1).

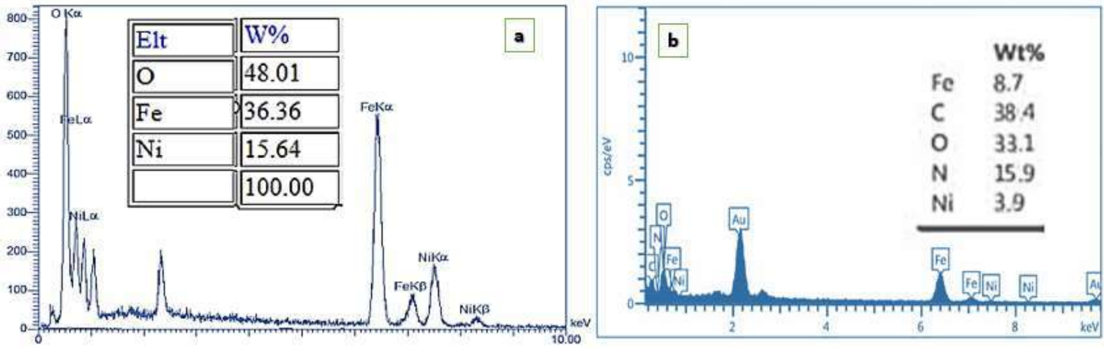

Elt	W%
O	48.01
Fe	36.36
Ni	15.64
	100.00

	Wt%
Fe	8.7
C	38.4
O	33.1
N	15.9
Ni	3.9

Fig.1. Elemental analysis of $NiFe_2O_4$ (a) and $NiFe_2O_4$@Chitosan (b)

References:

[1] S.R. Karnati, B. Høgsaa, L. Zhang, E.H. Fini, *Constr. Build. Mater,* 262 (2020) 120780.
[2] M.Mousavi-Ebadi, J.Safaei-Ghomi, (2024). *Front. Chem. 12*, 1395008.
[3] J. Safaei-Ghomi, M. Tavazo, H. Shahbazi-Alavi, *ZNB*, 74 (2019) 733-738.
[4] D. Kang, H. Zhang, Z. Wang, T. Zhao, T. Ginex, F. J. Luque, X. Liu, *J. med. Chem*. 62 (2019), ١٤٨٤-١٥٠١.
[5] S. Gopal Hegde, L. Koodlur, M. Narayanarao, *Synth. Commun*, 49 (2019), 34٥٣-٣٤٦٤.
[6] C. Rami, L. Patel, C. N. Patel, J. P. Parmar, *J. pharm. bioallied sci.*, 5(2013), 277-289.

Modified Fe_3O_4@SiO_2 core-shell nanoparticle catalyst containing copper and iron complex for facilitating Ullmann cross-coupling reactions

ARDALAN SARAFNIA, MOHAMMAD ABDOLLAHI-ALIBEIK

Department of Chemistry, Yazd University, Yazd 89158-13149, Iran

Keyword: nanoparticle catalyst, Fe_3O_4@SiO_2, Ullmann.

In recent years, the application of magnetic heterogeneous catalysts, particularly magnetic nanoparticles (MNPs), has garnered significant attention[1]. Consequently, magnetic nanoparticles featuring an iron oxide core and a silica shell serve as effective supports for the development of novel magnetic heterogeneous catalysts[2]. Additionally, Schiff base transition metal complexes have been extensively investigated as critical intermediates in the synthesis of diverse organic and inorganic compounds[3].

This study reports the preparation, characterization, and catalytic application of a novel catalyst based on magnetic nanoparticles for Ullmann-type coupling reactions. Magnetic iron oxide (Fe3O4) and Fe3O4@SiO2 core-shell nanoparticles were synthesized as the primary substrates. The desired catalyst was subsequently synthesized using a dendrimer ligand, followed by complexation with copper and iron metals.

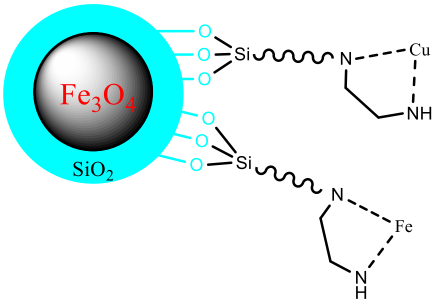

The new catalyst Fe3O4@SiO2@NEE/Cu-Fe[4] was employed in the Ullmann-type coupling reaction, yielding corresponding derivatives in good yields. The catalyst demonstrates the capability for multiple reusability, with only a moderate decrease in activity observed.

References:

[1] Esmaeilpour, M.; Javidi, J.; Dodeji, F. N.; Abarghoui, M. M. *Transition Met. Chem.* **2014**, *39*, 797.

[2] Zirak, M.; Abdollahiyan, A.; Eftekhari-Sis, B.; Saraei, M. *Cellulose* **2018**, *25*, 503.

[3] Uruş, S.; Purtaş, S.; Ceyhan, G.; Tümer, F. *Chem. Eng. J.* **2013**, *220*, 420.

[4] Abdollahi-Alibeik, M.; Gharibpour, N.; Ramazani, Z. **2020**, *43*, 184.

The 30th Iranian Seminar of Organic Chemistry
February 7-9, 2025, Iran University of Science and Technology, Tehran, Iran

One-Pot Photocatalytic synthesis of Benzimidazoles from o-nitroanilines, o-phenylenediamine and Alcohols under Visible light

Javad Samadi [a], Zahra Atharnia [a], Foad Kazemi *[a]

Affiliations: Department of Chemistry, Institute for Advanced Studies in Basic Sciences (IASBS), Zanjan, Iran.

Keyword: Photocatalytic, Benzimidazoles, o-Nitroaniline, o-Phenylenediamine, Alcohols

Introduction

Semiconductors play a key role in photocatalysis, utilizing light energy to drive reactions under mild and eco-friendly conditions [1]. A significant application is the photocatalytic conversion of o-phenylenediamines and o-nitroanilines into benzimidazoles, which are valued in medicinal chemistry for their antimicrobial, antifungal, anti-inflammatory, and anticancer properties [2]. Their stability and bioavailability make benzimidazoles indispensable in pharmaceutical research.

Method

All reactions were conducted in a one-pot batch system using titanium dioxide (TiO_2) as the photocatalyst. The starting materials (o-nitroanilines or o-phenylenediamine) were mixed with the solvent, sonicated for 3 minutes to form a suspension, and irradiated under optimized conditions. O-nitroaniline reactions used blue LED light in an argon atmosphere, while diamine reactions were stirred under sunlight. Reaction progress was monitored using standard analytical techniques.

Results and Discussion

As shown in Table 1, the synthesis of 2-methylbenzimidazole and 2-ethylbenzimidazole was achieved with excellent yields using ethanol and 1-propanol as solvents, respectively. The reactions proceeded efficiently under optimized conditions, highlighting the versatility of the photocatalytic method. Notably, these benzimidazole derivatives were synthesized at room temperature using a blue LED lamp as the light source, emphasizing the practicality and environmental compatibility of this approach.

Table 1: synthesis 2-methyl and 2-ethyl benzimidazole derivatives by TiO_2-P25 under blue LED light

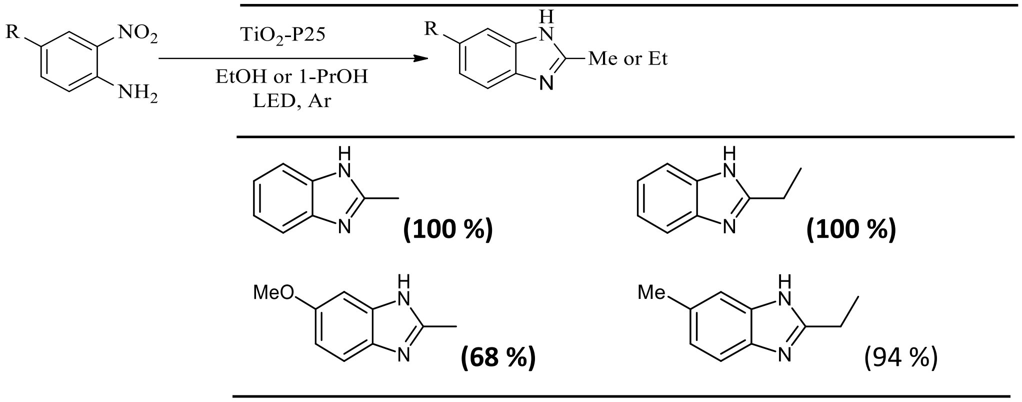

In addition, other benzimidazole derivatives were synthesized with excellent yields using o-Phenylenediamine and various alcohols under sunlight irradiation in an O_2 atmosphere. These results, summarized in Table 2, further demonstrate the efficiency and versatility of the developed photocatalytic method.

Table 2: synthesis of benzimidazol by o-Phenylenediamine and alcohol Under sunlight irradiation

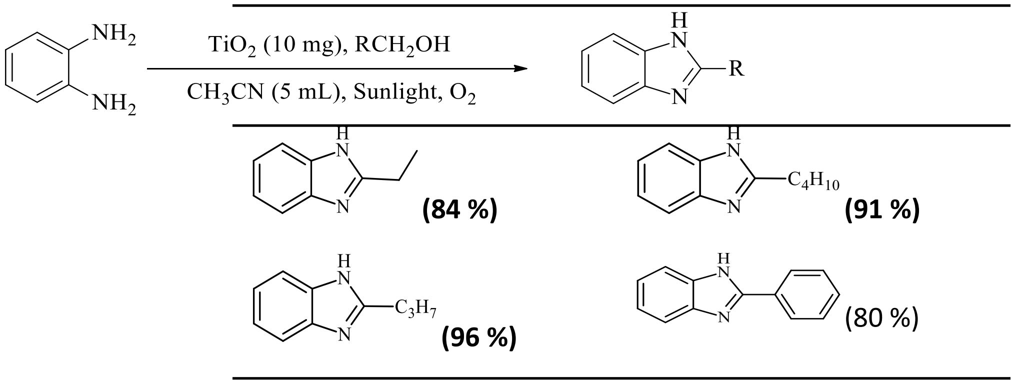

The synthesized products were characterized using ^1H and ^{13}C NMR spectroscopy in deuterated chloroform as the solvent. The NMR spectrum of one representative product is shown in Figure 1, confirming its structure.

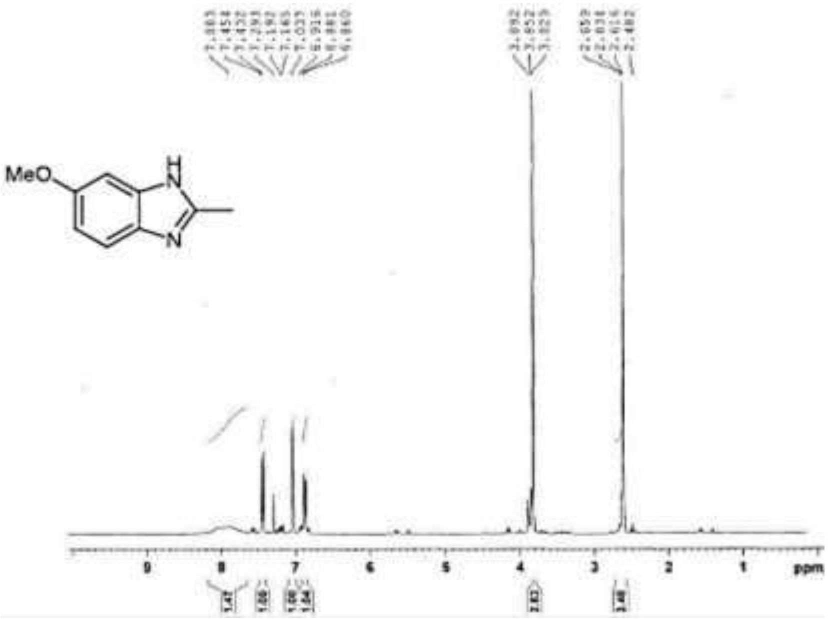

Figure 1:^{1}H NMR Spectra of 2-methyl-5-methoxybenzimidazole

References

[1] Balapure, Aniket, Jayati Ray Dutta, and Ramakrishnan Ganesan. "Recent advances in semiconductor heterojunctions: a detailed review of the fundamentals of photocatalysis, charge transfer mechanism and materials." RSC Applied Interfaces 1.1 (**2024**): 43-69.

[2] Mavvaji, Mohammad, and Senem Akkoc. "Recent advances in the application of heterogeneous catalysts for the synthesis of benzimidazole derivatives." Coordination Chemistry Reviews 505 (**2024**): 215714.

The 30th Iranian Seminar of Organic Chemistry
February 7-9, 2025, Iran University of Science and Technology, Tehran, Iran

Single-atom catalysts, an emerging field in chemical reactions; A DFT studies on the reaction mechanisms for various transformations

Authors: Hossein Tavakol

Affiliations: Department of Chemistry, Isfahan University of Technology, Isfahan, Iran

Keyword: Single-atom catalyst, Mechanism, DFT.

Modification of a support with a single metal atom in the form of doping or dispersion (adsorbed) on the surface is a powerful technique for achieving a high-performance catalyst, namely single-atom catalyst (SAC). Using SAC causes a larger available surface area, extraordinary catalytic activity, more selectivity, higher stability (versus aggregation), and low cost in comparison with metal nanoparticles [1]. The first SAC was introduced by Botao Qiao et al in 2011 as Pt/FeOx, which caused significant progress in this field as well as in the performance of chemical reactions [2]. After that, these perfect materials were investigated in the fields of oxygen reduction reaction (ORR), hydrogen evaluation reaction (HER) [3], CO2 oxidation [4], and water gas shift (WGS) reaction [5] in various experimental and theoretical studies. In the area of organic chemistry, several synthetic methods have also been developed employing SACs such as oxidation of the C−H bond of alkanes, oxidative esterification, oxidation of sulfides, alkenes epoxidation, oxidative dehydrogenation of heteroarenes, synthesis of imines, cyclohexene oxidation, alcohol ammoxidation, and alcohols oxidation.

To examine the applicability of SACs in organic transformations, DFT calculations were used via M06-2X/def2-SVP level of theory, employing Gaussian 09 program package. In this line, NBO calculations were performed and solvent effects have been considered using PCM model.

In the present work Ni, Co, and Cu atom or ions were decorated on the surface of various substrates such as graphene, graphyne, g-C3N4, and alumina to obtain the desired SACs. Then their catalytic effects in various reaction such as, aldol condensation, CO oxidation, CO2 reduction, and direct oxidation of benzene to phenol have been investigated and compared to obtain the most appropriate catalyst. Moreover, the possible mechanistic pathways for each reaction have been examined using the SACs and the most appropriate route was determined.

References:

[1] Yang, X.-F.; Wang, A.; Qiao, B.; Li, J.; Liu, J.; Acc. Chem. Res. 2013, 46 (8), 1740–1748.
[2] Liu, H.; Peng, X.; Liu, X. ChemElectroChem 2018, 5 (20), 2963–2974.
[3] Daghooghi, P.; Tavakol, H. T. Fullerenes Nanotubes Carbon Nanostruct. 2024, 1–15.
[4] Yin, Y.; Ge, X.; Ouyang, J.; Na, N. Nat Commun 2024, 15 (1), 2954.
[5] Saptal, V. B.; Ruta, V.; Bajada, M. A.; Vilé, G Angew Chem Int Ed 2023, 62 (34), e202219306.

The 30th Iranian Seminar of Organic Chemistry
February 7-9, 2025, Iran University of Science and Technology, Tehran, Iran

DFT Study on Tautomeric Stability and Reactivity of 1,3,5-Triazine-dithion

Mina Haghdadi, Setareh Alishah, Narjes Fallah , Sajedeh Karimi*

Department of Chemistry, Babol Branch, Islamic Azad University, Babol ,Iran

Keywords: 1,3,5-Triazine, Tautomeric conformations, thione-thiol, Theoretical calculations

Triazine derivatives have attracted considerable attention from scientists due to their diverse applications. Triazines are used as analytical reagents [1], dyes [2], and in the preparation of polymers [3]. Their significant applications span the fields of medicine, agriculture, and industry [4]. Additionally, the tautomeric equilibrium of substituted triazines has garnered interest. Tautomeric effects influence the reactivity of compounds in chemical processes and are crucial for many biological and biochemical processes.

In this study, we performed theoretical calculations of 1,3,5-triazine derivatives using the DFT B3LYP method to examine the tautomeric conformations of 1,3,5-triazine-2,4-thion-thiol derivatives. Full geometry optimizations were carried out using the 6-31G basis set.

In summary, 12 conformers, which are tautomers of each other, were identified. The energy results revealed a range of barriers and thermodynamic profiles with some pathways being energetically more favorable, while others required high activation energies. These findings underscore the complexity of the tautomerization process and its sensitivity to molecular configurations. The calculation results showed that the di-thione tautomer is the most stable, aligning well with experimental results. Furthermore, frontier orbital energy, atomic net charges, and reactivity indices were also analyzed and discussed.

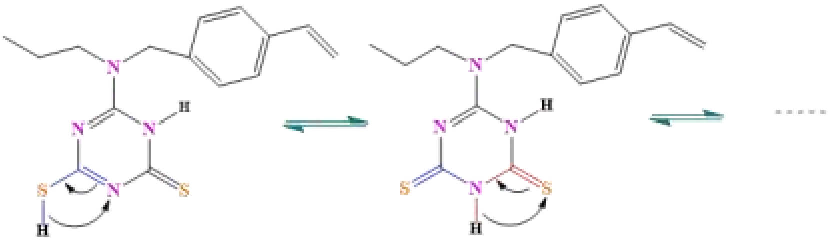

Scheme. thion−thiol tautomerization process of 1,3,5-triazine-2,4-dithion

References

[1] Busch, M. Ber. Dtsch. Chem. Ges. 1905, 38, 856.

[2] Colter, R. J.; Matzner, M. Ring Terming Polymerisation,Part-B-1. Heterocyclic Ring, Academic. New York,1972.

[3] Prasad, A. T.; Ramalingam, R. J.; Rao, A. B.; Diwan, P.V. Eur. J. Med. Chem. 1989, 24, 199.

[4] Bayrak, H.; Demirbas, A.; Bektas, H.; Demirbas, N.; Alpay-Karaoglu, S.; Demirbas, N. Turk. J. Chem. 2010, 34, 835

Synthesis of thieno[2,3-*b*]quinolines using 3-formyl-2-mercaptoquinoline and nitroepoxide

Sahar Harati Beiranvand*, Mohammad Sohrabi, Ahmad Takallou, Azizollah Habibi

Department of Organic and Polymer Chemistry, Faculty of Chemistry, Kharazmi University, Tehran, 49 Mofateh St., Tehran, IRAN, P. O. Box 15719-14911y

**E-mail: a.haratibeiranvand@gmail.com, habibi@khu.ac.ir*

Keywords: thiophene, 3-formyl-2-mercaptoquinoline, nitroepoxide

Heterocyclic compounds, with their significant and diverse roles in various fields, have always been an attractive subject for research. Sulfur- and nitrogen-containing heterocycles, in particular, play a crucial role in the pharmaceutical and therapeutic industries. Among them, thiophene and quinoline are noteworthy heterocycles with remarkable medicinal and biological properties, essential in the treatment of many serious and life-threatening diseases.[1-3] Considering these characteristics, we focused on synthesizing these biologically active compounds using novel methods. The core of this research involves the synthesis of fused thiophene rings from 3-formyl-2-mercaptoquinoline and nitro epoxide derivatives (Scheme 1). This reaction offers several advantages, including high yields, the absence of a need for catalysts, a short reaction time, and the facile synthesis of new thieno[2,3-*b*]quinoline derivatives.

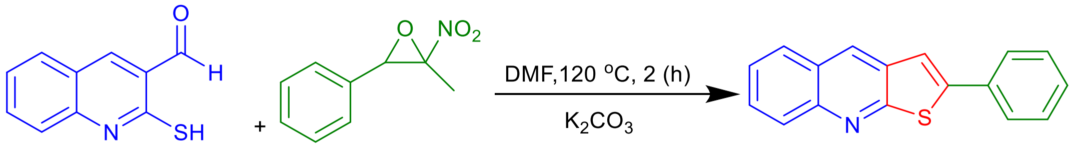

Scheme 1. Reaction pathway for the synthesis of thieno[2,3-b]quinolines

References

(1) Alizadeh, A.; Roosta, A. *Chemical Papers* **2018**, *72*, 2467-2478.

(2) Faghihi, Z.; Shiri, M.; Pourabed, R.; Heravi, M. M.; Zadsirjan, V.. *Polycyclic Aromatic Compounds* **2020**, 41 (10), 2120-2209.

(3) Ranjbari, M. A.; Tavakol, H. *The Journal of Organic Chemistry* **2021**, *86* (6), 4756-4762.

fabrication of the Ca-BTC MOF /polylactic acid/gelatin porous nanocomposite scaffold for bone tissue engineering application

Authors: Soghra Nikpour 1*, Zeinab Ansari-Asl 1, Tahereh Sedaghat 1 , Elham Hoveizi 2

[1] *Department of Chemistry, Faculty of Science, Shahid Chamran University of Ahvaz, Ahvaz, Iran*

[2] *Department of Biology, Faculty of Science, Shahid Chamran University of Ahvaz, Ahvaz, Iran*

Keyword: Metal-organic framework; Polylactic acid; Gelatine; Composite scaffold; Bone tissue engineering

The main aim of tissue engineering (TE) is replacement or regeneration of organs or tissues that are damaged by injuries or diseases. In this study, a novel porous composite scaffold, Ca-BTC MOF/PLA/Gelatine, was prepared by incorporating a Ca-based metal-organic framework (Ca-BTC MOF) into polylactic acid (PLA) and gelatin mixture (Scheme 1). PLA/Gelatine scaffold was also fabricated as a control. EDS elemental mapping and SEM images exhibited the homogeneous dispersion of the Ca-BTC MOF particles into the porous scaffold. Additionally, SEM images confirmed the interconnected porous morphology of the as-prepared scaffold. The obtained scaffold was evaluated in terms of structural and biocompatibility properties, as well as its ability to promote bone development. porous scaffold exhibited proper bone repair properties compared to the PLA/Gelatine scaffold that was tested as a control These findings suggest that the Ca-BTC MOF/PLA/Gelatine scaffold is a promising material for bone regeneration. Therefore By successfully loading Ca-BTC MOF into the PLA/Gelatine matrix, the as-obtained scaffold was able to act as a biocompatible material with bone regeneration capability.

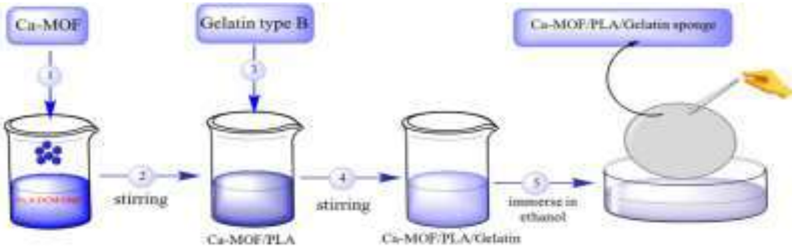

Scheme 1. Schematic procedure for fabrication of the Ca-BTC MOF/PLA/Gelatine composite scaffold.

References:

[1] Xue, N., Ding, X., Huang, R., Jiang, R., Huang, H., Pan, X., ... & Wang, Y. **(2022)**. Bone tissue engineering in the treatment of bone defects. Pharmaceuticals, 15(7), 879.

[2] Wong, H. L., Tsang, C. Y., & Beyer, S. **(2023)**. Metal–Organic Frameworks (MOFs) and Their Composites as Emerging Biomaterials for Osteoarthritis Treatment. Biomimetics, 8(1), 97.

[3] Ma, P. X. **(2004)**. Scaffolds for tissue fabrication. Materials today, 7(5), 30-40.

The 30th Iranian Seminar of Organic Chemistry
February 7-9, 2025, Iran University of Science and Technology, Tehran, Iran

Rhodium-Catalyzed Asymmetric Synthesis of Thioesters and Functionalized Morpholines

Azim Ziyaei Halimehjani,[a,*] Bernhard Breit [b,*]

[a] *Department of Chemistry, Sharif University of Technology, P.O. Box 11155-9516, Tehran, Iran. E-mail: azim.ziyaei@sharif.edu* [b] *Institut für Organische Chemie, Albert-Ludwigs-Universität Freiburg, Albert strasse 21, 79104 Freiburg im Breisgau (Germany).*

Keyword: Rhodium, Thioesters, Morpholines, aalenes, asymmetric synthesis

Activation of allenes with Rhodium catalyst is an important technique for the synthesis of branched allylic compounds. In this talk, I will discuss about the application of $[Rh(COD)Cl]_2$ as catalyst for regio- and enantioselective hydrothiolation of terminal allenes with thioacids for atom-economic synthesis of chiral branched allylic thioesters. In addition, intramolecular cyclization of nitrogen-tethered allenols will be discussed for the synthesis of functionalized morpholines in the presence of Rhodium catalyst. By using this strategy, various *N*-protected 2,5- and 2,6-disubstituted as well as 2,3,5- and 2,5,6-trisubstituted morpholines can be obtained *via* an atom-economic pathway with high to excellent yields, diastereo- and enantioselectivities.

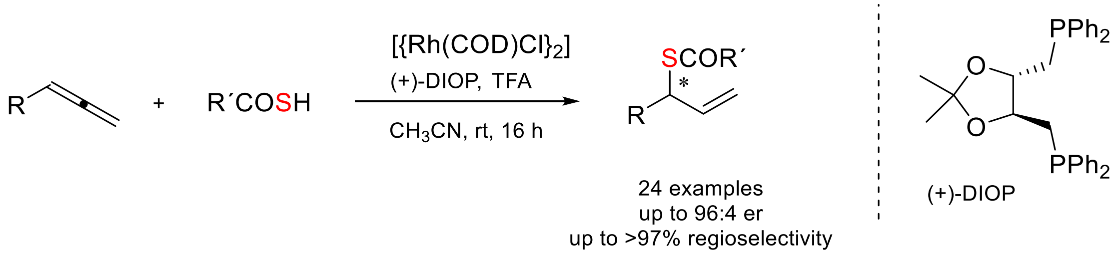

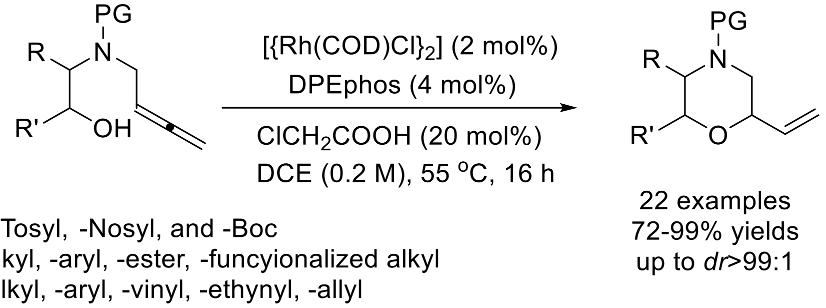

References: (a) Azim Ziyaei Halimehjani, Bernard Breit, *Chem. Commun*. **2022**, *58*, 1704-1707. (b) Azim Ziyaei Halimehjani, Bernard Breit, *Chem. Commun*. **2023**, *59*, 4376-4379.

The 30th Iranian Seminar of Organic Chemistry
February 7-9, 2025, Iran University of Science and Technology, Tehran, Iran

Mesoporous g-C_3N_4 prepared from urea and melamine as a semiconductive electrode material for supercapacitor applications

Authors: E. Jamshidi[a], M. Yaghoubi[a], F. Manteghi[a]*

Research Laboratory of Inorganic Chemistry and Environment, Department of Chemistry, Iran University of Science and Technology

Keywords: g-C_3N_4, supercapacitors, energy storage, mesoporous

Due to the considerable growth of global energy intensity to almost 2.1% in 2016, the efficient impact of renewable sources that control 50% of global energy intensity came to mind. Additionally, due to the increase in renewable energy sources usage until 2030, it is essential to keep global energy usage under surveillance to meet the Kyoto and Paris Agreement targets and control the global temperature rise average. By the way, a supercapacitor, which resembles a battery came to the eyes as a reliable high-capacitor energy storer due to its fantastic surface area, electrodes' slim dielectric layer space, and high capacity which lower the increase of economical contaminations and limitation in energy resources.[1] Carbon-based materials' notable electrochemical features which include excellent conductivity and stability, in addition to their low cost, porous structure, and high specific capacitance make them efficient candidates for SC electrode materials particularly for EDLCs.[2] Among various carbon-based materials used as SC electrode materials, graphitic carbon nitride (g-C_3N_4), a two-dimensional semiconductive provides numerous adsorption/desorption active sites, besides their other properties such as chemical stability and eco-friendly features that have drawn attention to them for supercapacitors applications.[3] In this work, we prepared a mesoporous graphitic carbon nitride (g-C_3N_4) with melamine and urea. In addition to electrochemical analyses like GCD (galvanostatic charge and discharge), CV (cyclic voltammetric potentiostatic), and EIS (FRA impedance potentiostatic), we also analyzed the structural features using SEM, FT-IR, XRD, and EDX. The electrochemical experiments on the as-prepared g-C_3N_4 indicate 124.44 F g^{-1} specific capacity at 2 A/g and 12.59 Wh kg^{-1} of energy density at a power density of 1618.71 W kg^{-1}, in conjunction with 123.52% stability after 6000 cycles at 5 A/g.

References

1.Kumar, Y.A., Roy, N., Ramachandran, T., Hussien, M., Moniruzzaman, M., and Joo, S.W. (2024). Shaping the future of energy: The rise of supercapacitors progress in the last five years. Preprint at Elsevier Ltd, https://doi.org/10.1016/j.est.2024.113040.

2.Yuan, C., Xu, H., A. El-khodary, S., Ni, G., Esakkimuthu, S., Zhong, S., and Wang, S. (2024). Recent advances and challenges in biomass-derived carbon materials for supercapacitors: A review. Preprint at Elsevier Ltd, https://doi.org/10.1016/j.fuel.2023.130795 https://doi.org/10.1016/j.fuel.2023.130795.

3.Thomas, S.A., Pallavolu, M.R., Khan, M.E., and Cherusseri, J. (2023). Graphitic carbon nitride (g-C3N4): Futuristic material for rechargeable batteries. Preprint at Elsevier Ltd, https://doi.org/10.1016/j.est.2023.107673 https://doi.org/10.1016/j.est.2023.107673.

The 30th Iranian Seminar of Organic Chemistry
February 7-9, 2025, Iran University of Science and Technology, Tehran, Iran

Revealing the ability of MOF (74)-polymer composite to improve carbon dioxide adsorption performance

Fateme Zeinali[a] (representing author), Amir Kazemi[a], Faranak Manteghi*[a] (corresponding author)

[a] *Research Laboratory of Inorganic Chemistry and Environment, Department of Chemistry, Iran University of Science and Technology, 16846-13114 Tehran, Iran*

Abstract

The global community is taking steps to drastically reduce greenhouse gas (GHG) emissions associated with climate change and global warming. There are different types of greenhouse gases, and their global warming potential is different. The best known GHG is CO_2. According to the US Environmental Protection Agency (EPA), CO_2 concentrations have increased dramatically since the beginning of the industrial age. Concentrations have increased from an annual average of 280 parts per million (ppm) in the late 1700s to more than 400 ppm in 2021, representing a 48 percent increase. Anthropogenic activities, including the combustion of fossil fuels such as coal, oil, and natural gas, are primarily responsible for this dramatic increase in CO_2 levels, which leads to numerous effects such as global temperature rise and ocean acidification. Today, the global temperature is on average 0.8-1.2 ˚C higher than pre-industrial levels, which is predicted to reach 1.5 ˚C by 2030-2050. Extensive research conducted in the last two decades, notable features of the framework, has highlighted metal-organic frameworks (MOFs) in terms of storage and separation.

However, the practical application and commercialization of MOFs have been limited to powder form due to their crystalline nature, creating challenges in their integration for various applications. In addition, certain types of MOFs show reduced performance under wet conditions. To overcome these limitations, there is the potential of combining MOFs with polymers to achieve desirable properties. Polymeric materials offer excellent solubility and mechanical properties for solid adsorbents such as powdered and crystalline MOFs.

In this research, in order to achieve a new structure of carbon dioxide-adsorbing MOF-polymer, polydopamine polymer was first synthesized and then added to Zn-MOF-74 precursors, and as a result, Zn-MOF-74 self-assembled around polydopamine. By solvothermal method, the core-shell structure of PDA@Zn-MOF-74 is formed. The results of structural tests such as PXRD, SEM, FTIR, and TEM showed that the synthesized adsorbent was successfully synthesized according to the previous data. The adsorption results showed that the maximum CO_2 adsorption capacity and the cyclic efficiency of the synthesized adsorbent were 8.17 and 96.8 mmol/g, respectively.

Keyword: MOF-74, MOF-Polymer, CO_2, gas adsorption

References:

1. Wei, K., et al., *Recent advances in CO_2 capture and reduction.* Nanoscale, 2022. 14(33): p. 11869-11891.

2. Xie, S., et al., *MOF-*74*-M (M= Mn, Co, Ni, Zn, MnCo, MnNi, and MnZn) for low-temperature NH3-SCR and in situ DRIFTS study reaction mechanism.* ACS applied materials & interfaces, 2020. 12(43): p. 48476-48485.

3. Yang, S., et al., *Enhancing MOF performance through the introduction of polymer guests.* Coordination Chemistry Reviews, 2021. 427: p. 213525.

4. Yang, S.-Y., et al., *Performances and Net CO2 Emission of Light Olefin Production Based on Biomass-to-Methanol and DMTO-II Technologies with CO_2 Capture and Sequestration.* ACS Sustainable Chemistry & Engineering, 2021. 9(44): p. 14670-14677.

5. Zhou, C., et al., *Amine-functionalized mesoporous monolithic adsorbents for post-combustion carbon dioxide capture.* Chemical Engineering Journal, 2021. 413: p. 127675.

6. Singh, J. and D.W. Dhar, *Overview of carbon capture technology: microalgal biorefinery concept and state-of-the-art.* Frontiers in marine science, 2019. 6: p. 29.

7. Song, K., et al., *Tailoring the crystal forms of the Ni-MOF catalysts for enhanced photocatalytic CO_2-to-CO performance.* Applied Catalysis B: Environmental, 2022. 309: p. 121232.

8. Sun, Y., et al., *Constructing a Highly Sensitivity SERS Sensor Based on a Magnetic Metal–Organic Framework (MOF) to Detect the Trace of Thiabendazole in Fruit Juice.* ACS Sustainable Chemistry & Engineering, 2022. 10(26): p. 8400-8410.

9. Vakili, R., et al., *Plasma-assisted catalytic dry reforming of methane (DRM) over metal-organic frameworks (MOFs)-based catalysts.* Applied Catalysis B: Environmental, 2020. 260: p. 118195.

10. Vinoth, S., W.-J. Ong, and A. Pandikumar, *Defect engineering of BiOX (X = Cl, Br, I) based photocatalysts for energy and environmental applications: Current progress and future perspectives.* Coordination Chemistry Reviews, 2022. 464: p. 214541.

The global economic prospect of the natural essential oil industry, the challenges of its supply and production in Iran

Mohammad Hossein Mohseni[a], Faranak Manteghi*[a], Hossein Ghafuri[b]

[a] *Research Laboratory of Inorganic Chemistry and Environment, Department of Chemistry, Iran University of Science and Technology, Tehran, 16846-13114, Iran*

[b] *Catalysts and Organic Synthesis Research Laboratory, Department of Chemistry, Iran University of Science and Technology, Tehran, 16846-13114, Iran*

Keywords: economy of natural essential oils, essential oil industry, demand of international markets, natural essential oils in Iran

Abstract:

The 20-year vision of economic development and non-oil exports of our country, Iran, and the need to pay attention to the role of its natural resources as a unique ecosystem in the world, creates a suitable platform for the development of exports and the increase of non-oil income of the country. Economic production and targeted processing of natural essential oils from God-given potential resources, compared to other sources, is less dependent on non-native complex technologies, foreign raw materials and imports in general. Therefore, in terms of stability, resilience and economic risk-taking, it is in more suitable conditions and political and international fluctuations have less negative impact on it. The direct but different entry of academics, especially scientists and researchers in the fields of chemistry and chemical engineering with trends related to this noble industry, as well as the use of specific beliefs for the synthesis of new products, can be a suitable model in providing the technical knowledge of scientific processing for international markets, and this is what farmers and artisans are looking for and cannot find. In addition, in order to keep the international markets dynamic, we must carefully identify the specific needs and demands of the consumers and in accordance with their desires and tastes, we should design the stages of production until the export of the products based on knowledge. In this regard, the technical know-how to produce competitive products in the field of natural essential oils is available on a laboratory scale, but it is important to note that the technical know-how is not a pre-prepared package, but according to the needs and as a result of the close relationship between the industry and the university. The statistics and reports of UNIDO, the World Bank and important economic centers of the United Nations show that developed countries with high per capita income create an added value of about 185 dollars per ton of vegetable products. While this figure in developing countries is close to 40 dollars, which means absolute raw sales. Also, 98% of the plant products of developed countries are placed in industrial processing, which is 38% for developing

countries. In 2024, the volume of the economic market of plants containing effective substances, including medicine, flavor, smell and taste, will be 296 billion dollars, of which about 26 billion dollars will be natural essential oils, and this figure will increase to 2030. It has predicted 430 and 42.5 billion dollars respectively.

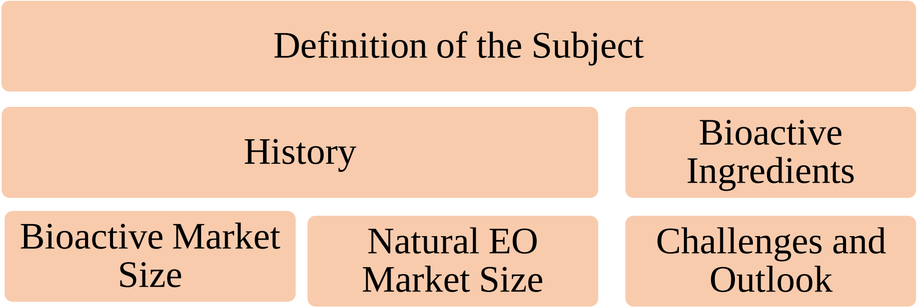

References:

١. Eziacka Mathew Mpelangwa, Jeremia Ramos Makindara, Olav Jull Sørensen and Kenneth Michael-Kitundu Bengesi, African Journal of Economic and Management Studies, **2021**, 13 (1), 1-14.
٢. Shilin Chen, Hua Yu, Hongmei Luo, Andre Steinmetz, Conservation and sustainable use of medicinal plants: Problems, progress, and prospects, Chinese Medicine, **2016**, 11, 37.
٣. Kemal Husnu Can Baser, Gerhard Buchbauer, Handbook of Essential Oils: Science, Technology, and Applications, Second Edition. **2015**, Taylor & Francis. ISBN 9781466590472.

The 30th Iranian Seminar of Organic Chemistry
February 7-9, 2025, Iran University of Science and Technology, Tehran, Iran

Designing New Heterogeneous Palladium Magnetic Nanocatalyst and its Catalytic Application in Suzuki and Stille Reactions

Sahar Safari, Arash Ghorbani-Choghamarani*, Arezo Monem

Department of Organic Chemistry, Faculty of Chemistry and Petroleum Science, Bu-Ali Sina University, Hamedan, 6517838683, Iran, a.ghorbani@basu.ac.ir or arashghch58@yahoo.com, saharsafari7725@gmail.com, arezomonem@yahoo.com

Keyword: : Magnetic nanoparticles, Heterogeneous catalyst, Suzuki reaction, Stille reaction, Zinc ferrite ($ZnFe_2O_4$)

Carbon-carbon cross-coupling reactions are vital in synthetic organic chemistry due to their diverse applications. They allow chemists to link carbon atoms and create complex molecules similar to natural substances [1-2]. In this study, new heterogeneous Palladium nanocatalysts immobilized on zinc ferrite magnetic nanoparticles ($ZnFe_2O_4$@SiO_2@CPTMS@PYA-Pd) were designed and synthesized. The structure and magnetic properties of this nanomagnetic material were analyzed by FT-IR, TGA, EDS, VSM, XRD, X-ray mapping, ICP-OES, and SEM techniques. This new magnetic Palladium nanocatalyst has outstanding properties such as acceptable chemical stability, low toxicity, and easy recycling. The $ZnFe_2O_4$@SiO_2@CPTMS@PYA-Pd exhibited excellent catalytic activity for Stille, and Suzuki cross-coupling reactions and biphenyl products were obtained with good to high conversion. The reported catalyst was efficiently recovered using a magnet and reapplied for at least five consecutive cycles while maintaining its catalytic activity throughout the C-C coupling reactions (Scheme 1).

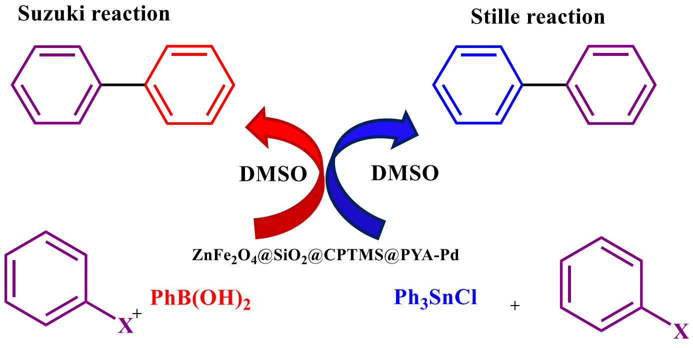

Scheme 1. Suzuki and Stille reactions

References:

١- A. Mohammadinezhad, B. Akhlaghinia, Fe3O4@Boehmite-NH2-CoII NPs: an inexpensive and highly efficient heterogeneous magnetic nanocatalyst for the Suzuki-Miyaura and Heck-Mizoroki cross-coupling reactions, Green Chem. 19 (2017) 5625–5641.

٢- M. Mohammadi, M. Khodamorady, B. Tahmasbi, K. Bahrami, A. GhorbaniChoghamarani, Boehmite nanoparticles as versatile support for organic–inorganic hybrid materials: synthesis, functionalization, and applications in eco-friendly catalysis, J. Ind. Eng. Chem. 97 (2021) 1–78.

The 30th Iranian Seminar of Organic Chemistry
February 7-9, 2025, Iran University of Science and Technology, Tehran, Iran

Biodiesel Production with Green Zinc Ferrite Catalyst via Esterification Reaction

Sahar Safari, Arash Ghorbani-Choghamarani*, Arezo Monem

Department of Organic Chemistry, Faculty of Chemistry and Petroleum Science, Bu-Ali Sina University, Hamedan, 6517838683, Iran, a.ghorbani@basu.ac.ir or arashghch58@yahoo.com, saharsafari7725@gmail.com, arezomonem@yahoo.com

Keywords: Magnetic nanoparticles, Esterification, Biodiesel, Heterogeneous Catalysis, Oleic acid, palmitic acid and myristic acid

Biodiesel is a promising renewable alternative to fossil fuels, offering a sustainable solution to energy needs. The transesterification of triglycerides into fatty acid methyl esters (FAME) is a widely accepted method for biodiesel production. The acid catalysts for the esterification of free fatty acids (FFAs) and the transesterification of triglycerides present a viable biodiesel synthesis approach from diverse and low-cost feedstock [1-2]. In this research, we report the synthesis and characterization of $ZnFe_2O_4@SiO_2–SO_3H$, a novel, environmentally friendly nanomagnetic solid acid catalyst. This catalyst incorporates sulfuric acid catalytic sites on the surface of $ZnFe_2O_4$ magnetic nanoparticles, which serve as the catalytic support [3]. The synthesized $ZnFe_2O_4@SiO_2–SO_3H$ magnetic nanoparticles (MNPs) were thoroughly characterized using various physicochemical methods, including FT-IR, FE-SEM, VSM, EDS, and X-ray mapping magnetometer analyses. The advantages of heterogeneous catalysts are particularly noteworthy, as they facilitate easier separation, exhibit lower corrosion rates, and offer potential for recycling. Furthermore, the catalytic activity of the recycled nanocatalyst was assessed over at least five cycles, demonstrating a negligible loss of activity, indicating its potential for sustainable biodiesel production (Scheme 1).

o

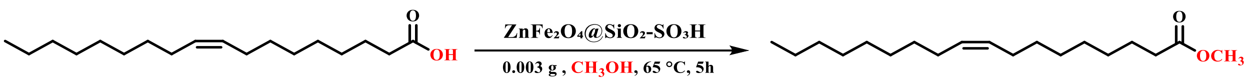

Scheme 1. **Esterification of Oleic Acid**

References:

١- Ghorbani-Choghamarani, A., Taherinia, Z., and Tyula, Y. A. Efficient biodiesel production from oleic and palmitic acid using a novel molybdenum metal–organic framework as efficient and reusable catalyst. Sci.Rep. ١٢, ١٠٣٣٨ (٢٠٢٢).

٢- Ma, F., & Hanna, M. A. Biodiesel production: a review. Bioresource technology. **70**, 1-15 (1999).

٣- Aghavandi, H., & Ghorbani-Choghamarani, A. ZnFe2O4@ l-Arginine-Ni: A novel, green, recyclable, and highly versatile catalyst for the synthesis of 1H-tetrazoles and oxidation of sulfides to the sulfoxides. Journal of Physics and Chemistry of Solids. **170**, 110952 (2022).

The 30th Iranian Seminar of Organic Chemistry
February 7-9, 2025, Iran University of Science and Technology, Tehran, Iran

The Effect of Deamidation on the Structure of Gluten

Atefeh Mousavi, Javad Safaei-Ghomi*

Department of Organic Chemistry, Faculty of Chemistry, University of Kashan, Kashan, I.R. Iran

** Corresponding author: +98 31 55912385, E-mail: safaei@kashanu.ac.ir*

Abstract

This study examines the structural changes in gluten proteins due to alkaline deamidation. It aims to compare the infrared properties of gluten before and after this process to highlight the induced structural changes.

Key words**:** Gluten, Deamidation, structural modification

١. Introduction

Gluten polymers feature two main domains: a beta-sheet-rich N-terminal repeat domain and a globular C-terminal domain rich in alpha-helices. Deamidation enhances the charge in the N-terminal domain and partially unfolds the C-terminal structure, leading to a decrease in alpha-helix content [1]. This modification converts glutamine and asparagine residues to glutamic acid and aspartic acid, significantly altering gluten's physicochemical properties and can be induced by acids, alkalis, and heat [2-6]. Alkaline deamidation promotes cross-link formation, such as disulfide bonds, enhancing gluten polymerization and creating fibrous microstructures while reducing cysteine content, which affects the disulfide bond network [7-11]. Thus, controlling deamidation conditions is essential for optimizing gluten's functional properties for food processing and developing new gluten-based products.

۲. Experimental

2.1 Material

Commercial wheat gluten powder used in this study was procured from Starch Company, Shiraz,

2.2. Deamidation by NaOH on gluten

A 25 mM NaOH solution was prepared in 70% ethanol. Gluten powder (10% w/v) was added to this solution and stirred at room temperature for 16h. The mixture was then heated to 35°C with continuous stirring until the ethanol evaporated.

2.3. Fourier Transform Infrared Spectroscopy

T-IR spectra were obtained using a Nicolet 550 Magna FT-IR spectrometer with KBr pellets, displaying wavenumber (cm^{-1}) on the X-axis and transmittance percentage on the Y-axis.

۳. Result and discussion

Wheat gluten is insoluble in water but can be dispersed when the pH is below or above its isoelectric point of approximately 7.3 [12]. This study offers a comparative analysis of the infrared (IR) spectra of gluten and its deamidated product, as shown in Figure 1.

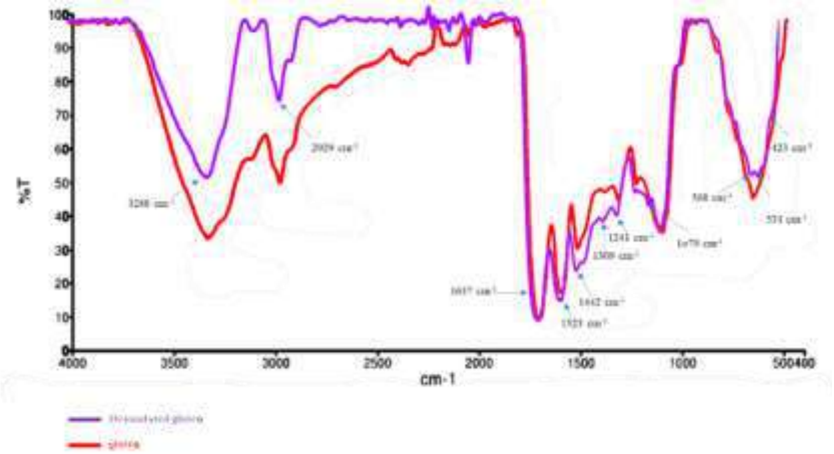

Figure 1: Comparison of spectra between gluten and the deamidation product

The fingerprint region (500-1500 cm^{-1}) shows significant differences in the IR spectra of gluten and deamidated gluten, indicating changes in hydrogen bonding, functional groups, and spatial structure after deamidation. In the 1500-4000 cm^{-1} range, variations in peaks related to functional groups such as hydroxyl (OH), amide (NH), and carbonyl (C=O) reflect changes in their content and intermolecular interactions. Alterations in N-H stretching peaks indicate modifications to the hydrogen bond network during deamidation, affecting the intensity and position of IR spectrum peaks, especially in the 1600-1700 cm^{-1} range.

٤. Conclusion

The comparison of FTIR spectra reveals that deamidation significantly alters the structure and properties of gluten. Key changes include the breaking of hydrogen bonds, alterations in functional group content, and modifications to the spatial structure of the gluten molecule. These findings enhance the understanding of the deamidation process and can improve the functional properties of gluten-containing products.

References

1. Wang, Y., Gan, J., Zhou, Y., Cheng, Y., & Nirasawa, S. (2017). Improving solubility and emulsifying property of wheat gluten by deamidation with four different acids: Effect of replacement of folded conformation by extended structure. *Food Hydrocolloids*, *72*, 105-114.
2. Abedi, E., & Pourmohammadi, K. (2021). Chemical modifications and their effects on gluten protein: An extensive review. *Food chemistry*, *343*, 128398.
3. Zhao, J., Tian, Z., & Chen, L. (2011). Effects of deamidation on aggregation and emulsifying properties of barley glutelin. *Food Chemistry*, *128*(4), 1029-1036.
4. Liao, L., Zhao, M., Ren, J., Zhao, H., Cui, C., & Hu, X. (2010). Effect of acetic acid deamidation-induced modification on functional and nutritional properties and conformation of wheat gluten. *Journal of the Science of Food and Agriculture*, *90*(3), 409-417.
5. Liao, L., Liu, T. X., Zhao, M. M., Zhao, H. F., & Cui, C. (2011). Aggregation behavior of wheat gluten during carboxylic acid deamidation upon hydrothermal treatment. *Journal of Cereal Science*, *54*(1), 129-136.
6. Liao, L., Han, X. Y., Zhao, M. M., Ni, L., Liu, Z. B., & Zhang, W. (2016). Effect of native aggregation state of soluble wheat gluten on deamidation behavior in a carboxylic acid/heat water solution. *Journal of Cereal Science*, *72*, 1-9.
7. Jansens, K. J., Lagrain, B., Brijs, K., Goderis, B., Smet, M., & Delcour, J. A. (2013). Impact of acid and alkaline pretreatments on the molecular network of wheat gluten and on the mechanical properties of compression-molded glassy wheat gluten bioplastics. *Journal of agricultural and food chemistry*, *61*(39), 9393-9400.
8. Cui, C., Hu, Q., Ren, J., Zhao, H., You, L., & Zhao, M. (2013). Effect of the structural features of hydrochloric acid-deamidated wheat gluten on its susceptibility to enzymatic hydrolysis. *Journal of agricultural and food chemistry*, *61*(24), 5706-5714.

9. Abe, R., Shimizu, S., Yasuda, K., Sugai, M., Okada, Y., Chiba, K., ... & Kumagai, H. (2014). Evaluation of reduced allergenicity of deamidated gliadin in a mouse model of wheat-gliadin allergy using an antibody prepared by a peptide containing three epitopes. *Journal of agricultural and food chemistry*, *62*(13), 2845-2852.
10. Wong, B. T., Zhai, J., Hoffmann, S. V., Aguilar, M. I., Augustin, M., Wooster, T. J., & Day, L. (2012). Conformational changes to deamidated wheat gliadins and β-casein upon adsorption to oil–water emulsion interfaces. *Food Hydrocolloids*, *27*(1), 91-101.
11. Li, T., Guo, X. N., Zhu, K. X., & Zhou, H. M. (2018). Effects of alkali on protein polymerization and textural characteristics of textured wheat protein. *Food Chemistry*, *239*, 579-587.
12. Gennadios, A., Brandenburg, A. H., Weller, C. L., & Testin, R. F. (1993). Effect of pH on properties of wheat gluten and soy protein isolate films. *Journal of agricultural and food chemistry*, *41*(11), 1835-1839.

The 30th Iranian Seminar of Organic Chemistry
February 7-9, 2025, Iran University of Science and Technology, Tehran, Iran

Successive paired electrochemical synthesis for late-stage modification of Nitrazepam and Molecular docking studies

Zahra Godini,[a] Davood Nematollahi*[a,b]

[a] *Faculty of Chemistry and Petroleum Sciences, Bu-Ali Sina University, Hamedan, Iran*

[b] *Planet Chemistry Research Center, Bu-Ali Sina University, Hamedan, Iran*

Keyword: Electrochemical synthesis; Nitrazepam; Cyclic voltammetry; late-stage modification Molecular docking

Introduction

Electrosynthesis is one of the best methods for the synthesis of molecules. Electrosynthesis is a green method when Electrons are produced using renewable energy, waste-free and sustainable. Electrosynthesis is carried out through the transfer of electrons, which are inherently clean. The time to perform electrochemical processes is usually shorter than the chemical one, and as a result, it minimizes the associated costs. Synthesis of new drug derivatives using, late-stage modification

(**LSM**), or called late-stage functionalization (**LSF**) of drugs has attracted our attention in this work. Pharmaceutical derivatives synthesized by this method can have better activity than the mother drug [1].

Method

Nitrazepam derivatives under controlled potential conditions using a simple cell equipped with ordinary graphite as cathode and anode electrodes, was carried out in water/ethanol mixture under mild conditions. After completion of electrolysis, it was allowed to evaporate at room temperature to one-third of the original volume, and the product was extracted with ethyl acetate and washed with chloroform, and collected. For electrochemical studies, a three-electrode system in an undivided cell has been used. The structure of the product was identified by FT-IR, ^{1}H NMR, ^{13}C NMR and MASS spectra [2].

Results and Discussion

We have investigated the electrochemical behavior of nitrazepam using cyclic voltammetry (CV) technique. In this study, in addition to looking at the oxidation and reduction mechanism of nitrazepam in an aqueous environment, we also tried to look at one of its metabolites .

Scheme1. Mechanism of reduction of nitrazepam

The mechanism of the reaction is that the nitro group of nitrazepam is reduced to amine on the surface of the cathode, and the amine created at the anode is oxidized and reacts with aryl sulfonic acid.

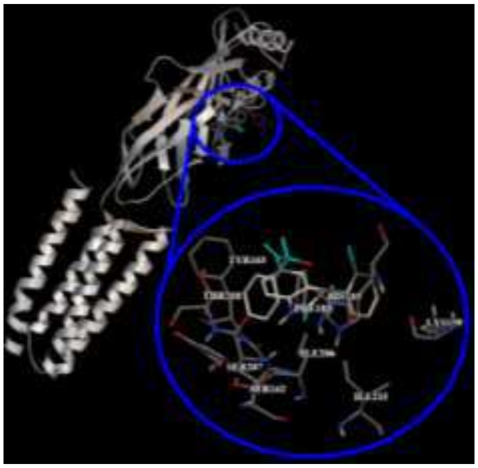

Scheme2. Interaction of Nitrazepam with Gamma-aminobutyric acid

In docking studies, synthesized derivative was docked and has a promising binding pattern in interaction with Gamma-aminobutyric acid. Based on this study, synthesized derivative can have a hydrogen bond with the nitrogen of THR208 and interact with other amino acids shown in **Scheme2**. The obtained data show that the compound under study shows a good fit inside the binding site.

References:

[1] Romero, Elvira, et al. "Enzymatic late-stage modifications: better late than never." *Angewandte Chemie International Edition* 60.31 (2021): 16824-16855

[2] *Lotfipour, Farideh, et al. "Electrochemical late-stage modification of hydralazine an antihypertensive drug. A green strategy for the synthesis of nano-structured new sulfonylhydrazine derivatives." Green Synthesis and Catalysis (2024).*

The 30th Iranian Seminar of Organic Chemistry
February 7-9, 2025, Iran University of Science and Technology, Tehran, Iran

Phenanthroline Ligand as a Versatile Building Block for the Construction of Supramolecular Architectures

Badri Z. Momeni[*], Rasa Daneshnia

Department of Inorganic Chemistry, Faculty of Chemistry, K.N. Toosi University of Technology, Tehran, Iran

E-mail address: momeni@kntu.ac.ir

Keywords: Phenanthroline; Hydrogen bonding; Crystal structure; Supramolecular assembly

The rigid 1,10-Phenanthroline (phen) core is a very popular bidentate ligand containing two nitrogen donor atoms oriented for metal cation chelation, which binds to all elements from s-, p- and d-block elements to lanthanide, and actinide elements and plays an important role in the development of coordination chemistry. 1,10-Phenanthroline decorated with various backbone substituents has been known to have a variety of applications, such as luminescent coordination scaffolds, catalysis, and sensors. In contrast to the widely used 1,10-phenanthroline and its derivatives, other isomers having different conformational features have been studied less. We report the improvement of 1,7-phenanthroline binding (especially hydrogen bonding) and its future applications in developing supramolecular assemblies. The tendency of 1,7-phenanthroline to form infinite N^+-H···N assisted chains and hence layered structures is presented.

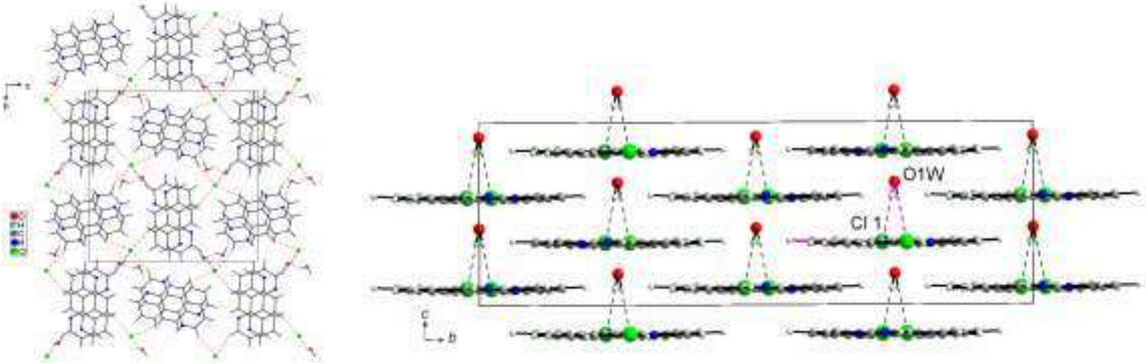

References

[1] B.Z. Momeni, A. Abd-El-Aziz, N. Ma, A.S. Abd-El-Aziz, J. Inorg. Organomet. Polym. Mater. 34 (2024) 2855.

[2] B.Z. Momeni, F. Shirvani, J. Janczak, J. Mol. Struct. 1317 (2024) 139155.

Synthesis of 5-substituted 1*H*-tetrazoles drivatives using a functionalized Cobalt-based metal-organic-framework catalyst

Pouria Bazvand [a], Ramin Ghorbani Vaghei[a,b], Sedigheh Alavinia[a]

[a]*Department of Organic Chemistry, Faculty of Chemistry and Petroleum Sciences, Bu-Ali Sina University, Hamedan 6517838683, Iran*

[b]*Department of Organic Chemistry, Faculty of Chemistry, University of Guilan, Rasht, Iran*

Keyword: Tetrazole, Cobalt, Metal-Organic-Framework, Benzonitrile, Sodium azide

Tetrazoles are a valuable class of heterocycles that have been recently used both as anticancer and antimicrobial agents. They have received increased attention due to their potential biological activities and industrial applications [1]. A versatile method for the preparation of tetrazole is based on [3+ 2] cycloaddition of the azide ion and organic nitriles in the presence of a catalyst [2-6].

We report here the functionalization of cobalt-based metal-organic frameworks with triazine and thiourea, followed by the immobilization of copper (I) iodide, which produces a new, green, and efficient [Co (BDC-NH_2)-TA-TU/Cu] catalyst for the synthesis of 5-substituted 1*H*-tetrazoles. XRD, FESEM, atomic absorption, TGA, N_2 absorption-desorption, and FT-IR analysis were recorded for the characterization of the [Co (BDC-NH_2)-TA-TU/Cu] structure. In synthesizing 5-substituted 1*H*-tetrazoles, [Co (BDC-NH_2)-TA-TU/Cu] shows superior yields in short reaction times at 120 °C. This catalyst also showed high thermal stability and recyclability, at least for 6 runs, without apparent loss of efficiency.

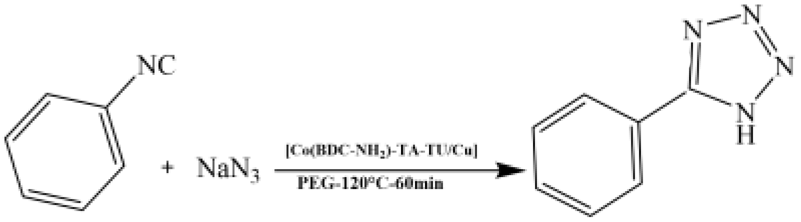

Scheme

References:

١- Zhang, J., Wang, S., Ba, Y., & Xu, Z. **2019**. *Tetrazole hybrids with potential anticancer activity.* Eur. J. Med. Chem., Vol. 178, 341-351.

٢- Habibi, D., Heydari, S., Afsharfarnia, M., & Rostami, Z. **2017**. *A versatile synthesis of arylaminotetrazoles by a magnetic Fe@ Phendiol@ Mn nano-particle catalyst and its theoretical studies.* Appl. Organomet. Chem., Vol. 31(12), e3826.

٣- Tamoradi, T., Ghorbani-Choghamarani, A., & Ghadermazi, M. **2017**. *Fe 3 O 4–adenine–Zn: a novel, green, and magnetically recoverable catalyst for the synthesis of 5-substituted tetrazoles and oxidation of sulfur containing compounds.* New J. Chem., Vol. 41(20), ١١٧١٤-١١٧٢١.

٤- Khorramabadi, V., Habibi, D., & Heydari, S. **2020**. *Facile synthesis of tetrazoles catalyzed by the new copper nano-catalyst.* Green Chem. Lett. Rev., Vol. 13(1), 50-59.

٥- Mohseni, E., Ghorbani-Choghamarani, A., Tahmasbi, B., & Norouzi, M. **2024**. *A new Schiff base 2-benzoylpyridine-based copper complex on boehmite nanoparticles as a recoverable nanocatalyst for the homoselective synthesis of 5-substituted tetrazoles.* RSC Adv., Vol. 14(23), 16269-16277.

٦- Heidarnezhad, Z., Ghorbani-Choghamarani, A., & Taherinia, Z. **2024**. *Magnetically recoverable Fe_3O_4@ SiO_2@ SBA-3@ 2-ATP-Cu: an improved catalyst for the synthesis of 5-substituted 1 H-tetrazoles.* Nanoscale Advances.

The 30th Iranian Seminar of Organic Chemistry
February 7-9, 2025, Iran University of Science and Technology, Tehran, Iran

Synthesis of 2,4,6-trisubstituted pyridines using cobalt-based metal-organic framework

Pouria Bazvand [a], Ramin Ghorbani Vaghei[a,b], Sedigheh Alavinia[a]

[a] *Department of Organic Chemistry, Faculty of Chemistry and Petroleum Sciences, Bu-Ali Sina University, Hamedan 6517838683, Iran*

[b] *Department of Organic Chemistry, Faculty of Chemistry, University of Guilan, Rasht, Iran*

Keyword: Pyridine, Cobalt, Metal-Organic-Framework

Compounds containing pyridine moieties, as one of the most inspiring and beneficial families of N-heterocycles, have gained the burgeoning attention of the society of researchers [1-3]. The plethora of utility of pyridines in natural products, functional materials, pharmaceuticals, coordination chemistry, and organic catalysis is undeniable [4-5]. In this paper, we have developed green, efficient, and powerful protocols for the preparation of 2,4,6-triarylpyridines in the presence of cobalt-based metal-organic frameworks Co (BDC-NH_2) under mild and solvent-free reaction conditions. These protocols furnished the desired products in short reaction times with good to high yields (60 min and 94%). Also, the nanocatalyst can be recycled and reused in both cases of the scrutinized one-pot multicomponent reactions with high turnover number and turnover frequency.

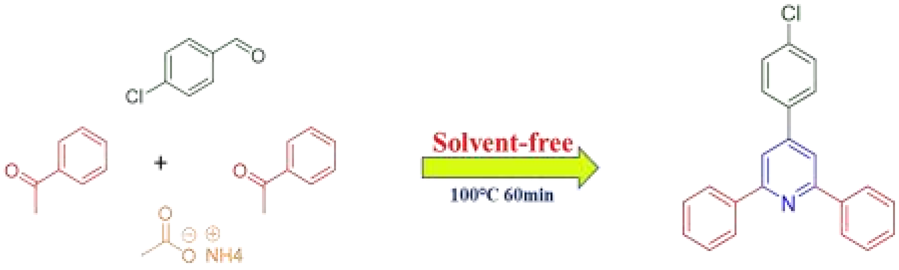

Scheme

References:

١- Azarifar, D., Mahmoudi-GomYek, S., & Ghaemi, M. **2018**. *Immobilized Cu (II) Schiff base complex supported on Fe3O4 magnetic nanoparticles: a highly efficient and reusable new catalyst for the synthesis of pyranopyridine derivatives. Appl.* Organomet. Chem., Vol. 32(12), e4541.

٢- Akbarpoor, T., Khazaei, A., Seyf, J. Y., Sarmasti, N., & Gilan, M. M. **2020**. *One-pot synthesis of 2-amino-3-cyanopyridines and hexahydroquinolines using eggshell-based nano-magnetic solid acid catalyst via anomeric-based oxidation. Res.* Chem. Intermed., Vol. 46, 1539-١٥٥٤.

٣- Karimi, F., Yarie, M., & Zolfigol, M. A. **2020**. *A convenient method for synthesis of terpyridines via a cooperative vinylogous anomeric based oxidation.* RSC Adv., Vol. 10(43), ٢٥٨٢٨_٢٥٨٣٥.

٤- Soleimani, E., Torkaman, S., Sepahvand, H., & Ghorbani, S. **2019**. *Ciprofloxacin-functionalized magnetic silica nanoparticles: as a reusable catalyst for the synthesis of 1 H-*

chromeno [2, 3-d] pyrimidine-5-carboxamides and imidazo [1, 2-a] pyridines. Mol. Divers., Vol. ٢٣, ٧٣٩-٧٤٩.

٥- Rakhtshah, J., & Yaghoobi, F. **2019**. *Catalytic application of new manganese Schiff-base complex immobilized on chitosan-coated magnetic nanoparticles for one-pot synthesis of 3-iminoaryl-imidazo [1, 2-a] pyridines.* Int. J. Biol. Macromol., Vol. 139, 904-916.

The 30th Iranian Seminar of Organic Chemistry
February 7-9, 2025, Iran University of Science and Technology, Tehran, Iran

Efficient Synthesis of tetrahydro benzopyrans in the presence of modified g-C_3N_4/Biochar as a green Nanocatalyst

Mohammad Nasir Shambayati 1[a], Maryam Hajjami 2[b]

Department of Organic Chemistry, Faculty of Chemistry and Petroleum Sciences, Bu-Ali Sina University, Postal code 6517838683, Hamedan, Iran. E-mail address, m.hajjami@basu.ac.ir or mhajjami@yahoo.com

Keyword: g-C_3N_4/Biochar, tetrahydro benzopyran, Nanocatalyst, Multicomponent reaction

Abstract

Design and synthesis of green and recyclable catalysts in order to improve the efficiency of organic chemistry reactions is a significant challenge. [1] Tetrahydro benzopyran are known to have diverse biological and pharmacological activities. [2] In this study, first, graphitic carbon nitride (g-C_3N_4) /biochar nanosheets with high surface area and chemical stability were synthesized. Afterwards, the surface of this nano-substrate was modified with polyethyleneimine to obtain g-C_3N_4 biochar/PEI. The synthesis of tetrahydro benzopyran derivatives was performed in reflux (water: ethanol) condition. The advantages of this reaction include easy catalyst preparation, separation and reusability, with good to excellent efficiency, and short reaction time.

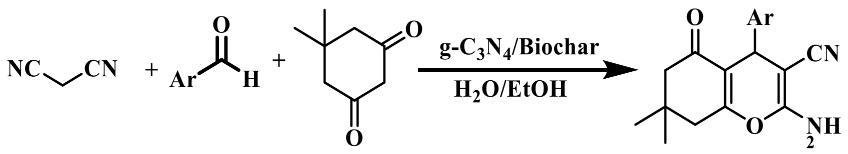

Scheme 1. Three-component reaction of dimedone, aldehydes and malononitrile in the presence of modified g-C_3N_4/Biochar

References:

1. Moradi, P., Hajjami, M. *RSC Advances* 2022 12, 13523-13534.

2.Trebše, P., Vraničar, L., Mušič, I., Polanc, S., Stevens, W. C., & Kočevar, M.. *Heterocycles*, 2000, *53*(5), 1111-1120.

The 30th Iranian Seminar of Organic Chemistry
February 7-9, 2025, Iran University of Science and Technology, Tehran, Iran

Synthesis and characterization of poly(2-[(2,4- dinitr (phenoxy)methyl]oxirane) as new a energetice polymer

Masoumeh Kiany 1, Yadollah Bayat2*.

Department of Chemistry and Chemical Engineering, Malek Ashtar University of Technology, Tehran, Iran.

Keyword: Polymerization. Energetic materials. Energetic polymers. 2,4-Dinitrofluorobenzene. ٢-[(٢،٤-Dinitro(phenoxy)methyl]oxirane. Glycidol. TGA. DSC.

Energetic materials are compounds or mixtures that store significant energy and must meet criteria such as environmental friendliness, high performance, thermal stability, and cost-effectiveness[1, 2]. They include explosives, pyrotechnics, and propellants, used in military and non-military applications like missile propulsion, mining, and automotive safety systems[3]. High-energy solid formulations, like plastic-bonded explosives, utilize flexible binders that incorporate granular materials[4, 5]. Polymers play a vital role in these compositions by reducing sensitivity to heat, shock, and abrasion while enhancing structural strength[6, 7]. Binders are divided into energetic and non-energetic types. Non-energetic binders such as hydroxyl-terminated polybutadiene (HTPB), polypropylene glycol(PPG) and others lack energetic functional groups[8]. Energetic binders, which incorporate high-energy moieties, examples of energetic binders such as Polyglycidyl nitrate (PGN)[9]and Poly(azidomethyl methyloxetane) (PAMMO). These compounds can be obtained either by polymerizing energetic monomers or by adding high-energy groups to existing polymers. In this paper, we chose the polymerization of an energetic monomer as the method for synthesizing a high-energy polymer. The objective was achieved in two stages(Scheme1). In the first stage, the monomer 2-[(2,4-dinitro(phenoxy)methyl]oxirane) was produced through the reaction between glycidol and 2,4-dinitrofluorobenzene at room temperature, with yield 43% . Subsequently, in the next stage, the polymer Poly(2-[(2,4-

Dinitro(phenoxy)methyl]oxirane) was synthesized at room temperature through the polymerization of this monomer, achieving a 62% efficiency. This project focuses on the synthesis of an energetic polymer, poly(2-((2,4-dinitrophenoxy)methyl)oxirane), with a low molecular weight (Mn = 1260 g/mol). This polymer was synthesized for the first time using a cationic ring-opening polymerization method with 2-[(2,4-dinitro(phenoxy)methyl]oxirane as the monomer and 1,4-Butanediol(BDO) as the initiator and boron trifluoride etherate ($BF_3.OEt_2$) as the catalyst. The polymer was characterized using FT-IR , ^{1}H-NMR and ^{13}C-NMR spectrometry and gel permeation chromatography (GPC). Its thermal properties were evaluated through thermogravimetric analysis (TGA) and differential scanning calorimetry (DSC). The newly synthesized polymer shows a glass transition temperature (Tg) of -9.5°C, which has the potential to be used as a plasticizer and binder.

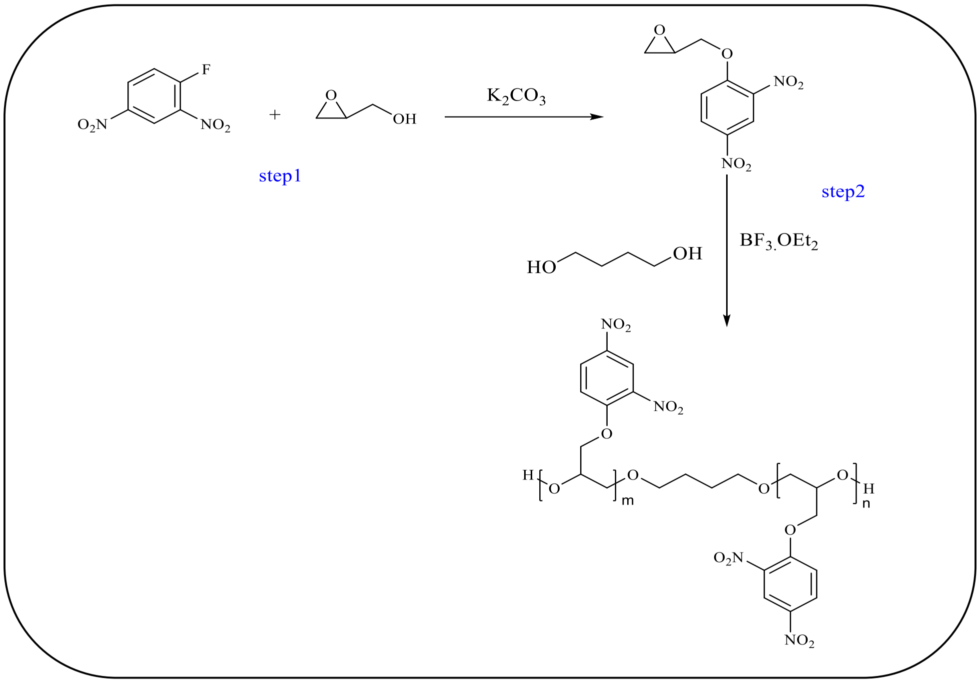

Scheme1

References:

1. J Dou, M Xu, B Tan, X Lu, H Mo, B Wang, N Liu, *Research progress of nitrate ester binders.* FirePhysChem. 2023. 3(1).54-77.

2. F Ghoroghchian, , Y Bayat, F Abrishami, *Preparation of the polyurethane elastomer based on polypropylene glycol-glycidyl azide polymer-polypropylene glycol.* Journal of Polymer Research2022. 29(11).472

3. G Oskueyan, Y Bayat, M Mostafavi, T Khanlari, *Synthesis and characterization of polypropylene glycol–polytetrahydrofuran–polypropylene glycol copolymer: investigation of effective parameters on the synthesis and preparation of elastomer.* Polymer Bulletin2024. 81(1).739-754.

4. Y Bayat, , S Jodar, T Khanlari, *Synthesis and thermal decomposition kinetics of tri-block copolymer ε-caprolactone/polybutadiene (PCL-PB-PCL); preparation of polyurethane network-based tri-block copolymer*. Journal of Polymer Research2022. 29(3)101.
5. Y Shan, S Huang, T Jiang, Y Cao, J Wang, Y Cao, W Zhang, *An effective strategy for balancing energy and sensitivity: design, synthesis, and properties of chimeric energetic molecules*. Journal of Materials Chemistry A 2025.
6. R Jiang, *Research Progress of Additive Manufacturing Technology in Energetic Material Field at Home and Abroad*. Journal of Materials Science and Chemical Engineering2024. 12(3) 51-59.
7. T Khanlari, Y Bayat, M Bayat, *Investigation of the Compatibility of a Novel Copolymer Based on Polypropylene Glycol/Polyglycidyl nitrate (PPG/PGN) with Plasticizers: Thermal, Rheological, Solubility Parameter and SEM*. Polymer Science, Series A 2020. 62:607-615.
8. CM Grégoire, O Mathieu, J Kalman, EL Petersen, *Review and assessment of the ammonium perchlorate chemistry in AP/HTPB composite propellant gas-phase chemical kinetics mechanisms*. Progress in Energy and Combustion Science2025. 106.101195.
9. M Alizadeh, Y Bayat, *Synthesis of a New Random Copolymer Based on Glycidyl Nitrate and Tetrahydrofuran: A Thermal, Kinetic, and Theoretical Study*. Central European Journal of Energetic Materials2024. 21(1).

The 30th Iranian Seminar of Organic Chemistry
February 7-9, 2025, Iran University of Science and Technology, Tehran, Iran

Cyclodextrin-Based Metal-Organic Frameworks (CD-MOF) as a Drug Delivery System

Sahar Mohajeri

Department of Chemistry, Ardabil Branch, Islamic Azad University, Ardabil, Iran

Keyword: Cyclodextrin, Metal–Organic Frameworks, Drug delivery.

Introduction

Coordination molecules known as metal-organic frameworks (MOFs) have a controllable function and a tunable structure. MOFs are widely used in many different industries, however their potential biological toxicity limits their employment in the food and biomedical industries. To solve this problem, researchers have concentrated on creating biocompatible MOFs [1–3]. Cyclodextrin-based metal-organic frameworks (CD-MOFs) have become a viable substitute among them. CD-MOFs are new MOFs that are edible, non-toxic, and renewable. They are made from naturally occurring carbohydrate cyclodextrin and alkali metal cations. CD-MOFs have been widely used in a variety of delivery methods, including the encapsulation of flavors, antibacterial agents, and nutraceuticals, because of their high specific surface area, adjustable porosity, and excellent biocompatibility. Although the field of CD-MOF materials is still in its early stages, they provide a promising direction for the development of MOF materials in the delivery field [4-7].

Method

Until today, vapor diffusion has been the most widely used method for creating CD-MOFs. However, there have also been reports of other techniques, such as ultrasonication synthesis and seed-mediated synthesis [8–11].

Results and Discussion

CDMOF-based MOF can be categorized into three categories. Based on the range of applicability of different types of CD-MOF, the sub-sections of CD-MOF have been arranged as follows (See Scheme 1):

1. α-CD-MOF

In contrast to γ and β-CD-MOF, α-CD-MOF has not been as thoroughly investigated for use in pharmaceutical applications. Certain medications can form inclusion complexes with α-CD-MOF, which is biocompatible. Using Na-α-CD-MOF has greatly improved 5-FU's drug loading efficiency and bioavailability. Similarly, α-CD-MOF has the ability to encapsulate menthol and improve its thermal stability. α-CD-MOF has been used for gas adsorption and storage stability applications in addition to medication delivery [12, 13].

2. *β-CD-MOF*

The laminated structure generated by β-CD-MOF can be synthesized utilizing β-CD and a contamination-free approach that does not use K^+ or Na^+. However, the low adsorption/desorption capacity caused by the cavities being stacked up in a layer covered by β-CD has reduced the loading capacity of β-CD-MOF. Therefore, sensing applications could make use of this type of MOF system [14, 15].

3. *γ-CD-MOF*

Among CDs, γ-CD can form the MOF with a wide variety of inorganic ligands such as NH_2-CD-MOF, KOH-CD-MOF, Na_2CO_3-CD-MOF.The high surface area and porosity, crystalline nature, definite structure, and host–guest complex formation properties of CDs make them suitable for the pharmaceutical application. The high solubility of γ-CD-MOFs could be used in for rapid dissolution and absorption of BCS-II class drugs. Moreover, CD-MOFs are cytocompatible and did not show any IC_{50} effect on various kinds of cells [16, 17].

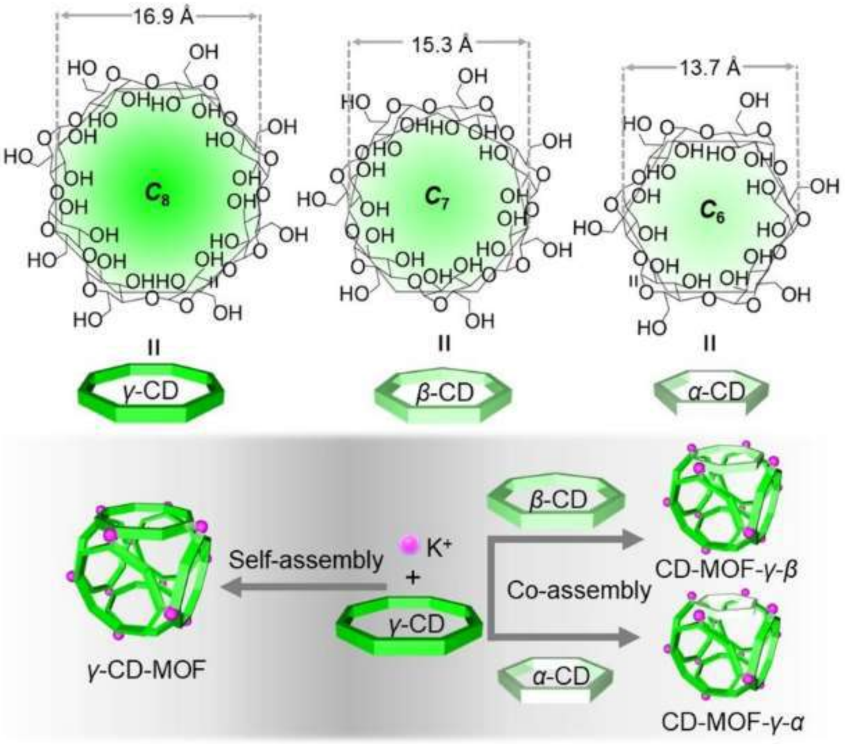

Scheme 1: Cyclodextrins and cyclodextrins-based metal-organic frameworks.

References

١. Dummert, S. V., Saini, H., Hussain, M. Z., Yadava, K., Jayaramulu, K., Casini, A., & Fischer, R. A. (2022). Cyclodextrin metal–organic frameworks and derivatives: recent developments and applications. *Chemical Society Reviews*, *51*(12), 5175-5213.

٢. Zhao, R. N., Zhu, B. W., Xu, Y., Yu, S. F., Wang, W. J., Liu, D. H., & Hu, J. N. (2023). Cyclodextrin-based metal-organic framework materials: Classifications, synthesis strategies and applications in variegated delivery systems. *Carbohydrate Polymers*, 121198.

٣. Kru̅kle-Be̅rziņa, K., Lends, A., & Boguszewska-Czubara, A. (2024). Cyclodextrin Metal–Organic Frameworks as a Drug Delivery System for Selected Active Pharmaceutical Ingredients. *ACS omega*, *9*(8), 8874-8884.

٤. Abuçafy, M. P., Mori, A. S., Caetano, B. L., Ribeiro, S. J. L., & Chiavacci, L. A. (2024). Cyclodextrin-metal-organic framework (CD-MOF)/organic-inorganic hybrid composite as a potential material for drug delivery devices. *Journal of Molecular Structure*, *1314*, 138717.

٥. Sadeh, P., Zeinali, S., Rastegari, B., & Najafipour, I. (2024). Functionalization of β-cyclodextrin metal-organic frameworks with gelatin and glutamine for drug delivery of curcumin to cancerous cells. *Heliyon*, *10*(9).

٦. Hamedi, A., Anceschi, A., Patrucco, A., & Hasanzadeh, M. (2022). A γ-cyclodextrin-based metal–organic framework (γ-CD-MOF): A review of recent advances for drug delivery application. *Journal of Drug Targeting*, *30*(4), 381-393.

٧. Liao, L. G., Ke, D., Li, G. C., Zhang, S., & Li, B. J. (2023). Cyclodextrin metal-organic framework as a broad-spectrum potential delivery vehicle for the gasotransmitters. *Molecules*, *28*(2), 852.

٨. Rajkumar, T., Kukkar, D., Kim, K. H., Sohn, J. R., & Deep, A. (2019). Cyclodextrin-metal–organic framework (CD-MOF): From synthesis to applications. *Journal of Industrial and Engineering Chemistry*, *72*, 50-66.

٩. Qiu, J., Li, X., Gref, R., & Vargas-Berenguel, A. (2020). Carbohydrates in metal organic frameworks: Supramolecular assembly and surface modification for biomedical applications. In *Metal-Organic Frameworks for Biomedical Applications* (pp. 445-465). Woodhead Publishing.

١٠. Qiu, C., Wang, J., Qin, Y., Fan, H., Xu, X., & Jin, Z. (2018). Green synthesis of cyclodextrin-based metal–organic frameworks through the seed-mediated method for the encapsulation of hydrophobic molecules. *Journal of agricultural and food chemistry*, *66*(16), 4244-4250.

١١. Qiu, C., McClements, D. J., Jin, Z., Wang, C., Qin, Y., Xu, X., & Wang, J. (2019). Development of nanoscale bioactive delivery systems using sonication: Glycyrrhizic acid-loaded cyclodextrin metal-organic frameworks. *Journal of colloid and interface science*, *553*, 549-556.

١٢. Dummert, S. V., Saini, H., Hussain, M. Z., Yadava, K., Jayaramulu, K., Casini, A., & Fischer, R. A. (2022). Cyclodextrin metal–organic frameworks and derivatives: recent developments and applications. *Chemical Society Reviews*, *51*(12), 5175-5213.

١٣. Hu, Z., Li, S., Wang, S., Zhang, B., & Huang, Q. (2021). Encapsulation of menthol into cyclodextrin metal-organic frameworks: Preparation, structure characterization and evaluation of complexing capacity. *Food Chemistry*, *338*, 127839.

١٤. Yang, D., Zhao, M., Huang, Y., Chen, L., Fang, J., Liu, J., ... & Zhao, C. (2024). β-Cyclodextrin metal-organic framework as a green carrier to improve the dissolution, bioavailability, and liver protective effect of luteolin. *International Journal of Pharmaceutics: X*, *7*, 100250.

١٥. Zhang, L., Zhang, M., Yang, P., Zhang, Y., Fei, J., & Xie, Y. (2023). Electrochemical Behavior of β-Cyclodextrin-Ni-MOF-74/Reduced Graphene Oxide Sensors for the Ultrasensitive Detection of Rutin. *Molecules*, *28*(12), 4604.

١٦. Singh, P., Feng, J., Golla, V. K., Lotfi, A., & Tyagi, D. (2022). Crosslinked and biofunctionalized γ-cyclodextrin metal organic framework to enhance cellular binding efficiency. *Materials Chemistry and Physics*, *289*, 126496.

١٧. Tian, B., & Liu, J. (2023). Cyclodextrin-metal-organic frameworks in molecular delivery, detection, separation, and capture: An updated critical review. *Carbohydrate Polymers*, *306*, 120598.

Cyclodextrins Based Nanoparticle System for Drug Delivery Application

Sahar Mohajeri

Department of Chemistry, Ardabil Branch, Islamic Azad University, Ardabil, Iran

Keyword: Cyclodextrin, Nanoparticle, Drug delivery.

Introduction

The cyclic oligosaccharides known as cyclodextrins (CDs) have special hydrophobic inner surfaces. Three parent α-CD, β-CD, and γ-CD, are employed in numerous medicinal applications and undergo additional chemical modification mainly to make them appropriate for parenteral delivery [1]. The ability of CDs to form inclusion complexes with a wide range of organic and inorganic lipophilic compounds gives them a unique advantage. This feature holds promise for a variety of applications, including gene transfer, medication administration, cancer treatment, and biosensing. The application of CDs as functional materials in drug delivery via nanoparticles (NP) has increased recently [2-4]. By adding CDs or their derivatives, NPs' characteristics can be usefully altered. Among the many advantages of CD-conjugated NPs (CD-NPs) are their enhanced drug solubility and ability to transport drugs to particular sites, like cancer cells, while lowering toxicity to healthy cells. Furthermore, CDs can get beyond NPs' drawbacks, namely their poor drug loading and encapsulation efficiency [5, 6].

Method

The creation of either nanospheres or nanocapsules depends on the preparation method. Drug loading can be done immediately during preparation (standard loading), with preloading (using drug: CD complexes that have already been generated), or with both (high loading). The graphical abstract shows the CD-NP preparation schematics. The following lists some techniques for creating these CD-based nanosystems.

Results and Discussion

Creating supramolecular nanoparticles based on CDs offers a fresh approach to biological molecule detection that can be used for biological events, health issues, and cell tracking. Through host-guest interaction, electrostatic interaction, and host-guest interaction in combination with other interactions, the supramolecular polymer created the nanoparticles. One of the most extensively researched moieties for the creation of nanoparticles is CD (see Scheme 1). Novel drug delivery systems were prepared by synthesizing polyrotaxane using quantum dots and gold nanoparticles. By hydrogen bonding two polymers (acrylamide) and PVA, Das and colleagues created a polymer complex [7].

Additionally, they created a macromolecular assembly by attaching β-CD by host–guest complexation. Increased bacterial activity was demonstrated by the supramolecular nanoparticles. Huskens and a colleague created a multivalent interaction between β-CD and p-tert-butylphenyl in supramolecular nanoparticles. Both repulsive electrostatic interactions between host and guest molecules and attractive supramolecular host–guest interactions regulated the size and stability of the particles. These particles may find application in bioimaging and medication delivery [8]. The use of CD-based nanoparticles in biomedical applications has been compiled by this group. In order to create a nanoparticle between poly-cyclodextrin and poly-PTX, Kim and his colleagues produced a supramolecular nanoassembly. This nanoparticle demonstrated biodegradability and markedly enhanced antitumor activity in a mouse model. Furthermore, a wide range of supramolecular nanoparticles have been created by various mechanisms, and researchers are becoming increasingly interested in CD-based nanoparticles for drug administration [9, 10].

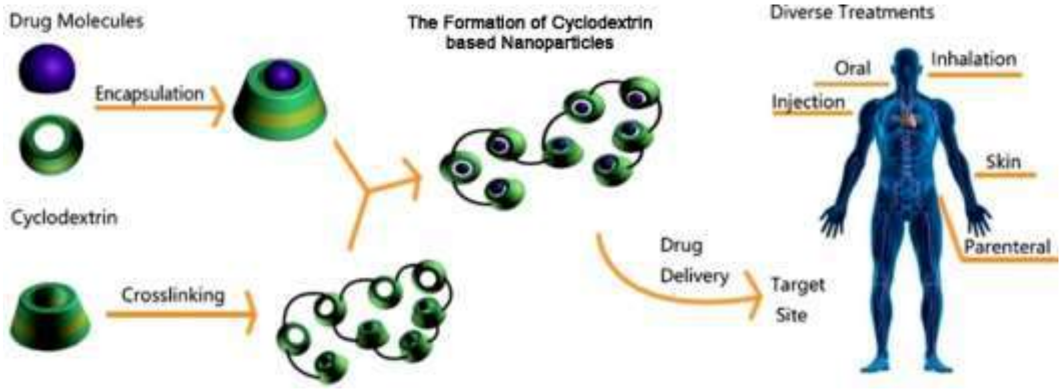

Scheme 1: Applications of cyclodextrin based nanoparticles.

References

١. Singh, P., & Mahar, R. (2024). Cyclodextrin in drug delivery: Exploring scaffolds, properties, and cutting-edge applications. *International Journal of Pharmaceutics*, 124485.

٢. Shelley, H., & Babu, R. J. (2018). Role of cyclodextrins in nanoparticle-based drug delivery systems. *Journal of pharmaceutical sciences*, *107*(7), 1741-1753.

٣. Soe, H. M. S. H., Loftsson, T., & Jansook, P. (2024). The application of cyclodextrins in drug solubilization and stabilization of nanoparticles for drug delivery and biomedical applications. *International Journal of Pharmaceutics*, 124787.

٤. Gadade, D. D., & Pekamwar, S. S. (2020). Cyclodextrin based nanoparticles for drug delivery and theranostics. *Advanced pharmaceutical bulletin*, *10*(2), 166.

٥. Liu, S., Xiong, Y., & Dong, F. (2024). Cyclodextrin metal–organic framework@ SiO_2 nanocomposites for poorly soluble drug loading and release. *RSC advances*, *14*(43), 31868-31876.

٦. Topuz, F., & Uyar, T. (2024). Recent Advances in Cyclodextrin-Based Nanoscale Drug Delivery Systems. *Wiley Interdisciplinary Reviews: Nanomedicine and Nanobiotechnology*, *16*(6), e1995.

۷. Mejia-Ariza, R., Graña-Suárez, L., Verboom, W., & Huskens, J. (2017). Cyclodextrin-based supramolecular nanoparticles for biomedical applications. *Journal of Materials Chemistry B*, *5*(1), 36-52.
۸. Suárez, L. G., Verboom, W., & Huskens, J. (2014). Cyclodextrin-based supramolecular nanoparticles stabilized by balancing attractive host–guest and repulsive electrostatic interactions. *Chemical communications*, *50*(55), 7280-7282.
۹. Namgung, R., Mi Lee, Y., Kim, J., Jang, Y., Lee, B. H., Kim, I. S., ... & Kim, W. J. (2014). Poly-cyclodextrin and poly-paclitaxel nano-assembly for anticancer therapy. *Nature communications*, *5*(1), 3702.
۱۰. Ang, C. Y., Tan, S. Y., Wang, X., Zhang, Q., Khan, M., Bai, L., ... & Zhao, Y. (2014). Supramolecular nanoparticle carriers self-assembled from cyclodextrin-and adamantane-functionalized polyacrylates for tumor-targeted drug delivery. *Journal of Materials Chemistry B*, *2*(13), 1879-1890.

The 30th Iranian Seminar of Organic Chemistry
February 7-9, 2025, Iran University of Science and Technology, Tehran, Iran

Magnetic Fe_3O_4 nanoparticles in melamine-based ternary deep eutectic solvent as a novel eco-compatible system for green synthesis of pyrido[2,3-*d*]pyrimidine derivatives

Sedigheh Alavinia, *[a] Ramin Ghorbani Vaghei[a,b]

[a] *Department of Organic Chemistry, Faculty of Chemistry and Petroleum Sciences, Bu-Ali Sina University, Hamedan 6517838683, Iran*

[b] *Department of Organic Chemistry, Faculty of Chemistry, University of Guilan, Rasht, Iran*

Keyword: Deep eutectic solvents, Pyrido[2,3-*d*]pyrimidine, Fe_3O_4, Melamine

Deep eutectic solvents (DESs) are among novel and more eco-friendly alternatives to ionic liquids (ILs) prepared by combining the components and the hydrogen bonds developed between them. The strong hydrogen bond interactions between the constituents of DESs make a considerable decline in the melting points in comparison to pure constituents. These green solvents have unique properties, making them a reliable and safe alternative to ILs and conventional organic solvents. In this study, we investigate the role of Fe_3O_4 nanoparticles (NPs) in Lactic acid:Melamine:NH_4Cl (as a novel deep eutectic solvent) in the green synthesis of pyrido[2,3-*d*] pyrimidine derivatives. The prepared DES was characterized using FT-IR, ^{1}H NMR, ^{13}C NMR, TGA/DTA, DSC and

physical properties, including viscosity, acidity, refractive index, surface tension, and density. The DES used during the experiments plays both catalytic roles and serves as a green environment for this reaction. In addition, magnetic DES can operate under very mild reaction conditions and be recycled easily with no significant catalytic activity loss. The fast and complete synthesis and high yield of the desired product are the remarkable benefits of this catalytic system.

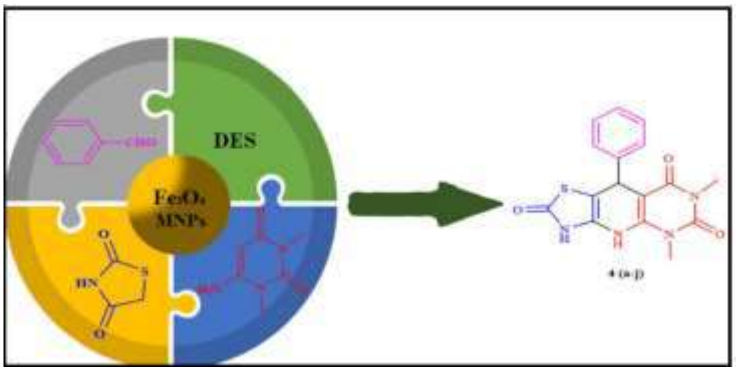

Scheme

References:

٤. A. P. Abbott, G. Capper, D. L. Davies, H. L. Munro, R. K. Rasheed, V. Tambyrajah, *Chem. Commun.*, 2001, **19**, 2010-2011;
٥. D. González-Martínez, V. Gotor, V. Gotor-Fernández, *Eur. J. Org. Chem.*, 2016, **2016**, 1513-1519;
٦. X. Marset, J. M. Pérez, D. J. Ramón, *Green Chem.*, 2016, **18**, 826-833

The 30th Iranian Seminar of Organic Chemistry
February 7-9, 2025, Iran University of Science and Technology, Tehran, Iran

Preparation and characterization of polyvinyl alcohol /Chitosan hydrogels reinforced with modified ZnO nanoparticles

Mohsen Hajibeygi, Negin Chegini

Introduction

Polyvinyl alcohol (PVOH) is a synthetic hydrophilic linear polymer that generally exists as a copolymer of vinyl alcohol and vinyl acetate. This material has been developed in the 1920s and is remarkable because of their recyclability and consideration of the natural continuation of their physical and chemical properties. PVA is a colorless, water-soluble synthetic resin employed principally in the treating of textiles and paper.

Inorganic nanostructures can be used to increase the thermal and mechanical resistance of polyvinyl alcohol. Another way to improve the properties of poly vinyl alcohol is hyrogel.

Hydrogels are three-dimensional polymers produced by chemical and/or physical reactions which produce “tie points” formed by covalent or ionic bonds, strong entanglements, crystallites or hydrogen bonds. They are prepared from linear or branched water-soluble polymers to form the corresponding hydrogels. One way to create hydrogels is through chemical crosslinking.

In this project, modified zinc oxide is used as a reinforcement and terephthalaldehyde as a chemical crosslinker.

Keyword: poly vinyl alcohol, Hydrogel, chemical crosslinking, Zno

Method

the surface of zinc oxide nanoparticles will be modified by vinyl silane structure, and radical polymerization reaction will be carried out on the surface of zinc oxide in the presence of acrylamide . for 5 and 8% solution :Aqueous solution of polyvinyl alcohol (60mL, 10% w/w) was mixed with chitosan (CH) solution (0.0375 or 0.06 gr chitosan dissolved in 10 mL acidified water by 2% acetic acid) in three-necked flask and stirred for 5 min, followed by addition of Terephthalaldehyde (TE) as a crosslinking agent (0.03 or 0.048 gr, compared to chitosan amount added). KOH solution (0.01 g/10 mL H2O) was drop wisely added and homogenized. The nanocomposites of cross-linked CH/PVA polymers were prepared by adding different zinc oxide nanoparticles ratios of 2.5 or 4 % to the homogenized CH/PVA. The prepared polymers and nanocomposites were poured in glass plates and kept for two days at room temperature. The obtained films were washed with water to eliminate unreacted Terephthalaldehyde and kept in de-ionized water at 25˚c.

Results and Discussion

Mechanism of hydrogel films are illustrated in below scheme.

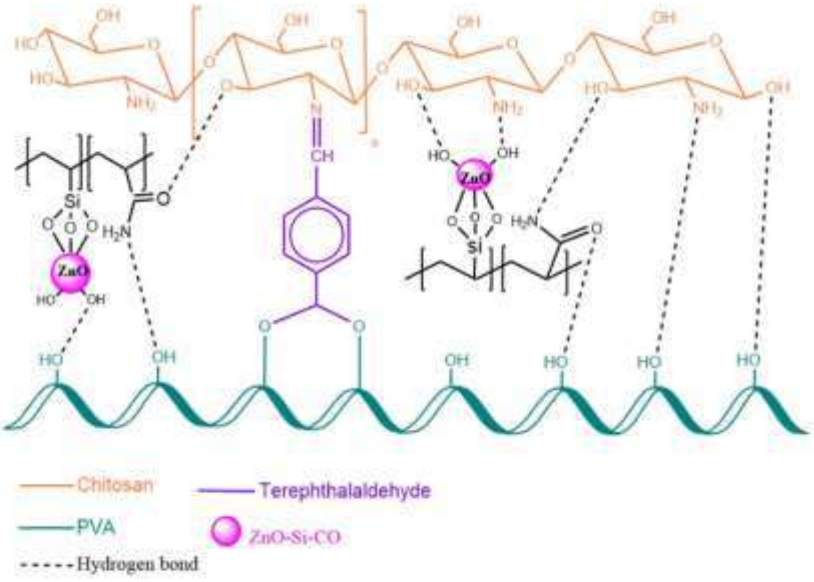

Thermal properti

The results are TGA and are given in the table below.

Sample	T$_5$ (°C)	T$_{10}$ (°C)	T$_{50}$ (°C)	C.Y [٣](%)	T$_{max1}$ (°C)
Pure PVA	255	274	320	2.782	302
PHZ$_5$[٤]	240	271	328	7.9375	315
PHZ$_8$	260	283	328	11/39	321

Comparison of the thermal behavior of PVA, PHZ$_5$, and PHZ$_8$ films showed that PHZ$_5$, PHZ$_8$ films have higher T50% and TMax1 than PVA, and even PHZ$_8$ has higher T5% and T10% than PHZ$_5$. The reason for this, in addition to the presence of chemical crosslinking, can be attributed to the high thermal stability of ZnO-Si-CO [٥]and its uniform dispersion in the chitosan/ poly vinyl alchohol matrix and hydrogen bonds between ZnO-Si-CO and the polymer matrix.

The results of DSC show that The T$_g$ of the PZH$_5$ film (87°C) is higher than that of pure PVA (78°C). The penetration of CH into PVA and its chemical crosslinking with TE and strong interactions such as hydrogen bonding between CH and PVA and hydrogen bonds existing in the presence of ZnO-Si-CO lead to a delay in the movement of molecular chain segments, which causes an increase in T$_g$.

Refrences:

---

[٣] Char yield

[٤] PHZ (P : poly vinyl alcohol, H: hybride of chitosan (chitosan + Terephthalaldehyde), Z (ZnO-Si-CO)

[٥] ZnO – Triethox vinyl silane-Copolymer

1- Nagarkar, R. and J. Patel, Polyvinyl alcohol: A comprehensive study. Acta Sci. Pharm. Sci, 2019. 3(4): p. 34-44

2- Muppalaneni, S. and H. Omidian, Polyvinyl alcohol in medicine and pharmacy: a perspective. J. Dev. Drugs, 2013. **2**(3): p. 1-5.

3- Adelnia, H., et al., Freeze/thawed polyvinyl alcohol h*ydrogels: Present, past and future.* European Polymer Journal, 2022. 164: p. 110974

The 30th Iranian Seminar of Organic Chemistry
February 7-9, 2025, Iran University of Science and Technology, Tehran, Iran

Prussian carbon obtained from sunflower stalks to destroy oxytetracycline drug

Iman Aliabadian[a], Nadiya Koukabi[*a], Eskandar Kolvari*[a], Kheibar Dashtian[*b]

[a] *Department of Chemistry, Semnan University, 35131-19111 Semnan, Iran*

[b] *Department of Chemistry, Iran University of Science and Technology, Tehran 16846- 13114, Iran*

[*] *E-mail:* n.koukabi@semnan.ac.ir, kolvari@semnan.ac.ir, kdasht68@gmail.com

Keywords: Oxytetracycline, Sunflower pith (SP), Degradation

In recent years, the issues of environmental pollution and energy scarcity have emerged as critical challenges in today's world due to the swift expansion of industrialization and urbanization, posing risks to survival. Antibiotics are a type of enduring contaminant, and oxytetracycline (OTC), a common tetracycline antibiotic and growth enhancer, has been extensively used in both medical treatment and animal husbandry. However, OTC cannot be fully metabolized in the human body and other living bodies, resulting in its massive release to the environment through hospital wastewater discharge, aquaculture, and human and animal feces. Moreover, traditional treatment methods such as adsorption, Fenton oxidation and biodegradation are not effective in OTC removal. Therefore, the environmental contamination caused by OTC poses a significant risk to both human health and ecosystems, making it essential to create innovative materials and technologies for the efficient removal of OTC pollution from the environment. More recently, light-driven photocatalytic technology has attracted much attention due to its stability, low energy consumption and ecofriendly nature, which has been considered as an promising technology [1].

In the cycle of production and harvesting, sunflower stalks are frequently regarded as waste materials with high volume due to the apparent lack of methods for converting them into value-added products. Additionally, research initiatives aimed at improving the utilization of sunflower stalks are notably scarce. The sunflower stalk consists of two mechanically separable components: the outer fiber, which accounts for 90% of the dry weight, and the inner pith, SP, which makes up 10% of the dry weight.Although the eight fraction of SP is relatively low, it covers most of the volume of the stalk due to its low density (0.035 g/cm^3).Therefore, this work aims to demonstrate production of AC from SP and demonstrate that SP porous structure increases the activation efficiency by offering potential activation sites that can result in high surface area ACs through alkaline hydroxide activation [2]. Pith material that is spongy (Fig. 1a) was extracted from the stalk through mechanical means and dried at 80°C. Before the carbonization process, the sunflower piths were crushed and sieved to collect SP particles sized 1mm or smaller.Initially, 1 gram of SPC was combined with the agent in a beaker containing 20 ml of distilled water. In all experiments, the SPC/Base weight ratio was set to 1:3. The mixtures were stirred for 1 hour to achieve uniformity and subsequently heated in an oil bath until dry. The dry powder blend was subsequently ground in the mortar swiftly to reduce moisture exposure and placed in a combustion boat. Activation occurred at 700 °C for 1 hour (with a heating rate of 10 °C/min) in an argon gas atmosphere, where the gas flow rate was set to 0.5 L/min. Once the activation heating cycle was finished, the sample was cooled in argon and subsequently washed with 0.1 M HCl, followed by rinsing with hot water until the filtrate reached neutrality to ensure that the residues of the activated agent and mineral substances were removed. The activated carbon made from sunflower pith (SPAC) was ultimately dried at 80^{o}C under vacuum for 24 hours and stored in a desiccator for subsequent analyses [3]. For advanced chemical analysis, elemental mapping and EDS analysis were conducted to assess the atomic distribution, surface elemental content, and chemical composition of the Sunflower stalk (Fig. 1b).

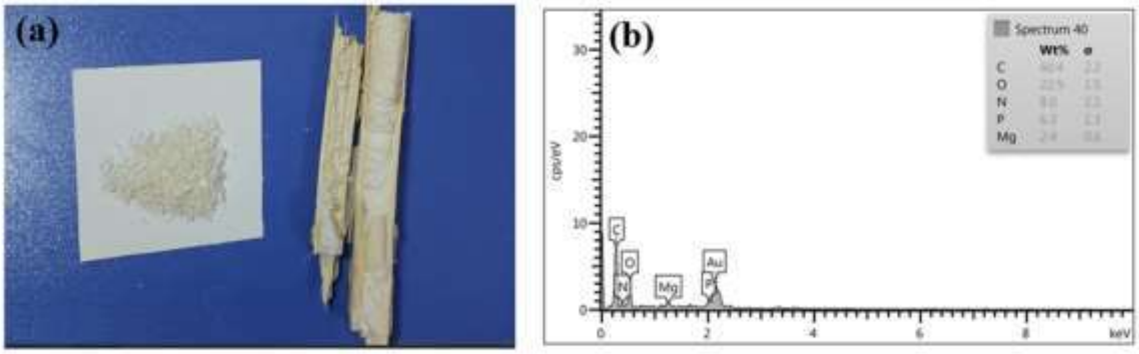

Fig1: Sunflower stalk and pith ,Powder form of SP (a), EDS spectra (b)

References:

1. Zhang, W., et al., *In Situ Construction of CdS/g-C3N4 Heterojunctions in Spent Thiolation@ Wood-Aerogel for Efficient Excitation Peroxymonosulfate to Degradation Tetracycline.* ACS Applied Materials & Interfaces, 2024.

2. Ma, J., et al., *Recent advances in photocatalytic degradation of tetracycline antibiotics.* Catalysts, 2024. **14**(11): p. 762.

3. Pek, İ., N. Kütük, and H. Daştan, *Cationic dye biosorption from aqueous solution using sunflower tray and process optimization.* Chemical Papers, 2024: p. 1-12

The 30th Iranian Seminar of Organic Chemistry
February 7-9, 2025, Iran University of Science and Technology, Tehran, Iran

Composite Hydrogels Loaded with Cerium-Containing Mesoporous Bioactive Glass Nanoparticles

Authors: Ali Rouhi Khatibi[a], Seyed Hamed Hashemi Kouchesfahani[a], Zahed Ahmadi*[a], Maryam Hosseini[a]

[a] *Department of Chemistry, Amirkabir University of Technology (Tehran Polytechnic), Tehran*

Keywords: Hydrogel, Mesoporous bioactive glass, Cerium, Wound healing

Introduction

Chronic wounds are challenging to heal due to limited natural healing mechanisms and bacterial infections, requiring moisture retention and infection prevention[1]. Hydrogels, such as those made from chitosan and gelatin, offer intrinsic and enhanced antibacterial properties when combined with agents like nanomaterials[2]. Bioactive materials like mesoporous bioactive glass nanoparticles (MBGN), doped with cerium (Ce), release therapeutic ions that promote antibacterial activity[3]. However, direct contact with MBGN may lead to adhesion to the wound bed, potentially causing lacerations and other adverse effects. To mitigate these issues, hydrogels loaded with MBGN can provide a safer alternative, avoiding the adverse reactions associated with MBGN alone[4], [5]. This study developed composite hydrogels of gelatin and chitosan, loaded with CeMBGN, to investigate their antibacterial properties against MRSA.

Method

Ce-doped mesoporous bioactive glass nanoparticles (CeMBGNs) were synthesized using a microemulsion-assisted sol-gel method.[3] Composite hydrogels of chitosan and gelatin, loaded with CeMBGNs, were prepared using EDC as a crosslinker[6].

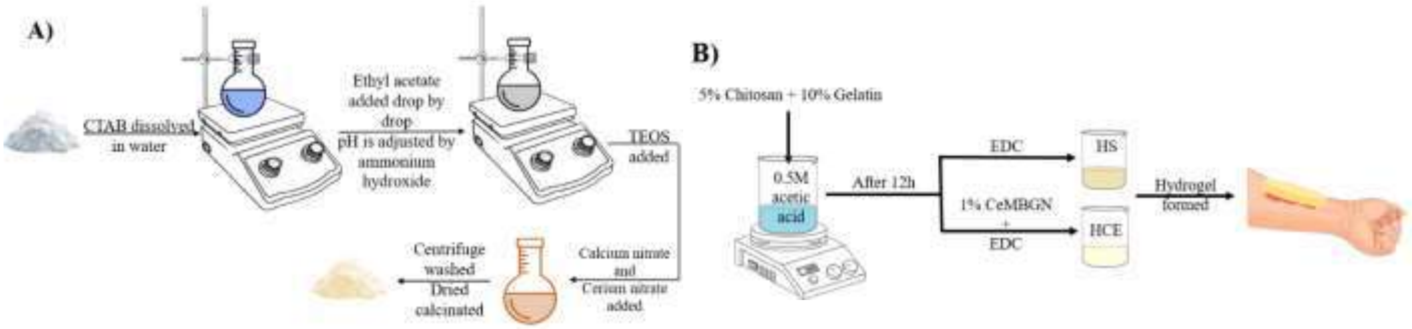

Figure 1: A) Synthesis of CeMBGN and B)Preparation of Hydrogels

Results and Discussion

The CeMBGN, with a theoretical composition of $50SiO_2$–$45CaO$–$5Ce_2O_3$, exhibited a spherical shape and a size of approximately 165 ± 35 nm. FTIR spectra revealed characteristic Si–O peaks. In the hydrogels, the disappearance of the broadband at 3355 cm^{-1} suggested the formation of hydrogen bonds between chitosan and gelatin. The hydrogels demonstrated rapid water absorption, with the CeMBGN-loaded hydrogel (HCE) achieving the highest swelling ratio. Staphylococcus aureus, a highly virulent and opportunistic pathogen commonly found on the skin, becomes particularly challenging to treat when methicillin-resistant (MRSA), leading to severe and persistent infections[7]. Antibacterial testing showed that HCE achieved a 98% reduction in MRSA.

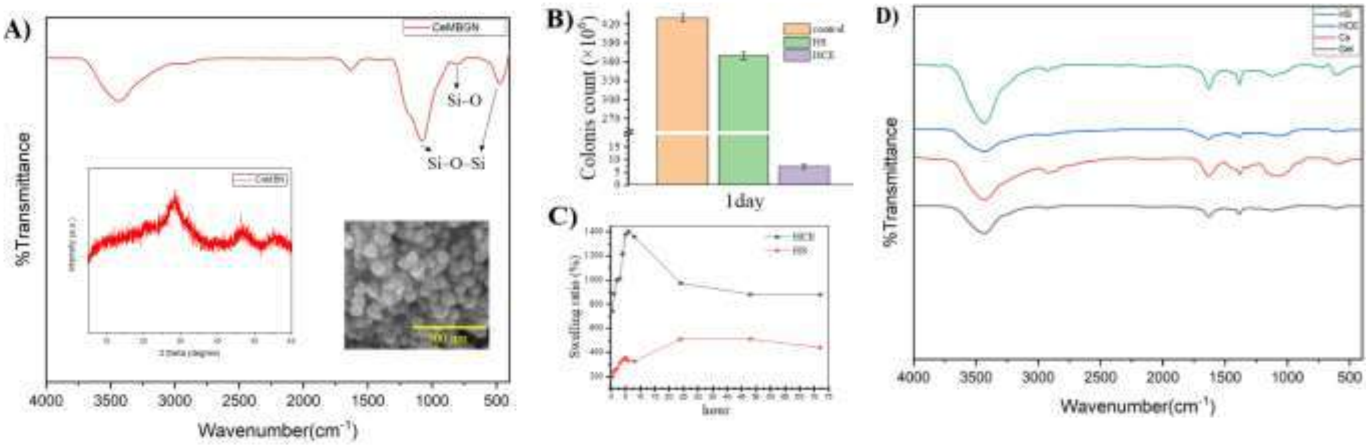

Figure 2: A)FTIR, XRD, and FESEM of CeMBGN B)Colonies count after treatment C)Swelling ratio (%) D)Hydrogels FTIR

References:

[1] X. Wei *et al.*, “Mesoporous bioglass capsule composite injectable hydrogels with antibacterial and vascularization promotion properties for chronic wound repair,” *J Mater Chem B*, vol. 10, no. 48, pp. 10139–10149, 2022, doi: 10.1039/d2tb01777f.

[2] O. Kapusta, A. Jarosz, K. Stadnik, D. A. Giannakoudakis, B. Barczyński, and M. Barczak, “Antimicrobial Natural Hydrogels in Biomedicine: Properties, Applications, and Challenges—A Concise Review,” *Int J Mol Sci*, vol. 24, no. 3, 2023, doi: 10.3390/ijms24032191.

[3] F. Kurtuldu *et al.*, “Cerium and gallium containing mesoporous bioactive glass nanoparticles for bone regeneration: Bioactivity, biocompatibility, and antibacterial activity,” *Materials Science and Engineering C*, vol. 124, May 2021, doi: 10.1016/j.msec.2021.112050.

[4] F. Bao *et al.*, “Bioactive Self-Pumping Composite Wound Dressings with Micropore Array Modified Janus Membrane for Enhanced Diabetic Wound Healing,” *Adv Funct Mater*, vol. 30, no. 49, Dec. 2020, doi: 10.1002/adfm.202005422.

[5] Y. H. Chen *et al.*, “Multifunctional injectable hydrogel loaded with cerium-containing bioactive glass nanoparticles for diabetic wound healing,” *Biomolecules*, vol. 11, no. 5, 2021, doi: 10.3390/biom11050702.

[6] B. Özkahraman, E. Tamahkar, N. İdil, A. Kılıç Suloglu, and I. Perçin, “Evaluation of hyaluronic acid nanoparticle embedded chitosan–gelatin hydrogels for antibiotic release,” *Drug Dev Res*, vol. 82, no. 2, pp. 241–250, Apr. 2021, doi: 10.1002/ddr.21747.

[7] M. Hosseini *et al.*, “Facile post modification synthesis of copper-doped mesoporous bioactive glass with high antibacterial performance to fight bone infection,” *Biomaterials Advances*, vol. 144, no. July 2022, p. 213198, 2023, doi: 10.1016/j.bioadv.2022.213198.

Synthesis and biological characterization of novel morpholine derivative of phencyclidine

Authors: Zahra Yarloo, Zahra Zaghari*

Department of Chemistry, Science and Research Branch, Islamic Azad University, Tehran, Iran

Kewords: Morpholine, Phencyclidine, Grignard reaction.

Aryl cyclohexyl amines are a semi-rigid molecules containing a cyclohexane ring with attached aromatic and amine groups.Many of them affect the central nervous system and display analgesic,stimulant,depressant and hallucinogenic effects because of specific binding sites in the brian[1,2]. They are also a non-competitive N-methyl-D-asparate (NMDA) receptor antagonist,has been demonstrated to produce psychomimetic effects on humans and to be a widely abused drug [3]. 1-(1-Phenyl cyclohexyl)piperidine, the first compound of this type is a synthetic drug with outstanding physiological properties.It is initially synthesized in the early 1950 s as a potential surgical anesthetic [4].1-(1-phenyl cyclohexyl)piperidine and it's derivatives (with changes in substitution on the molecule) have been synthesized and their pharmacological activities have been tested [5].

In this research, we synthesized 2-(N-morpholino methyl)-1-piperidino-cyano cyclohexane from 2-(N- morpholino methyl) cyclohexanone and potassium cyanide. The new derivative of 1-aryl cyclohexyl amines was prepared from this nitrile by replacement of the cyano group by aryl using Grignard reagent (scheme1).

The structure of nitrile compound and final product of reaction was confirmed by Mass, IR,^{13}C-NMR and ^{1}H-NMR.The analgesic properties of final compound were checked on male Syrian mice by formalin test.

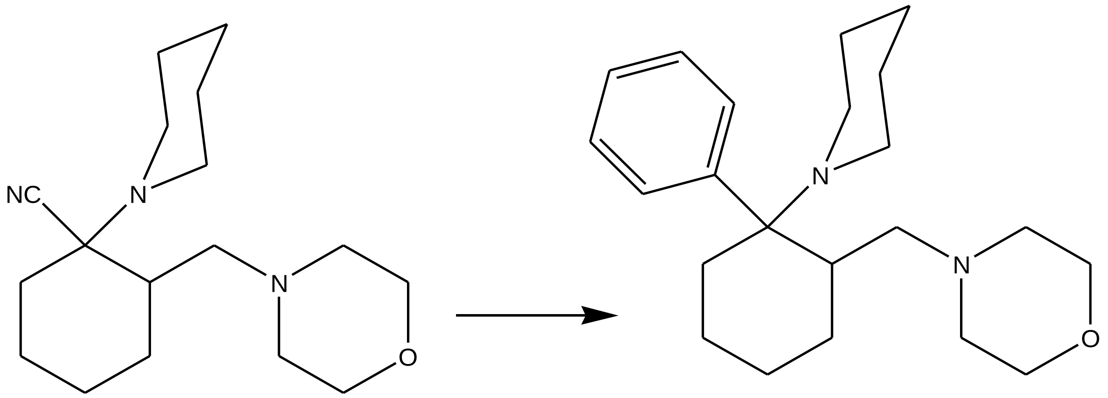

scheme1: Synthesis of 2-(N-morpholino methyl)-1-piperidino-cyano cyclohexane

References:

[1] . A.Ahmadi and et al, Mini Reviews in Medicinal Chemistry, Volume 17, Number 1, 2017, pp. 78-84(7)

[2]. A.Ahmadi and et al, Monatsh Chem, Volume 147, 2016, pp.457–464

[3]. M.Khalili and et al, Pharmaceutical Chemistry Journal, Volume 49, Number 9, 2015,pp. 613–619

[4] . R.Erard and et al,J.Psychedelic Drugs,Volume 12, 1980, pp.235–251

[5] . OA.Al-deeb,Arzneim-Forsch Drugs Res,Volume46, 1996, pp. 505–508

The 30th Iranian Seminar of Organic Chemistry
February 7-9, 2025, Iran University of Science and Technology, Tehran, Iran

Using the modified passerini reaction for the synthesis of novel N-methyl isatin derivatives

Authors: Zahra Zaghari*, Zahra Yarloo

Department of Chemistry, Science and Research Branch, Islamic Azad University, Tehran, Iran

Keyword: Multicompounet reactions(MCR), Passerini reaction, Isatin

The Passerini reaction is one of the multicompounent reactions (MCR) that is involving the reaction of aldehyde or the carboxylic acid and isocyanide ketones. In recent years, the success of Passerini reactions has been enhanced by new reactions or modifications of previous ones. Therefore, in this research, new sulfur depsipeptide compounds were prepared from N-methyl isatin derivatives by modified Passerini reaction. At the first, propyl thiouracil with α-bromo phenylacetic acid was reacted in presence of the 3-butyl-1-methyl imidazolium bromide as ionic liquid, then the resulting compound was reacted with cyclohexyl isocyanide and N-methyl isatin derivatives under solvent-free conditions. The novel sulfur depsipeptide derivatives of N-methyl isatin were obtained with yield of 86-92%(scheme1).

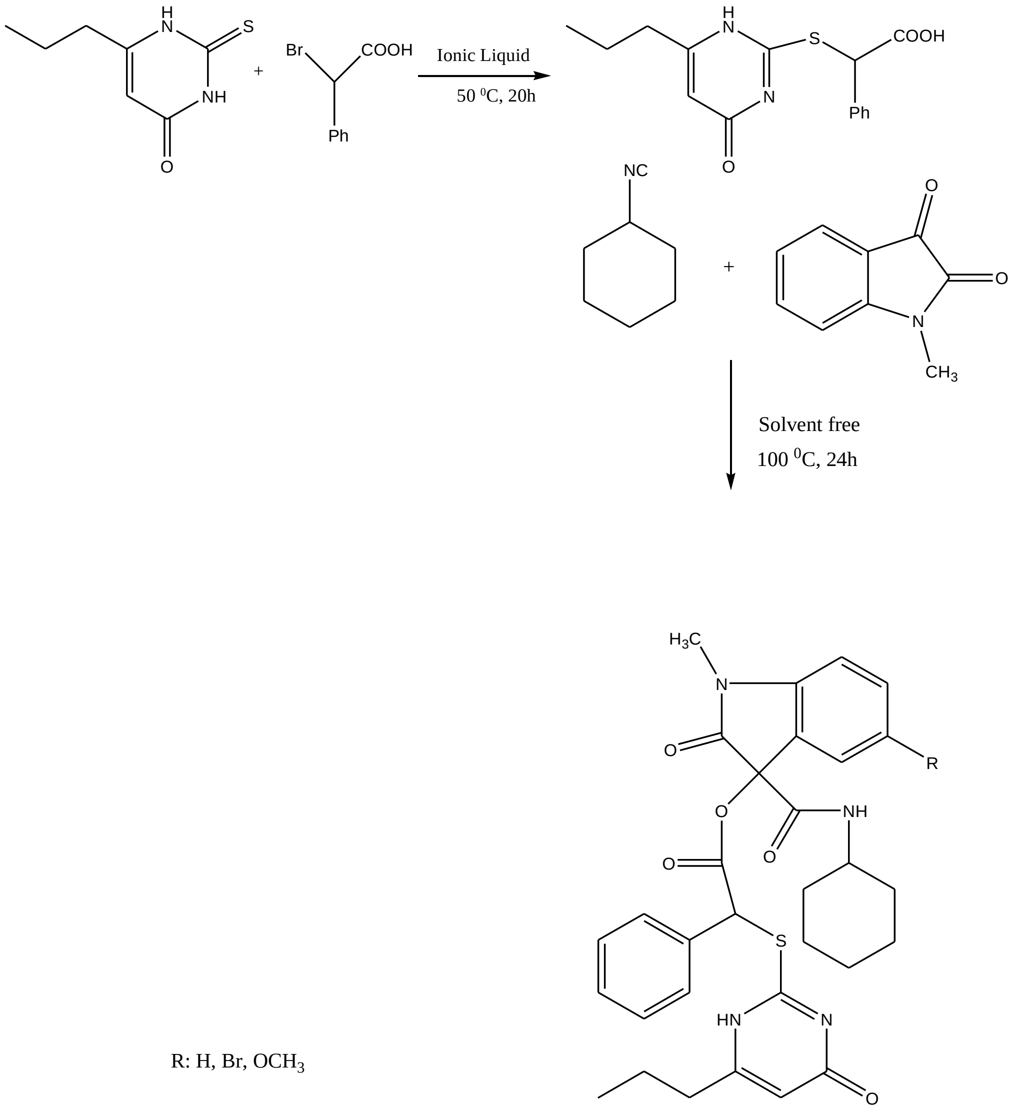

Scheme1: Synthesis of the novel sulfur depsipeptide derivatives of N-methyl isatin

References:

Moni, L., et al. Org. Lett. 18 (2016) 1638.

Kaicharla, T., et al. Green Chem. 15 (2013) 1608.

Sajadikhah, S.S., et al,. Research on Chemical Intermediates.41 (2015) 8665.

Bousquet, T., et al. Tetrahedron Lett. 53 (2012) 307.

The 30th Iranian Seminar of Organic Chemistry
February 7-9, 2025, Iran University of Science and Technology, Tehran, Iran

Investigation of the Catalytic Performance of Magnetic Metal-Organic Framework in Microwave-assisted Cross-Coupling Reaction

Mohammad Ali Irani[a], Mohammad Masoud Irani[a], Nadiya Koukabi*[a], Eskandar Kolvari[a], Kheibar Dashtian[b]

[a] *Department of Chemistry, Semnan University, 35131-19111 Semnan, Iran*

[b] *Department of Chemistry, Iran University of Science and Technology, Tehran 16846- 13114, Iran*

* *E-mail: n.koukabi@semnan.ac.ir*

Keywords: Cross-coupling reaction, Magnetic nanoparticles, Metal-organic framework, Microwave-assisted organic synthesis

The Sonogashira cross-coupling reaction is considered one of the most effective and efficient methodologies in organic synthesis, particularly for forming C–C bonds between terminal alkynes and aryl or vinyl halides [1]. Magnetite (Fe_3O_4) has emerged as a highly effective microwave absorber, attributable to its exceptional mechanical and chemical stability, tunable morphology, elevated Curie temperature, cost-effectiveness, and robust magnetic properties. However, its application is constrained by challenges such as agglomeration, eddy current losses, high density, and impedance mismatch, which adversely affect its performance as a standalone material. Furthermore, achieving efficient microwave absorption with low absorber loading remains a significant challenge [2]. To mitigate agglomeration, which arises from the high surface energy of magnetite and its susceptibility to oxidation—both of which can diminish magnetic performance—surface functionalization has been identified as an effective strategy. This process entails the application of organic or inorganic coatings that not only enhance stability but also facilitate further functionalization for practical applications [3]. The utilization of mesoporous solids, including metal-organic frameworks, in organic synthesis has attracted considerable interest. This can be attributed to their facile surface modification and functionalization, the capacity to accommodate catalytically active species at elevated concentrations with adequate dispersion, and their proficiency in facilitating reactions involving bulky molecules without the constraints of diffusion limitations. Furthermore, these materials enable the recapture of soluble active species, thereby contributing to the maintenance of catalyst stability. Consequently, their catalytic application offers clean, efficient, and sustainable methodologies for the synthesis of complex organic molecules [4]. The construction of Fe_3O_4-MOF composites demonstrates a strong synergistic interaction between Fe_3O_4 nanoparticles and the metal-organic framework, which significantly enhances the catalytic performance of the composite materials. Moreover, the incorporation of magnetic Fe_3O_4 nanoparticles offers a practical advantage by facilitating the efficient and convenient recovery of nanocatalysts, thereby improving their reusability and operational efficiency in catalytic applications [5]. Microwave-assisted organic synthesis (MAOS) is a widely accepted and innovative method in modern synthetic chemistry, having experienced significant growth over the past decade. Compared to cross-coupling techniques that use conventional heating, MAOS significantly reduces reaction times, produces cleaner reaction mixtures, and ultimately improves overall yields [6].

In the present study, aminated-Fe_3O_4 nanoparticles synthesized by a previous report [7] were incorporated with metal-organic framework precursors in an in-situ process to synthesize a magnetic metal-organic framework at ambient temperature, employing water as an environmentally friendly solvent. Subsequently, the magnetic metal-organic framework was employed in the Sonogashira cross-coupling reaction under microwave irradiation and solvent-free conditions (Scheme 1). The structural and physicochemical properties of the synthesized metal-organic framework were comprehensively assessed through a range of analytical techniques, including FT-IR, XRD, TGA, nitrogen adsorption and desorption, VSM, EDS, FE-SEM, and TEM. The advantages of the nanocatalyst produced encompass its capacity to sustain catalytic performance over three reaction cycles, high catalytic efficiency, decreased reaction times, facile separation, and mild operational parameters.

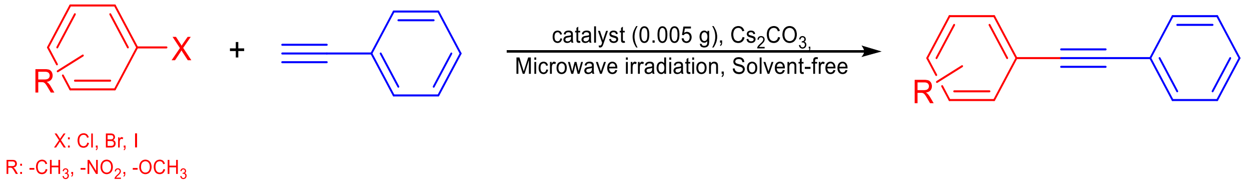

Scheme1: Sonogashira cross-coupling reaction catalyzed by magnetic metal-organic framework

References:

1. Huang, Y., et al., *Pd@HKUST-1@Cu(II)/CMC composite bead as an efficient synergistic bimetallic catalyst for Sonogashira cross-coupling reactions.* Carbohydrate Polymers, 2024. 324: p. 121531.

2. Wang, X., et al., *State of the art and prospects of Fe_3O_4/carbon microwave absorbing composites from the dimension and structure perspective.* Advances in Colloid and Interface Science, 2023: p. 102960.

3. Liu, S., et al., *Preparation, surface functionalization and application of Fe_3O_4 magnetic nanoparticles.* Advances in colloid and Interface Science, 2020. **281**: p. 102165.

4. Mastalir, Á. and Á. Molnár, *Coupling reactions induced by ionic palladium species deposited onto porous support materials.* Coordination Chemistry Reviews, 2022. **470**: p. 214696.

5. Chen, M., et al., *Enhanced degradation of tetrabromobisphenol A by magnetic Fe_3O_4@ZIF-67 composites as a heterogeneous Fenton-like catalyst.* Chemical Engineering Journal, 2021. **413**: p. 127539.

6. Gao, Y., Y. Liu, and D. Zou, *Microwave-assisted synthesis and environmental remediation: a review.* Environmental Chemistry Letters, 2023. **21**(4): p. 2399-2416.

7. Marandi, A. and N. Koukabi, *Fe_3O_4@TEA core-shell nanoparticles decorated palladium: A highly active and magnetically separable nanocatalyst for the Heck coupling reaction.* Colloids and Surfaces A: Physicochemical and Engineering Aspects, 2021. **621**: p. 126597.

The 30th Iranian Seminar of Organic Chemistry
February 7-9, 2025, Iran University of Science and Technology, Tehran, Iran

Microwave-Assisted Synthesis of Ag-Cu_2O/GLC as Efficient Nanocatalyst for the Solvent-Free Sonogashira Cross-Coupling Reaction

Mohammad Masoud Irani[a], Mohammad Ali Irani[a], Hadise Khoshkhoo Kakhki[a], Eskandar Kolvari*[a], Nadiya Koukabi[a], Kheibar Dashtian[b]

[a] *Department of Chemistry, Semnan University, 35131-19111 Semnan, Iran*

[b] *Department of Chemistry, Iran University of Science and Technology, Tehran 16846- 13114, Iran*

* *E-mail:* kolvari@semnan.ac.ir

Keywords: Sonogashira-coupling reaction, Graphene-like carbon, Ag-Cu_2O composite structure, Microwave Irradiation

Transition metal (TM)-catalyzed cross-coupling reactions represent some of the most versatile and reliable methodologies for synthesizing a diverse array of industrially significant fine chemicals. The application of transition metal nanocatalysts, particularly within the context of the Sonogashira cross-coupling reaction, has garnered significant attention owing to several advantageous properties, including (i) a high surface area, (ii) an increased number of surface atoms that facilitate the generation of additional catalytic active sites, and (iii) notable chemical stability [1]. Silver, in its metallic form, is particularly esteemed among the group of noble metals due to its advantageous properties, including atom-efficient utilization, low cost, ease of production, minimal toxicity, and widespread availability [2]. Additionally, silver nanoparticles (Ag NPs) possess distinct characteristics such as efficient reactivity, selectivity, long-term stability, and ease of recyclability in catalytic processes. Nonetheless, Ag NPs encounter challenges related to oxidation, instability, and agglomeration tendencies stemming from their high surface energy, which can compromise their catalytic efficacy and restrict their broader applications in organic synthesis [3]. Despite these challenges, the utilization of Ag NPs in a heterogeneous form has demonstrated an enhancement in the efficiency and selectivity of cross-coupling reactions [1]. Copper oxide (Cu_2O) is a commonly employed support for Ag NPs, attributable to its abundance, low cost, nontoxicity, and chemical stability [4]. The presence of silver at the Ag−Cu_2O interface significantly hinders the complete reduction of Cu_2O, thereby preserving Cu^+ sites and facilitating efficient C−C coupling reactions. However, Cu_2O is prone to instability, tending to reduce surface area over prolonged usage. The incorporation of Cu_2O with carbon-based materials can improve both nanoparticle dispersion and electron transfer, rendering carbon materials, particularly graphene, optimal support for precious metal nanoparticles [5]. Graphene, owing to its unique structure, outperforms traditional carbon supports like coal and graphite in catalysis. Consequently, there is increasing interest in developing cost-effective, scalable, and environmentally friendly carbon materials derived from biomass, which show promise in applications such as catalysis, energy storage, and fuel production [6]. Lastly, microwave-assisted synthesis methods are gaining traction for their energy efficiency, aligning with the principles of green chemistry to reduce environmental impact and enhance reaction control [7].

In this study, Ag-Cu_2O/graphene-like carbon (GLC) was successfully synthesized using sabja seeds activated with sodium hydroxide through a two-step microwave-assisted process involving reactions with silver and copper metal salts. The resulting catalyst was applied in the Sonogashira cross-coupling reaction (Scheme 1), demonstrating outstanding performance under optimized conditions. Comprehensive characterization of the nanocatalyst was carried out using various analytical techniques, including FT-IR, XRD, TGA, XPS, HR-TEM, FE-SEM, AAS, and EDS. The synthesized Ag-Cu_2O/GLC offers several key benefits, such as environmental sustainability, cost-effectiveness, and high catalytic efficiency.

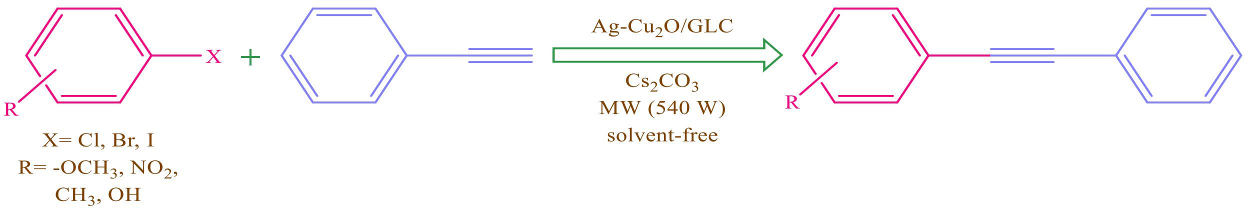

Scheme 1: Sonogashira cross-coupling reaction catalyzed by Ag-Cu_2O/GLC

References:

1. Ashraf, M., et al., *Transition metal nanoparticles as nanocatalysts for Suzuki, Heck and Sonogashira cross-coupling reactions.* Coordination Chemistry Reviews, 2023. **476**: p. 214928.

2. Pryshchepa, O., P. Pomastowski, and B. Buszewski, *Silver nanoparticles: Synthesis, investigation techniques, and properties.* Advances in Colloid and Interface Science, 2020. **284**: p. 102246.

3. Kargar, E. and A. Meshkini, *Improved photocatalytic disinfection performance of graphitic carbon nitride through hybridization with humic acid/zinc peroxide: A synergistic generation of antimicrobial reactive oxygen species.* Journal of Photochemistry and Photobiology A: Chemistry, 2024. **452**: p. 115577.

4. Torras, M. and A. Roig, *Copper oxide nanocubes wrapping metals by microwave synthesis.* Crystal Growth & Design, 2021. **21**(9): p. 5027-5035.

5. Irani, M.M., et al., *Ag–Cu_2O Supported Biomass-Derived rGO for Catalyzing Suzuki–Miyaura Cross-Coupling.* Langmuir, 2024. **40**(35): p. 18473-18485.

6. Kong, X., et al., *Synthesis of graphene-like carbon from biomass pyrolysis and its applications.* Chemical Engineering Journal, 2020. **399**: p. 125808.

7. Kumar, A., et al., *Microwave chemistry, recent advancements, and eco-friendly microwave-assisted synthesis of nanoarchitectures and their applications: a review.* Materials Today Nano, 2020. **11**: p. 100076.

The 30th Iranian Seminar of Organic Chemistry
February 7-9, 2025, Iran University of Science and Technology, Tehran, Iran

Adsorption of Moxifloxacin and Levofloxacin on lignin alkyl quaternized chitin/pectin nanofiber network hydrogel Nanocomposite

A.Alizadeh, R.Azhdari, A. Karbasi.

Faculty of Petroleum and gas, Yasuj University, Gachsaran, Iran

Abstract

The antibiotics are widely used to treat humans and animals then they enter the water through human and animal wastes water. One of the suitable ways of water purification is surface adsorption process using hydrogel nanocomposites consisting of natural polymer. The aim of this project is to investigate the adsorption mechanism of Moxifloxacin and Levofloxacin antibiotics using lignin alkyl quaternized chitin/pectin nanofiber network hydrogel Nanocomposite (CHPCQ). The experiment conditions were considered completely the same for both antibiotic adsorption modes. The effect of various parameters such as pH, initial concentration of antibiotics and different percentages of the hydrogel on removal processing was investigated. To study the adsorption isothermal data, the two-parameter models of Langmuir, Freundlich, Tempkin, and Dubinin-Rudushkevich (DR) and the three-parameter models of Redlich-Peterson (RP) and Sipes were investigated. The highest correlation coefficient was selected as the best adsorption isotherm model of each antibiotic. According to the obtained results from the adsorption data of MFX antibiotic, the data were more consistent with the Sips (۰/۹۹۹) and Langmuir (۰٫۹۹۹) models.The better matching of the data with the Sips and Langmuir models indicates the single-layer surface adsorption of MFX antibiotic and homogeneity of the adsorbent structure. Also, the highest correlation coefficient of LFX antibiotic adsorption was obtained for Langmuir (0.999) and Redlich-Peterson (0.940) models but were better described by the Langmuir model which this indicates the homogeneity of the adsorbent surface. The R_L parameter was obtained between zero and one, which shows the desirability of the adsorption process for this model.

Keywords: Antibiotic, Isotherm; Adsorption; Hydrogel, Chitin, Pectin, lignin alkyl quaternized.

1. Introduction

In general, the product or substance that is produced or taken from a microorganism and destroys the other microorganisms is called an antibiotic. The antibiotics are antimicrobial drugs that fights against the bacterial infections in humans and animals and are a biocide. Antibiotics are one of the most common drugs with incorrect use, that their structure includes sulfonamides and quinolones. The residues of active pharmaceutical compounds like human antibiotics are enter the urban wastewater, include domestic, hospital, and cause environmental risks such as genetic disorders in aquatics reproduction and they may also cause harm to human. Therefore, it is necessary to remove them from the wastewater. [1-5] In recent years, the surface adsorption method has been carried out using natural hydrogel nanoadsorbent.[5-7]Hydrogel or abgel is a network of hydrophilic polymer chains with a three-dimensional structure of hydraulic polymer chains which connected by crosslinks. For this reason, the integrity of its structure is not decomposed in the water.[8, 9] In fact, the nanoscale natural adsorbents with high specific surface area and high adsorption capacity produce less wastes that can be collected more easily. The production of bio-based nanopolymers has attracted the attention of most researchers due to their non-toxicity in the environment, their availability, the low cost of raw materials and their biodegradability as a tool to adsorb antibiotics from wastewater.[10-14] In order to fully investigate the surface adsorption reaction of antibiotics in wastewater, familiarity with the concept of the adsorption equilibrium isotherm is necessary. The adsorption isotherms with equilibrium data and adsorption properties describe how pollutants react with adsorbent materials and play a fundamental role in the optimization of adsorbent consumption. [15, 16] Chitin is a long and unbranched polysaccharide and after cellulose it is the most abundant natural polymer that produced by marine crustaceans such as crabs, shrimps and even some mollusca such as water snake. This compound with the formula $(C_8H_{13}O_5N)_n$ is a white substance similar to pieces of paper, where n is its degree of polymerization, and it is insoluble in water, alkaline substances and organic solvents. The structure of chitin is comparable to cellulose and has string-like bundles called microfibrils, that diameter is 3 to 30 nm. Therefore, these microfibrils are classified as nanofiberil. Chitin nanofiber is one of the thinnest and most delicate fibers which have interesting properties, such as renewability, high mechanical resistance, high specific surface area, cheap and abundant raw materials. [17-19] Pectins are plant cell wall structural polysaccharides composed mainly of galacturonic acid units with variations in composition, structure and molecular weight. This polysaccharide is often associated with other cell wall components such as cellulose, hemicellulose and lignin.[20] In general, pectins are located in the primary cell wall and middle lamella of many plants, being in the latter, the one with highest concentration, with a gradual decrease from the primary cell wall towards the plasma membrane. [21-23] Lignin is a complex polymer made of phenylpropane molecular units, which is in an amorphous form and mixed with holocellulose in plants in a layer around the cellulose. After cellulose, the lignin is the most common compound in the structure of woody and non-woody plants. The dry wood contains about 25% lignin in the cell wall and it is placed in the outer part of the cell. The lignin acts as a cell wall binder and binds the cell fibers containing the matrix together to strengthen the wood structure[24, 25]Quaternized alkyl lignin means quaternized alkyl lignin salts, since lignin is not soluble in water, it is quaternized and reacted with alkyl to turn it into a water-soluble substance. The different researchers worked on the equilibrium isotherm using and its derivatives (lignin + cellulose)[12, 26-30], chitin and its derivatives (chitosan)[30-34] adsorbents in nano and micro scale. In this project we used quaternized alkyl nanofiber network hydrogel as an adsorbent to remove Moxifloxacin and Levofloxacin antibiotics from aqueous solutions. Therefore, the purpose of this study is to investigate and compare adsorption isotherms, in order to fully understand the process of antibiotic surface adsorption using the investigated adsorbent. Two-parameter (Langmuir, Freundlich, Dubinin-Radushkevich and Tempkin) and three-parameter (Sipes and Redlich-Peterson) isotherms were used to investigate the adsorption isotherm. For each subject, the data of the models were compared with the laboratory data and the best model that had a better match with the laboratory data of antibiotic adsorption was determined.

2. Materials and method

2-1. Materials

The adsorbents of chitin/pectin/quaternized alkyl lignin nanofiber network hydrogel were prepared from polymer Nano-Novin CO. (Tehran, Iran). Antibiotics of LFX and MFX were obtained from Merck. Co (Darmstadt, Germany). The double-distilled water was used for experiments and dilution. 0.1 M solutions of NaOH and HCL were used to adjust the pH.

2-2. **Preparation of antibiotic standard solution**

1000ppm stock solution of LFX ($C_{18}H_{20}FN_3O_4$) and MFX ($C_{21}H_{24}FN_3O_4$) antibiotics were prepared. To prepare this solution, 1000 mg of antibiotic should be dissolved in 1 liter of double distilled water. Other test solutions were prepared from stock solution using double ionized distilled water.

2-3. General method of adsorption process

For equilibrium adsorption studies, a known amount of adsorbent was equilibrated with desired antibiotic solution at room temperature for definite time periods. At the end of the predetermined time intervals, the adsorbent was removed by simple filtration. The filtrate was analyzed for the residual (unadsorbed) antibiotic, spectrophotometrically.

The removal percentage and adsorption capacity of the adsorbent were calculated respectively through equation (1) and (2).

$$\%Removal = \left(\frac{\mathrm{C0 - Ce}}{\mathrm{C0}}\right) \times \text{١٠٠} \qquad (\text{١})$$

$$Qe = \left(\frac{\mathrm{C0 - Ce}}{\mathrm{W}}\right) \times V \qquad (\text{٢})$$

Where C_0 and C_e are the initial and equilibrium concentration of antibiotic in solution, respectively, W is the weight of adsorbent (g), and V is the solution volume. It should be noted that all the experiments were repeated three times and the average data and results were used.[16]

2-4. Adsorption isotherms

The accurate application of the adsorption process needs studies based on various adsorption isotherm models. Equilibrium relationships between CHPCQ and antibiotic are studied by adsorption isotherms. The applicability of the isotherm equations is compared through interpreting the correlation coefficient R^2. The isotherm studies were carried out by changing the initial antibiotic concentration from (3 to 15PPM) at pH = 7. After 150 min, the reaction mixture was analyzed for the residual antibiotics concentration. Next the two-parameter models of Langmuir, Freundlich, Tempkin, and Dubnin-Rudushkevich (DR) and the three-parameter models of Redlich-Peterson (RP) and Sipes were investigated. The Langmuir model (equation. 3) shows the single layer adsorption of adsorbate on a homogeneous adsorbent surface with a finite number of identical sites and with negligible interaction between adsorbed molecules.

$$\mathrm{q_e} = \frac{\mathrm{q_m \times C_e b}}{\text{١} + \mathrm{C_e b}} \qquad (\text{٣})$$

The important properties of the Langmuir isotherm is expressed in terms of equilibrium parameter RL (equation. 4), which is a dimensionless constant referred to as an equilibrium parameter.

$$Rl = \frac{\text{١}}{\text{١} + \mathrm{bCo}} \qquad (\text{٤})$$

Where Co is the initial concentration and b is the constant related to the energy of adsorption (Langmuir constant). The values of RL indicate the type of isotherm to be irreversible (RL = 0), favorable (0 < RL < 1), linear (RL = 1) or unfavorable (RL > 1). Freundlich model (equation. 5) confirms a heterogeneous adsorption surface with sites that have different unequal energy. This model is more widely applied but does not provide data on the single layer adsorption capacity in compared to the Langmuir model.

$$q_e = kfC_e\,{}^{\text{١}/n} \qquad (\text{٥})$$

The Tempkin isotherm (equation.6) express that the fall in the heat of adsorption is linear rather than logarithmic as showed in the Freundlich equation. The heat of adsorption of the molecules would decrease linearly with coverage due to adsorbate/adsorbate interaction.

$$q_e = B_T LnA_T + B_T LnC_e \qquad (٦)$$

The latest two-parameter model used in the analysis of isotherms was expressed by Dubinin and Radushkevich. The DR model (equation.7) was applied to estimate the porosity apparent free energy and characteristic of adsorption. The DR isotherm does not assume a homogeneous surface or constant adsorption potential. [16]

$$Lnq_e = Lnq_m - B\varepsilon^{٢} \qquad (٧)$$

Between the three-parameter isotherm models, the Redlich-Peterson model is often used for the liquid phase adsorption of heavy metals and organic compounds.[35, 36] The Sips isotherm (equation. 8) is also the integration of Freundlich and Langmuir isotherms, which is used to predict heterogeneous adsorption processes.[37, 38]

$$q_e = \frac{q_m C_e^{\beta_s}}{١ + a_{\beta s} C_e^{\beta_s}} \qquad (٨)$$

3. Findings and discussion

3-1. Effect of pH o**n antibiotic adsorption**

The pH of the system is important factor on the capacity of adsorbate molecule likely due to its effect on the surface properties of the adsorbent, ionization, and dissociation of the adsorbate molecule. The antibiotic removal was studied as a function of pH at a fixed concentration and adsorbent dosage. The percentage of antibiotic adsorption increases while pH increases from 3.0 to 11.٠. The maximum adsorption for two antibiotics occurred at pH =7(Fig 1.c). It can be due to the availability of negatively charged groups on the surface of the adsorbent in the adsorption process.

3.2. Effect of adsorbent dosage

To study the change in adsorption based on the amount of the CHPCQ adsorbent, in the conditions of antibiotics concentration (10 ppm) and pH = 7, the various amounts [(0.5 to 5.0) g] of CHPCQ were selected. With increasing the amount of adsorbent to 3.0 g, the adsorption capacity increases, but it decreases with increasing adsorbent amount (Fig 1.d). An increase in the adsorption with a high dosage of the adsorbent is due to an increased adsorbent surface area of pores and the availability of more adsorption sites.

3.3. Effect of Time of contact.

The relation between the adsorption of MFX and LFX with contact time was studied to identify the rate of antibiotics removal. The adsorption increases with increasing contact time. Then, the rate of adsorption becomes slow. The equilibrium was found to be nearly 150 min for 10 ppm of antibiotics. (Fig 1. a, b)

3-2- A**dsorption isotherm**

According to Fig. (2), the correlation coefficient (R^2) of the two-parameter models of Langmuir (0.999), Freundlich (0.910), Dubinin-Rudushkevich (0.606), tempkin (0.890) and the three-parameter models of Redlich-Peterson (0.940) and Sips (0.810) for LFX were obtained. Also, the correlation coefficient (R^2) of the two-parameter models of Langmuir (0.999), Freundlich (0.992), Dubinin-Rudushkevich (0.846) and tempkin (0.994) and the three-parameter models of Redlich-Peterson (0.996) and Sips (0.992) models for MFX were obtained. (Table 2). According to the correlation coefficients obtained for LFX, between the two-parameter models, the Langmuir isotherm model and between the three-parameter models, the Redlich-Peterson model has the highest R^2. This result shows that the adsorbate molecules are adsorbed on the surface of the adsorbent and the internal pores of the adsorbent are closed. Finally, the higher correlation coefficient for the Langmuir model shows that the adsorption of LFX on the adsorbent surface is homogeneous and monolayer. Also, all reactive sites on the surface of adsorbent have the same adsorption energy. [16]According to the correlation coefficients obtained for MFX, between the two-parameter models, the Langmuir isotherm model and between the three-parameter models, the Sips model has the highest R^2. Therefore, it can be concluded that the data are consistent with both Langmuir and Sips models, which confirm the homogeneity of the adsorbent structure and the monolayer surface adsorption process. [3, 16]. In this research, the separation factors of the Langmuir isotherm for LFX (R_L=0.32) and MFX (R_L=0.34) adsorption on the CHPCQ were between zero and one, which confirming thereby the favorable adsorption process. Also, the amount of E obtained from the Dubinin-Rudushkevich model for LFX was 8.57 kJ/mol and for MFX was 7.35 kJ/mol, which shows the adsorption process is physical.[39] The positive values of B_t for the adsorption of both LFX (+108.79) and MFX (+0.44) antibiotics indicate that the adsorption process by the desired adsorbent is exothermic.

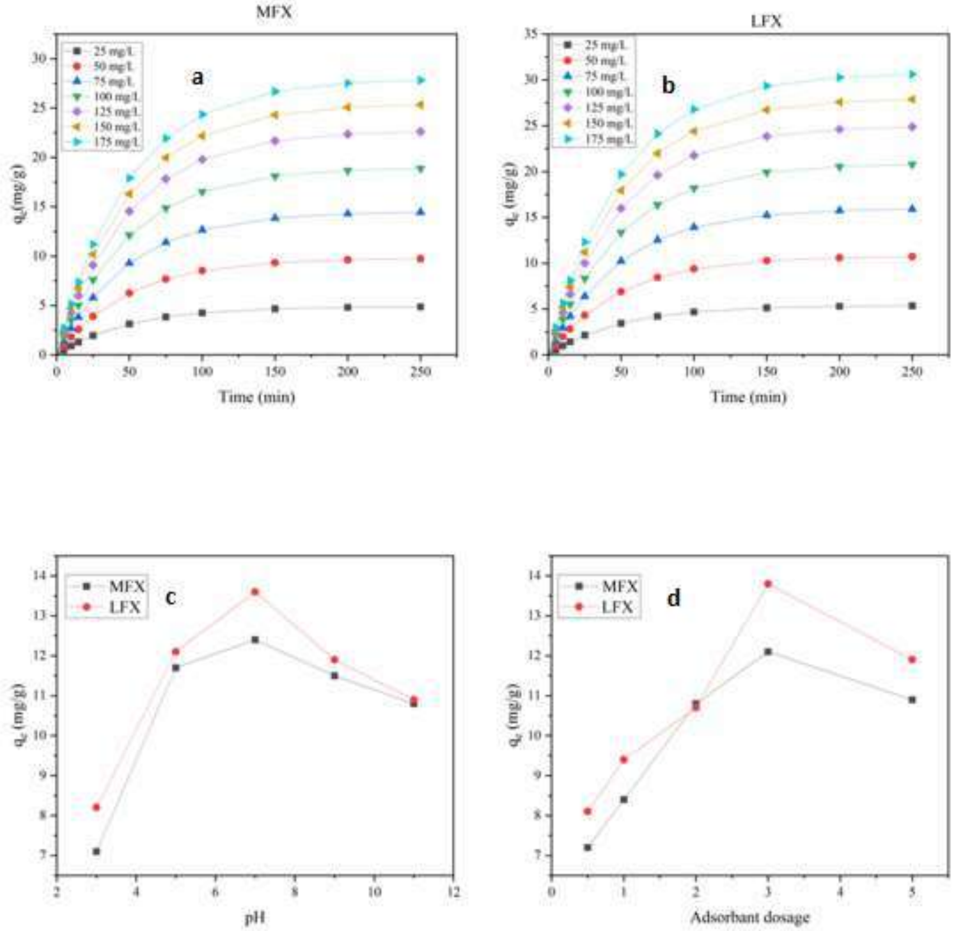

Fig.1. The plots of the effect of different parameters on the adsorption process: Time (MFX)(a), Time(LFX)(b), pH (c) and adsorbent dosage (d).

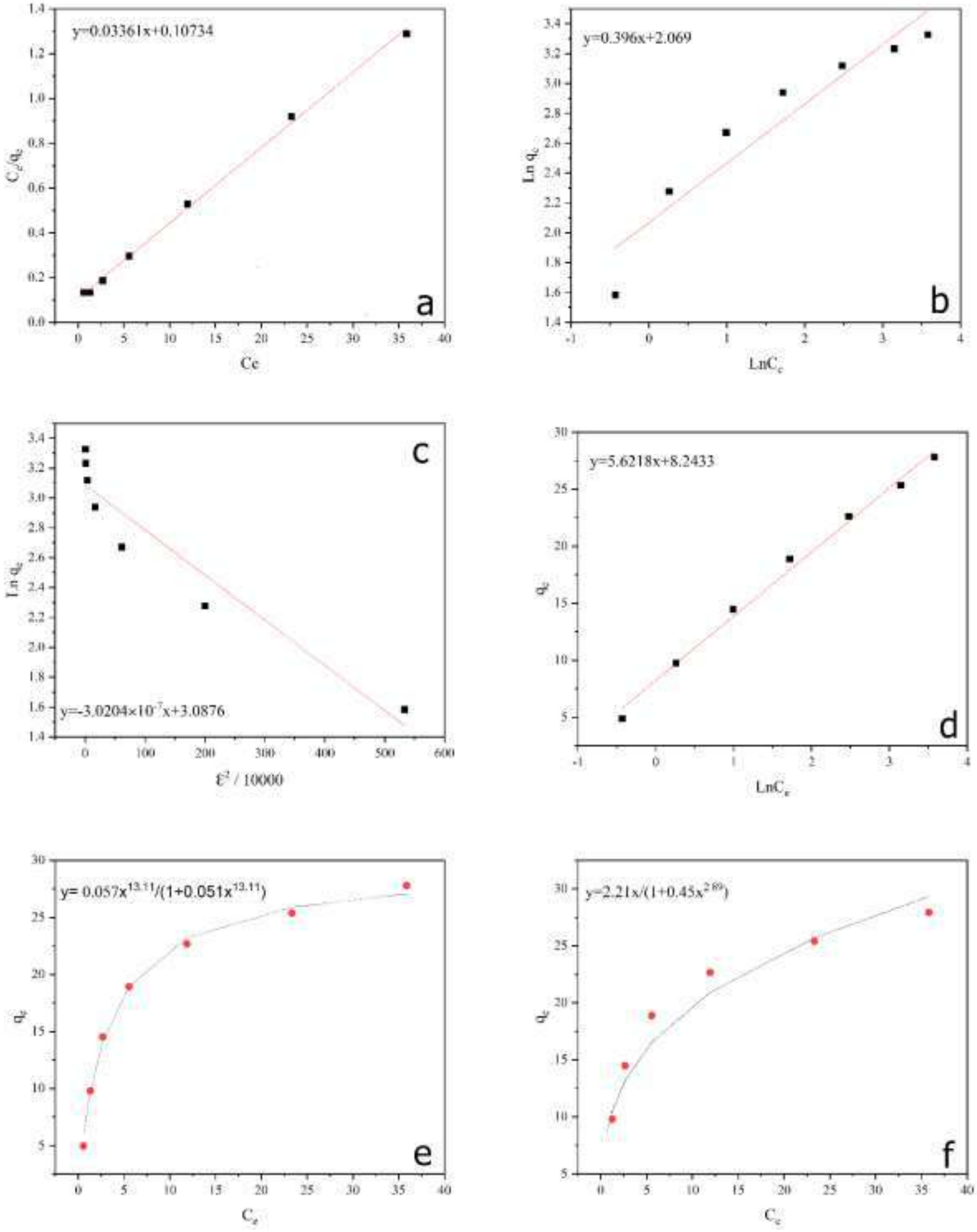

Fig.2. Langmuir (a), Freundlich (b), Dubinin- Rudushkevich (c), Tempkin (d), Sips (e) and Redlich-Peterson isotherm models plot for the adsorption of LFX.

Conclusions

The following conclusion may be drawn from the present investigation:

CHPCQ, with the special characteristics such as availability, inexpensiveness, large area, and the desired pores, is used for the removal of antibiotics such as MFX and LFX from its aqueous solution. The experimental data were in line with the Redlich-Peterson and Langmuir adsorption isotherms for LFX and Sips and Langmuir for MFX. The adsorption process is dependent on pH and adsorbent dosage and time. The separation factors of the Langmuir isotherm for LFX and MFX adsorption on the CHPCQ were between zero and one, which confirming thereby the favorable adsorption process. Also, the low amount of E obtained from the Dubinin-Rudushkevich model shows the adsorption process is physical. The positive values of B_t for the adsorption of both antibiotics indicate that the adsorption process by the desired adsorbent is exothermic.

References

1. Li, J., et al., *Carboxylated cellulose nanofiber/montmorillonite nanocomposite for the removal of levofloxacin hydrochloride antibiotic from aqueous solutions.* RSC advances, 2020. 10(69): p. 42038-42053.

2. Tao, J., et al., *Cellulose nanocrystals/graphene oxide composite for the adsorption and removal of levofloxacin hydrochloride antibiotic from aqueous solution.* Royal Society open science, 2020. **7**(10): p. 200857.

3. Nasuhoglu, D., et al., *Removal of the antibiotic levofloxacin (LEVO) in water by ozonation and TiO2 photocatalysis.* Chemical Engineering Journal, 2012. **189**: p. 41-48.

4. Iwuozor, K.O., et al., *Mitigation of levofloxacin from aqueous media by adsorption: a review.* Sustainable Water Resources Management, 2021. **7**: p. 1-18.

5. Geng, R., et al., *Adsorption of antibiotics by polydopamine-modified salecan hydrogel: Performance, kinetics and mechanism studies.* Chemical Engineering Journal, 2023. **454**: p. 140446.

6. Ma, J., et al., *Enhanced adsorption for the removal of antibiotics by carbon nanotubes/graphene oxide/sodium alginate triple-network nanocomposite hydrogels in aqueous solutions.* Chemosphere, 2020. **242**: p. 125188.

7. Yang, P., et al., *Graphene oxide modified κ-carrageenan/sodium alginate double-network hydrogel for effective adsorption of antibiotics in a batch and fixed-bed column system.* Science of The Total Environment, 2022. **837**: p. 155662.

8. Wichterle, O. and D. Lim, *Hydrophilic gels for biological use.* Nature, 1960. **185**(4706): p. 117-118.

9. Shrivastava, P., et al., *Magnetically responsive polymeric gels and elastomeric system (s) for drug delivery*, in *Smart Polymeric Nano-Constructs in Drug Delivery*. 2023, Elsevier. p. 129-150.

10. Hooshyar, S.P., et al., *Tailoring a new hyperbranched PEGylated dendrimer nano-polymer as a super-adsorbent for magnetic solid-phase extraction and determination of*

letrozole in biological and pharmaceutical samples. Journal of Molecular Liquids, 2021. 338: p. 116772.

11. Radmehr, S., et al., *Adsorption of nalidixic acid antibiotic using a renewable adsorbent based on Graphene oxide from simulated wastewater.* Journal of Environmental Chemical Engineering, 2021. **9**(5): p. 105975.

12. Das, L., et al., *Synthesis of hybrid hydrogel nano-polymer composite using Graphene oxide, Chitosan and PVA and its application in waste water treatment.* Environmental Technology & Innovation, 2020. **18**: p. 100664.

13. Almutairi, F.M., et al., *Application of chitosan/alginate nanocomposite incorporated with phycosynthesized iron nanoparticles for efficient remediation of chromium.* Polymers, 2021. 13(15): p. 2481.

14. Zong, X., et al., *Structure and process relationship of electrospun bioabsorbable nanofiber membranes.* polymer, 2002. **43**(16): p. 4403-4412.

15. Kardam, A., et al., *Nanocellulose fibers for biosorption of cadmium, nickel, and lead ions from aqueous solution.* Clean Technologies and Environmental Policy, 2014. **16**: p. 385-393.

16. Shokrollahi, A., et al., *Removal of bromocresol green from aqueous solution via adsorption on Ziziphus nummularia as a new, natural, and low-cost adsorbent: kinetic and thermodynamic study of removal process.* Journal of Chemical & Engineering Data, 2011. 56(10): p. 3738-3746.

17. Lehninger, A.L., D.L. Nelson, and M.M. Cox, *Lehninger principles of biochemistry*. 2005: Macmillan.

18. Sanjanwala, D., et al., *Polysaccharide-based hydrogels for drug delivery and wound management: a review.* Expert Opinion on Drug Delivery, 2022. **19**(12): p. 1664-1695.

19. Tang, W.J., et al., *Chitin is endogenously produced in vertebrates.* Current Biology, 2015. 25(7): p. 897-900.

20. Harholt, J., A. Suttangkakul, and H. Vibe Scheller, *Biosynthesis of pectin.* Plant physiology, 2010. **153**(2): p. 384-395.

21. Willats, W.G., et al., *Pectin: cell biology and prospects for functional analysis.* Plant molecular biology, 2001. **47**: p. 9-27.

22. Mellerowicz, E.J. and B. Sundberg, *Wood cell walls: biosynthesis, developmental dynamics and their implications for wood properties.* Current opinion in plant biology, 2008. 11(3): p. 293-300.

23. Van Buren, J., *Function of pectin in plant tissue structure and firmness.* The chemistry and technology of pectin, 1991: p. 1-22.

24. Sales, F., C. Abreu, and J. Pereira, *Catalytic wet-air oxidation of lignin in a three-phase reactor with aromatic aldehyde production.* Brazilian journal of chemical engineering, 2004. 21: p. 211-218.

25. Elvers, B., *Ullmann's encyclopedia of industrial chemistry*. Vol. 17. 1991: Verlag Chemie Hoboken, NJ.

26. Maia, L.C., L.C. Soares, and L.V.A. Gurgel, *A review on the use of lignocellulosic materials for arsenic adsorption.* Journal of Environmental Management, 2021. **288**: p. 112397.

27. Shen, X., et al., *Enhanced heavy metal adsorption ability of lignocellulosic hydrogel adsorbents by the structural support effect of lignin.* Cellulose, 2019. **26**: p. 4005-4019.

28. Othmani, A., et al., *Biochar and activated carbon derivatives of lignocellulosic fibers towards adsorptive removal of pollutants from aqueous systems: Critical study and future insight.* Separation and Purification Technology, 2021. **274**: p. 119062.

29. Landin-Sandoval, V., et al., *Physicochemical analysis of multilayer adsorption mechanism of anionic dyes on lignocellulosic biomasses via statistical physics and density functional theory.* Journal of Molecular Liquids, 2021. **322**: p. 114511.

30. Christou, C., et al., *Uranium adsorption by polyvinylpyrrolidone/chitosan blended nanofibers.* Carbohydrate polymers, 2019. **219**: p. 298-305.

31. Kausar, A., et al., *Kinetics, equilibrium and thermodynamics of dyes adsorption onto modified chitosan: a review.* Zeitschrift für Physikalische Chemie, 2021(0): p. 000010151520191586.

32. Saheed, I.O., W. Da Oh, and F.B.M. Suah, *Chitosan modifications for adsorption of pollutants–A review.* Journal of hazardous materials, 2021. **408**: p. 124889.

33. Huang, A., et al., *Adsorption characteristics of chitosan-modified bamboo biochar in Cd (II) contaminated water.* Journal of Chemistry, 2022. **2022**: p. 1-10.

34. Pathak, K., et al., *Biomedical applications of quaternized chitosan.* Polymers, 2021. 13(15): p. 2514.

35. Ouallal, H., et al., *Kinetic, isotherm and mechanism investigations of the removal of phenols from water by raw and calcined clays.* Heliyon, 2019. **5**(5): p. e01616.

36. Alouia, A., et al., *Biosorption of some pharmaceutical compounds from aqueous medium by Luffa cylindrica fibers: application of the linear form of the Redlich–Peterson isotherm equation.* Desalin Water Treat, 2021. **214**: p. 367-378.

37. Chen, X., et al., *Isotherm models for adsorption of heavy metals from water-a review.* Chemosphere, 2022: p. 135545.

38. Barakan, S., et al., *Thermodynamic, kinetic and equilibrium isotherm studies of As (V) adsorption by Fe (III)-impregnated bentonite.* Environment, Development and Sustainability, 2020. **22**: p. 5273-5295.

39. Belhaj, A.F., et al., *Experimental investigation, binary modelling and artificial neural network prediction of surfactant adsorption for enhanced oil recovery application.* Chemical Engineering Journal, 2021. **406**: p. 127081.

Nano Fe_3O_4 catalyzed selective, tandem, and oxidative conversion of alcohols to benzimidazoles

Samaneh Mohamadian[a], Ghasem Aghapour*[a]

[a] *School of Chemistry, Damghan University, Damghan 36716-41167 Iran;*
**E-mail: gh_aghapour@du.ac.ir*

Keyword: Alcohol, *o*-Phenylenediamine, Benzimidazole, Fe_3O_4 magnetic nanoparticles, *tert*-butyl hydroperoxide.

Benzimidazoles are considered as very important and attractive heterocycles in organic chemistry. The benzimidazole scaffold is present in the structure of many drugs and biologically active compounds having divers and valuable properties such as anticancer, antiparasite, antiviral, anti-inflammatory, antiulcer, antibacterial, anticonvulsant, antihypertensive, antifungal, antioxidant, antihistamine, and so on [1, 2]. Also, these nitrogen-containing heterocycles have industrial applications in addition to their pharmaceutical uses. For example, these compounds can act as corrosion inhibitors for some steels, pure metals and alloys [3]. In the present work, an efficient way is described for the synthesis of benzimidazole derivatives from the reaction of benzylic alcohols with *o*-phenylenediamine using *tert*-butylhydroperoxide ^tBuOOH as a mild oxidant, potassium cyanide and a catalytic amounts of iron oxide magnetic nanoparticles Fe_3O_4 MNPs in a tandem manner (Scheme 1). In continution, it was found that this oxidative conversion can be operable even in the presence of different other functional groups such as phenol, epoxide, pyridine ring, carboxylic acid and ester, sulfide, and nonbenzylic alcohol as well as THP and TMS ethers with excellent chemoselectivity. In addition, the Fe_3O_4 MNPs catalyst can be easily magnetically separated using an external magnet and then reused after washing with ethanol and drying for four times without a significant loss of its activity. Stability, ease preparation, non-toxicity, biocompatibility, cheapness, use in low amounts, ease separability, and also reusability of the nanomagnetic catalyst, catalytic and tandem nature, simple operation, good to excellent yields, use of a mild oxidant, excellent chemoselectivity and also easy work-up can be considered as main advantages of the present environment-friendly way.

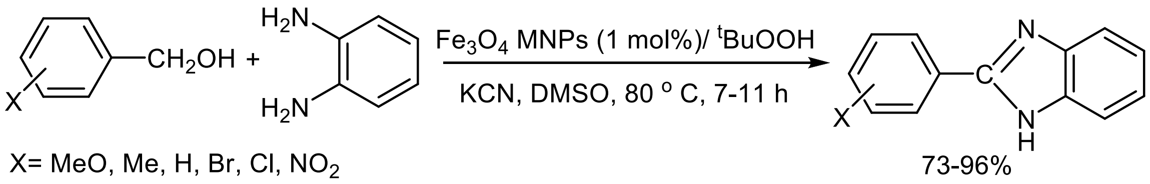

Scheme 1: Fe_3O_4 MNPs catalyzed synthesis of benzimidazoles from alcohols using $^tBuOOH/KCN$.

References:

[1] Kumar, R; Singh, G. *Pharmacophore* **2022**, *13*, 41.
[2] Raducka, A.; Czylkowska, A.; Gobis, K.; Szymanski, P.; Swiatkowski, M. *Materials* **2021**, *14*, 2958.
[3] Marinescu, M. *BMC Chem.* **2019**, *13*, 136.

The 30th Iranian Seminar of Organic Chemistry
February 7-9, 2025, Iran University of Science and Technology, Tehran, Iran

Graphene Quantum Dots Incorporated ZIF-67 for Stabilization of Au Nanoparticles: Efficient Catalyst for A^3-Coupling and Nitroarenes Reduction Reactions

Mahboobe Eskandari,[a] Mohammad Gholinejad,*[ab] José M. Sansano,[c] Zhwan Naghshbandi,[a]

[a] *Department of Chemistry, Institute for Advanced Studies in Basic Sciences (IASBS), P.O. Box 45195-1159, Gavazang, Zanjan 45137-66731, Iran. Email: gholinejad@iasbs.ac.ir*
[b] *Research Center for Basic Sciences & Modern Technologies (RBST), Institute for Advanced Studies in Basic Sciences (IASBS), Zanjan 45137-66731, Iran*
[c] *Departamento de Química Orgánica, Instituto de Síntesis Orgánica and Centro de Innovación en Química Avanzada (ORFEO-CINQA). Universidad de Alicante, Apdo. 99, E-03080-Alicante, Spain.*

Introduction:

Zeolitic imidazolate frameworks (ZIFs) are considered as new category of porous and crystalline materials having large pore volume, high surface area and advantage of easy functionalization are special class of metal organic frameworks (MOFs) [1]. Among them, ZIF-67 is prepared from tetrahedral cobalt cations and 2-methylimidazolate bridging ligand forming a cubic crystal symmetry in which the angle of Co-Im-Co is ~145˚ and unit cell parameters are a=b=c= 16.9589 ˚A. ZIF-67 has been used for an array of applications including separation, drug delivery, bioimaging, supercapacitors, and catalysis. However, modification of ZIF-67 with other components and ligands let them apply as support for immobilization of other transition metals and benefit from advantages of bimetallic catalysts [2].

Nowadays, typical method for preparation of propargylic amines include one-pot catalytic reaction of aldehydes, alkynes and amines [3], which is more efficient and easier than traditional methods including reaction of imine with Grignard or lithium acetylides [4]. Since, design of green and stable catalysts having high catalytic activity, selectivity and recyclability under low amount of expensive transition metals remains as a challenge in organic synthesis, in this study, we report an immobilization of Au nanoparticles on the ZIF-67 modified with GQD (ZIF-67/GQD@Au) for catalytic reduction of nitro compounds and A^3-coupling transformations under mild conditions in water.

Results and Discussion

To a 100 mL flask, $Co(NO_3)_2.6H_2O$, PVP and methanol were added. To the resulting mixture, solution of 2-methylimidazole was added and the mixture stirred at room temperature during 30 min. Subsequently, GQD is added to above solution and the suspension stirred at room temperature during 24 h. In the next step, ZIF-67/GQD was dispersed in ethanol and $NaAuCl_4.2H_2O$ solution was added to it and the resulting mixture was stirred at room temperature for 24 h under argon.

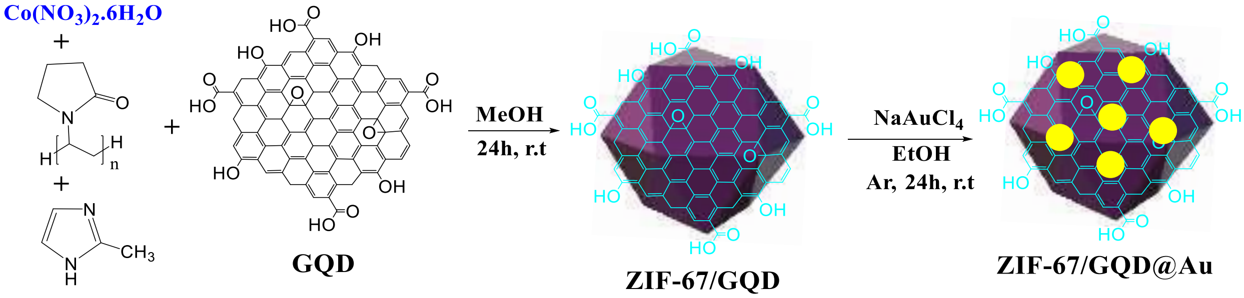

(Scheme): Schematic diagram for the preparation of ZIF-67/GQD@Au.

Conclusion:

In conclusion, the present study offered a new heterogeneous Au catalyst, in which ZIF-67 modified with graphene quantum dots as a green material to stabilize Au nanoparticles. ZIF-67 due to porous structure, excellent stability, high surface area and simple preparation utilize as a catalyst support, and also its synergetic affect with Au demonstrate great potential of ZIF-67/GQD@Au for catalytic application. In addition, presence of graphene quantum dots led to stability, high dispersity in water and reduction of Au(III) to Au nanoparticles. The prepared ZIF-67/GQD@Au is fully characterized and employed as an effective catalyst for nitroarene reduction and A^3-coupling reactions in water. This catalyst demonstrated excellent catalytic activity for reduction of the various nitroarenes with electron-donating group and electron-withdrawing substituents in the presence of $NaBH_4$ in H_2O/EtOH (1:1) at room temperature. Furthermore, this catalyst displayed high activity in the A^3-coupling reactions of amins, alkynes and aldehydes to prepare propargylamines in water. Comparing the catalytic performance of ZIF-67/GQD@Au with ZIF-67, ZIF-67/GQD and ZIF-67@Au revealed excellent efficiency of ZIF-67/GQD@Au. ZIF-67/GQD@Au indicated considerable catalytic recyclability and stability in both reduction and A^3-coupling reactions.

References:

[1] Y.X. Tan, F. Wang, J. Zhang, *Chem. Soc. Rev.* **2018**, *47*, 2130-2144. https://doi.org/10.1039/C7CS00782E.

[2] G. Kaur, R.K. Rai, D. Tyagi, X. Yao, P.Z. Li, X.C. Yang, S.K. Singh, *J. Mater. Chem. A.* **2016**, *4*, 14932-14938. https://doi.org/10.1039/C6TA04342A.

[3] M. Gholinejad, R. Khezri, S. Nayeri, R. Vishnuraj, B. Pullithadathil, *Mol. Catal*. **2022**, *530*, 112601. https://doi.org/10.1016/j.mcat.2022.112601.

[4] K. Lauder, A. Toscani, N. Scalacci, D. Castagnolo, *Chem. Rev*. **2017**, *117*, 14091-14200. https://doi.org/10.1021/acs.chemrev.7b00343.

The 30th Iranian Seminar of Organic Chemistry
February 7-9, 2025, Iran University of Science and Technology, Tehran, Iran

Extraction and characterization of polysaccharides from Trehala manna on *Cousinia stocksii*

Kiana Haji seyed javadi *[a], Mahdi Moridi Farimani [a], Elham Ahmadi [b]

[a] *Department of Phytochemistry, Medicinal Plants and Drugs Research Institute, Shahid Beheshti University, Tehran, Iran*

[b] *Department of Chemistry, Science Faculty, Golestan University, Gorgan, Iran*

Abstract:

"Mannas", that called "angabins" in Persian, are unique products of a dynamic insect-plant interaction and have various biological and ethno-medicinal importance. In this study, we investigated the isolation and characterization of trehala manna polysaccharides of *Cousinia stocksii* that serves as a host plant for the insect *Larinus trehalanus sp.* Hot water extraction was utilized to obtain the polysaccharides, and their molecular weight was determined through gel permeation chromatography (GPC). Furthermore, the monosaccharide composition was analyzed using gas chromatography (GC). The average molecular weight was about 800000 Da and galactose, fucose, deoxy-glucose, xylose, and arabinose monosaccharides were identified in the GC spectrum.

Keyword: *Cousinia stocksii*, *Larinus trehalanus*, trehala manna, polysaccharide

Introduction:

Carbohydrates are fundamental biomolecules widely distributed in nature, serving critical roles in both structural and metabolic functions across diverse organisms. Structurally, carbohydrates range from simple sugars to complex polysaccharides, and their functionality extends beyond providing energy. Due to their low toxicity and lack of significant side effects, polysaccharides play essential roles across food, pharmaceuticals, and materials industries and exhibit a diverse range of biological activities, such as immunomodulatory, anticancer, antioxidant, antimicrobial, and wound-healing properties. Among these, the anticancer potential of polysaccharides has been a focal point for extensive research.

Cousinia stocksii, a species from the Asteraceae family, has been traditionally used in medicine for hematuria and diarrhea. This plant serves as a host for the insect *Larinus trehalanus sp*. The female insects put their eggs individually on the host's stems, and cover them with their extinctions to protect the dryness and natural enemies. Once the eggs hatch, the larvae consume the plant's sap, leading to the formation of a gall known as trehala manna. Mannas are unique natural exudates produced through intricate plant-insect interactions. They are valued for diverse medicinal, culinary, and ecological significance, attributed to their complex sugar profiles and bioactive compounds. Beyond traditional uses, mannas have great potential in pharmacology and biodiversity preservation.

Materials and Methods:

Cousinia stocksii and trehala manna were collected from Kerman, Iran. The manna was mashed into smaller size and its polysaccharide extracted using hot distilled water and then freeze-dried. In order to obtain average molecular weight of polysaccharide and its constituent monosaccharides, gel permeation chromatography and gas chromatography were used, respectively. For the identification of monosaccharides using gas chromatography (GC), derivatization was performed via the silylation method.

Results and Discussion:

The results of GPC test showed an average molecular weight of 800000 Daltons and the result of the gas chromatography test after the derivatization of polysaccharide by the silylation method showed the presence of several monosaccharides including galactose, fucose, deoxy-glucose, xylose and arabinose.

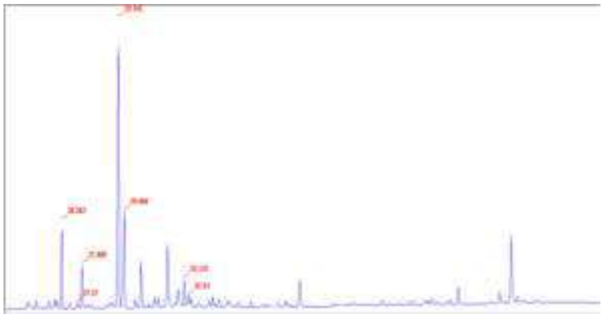

Figure 30 GC spectrum of trehala manna polysaccharide

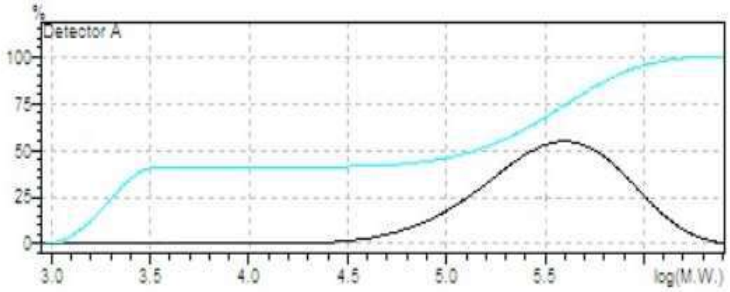

Figure 31 GPC spectrum of trehala manna polysaccharide

Conclusion:

In summary, the isolated polysaccharide was characterized with an average molecular weight of 800,000 Daltons, as determined by gel permeation chromatography. The monosaccharide composition analysis via gas chromatography after silylation derivatization revealed the presence of galactose, fucose, deoxy-glucose, xylose, and arabinose, emphasizing its structural complexity. These findings provide valuable insights into the biochemical properties of the polysaccharide.

References:

[1] X. Jia *et al.*, “Purification, structural characterization and anticancer activity of the novel polysaccharides from Rhynchosia minima root,” *Carbohydr Polym*, vol. 132, pp. 67–71, Jul. 2015, doi: 10.1016/j.carbpol.2015.05.059.

[2] S. Shahreyary-Nejad, S. Ali Asghar Fathi, F. M. Sc Student, and A. Professor, “Life history of the new weevil species producing trehala Larinus trehalanus (Col.: Curculionidae) on the medicinal plant Cousinia stocksii (Asteraceae) in Kerman region, Iran,” *Iranian Journal of Plant Protection Science*, vol. 48, no. 2, pp. 2017–2018, doi: 10.22059/ijpps.2017.212284.1006725.

[3] F. Ramezany, N. Kiyani, and M. Khademizadeh, “Persian Manna in the Past and the Present: An Overview,” *Am J Pharmacol Sci*, vol. 1, no. 3, pp. 35–37, Apr. 2013, doi: 10.12691/ajps-1-3-1.

The 30th Iranian Seminar of Organic Chemistry
February 7-9, 2025, Iran University of Science and Technology, Tehran, Iran

Synthesis of alkyl Polyglycosides (APG) Decyl glycoside and lauryl glycoside using acid catalyst by indirect method

1. Javad Askari Vartooni, 2.* Abbas Teimouri

Department of Chemistry, Payame Noor University, Isfahan, Iran, Email: chmjavadaskari@gmail.com

Keyword: Alkyl polyglycosides, PTSA, Decyl glycoside, lauryl glycoside

Alkyl polyglycosides (APG) are new surfactants that are excellent in terms of non-toxicity, safety and non-biodegradability and can be formulated with other surfactants. these surfactants have attracted more attention due to their non-sensitivity or very low sensitivity compared to some products with respect to consumer health and environmental compatibility because they do not contain sulfates and are prepared from renewable raw materials of glucose and fattybalcohol. [1-3].

alkyl polyglycosides are prepared from 1-decanol, 2-decanol, and octanol with glucose, which are soluble in water and exhibit good surface-active properties. these products exhibit suitable surface-active bonds due to the presence of a hydrophilic sugar moiety and a hydrophobic fatty alcohol residue. [4-5]

(APG) can be prepared directly (fisher) and indirectly through two steps of butanolysis and transesterification followed by neutralization and distillation, which was synthesized in a two-step process using glucose and fatty alcohols with different chain lengths. .[6- 13]

This process was carried out inside the reactor and also inside the laboratory flask at a certain temperature with different catalysts including zeolite and ptsa, etc. at a certain temperature.

alkyl polyglycosides were synthesized by various methods, and in one of the methods, it was synthesized by glucose and 2-decanol using zeolite catalyst and ptsa with a molar ratio of 1:6 and a mass ratio of 0.008 ptsa under optimal conditions with a reaction temperature of 120 ° c and a reduced pressure of 5 kpa with a relatively high yield, and h nmr, ftir, uv, and lcmass experiments were performed on it. Currently, researchers are still optimizing these surfactants, but to date, apgs are known as golden (green) surfactants.

Scheme:

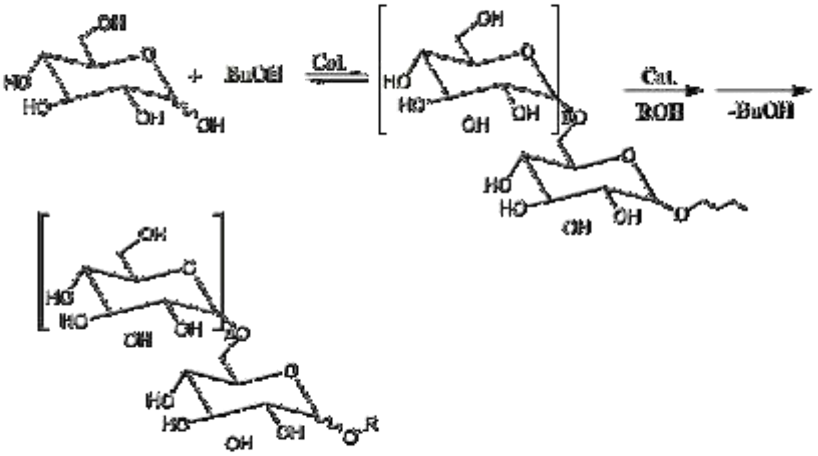

References:

[1] Piispanen, P.S. (2002). Synthesis and Characterization of Surfactants Based on Natural Products. Master Thesis, Kungl Tekniska Högskolan, Stockholm
[2]Rosen, M.J., & Dahanayake, M. (2000). *Industrial Utilization of Surfactant, Illinois*: AOCS Press, 1-85.
[3] Mehling, A., Kleber, M., & Hensen, H. (2007). Comparative studies on the ocular and dermal irritation of surfactants. *Food Chem. Toxicol., 14,* 747-758.
[4]Schmitt, T.M. (2001) Analysis of Surfactants. New York-Basel: Marcel Dekker Inc.
[5] R. Eskuchen, M. Nitsche in Alkyl Polyglycosides: Technology, Properties
and Applications (Eds.: K. Hill, W. von Rybinski, G. Stoll), Wiley-VCH,
Weinheim, 1997, Chapter 2.
[6] Ware, A.M., Waghmare, J.T., & Momin, S.A. (2007). Alkylpolyglycoside: Carbohydrate based surfactant. *J. Disper. Sci. Technol., 28*, 437-444.
[7] El-Sukkary, M.M.A., Syed, N., Aiad, I., & El-Azab, W.I.M. (2008). Synthesis and characterization of some alkyl polyglycosides surfactants. *J. Surfactants Deterg., 11(2)*, 129-13.
[8] Hill, K. (2009). Alkyl polyglycosides-where green meets performance. *Soft Journal*, *2*, 6-14

[9]Kurashima, K., Fujii, M., Ida, Y., & Akita, H. (2003). Enzymatic β-glycosidation of primary alcohols. *J. Mol. Catal. B-Enzym*., *26*(1-2), 87-98.
[10] Bastian, F., Suryani, A., & Sunarti, T.C. (2012). Peningkatan kecerahan pada proses sintesis surfaktan non ionik alkil poliglikosida (APG) berbasis tapioka dan dodekanol. *Reaktor Chem. Engineer. J., 14(3)*, 43-150.
[11] Chen, J., Li, J., Liu, K., Hong, M., You, R., Qu, P., Chen, M. (2019). Subcritical Methanolysis of Starch and Transglycosidation to Produce Dodecyl Polyglucosides. *ACS Omega*, *4(15)*, 16372-16377.
[12] Li, J. Y., Liu, Y. J., Zheng, G., Sun, Y., Hao, Y. N., & Fu, T. (2012). Preparation of Alkyl Polyglucoside Surfactants by One-Step. *Advanced Materials Research*, *550*, 75-79.
[13] Donat, R., & Demirel, V. (2022). Synthesis of some alkyl polyglycosides. *International Journal of Secondary Metabolite*.

The 30th Iranian Seminar of Organic Chemistry
February 7-9, 2025, Iran University of Science and Technology, Tehran, Iran

Innovative photocatalytic approach for methylene blue removal using g-C_3N_4/Bi_2O_3

Zolfa Afshari, Hakimeh Teymourinia, And Ali Ramazani *

Department of Chemistry, Faculty of Science, University of Zanjan, 45371-38791, Zanjan, Iran

Keywords: Graphitic carbon nitride (g-C_3N_4), photocatalyst, nanocomposite, dye degradation.

As industrial activities continue to rise, the influx of pollutants into water systems increases, resulting in a significant reduction of essential healthy water resources. This trend poses serious risks to environmental and human health, as well as to the broader ecosystem (Le, Le, Cheong, & Pung, 2022). Photocatalysts, particularly those based on nanomaterials, offer effective solutions for environmental pollution by utilizing light energy to degrade organic pollutants in water (Donga, Mishra, Abd-El-Aziz, & Mishra, 2021). In this study, we synthesized the nanocomposite g-C3N4-Bi2O3 through a hydrothermal method, followed by comprehensive characterization using techniques such as XRD, FE-SEM, FT-IR, and TEM. Our findings demonstrate that g-C3N4-Bi2O3 exhibits remarkable photocatalytic activity, achieving over 75% degradation of methylene blue dye in just 90 minutes. This highlights its potential for innovative applications in water purification and addressing water pollution challenges.

References:

Donga, C., Mishra, S. B., Abd-El-Aziz, A. S., & Mishra, A. K. (2021). Advances in graphene-based magnetic and graphene-based/TiO_2 nanoparticles in the removal of heavy metals and organic pollutants from industrial wastewater. *Journal of Inorganic and Organometallic Polymers and Materials, 31(2), 463-480.*

Le, A. T., Le, T. D. H., Cheong, K.-Y., & Pung, S.-Y. (2022). Immobilization of zinc oxide-based photocatalysts for organic pollutant degradation: A review. *Journal of environmental chemical engineering, 10*(5), 108505.

The 30th Iranian Seminar of Organic Chemistry
February 7-9, 2025, Iran University of Science and Technology, Tehran, Iran

Piperidine-4-carboxylic acid (PPCA) functionalized Fe_3O_4 nanoparticles (Fe_3O_4-PPCA): The efficient, green and reusable nanocatalyst for the synthesis of coumarin derivatives under solvent free conditions

Hassan Ghasemnejad-Bosra, Parsa Pourdadash-Miri

Department of Chemistry, Babol Branch, Islamic Azad University, Babol, Iran

Keyword: Piperidine-4-carboxylic acid (PPCA) functionalized Fe_3O_4 nanoparticles (Fe_3O_4-PPCA), substituted pyrano [2,3-h] coumarins, Solvent under, Green Catalyst

The coumarins (2*H*-1-benzopyran-2-ones) are important oxygen containing fused heterocycles used in drugs and dyes. Because of the great structural diversity of biologically active coumarins, it is not surprising that the coumarin ring system has become an important structural component in many pharmaceutical compounds. The synthesis of 3- substituted coumarins derivatives are currently of much interest, and various methods have been reported. [1-3]

Magnetic nano particles are efficient, readily available, high surface-area, resulting in high catalyst loading capacity and outstanding stability heterogeneous supports for catalysts. They show identical and sometimes even higher activity than their corresponding homogeneous analogues. More important, magnetic separation of the magnetic nano particles is more effective than filtration or centrifugation, simple, economical and promising for industrial applications. Among the various magnetic nano particles as the core, magnetic support, Fe_3O_4 nano particles are arguably the most extensively studied. [4-7]

The catalytic activity of Piperidine-4-carboxylic acid (PPCA) functionalized Fe_3O_4 nanoparticles (Fe_3O_4-PPCA) was investigated as a recoverable catalyst for the one-pot synthesis of novel substituted pyrano [2,3-*h*] coumarins linked to pyrazoline derivatives in high to excellent yield at room temperature under solvent free conditions (Scheme 1).

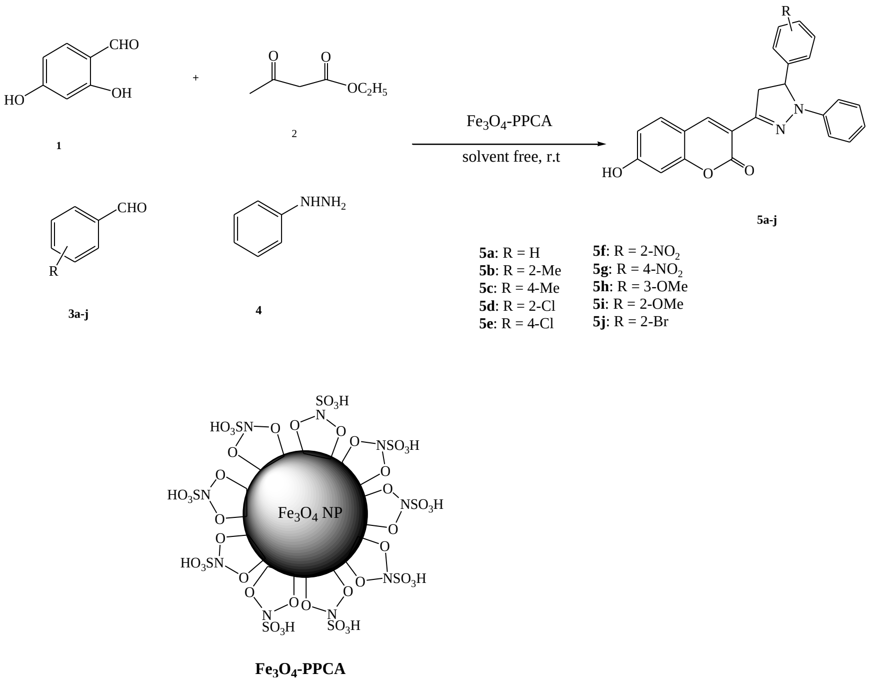

Scheme 1. Synthesis of pyrazolyl coumarins derivatives using Fe_3O_4-PPCA

We have developed a convenient methodology for the synthesis of coumarin linked to pyrazolines and pyrano [2,3-*h*] coumarins linked to 3-(1,5-diphenyl-4,5-dihydro-1*H*-pyrazol-3-yl)-chromen-2-one derivatives in high yields via a multi-component reaction protocol using Fe_3O_4-PPCA catalyst. This method has the advantages of low cost, short reaction time, high atom economy, convenience and efficiency. It also the characteristic aspects of this catalyst are rapid, simple and efficient separation by using an appropriate external magnet, which minimizes the loss of catalyst during separation and reusable for several times with little loss of activity.

References:

[1] Polshettiwar V, Luque R, Fihri A, Zhu H, Bouhrara M, Basset J. -M, *Chem. Rev.* 2011, 111: 3036.
[2] Patil P O, Bari S B, Firke S D, Deshmukh P K, Donda S T, Patil D A A, *Bioorg. Med. Chem.* 2013, 21: 2434.
[3] Khodabakhshi S, Karami B, *Tetrahedron Letter* 2014, 55: 7136.
[4] Shi Y, Zhou C -H, *Bioorg. Med. Chem. Lett.* 2011, 21: 956.
[5] Ghasemnejad-Bosra H, Faraje M, Habibzadeh S, Ramzaniyan-Lehmali F, *J. Serb. Chem. Soc.*, 2010, 75: 299.
[6] El-Aleem M A, El-Remaily A A, *Chin, J, Cat.,* 2015, 36: 1124.

[7] Shateriyan H, Aghakhanizadeh M, *Chin, J, Cat.*, 2013, 34: 1690.

The 30th Iranian Seminar of Organic Chemistry
February 7-9, 2025, Iran University of Science and Technology, Tehran, Iran

Computational Study of [3+2] Cycloaddition Reactions Between 2H-Azirines and Benzimidates Using DFT Study

Mina Haghdadi, Zahra Isazade, Parsa Pourdadash-miri*

Department of Chemistry, Babol Branch, Islamic Azad University, Babol ,Iran

Keywords: [3+2] cycloaddition reactions, DFT, azirine, benzimidate, regioselectivity.

Cycloaddition reactions, particularly [3+2] cycloadditions, are fundamental in the synthesis of heterocyclic compounds due to their versatility and efficiency[1]. These reactions are widely employed in the development of bioactive molecules and natural product synthesis, offering regioselective pathways to construct complex structures with high yields[2]. The interaction between dipoles and dipolarophiles facilitates these reactions, enabling the formation of five- or six-membered rings, often observed in pharmaceuticals, agrochemicals, and organic materials [3].

The [3+2] cycloaddition between azirines and benzimidates has garnered attention for its potential to produce diverse heterocyclic scaffolds under mild conditions [4]. However, understanding the mechanisms governing these reactions, particularly the influence of substituents on regioselectivity and product stability, remains a subject of theoretical and experimental investigation. This study employs Density Functional Theory (DFT) methods to explore these mechanistic pathways, offering insights into the reaction dynamics and factors affecting product formation. The article investigates the mechanisms of cycloaddition reactions, specifically [3+2] cycloadditions between 2H-azirines and benzimidates. Using computational methods within the Density Functional Theory (DFT) framework, with Gaussian software at the B3LYP/6-311G(d,p) level, the study examines transition states, intermediates, and product stabilities. The effects of substituents on product stability and reaction pathways were also analyzed. The findings indicate that the reactions are regioselective and occur via a stepwise mechanism.

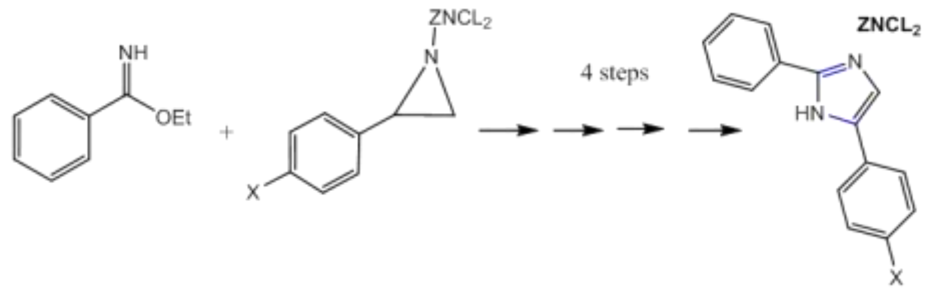

Scheme. The cycloaddition reaction of 2H-Azirines and Benzimidates in the presence of Lewis acid

References

١. Houk, K. N., & Gonzalez, J. (2001). "Mechanisms and Theoretical Studies of Cycloaddition Reactions." Angewandte Chemie International Edition, 40(8), 1340–1371.
٢. Domling, A., & Ugi, I. (2000). "Multicomponent Reactions with Isocyanides." Angewandte Chemie International Edition, 39(18), 3168–3210.
٣. Sustmann, R. (1971). "Regioselectivity and Frontier Molecular Orbital Theory." Tetrahedron Letters, 12(27), 2717–2720.
٤. Domingo, L. R., & Ríos-Gutiérrez, M. (2016). "Understanding the Reactivity of [3+2] Cycloadditions: A DFT Perspective." Chemical Reviews, 116(9), 4302–4372.

The 30th Iranian Seminar of Organic Chemistry
February 7-9, 2025, Iran University of Science and Technology, Tehran, Iran

Mechanistic and Computational Insights into the Regioselective Synthesis of N-Phenylpyrazoles via Cycloaddition Reactions

Mina Haghdadi , Ghazal Sina , Sarvin Easazadeh*

Department of Chemistry, Babol Branch, Islamic Azad University, Babol ,Iran

Keywords: DFT Study, Cycloaddition reaction, Zwitterionic thiolates,

The formation of carbon-carbon bonds remains a cornerstone of chemical synthesis, especially in the development of bioactive natural products and pharmaceuticals. Traditional methods for direct C-C bond formation often necessitate prefunctionalization, metal catalysts, or harsh reaction conditions. An alternative strategy involves the extrusion of small molecules, such as sulfur or nitrogen, concurrent with C-C bond formation. This approach provides a pathway to construct complex molecular scaffolds under relatively mild conditions, garnering significant attention from organic chemists [1].Nitrogen-containing heterocycles hold pivotal roles in the design of novel lead compounds for medical and pharmaceutical applications due to their broad-spectrum bioactivity. Among these, pyrazoles—particularly N-arylpyrazoles—are widely recognized as crucial pharmacophores in pharmaceuticals (e.g., Celebrex and Apixaban) and agrochemicals (e.g., Fipronil). Consequently, the development of novel synthetic methodologies to access these privileged heterocycles remains an active area of research [2-3].In this context, Chang et al. introduced a cycloaddition reaction between N-phenylhydrazonoyl chloride (a precursor of C-N-N dipoles) and pyridinium 1,4-zwitterionic thiolate, successfully synthesizing a diverse array of N-phenylpyrazole derivatives [4].

In the present study, we investigated the mechanistic details of these reactions through density functional theory (DFT) analysis. The results reveal that the reaction proceeds via an unusual [[3+3]-1] pathway, involving a formal [3+3] cascade cyclization followed by spontaneous ring contraction and sulfur extrusion from 4H-1,3,4-thiadiazine intermediates.

Additionally, the influence of substituents, both electron-withdrawing and electron-donating, was evaluated. The findings demonstrate that substituents on the aryl ring significantly affect reactivity. Thermodynamic and energetic analyses indicate that these cycloaddition reactions progress through a four-step process with complete regioselectivity. The reactivity indices and the polar nature of the cycloaddition reactions were further elucidated through the global electron density transfer (GEDT) values computed at the transition states. This comprehensive computational analysis sheds light on the mechanistic nuances of N-phenylpyrazole formation and offers valuable insights for designing novel synthetic approaches.

Scheme 1 Synthetic applications of pyridinium 1,4-zwitterionic thiolates and this work

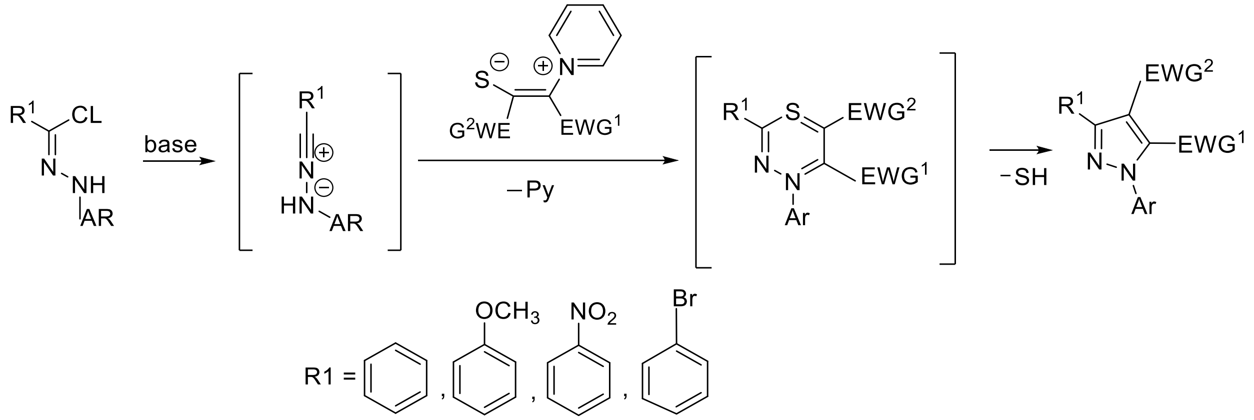

References

(1)F. Takahashi, K. Nogi and H. Yorimitsu, Intramolecular Desulfitative Coupling: Nickel-Catalyzed Transformation of Diaryl Sulfones into Biaryls via Extrusion of SO2, Org. Lett.,2018,**20**, 6601-6605
(2) B. Akkachairin, J. Tummatorn, N.Khamsuwan, C. Thongsornkleeb and S. Ruchirawat, DominoN2-Extrusion–Cyclization of Alkynylarylketone Derivatives for the Synthesis of Indoloquinolines and Carbocycle-Fused Quinolines, J. Org. Chem., 2018, **83**, 11254-11268
(3) S. A.Pujari, C. Besnard, T. Burgi and J. Lacour, A Mild and Efficient CH2-Extrusion Reaction for the Enantiospecific Synthesis of Highly Configurationally Stable Tröger Bases, Angew. Chem.Int. Ed., 2015, **54**, 7520-7523
(4) B. Cheng, B. Bao, W. Xu, Y. Li, H. Li, Synthesis of fully substituted pyrazoles from pyridinium 1,4-zwitterionic thiolates and hydrazonoyl chlorides via [[3+3]-1]pathway, J. Name., 2013, 1-3

The 30th Iranian Seminar of Organic Chemistry
February 7-9, 2025, Iran University of Science and Technology, Tehran, Iran

Antitumor performance of berberine-loaded cyclodextrin nanosponge-coated zinc oxide nanoparticles for 4T1 breast cancer therapy

Ali Abedi [a], Mostafa Arbabi [a], Elham Gholibegloo*[b]

[a] *Nanotechnology Research Center, Faculty of Pharmacy, Tehran University of Medical Sciences, Tehran 1416634793, Iran.*

[b] *Department of Synthesis Medicinal Organic Compounds, Institute of Medicinal Chemistry, Iranian Research Organization for Science and Technology (IROST), Tehran, Iran.*

Keyword: Zinc oxide nanoparticles, Cyclodextirn nanosponge, Berberine, Anti-cancer

Introduction:

Cancer treatment faces numerous challenges, especially in the precise and targeted delivery of drugs. Many efforts have been made to design smart drug delivery systems in recent years. This study explores a novel strategy that employs zinc oxide (ZnO) nanoparticles (NPs) coated with cyclodextrin nanosponges (CDNS) to enhance the delivery of berberine (BBR). BBR is a natural compound that has gained much attention from researchers in recent years due to its anti-cancer properties. It is very effective in controlling cancer cells by interrupting cell proliferation cycles and preventing angiogenesis, as well as inducing apoptosis. This performance is greatly improved, especially when used with advanced drug delivery systems. ZnO NPs enhance efficacy by inducing oxidative stress, which is a crucial factor in the cytotoxic effects of these NPs on cancer cells [1]. Meanwhile, CDNS facilitates controlled release and improves the stability of BBR, further enhancing its therapeutic potential [2, 3]. This modern approach promises to advance cancer treatment by increasing the precision of drug delivery and minimizing side effects.

Method:

Zinc acetate dihydrate ($Zn(CH_3CO_2)_2 \cdot 2H_2O$, 4 mmol) was dissolved in diethylene glycol (DEG, 40 mL) to prepare ZnO NPs with spherical morphology. The solution was transferred into a Teflon-lined stainless steel autoclave and heated from room temperature to 160 °C over 20 min. The temperature was maintained for 5 h. After completion, the reaction products were centrifuged at 5000 rpm for 30 min, washed with ethanol, and dried at 120 °C for 24 h. The synthesized ZnO NPs (0.5 g) were dispersed in dimethyl sulfoxide (DMSO, 10 mL). β-Cyclodextrin (β-CD, 1 mmol) was added to the dispersion, followed by triethylamine (Et_3N, 1 mL). The mixture was stirred for 3 h at room temperature. After that, epiclon (EPI, 8 mmol) was introduced, and the reaction was stirred for another 3 h. The coated ZnO NPs (ZnO@CDNS) were collected by centrifugation, washed with ethanol, and dried under vacuum for 24 h. BBR was loaded onto the coated ZnO NPs by preparing a solution of BBR in methanol (1 mL containing 2 mg BBR) and adding it dropwise to the ZnO@CDNS dispersion (0.6 g) in phosphate-buffered saline (PBS, 2 mL, pH 7.4). The mixture was shaken overnight at room temperature in the dark. The final BBR-loaded products (ZnO@CDNS/BBR) were separated by centrifugation at 8000 rpm for 10 min and washed twice with deionized water to remove any unloaded BBR.

Results and Discussion:

Several analytical methods were performed to confirm the structure and properties of the synthesized ZnOS@CDNS/BBR. Functional group interactions were established using FTIR, and proper coating of ZnO NPs with CDNS and BBR loading was ensured. Thermal stability was determined by TGA, while the detectable crystallinity of ZnO NPs was confirmed by XRD. Furthermore, SEM confirmed the detectable spherical morphology that the ZnO NPs were composed of. In addition, zeta potential analysis was also performed to evaluate the surface charge and colloidal stability. However, DLS was used to evaluate its hydrodynamic size distribution.

The presence and stability of loaded BBR were confirmed using UV-Vis spectroscopy as well as drug release kinetics in PBS at various pH, indicating controlled release behaviors for BBR. ZnO@CDNS/BBR was evaluated for its anti-cancer activity *in vitro* using MTT on 4T1 mouse breast cancer cells. The cells were subsequently incubated with different concentrations of ZnO@CDNS/BBR for 24, 48, and 72 h, followed by 4 h of incubation with MTT reagent. The formazan crystals produced were dissolved in DMSO and the absorbance was measured using a microplate reader at 570 nm. The findings indeed showed that ZnO@CDNS/BBR could significantly reduce the viability of 4T1 cancer cells in a dose- and time-dependent manner. In fact, at the highest concentration, ZnO@CDNS/BBR showed a significant reduction in cell viability, which indicates its potent anti-cancer activity.

References:

[1] Sawant VJ, Bamane SR. PEG-beta-cyclodextrin functionalized zinc oxide nanoparticles show cell imaging with high drug payload and sustained pH responsive delivery of curcumin in to MCF-7 cells. Journal of Drug Delivery Science and Technology. 2018 Feb 1;43:397-408.

[2] Gholibegloo E, Mortezazadeh T, Salehian F, Forootanfar H, Firoozpour L, Foroumadi A, Ramazani A, Khoobi M. Folic acid decorated magnetic nanosponge: An efficient nanosystem for targeted curcumin delivery and magnetic resonance imaging. Journal of colloid and interface science. 2019 Nov 15;556:128-39.

[3] Wang Y, Liu Y, Du X, Ma H, Yao J. The anti-cancer mechanisms of berberine: A review. Cancer management and research. 2020 Jan 30:695-702.

The 30th Iranian Seminar of Organic Chemistry
February 7-9, 2025, Iran University of Science and Technology, Tehran, Iran

Increasing the bioavailability Bergenin Isolated from Bergenia ciliata for Enhanced Antibacterial Activity

Kimia Rezaie[1], Soudeh Shiri[2*], Amir Asadzadeh[3]

[1] Department of Medical engineering, Urmia Branch Islamic Azad University, Urmia, Iran.

[2] Department of Organic Colorants, Institute of Color Science and Technology, Tehran, Iran.

[3] Department of Chemistry, Iran University of Science and Technology, Narmak, Tehran, Iran.

Address for correspondence: Institute of Color Science and Technology, Department of Organic Colorants, Tehran, Iran. Email address: soudehshiri1@yahoo.com

Abstract

Medicinal plants provide better compatibility with the human body due to their natural compounds. Bergenin, derived from *Bergenia ciliata*, has shown promise in managing diabetes, but its poor bioavailability limits effectiveness. To improve solubility and controlled release, niosomal carriers were used. This study evaluates bergenin-loaded niosomes, focusing on their antibacterial activity and mechanical properties, with scanning electron microscopy (SEM) employed for structural analysis.

Keywords: Bergenin, Niosomal carrier, Antibacterial Activity

1. Introduction

Bergenin, a bioactive compound from *Bergenia ciliata*, is a C-glycoside derived from 4-O-methyl gallic acid. Despite its therapeutic potential, its poor solubility and bioavailability restrict its use [1-3]. Niosomes, lipid vesicles made from cholesterol and non-ionic surfactants, offer an effective solution due to their enhanced stability, lower cost, and improved purity compared to liposomes. This study investigates the use of niosomal carriers to enhance the bioavailability and antibacterial properties of bergenin.

2. Experimental

2.1 Isolation and Extraction of Bergenin

Rhizomes of *Bergenia ciliata* were collected from Iran, dried, powdered, and subjected to ethanol extraction. One kilogram of powder was macerated in 4 liters of ethanol for three days at room temperature to produce a crude ethanol extract of bergenin.

2.2 Preparation of Niosomal Carriers

Non-ionic surfactant Span 60 and cholesterol were mixed at different ratios, dissolved in chloroform to form the organic phase. Bergenin (10 mg) was then combined with the surfactant-cholesterol mixture in a 1:1 ratio, dissolved in 2 mL of ethyl alcohol, and used to create the niosomal suspension.

3. Results and Discussion

The optimized niosomal formulation was analyzed using scanning electron microscopy (SEM) to assess its surface morphology, size, and shape. The SEM images confirmed that the niosomes had a smooth, well-formed structure with uniform size, meeting the desired formulation criteria. These findings suggest that the niosomal carriers are suitable for enhancing bergenin's solubility and bioavailability.

Refrences:

1. Ruby K, Chauhan R, Sharma S, Dwivedi (2012) J. Polypharmacological activities of Bergenia species. Int J Pharm Sci Rev 15:10–110

2. Venkatadri R, Guha G, Rangasamy AK (2011) Anti-neoplasticactivity of Bergenia ciliata rhizome. J Pharm Res 4:443–5

3. Haq IU, Mirza B, Park EJ, Burns BE, Marler LE, Kondratyuk TP (2013) Preliminary evaluation of cancer chemo preventive and cytotoxic potential of naturally growing ethanobotanically selected plants from Pakistan. Pharm Biol 51:316–28

The 30th Iranian Seminar of Organic Chemistry
February 7-9, 2025, Iran University of Science and Technology, Tehran, Iran

Synthesis of Bionanoparticles: A direct connection between bacteria and advanced catalysts for producing isochromeno[4,3-c]pyrazol-5(1H)-one

Maryam Robati[a], Eskandar Kolvari [a]*

a Department of Chemistry, Semnan University, P.O. Box 35131-19111, Semnan, Iran

⁎*Corresponding author, E-mail addresses: kolvari@semnan.ac.ir*

Keyword: Bacteria, Magnetic Nanoparticles, Bio-nanocomposite, Pyrazole fused to isocoumarins

One major challenge with nanocatalysts is their instability, often leading to aggregation and reduced catalytic efficiency. To address this, incorporating suitable supports can enhance their stability and improve access to active sites. Recent interest has grown in using natural materials, such as natural polymers and living cells, as catalysts and substrates for synthesizing various compounds, particularly heterocyclic compounds. Bacteria have a unique ability to grow and absorb metal ions even at high concentrations, thanks to functional groups like -NH_2 and -COOH in their cell membranes. The combination of bacterial cells with inorganic components leads to functional hybrids that can change material usage. For example, bacterial cells coated with metal nanoparticles can exhibit new functions. However, a challenge in loading nanoparticles onto bacterial cells is the lack of specific interactions, mainly due to the negative charge on both surfaces. The negative charge on Gram-positive and Gram-negative bacteria comes from teichoic acid and lipopolysaccharides, respectively. Loading methods aim to enhance contact between nanoparticles and bacterial surfaces and are categorized into two types. The first involves utilizing electrostatic interactions to precipitate cationic nanoparticles, resulting in the creation of cationic nanoparticle-labeled bacteria. The second method entails coating the bacterial surfaces with metal cations, followed by in situ synthesis of the nanoparticles. In this study, we examine the attachment of magnetic nanoparticles to the surface of E. coli bacteria using the first method: electrostatic attraction. This approach serves as an effective means of facilitating contact between bacterial surfaces and nanoparticles, which can subsequently be employed in the synthesis of pyrazole-fused isocoumarins [1,2].

In this study, using the first method, we attach magnetic nanoparticles synthesized according to previous protocols to the bacterial surface using electrostatic attraction. [3]. The washed bacteria were then reconstituted to their original volume using distilled water, after which the acidic nanoparticles were added dropwise to the solution over the course of one minute. The mixture of bacteria and nanoparticles washed using an external magnet, and dried in an oven. Comprehensive characterization of the Bac-Fe_3O_4 bio-nanocomposite was carried out using various analytical techniques. in the scheme 1, an overview of the Bac-Fe_3O_4 bio-nanocomposite can be seen in TEM analysis. (Scheme 1). The Bac-Fe_3O_4 bio-nanocomposite was isolated and used in the synthesis of pyrazole-fused isocoumarins (Scheme 2).

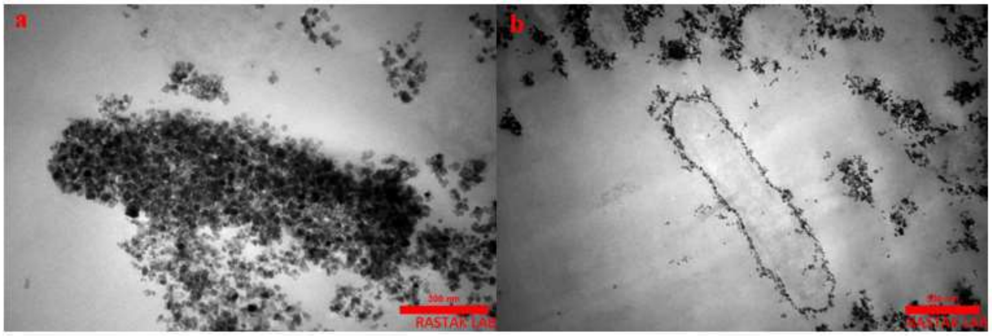

Scheme 1: TEM micrograph of Bac-Fe_3O_4 bio-nanocomposite

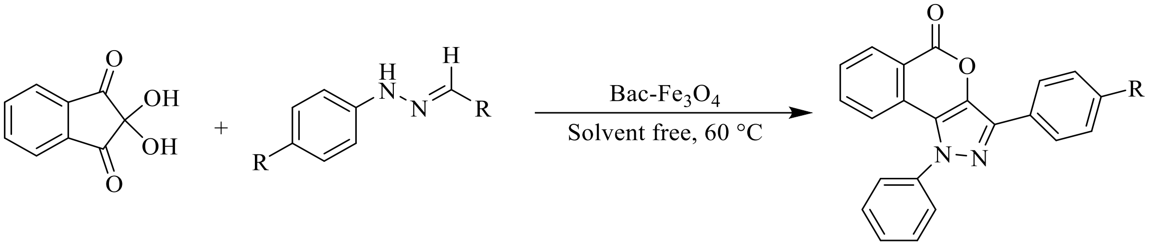

Scheme 12: Synthesis of pyrazole-fused isocoumarins by Bac-Fe_3O_4 bio-nanocomposite

References:

[1] Robati, M., et al., S. *Hierarchically assembled palladium catalysts: preparation of heterogeneous biocatalysts via a facial route for the Heck coupling reaction*. Transition Metal Chemistry, 2024, https://doi.org/10.1007/s11243-024-00617-3

[2] Devatha, C., et al., *Novel application of maghemite nanoparticles coated bacteria for the removal of cadmium from aqueous solution.* Journal of environmental management. 2020, https://doi.org/10.1016/j.jenvman.2019.110038

[3] Garjaei, S.S., et al., *Enhancing Photocatalytic Activity, Stability, and Separability of* TiO_2 *through Synthesis of* Fe_3O_4*@ Fibroin-*TiO_2 *Composite.* Chemistry Select, 2024, https://doi.org/10.1002/slct.202304658

The 30th Iranian Seminar of Organic Chemistry
February 7-9, 2025, Iran University of Science and Technology, Tehran, Iran

Evaluation of antioxidant properties of *polygonum aviculare L.* extract

Mahsa Fereydani [ab], Kambiz Larijani [a], Mohammad Hadi Givianrad [a*]

[a]*Department of Chemistry, Science and Research Branch, Islamic Azad University, Tehran, Iran*

[b] *Department of Chemistry, Faculty of Chemistry, Mazandaran University, Babolsar, Iran*

Keyword: *polygonum aviculare L.*, Maceration, Antioxidant, Flavonoid, Phenolic

Abstract

Introduction and Objective: *Polygonum aviculare* is an annual plant with small pointed leaves and pink flowers that grow in roadsides and shady areas. It has astringent properties and is used to treat diarrhea, remove kidney stones, and treat various ailments due to its high level of antioxidants. The study aimed to investigate the antioxidant properties of *Polygonum aviculare L.* plant extract.

Material and Methods: Initially, *Polygonum aviculare L.* hydroalcoholic extract was obtained by maceration and functional groups were determined by FT-IR. The extract's antioxidant activity was assessed using the free radical reduction method (DPPH), and its total phenolic and flavonoid content was measured.

Result: According to the findings, The FT-IR spectrum of this plant extract showed a broad and intense peak at 3416.09 cm-1 representing the stretching vibration of the hydroxyl group (OH) in water, phenolic compounds, and flavonoids. The peak observed at 2926.40 cm-1 corresponds to the presence of alkyl and CH groups, whereas the peak at 1616.91 cm-1 is associated with the C=O bond of the amide group and the C=C bond of aromatic rings. Additionally, the peaks at 1060.81 cm-1 are related to the presence of ether connections and the *Polygonum aviculare L.* extract contained a total phenolic content of 268.16 mg /g and a flavonoid content of 630 mg/g. The radical trapping activity was obtained IC_{50} = 202 / 68mg / L.

Conclusion: Our findings show that the hydroalcoholic extract of Polygonum aviculare L. has significant antioxidant activity and phenolic and flavonoid compounds and can be effective in the treatment of diseases such as cancer.

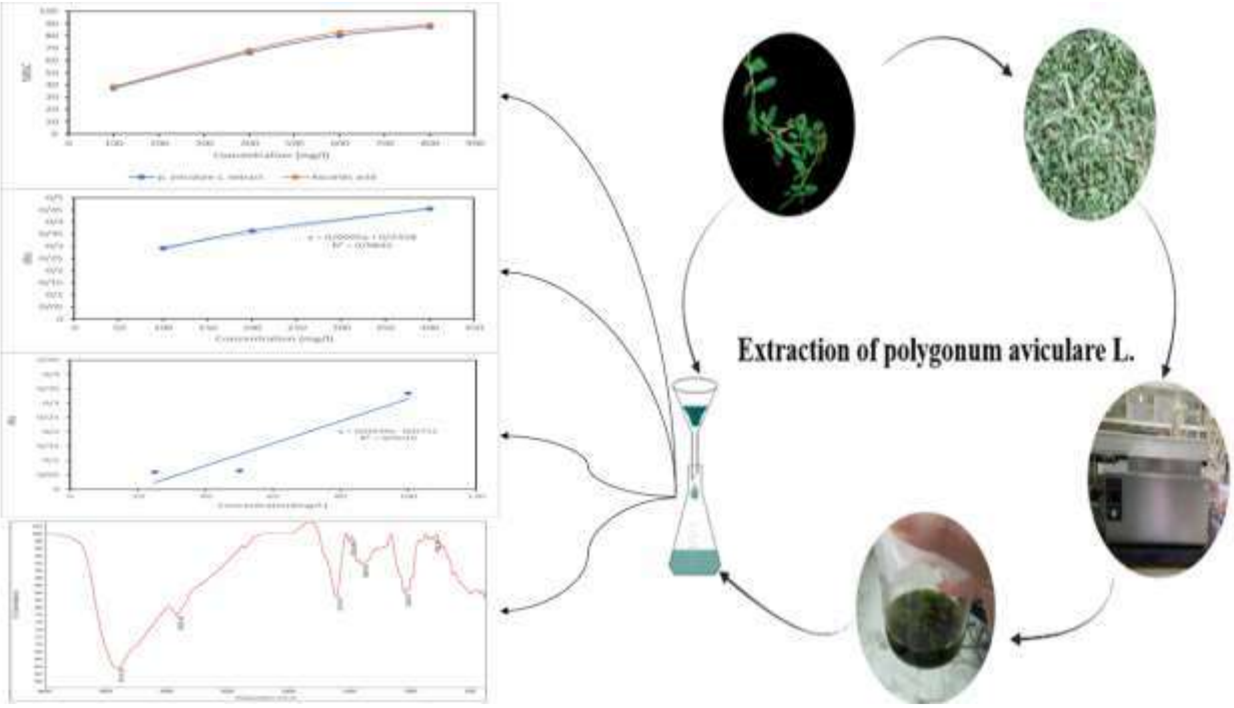

Figure 1. Polygonum aviculare L. extraction and evaluation of antioxidant properties of polygonum aviculare L. extract process. The obtained extract is green sludge in color and the efficient extraction efficiency was obtained 4.32%.

References:

١. Smith MA, Perry G, Sayre LM, Anderson VE, Beal MF, Kowall N. Oxidative damage in Alzheimer’s. Nature 1996; 382: 120-121.

٢. Kähkö nen MP, Hopia A, Vuorela HJ, Rauha J, Pihlaja K, Kujala T, et al. Heinonen M. Antioxidant activity of plant extracts containing phenolic compounds. J Agric Food Chem 1999; 47:3954-3962.

٣. Cerutti PA. Oxy-radicals and Cancer. Lancet 1994; 344:862-863.

٤. Kruawan K, Kangsadalampai K. Antioxidant activity, phenolic compound contents and antimutagenic activity of some water extract of herbs. Thai J Pharm Sci 2006; 30:28-35**.**

٥. Saboora A, Dadmehr K, Ranjbar M. Total phenolic and flavonoid contents and investigation on antioxidant properties of stem and leaf extracts in six Iranian species of wild Dianthus L. Iranian Journal of Medicinal and Aromatic Plants. 2013;29(2) :281-295.

٦. Sathishkumar R, Lakshmi P T V, Annamalai. A. Effect of drying treatment on the content of antioxidants in *Enicostemma littorale blume*. Research Journal of Medicinal Plant. 2009;3(3): 93-101.

٧. Lazarides M, Cowley K, Hohnen, P. Handbook of Australian Weeds. 7th ed. CSIRO Publishing;1997. p. 264.

The 30th Iranian Seminar of Organic Chemistry
February 7-9, 2025, Iran University of Science and Technology, Tehran, Iran

Green synthesis of graphene oxide nanoparticles by *Citrus Reticulate* peel extract and production of biodegradable and flame-retardant bioplastics based on chitosan

Delaram Takhti[a] , Anima Motamed[a] , Mahsa Fereydani[b*]

[a]*Department of Nanochemistry, Farzanegan 5's High School, Tehran, Iran*

[b] *Department of Chemistry, Faculty of Chemistry, Mazandaran University, Babolsar, Iran*

Keyword: *Graphene oxide nanoparticles, Citrus Reticulate peel, Chitosan, green synthesis, biodegradable*

Abstract

The increasing population and excessive plastic use in food packaging have led to significant environmental pollution. This project addresses these issues by designing and manufacturing biodegradable bioplastics based on chitosan, which decomposes naturally over time, offering a sustainable alternative to traditional plastics. *Citrus reticulate peel* extract was prepared using the maceration method, and graphene oxide nanoparticles were synthesized from a 2 mM solution of graphene oxide and the extract through a green method. The color change from yellow to black indicated successful nanoparticle formation. Field Emission Scanning Electron Microscopy (FESEM) and X-ray Diffraction (XRD) analyses were conducted to evaluate the morphological and crystalline properties of the nanoparticles. According to the results obtained from XRD and FESEM, the dimensions of the particles are between 20-50 nanometers. FESEM analysis also showed the nanoparticles' surface morphology, presenting both spherical and rod-like structures. Graphene oxide nanoparticles derived from the citrus extract and chitosan were utilized to enhance the thermal resistance of the bioplastics and reduce food spoilage. TGA investigated the thermal stability of bioplastic prepared by chitosan and synthesized graphene oxide nanoparticles and showed a weight loss of 14.78%. In this study, it was observed that the use of tangerine peel as a green source for the synthesis of graphene oxide nanoparticles was successful. The results also showed that a part of tangerine peel contains phenolic compounds that can act as a reducing agent for the synthesis of graphene oxide nanoparticles. Also, bioplastics containing these nanoparticles showed that they have good flame retardant and degradability properties that can be used in various environmental applications.

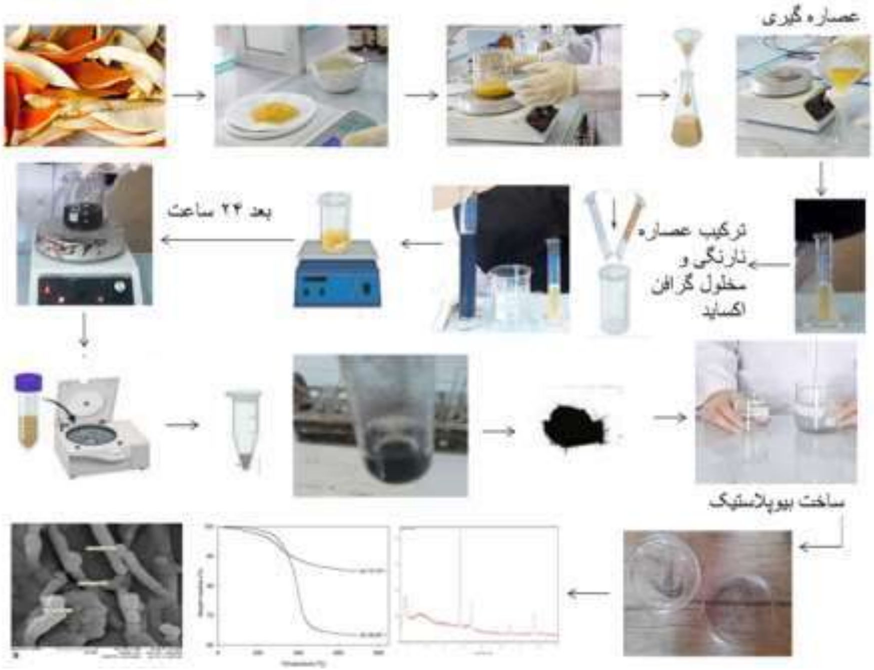

Figure 1. Steps for green synthesis of graphene oxide nanoparticles and the production of biodegradable bioplastics using them

References:

١. GHAREBEIGLOU M, IZADKHAH MSH, ERFAN NIYA H, ENTEZAMI A A. IMPROVING THE MECHANICAL AND THERMAL PROPERTIES OF CHEMICALLY MODIFIED GRAPHENE OXIDE/POLYPROPYLENE NANOCOMPOSITE. MODARES MECHANICAL ENGINEERING,2006, 16(8), 0-0.

٢. Jahed, E. , Almasi, H. , & Alizadeh khaled abad, M. Producing and optimizing the properties of chitosan-organic nanofiber biodegradable nanocomposite based containing O. vulgare subsp. gracile and C. copticum essential oils and its application on the oxidative stability of Canola oil. Iranian Food Science and Technology Research Journal, 2018, 14(5), 907-927. https://doi.org/10.22067/ifstrj.v14i5.71229

٣. Akhtar MS, Jutt DSR, Aslam S. et al. Green synthesis of graphene oxide and magnetite nanoparticles and their arsenic removal efficiency from arsenic-contaminated soil. Sci Rep 2024, 14, 23094. https://doi.org/10.1038/s41598-024-73734-9

٤. Karamali F, Asnaashari M, Farahmandfara R. Biodegradable packaging based on chitosan-potato starch biopolymer containing Apium graveolens seed extract for chicken fillets. FSCT 2023; 20 (137) :111-128

The 30th Iranian Seminar of Organic Chemistry
February 7-9, 2025, Iran University of Science and Technology, Tehran, Iran

Green synthesis of Ag-TiO_2 nanocatalysts by *Helianthus annuus* extract and evaluating their catalytic effect in removing sulfur from petroleum products

Fouzhan Khazaei[a], Zahra Atashbar Sarmi[a], Mahsa Fereydani[b*]

[a] *Department of Nanochemistry, Farzanegan 5's high school, Tehran, Iran*

[b] *Department of Chemistry, Faculty of Chemistry, Mazandaran University, Babolsar, Iran*

Keywords: Green synthesis, Nanocatalysts, Dibenzothiophene, Desulfurization, *Helianthus annuus*.

Abstract

Today, the oil industry is one of the most effective and largest industries and a major source of energy supply in the world and our country. The components of crude oil can include compounds such as thiols, sulfides, and thiophenes. The excessive sulfur content leads to corrosion and pollution. This study aims to synthesize Ag-TiO_2 desulfurization nanocatalysts using Helianthus annuus extract and evaluate their catalytic properties in removing sulfur from pollutants. Using the Maceration, Helianthus annuus extract was obtained, and silver nanoparticles were synthesized using a 2 mM $AgNO_3$ solution, while titanium dioxide nanoparticles were synthesized using a 2 mM $Ti(OH)_2$ solution through a green method. The color change of the first solution from yellow to brown indicates the formation of silver nanoparticles, and the color change of the second solution from yellow to pale yellowish-white suggests the formation of titanium dioxide nanoparticles. Field emission scanning electron microscopy (FESEM) and X-ray diffraction (XRD) were used to investigate the morphological and crystallographic properties of the nanoparticle's functional groups determined by Fourier-transform infrared spectroscopy (FT-IR) and the oxidation method was employed for desulfurization. The samples were analyzed using atomic absorption. Results showed that the nanoparticles had a well-defined crystalline structure with an average size of approximately 30-50 nanometers. FESEM images of Ag-TiO_2 nanocatalyst showed the nanoparticles were cubic and spherical. Increasing the weight of the nanocatalyst resulted in a larger number of active sites available for the reactants (97% for 22.5 ppm concentration of nanocatalyst), thereby improving the reaction conversion.

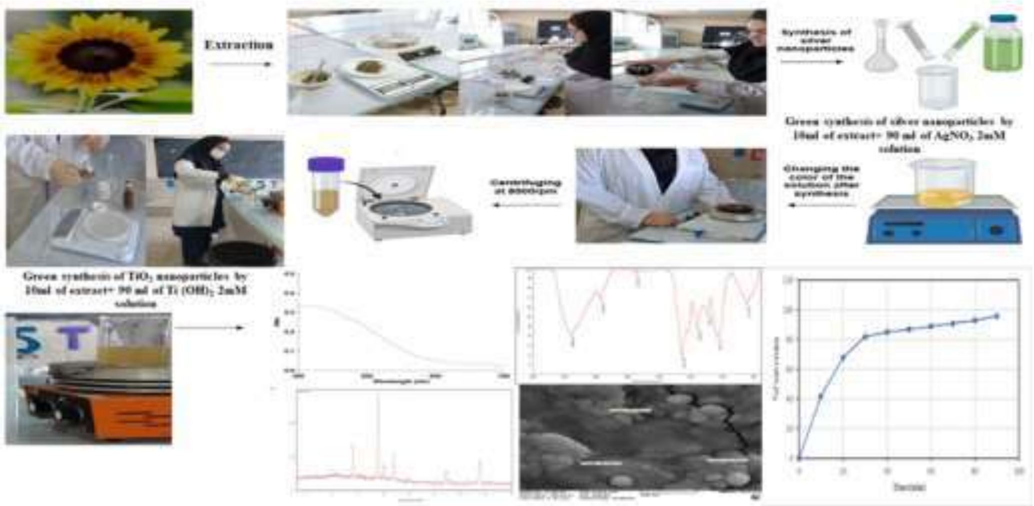

Scheme 1: Graphical abstract of the green synthesis process of Ag-TiO$_2$ nanocatalyst by *Helianthus annuus*.extract

References:

١. Mousavi S F, BAZYARI A, ALAVI AMLASHI S M. Oxidative Desulfurization of DBT over Vanadium-Based Catalysts. NASHRIEH SHIMI VA MOHANDESI SHIMI IRAN, 2022, 40, 4, 102, 101-109.

٢. NEISI AK, VOSOUGHI M, MOHAMMADI MJ, MOHAMMADI B, NAEIMABADI A, HASHEMZADEH B. PHYTOREMEDIATION OF BY HELIANTHUS PLANT. JOURNAL OF TORBAT HEYDARIYEH UNIVERSITY OF MEDICAL SCIENCES, 2014, 2(2), 55-65.

٣. HOJATKASHANI L. GREEN SYNTHESIS OF TITANIUM DIOXIDE NANOPARTICLES (TIO$_2$). THE APPLICATION OF CHEMISTRY IN ENVIRONMENT,2012, 3(11), 7-13.

٤. Shekari-Moghaddam R, Mohammadi M, Hekmatara SH, Darehkordi A, Salarizadeh P, Green Synthesis of Silver Nanoparticles by Cinnamon Extract and Evaluation of Their Photocatalytic Properties under Visible Light for Degradation of Methyl Orange Dye, Journal of Nano Materials, 2021, 13(45), 49-58. magiran.com/p2248098

٥. Biswajit S, Suman K, Sonali S, Green synthesis of nanosilver on TiO2 catalyst for application in the oxidation of thiophene, Chemical Engineering Science, 2019, Volume 199, Pages 332-341, ISSN 0009-2509, https://doi.org/10.1016/j.ces.2018.12.063.

Synthesis of palladium nanoparticles immobilized on functionalized chromium ferrite nanoparticles as efficient catalysts for cross-coupling reactions

Authors: Peyman Mohmadi, Arash Ghorbani-Choghamarani*, Arezo Monem

Affiliations*: Department of Organic Chemistry, Faculty of Chemistry and Petroleum Science, Bu-Ali Sina University, Hamedan, 6517838683, Iran, a.ghorbani@basu.ac.ir or arashghch58@yahoo.com, peyman.mohmadi120@gmail.com, arezomonem@yahoo.com.*

Keyword: magnetic nanoparticles, chromium ferrite, Heterogeneous Catalysis,Suzuki reaction

The use of magnetic nanocatalysts is a rapidly growing field for the development of sustainable and green processes. One of the main advantages of magnetic nanocatalysts is that they can be easily separated from the reaction medium using an external magnetic field and reused. This feature reduces costs and increases the efficiency of catalytic processes. Heterogeneous nanocatalysts are usually more stable than homogeneous catalysts and can perform well under harsh chemical reaction conditions [1-2]. Cross-coupling reactions, including Suzuki and Acetyl reactions, are considered important reactions in modern synthetic organic chemistry. They are used in various fields such as industry, pharmaceuticals, chemicals, pesticides, and polymers. In this study, the synthesis and characterization of palladium nanocatalysts immobilized on magnetic chromium ferrite nanoparticles were investigated [3]. Immobilization of palladium nanocatalysts on magnetic chromium ferrite nanoparticles leads to increased efficiency and stability in coupling reactions. Heterogeneous palladium nanocatalysts immobilized on chromium ferrite magnetic nanoparticles were characterized by various techniques such as FT-IR, EDX, ICP-OES, etc (Scheme 1).

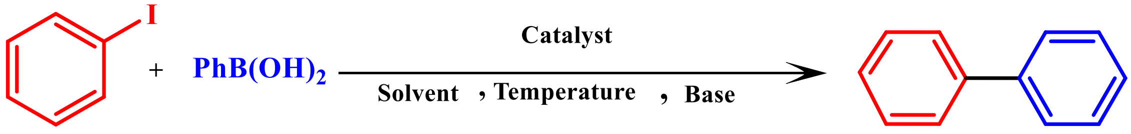

Scheme 1. Suzuki reaction

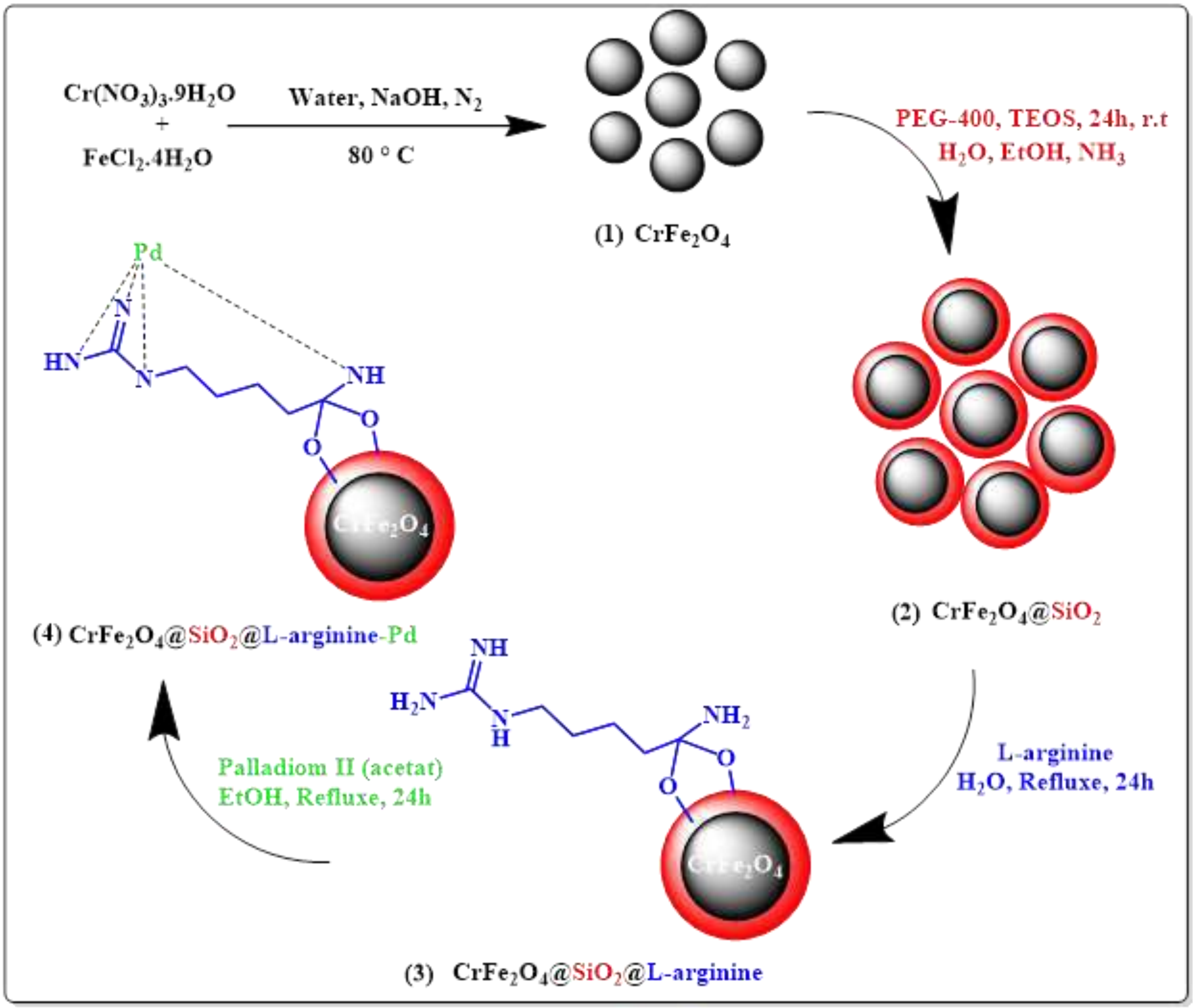

References:

١- Lu, F., Rodriguez-Garcia, J., Van Damme, I., Westwood, N. J., Shaw, L., Robinson, J. S., Warren, G., Chatzifragkou, A., McQueen Mason, S., Gomez, L., Faas, L., Balcombe, K., Srinivasan, C., Picchioni, F., Hadley, P., and Charalampopoulos, D. 2018. Valorisation strategies for cocoa pod husk and its fractions. Current Opinion in Green and Sustainable Chemistry 14: 80-88.

٢- Smith, J., et al. 2020. Palladium Nanocatalysts on Magnetic Nanoparticles for Suzuki Coupling Reactions. Journal of Catalysis 345: 123-130

٣- Ghorbani-Choghamarani, A., Tahmasbi, B., and Moradi, P. ٢٠١٦. Palladium–Spropyl-٢-aminobenzothioate immobilized on Fe_3O_4 magnetic nanoparticles as catalyst for Suzuki and Heck reactions in water or poly (ethylene glycol). Appl. Organomet. Chem., Vol. 306: 422-430

Synthesis of Triazoles in the Presence of 2,2'-Bipyridine-Based Copper Complex Stabilized on Magnetic Nanoparticles

Authors: Abolfazl Heydari[a], Meysam Yarie*[a], Morteza Torabi[a]

Department of Organic Chemistry, Faculty of Chemistry and Petroleum Sciences, Bu-Ali Sina University, Hamedan, Iran, myarie.5266@gmail.com

Keywords: 2,2'-bipyridine, Magnetic nanoparticles, triazole, copper complex

Magnetic nanoparticles serve as a support in catalytic systems, providing easy separation and reuse, thereby enhancing efficiency and reducing costs in chemical processes [1]. ۲،۲'-bipyridine plays a crucial role in catalysis by enhancing reaction rates and selectivity through its ability to form metal complexes [2,3]. Triazoles are important heterocyclic compounds that play a key role in drug development due to their antimicrobial properties [4,5]. In this study, the synthesis of triazole derivatives varied biological applications suchas by using a new copper complex catalyst we reported based on 2,2'-bipyridine immobilized on a magnetic support.

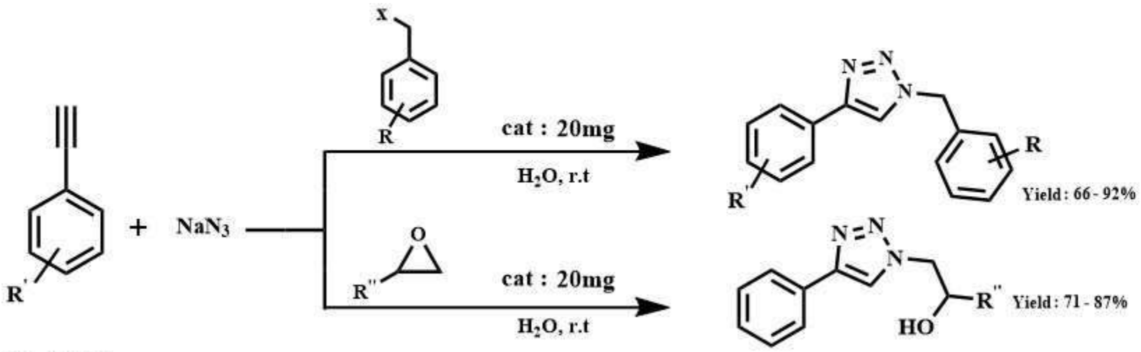

X = Cl, Br

R = 4-Cl, 4-Br, 4-Me, 4-Nitro, 3-Nitro, H

R' = H, 2-MeO

R''= Anisole, Ethyl, Phenyl, 1-Methoxybutane, 1-Methoxy-4-nitrobenzene

References:

1- Rossi, L. M., Costa, N. J. S., Silva, F. P., and Wojcieszak, R. **2014**. Green Chem., Vol. 16: 2906-2933.

2- Chawley, P., Suman, A. K., and Jagadevan, S. **2023**. In Persistent Pollutants in Water and Advanced Treatment Technology .pp. 213-233.

3- Zhang, B. **2019**. J. Med. Chem., Vol. *168*: 357-372.

٤- Sykam, K., Donempudi, S., and Basak, P. **2022**. J. Appl. Polym. Sci., Vol. *139*(32): 52771.

٥- Torabi, M., Zolfigol, M. A., and Yarie, M. **2023**. Arab. J. Chem., Vol. 16: 105090

The 30th Iranian Seminar of Organic Chemistry
February 7-9, 2025, Iran University of Science and Technology, Tehran, Iran

An efficient synthesis of 2-amino-6-alkoxy-4-arylpyridine-3,5-dicarbonitrile derivatives

Bagher Mohammadi[a,b]*, , Ali Ramazani [a] , Samira Darbidi [a]

[a] *Department of Chemistry, University of Zanjan, Zanjan, 45371-38791, Iran*

[b] *Department of Chemistry, Payame Noor University, P.O. Box 19395-3697 Tehran, Irant*

Keyword: Aryl pyridine, Potassium Sulfide, Malononitrile, Synthesis

Introduction

Pyridines are a significant class of organic compounds with diverse applications in pharmaceuticals, agrochemicals, and material science. The synthesis of these heterocyclic compounds has garnered extensive research interest due to their structural versatility and biological activity. Pyridine, a six-membered ring containing one nitrogen atom, serves as a fundamental scaffold in organic chemistry [1, 2].

Several synthetic strategies have been developed for the construction of pyridine derivatives, each offering unique advantages. Traditional methods include the Chichibabin synthesis, which involves the condensation of carbonyl compounds with ammonia or amines in the presence of a dehydrating agent. Modern approaches often employ transition metal-catalyzed reactions, such as palladium-catalyzed cross-couplings, to introduce various functional groups and appendages onto the pyridine ring[3, 4].

we would like to report herein a simple and mild method with higher atom economy for the preparation of highly functionalized of some poly-substituted pyridines (Scheme 1).

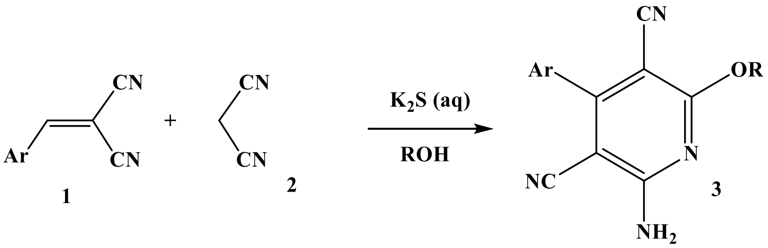

Scheme 1. Efficient Synthesis of highly substituted pyridines **3**.

Method

The reactions were carried out by adding arylidenmalononitrile 1, malononitrile 2 and potasium sulfide in alcoholic solvent. Then, the mixture was stirred at reflux condition. The reaction was complete within three hours to afford the highly substituted pyridines 3 in good yields. The product was filtered and dried. The structures of the products were confirmed by ^{1}H NMR, ^{13}C NMR, and IR spectroscopy.

Results and Discussion

A proposed mechanism is shown in Scheme 2. The first step may involve Michael addition of malononitrile anion **4** to arylidene malononitrile **2** to form intermediate **5**. This intermediate undergoing cyclization reaction will form cyclic intermediate 6, which undergoes imine isomerization along with oxidation [5] and produces highly substituted pyridine **3** (Scheme 2).

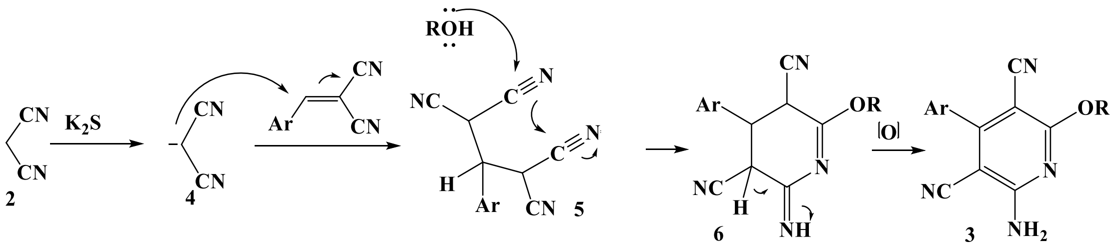

Scheme 2: Proposed mechanism for the formation of 2-amino-6-alkoxy-4-arylpyridine-3,5-dicarbonitriles **3**

In conclusion, the method has several advantages, including high yields of products, easy experimental workup, the use of simple and available starting materials, high atom economy, and eco-friendly and mild reaction conditions

References:

1. Alizadeh, S.R. and M.A. Ebrahimzadeh, *Antiviral activities of pyridine fused and pyridine containing heterocycles, a review (from 2000 to 2020).* Mini Reviews in Medicinal Chemistry, 2021. **21**(17): p. 2584-2611.

2. De, S., et al., *Pyridine: the scaffolds with significant clinical diversity.* Rsc Advances, 2022. 12(24): p. 15385-15406.

3. Arlan, F.M., et al., *Recent developments in the synthesis of polysubstituted pyridines via multicomponent reactions using nanocatalysts.* New Journal of Chemistry, 2021. **45**(28): p. 12328-12345.

4. Allaka, T.R. and N.K. Katari, *Synthesis of pyridine derivatives for diverse biological activity profiles: a review.* Recent Developments in the Synthesis and Applications of Pyridines, 2023: p. 605-625.

5. Sridhar, M., et al., *Novel ZnCl2-catalyzed one-pot multicomponent synthesis of 2-amino-*3, 5-dicarbonitrile-6-*thio-pyridines.* Tetrahedron Letters, 2009. **50**(27): p. 3897-3900.

The 30th Iranian Seminar of Organic Chemistry
February 7-9, 2025, Iran University of Science and Technology, Tehran, Iran

Development of Bio-hydrogels Reinforced with Ash for Efficient Oil-Water Separation

Parsa Pahlavani, Hamideh Sarreshtedar Aslaheh, Ahmad Poursattar Marjani*

Department of Organic Chemistry, Faculty of Chemistry, Urmia University, Urmia, Iran

**a.poursattar@urmia.ac.ir*

Keywords: Bio-coposite, Ash, oil/water separation

Introduction

It is known that all kinds of pollution can damage the environment, and one of these things is oil spills, which often happen because many industries pour wastewater into water, which causes these things to mix with the water and damage the environment in the world. This is the case in paint, textiles, and leather industries. Hydrogels have properties such as water absorption, and the ability to swell and change, which make them suitable for many pharmaceutical and medical applications [1]. This project aims to use water-absorbing hydrogels for water-oil separation.

Method

Mix biocomposites with ash in water in a flask. Heat until it reaches suitable viscosity. Dissolve the crosslinker in water and add it to the mixture. Then, add monomers and more water, combining well. Disperse on cotton fabric and let it dry for oil-water separation.

Results and discussion

Infrared spectroscopy (**IR**) was employed to analyze the functional groups in the bio-hydrogels. Incorporating ash into the hydrogel introduces a new peak at 688 cm^{-1}, attributed to Si–O or M–O (metal-oxygen) vibrations from silicates or metal oxides in the ash, confirming its successful integration. Other spectral changes, including enhanced O–H stretching at 3424 cm^{-1}, shifted C–H stretching at 2927 cm^{-1}, and intensified peaks at 1384 cm^{-1} (carboxylates) and 1273 cm^{-1} (C–O–C stretching), suggest improved hydrogen bonding, structural reinforcement, and cross-linking within the hydrogel matrix.

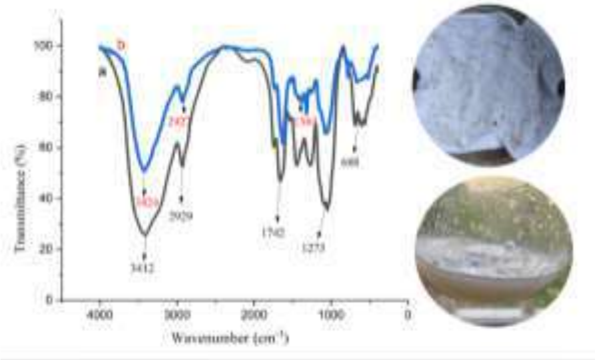

References

[1] Ejeromedoghene O, Abesa S, Akor E, Omoniyi AO. *Materials Today Communications.* 2023 Jun 1;35:106063.

The 30th Iranian Seminar of Organic Chemistry
February 7-9, 2025, Iran University of Science and Technology, Tehran, Iran

Synthesis and Modification of a Hematite Based Photocatalyst for Drug Degradation in Water

Sakineh Mohammadi, Hamideh Sarreshtehdar Aslaheh, Ahmad Poursattar Marjani*, Parsa Pahlavani

Department of Organic Chemistry, Faculty of Chemistry, Urmia University, Urmia, Iran

**a.poursattar@urmia.ac.ir*

Keywords: Green chemistry, Photocatalyst, Drug degradation, Hematite

Introduction

Water is an essential and scarce resource for life. Antibiotics can disrupt the microbial balance in wastewater and affect the degradation of organic materials. Methods for removing drugs from water include physical, biological, and photocatalytic processes that convert pollutants into harmless substances [1].

Method

In this study, the Ag@Fe_2O_3 photocatalyst was synthesized using chemical methods. Fe_2O_3 nanoparticles were enhanced by adding silver nitrate and using lavender essential oil to achieve optimal properties for environmental applications and renewable energy.

Results and Discussion

For the evaluation of the modified sample, FTIR analysis was discussed. The peak within specific wavenumber ranges indicates distinct chemical bond: 3200–3900 cm^{-1} signifies the O–H bond, 2925 and 2854 cm^{-1} represents the asymmetric and symmetric C–H bond, 1636 cm^{-1} is attributed to the C=O bond, 533 cm^{-1} region corresponds to the Metal-Oxygen bond (related to Iron Oxide).

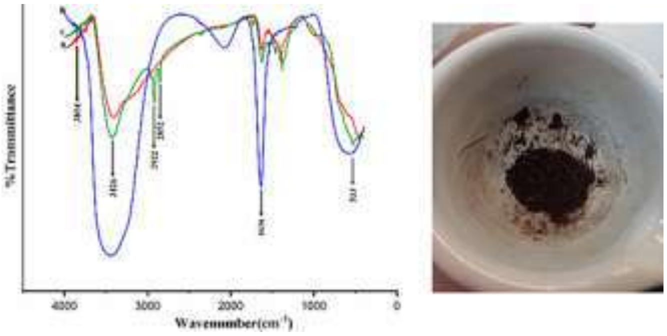

FTIR spectrum of Fe_2O_3 **(a)**, Lavender **(b)** and Ag@Fe_2O_3@Lavender **(c)**

References:

[1]. Sayadi MH, Ahmadpour N, Homaeigohar S. 2021 Feb;11(2):298.

Synthesis and application of carbon sphere designed by Zr-MOF as a catalyst for preparation of phenylnicotinonitriles

Zahra Torkashvand,[a] Milad Mohammadi Rasooll,[a] Hassan Sepehrmansourie [b] and Mohammad Ali Zolfigol*[a]

[a]Department of Organic Chemistry, Faculty of Chemistry and petroleum sciences, Bu-Ali Sina University, Hamedan 6517838683, E-Mail: zolfi@basu.ac.ir & mzolfigol@yahoo.com.
[b]Faculty of Converging Science and Technologies, University of Qom, Qom, Iran, 37185-359.

Keywords: Carbon sphere, Metal-organic frameworks, Porous catalyst, Phenylnicotinonitriles

Metal-organic frameworks (MOFs) as a group of porous materials are architectural structures consisting of the coupling of a metal group and an organic group. These structures are composed of metal elements that are ionic inside or outside their core and organic ligands that coordinate with metals [1]. MOFs are used in various fields such as storage and transport of gases, separation of materials, removal of pollutants from the environment, synthetic catalysis and pharmaceuticals [2]. Also, carbon spheres (CSs) are a category of organic compounds that synthesized in a green way and eventually don't lead to the production of pollution by interring the environment [3]. Additionally, CSs are very porous and in combination with the catalyst can cause a significant increase in the efficiency of the catalytic activity. so, we have succeeded in creating a greener and a more efficient catalyst by combining the carbon spheres with MOF. Pyridine-carbonitrile compounds are a class of organic compounds that are used in many medicinal substances with necessary properties in the context of the growth of body cells. In this report, the catalytic activity of CS@Zr-MOFs in the preparation of pyridine-carbonitriles was investigated as an important group of organic compounds with biological properties (**Scheme 1**).

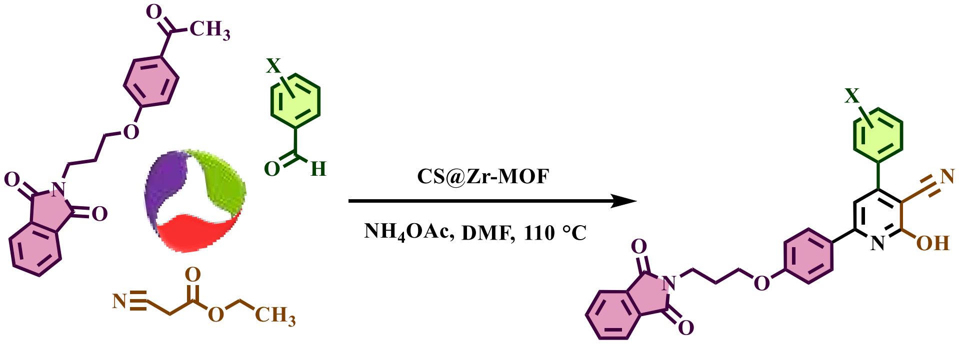

Scheme 1. Synthesis of pyridine-carbonitriles by CS@Zr-MOFs.

References:

(1) James, S. L. Metal-organic frameworks. Chemical Society Reviews, 2003, 32, 276-288.

(2)Zhou, H. C.; Long, J. R. Yaghi, O. M. Chemical reviews, 112, 673-674 (2012).

(3) Deshmukh, A. A., Mhlanga, S. D. & Coville, N. J. Carbon spheres. Mater. Sci. Eng. R 70, 1-28 (2010).

The 30th Iranian Seminar of Organic Chemistry
February 7-9, 2025, Iran University of Science and Technology, Tehran, Iran

Design and synthesis of Zr-MOF@Cu$(OAc)_2$ as a heterogeneous catalyst for the synthesis of pyrazolo[3,4-*b*]pyridine derivatives via a CVABO

Zahra Torkashvand,[a] Milad Mohammadi Rasooll,[a] Hassan Sepehrmansourie,[b] Mohammad Ali Zolfigol*[a] and Narges Alipour gomary [a]

[a]Department of Organic Chemistry, Faculty of Chemistry and petroleum sciences, Bu-Ali Sina University, Hamedan 6517838683, E-Mail: zolfi@basu.ac.ir & mzolfigol@yahoo.com.
[b]Faculty of Converging Science and Technologies, University of Qom, Qom, Iran, 37185-359.

Keywords: Heterogeneous catalyst, Anomeric effect, Metal-organic frameworks, Pyrazolo[3,4-*b*]pyridine.

In the last decade, significant progress has been made in the field of porous materials. Metal-organic frameworks (MOFs) are an amazing example of porous materials. The crystalline structure along with adjustable pores has made this category of porous compounds to be used in many fields, such as drug delivery, catalyst, photocatalyst, sensor and gas absorption [1]. The use of MOFs as a catalyst has attracted widespread scientific interest among scientists. Therefore, many organic compounds have been synthesized with the help of MOFs catalyst. Heterocycles are an important class of organic compounds that are widely used in the pharmaceutical, agricultural, and dye industries. Pyrazolo[3,4-*b*]pyridines have many medicinal and biological properties, such as anti-cancer, anti-bacterial, anti-fungal, etc. [2]. Therefore, for the synthesis of new pyrazolo[3,4-*b*]pyridines with biological cores, the Zr-MOF@Cu$(OAc)_2$ catalyst, which has a metal-organic framework support, has been used. These materials are synthesized under solvent-free conditions at 100 °C. The high reaction rate, short reaction time, high product yield, and catalyst separation capability are important features of the above research, which show the value of introducing this catalyst (**Scheme 1**).

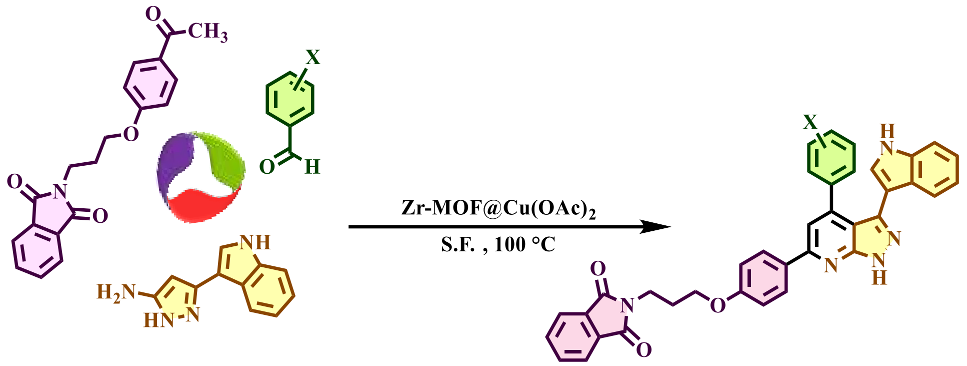

Scheme 1: Preparation of pyrazolo[3,4-*b*]pyridine derivatives using Zr-MOF@Cu(OAc)$_2$ as a catalyst.

References:

[1] Yang, F., Du, M., Yin, K., Qiu, Z., Zhao, J., Liu, C., ... & Pang, H. Small, (2022). 18(11), 2105715.

[2] Elsherif, M. A. Journal of Applied Pharmaceutical Science, (2021) 11(6), 118-124.

The 30th Iranian Seminar of Organic Chemistry
February 7-9, 2025, Iran University of Science and Technology, Tehran, Iran

The Synthesis of 6-Substituted Pyrido[2,3-*d*]pyrimidine-2,4(1*H*,3*H*)-diones Using Aminomethylene Malondialdehydes and 6-Aminouracils

Ahmad Rashidi*, Mehdi M. Baradarani
Department of Chemistry, Faculty of Science, University of Urmia, Urmia 57153-165, Iran

* *E-mail: rashidi.ahmad@gmail.com*

Keyword: Pyridopyrimidines, Aminouracil, Indolenine, Aminomethylene Malondialdehydes

In recent years, our research group has been developing a project centered on the synthesis of novel indolenines and bisindolenines, and reactions of them with the Vilsmeier reagent to produce aminomethylene malondialdehydes.[1-4] These malondialdehydes, as 1,3-dicarbonyl compounds, can be used to produce new heterocyclic systems.[1,3,4]

In this reaserch, we have extended our studies of aminomethylene malondialdehydes **1a-e** and demonstrated the synthesis of pyrido[2,3-*d*]pyrimidine-2,4-diones **3** by condensations with various 6-aminouracils **2a-c** (Scheme). After some preliminary experiments, it was found that a mixture of aminomethylene malondialdehyde **1a** and 6-aminouracil **2a** afforded 6-(3,3-dimethyl-3*H*-indol-2-yl) pyrido[2,3-*d*]pyrimidine-2,4(1*H*,3*H*)-dione **3a** in 79% yield in refluxing acetic acid for 12 h. Encouraged by this success, we extended this reaction to various aminomethylene malondialdehydes **1b–e** and 6-aminouracils **2b–c** under similar conditions (acetic acid at reflux), furnishing the respective compounds **3b–k** in good yields.

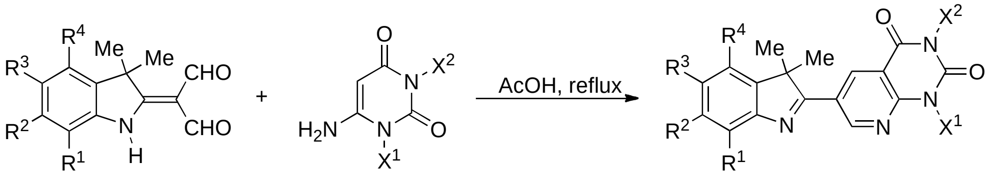

1a R^1, R^2, R^3, R^4=H
1b R^1=Cl, R^2, R^3, R^4=H
1c R^1=Me, R^2, R^3, R^4=H
1d R^1, R^2, R^4=H, R^3=OMe
1e R^1, R^3=H, R^2, R^4=Cl

2a X^1, X^2=H
2b X^1=Me, X^2=H
2c X^1=Me, X^2=Me

3a-k

References:

1. M. M. Baradarani, A. Afghan, F. Zebarjadi, K. Hasanzadeh, J. A. Joule, *J. Heterocyclic Chem.*, 2006, 43, 1591
2. M. Helliwell, A. Afgan, M. M. Baradarani, J. A. Joule, *Acta Crystallogr Sect E,* 2006, 62, o737
3. A. Rashidi, A. Afghan, M. M. Baradarani, J. A. Joule, *J. Heterocycl. Chem.,* 2009, *46*, 428
4. M. M. Baradarani, H. Zare Fazlelahi, A. Rashidi, J. A. Joule, *Arkivoc* 2018*, (iv), 114.*

The 30th Iranian Seminar of Organic Chemistry
February 7-9, 2025, Iran University of Science and Technology, Tehran, Iran

One-pot synthesis of bis spiro piperidines using nanocellulose/BF_3/Fe_3O_4 as catalyst

Authors: Parisa Moharrami Korblagh[a] , Abdolhamid Bamoniri*[a] , BiBi Fathemeh Mirjalili[b]

Corresponding author Email: bamoniri@kashanu.ac.ir

a) Department of Organic Chemistry, Faculty of Chemistry, University of Kashan, Kashan, Iran

b)Department of Chemistry, College of Sciences, Yazd University, Yazd, Iran

Keywords: Bis-spiro piperidine, Nanocellulose, One-pot synthesis, Boron tri fluride, Magnetite

Abstract

A highly impressive one-pot multicomponent synthesis of bis-spiro piperidine derivatives has been reported by performing the reaction of formaldehyde, aromatic aniline and dimedone [1].This reaction was performed in the presence of a catalyst in ethanol solvent at room temperature[2].

Using nanocellulose/BF_3/Fe_3O_4 as a Lewis acid and heterogeneous catalyst for the first time[3]. Nano-cellulose/BF_3/Fe_3O_4 has been synthesized and characterized with FE-SEM, TEM, FT-IR, TGA, BET, XRD and VSM analysis. The advantages of this catalyst are low reaction time, convergence, simplicity of operation, and recyclability. The beneficial features of this method are soft reaction position, no column chromatographic purification and high yield of products. All derivatives were distinguished by FT-IR and ^1H NMR spectroscopy.

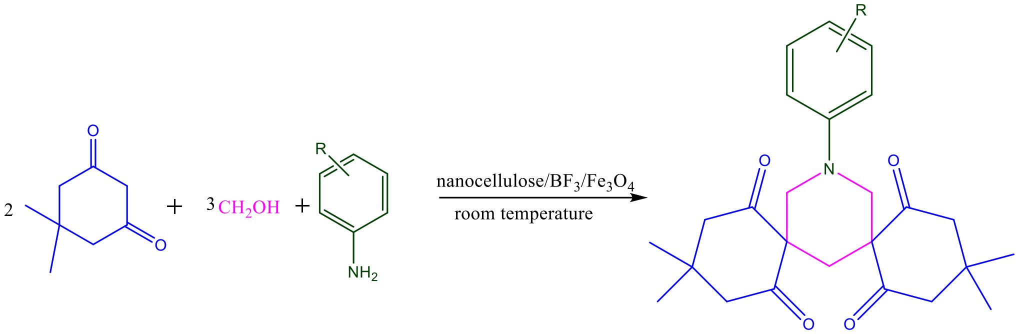

References:

[۱] B. M. Reddy, P. M. Sreekanth, P. Lakshmanan, Sulfated zirconia as an efficient catalyst for organic synthesis and transformation reactions. *J. Mol. Catal.*, **2005,** 237(1-2), 93-100.

[2] C. Mukhopadhyay, S. Rana, R. J. Butcher. $FeCl_3$ catalysed two consecutive aminomethylation at the α-position of the β-dicarbonyl compounds: an easy access to hexahydropyrimidines and its spiro analogues. *Tetrahedron Lett.*, **2011**, 52(32), 4153-4160.

[3] S. Azad, B.F. Mirjalili, Fe_3O_4@ nano-cellulose/TiCl: a bio-based and magnetically recoverable nano-catalyst for the synthesis of pyrimido [2, 1-b] benzothiazole derivatives. *RSC Adv.*, **2016**, 6(99), 96928-96962.

The 30th Iranian Seminar of Organic Chemistry
February 7-9, 2025, Iran University of Science and Technology, Tehran, Iran

Design of Organic Compounds with Lyotropic Liquid Crystal Properties for Applications in Green Chemistry: A Theoretical Descriptive Study

Dheyaa Adnan Hanoosh

E-Mail: Dia.adnan@gmail.com

PhD student in physical chemistry

Iran University of Science and Technology

Abstract

In the face of growing environmental challenges, green chemistry has emerged as a scientific approach to minimize the environmental impact of chemical processes by adopting sustainable materials and techniques. Lyotropic liquid crystals (LLCs) are promising candidates in this context due to their unique properties that combine the characteristics of liquids and crystalline materials, making them ideal for eco-friendly applications. This study focuses on the theoretical design and analysis of organic compounds with LLC properties, emphasizing their potential role in enhancing sustainable chemical processes.

The research explores the relationship between the chemical structure of LLCs and their unique physical properties, including self-assembly, phase transitions, optical behavior, and thermal stability. Key applications discussed include their use in improving chemical catalysis, reducing chemical waste, and advancing clean energy technologies, such as solar cells and pollutant removal systems. The study also proposes innovative design models and highlights the potential of LLCs in bridging theoretical principles with practical applications.

This research contributes to the fields of environmental science and applied chemistry by providing a comprehensive framework for utilizing LLCs to develop efficient and sustainable chemical processes. The findings underscore the importance of LLCs in supporting green chemistry goals, promoting environmental sustainability, and addressing industrial and ecological challenges.

Introduction

In light of the growing environmental challenges, green chemistry has emerged as a scientific approach aimed at reducing the environmental impact of chemical activities through the adoption of more sustainable materials and techniques. Lyotropic liquid crystals represent one of the promising fields in this context, as they possess unique properties that combine the characteristics of both liquids and crystalline materials, making them ideal for environmentally friendly applications.

Organic compounds with lyotropic liquid crystal properties are a key focus in scientific research due to their numerous advantages, including controllable physical properties, compatibility with environmental standards, and their potential use in innovative technologies such as chemical separation systems, enhanced catalyst efficiency, and nanomaterial fabrication. Moreover, these compounds could play a critical role in designing more efficient and cost-effective processes, supporting the transition to a sustainable future.

This research aims to design and analyze organic compounds with lyotropic liquid crystal properties using a theoretical approach based on collecting and analyzing data from previous studies. The focus will be on exploring the relationship between the chemical structure of these compounds and their unique physical properties, while highlighting their potential applications in green chemistry. We also seek to propose innovative design models that contribute to enhancing the scientific understanding of these materials and their role in supporting environmental sustainability.

This research serves as a new contribution to the field of environmental sciences and applied chemistry, aiming to bridge theoretical principles with practical applications to develop new materials that meet the demands and challenges of our time.

Definition and Physical Properties of Lyotropic Liquid Crystals

1. Definition: Lyotropic liquid crystals are organic or composite compounds that belong to the liquid crystal family, but are characterized by their ability to transition between clear liquid phases and liquid crystal phases depending on the concentration of the solvent and temperature. Unlike conventional liquid crystals that form over a specific temperature range, lyotropic liquid crystals depend on the concentration of the components in the solution for their formation.

These crystals are primarily composed of amphiphilic molecules (compounds with both hydrophilic and hydrophobic parts), allowing them to form liquid crystalline phases when dissolved in solvents. These materials exhibit unconventional properties due to their ability to self-organize in solvents, forming geometrically organized structures such as lamellar, cylindrical, or cubic phases in some cases.

2. Physical Properties: Lyotropic liquid crystals possess several unique physical properties that distinguish them from other materials:

A. Self-Assembly:

- Lyotropic liquid crystals have the ability to self-assemble, where their molecules organize themselves into specific geometric structures such as lamellar, cylindrical, or cubic phases. This self-organization enhances their ability to perform various vital functions in industrial applications such as filtration and chemical catalysis.

B. Interaction with Solvents:

- These crystals have the ability to form liquid crystalline phases and clear liquid phases in different solvents, and these phases vary depending on the solute concentration and temperature. Lyotropic liquid crystals exhibit unique properties like polarization and light refraction, which depend on the arrangement of molecules in the liquid crystal phase.

C. Phase Transition:

- This type of liquid crystal is characterized by dynamic transitions between phases when there is a change in concentration or temperature. For example, the material can transition from a liquid phase to a liquid crystal phase or vice versa, making them materials with variable properties based on the surrounding environment.

D. Optical Properties:

- Lyotropic liquid crystals possess the ability to interact with light in various ways, such as polarization and light diffraction. This makes them useful in optical applications such as liquid crystal displays and variable lenses.

E. Viscosity:

- The viscosity of lyotropic liquid crystals varies depending on temperature and concentration. In general, these materials have a lower viscosity compared to solid materials, which makes them suitable for applications that require flexible and easy movement of molecules.

F. Flexibility:

- Lyotropic liquid crystalline compounds exhibit high flexibility in their form and structure, allowing them to adapt to environmental conditions such as high or low temperatures, which enhances their applications in materials that require significant flexibility, such as biodegradable materials.

G. Thermal Stability:

- This type of liquid crystal has good thermal stability, allowing it to function across a wide range of temperatures without losing its liquid crystalline properties. However, at certain temperatures, it may transition into a liquid phase.

The 30th Iranian Seminar of Organic Chemistry
February 7-9, 2025, Iran University of Science and Technology, Tehran, Iran

The Relationship Between Green Chemistry and Lyotropic Liquid Crystals

1. How Can These Compounds Support Environmentally Friendly Chemical Processes?

Green chemistry is a scientific field that focuses on developing more sustainable and less harmful methods for chemical processes, through the adoption of safer materials and techniques. The importance of lyotropic liquid crystals in supporting these processes arises from their unique properties, which make them ideal for environmentally friendly applications.

A. Chemical Catalysis and Lyotropic Liquid Crystals:

- Lyotropic liquid crystals possess the ability to self-organize into specific geometric structures when dissolved in solvents, making them suitable as catalysts in chemical reactions. These compounds can improve reaction efficiency by providing a controlled and balanced environment for chemical interactions.

For example, lyotropic liquid crystals can act as green catalysts or green solvents to enhance chemical reactions without relying on harmful solvents or toxic materials. Compared to traditional solvents, these compounds can improve performance in reactions due to their chemical stability and ability to facilitate precise chemical interactions.

B. Reducing Chemical Waste:

- Environmental sustainability is one of the core goals of green chemistry, and lyotropic liquid crystals contribute to this by helping reduce chemical waste generated during chemical processes. When used as solvents or reaction systems, these compounds help reduce the need for organic solvents or toxic chemicals that are often harmful to the environment.

In processes such as chemical separation or extraction of active materials, lyotropic liquid crystals can be employed to reduce the volume of waste generated. This helps improve material consumption efficiency and reduces the environmental impact of the process.

2. Exploring Potential Applications in Waste Reduction and Clean Energy Production

A. Reducing Waste Using Lyotropic Liquid Crystals:

- Lyotropic liquid crystals can help reduce chemical waste in processes such as chemical separation, molecular recovery, and material recycling. These compounds have the ability to transition between liquid and liquid crystal phases, which allows for selective separation of chemicals during industrial processes.

For instance, in environmental reactions like purification or chemical filtration, lyotropic liquid crystals can be used to filter pollutants from liquids or gases more effectively, which reduces toxic waste and prevents its release into the environment.

- Other applications include their use in biological reactions, such as biocatalysis, where these compounds can improve environmental processing in industries like food production or environmental management. They help reduce the impact of chemical waste by minimizing the volume of materials disposed of.

B. Using Lyotropic Liquid Crystals in Clean Energy Production:

- Some lyotropic liquid crystals possess properties that make them suitable for use in clean energy production. For example, they can be employed in solar cells as part of the active systems that convert solar energy into electrical power. Lyotropic liquid crystals can enhance the efficiency of light absorption and conversion into energy.

- Ongoing research in this area has shown that lyotropic liquid crystals can be utilized in electronic devices that generate energy through electrical reactions, helping to improve energy efficiency and reduce dependence on traditional energy sources, such as fossil fuels.
- In the field of renewable energy, lyotropic liquid crystals may also contribute to the development of more efficient energy storage devices, such as flexible solar surfaces or modern batteries, boosting the ability to store renewable energy for later use.

Design of Organic Compounds:

1. Analyzing the Chemical Components Affecting Liquid Crystal Properties

Designing organic compounds with liquid crystal properties requires studying the chemical components that significantly influence how these compounds form and how their molecules organize to create liquid crystalline phases. Here's a detailed analysis of these components:

A. Amphiphilic Molecules:

- Amphiphilic molecules are one of the main components in the design of lyotropic liquid crystalline compounds. These molecules consist of a hydrophilic (water-loving) part and a hydrophobic (water-repelling) part. This dual characteristic allows them to self-organize in solvents, with the hydrophobic part aggregating together while the hydrophilic part interacts with the solvent.
- Importance: These molecules are crucial in forming liquid crystalline phases in solvents with certain ratios of hydrophilic and hydrophobic components. Careful design of amphiphilic molecules can help improve thermal stability, pressure responsiveness, and the ability to interact with other components in chemical reactions.

B. Molecular Engineering and Topological Distribution:

- The molecular structure of amphiphilic molecules (such as linear, cylindrical, or lamellar shapes) significantly impacts how the molecules organize in the liquid crystalline phase. Some molecules prefer forming cylindrical phases (such as the nematic phase), while others favor lamellar or cubic phases.
- Importance: By adjusting the molecular length and geometrical arrangement, researchers can design compounds with liquid crystalline properties that respond precisely to specific conditions like temperature, pressure, or solvent concentration.

C. Substitution Groups:

- The chemical groups introduced into molecules, such as alkyl groups, aromatic groups, or polar groups, affect the chemical stability and ability to form liquid crystalline phases.

- Importance: Selecting the right functional groups can enhance solvent interactions, increase stability, improve electrical conductivity, or achieve desirable dynamic behaviors such as interaction with radiation or chemical catalysis.

D. Environmental Effects:

- The effect of concentration, temperature, and pressure plays a crucial role in determining the phase that compounds will adopt. In some cases, these variables can be adjusted to achieve optimal molecular interactions.

2. Presentation of Proposed Models Based on Previous Literature

Based on existing research, several design models for organic compounds with liquid crystalline properties emerge as promising options in this field. Below are some of these proposed models:

A. Amphiphilic Molecule Model with Lamellar Phases:

- Properties: In this model, molecules are designed to form lamellar phases, where the molecules arrange in layers, allowing compounds to provide electrical response and high solvent interaction.
- Applications: These systems can be used in environmental applications like biological absorption or chemical filtration, where stability in layered structure and flexible interactions with solvents are needed.

B. Amphiphilic Molecule Model with Cylindrical Phases (Nematic Phase):

- Properties: In this model, molecules adopt a cylindrical shape, where the molecules align in parallel directions, improving electrical conductivity and light response.
- Applications: This model has applications in liquid crystal displays, where these compounds could be used to design high-efficiency devices or environmental sensors to measure changes in environmental conditions or chemical pressures.

C. Amphiphilic Molecule Model with Cubic Phases:

- Properties: Molecules self-assemble into cubic phases, which feature a highly stable arrangement of molecules that provide greater chemical stability when dealing with solvents or chemical reactions.
- Applications: This model may be useful in separation systems or filtration in industrial chemical reactions where chemical stability and reactivity are crucial.

D. Amphiphilic Molecule Model with Mixed Phases:

- Properties: Some compounds are designed to form mixed phases between cylindrical and lamellar, allowing the materials to respond flexibly to different conditions such as temperature or solvent concentration.
- Applications: This model can be used in separation technologies and industrial manufacturing where high-performance materials are required to function in changing environments, such as in green chemistry applications.

Comparative Study:

1. Comparison of Designed Compounds with Those Currently Used in Green Chemistry:

In this section of the research, we will conduct a comparison between the designed organic compounds and those currently used in green chemistry. The goal is to analyze the key differences between the new compounds and traditional ones currently in use in environmental and industrial applications, and highlight the advantages of the designed compounds in improving sustainable chemical processes.

A. Designed Lyotropic Liquid Crystal Compounds:

- The newly designed lyotropic liquid crystal compounds are based on self-interacting properties and precise physical response to environmental conditions. These compounds are characterized by their ability to adapt to solvents and chemical reaction conditions, which may enhance reaction efficiency and reduce the waste generated.
- In green chemistry, these compounds may offer environmental advantages such as:
    - Reducing the use of toxic solvents.
    - Improving selectivity in chemical reactions.
    - Utilizing renewable resources in design.

B. Compounds Currently Used in Green Chemistry:

- The traditional compounds currently used in green chemistry range from green solvents to environmental catalysts. Examples include:
    - Environmental solvents such as dimethyl sulfoxide (DMSO) and ethanol.
    - Biological catalysts or organic materials like enzymes that catalyze chemical reactions in sustainable environments.
- While these traditional compounds offer many benefits, they also have some limitations, such as:
    - Weak response to changing environmental conditions.
    - Higher energy consumption in certain processes.

    - Large waste production in some chemical reactions.

C. Comparison Between Designed and Traditional Compounds:

- Environmental Responsiveness: The designed compounds may show greater flexibility in handling multiple solvents and changing conditions (temperature, pressure), while traditional compounds tend to be more stable but less responsive.

- Reaction Efficiency: The newly designed compounds may enhance reaction efficiency, leading to reduced material and time usage, while traditional compounds may require more energy or additional solvents for some reactions.

- Environmental Sustainability: The new compounds may offer improved environmental sustainability by reducing waste or relying on renewable materials, compared to some traditional compounds that may contribute to environmental pollution due to toxic solvents or secondary chemicals.

2. Economic and Environmental Feasibility Analysis of These Compounds:

In this section of the research, an economic and environmental analysis will be performed to assess whether the designed lyotropic liquid crystal compounds could serve as sustainable economic and environmental alternatives compared to the compounds traditionally used in green chemistry.

A. Economic Feasibility:

- Initial Cost: The design of lyotropic liquid crystal compounds may require higher initial research investments to develop the chemical structure and production processes, which could lead to higher upfront costs compared to some traditional compounds.

- Operating Costs: On the other hand, if the designed compounds provide higher reaction efficiency or reduce the need for solvents and other materials, they may help in reducing operating costs in the long run.

- Long-Term Economic Sustainability: If the new compounds prove effective in reducing waste and increasing productivity, they could achieve economic gains over the long term, making them commercially viable.

B. Environmental Feasibility:

- Waste Reduction: Lyotropic liquid crystals could contribute to reducing chemical waste generated during chemical processes, particularly in processes that use toxic or non-degradable solvents.

- Pollution Reduction: By using green compounds, the environmental pollution caused by toxic chemicals can be reduced. Additionally, the reduced use of organic solvents decreases environmental risks.

- Overall Environmental Improvement: The design of organic compounds with lyotropic liquid crystal properties could help in reducing energy consumption in certain processes, contributing to an overall improvement in environmental efficiency.

C. Environmental and Economic Effectiveness Analysis:

- When comparing the designed compounds with traditional ones, we will look at the environmental impacts of manufacturing and using these compounds, along with the overall costs, including initial, operational, and waste disposal costs.

- The goal is to determine whether the designed lyotropic liquid crystals provide more sustainable solutions from both environmental and economic perspectives compared to the traditional compounds used in green chemistry.

Expected Results

١. Comprehensive Database of Organic Liquid Crystalline Compounds and Their Potential Applications in Green Chemistry:

  - The database is expected to include detailed information on organic liquid crystalline compounds that are significant in green chemistry. This information will cover molecular structures, liquid crystalline phases (such as nematic, smectic, and cubic phases), and their physical properties like viscosity and thermal stability.

  - For instance, previous studies on lecithin compounds have shown their liquid crystalline properties to be useful in chemical separation systems and environmentally friendly emulsifiers. Such compounds can be documented in the database, with details on their interactions with solvents and efficiency in reducing industrial waste.

  - Additionally, the database will include information on compounds studied for specific applications, such as amphiphilic molecules used in designing bio-membranes or biological filters.

٢. Design of Virtual Compounds with Enhanced Properties for Environmental Applications:

  - Using prior research and computational modeling tools like Material Studio, virtual compounds will be designed to improve molecular properties. These compounds will be tailored for applications such as enhancing catalyst efficiency or reducing energy consumption.

  - For example, compounds based on amphiphilic polymers can be designed to form liquid crystalline phases like lamellar phases, making them suitable for chemical separation processes that reduce pollution from liquid waste.

  - A prior study on Brij-type surfactants demonstrated the ability of these compounds to improve the performance of separation systems using liquid crystalline membranes. This concept can inspire the design of new compounds combining thermal stability and environmental flexibility.

٣. Proposing New Applications for These Compounds to Improve Sustainable Chemical Processes:

  - Based on data analysis and virtual designs, new applications will be proposed to enhance sustainable chemical processes. For instance:
    - Using compounds with liquid crystalline properties in clean energy production, such as in the design of flexible solar cells that rely on liquid crystals to improve light absorption.
    - Employing liquid crystalline compounds like those in hexagonal phases for environmental purification systems to remove pollutants from water.
  - Another example is the use of liquid crystalline compounds like ethoxylated polymer-based compounds in dynamic chemical separation processes, which have proven effective in reducing the need for harmful organic solvents.

Analysis and Importance of Expected Results:

- Developing a focused database will serve as a valuable tool for researchers and industrial practitioners working in green chemistry, helping them select the most suitable compounds for specific applications.
- The design of virtual compounds not only aims to reduce waste or improve chemical reactions but also provides practical solutions that can be tested and implemented on a large scale.
- The proposed new applications will open new horizons for the use of liquid crystalline compounds in improving environmental processes, contributing to advancing sustainability goals and providing integrated economic and environmental solutions.

The Importance of the Research

1. On the Scientific Level:

A. Bridging the Gap Between the Design of Organic Compounds and Their Applications in Green Chemistry:

- This research aims to bridge the gap between molecular design of organic compounds and their practical applications in green chemistry, a field focused on developing environmentally friendly processes that minimize negative environmental impacts.

- For example, previous studies on lecithin compounds and amphiphilic sulfonic acids have shown significant potential in chemical separation and environmental purification applications. Studying and analyzing these compounds can provide useful models for designing new ones.

B. Enhancing Theoretical Research on Liquid Crystalline Materials:

- Liquid crystalline materials are a multidisciplinary research area that combines physics, chemistry, and environmental studies. This research enhances the theoretical understanding of these materials by studying their interactions with solvents and their impact on environmental efficiency.
- An example includes studies on the properties of Brij-type surfactants, which form liquid crystalline phases when dissolved in aqueous solvents, making them valuable in separation and purification technologies.

2. On the Environmental Level:

A. Providing Innovative Solutions to Environmental Issues Using Eco-Friendly Organic Compounds:

- The research contributes to developing eco-friendly compounds as alternatives to traditional organic solvents that cause environmental pollution. Organic liquid crystalline compounds have the ability to self-organize, forming geometric patterns that help reduce waste and enhance reaction efficiency.
- For instance, amphiphilic polymers, such as ethoxylated polymers, have been shown to improve purification processes and treat polluted water. These compounds can reduce energy consumption and the use of toxic solvents.

B. Reducing Pollution from Industrial Processes:

- Studies on liquid crystalline hydrogels have demonstrated their effectiveness in absorbing pollutants from water, such as heavy metals and organic contaminants. These compounds can be used to design environmental filters that reduce industrial pollution.

3. On the Industrial Level:

A. Developing More Efficient and Sustainable Industrial Processes:

- This research seeks to introduce liquid crystalline compounds that enhance the efficiency of industrial processes such as chemical separation, energy production, and fluid purification.

- Example: Research on amphiphilic sulfonates has shown their effectiveness as separation agents in the food and pharmaceutical industries, paving the way for their application in major industries.

B. Reducing Costs and Improving Sustainability:

- The use of organic liquid crystalline compounds can reduce production costs by improving reaction efficiencies and lowering energy consumption.
- For instance, liquid crystals are used in flexible solar cells to enhance light absorption and improve energy conversion efficiency, making them an attractive option for renewable energy industries.

C. Advancing Manufacturing Techniques:

- Liquid crystalline compounds can be used to develop new materials with improved properties, such as adaptive smart materials or nano-membranes for separation and purification.
- Studies on liquid crystalline polymers have demonstrated their effectiveness in manufacturing high-performance membranes used in pharmaceutical and chemical industries.

Conclusions

The results of this research demonstrate that organic lyotropic liquid crystals (LLCs) offer significant potential in green chemistry due to their unique properties that combine the characteristics of both liquids and crystalline materials. These compounds can be utilized in sustainable chemical processes such as chemical separation and improving catalytic efficiency, which helps reduce the environmental impact associated with toxic solvents and chemicals. Additionally, the research shows that these compounds could play a critical role in clean energy production, such as their use in solar cells and energy storage devices, contributing to environmental sustainability.

Furthermore, potential applications of LLCs in chemical waste reduction have been analyzed by demonstrating their ability to reduce the reliance on harmful solvents and traditional chemicals, which is a crucial step towards a more sustainable industry. Using computational modeling to analyze the chemical structure of these compounds, innovative design models have been proposed that can be applied to achieve more effective and efficient environmental applications.

Based on these results, it can be concluded that lyotropic liquid crystals represent a promising tool for supporting the shift towards a sustainable future in various industries, including renewable energy, green catalysis, and chemical waste management .

Recommendations

Based on the results of the research, several future steps are recommended to enhance the use of lyotropic liquid crystal compounds (LLCs) in green chemistry:

١. Explore more amphiphilic compounds: Further studies should focus on designing new amphiphilic compounds with enhanced properties such as thermal stability and the ability to interact with various solvents. This will improve the environmental efficiency of chemical processes.

٢. Investigate industrial applications: More experiments should be conducted in chemical industries to test the effectiveness of LLCs in chemical separation, material purification, and clean energy production. These compounds should be applied in multiple industrial contexts such as water treatment and pollutant removal.

٣. Integrate computational modeling techniques: It is recommended to develop virtual design models using advanced computational techniques like Material Studio to analyze the impact of molecular structure on the physical properties of LLCs, thus accelerating the discovery of new applications.

٤. Collaboration between researchers and industries: Strengthening collaboration between researchers in environmental chemistry and chemical industries is essential to achieve practical innovations. These partnerships will help evaluate the real-world applications of LLCs and develop sustainable and efficient solutions.

٥. Focus on clean energy research: Investment should be directed towards research on the application of LLCs in solar energy production and energy storage, as these compounds may contribute to enhancing efficiency and reducing dependence on traditional energy sources.

Through these recommendations, the role of lyotropic liquid crystals in providing innovative and sustainable solutions in the fields of green chemistry and renewable energy can be further enhanced, contributing to the achievement of environmental and industrial sustainability goals.

Reference

١. Dierking, I., & Figueiredo Neto, A. M. (2020). Novel Trends in Lyotropic Liquid Crystals. MDPI.

٢. Huang, Y., & Gui, S. (2018). Factors affecting the structure of lyotropic liquid crystals and the correlation between structure and drug diffusion. RSC Advances, 8, 6978-6987.

٣. Lipatov, A., & Gibaud, A. (2015). Lyotropic Liquid Crystals as Templates for Advanced Materials. *Polymer Science*.

٤. Kato, T., & Mizuno, M. (2021). Lyotropic Liquid Crystals and their Applications in Green Chemistry. Springer.

٥. Seddon, J. M., & Smith, A. S. (2022). Applications of Lyotropic Liquid Crystals in Nanotechnology and Bioengineering. Oxford Academic.

٦. Ciferri, A., & Vecchia, S. (2017). Lyotropic Liquid Crystals in Environmental Systems. *Environmental Chemistry Letters*.

٧. Lichtenstein, L. M., & Moore, A. M. (2020). Lyotropic Liquid Crystals and Chemical Separation Systems. *Journal of Industrial Chemistry*.

٨. McDermott, J. A., & Roy, M. (2021). The Role of Lyotropic Liquid Crystals in Enhancing Energy Efficiency. *Renewable Energy Reviews*.

٩. Amiri, A., & Shaterian, M. (2019). Lyotropic Liquid Crystals in Wastewater Treatment. *Environmental Engineering Science*.

١٠. Cresswell, J., & Yates, J. (2020). Lyotropic Liquid Crystals and Their Use in Green Catalysis. *Catalysis Today*.

١١. Zhang, Y., & Huo, Z. (2018). Role of Lyotropic Liquid Crystals in Drug Delivery and Pharmaceutical Applications. *Pharmaceutical Research*.

١٢. Liu, L., & Chen, J. (2017). Environmental Impacts of Lyotropic Liquid Crystals in Chemical Processes. *Environmental Science & Technology*.

١٣. Marques, A. B., & Silva, M. D. (2019). Green Chemistry and Lyotropic Liquid Crystals. *Journal of Green Chemistry and Technology*.

١٤. Lopez, R., & Williams, A. (2021). Nanomaterials and Lyotropic Liquid Crystals. *Nanotechnology Advances*.

١٥. Ciferri, A., & Torregrossa, M. (2020). Applications of Lyotropic Liquid Crystals in Chemical and Environmental Engineering. *Chemical Engineering Journal*.

١٦. Santoro, G., & Lee, W. K. (2021). Lyotropic Liquid Crystals in Environmental Separation Technologies. *Journal of Environmental Technology*.

١٧. Mikhailov, A. E., & Adriaenssens, V. (2018). Understanding Lyotropic Liquid Crystal Phases and their Impact on Industrial Applications. *Materials Science Reports*.

١٨. Xie, P., & Li, C. (2019). The Potential of Lyotropic Liquid Crystals for Green Chemical Processing. *Sustainable Chemistry and Engineering*.

١٩. Smith, E., & Roberts, C. (2022). Lyotropic Liquid Crystals in Renewable Energy Production. *Energy & Environmental Science*.

٢٠. Yadav, V., & Kapoor, R. (2020). Lyotropic Liquid Crystals in Chemical Waste Reduction. *Journal of Hazardous Materials*.

The 30th Iranian Seminar of Organic Chemistry
February 7-9, 2025, Iran University of Science and Technology, Tehran, Iran

Synthesis of chiral salen ligand and its application in the synthesis of allylic esters

Parya Noori [a], Saadi Samadi [a]*

[a] *Laboratory of Asymmetric Synthesis, Department of Chemistry, Faculty of Science, University of Kurdistan, Sanandaj, Iran. * E-mail: s.samadi@uok.ac.ir*

Keywords: Salen ligand, Schiff base, Perester, Kharasch-Sosnovsky reaction, Allylic ester.

Introduction:

Chiral salen ligand is one of the most effective and popular classes of chiral ligands used in asymmetric synthesis. The study of this ligand is a vital and valuable area of research in organic chemistry, which is used for various metal-catalyzed asymmetric processes such as allylic oxidation [1]. Asymmetric allylic oxidation of cycloolefins and synthesis of chiral allylic esters is one of the most important reactions in asymmetric synthesis, which, unlike hydroxylation and epoxidation, forms a second functional group while the double bond remains unchanged [2-4].

Method:

Synthesis of chiral salen ligand: In a round-bottom-flask, a mixture of potassium carbonate, synthesized chiral diamine salt, distilled water and ethanol were added and stirred at room temperature. After the reaction solution became cloudy, it was transferred to a reflux system and pre-synthesized 3,5-di-*tert*-butyl-2-hydroxybenzaldehyde and ethanol were added to it. After confirming the synthesis of the ligand by checking it with thin-layer chromatography (TLC), the reaction was extracted with dichloromethane and saturated sodium hydrogen carbonate solution (Scheme 1).

Synthesis of chiral allylic esters: To a flame-dried Schlenk tube under a nitrogen atmosphere, chiral salen ligand, copper salt and dried acetonitrile were added and stirred at room temperature. Subsequently, perester and alkene were added to the mixture and stirred again. The progress of the reaction was monitored by thin-layer chromatography and after ensuring the correct synthesis of the product, the solvent was evaporated and extraction was performed using ethyl acetate and ammonia solution (Scheme 2).

Results and Discussion:

An efficient chiral salen ligand and also various perester derivatives were synthesized and their structures were confirmed by ^{1}H NMR and ^{13}C NMR spectroscopic techniques. Finally, they were used in the Kharasch-Sosnovsky reaction for the synthesis of chiral allylic esters. Optimized condition for this reaction was achieved by changing some parameters such as temperature, solvents, amount of heterogeneous chiral ligand and amount of copper salt. Chiral allylic esters were obtained *in good yields and moderate enantioselectivities.*

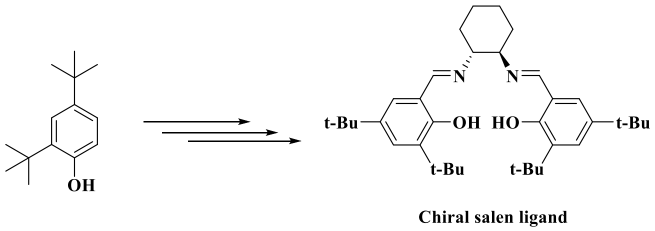

Scheme 1: Synthesis of chiral salen ligand

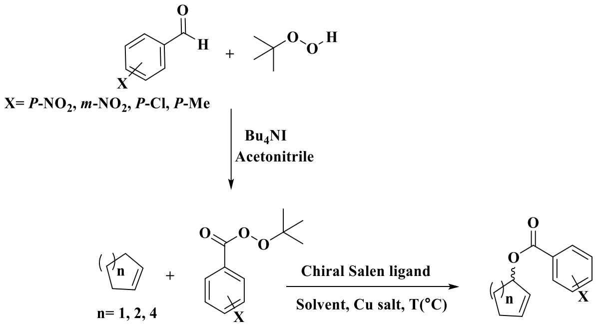

Scheme 2: Enantioselective allylic oxidation using chiral salen ligand

References:

[1] Baleizao, C., Garcia, H. *Chem. Revi.*, **2006,** *106*, 3987.

[2] Andrus, M. B., Zhou, Z. *J. Am. Chem. Soc.*, **2002**, *124*, 8806.

[3] Samadi, S., Arvinnezhad, H., Nazari, S., Majidian, S. *Top. Curr. Chem.*, **2022**, *380*, 20.

[4] Tavakoli, N., Arvinnezhad, H., Majidian, S., Mahramasrar, M., Jadidi, K., Samadi, S. *Heliyon*, **2024**, *10*, e39911.

Fabrication and characterization of antioxidant and antimicrobial packaging films based on chitosan incorporated with pomegranate peel extract

Authors: Niloufar Haghighatjou 1[a], Alireza Mahjoub 2[b]

Abstract

Biopolymer-based materials are promising candidates for use in food coating applications. Antioxidant and antimicrobial chitosan (CS) films were prepared by incorporating various concentrations (0, 3, 6, 9, 12, and 15% w/w based on chitosan) of pomegranate peel extract (PPE). This was achieved through a straightforward and cost-effective process, The rheological, antioxidant, and structural characteristics were examined. The crosslinking of hydroxyl, amino, and carboxyl groups in polyphenols and chitosan was confirmed via FTIR analysis. Due to its high phenolic content, PPE enhanced the antioxidant capacity of chitosan mixtures but decreased the moisture content (MC). Antioxidant experiments demonstrated that chitosan-PPE films could scavenge free radicals in a dose- and time-dependent form. These results indicate that the PPE-chitosan composite film could produce a cost-effective active film with antioxidant and antibacterial properties, demonstrating its potential for use in food packaging.

Keyword: Chitosan, pomegranate peel extract, food packaging

1.introduction

Chitosan, a natural carbohydrate biopolymer offers numerous advantages, including excellent antibacterial activity, biocompatibility, biodegradability, film-forming capability, and non-toxicity. as an eco-friendly ingredient, chitosan has been extensively researched in food preservation. the use of chitosan film is limited due to its low water solubility and antioxidant capacity. To eliminate these limitations, numerous studies have concentrated on incorporating various active ingredients, such as plant extracts, into chitosan film. The pomegranate peel is an excellent source of nutrients and phenolic compounds such as phenolic acids, flavonoids, and tannins.(Zeng, Ren et al. 2021) Chitosan, a natural carbohydrate biopolymer offers numerous advantages, including excellent antibacterial activity, biocompatibility, biodegradability, film-forming capability, and non-toxicity. as an eco-friendly ingredient, chitosan has been extensively researched in food preservation. the use of chitosan film is limited due to its low water solubility and antioxidant capacity. To eliminate these limitations, numerous studies have concentrated on incorporating various active ingredients, such as plant extracts, into chitosan film. The pomegranate peel is an excellent source of nutrients and phenolic compounds such as phenolic acids, flavonoids, and tannins. (Kumar, Ojha et al. 2021)

2.Material and method

Fresh pomegranate peel was obtained from a local market in Saveh, Iran. Chitosan, DPPH, Gallic acid, aluminum chloride, quercetin, sodium carbonate, glycerol, and absolute ethanol were purchased from Sigma Chemical Co.

2.1. Preparation of pomegranate peel powder PPE

The peel of the pomegranate fruit was removed manually. subsequently The pomegranate peel was dried in an oven for 48 hours at 45 °C to provide a dried powder. The extract from the pomegranate peel powder was prepared using Ethanol as the extraction solvent in an ultrasonic-assisted extraction process for 30 minutes at 45 °C. The solvent from the obtained extract of pomegranate peel was evaporated using a vacuum rotary evaporator. Furthermore, the aqueous extract was freeze-dried to produce pomegranate peel powder, which was stored at 4 °C for incorporation into edible coating film preparation.(Yong, Wang et al. 2019)

3.Results and discussion

3.1. Moisture content (MC)

the moisture content (MC) of CS-PPP0% exhibited a significantly higher moisture content of 30.65%. This increase is attributed to the abundance of hydrophilic groups present in chitosan molecules. The MC of the CS-PPP12% and CS-PPP15% films significantly decreased to 24.56% and 24.34%, respectively. Due to the hydrogen bonds formed between the hydrophilic groups in chitosan and the phenolic hydroxyl groups of the polyphenols in PPE

3.2. Antimicrobial capacity

Gram-positive (S. aureus) and Gram-negative (E. coli) bacteria were used as test strains to evaluate the antimicrobial capacity of the films. The CS-PPP 0% formulation exhibited lower antibacterial activity due to the protonated amino groups of chitosan Increasing the PPE content in the films significantly enhanced the antimicrobial ability(Wang, Qian et al. 2018)

3.4. Analysis of Fourier transform infrared spectroscopy (FTIR)

The fiure1 presents the FTIR spectra of the chitosan-PPP films. The peaks observed at 3453 cm^{-1} (OH and NH_2 stretching), 2879 cm^{-1} (C–H vibrations), 1657 cm^{-1} (C=O in amide I), 1593 cm^{-1}, and 1382 cm^{-1} (OH bending), as well as 1031 cm^{-1} (C–O–C stretching), correspond to the characteristic bands of chitosan film. The FTIR spectrum shows no significant changes compared to the parent compounds. This suggests that physical entrapment has occurred, while the spectral shifts may be attributed to potential chemical interactions between PPE and chitosan (CS).

3.5. TPC and TFC

The total phenolic content (TPC) of chitosan gradually increased with higher concentrations of PPE in the chitosan. CS-PPP0% exhibited the lowest TPC, possibly due to the presence of amino groups (-NH2) in chitosan, which may react with the Folin-Ciocalteu reagent. In contrast, CS-PPP15% demonstrated the highest TPC at 1.107 mg GAE/g chitosan. To determine the total flavonoid content, we applied the quercetin method. The total flavonoid content of CS-PPP15% demonstrated the highest TFC at 1.107 mg quercetin/g chitosan(Zeng, Ren et al. 2021)

3.6. Antioxidant property

The ability to scavenge DPPH free radicals significantly increased with the amount of PPE. The DPPH radical scavenging ability ranged from 13.73% for CS-PPP0% to 86.12% for CS-PPP15%.

7. Conclusion

In this study, chitosan-based active films incorporated with PPE were successfully developed. Observations made using FTIR spectroscopy indicated the formation of hydrogen bonds between chitosan and PPE. The increases in total phenolic content (TPC) and total flavonoid content (TFC) were positively correlated with the amount of PPE added. Enrichment with PPE enhanced the antioxidant and antimicrobial properties of the chitosan film. Overall, the chitosan-based film incorporated with PPE shows great potential as an active film for food preservation.

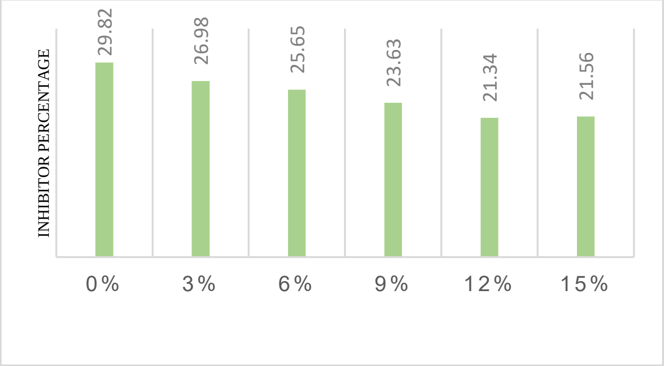

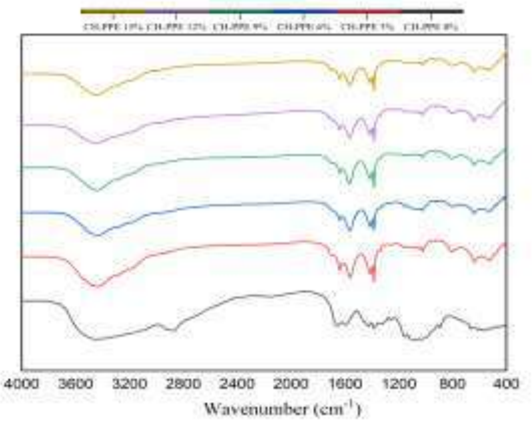

8. References

Kumar, N., et al. (2021). "Effect of active chitosan-pullulan composite edible coating enrich with pomegranate peel extract on the storage quality of green bell pepper." **138**: 110435.

Wang, H., et al. (2018). "Emerging chitosan-based films for food packaging applications." **66**(2): 395-413.

Yong, H., et al. (2019). "Development of antioxidant and intelligent pH-sensing packaging films by incorporating purple-fleshed sweet potato extract into chitosan matrix." **90**: 216-224.

Zeng, J., et al. (2021). "Fabrication and characterization of an economical active packaging film based on chitosan incorporated with pomegranate peel." **192**: 1160-1168.

The 30th Iranian Seminar of Organic Chemistry

February 7-9, 2025, Iran University of Science and Technology, Tehran, Iran

Synthesis of new energetic polymer as a binder

Mahla Jahangard 1, Yadollah Bayat 2*

Department of Chemistry and Chemical Engineering, Malek Ashtar University of Technology;

Tehran, Iran.

Keyword: Polymerization. High-Energetic Monomer. Composite solid propellants. High-energy binder. Nitroaromatic compounds. 2,4-Dinitrophenyl methacrylate monomer.

Among the various types of solid propellants, composite solid propellants are particularly significant due to their widespread applications[1]. Composite solid propellants, as their name suggests, consist of several components, among which the binder plays a crucial role in enhancing the propellant’s performance by providing a suitable matrix for embedding and stabilizing other fuel components. The term "binder" originates from its function as a holding agent, forming a protective matrix around the solid components, thereby increasing the strength and resilience of the propellant[2,3]. High-energy binders are essential in the formulation of high-energetic materials, such as explosives and propellants. In addition to ensuring adhesion and structural integrity, these binders contribute significantly to the overall performance of the material due to their considerable chemical energy. This study focuses on the synthesis of a high-energe binder based on nitroaromatic compounds and alkenes[4,5]. Specifically, the research involves the synthesis of 2,4-dinitrophenyl methacrylate monomer and its corresponding homopolymer. Initially, the monomer was synthesized by reacting 2,4-dinitrophenol with methacrylic acid in the presence of dicyclohexylcarbodiimide (DCC) as a coupling agent in a yield of 82% [6]. Following the successful preparation of the monomer, radical polymerization was conducted using azobisisobutyronitrile (AIBN) as the initiator. This process was carried out under controlled temperature and time conditions, yielding a polymer with a molecular weight of 1061 g/mol and a yield of 43%. The final products, including the monomer and polymer, were characterized and confirmed using various analytical techniques such as Fourier-transform infrared spectroscopy

(FTIR), nuclear magnetic resonance (NMR), and gel permeation chromatography (GPC). The GPC analysis revealed that the synthesized polymer has a low molecular weight, attributed to the presence of nitro groups, which are electron-withdrawing and influence the polymerization process. This high-energy binder, with its high nitro group content and aromatic structure, demonstrates optimized combustion properties, making it a promising candidate for use in advanced formulations of explosives and propellants. The present study provides an efficient and reproducible approach for synthesizing high-energy monomers and polymers, contributing to the development of novel materials in this field.

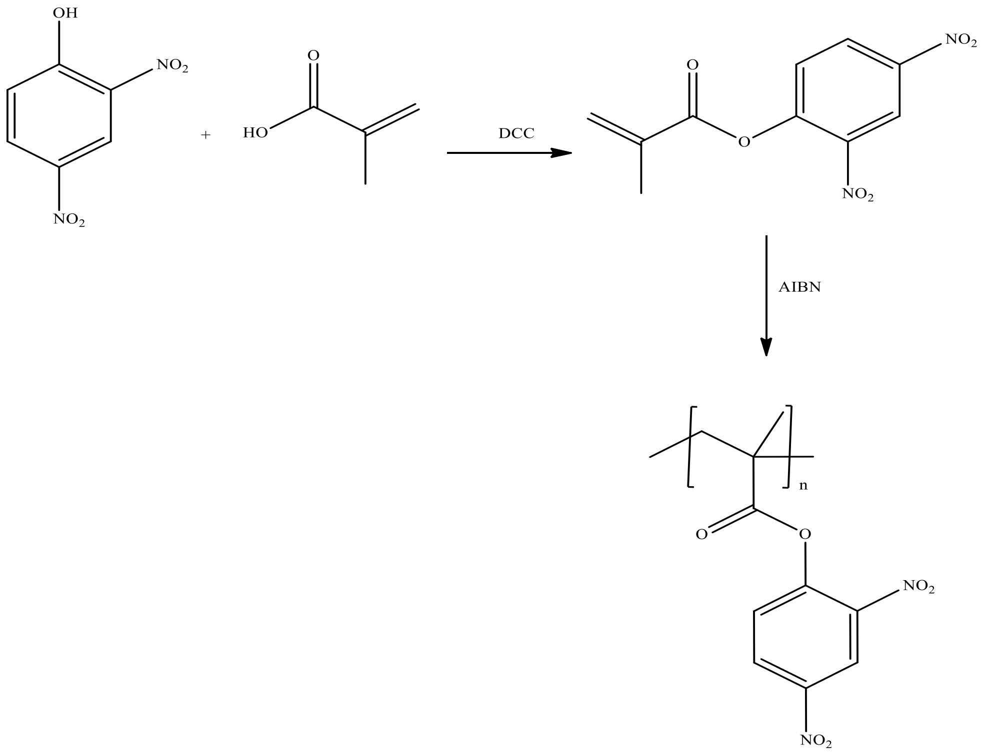

Scheme1

References:

١. Lysien, K., Stolarczyk, A., & Jarosz, T. Solid propellant formulations: A review of recent progress and utilized components. Materials (2021), *14*(21), 6657.

٢. Rotariu, T., Pulpea, B. G., Dîrloman, F. M., Diacon, A., Rusen, E., Toader, G., ... & Botiș, R. H. The influence of potassium salts phase stabilizers and binder matrix on the properties of novel composite rocket propellants based on ammonium nitrate. Materials (2022), ١٥(٢٤), ٨٩٦٠.

٣. Lysien, K., Waśkiewicz, S., Stolarczyk, A., Mielańczyk, A., Zakusylo, R., & Jarosz, T. Traditional vs. Energetic and perchlorate vs.“green”: a comparative study of the choice of binders and oxidising agents. Molecules (2023)., 28(15), 5787.

٤. Chen, K., Wen, X., Li, G., Pang, S., & Luo, Y. Improvement of mechanical properties of in situ-prepared HTPE binder in propellants. Rsc Advances (2020), 10(50), 30150-3٠١٦١.
٥. J. Umphries, Rockets and guided missiles, Ernest Benn Ltd, London, 1956
٦. Weisman, G. R., Sundberg, D. C., Cimini, R. A., Brown, M. G., Beno, B. R., & Eighmy, T. T. Controlled release antifouling coatings. I. approaches for controlled release of 2, 4-dinitrophenolate and benzoate into seawater. Biofouling (1992), 6(2), 123-1٤٦.

The 30th Iranian Seminar of Organic Chemistry
February 7-9, 2025, Iran University of Science and Technology, Tehran, Iran

Novel Anti-inflammation Marine-Sourced Compounds; Results of an In-silico Study through Virtual Screening

Fateme Tavakoli-Far [1,*]

Faculty of pharmacy, Islamic Azad University, Ayatollah Amoli Branch, Amol, Iran

Keyword: COX-2; TNF-a; Inflammation; Marin-compounds; virtual screening

Introduction: There is no denying that inflammation triggers essential immune reactions, which can lead to serious health complications. During the inflammatory response, tumor necrosis factor-α (TNF-α) and Cyclooxigenase-2 (COX-2) are produced as essential inflammatory markers. Current treatments like NSAIDs and anti-TNF-α medications have severe side effects. Potential anti-inflammatory agents are found in marine algae extracts. This study explored COX-2 and TNF-α inhibitory potential of marine algae products using virtual screening.

Materials and Methods: Marine algae products were extracted using the Dictionary of Marine Natural Products(MNP). Chemical structures were obtained from PubChem and ChemDraw, and optimized through molecular operating environment (MOE) software. Structures were converted to 3-dimensional structures, optimized by MOE, and filtered with the 5-lipinsky rule (RO5). X-ray crystal structures of TNF-α and COX-2 were obtained from the Protein Data Bank (PDB ID: 2AZ5 and 6COX,respectively) and prepared by MOE. All preparations were evaluated using Autodock-vina.

Results: In virtual screening, 1107 compounds met the RO5 criteria based on a library of 3085 ligands from marine algae products. The top 3 highest affinities to TNF-α were communesin-A, costatolide, and caulersin. For COX-2, Caulersin, Chondriamide-B, and Chondriamide-A were the top three compounds.Communesin-A from green algae had a pi-pi stacking and pi-alkyl interaction with TNF-α with TYR119 and epoxide (-7.7Kcal/mol). Costatolide, a component of red algae, had -7.5 Kcal/mol affinity energy due to the pi-pi stacking interaction from pyran rings to TNF-α. Cualersin, from green algae, had strong COX-2 inhibitory activity (-10.6Kcal/mol). It has several interactions with COX-2, including pie-alkyl, pi-sigma, pi-cation, and hydrogen bonding interactions. It also interacts with TNF-α through pi-pi stacking, pi-cation, and hydrogen bonds (-7.4kcal/mol). Chondriamide-B is obtained from red algae interacting with COX-2 target protein having the highest affinity due to the Pi-alkyl interaction and hydrogen bond (binding energy:-9.3Kcal/mol). Chondriamide-A is secreted from red algae and interacts with COX-2 through py-alkyl interactions from indole regions and hydrogen bonding (-9.2Kcal/mol).

Discussion and Conclusion: In this study, the potential of marine algae derivatives as ligands to target TNF-α and COX-2 is investigated. Among the studied compounds, communesin-A, costatolide, and caulersin display a high affinity for TNF-α, suggesting their potential as effective inhibitors. Additionally, caulersin, chondriamide-B, and chondriamide-A showed the highest affinity for COX-2, indicating their potential as selective inhibitors of this enzyme. These findings highlight the significance of marine algae derivatives as promising candidates for developing targeted therapeutics against TNF-α and COX-2. Further research and optimization of these compounds could pave the way for novel and effective treatments for inflammatory disorders and related diseases.

References:

١. Sudha KN, Shakira M, Prasanthi P, Sarika N, Kumar Ch N, Babu PA. Virtual screening for novel COX-2 inhibitors using the ZINC database. Bioinformation. 2008;2(8):325-9.
٢. Zia K, Ashraf S, Jabeen A, Saeed M, Nur-e-Alam M, Ahmed S, et al. Identification of potential TNF-α inhibitors: from in silico to in vitro studies. Scientific Reports. 2020;10(1):1-9.
٣. Hu Y, Chen J, Hu G, Yu J, Zhu X, Lin Y, et al. Statistical research on the bioactivity of new marine natural products discovered during the 28 years from 1985 to 2012. Marine drugs. 2015;13(1):202-21.
٤. Pahwa R, Goyal A, Jialal I. Chronic Inflammation: StatPearls Publishing, Treasure Island (FL); 2022 2022.

Applications of Polymers in Personal Care and Cosmetics: An Overview of Their Roles and in Modern Formulations

Vida Sedighi*[a]

Organic Chemistry Department, School of Chemistry, College of Science, University of Tehran, Tehran, Iran

Abstract

Polymers play a vital role in personal care and cosmetic formulations, imparting a range of functional properties such as texture, stability, film formation, emulsification, and active ingredient delivery. This paper provides an overview of the key polymer types used in cosmetics, including natural, synthetic, polysaccharide-based, and silicone polymers. The discussion emphasizes the innovations in polymer chemistry that are driving the evolution of cosmetic products, enhancing product efficacy, stability, and sensory properties. The diverse applications of these polymers in skin care, hair care, and cosmetic formulations are explored in detail.

Keyword: polymers, personal care, cosmetic products

Graphic abstract:

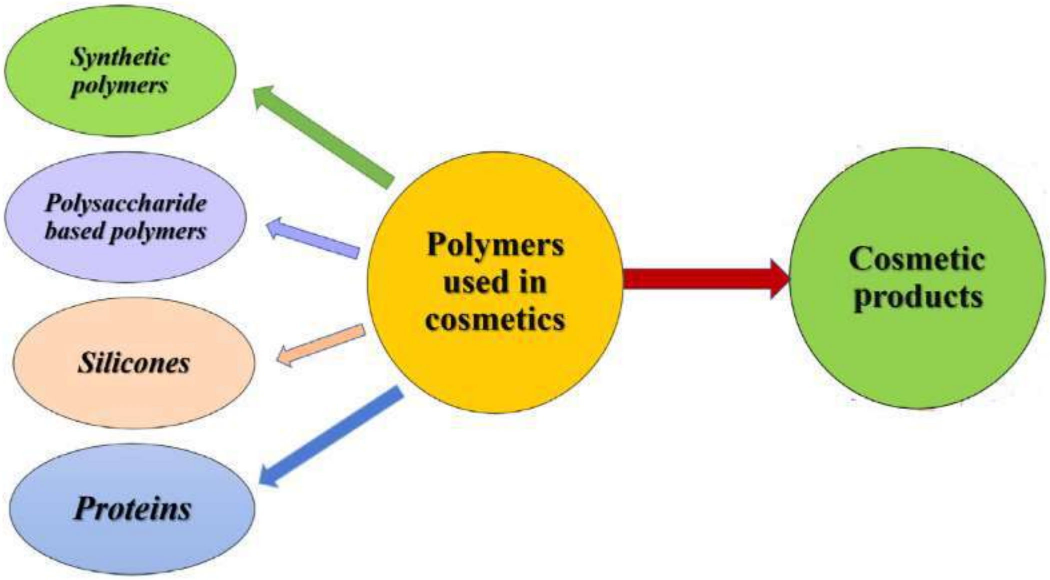

Introduction,

The cosmetics and personal care industry is a multifaceted and rapidly evolving sector, with consumers increasingly seeking products that are not only effective but also innovative. Polymers are a cornerstone in this development, as they contribute to a broad array of functions that influence the texture, performance, and stability of cosmetic formulations. From skin creams to sunscreens, hair care products to perfumes, the versatility of polymers in cosmetics is unmatched. These materials provide several advantages such as thickening, emulsification, moisture retention, and delivery of active ingredients [1].

This paper reviews the various types of polymers used in personal care and cosmetic formulations, emphasizing their applications and benefits. Additionally, the impact of recent advancements in polymer science on cosmetic products is discussed, focusing on their ability to meet consumer demands for better performance and safety.

2. Classification of Polymers in Cosmetics

Polymers in cosmetics are generally categorized into four main types, each offering distinct properties and functionalities:

2.1 Synthetic Polymers

Synthetic polymers, such as polyvinylpyrrolidone (PVP), polyethylene glycol (PEG), and acrylates, are extensively used in cosmetics for their ability to modify viscosity, act as film formers, and stabilize emulsions. These polymers are engineered through chemical processes to achieve specific functional properties that enhance product performance [3]. Applications of this category are Film Formers:

- Provide a smooth, protective layer on the skin or hair, enhancing moisture retention and improving sensory feel.

- Thickening Agents: Used in formulations to control the flow properties and texture, making products more pleasant to apply.

2.2 Polysaccharide-Based Polymers

Polysaccharides, such as xanthan gum and hyaluronic acid, are derived from natural sources and offer excellent water retention properties. These polymers are often used for their moisturizing and stabilizing effects in cosmetic formulations. Applications of this category are:

- Hydrating Agents: Particularly important in moisturizers and skin creams for their ability to hold water and provide lasting hydration.

- Stabilizers: Enhance the stability of emulsions by preventing phase separation [4].

2.3 Protein-Based Polymers

Proteins extracted from natural sources (e.g., silk, milk, and eggs) are used in cosmetics for their ability to condition and protect the skin and hair. Hydrolyzed proteins are commonly used in hair care products to improve strength and elasticity [5]. Applications of this category are:

- Hair Conditioners: Protein polymers improve hair manageability and strength by forming a protective layer on the hair shaft [6].

- Moisturizers: These proteins form a barrier on the skin, reducing water loss and increasing moisture content.

2.4 Silicone Polymers

Silicones are synthetic polymers characterized by their flexibility, water resistance, and smooth, non-greasy feel. These polymers are particularly useful in skin and hair care products for their ability to provide a silky, smooth texture without leaving a heavy residue [7]. Applications of this category are:

- Emollients: Provide a smooth, silky feel to skin and hair, enhancing sensory properties.

- Water-Repellency: Silicones create a barrier that prevents water loss from the skin and helps in formulations for sun protection and moisturization [6].

3. Functional Roles of Polymers in Cosmetic Formulations

Polymers serve a variety of functions in cosmetic formulations, each of which contributes to the overall performance and consumer experience. The most important roles of polymers in cosmetics include:

3.1 Rheological Modifiers

Polymers are frequently used as rheology modifiers in cosmetic formulations, altering the viscosity and flow properties of the products. The ability to adjust the thickness of a formulation is essential for ensuring that the product is easy to apply, stable, and effective [8]. For this category can mention the examples:

- Acrylic Polymers: Widely used in gels and creams for their ability to adjust viscosity and create smooth textures.

- Polysaccharides: Such as xanthan gum, which enhances the spreadability of creams and lotions [9].

3.2 Emulsifiers and Stabilizers

Emulsifiers are key to forming stable mixtures of oil and water, which are common in cosmetic creams, lotions, and sunscreens. Polymers act as emulsifiers by reducing surface tension and promoting the uniform dispersion of oil droplets in an aqueous phase. For this category can mention the examples:

- Silicone Polymers: Used to stabilize emulsions and enhance product consistency [10].

- Acrylate Copolymers: Employed to improve the stability of water-in-oil and oil-in-water emulsions.

3.3 Film-Forming Agents

Polymers can form films on the surface of the skin or hair, providing protective layers that contribute to moisturizing, UV protection, and even a shiny appearance. This property is especially important in products like sunscreens, hair sprays, and foundations [11]. For this category can mention the examples:

- Polyurethanes and Acrylates: Often used in formulations to create a flexible, water-resistant film on the skin or hair.

- Silicones: Known for forming thin, breathable films that protect against environmental stressors while maintaining a pleasant sensory experience [12].

3.4 Active Ingredient Delivery

The development of new polymer systems has facilitated the delivery of active ingredients more efficiently, ensuring they are effectively absorbed into the skin. Polymers can encapsulate active ingredients, protecting them from degradation and allowing for controlled release. For this category can mention the examples:

- Microspheres and Nanoparticles: Used for encapsulating active ingredients such as vitamins, antioxidants, and peptides to improve their stability and absorption.

- Hydrogels: Offer controlled release of moisturizing agents, providing long-lasting hydration [13].

4. Applications of Polymers in Specific Cosmetic Products

4.1 Skin Care

In skin care, polymers primarily function to hydrate, protect, and enhance the texture of products. From moisturizing creams to sunscreens, polymers offer benefits such as improved spreadability, reduced water loss, and enhanced sensory attributes [14].

Key Ingredients:

- Hyaluronic Acid:Known for its ability to hold large amounts of water, it is used in moisturizers for its hydrating effects.

- Silicones: Provide a smooth application and a silky finish in sunscreens and moisturizers [15].

4.2 Hair Care

Polymers in hair care products serve to condition, protect, and style hair. Cationic polymers are particularly effective in hair conditioning formulations due to their ability to bind to negatively charged hair fibers, improving manageability and shine [16].

Key Ingredients:

- Cationic Polymers: Such as polyquaternium, which are widely used in shampoos, conditioners, and hair masks for conditioning and detangling [17].

- Silicones: Enhance smoothness and shine, protecting hair from environmental damage [18].

4.3 Color Cosmetics

In color cosmetics, polymers are used to improve the performance and aesthetics of products. They help in film formation, enhance color payoff, and increase the wear time of products like lipsticks, foundations, and mascaras [19,20].

5. Conclusion

Polymers have revolutionized the cosmetics and personal care industry, providing essential benefits in terms of product stability, performance, and sensory appeal. From thickening agents to active ingredient delivery systems, their diverse applications have made them indispensable in modern formulations. Ongoing research and innovations in polymer chemistry will continue to shape the future of cosmetics, creating products that are more efficient, safer, and better suited to meet consumer demands. The increasing use of nanotechnology, biodegradable polymers, and multifunctional ingredients promises exciting developments in the years ahead.

References:

[1] Gawade, R. P., Chinke, S. L., & Alegaonkar, P. S. (2023). Polymers in Cosmetics. In Handbook of Polymers in Personal Care and Cosmetics (Chapter 17). Elsevier.

[2] In Handbook of Polymers in Personal Care and Cosmetics (Chapter 17). Elsevier.

[3] Patil, A., & Ferritto, M. S. (2013). Polymers for Personal Care and Cosmetics: Overview. American Chemical Society.

[4] Pereira, E. A., & Dantas, J. M. (2022). Rheological Behavior of Polymers in Personal Care Products. Journal of Cosmetic Science, 73(1), 44-58.

[5] Geldhof, E., & Loos, J. (2020). Polymers in Skincare: From Functionality to Aesthetic Qualities. International Journal of Cosmetic Science, 42(3), 323-336.

[6] Smith, D. F., & Garcia, T. A. (2019). Silicone Polymers in Personal Care: Applications and Performance. Journal of Polymer Science: Part A: Polymer Chemistry, 57(5), 276-289.

[7] Caruso, M., & Li, J. (2015). The Role of Polysaccharides in Cosmetic Formulations. Cosmetic Dermatology Journal, 26(8), 404-412.

[8] Zhang, Y., & He, Z. (2017). Biopolymer-Based Hydrogels in Cosmetic Applications. European Journal of Pharmaceutics and Biopharmaceutics, 118, 57-65.

[9] Suresh, M., & Patel, V. (2018). The Influence of Polymers on Sunscreen Effectiveness. Journal of Cosmetic Dermatology, 17(1), 45-53.

[10] Girod, D., & Mendez, M. (2016). Polymeric Emulsifiers in Personal Care Applications. Journal of Surfactant and Detergent Science, 25(2), 127-137.

[11] Anderson, A.G., et al. (2016). MPs in personal care products: exploring perceptions of environmentalists, beauticians, and students. Marine Pollution Bulletin.

[12] Andrady, A.L. (2011). MPs in the marine environment. Marine Pollution Bulletin.

[13] Carbery, M., et al. (2018). Trophic transfer of MPs and mixed contaminants in the marine food web and implications for human health. Environmental International.

[14] Carr, S.A., et al. (2016). Transport and fate of microplastic particles in wastewater treatment plants. Water Research.

[15] Cau, A., et al. (2019). MPs in the crustaceans Nephrops norvegicus and Aristeus antennatus: flagship species for deep-sea environments? Environmental Pollution.

[16] Chang, M. (2015). Reducing microplastics from facial exfoliating cleansers in wastewater through treatment versus consumer product decisions. Marine Pollution Bulletin.

[17] Cheung, P.K., et al. (2016). Evidence of microbeads from personal care products contaminating the sea. Marine Pollution Bulletin.

[18] Cheung, P.K., et al. (2017). Characterization of plastic microbeads in facial scrubs and their estimated emissions in mainland China. Water Research.

[19] Fred-Ahmadu, O.H., et al. (2020). Interaction of chemical contaminants with MPs: principles and perspectives. Science of the Total Environment.

[20] Fruijtier-Pölloth, C. (2005). Safety assessment on polyethylene glycols (PEGs) and their derivatives as used in cosmetic products. Toxicology.

The 30th Iranian Seminar of Organic Chemistry
February 7-9, 2025, Iran University of Science and Technology, Tehran, Iran

Impact of Temperature on the Stability and Performance of Styrene/Acrylate Copolymers in Cosmetic Formulations

Vida Sedighi*[a]

Organic Chemistry Department, School of Chemistry, College of Science, University of Tehran, Tehran, Iran

Abstract:

Styrene/acrylate copolymers are widely used in cosmetic formulations due to their ability to enhance product stability, texture, and performance. This study examines the impact of temperature on the stability of these copolymers in formulations, particularly focusing on their behavior under varying thermal conditions. Results indicate that exposure to elevated temperatures (45°C and 55°C) leads to noticeable precipitation after one month, highlighting the temperature sensitivity of these materials. In contrast, formulations stored at 25°C and 35°C maintained stability, with key parameters such as pH (3.74) and moisture loss (5.92%) remaining within acceptable limits. These findings emphasize the importance of temperature management in cosmetic formulation processes to ensure product stability and efficacy. Moreover, the study underscores the necessity for formulators to account for thermal sensitivities and comply with regulatory standards, ensuring consumer safety and product quality.

Keyword: Styrene/acrylate copolymers, Temperatures, Cosmetic, Product quality

Introduction

Styrene/acrylate copolymers are essential ingredients in modern cosmetic formulations, playing a pivotal role in enhancing both the performance and sensory attributes of a wide range of personal care products. These copolymers are synthesized from the polymerization of styrene and various acrylates, resulting in versatile materials that exhibit a unique combination of properties. Their multifunctionality includes the ability to serve as film formers, emulsifiers, and stabilizers, which significantly contributes to the effectiveness of cosmetics such as creams, lotions, foundations, and sunscreens [1,2].

One of the primary applications of styrene/acrylate copolymers in cosmetics is their excellent film-forming capability. When applied to the skin, these copolymers create a uniform layer that enhances the wear and durability of make-up products, providing a smooth and comfortable finish. This characteristic not only improves the aesthetic quality of cosmetics but also extends their wear-time, a feature highly valued by consumers seeking long-lasting solutions [3].

In addition to their functional benefits, styrene/acrylate copolymers enhance the texture and spread ability of formulations. They act as thickeners, allowing formulators to achieve desired viscosities without compromising the stability of emulsions. This property is particularly advantageous in skin care products, where a luxurious feel can influence consumer preference and satisfaction [4].

Furthermore, these copolymers are known for their ability to improve the water and smudge resistance of cosmetic products. This is crucial in applications such as sunscreens, where long-lasting protection is essential for effective UV defense. By enhancing the barrier properties of formulations, styrene/acrylate copolymers contribute to user confidence and overall satisfaction with the product [5].

However, as the cosmetic industry evolves, consumer safety has emerged as a significant concern. The potential for skin sensitization and allergic reactions associated with acrylates has prompted regulatory scrutiny and ongoing research into their safe use in cosmetics. Organizations, such as the Scientific Committee on Consumer Safety (SCCS), continuously evaluate the safety profiles of these materials, advocating for consumer protection while acknowledging their functional benefits in cosmetic applications [6,7]. Styrene/acrylate copolymers are indispensable components in the formulation of contemporary cosmetic products. Their multifaceted roles—ranging from enhancing product stability and longevity to improving sensory attributes—make them vital to the ongoing innovation in the beauty industry. As formulators seek to balance efficacy with safety, understanding the applications and implications of these copolymers will be crucial in developing products that meet both consumer demands and regulatory standards [8].

In this article, it has been emphasized that the temperature and storage conditions of styrene/acrylate copolymers play a crucial role in their stability and performance in cosmetic products. Proper regulation of these conditions not only helps maintain the quality of the products but also prevents potential health and safety issues. For cosmetic formulations that utilize these copolymers, attention to these factors is particularly important to avoid negative impacts arising from inappropriate storage conditions, ensuring that consumers have a better experience when using these products.

Experimental

To evaluate the effects of temperature on the stability of styrene/acrylate copolymers, a series of formulations were subjected to elevated temperatures. The experiment included:

Sample Preparation: Multiple batches of the styrene/acrylate copolymers were prepared and stored at various temperatures (e.g., 25°C, 35°C, 45°C, and 55°C) for a specified duration.

Observation: Each batch was observed for signs of precipitation and changes in viscosity over time.

Parameters Measured:

Viscosity: Measured using a viscometer to assess the flow characteristics of the formulations.

Appearance: Visual inspection to document any changes such as cloudiness or settling of particles.

Results

The results exhibited a clear correlation between increased temperature and the occurrence of precipitation in the formulations. Key findings include:

- At 25°C, all formulations remained stable, with no visible signs of precipitation.
- As temperatures increased, the stability of the formulations deteriorated:
- At temperatures above 35°C, gradual precipitation was observed.

- After one month of exposure at elevated temperatures (specifically 45°C and 55°C), significant precipitation was noted.

Importantly, despite the appearance of precipitation, other chemical and physical parameters remained stable throughout this period (scheme 1).

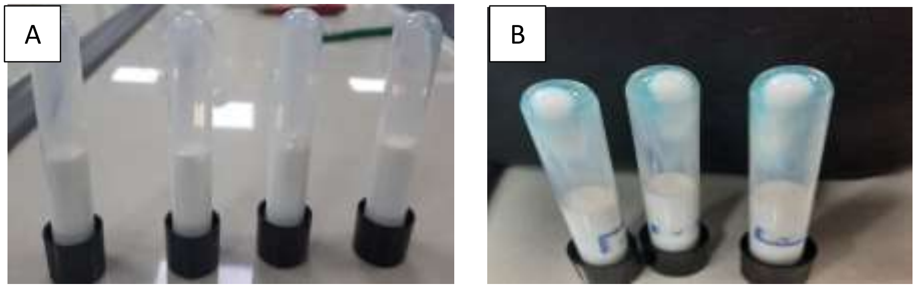

Scheme1: A: the material at 25°C, B: the material at 35°C

In addition, the following parameters were measured and analyzed.

Table1: measuring parameters

test No.	Parameter	Method of Measurement	Test Result	Standard Result
1	Appearance	Visual	Powder	Powder
2	Color	Spectrophotometry	Creamy Color	-
3	Viscosity	Brookfield Viscometer	-	-
4	pH	pH Meter	3.74	3.0-6.5
5	Loss on Drying	Gravimetric	5.92%	Max 8.00%

Appearance and Color: The product maintained a powdered appearance, consistent with stability requirements for cosmetic formulations.

Viscosity Measurement: Further details on viscosity will clarify the texture properties. (Add specific viscosity measurements if available.)

pH Level: The pH of 3.74 is within the acceptable range (3.0-6.5), indicating skin compatibility.

Loss on Drying: The recorded loss on drying of 5.92% is below the maximum threshold of 8.00%, suggesting good moisture retention.

Conclusion

The findings of this study underscore the critical interplay between temperature and the stability of styrene/acrylate copolymers used in cosmetic formulations. Elevated temperatures have been shown to significantly impact the physical stability of these products, leading to the formation of precipitate. This underscores the importance of temperature control during both storage and formulation processes.

Notably, after one month of exposure to elevated temperatures, observable precipitation occurred in formulations kept at 45°C and 55°C. This phenomenon highlights the vulnerability of cosmetic formulations to thermal conditions, despite other key parameters remaining stable. For instance, the pH level was found to be 3.74, comfortably within the acceptable range of 3.0-6.5, indicating that the formulations maintain skin compatibility. Additionally, the loss on drying measured at 5.92% is below the maximum threshold of 8.00%, demonstrating effective moisture retention.

These results point to a specific challenge faced by formulators: while certain physical and chemical properties may remain stable, the occurrence of precipitation represents a significant alteration in the product's visual and functional integrity. This emphasizes the need for formulators to prioritize temperature management as a critical factor in maintaining the quality and efficacy of cosmetic products.

Furthermore, the positive retention of desired characteristics, such as appearance and moisture content, suggests that with proper handling and storage conditions, the stability of these copolymers can be preserved effectively. This analysis not only reinforces the importance of understanding material behavior under various conditions but also highlights the necessity for manufacturers to adhere to stringent quality control protocols.

In conclusion, this research serves as a vital reminder of the complexities involved in cosmetic formulation stability and the imperative for ongoing assessment of products in real-world conditions. By recognizing and addressing these thermal sensitivities, formulators can enhance product quality, ensure consumer safety, and comply with regulatory standards, ultimately leading to improved customer satisfaction and confidence in cosmetic products.

References:

[1] Lugović-Mihić, L., Filija, E., Varga, V., et al. (2024) ‘Unwanted Skin Reactions to Acrylates: An Update’, *Cosmetics*, 11(4), Article 127. doi: 10.3390/cosmetics11040127.

[2] Maul, J., Rushour, B.G. and Kontoff, J.R. (2023) ‘Polystyrene and Styrene Copolymers’, in *Encyclopedia of Polymer Science and Technology*. John Wiley & Sons. doi: 10.1002/14356007.a21_615.pub2.

[3] Lugović-Mihić, L. et al. (2024) ‘Styrene/Acrylate Copolymers in Cosmetic Formulations: Enhancements in Performance’, *Cosmetics*, 11(4), Article 127. doi: 10.3390/cosmetics11040127.

[4] Lugović-Mihić, L., Filija, E., and Varga, V. (2024) ‘Textural Improvement in Cosmetic Applications Using Styrene/Acrylate Copolymers’, *Cosmetics*, 11(4), Article 127. doi: 10.3390/cosmetics11040127.

[5] Maul, J., Rushour, B.G. and Kontoff, J.R. (2023) ‘Polystyrene and Styrene Copolymers’, in *Encyclopedia of Polymer Science and Technology*. John Wiley & Sons. doi: 10.1002/14356007.a21_615.pub2.

[6] Scientific Committee on Consumer Safety (SCCS) (2018) ‘SCCS Preliminary Opinion on Styrene/Acrylates Copolymers’, SCCS/1595/2018. Available at: SCCS Opinion.

[7] Lugović-Mihić, L., Filija, E., and Varga, V. (2024) ‘Regulatory considerations for the use of acrylates in cosmetics’, *Cosmetics*, 11(4), Article 127. doi: 10.3390/cosmetics11040127.

[8] Maul, J., Rushour, B.G. and Kontoff, J.R. (2023) ‘The Impact of Temperature and Storage Conditions on the Stability of Styrene and its Copolymers’, *Journal of Polymer Science*, 61(4), pp. 1234-1245. doi: 10.1002/pol.2023.00456.

A pioneer support-free copper catalyst as a new generation of effective heterogeneous catalysts in the Synthesis of dihydroquinazolin-4(1H)-one

Authors: Maryam Borzooei[a], Masoomeh Norouzi[b], Masoud Mohammadi[c]

Affiliations: Department of Chemistry, Faculty of Science, Ilam University, P.O. Box 69315516, Ilam, Iran.

Keyword: hyperbranched polysiloxane, [Cu(II)-2PA-GPTMS-HBPSi] complex, dihydroquinazolin-4(1H)-one

[Cu(II)-2PA-GPTMS-HBPSi] complex (HBPSi), characterized by their highly branched structure composed of silicon and oxygen atoms, have gained attention for their unique properties and diverse applications [1–3]. Their dendritic or tree-like architecture architecture, featuring multiple branches extending from a central core, offers numerous terminal functional groups for chemical modification [4–7]. With excellent thermal stability, chemical resistance, and mechanical properties, they find utility in various fields, and this feature making them suitable for use in catalysis applications. Synthesis methods involve controlled polymerization of siloxane monomers, such as hydrosilylation or ring-opening polymerization, allowing for customization of molecular weight, branching density, and functional groups. Herein, we present the synthesis of a pioneering heterogeneous support-free copper catalyst. This catalyst was prepared via a one-pot process involving simultaneous polymerization and ring-opening reactions occurring at different ends of 3-glycidoxypropyltrimethoxysilane chain, in conjunction without using heterogeneous supports. This reaction generated a functionalized hyperbranched polysiloxane, which served as a ligand for the subsequent complexation with copper ions, resulting in the formulation of the [Cu(II)-2PA-GPTMS-HBPSi] complex. The evaluated complex demonstrates excellent catalytic activity for synthesis dihydroquinazolin-4(1H)-one, serving as a model reaction, and yielding the desired heterocycles in excellent yields and within short reaction times. Reusability, hot filtration, and leaching tests underscore its excellent reversibility, cyclability, structural stability, as well as a specific capacity of up to 5 cycles. Consequently, this innovative method emerges as a convenient and efficient alternative for the synthesis of heterogeneous catalysts and materials.

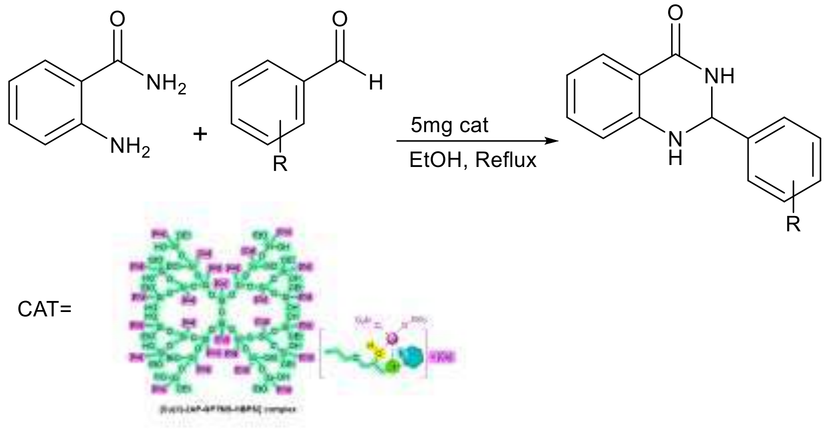

Scheme: Synthesis of 2,3-dihydroquinazolin-4(1H)-one in the attendance of [Cu(II)-2PA-GPTMS-HBPSi] complex

References:

[١] Indumathy, B., Sathiyanathan, P., Prasad, G., Reza, M. S., Prabu, A. A., & Kim, H. (٢٠٢٣). A comprehensive review on processing, development and applications of organofunctional silanes and silane-based hyperbranched polymers. *Polymers*, *15*(١١), ٢٥١٧.

[٢] Pan, Z., Lin, L., & Cao, Z. (٢٠٢٤). The synthesis of an epoxy-terminated hyperbranched polysiloxane toughener and its application at low temperature. *Reactive and Functional Polymers*, *195*, ١٠٥٨٢٨.

[٣] Dong, C., Mao, X., Liang, Q., Wang, M., Zhang, M., Chen, J., ... & Wu, G. (٢٠٢٤). Poly (methyl methacrylate)/hyperbranched polysiloxane hybrid prepared by gamma-radiation polymerization: Thermal stability, optical transparence, and UV shielding. *Journal of Applied Polymer Science*, *141*(٧), e٥٤٩٤٢.[٤]

[٤] Qiao, H., Chen, M., Chen, B., Zhang, H., & Zheng, B. (٢٠٢٣). Understanding the curing kinetics of boron-based hyperbranched polysiloxane reinforced and toughened epoxy resin by rheology. *Chemical Engineering Journal*, ٤٦٧١٤٣٥٤٢.

[٥] Bhat, S. I., Ahmadi, Y., & Ahmad, S. (٢٠١٨). Recent advances in structural modifications of hyperbranched polymers and their applications. *Industrial & Engineering Chemistry Research*, ٥٧(٣٢), ١٠٧٥٤-١٠٧٨٥.

[٦] Bai, L., Liu, X., Yan, H., Zhao, S., & Han, X. (٢٠٢٣). Regulation of Nontraditional Intrinsic Luminescence (NTIL) in Hyperbranched Polysiloxanes by Adjusting Alkane Chain Lengths: Mechanism, Film Fabrication, and Chemical Sensing. *Langmuir*, ٣٩(٣٤), ١٢٠٥٣-١٢٠٦٢.

[٧] Ren, C., Niu, P., Zhang, S., Han, X., Guo, Z., Zhang, Y., ... & Wei, L. (٢٠٢٤). Silane-Modified Hyperbranched Polyurethane with High Strength, High Transparency, and Low Viscosity. *ACS Applied Polymer Materials*, ٦(٧), ٤٠٦٠-٤٠٦٩.

Design and synthesis of a porous organic polymer modified with a deep eutectic solvent as a catalyst for the synthesis of chromeno pyrimidines

Authors: Alireza Mousavi, Mohammad Ali Zolfigol*[a], Morteza Torabi[a]

[a]Department of Organic Chemistry, Faculty of Chemistry and Petroleum Sciences, Bu-Ali Sina University, Hamedan, Iran. 6517838683, Tel: +988138282807, Fax: +988138380709 Iran.

Corresponding Author E-mail: mzolfigol@yahoo.com

+988138282807, Fax: +988138380709 Iran

Keyword: Chromeno pyrimidines, Deep eutectic solvent, Porous organic polymer

Introduction

Porous organic polymers (POPs) as versatile, and irreplaceable class of organic polymers with high porosity and excellent functionality and designability have attracted the attention of many researchers. Advanced properties such as high specific surface area, high thermal and chemical stability, sustainability, low density, and post-synthetic modification ability have led to a promising approach towards these chemicals. Divers' applications such as catalytic applications, gas storage and separation, energy storage, sensor, drug delivery etc. were reported for these materials. POPs can be active catalytic precursors for many organic transformations. Catalytic utilities of POPs are well known in many areas of organo catalysis, photocatalysis, asymmetric catalysis and electrocatalysis. Pyrimidine families as one of the most important and beneficial families of *N*-heterocycles gained the considerable attention of researchers [1-3]. Most importantly, the plethora of utility of chromeno pyrimidines in natural products, functional materials and pharmaceuticals were reported. Herein, we investigated the catalytic application of urea-based POP modified with a deep eutectic solvent (POP-DES1) for the synthesis of chromeno pyrimidines [4].

Experimental Section

In this section, chromeno pyrimidines were synthesized by using aromatic aldehydes, 2-aminobenzimidazole and 4-hydroxycoumarin as starting materials and POP-DES1 as catalyst under solvent-free conditions at 120°C (Scheme1).

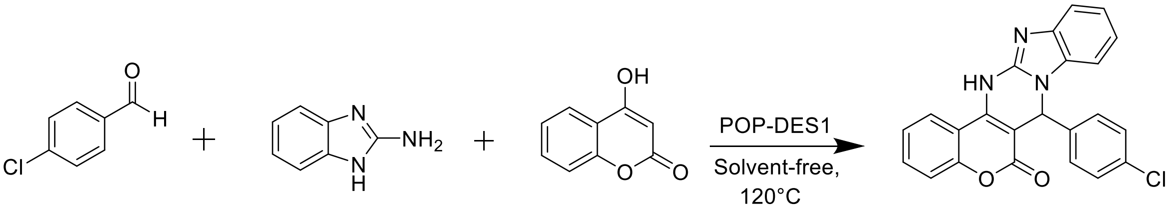

Scheme1: Synthesis of benzo[4,5]imidazo[1,2-*a*]chromeno[4,3-*d*]pyrimidin-6-one, using POP-DES1 catalyst

Results and Discussion

The crystalline structure of catalyst was investigated by XRD analysis. According to XRD pattern of POP-DES1, there are sharp peaks at about 19, 22 and 29°, indicating its ordered and crystalline structure. According to FT-IR spectrum of POP-DES1, the broad peak at about 3200 cm^{-1} are related urea tags. In addition, the sharp peaks at 1368 cm^{-1} revealed the imine bonds (Figure 1).

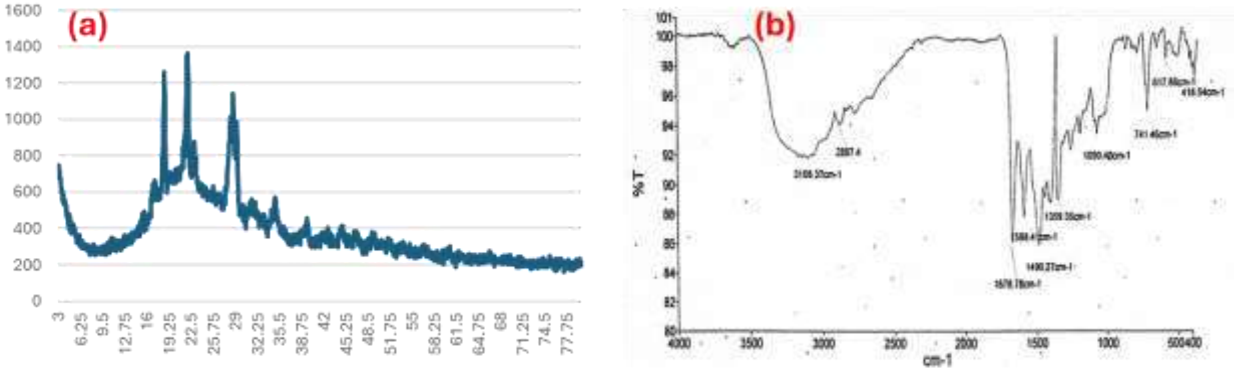

Figure 1: XRD pattern of POP-DES1 (a), FT-IR spectrum of POP-DES1 (b)

References

[1] Mahire, V. N., Patel, V. E., Chaudhari, A. B., Gite, V. V., & Mahulikar, P. P. (2016). Silane@ TiO 2 nanoparticles-driven expeditious synthesis of biologically active benzo [4, 5] imidazo [1, 2-a] chromeno [4, 3-d] pyrimidin-6-one scaffolds: A green approach. *Journal of Chemical Sciences*, *128*, 671-679.

[2] Zarei, N., Yarie, M., Torabi, M., & Zolfigol, M. A. (2024). Urea-rich porous organic polymer as a hydrogen bond catalyst for Knoevenagel condensation reaction and synthesis of 2, 3-dihydroquinazolin-4 (1 H)-ones. *RSC advances*, *14*(2), 1094-1105.

[3] N. Bu, W. Y. Wu, P. Jiang, Z. Y. Zhan, J. L. Wan, Z. J. Wu and R. Wan, Self-assembly and steric hindrance for further host– guest interactions of a tetrahedral cage Fe4 IIL4, Chem. Pap., 2021, 75, 4493–4499.

[4] Sabry, N. M., Mohamed, H. M., Khattab, E. S. A., Motlaq, S. S., & El-Agrody, A. M. (2011). Synthesis of 4H-chromene, coumarin, 12H-chromeno [2, 3-d] pyrimidine derivatives and some of their antimicrobial and cytotoxicity activities. *European journal of medicinal chemistry*, *46*(2), 765-۷۷۲.

The 30th Iranian Seminar of Organic Chemistry
February 7-9, 2025, Iran University of Science and Technology, Tehran, Iran

A new aza-crown macrocyclic fluorescence chemosensor (N3O2 donor atoms) for magnesium ions in aqueous ethanol solution

Mostafa Koolivand[a]*, Hesam Niknezhad[a] and Fariba Khanbabai[a]

Inorganic Chemistry Laboratory, Faculty of Chemistry, Bu-Ali Sina University, Hamedan, Iran

Keywords: aza-crown macrocycle, chemosensor, Mg^{2+}, fluorescence

Abstract : A new N_3O_2 aza-crown macrocyclic ligand (L) bearing two fluorophore naphthalene moieties was synthesized and characterized by IR, 1H and 13C NMR, DEPt-135, HSQCGP, microanalysis as well as mass spectrometry. Comparative studies on the effect of various metal cations such as Cr(III), Cu(II), Cu(I), Zn(II), Cd(II), Pb(II), Na(I), Ni(II), Co(II), Ba(II), Fe(II), Fe(III), Al(III), La(III), Au(III), Mg(II), Cs(I), Ca(II), Hg(II), K(I), Mn(II) and Ag(I) on fluorescence of L were investigated in aqueous ethanol. The macrocycle was found to be a sensitive and selective fluorescence chemosensors for Mg^{2+}. The binding constant value was established as 1.36 × 105 M ;+ along with 1:1 stoichiometry for Mg^{2+}- L. The detection limit was 2.51×10^{-8} M with a rapid response time. Chemical inputs of Mg^{2+} and Fe^{3+} ions satisfy the conditions of INHIBIT molecular logic gate.

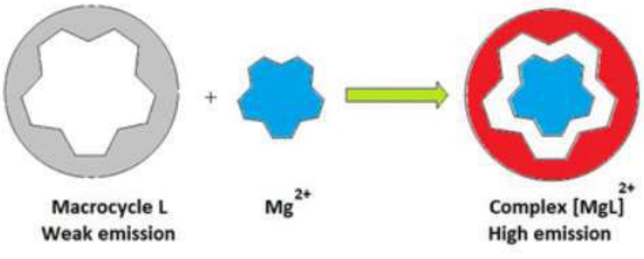

References:

۱- Abdollahi-Moghadam, M., Keypour, H., Azadbakht, R., & Koolivand, M. (2023). An experimental and theoretical study of a new sensitive and selective Al3+ Schiff base fluorescent chemosensor bearing a homopiperazine moiety. *Journal of Molecular Structure*, *1273*, 134289.
۲- Azadbakht, R., Moshiri, H., & Koolivand, M. (2024). Development of a highly selective and sensitive fluorescent chemosensory for zinc ion detection in aqueous ethanol solution: synthesis of a new aza-oxo macrocycle using high-dilution condition method. *Journal of Inclusion Phenomena and Macrocyclic Chemistry*, 1-11.
۳- Azadbakht, R., Moshiri, H., & Koolivand, M. (2024). Development of a highly selective and sensitive fluorescent chemosensory for zinc ion detection in aqueous ethanol solution: synthesis of a new aza-oxo macrocycle using high-dilution condition method. *Journal of Inclusion Phenomena and Macrocyclic Chemistry*, 1-11.

The 30th Iranian Seminar of Organic Chemistry
February 7-9, 2025, Iran University of Science and Technology, Tehran, Iran

An experimental and theoretical study of a new sensitive and selective Al^{3+} Schiff base fluorescent chemosensor bearing a homopiperazine moiety

Mostafa Koolivand[a]*, Hesam Niknezhad[a]

Inorganic Chemistry Laboratory, Faculty of Chemistry, Bu-Ali Sina University, Hamedan, Iran

Keywords: Schiff base, chemosensor, Al^{3+}, fluorescence

Abstract : Schiff base ligands can be considered key to designing fluorescent chemosensors due to their chromogenic properties. Here, we study this view and demonstrate that there is a remarkable fluorescence enhancement upon Al^{3+} addition to a new macroacyclic Schiff base ligand (H_2L) compared with 15 different metal ions, while the limit of detection (LOD) value is in good agreement with the values need for biological applications (2.1×10^{-9}M). Besides, we show that it can be a satisfactory linear relationship between the gradually added concentrations of Al^{3+} and the fluorescence intensity of H_2L. On the other hand, some transition shifts toward lower wavelengths were observed using the spectroscopic titration of H_2L with Al^{3+} ions. From the theoretical point of view, NBO analysis revealed that the band gaps varied from 1.715 eV for H_2L to 2.167 eV for $[AlL]^+$, confirming the blue shift upon complexation. The high difference in band gaps approved the occurrence of a significant electrochemical signal. Furthermore, the nature of bonds in H_2L and $[AlL]^+$ was investigated by the QTAIM method specifying the shared property of bonds in H_2L and the closed-shell metal-ligand interactions in $[AlL]^+$. Ellipticity (ε) measurements indicated that the π-character of imine bonding decreased via complexation.

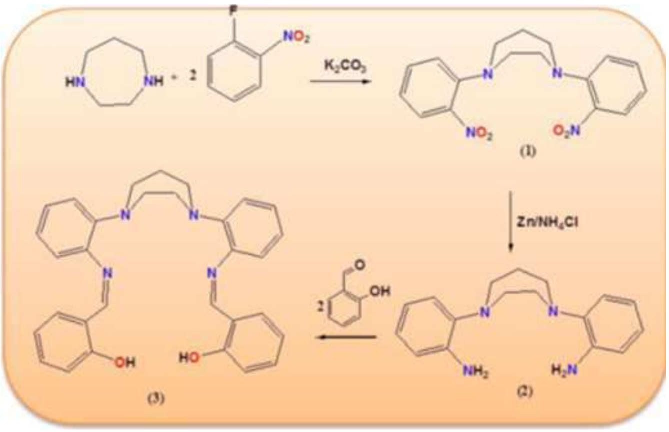

References:

١- Azadbakht, R., Chidan, N., Menati, S., & Koolivand, M. (2023). A new Azo-Schiff base dual-mode chemosensor: Colorimetric detection of cobalt ions and fluorometric detection of aluminum ions in aqueous ethanol solution. *Journal of Fluorescence, 33*(2), 527-538.

٢- Forooghi, K., Rudbari, H. A., Stagno, C., Iraci, N., Cuevas-Vicario, J. V., Kordestani, N., ... & Micale, N. (2024). Structural features and antiproliferative activity of Pd (ii) complexes with halogenated ligands: a comparative study between Schiff base and reduced Schiff base complexes. *Dalton Transactions*, *53*(25), 10571-10591.

٣- Golbedaghi, R., Ildiz, G. O., Azadbakht, R., & Fausto, R. (2022). A new tetramine bis (2-naphthol)-derivative fluorescent chemosensor for aluminum ion (Al3+). *Journal of Molecular Structure*, *1250*, 131775.

The 30th Iranian Seminar of Organic Chemistry
February 7-9, 2025, Iran University of Science and Technology, Tehran, Iran

Photocatalytic Suzuki–Miyaura Coupling Reaction Using a Novel Retrievable Magnetic photocatalyst

Authors: Gouhar Azadi[a], Mohammad Ghaffarzadeh[b]

[a]*Ilam Gas Company, Ilam, Iran*

[b]*Department of Organic Chemistry, Chemistry and Chemical Engineering Research Center of Iran (CCERCI), P.O. Box 14335-186, Tehran, Iran*

Keyword: Magnetic Photo-catalyst, Reusability, Coupling Reaction

Introduction

Sparked by the increasing energy crisis, much research has been focused on the development and utilization of renewable energy to supersede the limited fossil fuel. The potential of solar energy as a clean, economical, and accessible source of energy motivates new methods for converting solar energy into chemical energy. The development of photocatalytic methods for organic transformations is an important aspect of renewable energy technologies. Photocatalysis is currently considered as one of the most advanced, environmentally friendly, and promising technologies due to its excellent advantages such as efficiency, clean, energy-saving, and low cost [1]. The wide band-gap semiconductors (TiO_2, ZrO_2, ZnO etc.) have very wide application prospects in photocatalysis for varied reactions because they are high efficiency, low cost, and environment friendly, which have attracted great attentions [2,3]. In this photocatalytic system, TiO_2 is also a semiconductor that can absorb visible light and act as co-catalyst with Pd nanoparticle to facilitate C–C bond formation at room temperature.

Method

Synthesis of Pd-nanoparticle decorated L-arginine based Fe_3O_4@SiO_2@TiO_2

For the synthesis of Fe_3O_4@SiO_2@TiO_2@L-Arg, Fe_3O_4@SiO_2@TiO_2 (0.5g) was dispersed in 50 mL deionized water followed by sonication for 30 minutes, L-Arginine (1 g) was added to the suspended solid and the mixture was stirred at 90℃ for 24h. $Fe_{۳}O_{۴}$@$SiO_{۲}$@$TiO_{۲}$@L-Arg was separated using an external magnet and washed with distilled water several times, then dried in an oven overnight. To stabilize palladium on the surface of the product, Fe_3O_4@SiO_2@TiO_2@L-Arg (0.5 g) was dispersed in absolute ethanol (30 mL) for 15 minutes and then $Pd(OAc)_2$ (0.2 g) was added to the suspended solid. The mixture was stirred at reflux condition for 24 h. Finally, the product as a dark solid separated using an external magnet and dried at 60℃ to obtain Fe_3O_4@SiO_2@TiO_2@L-Arg@Pd as nano photocatalyst.

Results and Discussion

The magnetic nano-photocatalyst was synthesized by post-grafting approach, which the preparation process of Fe_3O_4@SiO_2@TiO_2@L-Arg@Pd is shown in scheme 1.

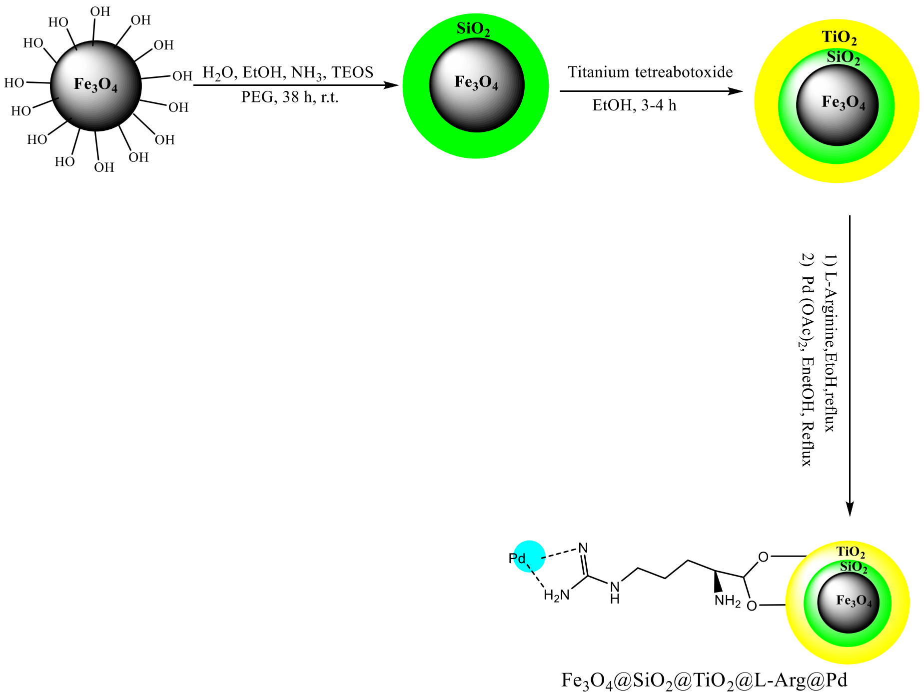

Scheme 1. Schematic illustration of the preparation process of Fe_3O_4@SiO_2@TiO_2@L-Arg@Pd.

The photocatalytic efficiency of the synthesized magnetic nano-photocatalyst was tested for the Suzuki coupling. The coupling of iodobenzene with phenylboronic acid was chosen as a model reaction to screen the catalytic activity of $Fe_3O_4@SiO_2@TiO_2$@L-Arg@Pd under visible light irradiation. Table 1 illustrates the results of the optimization studies.

Table 1. Different experimental conditions tested for the Suzuki reaction using $Fe_3O_4@SiO_2@TiO_2$@L-Arg@Pd.

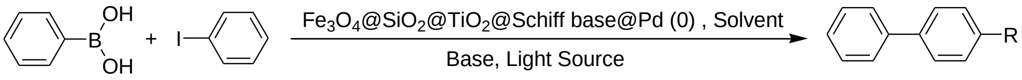

Entry	Solvent	Light source	Base	Catalyst (g)	Time (min)	Yield (%)
1	PEG	Blue LED 10W	K_2CO_3	0.02	20	55
2	PEG	White LED 10W	K_2CO_3	0.02	20	30
3	PEG	Green LED 10W	K_2CO_3	0.02	20	25
4	PEG	Blue LED 20W	K_2CO_3	0.02	20	98
5	PEG	Dark condition	K_2CO_3	0.01	120	10

[a]Reaction condition: iodobenzene (1 mmol), phenyl boronicacid (1 mmol), base (3 mmol). [b]Isolated yield. [c]Fe_3O_4, [d]$Fe_3O_4@SiO_2$, [e]$Fe_3O_4@SiO_2@TiO_2$.

References

١ . Juan C. Colmenares,a* Weiyi Ouyangb, Manuel Ojedab, Ewelina Kunaa, Olga Chernyayevaa, Dmytro Lisovytskiya, Sudipta Deb, Rafael Luqueb and Alina M. Balub*, N. Marina, A. E. Lanterna, J. C. Scaiano, *ACS Catal.* 2018, *8*, 7593–7597.
٢ . Y. Li, Y.-L. Li, B. Sa, R. Ahuja, *Catal. Sci. Technol.* 2017, *7*, 545–559.
٣ . G. Li, Q. Shi, S. J. Yuan, K. G. Neoh, E. T. Kang and X. L. Yang, Chemistry of Materials 22(4), 1309-1317 (2010).

The 30th Iranian Seminar of Organic Chemistry
February 7-9, 2025, Iran University of Science and Technology, Tehran, Iran

Synthesis of nanocomposites based on poly(amide-imide) and modified MOF for removal of Cr(VI) from aqueous media

Zahra Rafiee*

Affiliations: Department of Chemistry, Yasouj University, Yasouj 75918-74831, Islamic Republic of Iran

Keyword: Nanocomposite, Poly(amide-imide), MOF, Cr(VI)

Introduction

With the industrial growth, different pollutants are released in the environment which posing great threats to living beings; thus their removal is a pertinent issue. The heavy metals including mercury, cadmium, cobalt and chromium are most significant water pollutants [1]. Among these pollutants, chromium is one of the most dangerous heavy metals found in diverse industrial wastewaters [2,3]. Chromium in aqueous environment exists in two oxidation states of trivalent (Cr(III)) and hexavalent (Cr(VI)). Compare to Cr(III), Cr(VI) is found to be toxic and carcinogenic [4]. Different technologies have been offered for the removal of Cr(VI) from aqueous media [5]. Adsorption is the best technique among mentioned methods to remove dyes from aqueous solution due to its low cost, environmental friendly, easy operation, simple design and lack of contaminant byproducts [6]. The selection of the adsorbent plays a key role in adsorption method. Various adsorbents have been developed for the Cr(VI) removal from the aqueous solutions [7,8].

Method

Synthesis of Cu-BDC-MOF

0.498 g (3.00 mmol) of terephthalic acid was dissolved in 40 mL of DMF, and stirred for 15 min till a clear solution was formed. In another vessel, 2.42 g (10.00 mmol) of $Cu(NO_3)_2 \cdot 2H_2O$ was dissolved in 20 mL of DMF with stirring for 10 min at room temperature. Both solutions were mixed together, and then the mixture was transferred to a 150-mL Teflon-lined autoclave, sealed and heated in an oven at 100 °C for 12 h. After cooling, the resulting white crystalline solid was collected, washed by ethanol, and dried.

Preparation of Cu-BDC-MOF-NH_2

A mixture of 0.10 g of Cu-BDC-MOF, 30 mL of ethanol and 0.3 g of L-alanine was refluxed for 12 h under argon gas. After cooling, the reaction mixture was filtered to yield a blue precipitate which was washed with ethanol, and dried.

Preparation of Cu-BDC-MOF/PAI nanocomposites

Different weight percentages of modified Cu-BDC-MOF (5, 10 and 15 wt.%) were added to 0.2 g of PAI and the mixture was dispersed in 30 mL of absolute ethanol by stirring at room temperature for 30 min. Then, it was refluxed under argon atmosphere for 12 h. After cooling, the reaction mixture was filtered to yield a precipitate which was washed with ethanol, and dried.

Results and Discussion

Features of the resulting nanocomposites were investigated with FT-IR, XRD, SEM and TGA. According to the XRD results, highly crystalline Cu-BDC MOF is successfully inserted over polymer surface at which all the characteristic peaks of the MOFs appear in the XRD pattern of nanocomposite. No peak corresponding to impurities is detected which shows successful synthesis and compositing of the Cu-BDC-MOF and polymer. It is also evident that the prepared composites are binary hybrid nanocomposites rather than a physical mixture of the MOF with polymer. SEM images of nanocomposite show successful decoration of Cu-BDC-MOF over polymer surface. Furthermore, it was found that compared to bare Cu-BDC-MOF, which is in several microns, the presence of polymer results in well-dispersed and nano-sized Cu-BDC-MOF, resulting in MOF with higher surface area as well as formation of numerous pores between the MOF and the substrates, which are favorable for the adsorption of small molecules like organic pollutants. According to the findings of EDS analysis, the presence of the elements of Cu, C, and O in sample verify successful synthesis of the hybrid nanocomposite.

The removal of Cr(VI) was performed using Cu-BDC-MOF 15 wt.%. The amount of adsorbed heavy metal ions was calculated using the following equation:

$Q = (C_0 - C)V/m$

Q is the amount of metal ions adsorbed onto unit amount of sorbent (mg g^{-1}); C_0 and C are the concentrations (mg mL^{-1}) of metal ions in the primary solution and in the aqueous phase after adsorption, respectively; V is the volume of the aqueous phase (mL); and m is the weight of the sorbent (g). The influence of imperative parameters including contact time, pH and concentrations were assessed in this study.

Conclusions

This study examined Cr(VI) elimination from aqueous media via prepared Cu-MOF/PAI hybrid 15 wt.% as an absorbent. The optimum conditions were found to be initial dye concentration of 5 ppm, 0.016 g adsorbent, and pH = 9.5. The nonlinear pseudo-first-order model and linear Langmuir isotherm fitted the experimental results well.

References

[1] F. Fu, Q. Wang, J. Environ. Manag. 92 (2011) 407-418.
[2] B. Qiu, C. Xu, D. Sun, H. Yi, J. Guo, X. Zhang, H. Qu, M. Guerrero, X. Wang, N. Noel, Z. Luo, Z. Guo, S. Wei, ACS Sustain. Chem. Eng. 2 (2014) 2070-2080.
[3] N. Kumar, L. Reddy, V. Parashar, J. Catherine Ngila, J. Environ. Chem. Eng. 5 (2017) 1718-**1731.**
[4] J. Lopez-Luna, M. C. Gonzalez-Chavez, F. J. Esparza-Garcia, and R. Rodriguez-Vazquez, J. Hazard. Mater. 163 (20090 829-834.
[5] Y. Tan, J. Wang, L. Zhan, H. Yang, Y. Gong, *Sci Rep* 14 (2024) 4853.
[6] S. Daffalla, *Separations* 10 (2023) 260.
[7] J. Friday Amaku, R. Taziwa, *Chem. Pap.* 78 (2024) 5415-5431.
[8] Y. Qiu, Q. Zhang, B. Gao, M. Li, Z. Fan, W. Sang, H. Hao, X. Wei, Environ. Pollut. 265 (2020) 115018.

Fe_3O_4@SiO_2@$(CH_2)_3$Urea as a green and recyclable nanocatalyst for the synthesis of new naphthoazepines derivatives

Elham Ezzatzadeh*

Department of Chemistry, *Ardabil Branch, Islamic Azad University, Ardabil, Iran*

Keyword: Magnetic nanoparticles, Fe_3O_4@SiO_2@$(CH_2)_3$-Urea, Multicomponent reactions

Green chemistry plays a crucial role in organic transformations, prioritizing sustainability and reducing the environmental impact of chemical processes. It encompasses various principles such as maximizing yield, minimizing waste, using benign solvents and reagents, and promoting energy efficiency. Catalysis plays a crucial role in green chemistry by enhancing reaction efficiency and reducing the environmental consequences of chemical reactions. Recently, magnetic nanoparticles have attracted widespread research interest in organic synthesis owing to their high surface area, high stability, separability and reusability, low cost, convenient and cost-effective synthesis, and superparamagnetic properties [1]. In this research, a novel urea-immobilized silica-coated Fe_3O_4 MNP (Fe_3O_4@SiO_2@$(CH_2)_3$-Urea) a magnetically recoverable and metal-free nanocatalyst was designed and synthesized. Multiple techniques were employed to characterize this magnetic nanocatalyst such as FT-IR, XRD, FE-SEM, TEM, EDX, and VSM. This system was explored in a three-component reaction to newly synthesize naphthoazepines derivatives of 2-amino naphthol, electron-deficient acetylenic compounds, and alkyl bromide in water at room temperature. This method has various advantages, including clean reaction profiles, easy handling, a low-cost catalyst, no column purification, high yield, facile product isolation, and environmental compatibility (Scheme 1).

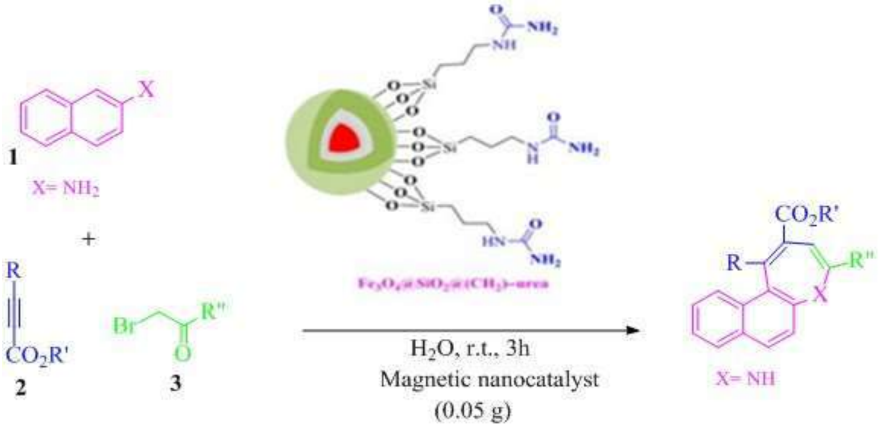

Scheme 1: The Fe_3O_4@SiO_2@$(CH_2)_3$-Urea catalyst for the synthesis of naphthoazepines derivatives

References:

[1] Ezzatzadeh, E., Hojjati, M., Parhami, A., & Hossaini, Z. (2024). One-Pot Multicomponent Synthesis of Substituted 1,6-Naphthyridine Derivatives Employing 4-Aminocumarin. *Applied Organometallic Chemistry*,38(12), e7718. https://doi.org/10.1002/aoc.7718

synthesis of pyrrole derivatives of using copeer iodide nanoparticles immobilized on functionalized copper based metal organic frameworks as novel catalyst

Yasamin Mirhadi 1*[a], Ramin Ghorbani-Vaghei 2[b], Sedighe Alavinia 3[c]

Depatmant of Organic Chemistry, Faculty of Chemistry and Petroleom Sciences, Bu-Ali Sina University, Hamedan 6517838683, Iran

**E-mail: ysmynmirhadi@gmail.com*

MOF, Pyrrole, heterocyclic compounds, metal–organic

The synthesis of novel heterocyclic compounds is of paramount importance among research studies, owing to their abundance, and extensive pharmaceutical and industrial application domains. Nitrogen-containing heterocycles as one of the most substantial categories of heterocyclic compounds are of eclectic pharmacological and biological performances. Pyrrole and its derivatives are widely circulated organic molecules having prime signifcance in natural products, synthetic chemistry, drugs, and the food industry. Some instances of Pyrrole are known to perform as antitumor. anti-infammatory, antibacterial, antioxidant, and antifungal agents. Besides, these compounds have been systematically employed in material science. Thus far, a good number of synthetic routes have been proposed and developed for the preparation of pyrroles and their derivatives. The classical methods utilized for the synthesis of pyrroles include Hantzsch, Knorr, Paal–Knorr, and Clauson-Kaas condensation reactions. How ever, despite their utility, such methods frequently sufer from some drawbacks such as multistep synthetic operations, severe reaction conditions, scarcity of the initiate materials, functional group compatibility, and region-specifcity. To overcome these challenges, various efcient strategies such as transition metal catalysis and multicomponent reactions (MCRs) have been developed.

Nanohybrid metal–organic frameworks (MOF) have recently been considered next-generation catalysts regarding their unique features like large surface-to-volume ratio, tailorable geometry, uniform pore sizes, and homogeneous distribution of active sites. In this report, we address the triazine-tetrazol modified 3D Cu-centred MOF Cu(NH_2-BCD) following a post-synthetic modification approach. The excellent chelating ability of triazine-aminopyridine was applied to immobilize Ni ions over the host matrix MOF. The as-synthesized material was physicochemically characterized using various analytical techniques like FT-IR, electron microscopy, EDS, elemental mapping, XRD, and ICP-OES. Subsequently, the material has been catalytically employed in synthesizing new Pyrrole derivatives.

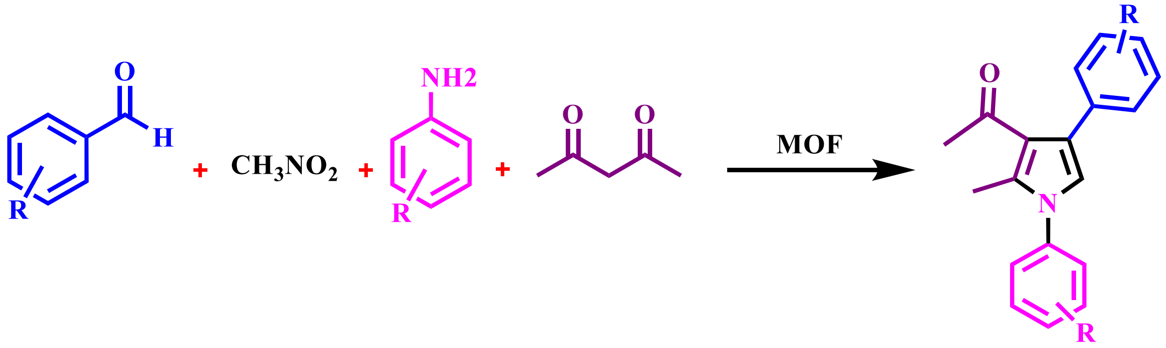

Scheme: Synthesis of pyrrole derivatives by MOF

References

(1) Mirzaei-Mosbat, M., Ghorbani-Vaghei, R., Karamshahi, Z., 2019, Springer Nature, 1613–1628
(2) Heidari, S., Alavinia, S., Ghorbani-Vaghei, R., 2023, *Sci Rep* **13**, 12964
(3) Pagadala, R., Maddila, S., Rana, S., Jonnalagadda, S,B., 2014, RSC Adv. **4**, 6602
(4) Alizadeh, A., Ghanbaripour, R., Zhu, L,G., 2014, Tetrahedron **70**, 2048
(5) Lonkar, S,P., Raquez, J,M., Ph Dubois, 2015, Nano-Micro Lett. **7**, 332
(6) Maiti, S., Biswas, S., Jana, U., 2010, J.Org. Chem. **75**, 1674

The 30th Iranian Seminar of Organic Chemistry
February 7-9, 2025, Iran University of Science and Technology, Tehran, Iran

Synthesis, Antimicrobial activity, and Molecular Docking Studies of Quinoxaline Derivatives

Elham Zarenezhad[1*]

[1] *Noncommunicable Diseases Research Center, Fasa University of Medical Sciences, Fasa, Iran*

Keyword: Cyclization, Quinoxaline, Molecular docking study.

Introduction: Quinoxalines, a significant class of nitrogen-containing heterocyclic compounds, have long captivated synthetic chemists due to their diverse applications in pharmacology (1-3). These valuable heterocycles have demonstrated a wide range of pharmacological activities. The quinoxaline core is a constituent of various antibiotic compounds, including levomycin, echinomycin, and actindeutin, which effectively inhibit the growth of Gram-positive bacteria. Additionally, triostin (I), which incorporates a quinoxaline ring, has exhibited potent antibacterial activity against Gram-positive bacteria by binding to the DNA of susceptible strains through the bifunctional intercalation of the quinoxaline moiety (4-6).

Method: This research focuses on the synthesis of O-oxime ethers containing amino cyclic residues. The process involved oximation of aromatic ketones followed by O-alkylation with epichlorohydrin to produce O-oxime ether adducts. Subsequent cyclization of these adducts with o-phenylenediamine resulted in the synthesis of novel quinoxaline compounds.

The synthesized compounds were evaluated for their in vitro antibacterial activity against standard strains of *Escherichia coli* and *Staphylococcus aureus*, and their efficacy was compared to reference drugs like tetracycline and penicillin. Additionally, molecular docking studies were conducted to understand the binding interactions of these compounds with bacterial targets.

Results and Discussion: All the synthesized compounds were evaluated for their anti-bacterial activities. Two compound **(5a**, **5b)** with 6.25 mg/cm^3 showed promising antibacterial activity against *S. aureus* .The docking results revealed that derivatives with smaller substituents, such as methyl and ethyl groups, exhibited the highest affinity and binding to the active sites of the tested bacterial proteins (*E. coli* Mur B (PDB ID: 2Q85) and *S. aureus* Gyrase B (PDB ID: 3G75))). This strong binding affinity likely contributes to the enhanced biological activity observed for these compounds (Scheme1).

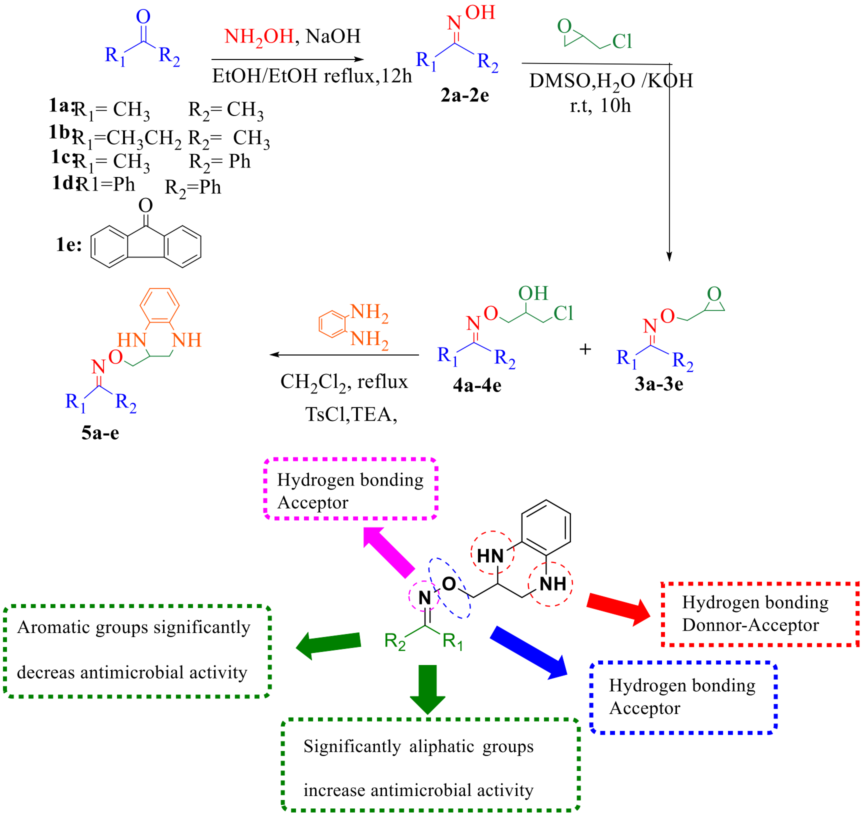

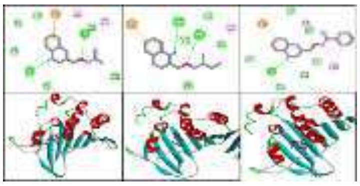

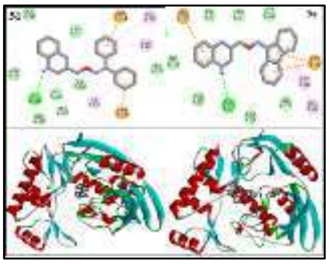

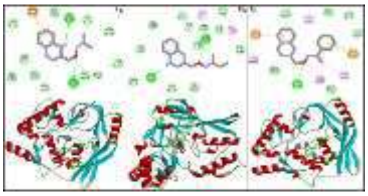

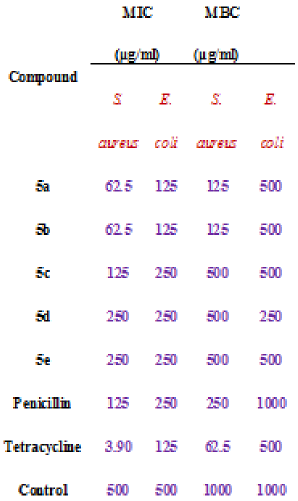

Compound	MIC (µg/ml)		MBC (µg/ml)	
	S. aureus	E. coli	S. aureus	E. coli
5a	62.5	125	125	500
5b	62.5	125	125	500
5c	125	250	500	500
5d	250	250	500	250
5e	250	250	500	500
Penicillin	125	250	250	1000
Tetracycline	3.90	125	62.5	500
Control	500	500	1000	1000

Scheme1

Refrences:

1. Husain A, Madhesia D. Recent advances in pharmacological activities of quinoxaline derivatives. J Pharm Res. 2011;4(3):924-9.
2. Tariq S, Somakala K, Amir M. Quinoxaline: An insight into the recent pharmacological advances. European journal of medicinal chemistry. 2018;143:542-57.
3. Mosslemin MH, Zarenezhad E, Shams N, Rad MNS, Anaraki-Ardakani H, Fayazipoor R. Green Synthesis of 5-aryl-(1 H, 3 H, 5 H, 10 H)-pyrimido [4, 5-b] quinoline-2, 4-diones Catalysed by 1, 4-diazabicyclo [2.2. 2] octane in Water. Journal of Chemical Research. 2014;38(3):169-71.
4. Ishikawa H, Sugiyama T, Kurita K, Yokoyama A. Synthesis and antimicrobial activity of 2, 3-bis (bromomethyl) quinoxaline derivatives. Bioorganic chemistry. 2012;41:1-5.
5. Kim YB, Kim YH, Park JY, Kim SK. Synthesis and biological activity of new quinoxaline antibiotics of echinomycin analogues. Bioorganic & medicinal chemistry letters. 2004;14(2):541-4.
6. El-Attar MA, Elbayaa RY, Shaaban OG, Habib NS, Wahab AEA, Abdelwahab IA, et al. Design, synthesis, antibacterial evaluation and molecular docking studies of some new quinoxaline derivatives targeting dihyropteroate synthase enzyme. Bioorganic chemistry. 2018;76:437-48.

Development and Characterization of Azo-Linked Phthalocyanine for Knoevenagel Condensation Reactions

Mohadeseh Janjan[a], Maliheh Safaiee *[a]

[a] *Department of Organic Chemistry, Faculty of Chemistry and Petroleum Sciences, Bu-Ali Sina University, Hamedan 6517838695, Iran*

Keyword: Azo-Linked Phthalocyanine, Knoevenagel Condensation

Aromatic azo compounds are characterized by their -N=N- double bonds and an extensive π electron conjugation system, which contribute to their diverse applications in functional materials[1]. The properties of these compounds are significantly influenced by the substituents attached to the aromatic rings. Azo-linked phthalocyanines, a novel class of compounds, have gained attention due to their unique structural and optical properties[2,3].

The Knoevenagel Condensation Reaction, first described by Emil Knoevenagel in the 1890s, is a classic organic synthesis method. It involves a nucleophilic addition between an aldehyde or ketone and a compound with active hydrogen, facilitated by a basic catalyst, leading to the formation of C–C bonds. In this context, we present a simple and efficient synthesis of azo-linked catalysts that incorporate accessible phthalocyanine and azo functional groups within their framework and characterize it. These catalysts are effectively utilized in Knoevenagel condensation reactions, as illustrated in Scheme 1.

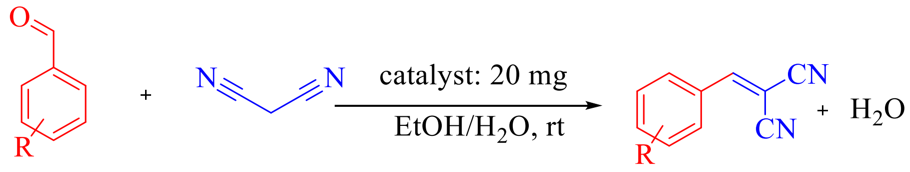

Scheme: Knoevenagel condensation reaction between different aldehydes and malonitrile catalyzed by azo-link phthalocyanine

References:

[1]. Zhao, M.-Y., Tang, Y.-F., and Han, G.-Z. *Recent Advances in the Synthesis of Aromatic Azo Compounds:Molecules* **2023**, *28, 6741.*

[2]. Saber, A. F., · Chen, K.-Y.; · EL-Mahdy, A. F. M.; Kuo, S.-W. **2021.**.*Designed azo-linked conjugated microporous polymers for CO2 uptake and removal applications, Journal of Polymer Research 28, 430.*

*[3]. Panić, B., Frey, T., Borovina, M., Konopka, K., Sambolec, M., Kodrin, I., & Biljan, I. (***2023***). Synthesis and characterization of benzene- and triazine-based azo-bridged porous organic polymers. Polymers, 15(1), 229.*

Multicomponent Reactions: Order, or Chaos? That Is the Question.

Mohammad Bagher Teimouri

Faculty of Chemistry, Kharazmi University, Mofateh Ave, 15719-14911 Tehran, Iran

Keywords: Multicomponent Reactions, Isocyanide, Chaos, Chromone

For over a century of active research, multicomponent reactions (MCRs) have been traditionally discovered "by-serendipity" or "by-analogy" [1-4]. As organic chemists, we have repeatedly observed that a very small change in the structure of one of the components or reaction conditions in a MCR can fundamentally alter the reaction process, leading to a new product that is completely different from our initial prediction. Even though we think we have sufficient control over all circumstances, we are still confused by the resulting chaos. Now the fundamental question is whether this situation is complete chaos or is there an order that we are unaware of.

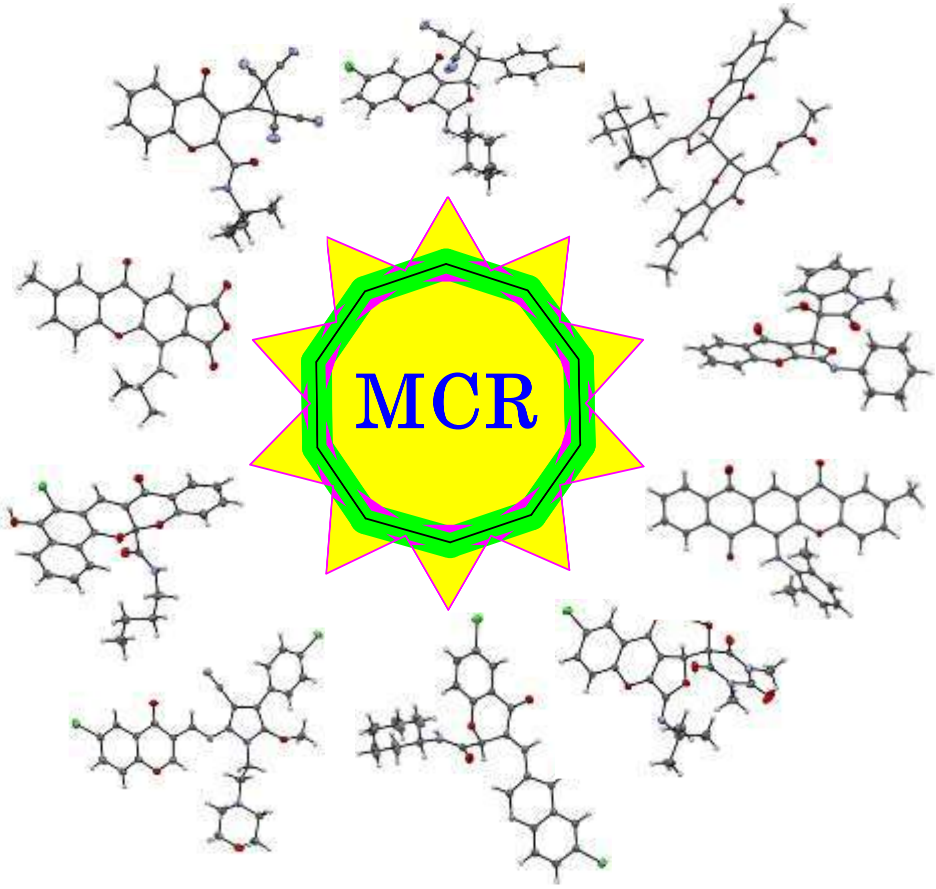

[1] Grzybowski, B. A., et al., *Nat. Comm.* **2024**, *15*, 10285. DOI: 10.1038/s41467-024-54611-5
[2] Dömling, A., *J. Org. Chem.* **2023**, *88*, 5242. DOI: 10.1021/acs.joc.2c00792
[3] Teimouri, M. B., et al., *J. Org. Chem.* **2024**, 89, 4657. DOI: 10.1021/acs.joc.3c02916
[4] Teimouri, M. B., et al., *Chem. Sci.*, **2025**, Advance Article. DOI: 10.1039/d4sc07275h

Designing of new functionalized imidazolium based ionic liquids attached to the antracene derivatives and investigation on the influence of intramolecular hydrogen bondings in anions on their intermolecular hydrogen bondings and some of the other properties: A DFT M06-2X-GD3 study

Authors: Farzad Alijani Chakoli, Khatereh Ghauri, Farhad Shirini *

Department of Organic Chemistry, Faculty of Chemistry, University of Guilan, P.O. Box 41335-19141, Rasht, Iran

**Corresponding author*

;E-mail addresses: shirini@guilan.ac.ir; fshirini@gmail.com

Keyword: Anthracene; Functionalized ionic liquids; M06-2X-GD3 functional; ECW; Gibbs free energy; NCI

1. Introduction

Ionic liquids (ILs) are different from traditional solvents because of their interesting and abnormal physical properties. They apply in many areas of chemistry especially in biochemistry, catalysis, synthesis, and material science [i-ii]. Also, by modifying the molecular structure of anions and cations in ILs green or designer solvents for academic researches and industrial applications can be obtained. These compounds generally consist of different inorganic anions and bulky organic cations [vi, viii], for example, cations based on tertiary ammonium or phosphonium ions or on heterocycles like pyridinium, pyrrolidinium, triazolium, or imidazolium [ix]. A new type of ionic liquids named as tunable aryl alkyl ionic liquieds, TAAILs, are prepared by a combination of aryl and alkyl groups at the N1 and N3 positions of the imidazole ring [x, xi]. In these compounds various substituents on the phenyl ring can be utilized to modify the attributes of the TAAILs for different applications [xiv].

2. Computational details

In the recent years, density functional theory (DFT) has been widely used to study the features of structural, electronic, energy and also description of the essence of H bonding interactions in ILs [xvii]. In this study, the geometries of all of the studied structures were quite optimized by the hybrid functional M06-2X [xviii] and 6-311++g(d,p) basis set [xxii] which have been commonly utilized in the study of cation-anion H bonding interactions in ILs. All the calculations reported in this study were performed with the Gaussian 09 program [xxiii]. To describe the stationary points, the calculate of zero-point vibrational energy (ZPVE) and thermochemical quantities, the analysis of vibrational frequency was applied at the same theoretical level of theory. For correcting of the basis set superposition error (BSSE) in the calculation of the interaction energies was used the counterpoise method (CP) [xxiv]. In addition, dispersion energies contribution

for the van der Waals interaction influences in the interaction energy of ILs was gained using the M06–2X–GD3 method and the 6-311++G(d,p) basis set. Electrostatic potential (ESP) maps [xxv,xxvi] for the free anions and cations were computed to predict the reaction center of every molecules with other ones. The NBO and AIM [xxvii] analysis were performed using version 3.1 of the NBO program[xxviii] and the AIM2000 package [xxix] at M06-2X/6-311++G(d,p) level of theory. The non-covalent interactions (NCI) calculations containing the plots of RDG versus the $\lambda_2 \times \rho(r)$ and RDG isosurfaces [xxx] were computed using Multiwfn [xxxi] and VMD [xxxii] programs.
In addition, the *UV-VIS absorption* of the ILs have been investigated using TD-DFT at the M06-2X-GD3/6-311++(d,p) level of theory in the gas phase. Finally, the solvent influence on the stability of ionic liquids was determined by using the polarizable continuum model PCM [xxxiii,xxxiv] at M06–2X-GD3/6-311++G(d,p) level of theory using optimized structures obtained in the gas phase of the ILs in five solvents including water, dimethylsulfoxide (DMSO), acetonitrile, methanol and cyclohexane. The Quantum chemical method of COSMO-RS to determine the electrochemical window (ECW) of ILs were performed at BVP86/TZVP level of theory in the acetonitrile solvent [xxxv,xxxvi].

4. Conclusions

In this study, the interaction energies, the features of structural, electronic and some of the physicochemical characteristics of two new series of ILs with the general formula of [X-AnMIM][A2] and [X-AnMIM][A3] ILs which in them anions are A2= $[(OHCH_2CH_2)_2CHO]^-$ and A3= $[(OHCH_2CH_2)_3CO]^-$, respectively, containing various substituents including NH_2, OH, OMe, H, Cl, CHO, CN and NO_2 on anthracene ring in the cationic part have been investigated. According to the optimized geometries and structural parameters of the ILs obtained at M06-2X-GD3/6-311++(d,p) level of theory, it can be inferred that the molecular structure, cation−anion interaction and intra and intermolecular hydrogen bonds of the ILs have significant effects on the studied ILs physicochemical properties. The change of the substituents on the anthracene ring of the cationic part and the change of anion from A2 with two intramolecular hydrogen bonds to A3 with three intramolecular hydrogen bonds has a significant effect on the energy values of the cation-anion interaction and features of optic and chemical of the ILs.

The 30th Iranian Seminar of Organic Chemistry
February 7-9, 2025, Iran University of Science and Technology, Tehran, Iran

Microbial polyhydroxyalkanoate (PHAs) production and comparison in three bacterial strains

Moosavi, S.M.[a], Mahmoodian, Sh.[a], Bagheripoor, L.[b], Yahyazadeh, S.[a], Montazer, Z.*[a]

[a]*Agricultural Faculty, Semnan University, Semnan, Iran*

[b]*Faculty of Veterinary, Semnan University, Semnan, Iran*

Abstract

Polyhydroxyalkanoates (PHAs) are biodegradable polymers with properties similar to petroleum-based plastics make them appropriate alternative to use in medical and industrial application like sustainable active food packaging. These polymers are produced in limited nutritional condition by many type of microorganisms. In this work microbial production of polyhydroxyalkanoate (PHAs) is surveyed and then compared in three strains of bacteria including *Cuprividus necator*, *Pseudomonas putida* and *Bacillus megaterium*. Result showed PHAs were produced and accumulated intracellulary in all strains, but are different in amount. Also mechanical and physical properties of the produced polymer are completely varied among bacterial strains.

Keywords: *Biodegradability, Green polymers, Microbial production*

Introduction,

One of the most promising green biopolymers to replace synthetic plastics are polyhydroxyalkanoates (PHAs). These biopolyesters are naturally synthesized by bacteria and stored as cytoplasmic granules of 0.2–0.5 μm diameter, providing carbon and energy for the bacteria under certain conditions (Porras et al., 2018) under limited condition of some nutritional components in media, the microorganisms assimilate the carbon source and store it as polymers called PHAs. Bacteria, fungi, and microalgae are known to produce PHAs by utilizing different substrates. Bioproduction of PHAs is a highly promising strategy for manufacturing biodegradable polymers using renewable resources as compared to its chemical method of production. PHAs find their application in various fields such as medical (slow drug-releasing carriers, tissue engineering, sutures, implants), agricultural (controlled release of pesticides, insecticides, and plant growth regulators), and food industries (active food packaging material), biofuels and as well in the manufacturing of disposables (bottles, bags, diapers, packaging, and lids) (Xu et al. 2021; Montazer et al., 2018).

The objects of this work are to survey the production of PHAs in three bacteria and comparison the amount and chemical structure to determine related medical and industrial applications.

Method

Bacteria strains

Three bacterial strains including *Cuprividus necator (10878 IBRC-M No.)*, *Pseudomonas putida (10847 IBRC-M No.)* and *Bacillus megaterium (10420 IBRC-M No.)* were prepared from Iranian bank of biological and genetic center (IBRC). *Escherichia coli* was prepared from veterinary faculty in Semnan University as negative control for PHA production.

Culture media

Minimal salt media (MSM) with limited composition described by Blunt et al. was prepared. Glucose was added into medium (1%) as sole carbon source and the medium was autoclaved. The final pH adjusted to 7.0. No-added carbon source media were prepared as negative control.

Bacterial growth and PHA production determination

Bacterial strains were activated on nutrient agar and then sub-cultured on Brain Heart Infusion Broth to reach up the suitable population number for inoculation in main media. Fifty microliter of one-day incubated tubed was inoculated in every individual minimal salt media containing glucose

Strains	Polymer type	Amount (g/L)	Physical state of PHA
Cuprividus necator	Hydroxybutyrate (3HB)	164±3.83^{a}	Soft
Pseudomonas putida	Hydroxyalkanoate	206±11.21^{a}	Rigid
Bacillus megaterium	Hydroxybutyrate (3HB)	18±1.95^{b}	Soft

in 30 minutes' intervals to measure the optical density at 600 nm (OD_{600}) with visible spectrophotometer (Biochrom WPA; Biovawe II; England) according to Uchida et al. (2000). all tubes were shaken gently to suspend the settled biomass. Growth curves of four bacteria were established too find the optimum time of maximum PHA production. PHA production was determined and compared by Sudan Black staining procedure according to Porras et al. (2018) and Nile Re staining under florescent microscope.

Statistical analysis

All data were subjected to statistical analyses using the R Core Team (2024) stats package. Mean variables were compared using Duncan's test, and correlations between variables were calculated by the Pearson Square method at probability level of 5% (R Core Team 2024). All experiments were done in three replicates.

Results and Discussion

Establishment of growth curves

All growth curve on glucose media was established in order to determine the microbial growth phases and optimize the maximum PHA production. Growth curves from bacterial turbidity at 600nm was achieved for four strains.

Determination and comparison of PHA production in cells

PHA production was confirmed by Nile red staining under florescent microscope in all strains can be seen in Figure 1 and compared by Sudan black absorbance by PHA in cells (Table 1).

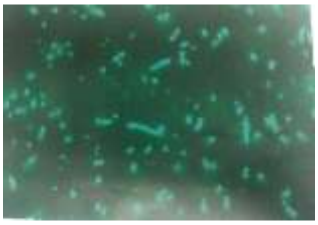

Figure 1- Glowing spots represent the PHB granules in *C.necator*. number of graunals are between 3 to 10.

Table 1- PHAs production and type of monomers in different bacterial strains.

References

[1] Porras, M. A., Villar, M. A., & Cubitto, M. A. (2018). Improved intracellular PHA determinations with novel spectrophotometric quantification methodologies based on Sudan black dye. *Journal of microbiological methods, 148,* 1–11.

[2] Xu, Z., Xu, M., Cai, C., Chen, S., & Jin, M. (2021). Microbial polyhydroxyalkanoate production from lignin by *Pseudomonas putida NX-1. Bioresource technology, 319,* 124210.

[3] Montazer, Z., Habibi Najafi, M. B., & Levin, D. B. (2019). Microbial degradation of low-density polyethylene and synthesis of polyhydroxyalkanoate polymers. Canadian journal of microbiology, 65(3), 224–234.

[4] Blunt, W., Lagassé, A., Jin, Z., Dartiailh, C., Sparling, R., Gapes, D. J., ... & Cicek, N. (2019). Efficacy of medium chain-length polyhydroxyalkanoate biosynthesis from different biochemical pathways under oxygen-limited conditions using Pseudomonas putida LS46. Process biochemistry, 82, 19-31.
[5] R Core Team (2024). _R: A Language and Environment for Statistical. Computing_. R Foundation for Statistical Computing, Vienna, Austria. <https://www.R-project.org/>.

The 30th Iranian Seminar of Organic Chemistry
February 7-9, 2025, Iran University of Science and Technology, Tehran, Iran

One-pot four component synthesis of functionalized benzo[α]phenazine derivatives in presence of Fe_3O_4 @SiO_2-n-propyl-NH_2 as an efficient and reusable nanocatalyst

Gholam Hossein Mahdavinia*[a]

[a] *Department of Chemistry, Marvdasht Branch, Islamic Azad University, Marvdasht, Iran.*

Keyword: 2-hydroxynaphthalene-1,4-dion, Benzo[α]phenazine , Magnetic nano catalyst, Fe_3O_4@SiO_2-n-propyl-NH_2

MCRs have been designed as a powerful synthetic tools for producing novel and complex elaborate biologically active compounds[1].The success of (MCRs) compared to divergent (linear) syntheses is due to their simple and efficient methodology[2], high productivity[3], lower cost[4], time saving manner[5], atom efficient nature[6], and lower energy requirement[7]. Multicomponent reactions have remarkable significance in combinatorial chemistry in the synthesis of drug-like molecules and pharmaceutical industry in the drug-discovery process and medicinal chemistry [8].

Among the nanoparticles (NPs) catalysis; magnetic nanoparticles (MNPs) play an important role in catalyzing a range of organic reactions [9]. In recent times interest in magnetic nanoparticles (MNPs) especially those which have core-shell components structures (magnetic core and functional shell) has increased considerably [10] in view of their high surface-to-volume ratio [11], high application in catalysis, environmental friendly nature and cost-effectiveness [12].

In continuation of our ongoing research concerning the development of new methods to the generation of heterocyclic compounds, in this research we would like to report a new and efficient methodology for synthesis of benzo[α]phenazine derivatives from a one-pot four component reaction of 2-hydroxynaphthalene-1,4-dion, *O*-phenylenediamine, aryl aldehyde and amide derivatives in ethanol.

In conclusion, an efficient and simple synthetic strategy for the one pot, four component synthesis of novel N-((6-hydroxybenzo[α]phenazin-5-yl)(phenyl)methyl)acetamide derivatives using ethanol as a cheap, safe and environmentally benign solvent and Fe_3O_4@SiO_2-n-propyl-NH_2 as a nano catalyst was identified for the first time. Particularly, distinguished advantages of this method are high yields, very straightforward isolation of product, short reaction times, low cost and simple procedure.

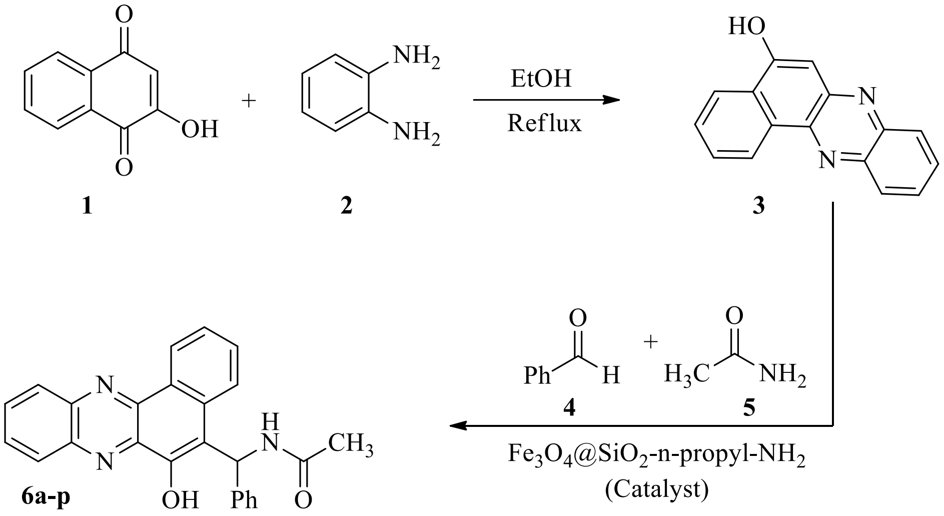

Scheme 1. Synthesis of N-((6-hydroxybenzo[α]phenazin-5-yl)(phenyl)methyl)acetamide

References:

[1] B. Dongare, S.; V .Chavan, H.; S. Bhale, P.; B. Mule, Y.; S. Kotmale, A.; P. Bandgar, B. *Chinese Chemical Letters* **2015**, *15*, 2.

[2] Amanpour, T.; Zangger, K.; Belaj, F.; Bazgir, A.; Dallinger, D.; Kappe, C.O. *Tetrahedron letters* **2014**, *14*, 3.

[3] Ghahremanzadeh, R.; Fereshtehnejad, F.; Bazgir, A. *Chem. Pharm. Bull.* **2010**, *58*, 516.

[4] El Aleem, M. A.; El-Remaily, A. A. *Chin. J. Catal.* **2015**, *36*, 1124.

[5] Ghahremanzadeh, R.; Fereshtehnejad, F.; Bazgir, A. *Chem. Pharm. Bull.* **2010**, *58*, 516.

[6] B. Dongare, S.; V .Chavan, H.; S. Bhale, P.; B. Mule, Y.; S. Kotmale, A.; P. Bandgar, B. *Chinese Chemical Letters* **2015**, *15*, 2.

[7] El Aleem, M. A.; El-Remaily, A. A. *Chin. J. Catal.* **2015**, *36*, 1124.

[8] Amanpour, T.; Zangger, K.; Belaj, F.; Bazgir, A.; Dallinger, D.; Kappe, C.O. *Tetrahedron letters* **2014**, *14*, 3.

[9] Zarnegar, Z.; Safari, J. *Journal Of Molecular Structure* **2014**, *1072*, 53-60.

[10] Sadeghzade, S. M.; Nasseri, M. A. *Catalyst Today* **2013**, *217*, 80-85.

[11] (a) Santra, S.; Rahman, M.; Roy, A.; Majee, A.; Hajra, A. *Catalyst Communication* **2104**, *49*, 52-57; (b) Sadeghzade, S. M.; Nasseri, M. A. *Catalyst Today* **2013**, *217*, 80-85.

[12] Rad-Moghadam, K.; Dehghan, N. *Journal Of Molecular Catalysis A: Chemical* **2014**, *392*, 97-104

The 30th Iranian Seminar of Organic Chemistry
February 7-9, 2025, Iran University of Science and Technology, Tehran, Iran

Schiff base ligands derived from o/m-anisidine and substituted salicylaldehyde and their Cu(II) complexes as anticancer drug candidates: X-ray crystallographic Studies

Nakisa Moini[a], Saeed Dehghanpour*[a], Hadi Amiri Rudbari*[b], Zahra Kazemi[b]

[a] *Department of Inorganic Chemistry, Faculty of Chemistry, Alzahra University, Tehran, Iran.*
[b] *Department of Chemistry, University of Isfahan, Isfahan, 81746-73441, Iran.*

Keyword: Schiff base, Cu(II) complexes, Crystallography

Introduction

According to the International Agency for Research on Cancer (IARC), cancer is the second leading cause of death worldwide, killing an estimated 10 million people in 2020 [1]. Different treatments, including radiotherapy and chemotherapy, can be used to treat this disease, quite often in combination with surgery. However, these treatments usually lead to severe side effects due to their lack of selectivity for cancer cells [2]. Therefore, further effort in the synthesis of new effective and less toxic anticancer drugs appears necessary. Coordination compounds were discovered as promising alternative agents to treat several types of cancer. Schiff bases ($R_1R_2C=NR_3$) are also interesting organic compounds containing an azomethine group (-CH=N-) or an imine group (-C=N-), that form very stable complexes, especially with transition metal ions. Therefore, metal complexes of Schiff bases have been widely designed and investigated for biomedical applications, such as antitumor, anti-inflammatory, antibacterial and antifungal activities [3]. Over the past decades, copper (II) complexes have shown a wide range of pharmacological activities, including anticancer activity. These compounds have shown different mechanisms in combating cancer cells [4]. An excellent example is Casiopeinas®, a family of planar copper coordination complexes with potent antineoplastic effects and low toxicity in normal cells, which has recently been the subject of phase I clinical trials in Mexico [5].

Method

According to the scientific articles, the best method for the synthesis of Schiff ligands is the reaction between the desired aldehyde and amine in methanol solvent and at ambient temperature (Figure 1) [6]. The most suitable method for the synthesis of the corresponding complexes is the reaction between copper acetate salt and the Schiff ligand in methanol solvent at ambient temperature with a ratio of 2:1.

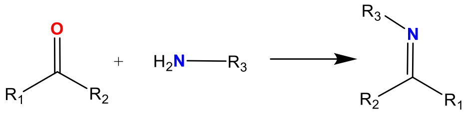

Figure 1. The general synthetic procedure of Schiff base ligands

Results and Discussion

In the first step of a research project to find a suitable anticancer drug, 62 Schiff base ligands and their Cu(II) complexes have been synthesized and characterized. SC-XRD data indicate that for o-anisidine derivatives the most likely structure is an octahedral or tetrahedral structures resulting from two Schiff ligands, where each Schiff ligand acts as a tridentate or bidentate ligands. Crystallographic results showed that the structural change depends on the substitution on the salicylaldehyde group. Also, the most likely structure for the complexes resulting from m-anisidine derivatives is a tetrahedral structure. Here, also each Schiff ligand acts as a bidentate ligand. In this case, the change in structure from octahedral to tetrahedral is due to the remoteness of the methoxy group present in m-anisidine derivatives, which cannot act as a metal donor group (Figure 2).

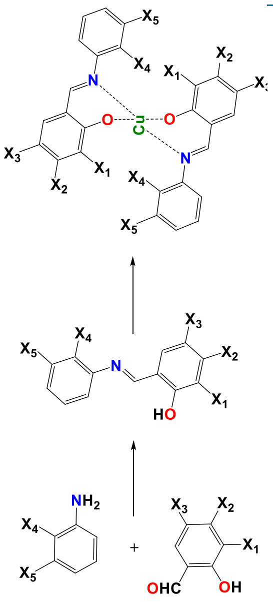

	Ligands						Complexes				
	X_1	X_2	X_3	X_4	X_5		X_1	X_2	X_3	X_4	X_5
1	H	H	H	OCH_3	H	**Cu1**	H	H	H	OCH_3	H
2	H	H	Cl	OCH_3	H	**Cu2**	H	H	Cl	OCH_3	H
3	H	H	Br	OCH_3	H	**Cu3**	H	H	Br	OCH_3	H
4	H	H	I	OCH_3	H	**Cu4**	H	H	I	OCH_3	H
5	Cl	H	Cl	OCH_3	H	**Cu5**	Cl	H	Cl	OCH_3	H
6	Br	H	Br	OCH_3	H	**Cu6**	Br	H	Br	OCH_3	H
7	I	H	I	OCH_3	H	**Cu7**	I	H	I	OCH_3	H
8	Br	H	Cl	OCH_3	H	**Cu8**	Br	H	Cl	OCH_3	H
9	H	H	NO_2	OCH_3	H	**Cu9**	H	H	NO_2	OCH_3	H

10	H	Me	H	OCH_3	H	**Cu10**	H	Me	H	OCH_3	H
11	H	H	Me	OCH_3	H	**Cu11**	H	H	Me	OCH_3	H
12	H	OMe	H	OCH_3	H	**Cu12**	H	OMe	H	OCH_3	H
13	H	H	OMe	OCH_3	H	**Cu13**	H	H	OMe	OCH_3	H
14	H	$N(C_2H_5)$	H	OCH_3	H	**Cu14**	H	$N(C_2H_5)$	H	OCH_3	H
15	OMe	H	NO_2	OCH_3	H	**Cu15**	OMe	H	NO_2	OCH_3	H
16	NO_2	H	OMe	OCH_3	H	**Cu16**	NO_2	H	OMe	OCH_3	H
17	H	H	H	H	OCH_3	**Cu17**	H	H	H	H	OCH_3
18	H	H	Cl	H	OCH_3	**Cu18**	H	H	Cl	H	OCH_3
19	H	H	Br	H	OCH_3	**Cu19**	H	H	Br	H	OCH_3
20	H	H	I	H	OCH_3	**Cu20**	H	H	I	H	OCH_3
21	Cl	H	Cl	H	OCH_3	**Cu21**	Cl	H	Cl	H	OCH_3
22	Br	H	Br	H	OCH_3	**Cu22**	Br	H	Br	H	OCH_3
23	I	H	I	H	OCH_3	**Cu23**	I	H	I	H	OCH_3
24	Br	H	Cl	H	OCH_3	**Cu24**	Br	H	Cl	H	OCH_3
25	H	H	NO_2	H	OCH_3	**Cu25**	H	H	NO_2	H	OCH_3
26	H	Me	H	H	OCH_3	**Cu26**	H	Me	H	H	OCH_3
27	H	H	Me	H	OCH_3	**Cu27**	H	H	Me	H	OCH_3
28	H	OMe	H	H	OCH_3	**Cu28**	H	OMe	H	H	OCH_3

29	H	H	OMe	H	OCH$_3$	**Cu29**	H	H	OMe	H	OCH$_3$
30	H	N(C$_2$H$_5$)	H	H	OCH$_3$	**Cu30**	H	N(C$_2$H$_5$)	H	H	OCH$_3$
31		OMe	H	NO$_2$	OCH$_3$	**Cu31**	OMe	H	NO$_2$	OCH$_3$	H
32		NO$_2$	H	OMe	OCH$_3$	**Cu32**	NO$_2$	H	OMe	OCH$_3$	H

6

Cu6

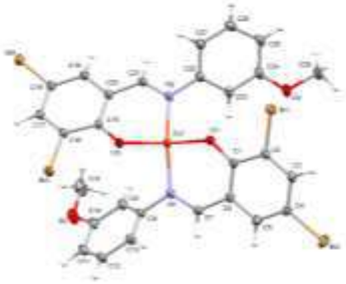

Cu22

Figure 2. Synthesized ligands and Cu(II) complexes in this work

References:

1. Piña-Sánchez, P., et al., *Cancer Biology, Epidemiology, and Treatment in the 21st Century: Current Status and Future Challenges From a Biomedical Perspective.* Cancer control, 2021. 28.
2. Mani, A., et al., *Structurally simple osmium (II) polypyridyl complexes as photosensitizers for photodynamic therapy in the near infrared.* Angewandte Chemie, 2023. **135**(20): p. e202218347.
3. Kanwal, A., et al., *A review on synthesis and applications of some selected Schiff bases with their transition metal complexes.* Journal of Coordination Chemistry, 2022. **75**(19-24): p. 2533-2556.
4. Santini, C., et al., *Advances in copper complexes as anticancer agents.* Chemical reviews, 2014. 114(1): p. 815-862.
5. Figueroa-DePaz, Y., et al., *Casiopeinas of third generations: synthesis, characterization, cytotoxic activity and structure–activity relationships of mixed chelate compounds with bioactive secondary ligands.* Molecules, 2022. **27**(11): p. 3504.
6. Boulechfar, C., et al., *Schiff bases and their metal Complexes: A review on the history, synthesis, and applications.* Inorganic Chemistry Communications, 2023. **150**: p. 110451.

Encapsulation of 5-fluorouracil and doxorubicin co-loaded layered double hydroxide with carboxymethyl starch as an efficient drug delivery system

Elaheh Ranjbar[a], Hassan Namazi[a,b*]

[a]*Polymer Research Laboratory, Department of Organic and Biochemistry, Faculty of Chemistry, University of Tabriz, Tabriz, Iran.*
[b]*Research Center for Pharmaceutical Nanotechnology, Biomedicine Institute, Tabriz University of Medical Science, Tabriz, Iran.*

Keywords: Carboxymethyl starch; Layered double hydroxides; drug delivery; colon cancer

Introduction

Recent decades have witnessed substantial advancements in the design of modern drug delivery systems characterized by unique biological, physical, and chemical properties[1]. Research indicates that nanocomposites enhanced with natural polymers show promising potential as drug delivery systems, particularly for the controlled and targeted release of anticancer agents within tumor environments. This study proposes a novel drug delivery system utilizing Carboxymethyl starch (CMS)-coated Layered Double Hydroxide (LDH) as a pH-sensitive biopolymer, facilitating controlled oral co-drug delivery and enhancing therapeutic efficacy in colon cancer treatment[2, 3].

Method

In the initial phase, LDH(Mg-Al) was synthesized using a straightforward co-precipitation method in an argon atmosphere at 90–95 °C. Subsequently, both 5-fluorouracil (5-Fu) and doxorubicin (DOX) were simultaneously loaded onto LDH(Mg-Al), utilizing STMP as a biocompatible chemical linker within the CMS biopolymer to create microspheres. The resulting CMS@LDH(Mg-Al)@DOX,5-Fu microspheres were then evaluated for their pH-controlled drug release profile and effectiveness against colon cancer cells.

Results and discuss

DOX and 5-Fu were loaded at approximately 38% and 75%, respectively, in the synthesized LDH(Mg-Al). The MTT assay conducted against Caco-2 cells demonstrated the biocompatibility of CMS/LDH(Mg-Al) and highlighted its sustained drug release capabilities due to the presence of CMS in the structure of CMS@LDH(Mg-Al)@DOX,5-Fu microspheres. This indicates that the formulation is promising for effective drug delivery in cancer treatment.

---

[*] Corresponding author: P.O. Box 51666, Tel: +98 4133393121, Fax: +98 4133340191, Email:namazi@tabrizu.ac.ir, ORCID: http://orcid.org/0000-0002-1977-4677.

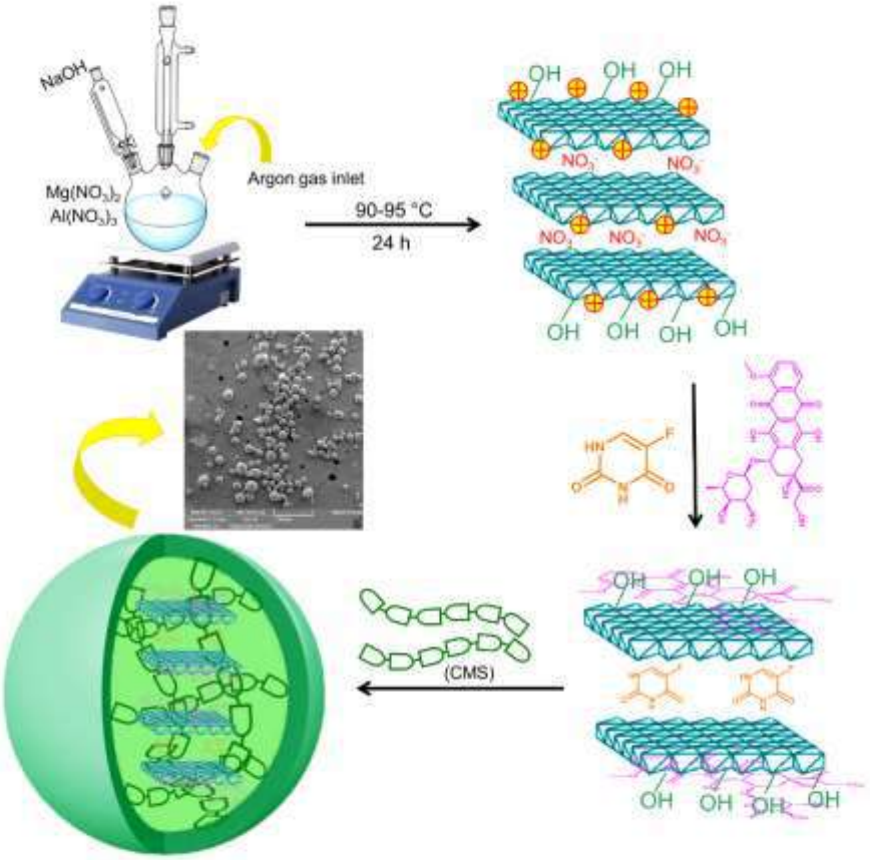

Scheme: Schematic illustration of the LDH(Mg-Al) synthesis, co-drug loading, coating of the LDH(Mg-Al)@DOX,5-Fu with CMS, and the proposed mechanism for the drug releases from CMS@LDH(Mg-Al)@DOX,5-Fu microspheres.

References:

[1] K. Saravanakumar, B. Sriram, A. Sathiyaseelan, A.V.A. Mariadoss, X. Hu, K.-S. Han, V. Vishnupriya, D. MubarakAli, M.-H. Wang, Synthesis, characterization, and cytotoxicity of starch-encapsulated biogenic silver nanoparticle and its improved anti-bacterial activity, International Journal of Biological Macromolecules 182 (2021) 1409-1418.
[2] M. Yadollahi, H. Namazi, S. Barkhordari, Preparation and properties of carboxymethyl cellulose/layered double hydroxide bionanocomposite films, Carbohydrate polymers 108 (2014) 83-90.
[3] X. Cai, Y. Wang, X. Du, X. Xing, G. Zhu, Stability of pH-responsive Pickering emulsion stabilized by carboxymethyl starch/xanthan gum combinations, Food Hydrocolloids 109 (2020) 106093.

Synthesis of a new biocompatible Fe_3O_4-PEG coated layered double hydroxide/doxorubicin loaded hydroxyapatite nanocomposite for targeted drug delivery to cancer cells

Elaheh Ranjbar[a], Hassan Namazi[a,b*]

[a]*Polymer Research Laboratory, Department of Organic and Biochemistry, Faculty of Chemistry, University of Tabriz, Tabriz, Iran.*
[b]*Research Center for Pharmaceutical Nanotechnology, Biomedicine Institute, Tabriz University of Medical Science, Tabriz, Iran.*

Keywords: Polyethylene glycol; Layered double hydroxide; Hydroxyapatite; pH-sensitive

Introduction

In the ongoing fight against cancer, the medical and scientific communities are continuously striving to enhance treatment strategies by improving efficacy and minimizing adverse effects [1, 2]. This study explores a novel approach leveraging advancements in materials science, nanotechnology, and biopolymers to address these challenges through the creation of a sophisticated pH-sensitive drug delivery system. Specifically, this study presents a biocompatible pH-sensitive system utilizing a nanocomposite of layered double hydroxide@hydroxyapatite doxorubicin coated magnetic Fe_3O_4-polyethylene glycol (LDH@HAp-DOX@Fe_3O_4-PEG) designed for the targeted delivery of doxorubicin (DOX) [3, 4].

Method

Initially, Mg-Al-Layered Double Hydroxide (LDH) nanocomposites were created through coprecipitation, followed by the encapsulation of HAp-DOX via sonication in an ultrasonic bath. Additionally, Fe_3O_4 nanoparticles underwent PEG modification after their preparation through co-precipitation using the same ultrasound-assisted technique. The resulting electrostatic interactions between the nanoparticles and the encapsulated LDH@HAp-DOX within the Fe_3O_4-PEG matrix led to the formation of a stable nanocomposite.

Results and discuss

The drug encapsulation efficiency (DEE) and drug-loading content (DLC) for HAp-DOX were determined to be approximately 78.1% and 7.8%, respectively. Furthermore, the system exhibited a significantly higher drug release rate of about 68.9% in a low-pH environment (pH 5) compared to only $\leq 40\%$ at pH 7.4, thereby confirming the pH-sensitive release behavior of the LDH@HAp-DOX@Fe_3O_4-PEG nanocomposite. This indicates that the nanocomposite is capable of targeted and efficient drug delivery under acidic conditions, which is often present in tumor microenvironments.

---

[*] Corresponding author: P.O. Box 51666, Tel: +98 4133393121, Fax: +98 4133340191, Email:namazi@tabrizu.ac.ir, ORCID: http://orcid.org/0000-0002-1977-4677.

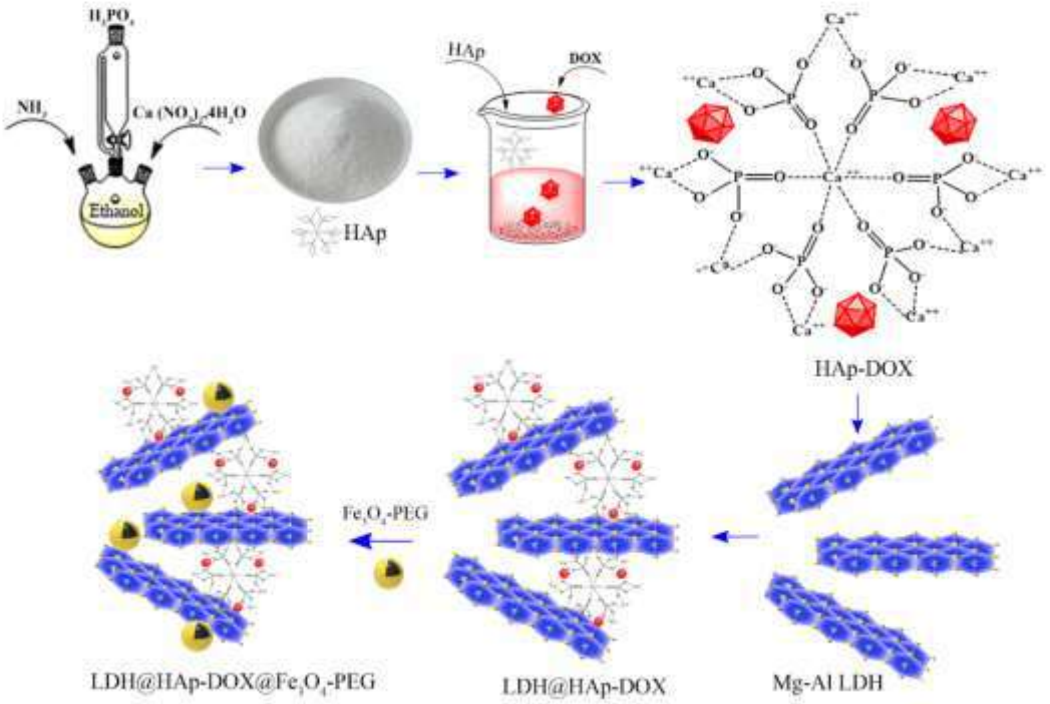

Scheme: Synthetic steps of new pH-responsive LDH@HAp-DOX@Fe_3O_4-PEG nanocomposites for delivery of DOX drug

References:

[1] H. Namazi, M. Pooresmaeil, R. Salehi, Construction of a new dual-drug delivery system based on stimuli-responsive co-polymer functionalized D-mannose for chemotherapy of breast cancer, European Polymer Journal 188 (2023) 111958.
[2] S. Javanbakht, N. Nazari, R. Rakhshaei, H. Namazi, Cu-crosslinked carboxymethylcellulose/naproxen/graphene quantum dot nanocomposite hydrogel beads for naproxen oral delivery, Carbohydrate polymers 195 (2018) 453-459.
[3] G.-Y. Lee, P.-Y. Lo, E.-C. Cho, J.-H. Zheng, M. Li, J.-H. Huang, K.-C. Lee, Integration of PEG and PEI with graphene quantum dots to fabricate pH-responsive nanostars for colon cancer suppression in vitro and in vivo, FlatChem 31 (2022) 100320.
[4] V. Gupta, S. Mohiyuddin, A. Sachdev, P. Soni, P. Gopinath, S. Tyagi, PEG functionalized zirconium dicarboxylate MOFs for docetaxel drug delivery in vitro, Journal of Drug Delivery Science and Technology 52 (2019) 846-855.

Improving the performance of cyclophosphamide anticancer drug by 18-crown-6 crown ether nanoparticle in drug delivery using quantum calculations and density functional theory (DFT)

AshkanBagheri*

Department of Applied Chemistry, Faculty of Science, Malayer University, Malayer, 65174, Iran

ashkanbagherichemist@gmail.com

Abstract: This study aimed to investigate the interaction between cyclophosphamide, a widely used chemotherapy drug, and 18-crown-6 nanoparticles for potential drug delivery applications, and investigated various thermodynamic parameters such as adsorption energy, enthalpy, Gibbs free energy, and solvent effects. These analyses determine to what extent crown ethers can act as a suitable carrier for cyclophosphamide. It was found that the adsorption process of cyclophosphamide onto 18-crown-6 is exothermic, which ultimately indicates the efficiency and effectiveness of this complex.

Keywords: cyclophosphamide, crown ether, 18-crown-6, drug delivery, DFT

Background: Cyclophosphamide is a widely used chemotherapeutic agent known for its efficacy in the treatment of various cancers including lymphoma and leukemia. However, its clinical use is often limited due to significant side effects and poor solubility, which can lead to adverse therapeutic outcomes. A type of crown ether, 18-crown-6, offers a promising solution by providing a biocompatible and non-toxic carrier for cyclophosphamide. Its high surface area and tunable porosity enable efficient drug loading and ensure that a sufficient amount of the drug reaches the target cells. The encapsulation process protects cyclophosphamide from degradation and increases its stability and bioavailability. Furthermore, crown ethers can be functionalized to improve targeting, allowing for selective delivery to cancer cells while minimizing exposure to healthy tissues. Controlled release mechanisms can be incorporated into the ether formulation, allowing for sustained drug release over time. Overall, the combination of cyclophosphamide and 18-crown-6 represents a significant advance in drug delivery systems aimed at improving treatment outcomes and patient quality of life in cancer treatment.

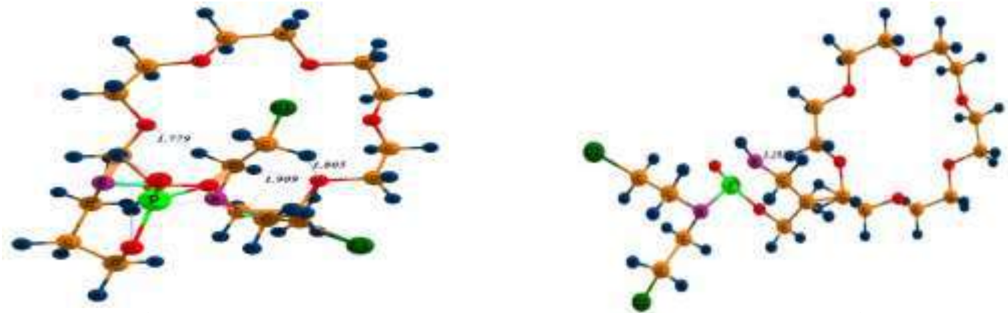

Fig1. Picture of the optimized structures related to the adsorption of cyclophosphamide to 18-Crown-6.

Methode : In this study, in order to improve the performance of cyclophosphamide in drug delivery based on quantum calculations and density functional theory method with b3lyp-6_311G(d,p) method, we investigated the interaction of cyclophosphamide drug and 18-crown-6 (encapsulated) ether tag. In this research, Gaussin 09 software and other computational software such as Spartan were used. The structure of the drug and optimized ether tag was displayed (Figure 1). Also, thermodynamic parameters such as adsorption energy, entropy, Gibbs free energy and solvent effect were calculated. And the results are shown in (Table 1).

Parameter	E_{ads}	HΔ	GΔ	E_{ads}(Solvent)
Complex	-68.07	-46.58	-51.93	**-59.17**

Table1. The values of adsorption energy, solvent medium adsorption energy, entropy and Gibbs free energy.

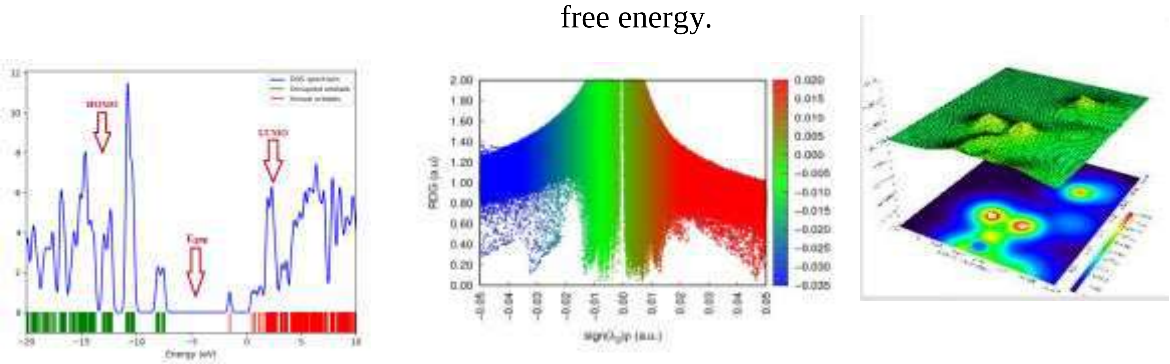

Fig2. Picture of the DOS plots,RDG , ELF to the adsorption of cyclophosphamide to 18-Crown-6.

Result: Considering the negative values of Gibbs free energy and enthalpy, it is shown that the interaction between cyclophosphamide and 18-crown-6 is spontaneous, exothermic and thermodynamically favorable. Furthermore, since the adsorption energy showed a negative value, this indicates a strong and favorable interaction between cyclophosphamide and 18-crown-6, which can lead to effective drug loading and controlled release. Furthermore, the solvent environment can significantly affect the interaction between the drug and the nanoparticle, with water potentially weakening the interaction between the drug and the nanoparticle.

Conclusion: Based on the computational analysis of the interaction between cyclophosphamide and 18-crown-6-ethertaji, it can be concluded that this compound has significant potential for enhancing drug delivery. The strong binding affinity between the drug and the nanoparticle, as indicated by the negative adsorption energy, indicates that the drug can be effectively loaded onto the nanoparticles. Furthermore, the favorable thermodynamic parameters point to a stable and spontaneous interaction. Also, the results of the effect of the solvent environment show that the placement of the drug-nano complex in an aqueous environment (blood) reduces the adsorption energy and also weakens the interaction between the drug and the nanoparticle, which indicates that when the complex enters the blood, it can more easily dissociate from its nanocarrier and bind to the target cell upon reaching the target tissue. However, it is important to note that computational studies provide valuable insights, but they need to be complemented by experimental validation. Further research, including experimental studies, is necessary to fully evaluate the efficacy and safety of this drug delivery system and reduce side effects. Ultimately, the integration of computational modeling and experimental validation could accelerate the development of innovative drug delivery systems.

Reference:

[1] Baker, J. R., & Lentz, T. L. (2019).** "Nanoparticle-based drug delivery systems for cyclophosphamide: A review." *Journal of Controlled Release*, 305, 153-1٦٥.

[2] Zhang, Y., et al. (2020).** "Targeted delivery of cyclophosphamide using liposomes: A novel approach to enhance therapeutic efficacy." *International Journal of Nanomedicine*, 15, 123-135.

[3] Khan, A. A., & Rahman, M. (2021).** "Formulation and evaluation of cyclophosphamide-loaded polymeric micelles for enhanced anticancer activity." *European Journal of Pharmaceutical Sciences*, 159, 105706.

[4] Huang, Y., et al. (2022).** "Smart drug delivery systems for cyclophosphamide: Challenges and opportunities." *Advanced Drug Delivery Reviews*, 178, 113968.

[5] Patel, M. M., & Desai, S. D. (2023).** "Cyclophosphamide: Mechanisms of action and drug delivery strategies." *Cancer Chemotherapy and Pharmacology*, 91(2), 301-3١٧.

The 30th Iranian Seminar of Organic Chemistry
February 7-9, 2025, Iran University of Science and Technology, Tehran, Iran

Carbohydrazide-based Schiff Base Linked Covalent Organic Framework as a Novel Peroxidase Mimic

Somaye Shahraki

Department of Chemistry, University of Zabol, Zabol, Iran

Nanomaterials with enzymatic properties (Nanozymes) have attracted much attention in recent years for various reasons such as good catalytic efficiency, high stability, low cost and good biocompatibility [1]. Here, we synthesized and characterized a novel covalent organic framework (COF) via the condensation reaction of triamine (benzene-1,3,5-triyltris(methaneylylidene))tri(methanedihydrazide, BTMTM) and terephthalaldehyde (Figure 1). In the presence of hydrogen peroxide (H_2O_2), the COF was able to catalyze the oxidation of 3,3',5,5'-tetramethylbenzidine (TMB) to a blue-colored oxidized product (ox-TMB), indicating its high peroxidase-like activity. Based on this phenomenon, the reported COF was used as a colorimetric probe for the sensitive and selective detection of H_2O_2 and glucose. The limit of detection (LOD) of H_2O_2 was calculated to be 7.5 μM in a linear range from 0.1 to 5 mM, while the LOD of glucose was evaluated to be 11.1 μM in the range of 0.1 to 0.25 mM. Therefore, the prepared COF can be used as a highly sensitive and selective peroxidase mimic for the detection of hydrogen peroxide-related molecules, indicating their great potential in biomedical applications.

Keyword: Covalent Organic Frameworks, Schiff Base, Peroxidase Mimic

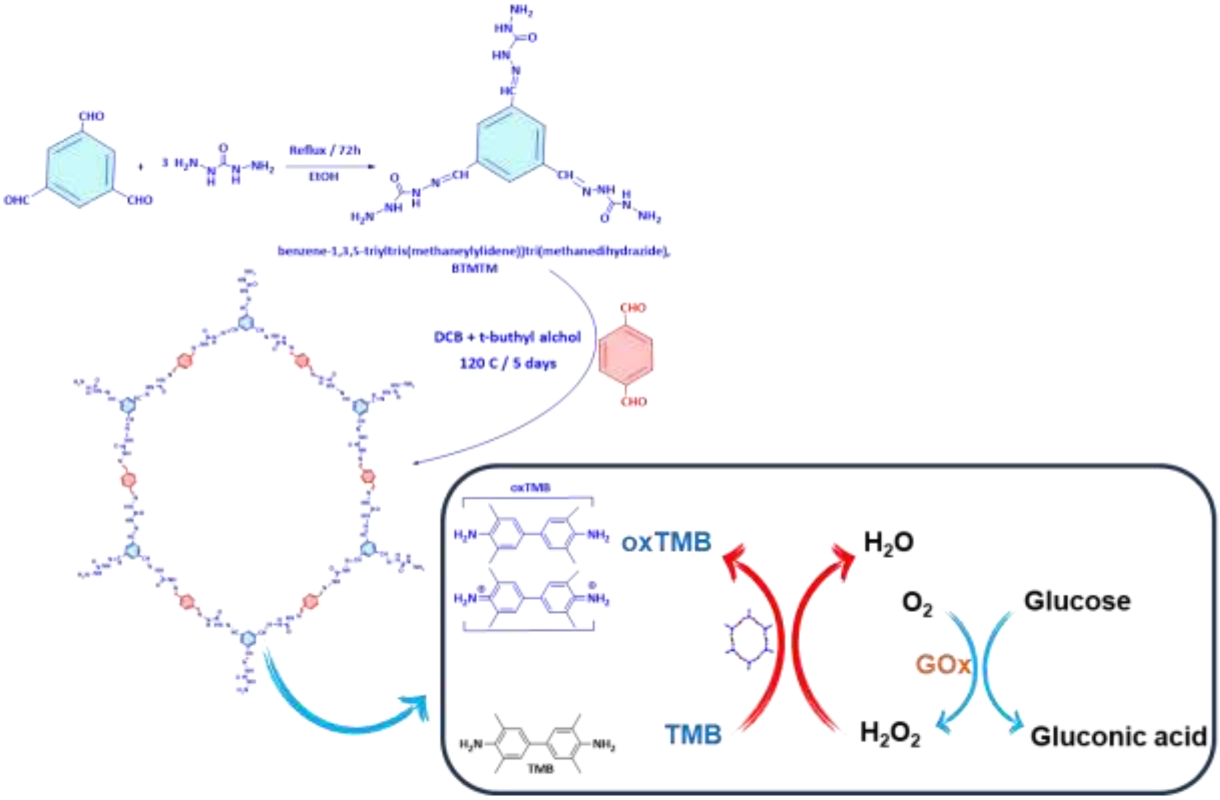

Figure 1. Schematic illustration of the formation of prepared COF and the colorimetric detection of glucose by it and glucose oxidase (GOx).

References:

[1] S. Shahraki, E. Vaziri, A.A. Saboury, K. Fan, Biomedical potential of nanozymes: Harnessing redox enzyme mimicry for theranostic applications, Coordination Chemistry Reviews 517 (2024) 215937.

The 30th Iranian Seminar of Organic Chemistry
February 7-9, 2025, Iran University of Science and Technology, Tehran, Iran

Schiff base-based oxime derivate as a highly selective fluorescent and colorimetric probe for Hg(II) ion

Somaye Shahraki

Department of Chemistry, University of Zabol, Zabol, Iran

Schiff bases are versatile, useful, cheap, readily available and easy-to-synthesize compounds that have attracted attention due to their wide range of applications [1, 2]. The Schiff base-based emission complex 4-((2-(hydroxyimino)-1-phenylpropylidene)amino)-3-((2-(hydroxyimino)-1-phenylpropylidene)amino)phenyl)(phenyl)methanone, HPAM, was synthesized from a facile condensation reaction and characterized by various spectroscopic techniques. The obtained ligand had strong fluorescence emission properties and could be used selectively and with high sensitivity for the detection of Hg(II) ions in aqueous solutions. The mechanism of fluorescence quenching was investigated and it was shown that the emission intensity of this fluorescence probe is quenched by a dynamic mechanism. The binding stoichiometry for the HPAM: Hg^{2+} complex was determined using the Benesi-Hildebrand plot and was discovered to be 1:1 Ratio. Also, the detection limit of HPAM ligand for Hg(II) ions was obtained to be as low as 1×10^{-6} M level, which was low enough for the detection of Hg(II) ions, which is widely distributed in biological and environmental systems.

Keyword: Fluorescent probe, Selectivity, Sensitivity, Schiff Base, Hg(II) ions

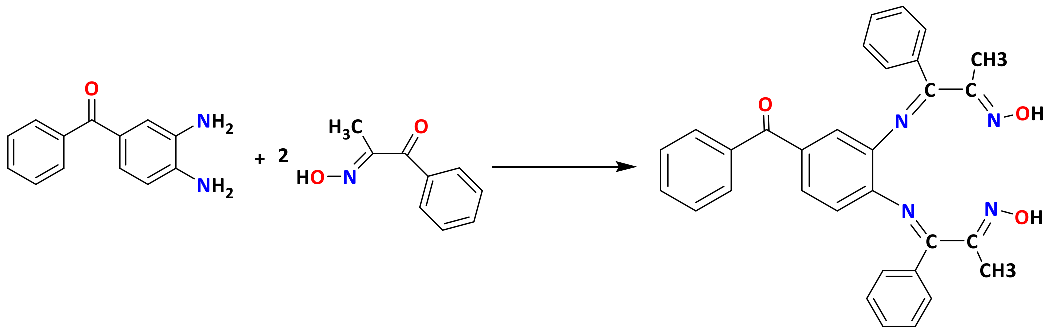

Figure 1. Design of fluorescent probe HPAM.

References:

[1] S. Shahraki, M.H. Majd, A. Heydari, Journal of Molecular Structure 1177 (2019) 536-544.
[2] S. Shahraki, Colloids and Surfaces B: Biointerfaces 218 (2022) 112727.

The 30th Iranian Seminar of Organic Chemistry
February 7-9, 2025, Iran University of Science and Technology, Tehran, Iran

Synthesis of polysubstituted imidazole-benzoxazinone conjugated derivatives and evaluation of their optical and electrochemical behaviors

Somayeh Rashtabad Jadidi [a], Zarrin Ghasemi [*a]
Department of Organic Chemistry and Biochemistry, Faculty of Chemistry, University of Tabriz, 51666-16471, Tabriz, Iran
Corresponding Author E-mail: z.ghasemi@tabrizu.ac.ir

Tell: +98-41-33393116

Abstract

This paper focuses on the synthesis of novel benzoxazinone derivatives containing polyaryl substituted imidazole moiety. The reaction of polysubstituted imidazolyl-based *o*-amino phenols with dimethyl acetylenedicarboxylate in ethanol gave corresponding benzoxazinones. The newly synthesized compounds were confirmed by spectroscopic techniques and analytical data. The optical and electrochemical behaviors of the newly synthesized compounds were also investigated.

Keywords: polysubstituted imidazole, *o*-aminophenol, benzoxazinone

1. Introduction

Benzoxazinone derivatives, are presented in a variety of pharmaceutical compounds and bioactive molecules like dopamine agonist activity, antimycobacterial, and intracellular calcium antagonist [1]. In addition to the medicinal applications, benzoxazinones have been used as dyes and key intermediates in the synthesis of organic semiconductors [2]. These compounds are also used in the agricultural sector as herbicides [3]. The synthesis and development of fluorescent organic compounds have always been considered by many scientists due to their technological applications [4-8]. On the other hand, organic supercapacitors as high-efficient and cost-effective electrochemical energy storage devices, have drawn most attention due to their unique features including eco-friendly, abundant, and simple principle [9]. 1,2,4,5-tetraarylimidazoles, which can be prepared *via* four-component condensation of 1,2-diketones, aryl aldehydes, primary amines, and ammonium acetate, are an important part of many bioactive molecules, conjugated and fluorescent materials, and metal-coordinating ligands [10,11]. Herein we report the design and synthesis of new polysubstituted imidazole linked benzoxazinone derivatives with related *o*-aminophenols and dimethyl acetylenedicarboxylate. The newly synthesized compounds were evaluated in view of optical and electrochemical properties.

2. Experimental Section

2.1. General procedure for the preparation of benzoxazinone compounds (4a,b)

A mixture of polysubstituted imidazole linked *o*-Aminophenols (**3a,b**) (1.0 mmol), and dimethyl acetylenedicarboxylate (1.0 mmol) in EtOH (5 mL) was stirred at room temperature. After 1 h, the solid product was separated, washed with EtOH, dried, and the desired products were obtained without further purification.

3. Results and Discussion

The starting materials, polysubstituted imidazole-based phenols **1a,b** were prepared by four-component reaction of benzil, ammonium acetate, *p*-aminophenol, and benzaldehyde derivatives in the presence of *p*-toluene sulfonic acid as catalyst [12]. Nitration of this compounds with nitric acid in acetic acid gave *o*-nitrophenols **2a,b** [13]. Iron in acetic acid and ethanol was then used to reduce the obtained compounds to give the corresponding *o*-aminophenols **3a,b** [13]. In the following, *o*-aminophenol compounds were treated with dimethyl acetylenedicarboxylate at room temprature in EtOH and benzoxazinone products **4a,b** were obtained in good yields (Scheme 1).

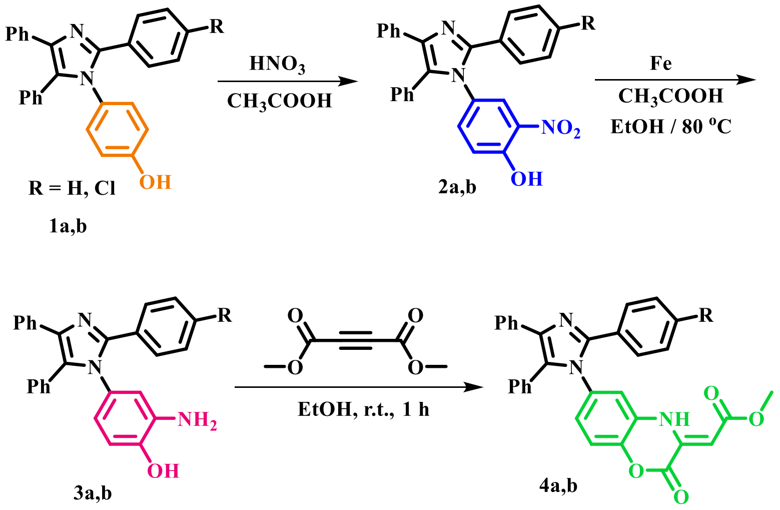

Scheme 1: Synthesis of benzoxazinone compounds **4a,b**

UV-Vis spectra of the synthesized molecules in ethanol (10^{-5} M) were studied. These compounds show an intense absorption band with a λ_{max} about 280 nm, corresponding to strong π-π^* transitions.

The fluorescence properties of the synthesized molecules were also showed the intense emission of blue light at about 390 nm (Figure 1). The emission quantum yields were also calculated using naphthalene as a standard (*Φ* = 0.23) and Maximum quantum yield is related to derivative **4b** (0.31).

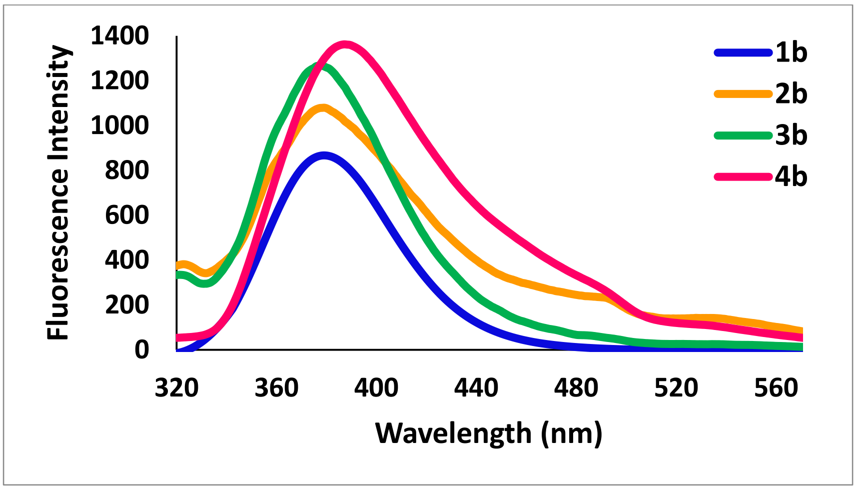

Figure 1. Fluorescence spectra of compounds **1a, 2a, 3a,** and **4a.**

The electrochemical performance of **4a/AC** supercapacitor in a two-electrode cell assembly with KOH (6 M) as electrolyte was evaluated at room temperature (Figure 2).

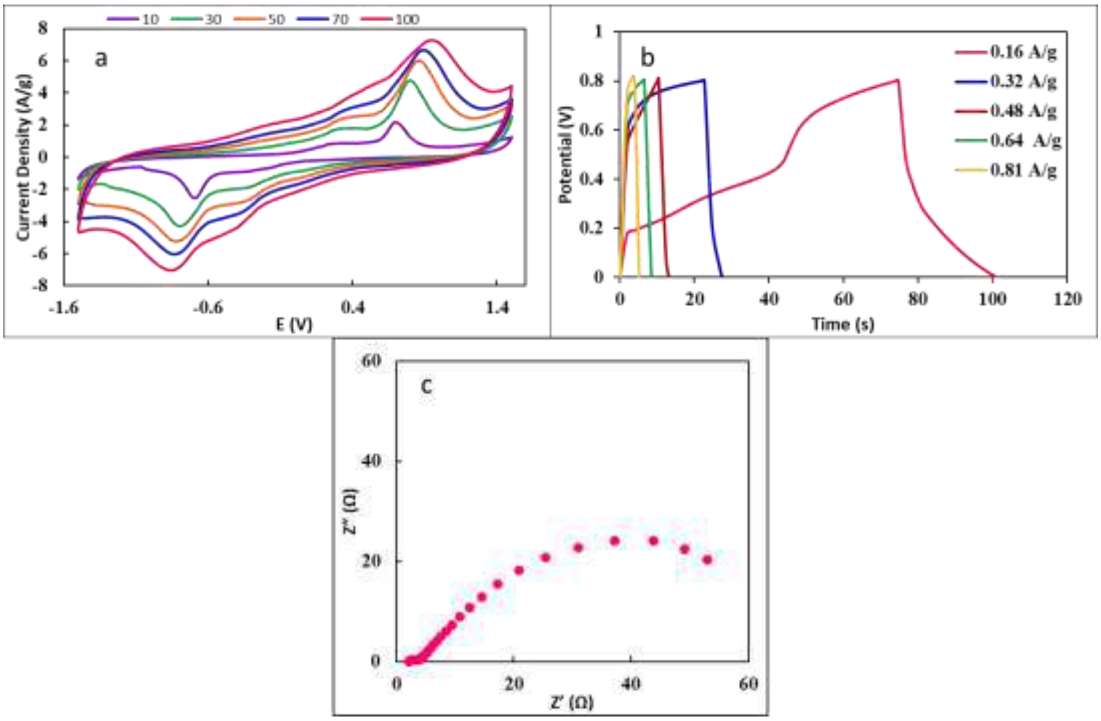

Figure 2. CV, GCD, and EIS curves using KOH (6 M) as electrolyte.

The specific capacitance obtained from CV curves of **4a** at scan rates of 10 mV s^{-1} was calculated **120.4 F g^{-1}. In addition, according to Figure 2(a), the capacitances decrease with increasing** scan rates.

Figure 4(b) shows the GCD curves for AC-based supercapacitor. In the GCD curves, the IR drop at the beginning of the discharge voltage indicates the internal resistance of the capacitors. As expected, the charge/discharge time decreased with increasing current density. As seen in Figure 2 (c) for sample **4a/AC**, the semicircle that appears at high frequencies is related to the charge transfer resistance (R_{ct}) at the current collector/electrolyte interface, and the curve observed at low frequencies was associated with ions penetration resistance path.

Table 1. Specific capacitance of **4a** in different scan rates**.**

	Scan rate (mV/s)	**4a/AC**
Specific capacity (F g^{-1})	10	120.4
	30	119.3
	50	105
	70	92.9
	100	82.3

Conclusion

In conclusion, a mild and efficient approach for synthesizing polysubstituted imidazole-baseds benzoxazinones has been successfully developed. The optical properties of all newly synthesized compounds were also investigated. As expected, among the synthesized compounds, the highest quantum yield (0.31) is related to benzoxazinone compound **4b**. Electrochemical behaviors of the newly synthesized compounds were also investigated and the capacitances decrease (120.4-82.3 F/g) with increasing scan rates (10-100 mV/s).

References

[1] Choudhary, G., Naganaboina, R.T. and Peddinti, R.K., 2014. *RSC Advances*, *4*(35), pp.17969-17979.

[2] Zampieri, D., Mamolo, M.G., Filingeri, J., Fortuna, S., De Logu, A., Sanna, A. and Zanon, D., 2019. *Bioorganic & Medicinal Chemistry Letters*, *29*(17), pp.2468-2474.

[3] Stepanova, E.E., Balandina, S.Y., Drobkova, V.A., Dmitriev, M.V., Mashevskaya, I.V. and Maslivets, A.N., 2021. *Archiv der Pharmazie*, *354*(2), p.2000199.

[4] Choudhary, G. and Peddinti, R.K., 2011. *Green Chemistry*, *13*(11), pp.3290-3299.

[5] Yavari, I., Adib, M. and Hojabri, L., 2002. *Tetrahedron*, *58*(34), pp.6895-6899.

[6] A.A. Fakhree, R. Mohammadzadeh, E. Alipour, and Z. Ghasemi, Rev. Chem. Intermed. 46 (2020) 2069-2082.

[7] Z. Wu, Y. Du, Q. Zhou, and L. Chen, Pestic. Biochem. Phys. 163 (2020) 51-63.

[8] B. Jie, H. Lin, Y. Zhai, J. Ye, D. Zhang, Y. Xie, X. Zhang, and Y. Yang, J. Chem. Eng. 454 (2023) 139931.

[9] Li, S., Wang, X., Hou, L., Zhang, X., Zhou, Y., Yang, Y. and Hu, Z., 2019. Graphene hydrogels functionalized non-covalently by fused heteroaromatic molecule for asymmetric supercapacitor with ultra-long cycle life. *Electrochimica Acta*, *317*, pp.437-448.

[10] S.S. Dipake, V.D. Ingale, S.A. Korde, M.K. Lande, A.S. Rajbhoj, and S.T. Gaikwad, RSC advances, 12 (2022) 4358-4369.

[11] C.K. Jadhav, A.S. Nipate, A.V. Chate, P.M. Kamble, G.A. Kadam, V.S. Dofe, V.M. Khedkar, and C.H. Gill, J. Chin. Chem. Soc. 68 (2021) 1067-1081.

[12] Z. Ghasemi, A. Mirzaie, R. Arabzadeh, Z. Fathi, and A.A. Fakhree, Synthesis and optical properties of novel 1, 2, 3-triazole derivatives possessing highly substituted imidazoles, J. Chem. Res. 43 (2019) 262-267, doi: 10.53555/jrtdd.v6i9s.2787.

[13] Jadidi, S.R. and Ghasemi, Z., 2025. Ultrasound-promoted synthesis of polysubstituted imidazole-linked benzoxazole derivatives and the investigation of their optical properties. *Journal of Molecular Structure*, *1321*, p.140071.

The 30th Iranian Seminar of Organic Chemistry
February 7-9, 2025, Iran University of Science and Technology, Tehran, Iran

Synthesis of new conjugated benzofuran derivatives based on polysubstituted imidazole and evaluation of their absorption and emission properties

Erfan Jalilzadeh Galeh [a], Zarrin Ghasemi *[a], Somayeh Rashtabad Jadidi [a]

Department of Organic Chemistry and Biochemistry, Faculty of Chemistry, University of Tabriz, 51666-16471, Tabriz, Iran

Corresponding Author E-mail: z.ghasemi@tabrizu.ac.ir

Tell: +98-41-33393116

Abstract

In this research, a series of ethyl *ortho*-hydroxy cinnamate based on polyarylimidazole were prepared through Wittig reaction. The S_N2 reaction on the hydroxy group with ethyl bromoacetate in the presence of K_2CO_3 to give the ether intermediate, was subsequently followed by an intramolecular Michael addition to produce dihydrobenzofuran derivatives. Oxidative dehydrogenation of the dihydrobenzofuran derivative was carried out with *N*-chlorosuccinimide in CCl_4, to give target benzofuran products. The newly synthesized compounds were confirmed by spectroscopic techniques, and their absorption and emission properties were recorded at a concentration of 10^{-5} M in ethanol and their emission quantum yields were calculated.

1. Introduction

Benzofuran is found in so many bioactive natural and synthetic chemicals. The significant uses of benzofuran derivatives in polymers, agriculture, and pharmaceuticals have attracted a lot of interest

[1-3]. The numerous drugs with properties such as antidepressants, antibacterial, antitumors, anti-inflammatory, and anticonvulsants, have benzofuran moiety in their structures [4-6]. The synthesis of highly fluorescent organic compounds with extended π conjugation has attracted the attention of researchers due to their many advantages and potential applications [7,8]. Oxygen-containing heterocyclic rings also exhibit very interesting optical properties [7]. The data from the literature and reaserch studies show that benzofuran derivatives are chromophores with good quantum yields, intense photoluminescence, beneficial electrochemical behaviors, thermal stability and blue-light emitting [9-12]. On the other hand, polysubstituted imidazoles have attracted the attention of many chemists due to their medicinal and luminescence properties [13]. These types of compounds are used in the preparation of organic light-emitting diodes (OLEDs), fluorescence probes, biological imaging, and also in the synthesis of drugs that act as anti-cancer, anti-allergic, anti-pain, and anti-fungal drugs [8]. Herein we report the design and synthesis of new benzofuran derivatives based on polysubstituted imidazole which have optical properties.

2. Experimental Section

2.1. General procedure for the synthesis of ethyl trans 2-hydroxy cinnamate derivatives based on polysubstituted imidazole compounds (2a-g)

A mixture of polysubstituted imidazole based on salicyaldehyde (2.5 mmol), phosphonium bromide salt (3.75 mmol) and pottasium carbonate (3.75 mmol) in DMF (3 mL) was stirred at room temperature for 2 hours. the solid product was separated after adding the water, washed with water, dried, and the desired products were obtained without further purification.

2.2. General procedure for the synthesis of ethyl (E)-3-(2-(2-ethoxy-2-oxoethoxy)phenyl)acrylate derivatives based on polysubstituted imidazole compounds (3a-g)

A mixture of Ethyl bromoacetate (2.5 mmol) and pottasium carbonate (3.5 mmol) was stirred at 60 ^{o}C for 3 hours. The solid product was separated after adding the water, washed with water, dried, and the desired products were obtained without further purification.

2.3. General procedure for the synthesis of dihydrobenzofuran derivatives (4a-g)

A mixture of **2a** (1.5 mmol), pottasium carbonate (5.25 mmol)) in DMF (3 ml) was stirred at 100 ^{o}C for 4 hours. Then Then, water was added to the reaction mixture and neutralized with several drops of hydrochloric acid solution. purification of the crude by column chromatography using n-hexane/EtOAc mixture, afforded the desired product **3a** in pure form.

2.4. General procedure for the synthesis of benzofuran derivatives (5a-g)

A mixture of **3a** (0.25 mmol) and *NCS* (0.5 mmol) in CCl_4 (2 ml) was stirred at room temperature for 5 hours After the completion of reaction as indicated by TLC, solvent was evaporated under reduced pressure The crude product purified by column chromatography using n-hexane/EtOAc (7:3) mixture afforded the desired product **4a** in pure form.

3. Results and Discussion

Deraivatives of Ethyl 2- hydroxycinnamtes **2a-g** were prepared with the Wittig reaction between correspounding salicylaldehydes **1a-g** and phosphonium bromide salt. Then the S_N2 reaction on the hydroxy group with ethylbromoacetate gave ethers **3a-g**, An intramolecular Michael addition and cyclization at 100 ^{o}C resulted in the formation of dihydrobenzofuran derivatives **4a-g**. Oxidative dehydrogenation of the dihydrobenzofuran derivatives were carried out with *N*-chlorosuccinimide in CCl_4, to produce the target benzofuran **5a-g** (Scheme 1).

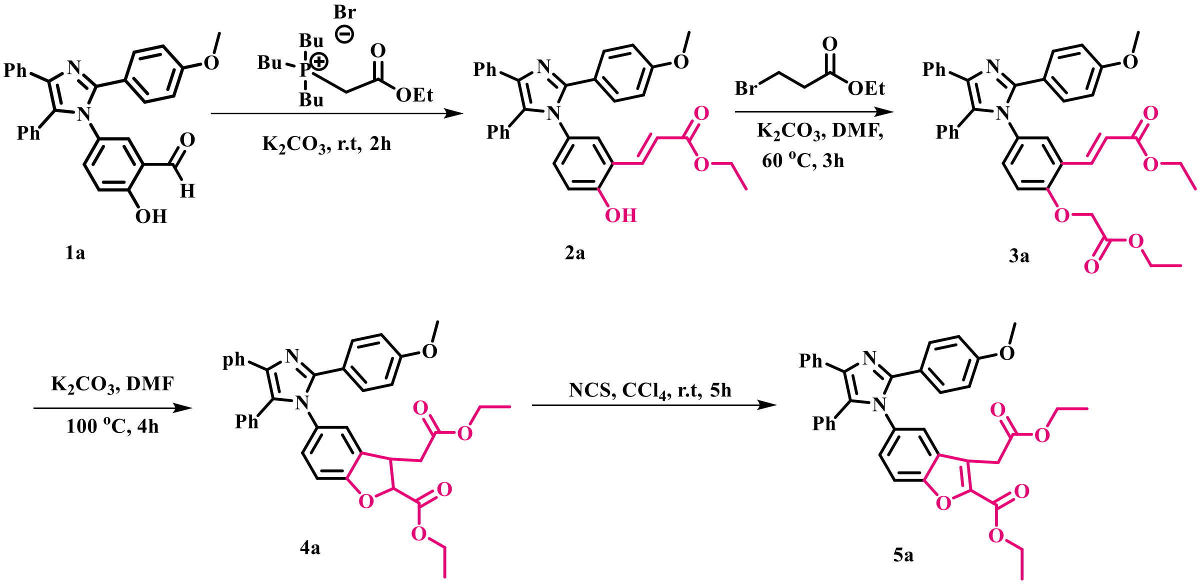

Scheme 1: synthesis steps of compounds 4a

UV-Vis spectra of the synthesized molecules in ethanol (10^{-5} M) were studied. These compounds show an intense absorption band with a λ_{max} about 280 nm, corresponding to strong π-π* transitions. The fluorescence properties of the synthesized molecules were also showed the intense emission of blue light at about 382 nm (Figure 1). The emission quantum yields were also calculated using naphthalene as a standard (Φ = 0.23) and Maximum quantum yield is related to derivative **5a** (0.54).

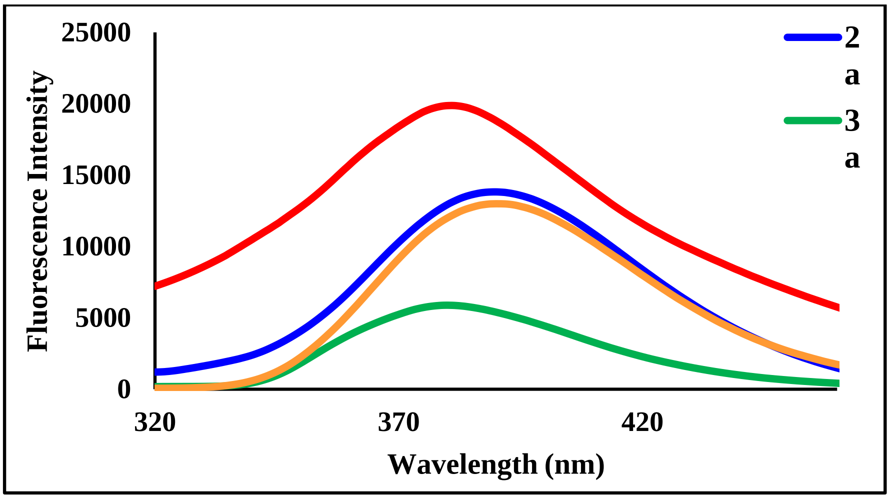

Figure 1. Fluorescence spectra of compouds **2a, 3a, 4a,** and **5a.**

Conclusions

In conclusion, a mild and efficient approach for synthesizing benzofuran based on polysubstituted imidazole has been successfully developed. The optical properties of all newly synthesized compounds were also investigated. As expected, among the synthesized compounds, the highest quantum yield (0.54) is related to benzofuran compound **5a**.

References

[1] Dawood KM. Benzofuran derivatives: a patent review, Expert Opin Ther Patents 23;2013:1133-1156.

[2] Yeung, KS. Furans and benzofurans, Topics Heterocycl Chem 2012;29:47-76.

[3] Shamsuzzaman KH, Bioactive Benzofuran derivatives: a review, Eur J Med Chem 2015;97:483-504.

[4] Zelova Hanakova HZ, Cermakova Z, et al. Evaluation of anti-inflammatory activity of prenylated Substances isolated from Morus alba and Morus nigra, J Nat Prod 2014;77:1297-1303.

[5] Nevagi R, Dighe SN and Dighe SN. Biological and medicinal significance of benzofuran, Eur J Med Chem 2015;97:561-581.

[6] Xu Z, Zhao S, Lv Z, et al. Benzofuran derivatives and their anti-tubercular, antibacterial activities. Eur J Med Chem 2019;162:266-276.

[7] Bodke, Y.D., Shankerrao, S. and Harishkumar, H.N., 2013. Synthesis of 2-(1-Benzofuran-2-yl)-4-(1, 3-benzoxazol-2-yl/1, 3-benzothiazol-2-yl) Quinolines as Blue Green Fluorescent Probes. Journal of Chemistry, 2013(1), p.794810.

[8] Zurnacı, M., Şener, İ., Gür, M. and Şener, N., 2023. Organic fluorescent compounds based on phenanthroimidazole: A review of highlight studies. Luminescence, 38(10), pp.1690-1701.

[9] Berlman, I., 2012. Handbook of florescence spectra of aromatic molecules. Elsevier.

[10] Hwu, J.R., Chuang, K.S., Chuang, S.H. and Tsay, S.C., 2005. New benzo [b] furans as electroluminescent materials for emitting blue light. Organic Letters, 7(8), pp.1545-1548.

[11] Xu, J., Nie, G., Zhang, S., Han, X., Pu, S., Shen, L. and Xiao, Q., 2005. Electrosyntheses of poly (2, 3-benzofuran) films in boron trifluoride diethyl etherate containing poly (ethylene glycol) oligomers. European polymer journal, 41(7), pp.1654-1661.

[12] Yang, J.X., Wang, X.L. and Xu, L.H., 2005. Studies on the synthesis and spectral properties of novel 4-benzofuranyl-1, 8-naphthalimide derivatives. Dyes and pigments, 67(1), pp.27-33.

[13] (a) Serdaliyeva, D., Nurgozhin, T., Satbayeva, E., Khayitova, M., Seitaliyeva, A. and Ananyeva, L., 2022. Journal of Clinical Medicine of Kazakhstan, 19(3), pp.11-15. J Clin Med Kazakhstan, 19(3), pp.11-15. (b) Umasankar, G., Ulla, H., Madhu, C., Reddy, G.R., Shanigaram, B., Nanubolu, J.B., Kotamarthi, B., Karunakar, G.V., Satyanarayan, M.N. and Rao, V.J., 2021. Journal of Molecular Structure, 1236, p.130306.

The 30th Iranian Seminar of Organic Chemistry
February 7-9, 2025, Iran University of Science and Technology, Tehran, Iran

In silico biological activity of a pyrido[2,3-d]pyrimidine derivative: DFT calculations, ADME-T analysis, and molecular docking simulation

Fateme Moradi-Chaleshtori[a], Mehran Feizi-Dehnayebi[a], Ghodsi Mohammadi Ziarani*,[a]

[a] *Department of Organic chemistry, Faculty of chemistry, Alzahra University, Tehran, 19938-93973, Iran.*

Keyword: biological activity, DFT calculation, ADME-T, molecular docking simulation

1. Introduction

Over the past years, uracil and its derivatives such as pyrido[2,3-d]pyrimidines have attracted attention due to their numerous biological activities such as antibacterial, anti-allergic and antimicrobial. On the other hand, nowadays, cancer causes more deaths than other diseases. For this reason, in this article, we present a compound of these derivatives in order to investigate their anti-cancer behavior through computational methods.

2. Method

*2.1. Synthesis of tetrahydropyrido[2,3-d]pyrimidine derivative (**4b**, Ar = 3-$NO_2C_6H_4$)*

The investigated compound was synthesized and characterized according to a previous paper [1].

2.2. Computational methods

Using the computational method of density functional theory (DFT), structural information, stability, and biological properties, as well as active sites on a compound for interaction with biological macromolecules can be investigated. The synthesized compound was analyzed using DFT calculations with the B3LYP functional method using the Gaussian 09W software package. DFT settings were selected using GaussView 6.0 software and the resulting file was used as input for structural optimization. The basis set used for all atoms is the 6-311g (d,p) basis set. On the other hand, a molecular docking simulation study was performed by AutoDock and AutoDock Tools software to investigate the anticancer property of the compound. Finally, the prediction of the pharmacological properties of the synthesized compound was performed by ADME-T analysis using OSIRIS DataWarrior 5.2.1 software.

3. Results and Discussion

The full geometry optimization of compound **4b** was achieved using the DFT/B3LYP/6-311g (d,p) method. The optimized geometry of this compound shows that the electronic energy in the ground state is -1161.16 Hartree, and its configuration is shown in Figure 1(a). On the other hand, the molecular electrostatic potential (MEP) map of this compound is shown in Figure 1(b). The MEP map is a very important method to show the reactive sites on the compound for electrophilic and nucleophilic attack. The MEP map of compound **4b** shows that the negative electrostatic potential (indicated by the red surface) is concentrated around the O1, O2, O3, O4, and N5 atoms, indicating that these regions are suitable targets for electrophilic reactions [2-5]. In addition, the positive electrostatic potential (blue surface) is concentrated on the hydrogens attached to N1, N2, and N4, indicating that these regions are ideal sites for nucleophilic reactions or biological interactions with macromolecules. The HOMO and LUMO molecular orbital analysis of compound **4b** is shown in Figure 1(c). The obtained energy gap for this compound is 3.91 eV. A smaller energy gap between the HOMO and LUMO levels indicates higher chemical reactivity and biological activity, along with a decrease in the stability of a compound [6-8]. This energy gap indicates that compound **4b** has high chemical reactivity and biological activity. For this reason, we performed molecular docking simulations of this compound with the target cell of breast cancer protein (PDB ID: 3HB5).

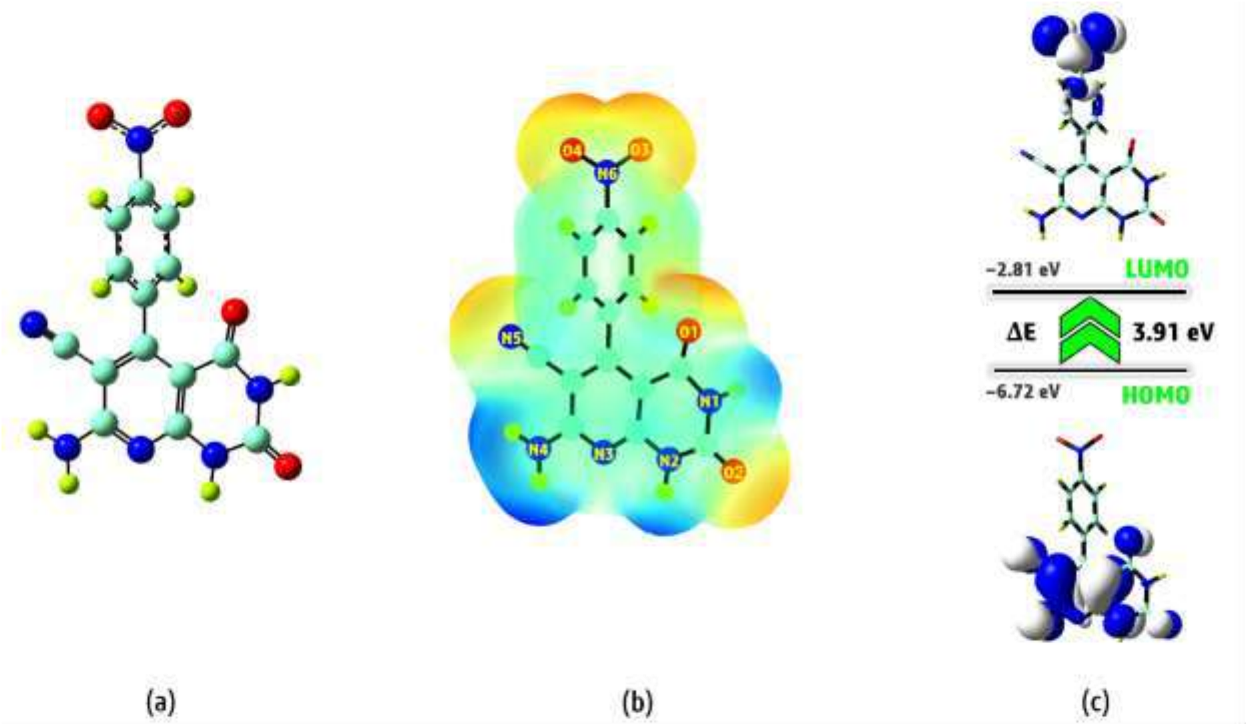

Figure 1. Optimized geometry (a), MEP map (b), and HOMO and LUMO surface (c) of the synthesized compound.

The best binding position with the highest negative binding free energy (strongest binding affinity) was selected for docking analysis. According to docking simulations, compound **4b** binds to the active site of breast cancer protein as shown in Figure 2. The binding affinity of this compound during interaction with breast cancer protein is -8.16 kcal/mol. Meanwhile, the binding affinity of cisplatin, a standard cancer drug, against this cancer cell was found to be -5.98. These results indicate that the synthesized compound has a higher binding affinity for breast cancer protein, which indicates a higher anticancer activity of this compound compared to cisplatin in terms of theoretical study. The best binding position of compound **4b** in interaction with 3HB5 protein was analyzed to reveal the interactions involved, and the findings are shown in Figure 2. Finally, the analysis related to the prediction of the pharmacological properties of this compound was performed by ADME-T analysis. Predictions show that there are no tumorigenic and mutagenic effects for this compound. Therefore, according to the computational results obtained, compound **4b** can be introduced as an effective agent on cancer cells and, it can be further analyzed for the in vitro analysis.

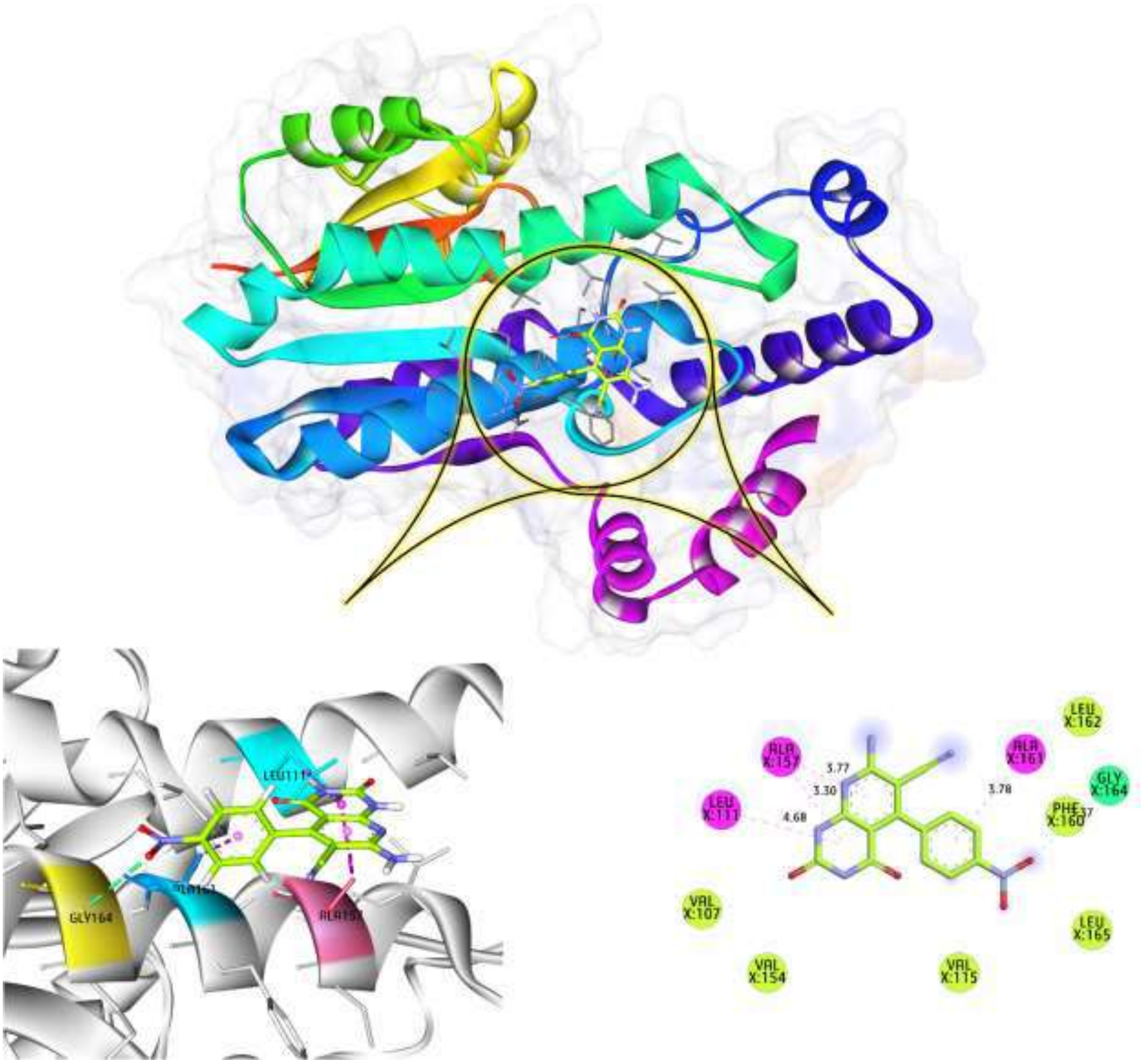

Figure 2. Docking simulation of compound **4b** on breast cancer protein.

4. Conclusion

In this paper, a *tetrahydropyrido[2,3-d]pyrimidine* derivative was synthesized. Various computational methods including DFT, molecular docking simulation and prediction of drug properties, were used to investigate the biological properties of this compound. The electrostatic potential map of this compound showed active sites for nucleophilic and electrophilic reactions. The energy gap between the HOMO and LUMO orbitals indicated that compound **4b** has high chemical reactivity and biological activity. On the other hand, the prediction of drug effects showed that there are no tumorigenic and gene mutagenic effects for this compound. According to the obtained results, it can be concluded that compound **4b** is a bioactive compound and effectively binds to the active site of breast cancer protein. Therefore, molecular docking simulation confirms the anticancer activity of this compound through its strong binding affinity to breast cancer protein. Given the promising computational results regarding the biological properties of this compound, laboratory methods can also be used to further investigate this compound.

5. References

[1] G.M. Ziarani, N.H. Nasab, M. Rahimifard, A.A. Soorki, One-pot synthesis of pyrido [2, 3-d] pyrimidine derivatives using sulfonic acid functionalized SBA-15 and the study on their antimicrobial activities, Journal of Saudi Chemical Society, 19 (2015) 676-681.

[2] M. Canakdag, M. Feizi-Dehnayebi, S. Kundu, D. Sahin, İ.Ö. İlhan, S.K. Alhag, L.A. Al-Shuraym, S. Akkoc, Comprehensive evaluation of purine analogues: Cytotoxic and antioxidant activities, enzyme inhibition, DFT insights, and molecular docking analysis, Journal of Molecular Structure, 1323 (2025) 140798.

[3] Parveen, Bushra, Saira Shahzadi, Saqib Ali, Mehran Feizi-Dehnayebi, Khurram Shahzad Munawar, Muhammad Ashfaq, and Muhammad Nawaz Tahir. "Synthesis, Spectral Characterizations, Computational Studies and Biological investigation of 4-(4-(2-hydroxyethyl) phenylamino)-4-oxobutanoic acid and its trimethyltin (IV) complex." Journal of Molecular Structure (2024): 138851.

[4] Ali El-Remaily, Mahmoud Abd El Aleem Ali, Mohammad Saleh Hussein Alzubi, Tarek El-Dabea, Rafat M. El-Khatib, Moumen S. Kamel, Mehran Feizi-Dehnayebi, and Ahmed M. Abu-Dief. "Insights into microwave-promoted synthesis of 3-methyl-4-phenyl-4, 9-dihydro-1H-pyrazolo [3, 4-d][1, 2, 4] triazolo [1, 5-a] pyrimidine derivatives catalyzed using new Pd (II), Cu (II), VO (II), and Ag (I) complexes as a heterogeneous catalyst and computational studies." Applied Organometallic Chemistry 38, no. 8 (2024): e7587.

[5] Abu-Dief, Ahmed M., Omran A. Omran, Mehran Feizi-Dehnayebi, Abdulmajeed Alqurashi, Inam Omar, Dalal Alhashmialameer, and Ahmad Desoky M. Mohamad. "Fabrication, structural elucidation, and DFT calculation of some new hydrophilic metal chelates based on NN′-(1-methyl-2-oxoindolin-3-ylidene) benzohydrazide ligand: Pharmaceutical studies and molecular docking approach." Applied Organometallic Chemistry 38, no. 9 (2024): e7593.

[6] T. Lanez, M. Feizi-Dehnayebi, E. Lanez, Assessment of the electrostatic binding of ferrocenylmethyl-nitroaniline derivatives to DNA: A combined experimental and theoretical study, Journal of Molecular Structure, 1308 (2024) 138386.

[7] Majumdar, Dhrubajyoti, Ankita Chatterjee, Mehran Feizi-Dehnayebi, Neelakanta Sarvashiva Kiran, Burak Tuzun, and Dipankar Mishra. "8-Aminoquinoline derived two Schiff base platforms: Synthesis, characterization, DFT insights, corrosion inhibitor, molecular docking, and pH-dependent antibacterial study." Heliyon 10, no. 15 (2024).

[8] Zahirović, Adnan, Selma Fetahović, Mehran Feizi-Dehnayebi, Renata Bešta-Gajević, Muamer Dizdar, Jelena Ostojić, and Sunčica Roca. "Substituent effect in salicylaldehyde 2-furoic acid hydrazones: Theoretical and experimental insights into DNA/BSA affinity modulation, antimicrobial and antioxidant activity." Journal of molecular structure 1312 (2024): 138628.

The 30th Iranian Seminar of Organic Chemistry
February 7-9, 2025, Iran University of Science and Technology, Tehran, Iran

Innovative Optical sensing of Al^{3+}: post-synthesis modification of UiO-66-NH$_2$

Fateme Moradi-Chaleshtori [a], Ghodsi Mohammadi Ziarani [a,*]

[a] *Department of Organic Chemistry, Faculty of Chemistry, Alzahra University, Tehran, 19938-93973, Iran.*

Keyword: Post-synthesis modification, 4-chloro-3-formyl coumarin, MOF, UiO-66-NH$_2$, Al^{3+}, F$^-$

Introduction

Metal-organic frameworks (MOFs) are coordination polymers formed from metal ions and organic ligands, distinguished by their highly crystalline structures [1]. They can undergo "post-synthetic modification," allowing for the adjustment of their properties by altering their linker or node components [2]. Recent developments have focused on MOFs' luminescent properties for detecting metals, explosives, and small molecules, facilitated by their unique pore arrangements and functional groups. Zr-based UiO-66-NH2 stands out among MOFs due to its structural diversity, water stability, and biocompatibility, making it ideal for selective sensing of cations and anions. Its fluorescence, primarily from the linker, can be enhanced by modifying the amino group with different organic moieties. The use of 4-chloro-3-formylcoumarin as a modifier is based on its strong fluorescence and structural versatility, although few sensors utilizing this compound have been developed [3- 5]. Aluminum (III) ions (Al$^{3+)}$ are hazardous and linked to neurological damage and Alzheimer's disease, prompting interest in MOF-based sensors for detection. Additionally, fluoride ions (F$^-$) are crucial in biology and health, with their imbalances causing serious conditions, necessitating sensitive detection methods due to low tolerance levels [6, 7]. We present a novel fluorescent chemosensor by incorporating 4-chloro-3-formylcoumarin into UiO-66-NH$_2$, aimed at enhancing sensing capabilities.

Method

All chemicals and solvents were acquired from Merck Company. Also, Fluorescence diagrams were composed with a Cary Eclipse Fluorescent Spectrophotometer.

Synthesis of UiO-66-NH$_2$

UiO-66-NH_2 was synthesized by dissolving $ZrCl_4$ and 2-NH_2-BDC in DMF, mixing the solutions, and heating the mixture in a Teflon-lined autoclave for 24 hours. After cooling, the product was centrifuged and washed with ethanol and acetone.

Modification of UiO-66-NH_2

To modify UiO-66-NH_2 was dispersed in ethanol, and 4-chloro-3-formylcoumarin was added to the upper solution. The mixture was refluxed, then centrifuged, washed, and dried to obtain UiO-66-N-CC.

Fluorescence Study

The fluorescence response for the product was investigated by preparing stock solutions of various metal ions and anions from nitrate and sodium/potassium salts in double-distilled water.

Results and Discussion

Fluorescence response of UiO-66-N-CC

To evaluate the performance of UiO-66-N-CC, its fluorescence spectra were analyzed with the addition of various ion solutions. A UiO-66-N-CC solution (0.02 g in 100 mL of ethanol) was excited at 300 nm, and fluorescence changes were recorded after adding 200 µL of different cations, including Ag^+, K^+, Pb^{2+}, Hg^{2+}, Cd^{2+}, Ni^{2+}, Ca^{2+}, Cu^{2+}, Mg^{2+}, Mn^{2+}, Co^{2+}, Zn^{2+}, Cr^{3+}, and Al^{3+}. Notably, the fluorescence emission increased with the addition of Al^{3+}. The selectivity behavior of the chemosensor UiO-66-N-CC was evaluated for its ability to detect Al^{3+} ions in the presence of various common interfering metal ions. The resulting emission was measured to assess the sensor's selectivity.

Conclusion

In summary, a novel mesoporous sensing material, UiO-66-N-CC, was successfully designed and synthesized, demonstrating significant potential as a highly selective sensor for specific metal ions. The unique structural properties of UiO-66-N-CC contribute to its effectiveness, enabling it to selectively recognize Al^{3+} ions even in the presence of various competing ions. The calculated LOD for Al^{3+} was good, highlighting the material's sensitivity and capability for practical applications in detecting trace levels of this ion in complex mixtures. These findings highlight the potential for UiO-66-N-CC to be employed in environmental monitoring, biomedical applications, and other fields where accurate detection of aluminum ions is crucial.

References:

[1] S.L. James, Metal-organic frameworks, Chemical Society Reviews 32(5) (2003) 276-288.

[2] B. Seoane, S. Castellanos, A. Dikhtiarenko, F. Kapteijn, J. Gascon, Multi-scale crystal engineering of metal organic frameworks, Coordination Chemistry Reviews 307 (2016) 147-187.

[3] X. Zhang, J. Qiao, J. Zhao, D. Xu, F. Wang, C. Liu, Y. Jiang, L. Wu, P. Cui, L. Lv, Q. Wang, W. Liu, Z. Wang, J. Liu, High-Efficiency Electromagnetic Wave Absorption of Cobalt-Decorated NH2-UIO-66-Derived Porous ZrO2/C, ACS Applied Materials & Interfaces 11(39) (2019) 35959-35968.

[4] J. Yang, Y. Dai, X. Zhu, Z. Wang, Y. Li, Q. Zhuang, J. Shi, J. Gu, Metal–organic frameworks with inherent recognition sites for selective phosphate sensing through their coordination-induced fluorescence enhancement effect, Journal of Materials Chemistry A 3(14) (2015) 7445-7452.

[5] Y. Song, Z. Chen, H. Li, Advances in coumarin-derived fluorescent chemosensors for metal ions, Current Organic Chemistry 16(22) (2012) 2690-2707.

[6] M. Arduini, F. Felluga, F. Mancin, P. Rossi, P. Tecilla, U. Tonellato, N. Valentinuzzi, Aluminium fluorescence detection with a FRET amplified chemosensor, Chemical communications (13) (2003) 1606-1607.

[7] S. Ayoob, A.K. Gupta, Fluoride in drinking water: a review on the status and stress effects, Critical reviews in environmental science and technology 36(6) (2006) 433-487.

The 30th Iranian Seminar of Organic Chemistry
February 7-9, 2025, Iran University of Science and Technology, Tehran, Iran

Heterocyclic-linked covalent organic frameworks: Design, synthesis and applications

Meysam Yarie*

Department of Organic Chemistry, Faculty of Chemistry and Petroleum Sciences, Bu-Ali Sina University, Hamedan, Iran. E-mail: myarie.5266@gmail.com, m.yarie92@basu.ac.ir

Keyword: Catalyst, Covalent Organic Frameworks, Reticular chemistry

In this speech, the focus is on the importance of the heterocycles which their formation leads to the construction of covalent organic frameworks (COFs). The main body of the speech, introduced the

most important heterocyclic linkers such as benzoxazole, chromenoquinoline, dioxane, imidazole, imide, oxadiazole, pyrazine, quinoline, thiazole, triazine, benzofuran, phthalocyanine, imidazopyridine, carbamate and thienopyridine. Heterocyclic chemistry, as a main subset of organic chemistry, serves a crucial role in the pillars of life. As an illustration, the nucleobases in the double-helix of DNA show the very important role of heterocyclic chemistry in our life. Also, heterocyclic molecules are frequently found in the main skeleton of other vital biomolecules such as RNA, proteins, enzymes, vitamins, chlorophyll and hemoglobin, which their proper functioning is necessary for our survival. Furthermore, heterocycle-based materials have an extended domain of applications in biological compounds, medicinal, functional materials, agriculture, sensors, energy storage, coordination chemistry, supramolecular chemistry, and catalyst. Therefore, it is not surprising that chemists have well understood their importance and have recently synthesized new COFs for different applications based on heterocycles which form during the linking of molecular building blocks [1-6].

In comparison with solo-bond formed COFs, heterocyclic-linked COFs have benefited from advanced linkages which give them new top-level standards such as superb complexity combined with adjustability, improved framework robustness, excellent structural periodicity and regularity, hydrogen bonding potentiality, functional diversity, exceptional porosity and crystallinity, post-synthetic modification capability, prominent thermal and chemical stability, and proper specific surface area. Due to these outstanding merits, a diverse range of performances in catalysis and photocatalysis processes, sensing materials, separation processes, gas and energy storage and conversion, optoelectronic devices, CO_2 photoreduction, environmental and contaminant remediation and drug delivery have been reported for them [7-8].

Despite the challenges ahead, such as the biodegradability and degradation mechanism in different chemical and environmental conditions, synthetic limitations of new methods, large-scale production for industrial and commercial purposes, and their usage for real applications, it is believed that the future is bright and these robust structures can find an excellent position in interdisciplinary sciences such as construction of bio-inspired and nature-mimicking molecular architectures and open a new window towards high-tech devices and technologies.

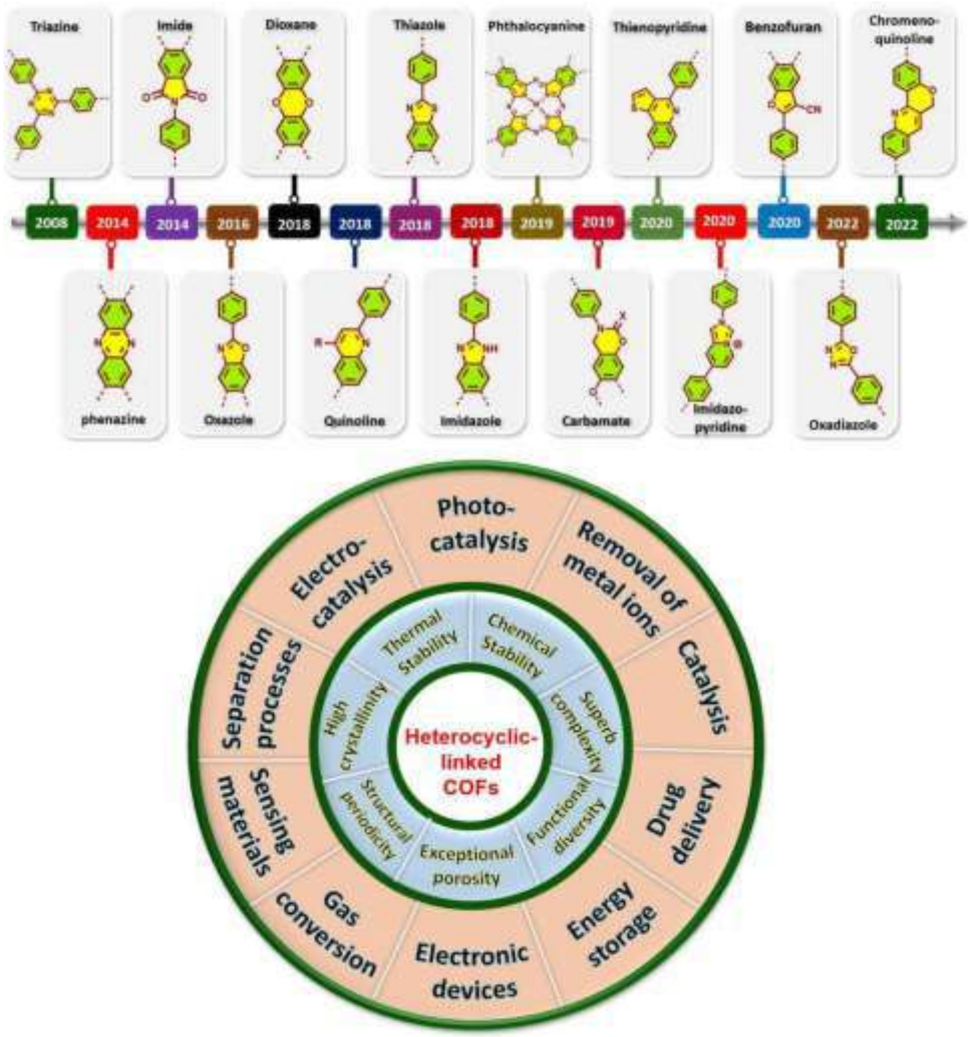

Scheme: The timeline of heterocyclic-linked COFs with representive linkages as well as their advantages and applications

References:

[1] O. M. Yaghi, J. Am. Chem. Soc. 138 (2016) 15507-15509.
[2] A. P. Cote, A. I. Benin, N. W. Ockwig, M. O'Keeffe, A. J. Matzger, O. M. Yaghi, Science 310 (2005) 1166-1170.
[3] Z. Wang, S. Zhang, Y. Chen, Z. Zhang, S. Ma, Chem. Soc. Rev. 49 (2020) 708-735.

[4] 16. W. Huang, W. Zhang, S. Yang, L. Wang, G. Yu, Small 20 (2023) 2308019.

[5] S. Ibáñez, M. Poyatos, E. Peris, Acc. Chem. Res. 53 (2020) 1401-1413.

[6] R. Nagarajan, C. Varadaraju, K. H. Lee, Dyes Pigm. 191 (2021) 109331-109420.

[7] Q. Guan, L. L. Zhou, Y. B. Dong, J. Am. Chem. Soc. 145 (2023) 1475-1496.

[8] X. Li, S. Cai, B. Sun, C. Yang, J. Zhang, Y. Liu, Matter 3 (2020) 1507-1540.

Synthesis of Novel Derivatives of Pyrimido[1,6-*a*]selenopheno[3,2-*d*]pyrimidine

Amin Mirfarah, Ali Shiri*

Department of Chemistry, Faculty of Science, Ferdowsi University of Mashhad, Mashhad, Iran

* *E-mail: alishiri@um.ac.ir*

Keyword: Selenophene, Pyrimidoselenophenopyrimidine, Heterocyclization

Introduction:

Selenophene and its derivatives are important heterocyclic compounds in medicinal chemistry due to their valuable pharmacological and biological activities such as antitumor [1], antibacterial [2], anticonvulsant [3], and antidepressant [4]. Selenophenopyrimidines are also another class of heterocyclic compounds with biological properties, particularly anticancer activity [5].

Method:

Initially, ۳-amino-2,4-dicyano-۵-(pyrrolidin-۱-yl)selenophene **(1)** was treated with 5-bromo-2,4-dichloro-6-methylpyrimidine **(2)** in tert-butanol as solvent. Potassium tert-butoxide was added, and the mixture was heated under reflux conditions to prepare the corresponding compound **(3)**. Then, compound **(3)** was reacted with different secondary amines in ethanol to form compounds **4(a-f)**. Eventually, the former compounds **4(a-f)** were treated with sodiumamide in DMF to obtain the corresponding cyclic products **5(a-f)** in good yields.

Results and discussion:

Our approach is based on using compound **(1)** as the starting material that was obtained via our previously published method [5]. In order to synthesize a novel heterocyclic system, compound **(1)** was reacted with 5-bromo-2,4-dichloro-6-methylpyrimidine **(2)** as a dielectrophile in the presence of t-BuOK/t-BuOH to give product **(3)**. (Scheme 1) The IR spectrum as well as the ^{1}H NMR and ^{13}C NMR spectra revealed the formation of an uncyclized product. The occurrence of heterocyclizations was performed after the substitution of chlorine atoms with appropriate secondary amines through nucleophilic aromatic substitutions and then treatment with sodium amide as a strong base to prepare the potential pharmacologically active compounds **5(a-f)**.

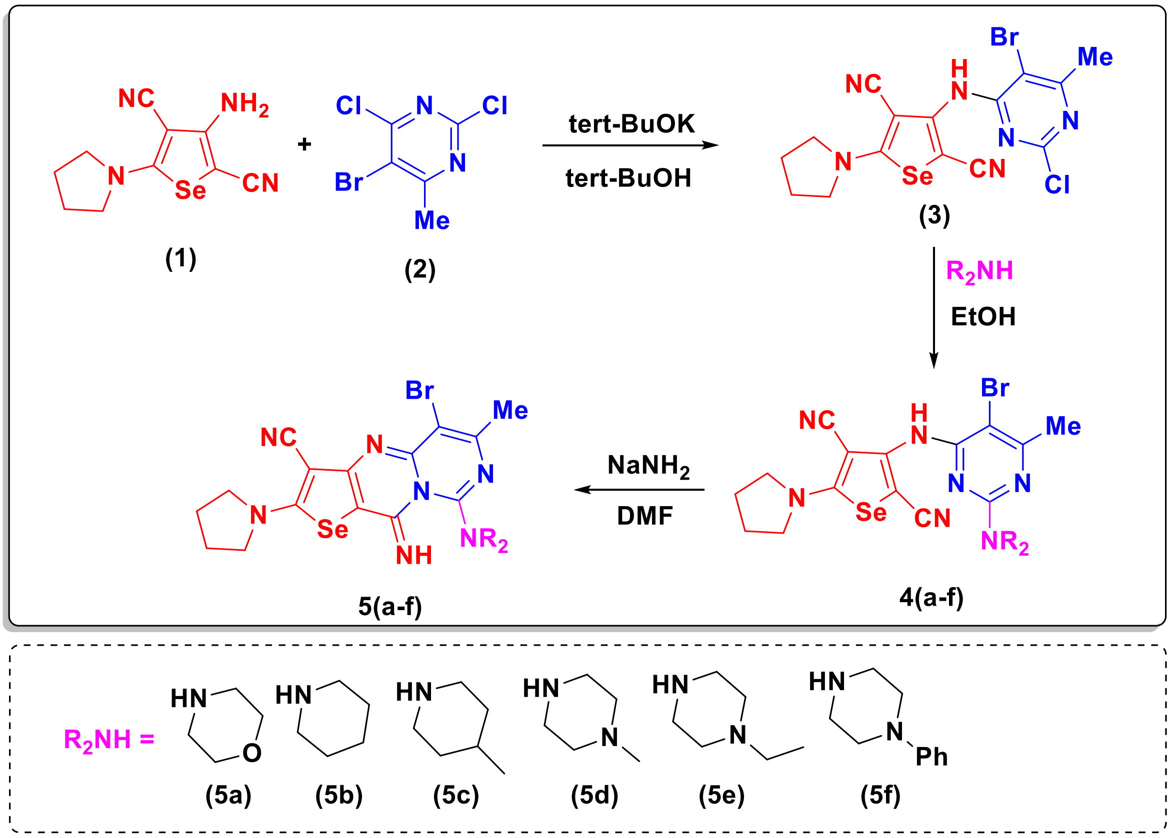

References:

[1] Adly ME, Gedawy EM, El-Malah AA, El-Telbany FA. Synthesis and anticancer activity of certain selenophene derivatives. Russian Journal of Organic Chemistry. 2019 Aug;55:1189-96.

[2] Wiles JA, Phadke AS, Bradbury BJ, Pucci MJ, Thanassi JA, Deshpande M. Selenophene-containing inhibitors of type IIA bacterial topoisomerases. Journal of medicinal chemistry. 2011 May 12;54(9):3418-25.

[3] Wilhelm EA, Gai BM, Souza AC, Bortolatto CF, Roehrs JA, Nogueira CW. Involvement of GABAergic and glutamatergic systems in the anticonvulsant activity of 3-alkynyl selenophene in 21 day-old rats. Molecular and cellular biochemistry. 2012 Jun;365:175-80.

[4] Velasquez D, Quines C, Pistóia R, Zeni G, Nogueira CW. Selective inhibition of MAO-A activity results in an antidepressant-like action of 2-benzoyl 4-iodoselenophene in mice. Physiology & behavior. 2017 Mar 1;170:100-5.

[5] Kohandel O, Sheikhi-Mohammareh S, Oroojalian F, Memariani T, Mague J, Shiri A. A Dimroth rearrangement approach for the synthesis of selenopheno [2, 3-e][1, 2, 4] triazolo [1, 5-c] pyrimidines with cytotoxic activity on breast cancer cells. Molecular diversity. 2022 Jun;26(3):1621-33.

Tunning the porosity of polystyrene-base beads with well-defined porogen synthesized via RAFT polymerization

Mahsa Khosravani Allahverdi[1], Nima Soltanieh[1], Abbas Rezaee Shirin-Abadi[1,*]

*[1] Chemistry and Petroleum Department, Shahid Beheshti University, Evin, Tehran, 19839-63113, Iran. * E-mail: ab_rezaee@sbu.ac.ir*

Keywords: Polymeric porogen, RAFT polymerization, Monodisperse porosity, Poly (styrene-*co*-divinyl benzene) beads, Well-defined porogen.

Introduction

In the late 1950s, studies on macroporous beads advanced for use as polymeric adsorbents, chromatographic media, and ion exchange resins. Porogens create porous structures, including solvating solvents, non-solvating solvents, and linear polymers. Linear polymers as porogens produce large pores (up to micrometer range) with high pore volume but low specific surface area (<10 m^2/g). This study used suspension polymerization to produce porous particles (50–2000 micrometers) with sizes influenced by monomer type, stabilizer concentration, and agitation intensity.

Building on prior methods like group transfer polymerization and ATRP, this study utilized RAFT polymerization to synthesize linear polymers with precise molecular weight, composition, and structure. RAFT employs a chain transfer agent to achieve controlled polymerization, enabling tailored properties for specific applications.

Experimental

Synthesis of RAFT agent: The synthesis of 2-cyanoprop 2-yl dithiobenzoate (CPDB) involved three main steps. First, sodium dithiobenzoate was prepared by reacting sodium methoxide, sulfur, and benzyl chloride in methanol under nitrogen at 67 °C, followed by extraction and purification using diethyl ether, HCl, and NaOH washes. Second, di(thiobenzoyl) disulfide was synthesized by adding potassium hexacyanoferrate(III) solution to sodium dithiobenzoate, forming a pink precipitate that was washed and vacuum-dried. Finally, CPDB was obtained by reacting di(thiobenzoyl) disulfide with AIBN in ethyl acetate at 75 °C for 18 hours under nitrogen. The crude product was purified via column chromatography, yielding a red oily residue.

Preparation of Polymeric Porogen: Linear polystyrene was synthesized by free radical polymerization and controlled radical polymerization (RAFT). A mixture of styrene, toluene, and benzoyl peroxide was refluxed for 7 hours. For the RAFT method, a combination of styrene, toluene, AIBN initiator, and 2-cyano-2-propyl benzodithioate was refluxed for 7 hours under a nitrogen atmosphere. After the reactions were completed in both methods, methanol was added as a non-solvent to precipitate the polymer.

Preparation of Porous Beads: Distilled water, polyvinyl alcohol, and calcium chloride were mixed and placed on a magnetic stirrer. Subsequently, the organic phase containing styrene and divinylbenzene as monomers, polystyrene as a porogen, toluene, and AIBN were added. The reaction mixture was stirred for 9 hours at 80°C.

Results and discussion

We employed gel permeation chromatography (GPC) to determine the molecular weight of the synthesized polymer. This technique enables precise analysis of the polymer's molecular weight distribution, offering valuable insights into its structural characteristics and suitability for specific applications. GPC indicated that the average molecular weight of the synthesized polystyrene was 2885 g/mol (Figure 1).

After suspension polymerization, the synthesized beads were analyzed with a scanning electron microscope, exposing significant pores within the structure (Figure 2).

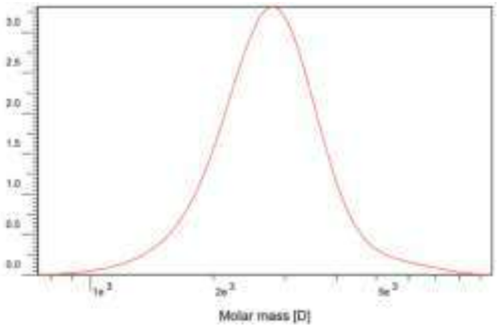

Fig 1) The distribution curve of the polystyrene prepared via RAFT polymerization.

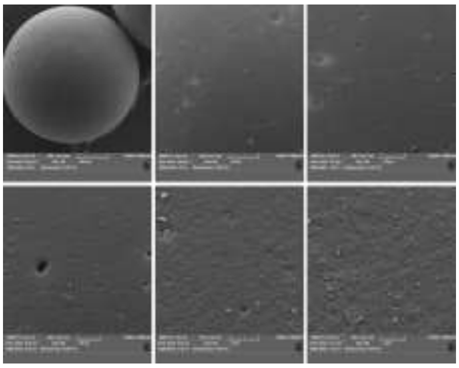

Fig 2) SEM micrographs of the porous polymer beads.

References

[1] Q.C. Wang, F. Švec, J.M.J. Fréchet, Fine control of the porous structure and chromatographic properties of monodisperse macroporous poly(styrene-co-divinylbenzene) beads prepared using polymer porogens, J Polym Sci A Polym Chem 32 (1994) 2577–2588.

[2] H.G. Yuan, G. Kalfas, W.H. Ray, SUSPENSION POLYMERIZATION, Journal of Macromolecular Science, Part C: Polymer Reviews 31 (1991) 215–299.

[3] D. Horák, J. Labský, J. Pilař, M. Bleha, Z. Pelzbauer, F. Švec, The effect of polymeric porogen on the properties of macroporous poly(glycidyl methacrylate-co-ethylene di methacrylate), Polymer (Guildf) 34 (1993) 3481–3489.

Design of Amino-palladium/biochar as an effective nanocatalyst in the Suzuki C–C coupling reaction

Seyedeh masoumeh shajiei, Maryam Hajjami*

Department of Organic Chemistry, Faculty of Chemistry and Petroleum Sciences, Bu-Ali Sina University, Postal code 6517838683, Hamedan, Iran. E-mail address, m.hajjami@basu.ac.ir or mhajjami@yahoo.com

Keyword: Amino-palladium, Biochar, Suzuki coupling reaction

Abstract

The synthesis of environmentally benign catalysts capable of being recovered and reused is a critical objective in advancing green chemistry practices within organic synthesis.[1] This reaction is an efficient method for constructing complex organic molecules, including natural product.[2] The Suzuki reaction is a versatile palladium-catalyzed cross-coupling reaction widely employed in organic synthesis for the efficient and selective formation of C-C bonds. This reaction is based on phenylboronic acid and aryl halide, utilizing catalytic amounts of palladium complexes under mild reaction conditions. In this study, amino palladium catalyst supported on biochar with high specific surface area and chemical stability was synthesized first. The synthesis of biphenyl derivatives was carried out using an efficient and recyclable catalyst, which was easily separable and significantly improved the reaction yield. **(Scheme1)**

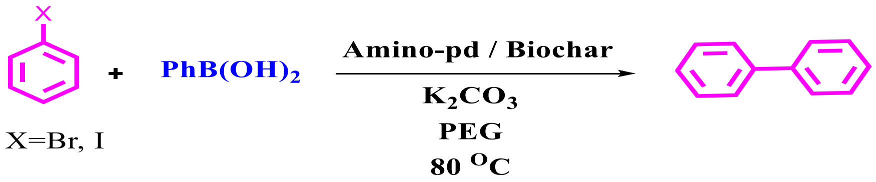

Scheme1: Carbon–carbon coupling reaction of aryl halides with $PhB(OH)_2$ in the presence of Amino-palladium/biochar

Reference:

(1) Moradi, P.; Hajjami, M. RSC Advances **2022**, 12, 13523-13534.

(2) Tamao, K.; Sumitani, K.; and Kumada, M. J. Am. Chem **1972**, 94, 4374-4376.

Mono-substituted vanadium heteropolyanion anchored on NiFe-layered double hydroxide for synthesis of cyclic carbonates from CO_2 cycloaddition with epoxides

Ahmad Shaabani[a,*], Hadi Hassani Ardeshiri[a]

[a]*Department of Organic Chemistry, Shahid Beheshti University, Daneshjou Boulevard, G.C., P.O. Box 1983963113, Tehran, Iran*

**Corresponding author: E-mail: a-shaabani@sbu.ac.ir (A. Shaabani); Tel./Fax: +98 212 990 2800*

Abstract

The increasing concentration of CO_2 in the atmosphere represents a significant environmental challenge, contributing to global warming and climate change. Nevertheless, the CO_2 fixation into cyclic compounds, such as cyclic carbonates, offers a promising strategy to both reduce atmospheric CO_2 levels and produce valuable chemicals for industrial applications. Herein, a new nanocomposite was synthesized *via* the immobilization of *mono*-substituted vanadium polyoxometalate ($[VW_{12}O_{40}]^{3-}$]) in the scaffold of $Ni_{0.75}Fe_{0.25}(CO_3)_{0.125}(OH)_2.0.38H_2O$ layered double hydroxide (LDH) to enhance the catalytic efficiency and selectivity of CO_2 conversion under mild reaction conditions. Various techniques were employed to investigate the characteristics of the intercalated polyoxometalate clusters in the layers of NiFe LDH in detail, including FT-IR, UV-vis, XRD, FE-SEM, and EDX. The $VW_{12}O_{40}$/LDH nanocatalyst demonstrates a significant capability in facilitating the cycloaddition reaction of CO_2 with epoxides in a solvent-free condition in the presence/absence of *tetra*-*n*-butylammonium bromide (TBAB) as a co-catalyst. Upon determining the optimal reaction parameters (model substrate = 228 μL), $VW_{12}O_{40}$/LDH nanocatalyst (10 mg), TBAB (3 mg), CO_2 (1 bar), temperature (70 °C), time (3 h)), five-membered cyclic carbonates derivatives were synthesized with an impressive yield ranging from 93% to 99%.

Keywords: CO_2 fixation, Polyoxometalate, Layered double hydroxide, Epoxides, Cyclic carbonates.

Graphical Abstract

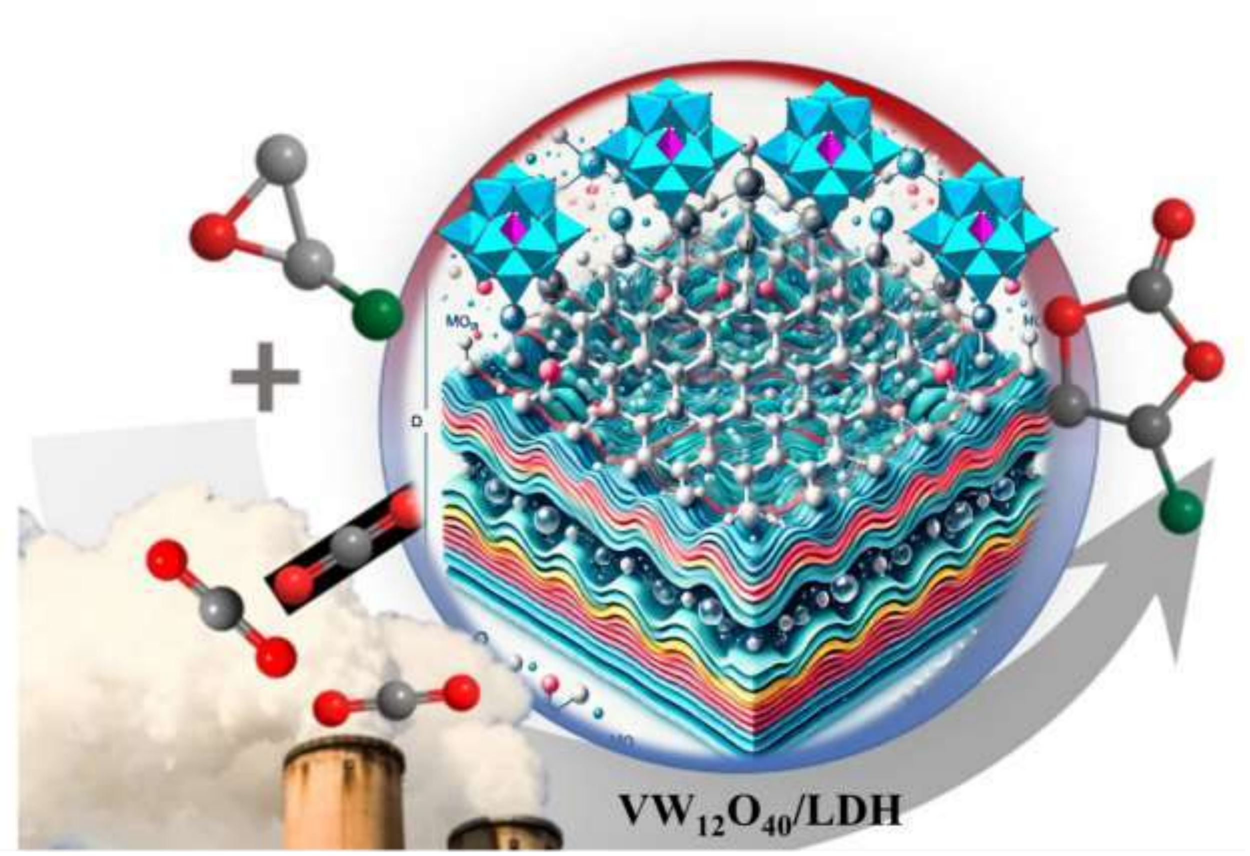

The 30th Iranian Seminar of Organic Chemistry
February 7-9, 2025, Iran University of Science and Technology, Tehran, Iran

Containment issues, effective management and optimal use of carbon dioxide in Iran

Ahmad Shaabani[a,b]

[a]*Department of Organic Chemistry, Shahid Beheshti University, Daneshjou Boulevard, G.C., P.O. Box 1983963113, Tehran, Iran*

[b] *Chemistry & Chemical Engineering Research Center of Iran (CCERCI), Pajohesh Blvd,17th Km of Tehran-Karaj Highway, Tehran, Iran.*

Abstract:

Carbon dioxide (CO_2) plays a crucial role in the two life cycle processes in Nature, namely photosynthesis-cellular respiration. These two processes exchange oxygen and carbon dioxide between living organisms and the environment. Photosynthesis and cellular respiration represent one of the most authentic and sustainable systems in Nature. However, human activities have increased the concentration of carbon dioxide in the atmosphere by about 40% since the Industrial Revolution. This disruption of the natural process has caused significant and irreparable damage to sustainable development worldwide. In 2023, official reports indicated that Iran produced and emitted over 20 billion tons of carbon dioxide. It is estimated that from the 71 billion cubic meters of gas consumed in power plants, approximately 118 billion kilograms, or 118 million tons, of carbon dioxide are released into the atmosphere annually. The economic value of this amount of carbon dioxide is almost equivalent to the total export of Iranian petrochemical products, which is $11.8 billion. Carbon dioxide is a crucial chemical compound with numerous applications across various industries, including food, chemicals, petrochemicals, pharmaceuticals, construction, refrigeration, and particularly in enhancing oil recovery (CO_2-EOR). Iran, with about 10 and 18 percent of the world's total oil and gas reserves, should make the chemical and petrochemical industries the main axis of the country's economic development. In this presentation, the status of carbon dioxide in Iran will be introduced, along with its management, applications, and optimal conversion into high-value-added products.

Keywords: Carbon dioxide, Photosynthesis, Cellular respiration, Iranian petrochemical products.

The 30th Iranian Seminar of Organic Chemistry
February 7-9, 2025, Iran University of Science and Technology, Tehran, Iran

Innovative Metal-Free Anthraquinone-based Photocatalyst: Investigating the Visible Light-Induced Photoisomerization of Stilbene

Mohammad Namjoo [a], Mona Hosseini-Sarvari *[a]

[a]*Nanophotocatalysis Lab., Department of Chemistry, Shiraz University, Shiraz 7194684795, Iran.*

Corresponded to: hossaini@shirazu.ac.ir

Keyword: Photocatalyst, Anthraquinone, Stilbene

Introduction

In recent years, there has been a growing interest in photocatalytic technologies that utilize semiconductors and photosensitizers responsive to visible light, primarily due to their potential applications in energy and environmental fields. Among the various photocatalysts that have emerged, non-metal photocatalysts, particularly anthraquinones (AQs), have gained considerable attention. AQs act as redox-active electron transfer mediators and photochemically active organic photosensitizers, effectively mitigating common challenges associated with traditional semiconductors, such as limited light utilization and poor carrier separation efficiency. The advantages of AQs include their abundant raw material availability, controllable synthesis processes, impressive electron transfer properties, and photosensitivity, making them suitable for applications in energy, medicine, and environmental management. For photocatalytic technology to be effective, ideal photocatalytic materials should be low-cost, non-toxic, sourced from abundant materials, highly efficient, stable, easily separable and recoverable, and capable of efficiently absorbing visible light. While noble metals like platinum and ruthenium exhibit excellent catalytic activity, their practical use is hindered due to their high costs and limited availability of raw materials. In contrast, AQs are recognized for their exceptional electron transfer capabilities, serving as redox mediators that enhance the anaerobic bioreduction of heavy metals and organic contaminants. Stilbenes or stilbenoids have various applications in pharmaceuticals, food preservatives, and food additives.The most recognized stilbenoid is resveratrol, but other noteworthy compounds include astringin and isorhapontin, which are derived from forest biomass and present opportunities for new product development. Stilbenes exist predominantly as trans isomers due to their greater thermodynamic stability, although trans-stilbenes can convert to the cis form under specific conditions, such as light irradiation. This study explores the effectiveness of an anthraquinone-based homogeneous photocatalyst for facilitating the photoisomerization of trans-stilbene to cis-stilbene under visible light without the use of an oxidant.[1–3]

Method

In a test tube and under the Ar atmosphere, Dry DMF as solvent was added to a mixture of photocatalyst (0.03g,0.04 mmol) and trans stilbene (0.1 mmol, 0.0180g). Then, the test tube containing the reaction mixture was placed inside the hand-made photoreactor , and irradiated by Blue LED lights from the bottom. After 24 h the mixture was extracted with EtOAc and H_2O (3:1). The combined organic layers were washed with brine and dried over Na_2SO_4.

Results and Discussion

Initially, we successfully synthesized the photocatalyst (PC) utilizing anthraquinone derivatives. Following the successful organic synthesis of the photocatalyst, we proceeded to employ it in a photoisomerization process. Both trans and cis stilbene are thermodynamically stable molecules, with the trans isomer exhibiting a slightly lower energy state by approximately 4.6 kcal/mol. Notably, the internal rotation (isomerization) barrier for stilbene is 48.3 kcal/mol. This substantial energy barrier hinders any isomerization around the double bond in the ground state; however, the photoisomerization from trans to cis has been widely studied. In the excited state, the lowest energy configuration of stilbene adopts a twisted conformation, characterized by a minimal barrier for internal rotation between the trans and twisted forms. By leveraging a homogeneous organic photocatalyst, we successfully surmounted this energy barrier, facilitating the conversion of trans stilbene to cis stilbene when exposed to blue light in the presence of the polar, aprotic solvent Dry DMF.(**Scheme** 1)

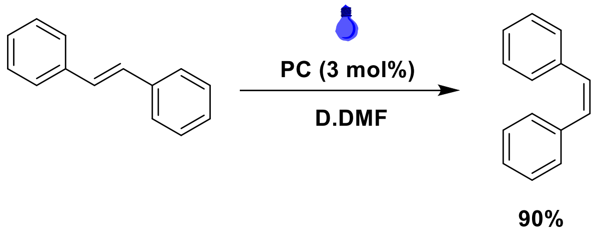

Scheme 1: Photoisomerization of trance stilbene

References:

(1) Latva-Mäenpää, H.; Wufu, R.; Mulat, D.; Sarjala, T.; Saranpää, P.; Wähälä, K. Stability and Photoisomerization of Stilbenes Isolated from the Bark of Norway Spruce Roots. *Molecules* **2021**, *26* (4), 1036.

(2) Chen, C.-X.; Yang, S.-S.; Pang, J.-W.; He, L.; Zang, Y.-N.; Ding, L.; Ren, N.-Q.; Ding, J. Anthraquinones-Based Photocatalysis: A Comprehensive Review. *Environ. Sci. Ecotechnology* **2024**, 100449.

(3) Xie, W.; Yu, Z.; Huang, H.; Jiang, R.; Yao, S.; Huang, J.; Hou, Y.; Yin, S.; Mo, R.; Wu, C. Anthraquinone-Based Polymer Modified BiVO4 Photoanode with Strong Electron-Withdrawing Functional Groups for Boasting Photoelectrochemical Water Oxidation. *J. Colloid Interface Sci.* **2024**, *665*, 977–987.

The 30th Iranian Seminar of Organic Chemistry
February 7-9, 2025, Iran University of Science and Technology, Tehran, Iran

Ultrasound-Assisted Green Synthesis of Heterocyclic and Heterocyclic Hybrid Isoxazolo[5,4-*b*]Pyridines *via* Multicomponent Reactions

Authors: Seyed Ali Hosseini[a], Abdolali Alizadeh[b]*

Corresponding author, Chemistry Department, Tarbiat Modares University, Tel.: +98 21 8800663; fax: +98 21 88006544; e-mail: aalizadeh@modares.ac.ir

Keyword: 5-Amino isoxazoles, Ultrasound (US) irradiation, Enamine Cyclization, Isoxazolo[5,4-*b*]pyridines, Multicomponent Reactions.

Introduction

One of the primary objectives in organic and medicinal chemistry is to design and synthesis significant bioactive molecules. Isoxazoles, a category of heterocyclic compounds, are prevalent in various medications and are also found in nature. These compounds demonstrate a broad spectrum of biological activities, such as antimicrobial, anticancer, antiviral, and anti-inflammatory effects [1-3].

Also, ultrasound irradiation has emerged as an efficient energy source for organic synthesis, facilitating multicomponent reactions while improving reaction rates and yields [4,5].

Results and Discussion

Here, considering our interest in the synthesis of organic compounds with the help of ultrasound we report the synthesis of isoxazolo[5,4-*b*]pyridines from by one-pot reaction of different combinations with 5-amino isoxazoles. We conducted three different studies in this field, all of which utilized enamine 5-amino isoxazoles and ultrasound irradiation.

In the first study, we commenced our exploration with the synthesis of intermediate 2-(2-oxo-2-arylethylidene)malononitrile **A** as a multifunctional synthon *via* the Knoevenagel condensation of phenylglyoxal and malononitrile in AcOH in the ultrasound irradiation and the reaction was completed after 20 min. The intermediate **A** was formed as a red liquid in solvent. In the next step, without further purification within a one-pot sequential process, elemental 5-amino-3-phenylisoxazole was added to the reaction mixture Interestingly, the intermediate **A** was consumed in 25 min under ultrasound irradiation and the reaction yielded a good amount 73% of the desired product. Also, in subsequent research, we synthesized intermediates 1,3-dimethyl-5-(2-oxo-2 arylethylidene)pyrimidine-2,4,6(1*H*,3*H*,5*H*)-trione and 2-(1,3-dioxo-1*H*-indene-2(3*H*)-ylidene)malononitrile from the reaction of arylglyoxal and barbituric acid, as well as ninhydrin and malononitrile. And we succeeded in synthesizing hybrid heterocyclic compounds pyrido[2,3-*d*]pyrimidines-fused isoxazoles and isoxazolo-fused indenopyridine using ultrasound irradiation.

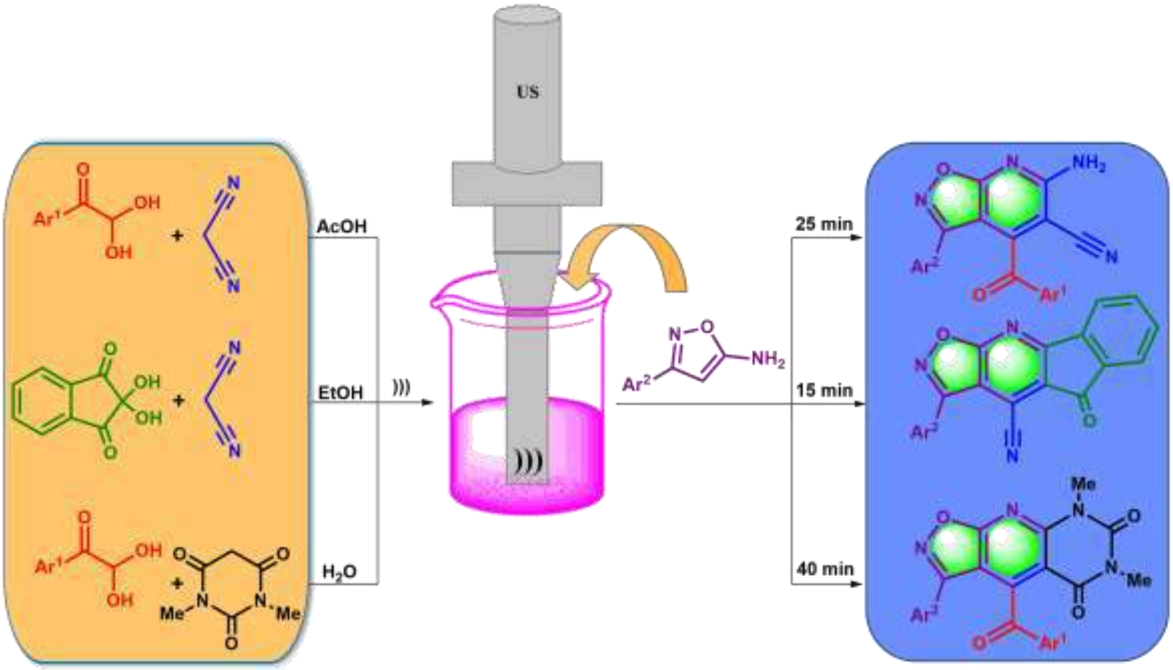

Scheme: synthesis of heterocyclic and heterocyclic hybrid isoxazolo[5,4-*b*]pyridines *via* multicomponent reactions

References:

[1] Wang, X.; Hu, Q.; Tang, H.; Pan, X. *Pharm.* **2023**, *16*, 228-263.

[2] Lamberth, C. *J. Heterocycl. Chem.* **2018**, *55*, 2035-2045.

[3] Tajbakhsh, M.; Naimi-Jamal, M. R.; Balalaie, S.; Rezaeian, M. *Sci. Rep.* **2022**, *12*, 19106.

[4] Javahershenas, R.; Nikzat, S. *Ultrason. Sonochem.* **2023**, *102*, 106741.

[5] Alizadeh, A.; Hasanpour, H.; Rezaiyehraad, R. *Chemistryselect* **2022**, *7*, e202203889.

The 30th Iranian Seminar of Organic Chemistry
February 7-9, 2025, Iran University of Science and Technology, Tehran, Iran

Catalytic synthesis of 1,5-dihydro-2*H*-pyrrol-2-one derivatives using a new covalent organic framework with sulfonic acid tags

Mohammad Amin Oghan, Mohammad Ali Zolfigol*, Maryam Hajjami*, Morteza Torabi

Corresponding Author E-mail: mzolfigol@yahoo.com & m.hajjami@basu.ac.ir

Department of Organic Chemistry, Faculty of Chemistry and Petroleum Science, Bu-Ali Sina University, Hamedan, 6517838683, Tel: +988138282807, Fax: +988138380709 Iran.
Keywords: Catalyst, COF, Multicomponent reaction, Pyrrole

Abstract

Covalent organic frameworks (COFs), constructed by organic building blocks, to make two and three dimensional geometry and are assembled with light elements (such as B, N, C, O) that are connected *via* strong covalent bonds [1]. On the other hand, *N*-heterocyclic compounds as important classes of natural and synthetics organic materials, have numerous biological activities [2]. Among *N*-heterocyclic compounds, 1,5-dihydro-2*H*-pyrrol-2-ones assuredly have considerable potential application in pharmaceutical industries and bioactive natural products owing to their notable biological properties such as anti-cancer, anti-tumor, anti-biotic and anti-diabetic [3]. In this study, we synthesized 1,5-dihydro-2*H*-pyrrol-2-one derivatives *via* multicomponent cyclo-condensation reaction of aldehydes, aryl amines and ethyl pyruvate as starting materials by using COF-SO_3H as heterogeneous active catalyst under mild reaction condition with excellent yields (Scheme 1). The synthesized pyrrol-2-one derivatives were characterized by using FT-IR and NMR analyses.

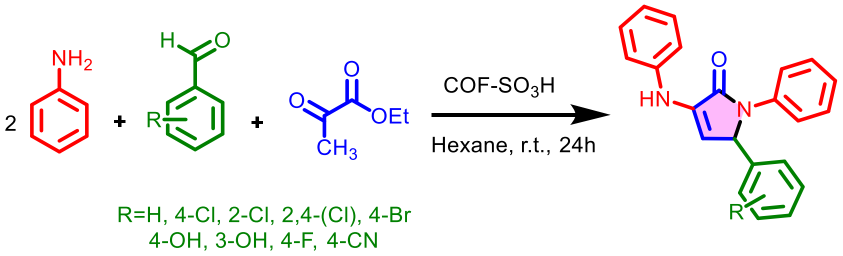

Scheme 1: Application of COF-SO_3H as a catalyst for preparation of 1,5-dihydro-2*H*-pyrrol-2-one derivatives

References

1. *Reticular Chemistry—Construction, Properties, and Precision Reactions of Frameworks.* Journal of the American Chemical Society, 2016. **138**(48): p. 15507.
2. Abbaspour, T., G. Firouzzadeh Pasha, and M. Tajbakhsh, *Synthesis of novel pyrrole derivatives from the multicomponent reaction using the new N-sulfonic acid modified poly (styrene-diethylenetriamine) as a solid acid catalyst.* Applied Organometallic Chemistry, 2023. **37**(1): p. 6933.
3. Brindisi, M., et al., *Anticancer potential of novel α, β-unsaturated γ-lactam derivatives targeting the PI3K/AKT signaling pathway.* Biochemical Pharmacology, 2021. **190**: p. 114659.

Efficacy of licorice extract in Acne vulgaris and Rosacea treatment

Farshad Akbarnejad

Scientific& Educational Department of Dr. Akhavi Laboratory Health Pharmaceutical Company, Tehran, Iran

Abstract

Licorice root has been used as a medicinal plant in Europe since prehistoric times, and the therapeutic use of the dried roots of different licorice varieties dates back to ancient Greece. According to in vitro and in vivo and clinical researches, several valuable medicinal properties such as anticancer, antiviral, strengthening the body's immune system, detoxification, sedative, treatment of digestive diseases, liver diseases treatment, treatment of heart diseases, atherosclerosis problems, and several other curative results have been confirmed. The purpose of the literature review is to investigate the effectiveness and safety of licorice derivatives in acne and rosacea, which may be useful for clinical trials on the dermatological effects of licorice and the development of complementary medicine in the future.

Keywords: Licorice, Acne, Rosacea, Anti-androgenic activities

Introduction

Licorice is one of the oldest medicinal plants that both its name and the plant have ancient origins. The records of its cultivation go back to the third century, that is, during the time of the Greeks and Romans era. Although at that time it was possible to extract from the plant's roots, its medicinal and commercial importance was understood. Licorice species are native to the Mediterranean and certain regions of Asia and are nowadays cultivated all over Asia and Europe. Glycyrrhiza species belongs to the Leguminosae family, which includes about 30 different species, including G. glabra, G. uralensis, G. inflata, G. eurycarpa, G. aspera and G. korshinskyi. Today, the development of technology practically led to the chemical analysis of its compounds, including the successful identification of the active ingredients like glycyrrhizin, chalcone, and glabridin, which made its medicinal importance known in more detail. Licorice contains more than 20 triterpenoids and approximately 300 flavonoids and is commonly used to treat some diseases.

Among its important active ingredients, it is a medicinal substance that is often used in clinical diseases. Chalcones are one of the main classes of flavonoids, which have various biological effects and are widely present in nature. Today, 42 chalcones have been identified in licorice, and play a key role in the licorice pharmacological effects. These compounds have many biological activities, including anticancer, anti-inflammatory, antiallergic, antibacterial, antioxidant, antiviral, antidiabetic, anti-depressant, hepatoprotective, etc. In the present century, licorice extract has found many uses, it is used as a flavoring, sweetener and as an effective medicinal ingredient. Glycyrrhizin is one of the sweetest compounds known, 60 times sweeter than sugarcane sugar. In addition, since ancient times, the dried roots and rhizomes of many licorice species have been used as medicinal plants.

Some useful medicinal properties include anti-cancer, anti-viral, strengthening the immune system, detoxifying, sedating, treating digestive diseases, liver diseases, treating heart disease, atherosclerosis, and many other medicinal effects based on in vitro, in vivo, and animals and human studies have been confirmed.

The first licorice was mentioned in the “The Code of Humnubari” around 2000 BC and the Assyrians made herbal pills from it. Ancient Egyptians used licorice to make sweet drinks.To quench thirst, soldiers used licorice extract on the battlefield. Records of the development of licorice's medicinal use date back to 500 BC. At that time this plant was called the grandfather of herbs. Hippocrates (460-370 BC), the father of medicine, discovered that licorice was an effective treatment for controlling ulcers and quenching thirst. Theophrastus (372-287 BC), a Greek botanist, in his book Historia Plantarum, called licorice sweet root and described its uses for coughs, asthma, and respiratory diseases. Pedanius Dioscorides (40-90 AD), a Roman physician and author of the Medicinal herbs Pharmacopoeia de Materia Medica, classified plants based on their nutritional and medicinal purposes.

Pliny the Great (23-79 AD), author of Naturalis Historia, described the medicinal uses of licorice for clearing the voice, suppressing coughs, alleviating asthma and digestive problems. Avicenna (c. 980-c. 1037), was a great polymath, who wrote very famous medical textbooks of his time, The Canon of Medicine and The Book of Healing. In the Canon of Medicine book, Ibn Sina considered licorice to be a medicine for wounds and ulcers.

Carl Linnaeus (c. 1707–c. 1778) first recognized three species of licorice, G. glabra, G. echinata, and G. hirsuta. Bolognese jurist Pietro de Crescenzi (c. 1230–c. 1320), an important historical figure and author of Ruralia commode or Liber ruralium commodorum, first documented the cultivation of licorice.

The earliest description of licorice was found in **"The Code Humnubari"** (2100 BC) and Assyrian herbal (2000 BC).

Hippocrates (460-370 BC) was a great Greek Physician referred as "Father of Medicine" and one of the outstanding personality in the history of medicine mentioned licorice could be used as effective remedy for control of ulcers and quenching of thirst.

Theophrastus (372-287 BC) is the "father of botany" and author of "Historia Plantarum", referred licorice as "Scythian roots" (sweet roots) and recommended licorice uses in cough, asthma and pectoral diseases.

Pedanius Dioscorides (c. 40 – 90 AD) written ***De Materia Medica*** and in his book he introduced the term "Glukurrhiza" for the roots and stem of *G. glabra*.

Pliny the Elder (23–79 AD) wrote encyclopedia "***Naturalis Historia***" and described medicinal uses of licorice for voice clearing, cough suppressant, asthma and carminative effects.

Abu Ali Sina (Avicenna) (c.980 - 1037) considered as "father of early modern medicine". He wrote very famous books ***The Canon of Medicine*** and **The Book of Healing** and recommended licorice as remedy for diseases of respiratory tract, stomach, voice clearing and reduce voice hoarseness etc.

Pietro de Crescenzi (c. 1230 – c. 1320) was the author of "*Ruralia Commode* or *Liber Ruralium Commodorum*" in which he firstly documented cultivation of licorice

Figure 1. Historical Development of Licorice.

Theophrastus is the first source of information about the use of licorice for the treatment of skin lesions, This source states that the use of licorice can help with skin problems,and he also found the prescription of licorice in honey to be useful for treating wounds.

In the current century, according to Ibn al-Bithaar, Dioscorides, its use is useful for the treatment of granulomas at the base of fingernails and toenails and foot ulcers. In his book of law, Ibn Sina considered licorice to be a medicine for wounds and ulcers.

The purpose of this review is to discuss the medical efficacy and safety of licorice in dermatology, which may help in the future clinical research and complementary medicine development of this plant in the field of dermatology. To date, 554 medicines containing licorice have been approved by the Chinese Food and Drug Administration.

Materials and methods

Data used in this study obtained from Springer, Hindawi, PubMed, ScienceDirect, Google Scholar, and other scientific sources. The data for this current study were collected, interpreted, and presented using keywords. This study paid more attention to the benefits of licorice in dermatology and did not include irrelevant papers. This review article discusses the medical efficacy and safety of Glycyrrhiza species in dermatology, and also mentions related research papers and their results.

Pharmacognosy

Licorice is a widely distributed herbaceous perennial shrub that reaches up to 2.5 meters in height. The leaves are compound and have four to seven pairs of leaflets and one terminal leaflet. The flowers are irregular and in yellow, purple or purple colors and in a complex form at the end of the flowering stems that are placed in the hermaphrodite inflorescence.

The fruit is two to three centimeters long and date-colored. The sides of the fruit are narrow and more or less pointed. Inside the fruit there are three to five rectangular brown beans. The genus Glycyrrhiza are able to fix nitrogen through symbiosis with rhizobium on the root surface, and are suitable for sandy and clay soils, but prefer moist soils. The healing activity of G. glabra have been well documented since ancient Egypt. The most consumed part of licorice is the roots and its leaves are agricultural waste. However, in the recent years, the studies of phytochemical compounds of G. glabra leaves show that similar to the roots, although in lower amounts, certain compounds are present in the leaves.

Phytochemistry

To date, more than 400 phytochemicals have been identified in the Glycyrrhiza genus.These molecules can be classified as saponins, flavonoids, chromenes, coumarins, dihydroxyacetone, coumestans, benzofurans, and dihydrophenanthrene among these, flavonoids and triterpenoid saponins are abundant in licorice roots and rhizomes. Licorice root has 50% dry weight and 5% to 15% metabolites and water-soluble sugars (glucose, sucrose and mannitol), 25 to 30% starch, 10% to 16% glycyrrhizin, 1% to 2% amines. asparagine, betaine and choline) and sterols (stigmasterol and beta-sitosterol). Glycyrrhizin (glycyrrhizic acid, glycyrrhizic acid) licorice root extract accounts for 10-25% and is considered the main active ingredient. Glycyrrhizin is a saponin ingredient consisting of a triterpenoid aglycone, glycyrrhetic acid (glycyrrhetinic acid, Enoxolone) conjugated to the disaccharide glucuronic acid. Both glycyrrhizin and glycyrrhetic acid can exist in 18α and 18β stereoisomers.

Flavonoids, which are liquiritin, isoliquiritin, liquiritigenin, and rhamnoliquiritin, and five new flavonoids, including glucoliquiritin, Liquiritin apioside, prenyllicoflavone A, shinflavanone, shinpterocarpin, and 1-methoxyphaseolin isolated from the dried roots.

Although the roots are the most commonly used part, phytochemical studies have also been conducted on the leaves, which are considered agricultural chemical waste. The studies showed that certain compounds in the roots are also detected in the leaves of G. glabra to a lesser extent. In general, alkaloids and tannins were not detected. The flavonoid and saponin compounds of G. glabra, G. inflata and G. uralensis species have cosmetic effects that some studies focused on them and their biological activities (Figure 1).

Flavonoids

Around 300 flavonoid ingredients have been isolated from licorice species.Flavonoids,made up of two benzene rings (ring A and ring B) via a C ring creating a tricarbon chain, are divided into flavonols, flavones, flavanones, flavanols, dihydroflavones, chalcones, isoflavones, depending on the position of ring C, its degree of oxidation and the connection site of ring B. Different types of flavonoids are isolated from G. glabra, G. uralensis and G. inflata. Flavonoids have been studied as cosmetically active ingredients such as flavonone, flavonol, flavone, isoflavone, isoflavones, isoflavones and chalcones. The flavonoids that have been investigated are those that exhibit cosmetic activities such as flavonones, flavonols, flavones, isoflavones, isoflavones, Isoflavones, and chalcones.Liquiritin is one of the most important flavonoids that is a phytochemical indicator of medicinal licorice species. Liquiritigenin is another flavonoid extract from Glycyrrhiza uralensis that has various medicinal properties, including antioxidant, anti-inflammatory, antibacterial and anti-aging effects. Pinocembrin and liquiritin apioside also related to the class of flavanones. Other flavonols include kaempferol, protensein and the flavone chrysoriol.

phytochemicaly, glabrin is a common isoflavone compound in G. glabra and accounts for 11% of the total flavonoid content. With glabidine, hispaglabrin A, glyaspirin C, glyaspirin D and 3-hydroxy-40-O-methylglabrin. From a phytochemical perspective, glabrin is a common isoflavone compound G. Glabra and with glabidine, hispaglabrin A , glyaspirin C, glyaspirin D and 3-hydroxy-40-O-methylglabrin accounts for 11 of the total flavonoid content.

Licorice isoflavones such as glabrin, dehydroglyaspirin C, dehydroglyaspirin D, isoflavones such as glycyrrhizoflavone, hemiquaisoflavone B, alloliquiisoflavone B, isoangstone A, and formonontin, as well as isoflavanones such as dihydroidzein and glycyrrhizinone have been investigated for cosmetic properties (Figure 2).

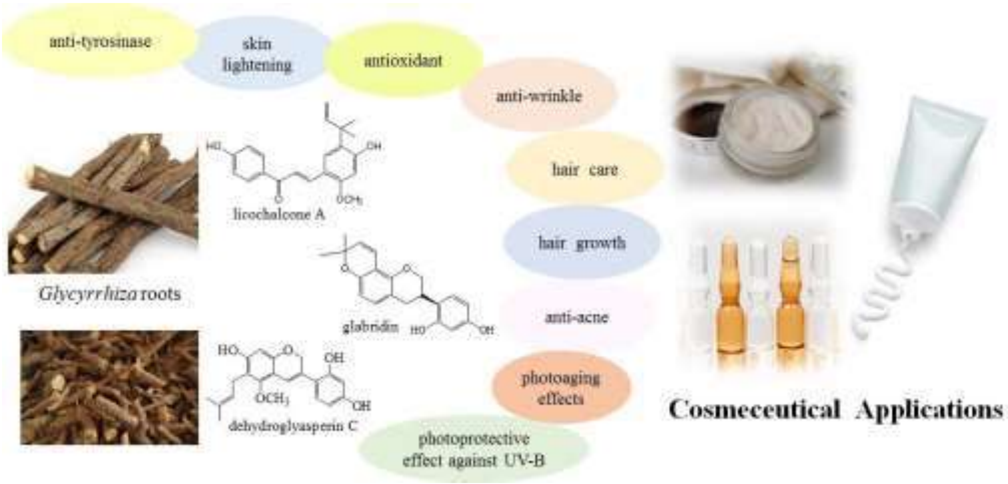

Figure2. Cosmetic applications of licorice isoflavones.

Chalcone has been reported frequently in licorice root. In this study the activities of isolico-ritigenin, isolicoritin, licochalcone A , licochalcone B, eicochalcone C, licochalcone D derivatives from Glycyrrhiza spp were discussed as effective ingredients for Cosmeceuticals formulation. Also, dibenzoylmethane, a structural analogue of curcumin (diferroylmethane), has been investigated for its cosmetic use. Among the flavonoids mentioned earlier, the main active ingredients of Glycyrrhiza licoricetin and isolicouritin are glycosides. Pharmacological properties of chalcones and their derivatives are mentioned in Figure 3.

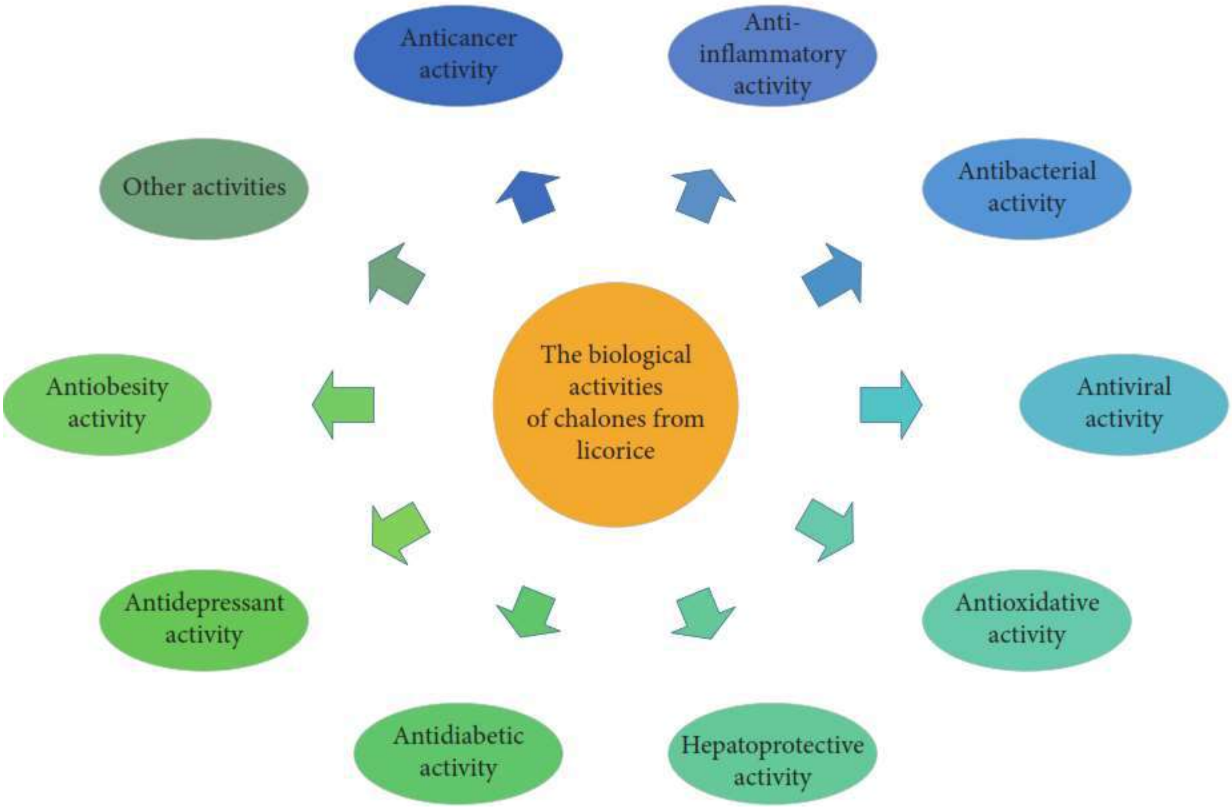

Figure 3. Pharmacological properties of chalcones and their derivatives

Saponins

More than 70 saponins have been recognized in licorice roots and their structures have been demonstrated in a recent study. Glycyrrhizinic acid or its salt, glycyrrhizin, has been reported as the major secondary metabolite that exists in Glycyrrhiza species. The main and abundant active cosmeceutical ingredients in the root of the plant are glycyrrhizin and glycyrrhetic acid.Glycyrrhetic acid exists as two isomers: the 18α form and the 18β form. As a sweetener, glycyrrhizin has been reported to be 30 to 50 times sweeter than sucrose.Glycyrrhizal saponins, which are composed of aglycone and half sugar, can be classified into several categories, in which glucuronic acid, glucose, rhamnose are the main characteristic parts of the sugar part. Licorice saponin G2 (also known as 24-hydroxyglycyrrhizin) is shown below (Figure 4).

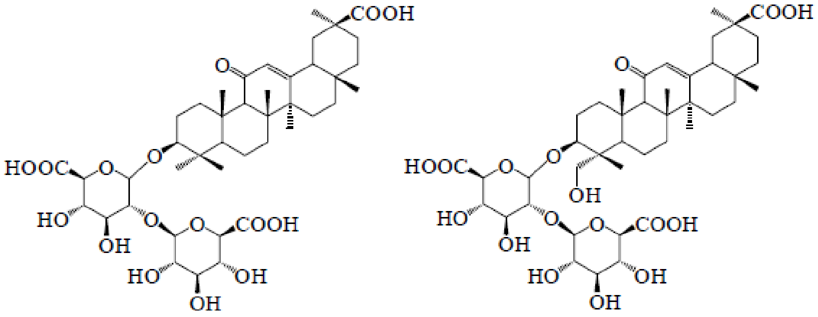

glycyrrhizinic acid licorice saponin G2

Figure 4. Licorice triterpenoids used in the cosmetic industry as active ingredients.

Polysaccharides

Among the biologically active components of glycyrrhiza plants, glycyrrhiza polysaccharides are more important.A recent report on their isolation, structural characterization, and biological activities. They are heteropolysaccharides mainly composed of arabinose, glucose, galactose, rhamnose, mannose, xylose, and galactronic acid in different ratios and types of glycosidic bonds. A preliminary research of the moisturizing capacity of polysaccharides showed that their water-holding capacity was greater than that of glycerol solutions, suggesting their potential for use as a moisturizing products in cosmetics.

Acne Vulgaris

Acne vulgaris, an acute multifactorial inflammatory disease, affects the pilosebaceous unit in the skin. This disease is usually seen in an area with high-density pilosebaceous units (face, neck, upper chest, shoulders, and back) and the presence of seborrhea, non-inflammatory lesions (open comedones or blackheads, and closed comedones or whiteheads), Inflammatory lesions (papules and pustules), and different degrees of scarring. The pathogenesis of acne includes the interaction between four main factors, including hypersborrhoea (excess production of sebum) by some androgens and changes in the fatty acid composition of sebum, hyperkeratinization in the follicle that leads to the formation of keratin plug (micro-comedone), colonization of the pilosebaceous unit. Acne is caused by Cutibacterium acnes (Propionibacterium acnes). Colony of Cutibacterium acnes (air-tolerant anaerobic bacteria) and the release of inflammatory mediators in response to the presence of Cutibacterium acnes, it was shown that Staphylococcus epidermidis (a facultative anaerobic bacterium) also plays a beneficial role by limiting the colonization of Cutibacterium acnes and inflammation. Licorice extract has anti-androgenic, anti-microbial, anti-inflammatory, antioxidant, brightening, and blood circulation-enhancing properties that can be effective with multiple anti-acne and anti-inflammatory post-blemish medicinal mechanisms.The components of licorice extract responsible for these medicinal activities have been studied in various studies in terms of molecular mechanisms and safety profile, as well as in vitro, in vivo, animal, and clinical studies. Licorice extract has a wide range of activity and can be considered an effective and safe option in anti-acne and anti-blemish treatment after inflammation. Glycyrrhizic acid is the key active ingredient of licorice extract, which is hydrolyzed to glycyrrhetinic acid in vivo.

Today, bacterial resistance is increasing due to improper use of antibacterial drugs.Therefore, it is very important to find new, safe and effective antibacterial drugs. Some herbal extract in licorice have antibacterial activity. Certain bacteria such as Coutibacterium acnes, Staphylococcus aureus, Staphylococcus epidermidis, and Streptococcus pyogenes play an important role in the pathogenesis of acne vulgaris by stimulating inflammatory processes. Licochalcone A, Licochalcone E and licorice root extract have antimicrobial properties against bacterial strain for acne. In vitro tests have indicated remarkable antibaterial function of licorice extract against Cutibacterium acnes, Staphylococcus aureus, Staphylococcus epidermidis, and Streptococcus pyogenes. The active methanolic extract of G. glabra indicated promising antibacterial effects against Staphylococcus aureus, Staphylococcus epidermidis, and Cutibacterium acnes, as demonstrated by in vitro screening. Another laboratory study showed antibacterial activity of G. glabra for two strains of Cutibacterium acnes with a minimum inhibitory concentration of 200 µg/ml for strain ATCC 6919 and a minimum inhibitory concentration of 100 µg/ml for strain ATCC 11827S. In addition, the minimum bacterial inhibitory concentration of licorice extract is 0.25 and 2.5 mg/ml against methicillin-sensitive Staphylococcus aureus and methicillin-resistant Staphylococcus aureus, respectively.

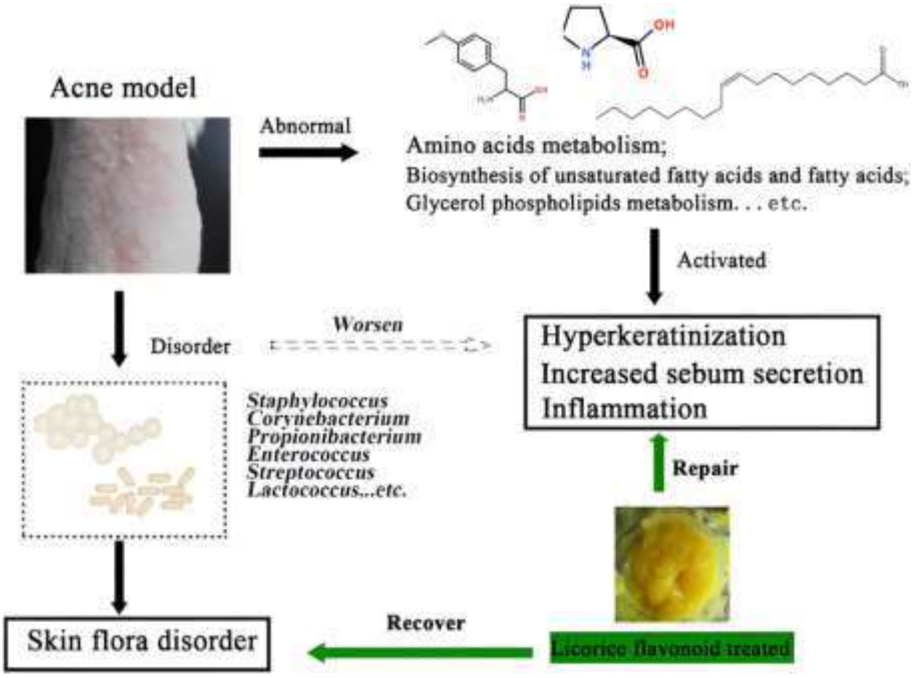

Figure 5- The mechanism of licorice flavonoids in healing acne vulgaris.

Regarding its antibacterial effect, laboratory studies have shown the inhibitory activity of aqueous and ethanol extracts of licorice on Staphylococcus aureus and Streptococcus pyogenes cultures, the first one indicated the strongest inhibition with a diameter of inhibition zone of 10-15 mm. Gupta et al. showed antibacterial activity against Gram-positive and Gram-negative bacteria. The results of the evaluation of the effectiveness of cosmetic products including glycolic acid, salicylic acid, gluconolactone and licochalcone A as an adjunctive treatment for adapalene in mild to moderate acne in a 28-day double-blind study on 25 people from each patient asked for two products including (1) a cosmetic product and health in combination with 0.1% adapalene and (2) 0.1% adapalene. The number of acne lesions, severity of acne, overall doctor and patient assessment of acne severity, visual analog brightness scale, skin biophysics, safety assessment and VISIA camera system were evaluated. The mean results did not show a difference in the reduction of inflammatory lesions on the seventh day, but there is no obstacle to using a cosmetic drug along with standard cure. However, this cosmetic product also reduces the complications of acne.

According to prior studies, isoliquiritigenin had a demonstrable inhibitory activity on methicillin-resistant Staphylococcus aureus. Licochalcone A, as one of the essential antibacterial ingedients which shows bactericidal activity against Staphylococcus aureus. Many studies show that G. glabra may be a potent remedy against acne. G. glabra indicated significant antibacterial activity against Cutibacterium acnes by inducing minimal resistance versus to the significant development of resistance in bacteria treated by erythromycin.

Multifactorial effects such as mechanisms are antimicrobial activity, moisturizing effect of licorice, anti-androgenic function, inhibiting PI3K-Akt signaling pathways, mitochondrial activity and regulating skin microbes has been suggested as a mechanisms related to the anti-acne effect.

In mice, Lakshmi et al., (2019) investigated the pharmacological effects of Licorice and concluded that in disease models, the volume and thickness of sebaceous glands were significantly increased compared to control animals and decreased when Licorice extract was used. Several articles report herbal formulations with anti-acne glycyrrhizin synergistic with anti-acne herbal formulations. The most recent of them was proposed by Keshri and Khare in 2020, although other synergistic formulas were proposed earlier.

Activation of NLRP3 (nucleotide-binding domain, leucine-rich Containing family, inflammasome containing pyrin-3) inflammasome by Cutibacterium acnes is a critical for inducing inflammation and exacerbating of acne lesions. The anti-acne activity of licochalcone A resulted in effective suppression of the NLRP3.

Under in vitro conditions, Cutibacterium acne has no bacterial resistance to licorice extract. It appears that Glycyrrhiza, in the treatment of acne has the potential to become a promising treatment. It seems that when topical cosmetic medications are correctly prescribed, they can improve acne treatment outcomes.

In a clinical study on 91 adult patients with mild acne, Federica Dal Oglio et al. (2019) evaluated the effectiveness and tolerability of a novel daily formula regimen in the remedy of mild facial acne.

In this study, patients were use a solution containing licochalcone A, salicylic acid and L-carnitine in the morning and a cream containing 10% complex of licochalcone A and hydroxy at night for 8 weeks. Clinical effectiveness with the Global Acne Grading System (GAGS) score and the number of comedone lesions, papules, and with the evaluation of the VISIA-CR tool (Canfield's Visia CR skin analysis imaging system: takes high-quality, standardized images of the face for clinical research) was evaluated in weeks 4 and 8.

In the fourth week, a statistically significant decrease was observed compared to the base of the global acne grading system. In addition, the average total number of comedones and papules decreased by 41% and 45%, respectively, compared to the baseline level and a significant decrease in the average sebum by 47%. At the 8th week, a statistically significant reduction compared to the Global Acne Grading System baseline, total number of comedones and papules (64% and 71%, respectively), along with a 52% reduction in excess sebum was also recorded. The results of this research show that the daily regimen based on licochalcone A solution, salicylic acid and L-carnitine or cream containing licochalcone A complex and 10% hydroxy is an effective aesthetic approach for mild acne treatment. A combination of 0.1% adapalene gel and moisturizer containing licochalcone A, L-carnitine and 1,2-decanediol also showed a synergistic effect in reducing inflammatory lesions without interfering with the effect of each of the active ingredients. Several chalcone derivatives showed anti-acne activity mainly as antibacterial and anti-inflammatory agents. Licochalcone A has been studied as a potent anti-inflammatory agent and has been combined with other active ingredients in several anti-acne formulations. A skin care formulation containing licochalcone A, L-carnitine, and 1,2-decanediol was evaluated in a 9-week, double-blind, randomized, placebo-controlled study to evaluate the independent efficacy of the formulation in volunteers with mild to moderately severe facial acne (10- 25 inflammatory lesions) were evaluated in 60 patients for 8 weeks, the results of this study showed that this formula can reduce pustular lesions, common lesions, total lesions and sebum level.

Antiandrogenic activities of licorice

An increase in androgen production in the sebaceous glands of the skin leads to an increase in sebum secretion and acne. Six major enzyme systems are involved in cutaneous androgen metabolism, namely steroid sulfatase, 3β-hydroxysteroid dehydrogenase, β-HSD17, steroid 5α-reductase, α-HSD 3, and aromatase. Licorice is known as an anti-androgen herb through various pharmacological mechanisms. Glycyrrhizin, licochalcone A and licorice root extract have anti-androgen activities. By blocking β-HSD3, β-HSD 17 in humans, licorice reduces testosterone production. Administration of high doses of pure licorice extract to male volunteers can significantly decrease serum testosterone levels, however, testosterone levels never fall below the normal range. In addition, licorice showed anti-androgenic properties in male rats due to increased testosterone metabolism, downregulation of androgen receptors, or activation of estrogen receptors. Licochalcone A inhibited 5 alpha-reductase and antagonized androgen receptors in vitro. Glycyrrhizin and glycyrrhetinic acid significantly reduced testosterone production by inhibiting β-HSD 17 in vitro and stimulating aromatase activity in vitro. Furthermore, in a Chinese clinical trial, glycyrrhizin reduced serum testosterone levels in women and was safe and effective in the treatment of postadolescent acne.

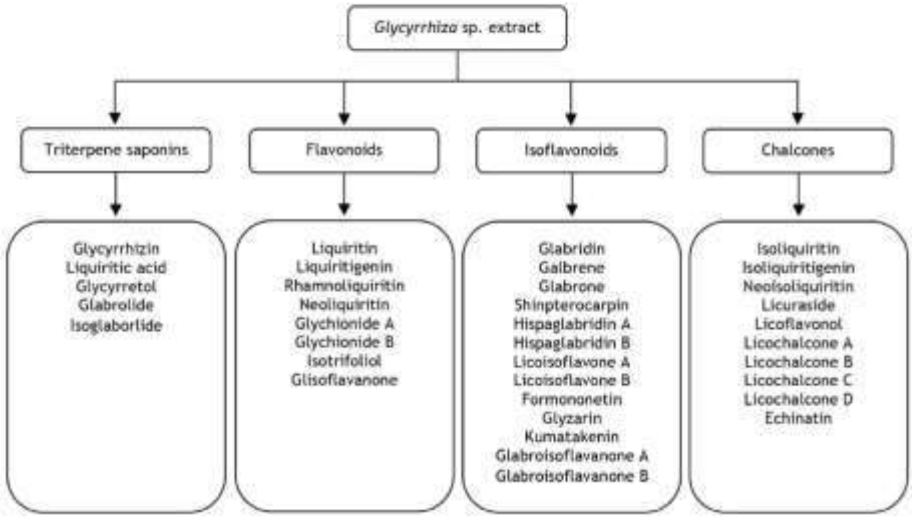

Figure 6. The main components of licorice extract

Acne rosacea

Rosacea is a multifactorial chronic inflammatory skin disorder characterized by persistent or periodic redness and several types of phymatosis changes in the central facial skin (cheeks, chin, nose, and central forehead). Based on the appearance of some of the main phenotypes, rosacea is divided into erythematotelangiectatic rosacea, papulopustular rosacea, glandular/hyperplastic rosacea, ocular rosacea, and other specific forms such as rosacea conglobata, rosacea fulminans, gram-aceacean neoester. Rosacea (Lupoid), Morbihan's disease and rosacea in children. The pathogenesis of rosacea is still not fully understood, but there are several factors that include (1) genetics, Haber syndrome with rosacea as one of the clinical features can be hereditary. (2) Environment Certain environmental factors can trigger rosacea, including extreme air temperature, sudden temperature changes, food (caffeine, alcohol, hot and spicy food), sunlight (ultraviolet and infrared rays), etc. . (3) overproduction of antimicrobial peptides (AMPs) by the innate immune system such as LL-37. (4) inflammation caused by oxidative stress produced by adaptive immune cells. (5) overexpression of toll-like receptors (TLRs). (6) inflammations caused by demodex folliculorum. and (7) neuroinflammation and vascular hyperactivity.

Hesperidin methylchalcone, licochalcone A and tetracarboxymethylnaringenin chalcone show significant activity in improving skin with rosacea. Clinical studies showed that topical formulations containing hesperidin methylchalcone can improve the condition of infected skin by reducing the proportion of dilated vessels, total vessel surface area and IL8 production. These formulas showed a complementary effect between each of the active ingredients in relieving inflammation and reducing redness. Another study reported that hesperidin methylchalcone has anti-inflammatory and analgesic activities, which are dual targets in the treatment of rosacea by inhibiting the potential receptor for vanilloid receptor type 1 (TRPV1), oxidative stress, TNF-α, production of interleukin (IL) 1β, IL -6 and IL-10), and NF-kB activity. Licochalcone A is a natural product of glycyrrhizin that shows strong activity in the treatment, especially in mild and moderate symptoms. In vivo studies have shown that skin care formulations containing licochalcone A provide various activities such as UVA/UVB protection, moisturizing, and redness concealing abilities that improve the appearance of skin with rosacea. These formulas showed high compatibility with sensitive skin and can be combined with other treatments such as metronidazole treatment. The moisturizing formula containing licochalcone A also increases skin hydration and reduces water loss through the skin. The most recent chalcone derivative used as an anti-rosacea is the stabilized form of naringenin chalcone, tetracarboxymethyl naringenin chalcone (TNC). TNC was obtained from naringenin chalcone by total esterification reaction of methyl chloroacetate. An in vitro study showed that tetracarboxymethylnaringenin chalcone significantly reduced LL-37, calcitriol, and several LL-37-induced inflammatory mediators in keratinocytes. Clinical testing also showed that the formulation containing tetracarboxymethylnaringenin chalcone as an active ingredient reduced the redness of rosacea-affected skin compared to untreated skin areas.

References

Ding Y, Brand E, Wang W, Zhao Z. Licorice: Resources, applications in ancient and modern times. Journal of Ethnopharmacology. 2022 Nov; 298:115594. DOI: 10.1016/j.jep.2022.115594. PMID: 35934191.

Raoufinejad K, Rajabi M, Sarafian G. Licorice in the Treatment of Acne Vulgaris and Post inflammatory Hyperpigmentation: A Review. J Pharm Care 2020; 8(4): 186-195.

Abraham J, Florentine S. Licorice (*Glycyrrhiza glabra*) Extracts-Suitable Pharmacological Interventions for COVID-19? A Review. *Plants*. 2021; 10(12):2600. https://doi.org/10.3390/plants10122600

Rudrapal M, Khan J, Dukhyil AAB, Alarousy RMII, Attah EI, Sharma T, Khairnar SJ, Bendale AR. Chalcone Scaffolds, Bioprecursors of Flavonoids: Chemistry, Bioactivities, and Pharmacokinetics. Molecules. 2021 Nov 26;26(23):7177. doi: 10.3390/molecules26237177.

Wang D, Liang J, Zhang J, Wang Y, Chai X. Natural Chalcones in Chinese Materia Medica: Licorice. Evid Based Complement Alternat Med. 2020 Mar 16;2020:3821248. doi: 10.1155/2020/3821248.

Maria Pia GD, Sara F, Mario F, Lorenza S. Biological Effects of Licochalcones. Mini Rev Med Chem. 2019;19(8):647-656. doi: 10.2174/1389557518666180601095420.

ÇOLAK F, GENİŞEL M, URAS İS (June 1, 2021) Evaluation of Glycyrrhiza Species as Medicinal Plant. Anatolian Journal of Biology 2 1 1–11.

Tibenda JJ, Du Y, Huang S, Chen G, Ning N, Liu W, Ye M, Nan Y, Yuan L. Pharmacological Mechanisms and Adjuvant Properties of Licorice Glycyrrhiza in Treating Gastric Cancer. *Molecules*. 2023; 28(19):6966. https://doi.org/10.3390/molecules28196966

Fiore C, Eisenhut M, Ragazzi E, Zanchin G, Armanini D. A history of the therapeutic use of liquorice in Europe. J Ethnopharmacol. 2005 Jul 14;99(3):317-24. doi: 10.1016/j.jep.2005.04.015.

Yang R, Yuan BC, Ma YS, Zhou S, Liu Y. The anti-inflammatory activity of licorice, a widely used Chinese herb. Pharm Biol. 2017 Dec;55(1):5-18. doi: 10.1080/13880209.2016.1225775.

Bayati Zadeh, J., Moradi Kor, Z., & Karimi Goftar, M. (2013). Licorice (Glycyrrhiza Glabra Linn) as a Valuable Medicinal Plant. *International Journal of Advanced Biological and Biomedical Research*, *1*(10), 1281-1288.

Pastorino G, Cornara L, Soares S, Rodrigues F, Oliveira MBPP. Liquorice (Glycyrrhiza glabra): A phytochemical and pharmacological review. Phytother Res. 2018 Dec;32(12):2323-2339. doi: 10.1002/ptr.6178.

Graebin CS. The Pharmacological Activities of Glycyrrhizinic Acid ("Glycyrrhizin") and Glycyrrhetinic Acid. Sweeteners. 2017 Jul 31:245–61. doi: 10.1007/978-3-319-27027-2_15.

Sharifi-Rad J, Quispe C, Herrera-Bravo J, Belén LH, Kaur R, Kregiel D, Uprety Y, Beyatli A, Yeskaliyeva B, Kırkın C, Özçelik B, Sen S, Acharya K, Sharopov F, Cruz-Martins N, Kumar M, Razis AFA, Sunusi U, Kamal RM, Shaheen S, Suleria HAR. *Glycyrrhiza* Genus: Enlightening Phytochemical Components for Pharmacological and Health-Promoting Abilities. Oxid Med Cell Longev. 2021 Jul 24; 2021:7571132. doi: 10.1155/2021/7571132.

Lu Q, Zou LF, Gao YZ, Ye T, Li MJ, Zhang YK, Liang B, Sun W, Xing DM. Liquiritigenin reverses skin aging by inhibiting UV-induced mitochondrial uncoupling and excessive energy consumption. J Cosmet Dermatol. 2023 Mar;22(3):1017-1030. doi: 10.1111/jocd.

Wang D, Liang J, Zhang J, Wang Y, Chai X. Natural Chalcones in Chinese Materia Medica: Licorice. Evidence-based Complementary and Alternative Medicine : Ecam. 2020 ;2020:3821248. DOI: 10.1155/2020/3821248.

Cerulli A, Masullo M, Montoro P, Piacente S. Licorice (*Glycyrrhiza glabra*, *G. uralensis*, and *G. inflata*) and Their Constituents as Active Cosmeceutical Ingredients. *Cosmetics*. 2022; 9(1):7. https://doi.org/10.3390/cosmetics9010007

Wahab S, Annadurai S, Abullais SS, Das G, Ahmad W, Ahmad MF, Kandasamy G, Vasudevan R, Ali MS, Amir M. Glycyrrhiza glabra (Licorice): A Comprehensive Review on Its Phytochemistry, Biological Activities, Clinical Evidence and Toxicology. Plants (Basel). 2021 Dec 14;10(12):2751. doi: 10.3390/plants10122751.

Ni Q, Gao Y, Yang X, Zhang Q, Guo B, Han J and Chen S (2022) Analysis of the network pharmacology and the structure-activity relationship of glycyrrhizic acid and glycyrrhetinic acid. Front. Pharmacol. 13:1001018. doi: 10.3389/fphar.2022.1001018

Shinu P, Gupta GL, Sharma M, Khan S, Goyal M, Nair AB, Kumar M, Soliman WE, Rahman A, Attimarad M, Venugopala KN, Altaweel AAA. Pharmacological Features of 18β-Glycyrrhetinic Acid: A Pentacyclic Triterpenoid of Therapeutic Potential. Plants (Basel). 2023 Mar 1;12(5):1086. doi: 10.3390/plants12051086.

Michael Zeece,Chapter six - Flavors,Editor(s): Michael Zeece,Introduction to the Chemistry of Food, Academic Press,2020,Pages 213-250,ISBN 9780128094341,https://doi.org/10.1016/B978-0-12-809434-1.00006-2.

Vasam M, Korutla S, Bohara RA. Acne vulgaris: A review of the pathophysiology, treatment, and recent nanotechnology based advances. Biochem Biophys Rep. 2023 Nov 23;36:101578. doi: 10.1016/j.bbrep.2023.101578.

Huang, C., Zhuo, F., Han, B. *et al.* The updates and implications of cutaneous microbiota in acne. *Cell Biosci* **13**, 113 (2023). https://doi.org/10.1186/s13578-023-01072-w

Cavallo I, Sivori F, Truglio M, De Maio F, Lucantoni F, Cardinali G, Pontone M, Bernardi T, Sanguinetti M, Capitanio B, Cristaudo A, Ascenzioni F, Morrone A, Pimpinelli F, Di Domenico EG.

Skin dysbiosis and Cutibacterium acnes biofilm in inflammatory acne lesions of adolescents. Sci Rep. 2022 Dec 6;12(1):21104. doi: 10.1038/s41598-022-25436-3.

Fournière M, Latire T, Souak D, Feuilloley MGJ, Bedoux G. *Staphylococcus epidermidis* and *Cutibacterium acnes*: Two Major Sentinels of Skin Microbiota and the Influence of Cosmetics. Microorganisms. 2020 Nov 7;8(11):1752. doi: 10.3390/microorganisms8111752.

Sedighinia F, Safipour Afshar A, Soleimanpour S, Zarif R, Asili J, Ghazvini K. Antibacterial activity of Glycyrrhiza glabra against oral pathogens: an in vitro study. Avicenna J Phytomed. 2012 Summer;2(3):118-24.

Nam C, Kim S, Sim Y, Chang I. Anti-acne effects of Oriental herb extracts: a novel screening method to select anti-acne agents. Skin Pharmacol Appl Skin Physiol. 2003 Mar-Apr;16(2):84-90. doi: 10.1159/000069030.

Rohinishree YS, Negi PS. Effect of licorice extract on cell viability, biofilm formation and exotoxin production by Staphylococcus aureus. J Food Sci Technol. 2016 Feb;53(2):1092-100. doi: 10.1007/s13197-015-2131-6.

Wang D, Liang J, Zhang J, Wang Y, Chai X. Natural Chalcones in Chinese Materia Medica: Licorice. Evid Based Complement Alternat Med. 2020 Mar 16;2020:3821248. doi: 10.1155/2020/3821248.

Ruan SF, Hu Y, Wu WF, Du QQ, Wang ZX, Chen TT, Shen Q, Liu L, Jiang CP, Li H, Yi Y, Shen CY, Zhu HX, Liu Q. Explore the Anti-Acne Mechanism of Licorice Flavonoids Based on Metabonomics and Microbiome. Front Pharmacol. 2022 Feb 8;13:832088. doi: 10.3389/fphar.2022.832088.

Lakshmi, J.N.; Supriya, P.; Soumya, P.L.; Vandana, P.; Babu, A.N. Pharmacological evaluation of liquorice for various dermatological disorders in mice. *Int. J. Pharm. Biol. Sci.* **2019**, *9*, 1253–1259

Yang G, Lee HE, Yeon SH, Kang HC, Cho YY, Lee HS, Zouboulis CC, Han SH, Lee JH, Lee JY. Licochalcone A attenuates acne symptoms mediated by suppression of NLRP3 inflammasome. Phytother Res. 2018 Dec;32(12):2551-2559. doi: 10.1002/ptr.6195.

Nasri H, Bahmani M, Shahinfard N, Moradi Nafchi A, Saberianpour S, Rafieian Kopaei M. Medicinal Plants for the Treatment of Acne Vulgaris: A Review of Recent Evidences. Jundishapur J Microbiol. 2015 Nov 21;8(11):e25580. doi: 10.5812/jjm.25580.

Dall'Oglio F, Fabbrocini G, Tedeschi A, Donnarumma M, Chiodini P, Micali G. Licochalcone A in Combination with Salicylic Acid as Fluid Based and Hydroxy-Complex 10% Cream for the Treatment of Mild Acne: A Multicenter Prospective Trial. Clin Cosmet Investig Dermatol. 2019 Dec 31;12:961-967. doi: 10.2147/CCID.S206935.

Copper (II) anchored on graphene oxide functionalized guanidine as a high-performance supercapacitor electrode

Samira Mohammadi 1[a] (representing author), Seyed Morteza Mousavi Khoshdel 2[*b] (corresponding author), Mohammad Ali Hedayati3 [c]

1,2 Industrial Electrochemical Research Laboratory, Department of Chemistry, Iran University of Science and Technology, Tehran, P.O. Box: 16846-13114, Iran, Iran, Email: mmousavi@iust.ac.ir*

3 School of Metallurgy & Materials Engineering, Iran University of Science and Technology, Tehran, P.O. Box: 16846-13114, Iran.

Keyword: Graphene oxide (GO), Copper (Cu), Anchored, Supercapacitor (SC).

1. Introduction

In response to the progressively extreme challenge of energy shortage, environmental pollution, and global warming, electrochemical energy storage devices like fuel cells, supercapacitors (SCs), and rechargeable batteries have developed as efficient solutions [1-4]. Over the past few decades, SCs have picked up significant prominence among Various electrochemical energy storage devices due to their high power density, high energy density, rapid charge/discharge capacitance, environmental friendliness, and suitable recyclability (more than 100000 cycles). Despite these advantages, the relatively low energy/power ratio of SCs has restricted their wide industrial application [3, 5-8].

According to the mechanism of energy storage/release of SCs, they are classified into three categories i) electrochemical double-layer capacitors (EDLCs), ii) pseudo-capacitors, and iii) hybrid SCs defined as their combinations. In the (EDLCs) category, the energy is stored and released by adsorption/desorption of anions and cations at the electrode/electrolyte surface. Therefore, the capacitance is highly proportional to the surface area of the electrode. while in the pseudo-capacitors mechanism, the capacitance is created by the Fast reversible Faradaic reactions [9-12]. Accordingly, tuning the porosity structure for controlling the specific surface area along with creating composite and incorporating heteroatoms onto the surface of electrode materials are critical strategies to enhance the energy density of SCs. These approaches enhance energy storage by increasing the contributions of electric double-layer capacitance (EDLC) and pseudo-capacitance [13]. Among various electrode materials, transition metal-based components have gained significant attention due to their high theoretical capacitance and excellent electrochemical activity [14-17]. Copper (Cu)-based components, particularly Cu (II) complexes, have emerged as promising candidates for SC applications owing to their multiple oxidation states, which facilitate rapid charge transfer and redox reactions.

2. GGO/Cu synthesis

Guanidine (0.5 g), dicyclohexylcarbodiimide (0.25 g), and 4-dimethylaminopyridine (0.25 g) were added 10 ml acetonitrile solvent and stirred for one hour at room temperature to obtain a clear solution. After that, 0.5 g GO, which synthesized by the modified Hummer method, was dispersed in the 5 mL acetonitrile and the obtained suspension was poured into the former solution and naturally stirred overnight. Finally, the powder was rinsed with acetonitrile several times and dried for 24 h at 70°C. 0.25 g of obtained guanidine-functionalized GO (GGO) was dispersed in the mixture of absolute ethanol and distilled water (volume ratio of 1:1). After that, copper acetate (0.25 g) was dissolved in the mixture by magnetic stirrer for 24 h at room temperature. After washing the obtained precipitate with water, it was dried at 70°C for 24 h (GGO/Cu)

3. Result and discussion

The CV analysis was conducted within the potential range of 0 to 0.45 V at various scan rates of 0.006 - 0.01 V s-1 which is presented in Fig. 4a. In Fig.4b, the non-linear nature of the GCD curves can be attributed to the existence of a GGO (electric double-layer capacitance) and copper (pseudo-capacitor) in the GGO/Cu composite. The GGO/Cu electrode showed a high specific capacitance of 1224 F g^{-1} in the potential window of 0 to 0.45 V at the current density of 2 A g^{-1}.

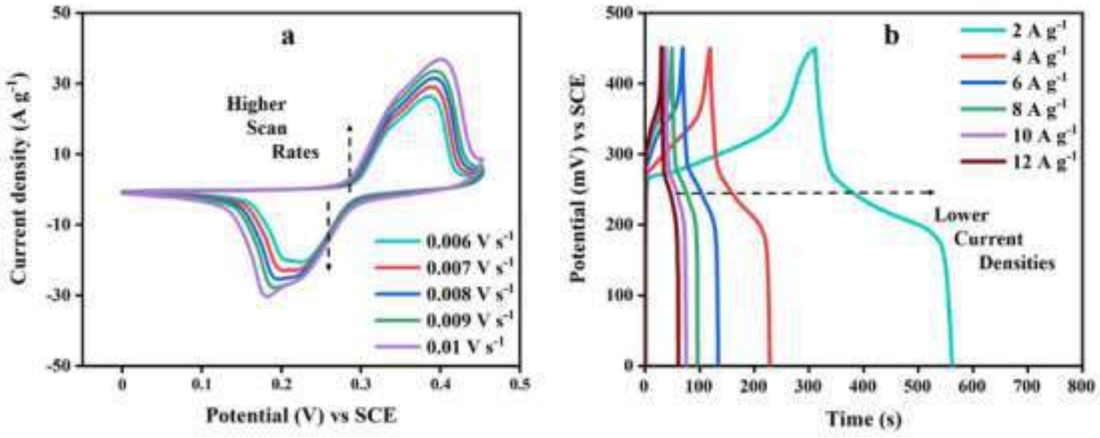

Fig. 1. (a) CV curve of GGO/Cu at various scan rates and (b) GCD curve of GGO/Cu at different current densities.

1. Yu, Z., et al., Graphene-supported Cu2O-CoO heterojunctions for high performance supercapacitors. Journal of Energy Storage, 2024. 77: p. 110009.

2. Feyie, E.K., et al., Electrodeposited Copper Tin Sulfide/Reduced Graphene Oxide Nanospikes for a High-Performance Supercapacitor Electrode. ACS omega, 2024. 9(8): p. 9452-9462.

3. Wang, Z., et al., One-step hydrothermal synthesis of Cu doped SnS2 quantum dots anchored on reduced graphene oxide (rGO) as high-performance electrodes for supercapacitors. Journal of Alloys and Compounds, 2024. 973: p. 172906.

The 30th Iranian Seminar of Organic Chemistry
February 7-9, 2025, Iran University of Science and Technology, Tehran, Iran

Sustainable Synthesis of Metal-Organic Framework Using Red Mud with application for organic pollutant removal

Mahdieh Chegeni[1*a], Mohanna Chegeni[1a]

[1a]Department of Chemistry, Faculty of Basic Sciences, Ayatollah Boroujerdi University, Boroujerd, Iran

Keyword: Metal-Organic Framework, Red Mud, Adsorbtion

This study presents the synthesis of a metal-organic framework (MOF) using trimesic acid (TCA) and red mud, an industrial waste by-product, for the adsorption of organic pollutants. The synthesis was carried out via a hydrothermal method, utilizing red mud as a sustainable metal precursor[1] and TCA as the organic linker. The structural and morphological properties of the synthesized MOF were characterized using Fourier-transform infrared spectroscopy (FTIR), scanning electron microscopy (SEM), X-ray diffraction (XRD), Brunauer–Emmett–Teller (BET) surface area analysis, Transmission Electron Microscopy (TEM), and Thermogravimetric analysis (TGA). The adsorption capacity of the MOF was evaluated for the removal of Methyl Orange (MO), from aqueous solutions (Scheme 1). Response Surface Methodology (RSM) was employed to optimize key experimental parameters, including MO concentration, contact time, MOF dosage, and pH.[2] A central composite design (CCD) was used to assess the interactive effects of these parameters and predict the optimal adsorption conditions. This study highlights the potential of using industrial waste and sustainable synthesis routes to develop effective adsorbents for environmental remediation.

Scheme 1: Adsorption of MO by TCA/Red mud MOF.

References:

1. W. Shi, H. Ren, X. Huang, M. Li, Y. Tang, F. Guo, Separation and Purification Technology 237 (2020) 116477.

2. S. Biswas, M. Bal, S.K. Behera, T.K. Sen, B.C. Meikap, Water 11(2) (2019) 325.

The 30th Iranian Seminar of Organic Chemistry
February 7-9, 2025, Iran University of Science and Technology, Tehran, Iran

وارنیش فلوراید

فاطمه عزیزی

چکیده

مهمترین و مؤثرترین راه برای پیشگیری از پوسیدگی دندان استفاده از ترکیبات فلوراید است. پوسیدگی دندان شایعترین بیماری مزمن دوران کودکی است. بسیاری از کودکان به‌دلیل وجود پوسیدگی دندانی فعال و کنترل نشده از سلامت دهانی و عمومی کافی برخوردار نیستند. تفاوت‌های فردی از قبیل شکل دندان‌ها، ظرفیت بافری بزاق و عادت‌های بهداشت دهان و دندان باعث ایجاد پوسیدگی با درجات متفاوت می‌شود .

واژه های کلیدی: فلوراید، پوسیدگی، بهداشت دهان و دندان، روش‌های پیشگیری

مقدمه

بهداشت دهان و دندان یکی از جنبه‌های سلامت است که با روش‌های جدید و صحیح آموزش می‌توان سلامت انسان‌ها و در نتیجه سلامت جامعه را فراهم نمود. در این راستا با شناخت بهتر از ساختار دندان و چگونگی عملکرد دندان می‌توان بسیاری از بیماری‌های دهان و دندان مانند پوسیدگی جلوگیری کرد.

شیمی فلوراید

فلوئور الکترونگاتیوترین عنصر در طبیعت و بسیار فعال است. معمولاً به‌صورت مولکولی F_2 مشاهده نمی‌شود بلکه به‌صورت نمک‌های فلور CaF_2 ، فلورایدآپاتیت یا Cryolite و $NaF\text{-}AlF_6$ می‌باشد. از نظرفیزیولوژیک، فلوراید منحصر به فرد است و مانند سایر هالوژنها رفتار نمی‌کند. این عنصر به تنهایی توسط اسکلت بدن جذب می‌شود و ید که توسط تیروئید جذب می‌شود. فلوئور در طبیعت بسیار گسترده است؛ در آب شیرین، آب دریا، سبزیجات، خون، شیر و ترکیبات آلی مشاهده می‌شود

فلوراید برای مهار یا حتی متوقف کردن پوسیدگی‌ها ثابت شده است. این ماده در سال ۱۹۱۶میلادی برای اولین بار توسط Blackمورد بررسی قرار گرفت و امروزه به صورت وسیعی از آن استفاده می‌شود.

پوسیدگی دندان

پوسیدگی دندان، یک بیماری میکروبیولوژیک عفونی است که منجر به فرسودگی و تخریب موضعی کلسیم از بافت‌ها می‌شود[۱]. عوامل مختلفی بر شروع و پیشرفت پوسیدگی دندان اثر دارد. برای ایجاد پوسیدگی نیاز به میزبان (دندان در محیط دهان)، محیط کشت غذایی(کربوهیدرات‌های قابل تخمیر، مواد قندی و نوشیدنی‌ها) و اسید حاصل از فعالیت میکروارگانیزم‌های کاریوژنیک است [۳،۲].

در فرایند پوسیدگی با از بین رفتن مواد معدنی در مینای دندان، حفره‌ی پوسیدگی ایجاد می‌شود. ازدست رفتن مواد معدنی وابسته به حضور پلاک (بیوفیلم[6]) و مواد قندی است که عامل اصلی بروز این بیماری می‌باشند. هنگامیکه سیر پیشرفت بیماری آرام باشد در ابتدا یک ضایعه‌ی اولیه تشکیل شده و اگر این ضایعات کنترل نشوند تخریب ساختار دندان اتفاق می‌افتد [٤] . پوسیدگی دندان در کودکان باعث درد و ناراحتی، عفونت استخوان فک، ایجاد رفتارهای منفی و عدم علاقه به حفظ و سلامت خوب دهان، نقص در عملکرد جویدن و زیبایی می‌شود [٥].

هنگامیکه دندان در معرض یک بستر مناسب (به‌طور معمول قند یا دسره‌ای شیرین) قرار می‌گیرد، باکتری‌های کاریوژنیک موجود در پلاک، اسید تولید می‌کنند؛ اگر این پروسه در یک زمان طولانی و کافی رخ دهد، ضایعه پوسیدگی گسترش می‌یابد. هرکدام از این عامل‌های عمده شامل تعدادی از عامل‌های ثانویه می‌باشد که می‌توان از آنها پیشگیری کرد. عدم پیشگیری باعث آسیب بیشتر دندان‌ها می‌شوند. ترکیب فلوراید وقتی داخل مینای دندان نفوذ می‌کند، مقاومت دندان را نسبت به پوسیدگی افزایش می‌دهد. از سوی دیگر کاهش در جریان بزاق به طور وسیعی ریسک پوسیدگی‌ها را بالا می‌برد [٦].

ارگانیسم‌های معلق آزاد به سرعت با جریان بزاق و بلع از دهان حذف می‌شوند. تنها تعداد کمی ازمیکروارگانیسم‌های اختصاصی که به‌طور عمده استرپتوکوک‌ها می‌باشند قادر به اتصال به سطوح دندانی هستند [۷]. استرپتوکک موتانس و استرپتوکک سوبرینوس باکتری‌های اصلی مسبب پوسیدگی در سطوح صاف و اکلوزال دندان‌ها می‌باشند؛ که با مسواک‌زدن دندان‌ها می‌توان پلاک دندانی را کنترل کرد و از بیماری پیشگیری نمود[۳].

فلوراید درمانی (فلوراید تراپی) برای ترمیم دندان‌ها

پزشکان در دندانپزشکی با استفاده از آب حاوی یک قسمت بر میلیون فلوراید، پوسیدگی دندان را کاهش می‌دهند. فلوراید درمانی با استفاده از خمیر دندان‌های حاوی فلوراید موجب تشکیل آپاتیت فلوراید در مینا و عاج دندان می‌شوند و انحلال پذیری آن را درمحیط اسیدی کاهش می‌دهند [۸]. یون‌های F^- در آب دهان و پلاسمای خون برای رشد طبیعی دندان و استخوان‌بندی

---

[6] Biofilm

مفید است[٩]. فلوراید آپ‌اتیت، برای ترمیم آسیب‌های دندانی و استخوانی، ساخت لایه خارجی دندان، بازسازی آرواره و غیره استفاده می‌شود. پیشنهاد شده است که مصرف حدود ١/ ٥ الی ٤ میلی‌گرم در روز می‌تواند خطر پوسیدگی دندان را کاهش دهد. فلوراید آپاتیت، لایه‌ی محافظ دندان (مینا) را تشکیل می‌دهد. تحقیقات فراوانی بر روی فلوراید آپاتیت انجام شده است؛ به این دلیل که فلوراید به پیشگیری از پوسیدگی دندان و پوکی استخوان مشهور می‌باشد.[١٠]. حضور مقادیرکمی یون فلوراید، رسوب کلسیم و فسفات را به میزان زیادی افزایش می‌دهد؛ مینای معدنی شده در اثر تشکیل فـلوراید آپاتیت در برابر اسید مقاوم‌تر ازهیدروکسی‌آپاتیت است و دندان را نسبت به حملات پوسیدگی ایمن‌تر می‌کند [١١]. در میان عناصر مختلف جانشین شده در ساختار هیدروکسی‌آپاتیت، فلوراید به شدت مورد توجه قرارگرفته است.

نتیجه گیری

شیوه‌های متعدد در کهن و امروزه به منظور پیشگیری و درمان پوسیدگی دندان شناخته شده است. همچنین محصولات متنوع با قابلیت ضد میکروبی وجود دارند. فلورایدتراپی به عنوان یکی از روش‌های پیشگیری همچنان رایج و در مدارس به‌کار می رود.

فلورایدتراپی برای دندان کودکان با ریسک بالای پوسیدگی، در فواصل ٣ تا ٦ ماهه استفاده می‌گردد و یک درمان موضعی در کودکان پیش دبستانی و کودکانی که نیاز به مراقبت‌های پزشکی خاص دارند، به‌کارگرفته می‌شود.

وارنیش فلوراید می‌تواند به تمام سطوح دندانی یا به‌طور انتخابی در نواحی با احتمال پوسیدگی بالاتر مانند نواحی دکلسیفیه (کمبود کلسیم)، شیار، فرورفتگی‌های عمیق و اطراف براکت‌های ارتودنسی به‌کاررود؛ در دندان‌های قدامی ماگزیلا در کودکان نیز استفاده می‌شود. وارنیش فلوراید به‌وسیله برس‌های یکبار مصرف نوک پنبه‌ای انجام می‌گیرد؛ لازم نیست قبل از مرخص کردن بیمار صبر کنیم تا وارنیش خشک شود چون وارنیش در تماس با مایعات دهانی سخت می‌شود. بعد از استفاده، دندان‌ها تا عصر آن روز یا روز بعد نباید مسواک زده شود تا در حداکثر تماس با دندان‌ها باقی بماند.

منابع

[1]Roberson T, Heymann HO, Swift Jr EJ. Sturdevant’s art and science of operative dentistry. Elsevier Health Sciences; n.d.

[2]Marinho VCC. Cochrane reviews of randomized trials of fluoride therapies for preventing dental caries. Eur Arch Paediatr Dent 2009, 10:183–91.

[3]Avery DR, McDonald RE. Dentistry for the Child and Adolescent. Mosby; 2004.

[4]Cury JA, Tenuta LMA. Enamel remineralization: controlling the caries disease or treating early caries lesions? Braz Oral Res 2009, 23:23–30.

[5]Koch G, Poulsen S, Espelid I, Haubek D. Pediatric dentistry: a clinical approach. John Wiley & Sons; 2017.

[6]Samaranayake LP. Microbiology of periodontal disease. Essent Microbiol Dent 3rd Ed Elsevier, Philadelphia, PA 2006:267–74.

[7]Zero DT, Fontana M, Martínez-Mier EA, Ferreira-Zandoná A, Ando M, González-Cabezas C, et al. The biology, prevention, diagnosis and treatment of dental caries: scientific advances in the United States. J Am Dent Assoc 2009, 140:25S-34S.

[8] Moreno EC, Kresak M, Zahradnik RT. Fluoridated hydroxyapatite solubility and caries formation. Nature 1974, 247:64–5.

[9] Alghamdi HS, AJA van Oirschot B, Bosco R, van den Beucken JJJP, Aldosari AAF, Anil S, et al, Biological response to titanium implants coated with nanocrystals calcium phosphate or type 1 collagen in a dog model. Clin Oral Implants Res 2013, 24, 475–83.

[10] Qu W-J, Zhong D-B, Wu P-F, Wang J-F, Han B. Sodium fluoride modulates caprine osteoblast proliferation and differentiation. J Bone Miner Metab 2008, 26:328–34.

[11] Fontana M, Zero DT. Assessing patients' caries risk. J Am Dent Assoc 2006, 137, 1231–9.

The 30th Iranian Seminar of Organic Chemistry
February 7-9, 2025, Iran University of Science and Technology, Tehran, Iran

Dopamine Neurotransmitter Determination Using a Graphite Sheet–Graphene Nanosensor

Mohammad Hossein Khajehpour (representing author), Ali Ghaffarinejad* (corresponding author)

Iran University of Science and Technology

Keyword: Dopamine sensor, Dopamine neurotransmitter, Graphene sensor, Electrochemical sensor, Neurotransmitter

Abstract

Measuring the amount of dopamine is very important for the diagnosis and prevention of many neurological and mental diseases like depression, Parkinson's, Huntington's, attention deficit hyperactivity disorder, Tourette's syndrome, etc. One of the best ways to measure dopamine is through electrochemical sensors. In this study, graphene oxide was electrochemically deposited and reduced on a graphite sheet. The electrode surface morphology was studied via scanning electron microscopy (SEM). The performance of the modified electrode in the detection of dopamine was investigated. The results show that the addition of reduced graphene oxide (rGO) on the electrode surface increases the dopamine oxidation current, decreases the overpotential, and reduces the charge transfer resistance. The efficiency of dopamine detection using this modified electrode was evaluated via cyclic voltammetry (CV), differential pulse voltammetry (DPV), and electrochemical impedance spectroscopy (EIS). The influence of the electrolyte pH, potential scan rate, electrode reproducibility, and selectivity was investigated. Also, for the stability test, the chronoamperometry (CA) technique was used and the results showed that the electrode has a good stability. The detection limit of this electrode was 68 nM and the linear range was 10^{-7} to 10^{-4} M. For real sample analysis, determination was achieved successfully in a dopamine ampoule. The preparation of this modified electrode is easy, fast and very cheap.

References: [1] Khajehpour, M.H., Ghaffarinejad, A. Dopamine neurotransmitter determination using graphite sheet–graphene nano-sensor. *Graphene and 2D mater* **9**, 125–135 (2024). https://doi.org/10.1007/s41127-024-00075-9

The 30th Iranian Seminar of Organic Chemistry
February 7-9, 2025, Iran University of Science and Technology, Tehran, Iran

One-pot and efficient procedure for the syntheis of new propellanes by reaction of acenaphthoquinone, malononitrile and 2-nitroethenamines

S. Mohammad Amin Razavi, Mohammad Reza Mohammadizadeh*

Department of Chemistry, Faculty of Bio- and Nano-Science and Technology, Persian Gulf University, Bushehr 75169, Iran; mrmohamadizadeh@pgu.ac.ir

Keyword: Acenaphthoquinone, Malononitrile, 2-Nitroethenamines, Propellanes

Propellanes are tricyclics compounds which one of their carbon-carbon single bonds are in common with their three-ring structure and can be find in naturally and non-naturally occurring products. [1-2] *Propellanes and their derivatives have attractive properties due to their unique structure so that* they have wide range of applications in biological, medicinal and organic chemistry. [3]

In continuous of our previous researches on the chemistry of acenaphthoquinone and 2-nitroethenamines [4], we wish to report here the results of our studies on the reaction of malonated acenaphthoquinone with 2-nitroethenamines. We found when 2-nitroetheneamines (**3**) were added to a mixture of acenaphthoquinone (**1**) and malononitrile (**2**) in ethanol under reflux conditions, propellane derivatives (**4**) synthesized in good to excellent yields (Scheme). The products (**4**) were characterized using their spectroscopic data. As a result of our efforts, we developed a new one-pot method for synthesis of some new propellanes having furane and pyrrole moieties.

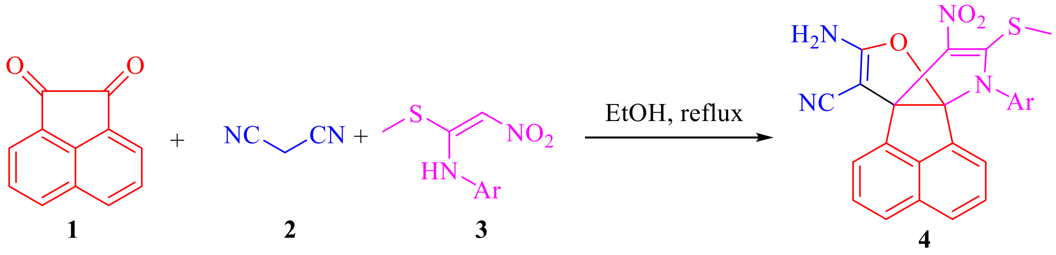

Scheme: One-pot synthesis of some new propellane derivatives

References:

[1] Zhang, L. J.; Yan, C. G. *Tetrahedron* **2013**, *69*, 4915.

[2] Kheilkordi, Z.; Ziarani, G. M. Badiei, A. *Polyhedron* **2020**, *178*, 114343.

[3] Beyrati, M.; Hasaninejad, A. *RSC advances* **2018**, *8*, 14171.

[4] Mousavi, S. H.; Mohammadizadeh, M. R.; Arimitsu, A.; Saberi, D.; Poorsadeghi, S.; Genta, K. *RSC Adv*. **2020**, *10*, 20552

The 30th Iranian Seminar of Organic Chemistry
February 7-9, 2025, Iran University of Science and Technology, Tehran, Iran

$Zr(HSO_4)_4$: Green Efficient, Recoverable and Reusable Catalyst for One-Pot Synthesis of 1,8-Dioxooctahydroxanthene Under Solvent-Free Conditions

Authors: Khalil Pourshamsian

Affiliations: Department of Chemistry, Tonekabon Branch, Islamic Azad University, Tonekabon, Iran

Keyword: Green chemistry, 1,8- dioxooctahydroxanthenes, $Zr(HSO_4)_4$, solid Brønsted acid.

Abstract

A green and highly efficient procedure for the one-pot synthesis of 1,8-dioxooctahydroxanthenes has been developed *via* cyclocondensation of arylaldehydes with excess dimedone using $Zr(HSO_4)_4$ as a recoverable and reusable heterogeneous catalyst under solvent-free conditions. The present method offers several advantages such as green, highly efficient, recoverable, reusable, simple work-up and simple purification of products.

Introduction

In recent years, synthetic chemists have shown tremendous interested in developing highly efficient transformation for the synthesis of xanthene derivatives due to their potential applications in the biological activities pharmaceutical and industrial applications. They are cited as active oxygen heterocycles possessing antibacterial. For example, they possess a large array of biological and therapeutic properties like anti-inflammatory [1], antiviral [2], antibacterial [3], as well as in photodynamic therapy [4] and as antagonists of the paralyzing action of zoxazolamine [5]. Xanthenes are also available from natural sources [6]. Besides some of them are served as Leuco-dyes [7], intracellular pH indicators and as fluorescent materials [8]. Many procedures are disclosed to synthesize xanthenes and benzoxanthenes like cyclodehydrations [9], trapping of benzynes by phenols [10], cyclocondensation between 2-hydroxy aromatic aldehydes and 2-tetralone [11]. Many syntheses of xanthene derivatives have been published; one of them is the condensation of aldehydes with cyclohexane-1,3-dione or 5,5-dimethylcyclohexane-1,3-dione to give 1,8-dioxooctahydroxanthene derivatives. This reaction has been conducted in the presence of strong protonic acids [12], Etidronic acid/MW [13], Lewis acids such as $InCl_3.4H_2O$ [14], $FeCl_3.6H_2O$ [15] and heterogeneous catalysts like Dowex-50W [16], $NaHSO_4.SiO_2$ [17], Ambertyst-15 [18], HBF_4/SiO_2 [19] and Sulfonic acid-functionalized LUS-1 [20]. Other catalysts such as Alum-promoted [21], Potash alum [22], boric acid [23], $ZrOCl_2.8H_2O$ [24], nano-Fe_3O_4 [25], $B(HSO_4)_3$ [26], TiO_2 [27], nano-TiO_2 [28], $BiVO_4$-NPs [29] and $InCl_3$ [30].

However, some of these methodologies have not been entirely satisfactory, with disadvantages such as low yields, prolonged reaction times, harsh reaction conditions and the requirement of expensive catalysis and use of toxic organic solvent. Therefore, to avoid these limitations, and to develop an alternate route for the synthesis of xanthene derivatives in improved yield, short reaction time, green approach and safe reaction conditions, using $Zr(HSO_4)_4$ as catalyst, has been attention. $Zr(HSO_4)_4$ is a low-coast solid Brønsted acid. There are no examples of the use of $Zr(HSO_4)_4$ for the synthesis of 1,8-dioxooctahydroxanthene derivatives. In this research we employed $Zr(HSO_4)_4$ as efficient, recoverable and reusable catalyst for synthesis of 1,8-dioxooctahydroxanthene derivatives *via* traditional route from cyclocondensation of dimedone and aromatic aldehydes in solvent-free conditions (Scheme 1).

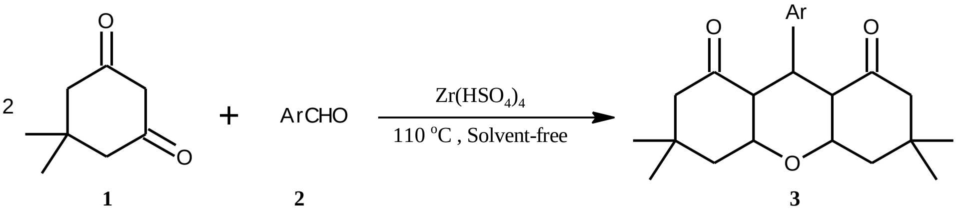

Scheme 1: synthesis of 1,8-dioxooctahydroxanthenes

EXPRIMENTAL

All the reagents experimental and aromatic aldehydes were purchased from Merck and used without further purification. Melting points were determined in open glass capillaries on an Electrothermal 9100s apparatus and are uncorrected.

The IR spectra were recorded with FT-IR Shimadzu IR-470 instrument using potassium bromide pellets. The ^{1}H-NMR spectra were determined on a Bruker Advance DRX-400 MHz instrument using TMS as the internal standard and $CDCl_3$ as solvent. Chemical shifts are expressed as δ(ppm) and the coupling constant as $J(H_2)$. The progress of reaction was monitored by TLC using 0.2 mm Merck silicagel GF254 pre-coated plates and visualized by UV-light (254 nm).

***General procedure for the preparation of 1,8-dioxooctahydroxanthene* (3a-j):** To a mixture of dimedone **1** (2 mmol) and aldehyde **2** (1 mmol) was added $Zr(HSO_4)_4$ which prepared as reported [ ] (20 mol%) and the mixture was allowed to stir at 110 °C for the total recorded time which indicated in Table 1. The progress of reactions was monitored by TLC (eluent: EtOAc/ Diethylether, 1:4). After completion of the reaction, the reaction mixture was cooled to room temperature. Then to mixture was added water and the product was extracted with ethyl acetate (3 × 5 mL). The organic layer was dried ($MgSO_4$) and evaporated in vacuum. The crude product recrystallized by EtOH 96% and purified. All the desired products were characterized by comparison of their physical data with those reported compounds. For the total confirmed of synthetic compounds, the spectral data given below. Selected spectral data for some products.

3,3,6,6-tetramethyl-9-phenyl-1,8-dioxooctahydroxanthene **(3a):** White powder, Yield (86%), mp 201-202 °C. FT-IR (ῡ, Cm^{-1}) (KBr disc): 3040 (CH$_{arom}$, Str.); 2990 (CH$_{aliph}$, Str.); 1605 (C=O Str.); 1540 (C=C Str.); 1360 (C-O Str.). ^{1}H NMR (400 MHz, $CDCl_3$) δ(ppm): 1.12 (6H, s, $2CH_3$); 1.26 (6H, s, $2CH_3$); 2.30-2.50 (8H, m, $4CH_2$); 5.58 (1H, s, CH); 7.11-7.13 (2H, d, CHO, ^3J = 6.8 Hz); 7.17-7.21 (1H, t, H$_p$, ^3J = 7.8 Hz); 7.27-7.31 (2H, dd, H$_m$, ^3J = 7.8 Hz , ^3J = 6.8 Hz).

3,3,6,6-tetramethyl-9-(4-methylphenyl)-1,8-dioxooctahydroxanthene **(3b):** White powder, Yield (81%), mp 173-175 °C. FT-IR (ῡ, Cm^{-1}) (KBr disc): 3080 (CH$_{arom}$, Str.); 2950 (CH$_{aliph}$, Str.); 1670 (C=O Str.); 1540 (C=C Str.); 1380 (C-O Str.). ^{1}H NMR (400 MHz, $CDCl_3$) δ(ppm): 1.01 (6H, s, CH_3); 1.11 (6H, s, CH_3); 2.15 (4H, dd, CH_2); 2.26 (3H, s, CH_3); 2.47 (4H, s, CH_2); 4.8 (1H, s); 7.02 (2H, d, CH$_{arom}$, ^3J = 8.2 Hz); 7.19 (2H, d, CH$_{arom}$, ^3J = 8.2 Hz).

3,3,6,6-tetramethyl-9-(4-methoxyphenyl)-1,8-dioxooctahydroxanthene **(3c):** Gray powder, Yield (82%), mp 238-239 °C. FT-IR (ῡ, Cm^{-1}) (KBr disc): 3080 (CH$_{arom}$, Str.); 3000 (CH$_{aliph}$, Str.); 1685 (C=O Str.); 1530 (C=C Str.); 1380 (C-O Str.). ^{1}H NMR (400 MHz, $CDCl_3$) δ(ppm): 1.01 (6H, s, CH_3); 1.11 (6H, s, CH_3); 2.22 (4H, dd, CH_2); 2.47 (4H, s, CH_2); 2.47 (1H, s, CH); 3.74 (3H, s, OCH_3); 6.7 (2H, d, CH$_{arom}$, ^3J = 8.4 Hz); 7.21 (2H, d, CH$_{arom}$, ^3J = 8.4 Hz).

3,3,6,6-tetramethyl-9-(3-methoxyphenyl)-1,8-dioxooctahydroxanthene **(3d):** White powder, Yield (92%), mp 159-160 °C. FT-IR (ῡ, Cm^{-1}) (KBr disc): 3100 (CH$_{arom}$, Str.); 3000 (CH$_{aliph}$, Str.); 1580 (C=O Str.); 1520 (C=C Str.); 1370 (C-O Str.). ^{1}H NMR (400 MHz, $CDCl_3$) δ(ppm): 1.12 (6H, s, CH_3); 1.25 (6H, s, CH_3); 2.30-2.48 (8H, m, CH_2); 3.75 (3H, s, OCH_3); 5.53 (1H, s, CH); 6.68-7.22 (4H, m, CH$_{arom}$).

Results and Discussion

In this research, the condensation of dimedones and various aldehydes in the presence of heterogeneous solid Brønsted acid catalyst of $Zr(HSO_4)_4$ for the synthesis of 1,8-dioxooctahydroxanthene derivatives has been studied (Scheme 1).

Table-1

Synthesis of 1,8-dioxooctahydroxanthene derivatives in the presence of $Zr(HSO_4)_4$

Entry	**R**	**Product**	**Time (min)**	**Yield^a (%)**
1	C_6H_5	3a	40	86
2	*p*-$CH_3C_6H_4$	3b	50	81
3	*p*- $CH_3OC_6H_4$	3c	55	82
4	*m*- $CH_3OC_6H_4$	3d	35	92
5	*p*-Cl C_6H_4	3e	40	88

6	*p*-NO_2 C_6H_4	3f	35	94
7	*p*-OHC_6H_4	3g	60	80
8	2-Cl-4-Cl-C_6H_4	3h	30	95
9	*p*-$(Me)_2N$ C_6H_4	3i	60	72
10	*m*-Cl C_6H_4	3j	40	88

a. Reaction condition: dimedone (2 mmol), aldehyde (1 mmol) and Zirconium persulfate (20 mol%) as catalyst

In order to optimize the reaction parameters, we investigated the catalytic activity of $Zr(HSO_4)_4$ in the synthesis of 1,8-dioxooctahydroxanthene derivatives under different reaction conditions. We examined the above reaction in several catalytic amounts and solvents using the condensation reaction of benzaldehyde and dimedone as a model reaction.

The results indicate that different solvents affected the efficiency of the reaction. As shown in table 2, among the tested solvents such as water, THF, $CHCl_3$, CH_3CN, CH_3CH_2OH and a solvent-free system, the best result was obtained after 40 min under solvent-free conditions in good yield (86%). When the same reaction was performed in the absence of the catalyst, the corresponding product was obtained in trace (<10%). Whereas, $Zr(HSO_4)_4$ in excess of 20 mol% did not improve the yield to a greater extent (Table 2, Entry 8).

The catalytic activity of the recycled $Zr(HSO_4)_4$ was also examined. $Zr(HSO_4)_4$ could be reused six times for the reaction without notable loss of activity (Table 2, Entry 7)(Figure 1).

Table-2

Screening of the catalyst and solvent for the reaction of benzaldehydes and dimedone catalyzed by $Zr(HSO_4)_4$ [a]

Entry	**Catalyst (mol%)**	**Solvent/condition**	**Time (min)**	**Yield[b] (%)**
1	20	water/reflux	120	trace
2	20	THF/reflux	120	trace
3	20	$CHCl_3$/reflux	120	20
4	20	CH_3CN/reflux	120	15
5	20	CH_3CH_2OH/reflux	100	55
6	10	solvent-free	100	68
7[c]	20	solvent-free	40	86, 85, 84,84,84,83
8	30	solvent-free	40	75

a. Reaction condition: dimedone (2 mmol), aldehyde (1 mmol) and Zirconium persulfate as catalyst

b. Isolated yield

c. Catalyst was reused six times

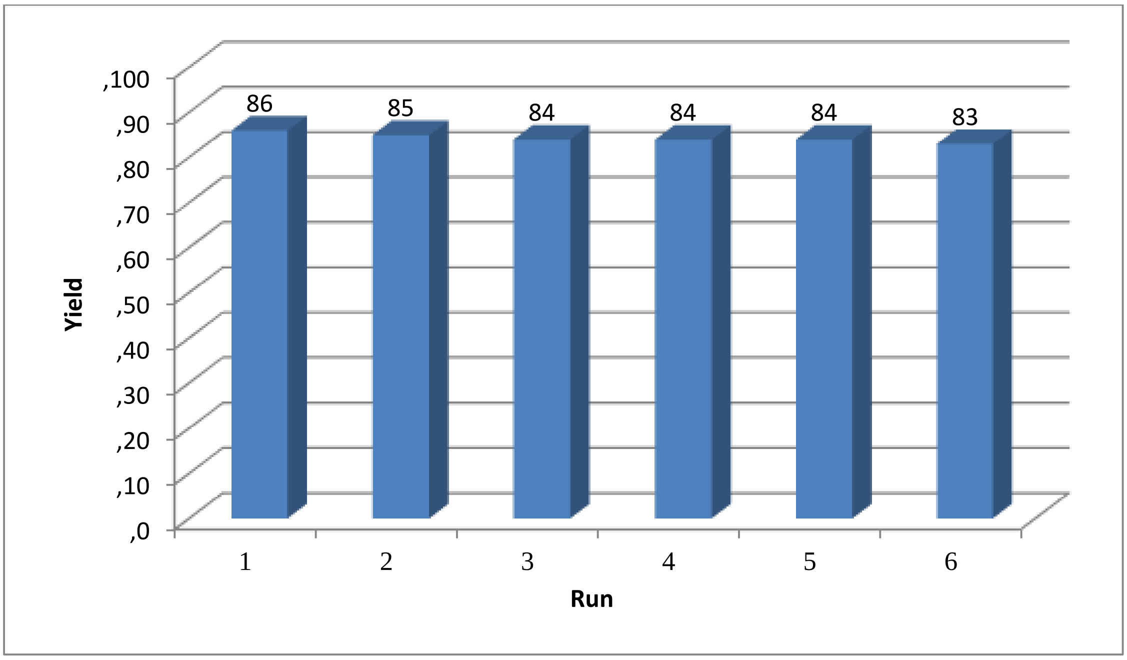

Fig 1. The reusability of $Zr(HSO_4)_4$ for the preparation of 3,3,6,6-tetramethyl-9-phenyl-1,8-dioxoocta hydroxanthene (3a)

The proposed mechanism is showed in Scheme 2. Initially SO_3H groups, as acid sites, are active in protonating the carbonyl group of aldehydes. This intermediate is attacked by dimedone to from knoevenagol products. In the next step, each of these intermediates is converted to the desired product via Micheal type additions and cyclization with the removal of a molecule of water.

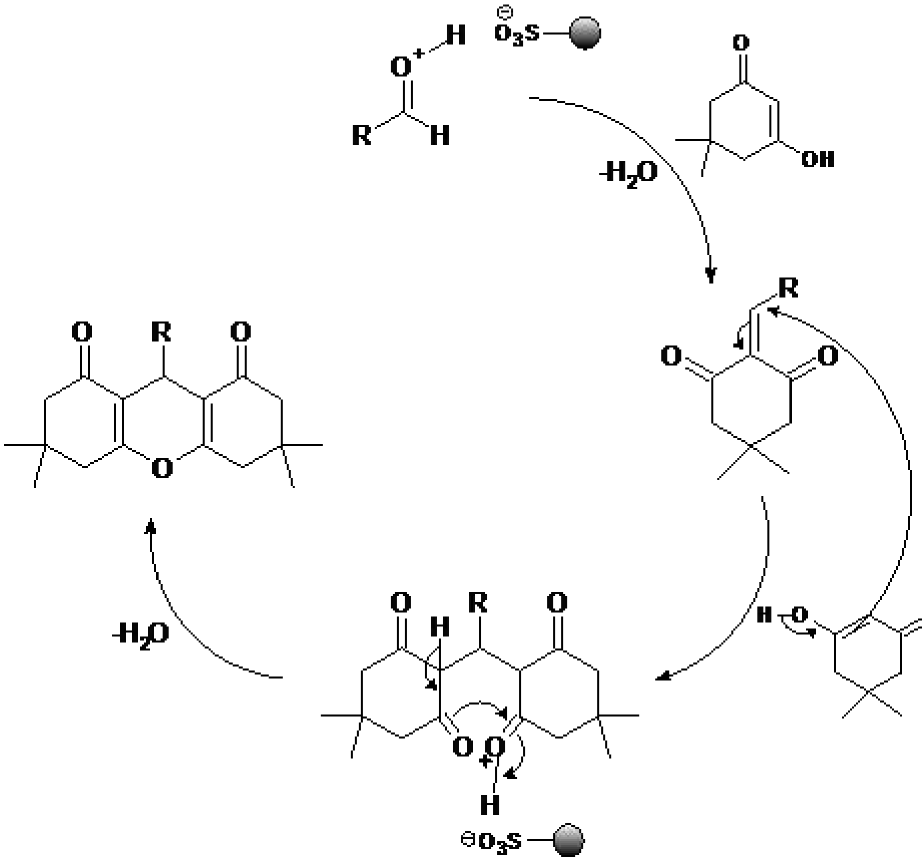

Scheme 2: Proposed mechanism for the synthesis of 1,8-dioxooctahydroxanthene in the presence of $Zr(HSO_4)_4$ as catalyst

All the products were characterized by ^{1}H NMR and IR spectra and compared with authentic samples.

Conclusion

In summary, we have developed a green efficient, recoverable and reusable protocol for the one pot synthesis of various 1,8-dioxooctahydroxanthenes employing $Zr(HSO_4)_4$ as catalyst. Some advantages of this protocol include a simple reaction set-up, high products yields and elimination of toxic solvents.

ACKNOWLEDGEMENTS

The author gratefully acknowledges the financial support from council of research and technology of Islamic Azad University. Tonekabon branch.

References:

[1] J. P. Poupelin, G. Saint-Rut, O. Foussard-Blanpin, G. Narcisse, G. Uchida-Ernouf, and R. Lacroix, *Eur. J. Med. Chem.*, **13**, 67 (1978).

[2] T. Hideo, JPn, Tokyo Koho, *Chem. Abstr*., **95**, 80922b (1981).

[3] R. W. Lambert, J. A. Martin, J. H. Merrett, , K. E. B. Parkesand, G.J. Thomas, *PCT Int. Appl*., Wo9706178, 1971: *Chem Abstr*., **126**, 212377y (1997).

[4] R.M. Ion, *Progr. Catal*., **2**, 55 (1997).

[5] G. Saint-Ruf, A. De, H. T. Hieu, *Bull. Chem. Ther*., **7**, 83 (1972).

[6] B. Ravindranath, and T.R. Seshadri, *Phytochemistry*., **12**, 2781(1973).

[7] A. Barner Jee, A.K. Mukherjee, *Stain Technol*., **56**, 83 (1981).

[8] C. G. Knight, T. Stephens, *Biochem. J.,* **258**, 683 (1989).

[9] A. Bekaert, J. Andrieux, M. Plat, *Tetra Lett*., **33**, 2805 (1992).

[10] D.W. Knight, P.B. Little, *Synlett.*, **10**, 1141 (1998).

[11] A. Jha, J. Beal, *Tetra Lett.*, **45**, 8999 (2004).

[12] F. Darviche, S. Balalaie, E. Chadegani, and P. Salehi, *Synth Commun*., **37**, 1059 (2007).

[13] P. V. Shitre, R. R. Harale, B. R. Sathe, M. S. Shingare, *Chemistry & Biology Interface.*, **6**, 137 (2016).

[14] X. Fan, X. Hu, X. Zhang, and J. Wang, *Can. J. Chem.*, **83**, 16 (2005).

[15] X-S. Fan, Y-Z. Li, X-Y. Zhang, X-Y. Hu, and J-J. Wang, *Chin. J. Org. Chem.*, **25**, 1482 (2005).

[16] G. I. Shakibaei, P. Mirzaei, and A. Bazgir, *Appl. Catal. A: Gen.*, **325**, 188 (2007).

[17] B. Das, P. Thirupathi, K.R. Reddy, B. Ravikath, and L. Nagarapu, *Catal. Commun.*, **8**, 535 (2007).

[18] B. Das, P. Thirupathi, I. Mahender, V.S. Reddy, and Y.K. Rao, *J. Mol. Catal. A: Chem.*, **247**, 233 (2006).

[19] Z.-H. Zhang, and X.-Y. Tao, *Aust. J. Chem.*, **61**, 77 (2008).

[20] M. Rahimifard, G. Mohammadi Ziarani, A. Badiei, S. Asadi, A. Abdolhasani Soorki, *Res. Chem. Inter.*, **42**, 3847 (2016).

[21] B. R. Madji, M. B. Ubale, J. V. Bharad, and M. S. Shingare, *S. Afr. J. Chem.*, **63**, 36 (2010).

[22] R. S. Aakruti, G. Meryl Maria, P. Iniyavan, A. Sreekath, V. Vijayakumar, *Int. J. ChemTech. Res.*, **6**, 3979 (2014).

[23] S. Rezayati, R. Hajinasiri, Z. Erfani, S. Rezayati, S. Afshari-Sharifabad, *Iran. H. Catal.*, **4**, 157 (2014).

[24] B. Massouri, M. Ahmadynezhad, M. R. Poor Heravi, *Lett. Org. Chem.*, **10**, 302 (2013).

[25] F. Nemati, S. Sabaqian, *J. Saudi. Chem. Soc.*, 2013, Available Online.

[26] H. Moghanian, A. Mobinikhaledi, and M. Deinavizadeh, *Res. Chem. Intermed.*, **10**, 1007 (2014).

[27] S. Kumari, A. Shekhar, and D. Pathak, *Chem. Sci. Trans.*, **3**, 652 (2014).

[28] S. Rahmani, A. Amoozadeh, *JNS.*, **4**, 91 (2014).

[29] A. Shoja, F. Shirini, M. Abedini, and M.A. Zanjanchi, *J. Nanostruct. Chem.*, **4**, 110 (2014).

[30] B. Karami, S. Nejati, K. Eskandari, *Cur. Chem. Lett.*, **4**, 169 (2015).

The 30th Iranian Seminar of Organic Chemistry

February 7-9, 2025, Iran University of Science and Technology, Tehran, Iran

Subject: Organic Chemistry

مهرداد برون

Abstract

Organic chemistry is part of the science of chemistry that studies hydrocarbons. For this reason, it is also called the chemistry of carbon compounds.

The suffix "organic" is reminiscent of the days when chemicals were divided into mineral and organic, depending on what source they came from. Minerals were those extracted from mines, and organic matter was those obtained from plant or animal sources, that is, materials produced by living organisms. In fact, until about 1850, many chemists believed that the origin of organic matter must be living organisms, and therefore these substances could never be synthesized from minerals.

Even after it became clear that these materials did not necessarily have to be obtained from living sources and could be synthesized in the laboratory, it was still appropriate to preserve the organic name for describing them and similar materials. This division between minerals and organic matter has been maintained to this day. In this article, we will examine this issue

key words

Isomerics, organic compounds, inorganic compounds, chemistry, organic chemistry, chemicals

مقدمه:

شیمی آلی بخشی از دانش شیمی است که به بررسی هیدروکربن‌ها می‌پردازد. به همین دلیل به آن شیمی ترکیبات کربن نیز گفته می‌شود.

پسوند «آلی» یادگار روزهایی است که مواد شیمیایی را بسته به این که از چه منبعی به دست می‌آمدند، به دو دسته معدنی و آلی تقسیم می‌کردند. مواد معدنی آنهایی بودند که از معادن استخراج می‌شدند و مواد آلی آنهایی که از منابع گیاهی یا حیوانی یعنی از موادی که توسط موجودات زنده تولید می‌شدند، به دست می‌آمدند. در واقع تا پیرامون سال ۱۸۵۰ بسیاری از شیمیدانان معتقد بودند که خاستگاه مواد آلی باید موجودات زنده باشند و در نتیجه این مواد را هرگز نمی‌توان از مواد معدنی سنتز نمود.

حتی پس از آن که مشخص شد این مواد لزوماً نبایستی از منابع زنده به دست آیند و می‌توان آنها را در آزمایشگاه سنتز کرد، باز هم مناسبت داشت تا نام آلی برای توصیف آنها و موادی همانند آنها حفظ شود. این تقسیم‌بندی بین مواد معدنی و آلی تا به امروز حفظ شده است.[۷]

شيمي آلي

مواد شیمیایی:[۸]

ماده ، به هر چیزی که حجمی را اشغال کند و جرمی داشته باشد، اطلاق می‌شود. مواد شیمیایی به موادی اطلاق می‌گردد که معمولا از طریق سنتز شیمیایی تهیه می‌شوند و یا اینکه منشأ طبیعی داشته و مواد اولیه تهیه سایر مواد شیمیایی به حساب می‌آیند.

طبقه بندی مواد شیمیایی:[۹]

مواد شیمیایی بطور عمده به دو گروه بزرگ مواد معدنی و مواد آلی تقسیم بندی می‌شوند. هر یک از این دو گروه ، در دو مبحث شیمی آلی و شیمی معدنی بررسی می‌شوند. در این مطالعه ، خواص فیزیکی و شیمیایی مواد آلی و معدنی ، منابع ، طریقه سنتز و ... مورد بررسی قرار می‌گیرند.

۱. مواد شیمیایی معدنی:[۱۰]

اگر شیمی آلی به عنوان شیمی ترکیبات کربن ، عمدتا آنهایی که شامل هیدروژن یا هالوژنها به علاوه عناصر دیگر هستند، تعریف شود، شیمی معدنی را می‌توان بطور کلی به عنوان شیمی عناصر دیگر در نظر گرفت که شامل همه عناصر باقیمانده در جدول تناوبی و همینطور کربن ، که نقش عمده‌ای در بیشتر ترکیبات معدنی دارد، می‌گردد.

شیمی آلی ـ فلزی ، زمینه وسیعی که با سرعت زیاد رشد می‌کند، به علت اینکه ترکیبات شامل پیوندهای مستقیم فلز - کربن را بررسی می‌کند دو شاخه را بهم مرتبط می‌سازد. همانطوری که می‌توان حدس زد، قلمرو شیمی معدنی با فراهم کردن زمینه‌های تحقیقی اساسا نامحدود ، بسیار گسترده است.

۲. مواد شیمیایی آلی:[۱۱]

در قدیم ، ماده آلی به ماده‌ای اطلاق می‌گردید که بوسیله بدن موجودات زنده ساخته می‌شد. تا اینکه در سال ۱۸۲۸ ، "وهلر"[۱۲] دانشمند آلمانی ، برای اولین بار جسمی به نام اوره[۱۳]را در آزمایشگاه از یک ترکیب معدنی به نام ایزوسیانات تهیه نمود و از آن پس معلوم شد که می‌توان مواد آلی را نیز در آزمایشگاه ساخت. امروزه بیش از یک میلیون نوع ماده آلی شناخته شده است که بسیاری از آنها را در آزمایشگاهها تهیه می‌کنند. مواد آلی ، به مواد غیر معدنی گفته می‌شود و با مواد معدنی تفاوتهای کلی در چند مورد دارند.

مقایسه مواد آلی و مواد معدنی:[۱۴]

مواد شیمیایی آلی و معدنی با همدیگر تفاوتهای کلی دارند که عبارتند از:

- در تمام مواد آلی حتما کربن وجود دارد، در صورتی که مواد معدنی بدون کربن بسیارند. ضمنا در ترکیبات آلی ، اتمهای کربن می‌توانند با یکدیگر ترکیب شوند و زنجیرهای طویل تشکیل دهند، در حالی‌که این خاصیت در عناصر دیگر خیلی کمتر دیده می‌شود.

---

[۷] http://fa.wikipedia.org

[۸] http://www.tebyan.ir

[۹] http://www.arsachem.persianblog.com

[۱۰] http://www2.dw-world.de

[۱۱] http://www.tebyan.ir

[۱۲] Wohler

[۱۳] $CO_2(NH)_2$

[۱۴] http://chem-2r1.blogfa.com

- مقاومت مواد آلی در برابر حرارت از مواد معدنی کمتر است.
- اغلب واکنش‌های میان مواد آلی کند و دو جانبه یا تعادلی هستند، در صورتی‌که اغلب واکنش‌های معدنی تند می‌باشند.
- در ترکیبات آلی ، ممکن است ۲ یا چند جسم مختلف با فرمولهای ساختمانی مختلف ، دارای یک فرمول مولکولی باشند که در این صورت به آنهاایزومر یا همفرمول گفته می‌شود. مثلا الکل معمولی[15] با جسمی به نام اتر اکسید متیل[16] همفرمول یا ایزومر است. زیرا هر دو دارای فرمول بسته یا مولکولی[17] هستند، در صورتی که پدیده ایزومری در ترکیبات معدنی وجود ندارد.

اهميت شيمي آلي:[18]

شیمی آلی اهمیت فوق‌العاده زیادی در تکنولوژی دارد و در واقع، شیمی رنگدانه‌ها و داروها، کاغذ و جوهر، رنگهای نقاشی و پلاستیکها، بنزین و تایرهای لاستیکی است؛ همچنین، شیمی غذایی است که می‌خوریم و لباسی است که می‌پوشیم.

شیمی آلی شالوده زیست‌شناسی و پزشکی است. ساختمان موجودات زنده، به غیر از آب، عمدتاً از مواد آلی ساخته شده‌اند؛ مولکولهای مورد بحث در زیست‌شناسی مولکولی همان مولکولهای آلی هستند. زیست‌شناسی در مقیاس مولکولی همان شیمی آلی است.

شاید دور از انتظار نباشد که بگوئیم ما در عصر کربن زندگی می‌کنیم. هر روزه، روزنامه‌ها ذهن ما را متوجه ترکیبات کربن نظیر کلسترول و چربیهای اشباع نشده، هورمونها و استروئیدها، حشره‌کشها و فرومونها، عوامل سرطان زا و شیمی درمانی، دي اِن اِي[19] ژنها می‌نمایند. به خاطر نفت، جنگها به راه افتاده است.

منابع بزرگ مواد آلي:[20]

دو منبع بزرگ مواد آلی که از آنها مواد آلی ساده تأمین می‌شوند، نفت و ذغال سنگ است. (هر دو اینها از مفهوم قدیمی «آلی» بوده و فراورده تجزیه (کافت) گیاهان و جانوران هستند). این ترکیبات ساده به عنوان مصالح ساختمانی در ساختن ترکیبات بزرگـتر و پیچیده‌تر مصرف می‌شوند.

نفت و زغال سنگ سوختهای فسیلی هستند که در طی هزاران سال بر روی هم انباشته شده وغیر قابل جایگزینی هستند. این مواد، بویژه نفت، جهت رفع نیازهای انرژی که به طور دائم در حال افزایش است، با سرعت خطرناکی مصرف می‌گردند. امروزه کمتر از ۱۰٪ نفت برای ساختن مواد شیمیائی مصرف می‌شود و قسمت اعظم آن برای تولید انرژی سوزانده می‌شود. خوشبختانه منابع دیگری برای ایجاد نیرو از قبیل منبع خورشیدی، گرمای زمین، باد، امواج، جزر و مد و انرژی هسته‌ای وجود دارد.

اما چگونه می‌توان منبع دیگری به جای مواد آلی پیدا نمود؟ البته در نهایت باید به جایی که سوختهای سنگواره‌ای از آنجا ناشی می‌شوند یعنی توده زیستی برگشت، اما این بار به طور مستقیم و بدون دخالت هزاران سال. توده زیستی قابل تجدید است و چنانچه به طور مناسب مصرف شود، تا زمانی که ما بر روی این سیاره بتوانیم وجود داشته باشیم آن هم باقی می‌ماند. در ضمن می‌گویند که نفت با ارزش‌تر از آن است که سوزانده شود.

تقسیم بندی مواد شیمیایی آلی:[21]

عناصر تشکیل دهنده ترکیبات شیمیایی آلی به ترتیب فراوانی مطابق زیر است:

فلزات , هالوژنها , As , P , S , N , O , H , C . فراوانترین چهار عنصر C , H , O , N عناصر اصلی سازنده مواد آلی به حساب می‌آیند. زیرا اغلب اجسام آلی از این چهار عنصر تشکیل یافته‌اند و با توجه به همین مطلب ، مواد آلی را به چهار دسته کلی تقسیم می‌کنیم:

---

[15] OH_5H_2C

[16] $-OCH_2CH_2$

[17] O_6C_2H -

[18] -http://chemtrain.persianblog.com

[19] –DNA

[20] -http://chemnew.persianblog.com

[21] –http://www.c60.persianblog.com

۱. هیدروکربنهای ساده:

ترکیباتی هستند که فقط از H , C درست شده‌اند و به همین دلیل ، هیدروکربن شده‌اند. آنها با فرمول کلی C_xH_y نمایش می‌دهند. بسته به اینکه y , x چه اعدادی باشند، هیدروکربنهای گوناگون یافت می‌شوند.

۲. هیدروکربنهای اکسیژن دار:

ترکیباتی هستند که از O , H , C درست شده اند و با فرمول کلی $C_xH_yO_z$ نشان داده می‌شوند.

۳. هیدروکربنهای نیتروژن‌دار:

ترکیباتی هستند که از N , H , C درست شده‌اند و با فرمول کلی $C_xH_yN_t$ نشان داده می‌شوند.

٤. هیدروکربنهای اکسیژن و نیتروژن دار:

ترکیباتی هستند که علاوه بر H ، C ، اکسیژن و نیتروژن و با فرمول کلی $C_xH_yO_zNt$ نمایش داده می‌شوند.

شیمی کربن:[۲۲]

موادی که از منابع آلی به دست می‌آیند، در یک خصوصیت مشترکند: همه آنها دارای عنصر کربن هستند.

امروزه اگر چه هنوز بسیاری از ترکیبات کربن به آسانی از منابع گیاهی و جانوری بدست می‌آیند، ولیکن بسیاری از آنها نیز سنتز می‌شوند. از ترکیبات گاهی از مواد معدنی مانند کربناتها و سیانیدها سنتز می‌شوند ولی غالباً از سایر مواد آلی تهیه می‌گردند.

علّت تمایز ترکیبات کربن با سایر ترکیبات:[۲۳]

چه خصوصیتی در ترکیبات کربن وجود دارد که آنها را از ترکیبات مربوط به صد و چند عنصر دیگر جدول تناوبی متمایز می‌سازد؟ لااقل قسمتی از این جواب به نظر می‌رسد که چنین باشد: تعداد بسیار زیادی از ترکیبات کربن وجود دارند که مولکولهای آنها می‌توانند بسیار بزرگ و پیچیده باشد.

تعداد ترکیباتی که دارای کربن هستند چندین برابر بیشتر از تعداد ترکیبات بدون کربن است. این مواد آلی در خانواده‌های مختلف قرار می‌گیرند، و معمولاً در بین مواد معدنی، همتایی ندارند.

مولکولهای آلی شامل هزاران اتم شناخته شده‌اند، و ترتیب قرار گرفتن اتمها حتی در مولکولهای نسبتاً کوچک بسیار پیچیده است. یکی از مسایل اصلی در شیمی آلی، آگاهی از طرز قرار گرفتن اتمها در مولکولها و یا تعیین ساختمان ترکیبات است.

راه‌های زیادی برای شکستن این مولکولهای پیچیده و یا نوآرایی آنها برای ایجاد مولکولهای جدید وجود دارد؛ روشهای مختلفی برای اضافه نمودن اتمهای جدید به این مولکولها و یا جایگزین نمودن اتمهای جدید به جای اتمهای قدیم وجود دارد. بخش کلان شیمی آلی به پژوهش در مورد این واکنشها اختصاص دارد، یعنی تشخیص این که این واکنشها کدامند، چگونه انجام می‌شوند و چگونه می‌توان از آنها برای سنتز یک ترکیب دلخواه استفاده نمود.

اتمهای کربن می‌توانند به میزانی که برای اتم هیچ عنصر دیگری مقدور نیست، به یکدیگر بپیوندند. اتمهای کربن می‌توانند زنجیرهایی شامل هزاران اتم و یا حلقه‌هایی با اندازه‌های متفاوت ایجاد نمایند؛ زنجیرها و حلقه‌ها می‌توانند دارای شاخه و پیوندهای عرضی باشند. به اتمهای کربن این زنجیرها و حلقه‌ها، اتمهای دیگری که عمدتاً هیدروژن و همچنین فلوئور، کلر، برم، ید، اکسیژن، نیتروژن، گوگرد، فسفر و سایر اتمهای گوناگون میپیوندد.

هر آرایش مختلف از اتمها مربوط به ترکیب متفاوتی است، و هر ترکیب یک رشته ویژگیهای شیمیایی و فیزیکی ویژه خود را دارد. از این رو غیر منتظره نیست که امروزه بیشتر از ده میلیون ترکیب شناخته شده کربن وجود داشته باشد و هر سال به این تعداد نیم میلیون ترکیب تازه افزوده گردد. تعجب‌آور نیست که بررسی این ترکیبات، رشته ویژه‌ای را در شیمی به خود اختصاص دهد.

---

[۲۲] -http://www.ketabekhoob.com

[۲۳] -http://www.creative-chemistry.org.uk

تأثیرات بد ترکیبات کربن:[24]

وقوع دو فاجعه بشریت را تهدید می‌کند و هر دو ناشی از تجمع ترکیبات کربن در جو است؛ یکی نازک شدن لایه ازن که عمدتاً به واسطه وجود کلروفلوئورو کربن ها است و دیگری پدیده گلخانه که به خاطر حضور متان، کلروفلوئور و کربن ها و سرآمد همه کربن دی‌اکسید است.

شاید به همین مناسبت بوده است که مجله سینس[25] در سال ۱۹۹۰، الماس را که یکی از فرمهای آلوتروپی کربن است به عنوان مولکول سال انتخاب کرده است. و مولکول آلوتروپ تازه‌یاب فولرن باکمینستر کربن ۶۰[26] است که هیجان بسیاری را در دنیای شیمی ایجاد کرده است، هیجانی که از زمان ککوله تاکنون دیده نشده است.

منابع:

1- http://www.physic-chemistry.blogfa.com

2- http://www.c60.persianblog.com

3- http://www.arsachem.persianblog.com

4- http://www.creative-chemistry.org.uk

5- http://www.ketabekhoob.com

http://fa.wikipedia.org6-

7- http://www.tebyan.ir

8- http://chemtrain.persianblog.com

9- http://chem-2r1.blogfa.com

10- http://chemnew.persianblog.com

11- http://www2.dw-world.de

---

[24] -http://www.physic-chemistry.blogfa.com

[25] –Science

[26] –buckminsterfullerene-C۶۰

Novel Cu(II)-Schiff base complex as an effective nanocatalyst for three-component synthesis of 5-aryl-pyrano[4,3-d]thiazolo[3,2-a]pyrimidines

Seyed Hadi Hosseyni Omam[a], Mehdi Khalaj*[a] and Seyed Mahmoud Musavi[a]

[a]*Department of Chemistry, Islamic Azad University, Buinzahra Branch, Buinzahra, Iran*

**E-mail: khalaj_mehdi@yahoo.com*

A novel $CuLCl_2$ complex (L = N-(3,4-dimethylphenyl)-pyridine-2-ylmethyleneamine) has been synthesized by two methods. The first method involved the preparation of a single crystal to determine the structure of the complex and $CuLCl_2$ nanoparticles were prepared by the second method. Single crystal X-ray diffraction, NMR, FT-IR, UV–Vis and elemental analysis have been used to characterize the single crystal of the complex (1) and XRD, scanning electron microscopy (SEM), transmission electron microscopy (TEM) and the corresponding particle size distribution histogram has been used to confirm the structure of $CuLCl_2$ nanoparticles (2). The catalytic performance of the complex 2 prepared has then been assessed in the synthesis of pyrano[4,3-d]thiazolo[3,2-a]pyrimidine derivatives through the three-component condensation of 4-hydroxy-6-methyl-2H-pyran-2-one, 5-methyl-2-aminothiazole and various aromatic aldehydes under solvent-free conditions in high yields. In addition, all the synthesized compounds were evaluated for their antibacterial activity against Staphylococcus aureus (gram-positive) and Escherichia coli (gram-negative) bacteria.[1-4]

(Scheme 1).

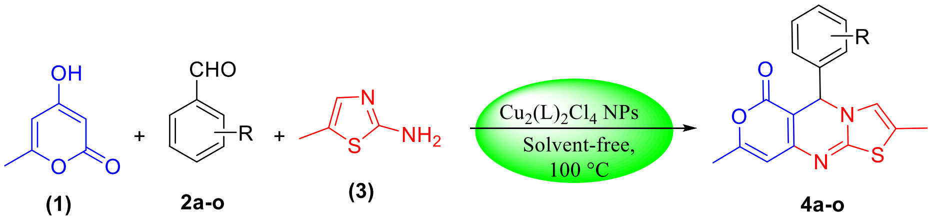

Scheme 1. Synthetic pathway of pyrano[4,3-d]thiazolo[3,2-a]pyrimidines (4a-o) by using 2 nano-particles.

References

(1)Khalaj, M.; Dehghanpour, S.; Mahmoudi, A.; Khalaj, A.; Lough, A.J. *Acta Crystallographica Section E* **2012**, *E68,* m920.

(2) Khalaj, M.; Arab-Salmanabadi, S. *Iranian Chemistry and Chemical Engineering Journal* **2021**, 41, 104, 27.

(3) Khalaj, M. *Arabian Journal of Chemistry* **2020**, *13*,7, 6403.

(4) Khalaj, M.; Musavi, S.M. *Scientific Reports* **2024**, *14*, 8870.

Density Functional Theory Insights into Pretomanid

Hossein Shirani[a,*] and Raha Dadashnezhad[b]

[*]*Corresponding author. E-mail: hossein_shirani@iust.ac.ir*

[a] *Department of Chemistry, Iran University of Science and Technology, P.O. Box 16846-13114, Tehran, Iran*
[b] *Department of Biotechnology, Kharazmi University, Tehran, Iran*

Introduction: Tuberculosis (TB), caused by Mycobacterium tuberculosis, is the leading infectious cause of death worldwide. Its management is increasingly challenging due to multidrug-resistant (MDR TB; resistant to isoniazid and rifampicin) and extensively drug-resistant (XDR TB; MDR TB with additional resistance to fluoroquinolones and at least one second-line injectable drug) strains [1]. Effective regimens rely on central drugs with strong bactericidal and sterilizing properties [2]. Pretomanid, an oral nitroimidazooxazine developed by TB Alliance under Novartis, is part of the BPaL regimen (bedaquiline, pretomanid, and linezolid) for rifampicin-resistant TB with fluoroquinolone resistance. It inhibits mycolic acid biosynthesis, disrupting M. tuberculosis cell walls and targeting non-replicating bacilli under anaerobic or hypoxic conditions [3]. Pretomanid is a bactericidal antibiotic that works by inhibiting mycobacterial cell wall synthesis and generating reactive nitrogen species, which contribute to bacterial killing. It is particularly effective against both actively replicating and dormant Mycobacterium tuberculosis under hypoxic conditions. The FDA's 2012 approval of bedaquiline, the first anti-TB drug with a novel mechanism in 40 years, revitalized TB drug development. Pretomanid, another breakthrough, has shown no serious adverse events (SAEs) in healthy subjects [4,5].

Methods: The molecular structure of Pretomanid was constructed using GaussView 5.0 and optimized via Gaussian 09 at the B3LYP/6-311+G level of theory. Geometry optimization was performed using gradient-based techniques within the density functional theory (DFT) framework, ensuring computational efficiency and accuracy. The optimized structure was confirmed as a minimum on the potential energy surface, with no imaginary frequencies observed.

Results: The molecular structure of Pretomanid was successfully optimized at the B3LYP/6-311+G level of theory using Gaussian 09. The optimized structure is illustrated in Figure 1, showcasing its geometrical arrangement.

Fig. 1. Pretomanid's optimized structure at the B3LYP/6-311+G theory level.

Table 1. Bond lengths, bond angles, and dihedral angles for Pretomanid, representing a selection of the calculated geometric parameters.

O8-N11	F2-C25	N9-C15	O4-C17	F1-C25-O6	O4-C17-C19	C14-O5-C15	C15-N10-C18	F1-C25-O6-C24	N9-C16-C18-N11	C14-C12-C13-N9	C20-C19-C17-O4
1.26167	1.40414	1.39226	1.47608	108.7	107.9	115.4	103.9	180	179.8	45	105.6

Thermodynamic properties were also calculated, with the electronic energy of the molecule found to be -1025.4 kcal/mol. The highest occupied molecular orbital (HOMO) energy was -0.26464 eV, while the lowest unoccupied molecular orbital (LUMO) energy was -0.10909 eV, resulting in a HOMO-LUMO gap (HLG) of 0.15555 eV. Mulliken atomic charges, spin density, and molecular orbital energies were analyzed. The dipole moment components were determined as X = 8.8161, Y = -0.8417, and Z = -1.0524, yielding a total dipole moment of 8.9185 Debye.

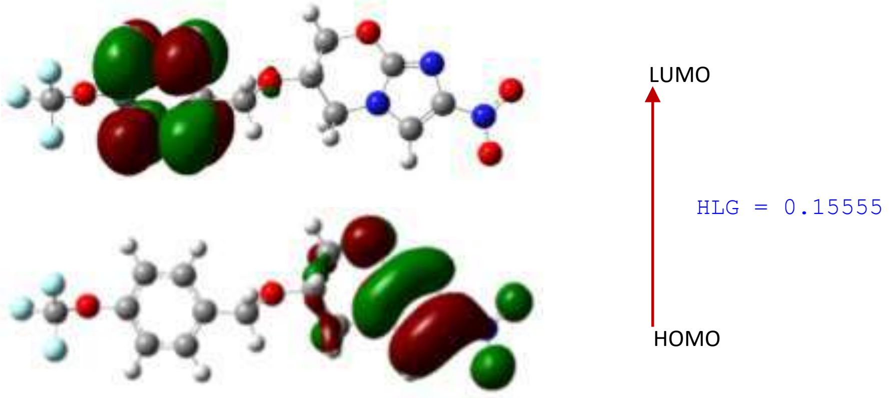

Fig. 2. The molecular orbital shapes of the HOMO and LUMO of the Pretomanid molecule at the B3LYP/6–311+G level.

Discussion: This theoretical study provides valuable insights into the chemical and pharmacological properties of Pretomanid. By leveraging an interdisciplinary approach, it paves the way for enhancing drug performance and developing similar compounds to achieve improved therapeutic outcomes.

Keywords: DFT, Pretomanid, Tuberculosis, TB, B3LYP/6-311+G; HOMO-LUMO gap

References:

[1] Stover CK, Warrener P, VanDevanter DR, et al. A small-molecule nitroimidazopyran drug candidate for the treatment of tuberculo- sis. Nature. 2000;405(6789):962–6.

[2] Van Deun A, Decroo T, Piubello A, de Jong BC, Lynen L, Rieder HL. Principles for constructing a tuberculosis treatment regimen: the role and definition of core and companion drugs. Int J Tuberc Lung Dis 2018;22:239e45.

[3] World Health Organization. Rapid Communication: key changes to the treat- ment of drug-resistant tuberculosis. Geneva: WHO; 2019. Available from: https://www.who.int/tb/publications/2019/WHO_RapidCommunicationMDR_TB2019.pdf?ua1⁄41.

[4] Winter H, Egizi E, Erondu N, Ginsberg A, Rouse DJ, Severynse-Stevens D, et al. Evaluation of pharmacokinetic interaction between PA-824 and midazolam in healthy adult subjects. Antimicrob Agents Chemother 2013;57:3699e703.

[5] Ginsberg AM, Laurenzi MW, Rouse DJ, Whitney KD, Spigelman MK. Assess-ment of the effects of the nitroimidazo-oxazine PA-824 on renal function in healthy subjects. Antimicrob Agents Chemother 2009;53:3726e33.

The 30th Iranian Seminar of Organic Chemistry
February 7-9, 2025, Iran University of Science and Technology, Tehran, Iran

Hyaluronic Acid and Hyaluronic Acid Nanogel: The Natural Moisturizer for Lipstick and Lip Balm

Mahla Firouzi Fariman, Ali Javid*

Department of Chemistry, Mashhad Branch, Islamic Azad University, Mashhad, Iran

Keyword: Hyaluronic Acid, Nano particles, Cosmetic, Lipstick, Lip balm.

Hyaluronic acid (HA) is a natural polymer that belongs to a group of heteropoly saccharides found in various human and animal tissues and through microbial sources [1]. Its structural characteristics and physical, chemical, and biological properties allow its use to be wide and cover several areas, mainly pharmaceutical, medical, dental, and aesthetics [2].

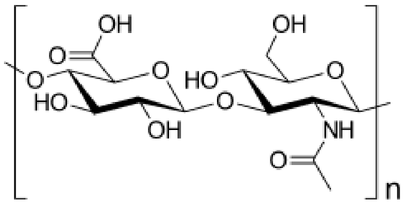

Scheme: HA structure

The physical, physicochemical, and biological properties of HA are directly linked to its molecular weight. Different covalent or non-covalent crosslinks in the three-dimensional structure of hydrogels enables them to absorb bulky volumes of water [3]. The properties of biological importance include high viscoelasticity, biocompatibility, hygroscopicity, and moisture retention abilities. Skin hydration ability, lubrication, and diminishing aging symptoms are among the physiological functions of our interest [4].

Regarding skincare products, HA has a clinically approved efficacy in fighting aging symptoms and counteracting the negative impact of skin chronic exposure to exosomes, external environmental challenges, such as sunrays, tobacco smoking, and pollution.

Nowadays, HA and derivatives are the most popular cosmetic agents with promising aesthetic results [5]. So, in recent years, HA has been used in products such as skin care products, sunscreen products, dermal fillers, hair care products, and nail care products. However, its use in lipstick has received less attention.

In this project, we used this acid, as well as its nanoparticles, in the lipstick and lip balm formulation. Synthesis of nano hyaluronic acid (nano-HA) can be approached through several methods, typically aimed at reducing the size of hyaluronic acid (HA) molecules while maintaining their biological activity. We chose the nanoprecipitation method. For this purpose, HA dissolved in a solvent (e.g., water) and then added a non-solvent (e.g., ethanol) to induce precipitation. The conditions (e.g., temperature, concentration) optimized to control the size of the resulting nanoparticles.

The quality of the resulting product was measured in comparison to a normal lipstick (control lipstick). The results emphasized the increase in lipstick quality and the improvement of lip texture.

References:

1. Graça, M.F.P.; Miguel, S.P; Cabral, C.S.D.; Correia, I.J. Hyaluronic acid—Based wound dressings: A review. *Carbohydr Polym.* 241, **2020**, 116364.
2. Gupta, R.C.; Lall, R.; Srivastava, A.; Sinha, A. Hyaluronic acid: Molecular mechanisms and therapeutic trajectory. *Front Vet Sci.* 6, **2019**, 1–24.
3. E. Caló, V.V. Khutoryanskiy, *Eur Polym J*, 65, **2015**, 252-267.
4. Haeusler H. Efficacy of a hyaluronic acid gel to improve the skin properties. *SOFW J*, 141, **2015**; 16–8.
5. Peng YP, Lin YW, Yang YY. System strategy to achieve full-face aesthetic with hyaluronic acid fillers: yes-lifting and pyramid-volumized approaches. Adv Oral Maxillofac Surg, 5, **2022**; 100209.

The 30th Iranian Seminar of Organic Chemistry
February 7-9, 2025, Iran University of Science and Technology, Tehran, Iran

The mechanical and adhesion characteristics of styrene based pressure sensitive adhesive with vinyl acetate monomer

Authors**:** Bahareh Rahimi Larki, Abdolhamid Bamoniri*

*Corresponding author email: bamoniri@kashanu.ac.ir
Department of Organic Chemistry, Faculty of Chemistry, University of Kashan, Kashan, Iran

Keywords: Pressure sensitive adhesives; Acrylic monomers; Silica nanoparticles; Vinyl acetate

Abstract

Monomers combination of vinyl acetate, butyl acrylate and acrylic acid to improve the mechanical properties due to the excessive crosslinking in the presence of vinyl acetate monomer and the adhesion failure was observed [1].By increasing of the peel and shear properties of the pressure sensitive adhesives by adding methyl acrylate monomer in the presence of 2-ethylhexyl acrylate monomer which these monomers are more expensive and less cost-effective among acrylic monomers [2]. Thus, in this paper a combination of vinyl acetate (to moderate the mechanical and adhesion traits), acrylate monomers (to reduce the glass transition temperature) and silica nanoparticles was used to produce the novel pressure sensitive adhesive usable in adhesive industry (scheme1). The properties of the polymer was characterized by attenuated total reflectance (ATR), scanning electron microscopy (SEM), glass transition temperature (Tg), peel determination and shear strength.

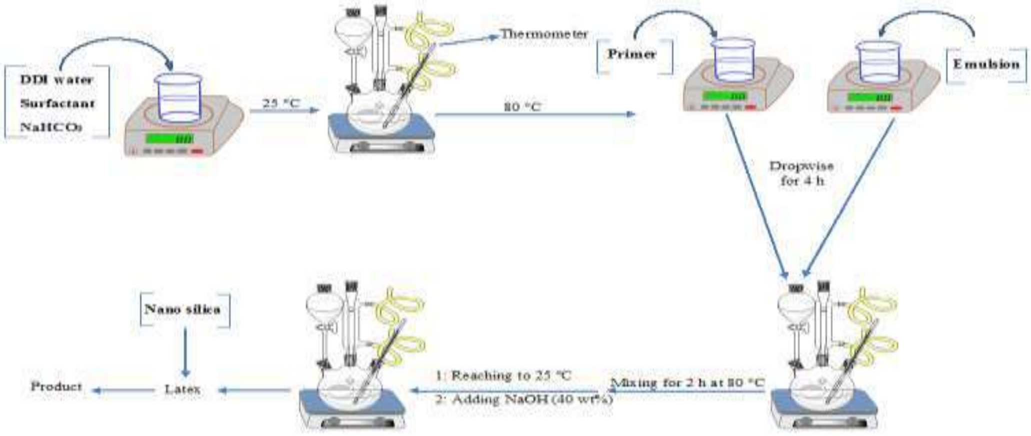

Scheme1. Preparation of the polymer

References

١. Jovanovic, R.; McKenna, T. F. Empirical modeling of butyl acrylate/vinyl acetate/acrylic acid emulsion-based pressure-sensitive adhesives. *Macromol. Mater. Engine.* **2004**, *289* (5), 467-474.
٢. Baek, S.-S.; Hwang, S.-H. Preparation and adhesion performance of transparent acrylic pressure-sensitive adhesives containing menthyl acrylate. *Polym. Bull.* **2016**, *73*, 687-701.

Synthesis and characterization of quantum dots using Bistort polyphenol as quenched fluorescence

Zahra Khajavi [a] , Fatemeh Rahmani[a] , Behnam Mahdavi*[a], Ehsan Koushki [b] ,Esmail Rezaei-Seresht[a]

[a]Department of Chemistry, Faculty of Science, Hakim Sabzevari University, Sabzevar, Iran

[b]Department of Physics , Faculty of Science, Hakim Sabzevari University, Sabzevar, Iran

Email: b.Mahdavi@hsu.ac.ir

Keyword: Bistort, Quantum dots, fluorescence

Abstract

Quantum dots (QDs) are classified into three classes: carbon, graphene, and semiconductor dots. There are many reports on the use of these materials as catalysts and supercapacitors. [1]. QDs have high potential for use as light-sensitive materials due to their high compatibility and high production of reactive oxygen species.

Bistort (*Persicaria bistorta*) is one of the most widely used medicinal plants in traditional medicine. N-epigall ocatechin is known as the main component of the plant as a remedy for ulcer inflammation, sore throat, and simple internal and external bleeding [2]. Bistort also contains other compounds such as albuminoids, starch, calcium oxalate, gallic acid, and vitamin C. [3] In this study, the extracted polyphenol bistort was used as the starting material for the synthesis of polyphenol quantum dots with a hydroalcoholic solvent by hydrothermal method.

Materials and Methods

A 0.05 gram of bistort hydroalcoholic extract powder was dissolved in 10 ml of 70% ethanol solvent. The mixture was poured into an autoclave and heated at 160 °C for 6 hours (CQDB). Also, the synthesis of iron-based quantum dots was carried out. For this purpose, 5 mL of iron nitrate solution (2M) was added to the plant extract and the synthesis was carried out under the same conditions (CQDBFe). After the synthesis process was completed, the fluorescence properties of the synthesized carbon quantum dots were examined using an UV lamp.

Results

Figure 1 a-b shows the fluorescence of the synthesized carbon quantum dots. According to the obtained results, CQDB shows a red fluorescence light. But CQDBFe shows a green fluorescence light. Furthermore, CQDB shows two bands at wavelengths of 231and 283 nm, which are related to the π→π*and n→π* transitions of C=C and C=O bonds, respectively. In Figure b, for CQDBFe, two consecutive bands are observed at wavelengths of ٤٧٩ and ٢٤٣ nm, respected to the π→π* and n→π* transitions of C-N and C=O bonds.

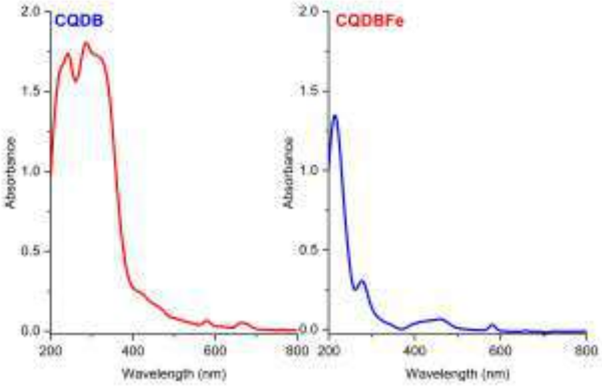

Figure1 UV-VIS spectroscopy of Bistort polyphenol

Figure2 (CQDB) (CQDBFe)

Conclusion

The results obtained show that the synthesis of carbon quantum dots in the presence of metal ions such as iron can be effective in their luminescence and therefore in their optical properties, that can introduced this material as sensor for various applications.

References:

1. Wu J, Chen X, Zhang Z, Zhang J. "Off-on" fluorescence probe based on green emissive carbon dots for the determination of Cu2+ ions and glyphosate and development of a smart sensing film for vegetable packaging. Microchimica Acta. 2022 Mar;189(3):131. Yang Y, Ding H, Li Z, Tedesco AC, Bi H.

2. Carbon dots derived from tea polyphenols as photosensitizers for photodynamic therapy. Molecules. 2022 Dec 6;27(23):8627.

3.Pawłowska KA, Hałasa R, Dudek MK, Majdan M, Jankowska K, Granica S. Antibacterial and anti-inflammatory activity of bistort (Bistorta officinalis) aqueous extract and its major components. Justification of the usage of the medicinal plant material as a traditional topical agent. Journal of ethnopharmacology. 2020 Oct 5;260:113077.

Synthesis and application of Ce-MOF@Cu as a porous catalyst in the synthesis of new diphenyl imidazole derivatives

Elham Tavakoli,[a] Hassan Sepehrmansourie,[b] Mohammad Ali Zolfigol,[a]* and Ardeshir Khazaei[a]*

[a]*Department of Organic Chemistry, Faculty of Chemistry and Petroleum Sciences, Bu-Ali Sina University, Hamedan 6517838683, Tel: +988138282807, Fax: +988138380709 Iran*

[b]*Faculty of Converging Science and Technologies, University of Qom, Qom, Iran, 37185-359.*

Keyword: Metal-organic frameworks; L-histidine; Imidazole

Metal-organic frameworks (MOFs) are porous crystalline materials which are composed of metal nodes combined with organic linkers, Variety in the choice of ligands, metal clusters and post-modification have made MOFs more feasible and designable. The post-modification approach has been explored in the development of diverse catalysts utilizing MOFs [1]. Amino acids, or protected amino acids, are significant chiral ligands in both synthetic and industrial contexts due to their affordability, natural occurrence, scalability, ease of modification, and stability in air. Among the amino acids, l-histidine is one of the strongest metal coordinating ligands and plays an important role in the binding of metal ions by proteins [2]. The main objective of the presented research is to design the architecture and synthesis of a Ce-based MOF that is modified with an amino acid group and finally copper metal is placed on it. The designed porous catalyst has been used in the synthesis of new imidazole compounds. Easy separation of the catalyst from the reaction medium, high yield of synthesized products, short reaction time, solvent-free and green reaction conditions are the most important features of the research. The synthesized compounds are likely to have medicinal properties due to their biological sections [3].

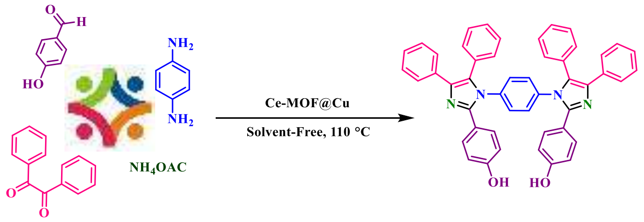

Scheme: Synthesis of new diphenyl imidazole derivatives with Ce-MOF@Cu as a porous catalyst.

References:

[**1**] Kitagawa, S. (2014). Metal–organic frameworks (MOFs). *Chemical Society Reviews*, *43*(16), **5415-5418.**

[**2**] Zeng, S., Wang, Y., Zhou, Y., Li, W., Zhou, W., Zhou, X., ... & Ren, L. (2022). Mixed-linker synthesis of L-histidine@ zeolitic imidazole framework-8 on amyloid nanofibrils-modified polyacrylonitrile membrane with high separation and antifouling properties. Separation and Purification Technology, 290, 120856.

[3] Singh, H., & Rajput, J. K. (2018). Co (II) anchored glutaraldehyde crosslinked magnetic chitosan nanoparticles (MCS) for synthesis of 2, 4, 5-trisubstituted and 1, 2, 4, 5-tetrasubstituted imidazoles. Applied Organometallic Chemistry, 32(1), e3989.

Catalytic Properties of Cobalt Tetraamino Phthalocyanine in Knoevenagel Condensation Reactions

Bahareh Vandaei[a], Maliheh Safaiee *[a]

[a] *Department of Organic Chemistry, Faculty of Chemistry and Petroleum Sciences, Bu-Ali Sina University, Hamedan 6517838695, Iran*

Keyword: Metal phthalocyanines, Knoevenagel, tetra amino Cobalt phthalocyanine

Metal phthalocyanines (MPcs) are a remarkable class of compounds with significant potential across various sectors due to their unique properties, including thermal stability, chemical inertness, vibrant colors, catalytic activity, and efficient electron transfer. Ongoing research promises further innovations in materials science, electronics, and biomedicine. The Knoevenagel condensation of benzylidenemalonitrile (BMN) derivatives with aryl aldehydes generates a diverse array of valuable organic intermediates that can be adapted for numerous synthetic transformations, particularly in the synthesis of biologically significant molecules such as carbohydrates, heterocycles, and enzyme inhibitors. In this context, we investigated the catalytic application of Cobalt tetraamino phthalocyanine in facilitating the Knoevenagel condensation of aldehyde derivatives with malononitrile, as illustrated in Scheme 1.

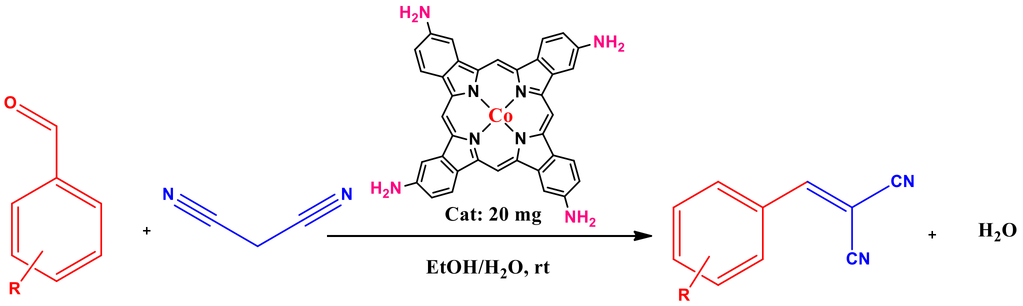

Scheme: Knoevenagel condensation reaction between different aldehydes and malonitrile catalyzed by tetra amino Cobalt phthalocyanine

References:

[1] Temizel, S., Çanak, T. Ç., & Sevim, A. M. **2020**. *Novel polymers with cobalt (II) phthalocyanine moieties as effective heterogeneous photocatalysts for visible-light-driven photodegradation of organic dyes in aqueous solutions. Journal of Photochemistry and Photobiology A*: Chemistry, 401, 112741.

[2] Sorokin, A. B. **2013**. *Phthalocyanine metal complexes in catalysis*. Chemical reviews, 113(10), 8152-8191.

[3] Hamad, O. A., Kareem, R. O., & Omer, P. K. **2024**. *Properties, Characterization, and Application of Phthalocyanine and Metal Phthalocyanine*. Journal of Chemical Reviews, 6(1).

The 30th Iranian Seminar of Organic Chemistry
February 7-9, 2025, Iran University of Science and Technology, Tehran, Iran

Synthesis of new azo-Schiff base molecules from benzocaine starting material

Marziyeh Farmani, Hamzeh Kiyani*, Mostafa Riahi

Department of Chemistry, Faculty of Science, Shahrekord University, Shahrekord, Iran

Keywords: Azo, Benzocaine, Schiff base

The discovery of azo compounds dates back to the mid-1800s. Azo dyes are a unique class of widely used photochromic molecules that reversibly photoisomerize between *cis* and *trans* geometric forms. The *trans*-to-*cis* photoisomerization occurs by ultraviolet irradiation whereas the opposite *cis*-to-*trans* occurs under blue light irradiation. They have numerous applications such as catalysis, photo-pharmacological, chemo-sensors, optical storage devices, optical switches, nonlinear optics, antifungal, pesticidal, antiviral, and anti-inflammatory. Furthermore, these attractive organic color compounds are also used in the food and textile industries. Azo-Schiff bases are photochromic molecules composed of azo systems coupled to Schiff bases. Like other azo dyes, these biphotochromic compounds have wide applications [1-4]. The azo compound **3** was synthesized by starting with benzocaine as the starting material in the presence of nitrous acid and then coupling it with salicylaldehyde. The pre-synthesized azo-aldehyde was reacted with various amines in ethanol at room temperature or reflux conditions. After several hours, the desired azo-Schiff base products (**4a**-**f**) were obtained in good yields. No column chromatographic purification was required to purify the synthesized compounds. They were isolated pure by simple filtration and washing the crude products subsequently with ethanol. If needed, recrystallization in ethanol is performed for further purification. The azo-Schiff base molecules **4a**-**f** were characterized using different spectroscopic techniques (UV-Vis, Fourier transform infrared, ^{1}H, and ^{13}C nuclear magnetic resonance (NMR), and the molecular structure is also confirmed by single-crystal X-ray diffraction measurement.

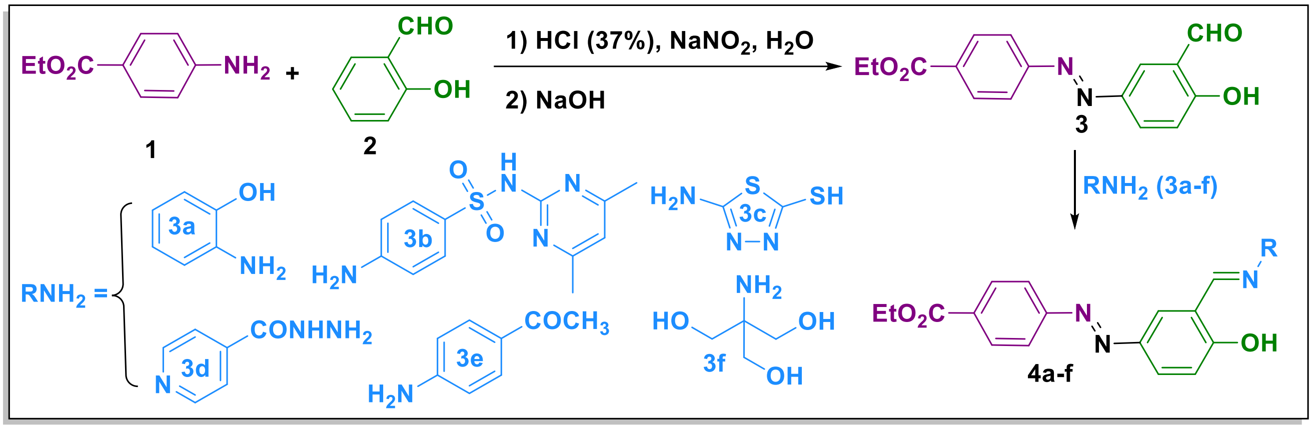

Scheme 1: Synthesize of azo-Schiff base molecules (**4a-f**)

References:

[1] E. Leonard, C. Takeda, T. Akitsu, *Colorants*, **2024**, 3, 53-72.
[2] N.O. Mahmoodi, F. Amouee, H.Y. Nyaki, H.T. Nahzomi, A. Ahmadi, *Polcycl. Aromat. Comp.*, **2024**, 44, 4724-4745.
[3] A.A. Beharry, G.A. Woolley, *Chem. Soc. Rev.*, **2011**, 40, 4422-4437.
[4] Z. Ma, J. Wu, Y. Tan, C. Tan, *Macromol. Rapid Commun.*, **2024**, 45, 2400048.

The 30th Iranian Seminar of Organic Chemistry
February 7-9, 2025, Iran University of Science and Technology, Tehran, Iran

Basicity enhancement of pyridinic amines using cation-π interaction: a comprehensive quantum study based on Density Functional Theory

Zohreh Mirjafary[1a] , Atefeh Javanmard Ghahfarokhi[2b] , Hamid Saeidian[3*c]

[a]*Department of Chemistry, Science and Research Branch, Islamic Azad University, Tehran, Iran, zmirjafary@srbiau.ac.ir*
[b]*Department of Science, Payame Noor University (PNU), P.O. Box: 19395-3697, Tehran, Iran*

Keywords: Proton–π interactions, Basicity, DFT calculations, AIM theory, Aromaticity

The cation-π interaction is a stabilizing force of a positive charge on the molecule containing this charge. Continuing previous work [1, 2], in the present study, for the first time, the effect of this interaction on the stability of conjugate acids of pyridine aromatic amines will be investigated. It is expected that this interaction will stabilize the conjugate acid and, as a result, increase the basicity of the designed structures. Therefore, the values of proton affinity (PA) and gas basicity (GB) will be calculated and compared using the reaction Scheme 1. Reactions in the gas phase as well as water and other solvents will also be considered. Due to the interaction of the proton with the π system of the aromatic ring, it is expected that the aromaticity of this ring will decrease in the conjugate acid compared to the original structure. Therefore, the aromaticity of this ring in the two structures will be measured with different parameters including HOMA, NICS, PDI, FLU, BI, *etc*. Since the cation-π interaction is a non-covalent interaction, the atom-in-molecule (AIM) theory will be used for this study. The best computational method will be obtained initially using experimental data or using several computational methods.

$$BH^+(g) \rightleftharpoons B(g) + H^+(g)$$

$$PA = \Delta H = H_B + H_{H^+} - H_{BH^+} \quad (1) \quad \text{and} \quad GB = \Delta G = G_B + G_{H^+} - G_{BH^+} \quad (2)$$

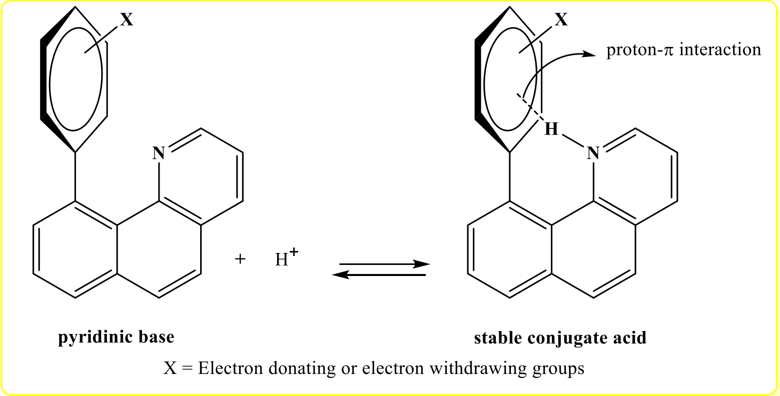

Scheme 1. Conjugate acid stability of a base using cation-π interaction

References

[1] Hajialiakbari, N., Saeidian, H., Mirjafary, Z., & Mokhtari, J. *Comput. Theor. Chem.* **2024**, 1241, 114881.

[2] Saeidian, H., Mirjafary, Z., Bakhtiari, A., & Rahmatabadi, Y. D. *J. Organometal. Chem.* **2024**, 1017, 123285.

The 30th Iranian Seminar of Organic Chemistry
February 7-9, 2025, Iran University of Science and Technology, Tehran, Iran

Quantum mechanical calculations on Tryvio drug

Hossein Shirani .[a,b,], Solaleh Rezaei .[b]

Corresponding Author E-mail: Hossein_shirani@iust.ac.ir
.[a]Department of Chemistry, Iran University of Science And Technology, P.O. Box 16846-13114, Tehran, Iran
.[b]Department of Microbiology, College of Biosience, Islamic Azad University, Tehran North Branch,Tehran ,Iran.

Abstract: This study investigates TRYVIO, a newly FDA-approved oral medication for uncontrolled hypertension and the first novel anti-hypertensive drug in nearly 40 years. Utilizing computational density functional theory, we analyze TRYVIO's chemical structure with Gaussian

Quantum mechanical calculations optimized by the B3LYP/6-311+G method. Our results provide insights into bond lengths, angles, dipole moments, and the HOMO-LUMO energy gap, contributing to a deeper understanding of TRYVIO's electronic properties and guiding future anti-hypertensive drug development.

Keywords: Tryvio, HOMO-LUMO Gap, B3LYP/6-311+G, DFT,Enthalpies,

Introduction

TRYVIO, a new prescription medicine, has made its way into the healthcare industry as a promising treatment for uncontrolled hypertension. This innovative drug received FDA approval on March 19, 2024, becoming the first oral antihypertensive medication with a unique mechanism of action in nearly 40 years. In this article, we will explore the computational study of density functional theory on TRYVIO, its chemical structure, and the various thermodynamic values obtained from quantum mechanical calculations, which is known as aprocitentan.

Method

To study TRYVIO's properties, we used computational software and followed these steps: drawing the chemical structure with the Gauss View program, performing Gaussian quantum mechanical calculations at the theoretical level, and optimizing the structure using the B3LYP/6-311+G method. Despite being time-consuming, these steps enabled us to obtain valuable data for further analysis.

Analysis and Discussion:

Using the computational data, we extracted various items crucial to understanding TRYVIO's properties: bond lengths of different atoms, angles of various bonds between atoms, dihedral angles, dipole moment and polar electric vector (6.8685), heat capacity, zero-point energy, enthalpy, and electronic energy, vibrational frequency, and HOMO-LUMO energy gap (-0.14554 eV). The HOMO-LUMO energy gap is essential for comprehending TRYVIO's electronic, optical, and redox properties.

Fig1. The calculated optimized structure of Tryvio at the B3LYP/6-311+G level.

Table1. Calculated Bond Length Values for Tryvio Molecule using B3LYP/6-311+G Computational Method .

C4-C5-N6	C4-C3-N2	N20-C22-N23	C1-O10-C11	C32-C27-C26	C3-C4-Br9
121.6	121.0	125.0	118.5	119.3	121.1

Table2.Calculated Bond Angle Values forTryvio Molecule using B3LYP/6-311+G Computational

Table3.Calculated Dihedral Angle Values for Tryvio Molecule using B3LYP/6-311+G

C4-Br9	C11-C12	C21-N36	S36-O42	C1-O10	C19-C25
1.93528	1.50376	1.40704	1.62492	1.35853	1.48669

Table4.Calculated Dipole Moments Values for Tryvio Molecule using B3LYP/6-311+G Computational.

C33-C29-C32-C27	C1-N2-C3-C4	N6-C1-N2-O10	C18-N20-C22-N23	C25-C26-C27-C32
-0.3	0.1	179.7	2.9	0.5

µ x	µ y	µ z	µ Tot
-2.1537	1.5614	-6.3324	6.8685

Table 5. Calculated zero-point Energies/ Enthalpies/ /CV /Hf Values for Tryvio Moleculeusing B3LYP/6-311+G Computational.

CV Cal/Mol-Kelvin	zero-point Energies (Kcal/Mol)	Enthalpies (Kcal/Mol)	Hf (kcal/Mol)
101.076	-4262863.982	-4262845.923	-4263051.713

HOMO	HLG	LUMO
-0.26004	-0.14554	-0.11450

Table6.Calculated HOMO-LUMO Energy Gap Values for TryvioMolecule using B3LYP/6-311+G Computational

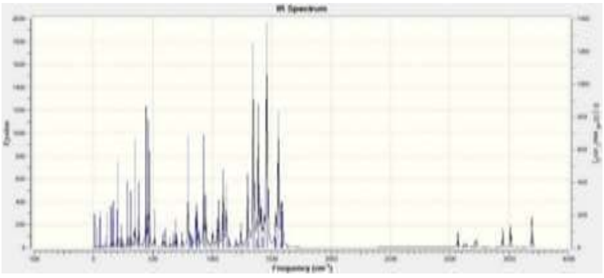

Fig2.Vibrational Frequency in IR Spectrum for Tryvio Molecule at B3LYP/6-311+G level. without encountering negative frequencies

Conclusion

This computational study of TRYVIO offers valuable insights into the drug's structure and properties. Understanding these aspects is vital for the development and optimization of innovative antihypertensive treatments. Further research could focus on the application of these findings and potential improvements for treating uncontrolled hypertension effectively.

References

[1] FDA Approves the First New Type of High Blood Pressure Drug In ... (verywellhealth.com)

[2] [PDF] US FDA approves Idorsia's once-daily TRYVIO (aprocitentan) (idorsia.com)

[3] Idorsia's once-daily TRYVIO™ (aprocitentan) is now available in the ... (prnewswire.com)

[4] Density Functional Theory (DFT) - MPI für Kohlenforschung (kofo.mpg.de)

[5] FDA Approves Aprocitentan (Tryvio) for Treatment-Resistant ... (hcplive.com)

The 30th Iranian Seminar of Organic Chemistry
February 7-9, 2025, Iran University of Science and Technology, Tehran, Iran

Synthesis of 1,8-dioxo-decahydroacridines catalyzed by Fe_3O_4@nano-coconut shell/$TiCl_4$

Motahare Hajihasani Bafghi[a], Abdolhamid Bamoniri*[a], Bi Bi Fatemeh Mirjalili[b]

[a] *Department of Organic Chemistry, Faculty of Chemistry, University of Kashan, Kashan, I.R.Iran*
[b] *Department of Chemistry, College of Science, Yazd University, Yazd, I.R.Iran*
Corresponding author Email: bamoniri@kashanu.ac.ir

Keywords: “Coconut shell”, “Magnetite”, “acridines”, “solvent free”

The preparation and design of catalysts based on magnetic biopolymers as green and biocompatible nano-catalysts have made many advantage. Fe_3O_4@nano-coconut shell/$TiCl_4$ as a biopolymer-based Lewis acid nano-catalyst from nano-coconut shell was prepared by adding $TiCl_4$ to Fe_3O_4@nano-coconut shell [1]. Synthesis of 1,8-dioxo-decahydroacridines by the one-pot pseudo three-component reaction of 4-bromobenzaldehyde , 5,5 dimethyl-1,3- cyclohexanedione and aniline in the presence of Fe_3O_4@nano-coconut shell/$TiCl_4$ at 80 °C under solvent-free conditions [2] (**Scheme**).

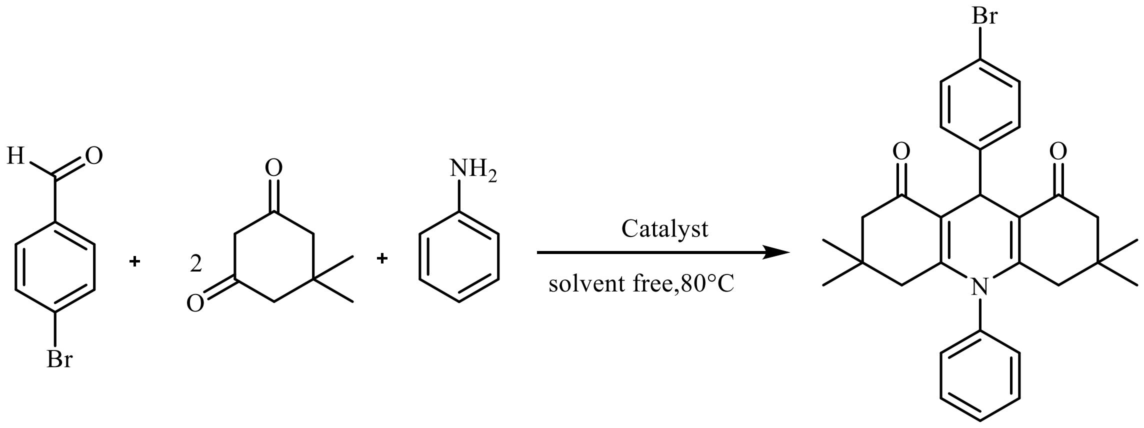

Scheme: Synthesis of 1,8-dioxo-decahydroacridines

References

[١] Tafti, A. D.; Mirjalili, B. B. F., Nano-Fe_3O_4@walnut shell/Cu(II) as a highly effective environmentally friendly catalyst for the one-pot pseudo three-component synthesis of 1, 3-oxazine derivatives under solvent-free conditions. *RSC Adv.* **2020,** *10* (53), 31874-31880.

[٢] Jin, T.-S.; Zhang, J.-S.; Guo, T.-T.; Wang, A.-Q.; Li, T.-S., One-pot clean synthesis of 1, 8-dioxo-decahydroacridines catalyzed by p-dodecylbenezenesulfonic acid in aqueous media. *Synthesis***, 2004**(12), 2001-2005.

The 30th Iranian Seminar of Organic Chemistry

February 7-9, 2025, Iran University of Science and Technology, Tehran, Iran

Novel magnetic nanocatalyst with morpholine moieties as catalyst for the synthesis of some pyranopyrimidinedione derivatives

Rojin Alavi[a] , Majid Rezaeivala[a,*], Ahmadreza Mousavi-zare[a]

[a] *Faculty of Chemical Engineering and Basic Sciences, Hamedan University of Technology, Hamedan,65155, Iran*

Keyword: Pyranopyrimidinedione, Magnetic Nanocatalyst, Morpholine, Green Chemistry.

Pyranopyrimidinediones are important heterocyclic compounds with a wide range of biological and pharmaceutical activities, such as antimicrobial, antiviral, and anticancer properties [1]. The synthesis of these compounds often requires efficient catalysts that can operate under mild, solvent-free conditions, in line with green chemistry principles [2]. Magnetic nanocatalysts, due to their high surface area, recyclability, and ease of separation, have attracted considerable attention [3]. In this work, first a polyamine with morpholine tags were synthesized [3] and then magnetic nanocatalyst containing morpholine moiety was prepared according literature method [4]. The novel nanocatalyst was characterized by FT-IR, XRD, FE-SEM, EDAX and AFM. The AFM image of nanocatalyst was shown in Fig.1. The catalytic performance of the novel nanomagnetic catalyst was examined in multicomponent preparation of pyranopyrimidinedione derivatives under mild reaction conditions (40 °C, solvent-free). The products were characterized by FT-IR, ^1H and ^{13}C NMR and melting point.

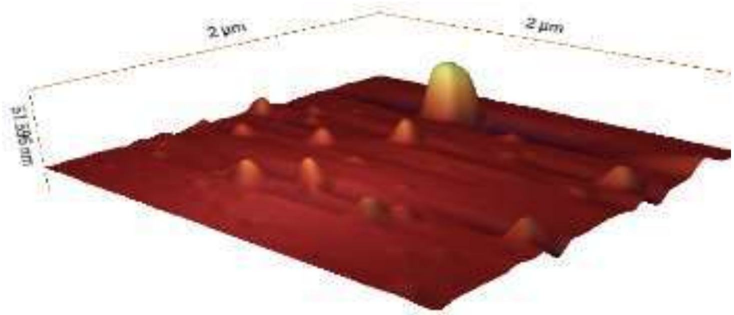

Fig.1: AFM image of nanomagnetic catalyst

References:

[1]. L. Amiri-Zirtol, T. S. Ahooie, E. Riazimontazer, M. A. Amrollahi and B.-F. Mirjalili, *Scientific reports*, 13 (2023) 17966.

[2]. S. D. Roy, K. C. Das and S. S. Dhar, *Inorganic Chemistry Communications*, 134 (2021) 109050.

[3]. A. Ali, T. Shah, R. Ullah, P. Zhou, M. Guo, M. Ovais, et al., *Frontiers in Chemistry*, 9 (2021) 629054.

[4]. M. A. Chegeni, M. Rezaeivala, S. Karimi and A. Berisha, *Journal of the Taiwan Institute of Chemical Engineers*, 152(2023)105127.

[5]. S. Kalhor, M. Yarie, M. Rezaeivala and M. A. Zolfigol, *Research on Chemical Intermediates,* 45 (2019) 3453.

The 30th Iranian Seminar of Organic Chemistry
February 7-9, 2025, Iran University of Science and Technology, Tehran, Iran

Fragmentation Pathways and Structural Characterization of *O*-alkyl *N*-(1-(dialkylamino))alkylidene phosphoramidofluoridates Related to the Chemical Weapons Convention With Using GC–MS/MS

Milad Bazzaz Rastkar[a], Seyed Esmaeil Hosseini*[a] , Davood Ashrafi [a], Fatemeh Mirbabaei [a], Mohammad Taghi Naseri[a]

[a]*Iran Defense Chemical Research Lab (DCRL), Department of Chemistry Shahid meysami Group, Alborz, Iran*

**E-mail:* s.e.hoseini.a@gmail.com

The electron ionization (EI) mass spectra a series of *O*-alkyl *N*-(1-(dialkylamino))alkylidene phosphoramidofluoridates, which are precursors of nerve agents, were studied for Chemical Weapons Convention (CWC) verification. General EI fragmentation pathways were constructed and discussed. Proposed fragment structures were confirmed through analyzing fragment ions of deuterated analogs[1-2]. The observed fragment ions are due to different fragmentation pathways such as hydrogen and McLafferty+1 rearrangement, alkene, amine and alkoxy elimination by α- or β-cleavage process. Fragment ions distinctly allow unequivocal identification of the interested compounds including those of isomeric compounds. The presence and abundance of fragment ions were found to depend on the size and structure of the alkyl group attached to nitrogen, phosphorus and oxygen atoms[3-4-5].

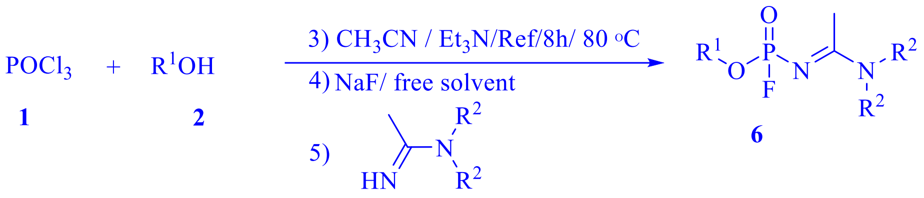

R^1: Me, Et, Pr, 1-But, 2-But, iso-But, Tert-But

R^2: Me, Et, Pr

Scheme 1. Synthesis of *O*-alkyl *N*-(1-(dialkylamino))alkylidene phosphoramidofluoridates

References

(1)Saeidian, H., Hosseini, S.E.,Amozadeh, A., Naseri, Mohammad Taghi., Babri, M. *International journal of Mass spectrometry* **2016**, *409*, 52.

(2)Noga, M., Jurowski, K. *Archives of Toxicology* **2023**, *97*, 661.

(3)Harvey, S., McMahon, L.,Berg, f. *Heliyon* **2020**, *6*, 3153.

(4)Aisyah Rahmania, T., Wisynu Kusuma Wardhani, E., Wardhani, E., Harahap, Y. *Pharmaceutical Sciences and Research* **2021**, *8*, 79.

(5)Jacquet, P., Remy, B., Bross, T., Van Grol, M., Gaucher, F., Chabriere, E., Konig, M., Daude., D. *International journal of Molecular Sciences* **2021**, *22*, 8152.

The 30th Iranian Seminar of Organic Chemistry

February 7-9, 2025, Iran University of Science and Technology, Tehran, Iran

Microsynthesis and Unambiguous Identification of *P*-alkyl *N*-(1-(dialkylamino))alkylidene phosphonamidic fluorides Related to the Chemical Weapons Convention With Using GC–MS/MS

Milad Bazzaz Rastkar[a], Seyed Esmaeil Hosseini*[a] , Davood Ashrafi [a], Fatemeh Mirbabaei [a], Mohammad Taghi Naseri[a]

[a]*Iran Defense Chemical Research Lab (DCRL), Department of Chemistry Shahid meysami Group, Alborz, Iran*

**E-mail: s.e.hoseini.a@gmail.com*

The present study was intended to develop suitable methods for unambiguous identification *P*-alkyl *N*-(1-(dialkylamino)) alkylidene phosphomimic fluorides. Since *O*-ethyl *N* -(1-(diethylamino)ethylidene)phosphoramidofluoridate (A234) have been added to the series of chemical compounds related to the Chemical Weapons Convention (CWC), These compounds, are banned as chemical weapon in the Organization for the Prohibition of Chemical Weapons (OPCW).[1-2] Due to synthesis of these compounds as a protected under the "top secret" program of some governments, no clear detailed investigation of the synthesis procures and data analysis of these compounds has been published[3]. For the first time, microsynthesis and EI-MS spectra a series of A related to CWC were collected and investigated with the aim of enriching the Organization for the Prohibition of Chemical Weapons Central Analytical Database (OCAD), which may be used in OPCW verification activities, on/off site analysis, and to improve synthesis and MS interpretation knowledge. The proposed mechanisms for the formation of the fragments were confirmed through the analysis of mass spectra of the structural isomers [4-5].

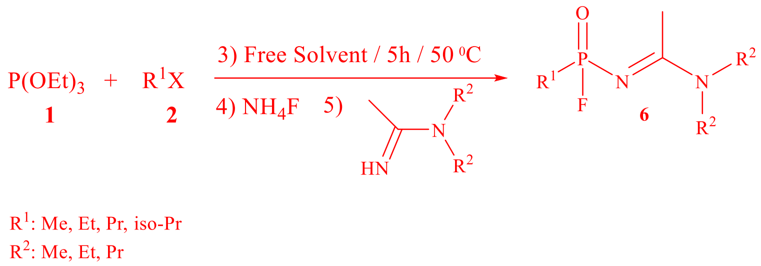

Scheme 1. Synthesis of *P*-alkyl *N*-(1-(dialkylamino))alkylidene phosphonamidic fluorides

References

(1)Eskandari, M.; Mousavi Faraz, S.; Hosseini, S.E., Moradi, Sh., Saeidian, H. *International journal of Mass spectrometry* **2022**, *472*, 116794.

(2)Nepovimova, E.; Kuca. *Food and chemistry toxicology* **2018**, *121*, 350.

(3)Yang Lee, J.; Chati Lim, k.; Suk kim, H. *Moleculees* **2021**, *26*, 1059.

(4)Hosseini, S.E., Saeidian, H., Amozadeh, A., Naseri, Mohammad Taghi., Babri, Babri. *Rapid Communication In Mass Spectrometry* **2016**, *30*, 2593.

(5)Bhakhoa, H., Rhyman, L., Ramasami, P. *Royal Society of chemistry* **2019**, *6*, 181831.

The 30th Iranian Seminar of Organic Chemistry
February 7-9, 2025, Iran University of Science and Technology, Tehran, Iran

Highly efficient and magnetically recoverable nanocatalyst based on ionic liquid immobilized on modified FSM-16

Azar Jahanbakhshi, Mahnaz Farahi*
Department of Chemistry, Yasouj University, Yasouj, Iran, Zip Code: 75918-74831.

Abstract: In this work, a recyclable magnetic catalyst, Fe_3O_4@FSM-16-SO_3/IL, based on FSM-16 was synthesized, characterized, and successfully employed as an effective catalyst in the synthesis of polyhydroquinoline derivatives. This synthesis involved a one-pot reaction of various aromatic aldehydes, dimedone, ethyl acetoacetate, and ammonium acetate.

Keyword: FSM-16, Ionic liquid, Magnetic nanoparticles, Polyhydroquinoline.

Introduction: Among the different mesoporous materials with structure and very regular pores, MCM-41 and FSM-16 have attracted much attention. FSM-16 structures have been prepared by intercalation of quarterly ammonium surfactant as a template into layered sodium silicate, kanemite, followed by calcination to remove the template, resulting in the formation of a hexagonal arrangement of channels with active surface silanol groups, high surface area, and uniform pore size. The combination of the properties of magnetic nanoparticles and mesoporous materials in a single material is particularly attractive from the point of view of catalysis because of possibility of combining the various functional groups with the advantages of the magnetic properties of magnetic nanoparticles. Immobilization of ionic liquids on suitable solid supports such as porous supports or magnetic nanoparticles would be a short cut to achieve better catalytic efficiency and recycling performance than current ionic liquid catalysts. To date, many ionic liquids supported on magnetic mesoporous materials have been prepared and used in many chemical reactions. Polyhydroquinoline derivatives, as an important class of *N*-heterocyclic compounds have become an important structural component in many pharmaceutical agents such as HIV protease inhibition, antitumor, neurotropic, antibacterial, MDR reversal, antimutagenic, antidiabetic, hepatoprotective, and vasodilator.

Method: The preparation of Fe_3O_4@FSM-16-SO_3/IL, involving the immobilization of an acidic ionic liquid on Fe_3O_4@FSM-16 nanocomposite, was carried out in several steps. Firstly, Fe_3O_4 nanoparticles were prepared and then coated with CTAB and kanemite (δ-$Na_2Si_2O_5$). The resulting product was calcined to produce Fe_3O_4@FSM-16. Subsequently, Fe_3O_4@FSM-16-SO_3H was prepared by the reaction of between Fe_3O_4@FSM-16 with chlorosulfunic acid. Then, the reaction of triethylamine with 1,4-butane sultone produced the ionic liquid (IL). Finally, the Fe_3O_4@FSM-16-SO_3/IL nanocatalyst was prepared by the electrostatic stabilization the IL on Fe_3O_4@FSM-16-SO_3H. Its catalytic application was investigated in the synthesis of polyhydroquinoline derivatives with the multicomponent reaction of aromatic aldehyde, dimedone, ethyl acetoacetate, and ammonium acetate (**Scheme**).

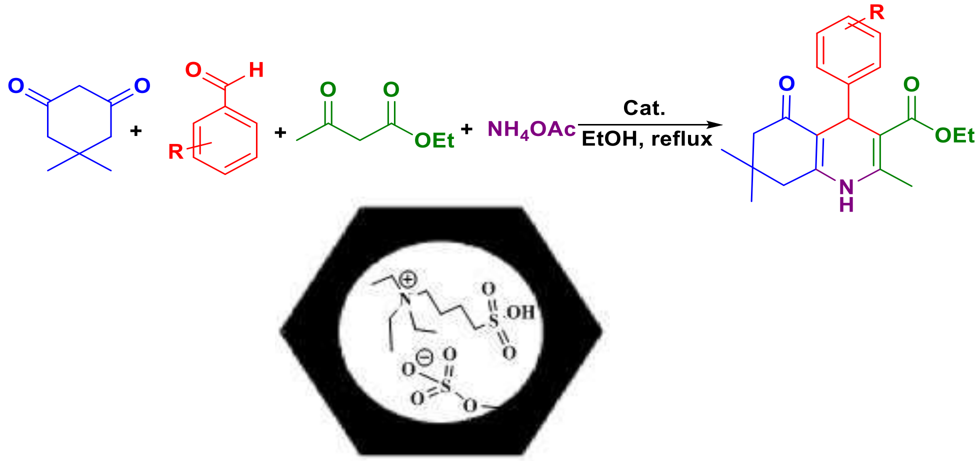

Cat=Fe_3O_4@FSM-16-SO_3/IL

Scheme: Synthesis of polyhydroquinoline derivatives using Fe_3O_4@FSM-16-SO_3/IL.

Results and Discussion: The synthesized nanocatalyst was characterized by XRD Low angle, TGA, FE-SEM, EDS, analyses.

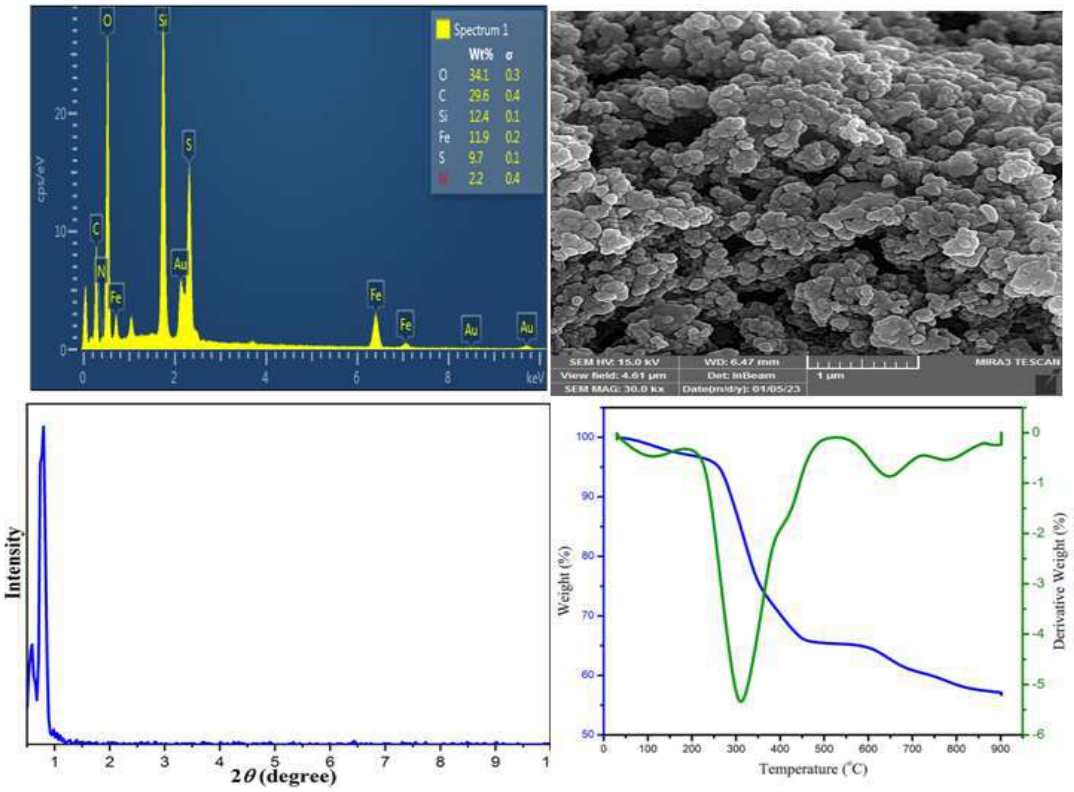

References:

1. M. Khorasani, B. Karimi and H. Vali, *React. Chem. Eng*., 2022, 7, 2618.
2. R. Pourhasan Kisomi, F. Shirini and M. Golshekan, *Appl. Organomet. Chem*., 2021, 35, 6212.
٣. S. Rostamnia and A. Hassankhani, *Synlett*, ٢٠١٤, ٢٥, ٢٧٥٣.
٤. R. Ghorbani-Vaghei and V. Izadkhah, *Appl Organomet. Chem*., ٢٠١٨, ٣٢, ٤٠٢٥.
5. R. R. Raslan, S. A. Hessein, S. A. Fouad and N. A. Shmiess, *J Heterocycl. Chem*., 2022, 59, 832.

The 30th Iranian Seminar of Organic Chemistry
February 7-9, 2025, Iran University of Science and Technology, Tehran, Iran

Novel magnetic FSM-16 supported ionic liquid/Pd complex as a high efficiency and recoverable nanocatalyst for the synthesis of pyrano[3,2-*c*]chromene-3-carbonitrile derivatives

Azar Jahanbakhshi, Mahnaz Farahi*
Department of Chemistry, Yasouj University, Yasouj, Iran, Zip Code: 75918-74831.

Abstract: In this research, Fe_3O_4@FSM-16/IL-Pd was successfully designed and synthesized via a new procedure of palladium (II) complex immobilization onto magnetic FSM-16 using an ionic liquid, as a novel heterogeneous nanocatalyst. Fe_3O_4@FSM-16/IL-Pd was used as a heterogeneous and efficient catalyst for the preparation of pyrano[3,2-*c*]chromene-3-carbonitrile derivatives.

Keyword: FSM-16, Fe_3O_4, Ionic liquid, Palladium, Pyrano[3,2-*c*]chromene**.**

Introduction: Chromene derivatives are oxygen-containing heterocyclic compounds with diverse pharmaceutical and biological properties which are widely distributed in nature. Chromenes demonstrate a diverse range of biological activities, such as anti anaphylactic activity, antimicrobial, anticancer properties, diuretic, and spasmolytic. During the past few decades, stabilized metallic nanoparticles have been utilized as heterogeneous catalysts in the transformation of organic functional groups and novel organic synthesis. Among various metal and metal oxide nanoparticles, Fe_3O_4 magnetic oxide nanoparticles (MNPs) owing to their inherent properties including superparamagnetism, a significant surface area, low toxicity, easy separation, recyclability through an external magnetic field, and reuse in chemical processes have garnered significant attention. Therefore, Fe_3O_4 magnetic nanoparticles are coated with a range of materials, including mesoporous silica materials, polymers, carbon nanotubes, and boehmite nanoparticles, resulting in the formation of core-shell structures. Among mesoporous silica compounds, FSM-16 (Folded Sheet Mesoporous) has attracted much interest due to its high pore volume, large surface area, surface silanol groups, and uniform pore diameter. An attractive approach for the fabrication of an effective solid catalyst, and recyclable is the covalent stabilization of ionic liquids on a heterogeneous solid surface, such as a suitable magnetic mesoporous.

Method: To prepare Fe_3O_4@FSM-16/IL-Pd nanocatalyst, firstly, Fe_3O_4@FSM-16 was prepared by the reported method. Next, IL_{DABCO} (Bis-PrSi/DABCO/Cl) was synthesized using the reaction of ١،٤-diazabicyclo[2.2.2]octane (DABCO) with 3-chloropropyltrimethoxysilane (CPTMS). In the following, the IL_{DABCO} was stabilized on the Fe_3O_4@FSM-16 surface through an organosiloxane bridge with free surface chloride ions. Finally, Fe_3O_4@FSM-16/IL was then reacted with $PdCl_2$ to prepare Fe_3O_4@FSM-16/IL-Pd nanocatalyst. Fe_3O_4@FSM-16/IL-Pd was used as a heterogeneous and efficient catalyst for the preparation of pyrano[3,2-*c*]chromene-3-carbonitrile derivatives via the reaction of 4-hydroxycoumarin, aldehyde, and malononitrile under solvent-free conditions (**Scheme**).

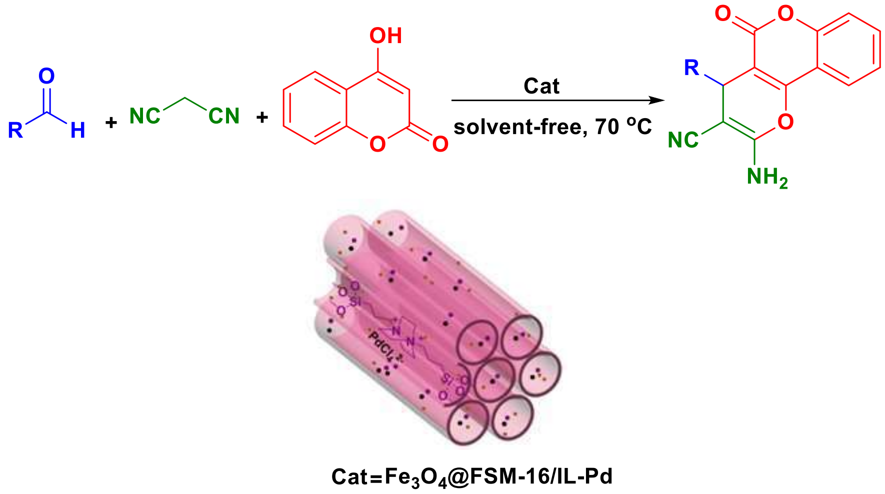

Scheme: Synthesis of pyrano[3,2-*c*]chromene-3-carbonitriles using Fe_3O_4@FSM-16/IL-Pd.

Results and Discussion: The synthesized nanocatalyst was characterized by VSM, TGA, FE-SEM, EDX analyses.

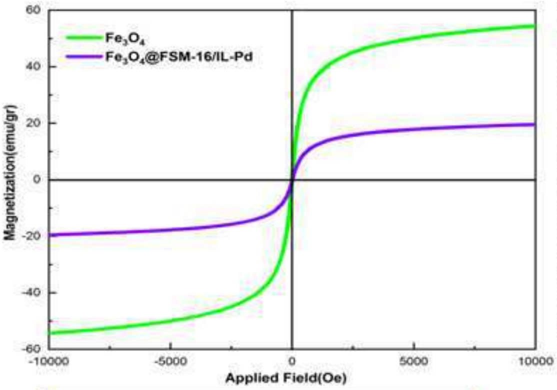

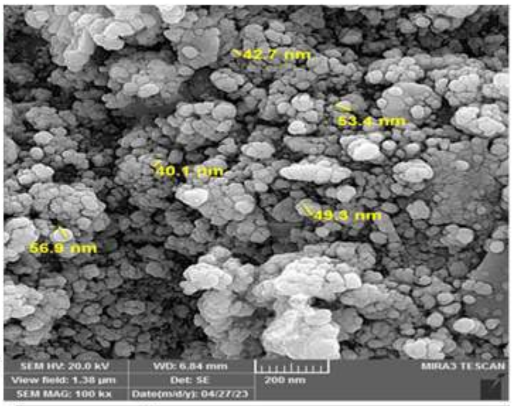

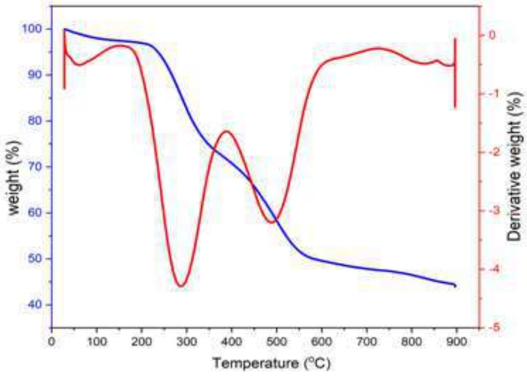

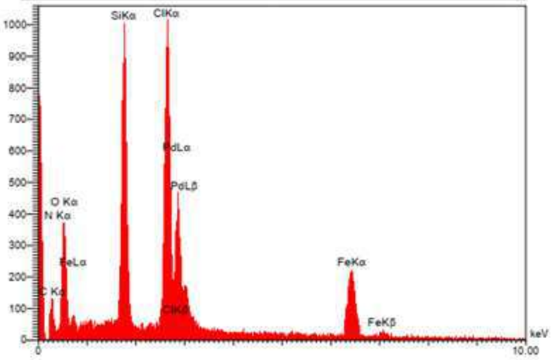

References:

1. S. Rostamnia, E. Doustkhah and B. Zeynizadeh, ***Micropor. Mesopor. Mater***., 2016, 222, 87.

2. M. Nasrollahzadeh, N. Motahharifar, Z. Nezafat and M. Shokouhimehr, ***J. Mol. Liq***., 2021, 341, 117398.

3. L. A. Bischoff, M. Drisch, C. Kerpen, P. T. Hennig, J. Landmann, J. A. Sprenger, R. Bertermann, M. Grüne, Q. Yuan, J. Warneke, X. B. Wang and M. Finze, ***Chem. Eur. J***., 2019, 25, 3560.

4. M. M. Abdullah, A. A. AlQuraishi, H. A. Allohedan, A. O. AlMansou and A. M. Atta, ***J. Mol. Liq***., 2017, 233, 508.

Efficient Synthesis of 2-Amino-4H-Chromene Derivatives by Sulfonated MIL-101(Fe) Catalyst

Faegheh Daraei-Ghadikolaei, Mostafa Ghafori-Gorab, Amir Kashtiaray, Ali Maleki*

Catalysts and Organic Synthesis Research Laboratory, Department of Chemistry, Iran University of Science and Technology, Tehran 16846-13114, Iran

Keyword: Chromene, MIL-101(Fe), Catalyst, Metal-Organic Frameworks

Chromene is an important bicyclic aromatic heterocyclic compound that successfully combines the structures of a benzene ring and a pyran ring. As an important chromene derivative, 2-amino-4H-chromene illustrates notable anti-cancer, anti-inflammatory, anti-microbial, and antioxidant properties [1]. The traditional synthesis of chromenes typically entails lengthy reaction time and stoichiometric reagents, toxic catalysts, high temperatures, and hazardous organic solvents, which can result in lower yields. The nature of the catalyst, in conjunction with other reaction parameters, significantly influences yield, selectivity, and overall applicability. There has been a collaborative effort to develop a catalyst that is not only cost-effective but also mild, versatile, and reusable [2]. Diverse catalytic systems, including polymers, zeolites, carbon-based catalysts, metal nanoparticles (NPs), and metal-organic frameworks (MOFs), are used for synthesizing 2-amino-4H-chromenes. MOFs, in particular, are gaining attention as heterogeneous catalysts due to their high surface area and dual Lewis and Brønsted acid characteristics, which enhance the synthesis of 2-amino-4H-chromene [3].

In this study, an innovative catalyst was prepared via sulfonation of NH_2-MIL-101(Fe). In order to prepare the catalyst initially, 2-amino terephthalic acid (0.206 g) and $FeCl_3 \cdot 6H_2O$ (0.76 g) were dissolved in DMF solvent and the reaction mixture was subjected to solvothermal conditions for 24h at 110°C. Subsequently, NH_2-MIL-101(Fe) was covalently sulfonated with 1,4-butane sultone (NH_2-MIL-101(Fe)-SO_3H) [4]. The prepared catalyst (NH_2-MIL-101(Fe)-SO_3H) was utilized to synthesize 2-amino-4H-chromene by the following reaction. A mixture of dimedone (1 mmol), malononitrile (1.1 mmol), and benzaldehyde (1 mmol) was dissolved in ethanol (2 ml) in the presence of 0.04 g of the prepared catalyst and the reaction was carried out over 2 hours at room temperature. This reaction achieved a 90% yield of 2-amino-4H-chromene. The catalyst's reusability was evaluated under optimal reaction conditions, demonstrating effectiveness for up to 5 cycles without any significant performance decrease.

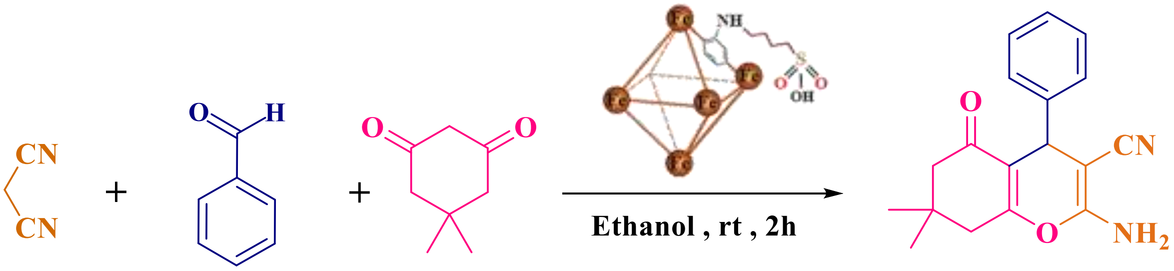

Scheme 1. Synthesis of 2-amino-4H-chromene derivatives using NH_2-MIL-101(Fe)-SO_3H catalyst

References

1. González-Rodal D, Przepiórski J, Peinado AL, Pérez-Mayoral E. Basic-carbon nanocatalysts in the efficient synthesis of chromene derivatives. Valorization of both PET residues and mineral sources. Chemical Engineering Journal. 2020 Feb 15;382: p.122795.

2. Pratap R, Ram VJ. Natural and synthetic chromenes, fused chromenes, and versatility of dihydro benzo [h] chromenes in organic synthesis. Chemical reviews. 2014 Oct 22;114(20): p.10476-526.

3. Jalili F, Sepehrmansourie H, Zarei M, Zolfigol MA, Khazaei A, As' Habi MA. Application of novel metal-organic frameworks containing sulfonic acid pending in the synthesis of chromene [4, 3-d] pyrimidines via back-to-back anomeric-based oxidation. Arabian Journal of Chemistry. 2024 Mar 1;17(3): p.105635.

4. Jin Y, Shi J, Zhang F, Zhong Y, Zhu W. Synthesis of sulfonic acid-functionalized MIL-101 for acetalization of aldehydes with diols. Journal of Molecular Catalysis A: Chemical. 2014 Mar 1; 383: p.167-71.

The 30th Iranian Seminar of Organic Chemistry
February 7-9, 2025, Iran University of Science and Technology, Tehran, Iran

4-amino coumarin as a novel coupling scaffold for the synthesis of some new azo dyes preferring hydrazone tautomeric structure

Enayatollah Moradi Rufchahi[a], Fatemeh Ashouri Mirsadeghi *[b]

Department of Chemistry, Faculty of Science, Islamic Azad University, Lahijan branch, P.O. Box: 1616, Lahijan, Iran

Keyword: 4-aminocoumarin, azo-coupling, solvatochromism, hydrazone, DFT

In recent years, some compounds having an en-amine functional group, such as 6-aminouracil and 1,3-dimethyl-6-aminouracil, have been used by several researchers as efficient intermediates to prepare relevant azo dyes and pigments [1-4]. The azo-hydrazone tautomerization capability exhibited by this category of heterocyclic azo dyes makes them suitable candidate compounds for investigating their solvatochromic and tautomeric properties in various organic solvents [5-8].

In this study, 4-Aminocoumarin was reacted as a new enamine-type coupling component with some diazonium salts derived from mono-substituted aromatic amines to afford the corresponding dyes. The structures of the obtained dyes were confirmed by infrared, nuclear magnetic resonance, and mass spectroscopic techniques. The outcomes of the study have revealed that the prepared dyes exist as hydrazone-imine tautomeric structures in both solid and solution states. The solvatochromism properties of dyes have been investigated in various solvents. The effects of acid and base on the visible absorption spectra of the dyes in ethanol were also studied, which showed that the spectral changes are clearly dependent upon the protonation-deprotonation of the dye molecules. Afterwards, the structures of the azo and hydrazone tautomeric forms of the dyes were optimized at B3LYP/6-311G level of theory. DFT calculations have performed to measure the stability (energy) of proposed azo and hydrazone tautomeric forms of the prepared dyes both in gas phase and in the solution state.

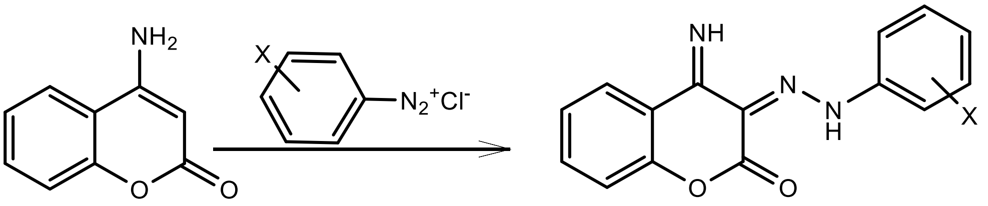

(١):X=4- NO_2	(٢):X= = 3-NO_2	(٣):X= 3-CN	(٤):X= 4-$COCH_3$
(٥):X= 4-F	(٦):X= 4-Cl	(٧):X= 3-Cl	(٨): X= 4-Br
(٩):X= -H	(**10**): X=4-C_2H_5	(**11**):X=4-n- C_4H_9	(**12**): 4-$NHCOCH_3$

Scheme1. Synthetic route to hydrazo-imine dyes **1-12**.

References:

[1] M.R. Yazdanbakhsh, M. Abbasnia, M. Sheykhan, L. Ma'mani, Journal of Molecular Structure 977 (2010) 266–273.

[2] H. Yousefi, A. Yahyazadeh, M. R. Yazdanbakhsh, M. Rassa, E. Moradi-e-Rufchahi, Journal of Molecular Structure 1015 (2012) 27–32.

[3] D. Debnath, S. Roy, B.-H. Li, Ch.-H. Lin, T. K. Misra, Spectrochimica Acta Part A: Molecular and Biomolecular Spectroscopy 140 (2015) 185–197.

[4] Z. Seferoğlu, N. Ertan, Central European Journal of Chemistry 6 (2008) 81-88.

[5] M. S. Masoud, S. A. Abou El-Enein, M. E. Ayad, A. S. Goher, Spectrochimica Acta Part A 60 (2004) 77–87.

[6] A. Purkayastha, A. Frontera, R. Ganguly, T.K. Misra, Journal of Molecular Structure, 1170 (2018) 70-81.

[7] I. Aprahamian, Chemical Communications 53 (2017) 6674-6684.

[8] S. Fotovati, G. Imanzadeh, A. Yahyazadeh, E. Moradi Rufchahi, Journal of Molecular Structure 1306 (2024) 137931.

A novel laccase-mediated system for treatment of phenolic pollutants

Seyed Hojjat Tayefi, Rafe Naijian, Mehdi Mogharabi*

Pharmaceutical Sciences Research Center, Mazandaran University of Medical Sciences, P.O. Box 48175-861 Sari 4847193698, Iran

Keyword: Laccase, Phenol, Enzyme immobilization, Wastewater treatment

Phenolic compounds are pervasive environmental pollutants that originate from industrial activities such as petrochemicals, pharmaceuticals, paper and pulp production, and textile manufacturing. These compounds are highly toxic, recalcitrant, and known to pose significant risks to both ecosystems and human health. Due to their stability and solubility in water, phenols are challenging to remove using conventional physical or chemical wastewater treatment methods. Therefore, the development of efficient, sustainable, and eco-friendly approaches for phenol remediation is of paramount importance [1]. Laccases, a class of multicopper oxidases, have emerged as promising biocatalysts for the removal of phenolic compounds from contaminated environments. These enzymes catalyze the oxidation of phenols to reactive radicals by reducing molecular oxygen to water, thereby initiating polymerization or degradation reactions that result in the removal of phenolic pollutants. Laccases exhibit a broad substrate specificity, making them suitable for the degradation of a wide range of phenolic compounds [2]. Moreover, their ability to function under mild conditions, coupled with their potential for immobilization and reuse, enhances their applicability in large-scale wastewater treatment processes [3]. This study explores the potential of laccase for the bioremediation of phenolic pollutants, focusing on optimizing its activity, enhancing its stability through immobilization techniques, and integrating it into advanced treatment systems to achieve sustainable phenol removal. This research involved the preparation of a magnetic cross-linked laccase aggregate employing superparamagnetic metal-organic frameworks, which was then applied to effectively remove phenol from the environment.

The results demonstrated that the magnetic cross-linked laccase aggregate maintained its activity over a wide pH range. Notably, ammonium sulfate positively impacted enzyme activity. It was determined that an optimal concentration range of 0.4–0.8% maximized enzyme activity while minimizing adverse effects from excessive cross-linking. The ideal conditions for efficient phenol removal were identified as a pH of 4.5 and a temperature of 45°C.

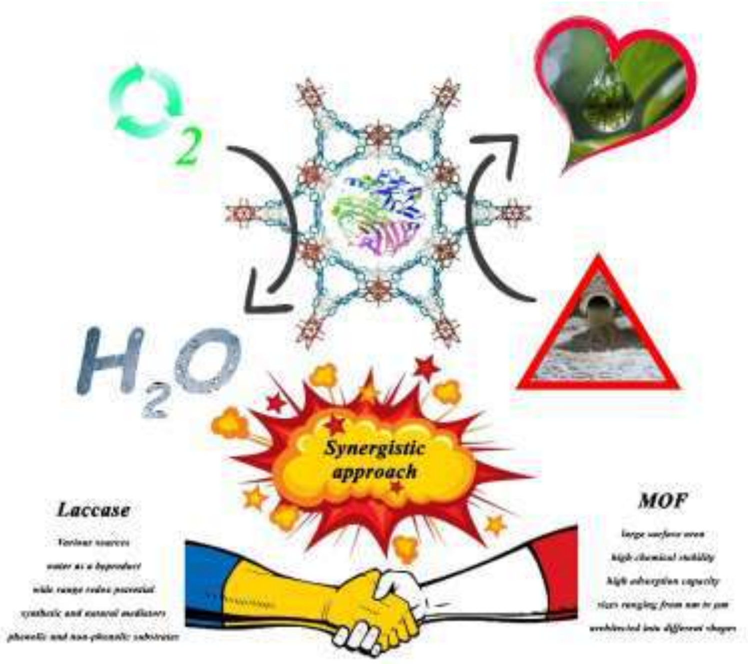

Scheme: laccase-MOF composite showed synergistic effect for remediation of phenolic pollutants.

In conclusion, the development and application of magnetic cross-linked laccase aggregates synthesized using superparamagnetic metal-organic frameworks demonstrate a promising approach for the efficient removal of phenolic pollutants. Future studies could explore scaling up the process and evaluating its performance in complex real-world wastewater matrices.

References:

1- Ren, S., Wang, F., Gao, H., Han, X., Zhang, T., Yuan, Y., & Zhou, Z. (2024). Recent progress and future prospects of laccase immobilization on MOF supports for industrial applications. Applied Biochemistry and Biotechnology, 196(3), 1669-1684.

2- Wang, H., Tang, L. X., Ye, Y. F., Ma, J. X., Li, X., Si, J., & Cui, B. K. (2024). Laccase immobilization and its degradation of emerging pollutants: A comprehensive review. Journal of Environmental Management, 359, 120984.

3- Almulaiky, Y. Q., Alkabli, J., & El-Shishtawy, R. M. (2024). Improving enzyme immobilization: A new carrier-based magnetic polymer for enhanced covalent binding of laccase enzyme. International Journal of Biological Macromolecules, 282, 137362.

Multi-component reactions of spiroindeno[1,*2-b*]quinoxaline in the presence of nano catalyst

S.F Hojati*, A. Rezvani, M. Mahamed

Department of Chemistry, Hakim Sabzevari University, Sabzevar, 96179-76487 Iran

Keyword: Multi-component Synthesis, Spiroindene, Functionalized carbon nanotube

Introduction

CNT-COOH, or group-functionalized carbon nanotubes, are a type of modified carbon nanotube where carboxyl, hydroxyl or epoxy groups (-COOH) are attached to the surface of CNT. Due to the biological activities of spiroindenes, such as antiviral and anticancer properties, and also due to the advantages of multi-component reactions, it was considered to use a cheap, non-toxic, and efficient catalyst for the synthesis of these compounds. In this study, four-component reactions were used to synthesize spiro[indeno[1,2-*b*]quinoxaline derivatives in the presence of functionalized carbon nanotubes.

Method

First, carbon nanotube was functionalized by nitric acid to yield CNT-COOH. Then, the synthesis of spiro[indeno[1,2-*b*]quinoxaline derivatives was carried out in two steps. First, phenylenediamine (1 mmol) and ninhydrin (1 mmol) were stirred in ethanol (15 mL) at room temperature for 10 min, and in the second step, malononitrile (1 mmol) and dimedone (1 mmol) were added to the reaction mixture at 80 °C along with 0.01 g of functionalized carbon nanotube as catalyst. The progress of the reaction was monitored using TLC. Finally, the catalyst was separated from the reaction product by centrifugation and washed several times with cold water.

Result and discussion

The IR spectrum of CNT-COOH (Figure 1) clearly confirms the presence of oxygen moieties on the carbon nanotube. The broad band at 3425 cm^{-1} is due to O-H stretching vibrations. The absorption band at 1730 cm^{-1} belongs to the C=O stretching vibration. The C-O stretching vibration is observed at 1156 cm^{-1}.

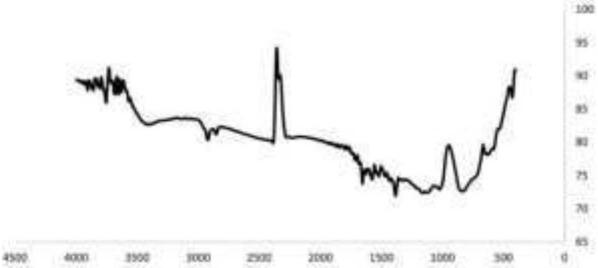

Figure 1. FT-IR spectrum of functionalized carbon nanotube (CNT-COOH)

After charactrization of CNT-COOH by FT-IR spectrum, its catalytic activity was incvestigated in the reaction of ninhydrin, phenylenediamine, malononitrile and dimedone to yield spiroindeno[1,2-*b*]quinoxallin (Scheme 1).

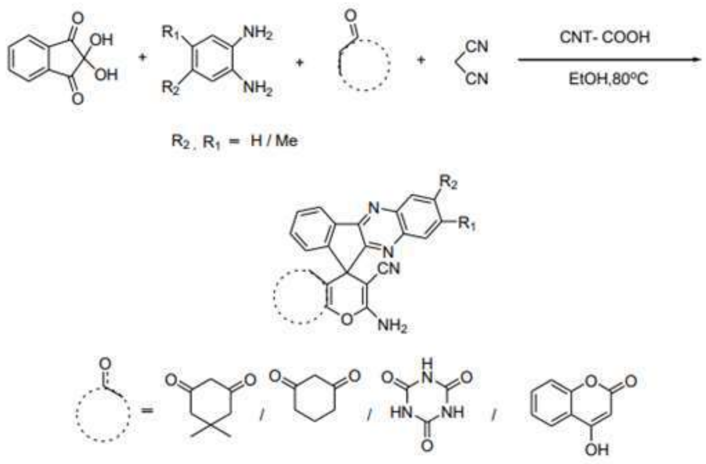

Scheme1. Synthesis of spiroindeno[1,2-*b*]quinoxallin derivatives in the presence of CNT-COOH catalyst

Reference:

1- Y. He, H. Guo, J. Tian, A simple three-component synthesis of spiro-pyran derivatives, *Journal of Chemical Research* **2011**, *35*, 1.

2- R. Singh, D. Bhardwaj, M.R. Saini, Recent advancement in the synthesis of diverse spiro-indeno[1,2-*b*] quinoxalines: a review, *RSC Advances* **2021**, *11*, 4760.

3- M. Salehpour, J. Azizian, H. Kefayati Clean synthesis of novel spiro[indene-2,2-[1,3,5]-oxathiazine]-1,3-diones in water, *Chinese Chemical Letters* **2017**, *28*, 1079.

The 30th Iranian Seminar of Organic Chemistry
February 7-9, 2025, Iran University of Science and Technology, Tehran, Iran

Extraction and determination of the organophosphorus pesticides in environmental samples by molecularly imprinted polymer using MEPS method and colorimetric detection

Arman Sharifi[a], Ramin Karimian*[a], Somayeh Payamani[b]

[a]*Chemical Injuries Research Center, Baqiyatallah University of Medical Sciences, Tehran, Iran.*

[b]*Department of Chemistry, University of Kurdistan, Sanandaj, Iran*

Keyword: organophosphorus pesticides, molecularly imprinted polymer, MEPS, colorimetric detection

Introduction: Residual pesticides-induced contaminated food products have become a global concern to food safety issues, health protection and public security [1,2]. Organophosphorus pesticides (OPPs) are widely used to improve agricultural products due to their effectiveness for eradicating insects [3]. Generally, cardiovascular diseases, asthma, dizziness, immunotoxicity, gastrointestinal disorders, nausea, impaired neurobehavioral functioning, cancer and reproduction ability reduction in men and even death have been reported for OPPs poisoning[4]. Although, a high level of 1 mg/kg has been set by the Food and Agriculture Organization of the United Nations for malathion in fruits. Therefore, the development of sensitive methods for the detection of organophosphate pesticides is essential.

Method: In this study, a system was developed for the extraction and colorimetric detection of malathion as a model organophosphate pesticide in environmental samples. In this regard, molecularly imprinted polymer was synthesized by sol-gel method using 3 aminopropyltriethoxysilane (APTES) as functional monomer and tetraethyl orthosilicate (TEOS) as crosslinker on glass powder substrate. Subsequently, the prepared adsorbent by microextraction in packed syringe (MEPS) method was used to extract malathion. Then, the extracted malathion was measured using a colorimetric detection method using silver nanoparticles. The mechanism of malathion detection is based on the aggregation of silver nanoparticles in the presence of malathion.

Results and Discussion: The prepared MIPs was characterized using Fourier-transform infrared spectroscopy (FTIR), field emission scanning electron microscopy (FESEM) and Thermogravimetric analysis (TGA). Different influencing parameters on extraction efficiency such as effect of the number of sample sorption/desorption cycles, type and volume of desorption solvent, pH of the sample solution and MIP amounts were optimized. Under optimal conditions, the colorimetric response of A_{555}/A_{400} was linear in the range of 0.01-5 mg/L. The detection limit of this method was 0.004 mg/L. The method was successfully applied for the detection of malathion in the environmental samples.

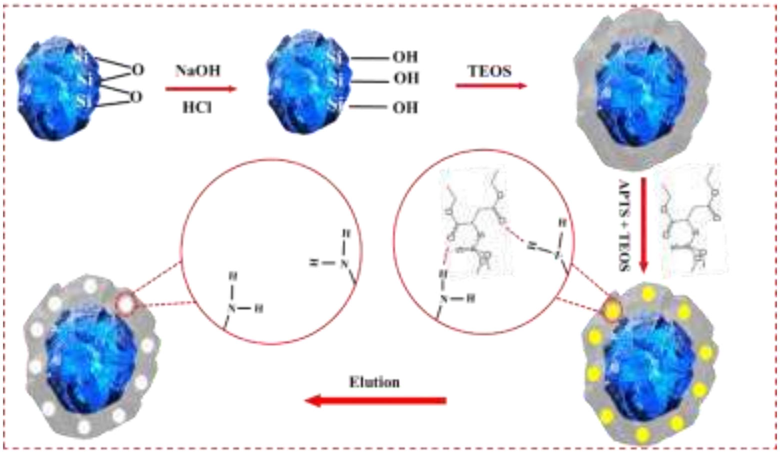

Scheme: Schematic diagram of malathion MIP preparation.

References:

[1] X. Li, P. Gan, R. Peng, C. Huang, and H. Yu, Determination of 23 Organophosphorous Pesticides in Surface Water Using SPME Followed by GC-MS, J. Chromatogr. Sci. 48, 183 (2010).

[2] R. Zhang, N. Li, J. Sun, and F. Gao, Colorimetric and Phosphorimetric Dual-Signaling Strategy Mediated by Inner Filter Effect for Highly Sensitive Assay of Organophosphorus Pesticides, J. Agric. Food Chem. 63, 8947 (2015).

[3] W. A. W. Ibrahim, H. R. Nodeh, and M. M. Sanagi, Graphene-Based Materials as Solid Phase Extraction Sorbent for Trace Metal Ions, Organic Compounds, and Biological Sample Preparation, Crit. Rev. Anal. Chem. 46, 267 (2016).

[4] E. Cequier, A. K. Sakhi, L. S. Haug, and C. Thomsen, Exposure to Organophosphorus Pesticides in Norwegian Mothers and Their Children: Diurnal Variability in Concentrations of Their Biomarkers and Associations with Food Consumption, Sci. Total Environ. 590, 655 (2017).

The 30th Iranian Seminar of Organic Chemistry
February 7-9, 2025, Iran University of Science and Technology, Tehran, Iran

Synthesis and characterization of xanthene derivatives catalyzed by a Metal-Organic framework Cu(BDC)

Hasti Tafti[a], Majid Rezaeivala[a,*], Ahmadreza Mousavi-zare[a]

[a] *Department of Chemical Engineering and Basic Sciences, Hamedan University of Technology, Hamedan 65155, Iran (email:mrezaeivala@hut.ac.ir).*

Keyword: Xanthene derivatives, Nanocatalyst , Green Chemistry, Cu-MOF.

Metal-organic frameworks (MOFs), a class of porous materials assembled from metal ions/clusters and organic ligands. MOFs have been utilized for many applications including gas storage, separations, chemical sensing, and drug delivery. In recent years, MOFs have demonstrated their potential application as heterogeneous catalysts, especially those using MOFs as a supporting matrix for metal nanoparticles (known as metal-MOFs) [1]. In this work we use Cu-MOF as nanocatalyst for synthesis and characterization of xanthene derivatives.

The catalyst Cu(BDC) was synthesized according to the literature procedure [2] and characterized by FT-IR, XRD, FE-SEM, TGA and TEM.

We have described a convenient and highly efficient synthesis of xanthene derivatives using Cu-MOF as a green and effective catalyst under solvent free condition. Excellent yields of product, short reaction time, mild reaction conditions, a simple workup procedure, and reusability of the catalyst are the important and valuable features of this catalyst. The resulting xanthene derivatives are of importance for organic and medicinal research. The products were characterized by FT-IR, 1H and ^{13}C NMR and melting point.

Scheme.Cu-MOF application

References:

[1]. Ghorbani-Vaghei, R., & Malaekehpoor, S. M. (2010). Facile One-Pot Synthesis of Tetrahydrobenzo [a] xanthene-11-one and Aryl-14 H-dibenzo [aj] xanthene. Organic Preparations and Procedures International, 42(5), 494-498.

[2]. Kassem, A. A., Abdelhamid, H. N., Fouad, D. M., & Ibrahim, S. A. (2019). Metal-organic frameworks (MOFs) and MOFs-derived CuO@ C for hydrogen generation from sodium borohydride. International Journal of Hydrogen Energy, 44(59), 31230-3١٢٣٨.

The 30th Iranian Seminar of Organic Chemistry
February 7-9, 2025, Iran University of Science and Technology, Tehran, Iran

Synthesis and characterization of some tetrahydrobenzopyrane derivatives catalyzed by a new magnetic nanocatalyst containing morpholine tags

Somayye Hasani[a], Majid Rezaeivala[a,*], Ahmadreza Mousavi-zare[a]

[a]*Faculty of Chemical Engineering and Basic Sciences, Hamedan University of Technology, Hamedan,65155, Iran (email:mrezaeivala@hut.ac.ir)*

Keyword: Magnetic nanocatalyst, Morpholine, Tetrahydrobenzopyran, Multicomponent reaction

Magnetic nanocatalysts labeled with morpholine are recognized as a novel tool in the field of chemical catalysis [1]. These nanocatalysts, by combining magnetic properties with the chemical characteristics of morpholine, provide easy separation and high efficiency in chemical reactions. The synthesized catalyst was examined using FT-IR, TGA, SEM, DLS, AFM, and TGA analysis. Tetrahydrobenzopyran derivatives are a group of heterocyclic compounds that are significant due to their extensive pharmaceutical and biological properties, such as anticancer, anti-inflammatory, anticoagulant, and anti-allergic activities [2].The magnetic nanocatalyst was synthesized by functionalizing Fe_3O_4 nanoparticles with a morpholine groups [1].

Tetrahydrobenzo pyran derivatives were synthesized with mentioned catalyst. The obtained data indicated that the products were synthesized with high efficiency and purity, short reaction time, mild conditions and easy separation of the catalyst by an external magnet are the superior advantages of this catalyst. The products were characterized by FT-IR, ^1H and ^{13}C NMR spectroscopy and melting point.

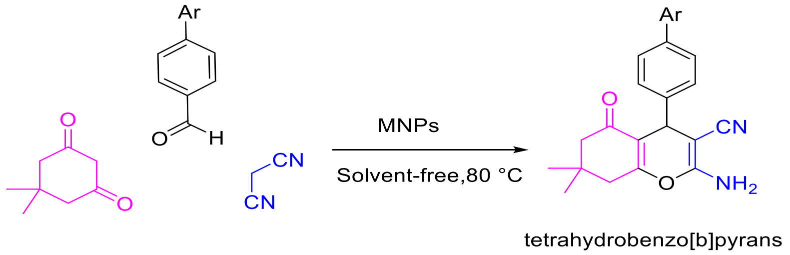

Scheme 1. Catalytic synthesis of tetrhydrobenzopyrane derivatives

References:

1. S. Kalhor, M. Yarie, M. Rezaeivala, and M. A. Zolfigol, " Novel magnetic nanoparticles with morpholine tags as multirole catalyst for synthesis of hexahydroquinolines and 2-amino-4, 6-diphenylnicotinonitriles through vinylogous anomeric-based oxidation" Research on Chemical Intermediates, 45 (2019) 3453-3480.

2. B. Maleki, H. Eshghi, M. Barghamadi, N. Nasiri, A. Khojastehnezhad, S. Sedigh Ashrafi, S., and O. Pourshiani, "Silica-coated magnetic $NiFe_2O_4$ nanoparticles-supported $H_3PW_{12}O_{40}$; synthesis, preparation, and application as an efficient, magnetic, green catalyst for one-pot synthesis of tetrahydrobenzo[b]pyran and pyrano[2,3-c]pyrazole derivatives" *Research on Chemical Intermediates*, 42 (2016) 3071-3093.

The 30th Iranian Seminar of Organic Chemistry
February 7-9, 2025, Iran University of Science and Technology, Tehran, Iran

Multi-component synthesis of spiro[indoline-3,4´-pyrano[2,3-*c*] pyrazole] using of $H_6P_2W_{15}Mo_3O_{62}$ catalyst

S. F. Hojati*, R. Shamsaei, F. Zeidabadinezhad

Department of Chemistry, Hakim Sabzevari University, Sabzevar, 96179-76487 Iran

Keyword: Heteropoly acid, Multi-component reaction, spiro[indoline-3,4´-pyrano[2,3-*c*] pyrazole]

Introduction:

Heteropoly anions are called heteropoly acids. These compounds are strong Brønsted acids and have two types of protons, indirect and direct. These protons are linked to the polyanion through strong bonds. Wells-Dawson's heteropoly acid (Scheme 1) has the general formula $[X_2M_{18}O_{62}]^{-6}$, in which the central X^{+n} atom is surrounded by a shelf of additional M atoms such as tungsten (VI), molybdenum or a mixture of these elements, each of which has MO_6 octahedral units. After the preparation and identification of $H_6P_2W_{15}Mo_3O_{62}$, it was used as a catalyst in the synthesis of spiro[indoline-3,4´-pyrano[2,3-*c*] pyrazole] derivatives.

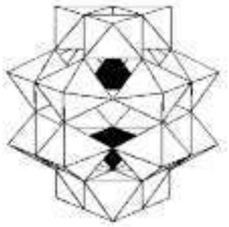

Scheme 1: The Wells- Dawson Structure

Method

synthesis of $H_6P_2W_{15}Mo_3O_{62}$

First, 5.7 gr of Na_2MoO_4 and 2 gr of Na_2WO_4 were dissolved separately in 16 and 5.2 ml of distilled water, then 0.575 gr of Na_2HPO_4 were dissolved in 2.5 ml of water. The three solutions were added together and heated to 100°C, then 4 ml of H_2SO_4 was slowly added to the solution. The resulting solution was kept for 8 hours at a temperature of 100 °C with stirring and the product was extracted with diethyl ether after cooling.

General method for the synthesis of spiro[indoline-3,4´-pyrano[2,3-*c*]pyrazole] in the presence of $H_6P_2W_{15}Mo_3O_{62}$ heteropoly acid

A mixture of hydrazine hydrate (1.5 mmol) and ethyl acetoacetate (1 mmol) along with 10 ml of water and catalyst (0.003 g) was poured into a 25 ml flask and stirred with a magnet for 10 minutes at room temperature. Then, isatin (1 mmol) and malononitrile (1 mmol) were added to the mixture and the progress of the reaction was followed by TLC. Then the product was separated by filtration and washed with distilled water.

Result and Discussion

$H_6P_2W_{15}Mo_3O_{62}$ was synthesized and successfully applied in the four- component condensation of isatin, malononitrile/ethylcyanoacetate, hydrazinehydrate and ethylaceto acetate. The corresponding spiro[indoline-3,4´-pyrano[2,3-*c*]pyrazole derivatives (Scheme 2) were generated in good to excellent yields. Short reaction times, high yields of products, easy work-up procedures, mild reaction condition in combination with non-toxicity, cheapness, efficiency and reusability of the catalyst are valuable advantages of the current work.

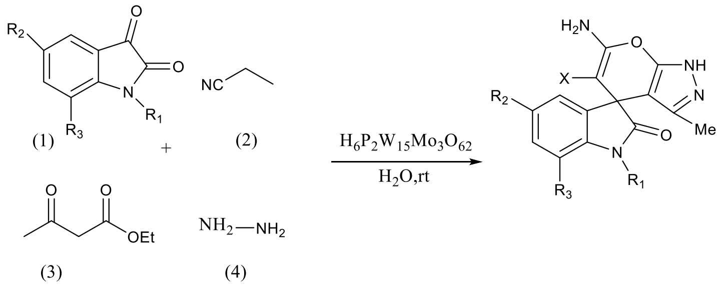

a)R_1=H,R_2=H,R_3=H,R_4=H,X=CN b)R_1=H,R_2=Cl,R_3=H,R_4=H,X=CN
c) R_1=H,R_2=Cl,R_3=H,R_4=Cl,X=CN d)R_1=H,R_2=Br,R_3=H,R_4=H,X=CN
e)R_1=H,R_2=NO_2,R_3=H,R_4=H,X=CN f)R_1=Me,R_2=H,R_3=H,R_4=H,X=CN
g)R_1=Bn,R_2=H,R_3=H,R_4=H,X=CN h)R_1=H,R_2=H,R_3=H,R_4=H,X=CO_2Et
j)R_1=H,R_2=Cl,R_3=H,R_4=H,X=CO_2Et k)R_1=H,R_2=Br,R_3=H,R_4=H,X=CO_2Et
l)R_1=H,R_2=Cl,R_3=H,R_4=Cl,X=CO_2Et m)R_1=H,R_2=NO_2,R_3=H,R_4=H,X=CO_2Et

Scheme 2. Synthesis of spiro[indoleine-3,4´-pyrano[2,3-*c*]pyrazole]derivatives in the presence of $H_6P_2W_{15}Mo_3O_{62}$

Reference:

١. S.F. Hojati, H. Raouf, Ionic liquid for one-pot synthesis of spiro[indoline-3,4′-pyrano[2,3-*c*]pyrazoles], *Organic Preparations and Procedures International* **2016**, *48*, 474.
٢. C. Wang, Y.H. Jiang, C.G. Yan, Convenient synthesis of spiro[indoline-3,4′-pyrano[2, 3-*c*]pyrazole] and spiro[acenaphthyl-3,4′-pyrano [2,3-*c*]pyrazoles] *via* four-component reaction, *Chinese Chemical Letters* **2015**, *26*, 889.
٣. G.A. Tsigdinos, Heteropoly compounds of molybdenum and tungsten, Springer, Berlin, Heidelberg, **1978**, 1.
٤. E. Rafiee, S. Eavani, Heterogenization of heteropoly compounds: a review of their structure and synthesis, *RSC Advance* **2016**, *6*, 46433.

The 30th Iranian Seminar of Organic Chemistry
February 7-9, 2025, Iran University of Science and Technology, Tehran, Iran

Preparation of polyurethanes based on acrylic polyols

Alireza Banan[a], Erfan Nourozpoor[a]

[a]Department of Chemistry, Faculty of Imam Hossein Comprehensive University, Tehran, Iran
bananjahromi@yahoo.com
[b]*Department of Chemistry, Faculty of Imam Hossein Comprehensive University, Tehran, Iran*
erfannourozpoor@gmail.com

Keywords: “TDI”, “DBTDL”, “polyurethane”, “acrylic polyols”

Polyurethanes (PUs) have been used extensively in coating industries because of their excellent abrasion resistance, low temperature flexibility, and high chemical, mechanical and physical properties [2]. The PU coatings are typically used for plastics, wood, aircraft topcoats, and automotive topcoats [1].

In this research, polyurethane coatings based on an acrylic resin and toluene diisocyanate (TDI) was prepared (Scheme 1) and the effect of preparation condition on the properties of the product was investigated. Dibutyl tin dilurate (DBTDL) was used as the catalyst and toluene was used as the solvent. The synthesis process was performed at different temperatures from 40 °C to 60 °C. It was found that by increasing the temperature, the synthesis process took place faster, but it also increases the possibility of the gelation and bubble formation. The formation of pin-holes has a negative effect on the properties of the prepared polyurethanes and decreases the tensile strength of the product.

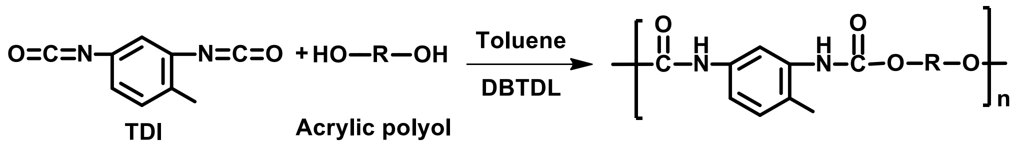

Scheme 1: Synthesis of polyurethane based on acrylic polyol and TDI.

References

1-Yadav, S., Zafar, F., Hasnat, A., & Ahmad, S. (2009). Poly (urethane fatty amide) resin from linseed oil—A renewable resource. Progress in Organic Coatings, 64(1), 27-32.

2-Ionescu, M. (2005). Chemistry and technology of polyols for polyurethanes. iSmithers Rapra Publishing.

The 30th Iranian Seminar of Organic Chemistry
February 7-9, 2025, Iran University of Science and Technology, Tehran, Iran

Preparation of Acrylic Resin

Alireza Banan[a], Erfan Nourozpoora

[a]Department of Chemistry, Faculty of Imam Hossein Comprehensive University, Tehran, ***Iranbananjahromi@yahoo.com***
[b]Department of Chemistry, Faculty of Imam Hossein Comprehensive University, Tehran, Iran
erfannourozpoor@gmail.com

Keywords: “acrylic resin”, “TEBAC”, “hydrogen peroxide”, “radical polymerization”

Acrylic resins have attracted much attention in automotive, construction, furniture and coating industries due to their unique features such as appropriate thermal properties, corrosion resistance, light stability, excellent mechanical properties and water resistance [1].

In this research, a low molecular weight acrylic resin containing hydroxyl groups was synthesized by free radical polymerization of ethyl acrylate and butyl acrylate monomers in toluene in the presence of hydrogen peroxide as an initiator (Scheme 1). However, since hydrogen peroxide is water soluble, it cannot be dissolved in the reaction medium. Thus, the polymerization also needs a phase transfer catalyst such as benzyltriethylammonium chloride (TEBAC) [2,3]. The polymerization reaction was carried out at different temperatures and different amounts of initiator in order to optimize the reaction condition and obtain the acrylic resin with desired structure and properties. The results revealed that the highest yield and the most appropriate molecular weight and functional groups were obtained at 100 °C using 1:5 ratio amount of the initiator to the solvent.

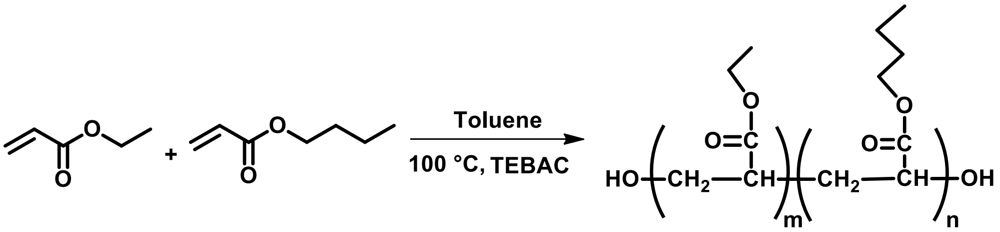

Scheme 1: The general scheme of acrylic resin synthesis.

References

1-Wang, L., Xu, F., Li, H., Liu, Y., & Liu, Y. (2017). Preparation and stability of aqueous acrylic polyol dispersions for two-component waterborne polyurethane. Journal of Coatings Technology and Research, 14, 215-223.

2-Tagle, L. H., Diaz, F. R., & Roncero, S. (1992). Polymerization by phase transfer catalysis. 14. Polyesters from terephthalic acid and related diacids with bisphenol A. Polymer international, 29(4), 265-268.

3-Thomas, J., Singh, V., & Jain, R. (2020). Synthesis and characterization of solvent free acrylic copolymer for polyurethane coatings. Progress in Organic Coatings, 145, 105677.

Synthesis of chiral (*R*)- and (*S*)-Betti bases and their applications in enantioselective Kharasch-Sosnovsky reaction

Mahvash Khosravy [a], Shiva Majidian [a], Saadi Samadi [a]*

[a] *Laboratory of Asymmetric Synthesis, Department of Chemistry, Faculty of Science, University of Kurdistan, Sanandaj, Iran. *E-mail: s.samadi@uok.ac.ir*

Keywords: Chiral Betti base, Chiral resolving reagent, Diastereomeric crystallization, Kharasch-Sosnovsky reaction, Chiral allylic ester.

Introduction:

The Betti reaction is one of the best-known multicomponent reactions, leading to the production of Betti bases. This kind of chiral ligand, due to its special structure, can chelate with metals, providing useful catalysts for a wide range of asymmetric syntheses [1-6]. Given the biological and chemical importance of chiral Betti bases, accurate methods for their separation are of great significance. Diastereomeric crystallization is a simple, scalable, and efficient method that typically uses natural (L)-tartaric acid as a chiral resolving reagent to prepare chiral Betti bases [1-6]. The oxidation of allylic C-H bonds in olefins with an oxidant in the presence of copper salts and chiral ligands, known as the enantioselective Kharasch-Sosnovsky reaction, is a powerful tool for the synthesis of chiral allylic esters [6, 7].

Method:

General procedure for synthesis of chiral Betti bases:

At first, 4-chlorobenzaldehyde was placed in a round bottom flask containing EtOH, *β*-naphthol, and NH_4OAc and stirred at room temperature. The resulting white precipitate (tautomeric mixture) was filtered and washed with cold ethanol. Then the obtained tautomeric mixture *was hydrolyzed* with dilute hydrochloric acid to give 1-(a-Amino-4-chloro benzyl)-2-naphthol. HCl salt. In continue a solution of Na_2CO_3 (2 M) was dropwise added to a suspension of 1-(a-Amino-4-chloro benzyl)-2-naphthol. HCl salt in water cooled in an ice bath. The aqueous phase was extracted by Et_2O and the racemic Betti base was produced. In the final step, a solution of (2*R*, 3*R*)-tartaric acid in ethanol: methanol mixture was added slowly to a solution of the racemic Betti base in ethanol and stirred. The obtained *S-RR* and *R-RR* diastereomeric salts were treated with aqueous solution of Na_2CO_3 (2 M) and stirred at room temperature (Scheme 1). The mixture was extracted with diethyl ether and chiral Betti bases were obtained in high yields [1-6].

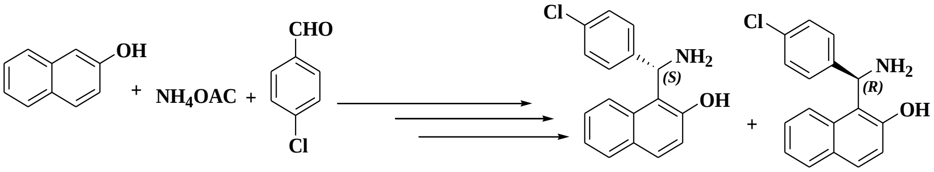

Scheme 1. Synthesis of chiral Betti bases

General procedure for asymmetric Kharasch-Sosnovsky reaction:

Under a nitrogen atmosphere, a 10 mL flame-dried Schlenk tube was charged with dried acetonitrile, $Cu(CH_3CN)_4PF_6$, and chiral Betti base and stirred at room temperature. Then alkene, benzoic acid derivatives and *tert*-Butyl hydroperoxide were added portionwise to the solution, respectively. When the reaction was completed, NH_4OH was added, and the aqueous layer was extracted with ethyl acetate (Scheme 2). Finally, purification of the residue by silica gel column chromatography resulted in the corresponding chiral allylic ester [6, 7].

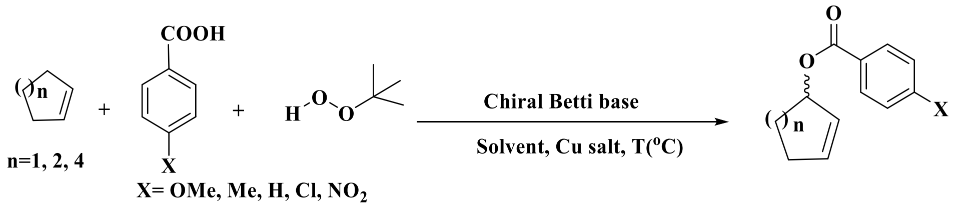

Scheme 2. Asymmetric allylic oxidation of olefins in the presence of chiral Betti bases

Results and Discussion:

A mixture of an acyclic Schiff base and two C-3 epimeric 1,3-naphthoxazine that are in equilibrium with each other was prepared by a three-component reaction of *β*-naphthol, 4-chlorobenzaldehyde, and ammonium acetate in ethanol at room temperature. Analyzing this mixture by ^{1}HNMR spectroscopy, revealed that the population of the *trans* isomer is higher than both the imine and *cis* forms, and also the ratio of the imine is more than the *cis* isomer. Then by acidic hydrolysis, all the isomers were converted into a stable racemic Betti base salt. The resulting salt was then neutralized with an alkali solution to give the racemic-free Betti base. Then, its enantiomers were separated by the diastereomeric crystallization method using (L)- tartaric acid. Finally, the copper complexes of the synthesized chiral Betti bases were used in the enantioselective Kharasch-Sosnovsky reaction, resulting in good yields of chiral allylic esters with moderate enantioselectivity.

References:

[1] Szatmari, I., Fulop, F., *Curr. Org. Chem.*, 2004, *1*, 155.
[2] Cardellicchio, C., Capozzi, M. A. M., Naso, F. Tetrahedron: Asymmetry, 2010, *21*, 507.
[3] Verkade, J. M. M., Van Hemert, L. J. C., Quaedflieg, P. J. L. M., Rutjes, F. P. J., *Chem. Soc. Rev.*, **2008**, *37*, 29.
[4] Szatmari, I., Martinek, T. A., Lazar, L., Koch, A., Kleinpeter, E., Neuvonen, K., Fülop, F. *J. Org. Chem.*, **2004**, *69*, 3645.
[5] Cimarelli, C., Mazzanti, A., Palmieri, G., Volpini, E., *J. Org. Chem.*, **2001**, *66*, 4759.
[6] Sehhat,Z., Mansoori, S., Arvinnezhad, H., Naghdi,Y., Samadi, S. *Mol. Catal.*, **2023**, *538*, 113011.
[7] Rezaei, A., Zheng, H., Majidian, S., Samadi, S., & Ramazani, A., *ACS Appl. Mater. Interfaces*, **2023**, *15*, 54373.

The 30th Iranian Seminar of Organic Chemistry
February 7-9, 2025, Iran University of Science and Technology, Tehran, Iran

Selenophenes and Selenazoles as Selenium-Containing Heterocycles: Synthesis and Characterization (A Review)

Ali Shiri*

Department of Chemistry, Faculty of Science, Ferdowsi University of Mashhad, Mashhad, Iran

* *E-mail:* alishiri@um.ac.ir

Keywords: Selenophene, Selenazole, Heterocyclization

Selenium-containing heterocycles have emerged as versatile frameworks with promising applications in medicinal chemistry due to their unique physicochemical properties and biological activities. This abstract consolidates our recent advanced methodologies for synthesizing selenium-enriched fused heterocycles, focusing on selenophene and selenazoles.

The first approach highlights the synthesis of selenopheno[2,3-e][1,2,4]triazolo[1,5-c]pyrimidines via Dimroth rearrangement, starting from hydrazinyl-selenopheno precursors. This multistep protocol employs electrophilic carbons (orthoesters and carbon disulfide) followed by S-alkylation to produce highly functionalized tricyclic compounds. [1] The other approach investigates the antioxidant properties of selenium-fused chalcogenophenes, specifically selenopheno[3,2-d]pyrimidines. Employing a base-promoted cascade cyclization of 3-amino-2,4-dicyano-5-(pyrrolidin-1-yl)selenophene with phenyl isothiocyanate, followed by S-alkylation, a series of functionalized derivatives were synthesized.[2] A complementary study extends this methodology to synthesize [1,3]selenazolo[5,4-e][1,2,4]triazolo[1,5-c]pyrimidines through acidic and basic Dimroth rearrangements. Starting from a selenazolo-pyrimidine scaffold, the strategy involves hydrolysis, cyclization, and selective alkylation.[3]

These studies collectively highlight the immense potential of selenium-containing heterocycles in anticancer and antioxidant applications, demonstrating the influence of structural modifications on bioactivity. The findings contribute to the growing interest in selenium-enriched frameworks for developing innovative therapeutic agents targeting oxidative stress, cancer, and other diseases.

References:

١) Kohandel O, Sheikhi-Mohammareh S, Oroojalian F, Memariani T, Mague J, Shiri A. A Dimroth rearrangement approach for the synthesis of selenopheno [2, 3-e][1, 2, 4] triazolo [1, 5-c] pyrimidines with cytotoxic activity on breast cancer cells. Molecular diversity. 2022 Jun;26(3):1621-33.

٢) Farzamnezhad I, Sheikhi-Mohammareh S, Beyzaei H, Yarmohammadi E, Shiri A. Synthesis of Novel DPPH-Free Radical Scavenger Se-Containing Fused Chalcogenophenes: 2-Alkyl-7-Cyano-4-Imino-3-Phenyl-6-(pyrrolidin-1-yl)-3, 4-Dihydroselenopheno [3, 2-d] Pyrimidines. Polycyclic Aromatic Compounds. 2024 Feb 7;44(2):807-17.

٣) **Sheikhi-Mohammareh S, Shiri A,·Mague J,** Dimroth rearrangement-based synthesis of novel derivatives of [1,3] selenazolo[5,4-*e*][1,2,4]triazolo[1,5-*c*]pyrimidine as a new class of selenium-containing heterocyclic architecture. Molecular Diversity, 2022, 26(2), 923–937.

The 30th Iranian Seminar of Organic Chemistry

February 7-9, 2025, Iran University of Science and Technology, Tehran, Iran

Green Synthesis of Copper Oxide Nanoparticles Using Oak Fruit Peel Extract and Their Catalytic Efficiency in 4-Nitrophenol Reduction

Authors: Shirin Havasipour, Saeid Taghavi Fardood*, Ali Naghipour*

Department of Chemistry, Faculty of Science, Ilam University, Ilam, Iran

[*]*E-mail: s.taghavi@ilam.ac.ir*

Keyword: Green Synthesis, Oak Fruit Peel Extract, 4-Nitrophenol Reduction

The exponential growth of the global population, agriculture, and industry has significantly increased environmental pollution, impacting air, soil, and water quality. Industrial wastewater contains toxic organic and inorganic pollutants, including synthetic dyes, hydrocarbons, aromatic nitro compounds, and phenols, originating from industries such as textiles, pharmaceuticals, and pesticides. Among these, 4-nitrophenol (4-NP) is a hazardous, non-biodegradable compound classified by the EPA as a priority pollutant due to its toxicity, water solubility, and resistance to oxidation (Hammett constant: 0.778) [1]. However, it can be reduced to its amino derivative, 4-aminophenol (4-AP), which is commercially valuable in the production of analgesics and antipyretics (e.g., acetaminophen, finasteride), as well as in photographic developers, plastics, corrosion inhibitors, fuel anti-corrosion lubricants, and various fine chemicals [2,3]. In this study, CuO nanoparticles were synthesized using the green sol-gel method, utilizing oak fruit peel extract as a natural stabilizing and reducing agent. The synthesized CuO nanoparticles were characterized by FTIR, XRD, TEM, FESEM, EDX, and BET techniques. Their catalytic activity was evaluated for the reduction of 4-nitrophenol to 4-aminophenol in the presence of $NaBH_4$. The reaction progress was monitored using UV-Vis spectroscopy. This study highlights the eco-friendly synthesis of nanoparticles, efficient catalysis, rapid reaction, and sustainable conditions.

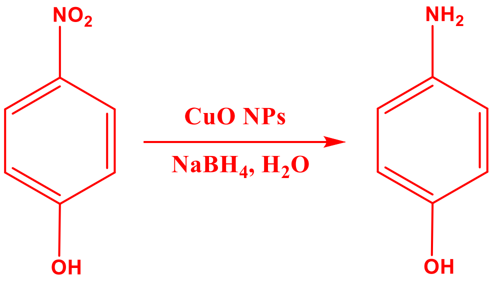

Scheme: Catalytic reduction of 4-nitrophenol to 4-aminophenol using CuO nanoparticles.

References

[1]. Liu, W.-J., Tian, K., Jiang, H., Yu, H.-Q.: *Green Chem.*, 2014, **16**, 4198.
[2]. Coşkuner Filiz, B.: *Adv. Powder Technol.*, 2020, **31**, 3845.
[3]. Sharma, A., Dutta, R.K., Roychowdhury, A., Das, D., Goyal, A., Kapoor, A.: *Appl. Catal., A*, 2017, 543, 257.

The 30th Iranian Seminar of Organic Chemistry
February 7-9, 2025, Iran University of Science and Technology, Tehran, Iran

Green Synthesis of SnO_2 Nanoparticles *via* Pomegranate Seed Extract for Efficient Dye Degradation

Authors: Shirin Havasipour, Jeyran Shams Beiranvand, Saeid Taghavi Fardood*, Ali Naghipour*

Department of Chemistry, Faculty of Science, Ilam University, Ilam, Iran

[*]*E-mail: s.taghavi@ilam.ac.ir*

Keyword: Green Synthesis, Tin Oxide Nanoparticles, Dye Degradation

Over the past few years, advances in nanoscience and nanotechnology have prompted high interest in semiconductor metal oxide nanoparticles for their photocatalytic capabilities in filtering out harmful contaminants from water and environment. The direct release of untreated industrial effluents into water bodies remains a critical environmental issue. Such wastes typically include non-biodegradable dyes, organic pollutants, and heavy metals, which are common because of their high use in cosmetics, paper, leather, textiles, printing, dyeing, and pharmaceuticals [1]. Thus, separating these chronic pollutants from wastewater to make it reuseable is a significant undertaking. Organic pollutants can be degraded into non-toxic molecules through photocatalysis under visible or ultraviolet light irradiation in the presence of an appropriate photocatalyst. This method is sustainable, cost-effective, energy-efficient, and generates minimal harmful by-products [2]. Among various semiconductor metal oxide nanoparticles, SnO_2 NPs are extensively employed as effective photocatalysts, owing to their abundance of active sites, high light absorption efficiency, and large surface area [3].

In this study, SnO_2 nanoparticles were synthesized via a green sol-gel method using pomegranate seed extract as a natural precursor. The synthesized nanoparticles were thoroughly characterized using various analytical techniques, including UV-Vis-DRS, BET, XRD, FESEM, TEM, and EDX. The photocatalytic activity of the nanoparticles for the degradation of congo red dye under visible light irradiation was investigated by varying the initial dye concentration, photocatalyst dosage, and irradiation time. The results demonstrated the significant ability of SnO_2 nanoparticles to effectively degrade congo red dye. This green synthesis method offers several advantages, including cost-effectiveness, simplicity, shorter processing time, environmental friendliness, and the potential for scalable production, making it a promising approach for dye degradation.

References

[1] V.V. Gawade, S.B. Teli, S.R. Sabale, R.V. Dhabbe, K.S. Dhanavade and K.M. Garadkar, *Res. Chem. Intermed.*, **2024**, *50*, 323.
[2] K. Gangwar and P. Jeevanandam, *J. Mol. Struct.*, **2023**, *1285*, 135423.
[3] D. Borah, P. Saikia, J. Rout, D. Gogoi, N.N. Ghosh and C.R. Bhattacharjee, *Mater. Today Sustain.*, **2024**, *26*, 100770.

The 30th Iranian Seminar of Organic Chemistry
February 7-9, 2025, Iran University of Science and Technology, Tehran, Iran

Efficient Photocatalytic Reduction of Cr(VI) Using Ce-BDC Immobilized on PVDF Film for Water Treatment

Zahra Valizadeh, Mohammad Hosseini, Vahid Safarifard[*]

Department of Chemistry, Iran University of Science and Technology, vsafarifard@ iust.ac.ir

Keywords: Photocatalysis, Metal-Organic Frameworks, Hexavalent chromium, Composite film.

Efficient and recyclable water treatment technologies are crucial for the practical removal of (Cr(VI)) from wastewater [1]. While metal-organic frameworks are widely used in water treatment due to their stability and multiple active sites, their powdered form presents challenges in reclamation, secondary pollution, and aggregation [2, 3]. This study addresses these issues by successfully loading Ce-based MOF onto a polyvinylidene fluoride (PVDF) film using the phase inversion method, resulting in a highly efficient photocatalyst for Cr(VI) reduction. The Ce-BDC/PVDF composite film offers two distinct advantages over powdered forms: enhanced process efficiency and stability, and minimized catalyst loss and recovery energy requirements [4]. The prepared photocatalyst demonstrated the ability to reduce 95.99% of chromium in solution within 120 min at pH 2 under visible light irradiation. Comprehensive characterization using XRD and FT-IR confirmed the formation of a composite structure, which effectively prevented charge carrier recombination and enhanced photocatalytic performance.

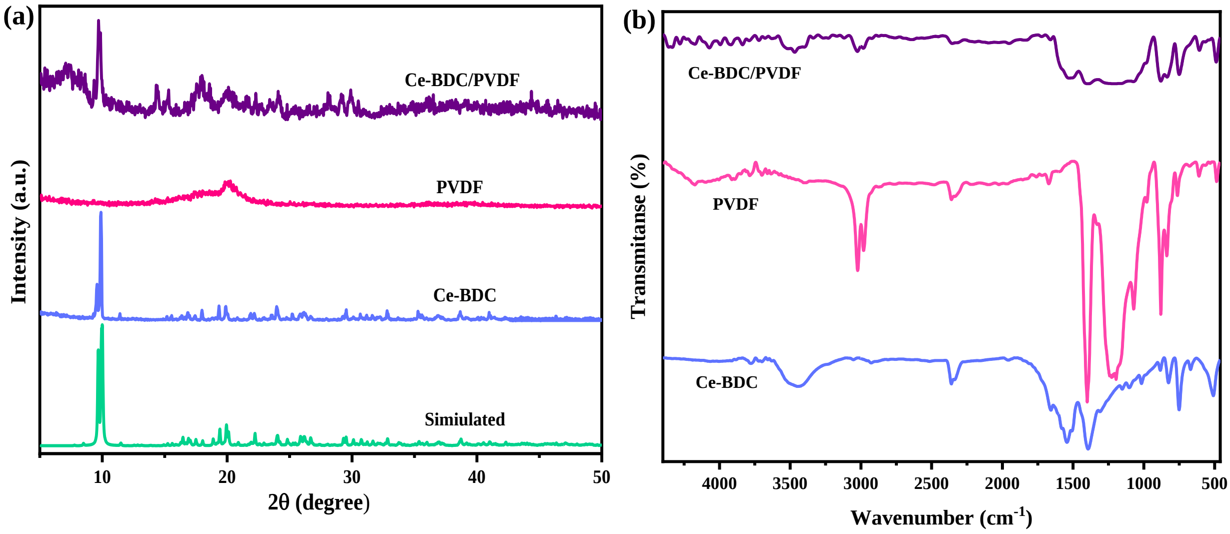

(a) PXRD patterns of Ce-BDC, PVDF and Ce-BDC/PVDF; **(b)** ATR spectra of Ce-BDC, PVDF and Ce-BDC/PVDF.

Refrences:

1. Zhang, Q., et al., *A porous Zr-cluster-based cationic metal–organic framework for highly efficient* $Cr_2O_7^{2-}$ *removal from water*. Chemical Communications, 2015. **51**(79): p. 14732-14734.
2. Dong, J., S.-L. Hou, and B. Zhao, *Bimetallic lanthanide-organic framework membranes as a self-calibrating luminescent sensor for rapidly detecting antibiotics in water*. ACS applied materials & interfaces, 2020. **12**(34): p. 38124-38131.
3. Kalaj, M., et al., *MOF-polymer hybrid materials: from simple composites to tailored architectures*. Chemical reviews, 2020. **120**(16): p. 8267-8302.
4. Saha, D., T.J. Hoinkis, and S.E. Van Bramer, *Electrospun, flexible and reusable nanofiber mat of graphitic carbon nitride: Photocatalytic reduction of hexavalent chromium*. Journal of colloid and interface science, 2020. **575**: p. 433-442.

Preparation and characterization of pH-sensitive nanocomposites based on metal-organic frameworks and carboxymethyl cellulose for the removal of pharmaceutical pollutants from wastewater

Mahdiyeh Ahmadi[a], Mohammad Hossein Alizadeh[a], Hassan Namazi[a,b*]

[a]*Polymer Research Laboratory, Department of Organic and Biochemistry, Faculty of Chemistry, University of Tabriz, Tabriz, Iran.*
[b]*Research Center for Pharmaceutical Nanotechnology, Biomedicine Institute, Tabriz University of Medical Science, Tabriz, Iran.*

Keywords: Water treatment; Magnetite; Hydrogel; Carboxymethyl cellulose; Nanocamposite.

Introduction

Water is one of the most fundamental and essential natural resources on Earth, crucial for the survival of all living organisms and human development. However, water pollution from various contaminants poses a serious threat to ecosystems, particularly impacting human life. Therefore, it is vital to develop and synthesize materials capable of removing these pollutants from water. One of the most cost-effective and accessible methods for water purification is the use of adsorbents. This research aims to synthesize a nanocomposite that includes a metal-organic framework, magnetic iron nanoparticles, and carboxymethyl cellulose, creating an affordable and biodegradable adsorbent for the removal of the cationic drug amiodarone [1].

Method

Initially, a magnetic metal-organic framework was prepared using $AgNO_3$ and $Cu(NO_3)_2$, along with the ligand 1,3,5-benzene tricarboxylic acid. Magnetic iron nanoparticles were synthesized through an in situ hydrothermal method. Carboxymethylcellulose polysaccharide and a Fe^{3+} crosslinker were used to create pH-sensitive nanocomposites designed for the drug removal of the cationic amiodarone [2].

Results and discuss

The removal percentages under fully optimal conditions for the adsorbents (5%)M/MOF(Cu-Ag)@CMC, (10%)M/MOF(Cu-Ag)@CMC, and (15%)M/MOF(Cu-Ag)@CMC were 64%, 66%, and 68%, respectively. Based on these results, the nanocomposite (5%)M/MOF(Cu-Ag)@CMC exhibits a shorter optimal contact time but has a lower removal percentage. In contrast,

---

[*] Corresponding author: P.O. Box 51666, Tel: +98 4133393121, Fax: +98 4133340191, Email:namazi@tabrizu.ac.ir, ORCID: http://orcid.org/0000-0002-1977-4677.

(15%)M/MOF(Cu-Ag)@CMC has a longer optimal contact time and a higher removal percentage. Additionally, the pH range for the drug when using (5%)M/MOF(Cu-Ag)@CMC is broader than that of the other nanocomposites. Therefore, the choice of adsorbent should be based on the specific conditions present.[3]

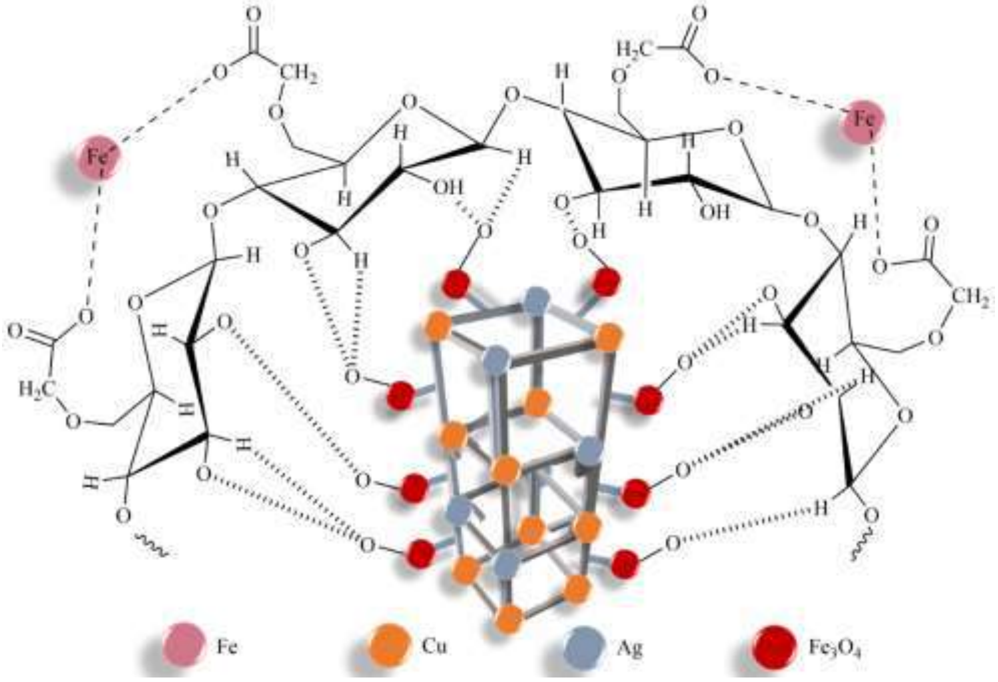

Scheme: Nanocamposite structure ((X%)M/MOF(Cu-Ag)@CMC).

References:

[1] B.S. Rathi, P.S. Kumar, D.-V.N. Vo, Critical review on hazardous pollutants in water environment: Occurrence, monitoring, fate, removal technologies and risk assessment, Science of the Total Environment 797 (2021) 149134.
[2] V.V.e. Butova, M.A. Soldatov, A.A. Guda, K.A. Lomachenko, C. Lamberti, Metal-organic frameworks: structure, properties, methods of synthesis and characterization, Russian Chemical Reviews 85(3) (2016) 280.
[3] N. Stock, S. Biswas, Synthesis of metal-organic frameworks (MOFs): routes to various MOF topologies, morphologies, and composites, Chemical reviews 112(2) (2012) 933-969.

Theoretical evaluation of Al-doped biphenylene nanosheet sensing properties toward gamma-butyrolactone

Lida Asadi 1*[a], Zohreh Saadati 2[b], · Mahboobeh Salehpour 3*[C]

Department of Chemistry, Omidiyeh Branch, Islamic Azad University, Omidiyeh, Iran

Keyword: biphenylene nanosheet, doping, gamma-butyrolactone, gamma-hydroxybutyrate, sensor, density functional theory (DFT).

Introduction

The rise of carbon-based 2D materials, like graphene, has driven interest in biphenylene nanosheets (BPH) due to their unique structural and electronic properties. Recently synthesized on gold substrates, BPH is composed of a periodic arrangement of four-, six-, and eight-membered carbon rings and exhibits metallic conductivity [1-5].

Gamma-butyrolactone (GBL), a precursor to gamma-hydroxybutyrate (GHB), is widely used in industry but poses risks as a drug of abuse. Detecting GBL with high sensitivity and selectivity remains a critical challenge [6]. This study evaluates the potential of pristine and Al-doped BPH nanosheets for GBL sensing using DFT methods**.**

Methods

The calculations were performed using the B3LYP functional and the 6-31+G(d) basis set, with dispersion corrections (DFT-D3). Adsorption energies (Eads) and electronic properties such as HOMO-LUMO gap (Eg) and charge transfer were calculated. Al doping was modeled by replacing a single carbon atom in BPH with aluminum.

Results and Discussion

Pristine BPH for GBL Sensing

The pristine BPH exhibited weak interaction with GBL, as evidenced by a low Eads (−12.30 kcal·mol^{-1}) and minimal changes in Eg (3.06 eV to 3.05 eV). These results indicate that BPH lacks the necessary sensitivity for GBL detection.

Enhanced Properties via Al Doping

Al doping introduced structural distortions and improved the electronic reactivity of BPH. The Eg of AlBPH decreased from 3.06 eV to 2.77 eV. Upon GBL adsorption, the Eads increased to −24.8 kcal·mol^{-1}, accompanied by a 23.7% reduction in Eg, enhancing the conductivity and sensitivity of the material.

Selectivity Toward GBL

AlBPH showed selective sensing capabilities for GBL. While the Eads for GHB was slightly higher (−29.2 kcal·mol^{-1}), the electronic response, particularly the Eg reduction, was more pronounced for GBL. This highlights AlBPH's potential as a selective nanosensor for GBL detection.

Results and discussion

This study demonstrated the feasibility of Al-doped biphenylene nanosheets as highly sensitive and selective sensors for gamma-butyrolactone detection. The substantial enhancement in adsorption energy and electronic response upon doping establishes a strong foundation for experimental validation and practical application in advanced sensing technologies [7-9].

References:

[1] Q. Fan, L. Yan, M.W. Tripp, O. Krejčí, S. Dimosthenous, S.R. Kachel, M. Chen, A.S. Foster, U. Koert, P. Liljeroth, Biphenylene network: A nonbenzenoid carbon allotrope, Science, 372 (2021) 852-856.
[2] M.A. Hudspeth, B.W. Whitman, V. Barone, J.E. Peralta, Electronic properties of the biphenylene sheet and its one-dimensional derivatives, ACS nano, 4 (2010) 4565-4570.
[3] P.A. Denis, Stability and electronic properties of biphenylene based functionalized nanoribbons and sheets, The Journal of Physical Chemistry C, 118 (2014) 24976-24982.
[4] H. Ge, G. Wang, Y. Liao, A theoretical investigation on the transport properties of armchair biphenylene nanoribbons, Chemical Physics Letters, 648 (2016) 97-101.
[5] P.A. Denis, F. Iribarne, Hydrogen storage in doped biphenylene based sheets, Computational and Theoretical Chemistry, 1062 (2015) 30-35.
[6] R. Beck, S. Mimica Matanović, L. Zibar, Gamma-hydroxybutyric acid, gamma-butyrolactone, and 1, 4-butanediol addiction: a serious health threat, Arhiv za higijenu rada i toksikologiju, 70 (2019) 149-150.
26.
[7] J. Beheshtian, M. Noei, H. Soleymanabadi, A.A. Peyghan, Ammonia monitoring by carbon nitride nanotubes: a density functional study, Thin solid films, 534 (2013) 650-654.
[8] E. Cagatay, P. Köhler, P. Lugli, A. Abdellah, Flexible capacitive tactile sensors based on carbon nanotube thin films, IEEE Sensors Journal, 15 (2015) 3225-3233.
[9] J. Blakemore, Solid State Physics, 2 nd, Edition by WB Saunders Company, (1974).

The 30th Iranian Seminar of Organic Chemistry
February 7-9, 2025, Iran University of Science and Technology, Tehran, Iran

Transition Metal-Decorated MgO Nanocages as Drug Carriers for the Chlormethine Drug

Lida Asadi 1*[a], Mahboobeh Salehpour 1[a], Zohreh Saadati 1[a], Asadollah Joata Bayrami 2[b]

[a] *Department of Chemistry, Omidiyeh Branch, Islamic Azad University, Omidiyeh, Iran*

[b] *Department of Basic Science, Omidiyeh Branch, Islamic Azad University, Omidiyeh, Iran*

Keyword: Metal oxide nanocages; transition metal-decorated nanostructures; density functional theory; chlormethine; targeted drug delivery; biosensors.

Introduction

Chlormethine (ClM) is an effective anticancer drug but causes adverse effects like bone marrow suppression and nausea [1-2]. Nanocarriers such as metal oxide nanocages offer solutions to enhance drug efficacy and minimize toxicity due to their high surface area, biocompatibility, and tunable properties. Among these, MgO nanocages, decorated with transition metals like Ni, Pd, and Pt, present promising opportunities in drug delivery by altering electronic properties and enabling controlled drug release [3]. DFT calculations provide valuable insights into drug-nanocarrier interactions, enabling optimization of nanostructures for better pharmacokinetics.

Computational details

All calculations employed the M06-2X functional with LANL2DZ and 6-311G(d,p) basis sets using Gaussian 09 software[4-5]. Vibrational frequency calculations confirmed structural stability, while molecular electrostatic potential (MEP) and natural bond orbital (NBO) analyses elucidated electronic behaviors. Adsorption energy, Gibbs free energy, and enthalpy were calculated to evaluate the nanocage-drug interactions [6].

Results and discussion

1. Structure and Electronic Properties

MgO nanocages exhibit a robust structure with a HOMO-LUMO energy gap (Eg) of 4.87 eV, indicating moderate chemical reactivity. Transition metal decoration (Ni, Pd, Pt) alters the nanocage properties, significantly influencing their electronic conductivity and reactivity:

- **Ni-MgO**: Decreases Eg to 4.76 eV, enhancing conductivity.
- **Pd-MgO**: Increases Eg by 10% (5.36 eV), suitable for ClM detection.
- **Pt-MgO**: Exhibits the largest Eg (5.70 eV), offering stability.

2. Adsorption Behavior

MEP analysis identified the reactive sites of ClM and TM-MgO nanocages. Adsorption of ClM involves non-covalent interactions:

- **Ni-MgO**: Moderate adsorption energy (-19.8 kcal/mol) ensures controlled release.
- **Pd-MgO**: Strongest adsorption (-29.8 kcal/mol), ideal for detection applications.
- **Pt-MgO**: Balanced interaction (-22.5 kcal/mol) with stable drug attachment.

3. Charge Transfer and Stability

NBO analysis reveals minor charge transfers (0.17–0.18 |e|) between ClM and nanocages, favoring reversible drug binding. Stabilization energies indicate weak donor-acceptor interactions, ensuring efficient drug release without compromising the nanocarrier's structure.

4. Drug Delivery Implications

The findings suggest that TM-MgO nanocages can enhance ClM's therapeutic performance by improving delivery efficiency and minimizing toxicity. Ni-MgO demonstrates significant potential for improving pharmacokinetics, while Pd-MgO can serve as a reliable Φ-type sensor for monitoring ClM levels.

Conclusions

Transition metal-decorated MgO nanocages hold significant promise as multifunctional platforms for drug delivery and biosensing. Future studies could explore their practical applications, focusing on in vitro and in vivo experiments to validate these computational insights. The combination of biocompatibility, enhanced electronic properties, and efficient drug adsorption highlights their potential in advanced cancer therapeutics.

References

[1] L.J. Geskin, M. Bagot, E. Hodak, E.J. Kim, Dermatology and Therapy 11 (2021) 1085.
[2] U. Wehkamp, M. Ardigò, E. Papadavid, C. Querfeld, N. Nikbakht, Advances in Therapy 39 (2022) 3979.
[3] S. Saha, M. Ali, M. Khaleque, M. Bacchu, M.A.S. Aly, M. Khan, Journal of Drug Delivery Science and Technology (2023) 104728.
[4] M. Frisch, F. Clemente, Scalmani, V. Barone, B. Mennucci, GA Petersson, H. Nakatsuji, M. Caricato, X. Li, HP Hratchian, AF Izmaylov, J. Bloino, G. Zhe (2009) 20.
[5] R. Dennington, T. Keith, J. Millam, (2009).
[6] S. Kaviani, S. Shahab, M. Sheikhi, V. Potkin, H. Zhou, Computational and Theoretical Chemistry 1201 (2021) 113246.

The 30th Iranian Seminar of Organic Chemistry
February 7-9, 2025, Iran University of Science and Technology, Tehran, Iran

Synthesis of chiral bisoxazoline ligands and their application in the simultaneous dehydrogenation and enantioselective allylic oxidation of alkanes to produce chiral allylic esters

Shiva Majidian[a], Saadi Samadi[a]*

[a] *Laboratory of Asymmetric Synthesis, Department of Chemistry, Faculty of Science, University of Kurdistan, Sanandaj, Iran. *E-mail: s.samadi@uok.ac.ir*

Keywords: Bisoxazoline, Chiral ligand, Dehydrogenation, allylic oxidation, Chiral allylic ester.

Introduction: Chirality has been one of the most important topics in the field of applied sciences, including medicine, pharmacy, environment, etc. Chiral compounds have different enantiomers, which usually have different biological activities and pharmacological properties. One way to access one of the enantiomers of chiral compounds is asymmetric synthesis and the use of chiral catalysts. Many catalysts have been designed and synthesized for this purpose, among which oxazoline-based ligands have very high catalytic capabilities and, as a class of efficient and powerful ligands, are increasingly and very seriously involved in asymmetric transformations. synthesis of chiral allylic esters is among the most important of these transformations [1-4]. These compounds are important intermediate and structural units in bioactive and medical molecules [5]. There are well-known methods to access these chiral compounds, but an interesting and rare reaction could be a combination of two well-known reactions involving the dehydrogenation of alkanes and the allylic oxidation of alkenes simultaneously [6, 7]. There is also no report on the use of chiral catalysts in this type of reaction to induce chirality.

Method:

Synthesis of **chiral bisoxazoline ligands** was carried out in several steps, as described below:

In the **first** step, chiral amino acids were reduced to the corresponding amino alcohols in a round-bottom flask under nitrogen atmosphere using sodium borohydride and iodine in tetrahydrofuran under reflux conditions.

In the **second** step, chiral bishydroxyamides were synthesized; for this purpose, 5-nitroisophthalic acid was converted to the diacyl derivative using thionyl chloride and a catalytic amount of *N*,*N*-Dimethylformamide (DMF) in dichloromethane, and then this mixture was slowly added to a solution of chiral amino alcohols and triethylamine in dichloromethane at 0 °C.

In the **last** step, the synthesized chiral bishydroxyamides were converted to chiral bisoxazoline ligands using 4-dimethylaminopyridine, triethylamine, and *p*-toluenesulfonyl chloride in dichloromethane.

Synthesis of chiral allylic esters via simultaneous dehydrogenation and allylic oxidation of alkanes: The synthesized bisoxazoline ligands were used to produce chiral allylic esters via simultaneous dehydrogenation and allylic oxidation of alkanes; for this purpose, to a flame-dried Schlenk tube under a nitrogen atmosphere, the chiral ligand and copper salt were added in dried benzene and stirred for 1 h. Then, benzoic acid derivatives, alkane and di-*tert*-butyl peroxide (DTBP) were added to the mixture and stirred again. The reaction progress was monitored by thin-layer chromatography (TLC) and the chiral product was finally extracted with ethyl acetate and water (Scheme 1).

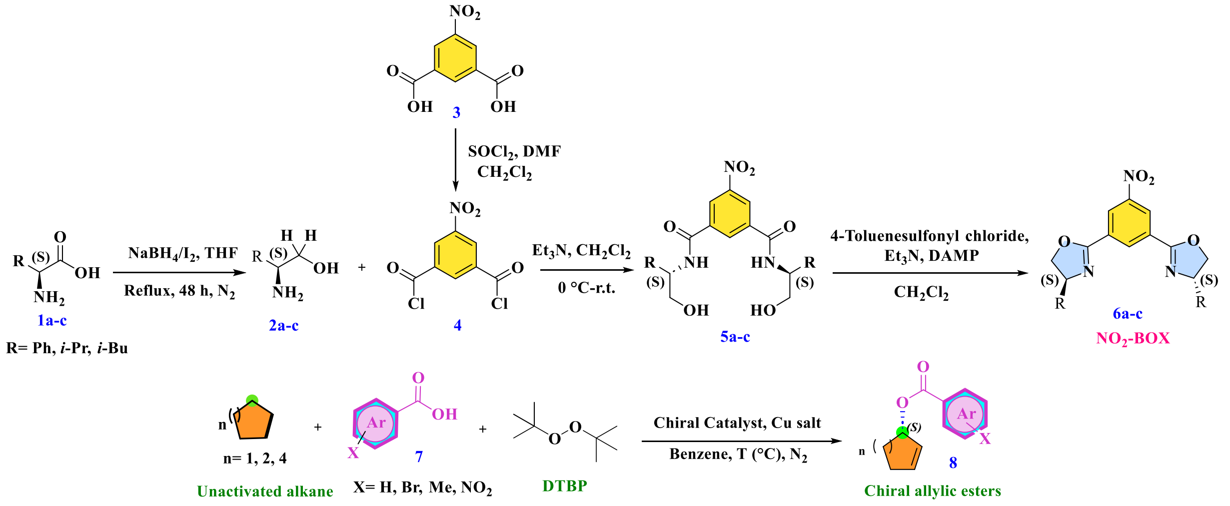

Scheme 1. Synthesis of chiral bisoxazoline ligands and their application in the simultaneous dehydrogenation and enantioselective allylic oxidation of alkanes

Results and Discussion: An efficient class of chiral bisoxazoline ligands were synthesized and purified through several steps and their structures were confirmed by ^{1}H NMR and ^{13}C NMR spectroscopic techniques (**Figure** 1). Finally, they were used as chiral catalysts for the synthesis of chiral allylic esters via simultaneous dehydrogenation and enantioselective allylic oxidation of unactivated cycloalkanes due to their greater availability and lower cost compared to the corresponding cycloalkanes in the presence of copper salts. Chiral allylic esters were obtained in high yields and moderate to good enantioselectivity.

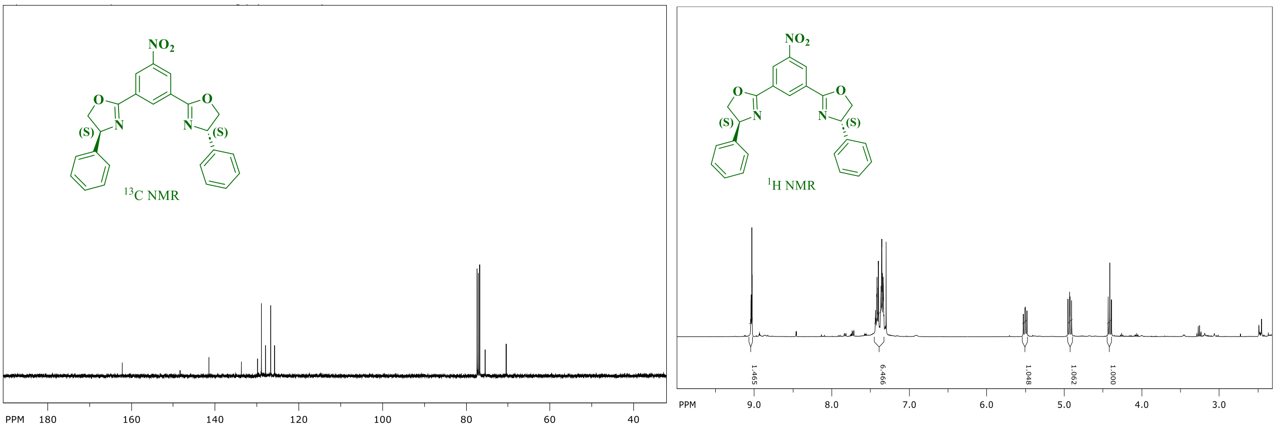

Figure 1. ^{1}H and ^{13}C NMR of chiral bisoxazoline ligand

References:

[۱] Russell, G. F., Hills, J. I. *Science* **1971**, *172*, 1043 .
[2] Brenna, E., Fuganti, C., Serra, S. *Tetrahedron: Asymmetry* **2003**, *14*, 1.
[3] Samadi, S., Arvinnezhad, H., Mansoori, S., Parsa, H. *Sci. Rep.*, **2022**, 12, 15038.
[4] Desimoni, G., Faita, G., Jorgensen, K. A. *Chem. Rev.*, **2006**, *106*, 3561.
[5] Lu, B., Zhu, F., Wang, D., Sun, H., Shen, Q., Shen. *Tetrahedron Lett.*, **2017**, 58, 2490.
[6] Tran, B. L., Driess, M., Hartwig, J. F. *J. Am. Chem. Soc.*, **2014**, 136, 17292.
[7] Majidian, S., Rashid, H. I., Naghdi, Y., Irani, M., Samadi, S. *Appl. Organomet. Chem.*, **2024**, e7857.

The 30th Iranian Seminar of Organic Chemistry
February 7-9, 2025, Iran University of Science and Technology, Tehran, Iran

Cu complex of supported on $CoFe_2O_4$ / HPA magnetic nanoparticles as a recyclable catalyst for the synthesis of polyhydroquinoline derivatives

Azam Habibollahi, Batol ZakeriNasab, Mohammad Ali Nasseri *

Department of Chemistry, College of Sciences, University of birjand, birjand, Iran

Keyword: Nanocatalyst, Polyhydroquinoline, Metal complexes

Catalysts play a key role in stability, as they allow chemical transformations to occur under milder conditions, thus conserving energy and minimizing the formation of by-products [1]. Metal Schiffbase complexes have excellent catalytic applications. The activity of these complexes can be varied by changing the type of ligands, metal ions and coordination sites of the ligands [2]. The importance of these catalysts is increasing due to their high performance, mild reaction conditions, good selectivity, reusability and easy working conditions. Researchers have investigated the meta-catalytic applications of transition metal complexes in organic reactions and the synthesis of various chemical compounds [3]. Polyhydroquinoline (PHQ) derivatives are important chemical compounds as they have been proposed as one of the most important drug classes for the treatment of cardiovascular diseases. They are also skin protectants and have the ability to modulate calcium channels [4].

In this study, a new heterogeneous Cu complex of supported on nanomagnetic $CoFe_2O_4$ / HPA was synthesized and identified by FT-IR, SEM, XRD, VSM, ICP, EDX techniques. Then, the applicability of the synthesized nanoparticles was tested as a recyclable catalyst for the synthesis of quinoline derivatives, an important class of potentially bioactive compounds. The products are obtained in good to high yields (75–95%) from one-pot reaction procedure involving benzaldehyde compounds, dicarbonyl , Ammonium acetate and keto ester under solvent-free conditions.

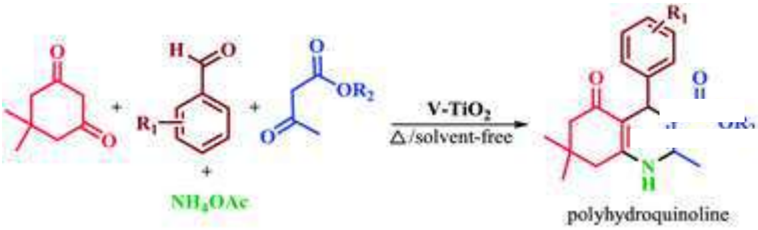

Scheme 1

References

[1] Centi, G., & Perathoner, S. (2009). Catalysis: role and challenges for a sustainable energy. *Topics in Catalysis*, *52*, 948-961.

[2] Juyal, V. K., Pathak, A., Panwar, M., Thakuri, S. C., Prakash, O., Agrwal, A., & Nand, V. (2023). Schiff base metal complexes as a versatile catalyst: A review. *Journal of Organometallic Chemistry*, 122825.

[3]Thakur, S., & Bhalla, A. (2024). Sustainable synthetic endeavors of pharmaceutically active Schiff bases and their metal complexes: A review on recent reports. *Tetrahedron*, 133836.

[4] Tamoradi, T., Ghadermazi, M., & Ghorbani-Choghamarani, A. (2018). Ni (II)-Adenine complex coated Fe3O4 nanoparticles as high reusable nanocatalyst for the synthesis of polyhydroquinoline derivatives and oxidation reactions. *Applied Organometallic Chemistry*, *32*(1), e3974.

The 30th Iranian Seminar of Organic Chemistry

February 7-9, 2025, Iran University of Science and Technology, Tehran, Iran

Synthesis of nano catalyst Cobalt ferrite@HAP/Cu Salen Complex for Preparation of spirooxindoles

Mohammad Ali Nasseri *, Batol Zakeri Nasab, Azam Habibollahi

Department of Chemistry, College of Sciences, University of birjand, birjand, Iran

Keyword: Nanocatalyst, Spirooxindoles, Hydroxyapatite

Hydroxyapatite is a major component of animal bones, and its synthetic form has many applications in chemical sensors, cancer cell inhibitors, lighting materials, tissue carriers, bioceramics, chromatography adsorbents, drug delivery agents, catalysts, catalyst supports and the dehydrogenation of alcohols, methane [1]. These properties are related to the different surface characteristics of Hydroxyapatite. It is known that the Hydroxyapatite surface has P-OH groups that act as adsorption sites. The adsorption properties of Hydroxyapatite are of particular importance for both environmental processes and industrial purposes [2,3]. Covalent surface modification of minerals using organic compounds is a useful method to obtain materials with special properties [4].

In this work, cobalt ferrite magnetic nanoparticles were synthesized and coated with HAP, then Cu salen complex was immobilized on $CoFe_2O_4$@HAP (Scheme 1). This catalyst was characterized using FT-IR, SEM, EDX, ICP and XRD techniques and used as a catalyst for the synthesis of spirooxindoles in exellent yield (Scheme 2).

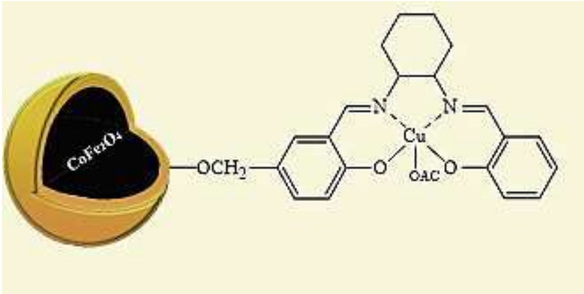

Scheme 1

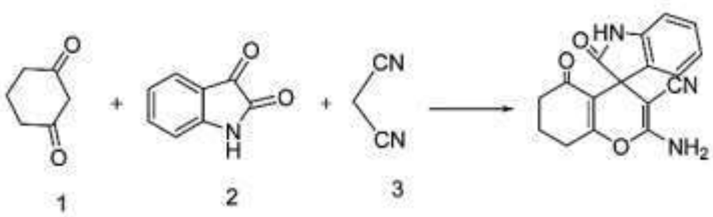

Scheme ٢

References

[1] Lopez, L., & Troisi, L. (1989). Electron-transfer chain isomerization of epoxides induced by one-electron oxidizing agents. *Tetrahedron letters*, *30*(23), 3097-3100.

[2] Saffar-Teluri, A. (2015). Direct covalent attachment of Mn (iii) salophen complex to the hydroxyapatite-encapsulated γ-Fe_2O_3 nanocrystallites: an efficient magnetic and reusable catalyst for oxidation of alcohols. *RSC advances*, *5*(86), 70577-70585.

[3] Dorozhkin, S. V., & Epple, M. (2002). Biological and medical significance of calcium phosphates. *Angewandte Chemie International Edition*, *41*(17), 3130-3146.

[4] Kim, T. G., & Park, B. (2005). Synthesis and growth mechanisms of one-dimensional strontium hydroxyapatite nanostructures. Inorganic chemistry, 44(26), 9895-9901.

The 30th Iranian Seminar of Organic Chemistry
February 7-9, 2025, Iran University of Science and Technology, Tehran, Iran

Synthesis, Characterization, and Photocatalytic Activity of CZn/TMU-21 Nanocomposite Derived from TMU-21 Metal-Organic Framework

Seyedeh Leyle Mirghaffari, Somayeh Tarasi and Ali Ramazani and Ali Morsali*

Department of Chemistry, Faculty of Science, University of Zanjan, Zanjan, Iran

E-mail: lailamirqafari@yahoo.com

In this study, the Metal-Organic Framework (MOF) TMU-21 was synthesized using a solvothermal method. This framework was subsequently used as a precursor to create the CZn/TMU-21 nanocomposite in an argon atmosphere furnace with water vapor. Various techniques, including X-ray diffraction (XRD), scanning electron microscopy (SEM), Fourier transform infrared spectroscopy (FT-IR), UV-Vis spectroscopy, and elemental mapping, were employed to characterize the structural and morphological properties of the nanocomposite. Methylene blue (MB) was used as a model organic pollutant to evaluate the photocatalytic activity of the CZn/TMU-21 nanocomposite under visible light irradiation. The results demonstrated that the nanocomposite achieved approximately 82% degradation of MB at a concentration of 10 ppm within 120 minutes, indicating significant photocatalytic activity. This performance enhancement is attributed to factors such as an increased specific surface area, a reduced band gap, improved charge separation and transfer, and the generation of hydroxyl and superoxide radicals.[1, 2].

Keywords: Metal-Organic Framework, Nanocomposite, Photocatalyst, Solvothermal.

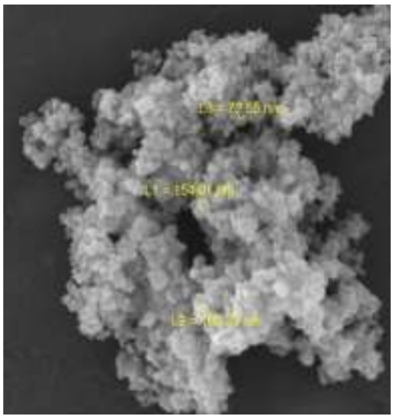

Fig.1: SEM Image of the CZn-TMU-21 Nanocomposite

References:

[1]. Yamini, Y. and M. Safari, Magnetic Zink-*based metal organic framework as advance and recyclable adsorbent for the extraction of trace pyrethroids.* Microchemical Journal, 2019. **146**: p. 134-141.

[2]. Tarasi, S. and A. Morsali, *Fabrication of transparent ultraviolet blocking films using nanocomposites derived from metal-organic frameworks.* Journal of Alloys and Compounds, 2021. 868: p. 158996.

The 30th Iranian Seminar of Organic Chemistry
February 7-9, 2025, Iran University of Science and Technology, Tehran, Iran

Investigations on the anticancer properties of Sorafenib loaded nano drug delivery systems containing *Lavandula angustifolia* essential oil against triple negative breast cancer cells

Mona Habibi-Kool-Gheshlaghi[a,b], Hossein Behboudi[c], Hasan Rafati*[b]

[a]*Department of Phytochemistry,* [b]*Department of Pharmaceutical Engineering,* [c]*Department of Biology, Medicinal Plants and Drugs Research Institute, Shahid Beheshti University, Tehran, Iran*

Keyword: Drug Delivery System, Nanoemulsion, Lavender, Breast Cancer

Introduction: There is an urgent need for research and development in cancer therapy for new molecular entities (NMEs) and more efficient drug delivery systems (DDSs)[1]. In the current study, a novel nanoformulation has been devised to modify various properties of sorafenib tosylate (SFT).

SFT is a multikinase inhibitor and an FDA-approved chemotherapic agent to treat breast cancer tumors. However, SFT is classified as a BCS class II drug with low bioavailability. It also often comes with multiple side effects and drug resistance in the prescribed doses[2]. Nanoemulsion (NE) is a biocompatible and thermodynamically stable DDS that has shown promising potential to improve the drug-loading efficiency, enhance bioavailability, and reduce toxicity with less side effects[3]. The main objective of this study was to prepare nanoformulations containing SFT and evaluate its' biological activities against MDA-MB-231 breast cancer cells.

Method: In this study, we prepared SFT-loaded bioactive *Lavandula angustifolia* essential oil using a high-energy rotor-stator homogenizer and investigated its physicochemical and biological properties. The shape, droplet diameter and size distribution of the proposed nanoformulations were characterized by DLS and TEM, while the surface charge was measured by a zetasize analyzer. GC-MS analysis was performed to determine the chemical composition of the essential oil. Moreover, the cytotoxicity of the raw materials and the nanoformulations were evaluated by the MTT assay on MDA-MB-231 triple-negative breast cancer cells and HUVEC uncancerous cell line for 24 hours.

Results and Discussion: prepared nanoformulations (droplet size <200 nm) were monitored over 300 days at 2-8°C, and their physicochemical properties as well as the biological activity were evaluated. Cytotoxicity evaluations presented in Figure 32, demonstrated that the nanoscale formulation combined with the biologically active lavender essential oil has significantly improved the cytotoxicity against MDA-MB-231 cells. Further investigations are recommended.

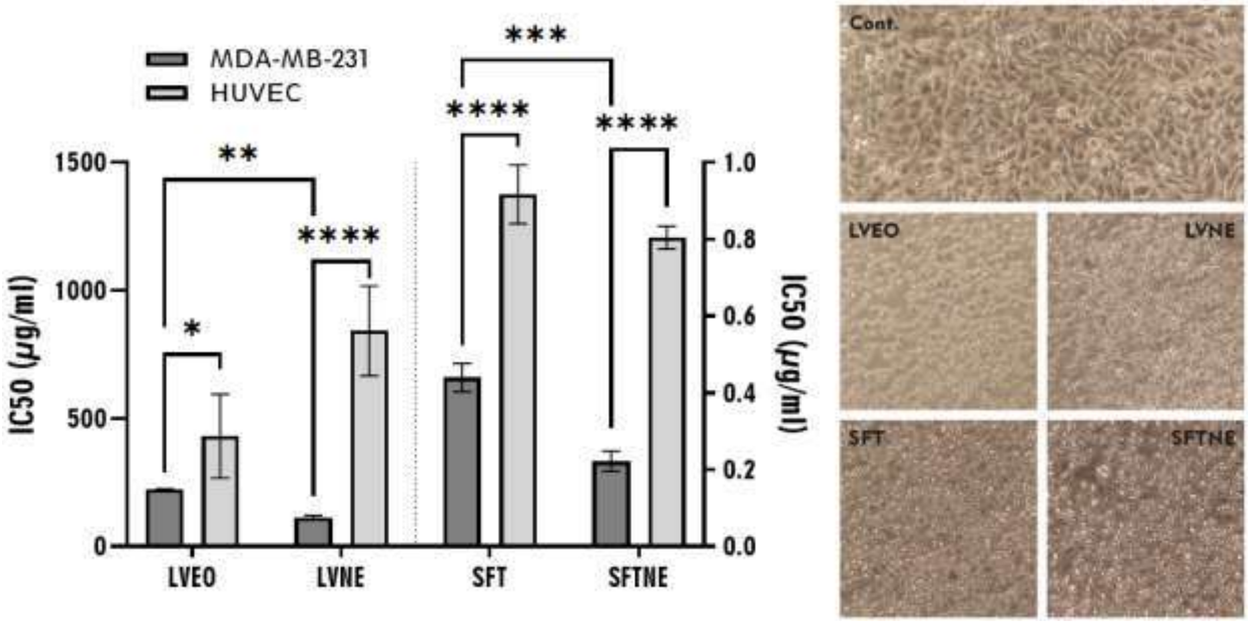

Figure 32 Effect of nanoscale formulation on both cancerous and normal cell lines

References:

1. Zhong H, Chan G, Hu Y, Hu H, Ouyang D. A comprehensive map of FDA-approved pharmaceutical products. *Pharmaceutics*. 2018;10(4). doi:10.3390/pharmaceutics10040263
2. Chaurawal N, Misra C, Abul Barkat H, et al. Oral sorafenib-loaded microemulsion for breast cancer: evidences from the in-vitro evaluations and pharmacokinetic studies. *Sci Rep*. 2022;12(1). doi:10.1038/s41598-022-17333-6
3. Ramalho ÍM de M, Bezerra GS, Ostrosky EA, et al. Chrysin-Loaded Microemulsion: Formulation Design, Evaluation and Antihyperalgesic Activity in Mice. *Appl Sci*. 2022;12(1). doi:10.3390/app12010477

The 30th Iranian Seminar of Organic Chemistry
February 7-9, 2025, Iran University of Science and Technology, Tehran, Iran

Modification of the surface of polyamide thin film membranes using an effective anti-chlorine polyester film

Mobina Moghadasi [۲۷*a], Yaghoub Mansourpanah [۲۸*b]

Membrane Research Laboratory, Lorestan University, Khorramabad, Iran

Keyword: Polyamide membrane, Polyester, Polymerization, Antichlorine properties

1.Introduction

Water and its scarcity have become one of the most important issues in life today[1]. Advanced membranes for water purification are rapidly being developed and updated [2]. Polyamide membranes are sensitive to oxidizing agents due to the presence of amide bonds (-CONH-) in their structure. Chlorine is one of these strong oxidizing agents that can break amide bonds and change the polymer structure. The critical downfall of polyamide membranes is their inherent sensitivity to oxidizing agents (such as chlorine) [3,4]. Ester bonds in polyesters are more resistant to oxidizing agents such as chlorine due to their carbonyl-oxygen structure and the absence of active hydrogen atoms nearby. For this reason, polyester membranes have been used to modify the surface of polyamide membranes.

2. Method

Polyethersulfone membrane was used as the support layer, which was made of 14% (PES), DMF, PVP, and Triton X-100. To form a thin layer, two aqueous and organic phases were used. First, the aqueous phase, which contains TEA, PIP, and CSA surfactant, was made up to volume in water, and the organic phase, which contains TMC, was made up to volume with hexane. First, the aqueous

---

[۲۷] mobina.moghaddasii@gmail.com
[۲۸] Mansourpanah.y@lu.ac.ir

phase was poured onto the support membrane, and after 5 minutes, the solution was removed, then the organic phase was added, and after 3 minutes, the organic phase was removed. To form the polyester layer, two aqueous and organic phases were used. First, the aqueous phase containing DHBA and NaOH was made up to volume in water, and the organic phase containing TMC was made up to volume with hexane. First, the aqueous phase was poured onto the support membrane and the solution was removed after 10 minutes. Then, the organic phase was added and the organic phase was removed after 10 minutes. (This step was repeated 2 times.) In the final step, the IPC solution in hexane was poured onto the membrane surface for 5 minutes.

3. Results and Discussion

In order to investigate the resistance of the synthesized membranes to chlorine, the performance of the membranes was investigated. As can be seen in Figure 1-a, the structure of the polyamide membrane was degraded after 6 hours of immersion in chlorine, resulting in increased flux, decreased NaCl salt rejection, and decreased Na2SO4 salt rejection. Figure 1-b shows the performance of a modified polyamide membrane or a polyester layer immersed in chlorine for different times. As can be seen, the polyester membrane was not degraded up to 42 hours and there was no significant change in flux and rejection, but from 48 hours onwards the membrane was degraded and flux increased and NaCl salt rejection and Na2SO4 salt rejection decreased.

As a result, the polyester membrane is more resistant to chlorine.

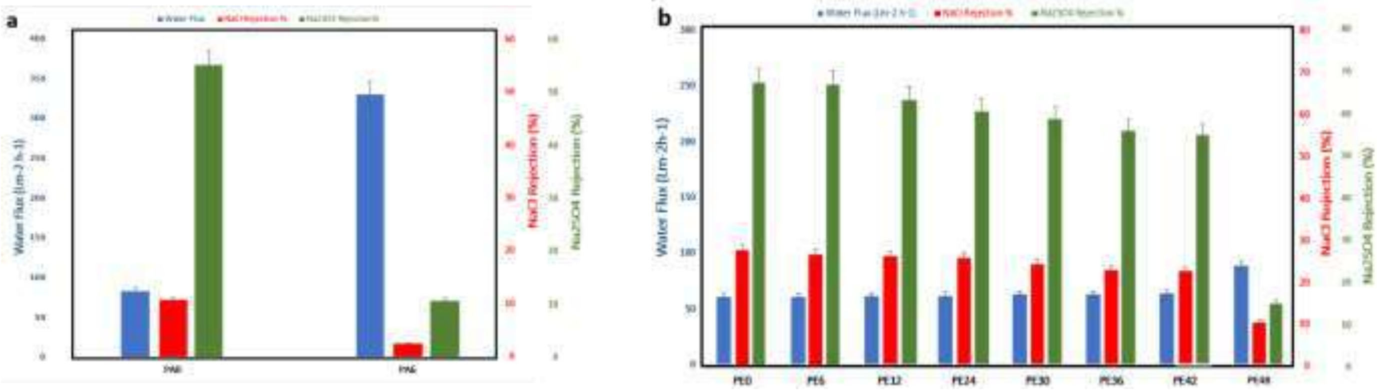

Figure 1- Performance diagram of a) polyamide membrane and b) polyester membrane immersed in chlorine.

Based on this research work, thin-film polyamide membranes were prepared by surface polymerization. The thin-film polyamide membranes were modified with a polyester layer and the resistance of the membranes to chlorine was examined. As observed, the resistance of the polyester membrane to chlorine increased compared to the unmodified polyamide membrane.

References:

١. Aziz, A.A., et al., *Tailoring the surface properties of carbon nitride incorporated thin film nanocomposite membrane for forward osmosis desalination.* Journal of Water Process Engineering, 2020. 33: p. 101005.

٢. Schafer, A., *Natural organics removal using membranes: principles, performance, and cost*. 2001: Crc Press.

٣. Gohil, J.M. and A.K. Suresh, *Chlorine attack on reverse osmosis membranes: Mechanisms and mitigation strategies.* Journal of Membrane Science, 2017. **541**: p. 108-126.

٤. Stolov, M. and V. Freger, *Degradation of polyamide membranes exposed to chlorine: an impedance spectroscopy study.* Environmental science & technology, 2019. **53**(5): p. 2618-2625.

The 30th Iranian Seminar of Organic Chemistry
February 7-9, 2025, Iran University of Science and Technology, Tehran, Iran

Synthesis and characterization of aluminum ferrite magnetic nanoparticles and investigation of its catalytic effects on reduction, and carbon-carbon coupling reactions

Parisa Moshfegh Monazah, Arash Ghorbani-Choghamarani,* Arezo Monem

Department of Organic Chemistry, Faculty of Chemistry and Petroleum Science, Bu-Ali Sina University, Hamedan, 6517838683, Iran, a.ghorbani@basu.ac.ir or arashghch58@yahoo.com, parisa.moshfegh4@gmail.com

Keywords: Heterogeneous Catalysis, magnetic nanoparticles, Aluminum ferrite ($AlFe_2O_4$), Suzuki reaction, Phenylamine

In recent years, magnetic nanocatalysts have attracted increasing attention. These nanocatalysts have diverse applications, including as adsorbents for dyes and pollutants in wastewater, as drug carriers, and as catalysts in various organic reactions [1]. In this work. we report the synthesis and identification of $AlFe_2O_4@SiO_2@n\text{-}pr@Xan\text{-}Cu(I)$ as a magnetic nanocatalyst. The structure of the mentioned nanocatalysts was confirmed using XRD ‹SEM ‹TGA ‹FT-IR ‹EDS ‹X-Ray Mapping techniques. Activation of $AlFe_2O_4@SiO_2@n\text{-}pr@Xan\text{-}Cu(I)$ in synthesizing biphenyl and phenylamine derivatives has been discussed here. This nanocatalyst was retrieved and reused four consecutive times without significantly reducing catalytic activity in the mentioned reactions. High yields, short reaction time, lack of toxicity, environmental compatibility, and easy purification methods are among the advantages of this research (Scheme 1-2).

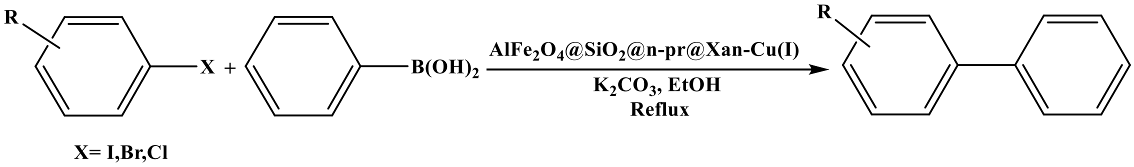

Scheme 1: Suzuki reaction

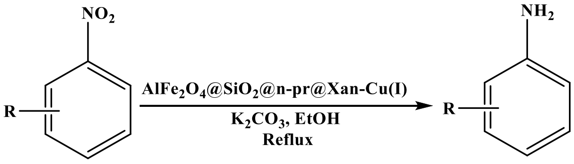

Scheme2: Reduction of nitrobenzene to aniline derivatives

References:

٤. Khanmohammadi-Sarabi, F., Ghorbani-Choghamarani, A., Aghavandi, H., & Zolfigol, M. A. (2022). $ZnFe_2O_4$@ SiO_2-ascorbic acid: Green, magnetic, and versatile catalyst for the synthesis of chromeno [2,3-*d*] pyrimidine-8-amine and quinazoline derivatives. *Applied Organometallic Chemistry*, *36*(8), e6768.

Hierarchical Cobalt Phosphide Catalysts from Metal-Organic Frameworks for Water Splitting

Ali Reza Oveisi[a,*], Esmael Sanchooli[b]

[a] *Department of Organic Chemistry, Faculty of Chemistry, Lorestan University, Khorramabad 68151-44316, Iran*

[b] *Department of Chemistry, Faculty of Sciences, Department of Chemistry, University of Zabol, 98615-538 Zabol, Iran*

Corresponding Author: oveisi.a@lu.ac.ir (A.R.Oveisi), Tel: +98-915-542-8132

Water splitting technology enables efficient hydrogen production through hydrogen evolution reaction (HER) and oxygen evolution reaction (OER). The hydrogen evolution reaction (HER) and oxygen evolution reaction (OER) in overall water splitting (OWS) depend critically on stable catalysts incorporating high-activity transition metal ions and alloys. Here, we synthesize Metal-P nanoparticle-embedded carbon nanotubes (Metal@CNT) via carbonization and phosphorization of an iron-organic framework composite with anchored Co-based coordination polymer (ZIF-67) (Figure 1). The photocatalyst demonstrates high HER activity (0.8 mmol/g H_2 evolution) under visible light in $MeOH/H_2O$ over 24 h. This strategy establishes a new pathway for developing precise and highly stable catalysts, featuring controlled morphology and enhanced durability for efficient water splitting applications.

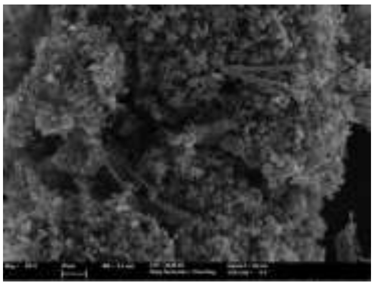

Figure 1. SEM image of the Metal@CNT.

References:

[1] H. Tabassum, W. Guo, W. Meng, A. Mahmood, R. Zhao, Q. Wang, R. Zou, *Adv. Energy Mater.* 2017, 7, 1601671.

[2] L. L. Chai, Z. Y. Hu, X. Wang, Y. W. Xu, L. J. Zhang, T.-T. Li, Y. Hu, J. J. Qian, S. M. Huang, *Adv. Sci.* 2020, 7, 1903195.

The 30th Iranian Seminar of Organic Chemistry
February 7-9, 2025, Iran University of Science and Technology, Tehran, Iran

Study of active ingredients and antibacterial effect of Malva and Stachys Schtschegleevii Sosn for preparation of ointment

Authors: Faranak Jamali Shabestari 1[a],Atisa Yazdanipour 2[b],Ali Niazi 3[*c]

Keyword: Malva, Stachys Schtschegleevii Sosn, active ingredients, antibacterial, ointment.

Introduction:

The use of chemicals, especially synthetic chemicals, in the production of pharmaceuticals can have various adverse effects on humans. In recent years, the use of medicinal plants in medical sciences has gained increasing attention. This research focuses on the investigation of active compounds, identification of key components, and the study of their medicinal properties.(1)

Superficial wounds are among the most common types of injuries in medical science, characterized by damage or abrasion to the skin while the underlying tissue remains intact. These wounds may be accompanied by bruising or redness. Historically, various methods and medications have been used for wound healing, prevention of bacterial and fungal infections, and reducing the likelihood of scarring. Such methods include honey dressings, antibiotic ointments, Betadine, and other approaches.(2)

In this study, the active compounds of medicinal plants (Stachys schtschegleevii spp.) and (Malva spp.) will be extracted and identified using various methods, including the Clevenger and Soxhlet techniques. The active compounds of these plants will be analyzed using GC-MS, and subsequently, they will be used to formulate a topical ointment.(3)

Method:

In this study, the extraction process was carried out using a Soxhlet apparatus. For each extraction, 10 to 15 grams of dried and ground plant material were used as the dry matter, along with 250 ml of 96% ethanol as the solvent.

The plant powder was placed in a medium-mesh fabric known as metqal and inserted into the Soxhlet chamber. On average, each extraction cycle took about 45 minutes, and to obtain a purer extract, three extraction cycles were performed.

The resulting extract was then analyzed for active compounds using the GC-MS device. For the antibacterial section, the zone of inhibition method, a relatively simple and commonly used technique, was employed. To ensure a comprehensive and precise analysis, two bacteria—one Gram-positive and one Gram-negative—were examined.

Results and Discussion: Results and Discussion will be ready in few weeks.

Refrences:

١. Yahya, R., & Ahmed, H. F. (2022). Article Review: Medical Plants: Their Compounds and the Biotechniques for Identifying and Separation of Them. Journal for Research in Applied Sciences and Biotechnology, 1(5), 68–74. https://doi.org/10.55544/jrasb.1.5.7
٢. Tashkandi, H. (2021). Honey in wound healing: An updated review. In Open Life Sciences (Vol. 16, Issue 1, pp. 1091–1100). De Gruyter Open Ltd. https://doi.org/10.1515/biol-2021-0084
٣. Shafodino, F. S., Lusilao, J. M., & Mwapagha, L. M. (2022). Phytochemical characterization and antimicrobial activity of Nigella sativa seeds. PLoS ONE, 17(8 August). https://doi.org/10.1371/journal.pone.0272457

The 30th Iranian Seminar of Organic Chemistry
February 7-9, 2025, Iran University of Science and Technology, Tehran, Iran

Evaluating the Cytotoxicity of Sorafenib Tosylate Loaded *Cymbopogon Citratus* Nanoemulsion on Liver Cancer Cells

Sepehr Saniepour Esfahani[a, c], Hossein Behboudi[b], Mona Habibi-Kool-Gheshlaghi[a,c], Hasan Rafati*[c]

[a] *Department of Phytochemistry, Medicinal Plants and Drugs Research Institute, Shahid Beheshti University, Tehran, Iran*

[b] *Department of Biology, Medicinal Plants and Drugs Research Institute, Shahid Beheshti University, Tehran, Iran*

[c] *Department of Pharmaceutical Engineering, Medicinal Plants and Drugs Research Institute, Shahid Beheshti University, Tehran, Iran*

Keywords: Liver Cancer, Drug Delivery, Nanoemulsion, Sorafenib, Lemongrass

Introduction: Liver cancer is the sixth most common cancer globally and ranks third in mortality rates. Hence finding new and non-invasive treatment methods for this malignancy is of utmost importance. Of the two major types of liver cancer, Hepatocellular Carcinoma (HCC) is the leading case in both incidence and mortality worldwide [1,2]. Current treatment methods, like resection, chemotherapy or radiotherapy, are usually limited by factors such as serious side effects, drug resistance and low effectiveness. Sorafenib Tosylate (SFB), a main chemotherapy agent used in treating HCC, also faces significant challenges, including side effects and low bioavailability. These limitations can be overcome using various drug delivery systems [3].

In recent years, nano-formulations have been used to address the above-mentioned restrictions and improve the effectiveness and biochemical properties of anti-cancer drugs. Among novel delivery systems, the nanoemulsion delivery method stands out due to its unique advantages, including 1) greater stability, 2) higher drug loading capacity, 3) improving the bioavailability of lipophilic drugs, 4) improving the cytotoxic effect of drugs by using essential oils as active nanoscale carriers [4,5]. Here, nanoemulsions were made using Lemongrass Essential Oil (LGEO) as the oil phase and Sorafenib Tosylate as the active compound. Cytotoxic, antioxidant and anti-inflammatory activities have also been reported for *Cymbopogon Citratus* Essential Oil (LGEO) major components like Citral, Limonene, Linalool and Geraniol. These formulations not only benefit from the advantages of nanoemulsions discussed earlier but are also enhanced by the aforementioned effects of LGEO. This study aimed to evaluate the effectiveness and cytotoxic effect of the proposed nanoemulsion on the HepG2 cell line.

Method: Nanoformulations were prepared through a high-energy method using a rotor-stator high-shear homogenizer, and the physicochemical properties of these formulations were optimized using Design Expert 13 experimental design software. The optimized nanoformulation (SFB-OP1) was characterized by a Dynamic Light Scattering (DLS) instrument for Polydispersity Index (PDI) and particle size (nm) monitoring, MTT cell viability assay to evaluate cytotoxic effects (IC_{50}) on HepG2 cell line, and Zetasizer for Zeta Potential (mV) measurement. GC-MS was also employed to identify the major active compounds present in Lemongrass Essential Oil.

Results and Discussion: SFB-loaded nanoemulsions were prepared and characterized using the techniques mentioned earlier. DLS results indicated a mean particle size of 124.09 ± 2.13 nm and a mean PDI of 0.25 ± 0.04 for the SFB-OP1 nanoformulation which was stable for the following 3 months. The collected data showed promising results, as the particle size was well below 200 nm usually considered for making ideal nanoformulations. The low polydispersity index (below 0.3) is also favourable as it indicates a narrow size distribution and that the optimized nanoemulsion is highly uniform and stable, which further supports its potential as a biocompatible and efficient drug delivery method. The results of Zeta Potential measurements for the SFB-OP1 nanoformulation indicated a slight negative surface charge (-2.09 ± 0.20 mV). This result aligns with the chemical structure of the drug loaded into the nanoformulation, as it may be because of the tosylate form of the anticancer agent Sorafenib. MTT assay results showed that HepG2 model cells treated with the

SFB-OP1 formulation present a notable decrease in cell viability. This formulation demonstrated a strong growth inhibition (IC_{50} = 0.58 ± 0.07 µg/mL), which is approximately doubled compared to the cytotoxicity of SFB drug when measured alone (IC_{50} = 1.14 ± 0.02 µg/mL). LGEO cytotoxicity was also measured for reference (IC_{50} = 35.76 ± 1.09 µg/mL). These observations may suggest the presence of a synergistic effect between SFB and LGEO, which increases the effectiveness of the nanoformulation compared to the conventional dosage form of SFB drug. Further in vivo studies on an animal model of cancer are recommended.

References:

[1] Li, Q., Cao, M., Lei, L., Yang, F., Li, H., Yan, X., ... & Chen, W. (2022). Burden of liver cancer: From epidemiology to prevention. Chinese Journal of Cancer Research, 34(6), 554.

[2] Guo, Q., Zhu, X., Beeraka, N. M., Zhao, R., Li, S., Li, F., ... & Liu, J. (2024). Projected epidemiological trends and burden of liver cancer by 2040 based on GBD, CI5plus, and WHO data. Scientific Reports, 14(1), 28131.

[3] Bray, F., Laversanne, M., Sung, H., Ferlay, J., Siegel, R. L., Soerjomataram, I., & Jemal, A. (2024). Global cancer statistics 2022: GLOBOCAN estimates of incidence and mortality worldwide for 36 cancers in 185 countries. CA: a cancer journal for clinicians, 74(3), 229-263.

[4] Rodríguez, F., Caruana, P., De la Fuente, N., Español, P., Gámez, M., Balart, J., ... & Céspedes, M. V. (2022). Nano-based approved pharmaceuticals for cancer treatment: present and future challenges. Biomolecules, 12(6), 784.

[5] Fofaria, N. M., Qhattal, H. S. S., Liu, X., & Srivastava, S. K. (2016). Nanoemulsion formulations for anti-cancer agent piplartine—Characterization, toxicological, pharmacokinetics and efficacy studies. International journal of pharmaceutics, 498(1-2), 12-22.

The 30th Iranian Seminar of Organic Chemistry
February 7-9, 2025, Iran University of Science and Technology, Tehran, Iran

A Quantum Mechanical Investigation on Dexlansoprazole

Hossein Shirani [a, b] and Fatemeh Sajedi Khanin [b]

[a] *Department of Chemistry, Iran University of Science and Technology, P.O. Box 16846-13114, Tehran, Iran*

[b] *Department of Microbiology, Faculty of Biological Sciences and Technology, University of Science and Culture, Tehran, Iran*

Keyword: Dexlansoprazole, DFT, B3LYP/6-311G, HOMO-LUMO gap

Introduction: Dexlansoprazole (also known as 1H-BENZIMIDAZOLE and LANSOPRAZOLE R-FORM) is a new-generation proton pump inhibitor (PPI) used for the management of symptoms associated with gastroesophageal reflux disease (GERD) and erosive esophagitis. Dexlansoprazole is the R-enantiomer of Lansoprazole, which is composed of a racemic mixture of the R- and S-enantiomers. Compared to the older generation of PPIs (which includes Pantoprazole, Omeprazole, and Lansoprazole), dexlansoprazole has a unique pharmacokinetic profile due to its delayed-release and dual-delivery release system: This aims to address some limitations of the older-generation PPIs, such as short plasma half-life and the need for meal-associated dosing. Dexlansoprazole inhibits the final step in gastric acid production by blocking the (H+, K+)-ATPase enzyme.

Methods: The study utilized quantum mechanics (QM) calculations conducted through the density functional theory (DFT) method with the GAUSSIAN 09 software. The structure of Dexlansoprazole the drug was first optimized through gradient procedures at both restricted Hartree-Fock (HF) and hybrid density functional B3LYP levels of theory using the 6-311G basis set. Examination of the results revealed that the optimized structure achieved in this research was situated at the minimum point on the potential energy surface, displaying no negative modes.

Results: This study conducted calculations for structural parameters like bond lengths, angles, and dihedrals, as well as thermodynamic parameters at the B3LYP/6-311G level of theory and provided.

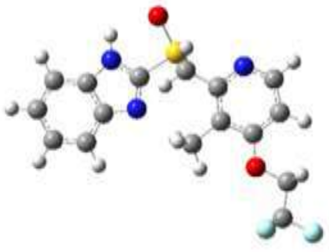

Scheme:

References: 1) Gaussian 09, Revision B.o1, M. J. Frisch et al., Gaussian, Inc., Wallingford CT, 2009

2) WHO - Essential Medicines: World Health Organization (WHO). Essential medicines list

3)FDA Approved Drug Products: DEXILANT (dexlansoprazole) Oral Delayed-release capsules or DEXILANT SOLUTAB (dexlansoprazole) delayed-release orally disintegrating tablets (October 2016)

4)TWI Pharmaceuticals: Dexlansoprazole MSDS

The 30th Iranian Seminar of Organic Chemistry
February 7-9, 2025, Iran University of Science and Technology, Tehran, Iran

A Quantum Mechanical Investigation on Inavolisib

Hossein Shirani[ab,*] and Mojdeh Karimi[b]

[*] *Corresponding author. E-mail: hossein_shirani@iust.ac.ir*

[a] *Department of Chemistry, Iran University of Science and Technology, P.O. Box 16846-13114, Tehran, Iran*
[b] *Department of Microbiology , College of Bioscience , Islamic Azad University, North Tehran Branch, Tehran, Iran*

Introduction: Inavolisib is a prescription medication used to treat certain types of breast cancer.Specifically it is indicated for adults with endocrine-resistant / PIK3CA-mutated /hormone receptor (HR)-positive / human epidermal growth factor receptor 2 (HER2)-negative / locally advancedor metastatic breast cancer.It is used in combination with Palbocicilib and Fulvestrant.

Methods: The study utilized quantum mechanics (QM) calculations conducted through the density functional theory (DFT) method with the GAUSSIAN 09 software(1). The structure of the Inavolisib drug was first optimized through gradient procedures at both restricted Hartree-Fock (HF) and hybrid density functional RB3LYP levels of theory using the 6-311G basis set. Examination of the results revealed that the optimized structure achieved in this research was situated at the minimum point on the potential energy surface, displaying no negative modes.

Figure 1 :Optimized structure of Inavolisib at the RB3LYP/6-311G level of theory.

Results: This study conducted calculations for structural parameters like bond lengths, angles, and dihedrals, as well as thermodynamic parameters at the RB3LYP/6-311G level of theory and provided the results. The electronic energy of the molecule was determined to be -923488.2 kcal/mole. Additionally, the mulliken atomic charge, spin density, and molecular orbital energies were calculated. The highest occupied molecular orbital (HOMO) was found to be -0.19846 eV and the lowest unoccupied molecular orbital (LUMO) was -0.03080 eV. The dipole moment in Debye was measured as X=-8.2609 , Y=-2.2774 , Z=-0.5325 , with a total of 8.5856.

Discussion: Optimization of the drug was performed using the RB3LYP/6-3**11G method. The** study focused on Inavolisib's electronic characteristics, specifically the energy difference between the HOMO and the LUMO. The HOMO-LUMO gap energy was determined to be 0.16766 eV. This provides insights into Inavolisib's electronic behavior, which could have applications in various fields.(2,3)

Keywords: Inavolisib ; DFT; RB3LYP/6-311G, HOMO-LUMO gap

References:

1) DrugBank Inavolisib : Wishart, D. S., Knox, C., Guo, A. C., Cheng, D., Shrivastava, S., Tzur, D., ... & Liu, P. (2018). DrugBank 5.0: a major update to the DrugBank database. Nucleic acids research, 46(D1), D1074-D1082.

2) Gaussian 09, Revision B.o1, M. J. Frisch et al., Gaussian, Inc., Wallingford CT, 2009

The 30th Iranian Seminar of Organic Chemistry
February 7-9, 2025, Iran University of Science and Technology, Tehran, Iran

Unique and outstanding catalytic behavior of porous HKUST-1 metal organic frameworks as an emerging and powerful catalyst in the synthesis of 2,3-dihydroquinazolin-4(1*H*)-one derivatives

Boshra Mirhosseini-Eshkevari,[1] Mohammad Ali Ghasemzadeh[1]*

[1]*Department of Chemistry, Qom Branch, Islamic Azad University, Qom, I. R. Iran,*

Corresponding author, E-mail address: qasemzade.a@gmail.com

Keyword: Metal-Organic Framework, Dihydroquinazolinone, Nanocomposite, Heterogeneous Catalyst.

1.Introduction

Metal-organic frameworks are a remarkable class of porous substances with outstanding attributes like excellent surface area, high thermal, chemical stability, and ultrahigh porosity. Thus, they are greatly used in sensors, separation medicinal, storage, and catalysis [1,2]

A significant interest has been attracted by multi-component reactions (MCRs) in organic syntheses since they can create the target products in a single operation with no isolation of the intermediates. Thus, the energy and reaction times are reduced [3,4] Organic reactions under circumstances without solvent have highly encouraged chemist's attention mainly from the green chemistry aspect. Green chemistry methods are considerable for reducing byproducts, produced waste, and energy cost. The potential MCRs in the absence of the solvent conditions using a nanostructure as catalyst could improve their efficacy economically and ecologically [5,6]

Quinazolin-4-ones are significant bicyclic heterocycles with significant pharmacological and biological properties like antifungal, analgesic, antidiabetic, antitumor, antibacterial, anticonvulsant and antihypertensive [7].

on the synthesis of novel heterogeneous catalysts, in this research we report how to prepare and use HKUST-1 MOF as a bifunctional acid-base catalyst for the producing of 2,3-dihydroquinazolin-4(1*H*)-ones by ternary condensation between isatoic anhydride, aldehydes, and primary amines under solvent-free conditions (Scheme 1).

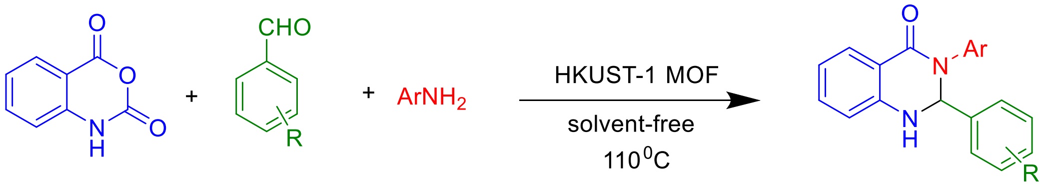

Scheme 1. Preparation of 2,3-dihydroquinazolin-4(1*H*)-ones using HKUST-1 MOF.

2. Method

2.1. Synthesis of HKUST-1 MOF

Porous HKUST-1 MOF was prepared using a novel hydro-thermal method. In a typical experiment, cupric nitrate hemipentahydrate (4.0 g) was dissolved into 250 mL deionized water. It was followed by the addition of Benzene-1,3,5 tricarboxylic acid (2.0 g) in a 250 mL of solvent consisting of equal parts of ethanol and deionized water and mixed thoroughly until it was completely dissolved. The resultant solution mixture was transferred into a 250 mL teflon-lined stainless steel autoclave. It was kept at 140°C for 21 h in oven to yield small crystals. Then the auto- clave was cooled down to room temperature naturally and the blue crystals were isolated by filtration. The suspension was washed with the mixture of deionized water several times and dried.

2.2. General preparation of 2,3-dihydroquinazolin-4(1H)-ones using HKUST-1 MOF

A mixture of isatoic anhydride, aldehydes, anilines with a molar ratio (1:1:1: mmol) in HKUST-**1** MOF (0.007 g) were mixed in the absence of any solvent at 110^{o}C for 10-**25 min. TLC w**as used to monitor the reactions progress. After completion, the HKUST-**1 MOF catalys**t was detached by the centrifugation. The retrieved heterogeneous catalyst was washed and dried for further runs. To obtain the corresponding heterocyclic product, the filtrated was placed in a rotary and the obtained residue was then rinsed with water and purified with ethanol by recrystallization to obtain pure products.

3. Results and Discussion

The procedure displayed in Figure 1 is used to synthesize the target catalyst including HKUST-**1** MOF. To characterize and confirm the structure, spectroscopic technique including FT-IR. The other two functional groups related to the HKUST-1 have appeared at 729 cm^{-1} (C–H). In general, the peaks detected between the wavenumber 700 to 1600 cm^{-1} confrmed the presence of benzene tricarboxylic acid (BTC) as the organic ligand in the structure.

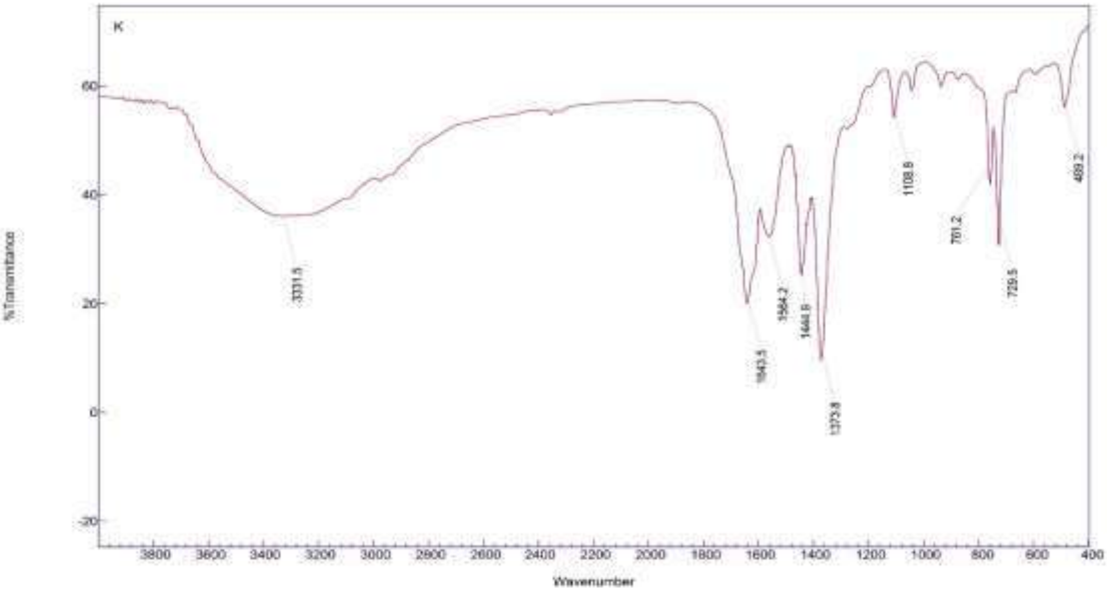

Figure 1. The FT-IR spectra of HKUST-1 MOF

References

[1] K. Farha and J.T. Hupp, *Acc. Chem. Res*. 2010, **43**, 1166-1175.

[2] M. Bosch, S. Yuan, W. Rutledge and H.-C. Zhou, *Acc. Chem. Res*. 2017, **50**, 857-865.

[3] A. Shaabani, A. Maleki, A. H. Rezayan and A. Sarvary, Molecular Diversity, 2011,15, 41-68.

[4] M. J. Climent, A. Corma and S. Iborra, RSC Advances, 2012, 2, 16-58.

[5] A. Kumar and R. A. Maurya, Tetrahedron, 2007, 63, 1946-1952.

[6] L. F. Tietze, T. Kinzel and C. C. Brazel, Acc.Chem. Res, 2009, 42, 367-378.

[7] J. Bartroli, E. Turmo, M. Alguero, E. Boncompte, M. L. Vericat, L. Conte, J. Ramis, M. Merlos, J. Garcia-Rafanell and J. Forn, J. Med. Chem. 1998, 41, 1869-1882.

The 30th Iranian Seminar of Organic Chemistry
February 7-9, 2025, Iran University of Science and Technology, Tehran, Iran

Efficient Synthesis of Xanthene Derivatives by Magnetic Biological Metal–Organic Frameworks Catalyst

Sepideh Faraji, Mostafa Ghafori-Gorab, Shabnam Ansari, Nazanin Nejatbakhsh, Ali Maleki*

Catalysts and Organic Synthesis Research Laboratory, Department of Chemistry, Iran University of Science and Technology, Tehran, Iran

Keyword: Xanthenes, Bio-MOF, Fe_3O_4, Catalyst

The synthesis of heterocyclic molecules like xanthenes is a vital challenge in both industry and research. Xanthenes derivatives play an important role in organic synthesis and they are highly regarded as dyes in laser technology as well as in the detection of biological molecules [1]. These compounds exhibit beneficial properties, including anti-inflammatory, antimicrobial, antiviral, and antitumor effects, which make them valuable in drug development [2,3]. Given the wide range of xanthenes applications, numerous synthetic methods have been explored. However, many of these methods rely on harsh reaction condition that are not environmentally friendly, generate considerable waste, and involve lengthy reaction times [4]. Therefore, it is important to find other methods to reduce mentioned limitations for the preparation of xanthene derivatives. Biological metal-organic framework (Bio-MOFs) are a type of metal-organic framework that incorporates biologically derived ligands, such as amino acids and proteins. These frameworks are characterized by their large surface area, high porosity, tunable chemical properties, and biocompatibility, making them particularly suitable for biomedical applications and catalysis. The distinct features of Bio-MOFs contribute to their effectiveness in various catalytic processes, including the synthesis of xanthenes. Utilizing Bio-MOFs in xanthenes synthesis, offers several advantages, including the ability to achieve high yields under mild conditions, reduced reaction times, and a decrease in unwanted by-product formation [4]. This study presents an efficient, and rapid method for synthesizing xanthenes derivatives by magnetic Bio-MOF-11 catalyst.

For the preparation of catalyst, Fe_3O_4 nanoparticles were initially synthesized using $FeCl_3\cdot 6H_2O$ and $FeCl_2\cdot 4H_2O$ salts in the presence of ammonia in the water. Subsequently, a metal-organic framework was synthesized by hydrothermally treating 0.90 mmol of cobalt acetate and 2.7 mmol of adenine with ethanol as the solvent at 100°C for 24 hours in the presence of 0.5g of Fe_3O_4 nanoparticles. Xanthenes were generated by combining 1 mmol of aldehyde with 2 mmol of dimedone in ethanol solvent at 75°C for 2h, utilizing 40 mg of catalyst. The products, which included electron-donating groups such as methyl and methoxy, as well as electron-withdrawing groups like nitro and chlorine, were obtained with efficiencies ranging from 85% to 98%. Notably, the catalyst maintained its effectiveness over five consecutive runs without a significant decline in reaction efficiency.

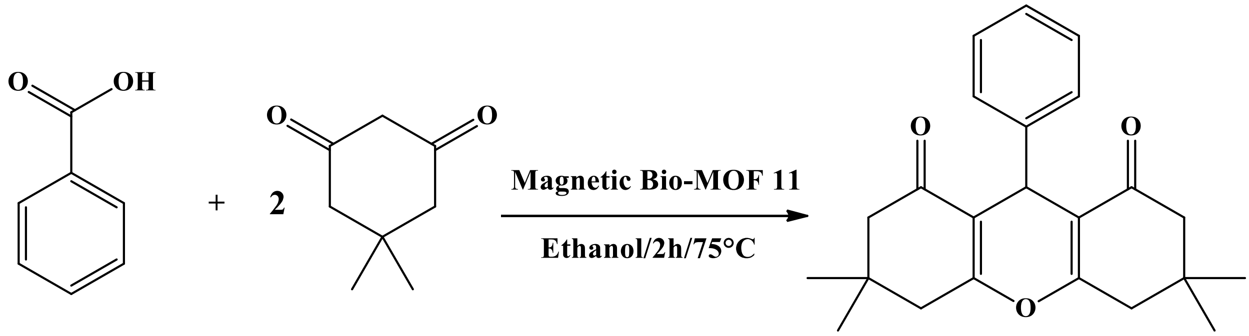

Scheme 1. Synthesis of Xanthene by Magnetic Bio-MOF-11 catalyst Catalyst.

References

١. Azizi N, Abbasi F, Abdoli-Senejani M. Natural acidic ionic liquid immobilized on magnetic silica: preparation and catalytic performance in chemoselective synthesis of dicoumarols and substituted xanthene derivatives. ChemistrySelect. 2018 Apr 9;3(13): p. 3797-802.

٢. Chaudhary A, Khurana JM. Advances in the synthesis of xanthenes: an overview. Current Organic Synthesis. 2018 May 1;15(3): p. 341-69.

٣. Kakeshpour A, Moradi A, Moradi F. Green Synthesis of Xanthenes: Utilizing Sulfonated Fructose as an Efficient and Eco-friendly Catalyst. Journal of Pharmaceutical Research International. 2024 Jun 6;36(7): p. 59-78.

٤. Li P, Ma F, Wang P, Zhang Z. Highly Efficient Low Melting Mixture Catalyzed Synthesis of 1, 8-Dioxo- Wang HS, Wang YH, Ding Y. Development of biological metal–organic frameworks designed for dodecahydroxanthene Derivatives. Chinese Journal of Chemistry. 2013 Jun;31(6): p. 757-63.

٥. biomedical applications: from bio-sensing/bio-imaging to disease treatment. Nanoscale advances. 2020;2(9): p. 3788-97.

$MgFe_2O_4@CeO_2$ Magnetic Nanoparticles: A Cost-Effective Catalyst for Solvent-Free Synthesis of 3,4-Dihydropyrimidin-2(1H)-ones

Authors: Saeid Taghavi Fardood*

Department of Chemistry, Faculty of Science, Ilam University, Ilam, Iran

E-mail: s.taghavi@ilam.ac.ir

Keyword: Core-Shell Nanoparticles, Solvent-Free Synthesis, Dihydropyrimidin Derivatives

The synthesis of 3,4-dihydropyrimidin-2(1H)-ones (Biginelli compounds) has garnered substantial interest due to their wide-ranging pharmacological applications, such as antiviral, antibacterial, antitumor, and antihypertensive activities. These compounds are also valuable as calcium channel blockers, α-1a-antagonists, and neuropeptide Y antagonists, making them crucial in the development of therapeutic agents [1,2]. The Biginelli reaction, a three-component condensation of ethyl acetoacetate, an aryl aldehyde, and urea, has proven to be an essential strategy for the synthesis of these bioactive molecules [3].

In this study, we present an efficient, environmentally friendly, and solvent-free one-pot synthesis of 3,4-dihydropyrimidin-2(1H)-ones using $MgFe_2O_4@CeO_2$ core-shell magnetic nanoparticles as a highly effective catalyst. These nanoparticles were synthesized via a green method, employing tragacanth gum as a stabilizer, and characterized using various techniques such as XRD, FESEM, TEM, EDX, and VSM analysis. The proposed synthesis offers several benefits, including high yields, short reaction times, mild conditions, simple work-up procedures, and excellent recyclability of the catalyst. This green approach emphasizes the potential of core-shell nanoparticles in the sustainable synthesis of valuable compounds, showcasing a significant advancement in green chemistry and nanotechnology for pharmaceutical applications.

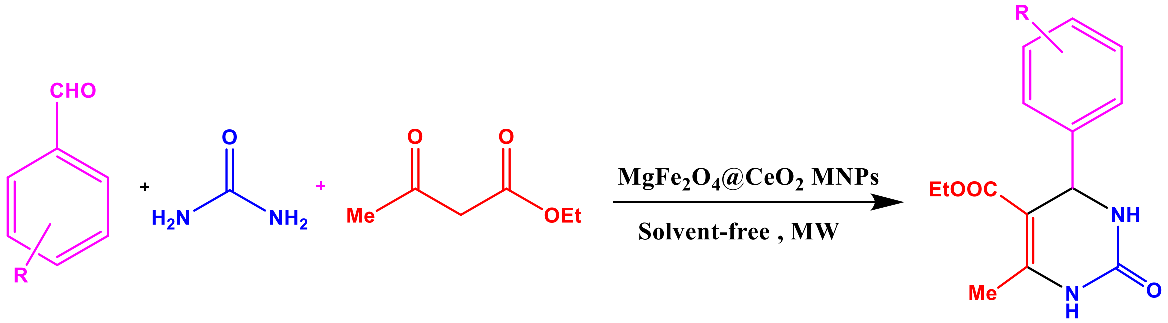

Scheme: Synthesis of 3,4-dihydropyrimidin-2(1H)-ones using $MgFe_2O_4@CeO_2$

References

[1]. Mohamadpour, F.: *Sci. Rep.*, 2023, **13**, 10262.
[2]. Merroun, Y., Chehab, S., El Hallaoui, A., Boukhris, S., Ghailane, R., Souizi, A.: *J. Mol. Struct.*, 2024, 1306, 137838.
[3]. Nasab, N.H., Raza, H., Hassan, M., Kloczkowski, A., Kim, S.J.: *J. Mol. Struct.*, 2023, **1286**, 135638.

The effects of Iranian dates fruit varieties on the total phenolic compounds and antioxidant activity of the extracts

Zarrin Nasri*

Department of Chemical Technologies, Iranian Research Organization for Science and Technology (IROST), P.O. Box 33535111, Tehran, Iran

Abstract

The effects of Iranian dates fruit varieties on the amount of phenolic compounds and antioxidant activity of the extracts were investigated. Five varieties of Iranian dates including Rabi, Zahedi, Dashtestan, Mazafati and Kharak were evaluated. The highest total extract and total phenolic compounds were related to Zahedi date; 78% and 603.82 GAE/100 gr of dry extract of date fruit, respectively. The highest antioxidant activity was related to the extract of Dashtestan date; 40.19.

Keyword: Date fruit; Iranian varieties; Total phenolic compounds; Aantioxidant activity

۱- Introduction

The antioxidant effects are mainly due to phenolic compounds such as flavonoids, phenolic acids and diterpenes. Reactive free radicals such as superoxide anion (O_2^{*-}), hydroxide radical ($^{*}OH$) and peroxyl radical (ROO^{*}) are specific reactants and are biological products of molecular oxygen reduction [1, 2]. The date fruit have a great ability to inhibit free radicals due to the presence of antioxidant compounds. Various types of phenolic compounds and flavonoids including flavones, flavanones and flavonol glycosides have been identified in dates. Flavonoids present in dates include Apigenin, Luteolin, Quercetin [3, 4]. More than one million tons of dates are produced in Iran annually, of which 600 thousand tons are date waste [5].

۲- Materials and Methods

The dates used in this research were purchased from the central distribution of Tehran. Extraction was carried out with distilled water solvent. The analysis of phenolic compounds was performed based on the Folin-Ciocalteu reagent method. The reduction products of metal oxide have a blue color that exhibits a broad light absorption with a maximum at 765 nm. The intensity of light absorption at this wavelength is proportional to the concentration of phenols. To measure the antioxidant activity of the date fruit extracts, the required amount of date fruit extract at different concentrations was added to 1.5 ml of DPPH (2,2-diphenyl-1-picrylhydrazyl) solution of appropriate concentration. The absorbance of the samples at 517 nm was measured by spectrophotometer.

$$\text{DPPH radical inhibition} = \frac{A_b - A_s}{A_b} * \text{۱۰۰} \qquad (\text{۱})$$

۳- Results and Discussion

Figure (1) shows the effect of date varieties on the total extract. The other process conditions included temperature: 70 °C, solvent to solid ratio: 20 ml/g, solvent volume: 100 cc, time: 120 min. The highest total extract is for Zahedi date, which is 78 wt%.

Figure (2) shows the effect of date varieties on the amount of total phenolic compounds in the extract. For three varieties of dates including Rabi, Zahedi and Dashtestan, the amount of total phenolic compounds are higher in comparison with the other two varieties. The highest amount of extracted phenolic compounds is for Zahedi; 603.82 GAE/100 gr of dry extract of date fruit.

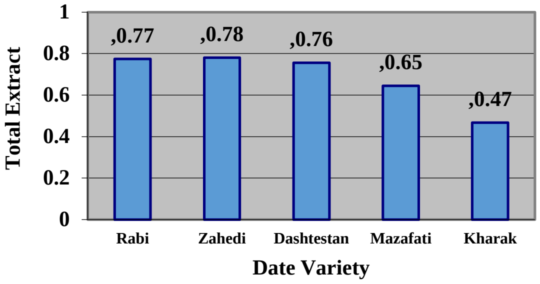

Figure (1) – The effect of date varieties on the total extract

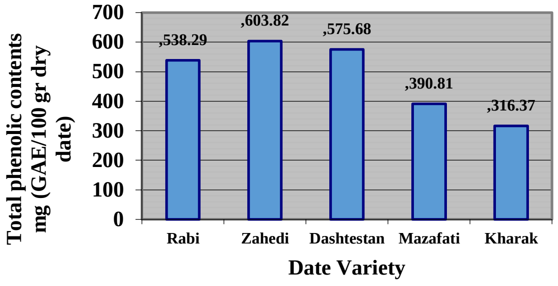

Figure (2) – The effect of date varieties on the total phenolic compounds

Figure (3) shows the effect of date varieties on the antioxidant activity of the extracts. The other process conditions are constant. The highest antioxidant activity is related to the extract of Dashtestan date and is equal to 40.19.

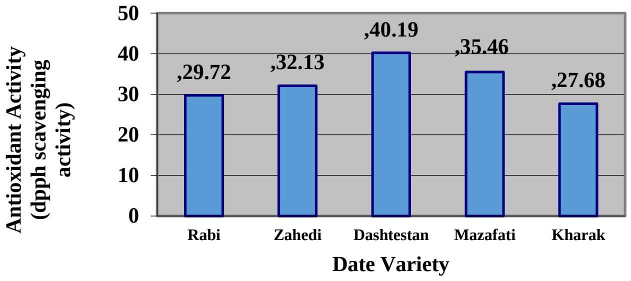

Figure (3) – The effect of date varieties on the antioxidant activity

Conclusions

The effects of five varieties of Iranian dates including Rabi, Zahedi, Dashtestan, Mazafati and Kharak on the amount of phenolic compounds and antioxidant activity of the extracts were evaluated. The highest amount of extracted phenolic compounds and antioxidant activity was related to Zahedi date; 603.82 GAE/100 gr of dry extract of date fruit and Dashtestan date; 40.19, respectively.

References

١) BiglariI, F., *Assessment of Antioxidant Potential of Date (Phoenix Dactylifera) Fruits from IRAN, Effect of Cold Storage and Addition to Minced Chicken Meat*, 2009, Universiti Sains Malaysia.

٢) Biglari, F., A.F.M. AlKarkhi, and A.M. Easa, *Antioxidant activity and phenolic content of various date palm (Phoenix dactylifera) fruits from Iran.* Food Chemistry 2008. 107: p. 1636–1641.

٣) Saafi, E.B., et al., *Phenolic content and antioxidant activity of four date palm (Phoenix dactylifera L.) fruit varieties grown in Tunisia.* International Journal of Food Science and Technology 2009. 44: p. 2314–2319.

٤) Allaith, A.A.A., *Antioxidant Activity of Bahraini Date Palm (Phoenix dactylifera L.) Fruit of Various Cultivars.* International Journal of Food Science and Technology, 2008. 43: p. 1033-1040.

٥) *"The value of Iranian dates increases 10 times with processing", 1388, Center of Trade Unions of food Industries of Iran.*

A One-pot Synthesis of *N*-Arylidene-2-Aryl-Imidazo[1,2-a] Pyridin-3-amines by $H_3PW_{11}MoO_{40}$ Catalyst

Fatemeh Mollaei, Mostafa Ghafori-Gorab, Maryam Jamili, Nazanin Nejatbakhsh, Ali Maleki*

Catalysts and Organic Synthesis Research Laboratory, Department of Chemistry, Iran University of Science and Technology, Tehran, Iran

Keyword: Imidazole [1,2-a] pyridine, Polyoxometalate, Multicomponent reaction, Catalyst

Imidazole pyridines represent a significant class of fused heterocyclic compounds renowned for their diverse biological activities. Owing to these properties, extensive research has focused on the synthesis of these heterocyclic compounds. The structural characteristics of the imidazole ring enhance its ability to participate in various drug-ligand interactions, facilitated by hydrogen bonds, van der waals forces, and hydrophobic interactions. Multicomponent reaction methods have been employed for the synthesis of imidazole [1,2-a] pyridines, with the Groebke-Blackburn–Bienaymé three-component reaction being a prominent technique introduced in 1998 [1-3]. Previous methods for synthesizing imidazole and pyridine derivatives through multicomponent reactions often depended on lewis acid catalysts such as $ZnCl_2$, Sc $(OTf)_3$, $MgCl_2$, and $ZrCl_4$. However, these approaches were limited by long reaction times and unsatisfactory yields. In contrast, polyoxometalates (POM) have proven to be effective catalysts in the synthesis of imidazoles and imidazole-pyridines. POM as a three-dimensional polyatomic anion that consists of transition metal oxyanions interconnected by shared oxygen atoms, demonstrated excellent catalytic activity due to their high acidity and strong oxidizing properties [4-5]. In this research, Keggin type $H_3PW_{11}MoO_{40}$ POM was prepared and used for the synthesis of imidazole pyridine compounds. In order to prepared the catalyst, $Na_2MoO_4 \cdot 2H_2O$, $Na_2WO_4 \cdot 2H_2O$, and $Na_3PO_4 \cdot 12H_2O$ salts were mixied in acidic media (pH 2.5) and heated at 90 °C for 2 h. Subsequently, purified with ether extraction. Imidazole [1,2-a] pyridine was synthesized via prepared catalyst. In this regard, 2 mmol of benzaldehyde, 1 mmol of toluene-4-sulfonyl methyl isocyanide (TsCHNC), and 1 mmol of 2-aminopyridine was combined with 20mg of catalyst in diethyl ether under reflux conditions. The mentioned reaction was purified through recrystallization and efficiency of 80% was obtained.

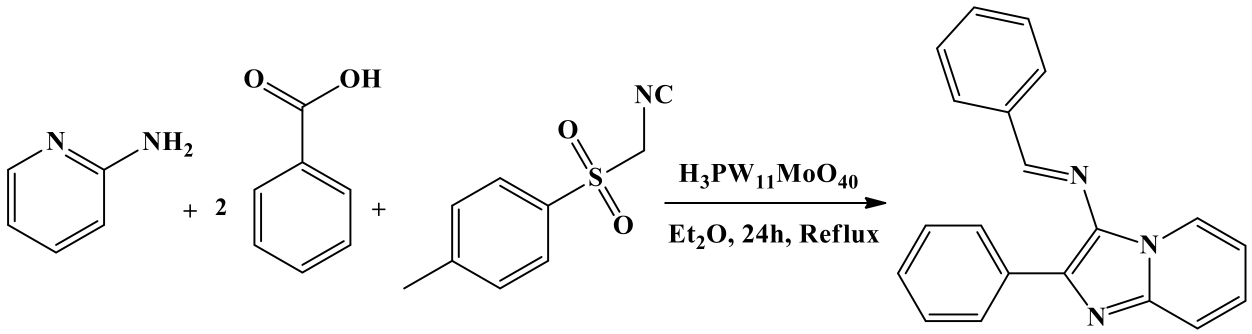

Scheme 1. Synthesis of *N*-Arylidene-2-Aryl-Imidazo[1,2-a] Pyridin-3-amines by $H_3PW_{11}MoO_{40}$ Catalyst.

References

١. Rahmati, A., A. Moazzam, and Z. Khalesi, A one-pot four-component synthesis of N-arylidene-2-aryl-imidazo [1, 2-a] azin-3-amines. Tetrahedron Letters, 2014. 55(29): p. 3840-3843.
٢. Alghamdi, S.S., et al., Imidazole as a promising medicinal scaffold: current status and future direction. Drug Design, Development and Therapy, 2021: p. 3289-3312.
٣. Boltjes, A. and A. Dömling, The Groebke-Blackburn-Bienaymé Reaction. European Journal of Organic Chemistry, 2019. 2019(42): p. 7007-7049.
٤. Reddy MR, Darapaneni CM, Patil RD, Kumari H. Recent synthetic methodologies for imidazo [1, 5-a] pyridines and related heterocycles. Organic & Biomolecular Chemistry. 2022;20(17): p. 3440-68.
٥. Krishnamoorthy R, Anaikutti P. Iodine catalyzed synthesis of imidazo [1, 2-a] pyrazine and imidazo [1, 2-a] pyridine derivatives and their anticancer activity. RSC advances. 2023;13(51): p. 36439-54.

The 30th Iranian Seminar of Organic Chemistry
February 7-9, 2025, Iran University of Science and Technology, Tehran, Iran

Acylketenes: Important Intermediates in the Synthesis of Heterocyclic Compounds

Neda Seyedi [a], Hassan Sheibani*[b]

[a]*Department of Chemistry, Faculty of Science, University of Jiroft, Jiroft, Iran*
[b]*Department of Chemistry, Shahid Bahonar University of Kerman, Kerman, 76169, Iran*
Email: hsheibani@uk.ac.ir

Keyword: Acylketenes, Heterocyclic Compounds, 2-diazo-1,3-diketones, 1,3-dioxin-4-ones, β-ketoacid

In organic chemistry, a *ketene* is an organic compound with carbon-carbon-oxygen cumulative double bonds, which they are known as a branch of cumulenes with replacement of one carbon with oxygen. Acylketenes are usually highly reactive molecules, which often prepare from 2-diazo-1,3-diketones, 1,3-dioxin-4-ones, β-ketoacid and malonic acid derivatives, which cannot be isolated or observed under ordinary reaction conditions [1] Acylketenes (α-oxoketenes) are extremely versatile synthetic reagents that have been employed in many syntheses. Therefore, there are considerable interests in the chemistry of ketenes due to fact that these compounds are the building blocks of a wide variety of heterocyclic compounds [2]. Their synthetically useful reactions are nucleophilic additions, [2+2] and [2+4] cycloaddition reactions to give four, five or six-membered ring systems. So, the ketene carboxylic acid derivatives such as (chlorocarbonyl)aryl ketenes are extraordinary stable and known as 1,3-bielectrophiles, which react with a wide variety of nucleophiles under mild experimental conditions, and have been used mainly for the synthesis of five- and six- membered heterocycles functionalized with oxo and hydroxyl groups in 1,3-positions [3].

References:

[1] H. Staudinger, S. Bereza, Chem. Ber. 1909, *42*, 4908–4918.

[21] H. Staudinger, *Ber. Dtsch. Chem. Ges.* **1905**, *38*, 1735–1739.

[3] H. Staudinger, *Chem. Ber.* 1911, *44*, 1619–1623.

The 30th Iranian Seminar of Organic Chemistry
February 7-9, 2025, Iran University of Science and Technology, Tehran, Iran

Synthesis of Triazin Compounds Using Acid Catalyst

Sobhan Yadegari Dokht, Neda Seyedi*

[a]*Department of Chemistry, Faculty of Science, University of Jiroft, Jiroft, Iran*
Email: nedaseyedi@ujiroft.ac.ir

Keyword: Catalyst, Triazine compound, Phytic acid, Graphitic carbon nitride

introduction:

Triazine is a six-membered heterocyclic ring containing three nitrogen atoms in which nitrogen replaces the carbon-hydrogen unit in the benzene ring. Based on the position of the nitrogen in the ring system, there are three isomer forms, 1,2,3-triazine, 1,2,4-triazine and 1,3,5-triazine [1].

Methods:

Phytic acid doped graphitic carbon nitride was synthesized [2]. For the synthesis of triazin compounds, the solution containing 2-aminobenzamide (0.10 mmol) in distilled water (10 ml) which is stirred with a magnetic stirrer at 0 °C, and then catalyst (15 mg) and n-butyl nitrite. (1.2 mmol) was added to the reaction mixture and stirred for 1.5 hours. The precipitated product was filtered and washed with distilled water. The crude product was purified by recrystallization from ethanol.

Results and Discussion:

All synthesized compounds were characterized by nuclear magnetic resonance spectroscopy. Based on the results, the prepared catalyst offers a sustainable, environmentally friendly and cost-effective method for the synthesis of triazine compounds (Scheme 1). High yield of products (95%), high speed and simplicity of the method are other advantages of the presented method.

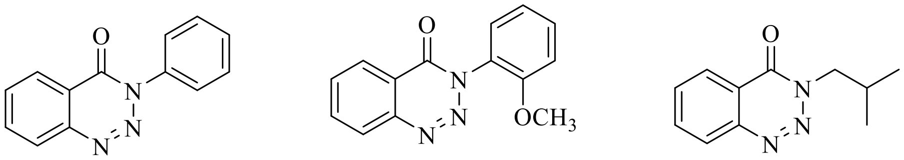

3a 3b 3c

Scheme 1. Synthesized Triazine Compounds

References:

[1] Al-Mulla, A. *Der Pharma Chemica*, **2017**, *9*(13), 141-147.

[2] B. Wang, H. He, H. Hao, P. Li, H. Cai, F. Shang, B. An, X. Li, S. Yang, Int. J. Hydrogen Energy. **2023**, 48(35):13097-13108.

The 30th Iranian Seminar of Organic Chemistry
February 7-9, 2025, Iran University of Science and Technology, Tehran, Iran

Degradation of methylene blue aqueous solution using clinoptilolite based catalyst

Elahe Moradi, Neda Seyedi*

[a]*Department of Chemistry, Faculty of Science, University of Jiroft, Jiroft, Iran*
Email: nedaseyedi@ujiroft.ac.ir
Keyword: Clinoptilolite, Tetracycline, Photocatalyst

introduction: Antibiotics are one of the most important pollutants in environments. Organic dyes are widely used in the industry.

Methods: 25 mL of 0.25 M zinc acetate solution made in ice cold water were taken in 50 mL Teflon lined vessels. Then, 1 g of clinoptilolite was added to reaction mixture and heated under continuous magnetic stirring for 3 h at 100°C. After that, the product was filtered, washed with deionized water and dried at 70 C for overnight. The prepared catalysis was investigated for degradation of methylene blue [1].

Results and Discussion: The photocatalytic degradation of Clinopetilolite/ZnO was investigated for degradation of methylene blue (MB) under ultraviolet-visible spectroscopy (UV). The photocatalytic maximum adsorption capacity of Clinopetilolite/ZnO composite was calculated as qm= 41.32 mg g^{-1} Scheme 1.

Scheme 1. UV–Vis absorbance spectra of MB Catalyzed

References:

J. Pavlovic, M. Opresnik, NN. Tusar, NZ. Logar, N. Rajic, Catalysts. **2022**, 12(2): 224.

The 30th Iranian Seminar of Organic Chemistry
February 7-9, 2025, Iran University of Science and Technology, Tehran, Iran

Introduction of a novel nickel-containing molten salt based on phenylendiammonium as the efficient and reusable catalyst for the reduction of carboxylic acids to alcohols

Farhad Shirini[a]*, Bahareh Abbas Khakiani, Negin Khajavi[b]
Department of Chemistry, College of Science, University of Guilan, Rasht

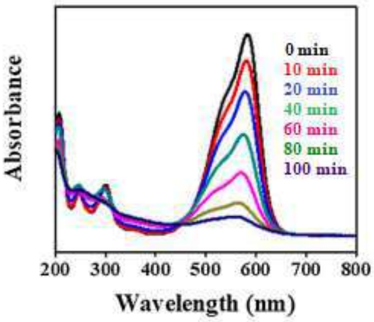

Abstract

Alcohols serve as crucial intermediates in the synthesis of fragrances, pharmaceuticals, detergents, emulsifiers, and lubricants. The conversion of carboxylic acids to alcohols is a significant reaction in organic synthesis, traditionally achieved using various borohydride systems [1]. However, many of the existing methods present drawbacks, including the use of toxic or costly catalysts, the requirement for additional reagents, harsh reaction conditions, the necessity for inert atmospheres (such as nitrogen or argon), prolonged reaction times, low yields, and the generation of mixed products. Furthermore, reliance on volatile organic solvents poses environmental concerns [2]. This study presents a novel approach for the homogeneous catalytic hydrogenation of carboxylic acids to alcohols using nickel. Recent advancements in green chemistry advocate for the use of molten salts as both catalysts and reaction media, owing to their high thermal stability, low vapor pressure, and

broad liquid range, which enhance reaction kinetics and selectivity [3]. A new green synthesis method utilizing a nickel-containing molten salt catalyst (TMPDNi) has demonstrated significant potential, achieving a 90% yield in approximately 30 minutes at 100 °C with water as the solvent (Scheme1). This method is both eco-friendly and efficient, underscoring the necessity for sustainable strategies in the production of valuable pharmaceutical compounds.

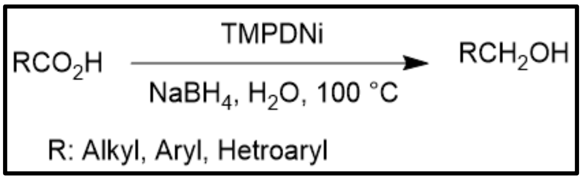

Scheme: Reduction of carboxylic acids to alcohols by nickel-containing molten salt.

Key words: Reduction, Molten salt, Nickel, Alcohol, Phenylendiammonium, Carboxylic acids

References:

[1] Zeynizadeh, B. and Zahmatkesh, K., (2003), Journal of Chemical Research, 2003, 522-525.

[2] Zeynizadeh, B., Sepehraddin, F., and Mousavi, H., (2019), Industrial & Engineering Chemistry Research, 58, 16379-16388.

[3] Laroum, R., & Debache, A., *Synthetic Communications*, 2018. *48*, p: 1876-188

2

The 30th Iranian Seminar of Organic Chemistry
February 7-9, 2025, Iran University of Science and Technology, Tehran, Iran

Fe_3O_4@sal-Cu as a highly efficient magnetic nano-catalyst for the synthesis of 2-substituted benzimidazoles under ultrasonic irradiation and solvent free condition

Roghayeh Ferdousian[a], Farahnaz K. Behbahani[a*], Bita Mohtat[a]

[a] *Department of Chemistry, Karaj Branch, Islamic Azad University, Karaj, Iran.*

Keyword: Fe_3O_4@sal-Cu, Nano-catalyst, Benzimidazoles, heterogeneous

Abstract: Fe_3O_4@Sal-Cu has been synthesized and characterized by XRD, SEM, EDX, VSM and FT-IR and employed as a novel, mild and efficient catalyst for the convenient preparation of benzimidazoles in good to excellent yields from the treatment of *o*-phenylenediamine with various aldehydes, respectively.

Introduction

Fe_3O_4@propyl-semicarbazide-salicyl aldehyde-Cu (Fe_3O_4@sal-Cu) nanocatalyst was synthesized and characterized by several methods including XRD, SEM, EDX, VSM and FT-IR analyses. The Fe_3O_4@sal-Cu has been used as an efficient recyclable magnetic catalyst for the preparation of benzimidazoles. The catalyst[1-6] was conveniently separated from the reaction mixture by an external magnet, and could be reused without any considerable change in catalytic activity. On base of the best our knowledge, Fe_3O_4@sal-Cu nano fine particles have not previously been used for the synthesis of 2-substituted benzimidazoles. Therefore, we wish to introduce Fe_3O_4@sal-Cu nano fine particles as a new catalyst for the preparation of 2-substituted benzimidazoles (Scheme 1).

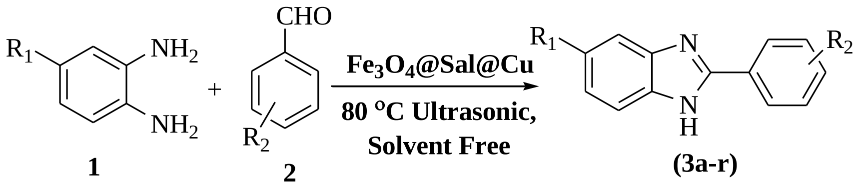

Scheme 1: Synthesis of 2-substituted benzimidazoles using Fe_3O_4@Sal@Cu

Results and discussion

To establish the generality of this method, the synthesis of various benzimidazoles was studied using different benzaldehydes and amines under optimized reaction conditions. Thus, a variety of aromatic aldehydes including electronwithdrawing and electron-donating groups were nvestigated using the new protocol. The results in Table 2 showed the reactions can be completed in relatively short period of times with good to excellent yields under solvent free conditions.

Experimental

General procedure for the synthesis of 2-substituted benzimidazoles: A mixture of benzaldehyde derivative (1 mmol), o-phenylenediamine derivative (1 mmol), Fe_3O_4@Sal@Cu (8 mg) was stirred at 80 °C under ultrasonic irradiation for an appropriate time. The completion of the reaction was monitored by thin layer chromatography (TLC). After completion of the reaction, boiling ethanol (10 ml) was addede and the catalyst was separated by external magnet. Then water was added and solid product was resulted and was filtrated and washed thoroughly with a water–ethanol mixture. All the product were were identified by characterization of their melting points by comparison with those authentic literature samples and also in some cases their FT-IR and ^{1}H NMR.

Conclusion

This method has several advantages like short reaction time, easy and quick work-up, to separate catalyst with external magnet and no leaching of the catalyst. Also, by using Fe_3O_4@Sal-Cu as catalyst, the mentioned reactions do not need toxic solvents and do not give environmentally harmful byproducts.

References

[1] Maleki, A., Aghaei, M., Hafizi-Atabak, H.R. and Ferdowsi, M.*Ultrason. Sonochem.* **2017**, *37*, 260-266.
[2] Maleki, A.; Aghaei, M.;. *Ultrason. Sonochem.* **2017**, *38*, 115-119.

[3] Karimirad, F.; Behbahani, F.K. *Inorg. Nano-Met. Chem.* **2021**, *51*, 656-666.

[4] Shokri, F. and Behbahani, F.K., *Inorg. Nano-Met. Chem.* **2021**, 1-10.
[5] Hasanzadeh, F.; Behbahani, F.K. *Russ. J. Org. Chem.* **2020**, *56*, 1070-1076.
[6] Ferdousian, R.; Behbahani, F.K.; Mohtat, B. *Mol. Divers.***2022**, 1-13.

The 30th Iranian Seminar of Organic Chemistry
February 7-9, 2025, Iran University of Science and Technology, Tehran, Iran

[TMBSPD][OMs]$_2$: An efficient recyclable ionic liquid for the synthesis of bis(indolyl)methanes from aldehydes or ketones and indoles at ambient temperature

M. Janmohammadi[a], F. K. Behbahani *[a]

[a]*Department of Chemistry, Karaj Branch, Islamic Azad University, Karaj, Iran.*

Keyword: TMBSPD][OMs]$_2$, Bis(indolyl)methanes, Friedel-crafts reaction, Recyclable

Abstract

An efficient synthesis of bis(indolyl)methanes from aldehydes and ketones with indoles through *N,N,N',N'*-Tetramethyl-*N,N'*-bis(sulfo)biphenyl-4,4'-diaminium mesylate '[TMBSPD][OMs]$_2$–catalyzed Friedel-Crafts alkylation is developed.

.

Introduction

Ionic liquids have attracted significant attention as dual reagents (catalyst and solvent) for a variety of the organic reactions due to their unique properties such as non-flammability, high solvent capacity, negligible volatility, high ion concentration and high chemical stability [1]. The wide range of anion and cation combinations represents the adjustable interactions and diverse applications of ionic liquids [2]. The basic and acidic ionic liquids could be designed to replace toxic liquid bases and liquid acids in chemical procedures [3]. In this communication, and continuing of our previous research on the organic transformations [4-6], here in we wish to report preparation of **bis(indolyl)methanes from indole and aromatic aldehydes using** [TMBSPD][OMs]$_2$ as a green catalyst in ethanol at room temperature (Scheme 1).

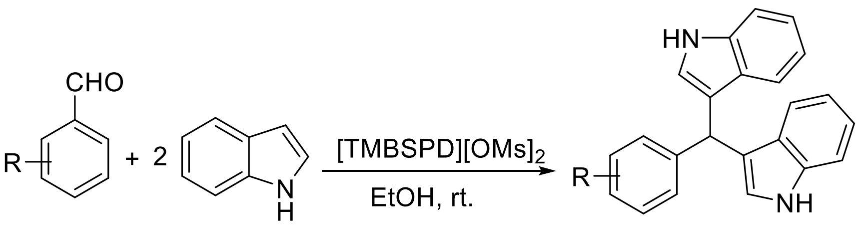

1a **2a** **3a-k**

Scheme 1: Manufacturing of bis(indolyl)methanes using [TMBSPD][OMs]$_2$

Results and discussion

To optimize the reaction conditions for synthesizing of 3,3'-((4-chlorophenyl)methylene)bis(1H-indole), the influence of the reaction temperature, the solvent, and the amounts of ionic liquid catalyst were studied in the reaction of 4-chlorobenzaldehyde, and indole (molar ratio: 1 : 2) as a model reaction. Finally, when the model reaction was accomplished in the presence of 4 mol% of [TMBSPD][OMs]$_2$ under the optimized conditions, the yield of **bis(indolyl)methane derivatives** were 86-90 %, respectively.

Experimental

General procedure for synthesis of bis(indolyl)methanes catalyzed by $[TMBSPD][OMs]_2$. *In one flask,* **indole (2 mmol), aldehyde, or ketone (1 mmol) ethanol (5 mL) and** $[TMBSPD][OMs]_2$ **(4 mol%, 0.16 mmol) was mixed and stirred magnetically at room temperature. After completion of the reaction, as flowed by TLC (hexane/ethyl acetate 4:1),** the water (10 mL) and ethyl acetate (2×15 mL) were poured into the reaction mixture and the product was extracted by separator funnel. The organic layer was separated and dried by Na_2SO_4. After filtration and evaporation of the solvent, the impure product was obtained and crystalized by ethyl acetate/ petroleum ether.

Conclusion

In summary, we have successfully developed a highly efficient, environment friendly and metal-free synthesis of BIMs. This green synthesis offers the corresponding products with good yields and excellent functional group tolerance.

References

[1] Hallett, J. P., and Welton, T., *Chem. Rev*. 2011, vol. 111, p. 3508. _

[2] Stenzel, O., Raubenheimer, H. G., and Esterhuysen, C., *J. Chem. Soc. Dalton Trans*., 2002, vol. 6, p. 1132.

[3] Hajipour, A. R., and Rafiee, F., *J. Iran. Chem. Soc*., 2009, vol. 6, p. 647.

[4] Hasanzadeh, F. and Behbahani, F.K., *Russian J. Org. Chem.*, 2020, vol. *56*, p.1070.

[5] Shekarchi, M. and Behbahani, F.K., *Russian J. Org. Chem.*,2020, vol. *56*, p.894.

[6] Arabpourian, K. and Behbahani, F.K., *Russian J. Org. Chem.*, 2019, vol. *55*, p.682.

The 30th Iranian Seminar of Organic Chemistry
February 7-9, 2025, Iran University of Science and Technology, Tehran, Iran

Ni-catalyzed synthesis of thioesters from aryl halides using chromium hexacarbonyl as CO source

Faezeh Roosta, Najmeh Nowrouzi*

Department of Chemistry, Faculty of Bio and Nano Science and Technology, Persian Gulf University, Bushehr 75169, Iran; nowrouzi@pgu.ac.ir

Keyword: **Thioester, Thiol, Nickel, Chromium hexacarbonyl**

Abstract

Thioesters are important structures that are widely used as active esters in the synthesis of amides, esters, aldehydes, and ketones [1]. These compounds are also more stable than acyl halides; hence, their purification and storage are easier. Although methods for the synthesis of thioesters from carboxylic acids or their derivatives are well known, they still require the use of anhydrous reagents

in stoichiometric amounts. Transition metal-catalyzed carbonylation reactions are an alternative method for the synthesis of unsaturated thioesters [2]. Metal carbonyls can serve as sources of carbon monoxide due to their ability to release CO upon decomposition or under certain conditions. These compounds, which consist of a metal center attached to one or more CO ligands, can release CO in several ways, such as thermal decomposition, photolysis, chemical reactions, and catalysis. These methods make metal carbonyls useful in various industrial and laboratory applications where CO is required. These compounds are more desirable than other carbonyl sources because breaking a C-C bond in organic carbonyls requires more energy than removing the carbonyl ligand. A wide range of carbonylation methods have been developed using $Cr(CO)_6$, $MO(CO)_6$, $W(CO)_6$ as carbonyl sources [3]. The protocol's key advantages include good yields, a simplified synthesis technique,synthesis of thioesters using thiols produced in the environment, lack of a need for any time-consuming work-up or column chromatography,and mild reaction conditions.

General Procedure

In this research project, various alkyl halides are first reacted with thiourea to produce thiol. After the production of the thiouronium salt in the environment, aryl halide, chromium hexacarbonyl, nickel catalyst, and base are added to the reaction mixture. In this reaction, chromium hexacarbonyl is used as a source of carbonyl group. The carbonyl group is added between the C-X bond with the help of nickel catalyst, and in the next step, the thioester is produced through a nucleophilic substitution process and then by reductive elimination (Scheme 1).

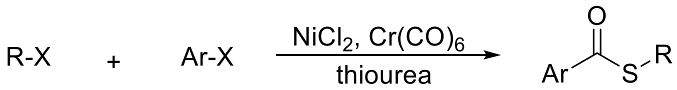

Scheme 1: One-pot synthesis of thioesters from aryl halides

References:

[1] Kazemi, M., Shiri, L. *J. Sulphur Chem*, **2015**, *36*, 613.

[2] Bongiardina, N. J., Long, K. F., Podgórski, M., Bowman, C. N. *J. Biol. Macromol.* **2021**, *54*, 8341.

[3] Odell, L. R.; Russo, F.; Larhed, M. *Synlett.* **2012**, *23*, 685.

The 30th Iranian Seminar of Organic Chemistry
February 7-9, 2025, Iran University of Science and Technology, Tehran, Iran

Polypyridyl materials as a versatile platform for light-emitting electrochemical cell

Babak Nemati Bideh*

Department of Inorganic Chemistry, Faculty of Chemistry and Petroleum Sciences, Bu-Ali Sina University, Hamedan, Iran

Keyword: Polypyridyl Material, Phenanthroimidazole-based ligand, Light-emitting electrochemical cell

Light-emitting electrochemical cells (LECs) are thin film lighting devices that consist of one or two ionic-based active layers sandwiched between two air-stable metal electrodes.These devices exhibit some interesting features that may make them more favourable compared with traditional organic light-emitting diodes (OLEDs), which allow the non-rigorous encapsulation of devices [1]. Among all-luminescent materials, ionic transition metal complexes (iTMCs) have received more attention due to their promising advantages such as their stable redox properties, and highly efficient phosphorescence nature of emission [1]. However, LEC devices suffer from low stability and long response time, limiting their practical applications. Chemical modification of iTMCs has been used to overcome these limitations. In our works, the phenanthroline with a fused imidazole unit with high chemical modification potential was employed as ligand and molecularly-engineered switches (Figure 1) [1-3].

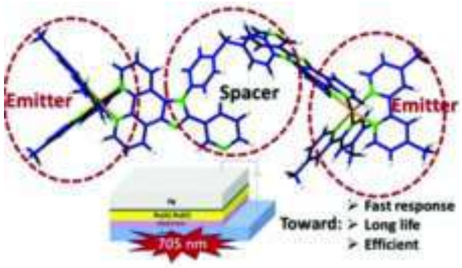

Figure 1: Near-infrared binuclear ruthenium (II) PI-based complex and LEC device [3].

In this context, a combinational approach such as electron donor/acceptor substitutions, various ancillary ligands, binuclearization strategy, and tethered ionic group is used for optimization of efficiency, stability, and response time of both ruthenium (II) and cyclometalated iridium (III) complexes-based LEC devices [1-4]. Our research confirms the advantages of employing these polypyridyl materials to modify iTMC emitters for LECs.

References

[1] Nemati Bideh, B.; Shahroosvand, H.; Nazeeruddin, M. K., High-Efficiency Deep-Red Light-Emitting Electrochemical Cell Based on a Trinuclear Ruthenium(II)–Silver(I) Complex. *Inorg. Chem.* 2021**,** *60*, 11915-11922.

[2] Nemati Bideh, B.; Moghadam, M.; Sousaraei, A.; Shahpoori Arani, B., Phenanthroimidazole as molecularly engineered switch for efficient and highly long-lived light-emitting electrochemical cell. *Sci. Rep.* 2023**,** *13,* 2287.

[3] Nemati Bideh, B.; Shahroosvand, H., New molecularly engineered binuclear ruthenium(ii) complexes for highly efficient near-infrared light-emitting electrochemical cells (NIR-LECs). *Dalton Trans.* 2022**,** *51*, 3652-3660.

[4] Mazaheri, Milad, Nemati Bideh, B.; Sousaraei, A., Binuclear cyclometalated Ir(iii) complexes with bis-bidentate butterfly-shaped ligands: synthesis, characterization, and application in efficient yellow–orange light-emitting electrochemical cells, *Dalton Trans.* 2024**, 53**, 17588-17594.

The 30th Iranian Seminar of Organic Chemistry
February 7-9, 2025, Iran University of Science and Technology, Tehran, Iran

Design of strong organic bases based on 9H-fluoren-9-imine scaffold: Harnessing cation–π interactions to engineer neutral superbases

Zohreh Mirjafary [a], Parsa Fallah [b], Hamid Saeidian [c]

[a]*Department of Chemistry, Science and Research Branch, Islamic Azad University, Tehran, Iran,* zmirjafary@srbiau.ac.ir

[b]*Department of Chemistry, Science and Research Branch, Islamic Azad University, Tehran, Iran,* Parsaw.1274@gmail.com

[c]*Department of Science, Payame Noor University (PNU), P.O. Box: 19395-3697, Tehran, Iran*

Keyword: Basicity, Cation–π interactions, DFT calculations, AIM theory

Amine basicity constitutes a fundamental aspect of organic chemistry, significantly influencing molecular interactions, reaction mechanisms, and various applications in fields such as pharmaceuticals, materials science, and environmental chemistry [1]. Basicity is fundamentally associated with the Gibbs free energy of protonation. The process of protonation is influenced by several factors, including inductive effects, resonance effects, solvent interactions, intramolecular hydrogen bonding, and the inherent instability of amines. Cation–π interactions refer to the attractive forces that occur between a positively charged cation and the electron-dense π-electron system of an aromatic ring [٢]. The strength of these interactions typically varies between ١ and ١٠ kcal/mol, positioning them alongside hydrogen bonds in terms of strength. In specific contexts, cation–π interactions may even exceed the strength of these more commonly recognized non-covalent interactions. In the present study new strategy is used to design of the strong neutral organic bases based on ٩H-fluoren-٩-imine scaffold. Proton–π interactions have been examined using density functional theory (DFT) calculations, employing various indices of aromaticity, including HOMA, NICS, PDI, BI, and FLU. Additionally, the atoms in molecules (AIM) theory have been utilized to investigate this noncovalent interaction.

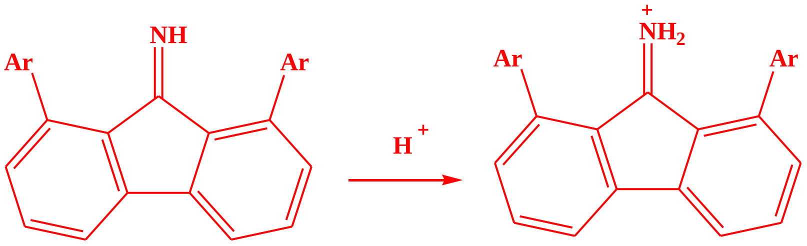

References:

[1]. H. Saeidian, Z. Mirjafary, *New J. Chem.* 2020, *44*, 12967-12977

[2] A. S. Mahadevi, G. N. Sastry, *Chem. Rev*. 2013, *113*, 3, 2100–2138

The 30th Iranian Seminar of Organic Chemistry
February 7-9, 2025, Iran University of Science and Technology, Tehran, Iran

Synthesis of Imidazole [1,2-a]Pyridine through Aza-Henry Reaction by MIL-١٠١(Fe) Catalyst

Bahareh Jadidi, Mostafa Ghafori-Gorab, Nazanin Nejatbakhsh, Amir Kashtiaray, Ali Maleki*

Catalysts and Organic Synthesis Research Laboratory, Department of Chemistry, Iran University of Science and Technology, Tehran, Iran

Keyword: Imidazole [1,2-a]pyridine, Aza-Henry, Metal–organic framework, Catalyst

Heterocycles are among the most diverse and intriguing classes of compounds in organic chemistry. Nitrogen-based heterocycles hold substantial significance in industrial studies. Imidazo[1,2-a]pyridines represent an important class of nitrogen-based heterocyclic compounds that effectively combine a pyridine with an imidazole ring [1]. These compounds illustrate various noteworthy biological activities, including anti-inflammatory, anti-protozoal, anti-bacterial, anti-cancer, anxiolytic, and anti-ulcer properties, among others [2]. Numerous synthetic methods have been established for the preparation of imidazole [1,2-a]pyridine. Among them, the Aza-Henry reaction standing out as one of the most efficient techniques. Many organic and metal-based catalysts have been employed in the Aza-Henry reaction as catalyst. In recent years, the development of metal-organic frameworks (MOFs) as heterogeneous catalysts with high Surface area, tunable pore sizes, chemical, and thermal stability brings an opportunity for advancements in the aza-Henry reaction.

In this study, MIL-101(Fe) was fabricated and used as an efficient catalyst for the synthesis of Imidazole [1,2-a]pyridines. In this regard, catalyst was prepared by combining 0.76 g of $FeCl_3 \cdot 6H_2O$ with 0.206 g of terephthalic acid in DMF solvent at 110 °C for 24 hours in an autoclave. After catalyst preparation and characterization, MIL-101(Fe) was used as a catalyst for the Aza-Henry reaction. The process involved the combination of 1 mmol of 2-aminopyridine, 1.1 mmol of benzaldehyde, 40 mg of the MIL-101(Fe) catalyst, at 110 °C for 18h in a mixture of nitromethane and DMF (2:1). Imidazo[1,2-a]pyridine was synthesized with an efficiency of 80%. Finally, the catalyst demonstrated effective reusability for up to five cycles without significant degradation in performance.

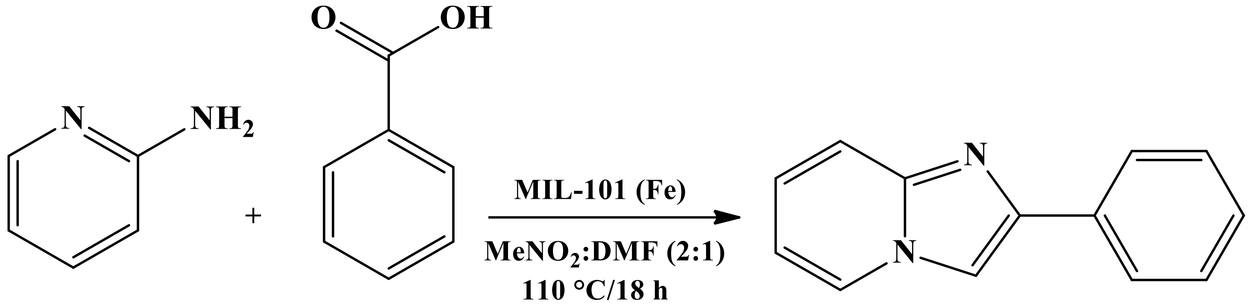

Scheme 1. Synthesis of Imidazole [1,2-a]pyridine through Aza-Henry reaction by MIL-101(Fe) catalyst.

References

1. Althagafi I, Abdel-Latif E. Synthesis and antibacterial activity of new imidazo [1, 2-a] pyridines festooned with pyridine, thiazole or pyrazole moiety. Polycyclic Aromatic Compounds. 2022 Aug 9;42(7): p. 4487-500.
2. Monir K, Kumar Bagdi A, Mishra S, Majee A, Hajra A. Copper (II)-Catalyzed Aerobic Oxidative Coupling between Chalcone and 2-Aminopyridine via C-H Amination: An Expedient Synthesis of 3-Aroylimidazo [1, 2-a] pyridines. Advanced Synthesis & Catalysis. 2014 Mar 24;356(5): p. 1105-12.

3. Saranya PV, Philip RM, Anilkumar G. Synthesis of imidazo [1, 2-a] pyridines via cobalt/iodine-catalyzed Ortoleva-King type approach. Tetrahedron Letters. 2024 Aug 15;146: p. 155188.

The 30th Iranian Seminar of Organic Chemistry
February 7-9, 2025, Iran University of Science and Technology, Tehran, Iran

Development of FTO-ZnO/Carbon Nanofiber Composites for Lithium-Ion Batteries with Organic Electrolytes: Enhancing Energy Storage Technology

Authors: Fatemeh Razi Astaraei 1[a], Mahsa Panahi Azar 2*[b]

[1]*Department of Renewable Energy Technologies and Energy Resources Engineering, School of Energy Engineering and Sustainable Resources, College of Interdisciplinary Science and Technology, University of Tehran, Tehran, Iran.*

[2]*Department of Renewable Energy Technologies and Energy Resources Engineering, School of Energy Engineering and Sustainable Resources, College of Interdisciplinary Science and Technology, University of Tehran, Tehran, Iran.*

Abstract

In this work, FTO-ZnO-CNF nanocomposites were synthesized and characterized as innovative anode materials for lithium-ion batteries. Zinc Oxide nanorods were fabricated through a hydrothermal process, with FTO add to PAN solution and integrated using electrospinning, followed by carbonization at 700°C for 2 hours. By Minitab software design experiments to optimize proportion of Zno-FTO salt in PAN solution. Electrochemical evaluations demonstrated an initial specific capacity of 1100 mAh/g at 0.1 mA/g and retention of 73% after 55 cycles. The rate performance revealed reversible capacity recovery from 600 mAh/g at 0.5 mA/g to 1000 mAh/g at 0.1 mA/g, showcasing excellent stability and reversibility. These properties were validated in CR2032 coin-cell configurations. The promising results highlight the FTO-ZnO nanocomposite as a scalable, high-performance anode material suitable for next-generation lithium-ion batteries.

Keyword: Lithium-ion Battery, Organic Electrolyte, Anode, Fluorine-Doped Tin Oxide, MiniTab

Introduction

Lithium-ion batteries (LIBs) are the cornerstone of modern energy storage technology, powering applications from portable electronics to electric vehicles. Their widespread adoption is attributed to their high energy density, long cycle life, and reliability. However, the conventional graphite anode—with a theoretical capacity of 372 mAh/g—limits the energy density achievable in current LIB systems, necessitating the development of alternative anode materials with enhanced capacity and performance metrics [1], [2]. This research investigates the potential of a novel composite comprising fluorine-doped tin oxide (FTO), zinc oxide (ZnO), and carbon nanofibers (CNFs), designed to address these limitations.

Organic electrolytes are an essential component of LIBs, offering high ionic conductivity and wide electrochemical stability windows. However, their inherent flammability and the formation of unstable solid-electrolyte interphases (SEI) pose significant safety challenges [3], [4]. Recent advances in electrolyte formulations—such as the incorporation of ionic liquids and gel polymer electrolytes—have shown promise in mitigating these risks while maintaining performance. The integration of a robust anode material like the FTO-ZnO-CNF composite with organic electrolytes could significantly enhance LIB safety, capacity, and rate performance [5].

FTO is a transparent conductive oxide widely utilized in electronic applications for its excellent electrical conductivity and chemical stability. In LIBs, FTO facilitates efficient electron transport, improving cycling stability and enhancing the overall performance of the anode [6], [7]. ZnO, a wide-bandgap semiconductor, offers a theoretical capacity of approximately 987 mAh/g, making it a promising candidate for increasing LIB energy density. However, its practical application is hindered by poor electrical conductivity and significant volume changes during lithiation and delithiation, leading to capacity fading [8], [9]. The inclusion of CNFs in the composite structure addresses these issues by providing a conductive framework with high mechanical strength and excellent surface area, which supports ion transport and buffers volume changes [10], [11].

The binder-free architecture of the FTO-ZnO-CNF composite eliminates the need for polymeric binders, which often impede ionic conductivity and add unnecessary weight. This design allows direct interaction between the active materials and the organic electrolyte, enhancing charge transfer kinetics and improving overall battery efficiency. The absence of binders also reduces the internal resistance of the electrode, enabling better rate capabilities and higher energy densities [12], [13].

The fabrication of this composite employs electrospinning, a versatile and scalable technique that ensures precise control over the morphology and distribution of the active materials. Electrospun nanofibers provide a porous structure, facilitating lithium-ion diffusion and increasing the number of active sites for electrochemical reactions. This structural advantage significantly enhances the composite's electrochemical performance and mechanical stability during repeated charge-discharge cycles [14], [15].

Safety is a critical consideration for LIBs utilizing organic electrolytes. The FTO-ZnO-CNF composite contributes to improved thermal stability and reduces the risk of dendrite formation, a common issue leading to short circuits and battery failure. Additionally, the structural integrity provided by CNFs ensures uniform lithium-ion flux, minimizing hotspots and uneven lithium plating [16], [17]. These properties make the composite an ideal candidate for high-performance and safe LIB systems.

The environmental impact of LIB materials is another important factor. The use of abundant and non-toxic materials like ZnO, combined with the potential recyclability of CNFs, aligns with the global push toward sustainable energy solutions. This composite addresses the need for eco-friendly materials while offering superior performance metrics [18], [19].

Future advancements in this field are likely to focus on optimizing the synthesis and integration of the FTO-ZnO-CNF composite with innovative organic electrolyte formulations. Potential strategies include doping with additional elements to enhance lithium-ion diffusion rates and applying surface coatings to protect against electrolyte degradation. These approaches aim to further improve the composite's capacity, cycling stability, and compatibility with organic electrolytes [20], [21].

In conclusion, the development of the FTO-ZnO-CNF composite represents a significant step forward in LIB technology, particularly for systems employing organic electrolytes. By combining the unique properties of FTO, ZnO, and CNFs, this composite addresses critical challenges such as low conductivity, capacity fading, and safety concerns. Its integration with advanced organic electrolyte formulations positions this material as a promising candidate for next-generation energy storage solutions.

Method

1. Synthesis of FTO Nanoparticles

The synthesis of fluorine-doped tin oxide (FTO) nanoparticles was performed using a sol-gel and thermal method. Initially, 2 g of tin(II) chloride pentahydrate ($SnCl_2 \cdot 5H_2O$) was dissolved in 1 mL of hydrochloric acid (HCl) at 70°C. Subsequently, 3 mL of ethanol was added. Separately, 0.5 g of ammonium fluoride (NH_4F) was dissolved in 3 mL of deionized water (DI). These two solutions were mixed under magnetic stirring at 70°C to ensure the complete reaction and evaporation of the solvents. Finally, the mixture was subjected to calcination at 450°C for 3 hours. The synthesized FTO nanoparticles were analyzed using X-ray diffraction (XRD), as depicted in Figure 1a, confirming the phase and crystallinity of the product.

2. Growth of ZnO Nanorods

Zinc oxide (ZnO) nanorods were synthesized through a hydrothermal method to ensure controlled morphology and cost-effectiveness. A precursor solution was prepared by dissolving 0.05 M zinc nitrate hexahydrate in 50 mL of DI water, and a second solution of 0.05 M hexamethylene tetramine (HMT) in 50 mL of DI water. These solutions were combined dropwise over 25 minutes under constant stirring to form a uniform and transparent solution. The resultant precursor was placed in an oven at 100°C for 3 hours to facilitate nanorod growth. After cooling to room temperature, the ZnO structures were collected via filtration, washed, and dried at 80°C for 2 hours. The XRD pattern, shown in Figure 1b, verified the successful synthesis.

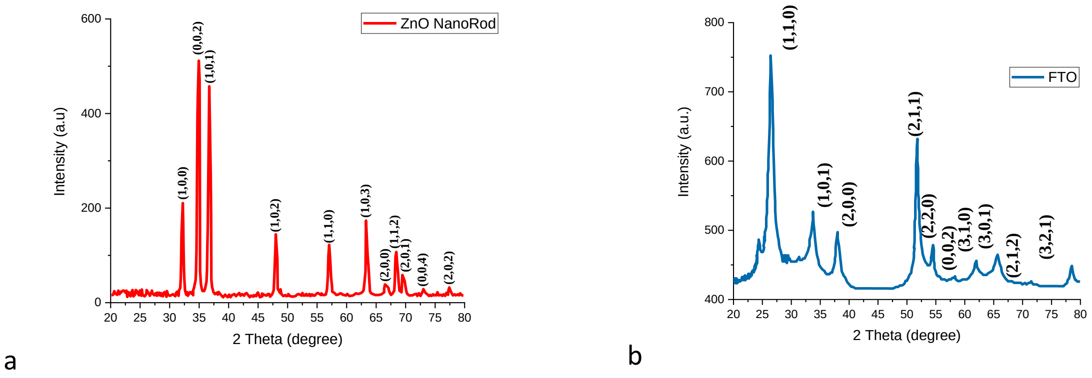

Figure 33 XRD patterns of (a) ZnO Nanorod (b) FTO Nanoparticles

3. Synthesis of FTO-ZnO-CNF Nanocomposite

The FTO-ZnO-carbon nanofiber (CNF) nanocomposite was prepared by electrospinning. Initially, an 8 wt.% solution of polyacrylonitrile (PAN) in dimethylformamide (DMF) was prepared and stirred at 60°C for 24 hours. Subsequently, FTO and ZnO were dispersed in the PAN solution, achieving a final metal salt concentration of 4 wt.% with a FTO:Zn weight ratio of 25:75. This mixture was stirred for another 24 hours at room temperature to ensure homogeneity.

Table 2 Key parameters of Electrospinning

Parameter	Measure
Voltage	15 kV
Distance	17 cm
Feed Rate	0.8 ml/h
Needle Diameter	Inner 0.84 mm Outer 1.27 mm
Time	10 h
Temperature of Pre-heating	180 C
Time of Pre-heating at Air	2 h
Carbonization Time in Argon Atmosphere	700 C
Time of Carbonization	6 h

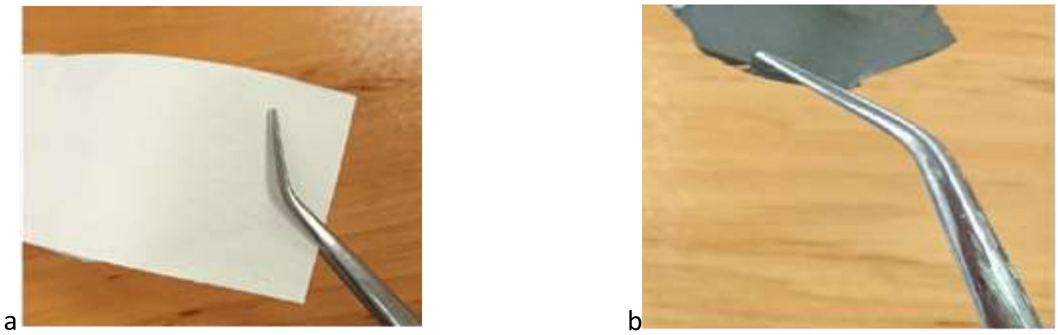

__Figure 34__ (a) As-prepared DMF-FTO-ZnO Nanofiber (b) Free-standing FTO-ZnO-CNF

The electrospinning setup consisted of a syringe and needle, a grounded aluminum collector, and a high-voltage power supply. The precursor solution was electrospun at room temperature with a 17 cm distance between the needle and the collector Figure 2a. Key parameters are summarized in Table 1. After spinning, the fibers were scraped off the substrate, stabilized at 280°C in air, and then carbonized in a tubular furnace under an argon atmosphere at 700°C for 2 hours Figure 2b. The XRD analysis of the resulting nanocomposite is illustrated in Figure 3d, and SEM and TEM images of the composite at different stages are shown in Figure 3a,b,c.

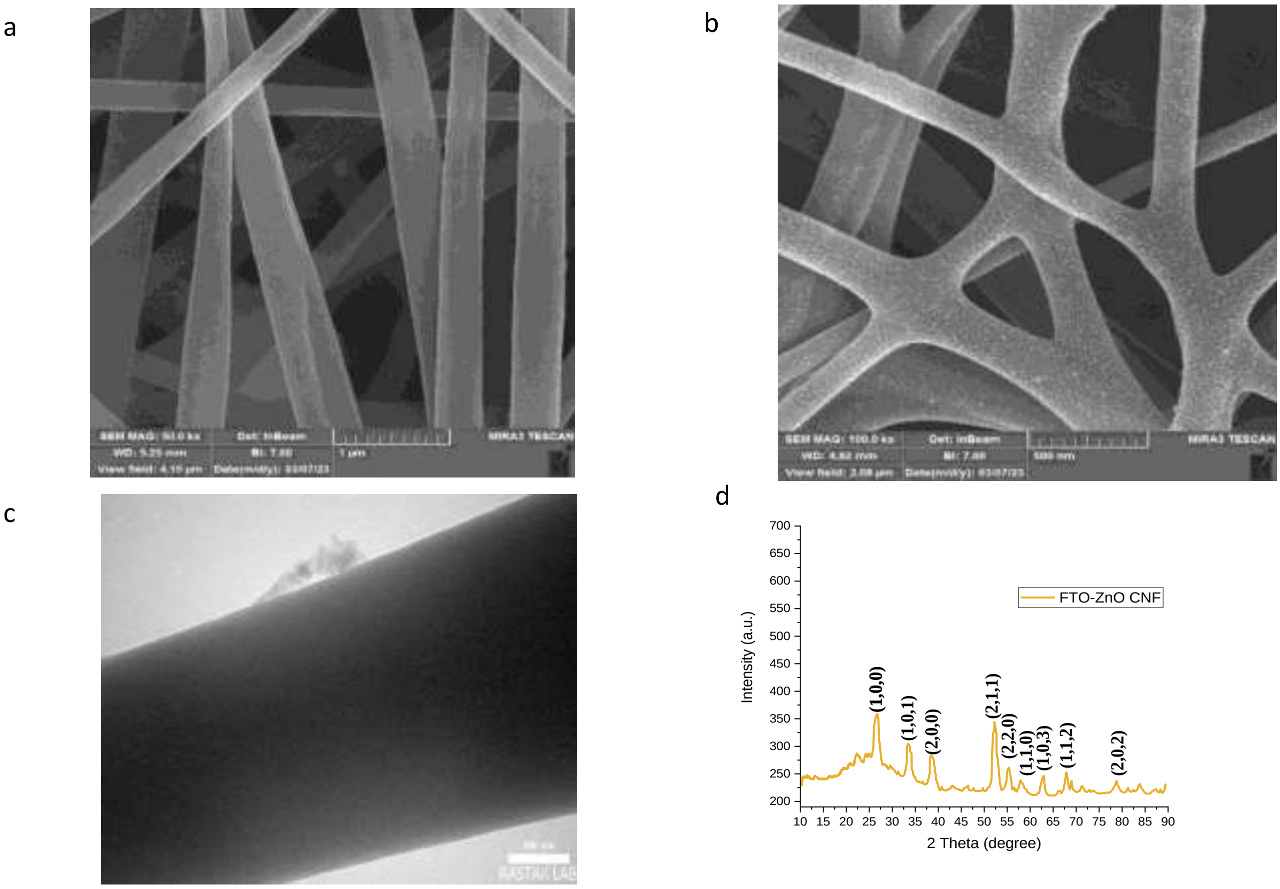

__Figure 35__ (a) SEM images of As-prepared FTO-ZnO-DMF Nanofiber (b) Free-standing FTO-ZnO-CNF (c)TEM image of Free-standing FTO-ZnO-CNF

4. Design of Experiments (DOE) and Statistical Analysis

Overview of Optimization Strategy

The optimization of the FTO-ZnO-CNF nanocomposite as an anode material for lithium-ion batteries was performed using a robust **full factorial design methodology** implemented in MiniTab software. This statistical approach is widely recognized for its ability to systematically evaluate all possible combinations of selected experimental factors, thereby enabling a comprehensive understanding of their individual effects and interactions. By employing this method, the experimental design ensures reliable conclusions about the optimal synthesis parameters and the resulting material performance.

Rationale for Selecting Factors

Two primary factors were identified for investigation based on their significant influence on the electrochemical performance of the anode material:

١. **Salt Concentration in PAN Solution (% by weight):**

This parameter affects the electrospinning process, influencing fiber formation, morphology, and uniformity. Variations in salt concentration alter the viscosity and conductivity of the solution, which in turn affect the deposition rate and structural integrity of the nanocomposite fibers.

٢. **Weight Ratio of FTO to ZnO (%):**

The ratio of these two materials determines the chemical and electrochemical properties of the composite. ZnO contributes to the structural stability and electronic properties, while FTO enhances electrical conductivity and contributes to the composite's ability to withstand repeated charge-discharge cycles. The weight ratio is critical to achieving a balance between these properties.

Definition of Levels

Each factor was examined at two levels, representing minimum and maximum practical limits derived from preliminary studies and literature reviews:

- **Salt Concentration in PAN:** 5% (low) and 15% (high).
- **FTO to ZnO Ratio:** 25% (low) and 75% (high).

The choice of these levels was guided by the need to explore the widest range of conditions without compromising process feasibility or material stability.

Design and Implementation of Full Factorial Design

A **full factorial design** was chosen due to its suitability for scenarios with a limited number of factors and levels, providing detailed insights into both main effects and interaction effects. The experimental matrix consisted of four unique combinations, as shown in Table 2:

Table 3 *Code of Designed Experiments*

Experiment Code	FTO-ZnO Ratio (%)	Salt Concentration (%)
FTO-ZnO525	25	5
FTO-ZnO575	75	5
FTO-ZnO1575	75	15
FTO-ZnO1525	25	15

This design provided a balanced approach to evaluating all possible combinations of the selected levels while minimizing the number of required experiments. The factorial approach also facilitates direct observation of interaction effects, which are critical in understanding the synergy between salt concentration and FTO-ZnO ratio.

Data Analysis and Statistical Methodology

The collected data were analyzed using MiniTab to determine the statistical significance of the factors and their interactions. Several advanced techniques were employed:

١. **Analysis of Variance (ANOVA):**

ANOVA was used to quantify the contributions of each factor and their interactions to the variance observed in the anode capacity. This analysis included the calculation of p-values and F-statistics to determine statistical significance at a 95% confidence level. The use of ANOVA ensured that the identified relationships between the factors and response variable (specific capacity) were both robust and reliable.

٢. **Response Surface Analysis:**

Though not explicitly part of a full factorial design, response surface plots were generated to visualize the interactions between factors. These plots provided insights into optimal operating conditions and clarified the nature of nonlinear interactions.

٣. **Residual Analysis:**

Residuals were examined to verify the assumptions of normality, homoscedasticity, and independence. This step was crucial to ensure the validity of the statistical model and the reliability of conclusions drawn from it.

٤. **Optimization Criteria:**

The primary optimization goal was to maximize the specific capacity of the anode material. The factor levels that produced the highest capacity, while maintaining acceptable cycle stability, were identified as optimal. Interaction plots were instrumental in identifying synergistic effects that could not be captured by main effect analysis alone.

Results and Discussion

1. Structural Analysis: X-ray Diffraction (XRD)

The structural properties of the synthesized FTO-ZnO-CNF nanocomposites were investigated using X-ray diffraction (XRD) analysis (Figure 4a). The results revealed distinct crystalline patterns corresponding to the compositions of the materials. As the mass percentage of FTO increased, the intensities of the diffraction peaks became more pronounced, reflecting enhanced crystallinity and better structural organization.

In contrast, higher concentrations of ZnO led to reduced peak intensities, indicating a potential decline in crystallinity due to the interaction between ZnO and CNFs, which may induce lattice distortions. Furthermore, broader diffraction peaks were observed at lower salt concentrations and higher CNF content, indicative of reduced crystallite size. These findings underline the critical role of FTO and ZnO proportions in tailoring the crystallinity and structural characteristics of the composite electrodes, which directly influence their electrochemical behavior.

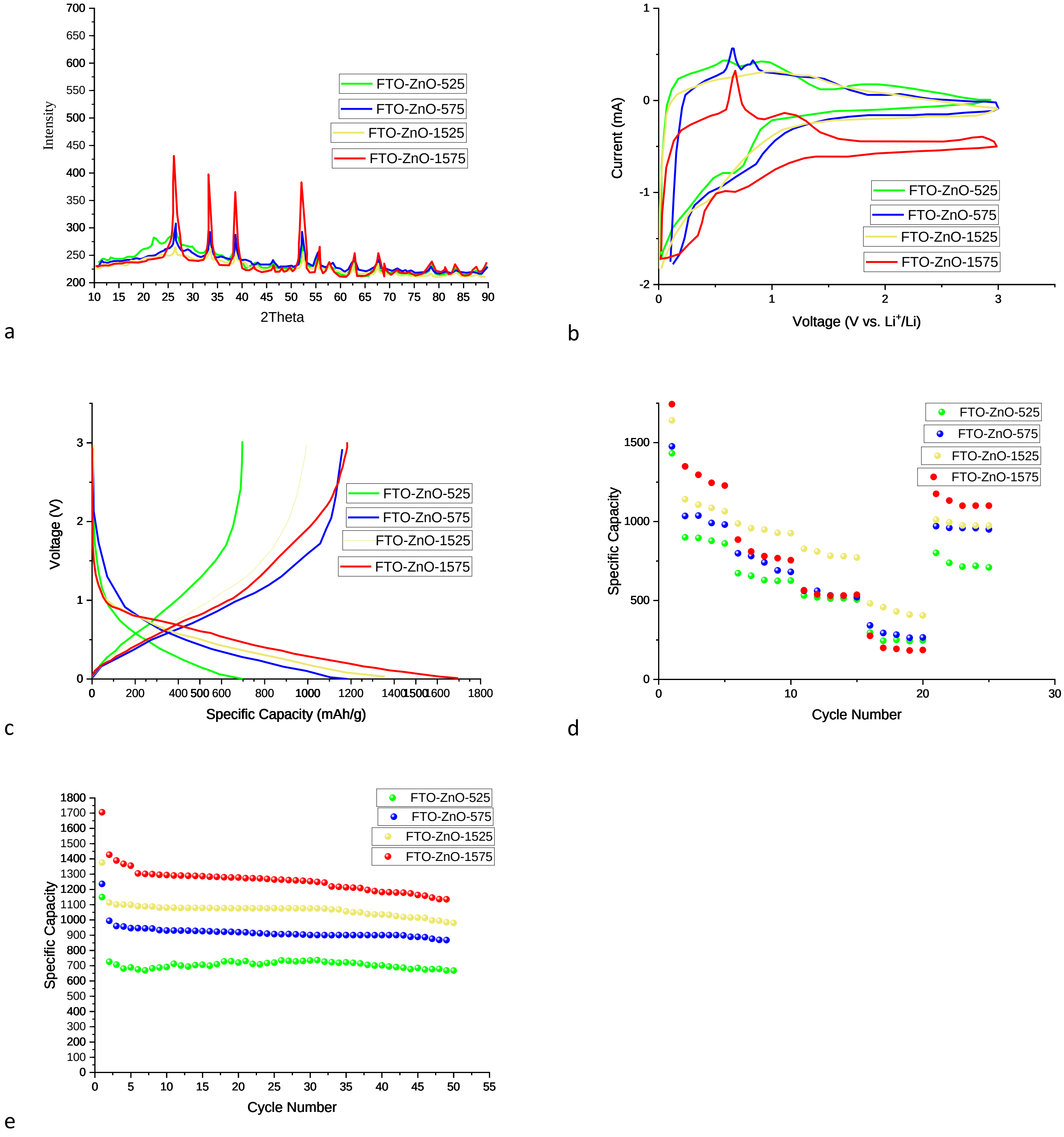

Figure 36 *(a) XRD Patterns of samples (b)Cyclic Voltammetry Curves of Samples (c)Charge-Discharge Curves of Samples (d) Rate Capability and Repeatability Curves of Samples (e)Cycle Stability Curves of Samples*

2. *Electrochemical Behavior: Cyclic Voltammetry (CV)*

The electrochemical properties of the nanocomposite electrodes were evaluated using cyclic voltammetry (CV), as illustrated in Figure 4b. During the first cathodic sweep (lithium insertion), irreversible peaks were observed at 0.52 V, 0.78 V, and 0.84 V. These peaks are primarily attributed to the formation of the solid electrolyte interphase (SEI) on the electrode surface, a phenomenon that is common in lithium-ion batteries (LIBs) and essential for stabilizing the electrode-electrolyte interface.

A reversible peak at approximately 0.34 V was observed in subsequent cycles, indicating the formation and decomposition of lithium-tin (Li-Sn) alloys. For electrodes with higher ZnO content, additional cathodic peaks appeared at 0.84 V and 0.3 V in the first scan, which can be ascribed to the reduction of ZnO and the associated SEI layer growth. Moreover, a broad peak at approximately 1.3 V is likely due to the reaction between Zn and Li2O, forming ZnO. The overlapping CV profiles in subsequent cycles suggest high reversibility of the lithiation/delithiation processes. These results confirm the ability of the FTO-ZnO nanocomposite electrodes to sustain reversible electrochemical reactions, a critical feature for long-term LIB performance.

3. Charge/Discharge Performance

The charge/discharge characteristics of the electrodes were studied through galvanostatic measurements over a voltage range of 0.01–3 V (Figure 4c). Among the synthesized samples, the FTO-ZnO-575 electrode demonstrated the highest initial Coulombic efficiency (>70%), significantly outperforming the other electrodes. This superior efficiency is attributed to the intimate contact between Sn particles and CNFs, which facilitates enhanced lithium-ion diffusion and reversible SnOx formation.

The presence of Li2O in the composite matrix further supports the reversible reactions, as Li2O undergoes repeated utilization during cycling. This interaction improves both the specific capacity and the electrochemical efficiency of the electrode. The consistent capacity retention in subsequent cycles highlights the robust performance of the FTO-ZnO-575 electrode under practical operating conditions.

4. Rate Capability Analysis

Rate capability is a critical parameter for evaluating the practicality of LIB electrodes, particularly under varying current densities. Figure 4d illustrates the rate performance of the four designed electrodes. The reversible specific capacities were determined to be 604.41, 897.74, 1175.75, and 943.45 $mAh \cdot g^{-1}$ for FTO-ZnO-525, FTO-ZnO-575, FTO-ZnO-1525, and FTO-ZnO-1575, respectively.

The superior rate capability of the FTO-ZnO-1525 and FTO-ZnO-1575 electrodes can be ascribed to the optimized interplay between salt concentration and the FTO/ZnO ratio. Higher salt concentrations facilitate better ionic conductivity, while the structural integrity of the nanocomposite ensures efficient lithium-ion transport pathways. These attributes collectively contribute to the enhanced electrochemical performance of these electrodes, particularly at high current densities.

5. Cycle Stability

The cycling stability of the electrodes was evaluated at a current density of 0.5 $A \cdot g^{-1}$ over multiple cycles (Figure 4e). The FTO-ZnO-1575 electrode exhibited the highest specific capacity retention, maintaining stable performance throughout the cycling test. Notably, FTO-ZnO-1525 showed a more pronounced capacity decline, likely due to volume expansion of Sn particles during cycling. This phenomenon, commonly associated with the lithiation of Sn-based materials, leads to mechanical stress and potential degradation of the electrode.

Despite these challenges, the FTO-ZnO-575 electrode demonstrated remarkable stability under high current densities, underscoring its potential for high-performance LIB applications. The combination of FTO and ZnO in the composite matrix significantly mitigates the effects of volume changes, thereby preserving the electrode’s structural and electrochemical integrity.

6. *Statistical and Optimization Analysis*

To identify the key parameters influencing the specific capacity of the FTO-ZnO nanocomposite anodes, statistical analysis was conducted using a full factorial experimental design. The analysis was aimed at quantifying the effects of salt concentration and the FTO/ZnO ratio on the specific capacity, as well as optimizing these parameters for maximum performance.

The statistical analysis of the experimental data, summarized in Table 1, highlights the significant impact of salt concentration (P = 0.034) and the FTO/ZnO ratio (P = 0.039) on specific capacity. The regression equation derived from the data is as follows:

Specific Capacity=259.4+35.83·Salt Percent+6.251·FTO-ZnO

The high R-squared value of 99.84% indicates excellent model accuracy and predictive reliability (Table 3). Optimization analysis using a full factorial design revealed that the maximum specific capacity of 1275.25 mAh·g^{-1} could be achieved with a salt concentration of 15% and an FTO/ZnO ratio of 75%. These parameters correspond to the composition of the FTO-ZnO-1575 sample, further validating the experimental findings and highlighting the sample's optimal performance.

Analysis of Variance (ANOVA)

The results of the ANOVA, presented in Table 1, demonstrate the significant impact of both independent variables on the specific capacity. The salt concentration (P = 0.034) and the FTO/ZnO ratio (P = 0.039) both exhibited P-values below the significance threshold of 0.05, indicating their statistically significant contribution to the model. Additionally, the F-value for the overall model was 305.50, signifying a highly robust predictive capability.

The ANOVA table also highlights the relative contribution of each parameter. The adjusted sums of squares (Adj SS) reveal that the salt concentration contributed approximately 57% of the total variability (Adj SS = 128,361), while the FTO/ZnO ratio accounted for the remaining 43% (Adj SS = 97,697). These results indicate that while both parameters are critical, salt concentration has a slightly more pronounced influence on specific capacity.

Table 4 *ANOVA Table*

Source	DF	Adj SS	Adj MS	F-Value	P-Value
Model	2	226058	113029	305.50	0.040
Linear	2	226058	113029	305.50	0.040
Salt-Percent	1	128361	128361	346.94	0.034
FTO-ZnO	1	97697	97697	264.06	0.039
Error	1	370	370		
Total	3	226428			

Regression Model and Predictive Accuracy

As it has said earlier the linear regression model derived from the experimental data is as follows:

Specific Capacity=259.4+35.83·Salt Percent+6.251·FTO-ZnO

The regression coefficients for salt concentration (35.83) and the FTO/ZnO ratio (6.251) highlight the positive contribution of both parameters to the specific capacity. Notably, the larger coefficient for salt concentration underscores its dominant role in enhancing the electrochemical performance of the nanocomposite anodes.

Table 5 *Model Summary*

S	R-sq	R-sq(adj)	R-sq(pred)
19.235	99.84%	99.51%	97.39%

The quality of the regression model was assessed through key statistical metrics summarized in Table 3. The coefficient of determination (R-Squared) was 99.84%, indicating that the model explains nearly all the variability in the experimental data. The adjusted R-Squared-adj (99.51%) and predicted R-Squared-pred (97.39%) further confirm the model's robustness, Table4, even when accounting for the number of predictors and potential overfitting. The standard error of the regression (S = 19.235) is relatively low, providing additional confidence in the model's precision.

Optimization Analysis

To determine the optimal parameter settings for maximum specific capacity, the data were analyzed using a full factorial optimization approach. The optimization results, visualized through contour and response surface plots (Figures 5 a,b), reveal a clear trend: the highest specific capacity of 1275.25 mAh·g^{-1} is achieved when the salt concentration is set to 15% and the FTO/ZnO ratio is 75%.

These findings align with the experimental results for the FTO-ZnO-1575 sample, which demonstrated superior electrochemical performance compared to other configurations. The optimization table confirms the desirability score of 0.985663, indicating near-ideal conditions for maximizing the specific capacity.

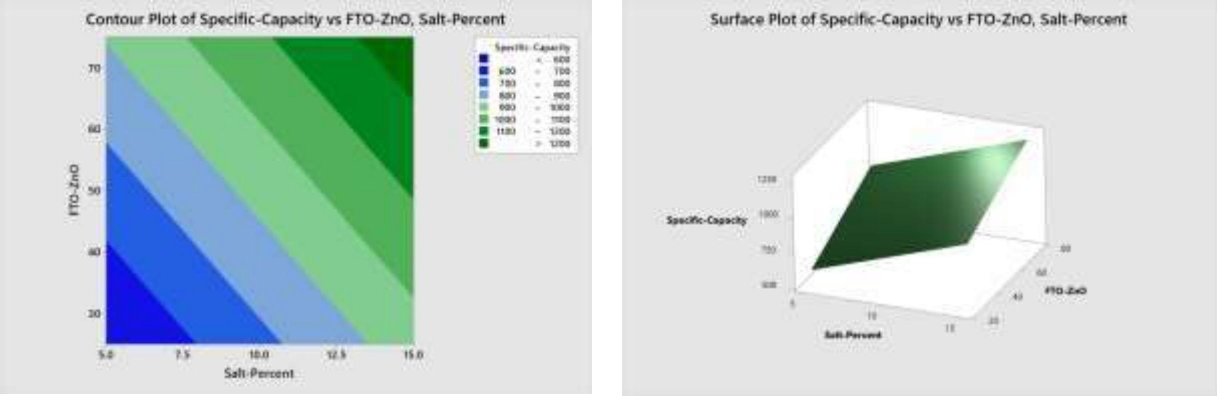

Figure 37 *(a)Countour plots (b)Surface plots*

Conclusion and Further Considerations

This study successfully synthesized and characterized FTO-ZnO nanocomposites as potential anode materials for lithium-ion batteries. The hydrothermal growth of ZnO nanorods combined with electrospinning of FTO yielded a uniform nanocomposite with desirable structural and electrochemical properties. The material exhibited an impressive initial capacity of 1100 mAh/g and a capacity retention of 73% after 55 cycles, confirming its long-term cycling stability. Rate capability tests indicated a reversible capacity recovery to 1000 mAh/g, demonstrating excellent adaptability to varying charge-discharge conditions. These findings suggest that the FTO-ZnO nanocomposite combines structural stability with superior electrochemical performance. Future research should focus on scaling production processes and integrating the composite into full-cell systems to explore its commercial viability as a sustainable, high-performance energy storage solution. While the current model is highly robust, it assumes linear relationships between the variables and specific capacity. Nonlinear interactions or secondary effects (e.g., particle size, distribution uniformity, and electrolyte interactions) may also play a role and should be explored in future studies. Incorporating advanced statistical techniques, such as response surface methodology (RSM) or machine learning models, could provide deeper insights and potentially uncover higher-order interactions.

References:

[1] V. Bui, T. Pham, J. Hur, and Y. Lee, "Review of ZnO binary and ternary composite anodes for lithium-ion batteries," *Nanomaterials*, vol. 11, no. 8, p. 2001, 2021, doi: 10.3390/nano11082001.

[2] T. Xia et al., "Facile in situ growth of ZnO nanosheets standing on Ni foam as binder-free anodes for lithium-ion batteries," *RSC Advances*, vol. 9, no. 34, pp. 19253–19260, 2019, doi: 10.1039/c9ra03373d.

[3] S. Wang et al., "Lithium chlorides and bromides as promising solid-state chemistries for fast ion conductors with good electrochemical stability," *Angewandte Chemie*, vol. 58, no. 24, pp. 8039–8043, 2019, doi: 10.1002/anie.201901938.

[4] Z. Liu et al., "Insights into quasi solid-state polymer electrolyte: The influence of succinonitrile on polyvinylene carbonate electrolyte," *Battery Energy*, vol. 2, no. 3, 2023, doi: 10.1002/bte2.20220049.

[5] X. Wang et al., "Ultrasonication-assisted fabrication of porous ZnO@C nanoplates for lithium-ion batteries," *Microstructures*, vol. 2, no. 3, p. 16, 2022, doi: 10.20517/microstructures.2022.11.

[6] H. Xu et al., "Fluorine-doped tin oxide nanocrystal/reduced graphene oxide composites as lithium-ion battery anode material," *ACS Applied Materials & Interfaces*, vol. 8, no. 6, pp. 14339–14349, 2015, doi: 10.1021/acsami.5b09538.

[7] J. Yuan et al., "Facile fabrication of three-dimensional porous ZnO thin films on Ni foams," *Materials Letters*, vol. 190, pp. 37–39, 2017, doi: 10.1016/j.matlet.2016.12.126.

[8] Y. Shen et al., "MXene/ZnO flexible freestanding film as a dendrite-free support in lithium metal batteries," *Journal of Materials Chemistry A*, vol. 10, no. 33, pp. 17199–17207, 2022, doi: 10.1039/d2ta04797g.

[9] B. Joshi et al., "Flexible, freestanding, and binder-free SnOx-ZnO/carbon nanofiber composites for lithium-ion battery anodes," *ACS Applied Materials & Interfaces*, vol. 8, no. 12, pp. 28583–28593, 2016, doi: 10.1021/acsami.6b01093.

[10] Z. Sadighi et al., "Atomic layer deposition ZnO-enhanced negative electrode," *Journal of the Electrochemical Society*, vol. 170, no. 1, p. 010512, 2023, doi: 10.1149/1945-7111/acaf3e.

[11] T. Xia et al., "High rate capability and cyclic stability of hierarchically porous SnO2/carbon nanofibers," *RSC Advances*, vol. 9, no. 1, pp. 1–7, 2019, doi: 10.1039/c9ra03373d.

[12] Z. Cao et al., "Perpendicular MXene arrays for dendrite-free lithium metal anodes," *Advanced Functional Materials*, vol. 30, no. 5, 2019, doi: 10.1002/adfm.201908075.

[13] Y. Zhao et al., "Nitrogen-doped carbon nanotubes coated with zinc oxide nanoparticles," *Beilstein Journal of Nanotechnology*, vol. 9, pp. 1677–1685, 2018, doi: 10.3762/bjnano.9.159.

[14] S. Sharma et al., "Versatile graphitized carbon nanofibers in energy applications," *ACS Sustainable Chemistry & Engineering*, vol. 10, no. 4, pp. 1334–1360, 2022, doi: 10.1021/acssuschemeng.1c06762.

[15] L. Liu et al., "Prospects of sulfide-based solid-state electrolytes modified by organic thin films," *International Journal of Energy Research*, vol. 2023, p. 1–7, doi: 10.1155/2023/2601098.

[16] P. Yao et al., "Review on polymer-based composite electrolytes for lithium batteries," *Frontiers in Chemistry*, vol. 7, 2019, doi: 10.3389/fchem.2019.00522.

[17] X. Yu and A. Manthiram, "A long cycle life, all-solid-state lithium battery," *ACS Applied Energy Materials*, vol. 3, no. 3, pp. 2916–2924, 2020, doi: 10.1021/acsaem.9b02547.

[18] J. Li et al., "Synergistic interface and mesopore engineering for enhanced performance," *Batteries & Supercaps*, vol. 4, no. 12, pp. 1858–1866, 2021, doi: 10.1002/batt.202100151.

[19] E. Thauer et al., "Novel synthesis and electrochemical investigations of ZnO/C composites," *Journal of Materials Science*, 2021, doi: 10.1007/s10853-021-06125-4.

[20] S. Ndruru et al., "Modification of cacao pod husk cellulose for lithium-ion batteries," *ChemistrySelect*, vol. 7, no. 44, 2022, doi: 10.1002/slct.202202510.

[21] V. Lazarenko et al., "Bi2Se3 nanostructured thin films for aqueous rechargeable lithium-ion batteries," *Batteries*, vol. 8, no. 10, p. 144, 2022, doi: 10.3390/batteries8100144.

The 30th Iranian Seminar of Organic Chemistry
February 7-9, 2025, Iran University of Science and Technology, Tehran, Iran

Synthesis of New Derivatives of Selenopheno[3,2-*d*]pyrimidine

Hanieh Salahshour, Iman Farzamnezhad, Seddigheh Sheikhi-Mohammareh, Ali Shiri*

Department of Chemistry, Faculty of Science, Ferdowsi University of Mashhad, Mashhad, Iran

* *E-mail: alishiri@um.ac.ir*

Keyword: Selenophene, Selenophenopyrimidine, Heterocyclization

Introduction:

Selenophenopyrimidines are heterocyclic compounds that have attracted considerable attention due to their unique chemical and pharmacological properties. The central core of selenophenopyrimidine has a stable and diverse structure, enabling the synthesis of various derivatives with different properties. These compounds show promise for pharmaceutical applications such as antitumor [1], antioxidant [2] and antimicrobial [3] activities.

Method:

This research describes an efficient multi step synthesis for novel 7-cyano-6-(pyrrolidin-1-yl)selenopheno[3,2-d]pyrimidine derivatives **(4a-e)**. Initially, compound **(1)** was prepared according to our previous reports[4]. Subsequent hydrolysis of compound **(1)** was converted to an amide, using concentrated sulfuric acid the carboxamide **(2)**, followed by cyclization with carbon disulfide to furnish the core structure 7-cyano-4-oxo-6-(pyrrolidin-1-yl)-2-thioxo-1,2,3,4-tetrahydroselenopheno[3,2-*d*]pyrimidine **(3)**. Finally, alkylation of this core scaffold led to a diverse array of dialkylated selenopheno[3,2-*d*]pyrimidine derivatives **(4a-e)** with potential applications, particularly in the pharmaceutical field.

Results and discussion:

This research synthesized novel derivatives of the selenophenopyrimidine. One of the most significant advantages of this synthetic approach is the simplicity of the procedures, high yields, and high purity of the products at each stage. One of the simplest synthetic steps involved the production of the final derivatives, which was achieved using the green solvent ethanol without the need for complex separation steps. Finally, a wide range of dialkyl derivatives was synthesized by reacting this compound with various alkyl halides. Ethanol instead of other toxic solvents is the advantage of this synthetic method, which is of great environmental importance and easy to use.

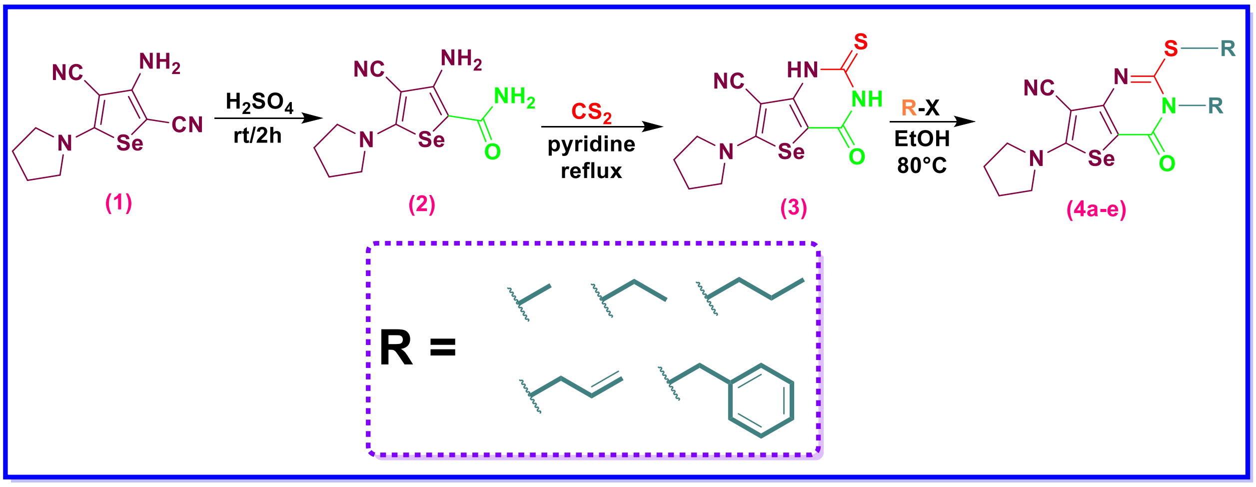

"The schematic process of the reaction"

References:

[1] Gouda MA, Salem MA. Recent advances in the chemistry of selenophenopyridine heterocycles: synthesis, reactivity and biological activity. Journal of Organometallic Chemistry. 2023 Oct 6:122899.

[2] Farzamnezhad I, Sheikhi-Mohammareh S, Beyzaei H, Yarmohammadi E, Shiri A. Synthesis of Novel DPPH-Free Radical Scavenger Se-Containing Fused Chalcogenophenes: 2-Alkyl-7-Cyano-4-Imino-3-Phenyl-6-(pyrrolidin-1-yl)-3, 4-Dihydroselenopheno [3, 2-d] Pyrimidines. Polycyclic Aromatic Compounds. 2024 Feb 7;44(2):807-17.

[3] Helal MH, Salem MA, Gouda MA. Recent advances in the Chemistry of Selenophenopyrimidine Heterocycles: Synthesis, Reactivity, and Biological Activity. Journal of Organometallic Chemistry. 2024 Aug 30:123343.

[4] Kohandel O, Sheikhi-Mohammareh S, Oroojalian F, Memariani T, Mague J, Shiri A. A Dimroth rearrangement approach for the synthesis of selenopheno [2, 3-e][1, 2, 4] triazolo [1, 5-c] pyrimidines

---

The 30th Iranian Seminar of Organic Chemistry
February 7-9, 2025, Iran University of Science and Technology, Tehran, Iran

Synthesis of SiO_3@Cu/ML Nanocatalyst and Its Application in the Hantzsch Reaction

Khadija Mansoori[1], Masoud Nasr-Esfahani*[2]

[1]PhD student in Organic Chemistry, Yasuj University

Kh.Mansoori1312@gmail.com

[2]Professor at Yasuj University

manas@yu.ac.ir

Keyword: Nanocatalysis, Hantzsch Reaction, SiO_3@Cu/ML Composite

Objective: The main goal of this study is to synthesize the SiO_3@Cu/ML nanocatalyst and investigate its application in the Hantzsch reaction. Silica, as a support material, possesses unique properties such as high thermal stability, large surface area, and the ability to undergo chemical modifications, making it a suitable candidate for designing heterogeneous catalysts [1]. On the other hand, copper nanoparticles, due to their cost-effectiveness, easy availability, and high catalytic activity in a wide range of chemical reactions, especially organic reactions, have attracted considerable attention [2]. By combining these two materials and utilizing suitable ligands, a powerful catalyst with enhanced capabilities for complex reactions can be designed. One of the key reactions in organic synthesis is the Hantzsch reaction, which is used to produce β-amino carbonyl compounds [3]. These compounds are valuable building blocks in the synthesis of pharmaceuticals, bioactive materials, and chemical industries [4]. Despite the high efficiency of this reaction, challenges such as prolonged reaction times, harsh reaction conditions, and difficulties in catalyst separation persist [2]. Therefore, the development of an efficient, stable, and recyclable nanocatalyst like SiO_3@Cu/ML could significantly address these issues. In this study, we focus on the design and synthesis of the SiO_3@Cu/ML nanocatalyst and evaluate its performance in the Hantzsch reaction. The primary aim of this research is to present an efficient, eco-friendly method that enhances the yield and reduces the costs of organic reactions.

Methodology: To synthesize the SiO_3@Cu/ML nanocatalyst, 3-CMPT was reacted with copper under reflux conditions at 78°C in diethyl ether. After washing and drying, ML was added, and the Cu/ML complex was synthesized by refluxing for three hours. Subsequently, the Cu/ML catalyst was supported on silica under reflux conditions. The catalyst was then employed in the Hantzsch reaction, conducted under reflux at 78°C in ethanol as the solvent.

Results: To determine the structure, morphology, and stability of the catalyst, several analyses were carried out, including FT-IR (for functional group identification), EDS (for elemental analysis), XRD and SEM (to study surface morphology), and TGA (for thermal stability evaluation). The catalyst's performance in the Hantzsch reaction was assessed by analyzing the reaction products using ^{1}H-NMR, ^{13}C-NMR, and FT-IR spectroscopy.

Conclusion: The results indicated that the synthesized nanocatalyst could efficiently catalyze the Hantzsch reaction under reflux conditions, with ethanol as solvent, completing the reaction within a short time (approximately 25 minutes). The reaction yields were consistently over 97%, demonstrating the high efficiency of this catalyst under optimized conditions. These features, coupled with its ease of recovery and reusability, make the SiO_3@Cu/ML nanocatalyst an effective and promising candidate for facilitating and improving Hantzsch reactions. The findings underscore that the designed nanocatalyst, by reducing reaction time and cost, can serve as a stable, efficient, and recyclable catalyst in chemical processes.

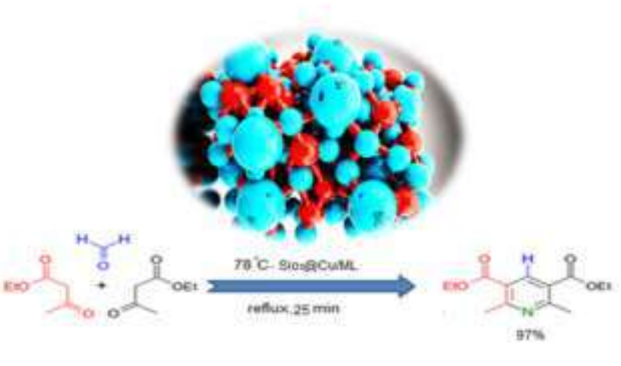

References:

[1]. Khodadadi, M., Rodriguez-Couto, S., Arghavan, F. S., & Panahi, A. H. (2020). Synthesis and characterization of feni3@ SiO_2@ TiO_2 nano-composite and its application as a catalyst in a photochemical oxidation process to decompose tetracycline. Desalination and Water Treatment, 195, 435-449.

[2]. Behrouzi, M., Rabiei, K., & Ghasemzadeh, S. (2024). GQDs@ SiO_3Pr Schiff-base complexes Co (II); As an eco-friendly environmental nanocatalyst for the synthesis of the amino carbonitrile chromenes. Journal of Organometallic Chemistry, 1022, 123413.

[3]. Ren, F., Li, S., Zheng, W., Song, Q., Jia, W., Nan, & Li, Y. (2022). Preparation of a novel heterogeneous palladium nanocatalyst based on carboxyl modified magnetic nanoparticles and its

applications in Suzuki-Miyaura coupling reactions. Colloids and Surfaces A: Physicochemical and Engineering Aspects, 642, 128611.

[4]. Hajizadeh, Z., Radinekiyan, F., Eivazzadeh-Keihan, R., & Maleki, A. (2020). Development of novel and green NiFe2O4/geopolymer nanocatalyst based on bentonite for synthesis of imidazole heterocycles by ultrasonic irradiations. Scientific Reports, 10(1), 11671.

The 30th Iranian Seminar of Organic Chemistry
February 7-9, 2025, Iran University of Science and Technology, Tehran, Iran

Synthesis of Al_2O_3@Ni-Cti Nanocatalyst and Its Application in Biginelli Multicomponent Reactions

Khadija Mansoori[1], Masoud Nasr-Esfahani*[2]

[1]PhD student in Organic Chemistry, Yasuj University

Kh.Mansoori1312@gmail.com

[2]Professor at Yasuj University

manas@yu.ac.ir

Keyword: Nanocatalyst, Biginelli Reaction, Al_2O_3@Ni-Cti, Multicomponent Reactions

Objective: The primary aim of this study is the synthesis of the Al_2O_3@Ni-Cti nanocatalyst and its application in Biginelli multicomponent reactions. Nanocatalysts are important in organic reactions due to their high surface area, uniform distribution of active sites, and tunable physical and chemical properties [1]. Among these, alumina nanoparticles, as a highly stable material with a large surface area, play a crucial role in developing heterogeneous catalysts. The Biginelli multicomponent reaction, one of the most renowned multicomponent reactions, is used for the synthesis of dihydropyrimidine derivatives (DHPMs). These compounds are of great importance due to their wide-ranging pharmaceutical properties, including anticancer, anti-inflammatory, and antiviral activities [2]. Despite the advantages of the Biginelli reaction, issues such as long reaction times, the need for harsh conditions, and low yields in the absence of efficient catalysts remain [3]. Therefore, designing and synthesizing a highly efficient nanocatalyst that can perform this reaction under mild conditions and in a short time with a high yield is of great significance. In this study, the Al_2O_3@Ni-Cti nanocatalyst was synthesized and characterized using various techniques, and its performance in accelerating the Biginelli reaction was evaluated.

Methodology: To synthesize the Al_2O_3@Ni-Cti nanocatalyst, the CMPT-3 compound was first reacted with nickel under reflux conditions at 78°C in diethyl ether. After the reaction was completed, the product was washed and dried. In the next step, the compound was modified by adding CTi to enhance its stability and activity. Finally, the Ni-CTi nanocatalyst was immobilized on the Al_2O_3support. This nanocatalyst was then applied in the Biginelli reaction, showing its ability to reduce reaction time and increase yield.

Results: To examine the structure, morphology, and stability of the synthesized nanocatalyst, several advanced techniques were employed. FTIR spectroscopy was used to identify surface functional groups, EDS for elemental composition analysis, XRD for crystal structure analysis, and SEM for surface morphology evaluation. The thermal stability of the nanocatalyst was assessed by TGA. The catalyst's performance in the Biginelli reaction was carefully studied through ^{1}HNMR, ^{13}CNMR, and FT-IR spectroscopy to determine its efficiency and quality in producing the desired products.

Conclusion: The results revealed that the synthesized nanocatalyst could complete the Biginelli reaction within a short time (approximately 20 minutes) and with ethanol as the solvent. The reaction yields in all experiments exceeded 93%, demonstrating the high efficiency of the catalyst. Furthermore, the catalyst showed excellent recyclability, with no significant loss in activity after multiple uses. These characteristics, combined with the fast reaction time and high yield, make the Al_2O_3@Ni-Cti nanocatalyst an economically viable, stable, and effective option for Biginelli reactions. This study highlights the potential of this catalyst to be widely used in chemical processes, reducing both reaction time and cost.

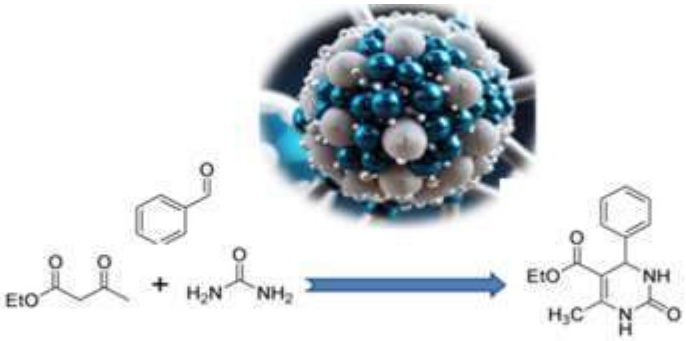

References:

[1]. Arlan, F. M., Marjani, A. P., Javahershenas, R., & Khalafy, J. (2021). Recent developments in the synthesis of polysubstituted pyridines via multicomponent reactions using nanocatalysts. New Journal of Chemistry, 45(28), 12328-12345.

[2]. Bhaskaruni, S. V., Maddila, S., Gangu, K. K., & Jonnalagadda, S. B. (2020). A review on multi-component green synthesis of N-containing heterocycles using mixed oxides as heterogeneous catalysts. Arabian Journal of Chemistry, 13(1), 1142-1178.

[3]. Daria, N., Ebrahimzadeh, K., & Darya, N. (2024). Fe3O4@SiO2@NCs@Al2O3 as a nanocatalyst for efficient one-pot synthesis of tetrahydrobenzo [b] pyran in water. Iranian Journal of Catalysis, 14(2).

Synthesis of Nano-Catalyst MGo@HZBn/Zn and Its Efficiency in Hantzsch Reactions

Khadija Mansoori[1], Masoud Nasr-Esfahani*[2]

PhD student in Organic Chemistry, Yasuj University

Kh.Mansoori1312@gmail.com

Professor at Yasuj University

manas@yu.ac.ir

Keywords: Nano-catalyst, Hantzsch reaction, Graphene-based catalysts, Multi-component reaction

The primary aim of this research is to synthesize the nano-catalyst MGo@HZBn/Zn and evaluate its application in one-pot, multi-component Hantzsch reactions. Graphene-based nano-catalysts are widely utilized in Hantzsch reactions for synthesizing dihydropyridine derivatives due to their high surface area, thermal stability, and active functional groups [1]. Stabilizing metal nanoparticles such as Cu, Pd, and Ni on graphene or its derivatives (e.g., graphene oxide) enhances reaction yields, accelerates reaction times, and reduces harsh reaction conditions [2]. Additionally, hybrid catalysts like graphene/Fe_3O_4 are particularly attractive due to their easy recyclability and green chemistry performance [3]. Functionalizing graphene with acidic groups or metal nanoparticles leads to efficient, stable, and environmentally friendly processes, making graphene an ideal candidate for optimizing the Hantzsch reaction [4].

Methodology: Graphene was synthesized from graphite using the Hummers' method [5], where H_2O_2 was employed to neutralize and eliminate hazardous by-products during the reaction. Subsequently, a mixture of $FeCl_2$ and $FeCl_3$ was utilized under basic magnetic conditions to prepare the intermediate. The linker 3-CTMS, zinc metal, and functional groups were then attached to the graphene framework. The resulting catalyst was employed in multi-component reactions under reflux conditions in ethanol after optimizing the reaction parameters.

Findings: The synthesized catalyst was characterized using various analytical techniques, including Fourier Transform Infrared Spectroscopy (FT-IR), Energy Dispersive X-ray Spectroscopy (EDS), X-ray Diffraction (XRD), Scanning Electron Microscopy (SEM), and Thermogravimetric Analysis (TGA). In addition, for the Hantzsch reaction, further analyses such as Proton Nuclear Magnetic Resonance (^{1}H-NMR), Carbon Nuclear Magnetic Resonance (^{13}C-NMR), and FT-IR were performed to identify the products and evaluate the catalyst's efficiency.

Conclusion: The results revealed that the synthesized catalyst exhibited excellent performance in the Hantzsch reaction. Under reflux conditions with ethanol as the solvent, the reaction was completed within an average of 20 minutes. Furthermore, the reaction yield consistently exceeded 95% in all cases. These findings indicate that the synthesized catalyst is highly effective for performing Hantzsch reactions under optimized conditions. Its outstanding performance, including short reaction times, high yields, and excellent reactivity, highlights its potential for efficient synthesis of Hantzsch derivatives in controlled and favorable conditions.

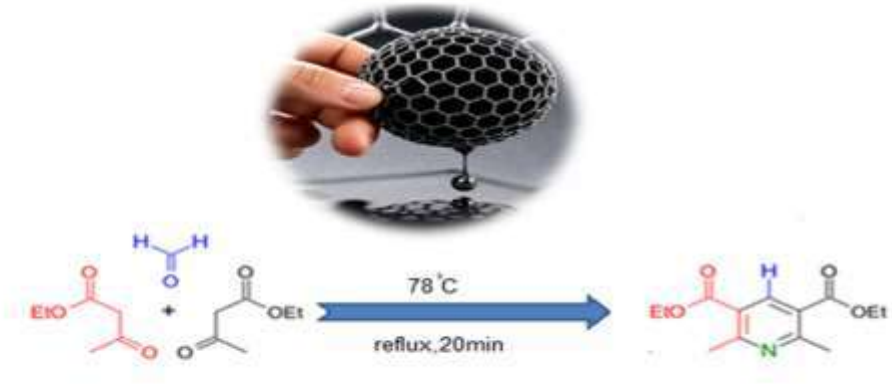

References:

[1]. Yan, Y., Shin, W. I., Chen, H., Lee, S. M., Manickam, S., Hanson, & Pang, C. H. (2021). A recent trend: application of graphene in catalysis. Carbon Letters, 31, 177-199.

[2]. Subramanian, H., Santhaseelan, H., Dinakaran, V. T., Devendiran, V., Rathinam, A. J., Mahalingam, & Mathimani, T. (2023). Hydrothermal synthesis of spindle structure copper ferrite-graphene oxide nanocomposites for enhanced photocatalytic dye degradation and in-vitro antibacterial activity. Environmental Research, 231, 116095.

[3]. Bogireddy, N. K. R., Ghafour El Hachimi, A., Muñiz, J., Elías, A. L., Lei, Y., Terrones, M., & Agarwal, V. (2021). Integration of nitrogen-doped graphene oxide dots with Au nanoparticles for enhanced electrocatalytic hydrogen evolution. ACS Applied Nano Materials, 4(11), 11513-11525.

[4]. Fauzi, A., Saifudin, A., & Rullah, K. (2023). Synthesis of Dihydropyrimidinone (DHPM) Derivatives through a Multicomponent Reaction (MCR) and Their Biological Activity.

[5]. Shahriary, L., & Athawale, A. A. (2014). Graphene oxide synthesized by using modified hummers approach. Int. J. Renew. Energy Environ. Eng, 2(01), 58-63.

The 30th Iranian Seminar of Organic Chemistry
February 7-9, 2025, Iran University of Science and Technology, Tehran, Iran

Evaluating the Anticancer Effect of a Chemotherapic Agent Loaded *Cymbopogon Citratus* Nanoemulsion on Leukemia

Mozhde Dadrasi[a], Hossein Behboudi[b], Mona Habibi-Kool-Gheshlaghi[a,b], Hasan Rafati*[c]

[a] *Department of Phytochemistry, Medicinal Plants and Drugs Research Institute, Shahid Beheshti University, Tehran, Iran*

[b] *Department of Biology, Medicinal Plants and Drugs Research Institute, Shahid Beheshti University, Tehran, Iran*

[c] *Department of Pharmaceutical Engineering, Medicinal Plants and Drugs Research Institute, Shahid Beheshti University, Tehran, Iran*

Keyword: Leukemia, Drug Delivery, Nanoemulsion, Nilotinib, Lemongrass

Introduction: Hematologic malignancies are cancers of the blood, and they include malignancies originating from blood-forming cells and immune system cells, including leukemia, lymphoma, and multiple myeloma. Leukemia is classified in two ways. First, based on cancer progression (chronic and acute), second, based on the types of leukemia cells present (lymphoid and myeloid cells).

In this study, chronic myeloid leukemia (CML) was chosen as a model cancer disease and the physicochemical and biological properties of the proposed drug delivery system were studied. The aim of this study was to investigate the combinational effect of lipophilic loading of Nilotinib HCl H_2O along with nanoscale formulations on model CML cell line compared to the individual treatments.

Methods: *Cymbopogon citratus* essential oil was chosen as a lipophilic carrier and characterized by GC-MS method. Nanoformulations were prepared using a high-energy method including a rotor-stator high shear homogenizer. The cytotoxicity of LG-EO and its formulations was assessed using MTT assay, which indicated cytotoxic effects (IC50) upon incubation for 24 hours. Dynamic Ligh Scattering (DLS) was used to obtain particle size and PDI, and Zetasizer for zeta potential assessment of the surface charge.

Results and Discussion: Nanoformulations were prepared using the above-mentioned methods. DLS results indicated a mean particle size of 180.53 ± 6.80 nm and a mean Polydispersity Index of *0.15 ± 0.06 for the optimized Nilotinib loaded LG-EO* nanoformulation. The stability of the optimized nanoformulation was also determined using DLS instrument. It was observed that the nanoformulation was stable for the following three months. The Zeta potential results indicated a surface charge of -2.58 ± 1.65 mV. The MTT results demonstrated that both LG-EO and its nano formulations significantly inhibited K562 cell viability in a dose-dependent manner. The optimized formulation containing both LG-EO and Nilotinib exhibited enhanced cytotoxicity (IC_{50} = 0.322 ± 0.004 *µg/mL*) compared to the blank nanoformulation (IC_{50} *= 113.804* ± 3.514 *µg/mL*). In contrast with the aforementioned formulations, the MTT results for raw materials indicated a noticeable difference, as the cell viability for the bulk LG-EO was observed to be 123.631 ± 4.486 µg/mL and *0.615* ± 0.001 *µg/mL for the bulk Nilotinib. Further investigations are under way to evaluate the* mechanism of anticancer activities of the pure and nanoformulations.

References:

[1] Kaur, G., & Singh, R. (2020). "Anticancer potential of lemongrass essential oil: A review." *Journal of Essential Oil Research*, 32(4), 345-356.

[2] Shafique, S., & Khan, M. I. (2021). "Nanoformulations for enhanced delivery of natural products in cancer therapy." *Pharmaceutical Nanocarriers*, 12(3), 213-227.

[3] Alzahrani, A., et al. (2022). "The role of reactive oxygen species in apoptosis induced by essential oils." *Molecules*, 27(5), 1500.

[4] Khameneh, B., et al. (2019). "Natural products for cancer therapy: A review." *Phytotherapy Research*, 33(9), 2348-2365.

[5] Jha, A., & Sharma, R. (2023). "Synergistic effects of natural compounds with chemotherapeutic agents in cancer treatment." *Current Cancer Drug Targets*, 23(1), 56-70.

The 30th Iranian Seminar of Organic Chemistry
February 7-9, 2025, Iran University of Science and Technology, Tehran, Iran

Preparation and Characterization of Activated Carbon from Gilsonite by KOH Chemical Activation

Fatemeh Ganjali [a], Mahboubeh Rabbani [b] (corresponding author), Ali Maleki [c] (corresponding author)

Department of Chemistry, Iran University of Science and Technology, Tehran 16846-13114, Iran

Abstract and Introduction

Increasing the industrial pollutants, like organic and inorganic dyes, etc., in water has gained the most significant concern due to the human health threats; their decontamination by porous materials via various methods, viz. adsorption, and degradation, is investigated [1, 2]. The asphalt of various optical textures, such as Gilsonite (GL), was activated by KOH at 900 ˚C to produce highly porous and nano-sized activated carbons (AC). The GL treatment eliminates volatile organic substances and produces an AC with high porosity. Additionally, the functional groups, crystallinity, and structural, morphological, and methylene blue (MB) adsorption-degradation properties of this nanomaterial were considered by FTIR, XRD, FESEM, and UV-Vis analyses. As a result, the AC substance demonstrated a very porous structure according to the FESEM images, corroborating the chemical activation by KOH in FTIR. The XRD pattern of GL represents sharp peaks at $2\theta \approx 26.7^\circ$, 31.9°, and 49.3°, while that of the AC demonstrates weak and broad peaks, indicating the mostly amorphous nature of the AC substance. The GL and AC (0.01 g) were applied in MB adsorption and degradation at 5.0 ppm, 10.0 mL of dye solution. The GL and AC adsorption-degradation efficiency is 31.35 and 46.20%, and 86.15 and 87.90%, respectively. According to the results, the degradation efficacy of the substances is much higher than their adsorption efficacy just by applying a white LED light (10.0 W) irradiation.

Keywords: Activated carbon, Alkali, Asphalt, Chemical activation, Gilsonite.

Method

The preparation method was employed, as reported in previous articles [3, 4]. First, the untreated GL was powdered via ball-milling and heated in a tube furnace at 400 ˚C for 3 h under nitrogen to dispel the oils and attain a stable structure. Then, it was cooled to an ambient temperature to reach the pre-treated GL. The pre-treated GL (0.25 g) was mixed in a mortar with KOH powder (1.0 g) with the KOH:GL proportion of 4:1 via grinding. The reaction was exerted in a quartz boat in a reaction furnace tube under N_2 conditions. After inserting the cold reaction tube in the furnace, it takes 5 min until the sample reaches 900 ˚C for 20 min under N_2 flow. At this stage, generating CO and CO_2 causes porosity in the structure. After the furnace temperature was cooled to 25 ˚C, the reaction products were separated from the quartz boat and rinsed with acetone and distilled H_2O to eliminate soluble salts and achieve a neutral pH. The AC was dried in the oven at 100 ˚C.

Results and Discussion

The AC substance exhibited a highly porous structure compared to the GL due to the FESEM images, confirming the chemical activation by KOH in FTIR. The XRD pattern of GL shows sharp peaks at $2\theta \approx 26.7^\circ$, 31.9°, and 49.3°, while that of the AC displays weak and broad peaks at $2\theta \approx 23^\circ$ and 40° related to the (0 0 2) and (0 1 0) planes, respectively. The sharp peak absence indicates the mostly amorphous nature of the AC substance [5]. The MB adsorption-degradation efficiency of the GL and AC (0.01 g) at 5.0 ppm, 10.0 mL dye solution was studied using UV-Vis curves, demonstrating a much higher MB degradation efficacy (86.15% (GL) and 87.90% (AC)) than adsorption (31.35% (GL) and 46.20% (AC)) under irradiating a 10.0 W LED light.

The schematic of the porous AC production from Gilsonite by KOH Chemical Activation

References

[1] Z. Chen, P. Weng, Y. Song, L. Zheng, Y. Tan, X. Yin, Loofah-inspired sodium alginate/carboxymethyl cellulose sodium-based porous frame for all-weather super-viscous crude oil adsorption and wastewater treatment in harsh environment, Carbohydrate Polymers 323 (2024) 121450.
[2] Z. Yang, Y.-W. Chen, Y.-F. Jin, Z. Jin, H.-S. Xie, X.-S. Cong, D.-G. Teng, Ni, Co-embedded MOF-derived N-doped bimetallic porous carbon for adsorption–photocatalytic degradation of organic dyes and antibiotics, ACS omega 9(10) (2024) 11356-11365.
[3] H. Javed, D.X. Luong, C.-G. Lee, D. Zhang, J.M. Tour, P.J. Alvarez, Efficient removal of bisphenol-A by ultra-high surface area porous activated carbon derived from asphalt, Carbon 140 (2018) 441-448.

[4] H. Marsh, D.S. Yan, T.M. O'Grady, A. Wennerberg, Formation of active carbons from cokes using potassium hydroxide, Carbon 22(6) (1984) 603-611.
[5] A.S. Jalilov, Y. Li, J. Tian, J.M. Tour, Ultra-high surface area activated porous asphalt for CO_2 capture through competitive adsorption at high pressures, Advanced energy materials 7(1) (2017) 1600693.

The 30th Iranian Seminar of Organic Chemistry
February 7-9, 2025, Iran University of Science and Technology, Tehran, Iran

Green and Environmentally Friendly Inhibitory Effect of Bitter Olive Plant Extract on Copper Corrosion in 3.5 wt.% Sodium Chloride Solution

Mahsa Esmaeilbeygi[1], Mohammad Mahdi Alemnezhad [1], Ali Ghaffarinejad[٢*,2]

[1] *Research Laboratory of Real Samples Analysis, Faculty of Chemistry, Iran University of Science and Technology (IUST), Tehran 1684613114, Iran*

[2] *Electroanalytical Chemistry Research Center, Iran University of Science and Technology (IUST), Tehran 1684613114, Iran*

Keyword: bitter olive fruit extract - biological corrosion inhibitors - electrochemical impedance spectroscopy - potentiodynamic polarization.

Introduction:

Copper and its alloys are essential metals widely used in industries such as chemical, agricultural, construction, and marine due to their versatility and properties. However, their frequent exposure to corrosive environments like saltwater, acid solutions, and chloride-containing systems makes them susceptible to corrosion. Corrosion, an oxidation process driven by thermodynamic energy shifts, poses significant challenges, necessitating effective prevention methods. Among various strategies, the use of green inhibitors derived from plant extracts has gained prominence for their non-toxic nature, cost-effectiveness, and high corrosion-inhibition efficiency, attributed to the presence of heteroatoms. This study explores the potential of bitter olive fruit extract (BOFE) as an environmentally friendly corrosion inhibitor for copper in a 3.5% NaCl solution [1-3].

Method:

The bitter olive fruit used in this study was collected, thoroughly washed with deionized water, and dried at 45°C for six hours. It was then ground into a fine powder with a particle size of 35 µm. The

---

[٢*] Corresponding authors:
Ali Ghaffarinejad: Email: Ghaffarinejad@iust.ac.ir; Tel: +98-21-77240652; Fax: +98-21-73021554

extract was prepared using deionized water and ultrasonication, where 4 g of powder was mixed with 100 mL of water, incubated at 70°C for 25 minutes, and filtered. Additionally, the Soxhlet method was employed, extracting 10 g of powder with 100 mL of ethanol at 90°C over 24 hours. Various concentrations of the extract, ranging from 2.5% to 20% (v/v), were tested for their corrosion inhibition efficiency in a 3.5% NaCl solution. Copper sheets polished to fine grades were used as test samples to evaluate the extract's effectiveness. Employing Electrochemical Impedance Spectroscopy (EIS) and Potentiodynamic polarization, the research assesses the extract's corrosion inhibition efficiency. Scanning Electron Microscopy (SEM) analyzes the surface changes. BOFE's effectiveness highlights its promise as a green, sustainable solution for corrosion mitigation.

Results and Discussion:

Potentiodynamic polarization and Electrochemical Impedance Spectroscopy (EIS) analyses were conducted to assess the corrosion inhibition efficiency of BOFE on copper in a 3.5% NaCl solution. Polarization curves revealed that increasing BOFE concentration reduced both corrosion current density and corrosion rate, indicating kinetic control of the corrosion process. Inhibition efficiencies (*IE%*) for 15% and 20% BOFE were 82.77% and 84.67%, respectively, with 15% being the optimal concentration for minimizing inhibitor usage. This concentration was subsequently employed in temperature-dependent studies (Fig. 1-b).

EIS data further confirmed the effectiveness of BOFE as a corrosion inhibitor. With increasing BOFE concentrations, polarization resistance (R_p) increased significantly, while double-layer capacitance (C_{dl}) decreased, reflecting the adsorption of BOFE molecules on the copper surface, forming a protective barrier. At the optimal concentration of 15%, R_p reached 0.426 kΩ.cm^2, and *IE%* was 84.1%. Higher concentrations, such as 20%, showed a slight improvement in R_p (0.569 kΩ.cm^2) and *IE%* (88.1%), but 15% remained the preferred concentration to balance efficiency and resource consumption. These findings underscore the potential of BOFE as a sustainable, high-performance green inhibitor for copper corrosion (Fig. 1-a).

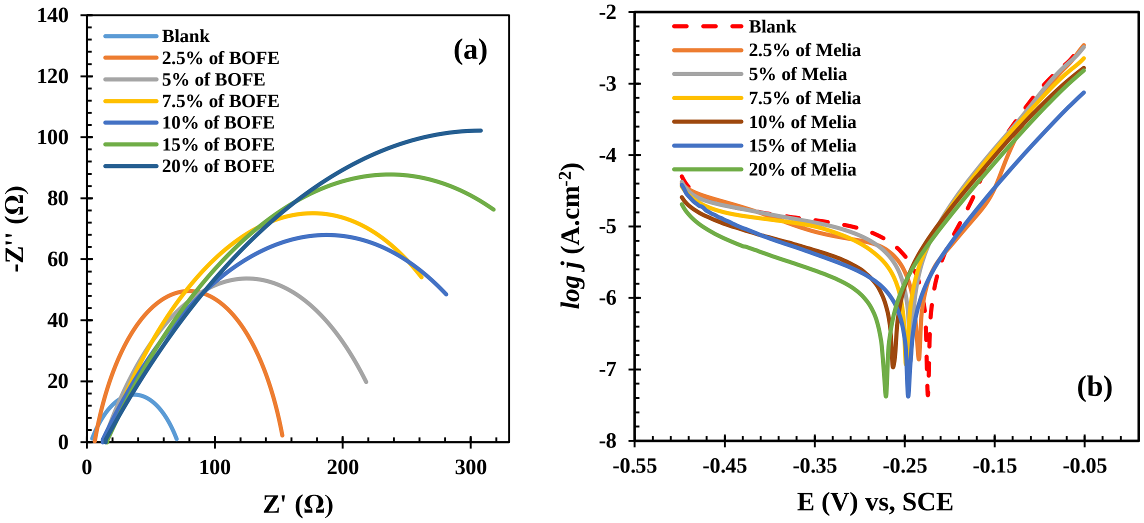

Figure 1. EIS and Potentiodynamic polarization curves for different concentrations of the BOFE in 3.5% NaCl solution.

The SEM images further validate the findings from the previous analyses, as shown in Figure 2. The application of the inhibitor significantly minimizes surface damage caused by corrosion, demonstrating its effectiveness in protecting the copper surface.

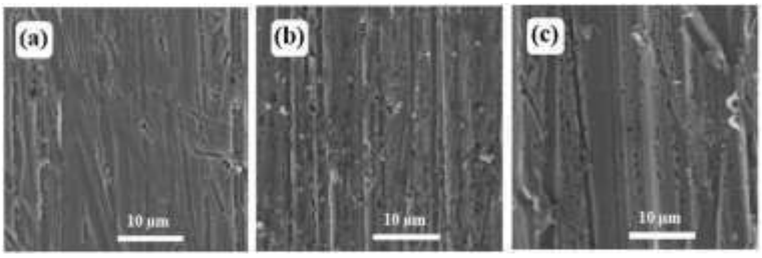

Figure 2. SEM images of the copper surface of (a) sanded state before immersion, (b) exposed to the 3.5 wt.% NaCl solution without (b), and with (c) BOFE for 24 hours.

References:

[1] H. Huang and X. Guo, Colloids Surf A Physicochem Eng Asp **598**, 124809 (2020).

[2] N. Benzbiria, S. Echihi, M.E. Belghiti, A. Thoume, A. Elmakssoudi, A. Zarrouk, M. Zertoubi, and M. Azzi, Mater Today Proc **37**, 3932 (2021).

[3] L. Feng, S. Zhang, Y. Qiang, Y. Xu, L. Guo, L. Madkour, and S. Chen, Materials **11**, 1042 (2018).

Comparison of phytochemical constituents of *Eucalyptus camaldulensis* essential oil collected from different habitats in Khuzestan Province

Zeinab Mazarei *, Ahmad Kooti

Department of Chemistry, Faculty of Sciences, Shahid Chamran University of Ahvaz, Ahvaz, Iran

Keyword: *Eucalyptus camaldulensis*, essential oil, monoterpenoids, sesquiterpenoids

Introduction: *Eucalyptus camaldulensis*, a perennial herb belonging to the *Myrtaceae* family, is indigenous to Australia and has been extensively cultivated across various regions of Iran. The leaves of *E. camaldulensis* are aromatic and possess an essential oil that has been documented to exhibit numerous therapeutic benefits. These benefits encompass analgesic, anti-inflammatory, antioxidant, anti-cancer, antiviral, and anti-diabetic properties (1).

Method: In this research, *Eucalyptus camaldulensis* leaves were collected from four cities: Ahvaz, Abadan, Dezful, and Bostan, located in Khuzestan province. Following the drying process, essential oils were extracted utilizing a Clevenger-type apparatus. The components of the essential oils were qualitatively and quantitatively identified through GC-MS analysis.

Results: The main constituents of the essential oil of *E. camaldulensis* identified as follows: Ahvaz: 1,8-cineole (36.6 %), (-)-Globulol (8.9 %) and (+)-Spatulenol (8.1 %). Abadan: 1,8-cineole (29.6 %), (-)-α-pinene (6.9 %), (-)-Globulol (15.8 %) and (+)-Aromadendrene (7.9 %). Dezful: 1,8-cineole (30.4 %), (-)-α-pinene (12.3 %), (-)-Globulol (5.6 %). Bostan: 1,8-cineole (32.4 %), (-)-α-pinene (12.4 %), (-)-Globulol (6.7 %) and (+)-Aromadendrene (7.3 %).

Discussion: A comparison of *E. camaldulensis* essential oils collected from different cities in Khuzestan reveals that while 1,8-cineole is the predominant compound as a monoterpenoid in these essential oils, they also possess notable quantities of sesquiterpene compounds, including Globulol and Aromadendrene.

References:

(1) Mondal, M., Quispe, C., Sarkar, C., Bepari, T. C., Alam, M. J., Saha, S., ... & Kundu, S. K. (2021). Analgesic and anti-inflammatory potential of essential oil of Eucalyptus camaldulensis leaf: in vivo and in silico studies. Natural Product Communications, 16(4), 1934578X211007634.

The 30th Iranian Seminar of Organic Chemistry
February 7-9, 2025, Iran University of Science and Technology, Tehran, Iran

Hybrid Copper-Based Perovskite/Metal-Organic Framework: An Efficient Catalyst for Triazole Synthesis and Visible-Light-Driven Photocatalysis

Saba Daliran*

Department of Organic Chemistry, Faculty of Chemistry, Lorestan University, Khorramabad 68151-44316, Iran

Email address: daliran.s@lu.ac.ir

Abstract

This research presents an innovative hybrid catalytic system combining a copper-based perovskite strategically grown within a zirconium metal-organic framework (MOF) through controlled in-situ synthesis. This hybrid system exhibits exceptional performance in copper(I)-catalyzed azide-alkyne cycloaddition (CuAAC) click reaction, producing regioselective 1,2,3-triazoles and photocatalytically degrading methyl orange pollutant. This enhanced activity stems from the synergistic interaction between the perovskite and MOF components, which improves copper ion accessibility and stabilization within the framework structure.

Keyword: Metal-organic framework, hybrid material, click reaction, catalysis, photocatalysis

1. Introduction

ABX_3 perovskites have emerged as promising semiconductors for photovoltaic and optoelectronic applications. Metal-organic frameworks (MOFs) offer complementary benefits through their crystalline structure and tunable porosity. The strategic combination of perovskites with MOF structures creates innovative hybrid materials that transcend the limitations of their individual components [1-3]. This research presents an innovative hybrid catalytic system combining a copper-based perovskite strategically grown within a MOF (UiO-66(Zr)-NH_2, Zr-MOF) through controlled in-situ synthesis.

2. Materials and Methods

$CsCu_2I_3$@MOF was prepared via antisolvent infiltration by dissolving CuI (1.2 mmol) and CsI (0.6 mmol) in acetonitrile (5 mL). After stirring at 60 °C for 5h, the filtered solution was transferred to activated MOF (40 mg) and heated at 50°C for 12h. For triazole synthesis, benzyl azide (1 mmol), phenylacetylene (1 mmol), and catalyst (15 mg) were combined in CH_2Cl_2 (3 mL) at room temperature.

3. Result and discussion

Field emission scanning electron microscopy (FESEM) imaging revealed well-defined octahedral crystals characteristic of the parent UiO-66-NH_2 framework (Fig. 1).

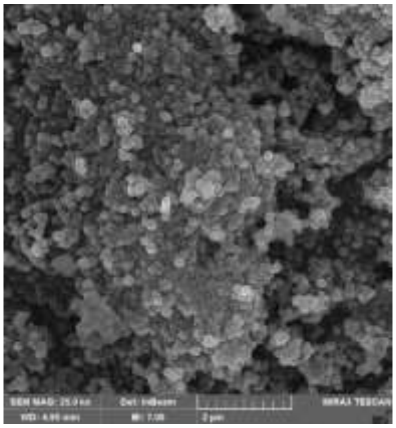

Figure 1. SEM images of $CsCu_2I_3$@MOF.

The catalytic performance of $CsCu_2I_3$@MOF was evaluated using CuAAC reaction between benzyl azide and phenylacetylene. Under ambient conditions in dichloromethane, the catalyst (15 mg) achieved 96% triazole yield in 20 min. Performance improved under reflux, reaching 97% yield with shorter reaction time. The material also demonstrated exceptional photocatalytic activity in removing methyl orange (MO) dye under visible-light irradiation, surpassing previously reported systems with an adsorption capacity of 972 mg g^{-1}.

Conclusion

We have successfully developed a multifunctional $CsCu_2I_3$@MOF hybrid material through post-synthetic modification of UiO-66(Zr)-NH_2. The material demonstrates exceptional catalytic activity in both click reactions and visible-light-driven pollutant degradation under green oxygen atmosphere. This work establishes a foundation for developing novel porous perovskite/MOF materials, advancing the field of heterogeneous catalysis and enabling new functional applications.

References:

[1] J. Qu, S. Xu, H. Shao, et al., Recent progress of copper halide perovskites: properties, synthesis and applications, Journal of Materials Chemistry C, 11 (2023) 6260-6275.

[2] S. Daliran, A.R. Oveisi, Y. Peng, et al., Metal-organic framework (MOF)-, covalent-organic framework (COF)-, and porous-organic polymers (POP)-catalyzed selective C-H bond activation and functionalization reactions, Chemical Society Reviews, 51 (2022) 7810-7882.

[3] S. Daliran, M. Khajeh, A.R. Oveisi, et al., $CsCu_2I_3$ Nanoparticles Incorporated within a Mesoporous Metal-Organic Porphyrin Framework as a Catalyst for One-Pot Click Cycloaddition and Oxidation/Knoevenagel Tandem Reaction, ACS Applied Materials & Interfaces, 14 (2022) 36515-36526.

Visible light-assisted Z-scheme n-type semiconductor anchored onto polyaniline for degradation antibiotic

Roshanak Asadpour1. Davood Habibi1*. Nafiseh Aghababaei 2

1. Department of Organic Chemistry, Faculty of Chemistry, Bu-Ali Sina University, Hamedan 6517838683, Iran.

2. Department of Chemical Engineering, Tafresh University, Tafresh, 39518 79611, Iran

Corresponding authors: davood.habibi@gmail.com

Keyword: Polyaniline, antibiotic, Photocatalytic degradation, water treatment

The most critical threat to air and water resources is antibiotic resistance [1]. The purpose of this research was to design a polyaniline-based photocatalyst for the removal of antibiotics from water. XRD, FTIR, FESEM, and EDX techniques were used to characterize the resultant samples. Ternary photocatalysts prepared with various ratios of polyaniline with in-situ hydrothermal treatment removed antibiotics with good efficiency. According to the results, antibiotic removal rates improved with increasing catalyst dosage, while decreasing with raised antibiotic concentration [2]. Furthermore, the kinetics during the degradation was also investigated. Degradation of antibiotic followed a first-order kinetic model and superoxide ions were the main species involved [3]. By utilizing the proposed photocatalyst, antibiotic can be efficiently and rapidly degraded. Therefore, synthetic antibiotics -contaminated wastewater can be treated with this economical and environmentally friendly photocatalyst.

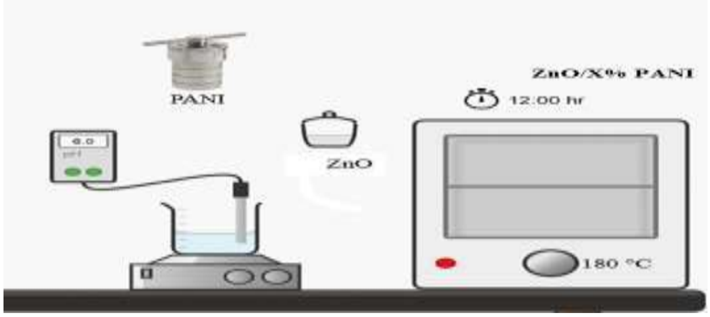

Scheme 1 : Diagram of the synthesis photocatalyst

References:

[1] A.R. Bhapkar, S. Bhame, A review on ZnO and its modifications for photocatalytic degradation of prominent textile effluents: Synthesis, mechanisms, and future directions, Journal of Environmental Chemical Engineering (2024) 112553.
[2] Ş.Ş. Türkyılmaz, N. Güy, M. Özacar, Photocatalytic efficiencies of Ni, Mn, Fe and Ag doped ZnO nanostructures synthesized by hydrothermal method: The synergistic/antagonistic effect between ZnO and metals, Journal of Photochemistry and Photobiology A: Chemistry 341 (2017) 39-50.
[3] T. Chankhanittha, V. Somaudon, T. Photiwat, S. Youngme, K. Hemavibool, S. Nanan, Enhanced photocatalytic performance of ZnO/Bi2WO6 heterojunctions toward photodegradation of fluoroquinolone-based antibiotics in wastewater, Journal of Physics and Chemistry of Solids 153 (2021) 109995.

The 30th Iranian Seminar of Organic Chemistry
February 7-9, 2025, Iran University of Science and Technology, Tehran, Iran

Aromaticity investigation of phosphorous analogs of 2-pyridone and 2-thiopyridone derivatives: A comprehensive DFT study on Schleyer hyperconjugative aromaticity

Marzie Baradaran Bagheri [a], Zohreh Mirjafary[a], Hamid Saeidian[b]

[a]*Department of Chemistry, Science and Research Branch, Islamic Azad University, Tehran, Iran, zmirjafary@srbiau.ac.ir*
[b]*Department of Science, Payame Noor University (PNU), P.O. Box: 19395-3697, Tehran, Iran*

Keywords: Hyperconjugation, DFT calculations, Schleyer aromaticity, 2-pyridone

The lone pair of electrons on the phosphorus atom within the five-membered phosphole ring exhibits a limited propensity to contribute to the ring's aromaticity. Phosphorus, being larger than nitrogen, experiences reduced orbital overlap with carbon atoms, resulting in a diminished formation of double bonds necessary for aromatic stabilization. Phosphorus readily undergoes pyramidal inversion, which disrupts the planarity of the structure, thereby precluding the establishment of aromatic character. The present study explores the influence of both electron-donating and electron-withdrawing groups on phosphorus, utilizing Schleyer's concept of aromaticity. This framework elucidates the interaction between the electrons of the P-X bond and the diene system within the 2-pyridone heterocycle. The hyperconjugation effect, characterized by the interaction between σ bonds and π* orbitals, is also considered. The HOMED index values, which are influenced by the introduction of bulky electron-donating groups such as trimethylsilyl on the phosphorus atom of the 2-pyridone and 2-thiopyridone heterocycles, are calculated as 0.595 and 0.823, respectively. Furthermore, DFT calculations indicated that the incorporation of electron-acceptor groups, such as BH_2, significantly enhances the planarity of the compounds, thereby increasing their aromaticity [1, 2].

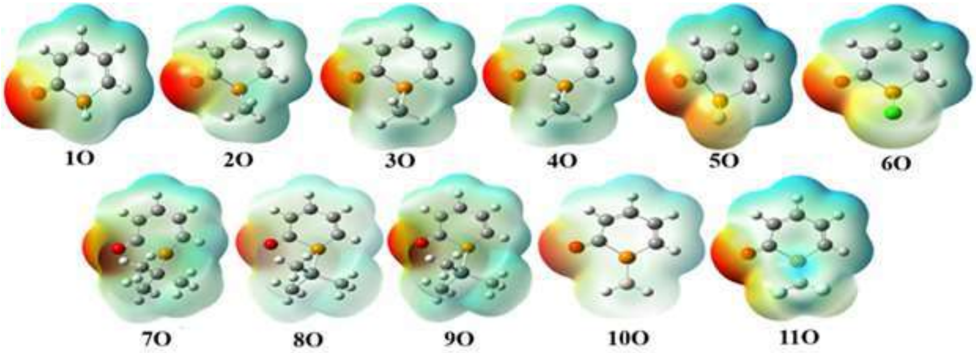

Fig. 1. Electrostatic potential map of phosphorous analogs of 2-pyridone scaffold.

References

[1] Saeidian, H., Asadabad, S.M.M., Szczepanik, D.W., Mirjafary, Z. *Inter. J. Quantum Chem*. **2024**, *124*, 27271.

[2] Solgi, L., Mirjafary, Z., Mokhtari, J., & Saeidian, H. *Chem. Phys. Lett*. **2023**, *821*, 140472.

The 30th Iranian Seminar of Organic Chemistry
February 7-9, 2025, Iran University of Science and Technology, Tehran, Iran

Eco-friendly Synthesis of Mn_2O_3 Nanoparticles for Catalytic Synthesis of 1,8-Dioxo-Octahydroxanthene Derivatives

Authors: Fatemeh Bozorgi, Saeid Taghavi Fardood*

Department of Chemistry, Faculty of Science, Ilam University, Ilam, Iran

**E-mail: s.taghavi@ilam.ac.ir*

Keyword: Mn_2O_3 Nanoparticles, Solvent-Free Synthesis, Xanthene Derivatives

Xanthene derivatives, particularly benzoxanthenes, represent a distinctive class of heterocyclic compounds characterized by an active oxygen atom. Benzoxanthene derivatives exhibit a wide range of pharmaceutical properties, including antiviral, antibacterial, and anti-inflammatory activities [1]. These compounds have also been explored for their potential as antagonists against zoxazolamine-induced paralysis and in photodynamic therapy. Additionally, xanthenes demonstrate notable spectroscopic properties, making them valuable as leuco-dyes in laser technologies and as fluorescent materials for biomolecule visualization. Consequently, the synthesis of xanthene and benzoxanthene derivatives has garnered significant attention from organic chemists due to their diverse biological and technological applications [2,3].

In this study, Mn_2O_3 nanoparticles were synthesized through a green method without using any organic chemicals. These nanoparticles were utilized as an efficient catalyst for the synthesis of 1,8-dioxo-octahydroxanthene derivatives via a solvent-free, multi-component reaction under microwave irradiation. Dimedone (2 mmol) and benzaldehyde (1 mmol) were used as starting materials (Scheme 1). The method offers several advantages, including environmental friendliness, high yields, and a simple work-up procedure. Furthermore, the Mn_2O_3 catalyst demonstrated excellent reusability, retaining high catalytic efficiency after several cycles.

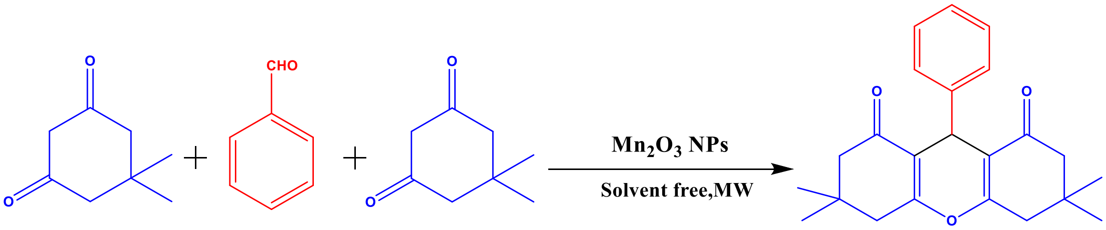

Scheme: Synthesis of Xanthene Derivatives using Mn_2O_3.

References

[1]. Parhad, A.R., Aute, D.S., Gadhave, A.G., Uphade, B.K.: *Polycyc. Aromatic Compounds*, 2024, 44, 5261.
[2]. Banerjee, B., Kaur, M., Sharma, V., Gupta, V.K., Kaur, J., Sharma, A., Priya, A., Singh, A.: *Res. Chem. Intermed.*, 2023, **49**, 4639.
[3]. Lodha, K., Wavhal, D., Bhujbal, N., Mazire, P., Bhujbal, S., Korde, A., Bagul, K., Roy, A., Meshram, R., Shinde, V.: *Results in Chemistry*, 2023, **5**, 100943.

The 30th Iranian Seminar of Organic Chemistry
February 7-9, 2025, Iran University of Science and Technology, Tehran, Iran

One-Pot Synthesis of Tetrahydropyrimidine Derivatives Using $MgFe_2O_4$ Nanoparticles as Catalyst

Authors: Fatemeh Bozorgi, Saeid Taghavi Fardood*

Department of Chemistry, Faculty of Science, Ilam University, Ilam, Iran

**E-mail: s.taghavi@ilam.ac.ir*

Keyword: Magnetic Nanoparticles, Solvent-Free Synthesis, Tetrahydropyrimidine Derivatives

Heterocyclic compounds, particularly pyrimidines, are crucial in pharmaceutical chemistry due to their broad range of biological and therapeutic properties. Pyrimidine derivatives, such as tetrahydropyrimidine derivatives, are integral components of nucleic acids and serve as key intermediates in the synthesis of various bioactive compounds [1]. These compounds are widely recognized for their bactericidal, fungicidal, analgesic, anti-inflammatory, and anti-tumor activities, contributing to their potential in drug discovery and development. Efficient synthetic routes for these derivatives are highly sought after due to their importance in medicinal chemistry and their applications in various disease treatments [2,3].

In this study, we present a green, solvent-free approach for the synthesis of tetrahydropyrimidine derivatives through a one-pot, three-component reaction. The reaction, which involves urea, ethyl acetoacetate, and various aldehydes, was catalyzed by magnetic $MgFe_2O_4$ nanoparticles under microwave irradiation. This method offers several advantages, including high yields, short reaction times, simple work-up procedures, and the use of a sustainable, recyclable catalyst. Furthermore, the magnetic $MgFe_2O_4$ catalyst demonstrated excellent reusability, maintaining high catalytic efficiency over multiple cycles.

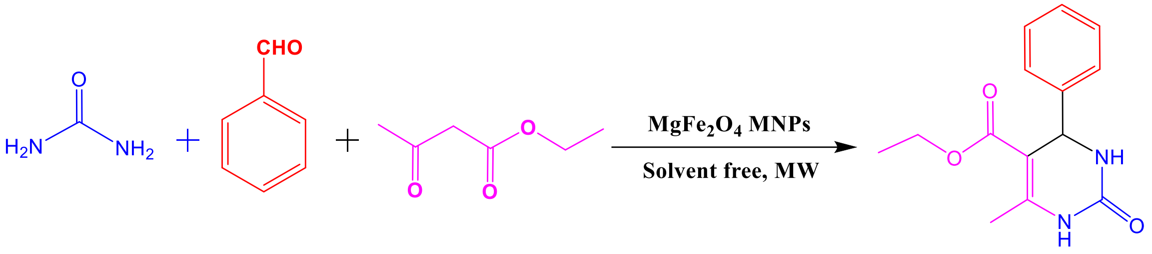

Scheme: Synthesis of tetrahydropyrimidine derivatives using $MgFe_2O_4$.

References

[1]. Balraj, G., Rammohan, K., Anilkumar, A., Sharath Babu, M., Ayodhya, D.: *Results in Chemistry*, 2023, **5**, 100691.
[2]. Moradnia, F., Taghavi Fardood, S., Ramazani, A.: *Appl. Organomet. Chem.*, 2024, **38**, e7315.
[3]. Lu, J., Bai, Y., Wang, Z., Yang, B., Ma, H.: *Tetrahedron Lett.*, 2000, **41**, 9075.

The 30th Iranian Seminar of Organic Chemistry
February 7-9, 2025, Iran University of Science and Technology, Tehran, Iran

DFT study of structural, vibrational and electronic properties of Poly(2-methoxy-5-(2-ethylhexyloxy)-1,4-phenylenevinylene)

Hossein shirani*a,b ,Yekta mohammadi

Corresponding Author E-mail: Hossein.shirani@iust.ac.ir

Department of Chemisrty, Iran University of science and Technology,P.O.BOX 16846-13114,Tehran,Iran

Department of Electrical engineering, North Tehran branch, Islamic Azad university, Tehran, Iran

Abstract: This sudy examines the properties of Poly(2-methoxy-5-(2-ethylhexyloxy)-1,4-phenylenevinylene) (MEH-PPV), a key conjugated polymer in organic solar cells. we analyze its molecular structure focusing on bond length and angles that affect its electronic properties. Our findings provide insights into MEH-PPV's charge transport capabilities and efficiency in photovoltanic applications. This research aids in optimizing organic materials for better energy conversation in solar technologies.

Keywords: MEH-PPV_energies_angles_bonds

Introduction

In recent years organic materials have garnered significant attention as promising candidates for solar energy production. Among these materials, conjugated polymers stand out due to their unique electrical and optical properties making them suitable for use in organic solar cells. One of the most notable of these polymers is Poly(2-methoxy-5-(2-ethylhexyloxy)-1,4-phenylenevinylene) , commonly known as MEH-PPV.

MEH-PPV, as a conjugated polymer with a specific structure, exhibits remarkable electrical and optical characteristics that renderit advantageous for solar cell applications. Its ability to facilitate charge transport and absorb light in the visible spectrum has led to extensive research and development in renewable energy technology.

Furthermore, the molecule structure of MEH-PPV significantly influence its electronic properties. Variations in bond length and angle can result in alterations to the HOMO and LUMO energy levels, which in turn affect energy conversion efficiency and the stability of solar cells.

Method

All calculations were executed utilizing the Gaussian 09 software. Initially, all clusters were sketched out with the GaussView 05 program. The refinement of the Poly(2-methoxy-5-(2-ethylhexyloxy)-1,4-phenylenevinylene) and the cluster was accomplished using Density Functional Theory (DFT). The configurations and various characteristics of the molecule andcluster were determined using the B3LYP theory and the G311 basis set.

Results & Discussion

Fig.1. The optimized structure of Poly(2-methoxy-5-(2-ethylhexyloxy)-1,4-phenylenevinylene) calculated at the B3LYP/6-31+G level.

Table 1. Calculated Bond length value for Poly(2-methoxy-5-(2-ethylhexyloxy)-1,4-phenylenevinylene) Molecule using B3LYP/6-31+G Computational mathod.

C4-O10	C2-C4	C1-O11	C20-C24	C5-C6
1.43000	1.39471	1.43000	1.54000	1.39514

Table 2. Calculated Bond Angles values for Poly(2-methoxy-5-(2-ethylhexyloxy)-1,4-phenylenevinylene) Molecule using B3LYP/6-31+G Computational.

C2-C3-C4	C21-C24-C26	C1-O11-C12	C5-C4-O10	C29-C39-C42
120	109.5	109.5	120	109.5

Table 3. Calculated Dihedral Angle values for Poly(2-methoxy-5-(2-ethylhexyloxy)-1,4-phenylenevinylene) Molecule using B3LYP/6-31+G Computational.

C3-c4-o10-c2	C24-c26-c29-	C2-c1-c11-c1	C4-c3-c16-c1	C21-c24-c32-
90.1	-178.1	90	58.6	31.4

Table 4. Calculated Dipole Moments values for Poly(2-methoxy-5-(2-ethylhexyloxy)-1,4-phenylenevinylene) Molecule using B3LYP/6-31+G Computational.

μ_x	μ_y	μ_z	μ_{tot}
0.4449	0.2000	-0.4681	-0.4681

Table 5. Calculated zero-point energies /enthalpies/s/cv values for Poly(2-methoxy-5-(2-ethylhexyloxy)-1,4-phenylenevinylene) Molecule using B3LYP/6-31+G Computational.

..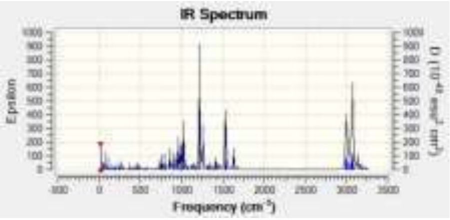

Fig. 2. The simulated IR spectra of the Poly(2-methoxy-5-(2-ethylhexyloxy)-1,4-phenylenevinylene) generated using the B3LYP/6-31+G level of theory.

Zero-piont energy (Joules/Mol)	Enthalpy (Kcal/Mol)	S (Cal/Mol-kelvin)	Cv (Cal/Mol-kelvin)
-813.469334	-813.446927	158.210	78.910

Conclusion

By drawing the structure of this molecule and calculating the bond lengths and angles and etc , we were able to better understand the geometric and electronic properties of this material. The main objective of this research was to investigate the structural impacts on the electrical and optical properties of MEH-PPV, which could enhance the performance of electronic and optical devices based on this polymer.

The results obtained showed that variations in molecule properties can significantly affect the electrical and optical behavior of the molecule. These findings may lead to the design and development of new materials with more desirable properties for various applications. Ultimately, it is hoped that this research will be a significant step toward advansing novel electronic and optical technologies.

References

1.G. Yu, J Gao, and A.J Heeger “Poly(2-methoxy-5-(2-ethylhexyloxy)-1,4-phenylenevinylene): A new Conjugated polymer for organic Electronics,” *Advanced materials*, vol.10,no.3,pp.215-219,1998.

2.H.wang, Y.zhang, and X. chen,”molecular structure and electronic properties of MEH-PPV: A theoretical study,”*Journal of Molecular Modeling8, vol.20,no.1,pp.123-130,2014 .

3. S.R.Forrest,”The path to a Universalphotonic Device,”*Nature photonics*, vol.1, no. 8, pp.457-459, 2007

The 30th Iranian Seminar of Organic Chemistry
February 7-9, 2025, Iran University of Science and Technology, Tehran, Iran

Evaluation of Hypromellose Phthalate as a Coating Agent for Microencapsulation of Probiotics by Spray-drying

Authors: Danial Gazalian[a] (representing author), Atousa Aliahmadi[b], Hasan Rafati*[a]

[a] Department of Pharmaceutical Engineering, Medicinal Plants and Drugs Research Institute, Shahid Beheshti University, Tehran, Iran

[b] Department of Biology, Medicinal Plants and Drugs Research Institute, Shahid Beheshti University, Tehran, Iran

Keywords: *Probiotics, Microencapsulation, Spray-drying, Hypromellose phthalate.*

In this study, we evaluated the potential of hypromellose phthalate (HPMCP) as a coating material for the microencapsulation of ***Lactobacillus plantarum*** through the spray-drying process. The aim was to enhance the survival rate of the probiotics in storage and simulated gastrointestinal fluids. Microcapsules were formulated using HPMCP alone and in combination with hypromellose (HPMC). We examined various physicochemical properties such as moisture content, solubility, particle size distribution, morphology, and flowability of the microparticles. Additionally, we assessed the viability of the encapsulated cells during storage and under simulated gastrointestinal conditions. Fourier-transform infrared spectroscopy (FT-IR) and differential scanning calorimetry (DSC) were utilized to study the interactions and thermal properties of the coating polymers. The results indicated that HPMCP significantly improved the survival rate of ***Lactobacillus plantarum*** during the spray drying process and provided superior acid resistance compared to unencapsulated cells. FT-IR analysis revealed strong hydrogen bonding among polymer chains, and DSC thermograms showed an increment in glass transition temperature, validating the formation of robust polymeric cross-linking networks. The encapsulated probiotics maintained >9 log CFU/g viable cell counts after 12 weeks of storage and >6 log CFU/g cells after 6 h of incubation in simulated gastrointestinal fluids, which is within the recommended range for probiotic efficacy. These findings demonstrate that HPMCP is a promising coating material for protecting probiotics, potentially enhancing their application in food and pharmaceutical industries.

References:

١. Bu, Wenyan, et al. "Encapsulation method of probiotic embedded delivery system and its application in food." *Food Hydrocolloids* (2024): 110625.

٢. Akanny, Elie, et al. "Development of enteric polymer-based microspheres by spray-drying for colonic delivery of Lactobacillus rhamnosus GG." *International Journal of Pharmaceutics* 584 (2020): 119414.

One-pot synthesis of spiro oxindoles using ZIF-8(Zn/Co)@g-C_3N_4 as catalyst

Authors: Hossein Mehri[a], Abdolhamid Bamoniri*[a] , BiBi Fathemeh Mirjalili[b]

Corresponding author Email: bamoniri@kashanu.ac.ir

a) Department of Organic Chemistry, Faculty of Chemistry, University of Kashan, Kashan, Iran

b)Department of Chemistry, College of Sciences, Yazd University, Yazd, Iran

Keywords: Spiro oxindoles, Antimicrobial, Nanocatalyst, ZIF-8 , Multicomponet.

Abstract

A series of novel spirooxindoles have been synthesized through 1,3-dipolar cycloaddition of an azomethine ylide generated from isatin[1] and sarcosine or L-proline with dipolarophile 1,4-naphthoquinone followed by spontaneous dehydrogenation[2]. Synthesized compounds were evaluated for their antimicrobial activities against eight bacteria and three fungi[3]. ZIF-8(Zn/Co)@g-C_3N_4 as a Lewis acid catalyst has been synthesized and characterized with FE-SEM, TEM, FT-IR, TGA, BET and XRD analysis. The advantages of this catalyst are low reaction time, convergence, simplicity of operation and recyclability. The beneficial features of this method are soft reaction position, no column chromatographic purification and high yield of products. All derivatives were distinguished by FT-IR and ^{1}H NMR spectroscopy.

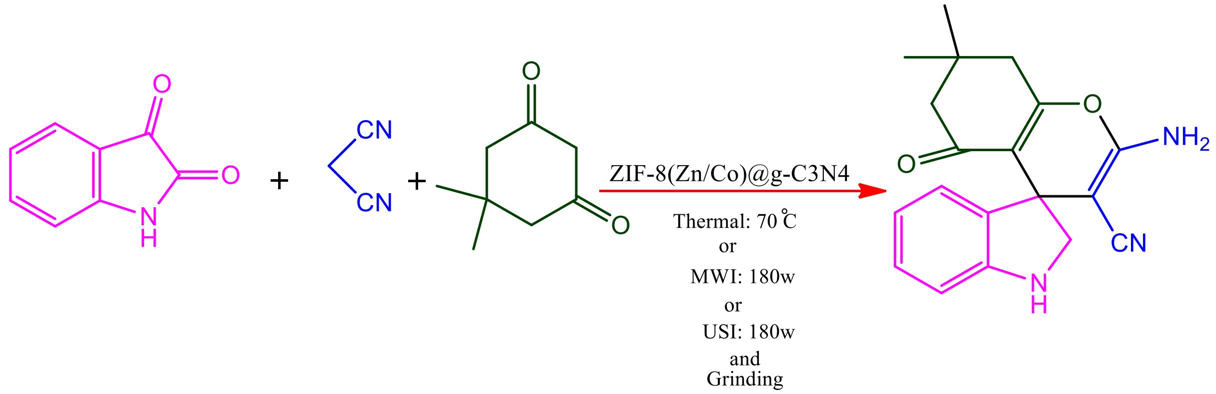

References:

[۱] A.V. Murashkina, A.Y. Mitrofanov, I. P. Beletskaya, Copper in cross-coupling reactions: Sonogashira- Hagihara reaction. *Russian. J. Org. Chem.*, **2019**, 55(2), 1445-58.

[2] R. Noreen, A. Hameed, T. Khalid, S. Batool, T. Farooq, Aqueous-mediated synthesis of bioactive spirooxindoles. Aqueous-Mediated Synthesis. *Green Synth. Catal.*, **2024**, 19 (2), 255-260.

[3] G. Sachdeva, J. Dhariwal, M. Vats, V. Rawat, Srivastava M, Srivastava A. Oxide Nanoparticles in Heterogeneous Catalysis. *J. Biophys. Chem.*, **2022**, 10(3), 15-50.

The 30th Iranian Seminar of Organic Chemistry
February 7-9, 2025, Iran University of Science and Technology, Tehran, Iran

Green Organic Inhibitors: Evaluating Ailanthus Altissima Seed Extract as an Eco-Friendly Solution for Copper Corrosion Prevention

Mohammad Reza Gholizadeh[1], Mohammad Mahdi Alemnezhad[1], Ali Ghaffarinejad[1,2]

[1] *Research Laboratory of Real Samples Analysis, Faculty of Chemistry, Iran University of Science and Technology (IUST), Tehran 1684613114, Iran*

[2] *Electroanalytical Chemistry Research Center, Iran University of Science and Technology (IUST), Tehran 1684613114, Iran*

Keyword: Copper corrosion; Green organic corrosion inhibitors; Electrochemical analyses

Introduction:

Corrosion of metals is a natural process that damages metals through reactions with their environment, adversely affecting their properties[1]. Copper and its alloys are valuable and widely used across various industries, including agriculture, electronics, construction, and marine engineering, due to their excellent thermal and electrical conductivity[2]. While copper typically exhibits good corrosion resistance in neutral environments by forming a passive protective layer, its susceptibility increases in the presence of oxygen or corrosive agents like chloride and sulfate ions, leading to pitting corrosion[3]. To extend the lifespan of metals, controlling corrosion rates through methods such as painting, coating, cathodic protection, and using inhibitors is crucial. Green organic inhibitors, which include natural ingredients such as leaf extracts, are an affordable and readily available option[4]. This study investigates the potential of ailanthus altissima seed extract (AASE) as an eco-friendly corrosion inhibitor for copper in 3.5 wt.% NaCl solution.

Method:

Plant seeds were collected, washed, dried at 40°C, and ground into powder. AASE was extracted using ultrasonic-assisted water extraction and Soxhlet extraction. The extracts were tested for corrosion inhibition effectiveness at concentrations of 2.5 to 20 v/v% on copper alloy sheets (UNS C16400). Corrosion behavior was analyzed using Potentiodynamic Polarization (PDP) and Electrochemical Impedance Spectroscopy (EIS) in a three-electrode setup at ambient temperature, with morphological changes examined via Scanning Electron Microscopy (SEM).

Result and Discussion:

PDP and EIS analyses were performed to evaluate the effectiveness of AASE as a corrosion inhibitor for copper in a 3.5 wt.% NaCl medium. Polarization curves demonstrated that increasing AASE concentration lowered both corrosion current density and corrosion rate, implying kinetic control of the corrosion process. The inhibition efficiencies (IE%) for 10 and 20 v/v% AASE were 83% and 92.41%, respectively. Thereby, 10% v/v AASE is the best concentration for reducing inhibitor consumption. (fig 1-a) EIS analysis confirmed the effectiveness of AASE as a corrosion inhibitor. As shown in Fig 1-b, with increasing AASE concentration, the polarization resistance (R_p) increased significantly, which means charge transfer resistance at the surface of the Cu electrode (R_{ct}) increased due to the formation of a protective barrier. In the EIS results, IE% for concentrations of 10 and 20 v/v% AASE was 83% and 93.4%, respectively. in conclusion, 10 v/v% AASE remained the preferred concentration to balance efficiency and resource consumption.

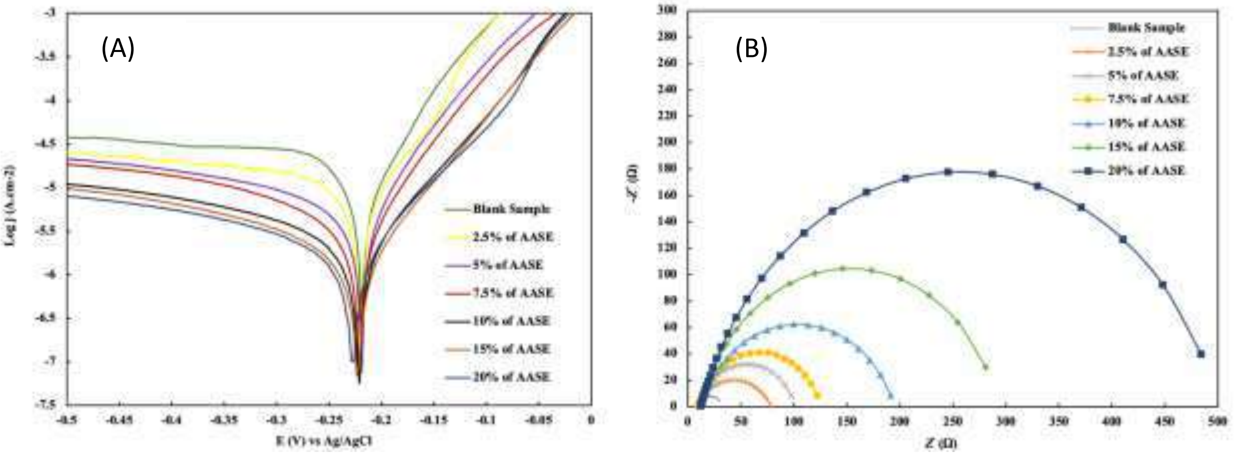

Figure 1: polarization curves (A) and EIS Nyquist plot (B) for Cu in 3.5 wt.% NaCl solution containing various AASE concentrations at 298 K.

The SEM images provide additional support for the earlier analyses, as illustrated in figure 2. The use of the optimum concentration of AASE greatly reduces surface corrosion damage, highlighting its efficacy in protecting the Cu surface.

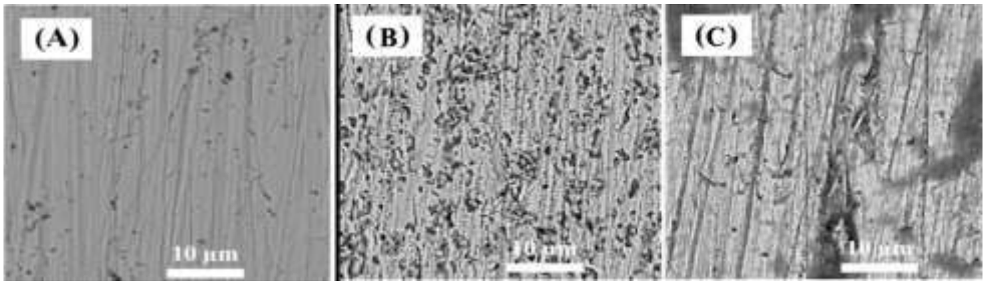

Figure 2: SEM images of blank Cu sheet sample (A), after 24h exposure to corrosive media without (B), and with (C) 10 v/v% AASE

References:

1. Zehra, S., Mobin, M. & Aslam, J. in *Environmentally Sustainable Corrosion Inhibitors* 3–23 (Elsevier, 2022).

2. Pareek, S., Jain, D., Behera, D., Sharma, S. & Shrivastava, R. *Mater Today Proc* **43**, 3303–3308 (2021).

3. Fateh, A., Aliofkhazraei, M. & Rezvanian, A. R. *Arabian Journal of Chemistry* **13**, 481–544 (2020).

4. Fekri, M. H., Omidali, F., Alemnezhad, M. M. & Ghaffarinejad, A. *Mater Chem Phys* **286**, 126150 (2022).

The 30th Iranian Seminar of Organic Chemistry
February 7-9, 2025, Iran University of Science and Technology, Tehran, Iran

Development and Evaluation of a Curcumin-loaded *Satureja khuzistanica* Nanoemulsion for Treating Ischemic Stroke

Faraz Maarefvand[a,d], Zinab Moradi Alvand[a,d], Samira Vahidi[b], Sepideh Khaksar[c], Hasan Rafati*[d]

[a] *Department of Phytochemistry, Medicinal Plants and Drugs Research Institute, Shahid Beheshti University, Tehran, Iran*

[b] *Department of Animal Science and Marine Biology, Faculty of Life Sciences and Biotechnology, Shahid Beheshti University, Tehran, Iran*

[c] *Department of Plant Sciences, Faculty of Biological Sciences, Alzahra University, Tehran, Iran*

[d] *Department of Pharmaceutical Engineering, Medicinal Plants and Drugs Research Institute, Shahid Beheshti University, Tehran, Iran*

Keyword: Ischemic stroke, Nano, Curcumin, *Satureja khuzistanica* Jamzad, MCAO

Introduction: Stroke affects 13.7 million people worldwide each year and is the second leading cause of death. Ischaemic stroke, which accounts for about 71% of all strokes globally, happens when there is damage to the brain due to a lack of blood flow and oxygen. Since multiple signaling pathways in the brain trigger neuroinflammation and oxidative stress following an ischemic stroke, using anti-inflammatory and anti-oxidant natural compounds presents a promising therapeutic strategy for this condition [1]. Curcumin, holds significant therapeutic potential due to its powerful anti-inflammatory and antioxidant properties. However, its poor water solubility and limited ability to cross the blood-brain barrier (BBB) greatly limit its biomedical applications. To solve this problem, various nanocarriers have been developed for delivering curcumin to brain, including nanoemulsions [2]. Similarly, *Satureja khuzistanica* Jamzad essential oil has demonstrated notable anti-inflammatory and antioxidant properties, further highlighting its potential as a therapeutic agent [3].In this study, we developed a nanoemulsion of *Satureja khuzistanica* Jamzad essential oil loaded with curcumin to investigate the potential synergistic effects of these two compounds.

Method: Nanoemulsion were prepared using a high-energy method with a rotor-stator high-shear homogenizer. The nanoemolsion was characterized using a Dynamic Light Scattering (DLS) instrument to determine the Polydispersity Index (PDI) and particle size (nm). This study includes five groups of adult male Wistar rats: 1. Sham Group, 2. Control Group, 3. Normal Curcumin Group: Rats were administered curcumin dissolved in normal saline with 1% DMSO following MCAO, 4. Nano Essential Oil Group: Rats were treated with nanoemulsion containing *Satureja khuzistanica* Jamzad essential oil without curcumin, 5. Nano Essential Oil + Curcumin Group: Rats were treated with a nanoemulsion containing *Satureja khuzistanica* essential oil loaded with curcumin. To induce focal cerebral ischemia, the Middle Cerebral Artery Occlusion (MCAO) procedure was used. The integrity of the blood-brain barrier (BBB) was assessed using the Evans Blue extravasation method. To evaluate the extent of infarction, 2,3,5-Triphenyltetrazolium chloride (TTC) staining was performed [2],[3]. The infarct volume was quantified using image analysis software to determine the percentage of damaged tissue relative to the total brain volume. Brain water content for wet and dried brain was measured to assess cerebral edema.

Results and Discussion: The nanoemulsion (SKJ+Curcumin) was successfully prepared and characterized. The particle size was determined to be approximately 196.65±0.0127 nm, with a Polydispersity Index (PDI) of 124±3.29, indicating a uniformly distributed nanoformulation. These properties suggest that the nanoemulsion is suitable for enhancing the stability and bioavailability of curcumin and *Satureja khuzistanica* essential oil. TTC staining revealed a significant reduction in infarct volume among the other treatment groups. The infarct volume was highest in the control group and significantly reduced in the Nano Essential Oil + Curcumin group. These results highlight the neuroprotective effects of the curcumin-loaded nanoemulsion. The Evans blue assay demonstrated reduced blood-brain barrier (BBB) disruption in the treatment groups. The dye leakage was highest in the control, while the Nano Essential Oil + Curcumin group showed the lowest leakage.

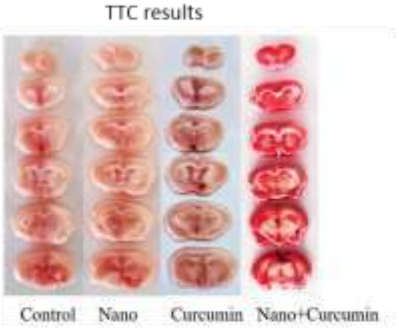

Brain water content, an indicator of cerebral edema, was significantly lower in the treatment group. The findings of this study demonstrate the therapeutic potential of the curcumin-loaded nanoemulsion in ischemic stroke. The Nano Essential Oil + Curcumin group consistently outperformed other groups across all metrics, including infarct volume, BBB integrity, and edema reduction. These results suggest that the combination of *Satureja khuzistanica* essential oil and curcumin has synergistic effects, likely due to their combined anti-inflammatory, antioxidant, and neuroprotective properties.

References:

[1] Campbell, B. C. V., De Silva, D. A., Macleod, M. R., Coutts, S. B., Schwamm, L. H., Davis, S. M., & Donnan, G. A. (2019). Ischaemic stroke. *Nature Reviews Disease Primers*, 5(1), 70. \

[2] Wang, Y., Luo, J., & Li, S.-Y. (2019). Nano-curcumin simultaneously protects the blood-brain barrier and reduces M1 microglial activation during cerebral ischemia-reperfusion injury. *ACS Applied Materials & Interfaces*, 11(4), 3763–3770.

[3] Abbasloo, E., Dehghan, F., Khaksari, M., Najafipour, H., Vahidi, R., Dabiri, S., ... & Asadikaram, G. (2016). The anti-inflammatory properties of *Satureja khuzistanica* Jamzad essential oil attenuate the effects of traumatic brain injuries in rats. *Scientific Reports*, 6, 31866.

The 30th Iranian Seminar of Organic Chemistry
February 7-9, 2025, Iran University of Science and Technology, Tehran, Iran

Synthesis of Metal Nanofibers via Electrospinning

Authors: Mohammad Jawad Akbar Heydary 1[a], Morteza Nasiri Azar1[a] , Saeed Bazgir2[b]

Abstract

In this work, a novel electrospinning method was used to synthesize polymer-metal (iron in this case) hybrid nano fibers, calcination process is then applied to these fibers to remove the polymer part to acquire metal nanofibers. The resulting fibers where then characterized by structural and functional analysis. The structural analysis of the fibers confirmed fiber diameter in 180 to 400 nanometer range and the functional analysis showed active surface area of 14 m2/gr.

Keyword: Electrospinning, Metal Nanofibers, Iron nanofibers, nanofiber synthesis

Introduction

Metal nanofibers are a class of advanced nanomaterials characterized by their high length to diameter ratio. Their unique properties such as high surface area to volume ratio, remarkable mechanical properties, functional reactivity and advanced thermal and electrical conductivity make metal nanofibers ideal materials for advanced applications such as energy storage devices, filtration systems and catalysts. These nanomaterials can be acquired by different methods such as chemical reduction, lithography and electrospinning. Their ease of integrity into complex systems along with precise control over their composition and morphology have gathered interest in recent years.

Materials and methods

Poly Vinyl Acetate (PVA) was supplied from Amirkabir Petro chemical company, Iran. Iron (III) Acetate was supplied from Amertat chemical company, Iran. Samples were prepared by solving 9 wt% PVA as the base solution, 0.5 ,1.0 and 1.5 ratio of iron salt were added and stirred for 24 hrs at 25℃. resulting in amber opaque solutions. metal-polymer solutions were then electro-spun. The optimum nozzle height were acquired at 25cm from collector, the optimum voltage was acquired at 20kv, collector speed was set at 40 rpm. Each sample were spun for 30 mins. After witch Samples were calcified for 3 hours at 600 ℃ to remove any polymer part. Acquired Metal nanofibers were then characterized via structural and functional analysis.

Results and discussion

Figure 1 presents the FESEM images [provided by MIRA3 (TESCAN, Korea) Field emission scanning electron microscopy Iran] of the acquired hybrid nanofibers. displaying a smooth surface and partial orientation morphology with mean diameter of 320 nanometers (calculated by imagj imaging software). Expansion of diameter was observed with the increase of metal salt concentration.

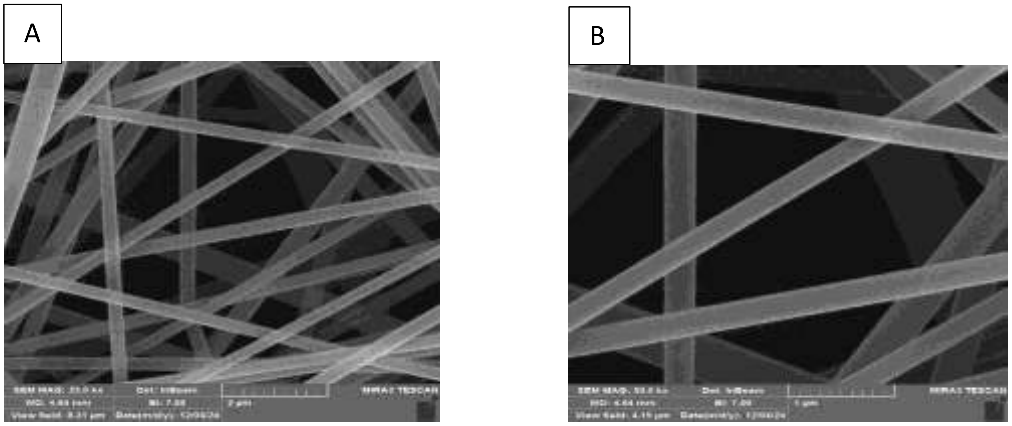

Figure 1:FESEM images of hybrid polymer-metal nanofibers with 25000 (A) and 50000 (B) magnification.

Figure 2 presents metal nanofibers after the calcination process.the resulting metal oxide nanofibers display a rough yet fibrous morpholgy. With mean diameter of 150 nanometers (calculated by imagj imaging software) the acquired metal nanofibers posses remarkable aspect ratios leading to significant functional and mechanical properties.

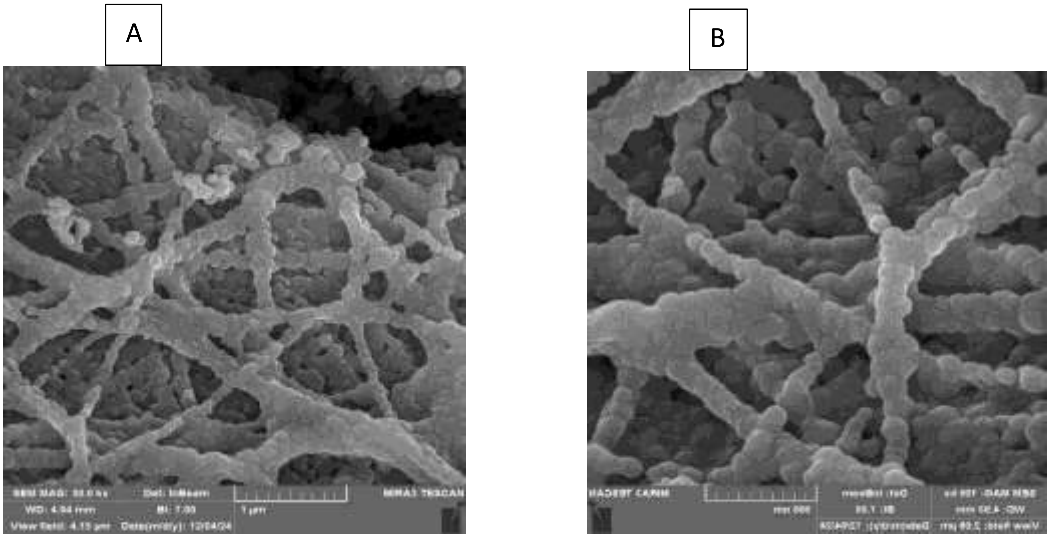

Figure 2:FESEM images of metal-oxide nanofibers with 50000 (A) and 100000 (B) magnification.

Brunauer-Emmett-Teller Surface Area & Porosity characterization and analysis presents the functional characterization of the metal-oxide nanofibers, with the mean specific active surface area of $14m^2$/gr and pore sizes in the 15 nanometer range and average pore volume of 0.07 m3/gr for pores less than 40 nanometers present these metal nanofibers with excellent reactivity surface and conducting properties.

References

١. Mortimer, Chris J. , The fabrication of iron oxide nanoparticle-nanofiber composites by electrospinning and their applications in tissue engineering, Biotechnol. J., 2012, vol. 7, 1860-6768

٢. Kyeong-Han N., et. al., Fabrication and characterization of the magnetic ferrite nanofibers by electrospinning process, Thin Solid Films, Volume 660, 2018, Pages 358-364,

٣. Nicolás T., et. al., Enhancing arsenic adsorption via excellent dispersion of iron oxide nanoparticles inside poly(vinyl alcohol) nanofibers, Journal of Environmental Chemical Engineering, 2021, Volume 9, Issue 1, 104664.

٤. Saikat Sinha R. et. al., A comprehensive review: electrospinning technique for fabrication and surface modification of membranes for water treatment application, Journal of RCS advances, 2016, vol 6, 85495-85514

Spherical nanostructured mixed Mo-Zr-Mn oxide: Synthesis, characterization, and application as heterogeneous catalyst for selective oxidation of sulfides to sulfoxides

Hoda Haghi [a], Alireza Sedrpoushan *[a]

[a] *Department of Chemical Technologies, Iranian Research Organization for Science and Technology (IROST), P.O. Box 33535111, Tehran, Iran.* (* *sedrpoushan@irost.ir*)

Abstract: A ternary metal oxide was synthesized using of Mo, Zr, Mn which are inexpensive and non-toxic metals. The composite was characterized using XRD, SEM, EDS and EM. The use of composite as a heterogeneous catalyst in the oxidation of sulfides with yield of 87 percent was examined.

Keyword: Metal oxide; Catalyst; Oxidation; Sulfide; Sulfoxide

Introduction: A significant challenge in organic chemistry is the selective oxidation of sulfides to sulfoxides. [1]. Transition metals are commonly utilized as catalyst, and their activity is based on the configuration of their outer electrons [2]. Hence, we presented an affordable mixed nano-metal oxides catalyst composed of Mo-Zr-Mn, which exhibits an enhanced surface area, physical-chemical interactions, and without additional support as a highly active. Also, we investigated the selective heterogeneous catalyst for our reactions utilizing H_2O_2 as a sustainable co-oxidant.

Method:

Catalysis preparation: The precursors of the metals in the proper quantities, $MoCl_5$ (1 mmol, 0.273g), $ZrCl_4$ (1 mmol, 0.233g), $MnCl_2.2H_2O$ (1 mmol, 0.125g), NH_4F (6 mmol, 0.253g) and urea (15 mmol) were dissolved at room temperature in distilled water (70 mL). Then, the solution was transferred into the autoclave and heated to 100 ^oC for 24 hours. After cooling the autoclave to room temperature, the resulting precipitate was washed with water and ethanol and dried for 12 hours. The resulting material was then calcinated at 350 ^oC to give the ternary nano catalyst.

Catalyst testing for sulfides: Catalytic oxidation of sulfides to corresponding sulfoxides, was investigated at 80 ^oC using a catalyst (15 mg), 30% H_2O_2 (4 mmol) as oxidant, and sulfide (0.5 mmol) in acetonitrile (5 mL) for 8 hours. The reactions were achieved to get the optimal point in different solvents, temperatures, and the molar ratios of substrate/oxidant. We were performed the oxidation reactions of sulfide in reflux conditions using thin-layer chromatography (TLC) (EtOAc/n-hexane) monitoring. Finally, the catalysis was filtered, washed with hot acetone, and dried in a vacuum desiccator to reuse and test the recycling capability.

Results and Discussion: We have the foundations for using XRD analysis to determine the structures of these compounds (Fig. 1). We were used the FESEM image to examine the shape and dimensions of the ternary Mo-Zr-Mn oxide catalyst at 1 µm, 200 and 500 nm (Fig. 2). Spherical structures with about 200 µm diameter have formed. The inner particles of the spherical structure have about 20 nm thickness.

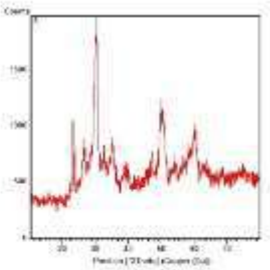

Fig.1: X-ray diffraction pattern

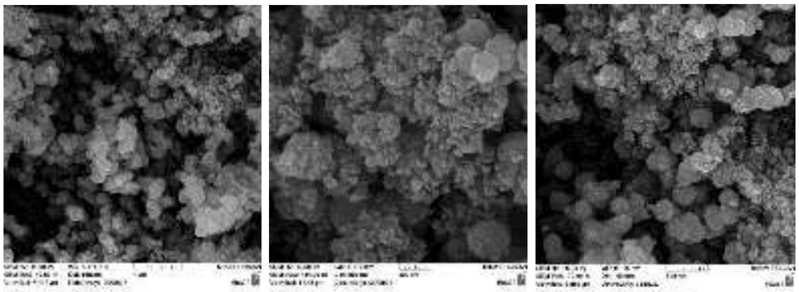

Fig.2: SEM images of Mo-Zr-Mn at 1 µm, 200 and 500 nm

Also, the presence of all three elements molybdenum, zirconium and manganese has been proven with EDS analysis (Fig. 3). Additionally, the presence of all three elements has been shown with color images (Fig. 4).

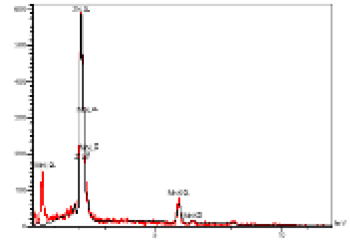

Fig.3: EDS of Mo-Zr-Mn

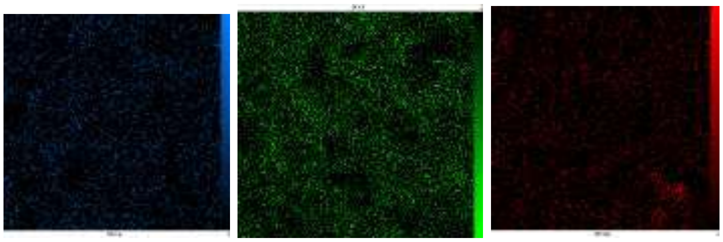

Fig.4: Elemental mapping images of Mo-Zr-Mn

Different types of sulfides were oxidized to sulfoxides under the optimized conditions (Table 1).

Table1: Oxidation of different sulfides to sulfoxides using Mo-Zr-Mn

Sulfide	Sulfoxide	Time (h)	(%) Yield
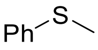	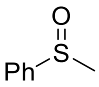	8	87
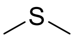	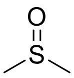	8	87
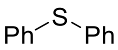	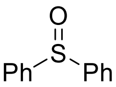	8	86
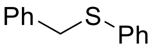	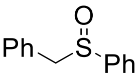	8	84

References: [1] J.N. Moorthy, K. Scnapati, K.N. Parida, J. Org. Chem. 75 (2010) 8416–8421.

[2] B. Bridier, J. Perez-Ramırez, J. Am. Chem. Soc. 132 (2010) pp. 4321.

The 30th Iranian Seminar of Organic Chemistry
February 7-9, 2025, Iran University of Science and Technology, Tehran, Iran

Preparation and Synthesis of the Magnetic Metal-Organic Framework (Fe_3O_4/UiO-66-NH_2): Investigation of magnetic and chemical properties

Leili Salahshour 1[a], Nader Bahramifar 2[b], 3*[c] *Ali Reza Oveisi*

1[a] M.S student, Environment Science, Faculty of Natural Resources and Marine Sciences, Tarbiat Modares University, Iran *l.salahshour@modares.ac.ir*

2 [b] *Faculty member, Faculty of Natural Resources and Marine Sciences, Tarbiat Modares University, Iran, nbahramifar@yahoo.com*

3[c] Faculty member, Department of Organic Chemistry, Faculty of Chemistry, Lorestan University, Iran, alir.oveisi@gmail.com*

Keyword: Metal organic frameworks (MOFs)- Nanocomposite- Magnetic properties-

Abstract:

This study provides a detailed method for synthesizing Fe_3O_4/Uio-66(NH_2), which exhibits unique magnetic and catalytic properties. A solvothermal approach is employed to achieve high crystallinity and uniform particle distribution. The synthesized nanocomposites were characterized using various techniques, including X-ray diffraction (XRD), scanning electron microscopy (SEM), Fourier-transform infrared spectroscopy (FTIR), and also Vibrating Sample Magnetometer technique (VSM), confirming the successful incorporation of Fe_3O_4 nanoparticles within the UiO-66-NH_2 framework. The application potential of Fe_3O_4/Uio-66(NH_2)was explored in environmental remediation and catalysis. The magnetic properties of Fe_3O_4 facilitated easy separation and recovery of the nanocomposites from aqueous solutions, making them ideal for repeated use in pollutant removal processes. Additionally, the catalytic performance of Fe_3O_4/Uio-66(NH_2)was evaluated in the degradation of organic pollutants, demonstrating high efficiency and stability under various conditions. This study highlights the versatility and effectiveness of Fe_3O_4/Uio-66(NH_2) nanocomposites, paving the way for their future applications in environmental and industrial fields. The findings underscore the importance of developing multifunctional materials that combine magnetic and catalytic properties for advanced technological applications.

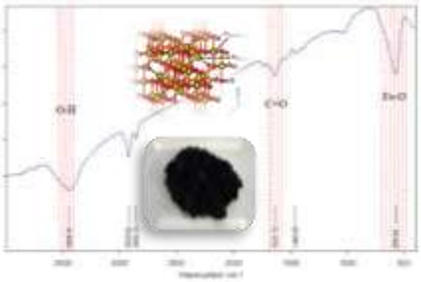

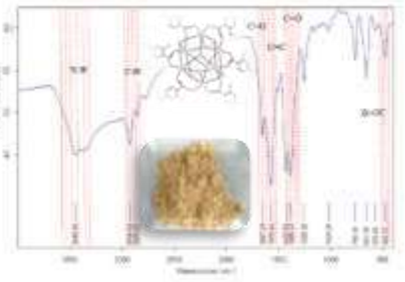

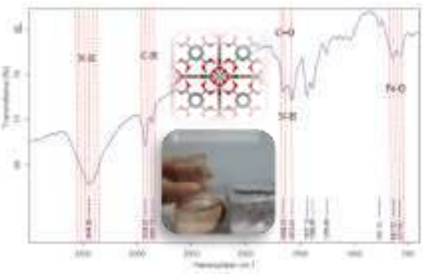

Fe_3O_4 + Uio66-NH_2 = Fe_3O_4/Uio66-NH_2

Fig. 1: Synthesis of Fe_3O_4/Uio66-NH_2

1-Introduction :

Metal-organic frameworks (MOFs) like UiO-66(NH_2) are effective in pollution control, owing to their high porosity, tunable structures, and large surface areas. UiO-66(NH_2) shows promise in environmental remediation and as a sustainable catalyst for various organic reactions, with advantages such as high catalytic performance and ease of magnetic separation. Despite these benefits, stability and scalability remain challenges. This study focuses on synthesizing a magnetic MOF (Fe_3O_4@UiO-66-NH_2) to improve stability and enable easy separation via an external magnetic field[1,2].

2. Experimental section

Fe_3O_4 NPs were prepared via a solvothermal method involving $FeCl_3.6H_2O$, ethylene glycol, sodium acetate, and EDTA-2Na. The Fe_3O_4/UiO-66-NH_2 composite synthesis included dissolving Fe_3O_4, $ZrCl_4$, and NH_2-H_2BDC in DMF, followed by sonication, mixing, dropwise HAc addition, reflux heating, and subsequent washing and drying.

3. Results and discussion

The Fe_3O_4/UiO-66-NH_2 composites demonstrate a saturation magnetization of 30 emu/g, indicating successful group immobilization on Fe_3O_4 MNPs. The composites exhibit significant magnetic properties, with Fe_3O_4/BAC/UiO-66 showing 44.06 emu/g, facilitating post-adsorption separation[3]. FTIR and XRD analyses confirm the presence of functional groups and well-maintained MOF crystals. SEM images reveal the composites' morphology and size, highlighting their environmental application potential and recyclability[4,5].

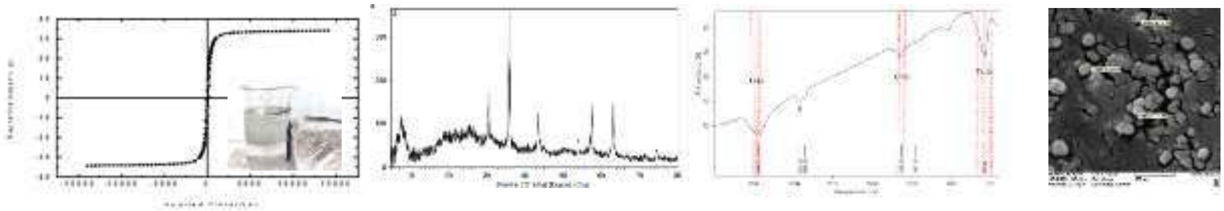

Fig. 2: (a)VSM, (b)XRD,(c)FTIR (d) SEM of Fe_3O_4/Uio66(NH_2),

[1] V. F. Yusuf, N. I. Malek, and S. K. Kailasa, “Review on Metal-Organic Framework Classification, Synthetic Approaches, and Influencing Factors: Applications in Energy, Drug Delivery, and Wastewater Treatment,” *ACS Omega*, vol. 7, no. 49, pp. 44507–44531, 2022, doi: 10.1021/acsomega.2c05310.

[2] Y. Qian, F. Zhang, D. J. Kang, and H. Pang, “A Review of Metal–Organic Framework-

Based Compounds for Environmental Applications," *Energy Environ. Mater.*, vol. 6, no. 3, pp. 1–30, 2023, doi: 10.1002/eem2.12414.

[3] Y. Li, Y. Xu, K. Guo, L. Kong, and Y. Zeng, "Recyclable magnetic-responsive AC/Fe3O4/UiO-66 adsorbents for removing elemental mercury from flue gas," *Sep. Purif. Technol.*, vol. 353, no. PB, p. 128395, 2025, doi: 10.1016/j.seppur.2024.128395.

[4] X. Zhang, Y. Zhang, T. Wang, and G. Zhang, "RSC Advances PAPER," pp. 24802–24810, 2019, doi: 10.1039/C9RA04714J.

[5] C. L. Luu, T. T. Van Nguyen, T. Nguyen, and T. C. Hoang, "Synthesis, characterization and adsorption ability of UiO-66-NH2," *Adv. Nat. Sci. Nanosci. Nanotechnol.*, vol. 6, no. 2, 2015, doi: 10.1088/2043-6262/6/2/025004.

The 30th Iranian Seminar of Organic Chemistry
February 7-9, 2025, Iran University of Science and Technology, Tehran, Iran

Green Synthesis of 3,4-Dihydropyrimidinones using Core-Shell Magnetic Nanoparticles as a Recoverable Catalyst

Nahal Sadri [a], Somayeh Soleimani-Amiri[a,۳], Behrooz Mirza [a]

[a] *Department of Chemistry, Karaj Branch, Islamic Azad University, Karaj, Iran*

Abstract: This study introduces a method for synthesizing Fe_3O_4@C@PrS-SO_3H nanoparticles, which serve as efficient, low-toxicity, cost-effective catalysts for organic synthesis. XRD confirmed their cubic magnetite structure, and SEM revealed an average particle size of ~30 nm. These catalysts were used in Biginelli multicomponent reactions to produce 3,4-dihydropyrimidin-2(1H)-ones (DHPMs) with a 91% yield under optimized conditions (20 wt% catalyst, ethanol reflux, 15 min reaction) using ethyl acetoacetate, benzaldehyde, and urea.

Keywords: Green synthesis, Biginelli condensation, 3,4-Dihydropyrimidinone, Magnetic nano-catalyst.

Introduction

3,4-Dihydropyrimidin-2(1H)-ones (DHPMs), important heterocyclic compounds in medicinal and synthetic chemistry, are synthesized via one-pot Biginelli condensation of aldehyde, urea, and β-keto ester, typically using acid catalysts. Traditional catalysts often involve harsh conditions, high costs, and prolonged reactions. Nano-catalysts, with high surface area and thermal stability, improve activity and enable easy removal [1]. Magnetic nanoparticles (MNPs) are particularly effective, offering high yields, selectivity, and magnetic separation [2, 3]. In this study,

---

[۳] Corresponding Authors: Somayeh Soleimani-Amiri: s.soleimani@kiau.ac.ir

Fe_3O_4@C@PrS-SO_3H nanoparticles were synthesized and used for green DHPM synthesis via Biginelli condensation, achieving high efficiency and short reaction times under ethanol reflux (Scheme 1).

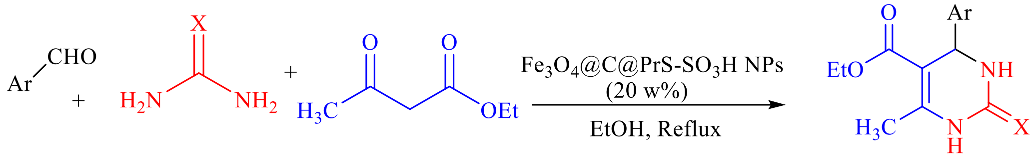

Scheme 1: Synthesis of 3,4-Dihydropyrimidinones using Fe_3O_4@C@PrS-SO_3H NPs.

Method

Materials from Sigma, Aldrich, Merck, Acros, and Alfa Aesar were used without further purification unless stated. XRD patterns were recorded on a Panalytical X'Pert Pro with Cu Kα radiation, and SEM analysis on a SIGMA VP-500-Zeiss. Melting points were measured with an Electrothermal IA 9200. FT-IR spectra (4000–400 cm^{-1}) were obtained using a Perkin Elmer spectrometer with KBr tablets, and NMR spectra on a Bruker Avance DRX-300 with DMSO-d_6.

Synthesis of Fe_3O_4@C@PrS-SO_3H NPs

Fe_3O_4@C@PrSH NPs were dispersed in dichloromethane, and Fe_3O_4@C@PrS-SO_3H NPs were synthesized by adding chlorosulfonic acid (0.8 mL) under nitrogen. The product was magnetically separated, washed with dichloromethane, and dried at 60°C.

General Synthesis Procedure of pyrimidin-2(1H) using Fe_3O_4@C@PrS-SO_3H NPs

Aromatic aldehyde (1 mmol), urea (1.5 mmol), ethyl acetoacetate (1 mmol), and Fe_3O_4@C@PrS-SO_3H NPs (20 wt%) were refluxed in ethanol. After cooling, the catalyst was magnetically separated, washed, dried, and reused. Products were characterized by melting points, FT-IR, and ^1H/^{13}C NMR.

Results and Discussion

Synthesis of 3,4-dihydropyrimidinones using Fe_3O_4@C@PrS-SO_3H NPs

The Biginelli condensation of aromatic aldehyde, urea, ethyl acetoacetate, and Fe_3O_4@C@PrS-SO_3H NPs in ethanol produced bioactive 3,4-DHPMs with excellent yields. Catalyst loading, temperature, and solvents were optimized. Various benzaldehydes with 20 wt% Fe_3O_4@C@PrS-SO_3H NPs in ethanol yielded 3,4-DHPMs (60–98%) within 15 minutes (Table 1).

Table 1. **One-pot synthesis of ۳،٤-DHPMs using Fe_3O_4@C@PrS-SO_3H NPs.**

Entry	Ar	Yield (%)	Time(min)	**M.P. (^oC)**
1	C_6H_5	91	15	**200-202**
2	4-$CH_3C_6H_4$	81	15	**206-208**
3	4-$OCH_3C_6H_4$	60	15	**194-196**
4	3-$NO_2C_6H_4$	98	15	**218-219**
5	4-$NO_2C_6H_4$	82	15	**205**
6	2-ClC_6H_4	77	15	**212-214**

7	3-ClC$_6$H$_4$	98	15	**183-185**
8	4-ClC$_6$H$_4$	77	15	**210-212**

Preparation and characterization of Fe_3O_4@C@PrS-SO_3H NPs

Fe_3O_4@C@PrS-SO_3H NPs were synthesized and characterized by FT-IR, XRD, and SEM. FT-IR identified functional groups including S–O bending (630 cm^{-1}), O=S=O stretching (1034, 1121, 1122 cm^{-1}), OH stretching (3384 cm^{-1}), C=C stretching (1639 cm^{-1}), C–O stretching (1082 cm^{-1}), and Fe–O stretching (570 cm^{-1}). SEM showed uniform spherical nanoparticles averaging 30 nm (Fig. 1a). XRD confirmed the Fe_3O_4 magnetite core's crystalline structure, matching reference code 98-011-1282 (Fig. 1b).

Conclusion

A green method was developed to synthesize 3,4-DHPMs via a one-pot reaction of aromatic aldehyde, ethyl acetoacetate, and urea using Fe_3O_4@C@PrS-SO_3H NPs in ethanol. This approach offers high yields, fast reactions, easy work-up, and a reusable magnetic catalyst. The NPs, synthesized cost-effectively and characterized by FT-IR, XRD, and SEM, were reused for five cycles with minimal activity loss.

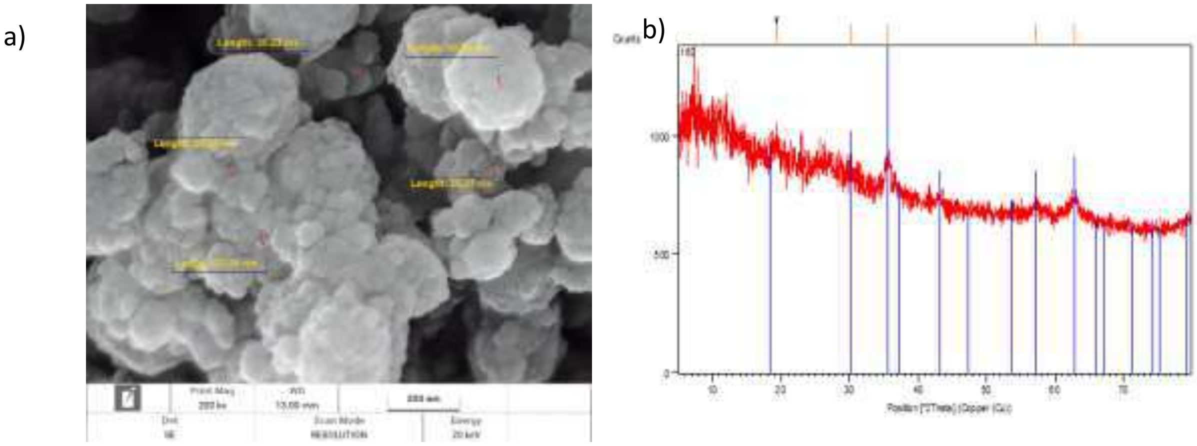

Figure 1. a) SEM image and b) XRD analysis of Fe_3O_4@C@PrS-SO_3H NPs.

References:

[1] S.P. Bahekar, P.B. Sarode, M.P. Wadekar, H.S. Chandak, Simple and efficient synthesis of 3,4-dihydropyrimidin-2(1H)-thiones utilizing l-proline nitrate as a proficient, recyclable and eco-friendly catalyst, Journal of Saudi Chemical Society, 21 (2017) 415-419.

[2] S.F. Taheri Hatkehlouei, B. Mirza, S. Soleimani-Amiri*, Solvent-free one-pot synthesis of diverse dihydropyrimidinones/tetrahydropyrimidinones using biginelli reaction catalyzed by Fe3O4@C@ OSO3H, Polycyclic Aromatic Compounds, 42 (2022) 1341-1357.

[3] M. Feizpour Bonab, S. Soleimani-Amiri, B. Mirza, Fe3O4@C@PrS-SO3H: A Novel Efficient Magnetically Recoverable Heterogeneous Catalyst in the Ultrasound-Assisted Synthesis of Coumarin Derivatives, Polycyclic Aromatic Compounds, 43 (2023) 1628-1643.

The 30th Iranian Seminar of Organic Chemistry
February 7-9, 2025, Iran University of Science and Technology, Tehran, Iran

Synthesis of Zinc Oxide Nanoparticles by Aqueous Extract of *Salvia reuterana* Boiss. and its Antimicrobial and Antioxidant Properties

Foroogh Mirzania[1,2*], Zahra Asgari[3], Iraj Salimikia [*2], Javad Ghasemian Yadegari [2]

[1]*Razi Herbal Medicines Research Center, Lorestan University of Medical Sciences, Khorramabad, Iran.* [2]*Department of Pharmacognosy, Faculty of Pharmacy, Lorestan University of Medical Sciences, P.O. Box: 6815144309, Khorramabad, Lorestan Province, Iran. Tel: +986633120239, fax: +986633120240. E-mail: Foroughmirzania@gmail.com.* [3]*Student Research Committee, Faculty of Pharmacy, Lorestan University of Medical Sciences.*

Keyword: *Salvia reuterana* Boiss., Zinc oxide nanoparticles, Antibacterial activity, Antifungal properties

Introduction: *Salvia reuterana* Boiss., is an endemic, perennial herbaceous plant of Iran, where it is known as Maryam-Goli-e-Isfahani. The plant is mainly found in the central and western Iran [1, 2]. In this research aqueous extract of this plant was used to produce zinc oxide nanoparticles (ZnO-NPs). ZnO-NPs as the most applicable nanoparticles that its therapeutic and pharmaceutical properties have recieved especial attention.

Method: To produce ZnO-NPs, leaf of *Salvia reuterana* were powdered and then macerated to obtain aqueous extract, After that, aqueous extract was used to reduce $Zn(NO_3)_2\ 6H_2O$ to produce ZnO-NPs. To confirm nanoparticles synthesis SEM, TEM, UV-Vis, FT-IR and XRD analyses were used. The synthesized ZnO-NPs were studied for antimicrobial activities by well diffusion, MIC and MBC methods. The antioxidant activity of the synthesized nanoparticles was also investigated.

Results: Analysis confirmed successful synthesis of ZnO-NPs by aqueous extract of *Salvia reuterana*. Sizes of ZnO-NPs were estimated between 30-100 nm. Antibacterial and antifungal experiments showed potent activities against *E.coli* with 32 and 32µg/ml for MIC and MBC respectively. The antioxidant properties of the synthesized nanoparticles were also significant when compared to ascorbic acid. IC_{50} of ZnO-NPs, extract and standard sample for DPPH test were: 93000, 600000 and 5.9 µg/ml respectively.

Discussion: The researchers conclude that the investigation of *Salvia reuterana* aqueous extract use in the green synthesis of ZnO nanoparticles which was conducted in the present study exhibits the economically viable and sustainable sources of production. The results of the tested nanoparticles also suggest immune enhancing potential since they showed good potency against E. coli while also having good antioxidant activity. The observed IC_{50} values for DPPH antioxidant activity are great, thus giving an impression that these nanoparticles can be used as future substitutes to the synthetic antioxidants. A further research direction includes studying how to apply these in medical purposes as well as scaling up their production.

References:

[1] Cozzolino, R.; Mari, A.; Ramezani, S.; Martignetti, A.; Piacente, S.; De Giulio, B., *Journal of Food Composition and Analysis*, **2021**, *100*, 103939.
[2] Mirzania, F.; Moridi Farimani, M.; Sarrafi, Y.; Nejad Ebrahimi, S.; Troppmair, J.; Kwiatkowski, M.; Stuppner, H. Alilou, M., *Frontiers in Chemistry*, **2022**, *9*,.1166-1177.

The 30th Iranian Seminar of Organic Chemistry
February 7-9, 2025, Iran University of Science and Technology, Tehran, Iran

Green Synthesis of Silver Nanoparticles by *Salvia palaestina*: Unlocking Potent Antimicrobial and Antioxidant Applications

Foroogh Mirzania[1,2*], Zahra Asgari[3], Iraj Salimikia [*2], Javad Ghasemian Yadegari [2]

[1]*Razi Herbal Medicines Research Center, Lorestan University of Medical Sciences, Khorramabad, Iran.* [2]*Department of Pharmacognosy, Faculty of Pharmacy, Lorestan University of Medical Sciences, P.O. Box: 6815144309, Khorramabad, Lorestan Province, Iran. Tel: +986633120239, fax: +986633120240. E-mail:* Forooghmirzania@gmail.com. [3]*Student Research Committee, Faculty of Pharmacy, Lorestan University of Medical Sciences.*

Keyword: Ag Nanoparticles, Green synthesis, *Salvia palestinea*, Antimicrobial, Antioxidant properties

Introduction: *Salvia palaestina* Benth. (English name: Palestinian sage; common Persian name: Maryam-goli-e-felestini), which is distinguished by panicle inflorescence with four to six flowers in each verticillate and pink or violet prominent bracts, is distributed in the western and southern provinces of Iran. *S. palaestina* is virtually used in daily basis with the breakfast tea to add its distinct pleasant flavor and good scent. In this study, *S. palaestina* was used to produce silver nanoparticles (Ag-NPs) and its antimicrobial and antioxidant effects also were investigated [1, 2]. Ag-NPs as the most applicable nanoparticles that its therapeutic and pharmaceutical properties have recieved especial attention.

Method: To produce Ag-NPs, leaf of *S. palestinea* were powdered and then macerated for obtaining aqueous extract. After that, aqueous extract was used to reduce Ag nitrate to Ag-NPs. To confirm nanoparticles SEM, TEM, UV-Vis, FT-IR and XRD were used. The synthesized Ag-NPs were studied for antimicrobial activities by well diffusion, MIC and MBC methods. The antioxidant activity of the synthesized nanoparticles was also investigated.

Results: Analysis of Ag-NPs confirmed successful synthesis by aqueous extract of *Salvia palestinea*. The size of Ag-NPs were estimated 30-80 nm in diameter. Antibacterial and antifungal experiments showed potent activities of Ag-NPs against Staphylococ aureus, E.coli and Candida albicans (16, 32 and 32 µg/ml for MIC respectively) and (32, 125 and 640 µg/ml for MBC respectively). The antioxidant properties of the synthesized nanoparticles were also moderately good compared to ascorbic acid. IC50 of Ag-NPs, aqueous extract and standard sample for DPPH test were: 3757, 5567 and 7 µg/ml respectively. According to the results and considering that various advantages of medicinal plants, it is expected that biosynthesized by *S. palestinea* would applied as antimicrobial agent.

Discussion: Elucidating the results points out that *S. palaestina* is capable of acting as an ecofriendly and efficient reducing agent during the synthesis of Ag-NP. The nanoparticles showed considerable antibacterial activity and were moderate antioxidants. These results emphasize the great promise of *S. palaestina* derived biosynthesized Ag-NPs as a potential biocontrol agent with antioxidant activity.

References:

[1] Saleh, B. (2021). TU-DAMD employment for molecular characterization of Salvia judaica and Salvia palaestina species. *Acta Biologica Szegediensis*, *65*(1), 11-16.

[2] Nakamura, S., Sato, M., Sato, Y., Ando, N., Takayama, T., Fujita, M., & Ishihara, M. (2019). Synthesis and application of silver nanoparticles (Ag NPs) for the prevention of infection in healthcare workers. *International journal of molecular sciences*, *20*(15), 3620-28.

The 30th Iranian Seminar of Organic Chemistry
February 7-9, 2025, Iran University of Science and Technology, Tehran, Iran

Synthesis of efficient, green, and reusable ammonium tribromide-based magnetic catalyst for biodiesel production

Setareh Esmaeili anvar, Arash Ghorbani-Choghamarani*, Arezo Monem

Department of Organic Chemistry, Faculty of Chemistry and Petroleum Science, Bu-Ali Sina University, Hamedan, 6517838683, Iran, a.ghorbani@basu.ac.ir or arashghch58@yahoo.com, Setare.esmaili@gmail.com, arezomonem@yahoo.com

Keywords: Biodiesel, $SrFe_2O_4$, Heterogeneous Catalysis, Magnetic nanoparticles, Esterification

Biodiesel is one of the most important fuels known for its biodegradability and capacity to reduce greenhouse gas emissions. This fuel is produced through the transesterification reaction of vegetable oils or animal fats with alcohol, typically involving acid, base, or enzyme catalysts [1]. This research uses magnetic catalysts to explore biodiesel synthesis as a green and sustainable fuel. Biodiesel, derived from vegetable oils and animal fats, can be an alternative to fossil fuels. Magnetic catalysts enhance efficiency and lower production costs due to their ease of separation and recovery. In this study, we examined the effects of various parameters on catalyst performance and biodiesel yield [2]. In this context, a new and environmentally friendly magnetic nanocatalyst ($SrFe_2O_4$) was synthesized and characterized using various techniques. This research contributes to the advancement of green technologies in the fuel industry and offers sustainable solutions for biodiesel production (Scheme 1).

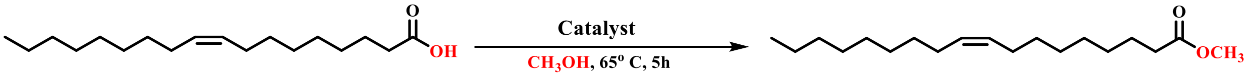

Scheme: Esterification of Oleic Acid

References:

۱- Jafari, A., Ghorbani-Choghamarani, A., & Aghavandi, H. (2024). Simple Synthesis of Novel Cr-EDTA-MOF: A Green, Reusable, and Versatile Catalyst for the Production of Biodiesel Fuel from Oleic Acid and Palmitic Acid. *ACS omega*, *9*(5), 5255-5264.
۲- Ghorbani-Choghamarani, A., Taherinia, Z., & Tyula, Y. A. (2022). Efficient biodiesel production from oleic and palmitic acid using a novel molybdenum metal–organic framework as efficient and reusable catalyst. Scientific Reports, 12(1), 10338.
۳- Khanmohammadi-Sarabi, F., Ghorbani-Choghamarani, A., Aghavandi, H., & Zolfigol, M. A. (2023). l-Methionine-Zr complex supported on magnetic ZnFe 2 O 4 as a novel, green, and efficient heterogeneous magnetic nanocatalyst for the synthesis of 1 H-tetrazole and polyhydroquinoline derivatives. New Journal of Chemistry, 47(9), 4252-4266.

Microcrystalline cellulose and cellulose-derived nutshell/zinc nanoparticles: Efficient and high performance microwave absorbing materials

Farbod Fazlalizadeh[a], Zahra Nezafat[a], Shahrzad Javanshir[*a], Reza Peymanfar [*b, c, d]

[a] *Pharmaceutical and Heterocyclic Chemistry Research Laboratory, Department of Chemistry, Iran University of Science and Technology, Tehran 16846-1**3114, Iran***

[b] *Department of Chemical Engineering, Energy Institute of Higher Education, Saveh, 39177-**67746, Iran***

[c] *Department of Science, Iranian Society of Philosophers, Tehran,13187-7**6511, Iran***

[d] *Sustainable Development of Industrial Laboratory (SDILAB) CO., Tehran, 15149-4**5511, Iran***

Keyword: Microwave absorption; Cellulose; Peanut shell; Zinc nanoparticles; Cryogel

Abstract

In this experimental research, fabrication of the pyrolyzed microcrystalline cellulose and cellulose-derived peanut shell/zinc nanoparticles (PMCC/Zn and PCDPS/Zn NPs) in the form of cryogel was reported. The prepared PMCC/Zn and PCDPS/Zn NPs were characterized using X-ray powder diffraction (XRD) and field emission scanning electron microscopy (FE-SEM). The microwave absorption performance of the PMCC/Zn and PCDPS/Zn NPs was evaluated by loading different amounts of the prepared materials in the polyvinyl chloride (PVC) as a absorbing matrix. The maximum reflection loss (RL_{max}) of the PMCC/Zn and PCDPS/Zn NPs are -81.93 and -56.34 dB at 25.65 and 25.43 GHz and thickness of 1 mm respectively. These fabricated absorbing materials have efficient absorption bandwidth (EAB) of 5.53 and 5.66 for PMCC/Zn and PCDPS/Zn NPs in the same thickness, respectively.

1. Introduction

Today, due to the increase in population and the industrialization of human life, the use of advanced electronic devices has also expanded [1,2]. Electronic devices include all types of 5-generation internet, satellites, military equipment, *etc.* These electronic devices, along with their many advantages, have a major disadvantage: they emit harmful electromagnetic waves into the environment. Electromagnetic waves are known to be the fourth most common pollutant in the world [3–5]. One of the most important ways to remove these types of pollutants is to use various types of electromagnetic wave absorbers. Various materials are used for this purpose, such as carbon compounds, natural polymers, metal nanoparticles, and so on [6–9]. One of the effective compounds for making electromagnetic wave absorbers is the conjugated carbon-based materials. Conductive carbon materials can be derived from natural compounds such as natural polymers. Cellulose is known as a type of natural polymer (polysaccharide) having rich source of carbon compounds obtaining naturally in nature, specially, peanut shells supply a rich source of cellulose [10–13].

In the present study, the PMCC/Zn and PCDPS/Zn NPs were fabricated. The synthesized PMCC/Zn and PCDPS/Zn NPs are in the form of cryogel. The prepared PMCC/Zn and PCDPS/Zn NPs NPs applied as an efficient and high-performance microwave absorbing/shielding material. For this aim, different amounts of the PMCC/Zn and PCDPS/Zn NPs were loaded in the PVC matrix.

2. Method

2.1 Materials and devices

All chemical materials were bought from Merck and Aldrich Co. and used without extra purification. Peanut shells were obtained from agricultural wastes in local areas in the North of Iran. The FE-SEM and XRD analyses were performed using Tescan Mira3 and D8 Advance X-ray diffractometer from Bruker devices, respectively. The microwave features of samples were identified by a vector network analyzer of Agilent technology (E8364A).

2.2 Preparation of PMCC/Zn and PCDPS/Zn NPs

For fabrication of PMCC/Zn, the MC was dissolved in NaOH and urea at -6 ºC. Then, the obtained mixture was freeze-dried at -50 ºC at a pressure of 0.1 atm for 24 h. In the next step, 1.7 g of MC cryogel was dispersed in 15 mL of DW, next, 0.0985 g of $Zn(OAc)_2.2H_2O$ was added at -8 ºC (sample B). In another beaker, 1.7 g and 1.1 g of NaOH and urea were dissolved in 10 mL DW, respectively. The solution was added to sample B and sonicated for 2 min (sample C). Finally, sample C was frozen for 24 hours following freeze-drying. The prepared MC/Zn cryogel was washed with DW and EtOH until its pH reached to 7, and then the achieved sample was pyrolyzed at a temperature of 900 ºC. For PCDPS/Zn NPs, all of the mentioned steps were repeated just the cellulose was extracted from peanut shells (PSs) (Figure 1).

Figure 1. Schematic pathway for synthesis of the PCDPS/Zn NPs.

2.3 Preparation of the microwave absorbent

The PVC was applied as a practical microwave-absorbing medium to fabricate microwave-absorbing films. Initially, PVC was dissolved in tetrahydrofuran (THF), then the fillers were separately loaded in the solution with 10 wt.% (sample/sample + polymer) using an overhead stirrer. Eventually, the microwave-absorbing films were prepared at 60º C in a k-band mold.

3. Results and Discussion

3.1 Characterization of the PMCC/Zn and PCDPS/Zn NPs

For characterization of the prepared PMCC/Zn and PCDPS/Zn NPs, the XRD and FE-SEM analyses were used. According to the XRD patterns, the synthesized materials have related peaks about Zn NPs at 2θ= 36.29, 38.99, 43.23, 54.33, 70.05º (JCPDS#: 00-004-0831) [14–16] as well as graphite. The peaks at 2θ= 26.3 are associated with the (002) Bragg diffraction of graphitic-like structure. Another peak located at 2θ= 43.2 is contributed to the (101) crystal plane of the ordered carbon structure (JCPDS#: 00-041-1487) [17–20]. According to FE-SEM analysis of the PMCC/Zn, PMCC has a plate structure that Zn NPs with semi-rod-like structure were loaded on the surface of it. In addition, the PCDPS/Zn NPs have a structure like PMCC/Zn with the difference that Zn NPs in the PMCC/Zn are more rod-like than PMCC/Zn NPs. In contrast, the cellulose in the PMCC/Zn is more smother than PCDPS/Zn NPs.

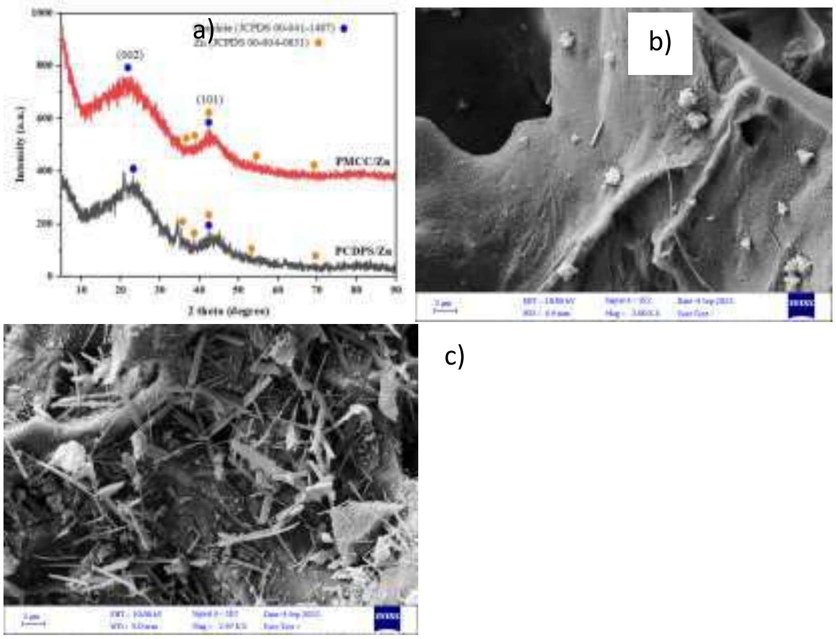

Figure 2. a) XRD patterns and FE-SEM images of the b) PMCC/Zn and c) PCDPS/Zn NPs.

3.2 Microwave absorbing performance

Microwave absorption and efficient bandwidth of the fabricated PMCC/Zn and PCDPS/Zn NPs are displayed in Figure 3. Microwave absorption of the PMCC/Zn and PCDPS/Zn NPs samples was evaluated by transmission line theory [21,22]. According to the results, the maximum reflection loss (RL_{max}) of the PMCC/Zn NPs was -81.93 dB at 25.43 GHz in thickness of 1 mm meanwhile the RL_{max} was -56.34 dB at 25.65 GHz in the same thickness for PCDPS/Zn NPs. The shielding performance is governed by absorption (SE_A)/reflection (SE_R)/total (SE_A+SE_R=SE_T) (Figure 3c). The essential mechanisms bringing microwave absorption of the samples are the interfacial/defect/dipole polarization and conductive loss due to the conjugated backbone. The multiple reflections and canceled waves are the other reasons behind the achieved RLs. The variety in electronegative elements and their dispersion in the polymeric backbone and the morphology of the pyrolyzed structures regulated the microwave absorbing capability of the samples.

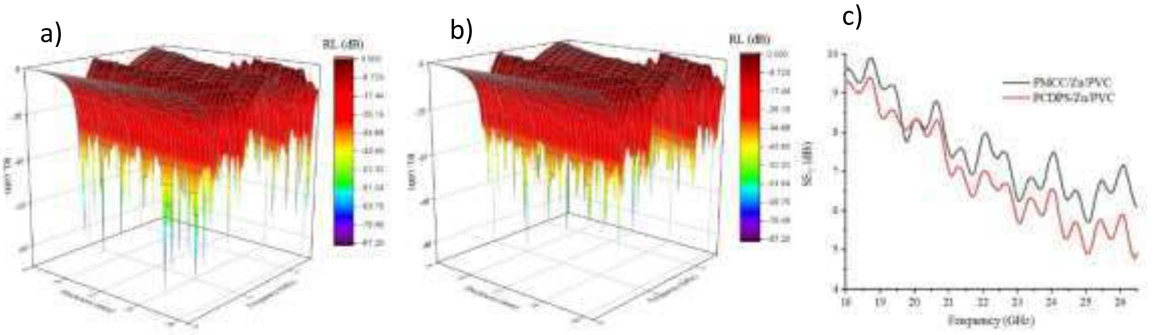

Figure 3. The 3D RL_{max} plots of the a) PMCC/Zn, b) PCDPS/Zn NPs, and c) shielding performance of the PMCC/Zn and PCDPS/Zn NPs.

4. Conclusion

In this experimental research, the PMCC/Zn and PCDPS/Zn NPs which have cryogel structure were fabricated. For this aim the peanut shell applied as source of the cellulose for one of the prepared composite. The synthesized cryogels were characterized using XRD and FE-SEM analyses. The PMCC/Zn and PCDPS/Zn NPs were applied as efficient microwave absorbents in k band using PVC as an absorbing matrix. The achieved results clarify that the morphology of the conjugated carbonaceous structure as well as they elemental composition play the pivotal role in tuning microwave absorbing performance.

References

[1] D. Zhang, T. Liu, J. Cheng, Q. Cao, G. Zheng, S. Liang, H. Wang, M.-S. Cao, Lightweight and high-performance microwave absorber based on 2D WS 2–RGO heterostructures, Nano-Micro Lett. 11 (2019) 1–15.

[2] R. Peymanfar, F. Azadi, Preparation and identification of bare and capped $CuFe_2O_4$ nanoparticles using organic template and investigation of the size, magnetism, and polarization on their microwave characteristics, Nano-Structures & Nano-Objects. 17 (2019) 112–122.

[3] M. Zhang, Q. Zheng, M.-S. Cao, C. Han, Regulating long-range travelling electrons for simultaneous electromagnetic absorption and interference shielding of Co@ C nanofibers, Carbon N. Y. 214 (2023) 118338.

[4] P. Wu, X. Kong, Y. Feng, W. Ding, Z. Sheng, Q. Liu, G. Ji, Phase Engineering on Amorphous/Crystalline γ-Fe_2O_3 Nanosheets for Boosting Dielectric Loss and High-Performance

Microwave Absorption, Adv. Funct. Mater. 34 (2024) 2311983.

[5] K. Chen, H. Wang, Y. Shi, M. Liu, Y. Feng, L. Fu, P. Song, Realizing balanced flame retardancy and electromagnetic interference shielding in hierarchical elastomer nanocomposites, J. Colloid Interface Sci. 653 (2024) 634–642.

[6] X. Meng, W. Lei, W. Yang, Y. Liu, Y. Yu, Fe_3O_4 nanoparticles coated with ultra-thin carbon layer for polarization-controlled microwave absorption performance, J. Colloid Interface Sci. 600 (2021) 382–389.

[7] M. Mariam, S. Noureen, S. Ali, U. Khalid, Unravelling the role of microwave absorber in color stripping of a dyed natural polymeric material with microwave assisted method, Cellulose. 31 (2024) 3855–3870.

[8] D. Gunwant, A. Vedrtnam, Microwave absorbing properties of carbon fiber based materials: A review and prospective, J. Alloys Compd. 881 (2021) 160572.

[9] E. Selseleh-Zakerin, A. Mirkhan, M. Shafiee, M. Alihoseini, M. Khani, B. Shokri, S.H. Tavassoli, R. Peymanfar, Plasma Engineering toward Improving the Microwave-Absorbing/Shielding Feature of a Biomass-Derived Material, Langmuir. (2024).

[10] P. Ganguly, S. Sengupta, P. Das, A. Bhowal, Synthesis of cellulose from peanut shell waste and its use in bioethanol production, Bioresour. Util. Bioprocess. (2020) 81–91.

[11] F. Zhang, N. Li, J.-F. Shi, L. Xu, L.-C. Jia, Y.-Y. Wang, D.-X. Yan, Recent progress on carbon-based microwave absorption materials for multifunctional applications: A review, Compos. Part B Eng. (2024) 111646.

[12] B. Wang, Q. Wu, Y. Fu, T. Liu, A review on carbon/magnetic metal composites for microwave absorption, J. Mater. Sci. Technol. 86 (2021) 91–109.

[13] S. Song, H. Li, P. Liu, X. Peng, Applications of cellulose-based composites and their derivatives for microwave absorption and electromagnetic shielding, Carbohydr. Polym. 287 (2022) 119347.

[14] H.J. Jung, R. Koutavarapu, S. Lee, J.H. Kim, H.C. Choi, M.Y. Choi, Enhanced photocatalytic degradation of lindane using metal–semiconductor Zn@ ZnO and ZnO/Ag nanostructures, J. Environ. Sci. 74 (2018) 107–115.

[15] K.I. Hassoon, S.H. Sabeeh, M.A. Khalaf, ZnO nano particles (NPs) properties prepared by liquid phase laser ablation (LPLA), Al-Nahrain J. Sci. 20 (2017) 70–77.

[16] N.T. Mai, T.T. Thuy, D.M. Mott, S. Maenosono, Chemical synthesis of blue-emitting metallic zinc nano-hexagons, CrystEngComm. 15 (2013) 6606–6610.

[17] A. Wotton, T. Yeung, S. Jennepalli, Z.L. Teh, R. Pickford, S. Huang, G. Conibeer, J.A. Stride, R.J. Patterson, Simultaneous Fe3O4 nanoparticle formation and catalyst-driven hydrothermal cellulose degradation, ACS Omega. 6 (2021) 10790–10800.

[18] J. Wang, Y. Wang, Z. Ma, L. Yan, Dissolution of highly molecular weight cellulose isolated from wheat straw in deep eutectic solvent of Choline/L-Lysine hydrochloride, Green Energy Environ. 5 (2020) 232–239.

[19] M.L. Nieva, M.A. Volpe, E.L. Moyano, Catalytic and catalytic free process for cellulose conversion: fast pyrolysis and microwave induced pyrolysis studies, Cellulose. 22 (2015) 215–228.

[20] L. Liu, S. Hu, K. Gao, Cellulose nanofiber based flexible N-doped carbon mesh for energy storage electrode with super folding endurance, Mater. Today Energy. 17 (2020) 100441.

[21] H. Sun, Y. Zhang, Y. Wu, Y. Zhao, M. Zhou, L. Liu, S. Tang, G. Ji, Broadband absorption of macro pyramid structure based flame retardant absorbers, J. Mater. Sci. Technol. 128 (2022) 228–238.

[22] M. Liu, B. Zhao, K. Pei, Y. Qian, C. Yang, Y. Liu, H. Cao, J. Zhang, R. Che, An Ion-Engineering Strategy to Design Hollow FeCo/$CoFe_2O_4$ Microspheres for High-Performance Microwave Absorption, Small. 19 (2023) 2300363.

The 30th Iranian Seminar of Organic Chemistry
February 7-9, 2025, Iran University of Science and Technology, Tehran, Iran

Magnetic Schiff Base Catalyst Incorporating Taxifolin and Ionic Liquid for the Efficient Conversion of Benzaldehyde Derivatives to Benzonitriles

Reza Sandaroos,*[a] Fahime Kazemi [a], Sanaz Naderia [a], Danial Mohammadia [a]
[a]*Department of Chemistry, Faculty of Sciences, University of Birjand, Birjand, Iran*

Abstract

A novel magnetic Schiff base-ionic liquid-Co(II) catalyst anchored on Fe_3O_4/SiO_2/3-CPTES nanoparticles was synthesized and evaluated for the selective oxidation of benzyl alcohol derivatives to nitriles. The catalyst integrates taxifolin, an ionic liquid, and cobalt (II) chloride to create a multifunctional and recyclable system. The structural and functional properties of the catalyst were confirmed using IR, XRD, VSM, TEM, FE-SEM, and EDX analyses. Reaction optimization revealed that the use of hydrogen peroxide as an oxidant under solvent-free conditions at 60°C provided the best results, with a nitrile yield of up to 85%. The catalytic system demonstrated excellent efficiency, particularly with electron-donating substituents such as OH, OMe, and Me, which enhanced reaction rates and yields. In contrast, electron-withdrawing groups like NO_2 and halogens reduced efficiency. Furthermore, the catalyst exhibited high reusability, maintaining performance even after six cycles, as confirmed by FT-IR analysis. This work presents a sustainable and efficient catalytic approach for nitrile synthesis, offering significant advantages in terms of green chemistry and operational simplicity. The catalyst's magnetic properties enable easy separation and recovery, making it a promising candidate for industrial applications.

Keywords: Schiff base-Co(II) complex, Fe_3O_4 nanoparticles, Ionic liquid, Benzaldehydes, Benzonitriles

Introduction

The selective oxidation of alcohols to aldehydes and ketones plays a crucial role in organic synthesis with applications in pharmaceuticals and industrial intermediates. Recent advancements in photocatalysis have utilized visible light as a sustainable energy source, but challenges like poor light absorption and limited catalyst recovery remain [1]. Magnetic Fe_3O_4 nanoparticles provide a promising solution due to their ease of separation and high surface area. Coating Fe_3O_4 with silica (SiO_2) enhances stability and creates a functional surface for modification. Functionalization with 3-CPTES facilitates the anchoring of catalytic species such as metal complexes or ionic liquids, enabling multifunctional catalyst design [2]. Incorporating ionic liquids (ILs) improves performance by preventing catalyst aggregation, stabilizing electron-hole pairs, and enhancing charge transfer [3]. Catalytic activity is further boosted by a Schiff base ligand derived from taxifolin, which strongly coordinates with cobalt ions, promoting charge transfer and redox activity. DFT calculations reveal that the ligand's reduced energy gap enhances visible light absorption and electron excitation [4]. Combining the Schiff base-Co(II) complex with Fe_3O_4/SiO_2/3-CPTES nanoparticles and ionic liquids creates a synergistic system. The Fe_3O_4 core ensures magnetic recovery, the silica shell adds chemical stability, the ionic liquid improves dispersion and charge transfer, and the Schiff base ligand enhances light absorption and catalytic efficiency [5]. This photocatalyst provides a stable, efficient, and reusable solution for visible-light-driven alcohol oxidation, advancing green and energy-efficient chemistry [6].

Experimental

Materials and instrumentation

The chemicals and solvents used were purchased from Merck. Fe_3O_4 magnetic nanoparticles, silica-coated iron oxide nanoparticles ($Fe_3O_4@SiO_2$ and functionalized iron oxide/silica nanoparticles with 3-chloropropyltriethoxysilane (Fe_3O_4/SiO_2/3-CPTES) were synthesized according to the literatures, respectively [7, 8, 9]. An Electrothermal 9100 device was used to measure the melting temperature. FT-IR spectra were recorded using a Therma Nicolet 370 instrument. NMR spectra were measured with a Bruker DPX-500 and DPX-250 instrument and

TMS as an internal standard. Thermogravimetric analysis (TGA) was performed under a nitrogen atmosphere using a TGA Q50 thermogravimetric analyzer. Transmission electron microscopy (TEM) images were acquired with a TOPCON-002B electron microscope. The morphology of the catalyst was examined using a MIRA3 TESCAN scanning electron microscope (SEM).

Synthesis of Imidazole Ionic Liquid

To a solution of N-methylimidazole, 164 mg (2 mmol), in 10 mL of ethanol, 3-bromopropylamine hydrobromide, 437 mg (2 mmol), was added, and the mixture was refluxed for 24 hours. After completion of the reaction and removal of the solvent, a milky mixture was observed. To this mixture, 1 mL of water was added, and the pH was adjusted to 8 using 1 N potassium hydroxide solution. The product was extracted using chloroform (5 × 20 mL). After removing the solvent, the residue was washed three times with a 1:1 mixture of ethanol and tetrahydrofuran to remove unreacted organic materials. Finally, the resulting precipitate was filtered (Scheme 1).

^{1}H-NMR of ionic liquid: 2.10 (m, 2H), 3.24 (t, 2H), 4.45(t, 2H), 4.58 (s, 3H), 5.78 (bs,2H), 7.32 (d,1H), 7.55(d, 1H), 9.85(s, 1H).

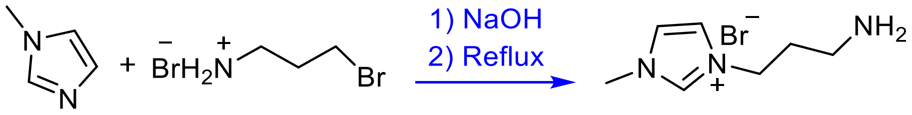

Scheme 1. Synthesis of imidazole ionic liquid

Synthesis of Schiff Base- ionic liquid @ Taxifolin (ligand)

The ionic liquid, 0.330 g (1.50 mmol), obtained in the previous step was dissolved in a mixture of ethanol (20 mL) and chloroform (20 mL), followed by the addition of one drop of formic acid. Subsequently, taxifolin, 0.450 g (1.50 mmol), was added to the reaction mixture, which was refluxed for 20 hours. The resulting yellow precipitate was collected after solvent removal, crystallized in ethanol, and obtained as the final product (yield: 69%) (Scheme 2).

^{1}H-NMR of taxifolin-ionic liquid schiff base ligand: 2.10 (m, 2H), 3.24 (t, 2H), 4.45 (t, 2H), 4.58 (s, 3H), 5.78 (bs, 2H), 9.0-12.0 (bs, 2H), 6.80-7.60 (m, 4H), 7.32 (d, 1H), 7.55 (d, 1H), 8.25 (s, 1H), 9.85 (s, 1H).

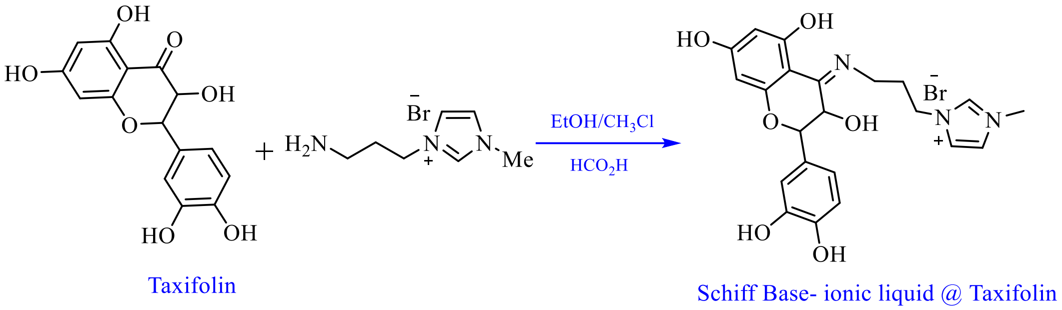

Scheme 2. Synthesis of taxifolin-ionic liquid schiff base ligand

Synthesis of Schiff Base- ionic liquid @ Taxifolin -Co (II)

A solution of the previously synthesized Schiff base ligand, 0.984 g (2 mmol), in 15 mL of THF was prepared under an inert argon atmosphere. To this solution, cobalt (II) chloride, 0.129 g (1 mmol), was added, and the reaction mixture was stirred at room temperature for 72 hours. The resulting blue precipitate was filtered and washed sequentially with ethanol and diethyl ether to afford the desired product with a yield of 85% (Scheme 3).

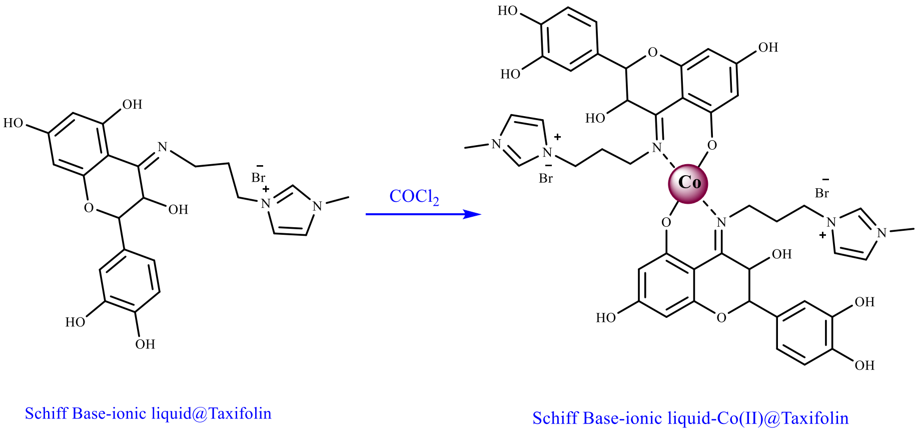

Scheme 3. Synthesis of schiff base- ionic liquid @ taxifolin -Co (II)

Synthesis of Schiff base of taxifolin/ionic liquid-Co(II)@ Fe_3O_4 SiO_2/3-CPTES

The previously synthesized Fe_3O_4/SiO_2/3-CPTES nanoparticles (1 g) were dispersed in dry toluene (40 mL) and sonicated for 30 minutes. Then, 34 mg of Schiff base of taxifolin/ionic liquid-Co(II) complex (0.5 mmol) was added to the mixture. 50 mg of Triethylamine (0.5 mmol) was added dropwise under continuous stirring, and the reaction mixture was refluxed at 105°C for 24 hours.

After completion of the reaction, the resulting product was separated using an external magnet, washed sequentially with distilled water and ethanol to remove unreacted materials, and dried in a vacuum oven at 80°C for 12 hours. (Scheme 6).

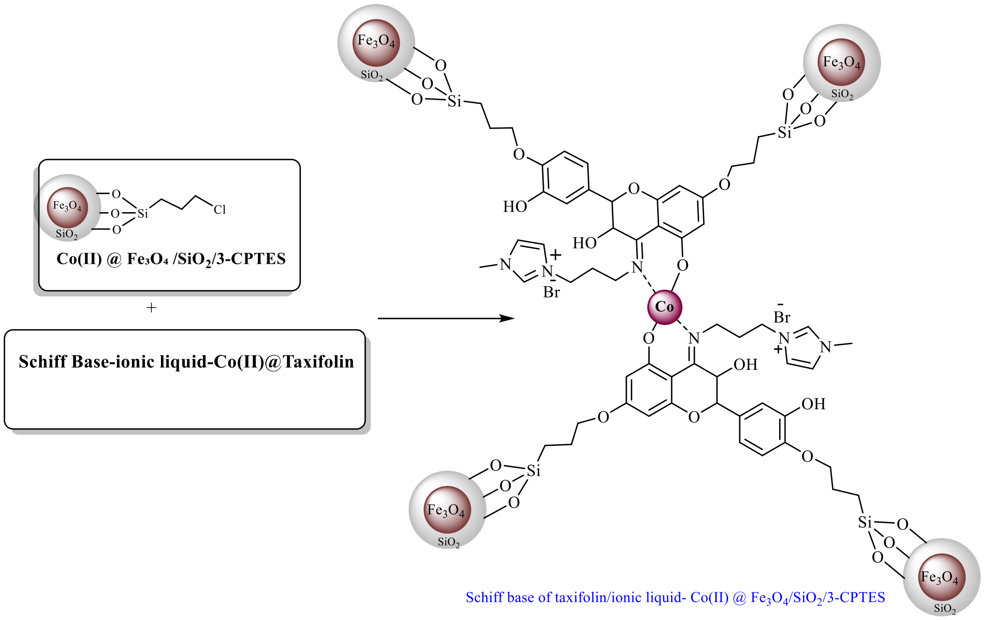

Scheme 4. Schiff base of taxifolin/ionic liquid- Co(II) @ Fe_3O_4/SiO_2/3-CPTES

Results and discussion

The IR spectra confirm the structural features of the synthesized materials (scheme 5). Absorption bands at 1570–1080 cm^{-1} (imidazole ring vibrations) and 3200–2900 cm^{-1} (C-H stretching) confirm the imidazole ring. The disappearance of NH_3^+ vibrations and the emergence of a 1625 cm^{-1} imine stretching band confirm ligand formation, with a 20 cm^{-1} shift in the catalyst indicating cobalt coordination. For Fe_3O_4 nanoparticles, Fe-O and hydroxyl vibrations are observed at 590 cm^{-1} and 3500 cm^{-1}, with C-O and Si-O bonds appearing at 1000–1250 cm^{-1}. XRD analysis shows crystalline iron oxide peaks and a broad 20°–30° amorphous region from catalyst deposition (scheme 6). VSM measurements reveal reduced magnetization upon cobalt complex incorporation: Ms values are 64.8, 40.3, and 34.0 emu/g for Fe_3O_4, Fe_3O_4/3-CPTES, and the catalyst, respectively (s. Despite reduced Ms, the catalyst maintains sufficient magnetic strength for efficient separation with an external magnet (scheme 7).

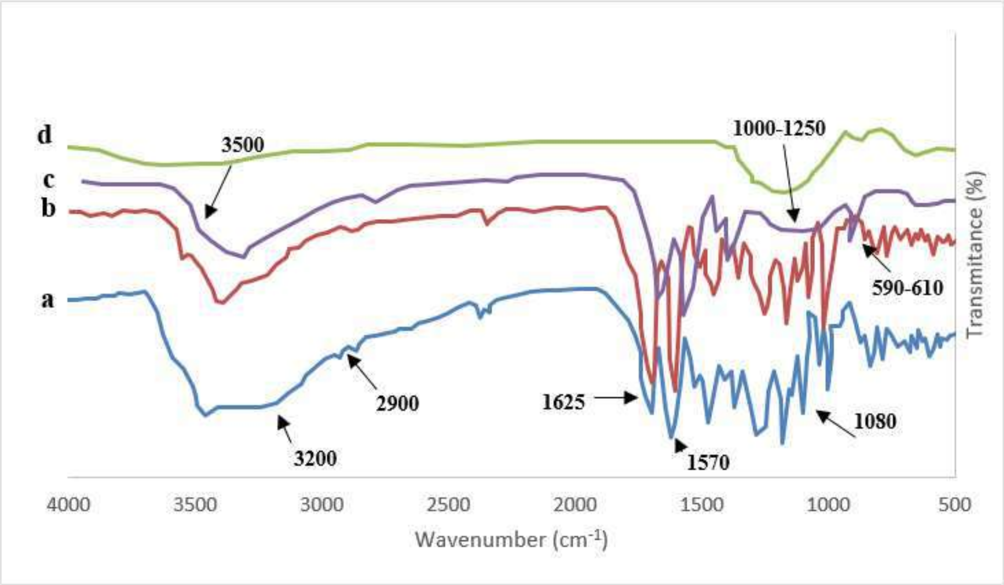

Scheme 5: The IR spectra of (a) the Ionic Liquid, (b) the Schiff base-ionic liquid@Taxifolin ligand, (c) the Schiff base-ionic liquid-CoCl(II)@Taxifolin@Fe_3O_4/3-CPTES catalyst, and (d) Fe_3O_4.

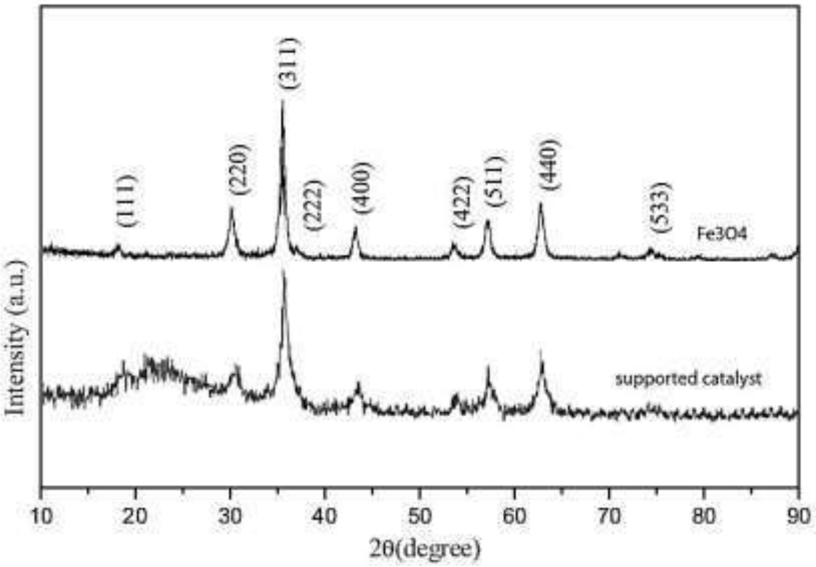

Scheme 5: The XRD spectrum of (a) the catalyst and (b) magnetic nanoparticles Fe_3O_4.

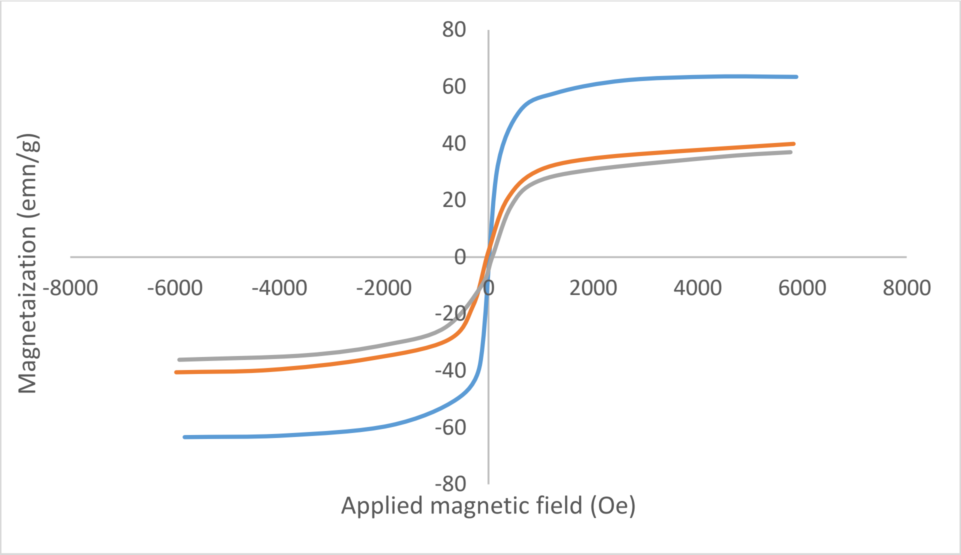

Scheme 6: The VSM spectrum of (blue) magnetic nanoparticles Fe_3O_4, (red) Fe_3O_4/3-CPTES, and (light blue) the Schiff base-ionic liquid-CoCl(II)@Taxifolin@Fe_3O_4/3-CPTES catalyst.

ICP analysis determined cobalt concentrations of 0.11 mol% for the homogeneous catalyst and 0.33 mol% for the heterogeneous catalyst. CHN analysis indicated the homogeneous catalyst contains 49.4% carbon, 4.33% hydrogen, and 7.86% nitrogen by weight, with a nitrogen-to-cobalt molar ratio of 4:1, confirming two ligand molecules in its structure. TGA of the heterogeneous catalyst showed weight loss stages of 3% at 100°C (water removal), 6% at 400°C (ligand decomposition), and 50% at 600°C (support degradation). Fe_3O_4 nanoparticles have a particle size of 12 nm, while the heterogeneous catalyst is approximately 25 nm, as confirmed by the Scherrer equation and TEM analysis (scheme 7).

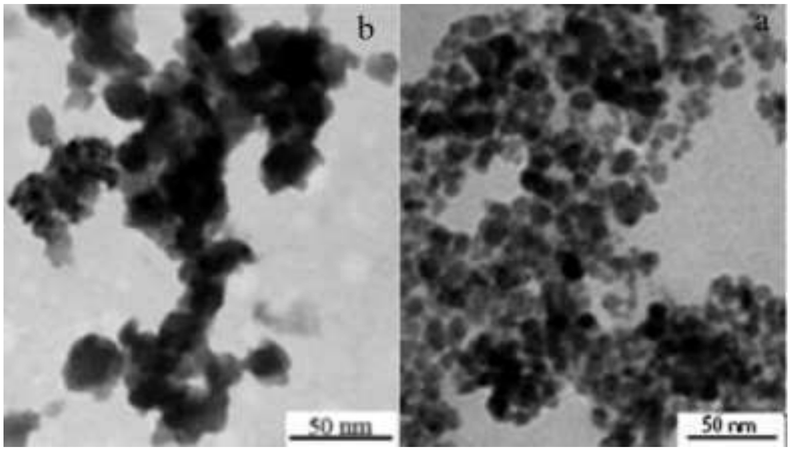

Scheme 7: The TEM image of (a) magnetic nanoparticles Fe_3O_4 and (b) the heterogeneous catalyst.

FE-SEM revealed uniform surface morphology of the heterogeneous catalyst (scheme 8a). EDX confirmed cobalt, nitrogen, oxygen, carbon, and iron in the catalyst (scheme 8b).

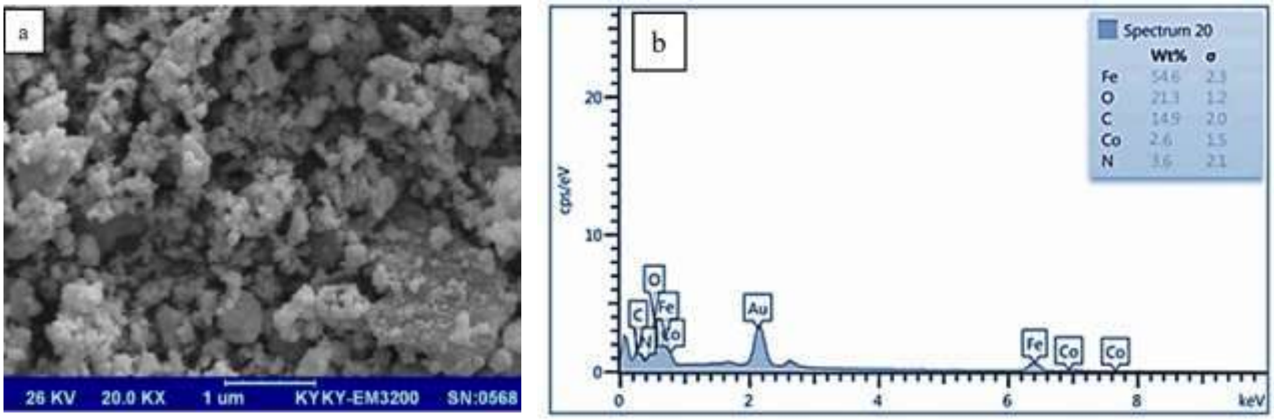

Scheme 8: The FE-SEM image (a) and EDX analysis (b) of the heterogeneous catalyst.

Results and Discussion

The heterogeneous catalyst was tested for benzonitrile synthesis. Without the catalyst, no reaction occurred at 50°C with H_2O_2. The cobalt complex showed the best results, as seen in Table 1.

To optimize the reaction temperature, the complex was tested at 40–80°C. Raising the temperature to 60°C improved nitrile yield with minimal effect on selectivity. However, higher temperatures reduced both the product yield and reaction selectivity (Table 2).

Table (1): Comparison of the Efficiency of Catalyst Components in the Nitrile Synthesis Reaction [a]

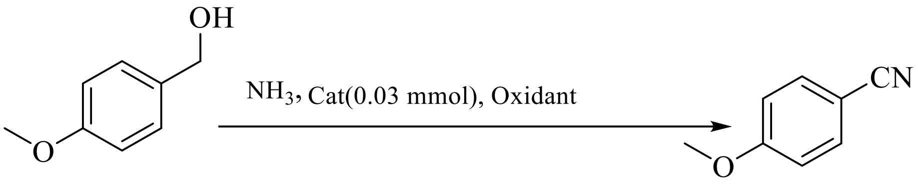

Catalyst	Nitrile Product Yield (%)	Benzoic Acid Yield (%)	Overall Yield (%)
Schiff base – ionic liquid@Taxifolin	2	2	2
Schiff base-ionic liquid-$CoCl_2$(II)@Taxifolin	6	9	15

Schiff base-ionic liquid-CoCl(II)@Taxifolin@Fe_3O_4/3-CPTES	85	10	95

[a] Reaction conditions: 4-Methoxybenzyl alcohol (0.125 mmol), Ammonia 25% (3 mmol), catalyst (1 mmol, heterogeneous catalyst: 1.03 g containing 0.03 mmol cobalt), Hydrogen peroxide (0.3 mmol), Solvent-free, 60°C, 1 hour.

Table (2): Effect of Temperature on the Nitrile Synthesis Reaction [a]

Temperature (°C)	Nitrile Yield (%)	Benzoic Acid Yield (%)	Overall Yield (%)
Ambient	47	10	57
40	54	15	69
50	67	20	87
60	80	15	95
70	75	20	95
80	70	25	95

[a] Reaction Conditions: 4-Methoxybenzyl alcohol (0.125 mmol), ammonia 25% (3 mmol), heterogeneous catalyst (1.03 g containing 0.03 mmol cobalt), oxidant: hydrogen peroxide (0.3 mmol, solvent-free, time: 1 hour.

To determine the optimal amount of catalyst, various quantities were tested for the nitrile synthesis reaction. The results indicate that using less than 0.03 g of the cobalt complex reduces the overall reaction efficiency, while amounts greater than 0.03 g slightly decrease the yield of the main product and increase the side product formation (Table 3).

Table (3): Effect of Catalyst Amount on Nitrile Synthesis Reaction [a]

Row	Catalyst Amount (g)	Nitrile Product Yield (%)	Benzoic Acid Yield (%)	Overall Yield (%)
1	0.25	70	10	80
2	0.3	85	15	95
3	0.35	85	20	95

[a] Reaction conditions: 4-Methoxybenzyl alcohol (0.125 mmol), Ammonia 25% (3 mmol), Hydrogen peroxide (0.3 mmol), Temperature 60°C, Solvent-free, 1 hour.

The reaction was further examined in the presence of various solvents, including water, ethanol, methanol, ethyl acetate, n-hexane, toluene, acetonitrile, and chloroform. The best efficiency was observed under solvent-free conditions, yielding 80% benzonitrile and 15% benzoic acid.

The effect of various oxidants on the reaction was investigated (Table 4). Using Oxone as a strong oxidant resulted in a 15% yield, likely due to its low solubility under the reaction conditions. Mild oxidants like oxygen led to low reaction yields. However, the use of hydrogen peroxide and TBHP as oxidants yielded the best results. Among these, hydrogen peroxide was chosen as the optimal oxidant for further research due to its lower cost and environmental benefits. Furthermore, hydrogen peroxide oxidant quantities ranging from 0.2 to 0.4 mmol were evaluated, with 0.3 mmol identified as the optimal amount (yielding 85% benzonitrile and 10% benzoic acid). A decrease in the oxidant amount had a negligible impact on the overall reaction efficiency, whereas an increase led to a reduction in overall efficiency and an increase in side product formation.

Table (4): Effect of Oxidants on Nitrile Synthesis Reaction [a]

Row	Oxidant	Nitrile Product Yield (%)	Benzoic Acid Yield (%)	Overall Yield (%)
1	TBHP	70	10	80
2	H_2O_2	80	15	95
3	Oxone	15	10	25
4	O_2	5	5	10
5	Free-oxidant	5	5	10

[a] Reaction conditions: 4-Methoxybenzyl alcohol (0.125 mmol), Ammonia 25% (3 mmol), Heterogeneous catalyst (1.03 g containing 0.03 mmol cobalt), Solvent-free, Temperature 60°C, 1 hour. [b] Tert-butyl hydroperoxide (TBHP), [c] Hydrogen peroxide (H_2O_2), [d] Oxygen (1 bar).

After optimizing the reaction conditions, the efficiency of this catalyst in synthesizing nitrile derivatives was examined (Table 5). The results indicate that electron-donating substituents such as OH, OMe, and Me increased the yield or reduced the reaction time. In contrast, electron-withdrawing substituents such as NO_2, Cl, and Br decreased the yield or extended the reaction time. Moreover, for a fixed substituent, ortho derivatives (due to steric hindrance) and meta derivatives (due to electronic effects) showed lower yields or longer reaction times. Overall, it appears that the oxidation step is the rate-determining step, and the presence of donating groups accelerates this step.

The reusability of the Schiff base-ionic liquid-CoCl(II)@Taxifolin@Fe_3O_4/3-CPTES catalyst in nitrile synthesis was evaluated. After the reaction, the catalyst was separated from the mixture using an external magnet, followed by washing four times with 1 mL ethyl acetate. It was then dried in a vacuum oven and reused for subsequent reactions. The results showed that even after six cycles of reuse, the catalyst's activity did not experience a significant decline. Additionally, FT-IR analysis of the catalyst after four cycles revealed no significant changes compared to its initial spectrum, confirming its structural stability.

Table (5): Efficiency of the Catalyst in Nitrile Derivatives Synthesis [a]

Row	Substituent	Reaction Time (h)	Nitrile Yield (%)	Overall Yield (%)
1	4-Me	2	85	90
2	4-Cl	4	75	80
3	2-OH	5	70	75
4	4-OH	2	90	95
5	benzaldehyde	6	60	65
6	4-OMe	2	88	93
7	2-OMe	5	70	75

[a] Reaction conditions: 4-Methoxybenzyl alcohol (0.125 mmol), Ammonia 25% (3 mmol), Heterogeneous catalyst (1.03 g containing 0.03 mmol cobalt), Hydrogen peroxide (0.3 mmol), Temperature 60°C, Solvent-free, 1 hour.

References:

1. Mastalir, A., et al., Preparation of monodispersed Pt nanoparticles in MCM-41, catalytic applications. Catalysis Communications, 2008. 9(5): p. 762-768.
2. Li, Y. and W. Shen, Morphology-dependent nanocatalysts: Rod-shaped oxides. Chemical Society Reviews, 2014. 43(5): p. 1543-1574.
3. Sulikowski, B., et al., Oxidative dehydrogenation of isobutane on MCM-41 mesoporous molecular sieves. Applied Catalysis A: General, 2002. 232(1-2): p. 189-202.

4. Nugent, B.M., R.A. Yoder, and J.N. Johnston, Chiral proton catalysis: a catalytic enantioselective direct aza-Henry reaction. Journal of the American Chemical Society, 2004. 126(11): p. 3418-3419.
5. Kalnin'sh, K., Electron and proton transfer in acid-base catalysis. Russian Journal of Applied Chemistry, 2007. 80: p. 934-940.
6. Mulla, S.A., et al., Activity of homogeneous transition metal catalysts for oxidative carbonylation of aniline to N, N′ diphenyl urea. Journal of Molecular Catalysis A: Chemical, 1997. 122(2-3): p. 103-109.
7. Elbashir, N.O., et al., Impact of cobalt-based catalyst characteristics on the performance of conventional gas-phase and supercritical-phase Fischer–Tropsch synthesis. Applied Catalysis A: General, 2005. 285(1-2): p. 169-180.
8. Gondal, M., et al., Production of hydrogen and oxygen by water splitting using laser induced photo-catalysis over Fe2O3. Applied Catalysis A: General, 2004. 268(1-2): p. 159-167.
9. Wahlen, J., et al., Disproportionation of hydrogen peroxide into singlet oxygen catalyzed by lanthanum-exchanged zeolites. Journal of Catalysis, 2005. 233(2): p. 422-433.

The 30th Iranian Seminar of Organic Chemistry
February 7-9, 2025, Iran University of Science and Technology, Tehran, Iran

Efficient Oxidation of Sulfides Using Bio-Based Cu (II) Catalyst

Reza Sandaroos,*[a] Sanaz Naderia [a]
[a]*Department of Chemistry, Faculty of Sciences, University of Birjand, Birjand, Iran*

Abstract

In this study, the efficiency of a novel catalyst system was evaluated for the oxidation of various sulfides, with a focus on the role of natural compounds, taxifolin and berberine, in enhancing catalytic performance. The solubility of these compounds in aqueous media facilitated their effective interaction with reactants, eliminating the need for toxic organic solvents and aligning with green chemistry principles. The reaction conditions were optimized by studying the effects of solvent type, oxidant amount, reaction time, and temperature. The results demonstrated that water was the most effective solvent, providing the highest yields and selectivity due to the superior solubility of the catalyst in polar protic media. Furthermore, the catalyst exhibited remarkable efficiency and selectivity across a wide range of sulfide substrates, converting them to sulfoxids under mild conditions. This work highlights the potential of integrating bio-based catalysts with environmentally friendly systems, offering a sustainable and efficient approach to organic synthesis.

Keywords: Taxifolin, Berberine, Sulfide oxidation, Aqueous solvent, Cu (II) catalyst

Introduction

The field of organic synthesis has been significantly transformed with the development of efficient catalytic systems and environmentally benign reaction conditions. The search for sustainable and efficient methods has led researchers to explore natural compounds with catalytic potential. Among these, taxifolin and berberine have garnered significant attention due to their unique structural properties, availability, and versatile applications. Taxifolin, a natural flavonoid, is renowned for its remarkable antioxidant properties, which also translate into its potential as an additive in catalytic processes to enhance reaction efficiency and selectivity [1, 2]. Similarly, berberine, an isoquinoline alkaloid, is widely studied for its biological activities and catalytic influence, making it a promising candidate for green chemistry applications [3].

One of the critical aspects of sustainable synthesis is the solubility of catalysts and reactants in environmentally friendly solvents. In this regard, the solubility of taxifolin and berberine in aqueous media provides a distinct advantage. Water, as an abundant, non-toxic, and green solvent, aligns perfectly with the principles of green chemistry and has been demonstrated to improve the reactivity and efficiency of many reactions [4, 5]. The ability of taxifolin and berberine to dissolve in water not only facilitates their effective interaction with reactants but also eliminates the need for hazardous organic solvents, thereby reducing the environmental footprint of chemical processes [6].

In addition to their solubility, taxifolin and berberine have been shown to enhance the catalytic performance in several organic transformations, such as oxidation and coupling reactions. Their inherent structural features, including multiple hydroxyl and aromatic groups, contribute to their ability to stabilize reaction intermediates and lower activation barriers [7]. Moreover, their compatibility with aqueous systems allows for mild reaction conditions, which are crucial for the synthesis of sensitive compounds and industrial-scale applications [8].

The exploration of these bio-based compounds as contributors to catalytic efficiency in water-based systems paves the way for greener and more sustainable organic synthesis. This study highlights the role of taxifolin and berberine in improving catalyst performance, focusing on their exceptional solubility and compatibility with aqueous media. By leveraging these properties, new opportunities for eco-friendly and efficient catalytic systems can be realized, addressing both environmental and industrial demands.

Experimental

Materials and instrumentation

The chemicals and solvents used were purchased from Merck. An Electrothermal 9100 device was used to measure the melting temperature. FT-IR spectra were recorded using a Therma Nicolet 370 instrument. ^{1}HNMR spectra were measured with a Bruker DPX-500 and DPX-250 instrument and TMS as an internal standard.

Synthesis of Berberine@propylamine

To a solution of 3.06 mmol (1.23 g) berberine derivative in 8 mL ethanol, 30 mmol of NaH was added while maintaining the reaction temperature at approximately 10°C. Subsequently, 3.06 mmol (0.66 g) of 3-bromo propylamine hydrogen bromide was introduced, and the mixture was warmed to room temperature. The reaction mixture was then refluxed for 16 hours. The progress of the reaction was monitored by TLC. After removing the solvent, the product was extracted from the aqueous phase using chloroform. The chloroform was evaporated, and the resulting white precipitate was crystallized with ethyl acetate and collected as the final product with a yield of 51% (Scheme 1).

^{1}H-NMR of berberine@propylamine: 1.95 (m, 2H), 3.25 (t, 2H), 3.58 (t, 2H), 4.12 (s, 3H), 5.65 (bs, 2H), 7.42 (d, 1H), 7.68 (d, 1H), 8.75 (s, 1H).

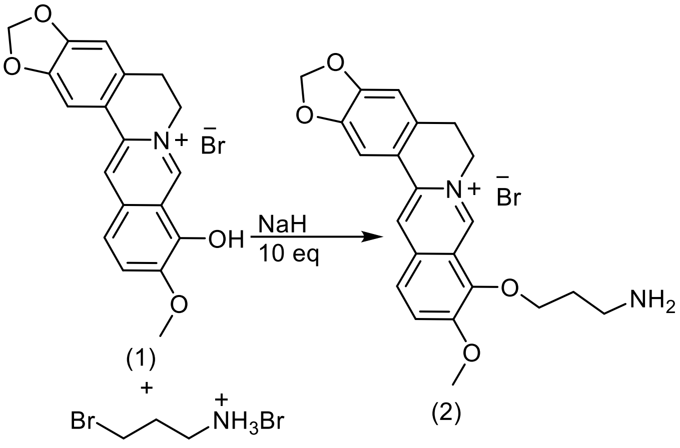

Scheme 1. Synthesis of berberine@propylamine

Synthesis of ligand

1.50 mmol (0.68 g) of the berberine@propylamine from the previous step was dissolved in a mixture of ethanol (20 mL), and a drop of formic acid was added. Subsequently, 1.50 mmol (0.45 g) of taxifolin was added to the reaction mixture, which was refluxed for 20 hours. The resulting yellow precipitate was crystallized in ethanol after solvent removal and collected as the final product with a yield of 71%. (Scheme 2).

^{1}H-NMR of ligand: 1.95 (m, 2H), 3.25 (t, 2H), 3.58 (t, 2H), 4.12 (s, 3H), 5.65 (bs, 2H), 6.20–6.80 (m, 4H, aromatic OH-bearing), 7.42 (d, 1H), 7.68 (d, 1H), 8.75 (s, 1H), 9.00–9.10 (s, 1H, aromatic OH-bearing).

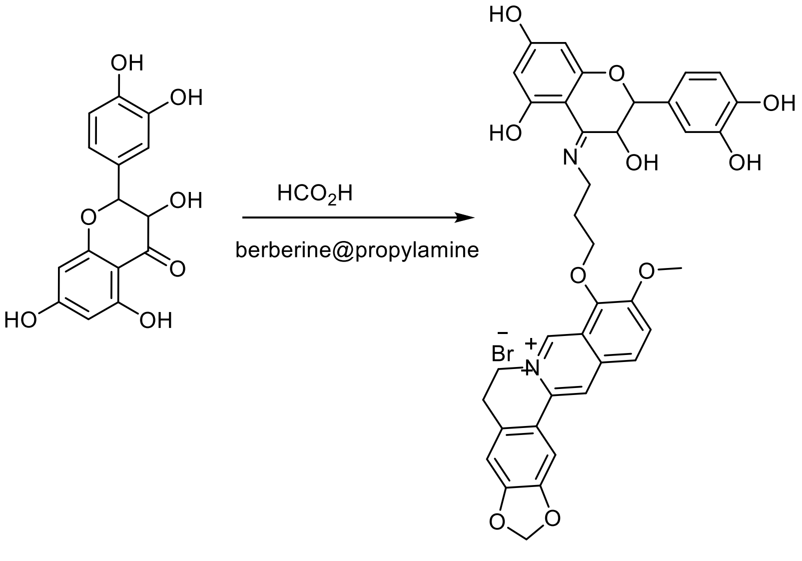

Scheme 2. Synthesis of ligand

Synthesis of Cu (II) Complex

1 mmol (0.48 g) of the ligand from the previous step was dissolved in 15 mL of THF under an inert argon atmosphere. Then, 1 mmol (0.18 g) of copper (II) acetate was added to the reaction vessel, and the mixture was stirred at room temperature for 72 hours. The resulting red precipitate was filtered and washed sequentially with ethanol and diethyl ether to afford the desired product with a yield of 72% (Scheme 3).

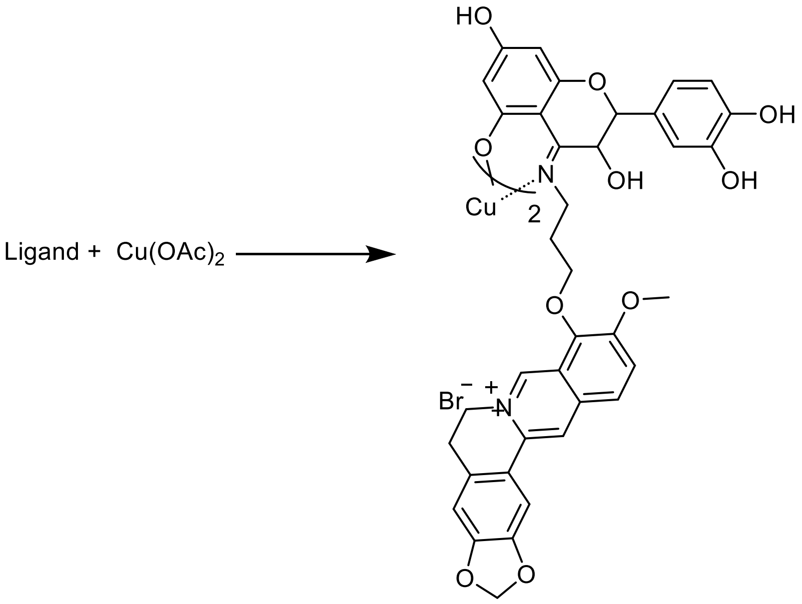

Scheme 3. Synthesis of Cu (II) Complex

Results and discussion

In the 1H-NMR spectrum of the ligand (scheme 4), a multiplet at 1.80 ppm corresponds to hydrogens a, while hydrogens f and b appear as triplets at 2.8 ppm and 3.2 ppm, respectively. Hydrogens c and d are observed as a triplet and a singlet at 4.0 ppm, hydrogen h as a multiplet at 4.4 ppm, and hydrogens g and i at 4.9 ppm, with hydrogens e appearing at 6.1 ppm. The IR spectra of berberine-propylamine (a), the ligand (b), and the catalyst (c) (scheme 5) show characteristic absorption bands at 2100 cm^{-1} and 3400 cm^{-1}, corresponding to $C=N^+$ and NH_2 stretching vibrations, confirming berberine's connection to propylamine. The disappearance of NH_2 stretching at 3400 cm^{-1} and the appearance of a new band at 1600–1580 cm^{-1} confirm the presence of an imine group in the ligand and catalyst. The imine stretching in the catalyst is shifted by approximately 20 cm^{-1} to lower frequencies, indicating complexation with copper. Elemental analysis (Table 1) further confirms the proposed structures, with a nitrogen-to-copper molar ratio of 4:1, indicating two ligand molecules in the catalyst structure.

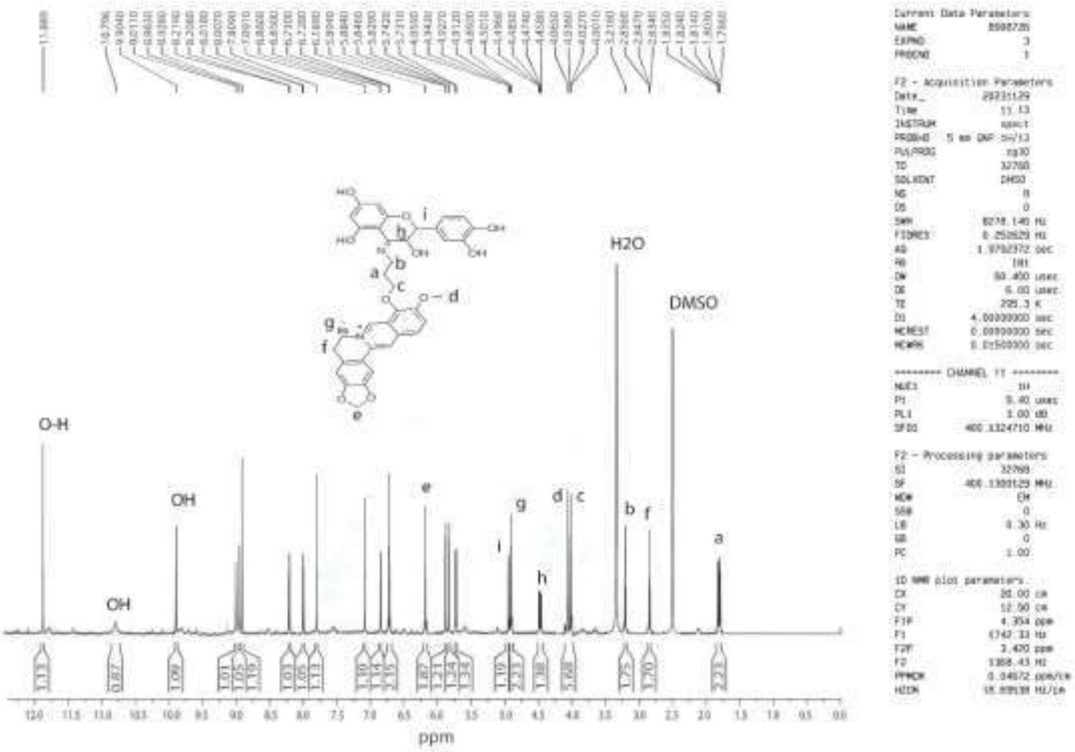

Scheme 4: The 1H-NMR Spectrum of the Ligand

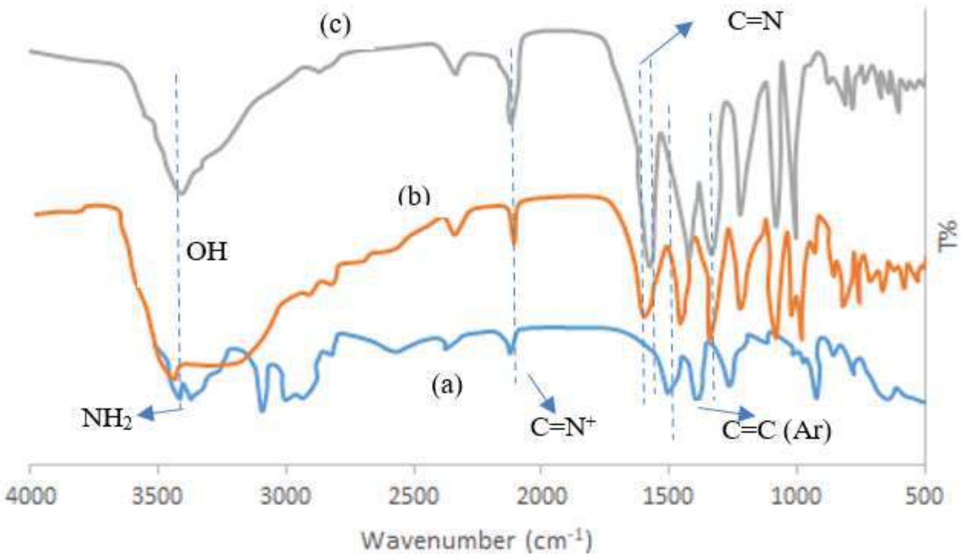

Scheme 5: The IR spectra of (a) berberine@propylamine, (b) ligand and (c) Cu (II) complex.

Table 1: CHN and ICP Analysis of Ligand and Catalyst

Element	**Percentage in Ligand**	**Percentage in Catalyst**
C	66.72	63.78
H	5.00	4.60
N	4.70	4.53
Cu[b]	-	4.01

[b] Measured by ICP

Scheme (6) shows the X-ray diffraction (XRD) patterns of the ligand (a) and the copper complex (b). The sharp and distinct peaks in both patterns confirm the polycrystalline nature of the samples. The XRD pattern of the ligand exhibits three prominent peaks at 2θ angles of 7°, 14°, and 21°, indexed as (001), (002), and (003), indicating its structural order. In contrast, the XRD pattern of the copper complex shows new peaks at 2θ angles of 15°, 17°, and 25°, indexed as (002), (200), and (140), demonstrating significant changes in peak positions and intensities compared to the ligand. These changes confirm the formation of the copper complex and structural rearrangements due to coordination between the ligand and Cu (II) ion, highlighting the successful synthesis of the complex

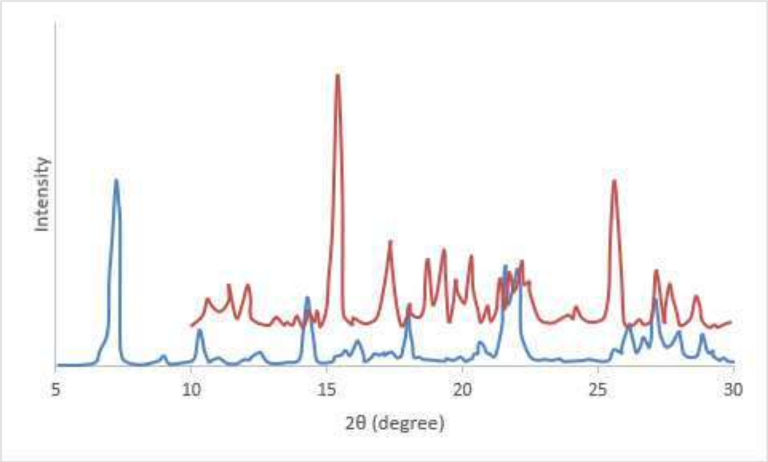

Scheme 6: The XRD analysis of the ligand (blue) and the copper complex (red).

In this section, the effect of the catalyst on the oxidation of sulfides was investigated. Methyl phenyl sulfide was used as a model substrate for this study (Table 2). The results indicated that in the absence of a catalyst, relatively good selectivity was observed; however, the yields were not significant. The use of 0.02 mmol of the copper catalyst resulted in a 72% yield with relatively good selectivity for sulfoxide synthesis. After testing various amounts of the catalyst, 0.01 mmol was determined to be the optimal amount. Using lower or higher amounts led to reduced yield and/or selectivity.

Table (2): Study of Catalyst Amount on Sulfide Oxidation [a]

Entry	**Catalyst**	**Conversion (%)**	**Sulfoxide (%)**	**Sulfone (%)**
1	None	12	75	25
2	0.02 mmol	72	80	20
3	0.05 mmol	79	49	51
4	0.01 mmol	85	90	10

[a] Reaction conditions: 0.30 mmol methyl phenyl sulfide, 1 mmol oxidant, 3 mL water, room temperature, reaction time: 30 minutes.

To optimize the reaction time, the oxidation of methyl phenyl sulfide was investigated in the presence of 0.01 mmol catalyst (optimal amount) at four different times: 15, 30, 45, and 60 minutes (Table 3). Except for the 15-minute time, which resulted in lower efficiency, no significant differences were observed in the other cases. However, considering the high value of time in industrial applications, the 30-minute duration was selected as the optimal reaction time.

Table (3): Effect of Time on Sulfide Oxidation [a]

Entry	**Time (min)**	**Conversion (%)**	**Sulfoxide (%)**	**Sulfone (%)**
1	15	80	90	10

2	30	85	90	10
3	45	85	88	12
4	60	86	89	11

[a] Reaction conditions: 0.30 mmol methyl phenyl sulfide, 1 mmol oxidant, 3 mL water, 100 mg catalyst, room temperature.

The effect of temperature on the oxidation reaction of methyl phenyl sulfide was studied, and the results are presented in Table 4. The findings indicate that 60°C is the optimal temperature for the oxidation process. Increasing or decreasing the temperature resulted in reduced efficiency and/or decreased selectivity.

Table (4): Effect of Temperature on Sulfide Oxidation [a]

Entry	Temperature (°C)	Conversion (%)	Sulfoxide (%)	Sulfone (%)
1	Room Temp	85	90	10
2	40	95	92	8
3	50	97	92	8
4	60	97	92	8
5	80	97	72	18

[a] Reaction conditions: 0.30 mmol methyl phenyl sulfide, 1 mmol oxidant, 0.10 mmol catalyst, 3 mL water, reaction time: 30 minutes.

To investigate the effect of oxidant amount, different amounts of oxone were used, and the best efficiency was achieved in the presence of 1 mmol of oxone (Table 5). Increasing or decreasing the amount of oxone resulted in reduced selectivity or reaction efficiency, respectively.

Table (5): Effect of Oxone Amount on Sulfide Oxidation [a]

Entry	Oxone (mmol)	Conversion (%)	Sulfoxide (%)	Sulfone (%)
1	0.5	84	90	10
2	1.0	91	92	8
3	1.5	99	69	31

[a] Reaction conditions: 0.30 mmol methyl phenyl sulfide, 1.0 mmol catalyst, 3 mL water, reaction temperature: 60°C, reaction time: 30 minutes.

To select the best oxidant, various oxidants, including UHP, H_2O_2, KIO_4, and Oxone, were evaluated. As shown in Table (6), Oxone demonstrated the highest efficiency (Entry 1).

Table (6): Evaluation of Different Oxidants [a]

Entry	Oxidant	Conversion (%)	Sulfoxide (%)	Sulfone (%)
1	Oxone	97	92	8
2	UHP	76	90	10
3	H2O2	29	92	8
4	KIO4	85	89	11
5	none	-	-	-

[a] Reaction conditions: 0.30 mmol methyl phenyl sulfide, 1.0 mmol catalyst, 3 mL water, reaction temperature: 60°C, reaction time: 30 minutes.

Subsequently, the reaction was performed in various solvents to select the best solvent for the reaction. The results clearly indicate that the highest yield is achieved in the presence of water (Table ٧). Other protic solvents, such as methanol and ethanol, also provided moderate yields. Furthermore, polar aprotic solvents (DMF, acetonitrile) resulted in better yields compared to non-polar solvents (toluene, hexane, etc.), which yielded lower efficiencies. It appears that the main factor behind this phenomenon is the better solubility of oxone in protic and polar aprotic solvents.

Table (7): Effect of Solvent Type on Sulfide Oxidation [a]

Entry	Solvent	Conversion (%)	Sulfoxide (%)	Sulfone (%)
1	H_2O	97	90	10
2	Toluene	20	90	10
3	CH_3CN	60	80	20
4	CH_3OH	83	90	10
5	DMF	85	90	10
6	n-Hexane	5	93	7
7	Dichloromethane	10	97	3
8	1,4-Dioxane	15	89	11
9	Solvent-free	20	87	13
10	CH_3CH_2OH	81	90	10

[a] Reaction conditions: 0.30 mmol methyl phenyl sulfide, 1.0 mmol oxone, 0.10 mmol catalyst, 3 mL solvent, reaction temperature: 60°C, reaction time: 30 minutes.

Finally, the efficiency of the catalyst for the oxidation of various sulfides was evaluated, and the results showed that all sulfides were converted to sulfone with high yield and selectivity (Table 8).

Table (8): Oxidation of Various Sulfides [a]

Entry	Sulfide	Conversion (%)	Sulfoxide (%)	Sulfone (%)
1	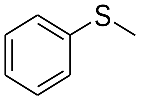	97	90	10
2	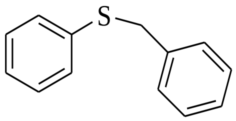	95	98	2
3	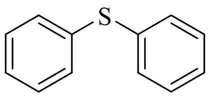	99	99	1
4	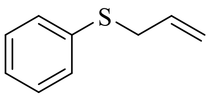	99	96	4

(a) Reaction conditions: 0.30 mmol methyl phenyl sulfide, 1.0 mmol oxone, 3 mL water, reaction temperature: 60°C, reaction time: 30 minutes.

References:

[1] Hagen, J.; *Industrial catalysis*. Wiley-Vch, Weinheim, Germany, 2006, 20.
[2] Gerard, M., Chaubey, A., Malhotra, B., Application of conducting polymers to biosensors, *Biosens. Bioelectron.* 17 (2002) 345–359.
[3] Zhao, L., et al., Berberine-Based Catalytic Systems: A Green Chemistry Approach, *Green Chemistry Letters and Reviews*, 11 (2018) 85–95.
[4] Kumar, R., Gupta, P., The Role of Aqueous Solvents in Sustainable Organic Synthesis, *Sustainable Chemistry Reviews*, 22 (2019) 245–260.
[5] Green, D., Patel, V., Water as a Solvent in Organic Catalysis, *Environmentally Friendly Synthesis Methods*, 9 (2017) 325–340.
[6] Johnson, H., Lee, M., Enhancing Solubility of Catalysts in Green Media, *Journal of Green Chemistry*, 18 (2021) 405–420.
[7] Wang, Y., Li, X., Natural Compounds as Catalysts in Organic Reactions, *Chemical Reviews*, 18 (2021) 975–990.
[8] Gupta, S., Rao, P., Bio-Based Catalysts in Aqueous Systems, *Journal of Sustainable Chemistry*, 16 (2020) 210–225

The 30th Iranian Seminar of Organic Chemistry
February 7-9, 2025, Iran University of Science and Technology, Tehran, Iran

Preparation of modified carbon nanomaterials via amination and their use as an additive to improve the tribological properties of lubricants

Safieh heidarzadeh 1[a], Mohammad.G Dekamin 2[b]

[a]*Department of Chemistry, Iran University of Science and Technology, Tehran 1684613114, Iran; s.heidarzadeh2019@gmail.com*

[b]*Department of Chemistry, Iran University of Science and Technology, Tehran 1684613114, Iran; mdekamin@iust.ac.ir*

Keyword: Monolayer graphene oxide, Dispersion stability, lubricant additive, friction and wear

Introduction: Graphene has attracted a great deal of attention in recent years because of its unique structure and remarkable mechanical, electrical, optical and thermal properties [1–3]. Friction and wear can lead to energy wastage, material losses and shorter life of moving components in mechanical processes. It is reported that the direct losses from tribological contacts are closed to 23% of total fuel energy lost [4]. In order to save energy as well as to protect the mechanical components, lubrication has been demonstrated as an effective method to reduce friction and wear in multiple industrial applications [5]. Liquid lubricant is one kind of versatile lubricant which has a wide range of uses. Nanomaterials are among the additives that have attracted increasing attention because they can be physically and chemically adsorbed on the surface and effectively improve the tribological properties of lubricating oil and significantly reduce friction and wear. Carbon nanomaterials, especially graphene has gained large interest in recent years as lubricating additives due to their low shear resistance between the layer structure, suitable size to enter the contact areas and good thermal conductivity to dissipate the heat generated during friction process [6-7]. So far, a number of studies have been conducted on the tribological behavior and lubrication mechanism of graphene as lubricating additives. Especially, it is highly necessary to ensure stable dispersion of graphene as lubricating additive in various base lubricants. One of the most effective ways to improve the dispersion stability of graphene is chemical modification. In this work, the chemical modification of graphene oxide with amines was investigated.

Method: Preparation and characterization of material GO was prepared via a modified Hummer's method while the graphite powder was used as raw material. The modified graphene (MG) was then prepared on the basis of GO. The dried GO (0.1 g) was dispersed in organic solvent by ultrasonication and mechanical stirring for 30 minutes. Then octadecylamine and acetic anhydride were added to the GO solution. The mixture was refluxed under the continuous stirring for 24 hours at 120 °C. Finally, the modified graphene was dried in vacuum drying chamber.This reaction was carried out in the presence of benzylamine, hexylamine, dodecylamine, and octadecylamine.

Results and Discussion: FTIR spectroscopy was also used in order to confirm the existence of alkyl chains. Figure is the FTIR result for GO. The peaks appeared at 1,735, 1,624, 1,381, and ۱,۰۷۳ cm–1 represent the C=O, C=C, C–O, and C–O–C, respectively, which are typical peaks of GO sample. As for MG sample, the typical peaks of C-H could be observed at 2,914 and 2,846 cm–1, the peaks appeared at 1,457 and 1,368 cm–1 represent CH3, and the typical peak of (CH2)n is at 710 cm–1, these results confirm the existence of long alkyl chains on graphene.

Conclusions: Carbon nanomaterials as additives in lubricants play an important role in creating new properties or compensating for the disadvantages of lubricants. The modified carbon nanotubes in this work were confirmed by FT-IR technique and their dispersion in base oil was investigated. Amination was performed with cyclic amines and linear amines, which resulted in an increase in the degree of GO depolarization by moving towards longer chain amines, resulting in increased dispersion in oil and further reduction in friction.

Scheme:

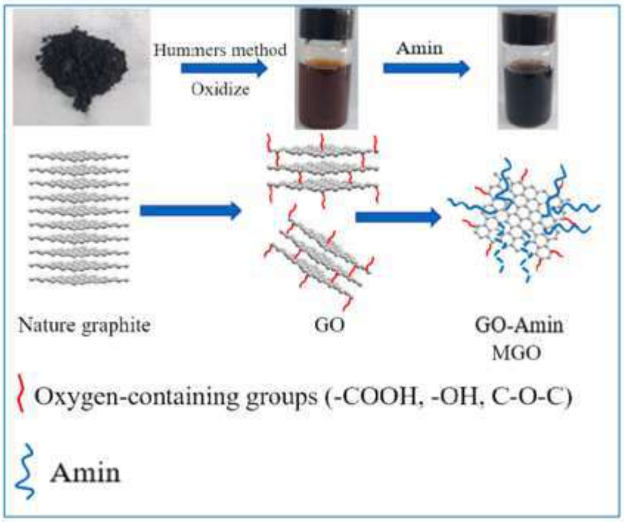

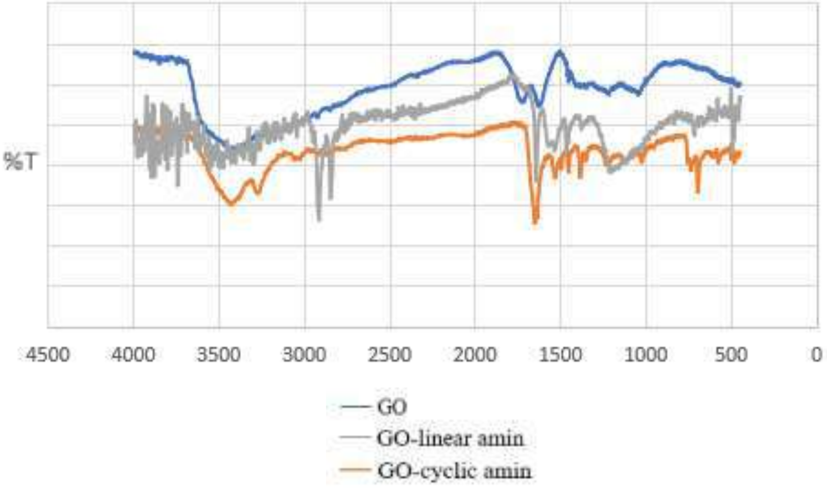

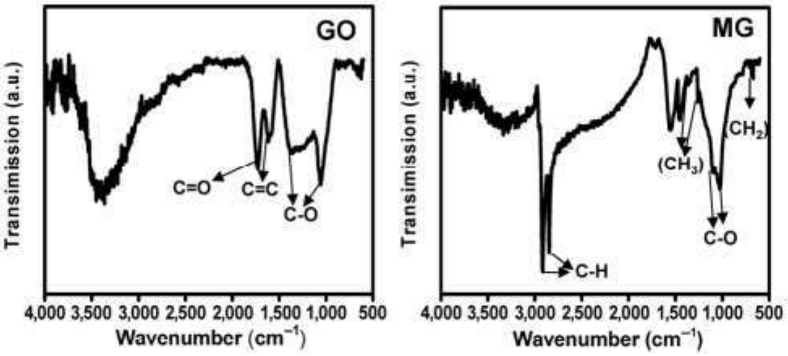

References:

[1] Wu H, Zhao J, Cheng X, Xia W, He A, Yun JH, et al. Friction and wear characteristics of TiO2 nano-additive water-based lubricant on ferritic stainless steel. Tribol Int 2018;117:24–38.

[2] Wu H, Zhao J, Xia W, Cheng X, He A, Yun JH, et al. Analysis of TiO2 nano-additive water-based lubricants in hot rolling of microalloyed steel. J Manuf Process 2017; 27:26–36.

[3] Sivakumar B, Ranjan N, Ramaprabhu S, Kamaraj M. Tribological properties of graphite oxide derivative as nano-additive: synthesized from the waster carbon source. Tribol Int 2020;142:105990.

[4] Gan C, Liang T, Chen D, Li W, Fan X, Tang G, et al. Phosphonium-organophosphate modified graphene gel towards lubrication applications. Tribol Int 2020;145: 106180.

[5] Li G, Yi S, Li N, Pan W, Wen C, Ding S. Quantitative analysis of cooling and lubricating effects of graphene oxide nanofluids in machining titanium alloy Ti6Al4V. J Mater Process Technol 2019;271:584–98.

[6] Huang S, He A, Yun JH, Xu XF, Jiang ZY, Jiao SH, et al. Synergistic tribological performance of a water based lubricant using graphene oxide and alumina hybrid nanoparticles as additives. Tribol Int 2019;135:170–80.

[7] Ahmad RTM, Hong SH, Shen TZ, Song JK. Water-assisted stable dispersal of graphene oxide in non-dispersible solvents and skin formation on the GO dispersion. Carbon 2016;98:188–94.

The 30th Iranian Seminar of Organic Chemistry
February 7-9, 2025, Iran University of Science and Technology, Tehran, Iran

Synthesis of modified graphene oxide as lubricating additive with high dispersion stability in oil

Safieh heidarzadeh 1[a], Mohammad.G Dekamin 2[b]

[a]*Department of Chemistry, Iran University of Science and Technology, Tehran 1684613114 , Iran; s.heidarzadeh2019@gmail.com*

[b]*Department of Chemistry, Iran University of Science and Technology, Tehran 1684613114 , Iran; mdekamin@iust.ac.ir*

Keyword: surface functionalization, silan, graphene oxide, lubricant additives, friction and wear, Dispersion stability

Introduction:

Statistics show that 23% of the world's energy is consumed to overcome friction between surfaces and rebuild worn parts (1).To reduce this problem, appropriate lubricants must be applied to the contact surfaces, which can form a layer with low shear resistance and eliminate direct contact between the surfaces (2).Lubricating oils are composed of base oils and additives in various types.In order to meet various needs such as ultra-low friction and high temperature and pressure resistance, new requirements have been imposed on lubricating oils, and lubricating additives have been greatly improved, thereby enhancing the tribological performance of lubricating oils (3).Among the common organic additives used to reduce friction and wear are dialkyl dithiophosphate and molybdenum dithiocarbamate, which have harmful and toxic emissions, so efforts have been made to replace them with other additives.Nanotechnology as an interface technology is considered one of the most promising strategies for this purpose (4).To date, a large amount of nanomaterials have been added to lubricating oils as additives. Among the advanced nanomaterials, carbon nanomaterials are the cheapest and most abundant in our country and not only affect the performance and thermal efficiency of the engine, but also have a major impact on the durability and wear of engine parts. Carbon nanomaterials include carbon nanotubes, fullerenes, graphene, graphene oxide, and carbon dots, which have been studied (5).

Method:

GO was synthesized according to modified hummer's technique.GO was modified with APTES (H2N(CH2)3Si(OCH2CH3)3) as follows: 20 mg of GO was dispersed in 20 ml of ethanol for 15 min using an ultrasonic bath. Then APTES (1 wt%) was added and refluxed at 75 C for 12 hr. The obtained product was washed with ethanol to remove additional APTES and dried at 60 C for 10 hr.

Results and Discussion:

In this work, graphene oxide and modified graphene oxide were investigated using FT-IR technique and the silane was well dispersed on the GO surface. Another feature of the recent study is the dispersion of this nanomaterial in base oil, which has a shelf life of up to two months and can therefore reduce friction and wear, and thus increase engine life.

Scheme:

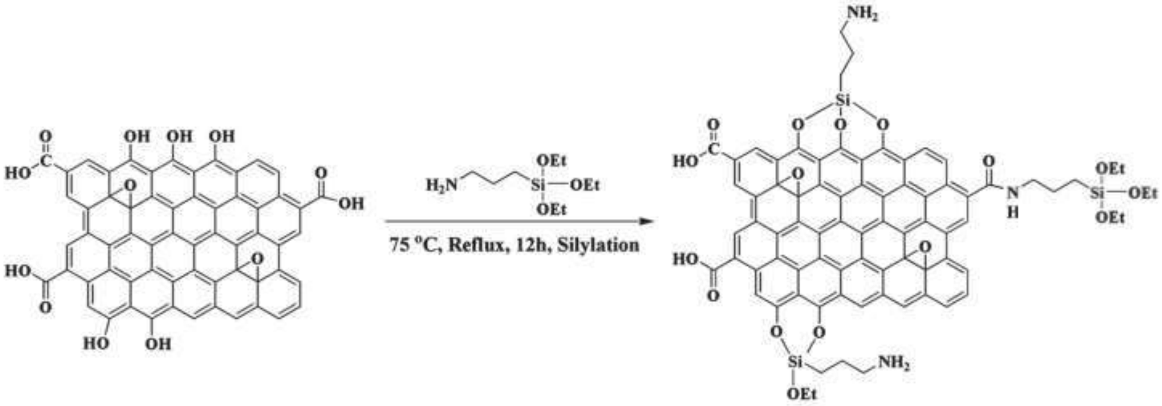

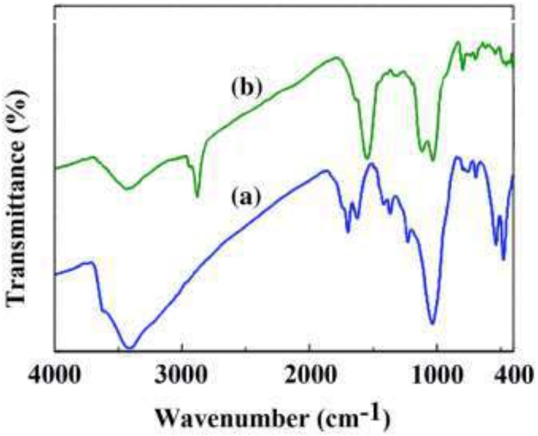

FT-IR spectra of GO (a) , MGO (b)

References:

1. Hatami M, Hasanpour M, Jing D. Recent developments of nanoparticles additives to the consumables liquids in internal combustion engines: Part I: Nano-fuels. Journal of Molecular Liquids. 2020;318:114250.
2. Patel J, Pereira G, Irvine D, Kiani A. Friction and wear properties of base oil enhanced by different forms of reduced graphene. AIP Advances. 2019;9(4).

3. Liu Y, Yu S, Shi Q, Ge X, Wang W. Graphene-family lubricant additives: Recent developments and future perspectives. Lubricants. 2022;10(9):215.
4. Akl S, Elsoudy S, Abdel-Rehim AA, Salem S, Ellis M. Recent advances in preparation and testing methods of engine-based nanolubricants: a state-of-the-art review. Lubricants. 2021;9(9):85.
5. Kumar VB, Sahu AK, Rao KBS. Development of doped carbon quantum dot-based nanomaterials for lubricant additive applications. Lubricants. 2022;10(7):144.
6. Suprakash S, Rashmi R. S. Covalently linked hexagonal boron nitride-graphene oxide nanocomposites as high-performance oil-dispersible lubricant additives. ACS Applied Nano Materials. 202٠;1١(٣):1٠٩٤١-١٠٩٥٣.

The 30th Iranian Seminar of Organic Chemistry
February 7-9, 2025, Iran University of Science and Technology, Tehran, Iran

چشم انداز اقتصاد جهانی صنعت اسانس های طبیعی و چالش های تامین و تولید آن در ایران

محمد حسین محسنی[1]،حسین غفوری[2] ،فرانک منطقی[3]

۱- دانشکده شیمی، دانشگاه علم و صنعت ایران mohseni_mo99@chem.iust.ac.ir

۲-دانشیار دانشکده شیمی، دانشگاه علم و صنعت ایران ghafuri@iust.ac.ir

۳-دانشیار دانشکده شیمی، دانشگاه علم و صنعت ایران f_manteghi@iust.ac.ir

چکیده

چشم انداز ۲۰ ساله توسعه اقتصادی و صادرات غیر نفتي کشور عزیزمان، ایران و ضرورت توجه به نقش منابع طبیعي آن به عنوان اکوسیستم منحصر به فرد جهان، ایجاد بستر مناسب برای توسعه صادرات و افزایش درآمدهاي غیر نفتي کشور را برجسته ترمي کند. تولید اقتصادی و فرآوری هدفمند اسانس های طبیعی از منابع بالقوه خدا دادی، نسبت به سایر منابع، وابستگی کمتری به فناوری‌های پیچیده غیر بومی، مواد اولیه خارجی و به طور کلی واردات دارد. بنابراین از نظر ثبات، تاب‌آوری و خطرپذیری اقتصادی در شرایط مناسب‌تری است و نوسانات سیاسی و بین‌المللی تاثیر منفی کمتری بر آن دارد. ورود مستقیم اما متفاوت دانشگاهیان، خصوصا دانشمندان و پژوهشگران حوزه شیمی و مهندسی شیمی با گرایش های مرتبط با این صنعت معظم و همچنین بکارگیری ایده‌های خاص برای سنتز محصولات جدید، می تواند الگویی مناسب در ارایه دانش فنی فراوری علمی برای بازارهای بین المللی باشد و این همان چیزی است که کشاورزان و صنعتگران جستجو می‌کنند و نمی‌یابند. علاوه بر این، برای پویا نگهداشتن بازارهاي بین المللي، می بایست نیاز و تقاضای مشخص مصرف کننده، دقیقا شناسایی و مطابق با میل و سلیقه آن ها، مراحل تولید تا صادرات محصولات را طراحی دانش بنیان نماییم. در این راستا، وجود دانش فنی تولید فرآورده‌های رقابتی در حوزه اسانس‌های طبیعی در مقیاس آزمایشگاهی در دسترس بوده اما توجه به این نکته مهم است که دانش فنی بسته‌ای از پیش آماده نیست، بلکه بر حسب نیاز و در نتیجه ارتباط تنگاتنگ صنعت و دانشگاه تولید می‌شود. آمار ها و گزارشات یونیدو، بانک جهانی و مراکز مهم اقتصادی سازمان ملل متحد نشان می دهد که کشورهای

توسعه یافته و با درامد سرانه بالا به طور میانگین در ازاء هر تن محصول گیاهی حدود ١٨٥ دلار ارزش افزوده ایجاد میکنند در حالیکه این رقم در کشورهای در حال توسعه تقریبا معادل ٤٠ دلار می باشد که به معنی خام فروشی مطلق است. همچنین ٩٨ درصد تولیدات گیاهی کشورهای توسعه یافته در فراوری صنعتی قرار میگیرند که این رقم برای کشورهای در حال توسعه ٣٨ درصد است. در سال ٢٠٢٤ حجم بازاراقتصادی گیاهان حاوی مواد موثره شامل دارو، طعم، بو و مزه بالغ بر ٢٩٦ میلیارد دلار بوده که از این مقدار حدود ٢٦ میلیارد دلار را اسانس های طبیعی به خود اختصاص داده و این آمار را در سال ٢٠٣٠ به ترتیب ٤٣٠ و ٥/٤٢ میلیارد دلار پیش بینی کرده است.

کلید واژه: اقتصاد اسانس های طبیعی، صنعت اسانس، تقاضای بازار های بین المللی، تولید اسانس طبیعی در ایران

jkguy
The 30th Iranian Seminar of Organic Chemistry
February 7-9, 2025, Iran University of Science and Technology, Tehran, Iran

Bovine serum albumin immobilized on the magnetic triazine-functionalized chitosan as an efficient nanocatalyst in the synthesis of 1,4-dihydropyridines and 3,4-dihydropyrimidinones

M. Amere,[a] Fatemeh Rafiee ,*[b]

[a, b] Department of Organic Chemistry, Factually of Chemistry, Alzahra University, Tehran, Iran.

Keyword: Chitosan, Bovine serum albumin, Multi-component reaction, Magnetic catalyst

There is considerable research on the expansion of biocatalysts in organic reactions is due to their high catalytic efficiency, selectivity, mild and environmentally friendly reaction conditions, simple operational procedures and low energy requirements [1-2]. Among the reported biocatalysts, commercially available and inexpensive bovine serum albumin (BSA) as most abundant protein of mammalian blood plasma has been used as an active and efficient catalyst or co-catalyst in various organic transformations [3]. In this research work, chitosan biopolymer was functionalized with 2,4,6-trichloro-1,3,5-triazine to produce new arms for further modification with BSA protein. The magnetization of biosupport was done through treatment of Fe_3O_4 nanoparticle with chitosan biopolymer that functionalized with chlorinated derivative of 1,3,5-triazine. BSA-immobilized on the magnetic chitosan support (Fe_3O_4@CSC-BSA (Scheme 1)) was applied as an efficient magnetic heterogeneous catalyst in the synthesis of dihydropyridine derivatives through Hantzsch reaction and dihydropyrimidinones by Biginelli reaction.

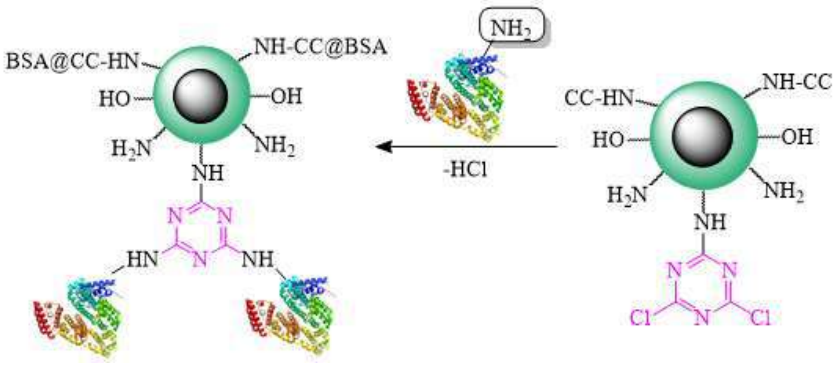

Scheme 1.

References:

1. Jumbam, N.D.; Masamba, W. Bio-catalysis in multicomponent reactions, *Molecules*, **2020**, 25, 5935.
2. Albanese, D.C.; Gaggero, N. Albumin as a promiscuous biocatalyst in organic synthesis, *RSC advances*, **2015**, 5, 10588-10598.
3. Sharma, U.K.; Sharama, N.; Kumar, R.; Sinha, A.K. Biocatalysts for multicomponent Biginelli reaction: Bovine serum albumin triggered wasted-free synthesis of 3,4-dihydropyrimidin-2-(1 H)-ones, *Amino Acids*, **2013**, 44, 1031.

The 30th Iranian Seminar of Organic Chemistry
February 7-9, 2025, Iran University of Science and Technology, Tehran, Iran

Tetra-substituted imidazole ligand for efficient green-emitting iridium(III) complex

Zahra Golbodaghi,[a] Babak Nemati Bideh*[a]

[a] *Department of Inorganic Chemistry, Faculty of Chemistry and Petroleum Sciences, Bu-Ali Sina University, Hamedan, Iran.* ***E-mail:*** *zahragolbodaghi@gmail.com, b.nemati@basu.ac.ir.*

Keyword: Imidazole-based ligand, Iridium complex, Green emitter

Ionic transition metal complexes are the most important materials used as emitters in the structure of optoelectronic devices such as OLEDs and LECs [1]. The electronic properties of diimine ligands in the structure of complex emitters play a crucial role in determining their efficiency and color emission. Five-membered nitrogen-rich heterocycle ligands-based iridium (III) complexes have afforded the most efficient LECs reported to date [2]. Here in, we have designed and synthesized the new imidazole-based ancillary ligand and its cationic cyclometalated iridium complex. In brief, the new 1, 2, 4, 5-tetrasubstituted imidazole ligand has been synthesized via the one-pot multi-component condensation of 2, 2'-pyridil with p-methylaniline, p-chlorobenzaldehyde, and ammonium acetate in glacial acetic acid under reflux. In following, the cyclometalated complex IrL was obtained by reacting the two equivalents of the imidazole ligand with one equivalent of the di-iridium chloro-bridged dimer $[Ir(ppy)_2(\mu\text{-}Cl)]_2$ (ppy: phenyl pyridine) in ethylene glycol under inert conditions as displayed in **Scheme 1**.

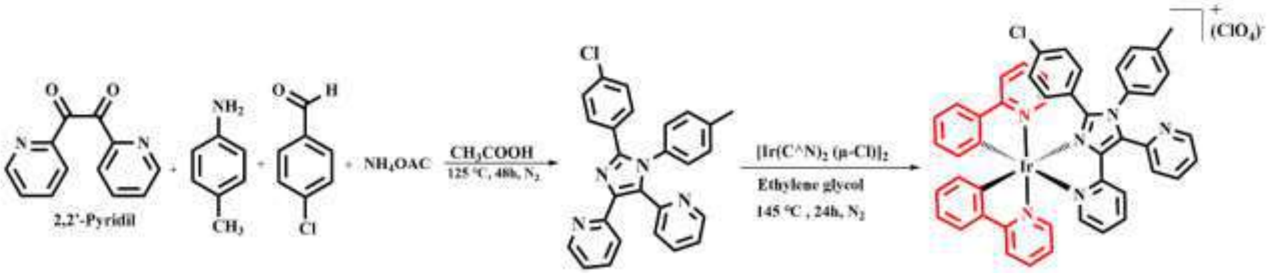

Scheme 1. Synthesis of imidazole dipyridyl-based ligand and its cyclometalated iridium(III) complex

In the DCM solution, the synthesized complex exhibits green color emission centered at 490, 515 nm with a PLQY of 17%. Moreover, the neat film of the complex shows intense yellow-green emission with a maxima emission of 540 nm. Overall, these emission properties show this material's high potential for synthesizing efficient emitters.

References:

[1] Pandit, V., Jang, J., Koodalingam, M., Ranasinghe, C. S. K., Gao, M., Burn, P. L., & Puttock, E. V. Effect of dendrimer generation and surface groups on the optoelectronic properties of green emitting bis-tridentate iridium (iii) complexes designed for OLEDs. *J. Mater. Chem. C*. 2023, *11*, 14134-14150.

[2] Karimi, S., Shahroosvand, H., Yaghoobi Nia, N., Di Carlo, A., & Nazeeruddin, M. K. Versatile electroluminescence color-tuning strategy of an efficient light-emitting electrochemical cell (LEC) by an ionic additive. *Inorg. Chem.* 2022, *61*, 20734-20742.

The 30th Iranian Seminar of Organic Chemistry
February 7-9, 2025, Iran University of Science and Technology, Tehran, Iran

Electrical and Structural Investigation of Masitinib; A DFT Study

Hossein Shirani[a,b,*] and Roxana Jahanian[b]

[*]*Corresponding author. E-mail:* hossein_shirani@iust.ac.ir

[a]*Department of Chemistry, Iran University of Science and Technology, P.O. Box 16846-13114, Tehran, Iran*
[b]*Faculty of Biosciences and Microbiology, Islamic Azad University, North Tehran Branch, Tehran, Iran*

Introduction

Masitinib is a drug that inhibits tyrosine kinases, a type of protein Masitinib (Figure 1) works by binding to and inhibiting specific receptors, including the stem cell factor receptor, platelet-derived growth factor receptor, fibroblast growth factor receptor, and focal adhesion kinas. It can inhibit tumor cell proliferation in cancer cells that overexpress these receptors and is used to treat various conditions, including Mast cell tumors in dogs, Multiple Sclerosis (MS), Amyotrophic Lateral Sclerosis (ALS) and other conditions [1-3]. The Density Functional Theory (DFT) calculations have not previously been performed on Masitinib. DFT is a commonly used computational method in quantum chemistry and physics. It investigates the electronic structures of atoms, molecules, and solids.

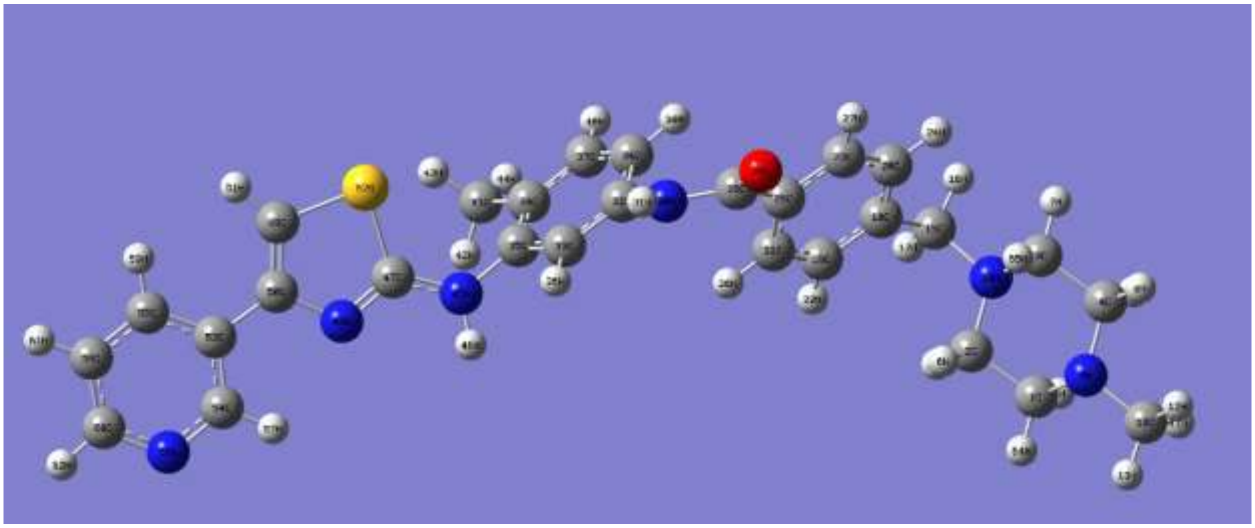

Figure 1: Optimized structure of Masitinib at the B3lyp/6-311++G(d,p) level of theory

Methods

We applied quantum mechanics computational methods to study Mastitinib, using the B3LYP/6-311++G(d,p) level of theory. Gaussian and GaussView programs were used for molecule optimization. Structural parameters such as bond angles and lengths were extracted, and vibrational frequencies were analyzed to obtain the IR spectrum.

Results

Since the interaction between drugs, ligands, and proteins is very important, the calculations and simulations of these interactions play a crucial role. Ultimately, this work can be used in experimental studies for drug delivery or targeted pharmaceutical applications. We focused on intra-molecular transitions with molecular orbitals, specifically HOMO and LUMO, and calculated the gap between them. The dipole moment and polarizability of the molecule in X, Y, and Z coordinates were computed, followed by the extraction of polarizability. The dipole moment is described as follows: μ_x;1.0666, μ_y;2.3175, μ_z;1.6279 Debye. Finally, we calculated and reported the polarizability in the XX, XY, and XYZ planes and the total polarizability. The Electronic energy has also been calculated (-1886.40873356 Hartree/particles). This theoretical investigation helps us understand the chemical and pharmacological applications of Mastitinib significantly better. With this interdisciplinary approach, we can take significant steps towards improving performance and producing similar drugs, ultimately achieving better outcomes.

Keywords: DFT, Masitinib, Molecular Orbitals, Polarizability

References

1. Boutin, J. A., et al. (2007). Masitinib: A selective inhibitor of c-Kit and PDGF receptor tyrosine kinases. Bioorganic & Medicinal Chemistry, 15(21), 6583-6595

2. Schmiegelow, M., et al. (2015). Masitinib: Chemical properties and pharmacological profiles. Journal of Medicinal Chemistry, 58(22), 9133-9142.

3. Gilbert, M., & Roush, W. R. (2009). Mechanisms and chemical properties of masitinib in treating cancer. Cancer Chemotherapy and Pharmacology, 64(3), 387-395.

The 30th Iranian Seminar of Organic Chemistry
February 7-9, 2025, Iran University of Science and Technology, Tehran, Iran

Removal of pharmaceutical pollutants with CdS immobilized on commercial PVC under UV irradiation

Soodabeh Hatami[1], Majid Abdous*[1], Nafiseh Aghababaei[2]

[1] *Department of Chemistry, Amirkabir University of Technology, 15875-4413, Tehran, Iran*

[2] *Department of Chemical Engineering, Tafresh University, Tafresh, 39518 79611, Iran*

Keyword: Polyvinyl chloride, optical stabilizer, advanced oxidation process, pharmaceutical contaminants

Abstract

In this study, the photostabilization of polyvinyl chloride (PVC) and its application in the removal of pharmaceutical contaminants using nanocomposites has been studied. As one of the most widely used industrial polymers, PVC is vulnerable to light and heat and requires stabilization. This study synthesized new PVC-based nanocomposites, and their photocatalytic properties for removing pharmaceutical contaminants via the advanced oxidation process (AOP) were investigated. The results show that PVC surface modification with CdS nanoparticles can significantly increase photostability. These nanocomposites also exhibit a high potential for removing pharmaceutical pollutants from water.

Introduction

Polyvinyl chloride, or PVC, is the world's second most widely used polymer due to its numerous applications in various industries. One of the most challenging aspects of its use is its sensitivity to light and heat. UV light irradiation may break the PVC structure and produce HCl, resulting in color change, reduced mechanical capabilities, and polymer degradation [1]. On the other hand, pharmaceutical poisoning of groundwater has become a major environmental issue [2]. As a potential approach for removing pharmaceuticals from the environment, photocatalytic polymer degradation offers very low operating costs, along with no toxic byproducts that cause secondary contamination.

Method

The hydrothermal technique was used to synthesize PVC/metal oxide nanocomposites. The photocatalytic reactor is used to perform photocatalytic activity under UV. HPLC measured pharmaceutical contaminants concentrations. The morphology and structure of composite studies were analyzed using FESEM, EDX, XRD, and FTIR assessments.

Results and Discussion

The XRD results showed that nanocomposite was formed. FESEM image indicated nanoparticle homogeneous dispersion inside the polymer matrix. Photocatalytic tests demonstrated that the produced nanocomposites can eliminate more than 88% of pharmaceutical pollutants within 60 minutes of UV light exposure. This work successfully produced innovative PVC-based nanocomposites with enhanced photocatalytic efficiency. These polymers demonstrated stronger photostability than pure PVC and were much more effective at removing pharmaceutical pollutants from aqueous environments.

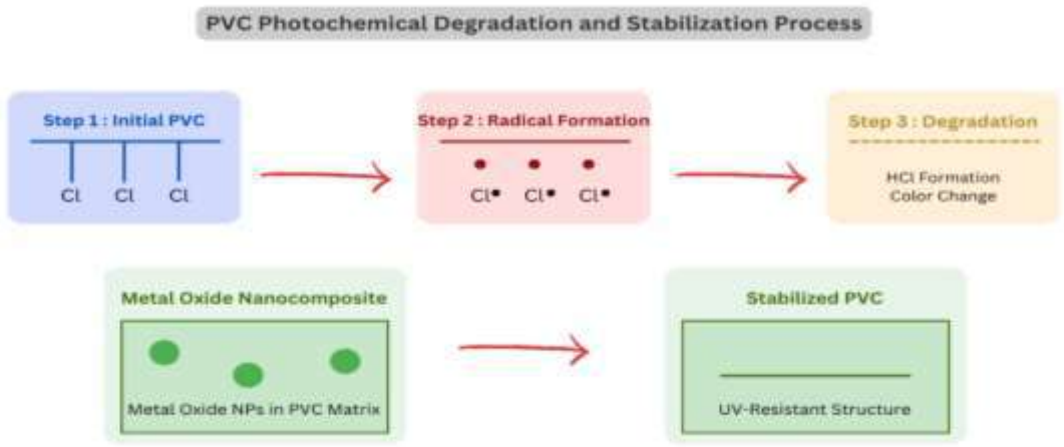

Scheme: PVC photochemical degradation and stabilization process.

References:

١. Heidari, A., & Montazer, M. (٢٠٢٠). A review on photo-stabilizing agents for polyvinyl chloride. Journal of Vinyl and Additive Technology, ٢٦(١), ٢٤-٣٧.

٢. Wang, Y., & Wang, Y. (٢٠٢١). Advanced oxidation processes for the removal of emerging contaminants in water: A review. Journal of Water Process Engineering, ٤٣, ١٠٢٢٢٥.

The 30th Iranian Seminar of Organic Chemistry
February 7-9, 2025, Iran University of Science and Technology, Tehran, Iran

Antioxidant, Antibacterial Activity, and Phytochemical Characterization of Ethanolic Extract of Flowers of *Lonicera caprifolium* L.

Reyhane Riazi[a], Mobina Jafari[a], Bahare Afshari[a], Mohadese Inanlou[a], Shahab Ojani*[b]

[a] *Department of Chemistry, Karaj Branch, Islamic Azad University, Karaj, Iran*

[b] *Institute of Nano Science and Nano Technology, University of Kashan, Kashan, Iran*

Keyword: *Lonicera caprifolium* L., Digestion method, Tannins, DPPH^0, *Staphylococcus aureus.*

Lonicera caprifolium L., a species of the Caprifoliaceae family, is recognized as edible and medicinal food [1]. Modern pharmacological studies have shown that of *L. caprifolium* has broad pharmacological properties, including antiviral, antiseptic, and anti-inflammatory effects [2]. The aim of this project was to antioxidant, antibacterial activity, and phytochemical characterization of ethanolic extract of flowers of *L. caprifolium*. In this project we use *of L. caprifolium* flowers and ethanol extract by digestion method. To this end, that the preliminary phytochemical analysis of six different chemical compounds Flavonoids (Alkaline Reagent Test), Phenols (Ferric Chloride Test), Tannins (Ferric Chloride Test), Saponins (Foam Test), Quinones (Sulfuric Acid Test) and Coumarins (10% NaOH) were tested in ethanolic extract. The total phenolic contents (TPC) and total flavonoid contents (TFC) of the extract were then measured using Folin Ciocalteu Reagent (FCR) and $AlCl_3$ methods, respectively. Total antioxidant activity was assayed by DPPH^0 free radical scavenging assay method. Also, the antibacterial potential was evaluated using the MIC and MBC technique. The screening of phytochemical of ethanolic extract of flowers of *of L. caprifolium* showed Flavonoids, Phenols, Tannins and Coumarins. Total phenolic content of ethanolic extracts of *of L. caprifolium* flowers was 439 mg GAE/g dry plant material. Also, total flavonoid content of methanolic extracts was 284 mg QE/g dry plant material. The value IC_{50} of ethanolic extract determined 5.67 mg/mL. **MIC and MBC of ethanolic extract of** flowers of *L. caprifolium* **on** *Staphylococcus aureus* **and** *Escherichia coli* **were (6.25 - 12.5), (12.5 - 50) mg/ml, respectively.** Therefore, *L. caprifolium* could be an excellent source for natural antioxidant and antibacterial agents for medical, pharmaceutical and nutraceutical applications.

References:

Gavit, A. A., Gagrani, M. B., Gurav, S. S., Ayyanar, M., Beldar, V. G., Tatiya, A. U., Surana, S. J., Firke, S. D., & Kalaskar, M. G. (2024). Chemical composition and biological activities of *Lonicera caprifolium* L. (Caprifoliaceae) essential oil. *Natural product research*, *38*(5), 719–726. https://doi.org/10.1080/14786419.2023.2193745.

Rahmati, M., Eghbali, S., Mokaber-Esfahani, M., & Taleghani, A. (2024). Volatile oil constituents, antioxidant and antibacterial activities of *Lonicera caprifolium* L. in different areas of Iran. *Natural product research*, 1–7. Advance online publication. https://doi.org/10.1080/14786419.2024.2369229.

The 30th Iranian Seminar of Organic Chemistry
February 7-9, 2025, Iran University of Science and Technology, Tehran, Iran

A Density Functional Theory Study of Litfulo

Hossein Shirani[a],* and Fatemeh Mahmoodi[b]

*Corresponding author. E-mail: shiranihossein@gmail.com

aDepartment of Chemistry, Iran University of Science and Technology, P.O. Box 16846-13114, Tehran, Iran

bDepartment of chemical engineering, College of engineering, Islamic Azad University, Tehran centeral Branch,Tehran,Iran

Introduction: LITFULO (Ritlecitinib) is a kinase inhibitor specifically indicated for the treatment of severe alopecia areata in adults and adolescents aged 12 years and older. This medication is designed to modulate the immune response and is effective in managing this autoimmune disorder characterized by significant hair loss.Despite the therapeutic benefits of LITFULO, awareness of its safety profile is essential. The use of this drug is associated with an increased risk of serious infections, including bacterial, fungal, viral, and opportunistic infections, which may lead to hospitalization or death. Notably, there is particular concern regarding tuberculosis (TB) infections, necessitating close monitoring for signs and symptoms of infection during the treatment period. LITFULO capsules contain ritlecitinib tosylate as the active ingredient. Ritlecitinib tosylate is described as a white to light pink solid that is well soluble in water.[۱]

Apart from the medical aspect, we decided to conduct Density Functional Theory (DFT) calculations to examine the subatomic interactions. [2]

Methods: By using the Gaussian09W and Gauss View software with the (B3lyp/6-311++g**) the level theory method, we performed DFT calculations on this drug and obtained notable data that provides us with valuable information.[3]

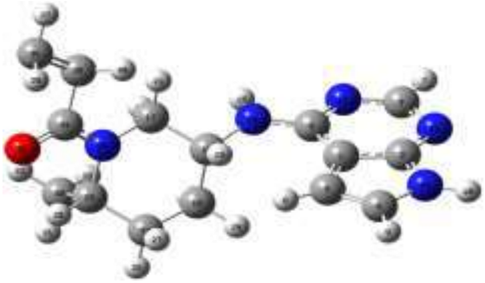

Fig.1. The optimized structure of fostemsavir at the B3lyp/6-311++g** level.

Table1. Calculated Bond Length Values for Litfulo Molecule using B3lyp/6-311++g** Computational Method.

N_{11}-C_3	C_2-N_{12}	C_4-N_{14}	C_1-C_5	C_{25}-N_{29}
1.33720	1.33641	1.36741	1.44115	1.47958

Table 2. Calculated Bond Angles Values for Litfulo Molecule using B3lyp/6-311++g** Computational Method.

N_{29}-C_{34}-O_{38}	N_{11}-C_4 -N_{14}	C_3-N_{12}-C_2	C_2-N_{13}-C_6	C_1-C_4-N_{14}
121.3	114.5	112.3	109.3	125.8

Table 3. Calculated Dihedral Angle Values for Litfulo Molecule using B3lyp/6311++g** Computational Method.

N_{11}-C_3-$N_{12}C_2$	C_{16}-C_{17}-N_{29}-C_{34}	C_{30}-C_{25}-C_{22}-C_{18}	N_{14}-C_{16}-C_{18}-C_{22}	O_{38}-C_{34}-N_{29}-C_{17}
0.05	-73.80	74.03	-175.26	174.24

Table 4. Calculated HOMO-LUMO Energy Gapvalues (eV) for fostemsavir molecule using B3lyp/6-311++g** computational.

HOMO	HLG	LUMO
-0.21695	0.16412	-0.05283

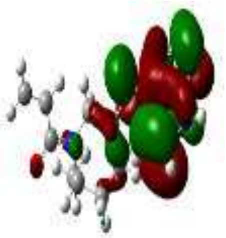

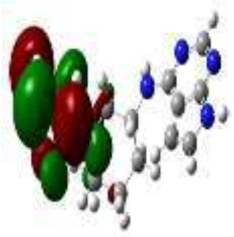

Table 5. Total electronic energy calculated in electron volts (eV) using DFT methods. The value represents the sum of orbital potential and kinetic energies of the electron with in the system.

HF	-933.5179002

Discussion: By performin these calculations and analyzing the obtained data, we discovered significant information about the behavior of this drug. This knowledge will aid in future research on this drug, highlighting the relationship between its chemical behavior and its side effects, which could ultimately lead to advancements in the industry.

Keywords: HOMO, LUMO, HLG , DFT, Litfulo , B3lyp/6-311 ++g**

References:

[۱] LITFULO. Prescribing Information. Pfizer; 2023

[۲] Drugsatfda.com

[۳] Frisch, M. J., Trucks, G. W., Schlegel, H. B., Scuseria, G. E., Robb, M. A., Cheeseman, J. R., ... & Fox, D. J. (2009). Gaussian 09, Revision D.01. Gaussian, Inc.

The 30th Iranian Seminar of Organic Chemistry
February 7-9, 2025, Iran University of Science and Technology, Tehran, Iran

Cyclometalating quinoxaline-based ligand for efficient deep-red emitter

Kokab Albaji,[a] Babak Nemati Bideh*[a]

[a] *Department of Inorganic Chemistry, Faculty of Chemistry and Petroleum Sciences, Bu-Ali Sina University, Hamedan, Iran.* ***E-mail:*** *kokabalbaji90@gmail.com, b.nemati@basu.ac.ir.*

Keyword: Quinoxaline-based ligand, Iridium complex, NIR emitter

Near-infrared IR emitters have attracted great attention because of their wide potential applications, such as biosensors, phototherapy devices, optical signal detectors, night vision devices, and optoelectronic devices such as OLEDs and LECs [1]. Cyclometalated iridium complexes are the most important group of red emitters with high emission efficiency which are widely used in optoelectronic devices [2]. Anyway, the type of cyclometalated ligands has a significant effect on the emission efficiency of this group of emitters. In this work, we have designed and synthesized the new cyclometalated iridium complex based on quinoxaline and imidazole material as cycometalating and ancillary ligands, respectively as shown in **Scheme 1**.

Scheme 1. Synthesis of imidazole dipyridyl-based ligand and its cyclometalated iridium(III) complex

In the DCM solution, the synthesized complex exhibits red color emission centered at 693 nm. Moreover, the neat film of the complex shows intense deep-red emission with a maxima emission of 726 nm. Cyclic voltammetry investigation indicates the good electrochemical stability of this emitter. Overall, these emission properties and good redox behavior show the high potential of quinoxaline ligands for synthesizing efficient emitters.

References: Times New Roman, Font size: 11, Align left, Arabic numeral

[1] Lin, Y. D., Lu, C. W., & Su, H. C, Long-Wavelength Light-Emitting Electrochemical Cells: Materials and Device Engineering, Chem. Eur. J. 2023, **29(10)**, e202202985.

[2] Housecroft, C. E., & Constable, E. C, Over the LEC rainbow: Colour and stability tuning of cyclometallated iridium (III) complexes in light-emitting electrochemical cells. Coordination Chemistry Reviews. 2017, **350**, 155-177.

The 30th Iranian Seminar of Organic Chemistry
February 7-9, 2025, Iran University of Science and Technology, Tehran, Iran

Synthesis and Analysis of E2,Z13-Octadecadienyl Acetate Molecule as a Component of the Sex Pheromone of Zeuzera pyrina (Walnut Tree Pest)

Mohammad Hadi Ghasemi*[a], Danial Namaki [a,b] , Elaheh Bohloulbandi[a], Zahra Kachoui[a]
a. Applied Chemistry Research Group-ACECR, Tehran University, Iran.
b. Pharmaceutical and Heterocyclic Compounds Research Laboratory Department of Chemistry Iran University of Science and Technology, Tehran

Abstract

Recent strategies in integrated pest management (IPM), uses chemicals to manipulate and control the behavior of insects. This group of compounds includes many insect repellants and attractants. Insect pheromones are special natural compounds that meet modern pest control requirements. Therefore, the practical application of insect pheromones, especially sex pheromones, has been extremely successful in controlling low pest populations and reducing long-term pest populations. Mass trapping and mating disruption strategies using sex pheromones have significantly reduced the use of conventional insecticides, thereby providing sustainable and environmentally friendly pest management in agricultural crops. The use of insecticides, which are an important part of agricultural and livestock production, may cause adverse consequences such as higher production costs, environmental pollution, and effects on non-target organisms. New strategies can reduce the use of insecticides. In this project, we first synthesized and analyzed the constituents of the sex pheromone of the Zeuzera pyrina. Then the appropriate formulation was prepared in the required number of plastic lures. In order to carry out field tests, lures were sent to different provinces in correspondence with the Plant Protection Organization. In order to check the pheromone traps and monitoring, periodic visits were made to the covered areas in the provinces. Also, according to the synthesis of the pheromone components of the Chilo suppressalis Walker, a rice worm, as part of the results of the lab phase of this project, all the above activities were also carried out regarding this pheromone.

Keywords: sex pheromones, integrated pest management, synthesis, Zeuzera pyrina

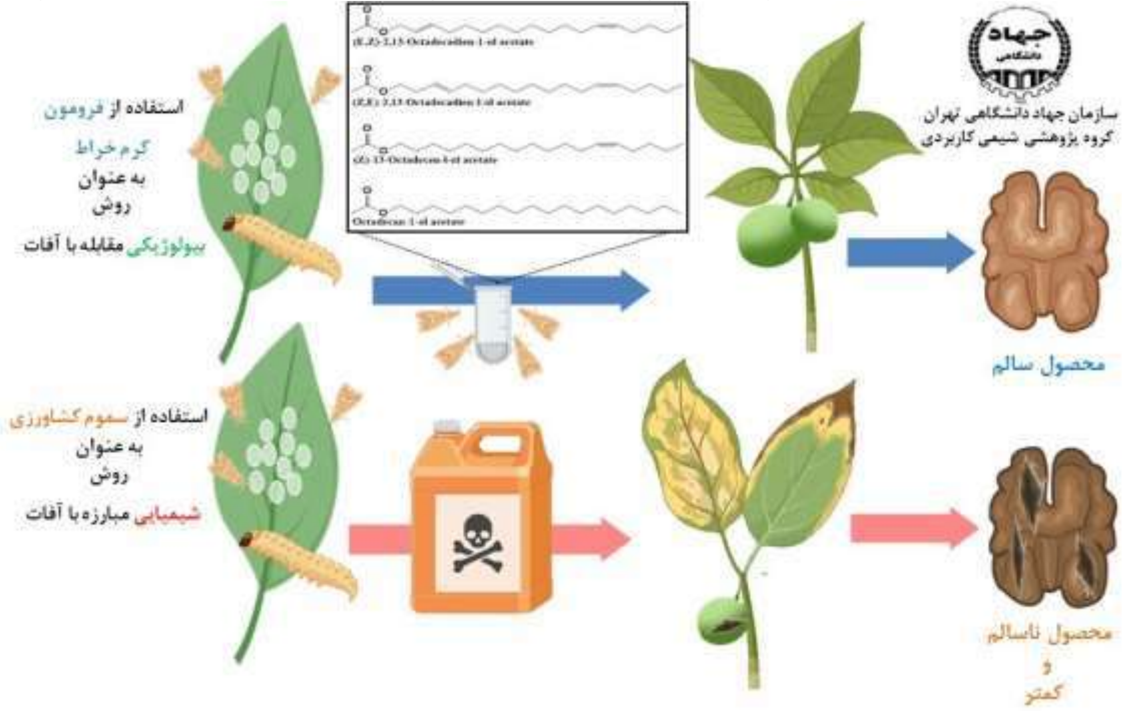

Introduction

Pheromone traps are a glue-coated surface such as a Delta trap or cone attached to a chamber in which the pheromone Louvre is embedded. Pheromone traps are used for insect population monitoring, mass insect hunting, and mating disorders [1]. For example, the pheromone of Zeuzera pyrina, implemented in the Applied Chemistry Group as a agrochemistry project, contains the following components [2-4].

(E,Z)-2,13-Octadecadien-1-ol acetate

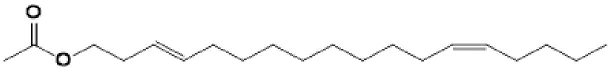

(Z,E)-2,13-Octadecadien-l-ol acetate

(Z)-13-Octadecen-l-ol acetate

Octadecan-1-ol acetate

Using pheromone traps is possible to saturate the environment with the sex pheromone of the female insect and disrupt mating, preventing the normal mating process and reducing the birth of this pest. These traps are able to hunt male insects. This procedure reduces the number of males and disrupts the birth of the pest.

Method

This phase involves laboratory activities of synthesis and analysis of one of four component that make up the sex pheromone of the Zeuzera pyrina.

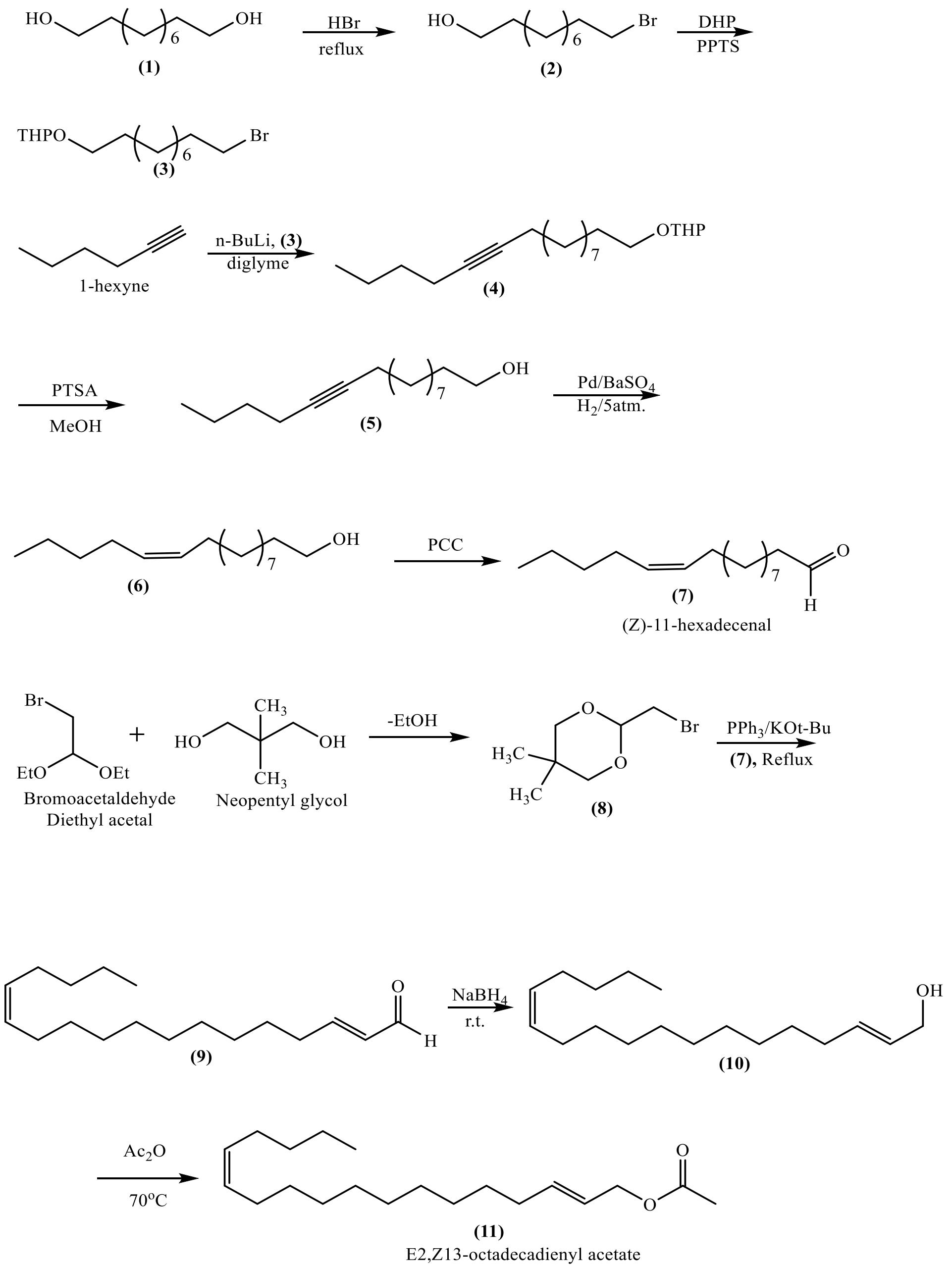

- Synthesis of 10-Bromo Decan-1-ol

To the solution of 5/2 g of 1,10 decandiol in 100 ml of toluene, the 5 ml of HBr 48% solution added and the mixture was refluxed for 24 h. The reaction progression process was followed up with TLC (normal hexane: ethyl acetate 9: 4). The resulting mixture washed with 1 molar solution of sodium hydroxide, 10% hydrochloric acid solution and NaCl solution several time. The organic phase was isolated and dried with sodium sulfate. Then the solvent was separated from the solution under a vacuum, the oily product obtained was applied in the next step.

- Protection of the alcoholic group

3/5 g of the oily product(10-Bromo Decan-1-ol) was added in 15 ml of dry THF in the presence of catalyst(pyridinium para-toluene sulfonate) in ice bath 1/65 ml of dihydropyran added dropwise. The mixture was stirred at room temperature for 24 h. The reaction progression process was followed up with TLC (normal hexane: ethyl acetate 9: 2). Then, washed with a solution of sodium bicarbonate and NaCl solution. The organic phase was dried with sodium sulfate overnight.

- Synthesis of 1-(tetrahydro-2'-pyranyloxy)-10-hexadecine

Added to the 5/5 ml 1-hexine mixture at 60 ml diglim, 30 ml n-butyl lithium added dropwise. The mixture was stirred for 30 minutes at the same temperature. Then 14 g of 1-(tetrahydro-2'-pyranyloxy) 10-Bromo Decan were quickly added to the mixture. Mixture was stirred for 5h at room temperature. Then 200 ml of water was added to the contents of the balloon, and the organic phase was separated and the aqueous phase was extracted with normal hexane. The solvent was separated from the solution under the vacuum.

- Deprotection the Pyran group

To a solution of 2g 1-(tetrahydro-2'-pyranyloxy)-10-hexadecine in 10 ml of methanol, several para-toluene sulfonic acid crystals were added. The mixture was stirred for 4 h at room temperature. The reaction progression process was followed up with TLC (normal hexane: ethyl acetate 9: 2). The reaction solvent was removed under the vacuum then Diethyl ether was added, the organic phase was drained with dry sodium sulfate. The solvent was separated from the solution under vacuum, the resulting raw product was purified with chromatographic column (hexane normal solvent: ethyl acetate 9:1)

- Synthesis of 2-Bromo-5,5-dimethyl 3,1-dioxane

A mixture of 19/78 g of bromoastaldehyde Diethyl acetal and 44/10 g of neopentyl glycol was reacted at a temperature of 90°C and under a relative vacuum for 10 h.

- Synthesis of E2,Z13-octadecadienyl acetate

٠/٧٧ g E2, Z13-octadecadion-ol and 8 ml of anhydride acetic was added and stirred in 70°C overnight. The reaction progression process was followed up with TLC (normal hexane: ethyl acetate 9: 4). After removing the solvent added Diethyl ether, the resulting solution was washed with Sodium bicarbonate solution, 10% hydrochloric acid solution. The organic phase was isolated and drained with dry Sodium sulfate. after removing the solvent, the residue was obtained as white solid (0.73 g), which were purified by a chromatographic column.

Results and Discussion

H_1NMR (500 MHz) of E2,Z13-octadecadien-1-ol acetate: δ 5.77 (dt, 1H), 5.55 (dtt, 1H), 5.4-5.25 (m, 2H), 4.5 (d, 2H), 2.06 (s, 3H), 2.1-1.9 (c, 6H), 1.42-1.2 (c, 18H), 0.89 (t, 3H) ppm; ^{13}C NMR (125 MHz) δ 170.9, 136.7, 129.8 (2C), 123.6, 65.3, 32.2, 31.9, 29.7, 29.54, 29.52, 29.4, 29.3, 29.16, 28.9, 27.2, 26.9, 22.3, 21.0, 13.99 ppm.

References:

١. Baker, T. C., & McNeil, J. N. (2001). Pheromone communication in moths: A review of the role of pheromones in mating behavior. *Journal of Chemical Ecology, 27*(6), 1107-1126. https://doi.org/10.1023/A:1010678718117

٢. El-Sayed, A. M. (2018). The use of pheromone traps for monitoring and controlling insect pests. *Insects, 9*(4), 130. https://doi.org/10.3390/insects9040130

٣. Suckling, D. M., & El-Sayed, A. M. (2012). Pheromone-based management of insect pests: A review. *Pest Management Science, 68*(3), 223-230. https://doi.org/10.1002/ps.2251

٤. Huang, Y. B., & Wu, Y. (2013). Field evaluation of pheromone traps for monitoring Zeuzera pyrina. *Journal of Pest Science, 86*(2), 175-182. https://doi.org/10.1007/s10340-012-0452-5

Core-Shell Strategies for Enhanced Photocatalytic Chromium Reduction: MOF-on-MOF Heterostructures on Steel Mesh

Authors: Nooshin Gholhovallahi Ardakan†, Parsa Azaddehghan†, Negin Khosroshahi, Vahid Safarifard*

Affiliations: Department of Chemistry, Iran University of Science and Technology, Tehran 16846-13114, Iran, E-mail: vsafarifard@iust.ac.ir

Keyword: Metal-organic frameworks; heterojunction; MOF-on-MOF; MOF-801;

Body Text: Integrating Ce-MOFs into MOF-on-MOF heterostructures with Zr-MOFs unlocks significant enhancements in photocatalytic Cr(VI) reduction under visible light. Positioning Ce-MOFs as the outer shell optimizes their activity, achieving near-complete Cr(VI) removal (~100%) within 2 hours at an initial concentration of 5 ppm. Immobilized on steel mesh substrates via a spraying method, these composites exhibit exceptional durability and reusability, with minimal leaching confirmed by ICP-OES analysis. This work presents a scalable, effective approach to designing mesh-based photocatalysts for addressing water purification challenges.

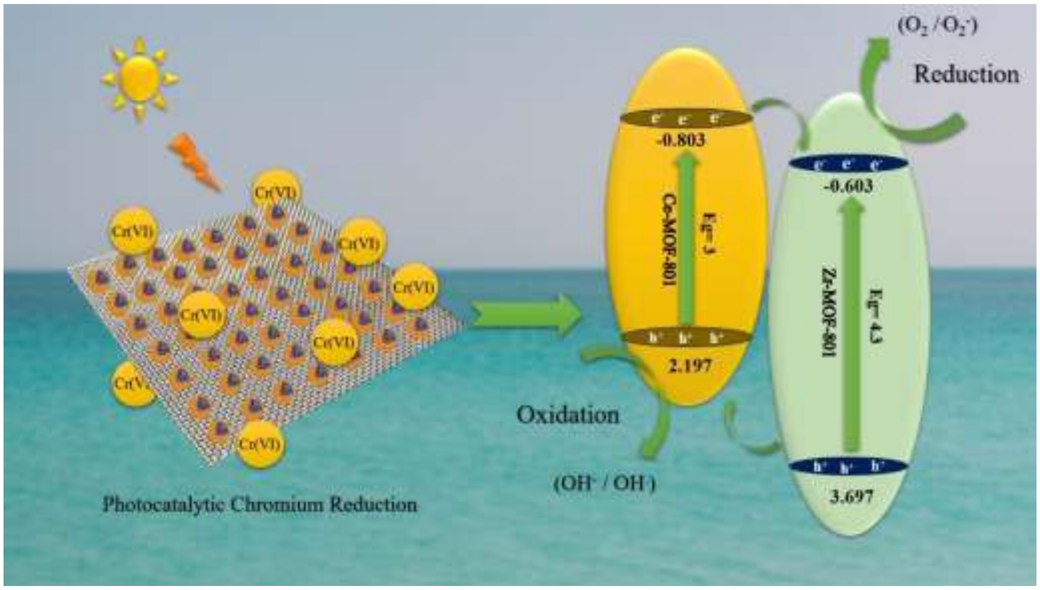

References:

[1] C. Liu, J. Wang, J. Wan, C. Yu, MOF-on-MOF hybrids: Synthesis and applications, Coordination Chemistry Reviews, 432 (2021) 213743.

[2] K. Poonia, S. Patial, P. Raizada, T. Ahamad, A.A.P. Khan, Q. Van Le, V.-H. Nguyen, C.M. Hussain, P. Singh, Recent advances in Metal Organic Framework (MOF)-based hierarchical composites for water treatment by adsorptional photocatalysis: A review, Environmental Research, (2023) 115349.

The 30th Iranian Seminar of Organic Chemistry
February 7-9, 2025, Iran University of Science and Technology, Tehran, Iran

Investigation of dibenzothiophene removal from oil and gas industries using DES/clay composite

Mohammad Gharajedaghi Hargalan, Abdolreza Abri*

Chemistry Department, Faculty of Basic Sciences, Azarbaijan Shahid Madani university, Tabriz, Iran
* E-mail: Ar.abri@yahoo.com

Abstract

The presence of organic sulfides in fuels has become a significant contributing factor to the formation of haze weather. The desulfurization of fuels has become a frontier scientific topic demanding urgent solutions. Research shows that acidic deep eutectic solvents (DESs) can provide a new route for the deep oxidation/extraction desulfurization of fuels because of their cheap and easily obtained raw materials, higher desulfurization efficiencies, environmentally friendly properties and simple synthetic procedures. Through smart design, a series of acidic DESs with different acidities were synthesized. The effects of various factors on the removal rate of dibenzothiophene (DBT) in n-octane simulated oil were investigated which showed a very high efficiency and was used up to six times cyclically. The characterization results of DESs through FT-IR and 1H NMR showed that DESs were formed by hydrogen bonding interaction.

Keyword: Desulfurization, DES(Deep eutectic solvent)

Introduction

The combustion of fuels containing sulfur compounds causes emission of toxic sulfur oxides (SOx), which are a one of the main air pollutants [1]. Due to this fact, many countries have issued stringent standards to control the sulfur content of fuel oil (mainly below 10 mg/L) Nowadays, hydrodesulfurization (HDS) is the most popular commercial technology used for removal of sulfur from fuels. HDS can effectively remove sulfur compounds, however, HDS process is not effective for removing cyclic organic sulfides such as thiophene (T), benzothiophene (BT), dibenzothiophene (DBT) and its derivatives.
In addition, HDS requires large quantities of hydrogen, a high temperature and pressure of the process, and expensive Cobalt–Molybdenum catalysts. This makes HDS a very costly technology for removal of sulfur compounds from fuels. Therefore, many research groups work on the development of new technologies for deep desulfurization, such as adsorptive desulfurization, bio-desulfurization, oxidative desulfurization or extraction. Extractive desulfurization is one of the most popular techniques. It follows from its low cost, high sulfur removal efficiency and simplicity of operation.[2-3]

Experimental

Three component eutectic solvents are synthesized from hydrogen bond binder (HBD) and hydrogen bond killer (HBA) and an acidic part.Simulated oils of dibenzothiophene (DBT), 4-methyldibenzothiophene (4MDBT), 6-4-dimethyldibenzothiophene (4,6-DMDBT) were prepared in n-octane solvent at different concentrations, and then the adsorbent was synthesized inside It was placed and the values and time were checked.

Results and discussion

Variables such as temperature, concentration, time and amount of adsorbent were investigated and using gas chromatography (GC) and UV devices and also by putting in the absorption formula, the amount of absorption of the synthesized adsorbent was interviewed and the results show that it is economical. This method is better than other methods.

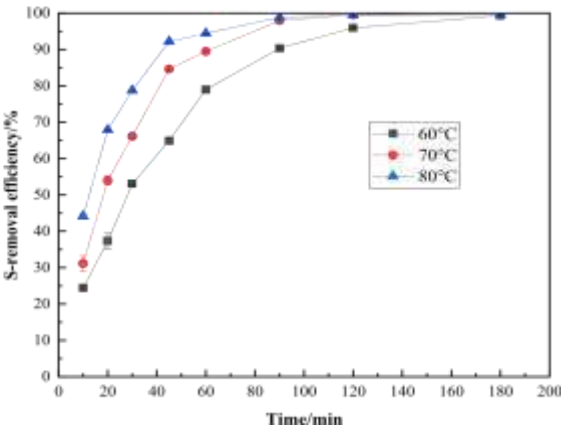

Conclusions

In this research, the adsorbent synthesized from deep eutectic solvents was tested on simulated oils, which had a very good efficiency, and XRD, FTIR, UV and TGA confirm this.

Acknowledgements

We thank the research office of Azarbaijan Shahid Madani University for financial support.

References

[1] International Energy Agency, Energy and air pollution, world energy outlook special report, https://www.iea.org/publications/freepublications/publication/WorldEnergyOutlookSpecialReport2016EnergyandAirPollution.pdf, Accessed date: 17 September 2018.

[2] S.A. Dharaskar, K.L. Wasewar, M.N. Varma, D.Z. Shende, K.K. Tadi, C.K. Yoo, Synthesis, characterization, and application of novel trihexyltetradecylphosphoniumbis (2,4,4-trimethylpentyl) phosphinate for extractive desulfurization of liquid fuel, Fuel Process. Technol. 123 (2014) 1–10, https://doi.org/10.1016/j.fuproc.2014.02.001.

[3] C.F. Mao, R.X. Zhao, X.P. Li, X.H. Gao, Trifluoromethanesulfonic acid-based DESs as extractants and catalysts for removal of DBT from model oil, RSC Adv. 7 (2017) 12805–12811, https://doi.org/10.1039/C6RA28448E.

The 30th Iranian Seminar of Organic Chemistry
February 7-9, 2025, Iran University of Science and Technology, Tehran, Iran

Magnetic Carboxymethyl Cellulose/Metformin-Based Hydrogel for Removal of Organic Pollutant from Environment

Authors: Shima Soltani, Zahra Nezafat, Akbar Mirzaei, Shahrzad Javanshir*

Keywords: Hydrogel, Organic pollutants, Reduction, Metformin, Carboxymethyl cellulose

Abstract

This study presents the synthesis and characterization of a magnetic carboxymethyl cellulose/metformin-based hydrogel (Fe_3O_4-CMC-Met-Cu (II)) for removal of organic pollutants, specifically targeting methylene blue (MB), Rhodamine B (RhB), and 4-nitrophenol (4-NP), which are significant environmental contaminants due to their toxicity and persistence. The hydrogel was thoroughly analyzed using various techniques, including field emission scanning electron microscopy (FE-SEM) and X-ray diffraction (XRD) analyses. The removal of organic pollutants were followed using ultra violet (UV) spectroscopy. This research highlights the innovative use of carboxymethyl cellulose and metformin in developing magnetic hydrogels, offering a promising solution for effective pollutant removal and contributing to the advancement of sustainable environmental cleanup technologies.

1. Introduction

Water contamination by organic pollutants has become a critical environmental issue, necessitating the development of efficient purification methods [1]. The rising levels of organic pollutants, such as industrial dyes and pharmaceutical residues, in water bodies have led to an increased demand for effective and eco-friendly water purification materials [2]. One promising approach in pollutant removal is the combination of adsorption with reduction processes. The advantages of this dual functionality include enhanced removal efficiency and the facilitation of recovery and reuse of the adsorbent material. Integrating reduction processes with adsorption can significantly improve the overall effectiveness of pollutant removal, as the reduced forms of pollutants often exhibit lower solubility and mobility in water [3]. Various catalysts have been utilized for reduction processes in water treatment, including noble metals like palladium, platinum, and gold, known for their high catalytic efficiency in reducing contaminants [4-5]. Despite their effectiveness, these catalysts often suffer from high costs and potential environmental concerns related to metal leaching. In the quest for more sustainable and cost-effective solutions, hydrogels have emerged as promising materials in water purification [6]. Hydrogels, particularly those based on carboxymethyl cellulose (CMC), offer several advantages over traditional catalysts [7]. CMC, a derivative of cellulose, is widely recognized for its biocompatibility, biodegradability, and excellent hydrophilicity. These properties make CMC an attractive candidate for hydrogel formation [8].

This study aims to develop and evaluate a novel Fe_3O_4-CMC-Met-Cu (II) hydrogel for its effectiveness in removal of organic pollutants from water. The incorporation of metformin is hypothesized to provide additional adsorption sites, enhancing the hydrogel's performance. The CMC-based hydrogels are synthesized with embedded magnetic nanoparticles and metformin, then characterized using techniques such as FE-SEM and XRD analyses.

2. Method

2.1 Chemicals and devices

All chemical materials were bought from Merck and Aldrich Co. The XRD and FE-SEM analyzes were accomplished on a Philips X'Pert diffractometer and TESCAN MIRA4 respectively.

2.2 Synthesis of Carboxymethyl Cellulose/Metformin Hydrogel

To synthesize the carboxymethyl cellulose/metformin hydrogel, 0.3 g of CMC was mixed with 10 mL of distilled water and stirred at room temperature for 30 min. In a separate container, 0.006 g of metformin was dissolved in 0.5 mL of distilled water [9]. The two solutions were then combined, and 1 mL HCl (1 M) was added to the mixture. The resulting mixture was stirred at 60°C for 3 h to ensure the reaction was complete. The formed hydrogel was washed repeatedly with a mixture of water and ethanol in a 2.5:1 ratio until the pH reached 7.

2.3 Synthesis of Fe_3O_4-CMC-Met-Cu (II) Hydrogel

The neutralized hydrogel from the previous stage was combined with 0.5 g of iron (II) chloride, 0.135 g of iron (III) chloride, 25 mL of distilled water, and 7.5 mL of ammonia solution in a flask. The mixture was stirred under an argon atmosphere at 60 °C. After 2 h, the reaction mixture was washed with water and ethanol in a 1:1 ratio and the magnetic hydrogel was dried at 60°C.

Subsequently, 0.117 g of copper(II)chloride was dissolved in 0.5 mL of distilled water. Then, 0.234 g the magnetic hydrogel obtained from the previous step, 25 mL of distilled water, and 25 mL of ethanol were placed in a flask and dispersed using an ultrasonic device. The copper(II)chloride solution was then added to the dispersed mixture and refluxed at 78 °C for 24

h. The reaction mixture was washed with water and ethanol in a 1:1 ratio and dried in an oven at 60 °C. The schematic of the synthesis process for the Fe_3O_4-CMC-Met-Cu (II) hydrogel and its structural schematic are shown in Figure 1.

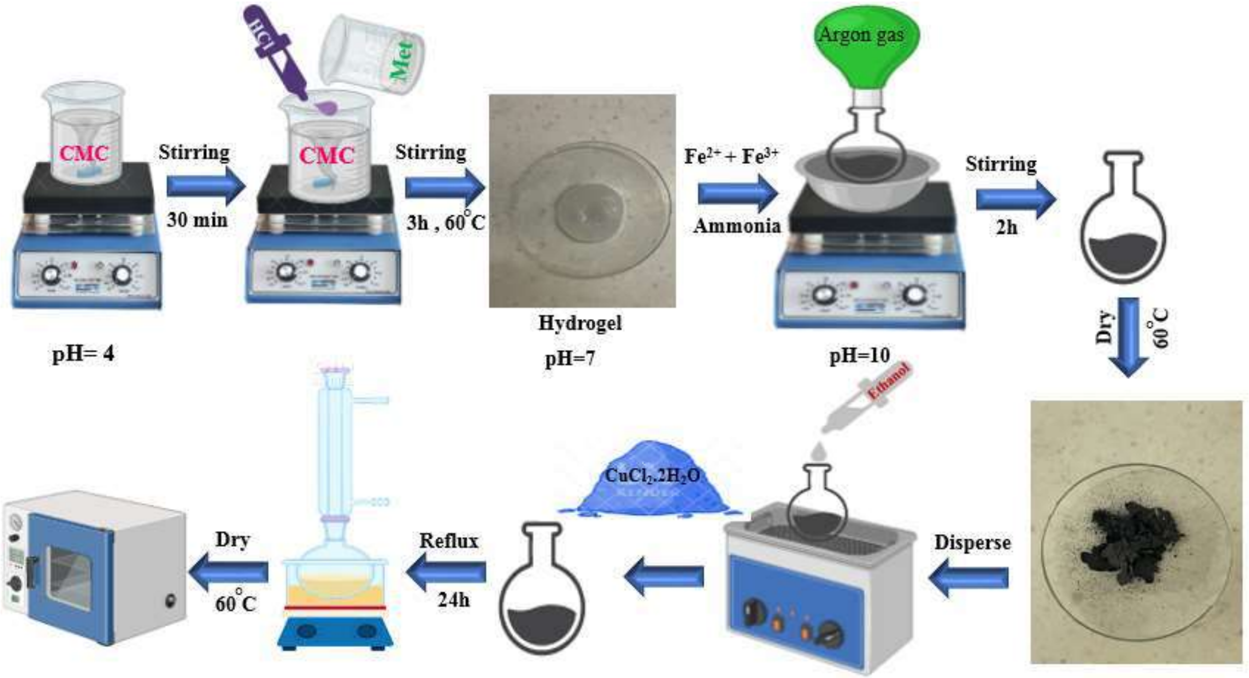

Figure 1. Schematic synthesis of the Fe_3O_4-CMC-Met-Cu (II) hydrogel

2.4 Reduction of Methylene Blue

A total of 0.005 g of the catalyst was added to 12.5 mL of methylene blue solution (100 ppm). Subsequently, 1 mL of freshly prepared sodium borohydride solution (0.05 M) was added to initiate the reduction reaction, and the mixture was stirred at room temperature. The blue color of the solution disappeared and turned colorless within 100 sec. After the reaction was completed, the catalyst was separated using an external magnet, and the changes in the adsorbance of the solution were measured using a UV-Vis spectrophotometer.

2.5 Reduction of Rhodamine B

A total of 0.01 g of the catalyst was added to 25 mL of rhodamine B solution (9.6 ppm). Subsequently, 1 mL of freshly prepared sodium borohydride solution (0.0052 M) was added to initiate the reduction reaction, and the mixture was stirred at room temperature. The purple color of the solution disappeared and turned colorless within 180 sec. After the reaction was completed, the catalyst was separated using an external magnet, and the changes in the adsorbance of the solution were measured using a UV-Vis spectrophotometer.

2.6 Reduction of 4-nitrophenol

A total of 0.01 g of the catalyst was added to 25 mL of 4-nitrophenol solution (350 ppm). Subsequently, 1 mL of freshly prepared sodium borohydride solution (0.249 M) was added to initiate the reduction reaction, and the mixture was stirred at room temperature. After the reaction was completed, the catalyst was separated using an external magnet, and the changes in the adsorbance of the solution were measured using a UV-Vis spectrophotometer.

3. Results and Discussion

3.1 Characterization of hydrogel

For characterization of the synthesized hydrogel we used XRD and FE-SEM analyses. The XRD pattern of the Fe_3O_4-CMC-Met-Cu (II) hydrogel indicates the presence of CMC and metformin (Figure 2). Specific peaks are seen at 2θ= 10.2, 11.2, 17.0, 19.0, 23.2, 25.2 and 27.3º which are related to crystalline metformin in hydrogel [10]. Furthermore, peaks related to magnetic particles are observed at 2θ= 30, 35, 43, 55, 58, 63, and 75º, confirming the presence of magnetic particles within the hydrogel (JCPDS Card No. 19-0629) [11].

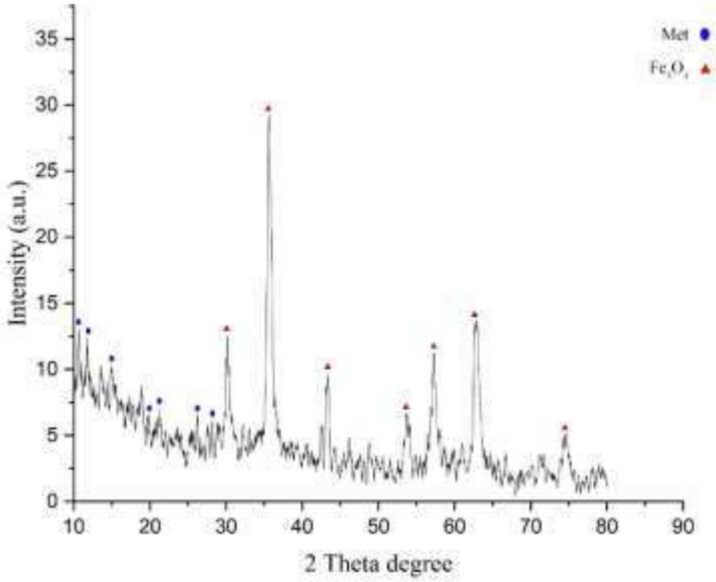

Figure 2. XRD pattern of the Fe_3O_4-CMC-Met-Cu (II) hydrogel

The FE-SEM images of the Fe_3O_4-CMC-Met-Cu (II) hydrogel are shown in Figure 3. The high-magnification image reveals a dense and porous network of small, nearly spherical particles with a rough and irregular surface, characteristic of typical hydrogels.

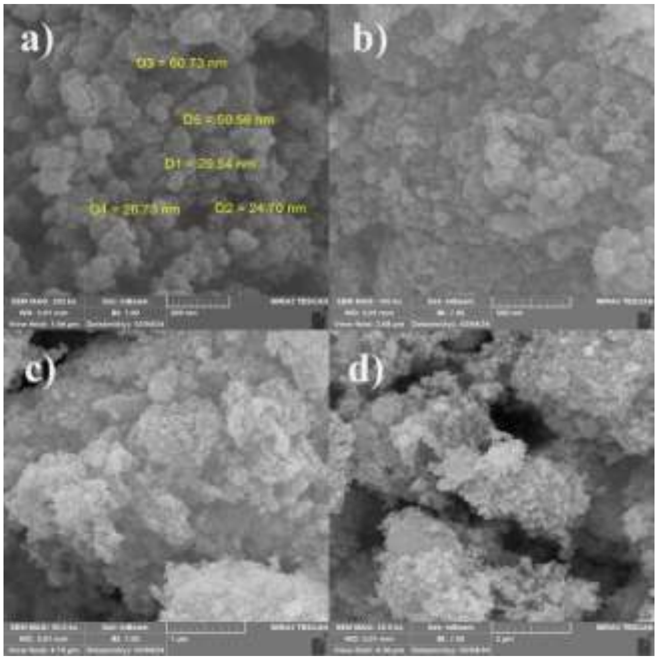

Figure 3. The FE-SEM images of the Fe_3O_4-CMC-Met-Cu (II) hydrogel.

3.2 Reduction of MB and RhB

For the reduction of MB and RhB solutions, the results indicate a direct correlation between the amount of catalyst and the reduction of MB. As shown in Table 1, increasing the amount of catalyst from 0.001 g to 0.005 g decreases the reduction time of MB from 4 seconds to "immediately," achieving reduction in a significantly shorter duration. In addition, as shown in Table 2, increasing the amount of catalyst from 0.005 g to 0.01 g decreases the reduction time of RhB from 5 min to 3 min. The UV-visible analyses of the MB and RhB displayed in Figure 4.

Table 1. The optimization of the amount of catalyst for reduction of MB.

Entry	$NaBH_4$ (M)	Catalyst (g)	Time (s)
1	0.5	0	12 h (No Reaction)
2	0	0.001	12 h (No Reaction)

3	0.5	0.001	4
4	0.5	0.002	4
5	0.5	0.003	3
6	0.5	0.004	2
7	0.5	0.005	Immediately

Table 2. The optimization of the amount of catalyst in the presence of reducing agent in reduction of RhB

Entry	$NaBH_4$ (M)	Catalyst (g)	Time (min)
1	0.005	0	720 (No Reaction)
2	0	0.005	720 (No Reaction)
3	0.005	0.005	5
4	0.005	0.007	4
5	0.005	0.009	3
6	0.005	0.01	3

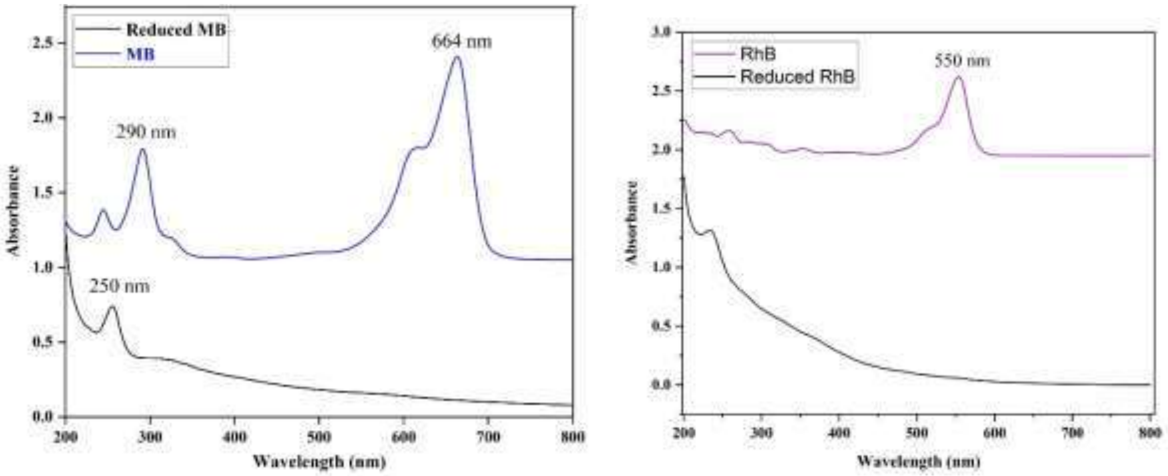

Figure 4. The V-Vis spectra of the (left) MB and (right) RhB.

3.3 Reduction of 4-NP

As shown in Table 3, increasing the amount of catalyst from 0.004 g to 0.01 g decreases the reduction time of nitrophenol from 8 minutes to 3 minutes, achieving reduction in a significantly shorter duration. These results indicate that increasing the catalyst amount reduces the reduction time, highlighting the importance of the catalyst in the process. The UV-visible spectrum was shown in Figure 5.

Table 3. The optimization of the amount of catalyst in the presence of reducing agent in reduction of 4-NP.

Entry	$NaBH_4$ (M)	Catalyst (g)	Time (min)
1	0.2	0	720 (No Reaction)
2	0	0.004	720 (No Reaction)
3	0.2	0.004	8
4	0.2	0.006	7
5	0.2	0.008	4
6	0.2	0.01	3

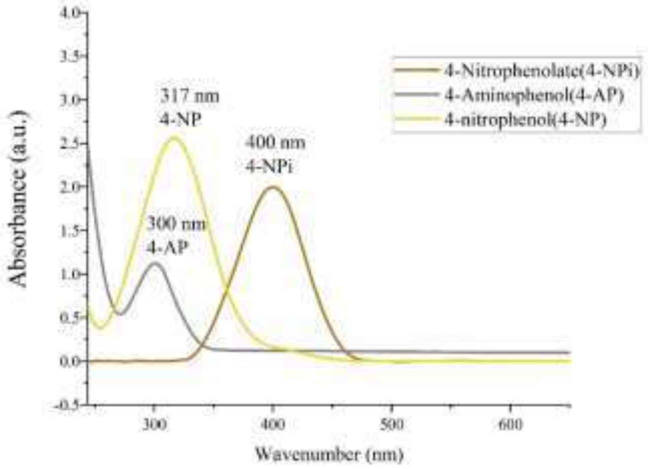

Figure 5. UV-Vis spectrum of nitrophenol and reduced 4-NP.

4. Conclusion

In this study, a magnetic hydrogel composed of carboxymethyl cellulose, metformin, and copper (II) was synthesized using a facile method. This hydrogel exhibits high performance for removal of the organic pollutants from aqueous solutions through the reduction of pollutants, as confirmed by UV-Vis spectroscopy. The hydrogel's characteristics were confirmed using various techniques, demonstrating its magnetic structure and the successful integration of magnetic nanoparticles and hydrogel. These attributes enhance the hydrogel's thermal and mechanical stability, improving its recyclability and reusability. The key findings indicate that the hydrogel is highly efficient in reducing NB, RhB and 4-NP.

References

[1] R. Kumar, M. Qureshi, et al. A review on emerging water contaminants and the application of sustainable removal technologies. *Case Studies in Chemical and Environmental Engineering*. 2022, 6, 100219.

[2] F. Lu and D. Astruc Nanocatalysts and other nanomaterials for water remediation from organic pollutants. *Coordination Chemistry Reviews*. **2020**, 408, 213180.

[3] J. Pathak and P. Singh Ultrafast catalytic reduction of organic pollutants using ternary zinc–copper–nickel layered double hydroxide. *Applied Organometallic Chemistry*. **2024**, 38, e7507.

[4] M. Danish, W.A. Khanday, et al. Application of optimized large surface area date stone (Phoenix dactylifera) activated carbon for rhodamin B removal from aqueous solution: Box-Behnken design approach. *Ecotoxicology and environmental safety*. **2017**, 139, 280-290.

[5] B.C. Choudhary, D. Paul, et al. Photocatalytic reduction of organic pollutant under visible light by green route synthesized gold nanoparticles. *Journal of Environmental Sciences*. **2017**, 55, 236-246.

[6] N. Bogireddy, U. Pal, et al. Green fabrication of 2D platinum superstructures and their high catalytic activity for mitigation of organic pollutants. *Catalysis Today*. **2021**, 360, 185-193.

[7] İ. Gözeten and M. Tunç Palladium nanoparticles supported on activated carbon (C) for the catalytic hexavalent chromium reduction. *Water, Air, & Soil Pollution*. **2022**, 233, 1-14.

[8] B. Kumar Green synthesis of gold, silver, and iron nanoparticles for the degradation of organic pollutants in wastewater. *Journal of Composites Science*. **2021**, 5, 219.

[9] Q. Ma, W. Wang, et al. Preparation of carboxymethyl cellulose-based hydrogel supported by two-dimensional montmorillonite nanosheets for methylene blue removal. Journal of Polymers and the Environment. 2021, 29, 3918-3931.

[10] İ. Gözeten and M. Tunç Palladium nanoparticles supported on activated carbon (C) for the catalytic hexavalent chromium reduction. Water, Air, & Soil Pollution. 2022, 233, 1-14.

[11] F. Fahim, A. Naseer, et al. A green approach for the determination of selected anti-diabetic drugs in pharmaceutical formulation by transmission FTIR spectroscopy. Journal of the Brazilian Chemical Society. 2014, 25, 2032-2038.

[13] K. Yang, X. Li, et al. Facile synthesis of novel porous graphene-like carbon hydrogel for highly efficient recovery of precious metal and removal of organic dye. *Applied Surface Science*. 2020, 528, 146928.

[14] P.O. Oladoye, T.O. Ajiboye, et al. Methylene blue dye: Toxicity and potential elimination technology from wastewater. *Results in Engineering*. **2022**, 16, 100678.
[15] N. Malatji, E. Makhado, et al. Synthesis and characterization of magnetic clay-based carboxymethyl cellulose-acrylic acid hydrogel nanocomposite for methylene blue dye removal from aqueous solution. *Environmental Science and Pollution Research*. **2020**, 27, 44089-44105.
[16] T. Guo, X. Fan, et al. Engineering shape of BiOCl nanosheets with improved visible-light response for superior photocatalytic degradation of Rhodamine B. *Journal of Alloys and Compounds*. **2023**, 948, 169586.
[17] A. Balakrishnan, G.J. Gaware, and M. Chinthala Heterojunction photocatalysts for the removal of nitrophenol: A systematic review. *Chemosphere*. **2023**, 310, 136853.
[18] I. Al-Qadsy, W.S. Saeed, et al. Novel metformin-based schiff bases: synthesis, characterization, and antibacterial evaluation. *Materials*. **2020**, 13, 514.
[19] C.B. Godiya, X. Cheng, et al. Carboxymethyl cellulose/polyacrylamide composite hydrogel for cascaded treatment/reuse of heavy metal ions in wastewater. *Journal of hazardous materials*. 2019, 364, 28-38.
[20] J. Ning, X. Luo, et al. Synergetic sensing effect of sodium carboxymethyl cellulose and bismuth on cadmium detection by differential pulse anodic stripping voltammetry. *Sensors*. **2019**, 19, 5482.
[21] Y.A. Faleh and N.D. Radhy Removal of Metformin hydrochloride from Aqueous Solutions by using Carboxymethyl cellulose-g-poly (acrylic acid-co-acrylamide) Hydrogel: Adsorption and Thermodynamic Studies. IOP Conference Series: Earth and Environmental Science. 2021, 790, 012062
[20] E.P. Rebitski, P. Aranda, et al. Intercalation of metformin into montmorillonite. *Dalton Transactions*. **2018**, 47, 3185-3192.
[21] H. Shagholani, S.M. Ghoreishi, and M. Mousazadeh Improvement of interaction between PVA and chitosan via magnetite nanoparticles for drug delivery application. *International journal of biological macromolecules*. **2015**, 78, 130-136.

The 30th Iranian Seminar of Organic Chemistry
February 7-9, 2025, Iran University of Science and Technology, Tehran, Iran

Effect of encapsulated sulfur toxicity on **S.aureus**

Firouzeh Yazdian Hossein Pour [A] , Esmaeil Rezaei Seresht [*A] ,Zahra Yazdan Panah[a], Eisa Kohan_Baghkheirati[b] ,Nafiseh Nemat_Shahi[b]

[a] *Department of Chemistry, Faculty of Science, Hakim Sabzevari University, Sabzevar, Iran*

[b] *Department of Biology, Faculty of Science, Hakim Sabzevari University, Sabzevar, Iran*

Email: e.rezaei@hsu.ac.ir

Keyword: 2-Hydroxy propyl-β-cyclodextrin , Sulfur, S.aureus

Introduction :

Elemental sulfur exists mainly as octa-sulfur. S_8 has low solubility in water (~19nM) .It has biologically accessible oxidation states from -2 to +6. Elemental sulfur is widely used as a diseases, and entering inhibits the electron transport chain for respiration by modifying thiol groups of important proteins (Glutathione).

Cyclodextrins are cyclic oligosaccharides consisting of a series of α-D-glucopyranose subunits joined by α-1,4-glycosidic bonds. Geometrically, CDs are distinguished by their hydrophilic circular truncated cone shape. This cavity(for β 262 $Å^3$) is suitable for the inclusion of appropriately sized hydrophobic guest molecules

Method :

Different concentrations of 2HPβCD/S_8 complexe in aqueous solution were synthesized at room temperature to investigate the effect of its toxicity on the strain of this bacterium.
S. aureus were grown in lysogeny broth (LB) at 37 centigrade with shaking. Fresh cells of S. aureus was grown overnight at 37 centigrade with shaking. The cells were transferred into 0/4 mL fresh medium in a 48-well plate. Sulfur complex at 0.2 and 0.5 mM concentrations were mixed with the cultures. Growth curves were plotted by measured OD600nm after incubating the plate in a microplate reader for 24 hours.

Results and Discussion :

These sulfur particles with a very small size in the angstrom range (~149 $Å^3$) were complexed with 2 hydroxy propyl β cyclodextrin, which causes more dissolution in the aqueous environment, more effectiveness with increasing concentration and increased degradation rate in S.aureus.

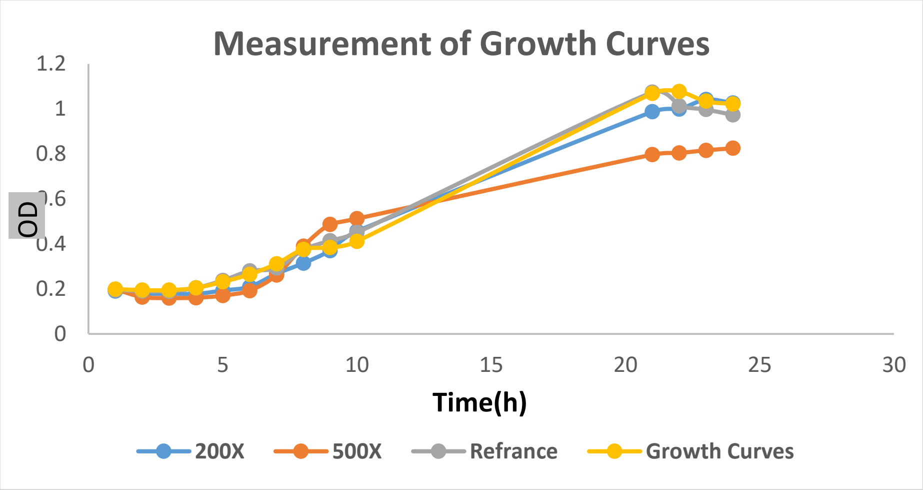

Fig 1: Measurement of Growth Curves for S.aureus

By increasing the concentration of sulfur complex, the rate of bacterial growth decreased compared to its normal growth. This result was obtained by decreasing the amount of OD according to the graph

References:

١. Poulson BG, Alsulami QA, Sharfalddin A, El Agammy EF, Mouffouk F, Emwas A-H, et al. Cyclodextrins: Structural, chemical, and physical properties, and applications. Polysaccharides. 2021;3(1):1-31.

٢. Wang T, Yang Y, Liu M, Liu H, Liu H, Xia Y, et al. Elemental sulfur inhibits yeast growth via producing toxic sulfide and causing disulfide stress. Antioxidants. 2022;11(3):576

The 30th Iranian Seminar of Organic Chemistry
February 7-9, 2025, Iran University of Science and Technology, Tehran, Iran

Preparation of magnetic nanoparticles modified with the amino acid tryptophan for drug delivery of riluzole

Authors: Shantia Mohammadzade [a], Atefeh Tamaddon [a*](corresponding author), Elham Moniri [b]

[a]*Department of Chemistry, Central Tehran Branch, Islamic Azad University, Tehran, Iran*

[b]*Department of Chemistry, Varamin (Pishva) Branch, Islamic Azad University, Tehran, Iran*

Keyword: riluzole, drug delivery, ALS, magnetic nanoparticles, tryptophan

Introduction :ALS (Amyotropic Latral Sclerosis) is a neurodegenerative disease that, in its advanced stages, leads to the death of the patient by the loss of vital muscles. A drug called Riluzole has been on the market since the 1990s to treat the disease.

Magnetic nanoparticles, as one of the pioneers in the pharmaceutical field, have attracted the attention of many medical researchers due to their limited harm, low toxicity, and various synthesis methods from simple and cost-effective materials. In the last few decades, the use of these nanoparticles and their surface modification with compounds for drug delivery to different parts of the body, including the brain and central nervous system, have been studied and investigated.

New approaches can improve the delivery of therapeutic molecules that are large in size or hydrophobic drug molecules. One strategy to enable the delivery of biologic drugs to the brain is to use nanoparticles encapsulated with large, hydrophobic molecules. In addition, specific antibodies can bind to the transferrin receptor on the surface of nanoparticles, enabling their targeted transport across the BBB (Blood Brain Barrier).

In this study, magnetic nanoparticles were prepared by co-precipitation method and their surface was modified with the amino acid tryptophan, which is a biocompatible protein. This surface modification was performed in 4 steps and at the end of each step, the results were evaluated by performing the tests such as; FTIR, TGA, SEM, EDX. After that, the drug was adsorbed and released by the synthesized nanosorbent and the study conditions were optimized.

Method: -Synthesis of the adsorbent: The desired adsorbent was synthesized in 4 steps:

Step 1: Synthesis of magnetic nanoparticles Fe_3O_4 by co-precipitation method.

Step 2: Coating with tetraethyl orthosilicate

Step 3: Creation of the epoxy structure

Step 4; Polymerization of Magnetic Nanostructure. For this part, the amino acid L-Tryptophan was chosen for polymerization.

At the end of each step, the necessary identification tests such as FTIR, TGA, SEM, EDX were performed to ensure that the desired product was obtained. For example, the SEM image for the final adsorbent (last step) can be seen in Figure 3.

-Investigating the variables affecting the drug adsorption process:

The optimal pH, temperature and time for the adsorption for a 20 mg/L solution of riluzole on 0.01 g of the synthesized adsorbent were obtained, and then the drug release in a simulated blood environment was investigated.

Results and Discussion:

From the results, it can be concluded that the synthesized adsorbent can be effective in delivering riluzole to the target tissue of this drug, which is the brain and nervous system, but more extensive studies are needed to reach certainty in this field. Because riluzole and its mechanism of action have not yet been fully identified and determined. This issue leads the work towards further research and synthesis.

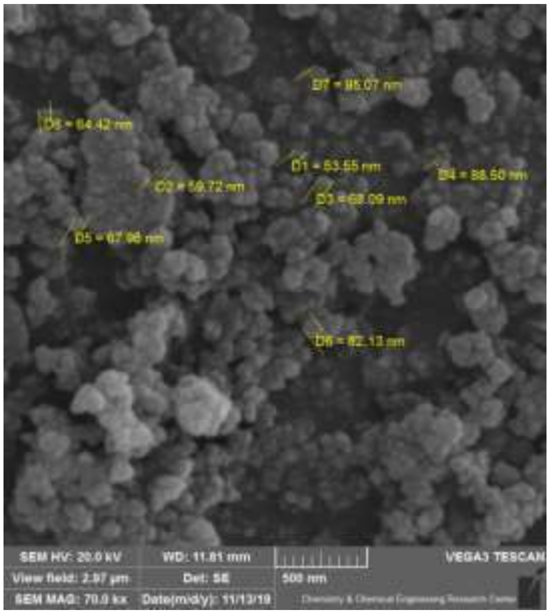

Fig. 3. SEM image of nanoparticles after coating with L-Tryptophan

References:

١- Gupta AK[1], Gupta M, Synthesis and surface engineering of iron oxide nanoparticles for biomedical applications,Biomaterials,2005,Volume 18,Pages:3995-4021

٢- Thi Kieu HanhTa,Minh-ThuongTrinh,Nguyen VietLong,Thi Thanh MyNguyen,Thi Lien ThuongNguyen[c]Tran LinhThuoc[b]Bach ThangPhan, DerrickMott, ShinyaMaenosono, HieuTran-Van,Van HieuLe, Synthesis and surface functionalization of Fe3O4-SiO2 core-shell nanoparticles with 3-glycidoxypropyltrimethoxysilane and 1,1′-carbonyldiimidazole for bio-applications,Colloids and Surfaces A: Physicochemical and Engineering Aspects,2016,Volume 504,Pages:376-383

٣- Sophie Laurent, Delphine Forge, Marc Port, Alain Roch, Caroline Robic, Luce Vander Elst and Robert N. Muller, Magnetic Iron Oxide Nanoparticles: Synthesis, Stabilization, Vectorization, Physicochemical Characterizations, and Biological Applications, Chemical Review, June 2008, Volume 108, Pages:2064–2110

٤- Massimo Masserini,Nanoparticles for Brain Drug Delivery,ISRN Biochemistry,2013,Volume 2013,Pages:685-700

٥- Louiza Bohn Thomsen,Maj Schneider Thomsen & Torben Moos, Targeted drug delivery to the brain using magnetic nanoparticles,Theraputic Delivery,2015,Volume 10,Pages:1145-1155

The 30th Iranian Seminar of Organic Chemistry
February 7-9, 2025, Iran University of Science and Technology, Tehran, Iran

Investigation and environmental effects of petroleum polyaromatic hydrocarbons (PAHs) in the Caspian Sea

Hadi babaei*,Siamak baghari

Agricultural Research, Education and Extension Organization (AREEO), Iranian Fisheries Science Research Institute, Inland Waters Aquaculture Research Center,Bandar Anzali, Iran

Abstracts

Polycyclic aromatic compounds(PAHs) are considered as priority organic compounds pollutants worldwide due to their high toxicity.These are the pollutants of soil and water which are very dangerous and lethal for the aquatic ecosystem.The presence or high level of PAHs is harmful for marine organisms and human health because these types of compounds have different properties such as toxicity, mutogenic, carcinogenic and estrogenic.In this study, the amount of petroleum compounds Naphthalene, Anthracene, Pyrene and Phenanthrene in the water and surface sediments of the Caspian Sea in Astara and Bandar Anzali regions were measured according to the ISIRI-18351 standard.Water samples were separated by liquid-liquid extraction method using normal hexane solvent and sediment samples after drying using solvent mixture (normal hexane and dichloromethane) by Soxhlet method and using gas mass chromatography (GC/MS) device was measured.The results showed that the maximum amount of Naphthalene,Anthracene,Pyrene and Phenanthrene compounds in water were 157.7,83.4,31.5 and 98.6 µg/l respectively and in surface sediments were 15.35,6.23,11.27 and respectively 11.76 ng/g was measured.In this research, to determine the origin of PAHs petroleum compounds in sediments, composition ratios were used, based on which the sediments of the study area had both pyrogenic (fuel) and petrogenic (petroleum) origin.The ecological risk (HQ) calculated in water for the petroleum compounds anthracene and pyrene was greater than 1, which indicates the ecological impact on the environment.

Keyword: Oil pollution, surface sediments, ecological risk (HQ), Caspian Sea

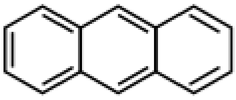
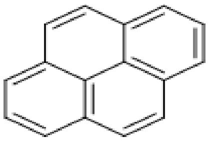
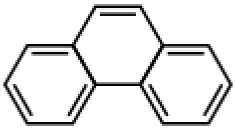

Anthracene Phenanthrene Pyrene

References:

-Mohammadi Zadeh,C.,Saify A and Shalikar, H.2010.Polycyclic Aromatic Hydrocarbons (PAHS) along the Eastern Caspian Sea Coast ,Global Journal of Environmental Research 4 (2):59-63.

- Peng,S.,2015.The nutrient, total petroleum hydrocarbon and heavy metal contents in the seawater of Bohai Bay,China:temporal–spatial variations, sources, pollution statuses, and ecological risks. Marine pollution bulletin, 95(1):445-51.

The 30th Iranian Seminar of Organic Chemistry
February 7-9, 2025, Iran University of Science and Technology, Tehran, Iran

Challenges and opportunities of green chemistry with emphasis on sustainable development

Hadi babaei[a]*,Fatmeh hamdi[b]

[a]Agricultural Research, Education and Extension Organization (AREEO), Iranian Fisheries Science Research Institute, Inland Waters Aquaculture Research Center,Bandar Anzali, Iran
[b]Deparment of Chemistry ,Faculty of Basic Sciences, University of Science and Technology, Tehran,Iran

Abstract

The realities of today's world indicate that countries cannot continue their healthy and optimal lives without paying attention to the issues of sustainable development.Our country is not an exception to this rule, for this reason, many efforts have been made in the last few decades at the international level to move towards sustainable development and to deal with existing and future challenges, and these actions are still ongoing.It is possible to create a balance in the use of natural resources, economic growth and environmental protection through the introduction of a green chemical process whose task is to design chemical processes and products that are harmless to human health and the environment.The concept of green chemistry is based on twelve principles that discuss the reduction or elimination of hazardous or harmful substances from the synthesis, production and use of chemical products, so the use of hazardous substances for human health and the environment is reduced or eliminated.Sustainable chemistry expands the scope of green

chemistry to include social, economic and environmental considerations,while green chemistry guarantees the achievement of these goals from a technical point of view.In this regard, legal and legal support and provision of financial resources for green chemistry training and implementation of green projects are essential prerequisites to make the path to sustainable development smoother.In our country, considering the large number of students and the high potential for working in environmental fields, it seems that by investing in green chemistry education in schools and universities and then on a wider level in society, it is possible to contribute to the development of green chemistry in the society and, accordingly, to sustainable development.

Keywords:Green chemistry, environment, challenges, schools, sustainable development

References:
- Anastas,P.T., & Warner, J. C. 1998.Green chemistry: theory and practice. New York: Oxford University.
- Collins,T. J. 2017. Review of the twenty-three year evolution of the first university course in green chemistry: teaching future leaders how to create sustainable societies. Journal of Cleaner Production, 140, 93–110.
- Welton, T. 2018. UN Sustainable Development Goals: How can sustainable/green chemistry contribute? There can be more than one approach. Current Opinion in Green and Sustainable Chemistry, 13, A7–A9.

The 30th Iranian Seminar of Organic Chemistry
February 7-9, 2025, Iran University of Science and Technology, Tehran, Iran

A new, efficient and green method for the synthesis of bis-indole derivatives using Equisetum arvense@$FeCl_3$

AMIR ABAS HAGHPANAH, SEYED MOHAMMAD VAHDA*

Department of Chemistry, Ayatollah Amoli Branch, Islamic Azad University, Amol, Iran

Keyword: Bis(indolyl)methane, E. arvenseA@$FeCl_3$, Green solid acid Catalyst, Aldehydes.

Bisindolylmethanes are one of the most important heterocyclic compounds that have many applications, including in organic syntheses and biological properties [1]. The most common process and some catalysts have been applied for this transformation containing {Fe_3O_4@SiO_2@$(CH_2)_3$-Urea-SO_3H/HCl} [2], $[MIMPS]_3PW_{12}O_{40}$ and $[TEAPS]_3PW_{12}O_{40}$ [3].

As part of our continuing program focused on the improvement of facile approaches in organic reactions [4], In the present study, we introduce a new catalyst named E. arvenseA@$FeCl_3$ as green solid acid catalyst for the efficient synthesis of bis(indolyl)methanes. The reaction of indole (1) with aldehydes (2) in ethanol afforded the corresponding bis(indolyl)methanes (3) in excellent yields (Fig. 1).

This reaction has been carried out in the presence of 20 mg of catalyst at room temperature. The reusability of the catalyst was demonstrated by a three-run test. Additionally, the catalyst poses several advantages including mild reaction conditions, cleaner reactions and shorter reaction times.

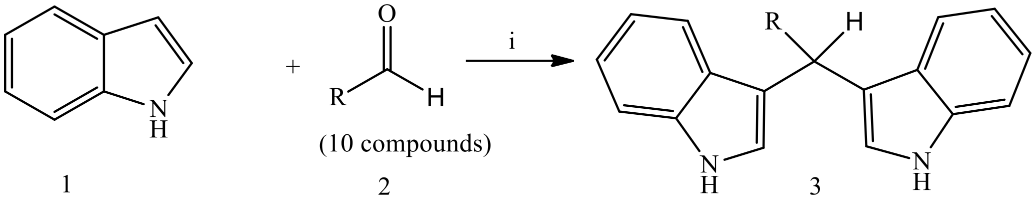

i= E. arvenseA@$FeCl_3$ (20 mg), C_2H_5OH (10 mL), r.t.

Fig. 1. Synthesis of bis(indolyl)methanes catalyzed by E. arvenseA@$FeCl_3$

References:

1. Athavale R., Gardi S., Choudhary F., Patil D., Chandan N., More P., (2024), Novel acidic ionic liquid [BEMIM][HSO4]: A highly efficient and recyclable catalyst for the synthesis of bis-indolyl methane derivatives, *Appl. Catal. A.* 669: 119505.

2. Zolfigol M. A., Ayazi-Nasrabadi R., Baghery S., (2016), The first urea-based ionic liquid-stabilized magnetic nanoparticles: An efficient catalyst for the synthesis of bis(indolyl)methanes and pyrano[2, 3-*d*] pyrimidinone derivatives. *Appl. Organometal. Chem.* 30: 273-281.

3 Vahdat S. M., Khaksar S., Baghery S., (2012), Sulfonated organic heteropolyacid salts: Recyclable green solid catalysts for the highly efficient and green synthesis of bis(indolyl)methanes in Water. *Lett. Org. Chem.* 9: 138-144.

۳. Chekin F., Vahdat S. M., Asadi M. J., (2016), Green synthesis and characterization of cobalt oxide nanoparticles and its electrocatalytic behavior. *Russ. J. Appl. Chem.* 89: 816-822.

The 30th Iranian Seminar of Organic Chemistry
February 7-9, 2025, Iran University of Science and Technology, Tehran, Iran

A new and efficient method for the oxidation of benzyl alcohols using H_2O_2 with Equisetum arvense@$FeCl_3$

Pardis Banasaz Navaei, Seyed Mohammad Vahda*

Department of Chemistry, Ayatollah Amoli Branch, Islamic Azad University, Amol, Iran

Keyword: Equisetum arvense, H_2O_2, Catalyst, $FeCl_3$, Oxidation of Benzyl Alcohols.

Equisetum arvense (Horse tail) is a medicinal plant that is a relic of prehistoric times and has existed on Earth for millions of years ago. The Equisetum's name is derived from the Latin word Equus meaning "horse" and seta means "hair" referring to tail. Horse tail is an herbaceous, permanent and harness plant with rhizome, and its rhizome carries two types of aerial stems, a stem that is red and appears in the early spring, and another stem that is green and infertile, and grows after the red stem. The medical consumption of the horse's tail is limited to its green stalk. Of course, there are many varieties of this plant in nature that are often not only unprotected but also harmful, but the species E. arvense, which, of course, is found in abundance in humid regions in Iran, has long been used for medical purposes [1].

The horse's tail contains flavonoids, iron oxides, phytosterols, and all kinds of minerals, and many medicines are produced, especially in European countries. Regarding the mineral composition of this plant, its pharmaceutical application in the modern pharmaceutical industry is mainly for the treatment of arthritis and rheumatism. These compounds play an important role in bone strengthening, and therefore sometimes powder from this plant is also used as a treatment for osteoporosis [2,3].

For this purpose, in this research, we try to use this plant as a natural catalyst for the oxidation of benzyl alcohols to the corresponding benzaldehyde derivatives due to the presence of various mineral substances in the horse tail plant. So, we introduce a new catalyst named E. arvenseA@$FeCl_3$ as green solid acid catalyst with H_2O_2 (30%) for the efficient synthesis of benzaldehydes. The reaction of various benzyl alcohol derivatives (1) with E. arvenseA@FeCl$_3$ catalyst and oxygenated water (30%) in CH$_3$CN afforded the corresponding benzaldehyde derivatives (2) in good to excellent yields (Fig. 1).

Also, This reaction has been carried out in the presence of 50 mg of catalyst at room temperature. The reusability of the catalyst was demonstrated by a three-run test. Additionally, the catalyst poses several advantages including mild reaction conditions, cleaner reactions and shorter reaction times.

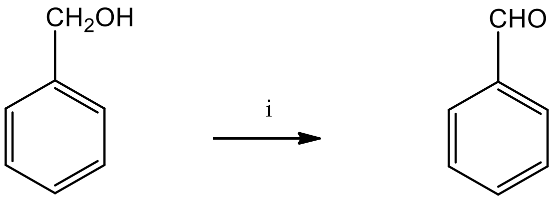

1 2

i= H_2O_2 (30%) (1 mL), E. arvenseA@FeCl$_3$ (50 mg), CH_3CN (10 mL), r.t.

Fig. 1. Synthesis of benzaldehyde derivatives catalyzed by E. arvenseA@FeCl$_3$ and H_2O_2

References:

١. Naccarato M, Yoong D, Gough KA. potential drug-herbal interaction between Ginkgo biloba and efavirenz. J Int Assoc Physicians AIDS Care (Chic). 2012; 11(2): 98–100.

٢. Sandhu NS, Kaur S, Chopra D. Equisetum aervens: Pharmacology and Phytochemistry - A review. Asian J Pharmaceut Clin Res. 2010; 3: 146-150.

٣. Sandhu NS, Kaur S, Chopra D. Pharmacognostic evaluation of Equisetum arvense Linn. Int J PharmTech Res. 2010; 2(2): 1460-1464.

The 30th Iranian Seminar of Organic Chemistry
February 7-9, 2025, Iran University of Science and Technology, Tehran, Iran

Passerini's multicomponent reaction and synthesis of Tris-cyclohexylamino-oxo-benzene 1,3,5-tricarboxylate using Nanocatalyst

Abbas Azimi-Roshan*

Department of Chemistry, Payam Noor University, Tehran, Iran

Keyword: Nanocatalyst, Tris-cyclohexylamino-oxo-benzene-1,3,5-tricarboxylate, Passerini reaction, antibacterial activity.

Isocyanide-based multicomponent reactions (IMCRs), which have been widely used in medicinal chemistry and synthetic chemistry, have become one of the mainstays in MCR chemistry [1]. The P-3CR commonly involves the reaction between carboxylic acids, isocyanides, and oxo components (aldehydes or ketones), followed by the Mumm rearrangement to produce α-acyloxy carboxamide structures in the one-pot conditions [2]. The α-acyloxy carboxamide moiety is often found in compounds with anticancer [3], antibacterial [4], antioxidant [5], HIV-1 inhibitor [6], and herbicidal properties. Therefore, the development of synthetically useful reactions taking place in water is of great interest. Due to the importance of macromolecules, we were interested in the synthesis of triscyclohexylamino- oxo-benzene-1,3,5-tricarboxylates via the Passerini approach under water conditions and Nano sodium bicarbonate (Scheme 1).

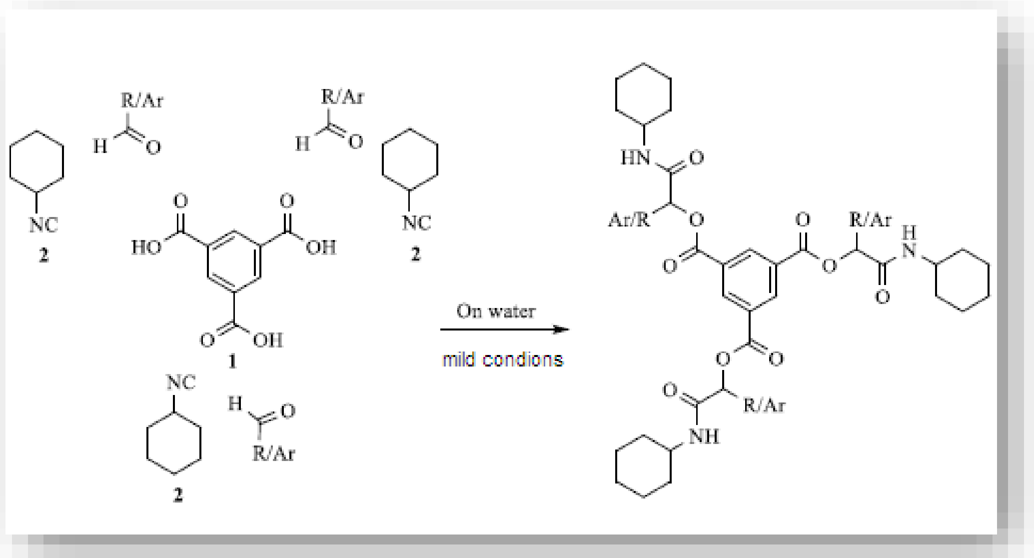

Scheme 1. Multicomponent synthesis of tris-cyclohexylamino-oxo-benzene-1,3,5-tricarboxylates.

In summary, we developed an efficient one-pot, multicomponent protocol for the synthesis of tris-cyclohexylamino-oxobenzene- 1,3,5-tricarboxylates using Nano sodium bicarbonate. The reaction proceeded smoothly and cleanly under Aqueous conditions. Therefore, it is considered to be a green chemistry method. The products were crystallized in ethanol solvent. Relatively faster production of target molecules with acceptable yields, mild reaction conditions, atom economy, and isolation of products using no column chromatography are some advantages of this synthetic method. This method does not use toxic solvents or expensive and time-consuming separation methods. This rapid method produced the products in short reaction times (15–20 min) and excellent yields (80–95 %) at room temperature. The structures of the products were deduced from their elemental analyses and spectroscopic data. Hence, it is considered environmentally friendly. Many compounds synthesized and reported demonstrated antibacterial properties against Gram-positive and Gram-negative species, such as P. aeruginosa and B. subtilis.

References

[1] Bao, L.; Li, M.; Zhang, L.; Xue, Y.; Dong, J.; Xu, X.. Org. Lett., 2023, 25(13), 2366-2371.

[2] Kumar, S.; Arora, A.; Kumar, S.; Kumar, R.; Maity, J.; Singh, B.K. Eur. Polym. J., 2023, 190, 112004.

[3] Ayoup, M.S.; Wahby, Y.; Abdel-Hamid, H.; Abu-Serie, M.M.; Ramadan, S.; Barakat, A.; Teleb, M.; Ismail, M.M.F. RSC Advances, 2023, 13(40), 27722-27737.

[4] Wu, Y.; Cheng, H.; Li, J.; Liu, J.; Sun, J.. J. Org. Chem., 2023, 88(15), 11186-11196.

[5] Wang, R.; Liu, Z.QTetrahedron Lett., 2015, 56(50), 7028-7033.

[6] Gravestock, D.; Rousseau, A.L.; Lourens, A.C.U.; Hoppe, H.C.; Nkabinde, L.A.; Bode, M.L. Tetrahedron Lett., 2012, 53(26), 3225- 3229.

The 30th Iranian Seminar of Organic Chemistry
February 7-9, 2025, Iran University of Science and Technology, Tehran, Iran

Synthesis of isocyanide-based 2-cyclohexylamino-2-oxo-1-arylaethyl/alkylthiophene-3-carboxylates using nanocatalyst

Abbas Azimi-Roshan*

Department of Chemistry, Payam Noor University, Tehran, Iran

Keyword: 2-cyclohexylamino-2-oxo-1-arylaethyl/alkylthiophene-3- carboxylates, Passerini reaction, nanocatalyst, antibacterial activity.

Multicomponent reactions (MCRs) are convergent reactions in which three or more reagents are combined to react in a one-pot procedure and are very efficient synthetic methods [1,2].

Isocyanide-based multicomponent reactions (IMCRs) have been of particular interest because of the large number of starting materials available as well as powerful tools in the modern drug discovery process and allow rapid, automated, and high-throughput generation of organic compounds [3]. The great potential of isocyanides for the development of multicomponent reactions lies in the diversity of bond forming processes available, their functional group tolerance, and the high levels of chemo-, regio-, and stereoselectivity are often observed [4]. MCRs that involve isocyanides are by far the most versatile reactions in terms of scaffolds and number of accessible compounds.Recent advances in the application of IMCRsin drug discovery summarize the various chemo types used to probe biological targets [6].

Therefore, we were interested in the synthesis of 2-cyclohexylamino-2-oxo-1-arylaethyl/alkylthiophene-3- carboxylates via the Passerini approach under mild conditions and using nanocatalyst (Scheme 1).

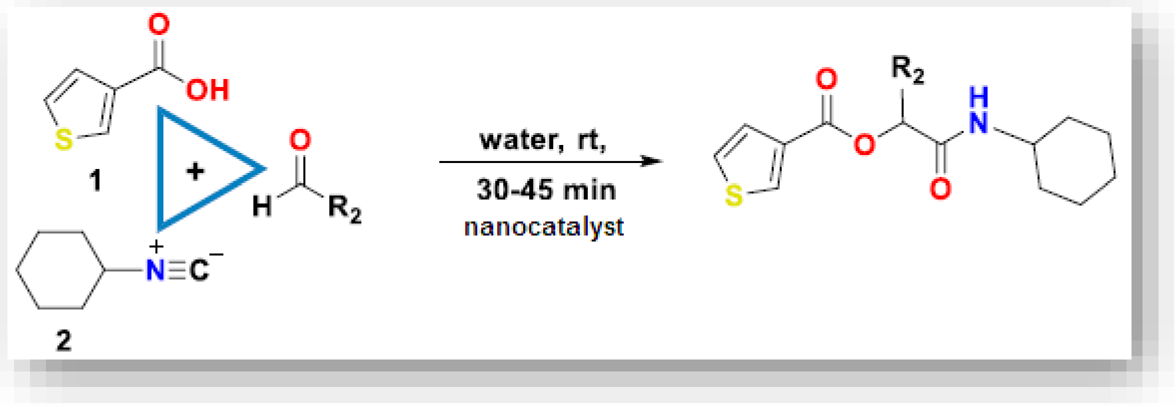

Scheme 1. Multicomponent synthesis of 2-cyclohexylamino-2-oxo-1-arylaethyl/alkylthiophene-3- carboxylates.

After the optimum conditions were successfully achieved, the generality and scope of the one-pot multicomponent reaction were explored. For this purpose, carboxylic acid and cyclohexylisocyanide were reacted with different aldehydes. Due to the special structure of these compounds mentioned above, some of the carbons and other sections of molecules appeared to doublet or multiplet. In molecule 4f, due to the presence of fluorine substituent, the multiplets were enhanced. It is worth noting that ^{1}H NMR and FT-IR spectra, as well as elemental analysis, all confirmed the structure of 2-cyclohexylamino-2-oxo-1-arylaethyl/alkylthiophene-3- carboxylates.

In summary, we developed an efficient one-pot, multicomponent protocol for the synthesis of 2-cyclohexylamino-2-oxo-1-arylaethyl/alkylthiophene-3- carboxylates under mild conditions and using nanocatalyst. The reaction proceeded smoothly and cleanly under mild conditions in water. Therefore, it is considered to be a green chemistry method. The products were crystallized in ethanol solvent. Relatively faster production of target molecules with acceptable yields, mild reaction conditions, atom economy, and isolation of products using no column chromatography are some advantages of this synthetic method. This method does not use toxic solvents or expensive and time-consuming separation methods. Hence, it is considered environmentally friendly. Many compounds synthesized and reported demonstrated antibacterial properties against Gram-positive and Gram-negative species.

References

1. M. Hasan, M. Zaman, A.A. Peshkov, N. Amire, A. Les, A.A. Nechaev, Y. Wang, S. Kashtanov, E.V. Van der Eycken, O.P. Pereshivko, V.A. Peshkov, Eur. J. Org. Chem. 2020 (2020) 3378.

2. E. Soleimani, M. Zainali, S. Samadi, Tetrahedron Lett. 52, 4186 (2011)

3. L. Weber, Curr. Med. Chem. 9, 1241 (2002)

4. M.M. Heravi, S. Moghimi, J. Iran Chem. Soc. 8, 306 (2011)

5. J.E. Biggs-Houck, A. Younai, J.T. Shaw, Curr. Opin. Chem. Biol. 14, 371 (2010)

6. I. Akritopoulou-Zanze, Curr. Opin. Chem. Biol. 12, 324 (2008)

7. P.T. Anastas, J.C. Warner, Green Chemistry: Theory and Practice (Oxford Univ. Press, New York, 1998)

The 30th Iranian Seminar of Organic Chemistry
February 7-9, 2025, Iran University of Science and Technology, Tehran, Iran

$P_2O_5/CuFe_2O_4$ as Magnetically Separable Solid Brønsted Acid Nanocatalyst for Synthesis of 1-Amidoalkyl-2-naphthols

Elnaz Ghafouri[a], Abdolhamid Bamoniri[a,*], Bi Bi Fatemeh Mirjalili[b]

Corresponding author: bamoniri@kashanu.ac.ir

[a] *Department of Organic Chemistry, Faculty of Chemistry, University of Kashan, Kashan, Iran*

[b] *Department of Chemistry, College of Science, Yazd University, Yazd, Iran*

Keywords: P_2O_5; Nanocatalyst; Multicomponent; Amidoalkyl naphthols; Solvent-less

ABSTRACT

Here, we have reported P_2O_5 decorated by $CuFe_2O_4$ as magnetically separable solid Brønsted acid nanocatalyst to prompt synthesis of 1-amidoalkyl-2-naphthols. Characterization of the nanocatalyst was carried out by XRD, FESEM, EDX, FTIR and Raman analyses. FTIR and Raman spectroscopy clearly reveal the presence of P_2O_5 on the surface of $CuFe_2O_4$ nanoparticles. The nanocatalyst was used to facilitate three-component synthesis of 1-amidoalkyl-2-naphthol under solvent free condition. The efficiency of the prepared nanocatalyst is 97% which could be attributed to the numerous Brønsted acid sites on the surface of nanocatalyst. Recyclability of the nanocatalyst was investigated under 5 successive runs. Different derivatives of amidoalkyl-2-naphthol were distinguished by FTIR and ^{1}H NMR spectroscopy.

INTRODUCTION

Owing to their superior pharmaceutical applications, 1-amidoalkyl-2-naphthol and its derivatives have been synthesized for many decades. They have offered variety of properties including nucleoside antibiotics and HIV protease inhibitors. Because of their importance, investigations for high yield synthesis of 1-amidoalkyl-2-naphthol derivatives are being developed [1]. Common synthesis method for 1-amidoalkyl-2-naphthol derivatives is a three-component condensation reaction between 2-naphthol, acetonitrile and aldehyde [2]. Different homogenous and heterogeneous catalysts, such as *p*-toluenesukfonic acid, phosphoric acid, SiO_2-$HClO_4$, $Fe(HSO_4)_3$, ZnO and AgI nanoparticles have been used to prompt the synthesis reaction of 1-amidoalkyl-2-naphthol [3].

Herein, we have introduced the synthesis of 1-Amidoalkyl-2-naphthols using $P_2O_5/CuFe_2O_4$ as magnetically separable solid Brønsted acid nanocatalyst. A schematic representation and FTIR spectrum has been provided for the 1-Amidoalkyl-2-naphthol derivative, as follows:

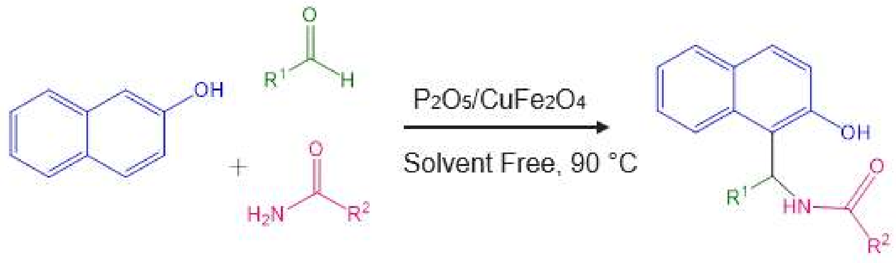

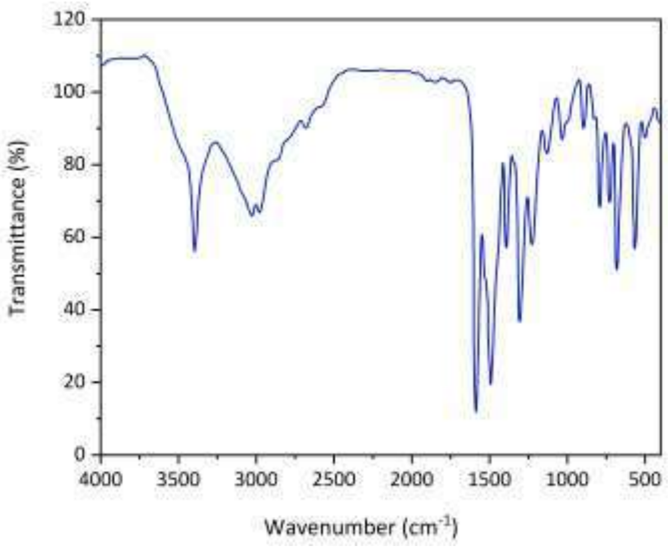

Wavenumber (cm^{-1})	Assignment
701	CH
753	CH
822	CH
1435	C=C
1627	C=O
3067	NH
3041	OH

FTIR and spectral data for N-[(2-Hydroxynaphthalene-1-yl)-(phenyl)-methyl]-benzamide.

References:

[1] K. Boudebbous, H. Boulebd, C. Bensouici, D. Harakat, R. Boulcina, A. Debache, Synthesis, docking study and biological activities evaluation of 1-Amidoalkyl-2-naphthol derivatives as dual inhibitors of cholinesterase and α-Glucosidase, *ChemistrySelect*, 5 (**2020**) 5515-5520.
[2] H. Taghrir, M. Ghashang, M.N. Biregan, Preparation of 1-amidoalkyl-2-naphthol derivatives using barium phosphate nano-powders, *Chinese Chem. Lett*., 27 (**2016**) 119-126.
[3] A.G. Woldegiorgis, X. Lin, Recent advances in the asymmetric phosphoric acid-catalyzed synthesis of axially chiral compounds, *Beilstein J. Org.Chem.*, 17 (**2021**) 2729-2764.

The 30th Iranian Seminar of Organic Chemistry
February 7-9, 2025, Iran University of Science and Technology, Tehran, Iran

Oxidation of Phenols in the Presence of Metalloporphyrin-based Magnetic Nanocatalysts

Fatemeh Nejabat*

Department of Chemistry, Amirkabir University of Technology, Tehran, Iran.

Email: F.nejabat@aut.ac.ir

Keyword: Metalloporphyrin, Oxidation, Phenol, Magnetic nanocatalyst, Fe_3O_4

Introduction

Oxidation of phenol is among the most significant chemical reactions with implications in various fields such as organic chemistry, environmental science and industrial applications. Since the oxidation of phenol can lead to the formation of potentially harmful byproducts, necessitating efficient and selective catalytic processes to manage these transformations.

Nowadays, heterogeneous catalysts play the key role in the science of catalyst production, and the various designs of catalysts are of interest. Recent advancements in nanotechnology and green chemistry have led to the development of new heterogenous nanocatalysts that offer improved performance and reduced environmental impact.

As catalyst supports, magnetic nanoparticles (MNPs) provide a range of advantages, including improved dispersion of active catalytic sites, enhanced stability against leaching, and the ability to facilitate the recycling of catalysts through simple magnetic separation techniques.

In this research, manganese porphyrin was attached onto the surface of MNPs via organic linkage and the catalytic efficiency of the prepared catalyst was evaluated in the oxidation of phenols in the mild condition.

Method

Porphyrin, metalloporphyrin and $Fe_3O_4@SiO_2-NH_2$ were prepared according to previously reported methods. Mn-porphyrin was attached onto the surface of magnetic support via amidic bond in the presence of coupling reagents (TBTU/DIPEA) as reported previously.

The efficiency of the prepared supported Mn-porphyrin was evaluated in the oxidation of 2,6-dimethyl phenol with H_2O_2 and the effect of time and temperature on the catalytic activity of $Fe_3O_4/SiO_2/NH_2$/MnTCPP in the mentioned reaction was monitored by UV-Vis and HPLC.

Results and Discussion

The prepared nanocatalyst were characterized by standard methods such as FTIR, SEM, TEM, VSM, XRD and TGA. Results proved the attachment of MnTCPP(OAc) onot the surface of functionalized magnetic nanoparticles

To study the catalytic activity of the prepared magnetic nano-catalyst, oxidation of 2,6-dimethyl phenol in the presence of $Fe_3O_4/SiO_2/NH_2$/MnTCPP with H_2O_2 in acetonitrile was studied as a model reaction. The effect of some parameters such as time, temperature and the nature of oxidant on the rate of oxidation of phenols was investigated.

The progress of the oxidation of 2,6-dimethyl phenol in CH_3CN was monitored at room temperature and at 40 °C in three consecutive times (1h, 2h and 4h) and the results show that the reaction progresses with time and the progress of the oxidation reaction is much higher at 40 °C than 25 °C.

The obtained results clearly proved high efficiency of $Fe_3O_4/SiO_2/NH_2$/MnTCPP in the oxidation of phenols in the mild condition.

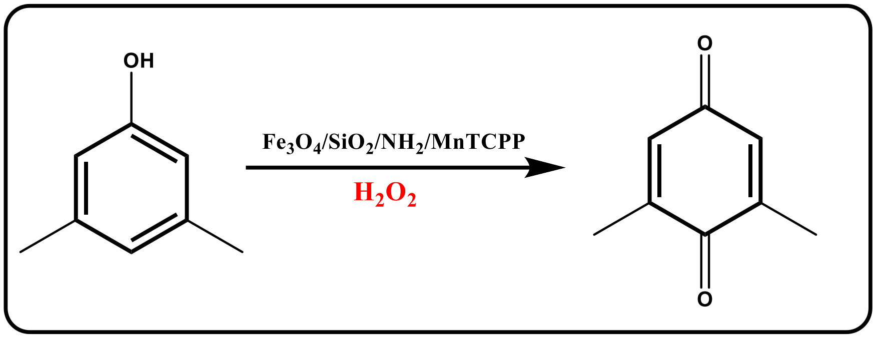

References:

[1] D. Dini, M. Hanack, K. M. Kadish, K. M. Smith, R. Guilard, "The Porphyrin hand book" Academic press, New York, Vol 17 (2003).

[2] F. Nejabat, S. Rayati, J. Ind. Eng. Chem., 69 (2019) 324.

[3] S. Sajjadifar, I. Amini, S. Habibzadeh, G. Mansouri, E. Ebadi, Chem. Methodologies, 4 (2020) 623.

[4] S. P. Gubin, “Magnetic Nanoparticles” John Wiley & Sons, Hoboken, NJ, (2009).

[5] P. Patoghi, A. Sadatnabi, D. Nematollahi, Sci. Rep., 13 (2023) 17582.

[6] M. Samani, M. H. Ardakani, M. Sabet, Res. Chem. Intermed., 48 (2022) 1481.

[7] S. Rayati, F. Nejabat, F. Panjiali, Catal. Commun., 122 (2019) 52.

[8] S. Rayati, D. Moradi, F. Nejabat, New J. Chem., 44 (2020) 19385.

[9] S. Rayati, S. Aghajani, F. Nejabat, P. Nafarieh, Polyhedron, 225 (2024) 116961.

The 30th Iranian Seminar of Organic Chemistry
February 7-9, 2025, Iran University of Science and Technology, Tehran, Iran

Supramolecular calix[4]arene as a pore-partitioning agent of MIL-101 for improved gas uptake

Saied Shafiei Navid [a], Rahman Hosseinzadeh [a*] (Corresponding author), Christoph Janiak [b]

[a] *Department of Organic Chemistry, Faculty of Chemistry, University of Mazandaran, Babolsar, Iran.*

[b] *Institut für Anorganische Chemie und Strukturchemie, Heinrich-Heine-Universität Düsseldorf, 40225 Düsseldorf, Germany.*

Keyword: Calix[4]arene, MIL-101 (Cr), Pore-partitioning, Gas uptake

p-Sulfonated calix[4]arene (SCA) as a bowl-shaped supramolecule with intrinsic cavity[1], was incorporated into the pores of MIL-101(Cr) as a micro-mesoporous material through adsorptive loading technique[2]. The utilizing the pore-partitioning of the MIL-101 (Cr) by SCA which possess the SO_3H and OH polar groups led to the SCA@MIL-101 (Cr) composite. The various measurements were used to investigate the success preparation of SCA@MIL-101 (Cr) such as FT-IR, PXRD, TGA, FE-SEM, EDS/MAPP, BET, and TEM analysis. The introduced organic-inorganic composite showed high affinity to CO_2 uptake than neat MIL-101 (Cr) without any involvement of amino functional groups which has been proved that have the highest affinity to CO_2 [3]. By adding a specified amount of SCA into the pores of MIL-101 (Cr), only trace amounts of SCA leached out, demonstrating the compatibility and close match between the size of SCA and the pores in MIL-101 (Cr).Though the prepared SCA@MIL-101 (Cr) composite showed lower BET surface area ($S_{BET} < 1100$ cm^3 g^{-1}) than MIL-101 (Cr) ($S_{BET} > 2700$ cm^3 g^{-1}), the composite was found to be more sensitive to CO_2 than the neat MOF. The CO_2 uptake values for SCA@MIL-101 (Cr) and MOF were reported to be 100 m^2 g^{-1} and 62 m^2 g^{-1}, respectively at 273K and 1 bar. Furthermore, the IAST selectivity results showed an increase for a 25:75 (v:v) molar CO_2/N_2 mixture from 5.6 (for MOF) to 23 (for composite) at 273K and 1 bar[4]. The results indicated that the prepared SCA@MIL-101 (Cr) composite could serve as a promising sorbent for greenhouse gases, such as methane and carbon dioxide.

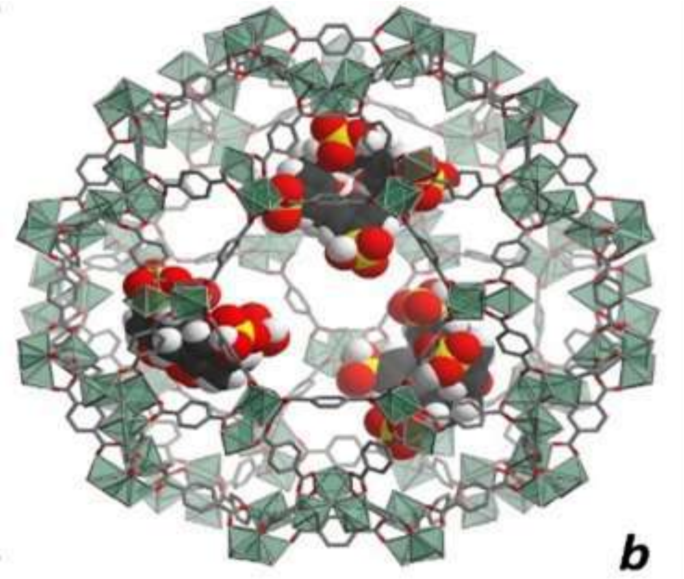

Scheme: The schematic incorporation of SCA molecules into the pores of MIL-101 (Cr).

References:

1. Zhang Q, Zhou Y, Ma J, Wang H, Li W. Synthesis and coating properties of sulfonated calixarene-based waterborne polyurethane hydrotalcite nanocomposite. Polymers for Advanced Technologies. 2023 May;34(5):1653-61.

2. Liang J, Gvilava V, Jansen C, Öztürk S, Spieß A, Lin J, Xing S, Sun Y, Wang H, Janiak C. Cucurbituril-Encapsulating Metal–Organic Framework via Mechanochemistry: Adsorbents with Enhanced Performance. Angewandte Chemie International Edition. 2021 Jul 5;60(28):15365-70.

3. Srivastava S, Kollemparembil AM, Zettel V, Claßen T, Gatternig B, Delgado A, Hitzmann B. Experimental investigation of CO2 uptake in CO2 hydrates formation with amino acids as kinetic promoters and its dissociation at high temperature. Scientific Reports. 2022 May 19;12(1):8359.

4. Nuhnen A, Janiak C. A practical guide to calculate the isosteric heat/enthalpy of adsorption via adsorption isotherms in metal–organic frameworks, MOFs. Dalton Transactions. 2020;49(30):10295-307.

The 30th Iranian Seminar of Organic Chemistry

February 7-9, 2025, Iran University of Science and Technology, Tehran, Iran

Choline chloride/ascorbic acid as an efficient medium/catalyst for the synthesis of quinazolinone derivatives

Zohreh Valipour[a], Shiva Zarei[a], Rahman Hosseinzadeh*[,a], Behrooz Maleki[a]

[a]Department of Organic Chemistry, Faculty of Chemistry, University of Mazandaran, Babolsar, Iran.

Keyword: Green chemistry, Organic synthesis, Quinazolinones, Three components reaction

Quinazolinones and its derivatives are an important class of heterocyclic compounds that have attracted much attention in organic and medicinal chemistry due to their wide presence in various natural alkaloids and bioactive natural products [1]. Normally, these compounds will be synthesized through three-component reactions of aldehydes, isatoic anhydrides, amines, or ammonium salts by various catalysts [2]. Accordingly, a large number of catalysts have been reported for the synthesis of quinazolinone derivatives under different conditions. Although the methods have significant merits and advantages, most of them suffer from one or more limitations, such as the use of toxic organic solvents, difficulties in catalyst preparation, laborious work-up procedure, long reaction times, and low yields. In last years, deep eutectic solvents (DESs) have been investigated as reaction media and catalysts for organic syntheses [3]. In our current work, we report the use of choline chloride/ascorbic acid (CC/AA) as a natural DES for the multicomponent-synthesis of quinazolinones (Scheme). The scope of this method was evaluated by employing various aromatic, and heterocyclic aldehydes. The desired products were achieved in high yield in a short reaction time. Also, the deep eutectic solvent CC/AA showed good recyclability and reusability

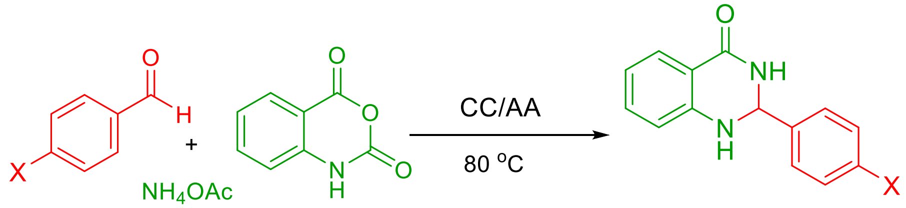

Scheme: Synthesis of quinazolinone derivatives

References:

[1] D. Sarma, B. Majumdar, B. Deori, S. Jain and T. K. Sarma. ACS omega. 2021, 6, 11902-11910

[2] M. Badolato, F. Aiello and N. Neamati. RSC adv. 2018, 8, 20894-20921

[3] Hooshmand, S. E.; Kumar, S.; Bahadur, I..; Singh, T.; Varma, R. S.. J. Mol. Liq.2022, 121013

The 30th Iranian Seminar of Organic Chemistry
February 7-9, 2025, Iran University of Science and Technology, Tehran, Iran

Heterogeneous layered double hydroxide catalyst for the selective and solvent-free oxidation of benzyl alcohol to benzaldehyde

Sama Maghoul[a], Seyed Saeed Mehrabi-Kalajahi*[a,b], Seyed Amir Hossein Vasigh*[a],Saeed Hajaghaei[a] and Behrouz Shaabani*[a]

[a] Faculty of Chemistry, Department of Inorganic Chemistry, University of Tabriz, Tabriz, Iran
[b]Department of Petroleum Engineering, Kazan Federal University, Kazan 420008, Russia

Keyword: Layered double hydroxide (LDHs); Aerobic oxidation; Benzyl alcohol; Heterogeneous catalysis; Highly selective

Introduction

Selective oxidation processes, vital for the production of fine chemicals on a large scale, frequently necessitate elevated temperatures and pressures, resulting in significant energy consumption and environmental damage. The transformation of benzyl alcohol into benzaldehyde is important due to its function as a crucial intermediate in numerous organic reactions. Conventional techniques utilize hazardous solvents and oxidizing agents, which present safety and environmental challenges[1,2]. To adhere to the principles of green chemistry, it is important to create catalysts that function effectively under milder conditions. Layered double hydroxides (LDHs) represent promising materials for boosting catalytic performance through synergistic interactions with metal nanoparticles[3,4]. We prepared several layered double hydroxides including Cu-Co-Fe-LDH, Zn-Co-Fe-LDH, Zn-Ni-Co-Fe-LDH, Cu-Ni-Co-Fe-LDH via co-precipitation for use as catalysts. The benzyl alcohol-free oxidation to benzaldehyde of this environmentally friendly method showed that Cu-Ni-Co-Fe-LDH achieved conversion rates of below 8% and 12.34% with selectivities as high as 99.60% and 92.31% under atmospheric and 10 atmosphere pressures, respectively, using molecular oxygen.

Method

For the synthesis of layered double hydroxides Cu–Co–Fe–LDH, Zn–Co–Fe–LDH, Zn–Ni–Co–Fe–LDH and Cu–Ni–Co–Fe–LDH coprecipitation method is used, in which 20 mmol of each salt (1:1:1 and 1:1:1:1 molar ratio) corresponding to the layered double hydroxide was taken and dissolved in 100 mL of deionized water. The resulting mixture was stirred under an inert Ar gas on a mechanical stirrer and a 1 M NaOH solution was refluxed for 12 h at 50 °C. The residue was washed three times with a mixture of water and ethanol and finally dried at 45 °C.

Results

In order to characterize the synthesized heterogeneous catalysts, XRD, Raman, SEM/EDS, TEM, BET and TG/DTG techniques were used.The study presents the characteristics of layered double hydroxides (LDHs). The Cu–Co–Fe–LDH sample shows typical peaks at various angles, indicating its structure. Similar peaks are noted for Zn–Co–Fe–LDH and Zn–Ni–Co–Fe–LDH, confirming their crystalline structures. FT-IR spectra reveal OH groups and $NO3^{-2}$ anions in the LDH structure. Raman spectra indicate specific vibration modes related to the cubic spinel structure, with notable peaks linked to O–Mo–O bending and nitrate ions. Trimetallic and tetrametallic double layer hydroxides (LDHs) act as efficient catalysts for the solvent-free oxidation of benzyl alcohol to benzaldehyde. TEM analysis reveals fewer clustered porous sheets in Cu–Ni–Co–Fe–LDH. Surface area and nitrogen isotherms were measured for adsorption potential. The nanosheets have a surface area of 122 m^2/g, thanks to their multi-layered structure preventing aggregation. Experiments were conducted under different conditions such as temperatures between 90 and 130 °C and reaction times between 5 and 48 h. The use of LDH significantly increased the conversion rate, with Cu-Ni-Co-Fe-LDH reaching a conversion rate of up to 12.34% and achieving more than 92% selectivity at 120 °C compared to previous catalysts. These LDHs show higher selectivity and efficiency, which is attributed to their redox coupling. And abundant active sites, which improve the adsorption and activation of benzyl alcohol, are essential for the dynamics of the reaction.

Discussion

The catalysts created showed exceptional results in the solvent-free aerobic conversion of benzyl alcohol into benzaldehyde. The synergy of multiple cationic active sites in the LDH and its exposed layered configuration significantly enhanced catalytic performance. Remarkably, Cu–Ni–Co–Fe–LDH emerged as the most effective catalyst for this oxidation reaction.

References

[1] X. Lan, T. Wang, Highly Selective Catalysts for the Hydrogenation of Unsaturated Aldehydes: A Review, ACS Catalysis 10 (2020) 2764–2790.
[2] S. Mehrabi-Kalajahi, Y. Orooji, S. Arefi-Oskoui, M.A. Varfolomeev, N.M. Khasanova, Y. Yoon, A. Khataee, Preparasion of layered V4AlC3 MAX phase for highly selective and efficient solvent-free aerobic oxidation of toluene to benzaldehyde, Molecular Catalysis 529 (2022) 112545.
[3] X. Dai, W. Yi, C. Yin, K. Li, L. Feng, Q. Zhou, Z. Yi, X. Zhang, Y. Wang, Y. Yu, X. Han, Y. Zhang, 2D-3D magnetic NiFe layered double hydroxide decorated diatomite as multifunction material for anionic, cationic dyes, arsenate, and arsenite adsorption, Applied Clay Science 229 (2022) 106664.
[4] A.E. Stamate, R. Zăvoianu, O.D. Pavel, R. Birjega, A. Matei, M. Dumitru, I. Brezeștean, M. Osiac, I.C. Marcu, The Influence of the Preparation Method on the Physico-Chemical Properties and Catalytic Activities of Ce-Modified LDH Structures Used as Catalysts in Condensation Reactions, Molecules 2021, Vol. 26, Page 6191 26 (2021) 6191.

The 30th Iranian Seminar of Organic Chemistry
February 7-9, 2025, Iran University of Science and Technology, Tehran, Iran

Selective and solvent-free oxidation of toluene to benzaldehyde by high entropy oxide composited with reduced graphene oxide

Sama Maghoul[a], Seyed Saeed Mehrabi-Kalajahi*[a,b], Seyed Amir Hossein Vasigh*[a], Behrouz Shaabani*[a]

[a] Faculty of Chemistry, Department of Inorganic Chemistry, University of Tabriz, Tabriz, Iran
[b]Department of Petroleum Engineering, Kazan Federal University, Kazan 420008, Russia

Keyword: High entropy oxides (HEO); Reduce graphene oxide; Toluene; Solvent-free; Benzaldehyde

Introduction

Reducing VOC emissions, like toluene, is crucial for the chemical sector. Toluene's conversion to benzaldehyde, a key chemical in various industries, is vital for environmental and industrial challenges[1]. Traditional methods of producing benzaldehyde are environmentally harmful. The focus is now on sustainable, solvent-free catalytic synthesis of benzaldehyde from toluene. Despite challenges in achieving high conversion rates, new catalysts and materials, including high-entropy alloys, show promise. These advancements highlight the importance of developing selective catalytic systems for green chemistry, aiming to efficiently convert toluene into valuable products[2,3]. In 2022, Fereja et al. developed a $(FeNiCoCrCu)_3O_4$ HEO nanostructure with oxygen vacancies and a large surface area, excelling in urea oxidation and oxygen evolution. Chen et al. created NiMgCuZnCoOx and PtNiMgCuZnCoOx HEOs with thermal stability for CO oxidation. In 2020, Feng's team introduced Co0.2Ni0.2Cu0.2Mg0.2Zn0.2O, a catalyst for benzyl alcohol conversion. Our research shows $(Fe, Co, Ni, Cu)_3O_4$ and $(CoFeMnCuNiCr)_3O_4$ on rGO outperform previous catalysts in solvent-free aerobic oxidation of toluene and benzyl alcohol[4,5]. This study presents a cost-effective and environmentally friendly method for the selective oxidation of toluene to benzaldehyde using HEO-rGO catalyst, achieving above 13% conversion and 90% selectivity at atmospheric pressure.

Method

The high entropy oxide $(Mn, Fe, Co, Ni, Cu)_3O_4$ was created by a conventional co-precipitation method. Sulfate salts were dissolved in deionized water, followed by the addition of PVP and ammonia solution. After being stirred, heated, and filtered, the mixture was calcined for five h at 1000°C. A 3:1 rGO/HEO mixture was created by adding 40 ml of DIW, ultrasonically sonicated for two hours, heated in a Teflon autoclave, filtered, cleaned, and dried in a hot oven. The precursor was calcined at 600°C for one h to obtain HEO-rGO.

Results

The best temperature for the formation of a nearly single-phase HEO is 1000 °C, according to the XRD patterns of rGO, $(MnFeCuCoNi)_3O_4$ HEO calcined at that temperature, and the HEO-rGO nanocomposite. In $(MnFeCuCoNi)_3O_4$ HEO, only 5 % CuO is formed as a secondary phase after calcination. $(CoFeMnCuNiCr)_3O_4$ HEO (8.357 Å) and Fe_3O_4 have larger lattice parameters than spinel HEO (8.343 Å). The FTIR spectrum of the rGO sample shows oxygen-containing groups such as O-H, which can be related to the OH stretching bond of the carboxylic acid. The FTIR spectrum of $(MnFeCuCoNi)_3O_4$ HEO shows bands related to the metal oxide stretching in the range of 550–1050 cm^{-1}. The peaks associated with O-H, C=O, and C-O become more intense in the spectrum of HEO-rGO. HEO−rGO and $(MnFeCuCoNi)_3O_4$ HEO nanoparticles demonstrated remarkable chemical stability up to 1000°C, according to TGA analysis. Below 140°C, moisture removal caused a 2.0 % mass loss in the HEO−rGO composite. 30 weight percent $(MnFeCuCoNi)_3O_4$ HEO was present in HEO−rGO samples.

Discussion

Synthesized $(MnFeCuCoNi)_3O_4$ HEO nanoparticles on rGO showed exceptional performance in solvent-free aerobic oxidation of toluene, with 18.0% conversion and 90.0% selectivity, demonstrating a novel method for heterogeneous catalysts.

References

[1] R. Rao, S. Ma, B. Gao, F. Bi, Y. Chen, Y. Yang, N. Liu, M. Wu, X. Zhang, Recent advances of metal-organic framework-based and derivative materials in the heterogeneous catalytic removal of volatile organic compounds, J. Colloid Interface Sci. 636 (2023) 55–72.
[2] L. Laasri, M. El Makhfi, Ecofriendly oxidation of benzyl alcohol to benzaldehyde using Zr-Ni/Natural phosphate as an efficient and recyclable heterogeneous catalyst, Mater. Today Proc. 31 (2020) S156–S161.
[3] S.S.M. Kalajahi, M. Hajimohammadi, N. Safari, Highly efficient, green and solvent-free photooxygenation of alkenes by air and visible light or sunlight in the presence of porphyrin sensitizers, React. Kinet. Mech. Catal. (2014).
[4] H. Chen, J. Fu, P. Zhang, H. Peng, C.W. Abney, K. Jie, X. Liu, M. Chi, S. Dai, Entropy-stabilized metal oxide solid solutions as CO oxidation catalysts with high-temperature stability, J. Mater. Chem. A. 6 (2018) 11129–11133.
[5] S.L. Fereja, Z. Zhang, Z. Fang, J. Guo, X. Zhang, K. Liu, Z. Li, W. Chen, High-Entropy Oxide Derived from Metal-Organic Framework as a Bifunctional Electrocatalyst for Efficient Urea Oxidation and Oxygen Evolution Reactions, ACS Appl. Mater. Interfaces . 14 (2022) 38727–38738.

The 30th Iranian Seminar of Organic Chemistry
February 7-9, 2025, Iran University of Science and Technology, Tehran, Iran

Effective removal of methylene blue dye from aqueous solution using magnetic nanoparticles functionalized with 1,4-butane sultone

Ghazaleh Mansourifard[a], Heshmatollah Alinezhad*[a], Ameneh Kiani*[a]

[a]Faculty of Chemistry, University of Mazandaran, Babolsar, Mazandaran 47416-13534, Iran

Keyword: Magnetic Fe_3O_4, Nanocatalyst, Organic dyes

ABSTRACT:

Wastewater contains organic compounds, including dyes, which have potential risks to the environment. Hence, these compound needs to be eliminated from the aqueous solution. In the present study, magnetic nanoparticles functionalized with 1,4-butane sultone (Fe_3O_4@1,4-butane sultone were used as an adsorbent to remove methylene blue dye (MB) from synthetic wastewater. To evaluate the parameters affecting adsorption, including the initial MB concentration, solution pH, contact time, and Fe_3O_4@1,4-butane sultone dose, batch experiments were carried out. Scanning electron microscopy (SEM), energy dispersive X-ray spectroscopy (EDX), and Fourier transform infrared (FTIR) were applied for characterizations of Fe_3O_4@1,4-butane sultone. The optimum conditions were obtained with an initial MB concentration of ۲۰ mg L−۱: solution pH~۹, for Fe_3O_4@1,4-butane sultone dose: 0.03 g, which caused 97.77% of MB removal. The results indicate that Fe_3O_4@1,4-butane sultone had a higher ability to remove MB than unfunctionalized-Fe_3O_4, probably due to its highly porous structure and rough surfaces that provide active sites and facilitate MB adsorption. These findings demonstrate the potential of the magnetic Fe_3O_4/1,4-butane sultone nanocomposite as a powerful adsorbent for the removal of methylene blue dye from aqueous solutions, offering promising prospects for the treatment of industrial wastewater.

The 30th Iranian Seminar of Organic Chemistry
February 7-9, 2025, Iran University of Science and Technology, Tehran, Iran

Synthesis of pseudo dendrimer polyglycerol-polyoxazoline-lysine and its antibacterial application

Behnaz Bastami[a] , Mohsen Adeli[b]*

[a]*Kish international campus, University of Tehran, Kish Island, Iran,*

[b]*Faculty of Science, Department of Chemistry, Lorestan University, Khorramabad, Iran,*

Corresponding author: adeli.m@lu-ac.ir

Keywords: Polyglycerol, polyoxazoline, pseudo dendrimer

Introduction

The use of polymeric materials as antibacterial agents has emerged as a promising approach due to their tunable structures and functionality[1]. Among these, dendrimers and pseudo-dendrimers stand out due to their branched architecture and high functionality, which can effectively interact with bacterial cell membranes and lead to bacterial eradication [2]. The aim of this study is to synthesize and investigate the antibacterial properties of polyglycerol-polyoxazoline-lysine pseudodendrimer. This study followed a four-step process to synthesize and modify hyperbranched polyglycerol (hPG). The procedure involved the polymerization and mesylation of hPG, followed by oxazoline polymerization and termination with lysine [3].

The synthesis involves a multi-step process where polyglycerol is first synthesized and functionalized with polyoxazoline through a ring-opening polymerization. Subsequently, lysine residues are conjugated to the resulting polymer via peptide bond formation. The resulting pseudo-dendrimer exhibits a highly branched architecture with a dense surface of functional groups, providing ample opportunities for interaction with bacterial membranes. In vitro, antibacterial assays demonstrate that the synthesized compound exhibits significant antibacterial activity against Gram-positive and Gram-negative bacteria, with minimal cytotoxicity towards mammalian cells. This novel pseudo-dendrimer represents a promising platform for developing new antibacterial agents, particularly in the context of rising antibiotic resistance. This research represents an important step towards the development of a new generation of antibacterial agents using polymeric structures, addressing the critical need for effective treatments against antibiotic-resistant bacterial infections [4-6].

Method

In this study, different characterization methods including FTIR, NMR, and SEM were used to identify the polyglycerol-polyoxazoline-lysine pseudodendrimer. Additionally, the antibacterial activity of this compound was evaluated through microbial culture tests to determine the minimum inhibitory concentration (MIC).

Results and Discussion

In this study, the pseudo-dendrimer polyglycerol-polyoxazoline-lysine was synthesized through a four-step reaction (fig 1).

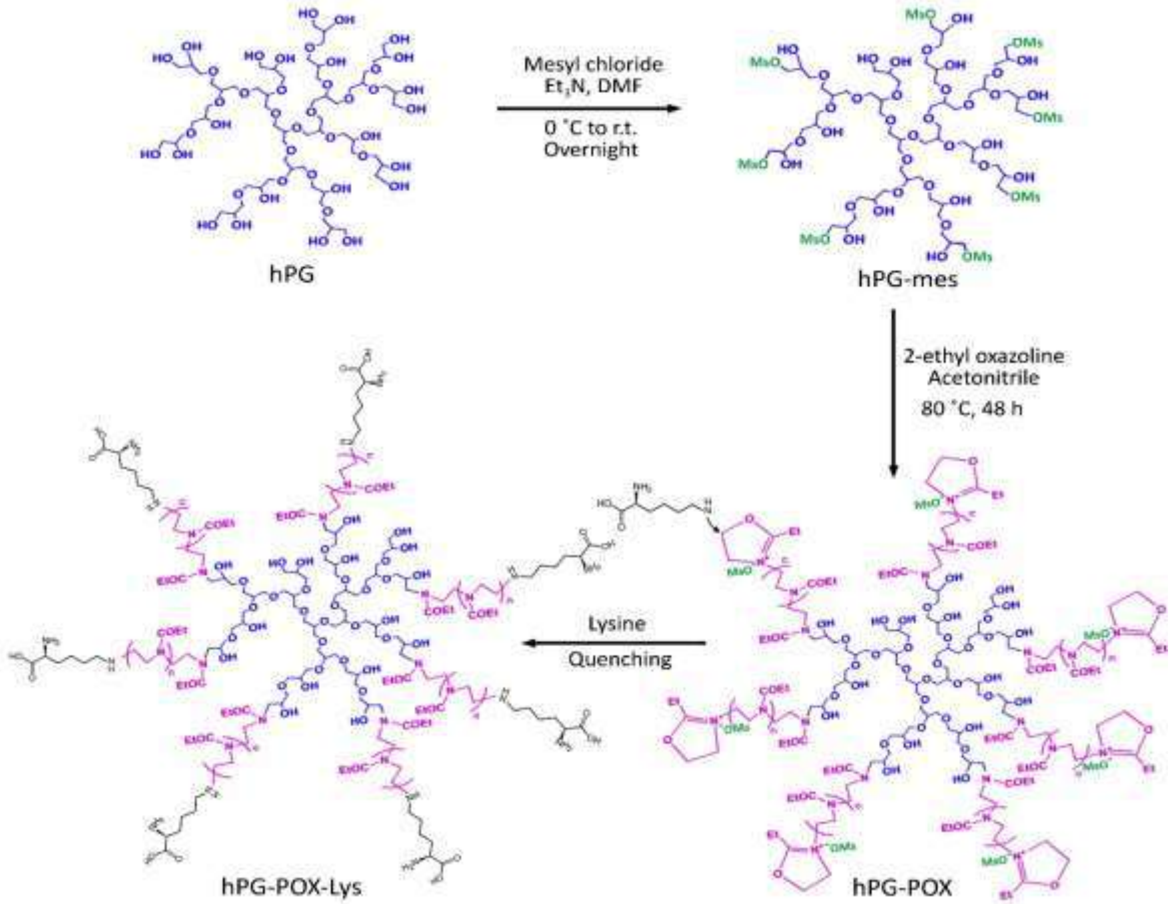

Figure 1. Synthesis of pseudo dendrimer polyglycerol-polyoxazoline-lysine (hPG-POX-Lys).

FT-IR spectra of the product indicated successful synthesis of the above-mentioned polymer with the desired functional groups (fig 2a). NMR spectra showed signals for different protons of the expected structure as assigned on fig 2b. SEM images revealed the morphology of the pseudo-dendrimer as spherical nanoparticles with dimensions of approximately 300-400 nm (fig 2c). MIC and MBC studies were conducted to determine the antibacterial capabilities of the pseudo-dendrimer against both Gram-positive and Gram-negative bacteria. The results showed that the tested combination exhibited good efficacy in laboratory conditions at concentrations below 0.19 mg/ml (equivalent to a concentration of 0.5 %) (fig 2d). Morphological studies using SEM indicated significant changes in the membrane of bacteria, including cell wall destruction and the formation of cracks and depressions. In contrast, the control groups, which included untreated E. coli and Staphylococcus aureus, appeared healthy, maintaining a normal shape and structure (fig 2e, 2f).

The results of this research demonstrate successful progress in the synthesis of the pseudo-dendrimer and its strong antibacterial properties at low concentrations. These findings not only confirm the potential of functionalized pseudo-dendrimers as novel antibacterial agents but also contribute to the development of effective and targeted drug nanoparticles for treating bacterial infections. Given the rise in antibiotic resistance, the results of this research may provide a new approach to combat bacterial infections and lay the groundwork for future studies in the design and synthesis of advanced pharmaceutical nanocarriers.

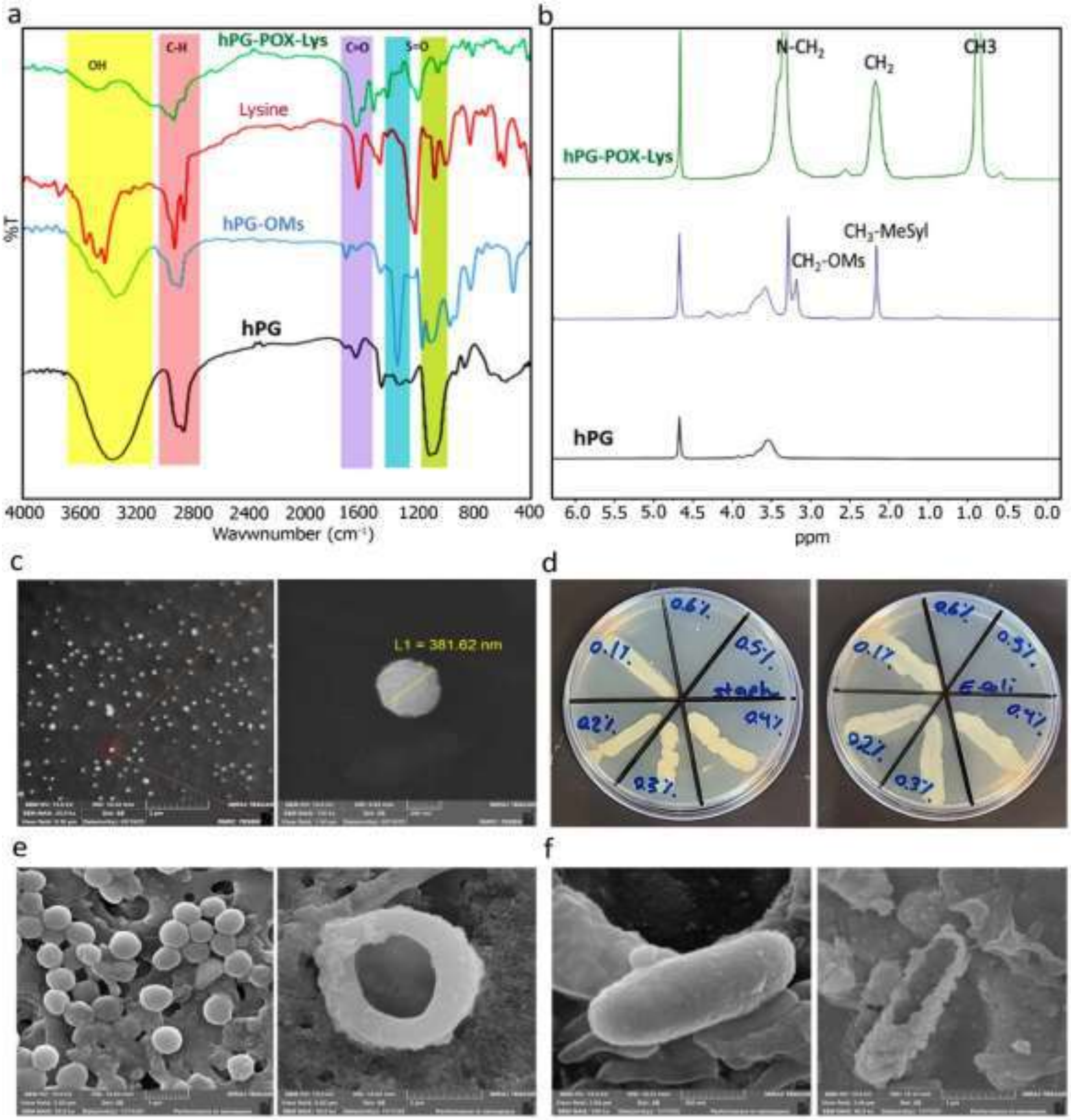

Figure 2. a) FT-IR spectra of hPG, hPG-OMs, Lys and hPG-POX-Lys, b) ^{1}HNMR spectra of hPG, hPG-OMs, and hPG-POX-Lys, c) SEM images of hPG-POX-Lys, d) MIC Determination of hPG-POX-Lys, e,f) Changes in the morphology of antibacterial after treatment with polymers.

References:

1. Aijaz, M.; Ahmad, M.; Ansari, M. A.; Ahmad, S., Antimicrobial Resistance in a Globalized World: Current Challenges and Future Perspectives. *International Journal of Pharmaceutical Drug Design* **2023,** *1* (1), 7-22.

2. Salam, M. A.; Al-Amin, M. Y.; Salam, M. T.; Pawar, J. S.; Akhter, N.; Rabaan, A. A.; Alqumber, M. A. A. In *Antimicrobial resistance: a growing serious threat for global public health*, 2023; MDPI: p 1946.

3. Chis, A. A.; Dobrea, C.; Morgovan, C.; Arseniu, A. M.; Rus, L. L.; Butuca, A.; Juncan, A. M.; Totan, M.; Vonica-Tincu, A. L.; Cormos, G., Applications and limitations of dendrimers in biomedicine. *Molecules* **2020,** *25* (17), 3982.

4. Bai, S.; Wang, J.; Yang, K.; Zhou, C.; Xu, Y.; Song, J.; Gu, Y.; Chen, Z.; Wang, M.; Shoen, C., A polymeric approach toward resistance-resistant antimicrobial agent with dual-selective mechanisms of action. *Science advances* **2021,** *7* (5), eabc9917.

5. Chen, S.; Huang, S.; Li, Y.; Zhou, C., Recent advances in epsilon-poly-L-lysine and L-lysine-based dendrimer synthesis, modification, and biomedical applications. *Frontiers in Chemistry* **2021,** *9*, 659304.

6. Gorzkiewicz, M.; Kopeć, O.; Janaszewska, A.; Konopka, M.; Pędziwiatr-Werbicka, E.; Tarasenko, I. I.; Bezrodnyi, V. V.; Neelov, I. M.; Klajnert-Maculewicz, B., Poly (lysine) dendrimers form complexes with siRNA and provide its efficient uptake by myeloid cells: model studies for therapeutic nucleic acid delivery. *International Journal of Molecular Sciences* **2020,** 21 (9), 3138.

The 30th Iranian Seminar of Organic Chemistry
February 7-9, 2025, Iran University of Science and Technology, Tehran, Iran

Synergistic Removal of Methylene Blue: NH2-UiO-66/PVDF Composite as a Sustainable Solution for Water Treatment

Authors: Ali Badihi, M. Reza Naimi-Jamal*, Roya Evazi

Affiliations: Research Laboratory of Green Organic Synthesis & Polymers, Department of Chemistry, Iran University of Science and Technology, 16846-13114 Tehran, Iran

Keyword: Dye, Metal-organic framework , PVDF polymer , Water purification

Body Text: This research focuses on tackling a persistent environmental issue caused by methylene blue, a widely used textile dye known for its toxicity and resistance to breakdown. To address this, a cutting-edge adsorbent was developed by combining NH2-UiO-66, a metal-organic framework, with a PVDF polymer. The composite was carefully studied using techniques like BET, FTIR, and XRD to understand its structure and properties. Its performance was tested under different conditions, such as pH, contact time, adsorbent amount, analyte concentration, and temperature, to find the sweet spot for maximum efficiency. The results were impressive, showing that this composite effectively removes methylene blue from water. By blending the strengths of MOFs and polymers, this innovative material offers a stable, high-performing, and environmentally friendly solution for cleaning contaminated water. This work opens up exciting possibilities for advancing sustainable approaches in water treatment.

The 30th Iranian Seminar of Organic Chemistry
February 7-9, 2025, Iran University of Science and Technology, Tehran, Iran

PEBAX based membranes containing metal organic framework with additional COOH groups for CO_2 separation

Elahe Ahmadi Feijani

Department of Applied Chemistry, Faculty of Chemistry and Petroleum Sciences, Bu–Ali Sina University, Hamedan 6517838695, Iran

Email: e.ahmadifeijani@basu.ac.ir

Abstract

This research explores the development and application of mixed matrix membranes (MMMs) embedded with MIL-121, a metal-organic framework (MOF) characterized by large pores and free carboxylic acid groups, to enhance gas separation efficiency. Gas separation tests revealed substantial enhancements in CO_2 permeability, which increased from 50.33 Barrer in the pristine PEBAX membrane to 95.29 Barrer in the PEBAX/MIL-121 (10 wt%) composite, without compromising N_2 exclusion.

Keywords: Gas separation, Membrane, MOF, CO_2 separation

۱ Introduction

Conventional separation methods such as distillation, adsorption, absorption, crystallization, and extraction are particularly energy-intensive compared to newer alternatives like membrane-based microfiltration, ultrafiltration, and nanofiltration [1]. Membranes have emerged as a promising solution to mitigate global warming by facilitating CO_2 separation, a major greenhouse gas [2]. Polymeric membranes, while advantageous due to their scalability and performance, face limitations in achieving an optimal balance between gas permeability and selectivity. A promising strategy to overcome this tradeoff involves fabricating hybrid or mixed matrix membranes (MMMs) by embedding inorganic or organic fillers within a polymer matrix. In this study, MIL-121, a MOF with carboxylic acid groups exhibiting strong CO_2-philic properties, was synthesized and incorporated into PEBAX matrices at 5 and 10 wt% loadings to enhance CO_2 separation performance.

۲ Methods

۲,۱ Material synthesis

MIL-121 was synthesized via a hydrothermal method. 1,2,4,5-benzenetetracarboxylic acid (0.8 g) and $Al(NO_3)_3\cdot 9H_2O$ (2.33 g) were dissolved in 60 mL of deionized water at 60 °C. The mixture was transferred to an autoclave and heated at 80 °C for 24 hours [3]. A 5 wt% PEBAX solution was prepared by dissolving the polymer in an ethanol-water mixture (7:3) under reflux conditions at 80 °C for 5 hours. For MMMs, the MOF filler was suspended in the ethanol-water mixture via vigorous stirring and sonication to prevent agglomeration. PEBAX was then added in a stepwise manner to ensure uniform dispersion. Membranes were cast onto petri dishes and dried at 80 °C for 3 hours.

۳ Results and Discussion

۳,۱ MOF and membranes characterizations

FT-IR analysis (Fig. 1a) revealed characteristic peaks corresponding to non-coordinated (-COOH) at 3019, 2684, and 2545 cm^{-1}, hydrogen-bonded -COOH at 3478 cm^{-1}, C=O of -COO- coordinated to Al^{+3} at 1617 cm^{-1}, and C=O of free -COOH at 1666 and 1759 cm^{-1}. Powder X-ray Diffraction analysis of MIL-121 (Fig. 1b) exhibited characteristic peaks at 2θ = 8.5, 12.9, 14.5, 17, 19.4, 21.9, 25.8, and 29.6° consistent with previously reported literature [3,4].

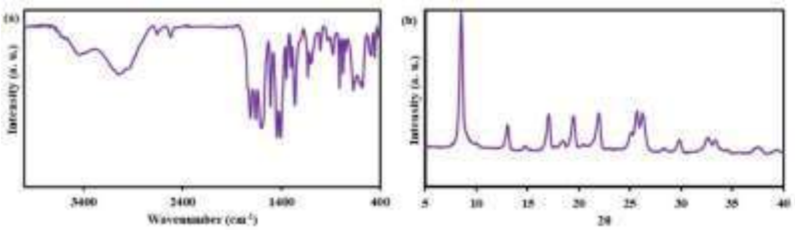

Fig. 1: FT-IR (a) and XRD (b) pattern of MIL-121

Fig. 2 presents the FT-IR and XRD of pure PEBAX and PEBAX/MIL-121 10 wt% membranes. The FT-IR spectrum of pure PEBAX exhibited a characteristic peak at 1113 cm^{-1} attributed to the C-O-C stretching of the flexible polyethylene oxide segment. Peaks at 3330, 1745, and 1664 cm^{-1} were observed, corresponding to the -N-H, O-C=O, and H-N-C=O functional groups of the rigid polyamide segments [5]. Compared to pure PEBAX, the spectra of the mixed matrix membrane displayed shifts and the emergence of new peaks. For instance, the peak at 1745 cm^{-1} shifted to 1750 cm^{-1} in the MMMs. These spectral changes can be attributed to interactions between the polar functional groups in the PEBAX backbone and the incorporated MIL-121. Fig. 2(b) presents the XRD patterns of the membranes. The pure PEBAX membrane displayed a broad peak in the 2θ range of 15 to 30°, indicative of its crystalline structure. The XRD patterns of the MMMs exhibited additional peaks characteristic of the crystalline structure of the incorporated MIL-121, confirming the preservation of the MOF's crystallinity within the membrane matrix.

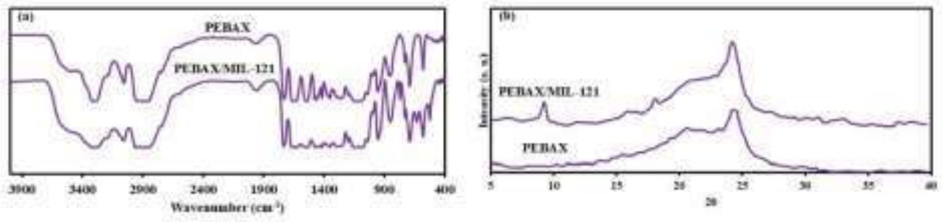

Fig. 2: FT-IR (a) and XRD (b) pattern of PEBAX and PEBAX/MIL-121 10 wt% membranes

٣,٢ Gas separation behavior

Pure gas permeation measurements were performed at a feed pressure of 2 bar and a constant temperature of 298 K and the results are displayed at Table 2. In PEBAX/MIL-121 large pores of MIL-121 provide paths for moving gas molecules especially for CO_2 molecules due to the interaction with the free –COOH groups in MOF’s structure. As shown in Table 2, CO_2 and N_2 permeabilities are increased with addition 5 and 10 wt% loading of MIL-121 into PEBAX matrix. This increase is more prominent for CO_2 compared to the N_2 and consequently the CO_2/N_2 selectivity is improved. In addition of MOF structure effect in observed gas behavior of MMMs, the interfacial region status should also be considered. Since with addition of 5 wt% of MOF to the PEBAX, CO_2/N_2 selectivity of the result MMM is not declined and the upward trend is continued with 10 wt% loading, absence of unselective voids formation at the interfacial region can be concluded. Thus, MIL-121 with additional COOH groups is not only effective in higher transfer of CO_2 but also can interact with PEBAX chains friendly. This compatibility between PEBAX chains and MIL-121 can be the reason of privileged observed mechanical properties of the MMMs. The commendable interaction between both polymer and MOF phases is responsible for uniform MOF particle dispersion which is an essential factor to achieve an ideal MMM.

Table 6: Gas permeability (Barrer) and CO_2/N_2 selectivity of the prepared membranes

	CO_2 permeability	N_2 permeability	CO_2/N_2 selectivity
PEBAX	50.33	2.62	19.20
PEBAX/MIL-121 5 wt%	76.31	2.86	26.68
PEBAX/MIL-121 10 wt%	95.29	2.93	32.52

٤ Conclusion

This study highlights the effective integration of MIL-121, a metal-organic framework, into PEBAX-based membranes for enhancing gas separation. The incorporation of MIL-121 at different loadings (5 wt% and 10 wt%) demonstrated significant improvements in gas permeability and CO_2/N_2 selectivity due to the MOF's large pores and additional functional carboxylic groups.

References:

[1] M.K. Mondal, H.K. Balsora, P. Varshney, Progress and trends in CO_2 capture/separation

technologies: A review, Energy. 46 (2012) 431–441. https://doi.org/10.1016/j.energy.2012.08.006.

[2] A.R. Kamble, C.M. Patel, Z.V.P. Murthy, A review on the recent advances in mixed matrix membranes for gas separation processes, Renew. Sustain. Energy Rev. 145 (2021) 111062. https://doi.org/10.1016/J.RSER.2021.111062.

[3] S. Chen, S. Mukherjee, B.E.G. Lucier, Y. Guo, Y.T.A. Wong, V. V. Terskikh, M.J. Zaworotko, Y. Huang, Cleaving Carboxyls: Understanding Thermally Triggered Hierarchical Pores in the Metal-Organic Framework MIL-121, J. Am. Chem. Soc. 141 (2019) 14257–14271. https://doi.org/10.1021/jacs.9b06194.

[4] C. Volkringer, T. Loiseau, N. Guillou, G. Férey, E. Elkaïm, A. Vimont, XRD and IR structural investigations of a particular breathing effect in the MOF-type gallium terephthalate MIL-53(Ga), J. Chem. Soc. Dalt. Trans. 53 (2009) 2241–2249. https://doi.org/10.1039/b817563b.

[5] G. Liu, L. Cheng, G. Chen, F. Liang, G. Liu, W. Jin, Pebax-Based Membrane Filled with Two-Dimensional Mxene Nanosheets for Efficient CO_2 Capture, Chem. – An Asian J. 15 (2020) 2364–2370. https://doi.org/10.1002/asia.201901433.

The 30th Iranian Seminar of Organic Chemistry
February 7-9, 2025, Iran University of Science and Technology, Tehran, Iran

Optimization and Characterization of Phytosynthesis of Silver Nanoparticles Using the Root Aqueous Extract of *Sambucus ebulus* L.

Fatemeh Fadaei [1], Jilla Saffari [2,*]

[1] MSc student in Organic Chemistry, Department of Chemistry, Islamic Azad University, Zahedan Branch, Zahedan, Iran

[2] Associate Professor of Inorganic Chemistry, Department of Chemistry, Islamic Azad University, Zahedan Branch, Zahedan, Iran

Phytosynthesis of silver nanoparticles (SNPs) is particular importance because of their environmental compatibility, low cost, avoidance of toxic and hazardous chemicals, and ability to be produced at room temperature. The present study aimed to biosynthesis and characterization of SNPs using root aqueous extract of *Sambucus ebulus* L. To biosynthesis of SNPs, fresh extract was prepared and added to $AgNO_3$ solution with concentration 2 mM. Effective parameters on synthesis of silver nanoparticles such as; pH, the volume of extract, silver ion concentration and reaction time were optimized by UV-Vis spectroscopy and characterization and studied to obtain individual shape and size of nanoparticles with FT-IR, XRD, and TEM. After adding the extract to the $AgNO_3$ solution, the color changed to brown that represents to successful synthesis of SNPs. SNPs showed maximum absorbance at 412 nm and they were spherical shape and the average size of them had been between 16-20 nm. Because of existing the antioxidant properties and many secondary compounds in plant, they have a role in reducing and stabilizing the nanoparticles

Keyword: Phytosynthesis, characterization, silver nanoparticles, *Sambucus ebulus* L.

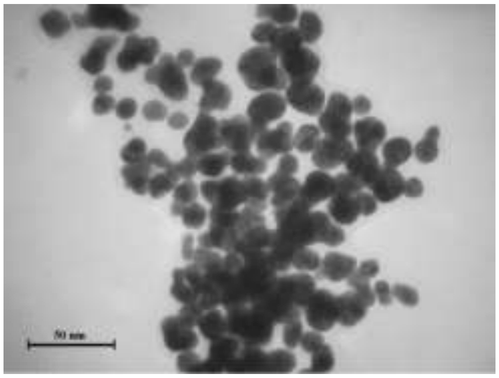

Figure: TEM image of SNPs biosynthesis by root aqueous extract of *Sambucus ebulus* L.

References: Azizian-Shermeh O., Jalali-Nezhad A.A., Taherizadeh M. Facile, Low-cost and rapid phytosynthesis of stable and eco-friendly silver nanoparticles using Boerhavia elegans (Choisy) and study of their antimicrobial activities. J. Inorg. Organomet. Polym. Mater. 2021; 31: 279-291. https://doi.org/10.1007/s10904-020-01691-7 23.

Synthesis of 3,4-dihydropyrano[3,2-c]chromene derivatives using a novel manganese-containing molten salt based on phenylene diammonium as an effective and recyclable catalyst

Amirhossein Fatehi Fard, Farhad Shirini*, Bahareh Abbas Khakiani

Department of Chemistry, College of Science, University of Guilan, Rasht

(E-mail: shirini@guilan.ac.ir , ١٢٣٦٥٤٧٩am@gmail.com)

One-pot multi-component reaction (MCR) strategies offer efficiency and high yield compared to traditional synthesis methods, making them a key focus of green chemistry. Among the compounds synthesized through these methods, 3,4-dihydropyrano[3,2-c]chromenes and their derivatives have wide applications in chemistry, biology, and pharmacology, displaying a range of activities such as spasmolytic, diuretic, anticoagulant, and anticancer effects. These compounds also show promise as cognitive enhancers for neurodegenerative diseases. The chromene scaffold serves as a significant template in medicinal chemistry, where derivatives demonstrate various biological activities, including anti-HIV, antitumor, antimalarial, and anti-Alzheimer effects. Notably, dihydropyrano[2,3-c]chromenes comprise a subclass exhibiting diverse activities, such as antimicrobial, anti-hyperglycemic, antioxidant, and inhibitors of important enzymes like acetylcholinesterase and Src kinase [1,2]. Also, recent developments in green chemistry support the use of molten salts as both catalysts and reaction media due to their high thermal stability, low vapor pressure, and extensive liquid range. These properties improve reaction kinetics and selectivity [3].

In this study, we employed a novel strategy that utilizes a Lewis acidic molten salt derived from phenylene diammonium containing manganese (TMPDMn) for the synthesis of 3,4-dihydropyrano[3,2-c]chromene derivatives (Scheme 1). The preparation of this catalyst is straightforward and offers several advantages, including easy separation, high product yield, and reduced reaction time.

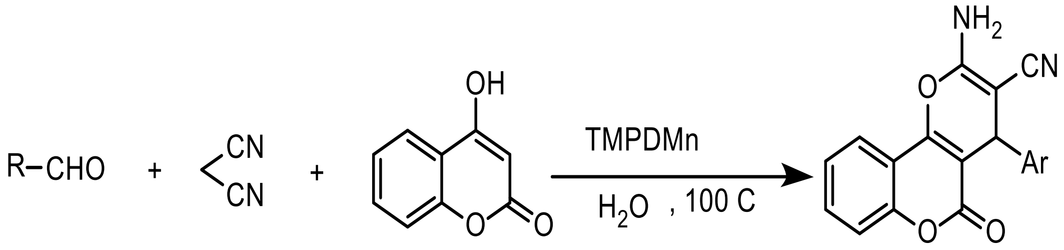

Scheme1. Synthesis of 3,4-dihydropyrano[3,2-c]chromenes catalyzed by TMPDMn

Keywords: Pyranochromenes, 4-Hydroxycoumarin, Molten salts, manganese

References:

[1]. Adami, E.; Marazzi-Uberti, E.; Turba, C. Arch. Ital. Sci. Farmacol. 1959, 9, 61-69.

[2]. Arvind, B. T.; Venkat, S. S.; Narayan, D. S.; Devanand, B. S. Bull. Environ. Pharmacol. Life Sci. 2012, 7, 30-33.

[3]. Manolov, I.; Maichle-Moessmer, C.; Danchev, N. Eur. J. Med. Chem. 2006, 41, 882-890.

The 30th Iranian Seminar of Organic Chemistry
February 7-9, 2025, Iran University of Science and Technology, Tehran, Iran

Catalytic application of Zr-L-histidine@GO/biochar nanocomposite for the synthesis of tetrahydrobenzopyrans

Sepideh Jalali-Mola, Maryam Hajjami*

Department of Organic Chemistry, Faculty of Chemistry and Petroleum Science, Bu-Ali Sina University, Hamedan, 6517838683, Iran, m.hajjami@basu.ac.ir or mhjjami@yahoo.com, s.jalalimola@gmail.com

Keywords: Graphene oxide, Biochar, Heterogeneous Catalysis, L-histidine

The use of catalysts across various fields is highly significant. Biochar nanoparticles represent one of the latest advancements in supports for immobilizing organic compounds. These materials are a type of porous substance produced through the pyrolysis of renewable resources and biomass in low-oxygen environments. In recent years, the diverse properties of nano-biochar, including its applications in catalysis, agriculture, and carbon capture, have gained considerable attention. Given that biochar is a carbon-rich solid, it is an effective option for managing agro-food industrial waste by converting it into biochar, which can serve as a biosorbent for treating soil and water. Modifying biochar with acids, alkalis, oxidizing agents, and metal ions enhances its properties [1,2]. Benzopyrans are a significant class of six-membered heterocycles containing oxygen atoms, which play a crucial role in creating structural components in natural products. They also demonstrate various biological activities, including anti-coagulation, anti-seizure, anti-shock, anti-tumor, and anti-allergy effects [3]. In this study, we investigated the use of Zr-L-histidine@GO/biochar as a catalyst for synthesis of benzopyran derivatives. This catalyst offers easy isolation and recyclability due to its heterogeneity, along with good to excellent efficiency.

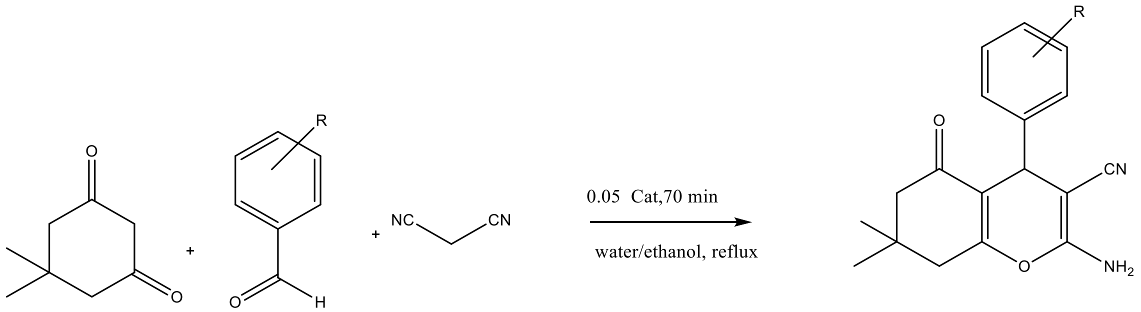

Scheme 1. synthesis of tetrahydrobenzopyrans in the presence of Zr-L-histidine@GO/biochar nanocomposite

References:

١- Farrokh, M., Hajjami, M., Zolfigol, M. A., & Jalali-Mola, S. (2024). Catalytic Application of Biochar Functionalized Copper-l-histidine for the Chemo and Homoselective Conversion of Cyanides to Amides and Reduction of Nitroarenes to anilines. *ACS omega*.Ghorbani-Choghamarani, A., Taherinia, Z., and Tyula, Y. A. **2022**. *Efficient biodiesel production from oleic and palmitic acid using a novel molybdenum metal–organic framework as efficient and reusable catalyst.* Sci.Rep., Vol. 12: 10338.

٢- Li, Z., Xing, B., Ding, Y., Li, Y., & Wang, S. (2020). A high-performance biochar produced from bamboo pyrolysis with in-situ nitrogen doping and activation for adsorption of phenol and methylene blue. *Chinese Journal of Chemical Engineering*, *28*(11), 2872-2880.

٣- Khodakarami, H., & Habibi, D. (2022). An amino-triethoxysilylpropyl-tetrazole-carboxamide-based Mn-complex as a capable nanocatalyst for the synthesis of tetrahydrobenzopyrans. *Catalysis Communications*, *172*, 106523.

The 30th Iranian Seminar of Organic Chemistry
February 7-9, 2025, Iran University of Science and Technology, Tehran, Iran

Effect of anionic and non-ionic surfactants on the formulation of hard gelatin capsule

RAMIN RAMEZANI KALMER [a], MOJGAN GHANBARI [a], SAMIRA GHOLIZADEH DOGAHEH [*a], DARIUSH SAMANDARIAN [a], MARYAM AGHAMOHAMMADSADEGH [a]

Affiliations: Iran Gelatin Capsule Mfg Co, 3351773415, Tehran, Iran

Surfactants play a vital role in the formulation of hard capsules used in pharmaceuticals. Sodium lauryl sulfate (SLS) is commonly used as an anionic surfactant in hard gelatin capsules due to its notable properties. One of the most substantial objectives of the present research study was to elucidate the impact of different surfactants on the surface properties of hard gelatin capsule solutions, especially on their surface tension and reducing the hard gelatin capsule defects. Consequently, different types of anionic, cationic, and neutral surfactants were tested to assess their impact on gelatin solutions. The tests revealed that lauryl glucoside and sodium olefin sulfonate were more effective in reducing defects compared to other surfactants used in the study.

Keyword: Hard gelatin capsule, anionic surfactant, non-ionic surfactant, sodium olefin sulfonate, lauryl glucoside.

1. Introduction

In the manufacturing of hard gelatin capsules, the presence of ingredients, especially surfactants, is crucial. Various additives are used in hard capsule formulations, including plasticizers, surfactants, antimicrobial agents, and preservatives. Studies have shown that surfactants with cationic or anionic functional groups perform better than their neutral counterparts [1,2]. In this study, Lauryl glucoside is considered a non-ionic surfactant with foaming, detergency, wetting characteristics, and emulsifying properties. Additionally, it demonstrates the alkaline and electrolyte features and surface tension reduction features. On the other hand, α-Olefin sulfonates are a group of anionic surfactants used as detergents. One of the most significant features of sodium C12 to C18 alpha-olefin sulfonates is their biodegradability and cost-effectiveness. In addition to these desirable ecological properties, low aquatic toxicity, as well as human toxicity, there are other positive and significant characteristics of sodium olefin sulfonate surfactants [4,5]. This research investigates the effect of different surfactants on the formulation of hard gelatin capsules, focusing on the physical and chemical properties of solutions containing ionic and non-ionic surfactants.

2. Method

To investigate the appropriate surfactant for the hard gelatin capsule, we have carried out different investigations over various surfactants. In a typical preparation procedure, different kinds of surfactants, including SLS, lauryl glucoside, sodium olefin sulfonate, Tween 80, Decyl glucoside, and Ditcrol AL40PG, with a weight ratio of 0.15 to dry gelatin were added to the solutions.

3. Results and discussion

With regard to the industrial application of hard capsule formulations and intrinsic properties of various forms of gelatin, the Surface tension assessment was performed on a wide range of different gelatin sources. Also noteworthy is the fact that a wide range of surfactants including the SLS, lauryl glucoside, sodium olefine sulfonate, decyl glucoside, ditcrol AL40 PG and Tween80 were employed to identify the effect of employed surfactants. Consequently, is seems that the sodium olefine sulfonate and lauryl glucoside can be employed for industrial manipulations with respect to hard capsule formulations.In Figure 1, images of hard gelatin capsules containing sodium olefin sulfonate and lauryl glucoside have been demonstrated.

a) **b)**

Figure 1: Produced hard gelatin capsules utilizing **a)** sodium olefin sulfonate and **b)** lauryl glucoside in formulation

One of the most important obtained results is that the lauryl glucoside and sodium olefine sulfonate possess superior efficacy in reducing the surface tension compared to SLS. With regard to the surface tension results, it is found out that the sodium olefine sulfonate displays the outstanding characteristic compared to the other surfactants. However, concerning the surface features of the prepared hard capsules sodium olefine sulfonate has outstanding properties. It is remarkable that the obtained experimental results have opened up opportunities toward the pharmaceutical application of SLS-free hard capsules utilizing sodium olefine sulfonate surfactant. Further, LOD and moisture content investigations have found out that the sodium olefine sulfonate surfactant possess lower moisture content that is appropriate for target applications. As a consequence, the current research demonstrates substantial implications for the development of novel drug delivery systems with lower side effects than current methods. Another significant aspect of this study is the suitability of these SLS-free hard capsules for target applications. Overall, the current research possesses the appropriate potential for industrial utilization.

References:

1- Berardi, A., Bisharat, L., Cespi, M., Basheti, I. A., Bonacucina, G., Pavoni, L., & AlKhatib, H. S. (2017). Controlled release properties of zein powder filled into hard gelatin capsules. Powder technology, 320, 703-713

2- Fakharian, M. H., Tamimi, N., Abbaspour, H., Nafchi, A. M., & Karim, A. A. (2015). Effects of κ-carrageenan on rheological properties of dually modified sago starch: Towards finding gelatin alternative for hard capsules. Carbohydrate polymers, 132, 156-163.

3- Cline, A., Uwakwe, L. N., & McMichael, A. J. (2018). No sulfates, no parabens, and the “no-poo” method: a new patient perspective on common shampoo ingredients. Cutis, 101(1), 22-26.

4- Ventura-Gayete, J. F., Reis, B. F., Garrigues, S., Morales-Rubio, Á., & de la Guardia, M. (2004). Multicommutation ATR-FTIR: determination of sodium alpha-olefin sulfonate in detergent formulations. Microchemical journal, 78(1), 47-54.

The 30th Iranian Seminar of Organic Chemistry
February 7-9, 2025, Iran University of Science and Technology, Tehran, Iran

Transition-metal-free Radical Approach for the Synthesis of Isothiocyanates by Pyridinium 1,4-Zwitterionic Thiolates as a Sulfur Source

Authors: Fatemeh Abdiyan Mobarakeh[a], Hormoz Khosravi[b], Alireza Akbari[c], Saeed Balalaie*[d]

Affiliations: [a]*Peptide Chemistry Research Institute, K. N. Toosi University of Technology, P.O. Box 15875-4416, Tehran 19697-64499, Iran, Email: balalaie@kntu.ac.ir*

Keyword: Pyridinium 1,4-Zwitterionic Thiolates, Functionalized Isothiocyanates, Transition-metal-free, Radical Approach

Body Text: Herein, we disclose a novel mild transition-metal-free approach to synthesizing diversely functionalized isothiocyanates from corresponding isocyanide precursors, achieving high to excellent yields (up to 97%). The current method sheds light on the reactivity of pyridinium 1,4-zwitterionic thiolates as an unprecedented sulfur source strikingly distinct from their previously known reactivity in ionic annulation reactions, showcasing an innovative approach to organic synthesis. The observed phenomenon has facilitated the development of this reagent as an effective sulfonation agent, eliminating the requirement for a catalyst and transition metal. In addition to experimental evidences, to further explore reaction mechanisms involved in the overall sulfuration process, density functional theory (DFT) calculations were carried out to obtain structures and energies of important intermediates relevant to this work.

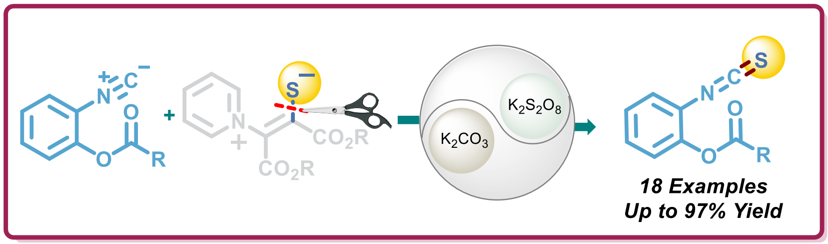

- Novel sulfonation reagent
- Transition-metal-free
- Unprecedented radical processes
- Mild reaction condition
- DFT calculations

Scheme: The synthesis of diversely functionalized isothiocyanates from corresponding isocyanides.

References: (a) Sun, S.; Wei, Y.; Xu, J. Microwave-Mediated Stereocontrolled Annulations of Diazo (Aryl) Methyl (Diaryl) Phosphine Oxides with Pyridinium 1, 4-Zwitterionic Thiolates. *Chem. Commun.* **2023**, *59*, 239–242. (b) Díaz-Jiménez, À.; Kennington, S. C. D.; Roglans, A.; Pla-Quintana, A. Copper (I) Iodide Catalyzed [3+ 3] Annulation of Iodonium Ylides with Pyridinium 1, 4-Zwitterionic Thiolates for the Synthesis of 1,4-Oxathiin Scaffolds. *Org. Lett.* **2023**, *59*, 239-242.

Synthesis of imidazole derivatives through multicomponent reaction strategy in the presence of new heterogeneous catalyst based on chitosan

Fereshteh Farhadpour [1], Mohammad G. Dekamin[1,*] Negin Rostami[1]

[1] Pharmaceutical and Heterocyclic Compounds Research Laboratory, Department of Chemistry, Iran University of Science and Technology, Tehran 16846-13114, Iran; fereshtehfarhadpoor1401@gmail.com; mdekamin@iust.ac.ir[1]; ne.rostami2016@gmail.com

[1,*]corresponding author: mdekamin@iust.ac.ir

Abstract

This research explores the efficient and sustainable synthesis of imidazole derivatives using novel catalytic methodologies. Here, the development of heterogeneous catalysts based on environmentally friendly materials like chitosan-based catalysts, for the synthesis of imidazole derivatives was reviewed. These catalysts offer advantages in terms of activity, selectivity, and reusability, contributing to a more sustainable chemical process.

Keyword: Chitosan, Imidazole derivatives, MCRs, Green Chemistry, Heterogeneous Catalysis

١. Introduction

Imidazole derivatives are one of the important nitrogen-containing five-membered heterocyclic compounds. This is due to their essential role as an important scaffold in diverse active pharmaceutical ingredients (APIs) and biologically active molecules such as histidine, histamine, biotin, losartan, miconazole and ketoconazole. Furthermore, they have been proved as efficient anti-cancer and anti-inflammation as well as anti-tuberculosis and antimicrobial compounds [1-5]. Hence, diverse applications of compounds containing imidazole as a moiety highlights the necessity of achieving efficient protocols for the synthesis of corresponding highly substituted derivatives. Following this issue, multi-component reaction (MCR) of benzyl or benzoin with aldehydes, primary amines and ammonium acetate is one of the most convenient protocols for synthesis of multi-substituted imidazole derivatives. [1].

2. **Methods**

2.1. General Procedure for the Synthesis of tetra-substituted imidazole derivatives in the presence of CS_Glu@Fe_3O_4

10.0 mg of the CS_Glu@Fe_3O_4 catalyst was added to a round-bottom flask containing benzyl or benzoin (1.0 mmol), aldehyde (1.0 mmol), primary amine (1.0 mmol) and ammonium acetate (1.75 mmol) in EtOH (2.5 ml) and the obtained mixture was heated under reflux conditions. The reaction progress was monitored by using thin layer chromatography and after completion of the reaction, the crude product was purified by crystallization in EtOH.

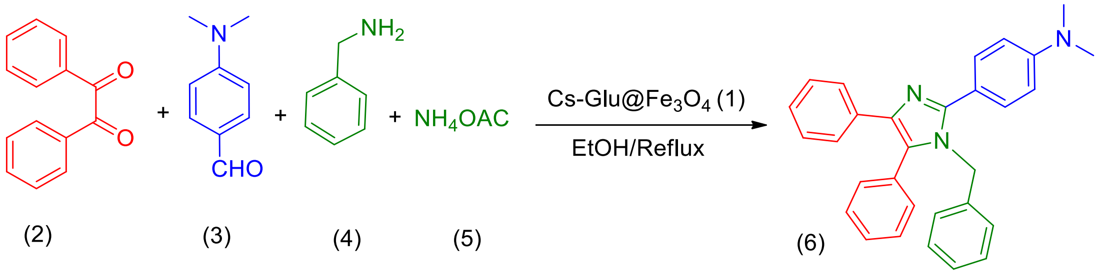

Scheme 1. Synthesis of 1,2,4,5-tetrasubstituted imidazole via one-pot four-component condensation between benzyl (2), 4-dimethylaminobenzaldehyde (3), ammonium acetate (5) and benzylamine (4) in the presence of CS_Glu@Fe_3O_4 (1) catalyst.

3. Results and Discussion

The reaction of benzyl (2), 4-dimethylaminobenzaldehyde (3), ammonium acetate (5) and benzylamine (4) was used as the model reaction **(**Scheme 1). The effect of different factors on the reaction rate was studied. According to the obtained results, it was concluded that using of the CS_Glu@Fe_3O_4 catalyst (1), which is a green catalyst can afford imidazole derivatives through the multicomponent reactions in a shorter reaction time compared to previous protocols. The corresponding product was obtained in high to excellent yields.

4. Conclusion

In summary, an efficient, environmentally benign, nonhazardous and expeditious protocol for the synthesis of highly-substituted imidazoles has been described in this work. The new catalyst was applied in the condensation of benzyl (or benzoin), aromatic carbocyclic and heterocyclic aldehydes, ammonium acetate and primary amines to afford the corresponding highly-substituted imidazoles, which are greatly important in numerous of biological and pharmacological compounds.

5. Acknowledgement

We are grateful for the financial support from The Research Council of Iran University of Science and Technology (IUST), Tehran, Iran is highly appreciated.

References:

1. Malihishoja, A., M.G. Dekamin, and M. Eslami, *Magnetic polyborate nanoparticles as a green and efficient catalyst for one-pot four-component synthesis of highly substituted imidazole derivatives.* RSC advances, 2023. **13**(24): p. 16584-16601.
2. Salimi, M., et al., *(Carboxy*-3-*oxopropylamino)*-3-*propylsilylcellulose as a novel organocatalyst for the synthesis of substituted imidazoles under solvent-free conditions.* RSC Advances, 2015. **5**(43): p. 33974-33980.
3. Thimmaraju, N. and S.M. Shamshuddin, *Synthesis of 2, 4, 5-trisubstituted imidazoles, quinoxalines and 1, 5-benzodiazepines over an eco-friendly and highly efficient ZrO 2–Al 2 O 3 catalyst.* RSC advances, 2016. **6**(65): p. 60231-60243.
4. Zarnegar, Z. and J. Safari, *Fe 3 O 4@ chitosan nanoparticles: a valuable heterogeneous nanocatalyst for the synthesis of 2, 4, 5-trisubstituted imidazoles.* RSC advances, 2014. **4**(40): p. 20932-20939.
5. Akbari, A., et al., *Novel magnetic propylsulfonic acid-anchored isocyanurate-based periodic mesoporous organosilica (Iron oxide@ PMO-ICS-PrSO3H) as a highly efficient and reusable nanoreactor for the sustainable synthesis of imidazopyrimidine derivatives.* Scientific Reports, 2020. **10**(1): p. 10646.

The 30th Iranian Seminar of Organic Chemistry
February 7-9, 2025, Iran University of Science and Technology, Tehran, Iran

Conversion of furfural as biomass to C-4 compounds with industrial value under iron-doped graphitic carbon nitride photocatalyst

Mohammad Bashiri [a], Mona Hosseini-Sarvari *[a]

[a]*Nanophotocatalysis Lab., Department of Chemistry, Shiraz University, Shiraz 7194684795, Iran.*

Corresponded to: hossaini@shirazu.ac.ir

Keyword: Photocatalyst, Furfural, Biomass

Introduction

Biomass, sourced from plants, animals, and microorganisms, is a renewable energy resource that includes materials like wood, crop residues, energy crops, and organic waste. Its importance is underscored by its ability to promote sustainable energy production and mitigate climate change. Biomass offers several benefits, including its renewability, the potential to reduce carbon dioxide emissions through a carbon-neutral cycle, and the enhancement of energy security by leveraging local resources. To ensure the sustainable use of biomass, it is crucial to adopt responsible sourcing practices, advance technology, and improve conversion processes to reduce environmental impacts and ensure long-term sustainability [1].

Photocatalysts play a crucial role in the degradation of biomass, especially in biomass conversion and waste management. They facilitate the breakdown of organic compounds in biomass, such as lignocellulosic materials and organic waste, by using light to speed up the degradation process [2]. The application of photocatalysts in biomass degradation provides a sustainable and environmentally friendly method, operating under milder conditions compared to conventional methods. This leads to lower energy consumption and reduced production of harmful byproducts. Moreover, photocatalysts enhance the efficiency of biomass degradation by increasing the rate of breakdown, which is advantageous for applications like biofuel production and waste treatment. Additionally, photocatalysis aids in the valorization of biomass by enabling the production of valuable chemicals or biofuels. Various types of photocatalysts can be tailored to target specific biomass components or optimize the degradation process for different feedstocks, allowing for customized strategies based on specific requirements and desired outcomes [3].

Method

A Pyrex glass tube was used to combine a nanocomposite of Fe^{III}/g-C_3N_4 (0.01 g), furfural (0.5 mmol), and a solvent mixture of MeCN/H_2O in a 1:1 ratio (3 mL). The reaction mixture was exposed to air and stirred at room temperature for a suitable period. After the reaction was completed, DMF (5–10 mL) was introduced into the mixture. The nanophotocatalyst was then isolated by centrifugation and meticulously washed with ethanol (3 mL×3).

Results and Discussion

The photoconversion of furfural into maleic acid and succinic acid has been effectively achieved using an Fe^{III}/g-C_3N_4 nanocomposite as a photocatalyst. Experimental findings highlight the efficiency of this nanocomposite in converting furfural under visible light. The superior photocatalytic activity of the Fe^{III}/g-C_3N_4 nanocomposite is due to the collaborative interaction between Fe species and g-C_3N_4. The Fe species function as co-catalysts, aiding in the separation of photogenerated electron-hole pairs and enhancing the production of reactive oxygen species (ROS), which are essential for the reaction. Furthermore, the distinctive structure and properties of g-C_3N_4, including its high surface area, stability, and ability to absorb visible light, enhance the overall photocatalytic performance. The integration of Fe and g-C_3N_4 in the photo-Fenton process results in heightened photocatalytic activity. The Fe^{III}/g-C_3N_4 nanocomposite serves as an effective catalyst, generating highly reactive hydroxyl radicals (•OH) under visible light. This photo-Fenton process is more environmentally friendly than traditional methods, as it does not require harmful chemicals or excessive energy, making it a greener option for furfural degradation. Additionally, it produces non-toxic byproducts, reducing environmental impact (**Scheme** 1).

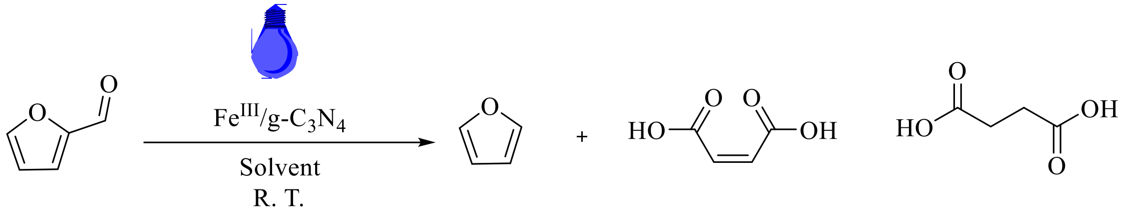

Scheme 1: Photoconversion of furfural

References:

[1]. T. Kalak, Potential use of industrial biomass waste as a sustainable energy source in the future, Energies 16 (2023) 1783.

[2]. R.A. Rather, A.W. Wani, S. Mumtaz, S.A. Padder, A.H. Khan, A.I. Almohana, S. F. Almojil, S.S. Alam, T.R. Baba, Bioenergy: a foundation to environmental sustainability in a changing global climate scenario, J. King Saud Univ. Sci. 34 (2022) 101734.

[3]. 3] A.I. Osman, L. Chen, M. Yang, G. Msigwa, M. Farghali, S. Fawzy, D.W. Rooney, P.- S. Yap, Cost, environmental impact, and resilience of renewable energy under a changing climate: a review, Environ. Chem. Lett. 21 (2023) 741–764.

The 30th Iranian Seminar of Organic Chemistry
February 7-9, 2025, Iran University of Science and Technology, Tehran, Iran

Synthesis and enantiomeric resolution of chiral Betti bases *via* chiral resolving agent

Rana Khezeli[a], Salar Tawana[a], Hamid Arvinnezhad[a], Saadi Samadi[a]*

[a]*Laboratory of Asymmetric Synthesis, Department of Chemistry, Faculty of Science, University of Kurdistan, Sanandaj, Iran. *Email:* s.samadi@uok.ac.ir.

Keywords: Chiral Betti base, L-(+)-tartaric acid, Chiral resolving agent

Introduction:

Betti bases, a subclass of amino alcohols, exemplify highly versatile scaffolds in synthetic organic chemistry. These compounds are typically synthesized via a three-component reaction involving β-naphthol, an aromatic aldehyde, and an amine, which provides a robust and efficient route to these multifunctional molecules. When a chiral amine or aldehyde is incorporated as a reactant, the resulting Betti bases exhibit chirality. Alternatively, chiral Betti bases can be obtained by enantiomeric resolution of racemic mixtures using chiral resolving agents. The latter approach is particularly advantageous due to its economic efficiency, circumventing the need for costly enantiomerically pure starting materials while enabling access to single-enantiomer products. Beyond their structural simplicity, chiral Betti bases serve as pivotal intermediates in constructing chiral bioactive molecules and as precursors for diverse chiral ligands integral to catalytic systems for asymmetric transformations. Their utility in enantioselective reactions, such as adding alkyl, alkenyl, and phenyl groups to carbonyl compounds, underscores their importance in synthesizing enantiomerically enriched products essential for pharmaceutical synthesis and fine chemical production, where stereochemical precision is critical [1-3].

Method:

Synthesis of racemic Betti bases:

In a round-bottom flask, benzaldehyde derivatives, β-naphthol, and pyrrolidine were dissolved in ethanol and refluxed for 24 hours. Reaction progress was monitored via TLC. Upon cooling to room temperature, the mixture was filtered and washed with ethanol, yielding pure racemic Betti base as a white-to-yellow solid.

Resolution of Betti bases using L-(+)-tartaric acid:

Under a nitrogen atmosphere at room temperature, the synthesized racemic Betti bases were added to a round-bottom flask containing acetone and L-(+)-tartaric acid. This mixture was stirred for six hours, producing diastereomeric salts. The resulting precipitate was filtered, dissolved in a mixture of aqueous sodium carbonate and dichloromethane, and stirred until fully dissolved. The organic layer was extracted, washed with brine, dried over magnesium sulfate, and evaporated under vacuum to yield (*S*)-(+)-Betti base.

For the isolation of the (*R*)-(-)-enantiomer, anhydrous oxalic acid was added to the filtrate under identical conditions and stirred for six hours. The precipitate underwent similar treatment with a sodium carbonate/dichloromethane mixture, yielding the (*R*)-(-)-Betti base [4, 5].

Results and Discussion:

Racemic Betti bases were synthesized through a one-pot, three-component reaction involving β-naphthol, pyrrolidine, and benzaldehyde derivatives in ethanol, a green solvent, under reflux conditions. The resulting white-to-yellow solid was washed with ethanol to yield pure racemic Betti bases. The formation of a new stereogenic center was confirmed by the appearance of characteristic signals at approximately 5 ppm and 70 ppm in the ^{1}H-NMR and ^{13}C-NMR spectra, respectively.

The chiral Betti bases were obtained by resolving the corresponding racemic mixture using L-(+)-tartaric acid, an inexpensive and environmentally friendly chiral resolving agent. Reaction with L-(+)-tartaric acid generated diastereomeric salts of the (*R*)- and (*S*)-enantiomers, which exhibited differential solubility. After filtration, the (*S*)-(+)-Betti base was obtained from the residue, while the filtrate contained the (*R*)-(-)-Betti base. Both enantiomers were subsequently purified by treating the salts with sodium carbonate to remove L-(+)-tartaric acid, yielding enantiomerically pure chiral Betti bases (Scheme 1).

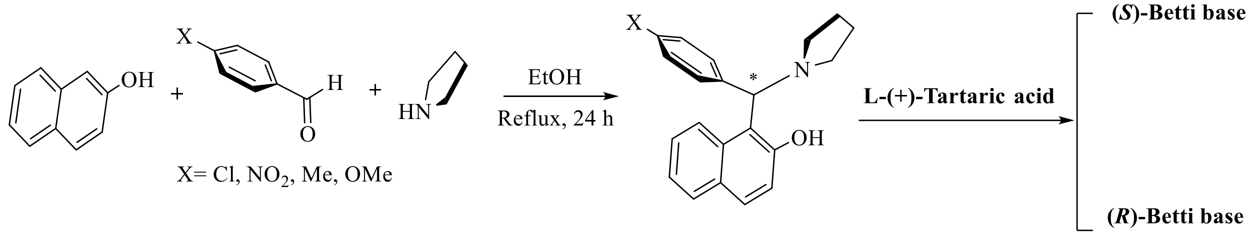

Scheme 1: Synthesis of racemic Betti bases and resolution of enantiomers

References:

[1]. Naso, F. *Substantia*, **2017**, *1*, 111.
[2]. Cardellicchio, C., Capozzi, M. A. M., Naso, F. *Tetrahedron: Asymmetry*, **2010**, *21*, 507.
[3]. Olyaei, A., Sadeghpour, M. *RSC Adv.*, **2019**, *9*, 18467.
[4]. Periasamy, M., Reddy, M. N., Anwar, S. *Tetrahedron: Asymmetry*, **2004**, *15*, 1809.
[5]. Sehhat, Z., Mansoori, S., Arvinnezhad, H., Naghdi, Y., Samadi, S. *Mol. Catal.*, **2023**, *538*, 113011.

The 30th Iranian Seminar of Organic Chemistry
February 7-9, 2025, Iran University of Science and Technology, Tehran, Iran

Palladium Nanoparticles-Decorated Porous MOF@ECH Over the Surface of *β*-CD: A Novel Efficient Catalyst in Cross-Coupling Reactions

Leila Mohammadi [a,*] and Mohammad Reza Vaezi [a,*]

Keyword: Palladium Nanoparticles, Metal Organic Framework, Cross-Coupling Reaction

In this study, UiO-66-NH_2, known for its inherent porous structure, hydrophilic properties, and high stability in aqueous environments, has been utilized to create a membrane with enhanced surface hydrophilicity, reduced cross-linking, and preferential pathways for water molecules through selected layers of UiO-66-NH_2 nanoparticles. Building on these promising results, this research aims to thoroughly evaluate and characterize the synthesized catalyst UiO-66-NH_2@1-Chloro-2,3-epoxypropane@ β-cyclodextrin@Pd-NPs. This catalyst is developed by combining UiO-66-NH_2 with epichlorohydrin (ECH) and β-cyclodextrin to cross-link and stabilize palladium nanoparticles on the substrate. The goal is to design a remarkably effective and novel green catalyst: UiO-66-NH_2@1-Chloro-2,3-epoxypropane@ β-cyclodextrin @Pd-NPs. This innovative catalyst has proven effective when employed in heterogeneous catalysis, demonstrating its flexibility in facilitating both C-C coupling and Carbonylative reactions. To this end, MOFs are ideal hosts. Given their permanent porosity, they offer significant advantages for confining metal nanoparticles, allowing the metal to retain its large and uniform potential, which benefits advanced catalytic applications. Recent studies have reported extensively on metallic MOF-nanoparticles (MOF@NP), highlighting their catalytic activity, which is largely attributed to the high activity and recyclability of metal nanoparticles immobilized within MOFs. The chemical environment surrounding the guest metal nanoparticles can be readily modified through functional group linkages, enhancing the catalytic performance by optimizing metal substitution within MOFs [1-3].

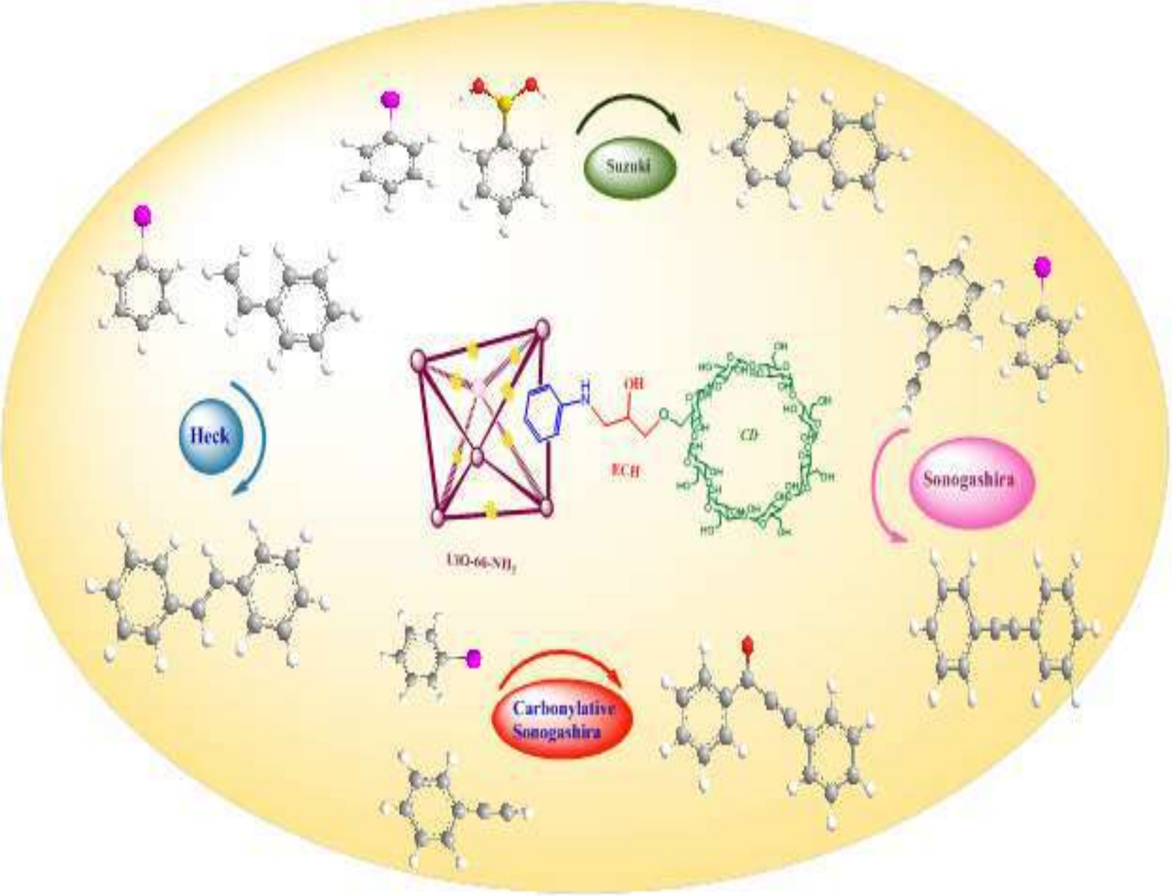

Scheme 1: UiO-66-NH_2@Epichlorohydrin@ β-Cyclodextrin **@Pd-NPs.**

References:

[1]. J. H. Park, F. Raza, S.-J. Jeon, H.-I. Kim, T. W. Kang, D. Yim & J.-H. Kim, *Tetrahedron Lett.* 2014, **55** (23), 3426-3430.

[2]. Z. J. Wang, S. Ghasimi, K. Landfester & K. A. Zhang, *Chem. Mater.* 2015, **27** (6), 1921-1924.

[3]. D. Dong, Z. Li, D. Liu, N. Yu, H. Zhao, H. Chen, J. Liu & D. Liu, *New J Chem.* 2018, **42** (11), 9317-9323.

Preparation of biodegradable-based supramolecule materials for improved pollution removal and catalyst

Hedieh Mokhtari[a], Mohammad Salehi[a], Saied Shafiei Navid[a], Rahman Hosseinzadeh[a*] (Corresponding author)

[a] *Department of Organic Chemistry, Faculty of Chemistry, University of Mazandaran, Babolsar, Iran.*

Keyword: Pollution removal, Chitosan, Supramolecule, Catalyst

Pollution removal including dyes, heavy metals, and aromatic residuals has attracted more attention in recent years due to the serious global health challenge in human society[1]. It has been proven that natural polymer (chitosan for example) can also be used as a green substrate in the field of pollutant removal[2]. In this research, a chitosan-based supramolecule (Chit@Sup) material was prepared with a lot of functional groups such as NH_2, OH, COOH, N=N, and SO_3H. The biodegradable chitosan was modified with two different supramolecules with instinct porosity. The prepared materials were characterized using different measurements such as FT-IR, PXRD, TGA, FE-SEM, and EDS/MAPP analysis. Due to the coexistence of chitosan and supramolecules in Chit@Sup, the removal efficiency of the prepared materials was higher than chitosan and supramolecule, individually for both dye and heavy metal removal. Furthermore, due to the presence of the sulfonated functional groups, the prepared composite showed a high catalytic activity as a Bronsted acid for the esterification of benzoic acid to the methyl and/or ethyl benzoate. The obtained results showed that the prepared materials could be served as a novel and capable sorbent for pollution removal as well as an acidic heterogenous catalyst.

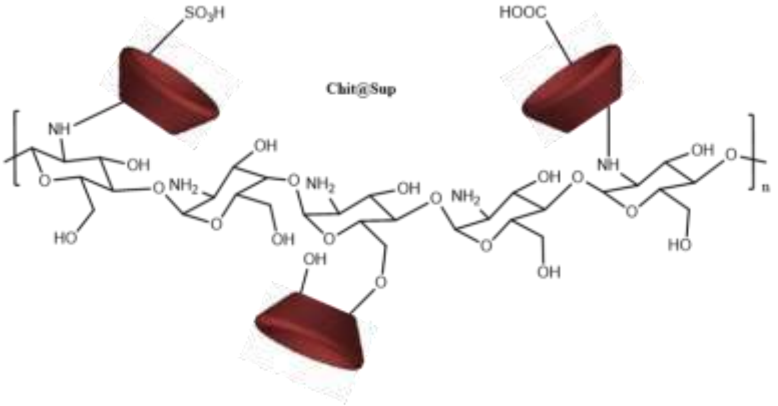

Scheme: The schematic representation of Chit@Sup structure.

References:

1. Muhaidin M, Naning FH, Saad JM, Wahi R, Zangina T. Heavy Metal Ion Adsorbent in Aqueous Solution: A Review on Chitosan and Chitosan Composites. J Adv Res MNE 2024; 18(1): 78-102.

2. Ishak S, Rosly NZ, Abdullah AH, Alang Ahmad SA. Fabrication of calix[4]arene/polyurethane for the adsorptive removal of cationic dye from aqueous solutions. Environ Monit Assess 2023; ١٩٥(١١): ١٣٠٣-١٣١١.

The 30th Iranian Seminar of Organic Chemistry
February 7-9, 2025, Iran University of Science and Technology, Tehran, Iran

One-pot synthesis of 3,4-dihydropyrimidin-2(1H)-ones catalyzed by acidic calix[4]arenes

Melika Hosseinzadeh[a], Rahman Hosseinzadeh[*,a], Ali Ahmadi[a], Mahmood Tajbakhsh[a]

[a]Department of Organic Chemistry, Faculty of Chemistry, University of Mazandaran, Babolsar, Iran.

Keyword: Multicomponent reactions, Biginelli reaction, 3,4-Dihydropyrimidin-2(1H)-ones, Calix[4]arenes,

One of the classical multicomponent strategies for synthesizing heterocycles is the Biginelli three-component condensation of aldehydes, *β*-keto esters, and urea or thiourea, which affords 3,4-dihydropyrimidin-2(1H)-(thi)ones (DHPM) [1]. Due to the broad spectrum of biological functions of DHPMs, numerous methods have been developed for synthesizing them over the past several decades. Although a large number of new catalysts have been reported [2], some of these methods suffer from one or more limitations. Among various macrocyclic compounds, calix[n]arenes have emerged as highly effective catalysts in numerous organic transformations. Calixarenes are macrocycles which formed from the condensation of p-substituted phenols with formaldehyde in basic medium. Since they can be modified at both the upper and lower rims, these characteristics make calixarenes suitable scaffolds for a wide array of applications [3]. We report here a effective method for synthesizing 3,4-dihydropyrimidin-2(1H)-ones using acidic-modified calix[4]arenes as an efficient, cost-effective, and reusable catalyst (Scheme).

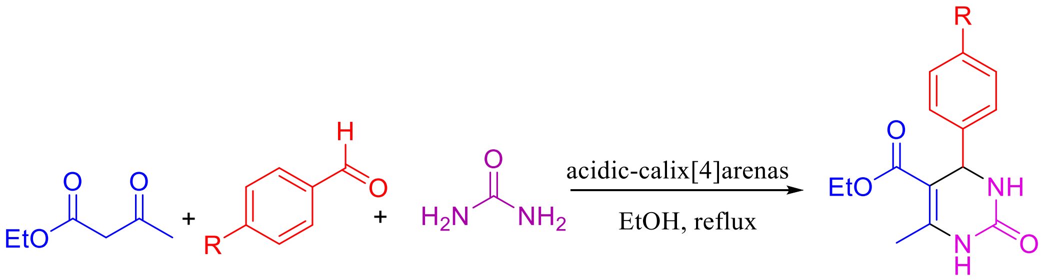

Scheme: Synthesis of 3,4-dihydropyrimidin-2(1H)-one's derivatives

References:

[1] S. Panda, S., Khanna, P., & Khanna, L. Current Organic Chemistry. 2012, 16(4), 507-520.
[2] H. Nagarajaiah, A.Mukhopadhyay, J. N. Moorthy. Tetrahedron Letters. 2016, 57(47), 5135-5١٤٩.

[3] L. Daniel , SA. Fernandes , AA. Sabino , Â De. Fátima. TetrahedronLett[Internet].2011; 52(48): 6328 30.

The 30th Iranian Seminar of Organic Chemistry
February 7-9, 2025, Iran University of Science and Technology, Tehran, Iran

Synthesis of new spirooxindoles and investigation of the biological activity of the products

Authors: Amir Reza Omidvar, Sakineh Asghari*, Leila Ghasempour and Mojtaba Mohseni

Department of Organic Chemistry, Faculty of Chemistry, University of Mazandaran, Babolsar,

Keyword: 2-Thiohydantoin, Spirooxindoles, Isatins, Antioxidant, Anti-bacterial

Introduction:

Heterocyclic compounds are a diverse group of organic compounds found in various natural sources, including hormones, alkaloids, antibiotics, and pharmaceutical drugs. Spiroxindole alkaloids are an important class of naturally occurring heterocyclic compounds, such as spirotriprostatin B, which are known for their diverse range of biological applications, especially their antimitotic activity.[5] In addition, various spiroxindole derivatives have been synthesized, which possess activities such as anticancer, antiviral, antibacterial [11,12], and antioxidant. Therefore, the important biological activities of spiroxindoles have led chemists to synthesize these compounds.[16] Since the structure of isatin and its derivatives is close to spiroxindole, they are considered as one of the primary reactants in multicomponent reactions leading to the production of spiroxindole. On the other hand, 2-thiohydantoin is a five-membered heterocyclic compound with different specific positions. Some derivatives of this compound have various biological properties such as antiviral, anticancer, [25] anti-HSV, anti-HIV, anti-gene mutagenic, anti-cancer. [30] antibacterial and antioxidant activities. Considering the numerous reported biological activities, we were encouraged to synthesize new spiroxindole derivatives including the hydantoin moiety and investigate their antibacterial and antioxidant activities. (Scheme 1)

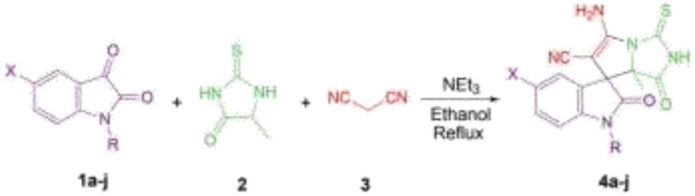

Scheme1: Preparation of spirooxindole derivatives 4a–j via one-pot reaction.

Method:

General procedure for the synthesis of compounds (4a-j): For the synthesis of products 4a-j, a mixture of isatin derivatives, malononitrile and NEt_3 in 10 mL of ethanol was refluxed at room temperature in the presence of 5-methyl-2-thiohydantoin for 4 h.

General method for the assessment of antioxidant activity: The use of DPPH radical spectrophotometry is a rapid and inexpensive method for measuring the radical scavenging activity of compounds. This assay is based on the ability of antioxidants to reduce DPPH, a stable free radical, to its non-radical form. DPPH reduction is evaluated at a wavelength of 517 nm. This was determined by preparing a solution of each compound in dimethyl sulfoxide (DMSO).

Antibacterial activity evaluation method: The antibacterial activity of the synthesized compounds 4a-j was tested in vitro using the Kirby-Bauer disk diffusion technique for antibacterial properties against two strains of Gram-positive bacteria, Staphylococcus aureus ATCC 35923 and Bacillus subtilis PTCC 1023, as well as two strains of Gram-negative bacteria, Escherichia coli PTCC 1330 and (Psev1330) PTCC. The exponential phase bacteria were established from existing cultures in Mueller-Hinton fresh broth and grown on an orbital shaker and 100 RPM overnight. The antibacterial effect of the synthesized compounds was compared with the known antibiotics gentamicin and chloramphenicol which were used as positive control and DMSO as negative control.

Results and Discussion:

A series of solvents (THF, DMF, toluene and EtOH) were used to determine the optimal conditions for the reaction. Also, the reactions were tested under reflux conditions and at room temperature. The highest yield (80%) was obtained when ethanol was used as the solvent in the reflux reaction. The reaction was also investigated in the presence of several bases such as K_2CO_3, $ZrCl_4$, DBU and NEt_3. The results showed that 20% NEt_3 gave a higher yield of the desired product than other bases. To evaluate the extent and scope of this reaction, the desired compounds were obtained in 65-90% yield. The structures of compounds 4a-j were determined using techniques such as IR, ^{1}H-NMR, ^{13}C NMR and mass spectra. The in vitro antioxidant activity of spiroxindole derivatives (4a-j) was measured using the DPPH radical scavenging assay based on the Blois method. The DPPH assay measures the ability of an antioxidant to donate an electron to a stable free radical. This process in the presence of antioxidants changes the color of the DPPH solution from dark purple to light yellow, as determined by measuring the decrease in absorbance at a wavelength of 517 nm. The degree of color change is proportional to the antioxidant activity of the compound.

All the synthesized compounds showed good to excellent DPPH scavenging power (59.65–94.03%). Among these compounds, compounds 4f–j showed higher antioxidant activity (84.85–94.30%) than compounds 4a–e (59.65–78.21%) and even higher than the standard compound (AA) with an activity of 82.3%. This could be due to the presence of chlorine heteroatoms only in compounds 4f–j. The antibacterial activity of the synthesized compounds was evaluated against two gram-positive bacteria as well as against gram-negative bacteria. Then, the results were compared with those of two standard antibacterial drugs, gentamicin and chloramphenicol. All compounds 4a–j showed higher antibacterial activity against Gram-positive bacteria compared to Gram-negative bacteria.

References:

[1] S. Karamthulla, S. Pal, M. N. Khan, L. H. Choudhury, RSC Adv. 2013, 3,15576–15581.

[2] D. L. Kong, J. Jiang, L. Y. Wu, X. H. Wang, Z. F. Shi, M. S. Wu, X. Wang, Q. Lin, Chin. J. Struct.Chem. 2016, 35,1849–1854.

[3] D. Kathirvelan, J. Haribabu, B. S. Reddy, C. Balachandran, V. Duraipandiyan, Bioorg. Med. Chem. Lett. 2015, 25, 389–399.

[4] S. A. Babu, R. Padmavathi, N. A. Aslam, V. Rajkumar, Nat. Prod. Chem. 2015, 46, 227–339.

[5] F. Wu, H. Jiang, B. Zheng, M. Kogiso, Y. Yao, C. Zhou, X. N. Li, Y. Song, J. Med. Chem. ٢٠١٥, ٥٨, ٦٨٩٩–٦٩٠٨.

[6] R. Raj, V. Mehra, J. Gut, P. J. Rosenthal, K. J. Wicht, T. J. Egan, M. Hopper, L. A. Wrischnik, K. M. Land, V. Kumar, Eur. J. Med. Chem. 2014, 84, 425– 432.

In situ synthesis of biomagnetic Fe_3O_4/CMC composite embedded with Ag nanoparticles and effectiveness in eliminating organic dyes from industrial wastewater

Authors: Mojtaba Azizi[a]*, Mahdi Jafari[b] and Sadegh Rostamnia[c]*

Affiliations: Organic and Nano Group (ONG), Department of Chemistry, Iran University of Science and Technology (IUST), PO Box 16846-13114, Tehran, Iran.

Keyword: biosynthesis; Fe_3O_4 Magnetic Nanoparticle; Carboxy Methyl Cellulose; Ag Nanoparticles; Dye Removal.

Introduction

Ionic dyes are commonly utilized across various industries, including textiles, printing, chemicals, pharmaceuticals, and food production. However, these dyes often contaminate water bodies through different channels, posing significant risks to both human health and aquatic life. Methylene blue (MB), a water-soluble cationic synthetic azo dye from the phenothiazine group, is particularly concerning due to its carcinogenic properties. Exposure to such dyes can lead to serious health issues, including skin disorders, allergies, and cancer. Moreover, even small quantities of these dyes can significantly tint large volumes of water. Hence, effectively removing MB from water is crucial for protecting the environment and public health [1].

Silver nanoparticles (Ag NPs) are valued for their beneficial characteristics, such as low cost, various crystal shapes, adjustable plasmon resonance, and a high surface-to-volume ratio. They serve multiple purposes, including catalysis, dye degradation, photocatalysis, antibacterial action, anti-cancer effects, biological applications, electrochemical functions, and drug delivery.

Similarly, magnetic Fe_3O_4 nanoparticles possess impressive magnetic and optical properties that vary with the application of a magnetic field. This versatility makes them ideal for uses in catalysis, heavy metal ion removal, dye removal, biodiesel production, electrocatalysis, and drug delivery. Additionally, they act as substrates for material growth and assist in separation processes.

This study explores the integration of carboxymethyl cellulose (CMC), a biopolymer, with Fe_3O_4 magnetic nanoparticles to serve as a substrate for regulating the growth of AgNPs, as illustrated in Scheme 1[2-8].

Method

Preparation of Fe_3O_4/CMC

The composite of magnetic nanoparticles, coated with the biopolymer carboxymethyl cellulose (CMC), was successfully synthesized using an in situ solvothermal method. Initially, ammonium acetate (0.385 g, 5 mmol) was incorporated into a solution composed of ethylene glycol (7 mL) and iron (III) chloride hexahydrate (135 mg, 0.5 mM) while being continuously stirred. Subsequently, CMC (Mw=90.0 kg/mol, purity= 99.5%) was added to the resulting brown mixture, which was stirred vigorously for 45 minutes. The homogeneous solution was then transferred to a stainless-steel autoclave lined with Teflon and subjected to heating at 200 ℃ for 12 hours. Following the cooling process, the resultant precipitate was isolated using an external magnetic field and thoroughly washed multiple times with deionized water and ethanol. Finally, the dark Fe_3O_4/CMC precipitate was dried at a temperature of 60 ℃.

Preparation of Euphorbia plant extract

The aerial parts of the flowering stage were thoroughly dried and subsequently ground to produce an extract from the Euphoria plant. The resulting powder was then immersed in ethanol, and the solution underwent filtration three times following a 36-hour period.

Preparation of Fe_3O_4/CMC-AgNPs

A total of 0.1 g of Fe_3O_4/CMC was suspended in 25 milliliters of deionized water. Subsequently, 100 ml of a silver nitrate solution, with a concentration of 10 mg.L−1, was introduced to the mixture and agitated for a period of 30 min. Following this, The Euphorbia plant extract solution was added gradually, and the mixture was stirred for 8 h at room temperature. The resulting magnetic precipitate was then rinsed with deionized water and ethanol, and subsequently dried at a temperature of 60°C.

Results and Discussion

To measure the saturation removal capacity of magnetic composite for cationic dye, methylene blue (MB) was chosen as a representative of cationic dyes in wastewater. Accordingly, 0.01-0.03 g of Fe_3O_4/CMC-Ag NPs magnetic composite was added to a conical flask (100 mL) containing 50 mL of dye solution (25-250 mg/L) and kept in a thermostatic shaker at 25 °C and 150 rpm. The supernatant was collected at different times for 135 min until the absorption equilibrium was reached, and the concentration of MB was determined using the characteristic light absorption peak at $\lambda = 616$ nm. The absorption capacity (Qt) of the dye species and their removal rate (Re) were calculated using the following equation using UV spectrophotometer [9,10]:

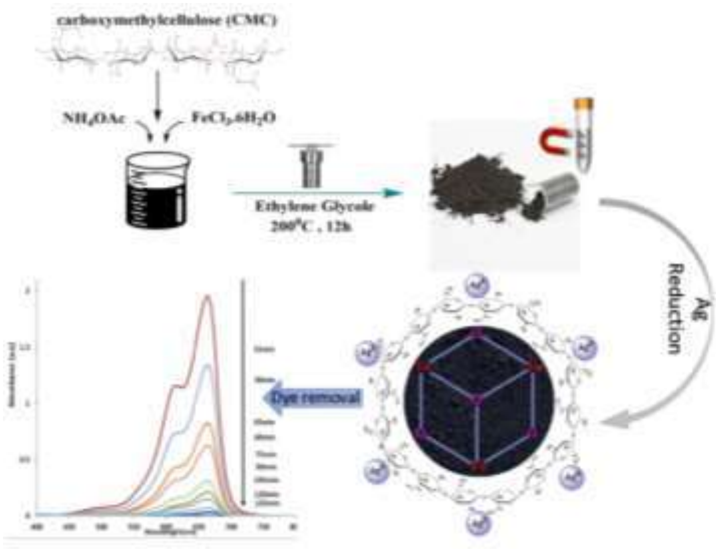

References:

١ M. Yan, W. Huang and Z. Li, *Int. J. Biol. Macromol.*, 2019, 136, 927–935.

٢ X. Jiang, W. Pan, Z. Xiong, Y. Zhang and L. Zhao, *J. Alloys Compd.*, 2021, 870, 159414.

٣ M. S. Yilmaz, *Microporous Mesoporous Mater.*, 2022, 330, 111570.

٤ A. Tanwar, P. Kalode, R. V, P. B.K., P. Doshi and D. Ottoor, *Mater. Today Commun.*, 2023, 35, 105922.

٥ R. Foroutan, S. J. Peighambardoust, S. Hemmati, A. Ahmadi, E. Falletta, B. Ramavandi and C. L. Bianchi, *RSC Adv.*, 2021, 11, 27309–27321.

٦ S. Dutta, B. Gupta, S. K. Srivastava and A. K. Gupta, *Mater. Adv.*, 2021, 2, 4497–4531.

٧ A. Ahmad, S. H. Mohd-Setapar, C. S. Chuong, A. Khatoon, W. A. Wani, R. Kumar and M. Rafatullah, *RSC Adv.*, 2015, 5, 30801–30818.

٨ F. Ahmadijokani, H. Molavi, M. Amini, A. Bahi, S. Wuttke, T. M. Aminabhavi, M. Kamkar, O. J. Rojas, F. Ko and M. Arjmand, *Chem. Eng. J.*, 2023, 466, 143119.

٩ H. Li, X. Cao, C. Zhang, Q. Yu, Z. Zhao, X. Niu, X. Sun, Y. Liu, L. Ma and Z. Li, *RSC Adv.*, 2017, 7, 16273–16281.

١٠ E. Jin, J. Kim, J. Nam, D. C. Yang, H. Jeong, S. Kim, E. Kang, H. J. Cho and W. Choe, *ACS Appl. Nano Mater.*, 2021, 4, 10068–10076.

Post-Synthetic Modification of IRMOF-3 with Schiff Bases for Encapsulating Pd Nanoparticles and use in Cross-Coupling Suzuki Reactions

Authors: Mojtaba Azizi*, Mahdi Jafari, and Sadegh Rostamnia*

Affiliations: Organic and Nano Group (ONG), Department of Chemistry, Iran University of Science and Technology (IUST), PO Box 16846-13114, Tehran, Iran.

Keyword: IRMOF-3, Pd NPs, Schiff-base, Suzuki reaction.

Introduction

Organic synthesis has long been an intriguing field in chemistry, particularly focusing on carbon-carbon synthesis strategies that produce more robust and complex molecules. Akira Suzuki, a Nobel Prize winner, is known for discovering Suzuki cross-coupling reactions, which have become one of the most commonly used methods for forming carbon-carbon bonds. The popularity of these reactions can be attributed to the availability, stability, and sustainability of the precursors, as well as the mild reaction conditions and their applicability to a diverse range of substrates with various functional groups.

Soluble palladium (Pd) complexes have been utilized to facilitate these reactions in both organic solvents and, more recently, aqueous environments. While homogeneous catalysts demonstrate excellent activity and selectivity, the challenging separation process has led researchers to explore heterogeneous catalysts.

Metal-organic frameworks (MOFs) are porous crystalline materials notable for their high surface area, adjustable structures, and permanent porosity. Among these, IRMOF-3, derived from amino functionalized terephthalic acid (H_2ATA) and octahedral $[Zn_4O]^{6+}$ inorganic nodes, has gained significant attention due to its high porosity and stability[1-7].

Method

Synthesis of IRMOF-3

To prepare IRMOF-3, 12.5 mmol of $Zn(NO_3)_2$ (2.36 g) and 4.1 mmol H_2ATA (0.74 g) were dissolved in 100 mL dry DMF. A Teflon-lined autoclave was used to seal the solution and keep it at 100 °C for 17 hours after being stirred for 60 min at room temperature. Following the formation of brown solids, DMF and $CHCl_3$ were used to wash the synthesized IRMOF-3, and then 60 °C vacuum drying was used to dry the solids.

Synthesis of IRMOF-3-SI

First, 1 g IRMOF-3 was dispersed in a 15 mL CH_2Cl_2 solution. In another vessel, 107 µL of salicylaldehyde (1mmol) was dissolved in a 15 mL CH_2Cl_2 solution and added to the dispersed IRMOF-3 solution. Finally, the yellow solid was collected by centrifugation and dried at 60 °C in a vacuum.

Synthesis of IRMOF-3-SI-Pd(II) and IRMOF-3-SI-Pd NPs

First, 0.5 g of synthesized IRMOF-3-SI and 20 mg $Pd(OAc)_2$ were added to a 6 mL acetonitrile solution. The mixture was vigorously stirred for six hours to stabilize Pd(II) ions in the MOF cavities. Then, the IRMOF-3-SI-Pd(II) was collected by centrifugation and dried at 60 °C in a vacuum.

Results and Discussion

General Suzuki cross-coupling procedure: Aryl halide (1 mmol), phenylboronic acid (1 mmol), and potassium carbonate (2 mmol) were dissolved in a 3 mL DMF/H_2O solution. Then, 0.5 mol% Pd encapsulated IRMOF-3 was added to this solution as a catalyst, and the solution was refluxed at 80 °C. Solid products were separated from the solution using CH_2Cl_2 and distilled water. Column chromatography was used for the purification of the products. The concentrated products were added to the silica gel column and extracted by EtOAc in an n-hexane (3:10) solution. The reaction between 4-bromoacetophenone and phenylboronic acid was selected as a model reaction to evaluate the effectiveness of three catalysts: IRMOF-3-SI-Pd(II), IRMOF-3-SI-Pd NPs reduced by $NaBH_4$, and alcohol. The results indicated that there were no significant differences in the catalytic activity among the three catalysts. The efficiencies of the products generated from all catalysts were comparable, with the only variation being the reaction time. The morphology of the synthesized metal-organic frameworks (MOFs) was analyzed using scanning electron microscopy (SEM). The images in Figures 3a and 3b illustrate the sheet-like morphology of bare IRMOF-3, as observed through optical photomicrographs and SEM analysis. This structure features noncovalent interactions, including hydrogen bonding, π-π interactions, and aromatic-metal interactions, which facilitate the aggregation of the MOF layers. The SEM image of IRMOF-3-SI shows that the sheet-like morphology remains intact even after its post-synthetic modification with salicylaldehyde. reveals the surface of IRMOF-3-SI-PdNPs, indicating that following the reduction of the Pd nanoparticles, the initially smooth surface of IRMOF-3 becomes markedly rough[8-9].

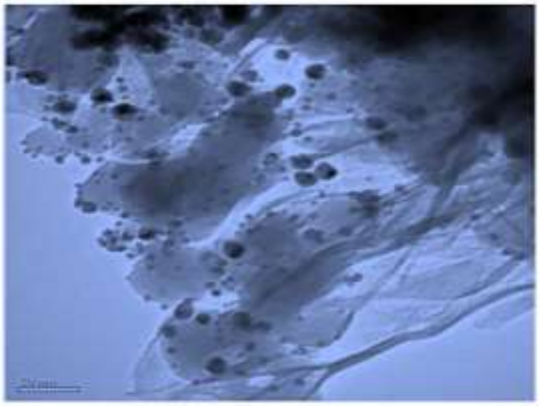

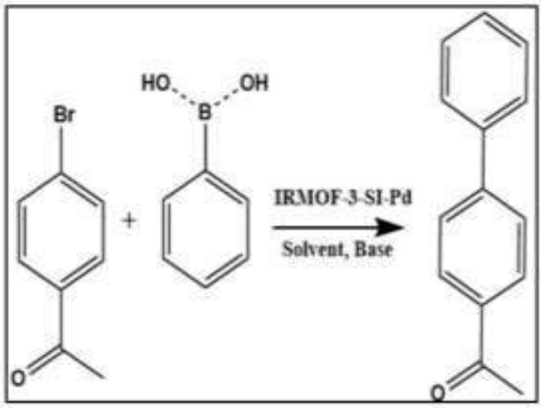

References:

١ J. C. González-Juárez and J. Jiménez-Becerril, *Radiat. Phys. Chem.*, 2006, **75**, 768–772.

٢ S. V Ley, D. E. Fitzpatrick, R. J. Ingham and R. M. Myers, *Angew. Chemie Int. Ed.*, 2015, **54**, 3449–3464.

٣ A. Fihri, M. Bouhrara, B. Nekoueishahraki, J.-M. Basset and V. Polshettiwar, *Chem. Soc. Rev.*, 2011, **40**, 5181–5203.

٤ S. Rostamnia and A. Morsali, *Inorganica Chim. Acta*, 2014, **411**, 113–118.

٥ S. Rostamnia and H. Xin, *Appl. Organomet. Chem.*, 2014, **28**, 359–363.

٦ X. Zhou, yi Zhang, X. Yang, L. Zhao and G. Wang, *J. Mol. Catal. A Chem.*, 2012, **s 361–362**, 12–16.

٧ S. Lyle, R. Flaig, K. Cordova and O. Yaghi, *J. Chem. Educ.*, DOI:10.1021/acs.jchemed.8b00265.

٨ E. Doustkhah, S. Rostamnia, H. G. Hossieni and R. Luque, *ChemistrySelect,* 2017, **2**, 329–334.

٩ Y. Hu, J. Zhang, H. Huo, Z. Wang, X. Xu, Y. Yang, K. Lin and R. Fan, *Catal. Sci. Technol*, DOI:10.1039/C9CY01940E.

The 30th Iranian Seminar of Organic Chemistry
February 7-9, 2025, Iran University of Science and Technology, Tehran, Iran

Synthesis and Biological Evaluation of Novel Chalcone-1,2,3-Triazole Hybrid Compounds

Khashayar Shadab[a], Maryam Esmkhani[a], Shiva Molaei[a], Shahrzad Javanshir[*a]

[a]*Heterocyclic Chemistry Research Laboratory, Department of Chemistry, Iran University of Science and Technology, Tehran, 16846-13114, Iran.*

Abstract

Chalcones are important compounds in organic chemistry, recognized for their high reactivity and diverse biological properties, including antimicrobial, anticancer, and anti-inflammatory activities. This study reports the synthesis of novel chalcone derivatives hybridized with a 1,2,3-triazole ring through a click chemistry approach. The synthesized compounds were characterized using ^{13}C-NMR, ^{1}H-NMR, and FT-IR spectroscopy, and evaluated for antibacterial properties via molecular docking studies.

Keywords: Chalcone, 1,2,3-Triazole, Click Chemistry, Antibacterial Activity, Hybrid Compounds

1. Introduction

Chalcones belong to the flavonoid family and are characterized by their α,β-unsaturated ketone structure, which enhances their reactivity as electrophiles and Michael acceptors. Due to their promising biological activities, chalcones have gained considerable attention in drug design and medicinal chemistry. This project aims to synthesize and evaluate novel chalcone-based compounds incorporating a 1,2,3-triazole scaffold, leveraging the advantages of click chemistry to explore potential therapeutic applications. [1-3]

2. Methodology

The synthesis of the target compounds was achieved through a three-step reaction process:

I)Claisen-Schmidt Condensation: The initial step involved the reaction of 4-aminoacetophenone with various aromatic aldehydes under alkaline conditions to form the chalcone structure. II) Diazotization and azide replacement: In the second step, the amino group in the chalcone was transformed into a diazonium salt, facilitating the replacement of the azide group using phenylacetylene as an alkyne source. III) Formation of 1,2,3-TriazoleThe final step involved a click reaction between the azide-containing chalcone and phenylacetylene, forming the 1,2,3-triazole ring.

3. Results and Discussion

The synthesis yielded six novel organic compounds featuring both chalcone and 1,2,3-triazole scaffolds. Characterization was performed using ^{13}C-NMR, ^{1}H-NMR, and FT-IR spectroscopy, confirming the structures of the synthesized compounds. The unique combination of chalcone and 1,2,3-triazole moieties enhances the potential for various biological activities. Molecular docking studies on these derivatives revealed promising antibacterial properties, indicating their potential application in treating bacterial infections.

4. Conclusion

This work successfully synthesizes novel chalcone-based compounds incorporating a 1,2,3-triazole scaffold, showcasing their potential for further biological evaluation and drug design applications. Future studies will explore these compounds' pharmacological properties and mechanisms of action.

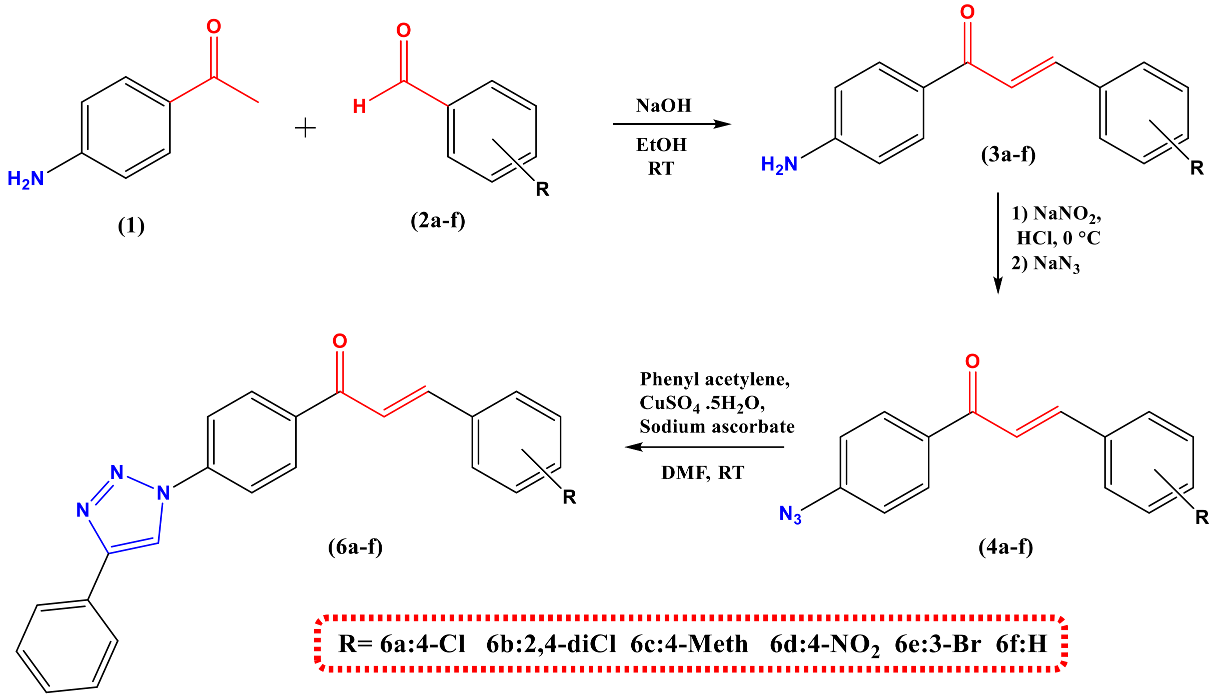

References

1. Ammohan A, Reddy JS, Sravya G, Rao CN, Zyryanov GV. "Chalcone synthesis, properties and medicinal applications: a review." *Environmental Chemistry Letters*. 2020;18:433-58.

2. Gomes MN, Muratov EN, Pereira M, Peixoto JC, Rosseto LP, Cravo PV, et al. "Chalcone derivatives: promising starting points for drug design." *Molecules*. 2017;22(8):1210.

3. Aboukhatwa, Shaimaa M., et al. "Terminators or guardians? Design, synthesis, and cytotoxicity profiling of chalcone-sulfonamide hybrids." *ACS Omega* 8.8 (2023): 7666-7683.

The 30th Iranian Seminar of Organic Chemistry
February 7-9, 2025, Iran University of Science and Technology, Tehran, Iran

Tandem transition-metal-free reaction of 2*H*-Azirine as a Versatile Building Block with Cyclic Anhydrides for the Synthesis of Oxaprozin Analoges

Reyhaneh Azimi [a], Kamran Amiri [a], S. Sina Hosseini [a], Alireza Ariafard [b], Frank Rominger [c], Hamid Reza Bijanzadeh [d], Saeed Balalaie *[a]

[a] *Peptide Chemistry Research Institute, K. N. Toosi University of Technology, P. O. Box 15875-4416, Tehran, Iran*
[b] *Research School of Chemistry, Australian National University, Canberra, ACT 2601, Australia*
[c] *Organisch-Chemisches Institut der Universität Heidelberg, Im Neuenheimer Feld 271, D-69121 Heidelberg, Germany*
[d] *Department of Environmental Sciences, Faculty of Natural Resources and Marine Sciences, Tarbiat Modares University, Noor, P.O. Box 46414-356, Iran.*

Keyword: 2*H*-Azirine, Anhydrides, Oxaprozin, Oxazole

Synthesis of Oxaprozin as a well-known non-steroidal anti-inflammatory drug has been a challenge for organic chemists. This study introduces a novel domino reaction of 2*H*-azirine with cyclic anhydrides under thermal conditions, enabling the efficient synthesis of oxaprozin analogs. The current process offers benefits such as transition-metal- and base-free reaction conditions, broad substrate scope, scalability, wide range substrate scope, high atom economy, and high bond-forming efficiency. The reaction mechanism was confirmed based on DFT calculations.

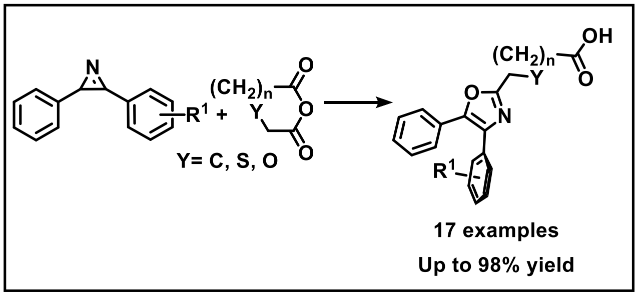

References:

١. Malandain, A.; Molins, M.; Hauwelle, A.; Talbot, A.; Loreau, O.; D'Anfray, T.; Goutal, S.; Tournier, N.; Taran, F.; Caillé, F.; Audisio, D., *J. Am. Chem. Soc*. **2023**, *145*, 16760-16770.
٢. Adouvi, G.; Nawa, F.; Ballarotto, M.; Rüger, L.A.; Knümann, L.; Kasch, T.; Arifi, S.; Schubert-Zsilavecz, M.; Willems, S.; Marschner, J.A.; Pabel, J.; Merk, D., *J. Med. Chem.* **2023**, *66*, 16762-16771.
٣. Saeifard, L.; Amiri, K.; Rominger, F.; Müller, T.J.J.; Balalaie, S., *J. Org. Chem.* **2023**, *88*, 12519-12525.

The 30th Iranian Seminar of Organic Chemistry
February 7-9, 2025, Iran University of Science and Technology, Tehran, Iran

Synthesis of New Derivatives of Pyrimido[4,5-*d*]pyrimidine

Ali Asaran-Darban, Seddigheh Sheikhi-Mohammareh, Ali Shiri*

Department of Chemistry, Faculty of Science, Ferdowsi University of Mashhad, Mashhad, Iran.

***E-mail**: alishiri@um.ac.ir

Keyword: Pyrimidine, Pinner/Dimroth Rearrangement, Heterocyclization, Pyrimidopyrimidine

Introduction:

Pyrimidopyrimidines are one of the most important heterocyclic compounds with biological activities. Considering the aromatic structure of this compound, the non-bonding electron pair on the nitrogen atom, and its ability to form ligands and hydrogen bonds, this class of heterocyclic compounds exhibit high reactivity and has a wide range of applications. [1] Some biological properties of pyrimidopyrimidines can be mentioned as antioxidant, antiaggeration [2] , antiviral and anticancer [3] properties.

Method:

The reaction of ethoxymethylenemalononitrile (**1**) with methyl thiourea (**2**) in ethanol in the presence of diisopropylethylamine results in the formation of the corresponding pyrimidine (**3**) through cyclization involving the deprotonation of the amino moiety of thiourea. Subsequently, an appropriate aromatic carboxylic acid is treated with pyrimidine (**3**) in refluxing phosphorous oxychloride leading to the formation of the relative amide. The resulting amide undergoes a Pinner cyclization followed by a Dimroth rearrangement to afford the corresponding derivatives (**4a-j**).

Results and discussion:

In this research, novel derivatives of the heterocyclic system pyrimido[4,5-*d*]pyrimidine were synthesized. One of the most important advantages of this work is the high yields and purity of the products, as well as the simplicity of preparation of both starting materials and the final product. Furthermore, considering the symmetrical structure of pyrimido[4,5-*d*]pyrimidine derivatives, the newly synthesized heterocyclic derivatives can be exploited in new pharmaceutical, biochemical activity, and catalytic fields.

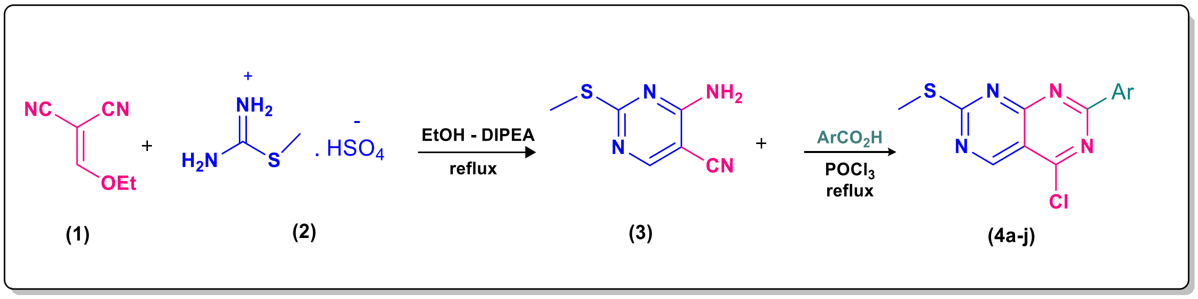

References:

[1]S.Sahrapeyma, F.Shirini and M.Mamaghani. "One-pot synthesis of pyrimido [4, 5-d] pyrimidine derivatives using a new DABCO-based ionic liquid catalyst." *Iranian Journal of Catalysis* 14.3 ,**2024**

[2] Ghada Ben, A., Maalej, E., Martin, H., Jacquinot, A. S., Barbanneau, N., Bernard, P. J., ... & Ismaili, L. (**2024**). Efficient Two-Step Synthesis of Novel Pyrimido [4, 5-d] Pyrimidines with Potent Neuroprotective, Antioxidant, and Aβ Anti-Aggregation Properties.

[3] Georgiou, E. A., Paraskevas, K., Koutra, C., Persoons, L., Schols, D., De Jonghe, S., & Kostakis, I. K. (2024). Exploring 4, 7-Disubstituted Pyrimido [4, 5-d] pyrimidines as Antiviral and Anticancer Agents. *Molecules*, *29*(23), 5549.

The 30th Iranian Seminar of Organic Chemistry
February 7-9, 2025, Iran University of Science and Technology, Tehran, Iran

Multi-component reaction synthesis of 2-amino-3-phenylsulfonyl-4-aryl-4*H*-benzo[*h*]chromene derivatives in the presence of Fe_3O_4@dextrin/OSO_3H nanocatalyst

Mehran Rezaie[a], Bahareh Sadeghi*[b], Morteza Rouhani[a]

[a]*Department of Chemistry, Science and Research Branch, Islamic Azad University, Tehran, Iran*

[b] *Department of Chemistry, Central Tehran Branch, Islamic Azad University, Tehran, Iran*

Keywords: chromenes; multicomponent reactions; dextrin, Fe_3O_4@dextrin/OSO_3H; Nanocatalyst

Introduction:

Recently, the use of multicomponent reactions (MCRs) has become a special and widely-recognized methodology in synthetic organic chemistry. In this context, the incorporation of chromene moieties into the frameworks of pharmaceuticals via the MCR method has proven to be an impressively productive technique, giving rise to compounds with antimicrobial and anticancer properties.[1] In particular, studies have shown that heterogeneous nanocatalysts, especially nanomagnetic catalysts, can be easily removed from reaction mixtures and re-used in new reactions. Among these catalysts we may note as examples $Fe_3O_4/SiO_2/TiO_2$,[2] and Fe_3O_4@SiO_2-SO_3H.[3]

We have found an innovative method for the synthesis of 2-amino-3-phenylsulfonyl-4-aryl-4*H*-benzo[*h*]chromenes. This process takes place through the one-pot MCR among aromatic aldehydes, phenylsulfonylacetonitrile and *α*-naphthol in the presence of Fe_3O_4@dextrin/OSO_3H as a readily available and highly efficient catalyst (Scheme 1).

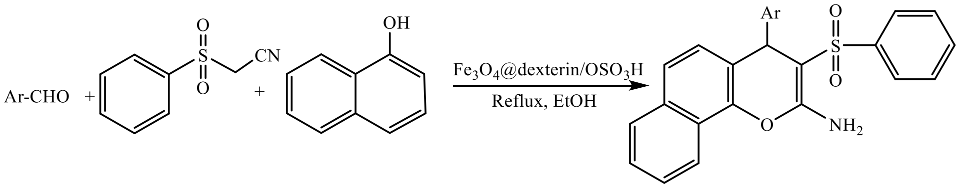

Scheme 1. Synthesis of 2-amino-3-phenylsulfonyl-4-aryl-4*H*-benzo[*h*]chromene derivatives in the presence of Fe_3O_4@dextrin/OSO_3H catalyst

Method:

2-Amino-3-phenylsulfonyl-4-aryl-4*H*-benzo[*h*]chromene derivatives were synthesized in the constant presence of Fe_3O_4@dextrin/OSO_3H as nanocatalyst. For this purpose, Fe_3O_4@dextrin/OSO_3H (3.0 mg) was incorporated into a mixed combination of phenylsulfonylacetonitrile (1.0 mmol), α-naphthol (1.0 mmol) and aromatic aldehyde (1.0 mmol). The materials were mixed and heated under reflux in ethanol (5mL) for the appropriate time, as monitored by TLC (n-hexane:ethyl acetate 3:1), generally 10-15 min. After completion of the reaction, the catalyst was then removed by magnet, and the product was recrystallized from the hot solution to afford the pure compound.

Results and Discussion:

The literature mentions several approaches to the synthesis of 2-amino-3-phenylsulfonyl-4-aryl-4*H*-benzo[*h*]chromenes. As useful as they have been in advancing the field, some of these methods suffer from high catalyst consumption, lengthy reaction times, or complex separation procedures. The importance of this area in synthesis justifies exploration of effective new procedures that can address these issues. We therefore examined the reactions of Scheme 1 using structurally-varied aldehydes, phenylsulfonylacetonitrile and α-naphthol in the presence of Fe_3O_4@dextrin/OSO_3H as a catalyst in refluxing ethanol. For identification of the structure of Fe_3O_4@dextrin/OSO_3H FT-IR spectra were recorded. Field emission scanning electron microscopy (FE-SEM) indicate that Fe_3O_4@dextrin/OSO_3H nanoparticles have a quasi-spherical shape and their size is about 20-46 nm.

References

1. A. M. El-Agrody, M. H. El-Hakim, M. S. Abd El-Latif, A. H. Fakery, E. S. M. El-Sayed and K. A. El-Ghareab, *Acta Pharm.*, **50**, 111 (2000).

2. N. Hazeri, S. Salahi, M. Lashkari, M. T. Maghsoodlou, E. Esmaeili-Shahri and E. Molashahi, *Org. Prep. Proced. Int.*, **50**, 375 (2018).

3. J. Safaei-Ghomi, Y. Fazeli-Mehrabani, A. Kareem Abbas and H. Shahbazi-Alavi, *Org. Prep. Proced. Int.*, **52**, 446 (2020).

The 30th Iranian Seminar of Organic Chemistry
February 7-9, 2025, Iran University of Science and Technology, Tehran, Iran

Fe_3O_4@kaolin/OSO_3H as a new nanomagnetic catalyst for synthesis of 3,9-diamino-5,10-dioxo-1-aryl-5,10-dihydropyrazolo[1,2-*b*]phthalazine-2-carbonitrile derivatives

Mahsa Sheykhhasani[a], Bahareh Sadeghi*[a], Ali Niazi[a]

[a] *Department of Chemistry, Central Tehran Branch, Islamic Azad University, Tehran, Iran*
*Corresponding Author; E-mail: bsadeghia@gmail.com

Keywords: phthalazine; nanomagnetic; kaolin, Fe_3O_4@kaolin/OSO_3H; Nanocatalyst

Introduction:

In particular, studies have shown that heterogeneous nanocatalysts, especially nanomagnetic catalysts, can be easily removed from reaction mixtures and re-used in new reactions. Among these catalysts we may note as examples Fe_3O_4@TiO_2/Cu_2O,[1] Fe_3O_4@SiO_2@ L-met@Ni (II),[2] and [Fe_3O_4@SiO_2-R-$NHMe_2$][H_2PO_4],[3] as a new catalyst for multicomponent reactions and heterocycle synthesis. In continuation of our research concerning the synthesis of novel catalysts for biologically active heterocycles, we now report on the use of kaolin, which can be an excellent bio-resource material, owing to the vast numbers and types of hydroxyl groups. Further to our work on the design of heterogeneous nanocatalysts for the production of heterocycles, we have found an innovative method for the synthesis of 3,9-diamino-5,10-dioxo-1-aryl-5,10-dihydropyrazolo[1,2-*b*]phthalazine-2-carbonitrile. This process takes place through the one-pot MCR among aromatic aldehydes, malononitrile and phtahalazine in the presence of Fe_3O_4@kaolin/OSO_3H as a readily available and highly efficient catalyst (Scheme 1).

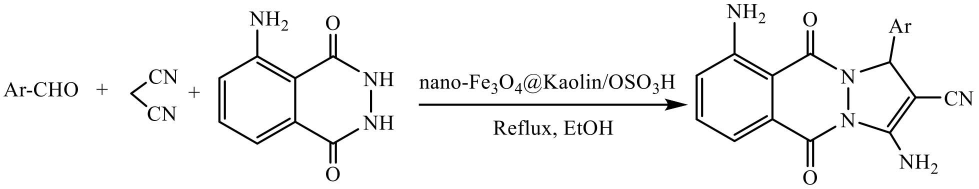

Scheme 1. Synthesis of 3,9-diamino-5,10-dioxo-1-aryl-5,10-dihydropyrazolo[1,2-*b*]phthalazine-2-carbonitriles in the presence of Fe_3O_4@kaolin/OSO_3H catalyst

Method:

General procedure for preparation of compounds

As seen in Scheme 2, the Fe_3O_4@kaolin/OSO_3H nanocatalyst were prepared in two-stages. Fe-SEM image indicate that Fe_3O_4@kaolin/OSO_3H nanoparticles have a quasi-spherical shape and their size is about 4-8 nm. Fe_3O_4@kaolin/OSO_3H NPs (0.008 g) was added to a stirred mixture of the aromatic aldehyde (1 mmol), malononitrile (1 mmol) and 5-amino-2,3-dihydro-phthalazine-1,4-dione (1 mmol) in EtOH (20 mL). The reaction mixture was then stirred for 10 min at reflux. The progress of the reaction was followed by TLC (n-hexane:ethylacetate). After completion of the reaction, the mixture was filtered to remove the catalyst. After evaporation of the solvent, the crude product was recrystallised from hot ethanol to obtain the pure compound.

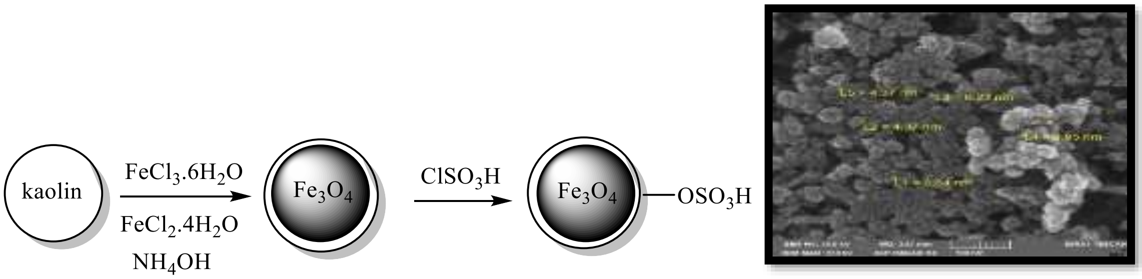

Scheme 2. Synthesis of Fe_3O_4@kaolin/OSO_3H nanocatalyst

Results and Discussion:

In summary, a novel acidic magnetic nanocatalyst (Fe_3O_4@kaolin/OSO_3H) has been developed to construct the 3,9-diamino-5,10-dioxo-1-aryl-5,10-dihydropyrazolo[1,2-*b*]phthalazine-2-carbonitrile derivatives. It may catalyze many organic reactions that require acidic catalysts to carry out. The benefits of this protocol consist of high performance, low catalyst loading, short reaction times and good consistent with green chemistry principles.

References

۱. A. Elhampour and F. Nemati, *Org. Prep. Proced. Int.*, **50**, 493 (2018).

2. M. Gholami Dehbalaei, N. Foroughifar, A. Khajeh-Amiri and H. Pasdar, *Org. Prep. Proced. Int.*, **52**, 171 (2020).

۳. N. Lotfifar, A. Zare and Gh. Rezanejade Bardajee, *Org. Prep. Proced. Int.*, **53**, 379 (2021).

The 30th Iranian Seminar of Organic Chemistry
February 7-9, 2025, Iran University of Science and Technology, Tehran, Iran

Fe_3O_4@feldspar/OSO_3H as a new nanomagnetic catalyst for synthesis of ethyl 3,9-diamino-1-argio-5,10-dioxo-5,10-dihydro-1*H*-pyrazolo[1,2-*b*]phthalazine-2-carboxylate derivatives

Zahra Boghratpour[a], Bahareh Sadeghi*[a], Marjaneh Samadizadeh

[a] *Department of Chemistry, Central Tehran Branch, Islamic Azad University, Tehran, Iran*
*Corresponding Author; E-mail: bsadeghia@gmail.com

Keywords: phthalazine; multi-component reactions; feldespar, Fe_3O_4@feldspar/OSO_3H; Nanocatalyst

Introduction:

Multi-component reactions (MCRs) provide rapid and efficient approach to organic transformations including diverse synthesis of polyfunctionalized heterocycles with significant biological and pharmaceutical importance. In particular, studies have shown that heterogeneous nanocatalysts, especially nanomagnetic catalysts, can be easily removed from reaction mixtures and re-used in new reactions. Among these catalysts we may note as examples Fe_3O_4@TiO_2/Cu_2O,[1] Fe_3O_4@SiO_2@ L-met@Ni (II),[2] and [Fe_3O_4@SiO_2-R-$NHMe_2$][H_2PO_4],[3] as a new catalyst for multicomponent reactions and heterocycle synthesis. In continuation of our research concerning the synthesis of novel catalysts for biologically active heterocycles, we now report on the use of feldespar, which can be an excellent bio-resource material, owing to the vast numbers and types of hydroxyl groups. Further to our work on the design of heterogeneous nanocatalysts for the production of heterocycles, we have found an innovative method for the synthesis of ethyl 3,9-diamino-1-argio-5,10-dioxo-5,10-dihydro-1*H*-pyrazolo[1,2-*b*]phthalazine-2-carboxylates. This process takes place through the one-pot MCR among aromatic aldehydes, ethyl cyanoacetate and phtahalazine in the presence of Fe_3O_4@feldspar/OSO_3H as a readily available and highly efficient catalyst (Scheme 1).

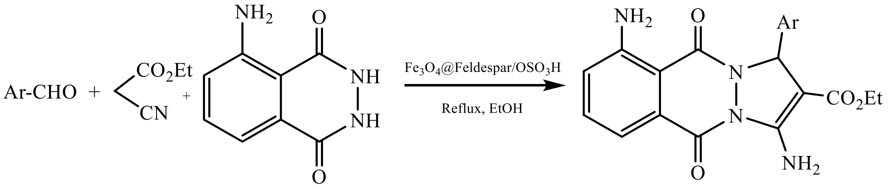

Scheme 1. Synthesis of ethyl 3,9-diamino-1-argio-5,10-dioxo-5,10-dihydro-1*H*-pyrazolo[1,2-*b*]phthalazine-2-carboxylates in the presence of Fe_3O_4@feldspar/OSO_3H catalyst

Method:

General procedure for preparation of compounds

Fe_3O_4@feldspar/OSO_3H NPs (0.006 g) was added to a stirred mixture of the aromatic aldehyde (1 mmol), ethyl cyanoacetate (1 mmol) and 5-amino-2,3-dihydro-phthalazine-1,4-dione (1 mmol) in EtOH (10 mL). The reaction mixture was then stirred for 15 min at reflux. The progress of the reaction was followed by TLC (n-hexane:ethylacetate). After completion of the reaction, the mixture was filtered to remove the catalyst. After evaporation of the solvent, the crude product was recrystallised from hot ethanol to obtain the pure compound.

Results and Discussion:

In summary, a novel acidic magnetic nanocatalyst (Fe_3O_4@feldspar/OSO_3H) has been developed to construct the ethyl 3,9-diamino-1-argio-5,10-dioxo-5,10-dihydro-1*H*-pyrazolo[1,2-*b*]phthalazine-2-carboxylate derivatives. It may catalyze many organic reactions that require acidic catalysts to carry out. The benefits of this protocol consist of high performance, low catalyst loading, short reaction times and good consistent with green chemistry principles.

References

١. A. Elhampour and F. Nemati, *Org. Prep. Proced. Int.,* **50**, 493 (2018).
2. M. Gholami Dehbalaei, N. Foroughifar, A. Khajeh-Amiri and H. Pasdar, *Org. Prep. Proced. Int.,* **52**, 171 (2020).
٣. N. Lotfifar, A. Zare and Gh. Rezanejade Bardajee, *Org. Prep. Proced. Int.,* **53**, 379 (2021).

The 30th Iranian Seminar of Organic Chemistry
February 7-9, 2025, Iran University of Science and Technology, Tehran, Iran

Investigating The Phytoremediation Potential of *Helianthus annuus* L. In Removing The Heavy Metals (Cd, Cr and Pb) From Water Sources

Ameneh Kordi-Todzil *, Mozhgan Taherizadeh, Houriyeh Rigi

Sistan and Baluchestan Province Water and Wastewater Company, Zahedan, Iran

Surface water pollution by heavy metals has become one of the major environmental and health challenges that threaten human health and other living organisms. This study investigated the ability of *Helianthus annuus L.* (sunflower) to absorb and accumulate heavy metals Cd, Cr, and Pb from aqueous solutions. Experiments were conducted in laboratory conditions with a solution containing an initial concentration of 100 mg/L of these metals, and the concentration of metals remaining in the solution and accumulated in plant tissue was measured daily for 14 days using an Atomic Absorption Spectrophotometer. The results showed that the absorption of metals by sunflower depended on the type of metal and time, with Cd being removed more efficiently by 75%, while Pb and Cr had a slower removal process (30% and 35%). Cd also accumulated most in the roots and stems, indicating its high mobility in the solution and plant absorption capacity. Cd accumulated moderately and remained mostly in the roots, and lower amounts were observed in the stems. Also, Pb remained mainly in the roots and had little transfer to other parts. These findings indicate that the plant can be used as an effective and cost-effective option in phytoremediation programs for treating water sources contaminated with heavy metals.

Keyword: Phytoremediation, *Helianthus annuus* L., Heavy Metals, Water Sources

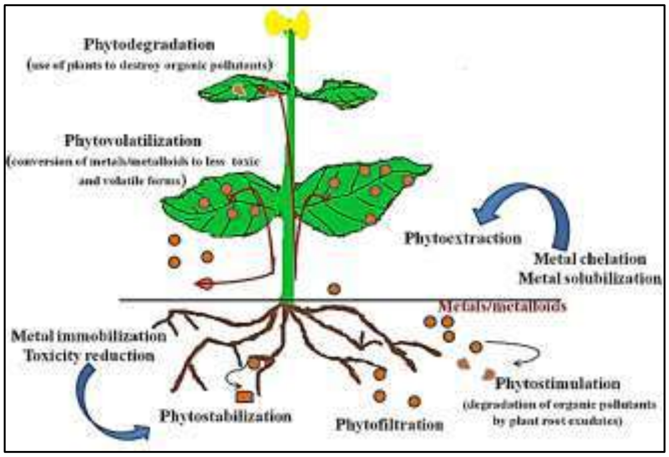

Scheme: Processes used in phytoremediation of heavy metals

References: Ali H., Khan E., Sajad M.A. Phytoremediation of heavy metals—Concepts and applications, Chemosphere, 91, (2013), 869-881

The 30th Iranian Seminar of Organic Chemistry
February 7-9, 2025, Iran University of Science and Technology, Tehran, Iran

Investigating the effect of pH and EDTA on improving the absorption of Pb by *Helianthus annuus* L.: An important method to increases the phytoremediation potential to remove the heavy metals using plants

Ameneh Kordi-Todzil *, Mozhgan Taherizadeh, Houriyeh Rigi

Sistan and Baluchestan Province Water and Wastewater Company, Zahedan, Iran

Heavy metals such as Pb pose major problems for human and environmental health due to their specific characteristics, including chemical stability and tendency to accumulate in the environment. Phytoremediation as a green technology uses plants to absorb, accumulate, and decompose pollutants in the environment. However, the absorption of heavy metals such as Pb by plants has challenges such as pH and lack of natural chelating agents in the environment, which reduce the availability of metals. This study was conducted to investigate the effect of pH and EDTA on Pb absorption by *Helianthus annuus* L. The plant was cultivated in a Pb solution with a concentration of 100 mg/L and in the pH range (4, 6, 8) and with/without the presence of EDTA. The results showed that acidic pH (pH: 4) and the presence of EDTA increased Pb absorption in

the roots and stems. Also, the reduction of Pb concentration in the solution in the presence of EDTA increased significantly. This study showed that pH and the presence of EDTA have a significant effect on Pb absorption by *Helianthus annuus* L.

Keyword: Phytoremediation, *Helianthus annuus* L., Heavy Metals, EDTA

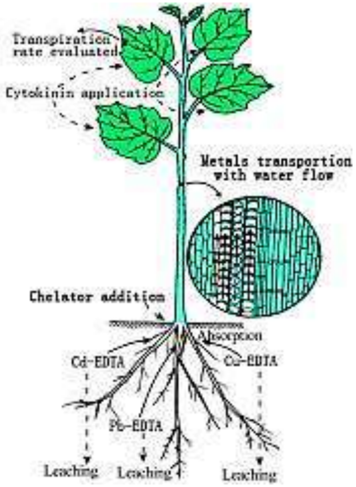

Scheme: The effect of chelator addition (EDTA) to Phytoremediation of heavy metals

References:

[1] Heidari R., Khayami M., Farboodnia T. Effect of pH and EDTA on Pb Accumulation in *Zea mays* Seedlings. Journal of Agronomy, 4 (2005) 49-54.

The 30th Iranian Seminar of Organic Chemistry
February 7-9, 2025, Iran University of Science and Technology, Tehran, Iran

Optimization, characterization and Investigation of Antibacterial Activities of Phytosynthesized Gold Nanoparticles Using Root Aqueous Extract of *Sambucus ebulus* L.

Mozhgan Taherizadeh, Ameneh Kordi-Todzil *, Horiyeh Rigi

Sistan and Baluchestan Province Water and Wastewater Company, Zahedan, Iran

The advantages of using biological methods include cheapness, non-toxicity and production of high-purity nanoparticles (NPs), short reaction time, and completeness [1]. The present study is the first report of the phytosynthesis of gold nanoparticles (GNPs) using an aqueous extract of the *Sambucus ebulus* L. After preparing the extract, 10 ml of it, was added to 40 ml of $HAuCl_4.3H_2O$ with a concentration of 2 mM, and the solution immediately changed color to purple. The parameters affecting the synthesis of nanoparticles, such as pH of the reaction, volume of the extract, concentration of gold (III) salt, temperature, and reaction time, were studied and optimized using UV-Vis spectrophotometry [2]. TEM images and XRD pattern were used to characterize the NPs. Finally, the antibacterial activity of the NPs on four pathogenic bacterial species were investigated by the MIC method. GNPs showed maximum absorption at 542 nm. It was found that the synthesized NPs are spherical in shape and their average size is between 15-20 nm. The results of the antibacterial activity of NPs showed that the have relatively good antibacterial activity against some bacteria. Plants have a high potential in reducing metal ions and stabilizing them due to their secondary compounds and antioxidant properties. In the present study, GNPs produced from the root aqueous extract of *Sambucus ebulus* L. had relatively high antibacterial properties.

Keyword: Phytosynthesis, Gold Nanoparticles, *Sambucus ebulus* L., Antimicrobial Activity

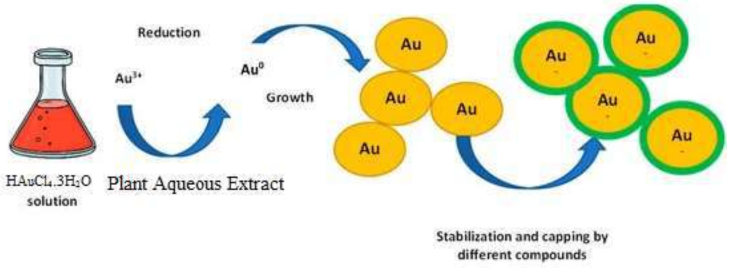

Scheme: Phytosynthesis of GNPs using aqueous extract of plants

References:

[1] Azizian-Shermeh O., Jalali-Nezhad A.A., Taherizadeh M. Facile, Low-cost and rapid phytosynthesis of stable and eco-friendly silver nanoparticles using *Boerhavia elegans* (Choisy) and study of their antimicrobial activities. J. Inorg. Organomet. Polym. Mater. 2021; 31: 279-291. https://doi.org/10.1007/s10904-020-01691-7 23.

[2] Azizian-Shermeh O., Valizadeh M., Taherizadeh M., Beigomi, M. Phytochemical investigation and phytosynthesis of ecofriendly stable bioactive gold and silver nanoparticles using petal extract of saffron (*Crocus sativus* L.) and study of their antimicrobial activities. Appl. Nanosci. 2020; 10: 2907-2920. https://doi.org/10.1007/s13204-019-01059-5.

Investigation of Substituent Effect by the Synthon Approach in Crystal Structure Prediction

Ali Reza Keramati, Alireza Salimi*
Department of Chemistry, Faculty of Science, Ferdowsi University of Mashhad, Mashhad, Iran
**E-mail: salimi-a@um.ac.ir*

Keyword: Crystal Structure Prediction, Synthon Approach, Crystal Engineering, Substituent Effect

Crystal engineering has emerged as a vital discipline to address the growing need for rational approaches to understanding solid-state structures of both fundamental and practical importance. This field aims to elucidate intermolecular interactions and recognition phenomena, particularly in the context of crystal packing[1].

In this study, we examine the impact of molecular substitutions in a series of benzoate derivatives containing halogen substituents on crystal structure prediction. Specifically, three configurations of a molecule were analyzed using a crystal engineering framework to streamline the prediction process and enhance its efficiency. Database searches highlighted the pivotal role of halogen bonding ($N–X\cdots OC$; X = Cl, Br, I) as a fundamental synthon[2]. Through the synthon approach, key influence of interactions, such as $NH_2\cdots O$ and $CH_3\cdots Br$, were identified. These interactions correspond to critical graph sets, including C(6) and $R_2^2(12)$, which aid in determining suitable crystal structures. Among these, the $NH_2\cdots O$ interaction emerged as a key factor in ranking predicted CSP structures and exhibited strong agreement with experimental data from the Cambridge Structural Database. The identified synthons act as representative structural units, bridging the information gap between isolated molecules and their resultant crystal structures[3]. This study underscores the potential of the synthon approach to advance the predictive accuracy and efficiency of CSP methodologies.

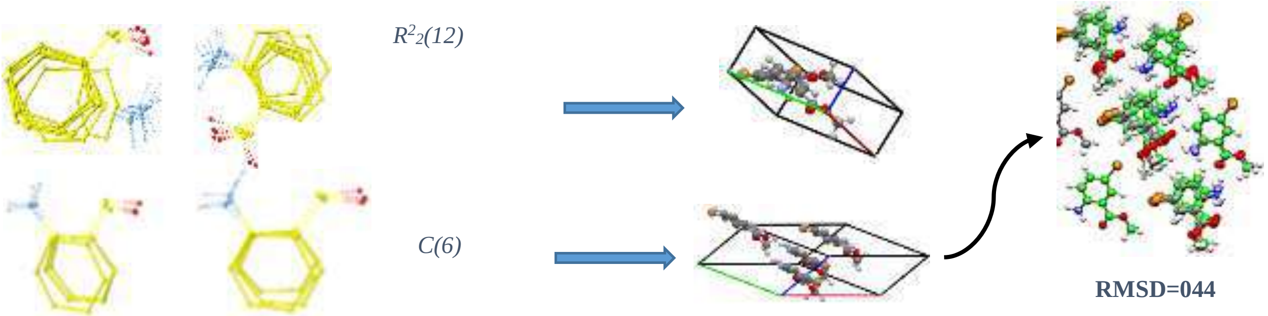

Figure 38 These two common states illustrate the synthon approach to crystal structure due to the $NH_2\cdots O$ interaction, organized from right to left as head-to-tail and head-to-head arrangements. Additionally, the compatibility of the structure containing the C(6) synthon with the Cambridge database has been assessed.

References:

۱) Desiraju, G. R. *Angew. Chem., Int. Ed.* **1995**, *34* (21), 2311-2327.

۲) Abardeh, Z. M.; Salimi, A.; Oganov, A. R. *CrystEngComm* **2022**, *24* (34), 6066-6075.
۳) Sarma, J.; Desiraju, G. R. *Cryst. Growth Des* **2002**, *2* (2), 93-100.

The 30th Iranian Seminar of Organic Chemistry
February 7-9, 2025, Iran University of Science and Technology, Tehran, Iran

Enhanced CO_2 separation using PEBAX/PDDA blend membranes

Seyed Alireza Saeidi, Elahe Ahmadi Feijani*

Department of Applied Chemistry, Faculty of Chemistry and Petroleum Sciences, Bu–Ali Sina University, Hamedan 6517838695, Iran

*Corresponding author Email: e.ahmadifeijani@basu.ac.ir

Abstract

This study focuses on the development and characterization of PEBAX-based membranes modified with poly(diallyldimethylammonium chloride) (PDDA) to enhance CO_2 separation performance. Membranes were fabricated by blending PEBAX-1657 with 10 wt% and 20 wt% PDDA using the solution casting method. Gas permeability measurements indicated that incorporating 10 wt% PDDA increased CO_2 permeability compared to pristine PEBAX, with improved CO_2/N_2 selectivity due to enhanced free volume and facilitated transport through amine functionality. However, at 20 wt% PDDA, reduced permeability was observed, attributed to increased crystallinity and reduced gas diffusivity and solubility.

Keyword: Gas separation, Membrane, PEBAX, CO_2 separation

۱ Introduction

The escalating consumption of fossil fuels has resulted in a rapid increase in atmospheric CO_2 concentrations. To mitigate this issue, various carbon capture, utilization, and storage technologies are being explored. Post-combustion CO_2 capture is considered particularly attractive due to its potential for retrofitting into existing power plants. While conventional technologies such as amine scrubbing, regenerative solvents, and cryogenic distillation can achieve high CO_2 capture rates (90%) with acceptable purity (80%), their significant energy penalties hinder large-scale implementation [1]. Membrane gas separation offers a promising alternative to conventional technologies, characterized by moderate energy requirements and simplified operation and maintenance. Polymeric materials currently dominate membrane-based gas separations, with gas transport primarily governed by the solution-diffusion mechanism [2]. Membrane performance is critically dependent on both selectivity and permeability, however, these two properties often exhibit an inverse relationship, posing a significant challenge for industrial applications [3]. To overcome this limitation, there is a strong need for materials that exhibit both high separation performance and exceptional durability. Recent advancements in materials science have shown promise in this area, including polymers of intrinsic microporosity (PIMs), thermally rearranged polymers, organic/inorganic hybrid materials (mixed matrix membranes), and facilitated transport materials [4]. Block copolymers such as poly(ether-block-amide) (PEBAX), widely employed in gas separation applications, exhibit a distinct phase-separated morphology consisting of soft polyether (PE) and rigid polyamide (PA) segments. Among various PEBAX grades, PEBAX-1657, with a 60/40 wt% ratio of PEO to PA, has demonstrated superior CO_2 selectivity over light gases like N_2 and CH_4 [5,6]. The CO_2 separation performance of PEBAX-1657 can be further enhanced by incorporating amine-functionalized compounds. These compounds, containing positively charged nitrogen atoms, can interact with the negatively charged central oxygen atom of CO_2 molecules through Lewis acid-base interactions, thereby enhancing CO_2 permeation. In this study, PEBAX-1657 was blended with poly(diallyldimethylammonium chloride) (PDDA), a cationic polyelectrolyte, to introduce amine functionality. PEBAX/PDDA blend membranes were fabricated using the solution casting/solvent evaporation method, and their CO_2 and N_2 permeability coefficients were subsequently investigated.

۲ Methods

۲,۱ Membrane preparation

PEBAX/PDDA blend membranes were produced in two weight percent, 10 and 20% of PDDA. Proper amount of PEBAX was dissolved in mixture of 7 ml ethanol and 3 ml H_2O by stirring at ۸۰ ℃ under reflux for 5h. Then the required value of PDDA was added to the PEBAX solution and the result mixture was allowed to be mixed for 2h at room temperature. The prepared PEBAX/PDDA solution was decanted into a petri dish with diameter of 8 cm. The result film was achieved by placing petri dish in oven at 80℃ for 3h.

۳ Results and Discussion

۳,۱ FT-IR analysis

Fig. 1 shows the FT-IR spectra of pure PEBAX, pure PDDA, PEBAX/PDDA 10 wt% and PEBAX/PDDA 20 wt%. The FT-IR spectrum of the pristine PEBAX membrane revealed characteristic peaks corresponding to its functional groups. The C-O-C stretching vibration of the flexible polyethylene oxide segment appeared at 1113 cm^{-1}. Additionally, peaks associated with the rigid polyamide segment were observed, inclusive of the N-H bending vibration at 1540 cm^{-1} and the N-H, O-C=O, and H-N-C=O stretching vibrations at 3330, 1745, and 1664 cm^{-1}, respectively [7,8]. FTIR spectroscopy of PDDA revealed characteristic peaks at 3447, 2932, 2867, 1640, 1471, and 1252 cm^{-1}. The band observed at 3447 cm^{-1} can be attributed to either $-NR_3^+$ stretching vibrations or the presence of hydroxyl groups. The peaks at 2932, 2867, and 1471 cm^{-1} are characteristic of C-H stretching vibrations. Furthermore, the bands at 1640 and 1252 cm^{-1} correspond to the deformation vibration of $-NR_3^+$ and C-N stretching vibrations, respectively [9,10].

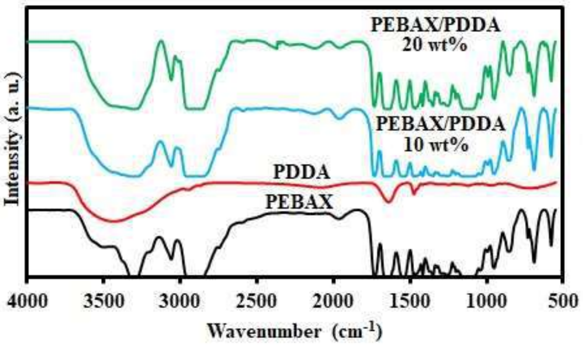

Fig. 3: FT-IR of the materials

۳,۲ Gas permeability behavior

The pure gas permeation results of the prepared membranes are included in Fig. 2. Gas permeation measurements for CO_2 and N_2 were conducted at 30 °C and a feed pressure of 3 bar. Gas transport through polymeric membranes is governed by two primary mechanisms: solution and diffusion. The diffusion mechanism primarily differentiates penetrants based on their molecular size. Smaller molecules, with lower kinetic diameters, generally exhibit higher diffusivity through the polymer matrix. The solution mechanism, on the other hand, is significantly influenced by the gas's solubility within the polymer. Gas solubility is directly correlated with its condensability, which is often characterized by the gas's critical temperature. Gases with higher critical temperatures exhibit stronger intermolecular forces and tend to condense more readily within the polymer matrix, resulting in higher solubility. In this context, CO_2, possessing a smaller kinetic diameter and a higher critical temperature than N_2, exhibits both higher diffusivity and higher solubility within the polymer matrix. These combined factors contribute to the observed higher permeability of CO_2 compared to N_2 through the prepared membranes [11]. Thus the permeability of CO_2 in all membranes was higher than the permeability of N_2. PEBAX/PDDA 10 wt% showed higher gas permeability compared to neat PEBAX especially for CO2. In this weight ratio of PEBAX and PDDA, the PDDA could play the role of a plasticizer for PEBAX chains and increased the free volume between PEBAX chains. This free volume could effectively transfer gas molecules in favor of CO_2 against N_2 due to the interaction of nitrogen atoms of PDDA and the PE segments of PEBAX. By adding 20 wt% of PDDA into the Pebax matrix, the CO2 permeability was reduced compared to pure Pebax. The permeability of carbon dioxide was dropped from 116.22 barrer in neat Pebax to 79.03 barrer in PEBAX/PDDA 20 wt%). Since PEBAX is a semi-crystalline copolymer, addition 20 wt% of PDDA might influence the degree of PEBAX crystallinity. Considerable decrease of gas permeability of PEBAX/PDDA 20 wt% relative to that of neat PEBAX indicated crystallinity level of PEBAX/PDDA 20 wt% could be higher than that of neat PEBAX. Crystalline parts in membrane could play obstacle role against gas transport and therefore gas permeability was decreased. PDDA chains could interact with PEBAX chains in order to increase the arrangement of the PEBAX chains. The higher regularity led to higher packed structures of the membrane. The free volume between chains decreased and the gas diffusivity was declined. In addition of gas diffusivity decrease, gas solubility could also be diminished. For description of gas solubility decrease, it could be mentioned that PEBAX and PDDA were busy to interact with each other and there was less functional groups for interaction with gases consequently the gas solubility could decrease. The decrease in gas diffusivity and solubility was prominent for CO_2 in comparison with N_2 and therefore CO_2/N_2 selectivity was enhanced relative to both neat PEBAX and PEBAX/ PDDA 10 wt%.

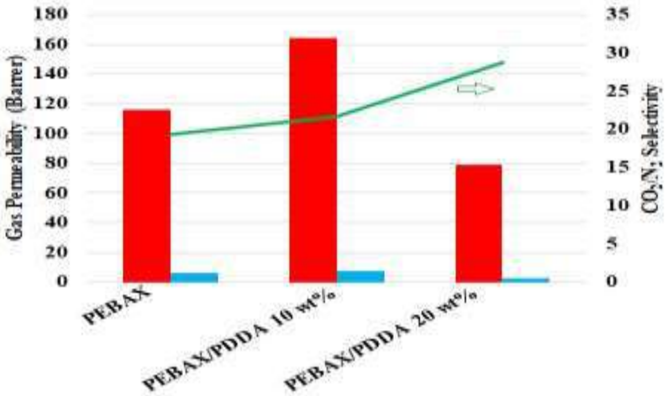

Fig. 4: Gas permeability and selectivity of the prepared membranes

٤ Conclusion

In this study, the successful modification of PEBAX-1657 membranes with poly(diallyldimethylammonium chloride) (PDDA) for enhanced CO_2 separation was demonstrated. The incorporation of 10 wt% PDDA significantly improved CO_2 permeability and selectivity due to increased free volume and facilitated transport enabled by amine functionalities. However, higher PDDA content (20 wt%) reduced permeability, likely due to increased membrane crystallinity, which limited gas diffusivity and solubility.

References:

[1] P. Viebahn, V. Daniel, H. Samuel, Integrated assessment of carbon capture and storage (CCS) in the German power sector and comparison with the deployment of renewable energies, Appl. Energy. 97 (2012) 238–248.

[2] R.W. Baker, B.T. Low, Gas separation membrane materials: A perspective, Macromolecules. 47 (2014) 6999–7013.

[3] L.M. Robeson, The upper bound revisited, J. Memb. Sci. 320 (2008) 390–400.

[4] R. Sidhikku Kandath Valappil, N. Ghasem, M. Al-Marzouqi, Current and future trends in polymer membrane-based gas separation technology: A comprehensive review, J. Ind. Eng. Chem. 98 (2021) 103–129.

[5] Y. Wu, D. Zhao, J. Ren, Y. Qiu, Y. Feng, M. Deng, Effect of triglyceride on the microstructure and gas permeation performance of Pebax-based blend membranes, Sep. Purif. Technol. 256 (2021) 117824.

[6] P. Taheri, M.S. Maleh, A. Raisi, Cross-linking of poly (ether-block-amide) by poly (ethylene glycol) diacrylate to prepare plasticizing-resistant CO_2-selective membranes, J. Environ. Chem. Eng. 9 (2021) 105877.

[7] P. Bernardo, G. Clarizia, Enhancing gas permeation properties of Pebax® 1657 membranes via polysorbate nonionic surfactants doping, Polymers (Basel). 12 (2020).

[8] G. Liu, L. Cheng, G. Chen, F. Liang, G. Liu, W. Jin, Pebax-Based Membrane Filled with Two-Dimensional Mxene Nanosheets for Efficient CO_2 Capture, Chem. – An Asian J. 15 (2020) 2364–2370.

[9] L. Zhang, D. Yi, J. Hao, Poly (diallyldimethylammonium) and polyphosphate polyelectrolyte complexes as an all-in-one flame retardant for polypropylene, Polym. Adv. Technol. 31 (2020) 260–272.

[10] A. Mehta, J.P. Pandey, G. Sen, Synthesis of Diallyl dimethyl ammonium chloride grafted polyvinyl pyrrolidone (PVP-g-DADMAC) and its applications, Mater. Sci. Eng. B. 263 (2021) 114750.

[11] W. Zhu, Y. Qin, Z. Wang, J. Zhang, R. Guo, X. Li, Incorporating the magnetic alignment of GO composites into Pebax matrix for gas separation, J. Energy Chem. 31 (2019) 1–10.

The 30th Iranian Seminar of Organic Chemistry
February 7-9, 2025, Iran University of Science and Technology, Tehran, Iran

Synthesis of dihydropyrimidinone derivatives through multi-component Biginelli reaction strategy in the presence of a heterogeneous catalyst based on chitosan

Authors: Narges porghafari1 [1], **Mohammad G. Dekamin[1,*]** and Negin Rostami [1]

Pharmaceutical and Heterocyclic Compounds Research Laboratory, Department of Chemistry, Iran University of Science and Technology, Tehran 16846-13114, porghafarinarges8@gmail.com, corresponding author: mdekamin@iust.ac.ir

Abstract:

L-glutamine-functionalized chitosan (Cs-L-glutamine) was used as a new and efficient catalyst for the synthesis of dihydropyrimidinones derivatives. In this regard, some dihydropyrimidinones (DHPM) derivatives were synthesized under reflux conditions as a three-component condensation of an aldehyde, b-ketoester, and urea in ethanol solvent. This method has the prominent features such as green solvent, high yield with short reaction time, easy separation, and no need for purification using chromatography columns. This bio-based (Cs-L-glutamine) nanocatalyst contains appropriate basic active sites to act as a multifunctional catalyst. Furthermore, the (Cs-L-glutamine) network, as a heterogeneous catalyst, illustrated magnificent reusability.

Keyword: Chitosan-based catalyst; Green chemistry; dihydropyrimidinones derivatives; Biginelli reaction; Heterogeneous; Multicomponent reactions (MCR)

١. Introduction

Multicomponent reactions (MCRs) simultaneously engage three or more components, resulting in products that incorporate the elements of all starting materials in their frameworks. This integrative nature of MCRs is attractive when a rapid increase in molecular diversity is desired.[1]. These reactions often referred to as green as they are expeditious and consequently give an improvement in the development of new synthetic procedures[2]. MCRs have played a central role in the development of modern synthetic methodology due to its selectivity, synthetic convergency and atom-economy for pharmaceuti-cal and drug discovery research. MCRs are cornerstones of both combinatorial chemistry and diversity-oriented synthesis. Combinatorial chemistry is helpful to introduce structural variations in targeted compounds of interest whereas Diversity oriented synthesis is helpful to explore chemical structure space in search of new bioactive small molecules. Both approaches are benefit from the complexity-generating characteristics of MCRs. An-other important feature of these reactions implies that the diminution of waste production because of reducing synthetic or isolation steps along with saving time. Significant ad-vantages were offered by the multi component strategies over conventional linear-type syntheses. Therefore, MCRs have gained tremendous importance in the synthesis of drug moieties[3]. Biginelli reaction is the well-known reaction among the multi- component reaction[4]. The classical version of Biginelli reaction involves the ac-id-catalyzed, three-component reaction between benzaldehyde; ethyl acetoacetate (EAA), and urea in ethanol at reflux condition inciting the formation of Biginelli adduct. The rising interest in the Biginelli reaction is basically a direct result of the therapeutic and pharmacological properties of Biginelli adducts, specifically, DHPMs. Besides, various DHPMs had been seen to flaunt a huge spectrum of biological activities including antimalarial, antileishmanial, antitubercular, antiviral, antidiabetic, antiproliferative, anticancer, calcium channel inhibition, antioxidant, antimicrobial, antitumor, anti-inflammatory, anti-hypertensive, antineoplastic activities, and etc.[2].

The aim of this study is to synthesis dihydropyrimidinones derivatives by a green-based chitosan catalyst under optimal laboratory conditions through a MCR strategy namely Biginelli synthesis. Chitosan is a natural, biodegradable, and non-toxic poly-saccharide derived from chitin, which is the primary component of the exoskeletons of crustaceans like shrimp and crabs[5].

Chitosan can be modified to create porous structures, which increase the surface area available for catalytic reactions[6]. In many cases, chitosan-based catalysts can be recovered and reused, reducing waste and minimizing environmental impact[7, 8]. Chitosan's properties can be tailored through various modifications, such as cross-linking, grafting, and functionalization[9, 10]. Overall, chitosan's unique properties and versatility make it a promising material for developing sustainable and efficient catalysts for a wide range of applications.

2. Materials and Methods

2.1. Materials

All chemical reagent were purchased from Merck. Chitosan (MW =100,000–300,000 Da) was purchased from Acros Organics. To determine the completion of the reaction, analytical thin-layer chromatography (TLC) was performed on pre-coated silica-gel plates (Merk Silica Gel F254). Product stains were detected eighter under UV light or by placing in an iodine chamber. Also, melting points were determined in open capillaries using an Electrothermal 9100 apparatus. Chitosan (Medium molecular weight, provided by Sig-ma-Aldrich) was used.

2.1. Methods

General procedure for the synthesis of dihydropyrimidinones

In a 10 ml round-bottom flask, aldehyde (**2**) (1 mmol), ethyl acetoacetate (**3**) (1mmol), urea **(4)** (1.5 mmol), and catalyst (**1**) (15 mg) were added in a 5 mmol of ethanol. Then, the obtained mixture was refluxed for 7 h and after that the mixture was cold at the room temperature. The reaction progress was monitored by using thin layer chromatography and after completion of the reaction, the crude product was purified by crystallization in EtOH. Also, the separated catalyst 4 was used for the next reactions.

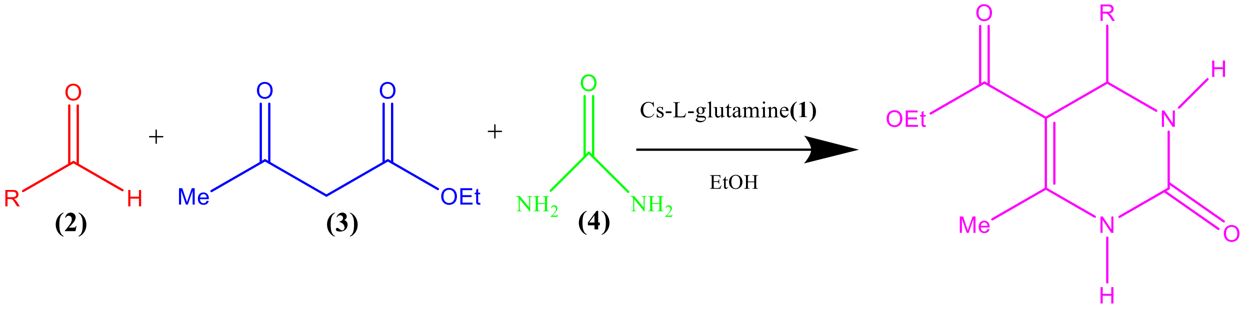

(5)

Scheme 1. Synthesis of dihydropyrimidinones via one-pot three component condensation of aldehyde **(2)**, ethyl acetoacetate **(3)**, urea **(4)** in the presence of Cs-L-glutamine catalyst.

٢. Results and Discussion

The general scheme for the multicomponent synthesis of dihydropyrimidinone derivatives has been shown in Scheme 1. The reaction of aldehyde (**2**), ethyl acetoacetate (**3**) and urea (**4**) were used as the model reaction. The effect of different factors on the reaction rate was studied. According to the obtained results, it was concluded that using of the Cs-L-glutamine catalyst (4) can afford dihydropyrimidinone derivatives through the multicomponent Biginelli reactions in a shorter reaction time compared to previous protocols. By using spectroscopic analyses such as FTIR spectroscopy, the structure of products was identified and confirmed.

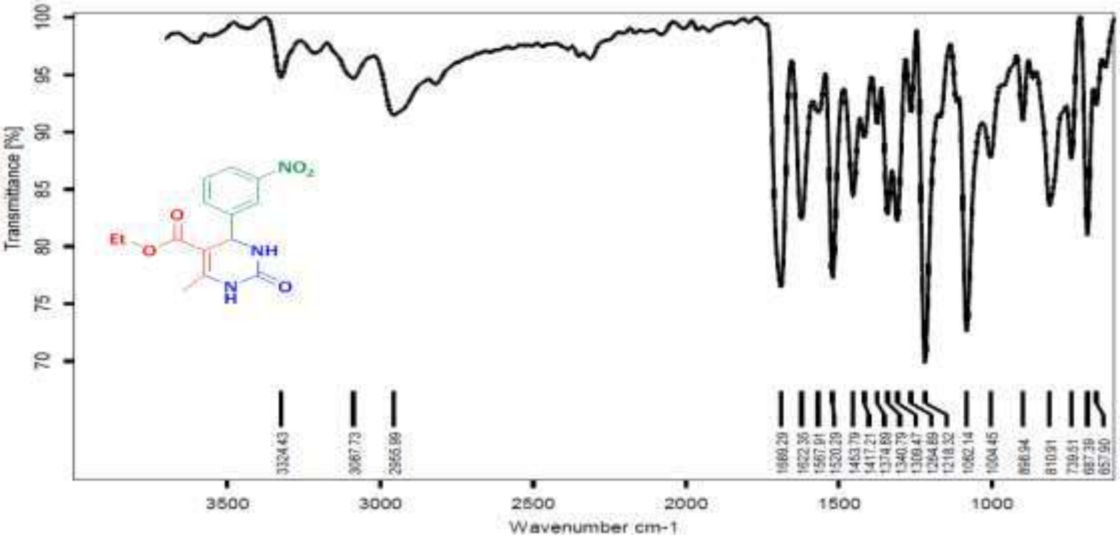

Fig. 2. FT-IR spectrum of 5-Ethoxycarbonyl–6-methyl-4-(3-nitrophenyl)–3,4-dihydropyrimidin-2(1*H*)-one.

٣. Conclusion

Briefly, the inexpensive and eco-friendly Cs-L-glutamine catalyst, which is easily pre-pared, has advantages such as low catalyst loading, high efficiency, good recyclability, and reusability, at least for five runs, for the synthesis dihydropyrimidinone derivatives through the multicomponent reaction strategy.

Acknowledgments

We are grateful for the financial support from The Research Council of Iran University of Science and Technology (IUST), Tehran, Iran

References:

1. Rotstein, B.H., et al., Small heterocycles in multicomponent reactions. Chemical reviews, 2014. 114(16): p. 8323-8359.

2. Adole, V.A., Synthetic approaches for the synthesis of dihydropyrimidinones/thiones (biginelli adducts): a concise review. World journal of pharmaceutical research, 2020. **9**(6): p. 1067-1091.
3. Anjaneyulu, B., D. Rao, and A. GB, Mini review: Biginelli reaction for the synthesis of dihydropyrimidinones. Int. J. Eng. Technol. Res, 2015. **3**(6): p. 26-37.
4. Chopda, L.V. and P.N. Dave, Recent advances in homogeneous and heterogeneous catalyst in Biginelli reaction from 2015-19: A concise review. ChemistrySelect, 2020. **5**(19): p. 5552-5572.
5. Cheung, R.C.F., et al., Chitosan: an update on potential biomedical and pharmaceutical applications. Marine drugs, 2015. **13**(8): p. 5156-5186.
6. Fletes-Vargas, G., et al., Porous chitosan hydrogels produced by physical crosslinking: physicochemical, structural, and cytotoxic properties. Polymers, 2023. **15**(9): p. 2203.
7. Dohendou, M., M.G. Dekamin, and D. Namaki, Pd@ l-asparagine–EDTA–chitosan: a highly effective and reusable bio-based and biodegradable catalyst for the Heck cross-coupling reaction under mild conditions. Nanoscale Advances, 2023. **5**(9): p. 2621-2638.
8. Fattahi, B. and M.G. Dekamin, Cu (II)/citric acid grafted to chitosan by dendritic units of melamine as a novel and highly efficient heterogeneous catalyst for the synthesis of 2-aminobenzothiazole derivatives. Colloid and Interface Science Communications, 2023. **54**: p. 100711.
9. Kluczka, J., Chitosan: Structural and Chemical Modification, Properties, and Application. *2023, MDPI. p. 554.*
10. Rostami, N., et al., Chitosan-EDTA-Cellulose network as a green, recyclable and multifunctional biopolymeric organocatalyst for the one-pot synthesis of 2-amino-4 H-*pyran* derivatives. Scientific Reports, 2022. **12**(1): p. 8642.

The 30th Iranian Seminar of Organic Chemistry
February 7-9, 2025, Iran University of Science and Technology, Tehran, Iran

Kinetic study of asparaginase and its application in the removal of acrylamide resulting from the Maillard reaction in the food industry

Mohammadhossein Aghabarari[1a], Maryam Mohadjerani[2*b]

[1]*MSc, Department of molecular and cell Biology, Faculty of Basic Science, University of Mazandaran, Babolsar, Mazandaran*

[2]*Associate Prof., Department of molecular and cell Biology, Faculty of Basic Science, University of Mazandaran, Babolsar, Mazandaran*

During the heating process, the amino acid asparagine, which is naturally present in starchy foods, undergoes a chemical process called the Maillard reaction. This reaction is the main cause of browning and crisping of baked or fried foods. Unfortunately, carcinogens such as acrylamide and

some heterocyclic amines are also formed during the Maillard reaction. Apart from its numerous applications, acrylamide is a known toxin that causes a range of toxicities. These adverse effects include its damaging effects on the nervous system, fertility, and the possibility of mutagenic and carcinogenic effects through the production of epoxides (glycidamides). Asparaginase is an enzyme that catalyzes the hydrolysis of asparagine to aspartic acid (Figure 1). The presence of asparaginase has been reported in various organisms, including animals, plants, and microorganisms (bacteria, fungi, algae, yeasts, and actinomycetes) other than humans. In the food industry, the use of asparaginase reduces acrylamide production. The aim of this study is to investigate the kinetic properties of the asparaginase enzyme and inhibit acrylamide production in the Maillard reaction. In this study, the asparaginase enzyme was partially isolated from the liver using homogenization, centrifugation, precipitation with ammonium sulfate, and dialysis at 4°C. After extraction, the enzyme activity was estimated by the Nessler reagent (2). In this study, the specific activity of the asparaginase enzyme isolated from the liver was determined to be 2.77 U/mg. The optimum pH of the enzyme was 6.5 and the optimum temperature was 35°C. The kinetic parameters Km and Vmax of the enzyme were 127.295 mM and 3.639 mM/min, respectively. Since the asparaginase enzyme can reduce acrylamide in the food industry, the study of the kinetics of this enzyme under different conditions such as ions, natural compounds, etc. should be of interest to researchers for more extensive studies.

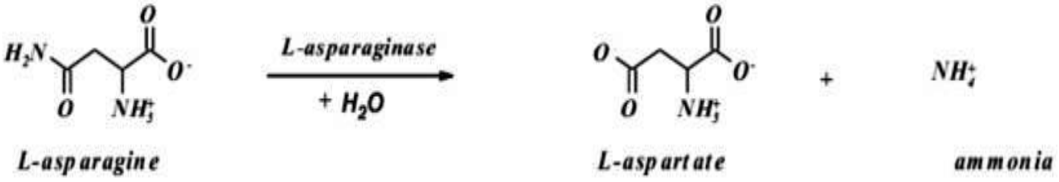

Scheme1: Catalyzed reaction by Asparaginase

Keyword: Acrylamide, Kinetic parameters, Asparaginase

References:

1)Röhm, K. H., & Van Etten, R. L. (1986). The 18O isotope effect in 13C nuclear magnetic resonance spectroscopy: mechanistic studies on asparaginase from Escherichia coli. Archives of biochemistry and biophysics, 244(1), 128-136.

2)Ren, J., He, F., & Zhang, L. (2010). The construction and application of a new PPY-MSPQC for l-asparaginase activity assay. Sensors and Actuators B: Chemical, 145(1), 272-277.

3)Nguyen, T. T. H., Nguyen, C. T., Le Nguyen, T. S., & Do, T. T. (2016). Optimization, purification and characterization of recombinant L-asparaginase II in Escherichia coli. African Journal of Biotechnology, 15(31), 1681-1691.

4-Methyl Benzoic Acid-Controlled Divergent Radical Cyclization of 1,6-Enynes to Access 1-Indanones and 1H-Cyclopropa[*b*]naphthalene-2,7-diones under Copper(I)-Catalyzed Reaction

Elmira Jamshidi,[a] Saideh Rajai-Daryasarei,[a] Robert Stranger,[b] Alireza Ariafard,*[,b] Frank Rominger,[c] Saeed Balalaie*[, a]

[a] *Peptide Chemistry Research Institute, K. N. Toosi University of Technology, P.O. Box 15875-4416, Tehran, Iran, Email: balalaie@kntu.ac.ir*

[b] *Research School of Chemistry, Australian National University, Canberra, ACT 2601, Australia*

[c] *Organisch-Chemisches Institut der Universität Heidelberg, Im Neuenheimer Feld 271, 69120 Heidelberg, Germany*

Keyword: Radical cyclization, 1,6-Enynes, Copper, 4-Methyl benzoic acid, 1-Indanones

Abstract: Radical cyclization reactions are a powerful tool for assembling valuable target molecular architectures.[1] Herein, 1-indanone derivatives are efficiently synthesized *via* a radical cyclization reaction of 1,6-enynes, using TBHP as both oxidant and reactant, in the presence of Cu(I) as the catalyst and 4-methyl benzoic acid as the cocatalyst. Interestingly, we found through mechanistic studies and DFT calculations that the synthesis of 1-indanones requires a combination of copper salt and 4-methylbenzoic acid as a prerequisite, and the removal of the 4-methylbenzoic acid cocatalyst leads to the exclusive formation of a different product, namely strained 1*H*-cyclopropa[*b*]naphthalene-2,7-diones **4**.

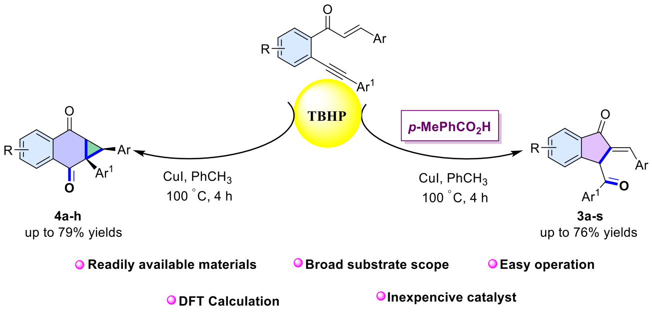

Scheme 1: Synthesis of 1-indanones and 1*H*-cyclopropa[*b*]naphthalene-2,7-diones

References:

1. a) Z.-J. Shen, Y.-N. Wu, C.-L. He, L. He, W.-J. Hao, A.-F. Wang, S.-J. Tu, B. Jiang, *Chem. Commun.* **2018**, *54*, 445-448; b) T.-S. Zhang, W.-J. Hao, R. Wang, S.-C. Wang, S.-J. Tu, B. Jiang, *Green Chem.* **2020**, *22*, 4259-4269; c) Y. Xia, S. Ochi, G. Dong, *J. Am. Chem. Soc.* **2019**, *141*, 13038-13042.

The 30th Iranian Seminar of Organic Chemistry
February 7-9, 2025, Iran University of Science and Technology, Tehran, Iran

Efficient degradation of 1,4- Dioxane in sodium lauryl ether sulfate (Behdapon)

Z. Hoseini[1], A. Fazli[1], S. Habibzadeh[2*]

[1] *Research and Technology Development, Behdash chemical Co, Lia industrial Park, Qazvn, Iran.*

[2] *Department of Chemical Engineering, Amirkabir University of Technology, Tehran, Iran.*

[*] *z.hoseini25@gmail.com*

Abstract

The degradation of 1,4-dioxane (dioxane) as a contaminate impurity in sodium lauryl ether sulfate (SLES) 70% produced by BEHDASH CHEMICAL COMPANY under trade name of BEHDAPON has been investigated. The oxidative degradation was performed by hydrogen peroxide in combination with UV irradiation. Result showed in the presence of UV light, hydrogen peroxide demonstrated a high efficiency in degradation. This method could provide a cost effective solution to the dioxane challenge in the detergents and personal care industry.

Keywords: ١،٤- Dioxane, sodium lauryl ether sulfate, detergent, oxidation processes

Introduction

1,4-Dioxane is a water soluble cyclic ether and an industrial chemical contaminate for human health and the environment. Dioxane is a common by-product inevitably occur in the synthesis of ethoxylated surfactants such as Sodium lauryl ether sulfate (SLES) which is used in finished consumer products (cosmetic, personal care, and cleaning products). For this reasons dioxane is found as an impurity in deodorants, shampoos, toothpastes, cleaning products, paints, etc. SLES is one of the most prominent anionic surfactants in the formulating of several commercial detergents and personal care products. SLES Production involves 3-step process: The first step consists of a reaction between lauryl alcohol and numerous ethylene oxide molecules. Ethylene oxide is reacted with the alcohol, which increases the molecule's solubility in water. But sometimes, the newly formed ethoxylate is decomposed into dioxane and an alcohol molecule. Ethylene oxide can also dimerize to form dioxane.

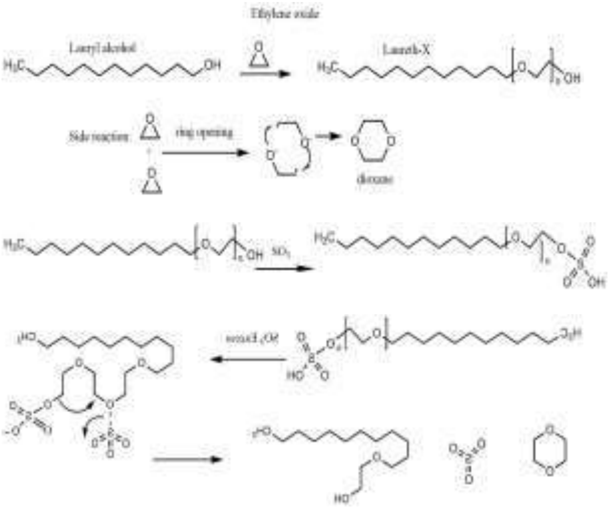

The second stage involves the sulfatization of lauryl alcohol using SO_3, followed by neutralization reaction with caustic soda and generate the liquid SLES that concentration is 70%. During this stage, SO_2 in the structure induces an intermolecular substitution reaction, leading to the cleavage of the ethoxylated chain and the formation of dioxane. The amount of dioxane allowed in consumer products by the Ministry of Health in Iran is lower than 50 ppm. The produced SLES may contain a higher amount of dioxane than the specified limit. Degassing can reduce dioxane by ~50%**.** Among the technologies capable of removing dioxane, the most effective is carbon adsorption and air stripping. Since dioxane is very hydrophilic and water soluble and has a very low vapor pressure, carbon adsorption and air stripping are not feasible and cost effective. Therefore, chemical treatments should be considered as an alternative. Several studies examined the removal of dioxane in aqueous solutions by advanced oxidation processes with ozone, Fenton's reagent, H_2O_2/ozone and so on. All these studies showed, neither hydrogen peroxide nor ozone alone readily oxidize dioxane. Suh and et al. demonstrated the advanced oxidation processes using ozone and hydrogen peroxide to effectively remove dioxane, a problematic water pollutant. In the present research, for the first time, we have developed a new method with the use of H_2O_2 to degrade dioxane, under processes induced by uv light for the reducing of dioxane in SLES 70% (Behdapon), which is low cost, no organic consumption and good repeatability [1-3].

Experimental

The experimental setup included a beaker equipped with a 15 W UV (λ_{max}=253.7 nm) lamp positioned horizontally above the sample, ensuring a consistent distance (7 cm) for uniform light exposure, was used as the reactor at different time intervals. The 300 ppm concentration of dioxane, with an optimized quantity of H_2O_2 was sampled at 0-15 minutes to monitor the degradation efficiency. The degradation was analyzed using GC, thereby assessing the effectiveness of UV irradiation in the advanced oxidation process.

Results and discussion

The effect of the addition of H_2O_2 on the photocatalytic dioxane oxidation was investigated in fig. 1. Several tests have confirmed addition of H_2O_2 to the SLES would enhance the degredation reaction by generating hydroxyl radicals (HO•) where 0.03 wt% increased in the degradation rate of 3.69 times for dioxane and the addition of 0.07 wt% H_2O_2 increased the photocatalysis by 4.03 times. However, in the SLES product, adding hydrogen peroxide and the generation of free radicals are limited. Considering this, the controlled amount of free oxidant HO• is maintained at around 40 ppm. This optimal level is achieved with 0.03% hydrogen peroxide.

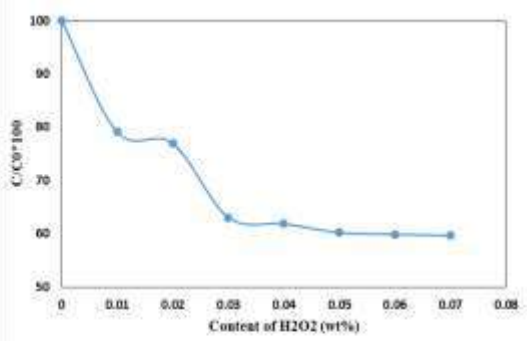

Fig 1. The degadation of dioxane vs H_2O_2 in SLES

According to fig. 2, the degradation of dioxane is notably improved when UV photolysis is combined with H_2O_2 in comparison with pure H_2O_2 and UV light. The necessary concentration of H_2O_2 is largely influenced by the molar ratio of H_2O_2 to dioxane. The removal efficiency of dioxane was 49.29% using H_2O_2 /UV at reaction time of 15 min and 0.03 wt% H_2O_2 concentration while the removal amounts under pure UV irradiation were 3%, and pure hydrogen peroxide were 36.94%. The impact of treatment time on the enhancement of degradability for a specific initial concentration of dioxane (300 ppm) is illustrated in Fig. 7. The data indicate that the degradability of the dioxane in SLES improves as the treatment time is extended. Notably, a significant enhancement is observed when the time is increased from 0 to 15 min .After 15 minutes, the concentration of dioxane shows a negligible decrease. Therefore, 15 minutes is considered an industrial optimal time.

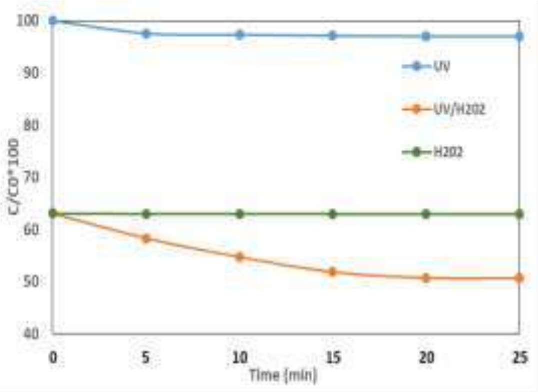

Fig 2. The degradation processes of dioxane in SLES by UV, UV/H_2O_2 and H_2O_2

Conclusions

The study concludes that the H_2O_2 advanced oxidation process is an effective method for the removal of dioxane-contaminated products. The analysis demonstrated that optimization of H_2O_2 at a quantity of 0.03 wt% for the degradation of 300 ppm dioxane, when combined with UV, exhibited the highest degradation rate compared to other tested processes which is viable, cost-effective, and environmentally friendly approach for the treatment of SLES product containing dioxane.

Acknowledgements

The authors gratefully acknowledge the financial support from Behdash Chemical Company.

References

[1] Gulyas H, von Bismarck R, Hemmerling L. Treatment of industrial wastewaters with ozone/hydrogen peroxide. Water Sci Technol 1995; 32(7):127–34.

[2] Suh, J.H., & Mohseni, M. (2004). A study on the relationship between biodegradability enhancement and oxidation of 1,4-dioxane using ozone and hydrogen peroxide. *Water Research*, 38(12), 2596-2604.

The 30th Iranian Seminar of Organic Chemistry
February 7-9, 2025, Iran University of Science and Technology, Tehran, Iran

Title: Efficiant Approach for The Synthesis of Conjugated Peptide Containing Ethyleneglycol as Linker

Authors: Zahra Bigdeli, Alireza Akbari, Saeed Balalaie *

**Peptide Chemistry Research Institute, K. N. Toosi University of Technology, P. O. Box 15875-4416, Tehran, Iran*

Keyword: Conjugated Peptide, Linker, Polyethylene glycol, Peptide Stability

Peptide conjugation is an important strategy to access bioactive molecules and could improve their biological activities. One of the important approach for the synthesis of conjugated peptides is related to attaching polyethyleneglycol at various positions that improve peptide stability, solubility and bioavailability. In the last years, the new conjugated peptides that contain peptides, linkers and other bioactive molecules such as carbohydrates and nucleotides have been extended. In this regard finding suitable and efficient approaches for the synthesis of these compounds are interesting subject in organic synthesis. Herein, we wish to report an efficient approach for the synthesis a bioactive peptide segment that has a long linker. The linker contains a ethyleneglycol and also an alkyl moieties. The synthesis of peptides was done through solid phase peptide synthesis (SPPS) approach and putting the linker on the side chain of lysine was done in the solution phase. The synthesized peptide was purified using preparative HPLC and was determined based on HR-MS(ESI) data. This segment is a part of semaglutide that used for the treatment of type-2 diabetes. The synthesis of conjugated peptides containing different linkers is in progress in our lab.

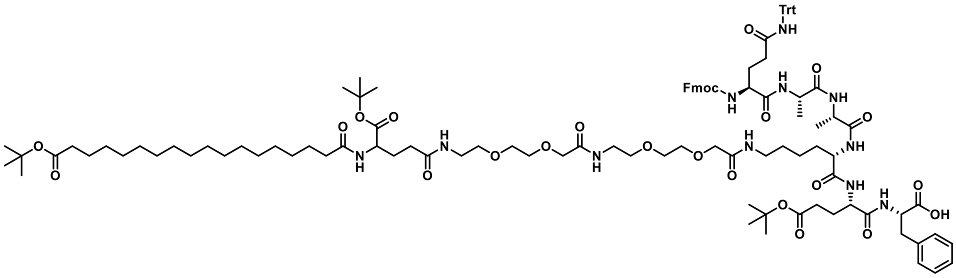

Fmoc-Gln(Trt)-Ala-Ala-Lys[PEG2-PEG2-*γ*-Glu(*α*-O*t*Bu)-Oct(O*t*Bu)]-Glu(O*t*Bu)-Phe-OH

References:

١) K. Bugatti *ChemBiochem.* **2023**,24. e202300254.

٢) M. Srinivasarao, P.S, Low *Chem. Rev.* **2017**,117,12133.

٣) X. Zhong, J. Yan, X. ding, C. Su, Y. Xu, M. Yang, *Bioconjugate Chem.***2023**, 34,457.

The 30th Iranian Seminar of Organic Chemistry
February 7-9, 2025, Iran University of Science and Technology, Tehran, Iran

Synthesis of dialkylaminoarylated indoles in the presence of nickel oxide/aluminum oxide nano catalyst as a recyclable catalyst

Bita Baghernejad*[a]

[a]*Department of Chemistry, School of Sciences, Payame Noor University(PNU), Tehran, Iran*

E-mail address:bitabaghernejad@pnu.ac.ir & bitabaghernejad@yahoo.com

Keyword: indole, formaldehyde, tertiary aromatic amines, nickel oxide/aluminum oxide, nanocatalyst

Introduction

Multi-component reactions (MCRs) have offered many fascinating and challenging transformations in organic synthesis.[1] The atom-economy, convergent character, operational simplicity, structural diversity, and complexity of the molecules are the major advantages associated with multi-component reactions. Besides this multi-component reactions are emerging as a powerful tool in the synthesis of biologically important compounds.[2] Thus, the discovery of novel multi-component reactions is of much importance. Most of the previously known MCRs were invented by serendipity rather than logically designed multi-component reactions. Recently, much effort is devoted for rational design of new multi-component reactions. There are three major ways of designing new MCRs such as combinatorial chemistry, MCR sequences, and smallest atom connectivity. We wish to report here a new multi-component reaction involving indoles, formaldehydes, and tertiary aromatic amines for the synthesis of dialkylaminoarylated indoles. Substituted 3-alkyl indole moieties are of much importance as they are widely distributed in nature and reveal a broad range of biological activity.[3] Indoles with substituents at the 3-position are considered as venerable pharmacophores[4] in drug discovery as well as found in various ranges of natural products such as 5-HT$_1$B/1D receptor agonist activities used in the treatment of migraine, aromatase inhibitor for breast cancer II[5] and HIV-1 integrase inhibitor[6]. The immense potential of indole nucleus as drug candidates prompted us to design a novel substituted 3-alkyl indole based on multi-component reactions.

In continuation of our work on MCRs, we report here a novel multi-component reaction of indoles, formaldehydes, and tertiary aromatic amines for the synthesis of dialkylaminoarylated indoles using nickel oxide/aluminum oxide nano catalyst as a catalyst (Scheme 1).

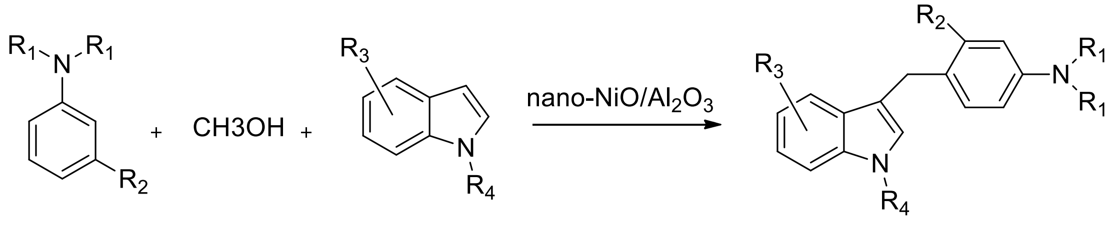

(Scheme 1)

Method

Preparation of nano nickel oxide/aluminum oxide:

0.08 mol of hexahydrate nickel nitrate, 0.32 mol of urea are dissolved in 100 ml of deionized water. The mixture was stirred at room temperature with a magnetic stirrer until a homogeneous solution was obtained. Then 32.64 grams of γ-Al_2O_3 is added to the homogeneous solution and placed in an oil bath at a temperature of 115 degrees Celsius for 2.5 hours. After the reaction was complete, the reaction mixture was cooled to room temperature and then filtered. The sediment was washed with deionized water to remove possible adsorbed ions and chemicals. Then it was placed in a 90 ^{0}C oven for six hours to dry completely. Finally, it is calcined for one hour at a temperature of seven hundred degrees Celsius. The dimensions of nanoparticles were determined by TEM and SEM(Figure 1,2) [6].

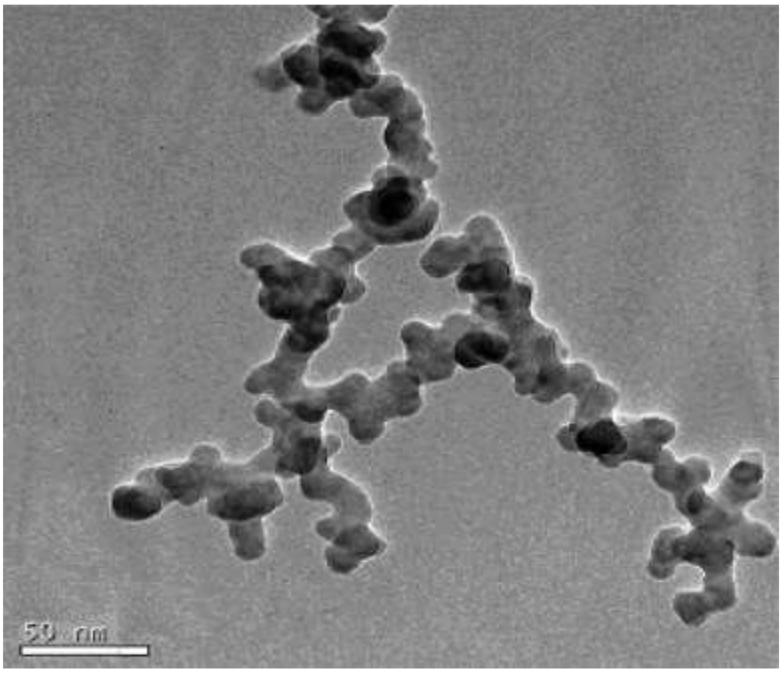

Figure 1.TEM of nano-NiO/Al_2O_3

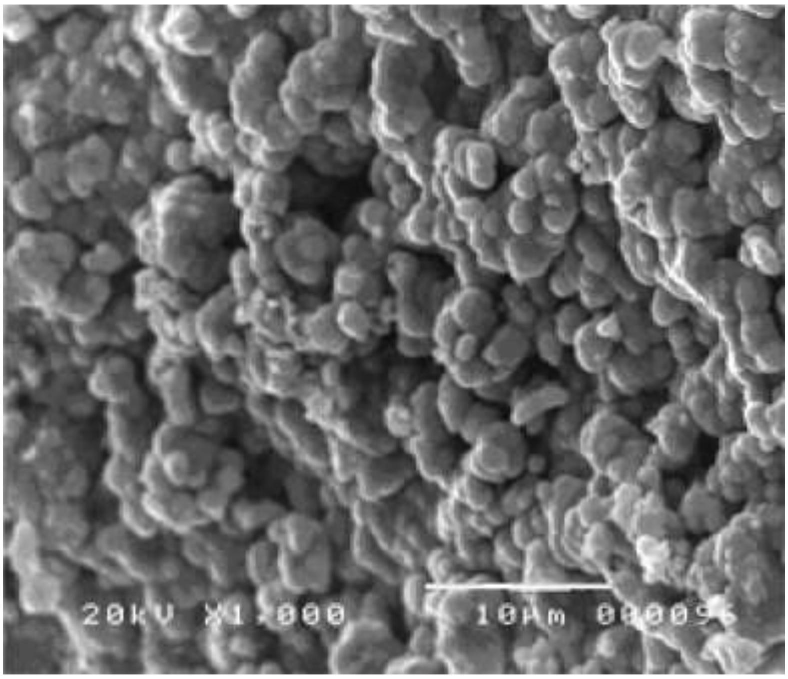

Figure 2. SEM of nano-NiO/Al_2O_3

Preparation of dialkylaminoarylated indoles

In a 25 ml flask, Indole (1.0 mmol), formaldehyde (1.0 mmol), N,N-dialkylaniline (1.0 mmol), nano-NiO/Al_2O_3 (0.05 g) and MeOH (5 mL), were mixed. The mixture was stirred by a magnetic stirrer at room temperature. The progress of the reaction was monitored using TLC in a mixture of n-hexane and ethyl acetate in a ratio of 1:3. After the reaction was complete, the contents of the balloon were filtered by filter paper. The product is soluble in methanol and the catalyst is insoluble, so the catalyst was easily separated by filter paper. By adding water and boiling the mixture, the desired product was withdrawn as a solid powder. The structure of the known samples was confirmed by comparing their spectral and physical data with references.

Results and Discussion

We have established a one-pot reaction of various indoles, formaldehyde, various N,N-dialkylanilines in methanol in the presence of nickel oxide/aluminum oxide nano catalyst as recyclable catalyst in good yields for synthesizing of dialkylaminoarylated indoles (Table 1). By examining the reaction time and the yield of the obtained products, it can be said that the presence of electron-donating or electron-donating substitutions does not cause noticeable changes in the reaction time and the yield of the products.

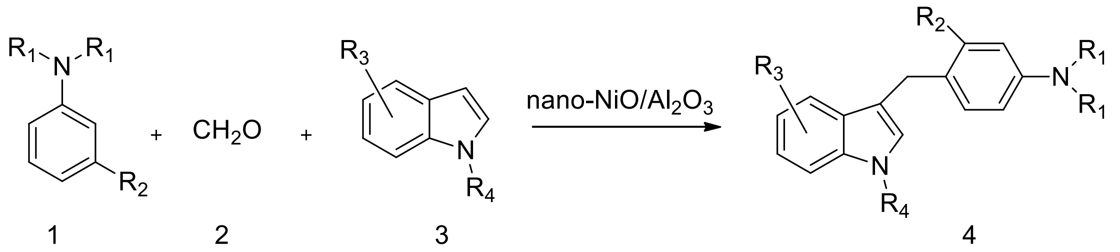

Table 1. nano-nickel oxide/aluminum oxide catalyzed the preparation of dialkylaminoarylated indoles

Entry	R1	R2	R3	R4	Product	Time (min)	Yield(%)
1	CH_3	H	H	H	4a	20	94
2	C_2H_5	H	H	H	4b	20	93
3	CH_3	CH_3	H	H	4c	20	94
4	CH_3	H	H	H	4d	20	91
5	CH_3	H	H	CH_3	4e	20	92
6	C_2H_5	H	Br	H	4f	20	92
7	CH_3	CH_3	Br	H	4g	20	94

We tested the synthesis of compound **4a** in the presence of different solvents to compare the effects of the solvent on the reaction. As you can see in the table 2, the best efficiency and the shortest time were obtained in methanol (Table 2).

Table 2. Synthesis of 3a using different solvents

Entry	Solvent	Yield(%)^a
1	THF	68
2	C_2H_5OH	91

3	CH_3CN	90
4	EtOAc	88
5	water	90
6	methanol	94
7	Solvent-free	91

[a]Yields were analyzed by GC

After the completion of the model reaction, 10 ml of ethyl acetate was added to the contents on the flat paper that has a catalyst. The mixture was stirred using a magnetic stirrer at room temperature for 5 minutes. The reaction mixture was filterated and because the catalyst was insoluble in ethyl acetate solvent, it remains on the filter. Then, in order to reuse the catalyst, the material on the filter was washed several times with acetone. After drying it to check the power of the catalyst, the reaction was repeated with it (Table 3). As seen in the Table 4, the reaction can be performed up to five times with good efficiency by the recycled catalyst.

Table 3. Comparison of catalyst recycling for synthesis of **4a**

Entry	Time(min)	Yield (%)[a]
First run	15	94
Second run	15	92
Third run	15	90
Fourth run	15	89
Fifth run	15	88

(a) Isolated yields

Conclusion

Dialkylaminoarylated indoles are heterocyclic compounds that have been of great interest due to their antibacterial and antiviral properties. Due to the extraordinary applications that these compounds have, they have received attention and various synthetic methods have been developed to prepare them. In this regard, we tried to obtain dialkylaminoarylated indoles in suitable conditions with small amounts of nano-oxidnical/aluminum oxide catalyst.

This method has many advantages such as:

1-Since the catalyst used is a solid nano catalyst, it is considered a useful method in chemistry.

2-Products are separated by simple filtering with filter paper and the percentage of products lost during the purification process is very small.

3-The catalyst used does not dissolve in any solvent and its separation is very easy.

References:

1. (a)Multicomponent Reactions; Zhu, J., Bienaymé, H., Eds.; Wiley-VCH: Weinheim, 2005; Reviews: (b) Dömling, A. Chem. Rev. 2006, 106, 17; (c) Ramón, D. J.; Yus, M. Angew. Chem., Int. Ed. 2005, 44, 1602; (d) Simon, C.; Constantieux, T.; Rodriguez, J. Eur. J. Org. Chem. 2004, 4957; (e) Orru, R. V. A.; de Greef, M. Synthesis 2003, 1471; (f) Bienaymé, H.; Hulme, C.; Oddon, G.; Schmitt, P. Chem.-Eur. J. 2000, 6, 3321; (g) Ulaczyk-Lesanko, A.; Hall, D. G. Curr. Opin. Chem. Biol. 2005, 9, 266.

2. (a) Weber, L. Curr. Med. Chem. 2002, 9, 2085; (b) Hulme, C.; Gore, V. Curr. Med.Chem. 2003, 10, 51–80.

3. For a recent review of indole containing natural products, see: (a) Faulkner, D. J. Nat. Prod. Rep. 1999, 16, 155; (b) Lounasmaa, M.; Tolvanen, A. Nat. Prod. Rep. 2000, 17, 175.

4. (a) Sundberg, R. J. In Indoles; Academic Press: San Diego, 1996; (b) Sundberg, R. J. In The Chemistry of Indoles; Academic Press: New York, 1970.

5. (a) Le´ ze´ , M.-P.; Le Borgne, M.; Marchand, P.; Loquet, D.; Kogler, M.; Le Baut, G.; Palusczak, A.; Hartmann, R. W. J. Enzyme Inhib. Med. Chem. 2004, 19, 549; (b) Le Borgne, M.; Marchand, P.; Delevoye-Seiller, B.; Robert, J.-M.; Le Baut, G.; Hartmann, R. W.; Palzer, M. Bioorg. Med. Chem. Lett. 1999, 9, 333.

6. (a) Deng, J.; Sanchez, T.; Neamati, N.; Briggs, J. M. J. Med. Chem. 2006, 49, 1684; (b) Contractor, R.; Samudio, I. J.; Estrov, Z.; Harris, D.; McCubrey, J. A.; Safe, S. H.; Andreeff, M.; Konopleva, M. Cancer Res. 2005, 65, 2890.

7. Li, J., Yan, R., Xiao, B., Tee Liang, D., Du, L., Environ. Sci. Technol. 2008, 42, 6224.

Multicomponent synthesis of pyrimido[4,5-b] quinolones in the presence of nickel oxide/aluminum oxide nano catalyst as a recyclable catalyst

Bita Baghernejad*[a]

[a]*Department of Chemistry, School of Sciences, Payame Noor University(PNU), Tehran, Iran*

E-mail address:bitabaghernejad@pnu.ac.ir & bitabaghernejad@yahoo.com

Keyword: aldehyde, 6-amino-1,3-dimethyluracil, dimedone, nickel oxide/aluminum oxide, nanocatalyst

Introduction

Pyrimido[4,5-*b*]quinolones are important compounds in medicinal chemistry due to some biological properties such as antifungal[1], antimalarial[2], anticancer[3,4], antiviral[5], antihistaminic[6], anti-oxidant, anti-microbial[7], and anti-inflammatory activities[8,9].

The one pot multi-component synthesis of pyrimido[4,5-*b*]quinolones by the reaction of aldehyde with dimedone and 6-amino-1,3-dimethyluracil is an important method for the preparation of these compounds[10].

Multi-component reactions are notable for the chemists due to prepare of the target product in one step without the produce of side products. High atomic economy, high yields, short reaction times, saving energy, reaction times, materials and solvents and compliance with green chemistry protocols are some important advantages of these reactions[11,12].

Various catalysts were used in the multi-component synthesis of pyrimido[4,5-*b*]quinolines such as[TSSECM][13], SBA-15/PrN($CH_2PO_3H_2$)$_2$[14], Nano-[Fe_3O_4@SiO2/N-propyl-1-(thiophen-2-yl)ethanimine][ZnCl2][15],[H2-DABCO][ClO_4]$_2$[16], nano-[Fe3O4@- SiO2@R-HMe2][H2PO4][17], *N*,*N*-diethyl-*N*-sulfoethanaminium chloride[18], Fe3O4@Cellulose sulfuric acid[19], [bmim]Br[20], nanocrystalline MgO[21], glycolic acid-supported cobalt ferrite[22], Agar-entrapped sulfonated DABCO[23],[$C_4(DABCO)_2$]·2OH[24], DABCO[25],Nano-[Cu-4C3NSP]$(Cl)_2$[26]. Most of the reported methods are performed by acidic or basic catalysts. In the presented work, the preparation of pyrimido[4,5-b]quinolines was reported in the presence of nano nickel oxide/aluminum oxide as a neutral compound which is commercially available. This method was carried out under mild reaction condition.

In continuation of our work on MCRs, we report here a novel multi-component reaction of aldehydes, dimedone, 6-amino-1,3-dimethyluracil for the synthesis of Pyrimido[4,5-*b*]quinolones using nickel oxide/aluminum oxide nano catalyst as a catalyst (Scheme 1).

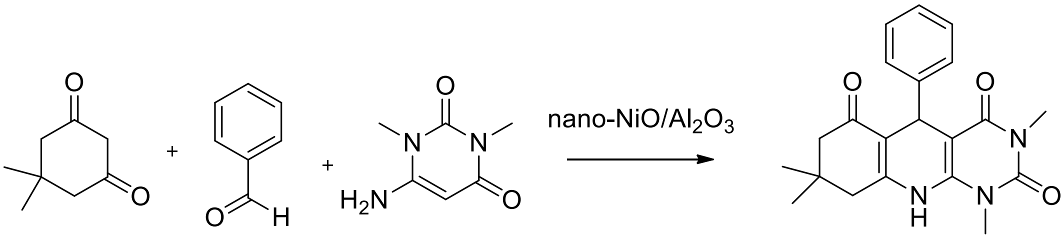

(Scheme 1)

Method

Preparation of nano nickel oxide/aluminum oxide:

0.08 mol of hexahydrate nickel nitrate, 0.32 mol of urea are dissolved in 100 ml of deionized water. The mixture was stirred at room temperature with a magnetic stirrer until a homogeneous solution was obtained. Then 32.64 grams of γ-Al_2O_3 is added to the homogeneous solution and placed in an oil bath at a temperature of 115 degrees Celsius for 2.5 hours. After the reaction was complete, the reaction mixture was cooled to room temperature and then filtered. The sediment was washed with deionized water to remove possible adsorbed ions and chemicals. Then it was placed in a 90 ^{0}C oven for six hours to dry completely. Finally, it is calcined for one hour at a temperature of seven hundred degrees Celsius. The dimensions of nanoparticles were determined by TEM and SEM(Figure 1,2) [27].

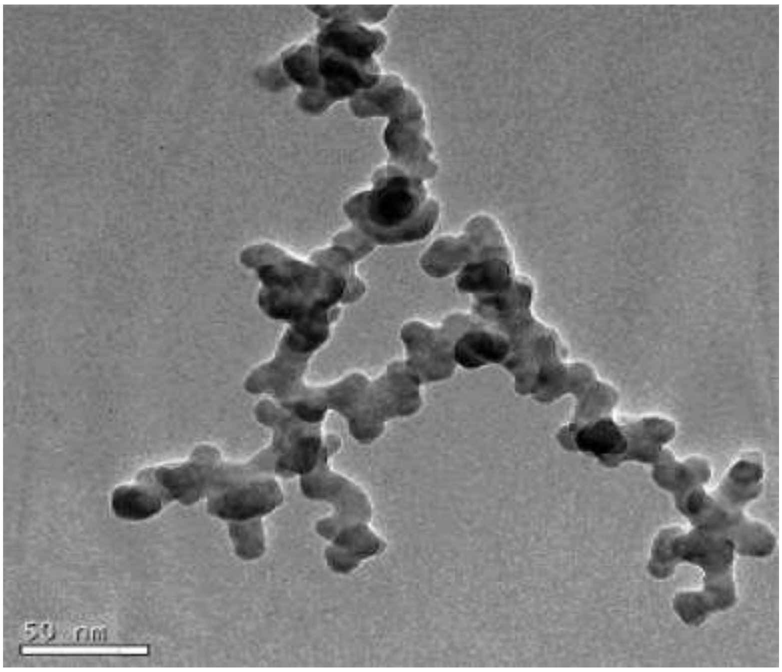

Figure 1.TEM of nano-NiO/Al_2O_3

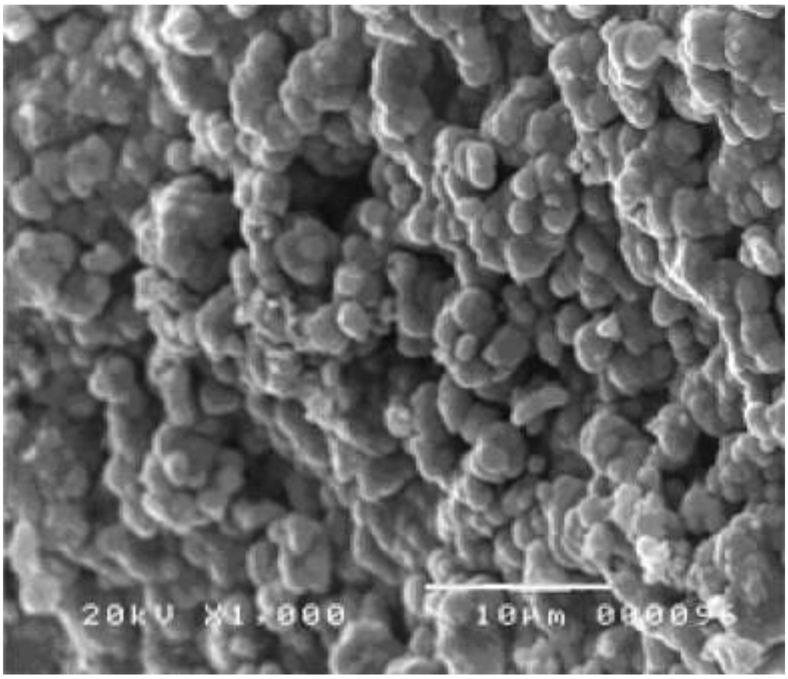

٦

Figure 2. SEM of nano-NiO/Al_2O_3

Preparation of pyrimido[4,5-b] quinolones

In a round-bottomed flask which connected to a reflux condenser, aromatic aldehydes (1 mmol), dimedone (1 mmol, 0.140 g), 6-amino-1,3-dimethyluracil (1 mmol, 0.155 g) and nano-NiO/Al_2O_3 (0.05g) as a catalyst were added and stirred in ethanol (5 mL) as a solvent under reflux condition for appropriate time (Table 1). After completion of the reaction as monitored by TLC, the solvent was removed and finally, the desired product was purified by the recrystallization in aqueous ethanol (70%).

Results and Discussion

We have established a one-pot reaction of various adldehyde, dimedone, 6-amino-1,3-dimethyluracil in ethanol in the presence of nickel oxide/aluminum oxide nano catalyst as recyclable catalyst in good yields for synthesizing of pyrimido[4,5-b] quinolones (Table 1). By examining the reaction time and the yield of the obtained products, it can be said that the presence of electron-donating or electron-donating substitutions does not cause noticeable changes in the reaction time and the yield of the products.

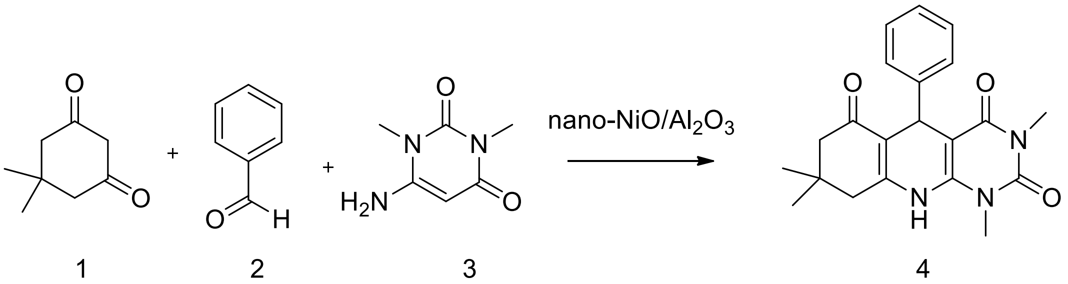

Table 1. nano-nickel oxide/aluminum oxide catalyzed the preparation of pyrimido[4,5-b] quinolones

Entry	Aldehydes	Product	Time (min)	Yield(%)
1	benzaldehyde	4a	30	97
2	4-chlorobenzaldehyde	4b	30	98
3	2-chlorobenzaldehyde	4c	30	97

4	4-methylbenzaldehyde	4d	30	96
5	4-methoxybenzaldehyde	4e	30	96
6	3-nitrobenzaldehyde	4f	30	98
7	4-nitrobenzaldehyde	4g	30	98

We tested the synthesis of compound **4a** in the presence of different solvents to compare the effects of the solvent on the reaction. As you can see in the table 2, the best efficiency and the shortest time were obtained in ethanol (Table 2).

Table 2. Synthesis of 3a using different solvents

Entry	Solvent	Yield(%)[a]
1	THF	68
2	C_2H_5OH	97
3	CH_3CN	92
4	EtOAc	88
5	water	90
6	methanol	94
7	Solvent-free	91

[a]Yields were analyzed by GC

After the completion of the model reaction, 10 ml of ethyl acetate was added to the contents on the flat paper that has a catalyst. The mixture was stirred using a magnetic stirrer at room temperature for 5 minutes. The reaction mixture was filterated and because the catalyst was insoluble in ethyl acetate solvent, it remains on the filter. Then, in order to reuse the catalyst, the material on the filter was washed several times with acetone. After drying it to check the power of the catalyst, the reaction was repeated with it (Table 3). As seen in the Table 4, the reaction can be performed up to five times with good efficiency by the recycled catalyst.

Table 3. Comparison of catalyst recycling for synthesis of **4a**

Entry	Time(min)	Yield (%)[a]
First run	15	97
Second run	15	93
Third run	15	90
Fourth run	15	88
Fifth run	15	87

(b) Isolated yields

conclusion

In summary, nano-nickel oxide/aluminum oxide was used as a heterogeneous catalyst for the synthesis of pyrimido[4,5-*b*]quinolones derivatives in neutral condition. The products were prepared in high yields and short reaction times. The recyclability of catalyst, commercially availability of the catalyst, short reaction times and the avoidance of harsh acidic conditions are important advantages of this work.

References:

1. Valderrama, J. A. *et al.* Studies on quinones. Part 44: Novel angucyclinone N-heterocyclic analogues endowed with antitumoral activity. *Bioorg. Med. Chem.* **16**, 10172–10181 (2008).

2. Alqasoumi, S. I., Al-Taweel, A. M., Alafeefy, A. M., Noaman, E. & Ghorab, M. M. Novel quinolines and pyrimido [4, 5-*b*] quinolones bearing biologically active sulfonamide moiety as a new class of antitumor agents. *Eur. J. Med. Chem.* **45**, 738–744 (2010).

3. Nair, V., Chi, G., Shu, Q., Julander, J. & Smee, D. F. A heterocyclic molecule with significant activity against dengue virus. *Bioorg.Med. Chem. Lett.* **19**, 1425–1427 (2009).

4. Alagarsamy, V. Synthesis and pharmacological investigation of some novel 2-methyl-3-(substituted methylamino)-(3H)-quinazolin-4-ones as histamine H1-receptor blockers. *Pharmazie* **59**, 753–755 (2004).

5. El-Gazzar, A. B. A., Hafez, H. N. & Nawwar, G. A. M. New acyclic nucleosides analogues as potential analgesic, anti-inflammatory, anti-oxidant and anti-microbial derived from pyrimido [4, 5-*b*] quinolones. *Eur. J. Med. Chem.* **44**, 1427–1436 (2009).

6. Alagarsamy, V. *et al.* Synthesis and pharmacological investigation of some novel 2-phenyl-3-(substituted methyl amino) quinazolin-4 (3H)-ones as H1-receptor blockers. *Pharmazie* **57**, 306–307 (2002).

7. Baghernejad, B. & Harzevili, M. R. Nano-cerium oxide/aluminum oxide: An efficient and useful catalyst for the synthesis of tetrahydro[a]xanthenes-11-one derivatives. *Chem. Methodol.* **5**, 90–95 (2021).

8. Moosavi-Zare, A. R., Goudarziafshar, H., Jalilian, Z. & Hosseinabadi, F. Efficient pseudo-six-component synthesis of tetrahydropyrazolopyridines using [Zn-2BSMP]Cl2. *Chem. Methodol.* **6**, 571–581 (2022).

9. Abedini, E. & Shaterian, H. R. L-Leucine supported on silica gel encapsulating γ-Fe2O3 nanoparticles: A new recoverable magnetic catalyst for preparation of 1, 3-thiazole derivatives. *Eurasian Chem. Commun.* **5**, 228–245 (2023).

10. Baghernejad, B. & Taromsari, S. M. H. Aqueous media preparation of 2-amino-4H-benzopyran derivatives using cerium oxide nanoparticles as a recyclable catalyst. *Asian J. Green Chem.* **6**, 194–202 (2022).

11. Muhiebes, R. M., Fatolahi, L. & Sajjadifar, S. L-proline catalyzed multicomponent reaction for simple and efficient synthesis of tetrahydropyridines derivatives. *Asian J. Green Chem.* **7**, 121–131 (2023).

26. Deb, M. L., Borpatra, P. J. & Baruah, P. K. A one-pot catalyst/external oxidant/solvent-free cascade approach to pyrimidines via a 1,5-hydride transfer. *Green Chem.* **21**, 69–74 (2019).

12. Zare, A., Dianat, M. & Eskandari, M. M. A novel organic–inorganic hybrid material: production, characterization and catalytic performance for the reaction of arylaldehydes, dimedone and 6-amino-1,3-dimethyluracil. *New J. Chem.* **44**, 4736–4743 (2020).

13. Jalili, F., Zarei, M., Zolfigol, M. A., Rostamnia, S. & Moosavi-Zare, A. R. SBA-15/PrN(CH2PO3H2)2 as a novel and efficient mesoporous solid acid catalyst with phosphorous acid tags and its application on the synthesis of new pyrimido[4,5-b]quinolones

and pyrido[2,3-*d*]pyrimidines via anomeric based oxidation. *Microporous Mesoporous Mater.* **294**, 109865–109897 (2020).

14. Esmaili, S., Moosavi-Zare, A. R. & Khazaei, A. Nano-[Fe3O4@SiO2/N-propyl-1-(thiophen-2-yl)ethanimine][ZnCl2] as a nano magnetite Schiff base complex and heterogeneous catalyst for the synthesis of pyrimido[4,5-*b*]quinolones. *RSC Adv.* **12**, 5386–5394 (2022).

15. Shirini, F., Langarudi, M. S. N., Daneshvar, N., Jamasbi, N. & Irankhah-Khanghah, M. Preparation and characterization of [H2-DABCO][ClO4]2 as a new member of DABCO-based ionic liquids for the synthesis of pyrimido[4,5-*b*]-quinoline and pyrimido[4,5-*d*]pyrimidine derivatives. *J. Mol. Struct.* **1161**, 366–382 (2018).

16. Zare, A., Lotfifar, N. & Dianat, M. Preparation, characterization and application of nano-[Fe3O4@-SiO2@R-NHMe2][H2PO4] as a novel magnetically recoverable catalyst for the synthesis of pyrimido[4,5-*b*]quinolones. *J. Mol. Struct.* **1211**, 128030 (2020).

17. Zare, A. & Dianat, M. A highly efficient and green approach for the synthesis of pyrimido[4,5-*b*]quinolines using N, N-diethyl-N-sulfoethanaminium chloride. *Z. Naturforsch.* **76**, 85–90 (2021).

18. Osanlou, F., Nemati, F. & Sabaqian, S. An eco-friendly and magnetized biopolymer cellulose-based heterogeneous acid catalyst for facile synthesis of functionalized pyrimido[4,5-*b*]quinolines and indeno fused pyrido[2,3-*d*]pyrimidines in water. *Res. Chem. Intermed.* **43**, 2159–2174 (2017).

19. Shi, D.-Q. *et al.* An Efficient synthesis of pyrimido[4,5-*b*]quinoline and indeno[2′,1′:5,6]pyrido[2,3-d]pyrimidine derivatives via multicomponent reactions in ionic liquid. *J. Heterocyclic Chem.* **45**, 693–702 (2008).

20. Rad, A. M. & Mokhtary, M. Efficient one-pot synthesis of pyrido[2,3-d]pyrimidines catalyzed by nanocrystalline MgO in water. *Int. Nano Lett.* **5**, 109–123 (2015).

21. Gholami, A., Mokhtary, M. & Nikpassand, M. Glycolic acid-supported cobalt ferrite-catalyzed one-pot synthesis of pyrimido[4,5-b]quinoline and indenopyrido[2,3-d]pyrimidine derivatives. *Appl. Organomet Chem.* **34**, e6007 (2020).

22. Moghaddampour, I. M., Shirini, F. & Langarudi, M. S. N. Agar-entrapped sulfonated DABCO: Agelly acidic catalyst for the acceleration of one-pot synthesis of 1,2,4-triazoloquinazolinone and some pyrimidine derivatives. *J. Mol. Struct.* **1226**, 129336 (2021).

23. Jolodar, O. G., Shirini, F. & Seddighi, M. Efficient synthesis of pyrano[2,3-*d*]pyrimidinone and pyrido[2,3-d]pyrimidine derivatives in presence of novel basic ionic liquid catalyst. *Chin. J. Catal.* **38**, 1245–1251 (2017).

24. Esmaili, S., Moosavi-Zare, A. R., Khazaei, A. & Najafi, Z. The synthesis of novel pyrimido[4,5-*b*] quinolines containing benzyloxy and 1,2,3-triazole moieties by DABCO as a basic catalys. *ACS Omega* **7**, 45314–45324 (2022).

25. Moosavi-Zare, A. R., Goudarziafshar, H. & Bahrami, Z. Nano-[Cu-4C3NSP](Cl)2 as a new catalyst for the preparation of pyrimido[4,5-*b*]quinoline derivatives. *Res. Chem. Intermed.* **49**, 507–523 (2023).

26. Azimi, S. C. Cellulose sulfuric acid catalyzed multicomponent reaction for efficient synthesis of pyrimido and pyrazolo[4,5-*b*] quinolines under solvent-free conditions. *Iran. J. Catal.* **4**, 113–120 (2014).

27. Li, J., Yan, R., Xiao, B., Tee Liang, D., Du, L., Development of nano-niO/Al2O3 catalyst to be used for tar removal in biomass gasification. *Environ. Sci. Technol*. 42, 6224-6229 (2008).

The 30th Iranian Seminar of Organic Chemistry
February 7-9, 2025, Iran University of Science and Technology, Tehran, Iran

A highly efficient synthesis of 2,4-diamino-6-arylpyrimidine-5-carbonitrile derivatives in the presence of nickel oxide/aluminum oxide nano catalyst as a recyclable catalyst

Bita Baghernejad*[a]

[a]*Department of Chemistry, School of Sciences, Payame Noor University(PNU), Tehran, Iran*

E-mail address:bitabaghernejad@pnu.ac.ir & bitabaghernejad@yahoo.com

Keyword: aldehyde, 2,4-diamino-6-arylpyrimidine-5-carbonitrile, malononitrile, nickel oxide/aluminum oxide, nanocatalyst

Introduction

Pyrimidines and their derivatives are of considerable interest as they possess a wide range of biological properties, such as antibacterial [1], antimicrobial [2], antiviral [3], antihypertensive [4], antimalarial [5], and antitumor [6]. In addition, they can be used as integral backbones of several calcium blockers, antihypertensive agents, α-1aantagonists, and neuropeptide Y antagonists [7]. There are some examples for the syntheses of 2,4-diamino-6-arylpyrimidine-5-carbonitrile in the literature via the condensation reaction of aromatic aldehydes, malononitrile, and guanidine hydrochloride or carbonate [8–12]. Although these procedures have their advantages, research for a simple, efficient, and environmentally friendly procedure that afforded the desired products in higher yields is still strongly desired. In view of the biological significance of pyrimidinones mentioned above and with the fact that , nano-nickel oxide/aluminum oxide make the development of a new catalytic procedure possible for organic transformations under milder reaction conditions, we investigate a , nickel oxide/aluminum oxide as catalyst for the synthesis of a series of 2,4-diamino-6-aryl-5-pyrimidinecarbonitriles. It was found that the nano-nickel oxide/aluminum oxide is an effective promoter for the synthesis of 2,4-diamino-6-arylpyrimidine-5-carbonitrile under solvent-free conditions (Scheme 1).

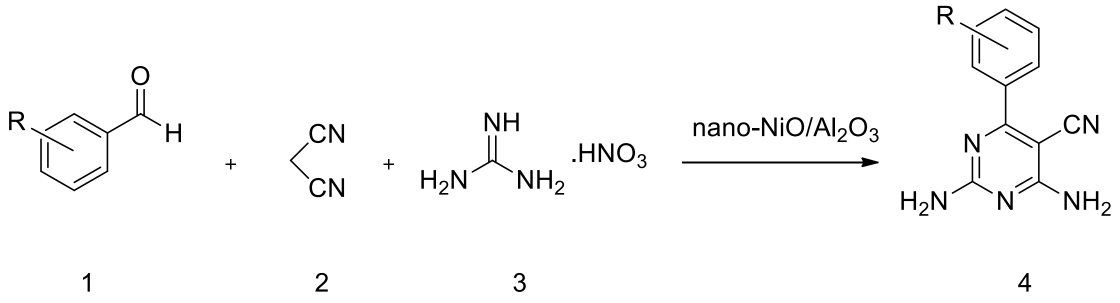

Scheme 1. synthesis of 2,4-diamino-6-arylpyrimidine-5-carbonitrile derivatives

Method

Preparation of nano nickel oxide/aluminum oxide:

0.08 mol of hexahydrate nickel nitrate, 0.32 mol of urea are dissolved in 100 ml of deionized water. The mixture was stirred at room temperature with a magnetic stirrer until a homogeneous solution was obtained. Then 32.64 grams of γ-Al_2O_3 is added to the homogeneous solution and placed in an oil bath at a temperature of 115 degrees Celsius for 2.5 hours. After the reaction was complete, the reaction mixture was cooled to room temperature and then filtered. The sediment was washed with deionized water to remove possible adsorbed ions and chemicals. Then it was placed in a 90 ^{0}C oven for six hours to dry completely. Finally, it is calcined for one hour at a temperature of seven hundred degrees Celsius. The dimensions of nanoparticles were determined by TEM and SEM(Figure 1,2) [13].

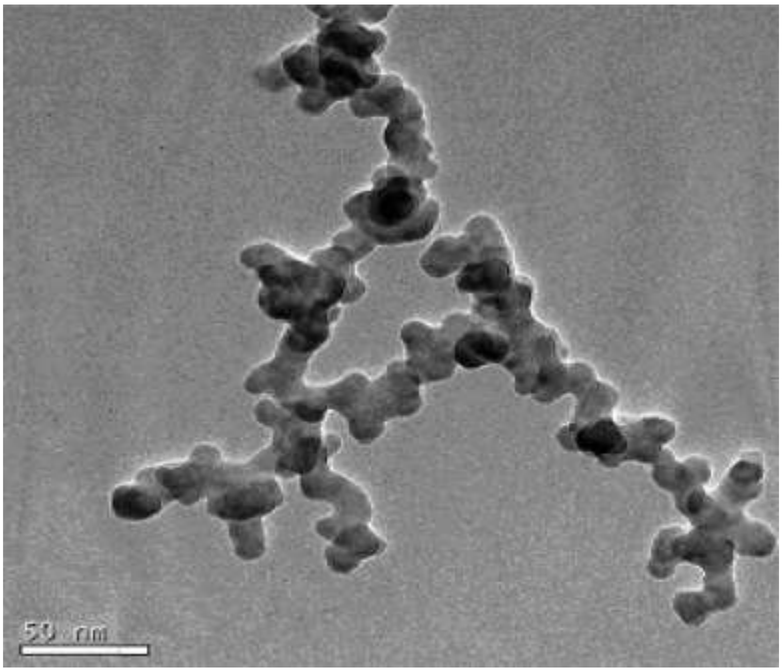

Figure 1.TEM of nano-NiO/Al_2O_3

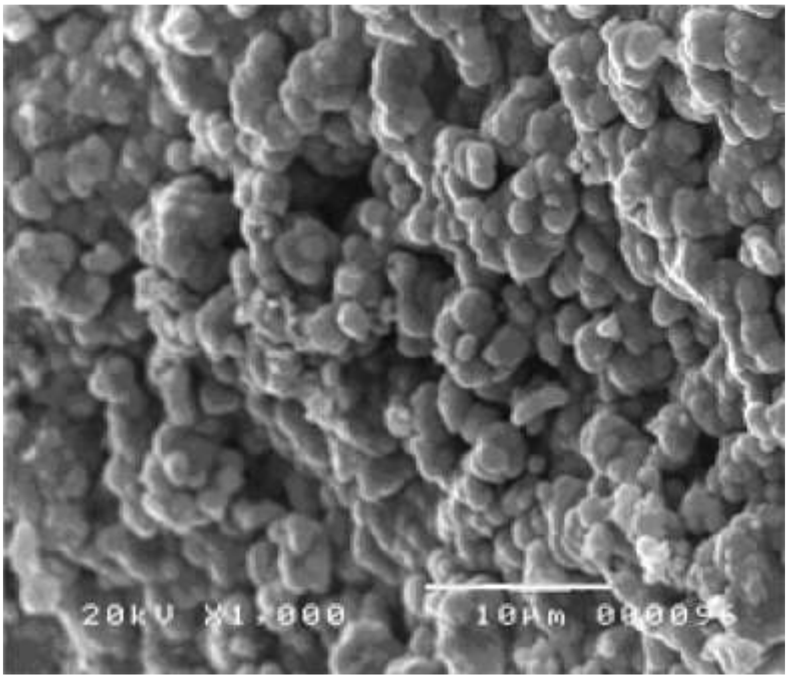

٧

Figure 2. SEM of nano-NiO/Al_2O_3

Preparation of 2,4-diamino-6-arylpyrimidine-5-carbonitrile

A mixture of aromatic aldehydes (1 mmol), malononitrile (1.2 mmol), guanidine nitrate (1.2 mmol), and nano-NiO/Al_2O_3 (0.05g) was stirred at 80°C for about 2 h. The progress of the reaction was monitored by thin-layer chromatography (acetone–petroleum ether,1 : 3). Upon completion of the reaction, hot ethanol (5 mL) was added to the reaction mixture, and the catalyst was filtered and dried in air at ambient temperature for reuse. The organic solution was poured into the ice-cold water (5 mL) and the solid was removed by filtration and then recrystallized from EtOH–H2O to give the pure product in high yield.

Results and Discussion

We have established a one-pot reaction of various adldehyde, malononitrile, guanidine nitrate in the presence of nickel oxide/aluminum oxide nano catalyst as recyclable catalyst in good yields for synthesizing of 2,4-diamino-6-arylpyrimidine-5-carbonitrile (Table 1). By examining the reaction time and the yield of the obtained products, it can be said that the presence of electron-donating or electron-donating substitutions does not cause noticeable changes in the reaction time and the yield of the products.

Table 1. nano-nickel oxide/aluminum oxide catalyzed the preparation of 2,4-diamino-6-arylpyrimidine-5-carbonitrile

Entry	Aldehydes	Product	Time (min)	Yield(%)
1	benzaldehyde	4a	20	96
2	4-chlorobenzaldehyde	4b	20	97
3	2-chlorobenzaldehyde	4c	20	96
4	4-methylbenzaldehyde	4d	20	95
5	4-methoxybenzaldehyde	4e	20	96
6	3-nitrobenzaldehyde	4f	20	97
7	4-nitrobenzaldehyde	4g	20	97

We tested the synthesis of compound **4a** in the presence of different solvents to compare the effects of the solvent on the reaction. As you can see in the table 2, the best efficiency and the shortest time were obtained in solvent-free condition (Table 2).

Table 2. Synthesis of 3a using different solvents

Entry	Solvent	Yield(%)[a]
1	THF	68
2	C_2H_5OH	92
3	CH_3CN	92
4	EtOAc	88
5	water	90
6	methanol	93
7	Solvent-free	96

[a] Yields were analyzed by GC

After the completion of the model reaction, 10 ml of ethyl acetate was added to the contents on the flat paper that has a catalyst. The mixture was stirred using a magnetic stirrer at room temperature for 5 minutes. The reaction mixture was filterated and because the catalyst was insoluble in ethyl acetate solvent, it remains on the filter. Then, in order to reuse the catalyst, the material on the filter was washed several times with acetone. After drying it to check the power of the catalyst, the reaction was repeated with it (Table 3). As seen in the Table 4, the reaction can be performed up to five times with good efficiency by the recycled catalyst.

Table 3. Comparison of catalyst recycling for synthesis of **4a**

Entry	Time(min)	Yield (%)[a]
First run	15	96
Second run	15	93

Third run	15	90
Fourth run	15	88
Fifth run	15	87

(c) Isolated yields

Conclusion

In conclusion, we found a novel solvent-free approach for the synthesis of 2,4-diamino-6-arylpyrimidine-5-carbonitrile derivatives. Meanwhile the new method also expands the application of the nano-NiO/Al_2O_3 in organic synthesis. Compared with previous methods, this method has the advantages of high yields, mild reaction conditions, short reaction time, easy work-up, inexpensive reagents, and environmentally friendly procedure

References:

[1] D. Jabli, K. Lahbib, K. Dridi, M. Lotfi Efrit, *J. Pharm. Chem. Biol. Sci*. **2015**, *3*, 178.

[2] A. S. M. Hossan, H. M. A. Abu-Melha, M. A. Al-Omar, A. E. G. E. Amr, *Molecules* **2012**, *17*, 13642.

[3] W. Wierenga, *Pharmacol. Ther*. **1985**, *30*, 67.

[4] K. S. Atwal, B. N. Swanson, S. E. Unger, D. M. Floyd, S. Moreland, A. Hedberg, B. C. O'Reilly, *J. Med. Chem*. **1991**, *34*, 806.

[5] A. Agarwal, K. Srivastava, S. K. Puri, P. M. Chauhan, *Bioorg. Med. Chem*. **2005**, *13*, 4645.

[6] W. Chen, J. Feng, H. Tu, *Front. Chem. China* **2007**, *2*, 127.

[7] G. C. Rovnyak, S. D. Kimball, B. Beyer, G. Cucinotta, J. D. DiMarco, J. Gougoutas, A. Hedberg, M. Malley, J. P. McCarthy, *J. Med. Chem*. **1995**, *38*, 119.

[8] M. B. Deshmukh, P. V. Anbhule, S. D. Jadhav, S. S. Jagtap, D. R. Patil, S. M. Salunkhe, S. A. Sankpal, *Indian J. Chem*. **2008**, *47b*, 792.

[9] H. Sheibani, A. S. Saljoogi, A. Bazgir, *Arkivoc*. **2008**, *2*, 115.

[10] H. Sheibani, M. Seifi, A. Bazgir, *Synth. Commun*. **2009**, *39*, 1055.

[11] L. Rong, H. Han, L. Gao, Y. Dai, M. Cao, S. Tu, *Synth. Commun*. **2010**, *40*, 504.27.

[12] S. Abdolmohammadi, R. Ghiasi, S. Ahmadzadeh-Vatani, Z. Naturforsch. **2016**, 71b, 777.

[13] Li, J., Yan, R., Xiao, B., Tee Liang, D., Du, L., *Environ. Sci. Technol*. **2008**, 42, 6224.

Facile Synthesis of Quinazolinones through a Tandem Reaction of Isatoic Anhydrides and Isocyanides

Farshad Fahami,[a] Kamran Amiri,[a] Sattar Mirzaie,[a] Frank Rominger,[b] Saeed Balalaie*,[a]

[a] *Peptide Chemistry Research Institute, K. N. Toosi University of Technology, P.O. Box 15875-4416, Tehran, Iran, Email: balalaie@kntu.ac.ir*

[b] *Organisch-Chemisches Institut der Universität Heidelberg, Im Neuenheimer Feld 271, 69120 Heidelberg, Germany*

Keyword: isocyanides, Isatoic anhydride, Quinazolinones,[4+2] cycloaddition reaction, Tandem reaction

Abstract: Developing new methodologies that provide easy access to heterocyclic backbones has always been of considerable interest. Quinazolinones are key constituents of many pharmaceutical agents and biologically active natural products. In this regard, finding an efficient synthetic pathway is an interesting subject in organic synthesis. Due to the importance of isocyanides, our group has been involved in the development of novel reactions based on these compounds. Herein, we wish to report the synthesis of quinazolinone derivatives *via* the reaction of isatoic anhydrides and isocyanides. The reactions were carried out under metal-free conditions in toluene at 80 °C. In most cases, isocyanides participate in [4+1] cycloaddition reaction, but in this case, isocyanides participated in hetero-Diels-Alder cycloaddition reaction via ring-opening of isatoic anhydride. The structure of the products was confirmed using spectroscopic data and X-ray crystallographic analysis.

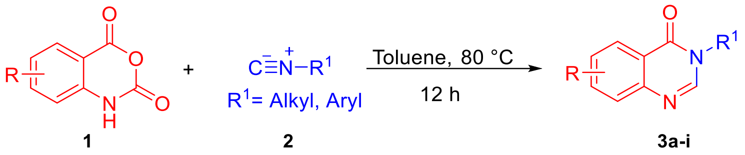

Scheme 1: Synthesis of quinazolin-4(3*H*)-one scaffold

References:

1. a) Shvekhgeimer, M.-G. A. *Chem. Heterocycl. Compd.* **2001**, *37*, 385; b) V. Nenajdenko, Isocyanide Chemistry: Applications in Synthesis and Material Science, John Wiley & Sons, ۲۰۱۲; c) J.-R. Chen, X.-Q. Hu, L.-Q. Lu and W.-J. Xiao, *Chem. Rev.*, ۲۰۱۵, *115*, ۵۳۰۱.

Preparation of antibacterial film based on chitosan, PVA and silver nanoparticles using laser ablation

Zahra Zareifarja[a], Atefeh Nasri[a], Babak Jaleh[a], Fatemeh Goharpour[a] and Hossein Zhaleh[b]

[a] *Department of Physics, Faculty of Science, Bu-Ali Sina University, 65174, Hamedan, Iran*
[b]*Department of Biology, Faculty of Science, Bu-Ali Sina University, 65174, Hamedan, Iran*

Abstract

Herein, an antibacterial film containing of chitosan (CS), polyvinyl alcohol (PVA), and silver nanoparticle (Ag NPs) was synthesized by a simple laser ablation in air (LAA) method of in-situ synthesis of Ag NPs. This is a cost-effective, easy, quick and in situ strategy to prepare CS/PVA film loaded with Ag NPs. This approach of formation of CS/PVA/Ag films is proved to be an excellent 'green approach' for the synthesis of metal nanoparticle composite films. The presence of Ag NPs was confirmed from the microscopic images of the film. The developed CS/PVA/Ag film demonstrated excellent antibacterial action against Escherichia coli. These films can be used as antimicrobial packaging materials.

Keyword: Chitosan, PVA, Antibacterial films, Ag NPs

Introduction

The increasing global population and the growing demand for plastic packaging in industrial applications, medical products, and other sectors have turned the use of non-degradable plastics into a significant environmental problem. Conventional plastics, due to their long lifespan after disposal, contribute substantially to environmental pollution, causing considerable damage to marine and terrestrial ecosystems. This necessitates the development of biodegradable alternatives. Furthermore, extending the shelf life of food products and preventing spoilage remains a major challenge. Widespread use of biodegradable plastics can substantially reduce pollution from non-degradable plastics and positively impact natural ecosystems [1,2]. Utilizing abundant and inexpensive raw materials such as CS biopolymer, which is extracted from natural sources, can reduce production costs and offer economic advantages. Therefore, research into the production of biodegradable films based on CS and PVA contributes to mitigating environmental problems. Ag NPs can further enhance the properties of CS and PVA based films.

Method

At first, 0.5 g of CS and 2 g of PVA were separately dissolved in 50 ml of distilled water. Acetic acid (3%) was used as a solvent to dissolve the CS, while the PVA solution was prepared at 50 °C. They were placed on a magnetic stirrer for 2 hours to achieve a uniform solution.

After 2 hours, the PVA solution is added to the CS solution and stirred again for 30 minutes. Then, 1 mL of glycerol was added and allowed to mix for 2 hours. Finally, the resultant solution was poured into a suitable glass petri dish and dried at room temperature to fabricate the CS/PVA film. To preparation of CS/PVA/Ag film, after the formation of the desired CS/PVA film, Ag NPs were simultaneously synthesized and deposited on the surface of the CS/PVA film using the LAA method with a fiber laser (1064 nm, 30 W). The LAA process was done continuously for 15 min. Finally, the film was dried at room temperature.

Results and Discussion

Antibacterial activity was investigated in laboratory condition by placing pieces of film measuring 8×8mm on muller_hinton agar medium inoculated with Escericha Coli. Antibacterial activity was seen in sample B against E.Coli compared to A sample.

Fig. 1. Zone inhibition of CS/PVA discs (A) and CS/PVA/Ag discs (B) in petri plates with culture of E. coli.

References

1. Alvarez, M. F. 2000. Review: Active food packaging. Food Science and Technology International, 6(2), 97–108.

2. Abedi-Firoozjah, Reza, et al. PVA/starch films: An updated review of their preparation, characterization, and diverse applications in the food industry. Polymer testing, 2023, 118: ۱۰۷۹۰۳.

The 30th Iranian Seminar of Organic Chemistry
February 7-9, 2025, Iran University of Science and Technology, Tehran, Iran

Synthesis of naproxen

Mansureh Hesernavi[a], Yaghoub Sarrafi*[a] Mohammad Eghtedari[b]

[a]*Department of Organic Chemistry, Faculty of Chemistry, University of Mazandaran, Babolsar, Iran.*

[b]*Chemistry and Chemical Engineering Research Center of Iran, Tehran, Iran*

Keyword: Naproxen, Nonsteroidal anti-inflammatory Drug (NSAID),

Non-steroidal anti-inflammatory drugs (NSAIDs) are among the most widely used medical drugs. These drugs cause cyclooxygenase and have three important features: reduction, pain relief, and fever reduction. This group is anti-inflammatory in high doses. NSAIDs are suitable because they are non-narcotic and do not cause side effects1.Naproxen is one of the strongest and best drugs this family. drug (S-naproxen) was first synthesized by Syntex company starting from 2-naphthol molecule2. Naproxen is one of the imported drugs of the country. It is used to relieve pain and inflammatory diseases such as rheumatism and fever3. In our current work, 2-acetyl-6-methoxynaphthalene was prepared as a precursor for the synthesis of naproxen in the Friedel-Crafts reaction.

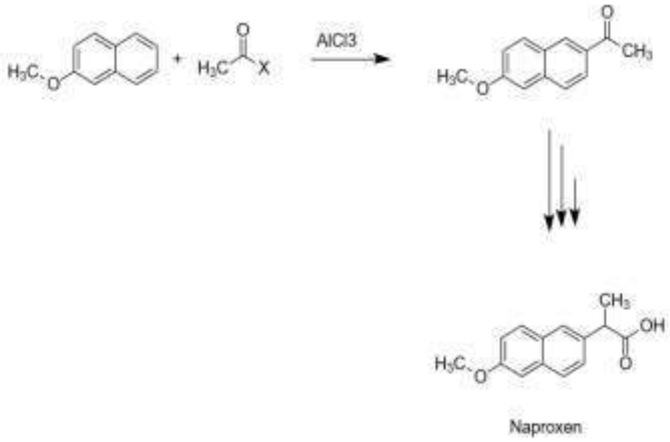

Scheme: Naproxen synthesis starting from 2-methoxynaphthalene molecule

References

1. Raauf, A. M., Raauf, S. S., & Abed, N. K. (2019). Non-Steroidal Anti-inflammatory Drugs (NSAIDs): Synthesis of Ibuprofen, Naproxen and Nabumetone. Al Mustansiriyah Journal of Pharmaceutical Sciences, 19(3), 19-27.

2. Harrington, P. J., & Lodewijk, E. (1997). Twenty years of naproxen technology. Organic Process Research & Development, 1(1), 72-76.

3. Kamaruddin, A. H., Uzir, M. H., Gonawan, F. N., & Lau, S. Y. (2015). Dynamic Enzymatic Kinetic Resolution of NSAIDS. Advances in Bioprocess Technology, 317-355.

The synthesis of arylidene isatin-hydrazone as a chemosensor

Zahra Panahande*, Ghodsi Mohammadi Ziarani

Department of Organic Chemistry, Faculty of Chemistry, Alzahra University, Tehran, Iran

Keywords: Multicomponent reaction, Nanocatalyst, Chemosensor, Fluorescence spectroscopy, Hg^{2+}

Introduction

Similar to carbonyl compounds, hydrazones can take part in metal reactions, free radical reactions, and cycloaddition reactions. Hydrazone derivatives that have the functional group -CH=N-NH- are easy to manufacture and show promise as sensors. Among its many forms, mercury is a heavy metal that can be found in salts, ions, and organic-inorganic complexes. Because of its special characteristics, which include its extreme biological toxicity, excellent water solubility, and permanence, this element poses a risk to the nervous system and endocrine organs. Exposure to mercury ions (Hg^{2+}) for an extended period, even at extremely low concentrations, can impair brain processes like vision and movement [1-3].

Material

All materials and solvents were grade-quality and purchased commercially. Fluorescence diagrams were composed using a Cary Eclipse fluorescent spectrophotometer.

The synthesis of 4-fluorobenzaldehyde-N-(2-oxo-1,2-dihydro-3H-indole-3-indole-3-ylidene)hydrazone

Arylidene isatin-hydrazone was synthesized through the reaction of isatin (1 mmol), hydrazine hydrate 80% (5 mL), and 4-fluorobenzaldehyde (1 mmol) using nanocatalyst (0.02 g) under reflux conditions. After the completion of the reaction (detected by TLC), the reaction mixture was filtered. The resulting solid was dissolved in EtOH and filtered to remove the insoluble nanocatalyst, to afford the pure product (Scheme 1).

Result and Discussion

Arylidene isatin-hydrazone was synthesized through the reaction of isatin-hydrazone and 4-fluorobenzaldehyde in the presence of a nanocatalyst under reflux conditions. After purification, arylidene isatin-hydrazone was gained and it was characterized using various techniques (Scheme 1).

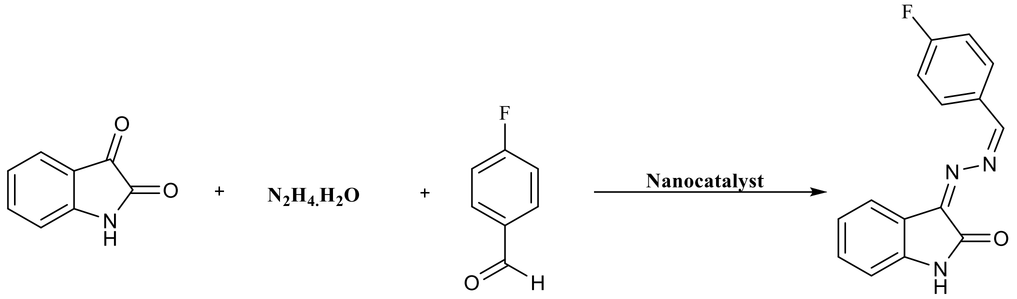

1 2 3 4

Scheme 1. The synthesis of arylidene isatin-hydrazone

Fluorescence study for arylidene isatin-hydrazone

The sensing ability of arylidene isatin-hydrazone (10^{-3} M, 2.5 mL) was investigated in the presence of various cations such as K^+, Ca^{2+}, Na^+, Cu^{2+}, Zn^{2+}, Cr^{3+}, Fe^{3+}, Mn^{2+}, Co^{2+}, Al^{3+}, Pb^{2+}, Ag^+, Cd^{2+}, Ni^{2+}, Hg^{2+}, and Mg^{2+}. Upon the addition of 200 µL metal ions, only when Hg^{2+} was added, the fluorescence intensity was changed, while the other metal ions presented a weak fluorescent emission intensity.

References:

[1] W. Anbu Durai, A. Ramu, A. Dhakshinamoorthy, A Visual and Ratiometric Chemosensor Using Thiophene Functionalized Hydrazone for the Selective Sensing of Pb^{2+} and F^- Ions, J Fluoresc, 31 (2021) 465-474. http://doi.org/10.1007/s10895-020-02673-1.
[2] A.C. Sotolongo, M.M. Messina, F.J. Ibañez, R.G. Wuilloud, Hybrid ionic liquid-3D graphene-Ni foam for on-line preconcentration and separation of Hg species in water with atomic fluorescence spectrometry detection, Talanta, 210 (2020) 120614. https://doi.org/10.1016/j.talanta.2019.120614.
[3] D. Chang, L. Li, L. Shi, Y. Yang, Hg^{2+} detection, pH sensing and cell imaging based on bright blue-fluorescent N-doped carbon dots, Analyst, 145 (2020) 8030-8037. http://doi.org/10.1039/D0AN01487G.

The 30th Iranian Seminar of Organic Chemistry
February 7-9, 2025, Iran University of Science and Technology, Tehran, Iran

The synthesis of a chemosensor imidazole-based for detecting Ag^+ ions

Mohammad Goodarzi*, Ghodsi Mohammadi Ziarani, Zahra Panahande

Department of Organic Chemistry, Faculty of Chemistry, Alzahra University, Tehran, Iran

Keywords: Imidazole, Nitration, Chemosensor, Fluorescence spectroscopy, Ag^+

Introduction

The one-ring combination between electron-deficient and electron-rich characteristics is an attractive feature common to the imidazole heteroaromatic ring. The 5-membered ring has two nitrogen atoms, one of which is an electron donor and the other is an electron acceptor [1]. Nowadays, imidazole-based chemosensors have attracted much attention due to their remarkable biological activity, as they can show greater affinity, selectivity, and hydrogen bond formation with ions, which causes their detection [2, 3]. The design and synthesis of chemosensors, which have characteristics such as high efficiency, sensitivity, select ability, and cost-effectiveness for the detection of heavy metal ions and other environmental pollutants, are in high demand [4]. In the past decades, Ag^+ has been used as one of these metal ions with properties such as malleability, flexibility, and high electrical and thermal conductivity in various fields such as photographic film processing and electroplating. Ag metal is not dangerous for humans, but its salts are poisonous. Also, Ag^+ can bind with imidazole and cause adverse effects on human health. fluorescent chemosensors compared to traditional methods have distinct advantages for the detection of converted metal ions [5, 6].

Material

All materials and solvents were purchased commercially and in grade quality. Also, fluorescence diagrams were composed with a Cary Eclipse fluorescent spectrophotometer.

Synthesis of 2-methyl-4(5)-nitroimidazole

In a flask, distilled H_2O (1 mL) and concentrated H_2SO_4 (0.2 mL, 3 mmol) were added and stirred. Then 2-methylimidazole (0.82 g, 1 mmol) and $NaNO_3$ (0.2 g, 1 mmol) were added to the reaction mixture. NH_3 was added to the obtained solution, and a white precipitate was obtained. Finally, the precipitate obtained was washed with distilled H_2O and dried.

Result and discussion

Nitration of 2-methylimidazole

2-methylimidazole was nitrated using H_2SO_4 under controlled temperature conditions in the presence of $NaNO_3$. After purification, 2-methyl-4(5)-nitroimidazole was gained as white crystals and it was characterized using different methods (Scheme 1).

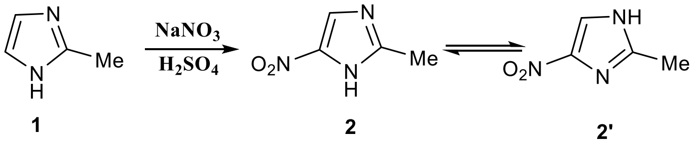

Scheme 1. Nitration of 2-methylimidazole

Fluorescence study for 2-methyl-4(5)-nitroimidazole

The sensing activity of 2-methyl-4(5)-nitroimidazole (10^{-3} M, 2.5 mL) in H_2O was studied in the presence of various cations such as K^+, Al^{3+}, Cd^{2+}, Na^+, Cr^{3+}, Ag^+, Mn^{2+}, Pb^{2+}, Mg^{2+}, Co^{2+},

Hg^{2+}, Zn^{2+}, Ni^{2+}, Ca^{2+}, and Cu^{2+}. Upon the addition of 200 μL cations, when Ag^{+} was added, the fluorescence intensity was changed.

References

[1]. Al Sharif, O. F.; Nhari, L. M.; El-Shishtawy, R. M.; Asiri, A. M. Imidazole-based fluorophores: Synthesis and applications. *Mater. Today. Chem.* **2023**, *29*, 101453. DOI: https://doi.org/10.1016/j.mtchem.2023.101453.

[2]. Batool, M.; Afzal, Z.; Saleem Khan, I.; Solangi, A. R. Exploring the Mechanism of Anionic Chemosensing by Imidazoles: A Review. *Crit. Rev. Anal. Chem.* **2023**, 1-9. DOI: https://doi.org/10.1080/10408347.2023.2210680.

[3]. Bag, R.; Sikdar, Y.; Sahu, S.; Islam, M. M.; Mandal, S.; Goswami, S. Benzimidazole-acid hydrazide Schiff–Mannich combo ligands enable the nano-molar detection of Zn^{2+} in semi-aqueous media, HuH-7 cells, and plants via a fluorescence turn-on mode. *New. J. Chem.* **2022**, 46 (33), 16161-16171. DOI: https://doi.org/10.1039/D2NJ02875A.

[4]. Khan, E.; Khan, S.; Gul, Z.; Muhammad, M. Medicinal importance, coordination chemistry with selected metals (Cu, Ag, Au) and chemosensing of thiourea derivatives. A review. *Crit. Rev. Anal. Chem.* **2021**, *51* (8), 812-834. DOI: https://doi.org/10.1080/10408347.2020.1777523.

[5]. Prabakaran, G.; Narmatha, G.; Velmurugan, K.; Basith, A.; Karthick, R.; Velraj, G.; Kumar, R. S.; Nandhakumar, R. Imidazole derived PET based reversible dual fluorescent chemosensor: Sensing of zinc and carbonate ions and their usage on real samples and live cells. *J. Mol. Struct.* **2024**, *1295*, 136684. DOI: https://doi.org/10.1016/j.molstruc.2023.136684.

[6]. Renhart, P.; Summer, F.; Grun, F.; Posch, C.; Eder, A. The tribological performance of silver in aircraft turbine load cases. *Tribol. Int.* **2021**, *163*, 107184. DOI: https://doi.org/10.1016/j.triboint.2021.107184.

[7]. Xu, K.; Perez-Rafols, C.; Cuartero, M.; Crespo, G. A. Electrochemical detection of trace silver. *Electrochim. Acta.* **2021**, *374*, 137929. DOI: https://doi.org/10.1016/j.electacta.2021.137929.

The 30th Iranian Seminar of Organic Chemistry
February 7-9, 2025, Iran University of Science and Technology, Tehran, Iran

Synthesis of Spiro indeno[1,2b]pyrido-[2,3d]pyrimidine-5,3`-indoline in the presence of nanocatalyst and its application as a chemosensor to detect Hg^{2+}

Shiva Shaabani*, Ghodsi Mohammadi Ziarani, Zahra Panahande

Department of Organic Chemistry, Faculty of Chemistry, Alzahra University, Tehran, Iran

Keywords: Multicomponent reaction, Nanocatalyst, Chemosensor, UV-Vis spectroscopy, Hg^{2+}

Introduction

A multicomponent reaction is a group of chemical reactions in which more than two raw materials, at least three reactants, react with each other to produce one product.

Multicomponent reactions (MCRs) have appeared as suitable and useful tools in organic reactions because they allow the reactions to make several chemical bonds in one sequence without labor-consuming reaction condition optimization, for this reason reducing waste production, cost, and labor consumption. The unique feature of MCR includes the synthesis of highly effective molecules for various fields such as chemosensors[1-3]. Toxic ions in the environment have caused global environmental and biological health problems due to their toxicity and stability. The presence of heavy metal ions in water can have severe consequences for both the ecosystem and public health. Among these heavy metals, Hg^{2+} is the most hazardous pollutant that is known. In particular, the accumulation of Hg^{2+} in the human body, even at a very low concentration, can cause a different kind of disease, namely digestive, kidney, and neurological illness. So, the development of highly sensitive detection methods is essential, and optical sensors offer significant advantages, such as portability, easy usage, and flexibility, making them important tools in this way [4, 5].

Material

All materials and solvents were grade quality and purchased commercially. The UV-vis absorption spectra were afforded from an Analytic Jena Specord S600 Spectrophotometer.

Synthesis of spiro indeno[1,2b]pyrido-[2,3d]pyrimidine-5,3`-indoline (4)

Spiro indeno[1,2b]pyrido-[2,3d] pyrimidine-5,3`-indoline was prepared through the reaction of indandione 1 (1 mmol), isatin derivatives 2 (1 mmol), and 6-amino uracil 3 (1 mmol) using nanocatalyst. Completion of the reaction was detected by using TLC, ethyl acetate: n-hexane (1:1). Then, the nano-catalyst was filtrated, and an orange precipitate appeared with 98% yield.

Result and discussion

Preparation of spiro indeno[1,2b]pyrido-[2,3d]pyrimidine-5,3`-indoline

Spiro indeno[1,2b]pyrido-[2,3d]pyrimidine-5,3`-indoline was prepared through the reaction of indandione, isatin derivatives, and 6-amino uracil using a nanocatalyst. After purification, the aim product was characterized using various techniques (Scheme 1).

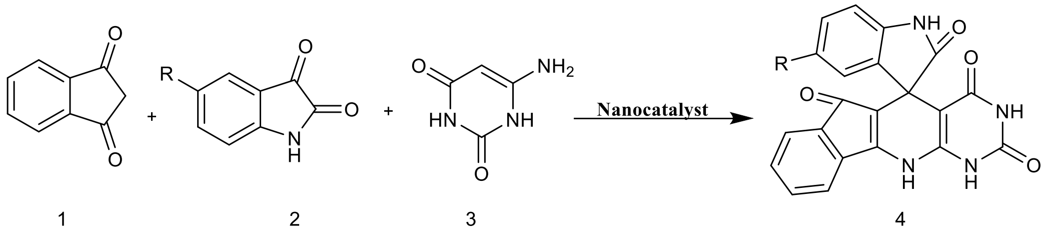

Scheme 1. The Synthesis of spiro indeno[1,2b]pyrido-[2,3d] pyrimidine-5,3`-indoline

Fluorescence study for compound 4

The sensing ability of compound 4, 2.5 mL of this chemosensor 4 (10^{-3} M) in EtOH in the presence of various cations Cd^{2+}, Cr^{3+}, Al^{3+}, Mn^{2+}, Hg^{2+}, Pb^{2+}, Cu^{2+}, Ni^{2+}, Co^{2+}, Fe^{2+}, Fe^{3+}, Zn^{2+}, Mg^{2+}, Ca^{2+}, Ag^{2+}, k^+ and Na^+ was studied via UV-Vis spectroscopy. In UV-Vis absorbance, when the Hg^{2+} solution was added, it created a considerable change. This change in absorbance shows that this compound can be applied with selectivity and sensitivity to detect Hg^{2+} ions.

References

[1] Preeti, K.N. Singh, Metal-free multicomponent reactions: a benign access to monocyclic six-membered N-heterocycles, Org. Biomol. Chem., 19 (2021) 2622-2657. http://doi.org/10.1039/D1OB00145K.

[2] H.A. Younus, M. Al-Rashida, A. Hameed, M. Uroos, U. Salar, S. Rana, K.M. Khan, Multicomponent reactions (MCR) in medicinal chemistry: a patent review (2010-2020), Opin. Ther. Pat., 31 (2021) 267-289. http://doi.org/10.1080/13543776.2021.1858797.

[3] G. Mohammadi Ziarani, Z. Panahande, A. Badiei, Synthesis of spiro-oxindole-based chemosensor for detection of Hg^{2+} ions using SBA-Pr-N-IS-Bu-SO_3H, Inorg. Chem. Commun., 164 (2024) 112398. https://doi.org/10.1016/j.inoche.2024.112398.

[4] A. Bashir, T. Manzoor, L.A. Malik, A. Qureashi, A.H. Pandith, Enhanced and selective adsorption of Zn (II), Pb (II), Cd (II), and Hg (II) ions by a dumbbell-and flower-shaped potato starch phosphate polymer: a combined experimental and DFT calculation study, ACS. Omega., 5 (2020) 4853-4867. https://doi.org/10.1021/acsomega.9b03607.

[5] P. Mohanty, P.P. Dash, S. Naik, R. Behura, M. Mishra, H. Sahoo, S.K. Sahoo, A.K. Barick, B.R. Jali, A thiourea-based fluorescent turn-on chemosensor for detecting Hg^{2+}, Ag^{+} and Au^{3+} in aqueous medium, J. Photochem. Photobiol. A., 437 (2023) 114491. https://doi.org/10.1016/j.jphotochem.2022.114491.

The 30th Iranian Seminar of Organic Chemistry
February 7-9, 2025, Iran University of Science and Technology, Tehran, Iran

Development of MOF-MXene composite for the removal of *P*-nitrophenol

Roya Evazi 1[a], Ali Badihi, Mohammad Reza Naimi-Jamal 2*[a]

Affiliations: Department of Chemistry, Iran University of Science and Technology, 16846-13114 Tehran, Iran

Keyword: Adsorption, Methylene blue, MXene, NH2-MIL-101(Al), MXene@NH2-MIL-101(Al), Composite

ABSTRACT: MXene has a multilayer structure, which can be peeled and layered into single or multilayer nanosheets, and it possesses multiple functional groups that can be easily modified. NH2-MIL-101(Al), a kind of metal−organic framework material, was synthesized by the solvent hydrothermal method using aluminum ion as the center metal and 2-Aminoterephthalic acid as the organic ligand. In this paper, NH2-MIL-101(Al) was grown in situ on Ti3C2Tx MXene to synthesize the MXene@NH2-MIL-101(Al) composite, which

combined the advantages of both MXene and NH2-MIL-101(Al). newly synthesized adsorbent was characterized by utilizing powder X-Ray diffraction analysis, Fouriertransform infrared spectroscopy, and scanning electron microscopy. Exceptional adsorption properties of MXene@NH2-MIL-101(Al) composite were verified by adsorption of methylene blue (MB). Adsorption process was studied by applying different optimization parameters such as pH, contact time, adsorbent dose, and initial concentration of MB. Results showed that MXene@MOF composite have best adsorption performance with removal rate of 97% for MB. two kinetic models pseudo-first order, pseudo-second order were applied, and results showed that kinetic process was well described by pseudo-second-order kinetic model for MB. two different isotherm models are used such as Langmuir, Freundlich, the study shows that the Langmuir isotherm model describes well for the adsorption of MB.

Scheme: center

References: Times New Roman, Font size: 11, Align left, Arabic numeral

---

The 30th Iranian Seminar of Organic Chemistry
February 7-9, 2025, Iran University of Science and Technology, Tehran, Iran

Fabrication of a magnetic Mn (II) cross-linked chitosan-amine/glutaraldehyde nanocomposite for the rapid degradation of dyes and aerobic selective oxidation of ethylbenzene

Behzad Bornas, Alireza Faraji *, Fatemeh Ashouri

aDepartment of Nano Chemistry, Faculty of Pharmaceutical Chemistry, Tehran Medical Sciences, Islamic Azad University, Tehran, IranbDepartment of Organic Chemistry, Faculty of Pharmaceutical Chemistry, Tehran Medical Sciences, Islamic Azad University, Tehran, Iran. Behzadbornas8@gmail.com, alireza_ch57@yahoo.com

Keyword:

Degradation, Aerobic oxidation, Advanced oxidation process, Water treatment, Methyl orange

Owing to the great demand for using sustainable, renewable, and widely available materials in catalytic systems for the conversion of waste/toxic material to high value-added and harmless products, biopolymers derived from natural sources have demonstrated great promise as an alternative to state-of-the-art materials that suffer from high costs and limitations. These have encouraged us to design and fabricate a new super magnetization of Mn–Fe3O4–SiO2/amine-glutaraldehyde/chitosan bio-composite (MIOSC-N-et-NH2@CS-Mn) for advanced/aerobic

oxidation process. The morphological and chemical characterization of the as-prepared magnetic bio-composite was assessed using ICP-OES, DR UV-vis, BET, FT-IR, XRD, FE-SEM, HR-TEM, EDS, and XPS techniques. The PMS + MIOSC-N-et-NH2@CS-Mn system was capable of degrading methylene orange (98.9% of removal efficiency) and selectively oxidizing ethylbenzene to acetophenone (conversion 93.70%, selectivity 95.10% and TOF 214.1 (103 h−1) within 8.0 min and 5.0 h, respectively. Moreover, MO was efficiently mineralized (TOC removal of ~56.61) by MIOSC-N-et-NH2@CS-Mn with 60.4%, 5.20, 0.03 and 86.02% of the synergistic index, reaction stoichiometric efficiency, specific oxidant efficiency, and oxidant utilization ratio in wide pH ranges, respectively. An understanding of its vital parameters and relationship of catalytic activity with structural, environmental factors, leaching/heterogenicity test, long-term stability, inhibitory effect of anions in water matrix, economic study and response surface method (RSM) were evaluated in detail. Overall, the prepared catalyst could be employed as an environmentally friendly and low-cost candidate for the enhanced activation of PMS/O2 as an oxidant. Additionally, MIOSC-N-et-NH2@CS-Mn exhibited great stability, high recovery efficiency, and low metal leaching, which eliminated the harsh condition reaction and supplied practical application performance for water purification and selective aerobic oxidation of organic compounds (Scheme 1).

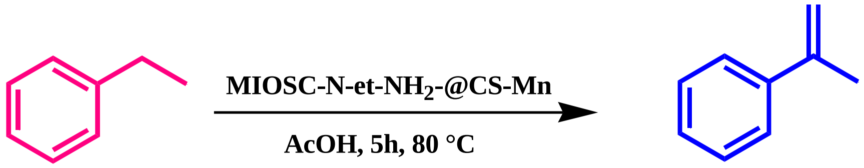

Scheme 1. Synthesis of derivatives of Acetophenone

References:

۴- Habibi, D., Faraji, A. R., Arshadi, M., Heydari, S., & Gil, A. 2013. Efficient catalytic systems based on cobalt for oxidation of ethylbenzene, cyclohexene and oximes in the presence of N-hydroxyphthalimide. Appl. Catal., Vol. 466: 282-292.

۵- Habibi, D., Faraji, A. R., Arshadi, M., Veisi, H., & Gil, A. **2014**. *Manganese nanocatalyst and N-hydroxyphthalimide as an efficient catalytic system for selective oxidation of ethylbenzene, cyclohexene and oximes under aerobic condition.* J. Mol. Catal. A Chem., Vol. 382: 41-54.

The 30th Iranian Seminar of Organic Chemistry
February 7-9, 2025, Iran University of Science and Technology, Tehran, Iran

Triphenylamine-Assisted Fabrication of Copper (I) Oxide Nanoparticles: A Facile and Low Cost Synthesis Route

Omid Azizian-Shermeh, Ali Reza Modarresi-Alam *, Ebrahim Mollashahi, Sahar Shabzendedar

Organic and Polymer Research Laboratory, Department of Chemistry, Faculty of Sciences, University of Sistan and Baluchestan, Zahedan, Iran

Nanomaterials (NMs) refers to particles size less than 100 nm, which have unique properties and extensive applications as drug delivery devices, antimicrobial agents, catalysts and electrical conductors [1]. Among all NMs, interest in copper (I) oxide (Cu_2O) NPs with specific size and shape stems from their optical and electronic properties and beneficial antimicrobial properties [2]. This present study is the first report of synthesis of Cu_2O NPs with triphenylamine (TPA) assisted. For the synthesis of Cu_2O NPs, Cu $(ClO_4)_2.6H_2O$ and TPA were dissolved in acetonitrile (MeCN) [3]. After 12 hours, K_2CO_3 and double distilled water were added to the mixture. After filtration, washing, and drying, precipitation of Cu_2O NPs remained. The synthesized Cu_2O NPs was characterized by different techniques including UV–Vis spectroscopy, XRD, FT-IR spectroscopy, TEM, SEM, EDX, and AFM. The XRD pattern and TEM analysis revealed spherical and cavity, stable, and uniform Cu_2O NPs with the range particle size of about 3-33 nm. The results showed that TPA has the ability to synthesize Cu_2O NPs with uniform morphology and small size with many applications.

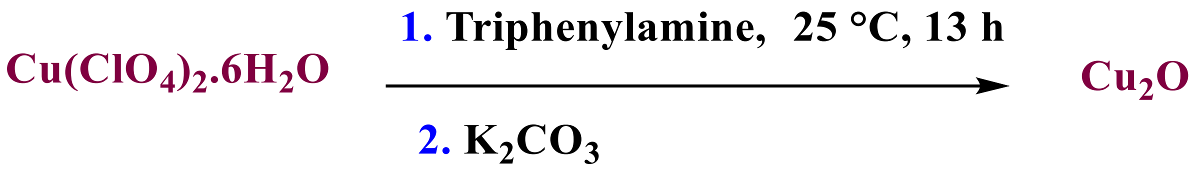

Scheme. Synthesis of Cu_2O nanoparticles in the presence of triphenylamine.

Keyword: Triphenylamine, Copper (I) Oxide Nanoparticles, XRD, TEM, SEM, AFM

References:

[1] Azizian-Shermeh O., Einali E., Ghasemi A. Rapid biologically one-step synthesis of stable bioactive silver nanoparticles using Osage orange (*Maclura pomifera*) leaf extract and their antimicrobial activities, Adv. Powder Technol, 28, (2017) 3164–3171.
[2] Mallik M., Monia S., Gupta M., Ghosh A., Toppo M.P., Roy H. Synthesis and characterization of Cu_2O nanoparticles, J. Alloys Compd, 829, (2020), 154623.
[3] Sreenath, K., Suneesh, Ch.V. Kumar, V.K.R., Gopidas K.R. Cu (II)-Mediated Generation of Triarylamine Radical Cations and Their Dimerization. An Easy Route to Tetraarylbenzidines, J. Org. Chem. (2008), 73, 3245-3251

The 30th Iranian Seminar of Organic Chemistry
February 7-9, 2025, Iran University of Science and Technology, Tehran, Iran

Synthesis and Characterization of Novel Superparamagnetic Nanocomposite of Poly (N-(sulfophenyl) aniline) and Fe_3O_4 for the Photovoltaic Activity in fabrication of New Generation Magnetic Solar Cells

Omid Azizian-Shermeh, Ali Reza Modarresi-Alam*, Ebrahim Mollashahi, Sahar Shabzendedar

Organic and Polymer Research Laboratory, Department of Chemistry, Faculty of Sciences, University of Sistan and Baluchestan, Zahedan, Iran

Research indicates that the use of an inexpensive and efficient semiconductor can have an important effect on the development of a hybrid solar cell. Moreover, the function of solar cells has also had a noticeable increase by using nanocomposites recently [1]. The poly (N-(sulfophenyl) aniline) (PSA) [2] and superparamagnetic nanocomposite of it (SNCPSA) were synthesized by a simple room temperature solid-state mechanochemical reaction. For this aim; $FeCl_3.6H_2O$ was mixed with diphenylamine-4-sulfonic acid barium salt and grinding for 1 h. The mixture was divided into two equal parts. The first part was filtration by a centrifuge and washed (workup) with H_2O and HCl. After drying, PSA was obtained [2]. The second part was washed (workup) with H_2O and NaOH to prepare SNCPSA similar to our previous reports on the fabrication of **“New Generation Magnetic Solar Cells”** [3,4]. After drying, the superparamagnetic nanocomposite of poly (N-(sulfophenyl) aniline) (SNCPSA) was obtained. The products characterized and studied with cyclic voltammetry (CV), UV-Vis and FT-IR spectroscopy and they were confirmed the successfully synthesis of PSA and SNCPSA. The photovoltaic properties of the cells have been evaluated with a solar simulator and the I-V characteristics and power conversion efficiency (PCE) of the samples were examined and discussed. The PCE values for the 2 samples were found to be in the range of 0.15–0.54 %. Results showed that, this kind of conjugated polymer should be a promising material in the application of polymer solar cells.

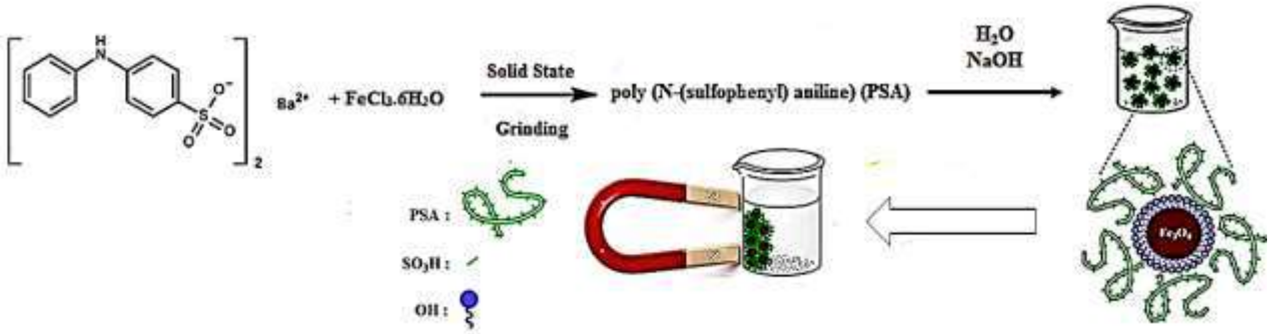

Scheme. Synthesis of PSA and SNCPSA

Keyword: Diphenylamine-4-Sulfonic Acid Barium Salt, Photovoltaic Activity, Superparamagnetic Nanocomposite, Poly (N-(sulfophenyl) aniline)

References:

[1] Socol M., Preda N. Hybrid nanocomposite thin films for photovoltaic applications: a review, Nanomaterials, 11, (2021), 1117.

[2] Yarmohamadi-Vasel, M., Modarresi-Alam, A.R., Noroozifar, M., Shabzendedar, S., Gholizadeh, S., Valadbeigi, E. Mechanochemical synthesis and characterization of poly [(aniline-*co*-*N*-(4-sulfophenyl) aniline] nanofibers and its nanocomposite with titanium dioxide

nanoparticles and study of their efficiency in hybrid solar cell, Synthetic Metals, 309, (2024), ۱۱۷۷۶۷.

[3] F. Sadegh, A. R. Modarresi-Alam, M. Noroozifar, and Kagan Kerman, A facile and green synthesis of superparamagnetic Fe3O4@PANI nanocomposite with a core–shell structure to increase of triplet state population and efficiency of the solar cells, Journal of Environmental Chemical Engineering, (2021), 9, 104942.

[4] Shabzendedar S., Modarresi-Alam A.R, Noroozifar., Kerman K., Core-shell nanocomposite of superparamagnetic Fe_3O_4 nanoparticles with poly(m-aminobenzenesulfonic acid) for polymer solar cells, Organic Electronics, (2020), 77, 105462.

The 30th Iranian Seminar of Organic Chemistry
February 7-9, 2025, Iran University of Science and Technology, Tehran, Iran

Innovations in Fabrication of New Generation Photovoltaics cells and Batteries: Polyaniline-Enhanced Polymer Cells Focusing on the Transitions from Fossil Fuels to Renewable Energy Sources

Ali Reza Modarresi-Alam[1,*]
Organic and Polymer Research Laboratory, Department of Chemistry, Faculty of Science, University of Sistan and Baluchestan, Zahedan, Iran.
**E-mail:* modaresi@chem.usb.ac.ir

Keywords: Polyanilines, Superparamagnetic Nanocomposites, Singlet Fission, New Generation Photovoltaics cells and Batteries.

Nowadays, the use of renewable energies is very important to provide the required energies of human life and solar cells are one of the most widely used means of using solar energy as well as self-charging batteries for energy storage. So, in recent years many studies have been done in this field to increase efficiency of solar cells and capacities of these batteries. According to our recent papers, superparamagnetic nanocomposites of polyaniline are very effective in increasing solar cell efficiency (η) and can improve their performance. Thus, studying and construction of new superparamagnetic solar cells using novel homopolymers, copolymers or nanocomposites of Fe_3O_4 and aniline, and its derivatives, are important.

The prepared solar cells in this discovery **can be turned into new self-charging batteries with minor modifications that can open a new window for energy storage.**

These devices have further advantages, for example the use of a new flexible transparent electrode made of PANI, easy and green overall processing conditions, lower fabrication cost, very simple cell structure and high material stability, which is very significant in the fabrication of solar cells and related batteries.

Furthermore, magnetic property of the cells can be used for shift of cells in various places automatically and fix them without using glue and in especial frame work.

In this lecture, I wish to describe the development of our recent works on the application of the novel superparamagnetic core-shell nanocomposites of PANI derivatives and Fe_3O_4 nanoparticles in ***"the new generation magnetic solar cells and self-charging batteries"***. It can be confirmed by different mechanisms such as spin-orbit coupling and singlet fission (SF) which can increase the triplet state of excitons and/or trimerons formation. The other factors influencing the source of this great success is explained.

Referances:

١) Sahar Shabzendedar, Ali Reza Modarresi-Alam, Farideh Paymozd, Mazaher Yarmohamadi-Vasel, Fariba Kaedi, Yuning Li, Solar cells containing two novel superparamagnetic nanocomposites of Fe3O4-TiO2-poly(m-aminobenzenesulfonic acid, Synthetic Metals, 295, 2023, 117335, https://doi.org/10.1016/j.synthmet.2023.117335.

٢) Fatemeh Sadegh, Ali Reza Modarresi-Alam, Yuning Li, Improving the efficiency of polymer solar cell by using a new magnetic nanocomposite of polyaniline-Fe_3O_4-TiO_2, Nano-Structures&Nano-Objects, **2023, 36, 101033 (1-13). doi.org/10.1016/j.nanoso.2023.101033.**

٣) Sahar Shabzendedar, Abdolhamid Bahrpeyma, Amirreza Kheirkhah, Ali Reza Modarresi-Alam, Fatemeh Sadegh, Study on the synthesis, properties, and efficiency of two new superparamagnetic nanocomposites of poly(m-aminobenzenesulfonic acid) and TiO_2 in P-N junction hybrid solar cells, Polymer Bulletin, 2022, 79, 3395-3418, https://doi.org/10.1007/s00289-021-03986-2.

٤) Fatemeh Sadegh, Ali Reza Modarresi-Alam, Negar Sadegh, Abdolhamid Bahrpeyma, Sahar Shabzendedar, Kagan Kerman, and Meissam Noroozifar, Simple and green route for fabrication of a nanostructured of the graphene-Fe_3O_4@PANI for the photovoltaic activity, Electrochimica Acta, 2021, 399, 139327, https://doi.org/10.1016/j.electacta.2021.139327.

٥) F. Sadegh, A. R. Modarresi-Alam, M. Noroozifar, and Kagan Kerman, A facile and green synthesis of superparamagnetic Fe3O4@PANI nanocomposite with a core–shell structure to increase of triplet state population and efficiency of the solar cells, Journal of Environmental Chemical Engineering, 2021, 9, 104942. https://doi.org/10.1016/j.jece.2020.104942.

٦) Sahar Shabzendedar, Ali Reza Modarresi-Alam, Meissam Noroozifar, Kagan Kerman, Core-shell nanocomposite of superparamagnetic Fe_3O_4 nanoparticles with poly(m-aminobenzenesulfonic acid) for polymer solar cells, Organic Electronics, 2020, 77, 105462, https://doi.org/10.1016/j.orgel.2019.105462.

The 30th Iranian Seminar of Organic Chemistry
February 7-9, 2025, Iran University of Science and Technology, Tehran, Iran

Synthesis & characterization of aminated polyhedral oligomeric silsesquioxane (POSS-NH_2) nanoparticles

Authors: Farzaneh Sadrykia[a] (representing author), Peyman Najafi Moghadam *[a] (corresponding author), Hamed Hamishehkar [b]

Affiliations:

[a] *Department of Organic Chemistry, Faculty of Chemistry, Urmia University, Urmia, Iran*

[b] *Drug Applied Research Center, Tabriz University of Medical Sciences, Tabriz, Iran*

Keyword: 3-aminopropyl triethoxy silane (APTES), polyhedral oligomeric silsesquioxane, aminated POSS

Introduction

Incompletely condensed polyhedral oligomeric silsesquioxanes (POSS) are nano sized particles (1-3 nanometer) with this formula: $(RSiO_{1.5})_n$. Fully-condensed silsesquioxanes or incompletely-condensed silsesquioxanes can be made with different methodologies [1].

Method

The nano sized heptaphenyltricycloheptasiloxane trisodium silanolate $[Na_3O_{12}Si_7(C_6H_5)_7]$ molecules (HPSTS molecules) were synthesized by hydrolysis and condensation method [2]. In this method incompletely condensed POSS molecules were synthesized by using phenyltrimetoxysilane $[C_6H_5Si(OCH_3)_3]$ and sodium hydroxide (NaOH) in THF solution. Then at second step, POSS-NH_2 nanoparticles were synthesized. Briefly, 1 g of HPSTS was dissolved in a flask containing 150 ml of dry toluene solvent. Also, 467µl of APTES reagent was dissolved in 5 ml of dry toluene and added dropwise to the flask containing the HSPST solution. Then, the reaction system was refluxed for 8 hours in a magnetic stirrer at 90 ° C. Finally, all the solvent and volatiles were removed by rotary evaporation. The resulting product was washed with water and then with acetonitrile. Then, it was placed in an oven at 60 ° C for 24 hours to dry (scheme 1).

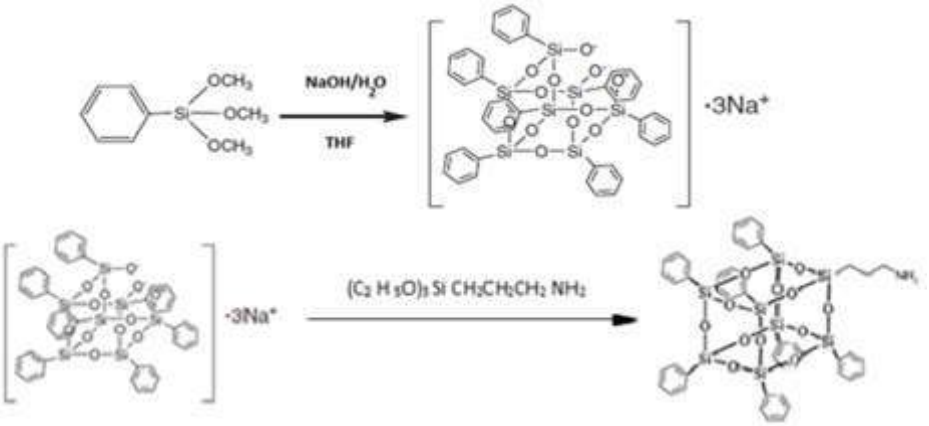

Scheme1. Synthesis of aminated POSS (POSS-NH2) nanoparticles

Results and Discussion

The FT-IR spectra of synthesized POSS-NH2 is shown in scheme 2. The strong peak at around 1130 cm -1 is related to Si-O-Si stretching vibration. The stretching vibration of phenyl groups appears at 1430 and 1597 cm^{-1}. Also, the peaks related to C-H stretching vibration of phenyl groups are shown at 3000-3100 cm $^{-1}$. The C-H vibration of propyl groups is appeared at 2800-2900 cm^{-1}. Also the stretching vibration of NH_2 at about 3360 is shown in this figure.

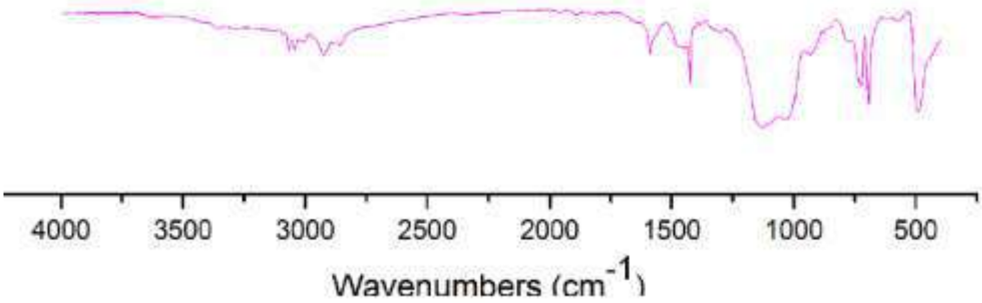

Scheme2. The FT-IR spectra of POSS-NH_2

References:

[1] Li G., Wang L., Ni H., Pittman C. U. (2001). Polyhedral oligomeric silsesquioxane (POSS) polymers and copolymers: A review. Journal of Inorganic and Organometallic Polymers, 11:123-154.

[2] Ohno K., Sugiyama S., Koh K., Tsujii Y., Fukuda T., Yamahiro M., Oikawa H., Yamamoto Y., Ootake N., Watanabe K. (2004). Living radical polymerization by polyhedral oligomeric silsesquioxane-holding initiators: Precision synthesis of tadpole-shaped organic/inorganic hybrid polymers. Macromolecules, 37(23):8517-8522.

The 30th Iranian Seminar of Organic Chemistry
February 7-9, 2025, Iran University of Science and Technology, Tehran, Iran

Times New Roman Bold, Font size: 14, Centre, Sentence case

Hamid Rashidianfar1[a], Adel Bahman 2[b] (Hamid Rashidianfar), Author 3*[c] (Hamid Rashidianfar)

1Payame Noor University, Mashhad, Iran - Department of Chemistry, Organic Chemistry

2University of Isfahan, Iran - Department of Chemistry

Abstract

Biofilm growth in industrial systems, including wastewater treatment plants, marine industries, and power plants, is a significant challenge that reduces equipment efficiency, increases maintenance costs, and poses environmental risks. This study investigates the properties, applications, and challenges of using polymeric and acrylic paints to prevent biofilm growth. Due to their chemical, mechanical, and environmental properties, these coatings are recognized as one of the most effective solutions for protecting industrial surfaces and enhancing system performance. This review analyzes credible scientific sources and examines the role of antimicrobial agents such as silver, copper, and zinc oxide nanoparticles in improving the efficiency of these coatings. Results show that the use of these coatings in various industries, especially under harsh environmental conditions, can prevent biofilm growth and extend the service life of equipment. However, challenges such as high production costs and the environmental impacts of chemical components require further research. Future perspectives in this field include the development of smart coatings, environmentally friendly formulations, and cost reduction strategies.

Keyword: Acrylic paints, polymeric coatings, biofilm, antimicrobial agents, industrial coatings, corrosion prevention, environmental management, nanotechnology.

1. Introduction

Biofilms are complex aggregations of microorganisms that adhere to surfaces and create a protective extracellular polymeric matrix. These structures cause significant problems in industrial environments, particularly in wastewater and industrial effluent systems [1, 2]. Such issues include reduced equipment efficiency, increased maintenance and repair costs, and health risks due to microbial growth. The high resistance of biofilms to disinfectants and environmental conditions presents serious challenges for their removal [2, 3].

One of the innovative and effective solutions to combat biofilm formation is the use of protective polymer-based coatings. Among these, acrylic paints have gained particular attention due to their unique properties, such as high chemical and mechanical resistance, optimal drying speed, and adhesion to diverse surfaces [4]. In addition to providing a physical protective layer, these paints can effectively prevent biofilm growth and spread through chemical modifications and the incorporation of antimicrobial agents [5].

Coating industrial surfaces with acrylic paints containing active nanoparticles, such as silver, copper, or zinc oxide, represents a significant advancement in inhibiting microbial growth. Nanoparticles, due to their antibacterial and antifungal properties, limit microbial growth through the release of active ions [6, 7]. Furthermore, advances in smart material technologies have enabled the design of coatings that activate under specific biological conditions, providing targeted responses [7].

In industrial wastewater systems, in addition to reducing biofilm growth, protecting surfaces from corrosion is also necessary. Acrylic paints, with their protective and environmentally friendly properties, are considered one of the best options for this application. Studies have shown that combining antimicrobial agents with water-resistant structures can significantly enhance the durability and performance of these coatings in industrial environments [8, 9].

This article aims to comprehensively review the application of polymeric and acrylic paints for coating industrial wastewater surfaces, analyzing their role in preventing biofilm growth and improving industrial system performance. Additionally, the benefits, challenges, and future prospects of this method are discussed to provide a foundation for further research in this field.

2. Methodology

This study was conducted as a review aimed at compiling and analyzing existing information about the use of polymeric and acrylic paints to prevent biofilm growth on industrial wastewater surfaces. The research process involved the following steps:

2.1 Literature Search

Relevant scientific sources were collected from reputable databases, including Google Scholar, ScienceDirect, PubMed, and Scopus. Searches were conducted using the following keywords:

Biofilm

Acrylic coatings

Polymer paints

Antimicrobial surfaces

Industrial wastewater management

2.2 Selection of Relevant Articles

Inclusion criteria: Published articles that provide information related to the application of polymeric paints in preventing biofilm growth.

Article types: Laboratory studies, previous review articles, and industrial reports.

2.3 Review and Data Extraction

Information was extracted from 42 selected articles on the following topics:

Physical and chemical properties of polymeric and acrylic paints.

Effectiveness of these coatings in preventing biofilm growth.

Advantages and limitations of using these paints in industrial environments.

2.4 Data Analysis and Synthesis

The extracted information was descriptively analyzed and categorized based on the main topics of the article, including the properties of acrylic paints, application challenges, and advancements in technology.

3. Scientific and Conceptual Background

Biofilm growth is one of the most significant challenges in industrial systems, particularly in wastewater management. Biofilms are clusters of microorganisms that adhere to surfaces and produce an extracellular polymeric substance (EPS) matrix, creating a protective environment. This complex matrix allows biofilms to exhibit high resistance to disinfectants and environmental conditions [10]. The presence of biofilms can lead to reduced efficiency in water and wastewater transfer systems, bio-corrosion, and increased maintenance costs [8].

The use of protective coatings, particularly polymer-based ones, has emerged as an effective solution to prevent biofilm formation. Polymeric paints, including acrylic ones, have gained significant attention in recent years due to their unique properties such as chemical resistance, favorable mechanical characteristics, and fast drying times [11]. These paints not only prevent the initial adhesion of microorganisms to the surface but also show enhanced effectiveness in preventing biofilm formation when active antimicrobial compounds are added [12].

In addition to mechanical issues, biofilms pose health risks. In industrial wastewater systems, biofilm growth can lead to water contamination and the spread of pathogens, posing a serious threat to public health [8]. Therefore, research and development in new technologies to prevent biofilm growth have become increasingly important.

Acrylic paints are recognized as one of the most effective options for industrial surface coatings due to their high ability to create homogeneous and durable coatings. With their advanced formulations, these paints can withstand extreme temperature variations, humidity, and chemical exposure [13]. Furthermore, the addition of antimicrobial nanoparticles such as silver, copper, or zinc oxide to these coatings has significantly enhanced their antibacterial properties [14].

In recent decades, extensive research has been conducted to prevent biofilm formation. Early studies primarily focused on the use of disinfectants. However, with the advent of nanotechnology and advances in polymer chemistry, the focus has shifted toward designing advanced coatings. These coatings not only prevent initial adhesion but also create an impermeable layer that provides an unfavorable environment for microbial growth [15]. Given the detrimental effects of biofilms across various industries and the success of polymeric coatings in preventing them, it can be concluded that this method is one of the best preventive options in industrial system management. The subsequent sections will delve deeper into the technical and practical characteristics of these coatings.

4. Properties of Polymeric and Acrylic Paints

Polymeric and acrylic paints have gained a prominent position in various industries, especially in industrial and environmental applications, due to their unique properties. These paints are made from synthetic polymer compounds and play a critical role in protecting and optimizing the performance of industrial systems due to their physical, chemical, mechanical, and environmental features [16].

One of the outstanding features of acrylic paints is their high adhesion, which enables them to bond strongly to various surfaces, including metal, concrete, and plastic. This property makes them ideal for coating surfaces in industrial environments [16, 17]. Additionally, the chemical structure of acrylic paints provides excellent resistance to water absorption, allowing them to maintain stable performance in humid conditions. This water resistance, combined with high chemical stability against acids, alkalis, and other industrial chemicals, makes these paints suitable for use in harsh environments [18].

Mechanically, these paints exhibit excellent resistance to impact and abrasion, which is particularly important for surfaces exposed to strong water currents or suspended particles. Furthermore, the high flexibility of acrylic paints allows them to adapt to thermal and mechanical changes without cracking or breaking, making them one of the most reliable options for industrial surface coatings [19].

Another significant property of polymeric and acrylic paints is their corrosion resistance. These paints form an impermeable layer that prevents direct contact between the surface and corrosive agents. Studies have shown that these coatings maintain their performance for extended periods under harsh environmental conditions, preventing damage caused by corrosion. This feature is particularly valuable in the oil and gas industries, wastewater treatment plants, and marine industries [20].

Moreover, the antimicrobial properties of acrylic paints, enhanced by active additives such as silver, copper, or zinc oxide nanoparticles, play a key role in preventing biofilm growth. These paints effectively inhibit the initial adhesion of microorganisms and suppress their growth, thereby preventing biofilm formation. This antimicrobial property makes acrylic paints particularly suitable for industries where cleanliness and hygiene are critical, such as the food and pharmaceutical sectors [21].

From an environmental compatibility perspective, many acrylic paints are free of volatile organic compounds (VOC), making them safer for the environment. Additionally, these paints can be designed to minimize negative environmental impacts, making them a suitable option for industries sensitive to environmental issues [22].

Finally, the fast-drying characteristic of acrylic paints is a key feature that reduces coating operation times and enhances efficiency in industrial processes. This property is especially significant in projects with tight execution timelines.

5. Mechanism of Polymeric Paints

Polymeric and acrylic paints combine physical, chemical, mechanical, and environmental features, making them a powerful tool for addressing challenges such as corrosion and biofilm growth in industrial settings. These features optimize their use in industries like wastewater treatment plants, power plants, and marine industries, enhancing efficiency, reducing costs, and contributing to environmental preservation.

One of the key features of polymeric and acrylic coatings is their ability to create low-surface-energy surfaces, which prevent microbial adhesion. Acrylic polymers, due to their molecular structure, have hydrophobic chains [23]. These hydrophobic groups reduce surface energy, lowering the interaction between microbial cells and the coating. This interaction reduction prevents microorganisms from forming strong bonds with the surface, which is the initial step in biofilm formation. Furthermore, this hydrophobicity ensures that water molecules and dissolved substances cannot easily interact with the surface, creating an environment unsuitable for microbial growth and accumulation [23, 24].

In addition to reducing surface energy, acrylic coatings prevent biofilm formation by modifying the physical structure of the surface. These coatings are typically designed with extremely low surface roughness, significantly reducing the potential adhesion points for microbial cells. Some engineered coatings also feature complex surface structures, further minimizing microbial adhesion. Even when microorganisms contact the surface, such designs inhibit colony formation and the accumulation of extracellular polymeric substances (EPS) [25, 26].

A crucial chemical feature of these coatings is their ability to release antimicrobial agents in a controlled manner. These coatings are often fortified with active compounds like silver nanoparticles, copper, or organic antimicrobial agents. These compounds are gradually released from the polymeric matrix and attack microbial cell surfaces. The primary mechanism involves disrupting the microbial cell wall and membrane, preventing cell survival and biofilm formation. Controlled release ensures prolonged effectiveness, reducing the need for frequent reapplication [21, 27].

Acrylic coatings actively inhibit biofilm formation by interfering with biological processes. Biofilm formation typically involves two stages: initial adhesion and EPS matrix accumulation [4]. These coatings disrupt intercellular communication (Quorum Sensing) by altering surface properties and emitting inhibitory signals. This communication system is crucial for microorganisms to coordinate colony formation and enhance resistance. Thus, these coatings effectively disrupt the coordination needed for biofilm formation [28].

Polymeric and acrylic coatings can adjust their hydrophilic and hydrophobic properties, a key mechanism for biofilm prevention. Hydrophilic coatings typically retain a thin water layer on their surface, acting as a physical barrier against direct microbial contact. In contrast, hydrophobic coatings repel water and nutrients, creating an environment unsuitable for microbial growth. This adjustable property is a significant advantage, depending on the application and industrial setting [29].

Certain types of acrylic coatings incorporate catalytic materials like titanium oxide. These materials, upon light exposure, generate reactive oxygen species (ROS) that damage microbial cell walls. This photocatalytic process is especially effective in light-accessible environments and can simultaneously eliminate multiple microbial species. Catalytic reactions also prevent EPS matrix accumulation, keeping the surface clean [30, 31].Some polymeric coatings contain compounds that disrupt microbial cell division processes. These compounds interfere with metabolic activities, preventing cell replication and biofilm formation at early stages. They may also deactivate key enzymes required for EPS production [32].

Acrylic coatings, due to their combination of physical, chemical, and biological properties, are among the most effective solutions for preventing biofilm formation. By creating surfaces unsuitable for adhesion, releasing antimicrobial agents, and interfering with biological processes, these coatings enhance performance and reduce maintenance costs in various industries. However, developing more durable and environmentally sustainable coatings remains a critical challenge.

6. Role of Antimicrobial Agents in Acrylic Paints

Adding antimicrobial agents to acrylic paints is an innovative strategy to enhance the efficiency of these coatings in preventing microbial growth and biofilm formation. These agents are particularly effective in industrial and environmental settings where contamination risk is high. This section examines various antimicrobial agents, their mechanisms, and their impact on reducing biofilm formation [22].

Acrylic paints containing metallic nanoparticles like silver, copper, and zinc oxide are among the most advanced antimicrobial coatings. Silver nanoparticles, known for their potent antibacterial properties, are widely used in acrylic paints. They disrupt bacterial cell walls and enzymatic functions, halting microbial growth. Copper nanoparticles, being more cost-effective yet similarly effective, are also gaining traction. Zinc oxide, by releasing active ions and generating reactive oxygen species, exhibits significant antimicrobial effects. Additionally, organic compounds like quaternary ammonium salts and isothiazolinones are extensively used to prevent fungal and bacterial growth in acrylic paints [33].

The mechanisms of antimicrobial agents in these paints involve three main processes: releasing active ions, initiating oxidative reactions, and disrupting microbial membranes. Metallic nanoparticles like silver and copper continuously release active ions that impair microbial metabolic functions. These agents generate ROS, which damage essential microbial components such as DNA and proteins. Furthermore, they penetrate microbial membranes, causing intracellular leakage and cell death [21, 33].These antimicrobial agents play a crucial role in reducing biofilm formation. They lower the surface energy of acrylic paints, preventing the initial adhesion of microorganisms. Additionally, by inhibiting cell replication, they limit microbial colony expansion and reduce EPS production, the structural basis of biofilms. These effects significantly hinder biofilm formation and stability [19, 21].

The advantages of using antimicrobial agents in acrylic paints include increased coating durability, reduced equipment maintenance costs, and environmental protection. These agents extend the paint's lifespan against biological contamination and reduce the need for frequent chemical disinfectants. These features make these paints not only economically viable but also environmentally friendly [33].However, challenges such as the high cost of metallic nanoparticle production, environmental compatibility, and maintaining long-term effectiveness remain significant limitations. Developing sustainable and environmentally friendly compositions to enhance the efficiency of these paints remains a priority for research [19].Advancements in modern technologies, such as nanotechnology, encapsulation of antimicrobial agents, and the design of smart coatings responsive to environmental stimuli, are crucial for improving these paints' performance. These technologies can enhance efficiency and reduce costs, expanding their applications across industries like wastewater treatment, marine industries, and power plants [19].

Acrylic paints containing antimicrobial agents, as a novel and efficient solution, hold great potential for combating biofilm growth while addressing environmental and industrial challenges. With their high performance and environmental sustainability, these coatings serve as an effective tool for managing industrial systems [19, 21].

7. Industrial Applications

Acrylic and polymeric paints, due to their unique properties, have found extensive applications across various industries. These coatings not only combat challenges like corrosion, biofilm growth, and biological contamination but also enhance the overall efficiency of industrial systems. Below are the major industrial applications of these paints [34]:

1. Water and Wastewater Treatment Plants

In water and wastewater treatment plants, acrylic paints are used to coat storage tanks and piping systems. These coatings create a layer resistant to water and chemicals, preventing biofilm growth and surface corrosion [35]. The use of these paints extends the lifespan of equipment while reducing maintenance and repair costs. Additionally, they prevent blockages and pressure drops in piping systems, thereby improving the overall performance of treatment plants [36].

2. Oil and Gas Industry

Polymeric and acrylic paints are widely used in the oil and gas industry to protect equipment from harsh environmental conditions. These paints are effective in coating offshore equipment exposed to high humidity and salinity [16]. Furthermore, in oil and gas pipelines, these coatings prevent biological deposits and microbial corrosion, enhancing the efficiency of transportation operations. Fuel storage tanks are also coated with these paints to protect them from chemical and biological degradation [37].

3. Food and Pharmaceutical Industries

In the food and pharmaceutical industries, where maintaining hygienic standards is crucial, antimicrobial acrylic paints are used to coat internal surfaces of equipment. These coatings prevent the growth of bacteria and fungi, minimizing the risk of contamination in products. Additionally, acrylic paints with smooth and non-adhesive surfaces facilitate equipment cleaning and prevent the spread of biological contaminants [37].

4. Power Plants

Cooling systems in power plants are continuously exposed to biological deposits and biofilms. Polymeric and acrylic paints are used to coat these systems, preventing deposit formation and improving the efficiency of thermal systems. Additionally, these paints protect turbines and sensitive equipment in power plants from corrosion and biological contamination [38].

5. Maritime and Shipping Industries

In the shipping industry, antimicrobial acrylic paints are applied to ship hulls. These coatings prevent the formation of biofilms and algae, reducing hull friction and optimizing fuel consumption. Furthermore, in offshore oil platforms, these paints provide reliable protection against marine conditions due to their high durability [39].

6. Construction Industry

Acrylic paints are used for interior and exterior coatings of industrial buildings. These coatings reduce mold and fungal formation, creating more hygienic environments. They also enhance the durability of concrete structures by protecting them against corrosion and erosion [39].

7. Chemical Industry

In the chemical industry, these paints are applied to tanks and pipes used for transferring corrosive chemicals. The high resistance of these paints to chemicals and microorganisms improves the safety and longevity of the equipment [21].

8. Benefits and Achievements

The use of acrylic and polymeric paints across various industries offers numerous advantages:

Prolonged Equipment Lifespan: By reducing corrosion and biofilm growth, these paints significantly extend the life of equipment.

Lower Maintenance Costs: Reduced cleaning and maintenance requirements decrease operational expenses.

Enhanced Industrial Productivity: These coatings boost system efficiency by minimizing biological contamination [21].

Acrylic and polymeric paints, due to their exceptional properties, are widely applied in a variety of industries. These coatings not only improve system performance but also mitigate environmental and economic impacts caused by biological issues, providing an innovative solution to industrial challenges [40].

8. Future Prospects and Recommendations

Recent advancements in the use of acrylic and polymeric paints to prevent biofilm growth highlight the potential for developing novel technologies and creative applications. Below are future perspectives and recommendations for research and improvement in this field [40]:

One future direction is the development of nanocoatings using smart nanoparticles. These nanoparticles can provide controlled release of antimicrobial agents, enhancing the durability and effectiveness of acrylic paints. Nanocoatings, due to their high surface-to-volume ratio, offer optimized antimicrobial performance. Additionally, incorporating eco-friendly compounds like plant extracts and biopolymers could replace current chemical agents, reducing environmental impact [41].

Designing smart coatings that respond to environmental changes such as pH, temperature, or pressure is an exciting area for future research. These coatings could activate antimicrobial effects under specific biological conditions. Furthermore, developing self-healing acrylic paints could enhance the durability of these coatings against mechanical or chemical damage, improving their industrial applications [41].

To address environmental sustainability, reducing volatile organic compounds (VOC) in paint formulations is a priority. Developing recyclable paints could lower industrial waste disposal costs and strengthen environmental sustainability. Additionally, assessing the long-term effects of metallic nanoparticles on the environment and living organisms is critical to ensuring the safety and sustainability of this technology [41].

Antimicrobial acrylic and polymeric paints could find use in industries beyond their current domains:

Medical Industry: Coating hospital equipment and pharmaceutical packaging to reduce hospital-acquired infections [42].

Food Industry: Designing coatings that prevent microbial growth in production and packaging equipment to improve product safety and quality.

Marine Industry: Further research on enhancing antifouling coatings could reduce fuel consumption and maintenance costs in ships [42].

Developing more precise laboratory methods to evaluate the efficacy of antimicrobial agents and conducting long-term tests in real-world conditions are essential for ensuring the durability and effectiveness of these paints. Using mathematical models and computer simulations could facilitate predicting the behavior of these coatings under different environmental conditions [42].

Interdisciplinary Research: Collaboration between polymer chemistry, environmental engineering, and microbiology experts to develop innovative technologies.

Cost Reduction: Using cheaper raw materials and optimizing production processes to reduce the cost of these paints.

Exploration in New Industries: Feasibility studies on using acrylic paints in renewable energy and energy storage industries to create new opportunities.

9. Conclusion

Polymeric and acrylic paints play a vital role in preventing biofilm growth and protecting industrial surfaces, significantly improving the performance and productivity of various industries. This study comprehensively explored the properties of these paints, the role of antimicrobial agents, industrial applications, challenges, and future perspectives.Acrylic paints, with their chemical and mechanical properties, stand out as one of the best options for biofilm prevention. Adding antimicrobial agents like metallic nanoparticles significantly enhances their effectiveness in controlling microbial growth. The diverse applications of these paints in industries such as wastewater treatment, marine industries, and power plants demonstrate their versatility and high performance.

While challenges such as high production costs, especially for metallic nanoparticles, remain limitations, developing sustainable and affordable compositions will be crucial. Future advancements in formulations and innovative technologies promise a sustainable and efficient future for this field.Acrylic and polymeric paints, combining favorable physical, chemical, and environmental properties, are a powerful tool for biofilm management and surface protection. These coatings improve industrial system productivity and reduce environmental and operational costs, playing a key role in resource management and industrial infrastructure preservation. Advancements in this field can pave the way for a more sustainable and optimized future across various industries.

Reference

1. Wimpenny, J. An overview of biofilms as functional communities. Cambridge; Cambridge University Press; 1999.

2. Verma, S., A. Kuila, and S. Jacob, Role of biofilms in waste water treatment. Applied Biochemistry and Biotechnology, 2023. 195(9): p. 5618-5642.

3. Carrascosa, C., et al., Microbial biofilms in the food industry—A comprehensive review. International Journal of Environmental Research and Public Health, 2021. 18(04): p. 2014.

4. Jansen, B. and W. Kohnen, Prevention of biofilm formation by polymer modification. Journal of industrial microbiology and biotechnology, 1995. 15(4): p. 391-396.

5. De Carvalho, C.C., Biofilms: recent developments on an old battle. Recent patents on biotechnology, 2007. 1(1): p. 49-57.

6. Bellotti, N., et al., The application of bioactive compounds from the food industry to control mold growth in indoor waterborne coatings. Colloids and Surfaces B: Biointerfaces, 2013. 104: p. 140-144.

7. Tiller, J.C., Coatings for prevention or deactivation of biological contamination, in Developments in surface contamination and cleaning. 2008, Elsevier. p. 1013-1065.

٨. Mattila-Sandholm, T. and G. Wirtanen, Biofilm formation in the industry: a review. Food reviews international, 1992. 8(4): p. 573-603.

9. Kokilaramani, S., et al., Microbial influenced corrosion of processing industry by re-circulating waste water and its control measures-A review. Chemosphere, 2021. 265: p. 129075.

10. Vishwakarma, V., Impact of environmental biofilms: Industrial components and its remediation. Journal of basic microbiology, 2020. 60(3): p. 198-206.

١١. Lisoń, J., et al., Perspectives in prevention of biofilm for medical applications. Coatings, 2022. 12(2): p. 197.

12. De Carvalho, C.C.C.R., Biofilms: recent developments on an old battle. Recent patents on biotechnology, 2007. 1(1): p. 49-57.

13. Gaylarde, C.C. and L.H.G. Morton, Deteriogenic biofilms on buildings and their control: a review. Biofouling, 1999. 14(1): p. 59-74.

14. Breitbach, A.M., J.C. Rocha, and C.C. Gaylarde, Influence of pigment on biodeterioration of acrylic paint films in Southern Brazil. Journal of coatings technology and research, 2011. 8: p. 619-628.

15. Bogdan, S., et al., Natural products to control biofilm on painted surfaces. Pigment & Resin Technology, 2018. 47(2): p. 180-187.

16. Friel, J.M. and E. Nungesser, Acrylic polymers as coatings binders. Paint and coating test manual-Fourteenth edition of the Gardner-Sward Handbook, 1995: p. 39-52.

17. Iezzi, R.A., S. Gaboury, and K. Wood, Acrylic-fluoropolymer mixtures and their use in coatings. Progress in organic coatings, 2000. 40(1-4): p. 55-60.

18. Learner, T. Modern paints: uncovering the choices. in Modern paints uncovered: proceedings from the modern paints uncovered symposium. 2007. Los Angeles: Getty Conservation Institute.

19. Weiss, K.D., Paint and coatings: A mature industry in transition. Progress in polymer science, 1997. 22(2): p. 203-245.

20. Buchheit, R.G., Corrosion resistant coatings and paints, in Handbook of environmental degradation of materials. 2005, Elsevier. p. 367-385.

21. Gupta, S., et al., Antimicrobial polymeric paints: An up-to-date review. Polymers for Advanced Technologies, 2021. 32(12): p. 4642-4662.

22. Iscen, A., et al., Acrylic paints: An atomistic view of polymer structure and effects of environmental pollutants. The Journal of Physical Chemistry B, 2021. 125(38): p. 10854-10865.

23. Awaja, F., et al., Adhesion of polymers. Progress in polymer science, 2009. 34(9): p. 948-968.

24. Shirtcliffe, N.J., G. McHale, and M. I. Newton, The superhydrophobicity of polymer surfaces: recent developments. Journal of Polymer Science Part B: Polymer Physics, 2011. 49(17): p. 1203-1217.

25. Yang, J., et al., A mechanically robust slippery coating for anti-corrosion, Photothermal deicing, and anti-sticking applications. Surface and Coatings Technology, 2022. 438: p. 128395.

٢٦. Yong, Q., et al., Advances in polymer-based matte coatings: A review. Polymers for Advanced Technologies, 2022. 33(1): p. 5-19.

27. Trojer, M.A., et al., Use of microcapsules as controlled release devices for coatings. Advances in colloid and interface science, 2015. 222: p. 18-43.

28. Zhang, P., et al., Biofilm inhibition and elimination regulated by cationic conjugated polymers. ACS applied materials & interfaces, 2017. 9(20): p. 16933-16938.

29. Ahmad, D., et al., Hydrophilic and hydrophobic materials and their applications. Energy Sources, Part A: Recovery, Utilization, and Environmental Effects, 2018. 40(22): p. 2686-2725.

30. Fleischmann, C., M. Lievenbrück, and H. Ritter, Polymers and dyes: developments and applications. Polymers, 2015. 7(4): p. 717-746.

31. Borjigin, T., et al., Low-cost and recyclable photocatalysts: Metal oxide/polymer composites applied in the catalytic breakdown of dyes. Photochem, 2022. 2(3): p. 733-751.

32. Mahmoudi, M., et al., Effect of nanoparticles on the cell life cycle. Chemical reviews, 2011. 111(5): p. 3407-3432.

33. Farsinia, F., et al., Antimicrobial waterborne acrylic paint by the additive of graphene nanosheets/silver nanocomposite. Materials Chemistry and Physics, 2023. 297: p. 127355.

34. Procopio, L.J., Acrylic Coatings. 2015.

35. Hamilton, J.D., K.H. Reinert, and J.E. McLaughlin, Aquatic risk assessment of acrylates and methacrylates in household consumer products reaching municipal wastewater treatment plants. Environmental technology, 1995. 16(8): p. 715-727.

36. Viktoryová, N., A. Szarka, and S. Hrouzková, Recent developments and emerging trends in paint industry wastewater treatment methods. Applied Sciences, 2022. 12(20): p. 10678.

37. Keefe, M., et al., Art and Industry: Novel Approaches to the Evaluation and Development of Cleaning Systems for Artists' Acrylic Latex Paints. CoatingsTech, 2011. 8(9).

38.	Kaew-on, N., Formulations of primer, acrylic paint and pastel in traditional Thai style colour. 2017.

39.	Almeida, E., T.C. Diamantino, and O. de Sousa, Marine paints: the particular case of antifouling paints. Progress in organic coatings, 2007. 59(1): p. 2-20.

40.	DeFusco, A., K.C. Sehgal, and D.R. Bassett, Overview of uses of polymer latexes, in Polymeric Dispersions: Principles and Applications. 1997, Springer. p. 379-396.

٤١.	Jones, F.N., et al., Artist paints—an overview and preliminary studies of durability. Progress in Organic Coatings, 2005. 52(1): p. 9-20.

42.	Escorteganha, M.R., et al., INTERDISCIPLINARY STUDIES OF THE" VISTA DO DESTERRO" PAINTING: HISTORICAL APPROACH, ANALYSIS OF MATERIALS AND PRESERVATION/RESTORATION TECHNIQUES. International Journal of Conservation Science, 2015. 6(3).

The 30th Iranian Seminar of Organic Chemistry
February 7-9, 2025, Iran University of Science and Technology, Tehran, Iran

Synthesis of novel phospholipid based on succinic anhydride for nano liposomal encapsulation of omega-3

Fatemeh Tabibzadeh[a], Elaheh Mosaddegh*[a,b] and Ismaeil Haririan[c]

[a]*Department of Chemistry, Graduate University of Advanced Technology, PO Box 76315-117, Kerman, Iran*

[b]*Department of New Materials, Institute of Science and High Technology and Environmental Sciences, Graduate University of Advanced Technology, PO Box 76315-117, Kerman, Iran*

[c]*Department of Pharmaceutical Biomaterials, Faculty of Pharmacy, Tehran University of Med. Sci. (TMS), P.O. Box: 14155-6451, Tehran, Iran.*

Keywords: Phospholipid, Liposome, Omega-3, encapsulation, drug delivery

Introduction: Omega-3 (ω-3) polyunsaturated fatty acids (PUFAs) are known to have beneficial effects on human health. Numerous studies have demonstrated the potential role of omega-3 PUFAs, especially eicosapentaenoic acid (EPA) and docosahexaenoic acid (DHA), in helping to prevent chronic diseases [1]. The World Health Organization (WHO) recommends that adults consume 200-500 mg of DHA and EPA [2]. The rise in awareness of EPA and DHA's health benefits has led to a growing demand for dietary supplements. Enhancing foods with oils rich in EPA and DHA is difficult due to issues with lipid oxidation

[3]. A key requirement for successfully developing foods rich in omega-3 PUFA is to prevent or delay lipid oxidation as much as possible [4]. One method of protecting lipids from oxidation is to microencapsulate the lipid to be protected [3]. Micro- and nano-encapsulation is a promising approach to protect core materials (PUFA) against environmental factors such as oxygen, light, and transition metals, thus improving their oxidative stability and biological activity [2]. One of the most useful delivery systems for lipophilic bioactive substances is through lipid-based encapsulation systems. Phospholipids are excellent emulsifiers because they have a glycerol backbone attached to two fatty acids (hydrophobic) and one phosphoric acid (hydrophilic) [5]. Phospholipids are characterized by their exceptional biocompatibility and distinct amphiphilic properties. These attributes render them particularly suitable for use as pharmaceutical excipients, leading to a broad spectrum of applications in drug delivery systems. Upon introduction into an aqueous environment, phospholipids undergo self-assembly, resulting in the formation of various supramolecular structures that are influenced by their specific properties and environmental conditions. Notably, phospholipids tend to form liposomes, which serve as effective drug carriers in therapeutic applications [6]. Liposomes can be made from both natural and synthetic phospholipids. The phospholipid composition strongly influences liposome properties, including particle size, hardness, fluidity, stability, and electrical charge. Liposomes are the safest and most suitable drug delivery system for humans due to their biocompatibility, biodegradability, and low toxicity [7]. The main advantage of liposome microencapsulation systems over other microencapsulation systems is that the materials encapsulated in the microcapsules exhibit much higher water activity compared to other microencapsulation systems [5]. Thin-layer hydration is the oldest, most common, and simplest method to prepare liposomes. Regarding drug loading into liposome systems, lipophilic drugs can be solubilized with phospholipid mixtures before thin film formation, while hydrophilic drugs can be introduced into hydration media and then incorporated into liposomes during the hydration process [8].

In this research a new cationic phospholipid based on succinic anhydride has been designed for use in formulating liposomes that contain omega-3, enhancing the stability of omega-3. Cationic lipids possess a greater ability for transport, and cationic liposomes loaded with drugs can effectively adsorb negatively charged macromolecules. Compounds are used as preservatives to enhance the stability of liposomes. Additionally, natural polysaccharides aid in deep cellular penetration through the cell wall structure, while compounds are also utilized as flavorings to improve aroma and taste. The structure of the phospholipid was confirmed through NMR analysis, while the liposome formulation was verified using SEM and TEM analysis. Additionally, the drug loading and release were thoroughly investigated.

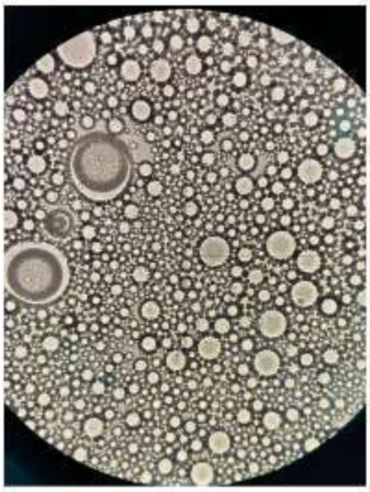

Scheme 1. TEM image of nano liposomal omega-3

Results and Discussion: This study synthesized A novel phospholipid based on succinic anhydride. The success of the synthesis was proven by structural analyses using FT-IR, ^{1}H NMR, ^{13}C NMR, and ^{31}P NMR. The new phospholipid was used in the liposome structure with the formulation of phospholipid/cholesterol/Tween 60/Span 60/polysaccharide. The TEM analyses, which resulted in liposomes with dimensions of DLS, 7 nm, called nano. The synthesized nanoliposome was successful in increasing the stability of omega-3 which showed no sedimentation after several months.

References:

1. Padial-Domínguez, M., et al., *Protein-derived emulsifiers with antioxidant activity for stabilization of omega-3 emulsions.* Food Chemistry, 2020. **329**: p. 127148.

2. Saini, R.K., et al., *Omega*-3− 3 polyunsa*turated fatty acids (PUFAs): Emerging plant and microbial sources, oxidative stability, bioavailability, and health benefits—A review*. Antioxidants, 2021. **10**(10): p. 1627.
3. Arab-Tehrany, E., et al., *Beneficial effects and oxidative stability of omega*-3 long-*chain polyunsaturated fatty acids.* Trends in Food Science & Technology, 2012. **25**(1): p. 24-33.
4. Jacobsen, C., A.-D. Sørensen, and N.S. Nielsen, *Stabilization of omega*-3 oils and *enriched foods using antioxidants*, in *Food enrichment with omega-3 fatty acids*. 2013, Elsevier. p. 130-149.
5. Barrow, C., et al., *Spray drying and encapsulation of omega-3 oils,* in *Food enrichment with omega-3 fatty acids*. 2013, Elsevier. p. 194-225.
6. Li, J., et al., *A review on phospholipids and their main applications in drug delivery systems.* Asian journal of pharmaceutical sciences, 2015. **10**(2): p. 81-98.
7. Grazia Calvagno, M., et al., *Effects of lipid composition and preparation conditions on physical-chemical properties, technological parameters and in vitro biological activity of gemcitabine-loaded liposomes.* Current drug delivery, 2007. **4**(1): p. 89-101.
8. Lombardo, D. and M.A. Kiselev, *Methods of liposomes preparation: Formation and control factors of versatile nanocarriers for biomedical and nanomedicine application.* Pharmaceutics, 2022. **14**(3): p. 543.

Synthesis and Characterization of Folic Acid-Targeted Nanoniosomes for Controlled Delivery of Doxorubicin: A Novel Lipid-Based Formulation

Saideh Mahdavi,[a] and Elaheh Mosaddegh*[a,b]

[a] *Department of Chemistry, Graduate University of Advanced Technology, PO Box 76315-117, Kerman, Iran*

[b] *Department of New Materials, Institute of Science and High Technology and Environmental Sciences, Graduate University of Advanced Technology, PO Box 76315-117, Kerman, Iran*

Keywords: Nanoniosomes, Doxorubicin, Targeted Drug Delivery, Folic Acid, Controlled Release, TEM.

Abstract: In this study, a novel branched lipid derived from ethanolamine was synthesized and characterized using FTIR and NMR spectroscopy. The lipid, combined with Span 60, Tween 60, polysaccharides, and cholesterol, was utilized to fabricate nanoniosomes for encapsulating doxorubicin. The structure of the nanoniosomes was characterized before and after drug loading using transmission electron microscopy (TEM) and dynamic light scattering (DLS), confirming their nanoscale size and uniformity. For targeted drug delivery, the nanoniosomes were functionalized with folic acid on their surface. Drug release studies conducted using a dialysis bag indicated sustained and controlled release of doxorubicin in the optimized formulation. These findings suggest that the designed nanoniosomes have significant potential for targeted cancer therapy.

Introduction: The development of nanocarriers for targeted drug delivery has revolutionized the field of cancer therapy, addressing the limitations of conventional treatments, such as systemic toxicity and poor bioavailability [1-3]. Nanoniosomes, non-ionic surfactant-based vesicles, have emerged as a promising platform for encapsulating and delivering chemotherapeutic agents due to their biocompatibility, stability, and ease of functionalization [4,5].

In this study, we synthesized a novel branched lipid derived from ethanolamine and incorporated it into the formulation of nanoniosomes along with Span 60, Tween 60, polysaccharides, and cholesterol. The niosomes were subsequently functionalized with folic acid to achieve targeted delivery of doxorubicin to folate receptor-expressing cancer cells. The structural and functional characteristics of the lipid and the formulated nanoniosomes were thoroughly investigated, along with drug release and targeting efficiency.

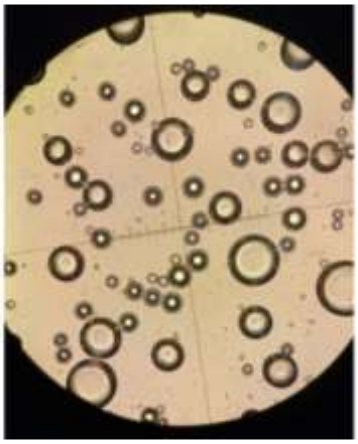

Scheme 1. Encapsulated doxorubicin in novel nanoniosome

Materials and Methods

1. Synthesis of the Branched Lipid

The branched lipid was synthesized through a multi-step reaction involving ethanolamine and fatty acid derivatives. The chemical structure was confirmed by FTIR, which showed characteristic peaks for amine and ester groups, and NMR spectroscopy, which confirmed the molecular structure of the synthesized lipid.

2. Preparation of Nanoniosomes

Nanoniosomes were prepared using the thin-film hydration method:
Step 1: A mixture of the branched lipid, Span 60, Tween 60, cholesterol, and appropriate polysaccharide was dissolved in chloroform.
Step 2: The solvent was evaporated under reduced pressure to form a thin lipid film on the walls of a round-bottom flask.
Step 3: The film was hydrated with phosphate-buffered saline (PBS) at 60°C with constant vortexing, followed by sonication to reduce particle size.

3. Drug Encapsulation

Doxorubicin was incorporated into the niosomes during the hydration step. Encapsulation efficiency was determined spectrophotometrically. Finally, folic acid was covalently conjugated to the surface of nanoniosomes using a PEGylation approach. The success of functionalization was confirmed using FTIR analysis.

Results and Discussion

FTIR spectra confirmed the presence of amine and ester groups, while NMR analysis verified the expected molecular structure. The lipid demonstrated excellent solubility and compatibility with other formulation components.TEM images revealed spherical niosomes with smooth surfaces, while DLS analysis showed an average size of 25 nm, suitable for enhanced permeability and retention (EPR) effects. Encapsulation efficiency of doxorubicin was approximately 85%, indicating effective drug loading.

FTIR spectra showed characteristic peaks corresponding to folic acid, confirming successful conjugation to the niosome surface. This functionalization enhances the ability of the nanoniosomes to target cancer cells expressing folate receptors.

The drug release profile demonstrated a sustained release pattern over 72 hours. Initial rapid release was attributed to surface-adsorbed doxorubicin, followed by a controlled release phase due to diffusion through the lipid bilayer. The functionalized nanoniosomes showed great potential for targeted delivery, reducing off-target effects and enhancing therapeutic efficacy. The branched lipid and folic acid conjugation played key roles in improving stability, targeting capability, and drug release kinetics.

٧,١,١ Conclusion

This study successfully demonstrated the synthesis of a novel branched lipid and its application in the formulation of folic acid-functionalized nanoniosomes for the targeted delivery of doxorubicin. The nanoniosomes exhibited excellent structural properties, high drug encapsulation efficiency, and sustained release behavior, making them a promising candidate for cancer therapy.

References:

١. Bangham, A. D., & Horne, R. W. (1964). Negative staining of phospholipids and their structural modification by surface-active agents as observed in the electron microscope. *Journal of Molecular Biology, 8*(5), 660–668.
٢. Uchegbu, I. F., & Florence, A. T. (1995). Non-ionic surfactant vesicles (niosomes): Physical and pharmaceutical chemistry. *Advances in Colloid and Interface Science, 58*(1), 1–55.
٣. Torchilin, V. P. (2005). Recent advances with liposomes as pharmaceutical carriers. *Nature Reviews Drug Discovery, 4*(2), 145–160.
٤. Tavano, L., Muzzalupo, R., Picci, N., & de Cindio, B. (2013). Co-encapsulation of antioxidants into niosomal carriers: Gastrointestinal release studies for nutraceutical applications. *Colloids and Surfaces B: Biointerfaces, 102,* 550–556.
٥. Kulkarni, S. A., & Feng, S. S. (2013). Effects of surface modification on delivery efficiency of biodegradable nanoparticles across the blood-brain barrier. *Nanoscale, 5*(6), 2589–2597.

The 30th Iranian Seminar of Organic Chemistry
February 7-9, 2025, Iran University of Science and Technology, Tehran, Iran

Effect of Surface Modification on the Physiochemical Properties of Polylactic Acid and Reduced Graphene Oxide Composite

Authors: Maryam Poostchi 1[a], Amin Dolatabadi 2[b], Aliasghar Behnamghader 3*[c]

Affiliations:

[1a]*Biomaterials Group, Department of Nanotechnology and Advanced Materials, Materials and Energy Research Center (MERC) Tehran, Iran* m.poustchi@merc.ac.ir

[2b]*Biomaterials Group, Department of Nanotechnology and Advanced Materials, Materials and Energy Research Center (MERC) Tehran, Iran* a.dolatabadi@merc.ac.ir

[3c] *Biomaterials Group, Department of Nanotechnology and Advanced Materials, Materials and Energy Research Center (MERC)* Tehran, Iran behnamghader@yahoo.com

Keyword: Polylactic acid-rGO composite, physical and chemical characterization, reduced oxide graphene, chemical surface modification

ABSTRACT

Given the increasing use of polymeric composite in tissue engineering, electroconductive composites take higher attention, especially in the field of bone and nerve tissue engineering. Polylactic acid-reduced graphene oxide composite based scaffolds are widely used in tissue engineering while lack of hydrophilic groups on their surface limit their biocompatibility. In the field of tissue engineering, it would be necessary to modify surface of the composite to improve cell adhesion. In this research, composite samples were prepared and modified with NaOH solution at different timepoints. The effect of surface modification on the physicochemical properties was investigated using Fourier transform infrared spectroscopy – attenuated total reflectance (FTIR-ATR), scanning electron microscope (SEM) and optical microscopy (OM) experiments. It was found that chemical surface modification with sodium hydroxide increased surface roughness at the microscale and changed the surface morphology at the nanoscale. FTIR-ATR results also indicated creation of O-H bonding in the modified composites which confirms the enhancing wettability of the composites. NAOH modification can play a significant role in enhancing cell attachment in tissue engineering by changing the surface morphology and chemical properties.

۱. Introduction

Scaffolds play an essential role in tissue engineering by mimicking the extracellular matrix, providing a three-dimensional structure that supports cell growth, proliferation, and differentiation. The ideal scaffold must possess several key properties to facilitate tissue regeneration: biocompatibility to avoid immune responses, biodegradability to allow gradual tissue replacement, mechanical strength to maintain structural integrity, and porosity to support nutrient and waste exchange [1], [2].

Polylactic acid (PLA), a widely used biomaterial in tissue engineering, exhibits excellent biocompatibility, biodegradability, and mechanical properties, making it an ideal candidate for scaffolds. However, its inherent lack of electrical conductivity limits its use in specific applications like neural and cardiac tissue engineering, where electrical stimulation is crucial [3] This challenge has led to the increasing incorporation of reduced graphene oxide (rGO) into PLA-based scaffolds, as rGO provides enhanced electrical conductivity while maintaining the favorable properties of PLA. Recent studies show that PLA/rGO composites are gaining popularity due to their potential to improve tissue regeneration, especially in tissues requiring electrical conductivity [4].

Although PLA/rGO composites demonstrate favorable mechanical and electrical properties, a substantial limitation lies in their inherently poor surface hydrophilicity. This characteristic is paramount in tissue engineering, as hydrophilic surfaces facilitate protein adsorption and cell adhesion, which are indispensable for cell proliferation and tissue growth. The hydrophobic nature intrinsic to both PLA and rGO can impede cell attachment, necessitating surface modification to enhance the scaffold's biocompatibility and bioactivity [5], [6]. Chemical surface modification represents a prevalent strategy for improving the hydrophilicity and functionalization of composite scaffolds. By introducing functional groups or altering the surface chemistry, it is feasible to augment the interaction between the scaffold and biological tissues [7]. Diverse chemical treatments have been implemented, including acid treatments, plasma modifications, or grafting of bioactive molecules. Among these, NaOH treatment has demonstrated particular efficacy. NaOH induces hydrolysis on the PLA surface, generating hydroxyl (-OH) and carboxyl (-COOH) groups, which enhance surface hydrophilicity and facilitate the binding of bioactive molecules such as peptides or proteins [8], [9]

NaOH treatment is favored for several reasons: it is simple, cost-effective, and efficient in introducing functional groups on both PLA and rGO surfaces without causing significant damage to the composite's structure. Moreover, the mild conditions of NaOH treatment minimize the risk of degrading the polymer matrix, making it an ideal choice for applications where scaffold integrity must be maintained [10], [11].

Based on existing literature and established practices in the surface modification of PLA/rGO composites, a 1 molar (1 M) NaOH solution is frequently considered an optimal concentration

[12]. This concentration provides a balanced approach, effectively modifying the surface while preserving the bulk properties of the composite. It is sufficiently potent to induce hydrolysis on the PLA surface, generating hydroxyl (-OH) and carboxyl (-COOH) groups, without causing excessive degradation [13]. Treatment with 1 M NaOH has been demonstrated to significantly reduce contact angles, indicative of enhanced hydrophilicity. Moreover, it can increase surface roughness, promoting cell adhesion. Unlike higher concentrations, 1 M NaOH typically does not substantially alter the bulk mechanical properties of the scaffolds [14]. The functional groups generated by this treatment facilitate the binding of bioactive molecules, such as successful gelatin coupling. Notably, 1 M NaOH has been effectively employed across various treatment durations, ranging from 1 to 96 hours, offering flexibility in processing. While requiring prudent handling, NaOH (1 M) is less hazardous compared to higher concentrations, making it a suitable choice for laboratory applications. Furthermore, its affordability and widespread availability render 1 M NaOH a cost-effective option for surface modification [15].

This research aims to investigate the effects of chemical surface modification by NaOH solution on the physical, chemical, and morphological properties of PLA-rGO composites. Adequate analyses such as contact angle (CA), scanning electron microscopy (SEM), optical microscopy (OM), and Fourier transform infrared spectroscopy (ATR-FTIR) were utilized to characterize the surface properties of the composites.

۲. **Material and methods**

2.1 Materials

Reduced graphene oxide (rGO) powder was obtained from previous research [16]. PLA, purchased from Chemie Kas GmbH, along with dichloromethane (DCM) and sodium hydroxide (NaOH), supplied by Merck and Sigma-Aldrich respectively, were utilized in this study. All materials were used as received, without further modification.

2.2. **Methods**

2.2.1Preparation of polylactic acid/rGO composite

Preparation of polylactic acid/rGO composites via the solution casting method. The process began by dissolving 2.5 grams of PLA granules in 15 milliliters of DCM at room temperature to create a uniform polymer solution. To ensure a homogenous dispersion of rGO, a key conductive component, 0.1% w/w rGO relative to the PLA was first dispersed in 4 milliliters of DCM before being incorporated into the PLA solution. The mixture was stirred thoroughly to achieve a uniform distribution of rGO throughout the matrix. Afterward, the solution was poured into a flat glass mold and allowed to dry, enabling the DCM to evaporate. To ensure complete solvent removal, the samples were placed in a vacuum oven for 6 hours. The final composite specimens, with dimensions of 7 mm × 7 mm × 0.3 mm, were used for subsequent analyses. The samples were named as presented in table 1.

Table 1. Samples name and description.

Sample Name	**Description**
PLA-0	PLA-rGO untreated
PLAG-1	PLA-rGO treated with NaOH 1 molar for 1 hour
PLAG-2	PLA-rGO treated with NaOH 2 molar for 1 hour
PLAG-3	PLA-rGO treated with NaOH 3 molar for 1 hour

2.2.*2 Surface treatment* of polylactic acid/rGO composite

NaOH solutions at different concentrations (1, 2, and 3 M) were prepared by dissolving certain amount of NaOH in distilled water. To surface treatment of PLA-rGO composite, each sample were soaked in 50 ml NaOH solution in 37˚c for 1 hour, while they were shaking. After 1 hour, samples were removed from solution and washed with DI water for several minutes and dried at 37˚ c for 24 hours.

٣. **Characterization**

3.1 Wettability Test

The wettability test was conducted using a contact angle goniometer developed at the Iran Materials and Energy Research Institute. For this purpose, 4 microliters of deionized water were dropped onto the surface of each sample (10 × 10 mm^2). Subsequently, images of these droplets were captured using a DFK 23U618 USB 3.0 industrial color camera equipped with a ×2 lens. The angles around the image were analyzed, and the average values were used to determine the final contact angle. The wettability test was performed to investigate the effect of rGO content on the surface hydrophilicity of the composite samples.

3.2 Fourier Transform Infrared Spectroscopy (ATR-FTIR) Analysis

Fourier transform infrared spectroscopy (ATR-FTIR) is a technique that utilizes the absorption of infrared radiation to study the vibrational modes of molecules and polyatomic ions. In this study, ATR-FTIR was employed to investigate the interactions between rGO and PLA chains in the composite material. The infrared spectra were recorded over a wavenumber range of 4000-400 cm^{-1} with a resolution of 4 cm^{-1}. The measurements were performed using an ATR-FTIR spectrometer model Equinox 55 (Bruker, Germany) located at the Iran Polymer and Petrochemical Research Institute.

3.3 Scanning Electron Microscopy (SEM) Analysis

Scanning electron microscopy (SEM) was employed to investigate the surface morphology of the composite material, including the distribution of rGO particles and the effect of rGO content on the surface morphology. The SEM analysis was performed using a TESCAN MIRA3 SEM instrument (EHT= 20.0kv, WD =19 mm, magnification =×300) Prior to imaging, the samples were mounted on aluminum stubs and sputter-coated with platinum for 3 minutes. SEM images were randomly captured from the sample surfaces and analyzed using ImageJ software.

3.4 **Optical Microscopy (OM) Analysis**

To investigate the surface morphology and the distribution of rGO particles on the composite surface before and after surface modification, an optical microscope located at the Materials and Energy Research Center was utilized. Images were randomly captured from the sample surfaces. The equipment was an Olympus BX61 model, equipped with a 10MP mu1003 camera.

4. Results and Discussion

4.1 Wettability Test

The static water contact angle was employed to assess the change in wettability of pure polylactic acid surfaces and PLA/rGO composites before and after surface modification. The contact angle, formed at the three-phase solid/liquid/gas interface, offers a simple and convenient method for evaluating the hydrophilicity and/or hydrophobicity of film materials. Figure 1 displays an image of a water droplet on the surface of the PLA/rGO composite. The average water contact angle on the composite surface, before treatment, was calculated as 76.6degrees. After surface modification of the composite with NaOH 1M for 1 hour, its contact angle decreased to 62.5 degrees. However, after surface modification with NaOH 2M and NaOH 3M for 1 hour, the contact angle increased to 76.5 and 84 degrees, respectively

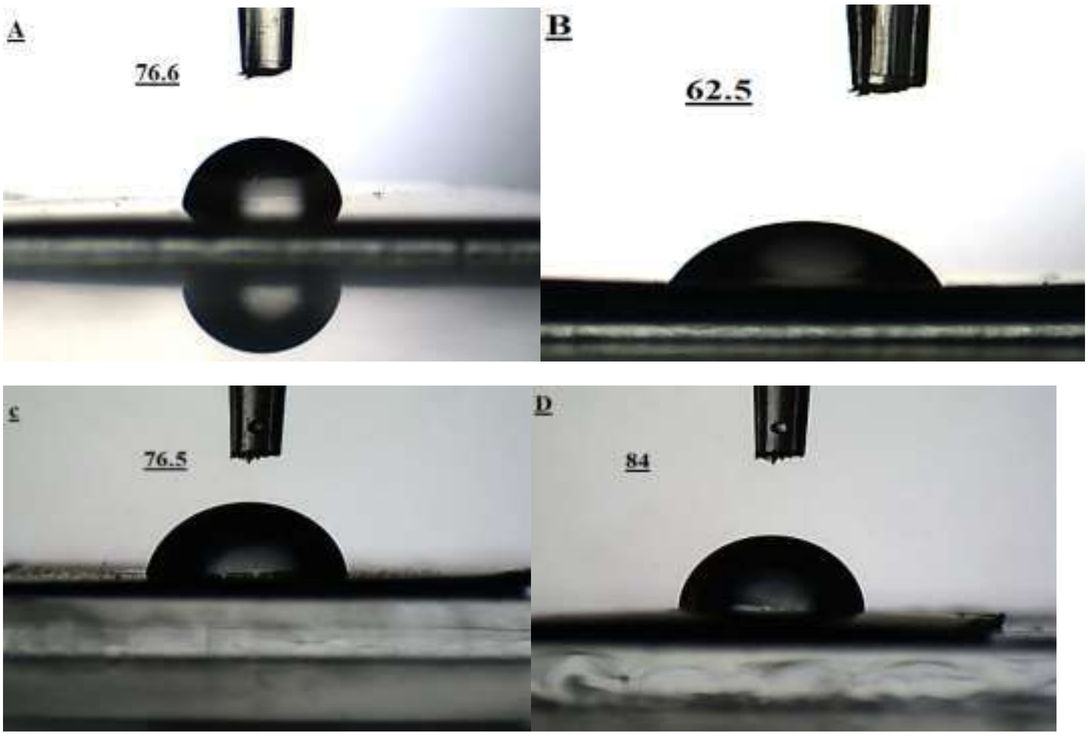

Figure 1. *The water contact angle on the surface of the composite sample before (a) and after (b) surface modification with 1 M NaOH for 1 hour. The sample after surface modification with 2 M NaOH (c) and 3 M NaOH (d) for 1 hour.*

As evident from the graph, the contact angle increases with an increase in the surface modification duration, indicating an enhancement in the hydrophobicity of the surface. The lowest contact angle value, signifying the highest hydrophilicity of the composite, was obtained at a concentration of 1 M for a duration of 1 hour. Increasing NaOH concentration resulted in decrease in hydrophilicity which might be attributed to the increase of rophness and change in surface morphology .

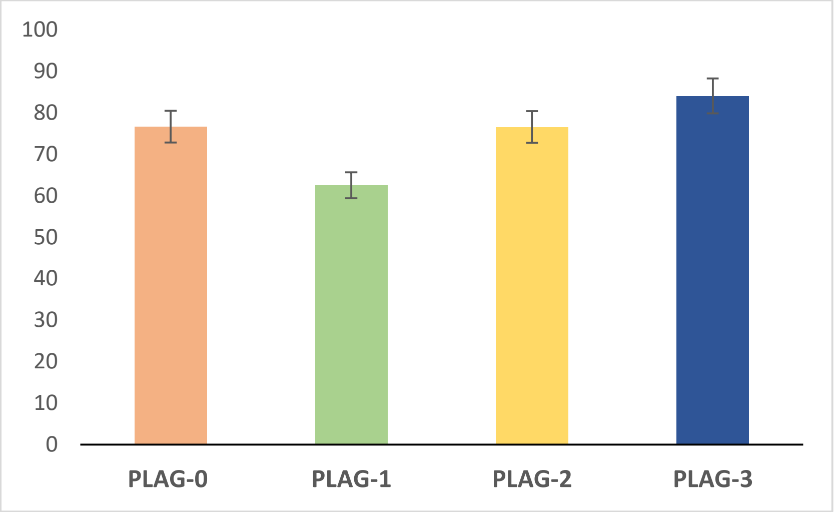

Figure 2. *Investigation of the contact angle of PLA/rGO composite after treatment with different concentration of NaOH.*

4.2 Fourier Transform Infrared Spectroscopy (ATR-F*TIR) Analysis*

ATR-FTIR analysis is presented in Figure 3 for the surface of samples before and after treatment with NaOH solution. PLA-rGO composite exhibited four characteristic peaks of PLA in the wavenumber range of 500 to 4000 cm^{-1}. These peaks correspond to C-H stretching vibrations in the 2850-3000 cm^{-1} region, ester C=O stretching at 1740-1750 cm^{-1}, C-O stretching at 1000-1100 cm^{-1}, and C-H bending vibrations around 1400-1500 cm^{-1}, as reported in the literature. These peaks are clearly observed in the PLAG-0 spectrum at 2990, 2946 (C-H), 1745 (C=O), 1079, 1126, 1179 (C-O-C), and 1452 cm^{-1}. Additionally, peaks characterize the amorphous and crystalline regions of the polymer at 865 and 757 cm^{-1}, respectively [17]. As shown in the Figure 3, the PLAG composite after NaOH treatment exhibits peak at 1268 cm^{-1} (C-O-C stretching vibration of ester linkage) in lower intensity, indicating the breakdown in PLA chain.

A broad and weak peak in the 3500 cm^{-1} regions, indicating the formation of O-H groups in the polymer chain. Overall, the intensity of the characteristic peaks of oxygen-containing polylactic acid changed after surface modification with NaOH, suggesting a change in the structure of the polymer molecular chains [18]

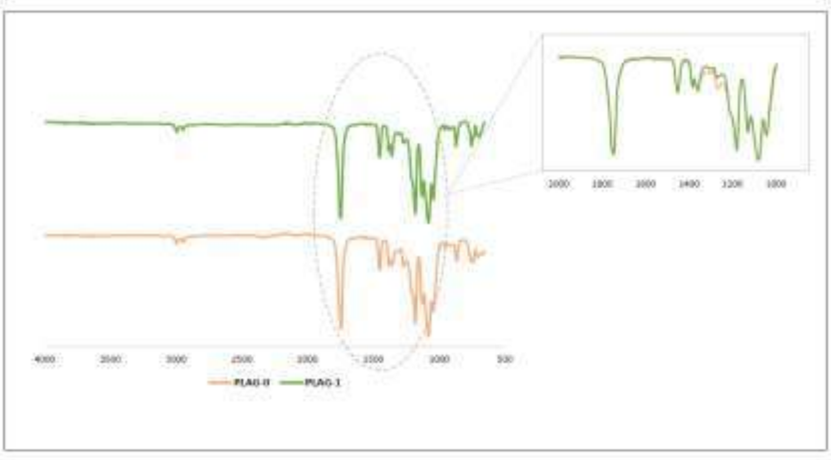

Figure. 3. *ATR-FTIR spectra of PLA/rGO composite after surface modification.*

4.3 Scanning Electron Microscopy (SEM) Analysis

PLA/rGO surfaces etched with 1 M NaOH for 1 hour exhibited significant changes in surface morphology compared to unmodified samples. As expected, an increase in surface roughness with the formation of grooves, pits, and depressions of varying sizes and depths was observed, as evident in Figure 4. The treated surface displayed notable topographical changes in comparison to the relatively smooth unmodified PLA/rGO surface.

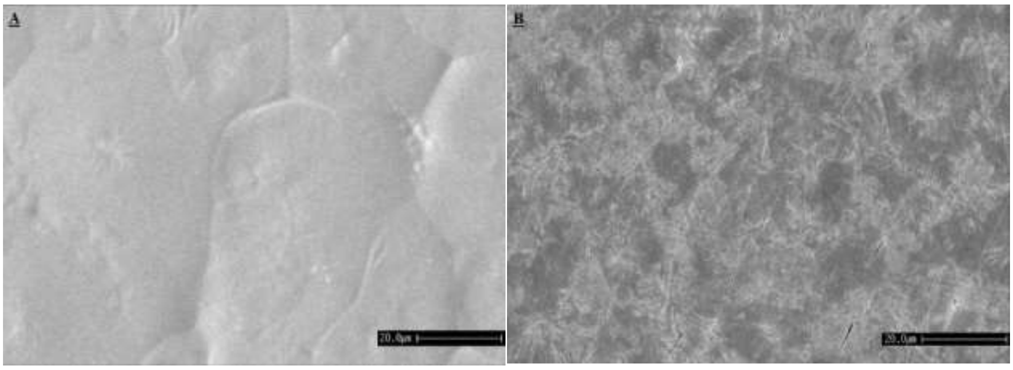

Figure. 4 *SEM images of the PLA/rGO composite before (A) and after (B) surface modification.*

4.4 Optical Microscopy (OM) Analysis

In Figure 5, the surface of the PLA/rGO scaffold underwent a transformation into a rough surface after surface modification with NaOH 1 M. This alteration can be attributed to the chemical etching of the PLA surface. The surface degradation induced by the NaOH solution resulted in increased surface roughness, consequently enhancing the contact angle and promoting the hydrophilicity of the composite [19].

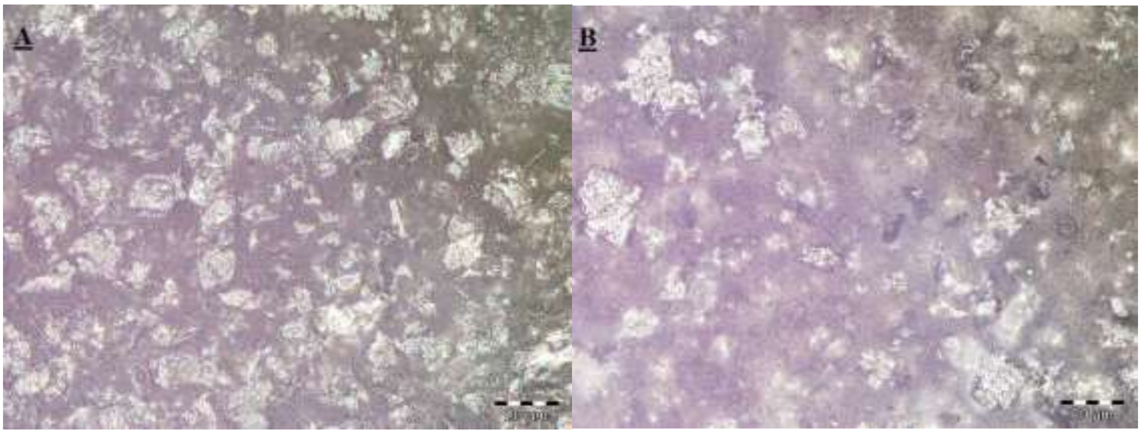

Figure 5. *Optical Microscopy images of the PLA/rGO composite before (A) and after (B) surface modification.*

5. Conclusions

This study systematically examined how varying NaOH solution concentrations and modification durations affect the surface, physical, and chemical properties of PLA- rGO composites. The preparation process commenced with the synthesis of rGO, which was incorporated into the PLA matrix at a 1% concentration. The composite was fabricated using a solution casting method and subsequently cut into 10 mm × 10 mm pieces for detailed analysis.

Contact angle measurements revealed that surface modification using a 1 molar NaOH solution for 1 hour decreased the contact angle to 62.5 degrees, enhancing surface wettability. However, modification with 2 molar NaOH 2M for 1 hour slightly increased the contact angle to 76.6 degrees. The surface treatment using a 3 molar NaOH solution for 1 hour resulted in a significant increase in the contact angle to 84 degrees, suggesting a trend toward increased hydrophobicity with higher NaOH concentrations. These findings suggest that while NaOH treatment can effectively alter surface properties, the concentration and duration of exposure play critical roles in determining the final wettability and surface characteristics of PLA/rGO composites.

The surface morphology of the composite was examined using both OM and SEM. The SEM images indicated significant changes in the surface morphology compared to the unmodified samples. An increase in surface roughness was expected, with the formation of grooves, pits, and depressions of varying sizes and depths which were approved through the SEM examination at higher magnifications. As observed in the report, the optical microscopy images corroborated these findings.

The results obtained from ATR-FTIR analysis of the polylactic acid composite modified with sodium hydroxide indicated a change in the intensity of the characteristic peaks associated with ester linkage in PLA after surface modification with NaOH. This suggests a change in the molecular structure of the polymer chains. This result implies the possible breaking C-O-C bonds within the polymer chain.

In summary, based on the results of this research, the improvement in surface properties and wettability makes the application of these composites in tissue engineering promising. Having suitable substrate materials for biomedical applications, from the standpoint of chemical and physicochemical properties, in the field of tissue repair does not fulfill all the necessary application requirements. Achieving these properties at the point of impact, which is the target tissue environment, often encounters significant challenges such as the application of biological interface compounds or biological responses like immune system reactions. Despite of the sucess of this research in decreasing of hydrophobicity of PLA-rGO composites through NAOH chemical etching, applying the composites in neural tissue engineering needs more chemical and physicochemical modification such as plasma surface treatment and In-Vitro biological researches in real condition.

References:

[1] I. Pattanayak, Y. Alex, and S. Mohanty, “Advancing strategies towards the development of tissue engineering scaffolds: a review,” *Journal of Materials Science 2023 58:32*, vol. 58, no. 32, pp. 12847–12898, Aug. 2023, doi: 10.1007/S10853-023-08798-5.

[2] G. Kandhola *et al.*, “Nanomaterial-Based Scaffolds for Tissue Engineering Applications: A Review on Graphene, Carbon Nanotubes and Nanocellulose,” *Tissue Eng Regen Med*, vol. 20, no. 3, pp. 411–433, Jun. 2023, doi: 10.1007/S13770-023-00530-3/METRICS.

[3] A. Indurkar, A. Pandit, R. Jain, and P. Dandekar, “Plant-based biomaterials in tissue engineering,” *Bioprinting*, vol. 21, p. e00127, Mar. 2021, doi: 10.1016/j.bprint.2020.e00127.

[4] J. D. Jovanovic, S. N. Blagojevic, and B. K. Adnadjevic, “The Effects of rGO Content and Drying Method on the Textural, Mechanical, and Thermal Properties of rGO/Polymer Composites,” *Polymers (Basel)*, vol. 15, no. 5, p. 1287, Mar. 2023, doi: 10.3390/polym15051287.

[5] S. Singh, S. Kumar, and V. Khanna, “A review on surface modification techniques,” *Mater Today Proc*, Jan. 2023, doi: 10.1016/j.matpr.2023.01.010.

[6] A. F. Ahmad *et al.*, “Chemically Reduced Graphene Oxide-Reinforced Poly(Lactic Acid)/Poly(Ethylene Glycol) Nanocomposites: Preparation, Characterization, and Applications in Electromagnetic Interference Shielding.,” *Polymers (Basel)*, vol. 11, no. 4, Apr. 2019, doi: 10.3390/polym11040661.

[7] J. Shi *et al.*, “Crystallinity Dependence of PLLA Hydrophilic Modification during Alkali Hydrolysis,” *Polymers (Basel)*, vol. 15, no. 1, p. 75, Jan. 2023, doi: 10.3390/POLYM15010075/S1.

[8] M. Schneider *et al.*, “Surface Etching of 3D Printed Poly(lactic acid) with NaOH: A Systematic Approach,” *Polymers (Basel)*, vol. 12, no. 8, p. 1711, Jul. 2020, doi: 10.3390/polym12081711.

[9] M. A. Kaysar *et al.*, “Impact of NaOH Treatment on the Chemical, Structural, Physico-mechanical, and Thermal Characteristics of Jute Species,” *Fibers and Polymers*, vol. 25, no. 5, pp. 1765–1777, May 2024, doi: 10.1007/S12221-024-00542-3/METRICS.

[10] S. S. Park *et al.*, “Facile Surface Treatment of 3D-Printed PLA Filter for Enhanced Graphene Oxide Doping and Effective Removal of Cationic Dyes,” *Polymers 2023, Vol. 15, Page 269*, vol. 15, no. 2, p. 269, Jan. 2023, doi: 10.3390/POLYM15020269.

[11] R. Donate, M. E. Alemán-Domínguez, and M. Monzón, “On the Effectiveness of Oxygen Plasma and Alkali Surface Treatments to Modify the Properties of Polylactic Acid Scaffolds,” *Polymers 2021, Vol. 13, Page 1643*, vol. 13, no. 10, p. 1643, May 2021, doi: 10.3390/POLYM13101643.

[12] M. Choi *et al.*, “Surface Modification of Sulfur-Assisted Reduced Graphene Oxide with Poly(phenylene sulfide) for Multifunctional Nanocomposites,” *Polymers (Basel)*, vol. 14, no. 4, p. 732, Feb. 2022, doi: 10.3390/polym14040732.

[13] S.-S. Park *et al.*, “Facile Surface Treatment of 3D-Printed PLA Filter for Enhanced Graphene Oxide Doping and Effective Removal of Cationic Dyes,” *Polymers (Basel)*, vol. 15, no. 2, p. 269, Jan. 2023, doi: 10.3390/polym15020269.

[14] D. Yadav, G. R. Selokar, A. Agrawal, V. Mishra, and I. A. Khan, “Effect of Concentration of NaOH Treatment on Mechanical Properties of Epoxy/Sisal Fiber Composites,” *IOP Conf Ser Mater Sci Eng*, vol. 1017, no. 1, p. 012028, Jan. 2021, doi: 10.1088/1757-899X/1017/1/012028.

[15] S. Sitthisang *et al.*, “Nanomechanical mapping of PLA hydroxyapatite composite scaffolds links surface homogeneity to stem cell differentiation,” *Sci Rep*, vol. 14, no. 1, p. 21097, Sep. 2024, doi: 10.1038/s41598-024-72073-z.

[16] A. Behnamghader, M. Poostchi, and S. Hosseinpour, “Comparison of the effect of oxygen and nitrogen plasma treatments on the surface activation of PLA/rGO composites,” *Surfaces and Interfaces*, vol. 51, p. 104741, Aug. 2024, doi: 10.1016/j.surfin.2024.104741.

[17] G. Fredi, M. Karimi Jafari, A. Dorigato, D. N. Bikiaris, and A. Pegoretti, “Improving the Thermomechanical Properties of Poly(lactic acid) via Reduced Graphene Oxide and Bioderived Poly(decamethylene 2,5-furandicarboxylate),” *Materials*, vol. 15, no. 4, p. 1316, Feb. 2022, doi: 10.3390/ma15041316.

[18] A. Abdulkareem *et al.*, “Surface Modification of Poly(lactic acid) Film via Cold Plasma Assisted Grafting of Fumaric and Ascorbic Acid.,” *Polymers (Basel)*, vol. 13, no. 21, Oct. 2021, doi: 10.3390/polym13213717.

[19] M. Inchingolo *et al.*, “Polycaprolactone in Bone Tissue Engineering: A Comprehensive Review of Innovations in Scaffold Fabrication and Surface Modifications,” *Journal of Functional Biomaterials 2024, Vol. 15, Page 243*, vol. 15, no. 9, p. 243, Aug. 2024, doi: 10.3390/JFB15090243.

The 30th Iranian Seminar of Organic Chemistry
February 7-9, 2025, Iran University of Science and Technology, Tehran, Iran

Synthesis of carbon quantum dots using aquatic organism waste and investigation of its chemical, physical and optical properties in a hydrogel substrate

Authors: Sara Zadehsebardi[a], Shiva Molaei[a], Ghazaleh Mirzaei[a], Mohsen Omrani[b], Shahrzad Javanshir*[a], M-Reza Naimi-Jamal*[b]

[a]*Heterocyclic Chemistry Research Laboratory, Department of Chemistry, Iran University of Science and Technology, Tehran, 16846-13114, Iran*

[b]*Research Laboratory of Green Organic Synthesis and Polymers, Department of Chemistry, Iran University of Science and Technology, Narmak, Tehran, Iran*

Keyword: Carbon quantum dots, Hydrogel, Drug delivery, Doxorubicin, Cancer therapy

This research explores the interdisciplinary integration of Quantum-Hydrogel composites and smart materials and their applications in a range of fields, including biomedicine. The Hydrogel is composed of Carboxymethyl cellulose and Polyvinyl alcohol, and Carbon Quantum Dots extracted from natural sources were used in its construction. The synthesized Hydrogel has been used for targeted drug delivery of the drug Doxorubicin to treat cancer tumors.

1. Introduction

Conventional and traditional cancer treatments include surgical intervention, through which tumor tissues can be directly or partially destroyed. Radiotherapy may be used synergistically with chemotherapy or alone for local treatments, or as an adjuvant to surgical treatment. Chemotherapy, widely used as an adjuvant therapy, can be administered before or after surgery or for cancers that may be unsuitable for surgical intervention. It is characterized by its ability to work throughout the body rather than in a localized area alone.

Novel drug delivery systems that exhibit excellent properties for loading, releasing, tracking, and targeting chemotherapeutic drugs are gaining increasing importance. In recent years, the development of nanotechnology-based cancer therapies has accelerated rapidly, utilizing graphene, quantum dots, carbon nanotubes, dendrimers, liposomes, and nanoparticles as drug delivery agents. Carbon quantum dots (CQDs), composed mainly of carbon, can be prepared using a green synthetic strategy and non-toxic chemicals, including environmentally friendly solvents. Recently, the use of carbon quantum dots in cancer therapy has shown impressive results due to their attractive properties, such as biocompatibility and low toxicity.[1-3]

Delivery using injectable biodegradable hydrogels has also attracted significant attention because they can provide continuous and controlled delivery of the drug to the target tumor site while minimizing the adverse effects of systemic drug exposure. Furthermore, local treatment with injectable hydrogels can reduce the amount of drug required and increase the quantity that reaches the tumor site.[1-3]

2. Methodology

In this study, we have used the preparation of a drug composite with antitumor properties (Hydrogel/CQD/DOX), with the aim of providing a new and efficient strategy for cancer treatment. Carbon quantum dots prepared from the bones of aquatic organisms and a Hydrogel prepared from Carboxymethyl cellulose(CMC) and Polyvinyl alcohol(PVA) were combined to form a hydrogel with fluorescent properties. This nanocomposite was used as a drug carrier with high fluorescence properties for the drug Doxorubicin (DOX). (Figure 1)

3. Result and discussion

Through a wide range of analytical techniques such as FT-IR, PL, FE-SEM, TGA, UV-VIS, Zeta Potential, the swelling of the hydrogel, the loading and release of the drug were investigated. The results showed that the particle size was below 10 nm and the drug release continued to 89.74% in 144 hours in a tumor simulation environment.

4. Conclusion

In general, drug delivery systems are more likely to have slow and controlled release in addition to high loading. This hydrogel/carbon quantum dot had all of these characteristics and could be a very suitable and promising option in the future for drug delivery, especially in the field of cancer drugs.

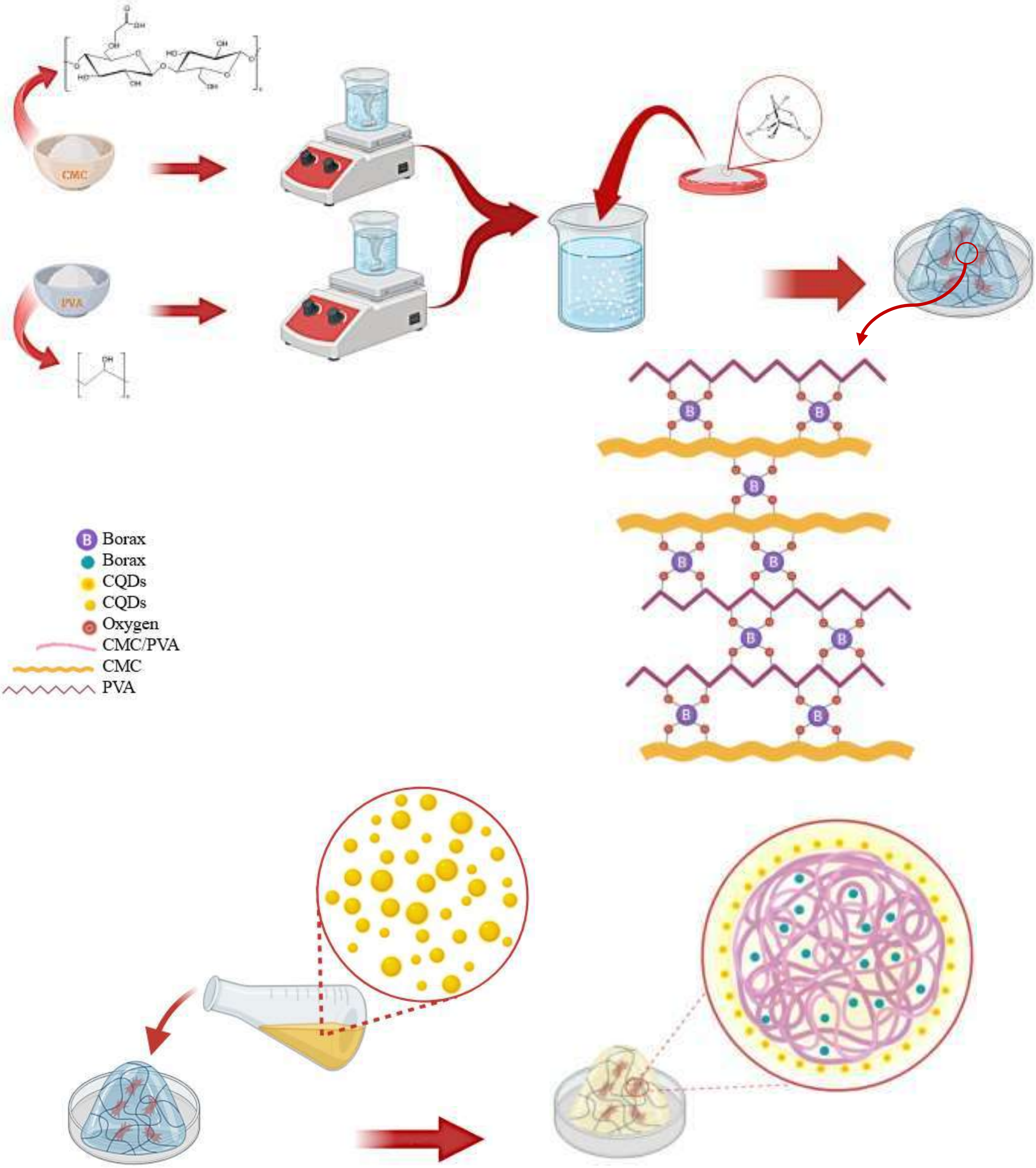

(Figure 1) Image of the synthesis of Hydrogel/CQDs and its structure

References:

١. Yuan, Y., et al., *Doxorubicin-loaded environmentally friendly carbon dots as a novel drug delivery system for nucleus targeted cancer therapy.* Colloids and Surfaces B: Biointerfaces, 2017. **159**: p. 349-359.
٢. Norouzi, M., B. Nazari, and D.W. Miller, *Injectable hydrogel-based drug delivery systems for local cancer therapy.* Drug discovery today, 2016. **21**(11): p. 1835-1849.
٣. Bhattacharya, T., G.H. Shin, and J.T. Kim, *Carbon dots: Opportunities and challenges in cancer therapy.* Pharmaceutics, 2023. **15**(3): p. 1019.

The 30th Iranian Seminar of Organic Chemistry
February 7-9, 2025, Iran University of Science and Technology, Tehran, Iran

Magnetic silica supported Schiff-base/Fe complex as a durable and efficient catalyst for the synthesis of pyrazolo[b]phthalazine diones

Afsaneh Sadatzadeh, Dawood Elhamifar*, Shiva Kargar, and Fatemeh Kiani

Department of Chemistry, Yasouj University, Yasouj, 75918-74831, Iran

Keyword: Magnetic nanocatalyst, Schiff-base, Pyrazolo[b]phthalazine diones

Introduction

Pyrazolo[b]phthalazine diones are one of the most significant compounds that considered the main structure of many biological materials. To date, several methods for the production of these compounds have been developed. However, the most of these approaches exhibit limitations such as challenging product and catalyst separation, low yields, harsh reaction conditions, and long reaction times. Magnetic nanocomposite materials have gained significant attention as the supporting materials for the homogeneous catalysis because there is no need for tedious separation methods such as centrifugation, extraction, and filtration and can be recovered rapidly by using an external magnet. Meanwhile, Schiff-base ligands have attracted considerable interest in the fields of chemistry and materials science due to their effective complexation with diverse transition metal ions, exceptional solubility, and outstanding catalytic efficacy. Accordingly, herein, magnetic core-shell structured silica supported Schiff-base/Fe is prepared and applied as an efficient catalyst for the synthesis of pyrazo(b)phthalazines.

Method

Firstly Fe_3O_4@silica was dispersed in toluene at 25 °C. After complete dispersion of this material, 3-aminopropyltrimethoxysilane was added and the obtained mixture was refluxed for 24 h. The solid material was then collected with a magnet, and dried at 70 °C. Next, Fe_3O_4@silica-NH_2 was dispersed in toluene at 25 °C. Subsequently, isatin was added to the reaction vessel and this was refluxed for 24 h. Afterwards, it was collected, dried at 70 °C and denoted as Fe_3O_4@silica/SB. Next, the Fe_3O_4@silica/SB was added in DMSO while sonicating at 25 °C. Next, it was treated with $FeCl_3.6H_2O$ and allowed to stir at 25 °C for 24 h and denoted as Fe_3O_4@silica/SB-Fe.

Results and Discussion

The FTIR measurement of all samples indicated a distinct absorption peak for the Fe-O bond at 584 cm-1 and a stretching vibration of the O-H bond at 3425 cm^{-1}. The absorption bands were obtained at 2859–2934 and 1458 cm^{-1}, corresponding to the aliphatic C-H stretching and bending vibrations of the propyl amines and silica. The successful surface modification of Fe_3O_4@silica with (3-aminopropyl)trimethoxysilane was confirmed by the presence of the Si–O–Si signals at 809 and 1025 cm^{-1} (Figures 1b-1c). Furthermore, the peak appeared at 1618 cm^{-1} corresponds to the C=N bond, showing that the isatin-Schiff-base (SB) ligand was successfully immobilized onto the material surface (Figures 1b and 1c).

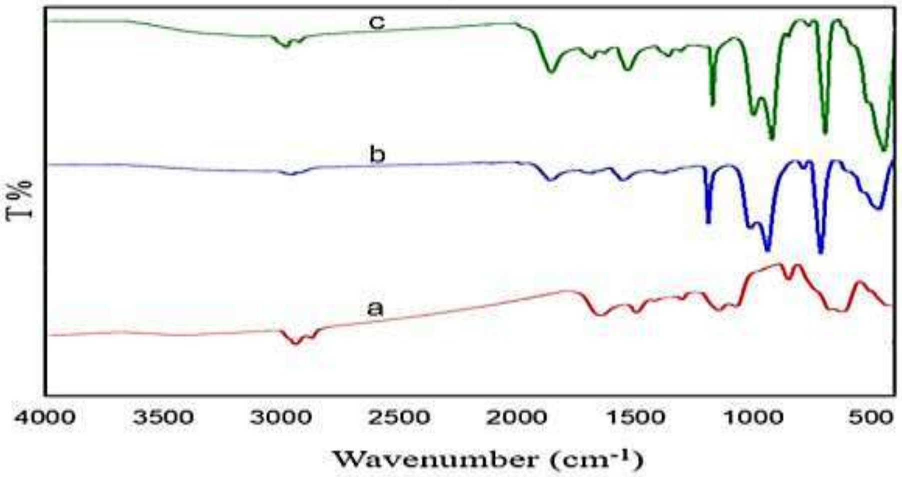

Figure 1. The FTIR of a) Fe_3O_4@silica-NH_2, (b) Fe_3O_4@silica/SB and (c) Fe_3O_4@silica/SB-Fe

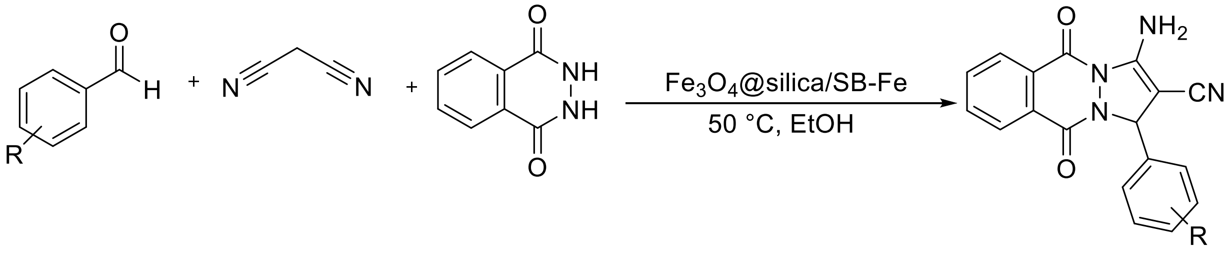

Entry	Aldehyde	Time (min)	Yield (%)
1	C_6H_5	25	95
2	4-Me-C_6H_4	45	84
3	4-Br-C_6H_4	30	92

References:

[1] B. Szczęśniak, J. Choma, M. Jaroniec, Gas adsorption properties of graphene-based materials, Adv Colloid Interface Sci 243 (2017) 46–59.

[2] M.-C. Liu, Y. Xu, Y.-X. Hu, Q.-Q. Yang, L.-B. Kong, W.-W. Liu, W.-J. Niu, Y.- L. Chueh, Electrostatically charged MoS2/graphene oxide hybrid composites for excellent electrochemical energy storage devices, ACS Appl Mater 10 (2018) 35571–35579.

[3] S. Kumari, A. Shekhar, D.D. Pathak, Graphene oxide–TiO2 composite: an efficient heterogeneous catalyst for the green synthesis of pyrazoles and pyridines, New J Chem 40 (2016) 5053–5060.

The 30th Iranian Seminar of Organic Chemistry

February 7-9, 2025, Iran University of Science and Technology, Tehran, Iran

Magnetic silica supported amine/H$_3$PW$_{12}$O$_{40}$: An effective and extremely stable nanocatalyst for the synthesis of pyrano[2,3-d]pyrimidines

Shiva Kargar, Dawood Elhamifar* and Fatemeh Taheri

Department of Chemistry, Yasouj University, Yasouj, 75918-74831, Iran

Keyword: Magnetic composite, Nanocatalyst, Pyrano[2,3-d]pyrimidine, Phosphotungstic acid

Introduction

Heteropolyacids (HPAs) are a category of polyoxometalates (POMs) that have been widely employed as effective catalysts owing to their superior electron capture, solubility in polar solvents, and remarkable stability. The Keggin type heteropolyacid (KHPA)-based catalysts have gained significant attention owing to their high Brønsted and Lewis acidity, resistance to corrosion, excellent thermal stability, and structural variety [1]. For instance, 12-tungstophosphoric acid (H3PW12O40, PTA) is a KHPA that has been widely used as a superacid catalyst in several chemical and industrial processes. Meanwhile, magnetic materials with outstanding advantages of high thermochemical stability, biocompatibility, easy functionalization and high surface area have also gained interest as promising supports for PTAs [2]. On the other hand, pyrano[2,3-d]pyrimidines, are among the most significant compounds in the field of organic chemistry due to their anticancer, antifungal, spasmolytic, antimalarial, and anticoagulant properties [3]. Accordingly, herein, a novel magnetic silica supported propylamine/H3PW12O40 is prepared and has been applied as an effective catalyst for the synthesis of pyrano[2,3-d]pyrimidines.

Method

Firstly, $Fe_3O_4@SiO_2$ was dispersed in toluene for 15 min. Then it was treated with 3-aminopropyltrimethoxysilane and refluxed for 24 h. The resulting material was magnetically separated, washed with EtOH and water, and dried at 70 °C for 6 h. Then, the resulting $Fe_3O_4@SiO_2$/Ap was dispersed in methanol for 20 min. Next, the heteropoly phosphotungstic acid was added to the reaction vessel, and it was allowed to reflux for 12 h. The product was separated magnetically, washed with water and EtOH, dried at 70 °C, and denoted as $Fe_3O_4@SiO_2$/Ap-PTA.

Results and Discussion

FT-IR analysis was conducted to identify the functional groups in the synthesized nanomaterials. For all samples, the peaks observed at 3388 and 575 cm^{-1} are assigned to the OH and Fe–O bands, respectively. Also, the peaks at 826 and 1080 cm-1 are due to the Si–O–Si bonds, indicating the formation of the SiO_2 shell. The successful grafting of 3-aminopropyltrimethoxysilane was confirmed by C–H bond vibrations at 2856–2898 cm^{-1}. Additionally, the characteristic peaks of W=O (941 cm-1) and W–O–W (806 cm-1) prove the successful immobilization of $H_3PW_{12}O_{40}$ onto the material surface (Figure 1c).

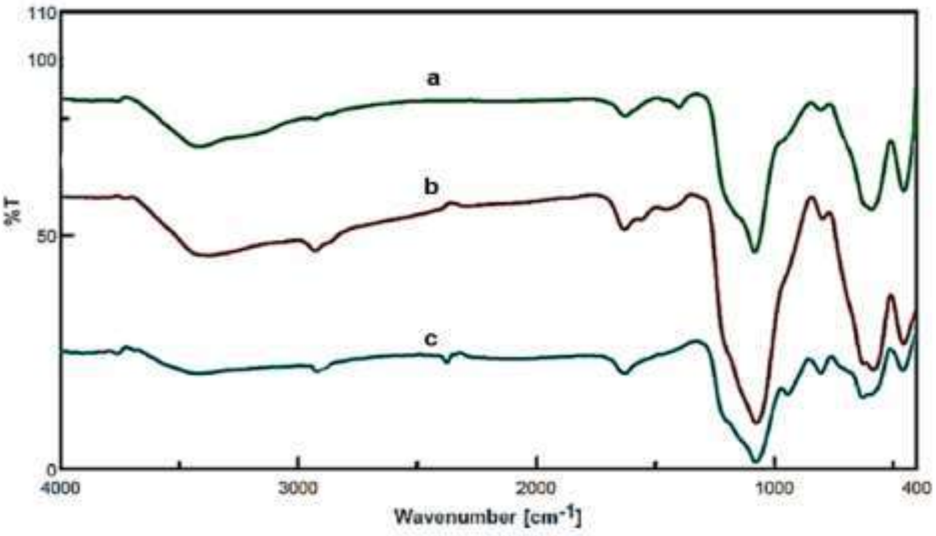

Figure 1. FT-IR spectra of a) $Fe_3O_4@SiO_2$ b) $Fe_3O_4@SiO_2$/AP c) $Fe_3O_4@SiO_2$/AP-PTA

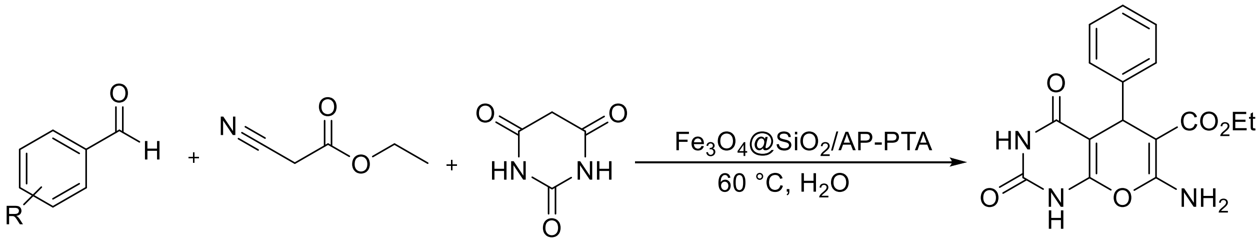

Entry	Aldehyde	Time (min)	Yield (%)
1	C_6H_5	30	93

2	4-Me-C_6H_4	55	81
3	4-Cl-C_6H_4	20	96

References:

[1] D. Wang, L. Liu, J. Jiang, L. Chen, J. Zhao, Polyoxometalate-based composite materials in electrochemistry: state-of-the-art progress and future outlook, Nanoscale 12 (2020) 5705–5718.

[2] Y.L. Hu, J.R. Li, C. Chen, X.B. Liu, Q. Rong, Novel and sustainable synthesis of tetrahydrobenzo [b] pyrans using magnetic zinc ferrites modified SBA-15 supported ionic liquids as efficient and reusable catalysts, Sustain. Chem. Pharm. 29 (2022), 100779.

[3] M. Biglari, F. Shirini, N.O. Mahmoodi, M. Zabihzadeh, M. Mashhadinezhad, A choline chloride-based deep eutectic solvent promoted three-component synthesis of tetrahydrobenzo [b] pyran and pyrano [2, 3-d] pyrimidinone (thione) derivatives, J. Mol. Struct. 1205 (2020), 127652.

The 30th Iranian Seminar of Organic Chemistry
February 7-9, 2025, Iran University of Science and Technology, Tehran, Iran

Magnetic core-shell structured silica supported Cu complex as a highly stable nanocatalyst for the synthesis of tetrahydrobenzo[b]pyrans

Parivash Bazmayoun, Dawood Elhamifar* and Shiva Kargar

Department of Chemistry, Yasouj University, Yasouj, 75918-74831, Iran

Keyword: Magnetic composite, Nanocatalyst, Tetrahydrobenzo[b]pyran, Core-shell

Introduction

Magnetic nanocomposites are important group of nanomaterials that have a variety of applications, including catalysis, drug delivery, plasmonics, and magnetic resonance imaging (MRI). However, due to their sensitivity to acidic and basic environments and their tendency to aggregate, the stability of Fe_3O_4 NPs has remained a challenge [1]. Therefore, a protection layer is required as the stabilizer, which prevents direct contact between the nanoparticles and prevent them from oxidation. Among different shells, silica shells with adjustable porous structure have gained a lot of attention due to their high surface area and accessible pore volume

[2]. On the other hand, tetrahydrobenzo[b]pyrans are very important in the preparation of biologically active compounds with anti-bacterial, antitumor, anti-allergic, and anti-cancer properties [3]. Accordingly, herein, a novel magnetite core-shell structured silica supported Cu complex is prepared and has been applied as an effective catalyst for the synthesis of pyrans and delivered corresponding products in high yields.

Method

Firstly, Fe_3O_4 nanoparticles were dispersed in a mixture of water and ethanol at 25 ℃. The ammonia, TMOS (0.6 mL) was added dropwise, and the mixture was stirred for an additional 2 h. The mixture was then heated to 100 °C under static conditions for 72 h, and then it was magnetically collected, and dried at 70 ℃. The resulting Fe_3O_4@SiO_2 nanocomposite was then dispersed in toluene at 25 ℃. (Methyl-propyl)-imidazolium chloride ionic liquid was added, and it was refluxed for 24 h. The solid material was collected and dried at 70 ℃. Finally, Fe_3O_4@SiO_2/IL was dispersed in DMSO at 25 ℃, followed by the addition of $Cu(OAc)_2$. The mixture was stirred for 24 h, and the resulting material was magnetically collected and dried at 70 ℃.

Results and Discussion

All samples showed two peaks at 3386 and 578 cm^{-1}, corresponding to the O-H and Fe-O bonds, respectively. Additionally, the signals at 2923, 2857, and 1446 cm^{-1} are attributed to the vibrations of CH_2 moieties. It is also important to note that the successful surface modification with the SiO_2 shell was proved by the appearance of the Si–O–Si bonding peaks at 1087 and 817 cm^{-1} (Figure 1b and 1c). Also, the characteristic peak of C=N bonds at 1690 cm^{-1} confirming successful grafting of IL onto the material surface (Fig. 1c).

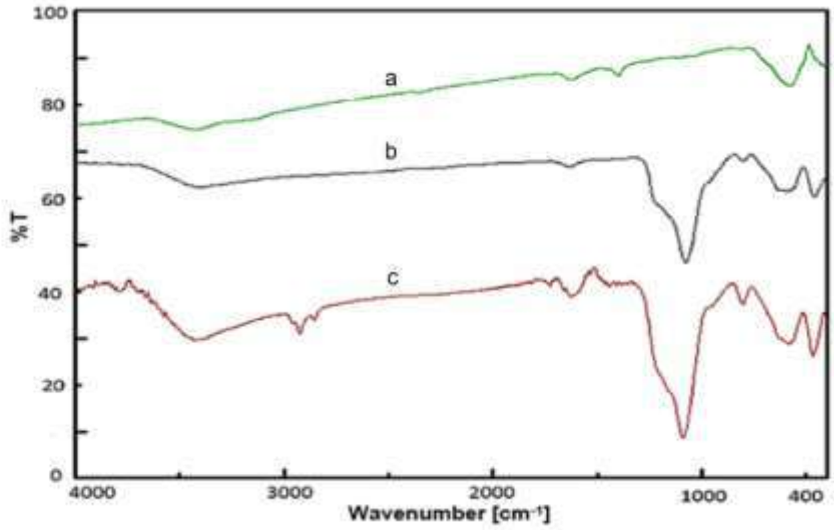

Figure 1. FT-IR spectra of a) Fe_3O_4@SiO_2 b) Fe_3O_4@SiO_2/IL c) Fe_3O_4@SiO_2/IL-Cu

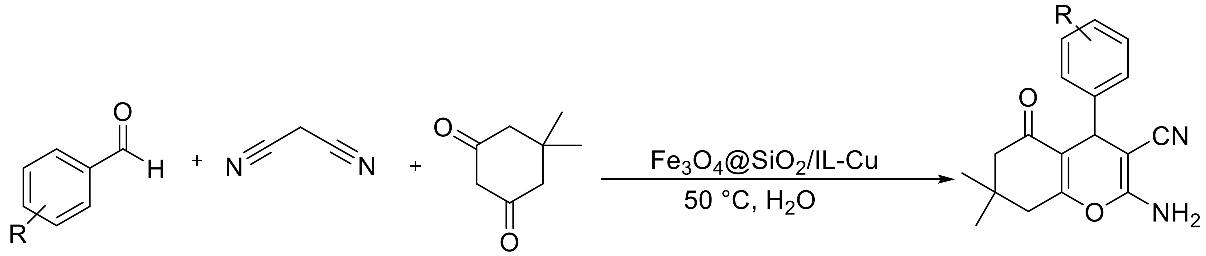

Entry	Aldehyde	Time (min)	Yield (%)
1	C_6H_5	25	96
2	4-Me-C_6H_4	45	87
3	4-MeO-C_6H_4	55	85

References:

[1] R. Mirbagheri, D. Elhamifar, J. Alloys Compd., 2019, 790, 783.

[2] S. P. Schwaminger, R. Surya, S. Filser, A. Wimmer, F. Weigl, P. Fraga-García, S. Berensmeier, Sci. Rep., **2017**, 7, 12609.

[3] W. Wu, Z. Wu, T. Yu, C. Jiang, W.-S. Kim, Sci. Technol. Adv. Mater., **2015**, 16, 023501.

The 30th Iranian Seminar of Organic Chemistry
February 7-9, 2025, Iran University of Science and Technology, Tehran, Iran

Graphene oxide supported IL/Mo complex as a highly stable and robust nanocatalyst for the synthesis of tetrahydrobenzo[b]pyrans

Yasaman Daghagheleh, Dawood Elhamifar* and Shiva Kargar

Department of Chemistry, Yasouj University, Yasouj, 75918-74831, Iran

Keyword: Graphene oxide, Nanocatalyst, Tetrahydrobenzo[b]pyran, Ionic liquid

Introduction

Graphene-based carbon nanomaterials have gained significant attention for their stability, thermal conductivity, and mechanical strength, with applications in catalysis, adsorption, and electronics. The large surface area of graphene and its π-electron system make it a promising catalyst support, but its practical use is limited by sheet stacking due to π-π interactions and van der Waals forces [1]. Graphene oxide (GO), with its hydrophilic functional groups (e.g., hydroxyl, epoxide, carboxyl), overcomes these limitations by preventing aggregation and increasing interlayer spacing. These groups also enable chemical functionalization, making GO a highly attractive material for catalyst support [2]. Meanwhile, Ionic liquids (ILs) due to their thermal stability, tunable hydrophobicity, negligible vapor pressure, and high conductivity have gained considerable attention. Moreover, their polar and ionic properties make them excellent stabilizers for charged and polar catalysts, including transition metal complexes. Accordingly, Herein, graphene oxide supported IL/Mo complex is prepared and applied as a robust catalyst for the synthesis of tetrahydrobenz[b]pyrans.

Method

Firstly, GO was synthesized using the modified Hummers method. For preparation of GO/IL, GO was ultrasonically dispersed in toluene, mixed with 1-methyl-3(3-trimethoxysilylpropyl)-imidazolium chloride, and refluxed for 24 h. The resulting material was filtered, washed with water and EtOH and dried at 70 °C for 7 h. Next, GO-IL was dispersed in acetone (30 mL). After 20 min, the $MoO_2(acac)_2$ was added to the reaction vessel and it was allowed to stir at 25 °C for 24 h. The product was filtered, washed with water and EtOH, dried at 70 °C, and designated as GO-IL/Mo.

Results and Discussion

FT-IR analysis identified functional groups in the materials. For GO, a strong peak at 3500 cm^{-1} corresponds to OH stretching. The other peaks at 1725, 1623, 1288, and 1078 cm^{-1} are attributed to carboxyl (C=O), aromatic (C=C), epoxy (–C–O), and alkoxy (–C–O) groups, respectively (Figure 1a-1c). GO/IL displayed aromatic and aliphatic C–H bands at 3124 and 2943 cm^{-1}, along with Si–O and C=C bands at 1034 and 1645 cm^{-1}, confirming ionic liquid grafting (Figure 1b and 1c). In GO/IL-Mo, the Mo=O bands at 906 and 942 cm^{-1} confirm successful MoO2(acac)2 immobilization (Figure 1c).

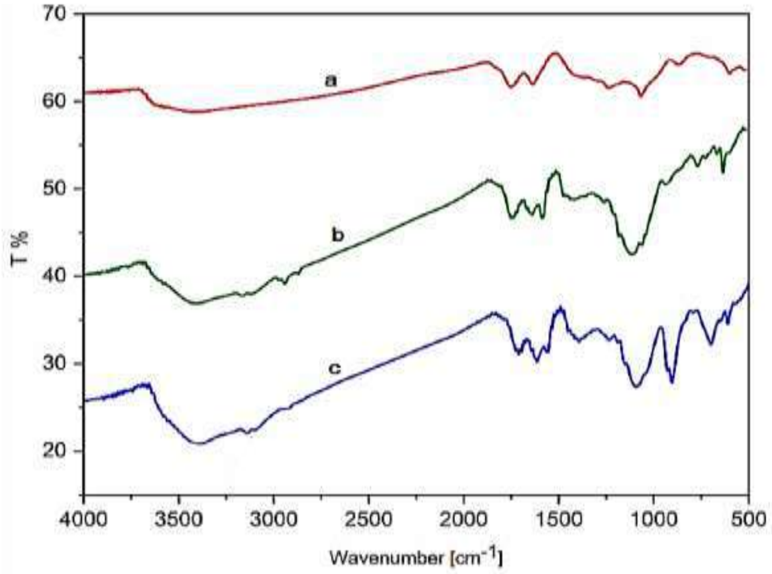

Figure 1. FT-IR spectra of a) GO b) GO/IL c) GO/IL-Mo

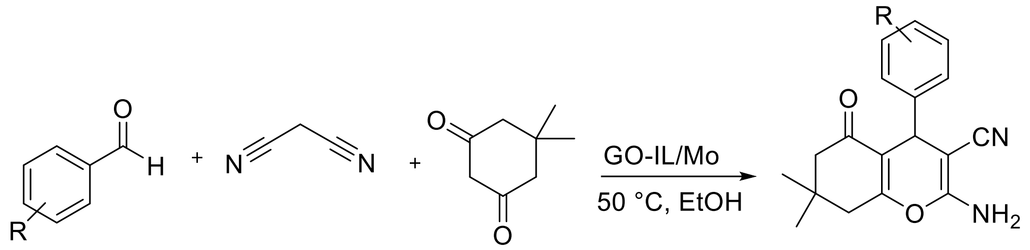

Entry	Aldehyde	Time (min)	Yield (%)
1	C_6H_5	25	93
2	4-Me-C_6H_4	50	88
3	4-MeO-C_6H_4	60	90

References:

[1] M. Jafary-Zadeh, Y.-W. Zhang, Molecular mobility on graphene nanoroads, Sci Rep 5 (2015) 12848. [2] P.L. Yap, S. Kabiri, Y.L. Auyoong, D.N. Tran, D. Losic, Tuning the Multifunctional Surface Chemistry of Reduced Graphene Oxide via Combined Elemental Doping and Chemical Modifications, ACS omega 4 (2019) 19787–19798.

[3] M. Piltan, Preparation of 1H-pyrazolo [1, 2-b] phthalazine-5, 10-diones using ZrO2 nanoparticles as a catalyst under solvent-free conditions, Heterocyclic Communications 23 (2017) 401–403.

The 30th Iranian Seminar of Organic Chemistry

February 7-9, 2025, Iran University of Science and Technology, Tehran, Iran

Mechanistic Insights into Flavin Reductase-Catalyzed Tetraketone Synthesis: Role of Serine 49 in Enzyme Promiscuity

Authors: Hamid Reza Kalhor [a], and Amene Navaser [a]

a) Biochemistry and Chemical Biology Research Laboratory, Chemistry Department, Sharif University of Technology, Tehran, Iran, kalhor@sharif.edu
Amenenavaser@gmail.com

Keyword: biocatalysis, hydrogen bond, site-directed mutagenesis, enol formation.

Biocatalysis, the use of enzymes as catalysts, has emerged as a transformative approach in the synthesis of organic compounds due to its high specificity, selectivity, and environmental sustainability [1]. Enzymes, which drive almost all biochemical reactions in living organisms, offer significant advantages over traditional chemical catalysts, including mild reaction conditions and fewer by-products. A particularly intriguing aspect of enzymatic catalysis is enzyme promiscuity, which refers to the ability of an enzyme to catalyze reactions with non-native substrates or catalyze multiple reaction types at a single active site. This phenomenon expands the scope of enzyme applications beyond their natural functions [2]. Enzyme promiscuity has gained substantial attention for its potential in drug discovery, chemical synthesis, and industrial applications, particularly within the pharmaceutical and fine chemical industries. The development of promiscuous enzymes is enabling the creation of novel synthetic routes, offering a sustainable alternative to traditional chemical processes.

Flavin reductase (EC 1.5.1.30) from *Escherichia coli* is an NAD(P)H-dependent enzyme that catalyzes the reduction of riboflavin. In previous studies, we demonstrated that recombinant flavin reductase, in the absence of NADH, is capable of catalyzing the Knoevenagel-Michael addition cascade, resulting in the production of tetraketones. In the present work, we further investigated the mechanism of this enzymatic reaction and identified the key residues involved through both experimental and computational approaches. Molecular docking and molecular dynamics simulations were employed to pinpoint critical residues that contribute to tetraketone synthesis. Site-directed mutagenesis experiments revealed that the side chain of serine 49 forms a hydrogen bond with the carbonyl oxygen of dimedone, thereby facilitating enol formation and promoting the reaction. These findings provide deeper insight into the catalytic mechanism of flavin reductase and its potential for synthetic applications.

References:

Carette, Noëlle, et al., *Nature nanotechnology*, 2007.

Taglieber, Andreas, et al., *Angewandte Chemie*, 2007.

Tawfik, Dan S., *The FEBS journal*, 2020.

Navaser, Amene, Hamid R. Kalhor, and Fatemeh Hayati., *Heliyon*, 2023.

The 30th Iranian Seminar of Organic Chemistry
February 7-9, 2025, Iran University of Science and Technology, Tehran, Iran

Title: Bioinspired Versatile Lysine Modified Carbon Quantum Dot Catalysis in Organic Synthesis Using Earth-abundant Starting Materials

Authors: Hamid R. Kalhor*, Masumeh Salehi, Morteza Hasani

Kalhor@sharif.edu

Affiliations: Sharif University of Technology

Keyword: Organic Synthesis, CQD-catalysis, Bioinspired Catalysis, Enzyme Mimic, Carbonylation

Carbon Quantum Dots (CQDs) have recently been recognized as rising catalysts in organic synthesis. Their promising characteristics in catalysis make them potential candidates in place of metal- and organocatalysis [1]. We previously conceptualized that the long amino arm of lysine residue could provide catalytic accessibility to the substrates. As a result, a Lysine functionalized CQD was developed for the condensation of amines and urea [2]. Here, it was reported that Lys-CQD could be also a versatile catalyst in challenging organic reactions, mostly by using renewable and earth-abundant precursors. To that end, we disclosed the high efficiency of Lys-CQD catalysis in heightening the reactivity of chemically stable and yet naturally abundant carbonyl bearing precursors, such as DMF and urea. As a result, metal-free Lys-CQD catalyzed reaction of different aromatic amines with DMF was experimented. DMF was used both as the carbonyl bearing substrate and the solvent of the reaction, and the corresponding formamide products were synthesized in a sustainable manner. Next, aiming at providing a feasible synthetic route for some bioactive amide compounds, the condensation of different aniline derivatives with vinyl acetate was investigated. It was found that metal-free Lys-CQD catalyst is perfectly capable of catalyzing the reaction, thereby yielding a number of amide products in the reaction. As amide compounds are of paramount importance in medicinal chemistry, we also synthesized several known drugs, such as acedoben and acetaminophen in gram-scale synthesis. In brief, Lys-CQD catalyst could be recognized as a multi-functional catalyst in organic synthesis. In particular, it is a catalyst of great potential in sparking off the reactivity of carbonyl bearing molecules.

References:

[1] *ACS Catal.* 2021, 11, 17, 10778–10788.

[2] *ACS Catal.* 2020, 10, 15, 8090–8105.

The 30th Iranian Seminar of Organic Chemistry
February 7-9, 2025, Iran University of Science and Technology, Tehran, Iran

Degradation of ciprofloxacin antibiotic using Ga$_{5.0}$S$_{10.0}$@TiO$_2$@g-C$_3$N$_4$ as a high-performance visible light-activated photocatalyst

Razieh Nejat

Department of Chemistry, Kosar University of Bojnord, Bojnord, Islamic Republic of Iran

Fax: (+98)-58-3242740, phone: (+98)-58-32262863. P.O. Box 9415615458; Email: organochem.nejat@kub.ac.ir

**Corresponding author: organochem_nejat@yahoo.com*

Keyword: photocatalyst, ciprofloxacin, $Ga_{5.0}S_{10.0}$@TiO_2/g-C_3N_4.

Abstract— A unique photocatalyst was developed by combining Ga- and S-co-doped TiO_2 with graphitic carbon nitride (g-C_3N_4), resulting in the $Ga_{5.0}S_{10.0}$@TiO_2/g-C_3N_4 composite. This composite was effectively employed to degrade ciprofloxacin under visible-light irradiation. The $Ga_{5.0}S_{10.0}$@TiO_2/g-C_3N_4 composite outperformed bare g-C_3N_4 by up to three times. Experimental results showed that optimal degradation of ciprofloxacin (CIP) was achieved after 180 minutes using a concentration of 40 mg L^{-1} CIP and 0.1 g L^{-1} of $Ga_{5.0}S_{10.0}$@TiO_2/g-C_3N_4. This research provides valuable insights into the development of cost-effective co-catalysts that enhance the photocatalytic performance of established materials, contributing to improved efficiency in photocatalytic systems.

١. INTRODUCTION

Fluoroquinolone antibiotics (FQs) are extensively employed worldwide for disease treatment and animal husbandry. Among the most commonly used FQs, ciprofloxacin (CIP) has become a notable contaminant in aquatic ecosystems [1]. Due to its high production and widespread use, CIP concentrations can reach levels of mg L^{-1} in water; for example, measurements have indicated concentrations ranging from 0.848 to 5.286 mg L^{-1} in municipal sewage in Spain, with levels of 3.35, 2.10, and 5.93 mg L^{-1} found in animal farm effluent, pond water, and river water in Jiangsu Province, China, respectively. Furthermore, tap water in Guangzhou, China, has been reported to contain CIP levels between 6.0 and 679.7 ng L^{-1} [2-4]. However, it is estimated that 50% to 80% of these oral antibiotics are discharged into the environment, primarily through feces and urine, both in their active forms and as metabolites. Studies have shown that even trace levels of CIP (ng L^{-1}) can lead to increased bacterial resistance, potentially reducing the therapeutic effectiveness against pathogens in both humans and animals. Consequently, there is an urgent need to develop fast and effective treatment technologies to remove CIP from wastewater.

Conventional methods, such as adsorption and biological degradation, are insufficient for effectively removing ciprofloxacin (CIP) and reducing its toxicity. Moreover, the adsorbed CIP and activated sludge require additional treatment. In contrast, advanced oxidation processes (AOPs)—including chlorination, photocatalysis, and ozonation—are recognized for their effectiveness in degrading CIP due to their strong oxidation capacity and high selectivity. Notably, photocatalysis has garnered increasing attention because of its high efficiency and low cost [5-7].

g-C_3N_4 has emerged as an excellent metal-free photocatalyst, featuring stable physicochemical properties and an abundant material source. Recent studies have demonstrated its potential for photocatalytic degradation of synthetic dyes, including methyl orange and Rhodamine B.

Therefore, it is worthwhile to investigate the effectiveness of g-C_3N_4 for the photocatalytic degradation of antibiotics. The aim of this study is to develop a novel step-scheme photocatalyst, $Ga_{5.0}S_{10.0}$@TiO_2-g-C_3N_4, specifically engineered for the visible light-induced degradation of ciprofloxacin [8-10].

2. EXPERIMENTAL

2.1. Materials and Physical Techniques

In this work, chemicals were obtained from Merck, Sigma-Aldrich, and Fluka chemical companies and used without further purification. FTIR spectra obtained in the range of 4000 cm^{-1} to 400 cm^{-1} using a NICOLET IR100 spectrophotometer. UV/Vis diffusive reflectance (UV/Vis DRS) measurements were carried out using a Thermo Scientific Evolution 300/600 UV-Visible spectrophotometer (USA), following established protocols described in the literature. The light source used for the experiments had a specific wavelength of 360.0 nm. Visible illumination, on the other hand, was provided by a 400 W lamp, specifically a high-pressure mercury-vapor lamp, with a wavelength of 546.8 nm. All measurements were performed at room temperature. The sample was analyzed using a GC-MASS AGILENT 7890A gas chromatography instrument.

A solution was prepared by dissolving 0.1 mol of titanium isopropoxide in isopropanol, with acetic acid added to adjust the pH to 5. After stirring for 360 minutes, the sol was aged for 48 hours, air-dried at 100°C, and calcined at 500°C for 3 hours to produce nanocrystalline TiO_2 nanoparticles. For Ga and S-doped TiO_2, stoichiometric amounts of thiourea and $Ga(NO_3)_3$ were dissolved in isopropanol and deionized water) and stirred for 20 minutes before being added to the Ti sol and stirred for another 60 minutes. g-C_3N_4 was synthesized by annealing thiourea at 550°C for 3 hours; 1.0 g of g-C_3N_4 was then mixed with 50 ml of ethanol and sonicated for 2 hours. Finally, 0.01 g of (GaxSy@TiO_2) was added, the mixture was sealed and stirred for 6 hours, and the solid phase was filtered and dried at 120°C.

3. PHOTOCATALYTIC

The photocatalytic activities of $Ga_{5.0}S_{10.0}$@TiO_2-g-C_3N_4, were evaluated using 0.1 g of catalyst, H_2O_2, and a 20 ml aqueous solution of CP at a concentration of 40 mg L^{-1}. An adsorption reaction was initiated by stirring the CP solution in the dark to achieve equilibrium with the catalyst. The mixture was then irradiated for 120 minutes using a 400 W high-pressure mercury vapor lamp at a wavelength of 546.8 nm, with the temperature maintained 25 ºC. After 30 minutes, approximately 5 mL of the reaction mixture was centrifuged to separate the catalyst, and the supernatant containing ciprofloxacin was analyzed using a UV spectrophotometer.

Figure 1 shows a reduction in the absorption peak at 275 nm as degradation occurs. After 180 minutes of irradiation, the degradation efficiency achieved an impressive 99%, confirming the effective photodegradation of ciprofloxacin with the photocatalyst.

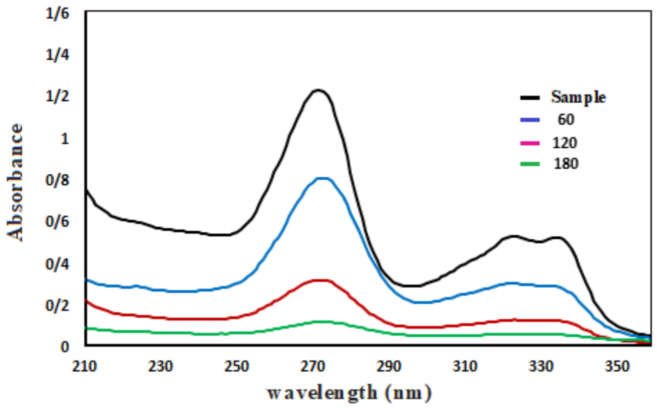

Figure 1. UV–visible absorption spectra of ciprofloxacin elimination with Ga$_{5.0}$S$_{10.0}$@TiO$_2$/g-C$_3$N$_4$, (CP) =40 mg L-1, [cat.]=0.1 g, H_2O_2

FT-IR spectroscopy of the Ga$_{5.0}$S$_{10.0}$@TiO$_2$/g-C$_3$N$_4$ composite revealed key peaks in the 400-4000 cm^{-1} range. The composite retains all characteristic peaks of both TiO$_2$ and g-C$_3$N$_4$, confirming the successful loading of Ga$_{5.0}$S$_{10.0}$@TiO$_2$ onto g-C$_3$N$_4$. In pure g-C$_3$N$_4$, peaks between 1200-1700 cm^{-1} correspond to CN stretching vibrations, and the peak at 805 cm^{-1} is linked to triazine breathing vibrations. Additionally, peaks at 3100-3350 cm^{-1} indicate N–H bond stretching, while the TiO$_2$ spectrum shows a peak around 520 cm^{-1} for Ti–O stretching (Figure 2).

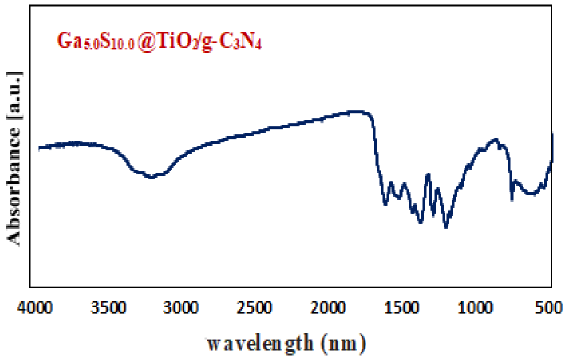

Figure 2. FT-IR Analysis: Ga$_{5.0}$S$_{10.0}$@TiO$_2$ Spectram.

XRD measurements of Ga$_{5.0}$S$_{10.0}$@TiO$_2$/g-C$_3$N$_4$ were conducted to evaluate their presence, crystallinity, and purity, as shown in Figure 3. The characteristic peaks of g-C$_3$N$_4$ and TiO$_2$ in the catalyst spectrum remained unchanged, indicating the successful loading of Ga$_{5.0}$S$_{10.0}$@TiO$_2$ onto g-C$_3$N$_4$. Additionally, the XRD pattern of the doped sample reveals a decrease in the intensity of the crystal planes, suggesting effective incorporation of gallium and sulfur into the TiO$_2$ lattice. Notably, no peaks associated with dopant impurities were detected in the diffraction spectra of the co-doped nanocomposite, confirming the high purity of the doped samples.

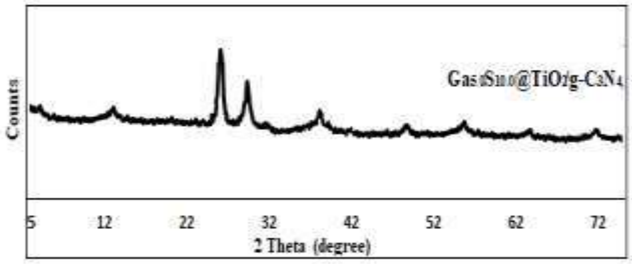

Figure 3. XRD Analysis: $Ga_{5.0}S_{10.0}@TiO_2$ Spectram.

CONCLUSIONS

In summary, $Ga_{5.0}S_{10.0}@TiO_2\text{-g-}C_3N_4$ resulted in the development of a highly effective photocatalyst. This photocatalyst exhibited exceptional performance in the removal of ciprofloxacin under VIS light irradiation. The presence of $Ga_{5.0}S_{10.0}@TiO_2$ in the composite probably caused the reduction of the carrier recombination rate and the enhancement of photocatalytic degradation of ciprofloxacin. This project holds promise in providing an efficient and environmentally friendly technology for antibiotics treatment, utilizing $Ga_{5.0}S_{10.0}@TiO_2\text{-g-}C_3N_4$ under VIS light.

ACKNOWLEDGMENT

The study was supported by Kosar University of Bojnord with the grant number (NO. 0308072613).

References:

[1] Golet, E.M., Alder, A.C., Hartmann, A., Ternes, T.A., Giger, W., 2001. Trace determination of fluoroquinolone antibacterial agents in urban wastewater by solidphase extraction and liquid chromatography with fluorescence detection. Anal. Chem. 73, 3632-3638.

[2] Gothwal, R., Shashidhar, T., 2015. Antibiotic pollution in the environment: a review. Clean 43, 479-489.

[3] Watkinson, A.J., Murby, E.J., Kolpin, D.W., Costanzo, S.D., 2009. The occurrence of antibiotics in an urban watershed: from wastewater to drinking water. Sci. Total Environ. 407, 2711-2723.

[4] Guo, H.G., Gao, N.Y., Chu, W.H., Li, L., Zhang, Y.J., Gu, J.S., Gu, Y.L., 2013. Photochemical degradation of ciprofloxacin in UV and UV/H_2O_2 process: kinetics, parameters, and products. Environ. Sci. Pollut. Res. 20, 3202-3213.

[5] Chang, F., Zheng, J.J., Wang, X.F., Xu, Q., Deng, B.Q., Hu, X.F., Liu, X.Q., 2018. Heterojuncted non-metal binary composites silicon carbide/g-C_3N_4 with enhanced photocatalytic performance. Mater. Sci. Semicond. Process. 75, 183-192.

[6] Chen, M.J., Yao, J., Huang, Y., Gong, H., Chu, W., 2018. Enhanced photocatalytic degradation of ciprofloxacin over Bi_2O_3/$(BiO)_2CO_3$ heterojunctions: efficiency, kinetics, pathways, mechanisms and toxicity evaluation. Chem. Eng. J. 334,
453-461.

[7] De Witte, B., Dewulf, J., Demeestere, K., Van Langenhove, H., 2009. Ozonation and advanced oxidation by the peroxone process of ciprofloxacin in water. J. Hazard Mater. 161, 701-708.

[8] Deng, J., Xu, M.Y., Feng, S.F., Qiu, C.G., Li, X.Y., Li, J., 2019. Iron-doped ordered mesoporous Co_3O_4 activation of peroxymonosulfate for ciprofloxacin degradation: performance, mechanism and degradation pathway. Sci. Total Environ.
658, 343-356.

[9] Zhu, S.S., Li, X.J., Kang, J.K., Duan, X.G., Wang, S.B., 2019. Persulfate activation on crystallographic manganese oxides: mechanism of singlet oxygen evolution for nonradical selective degradation of aqueous contaminants. Environ. Sci. Technol. 53, 307-315.

[10] Yang, B., Mao, X.H., Pi, L., Wu, Y.X., Ding, H.J., Zhang, W.H., 2017. Effect of pH on the adsorption and photocatalytic degradation of sulfadimidine in Vis/g-C_3N_4 progress. Environ. Sci. Pollut. Res. 24, 8658-8670.

The 30th Iranian Seminar of Organic Chemistry
February 7-9, 2025, Iran University of Science and Technology, Tehran, Iran

Gallium and Sulfur Co-Modified TiO_2 Nanocomposites on g-C_3N_4 as photocatalyst for degradation of Tetracycline

Razieh Nejat

Department of Chemistry, Kosar University of Bojnord, Bojnord, Islamic Republic of Iran

Fax: (+98)-58-3242740, phone: (+98)-58-32262863. P.O. Box 9415615458; Email: organochem.nejat@kub.ac.ir

**Corresponding author: organochem_nejat@yahoo.com*

Keyword: photocatalyst, Tetracycline, TiO_2, Gallium, Sulfur.

Abstract— A novel photocatalyst was formulated by integrating Ga- and S-co-doped TiO_2 with graphitic carbon nitride. This composite successfully facilitated the degradation of tetracycline under visible-light irradiation, achieving optimal degradation after 180 minutes with a concentration of 20 mg L^{-1} tetracycline and 0.1 g L^{-1} of catalyst. The gallium and sulfur co-modified TiO_2 nanocomposite on g-C_3N_4 demonstrated nearly threefold improvement over bare g-C_3N_4. This study offers important insights into the development of cost-effective catalysts that enhance the photocatalytic efficiency of established materials, contributing to better outcomes in photocatalytic systems.

INTRODUCTION

The prevalent presence of pharmaceutical compounds, especially antibiotics, constitutes a serious environmental challenge due to their widespread application in humans and animals. Antibiotics, such as tetracycline, are long-lasting pollutants in water sources and represent a substantial environmental hazard [1-3]. Tetracycline necessitates prompt attention because of its considerable use in human medicine, agriculture, and livestock management [4]. It can taint water through various pathways, making it vital to prioritize its removal over other pharmaceuticals, as it does not offer multiple uses.

Tetracycline is a broad-spectrum antibiotic effective against gram-positive and gram-negative microorganisms, as well as mycoplasma and protozoan parasites [5]. It is commonly used in aquaculture as a growth promoter to improve nutrient absorption, helping farmers boost yield [6]. However, ongoing use and insufficient treatment have led to its presence in various water sources [7].

Tetracycline enters the environment through urine and feces and tends to remain unchanged due to limited metabolic processing. Traditional wastewater treatment methods often do not fully remove it, posing a significant long-term risk to both plants and animals. Therefore, developing effective remediation technologies is essential for eliminating tetracycline from wastewater.

Photocatalytic technology is a key method for eliminating tetracycline due to its high efficiency, low cost, and suitability for solar-light-induced degradation. Graphitic carbon nitride (g-C_3N_4) was chosen as a catalytic material for its metal-free nature, stability, and visible light efficiency. As a visible light-activated semiconductor, g-C_3N_4 has a band gap of 2.7 eV, allowing for effective light absorption.

While it offers good chemical and thermal stability, its catalytic performance is limited by high charge carrier recombination, small surface area, and low reusability. These issues can be addressed through strategies like doping, co-doping, and heterojunction structures.

The aim of this study is to develop a novel photocatalyst, Gallium and Sulfur Co-Modified TiO_2 Nanocomposites on g-C_3N_4, specifically engineered for the visible light-induced degradation of Tetracycline.

2. EXPERIMENTAL

2.1. Materials and Physical Techniques

In this work, chemicals were obtained from Merck, Sigma-Aldrich, and Fluka chemical companies and used without further purification. FTIR spectra obtained in the range of 4000 cm^{-1} to 400 cm^{-1} using a NICOLET IR100 spectrophotometer. UV/Vis diffusive reflectance (UV/Vis DRS) measurements were carried out using a Thermo Scientific Evolution 300/600 UV-Visible spectrophotometer (USA), following established protocols described in the literature.

The light source used for the experiments had a specific wavelength of 360.0 nm. Visible illumination, on the other hand, was provided by a 400 W lamp, specifically a high-pressure mercury-vapor lamp, with a wavelength of 546.8 nm. All measurements were performed at room temperature. The sample was analyzed using a GC-MASS AGILENT 7890A gas chromatography instrument.

A solution was prepared by dissolving 0.1 mol of titanium isopropoxide in isopropanol, with acetic acid added to adjust the pH to 5. After stirring for 120 minutes, the sol was aged for 48 hours, air-dried at 100°C, and calcined at 500°C for 3 hours to produce nanocrystalline TiO_2 nanoparticles.

For Ga and S-doped TiO_2, stoichiometric amounts of thiourea and $Ga(NO_3)_3$ were dissolved in isopropanol and deionized water and stirred for 20 minutes before being added to the Ti sol and stirred for another 60 minutes.

g-C_3N_4 was synthesized by annealing thiourea at 550°C for 3 hours; 1.0 g of g-C_3N_4 was then mixed with 50 ml of ethanol and sonicated for 2 hours. Finally, 0.01 g of (GaxSy@TiO_2) was added, the mixture was sealed and stirred for 6 hours, and the solid phase was filtered and dried at 120°C.

3. PHOTOCATALYTIC EXPERIMENTS

Figure 1 illustrates the combined effect of light irradiation and the catalyst on tetracycline degradation, highlighting their impact on process efficiency. In the absence of the catalyst under visible (VIS) light irradiation, no degradation of tetracycline occurs. However, a partial reduction in tetracycline concentration (about 15%) is noted when the reaction is conducted in the dark, likely due to the adsorption of tetracycline molecules onto the catalyst's surface. When the tetracycline solution containing the catalyst is exposed to VIS light, degradation efficiency significantly increases to 98%.

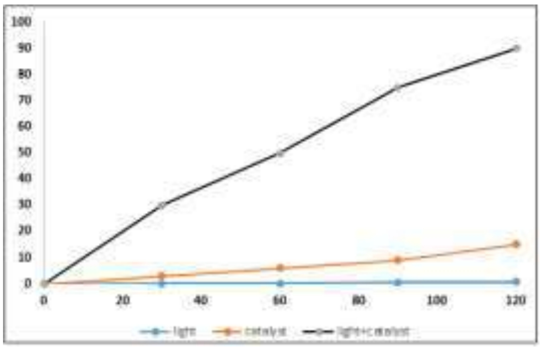

Figure 1. Impacts of VIS light, (VIS light + cat.) on Tetracycline degradation.

Furthermore, the impact of various VIS light-driven catalysts on tetracycline degradation was analyzed (Figure 2). The study included pristine g-C_3N_4 as a reference photocatalyst, assessing its photoactivity in catalyzing tetracycline degradation in water. The photocatalytic activity of gallium and sulfur co-modified TiO_2 nanocomposites on g-C_3N_4 was found to be significantly higher than that of pure g-C_3N_4 for tetracycline degradation under VIS light. This suggests that the incorporation of gallium and sulfur co-modified TiO_2 enhances the photoactivity of the g-C_3N_4 catalyst by improving absorption in the VIS light region, exhibiting better adsorption of tetracycline molecules, and facilitating efficient separation of photogenerated charges.

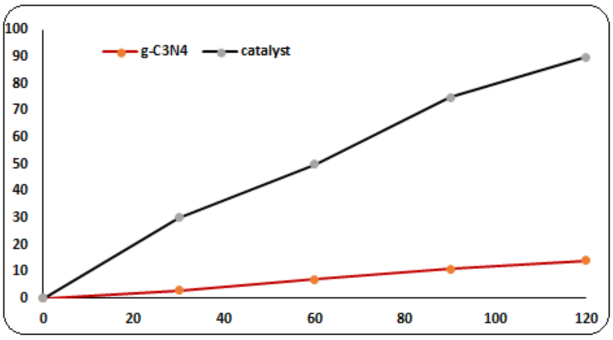

Figure 2. Effects of various VIS light-driven catalysts on Tetracycline degradation.

Figure 3 shows a positive correlation between the tetracycline removal rate and catalyst dosage within the range of 0.01 g/L to 0.15 g/L. The highest degradation yield is achieved with 0.1 g of catalyst under VIS light irradiation. Decreasing the catalyst amount leads to lower yields, while increasing the dosage beyond 0.1 g results in only marginal improvements in degradation efficiency.

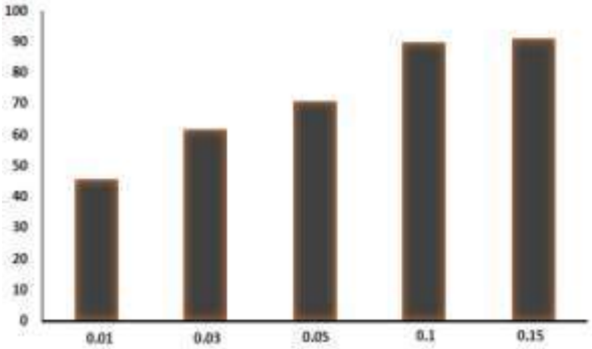

Figure 3. Effect of the catalyst dosage for Tetracycline degradation by catalyst.

The photocatalytic activities of Gallium and Sulfur Co-Modified TiO_2 Nanocomposites on g-C_3N_4, were evaluated using 0.1 g of catalyst, H_2O_2, and a 50 ml aqueous solution of Tetracycline at a concentration of 20 mg L^{-1}. An adsorption reaction was initiated by stirring the Tetracycline solution in the dark to achieve equilibrium with the catalyst. The mixture was then irradiated for 120 minutes using a 400 W high-pressure mercury vapor lamp at a wavelength of 546.8 nm, with the temperature maintained 25 °C. After 30 minutes, approximately 5 mL of the reaction mixture was centrifuged to separate the catalyst, and the supernatant containing Tetracycline was analyzed using a UV spectrophotometer. After 120 minutes of irradiation, the degradation efficiency achieved an impressive 90%, confirming the effective photodegradation of Tetracycline with the photocatalyst.

FT-IR spectroscopy of the Gallium and Sulfur Co-Modified TiO_2 Nanocomposites on g-C_3N_4 revealed key peaks in the 400-4000 cm^{-1} range. The composite retains all characteristic peaks of both TiO_2 and g-C_3N_4, confirming the successful loading of GS@TiO_2 onto g-C_3N_4. In pure g-C_3N_4, peaks between 1200-1700 cm^{-1} correspond to CN stretching vibrations, and the peak at 805 cm^{-1} is linked to triazine breathing vibrations. Additionally, peaks at 3100-

3350 cm^{-1} indicate N–H bond stretching, while the TiO_2 spectrum shows a peak around 520 cm^{-1} for Ti–O stretching (Figure 4).

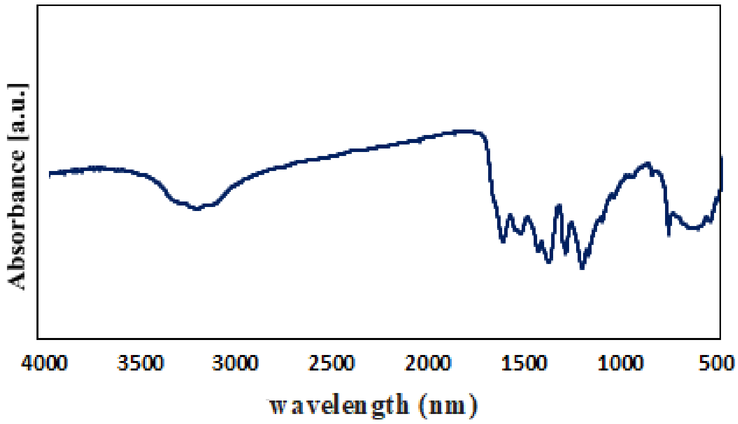

Figure 4. FT-IR Analysis: catalyst Spectram.

CONCLUSIONS

In summary, Gallium and Sulfur Co-Modified TiO_2 Nanocomposites on g-C_3N_4 resulted in the development of a highly effective photocatalyst. This photocatalyst exhibited exceptional performance in the removal of Tetracycline under VIS light irradiation. The presence of GaS@TiO_2 in the composite probably caused the reduction of the carrier recombination rate and the enhancement of photocatalytic degradation of Tetracycline. This project holds promise in providing an efficient and environmentally friendly technology for antibiotics treatment, utilizing GaS@TiO_2 on g-C_3N_4 under VIS light.

ACKNOWLEDGMENT

The study was supported by Kosar University of Bojnord with the grant number (NO. 0308072613).

References:

[1] Ben, Y., Fu, C., Hu, M., Liu, L., Wong, M.H., Zheng, C., 2019. Environ. Res. 169, 483–493..
[2] Guo, Y., Li, M., Huang, X., Wu, Y., Li, L., 2021
[3] Habibi-Yangjeh, A., Mousavi, M., 2018 Adv. Powder Technol. 29, 1379–1392.
[4] Li, X., Qiu, Y., Zhu, Z., Zhang, H., Yin, D., 2022. Chem. Eng. J. 429, 132130..
[5] Gopal, G., Alex, S.A., Chandrasekaran, N., Mukherjee, A., 2020.
[6] Xu, L., Zhang, H., Xiong, P., Zhu, Q., Liao, C., Jiang, G., 2021. Sci. Total Environ. 753, 141975
[7] Scaria, J., Anupama, K.V., Nidheesh, P.V., 2021 .SCITOTENV.2021.145291.

Binary CQD-catalysis for Regioselective Synthesis of Unsymmetric Azoxy Arenes; The Role of H-bond Acceptor in Tuning the Regioselectivity

Authors: Hamid R. Kalhor*, Morteza Hasani.

Kalhor@sharif.edu

Affiliations: Sharif University of Technology

Keyword: Cooperative CQD Catalysis, Unsymmetric Azoxy Arenes, Cross coupling reactions, Hydrogen Bond Acceptor Mechanism

Control over the selectivity of constitutional isomers in unsymmetric azoxy arenes has been a formidable challenge for organic chemistry [1-2]. In continuation of our ongoing interest in carbon quantum dot (CQD) catalysis, we developed a binary CQD-catalysis and an H-bond acceptor (HBA) mechanism to rise to the challenge of the regioselective synthesis of unsymmetric azoxybenzenes. As such, in the oxidative coupling of anilines, first, the product selectivity to azoxy arenes was controlled by an asparagine-modified CQD catalyst [1,3]. The successful control over the product selectivity was achieved by the inspiration provided by the enzyme engineering, where substitutions of functional amino acids bring about significant improvements to the enzyme (or Bioinspired catalyst).

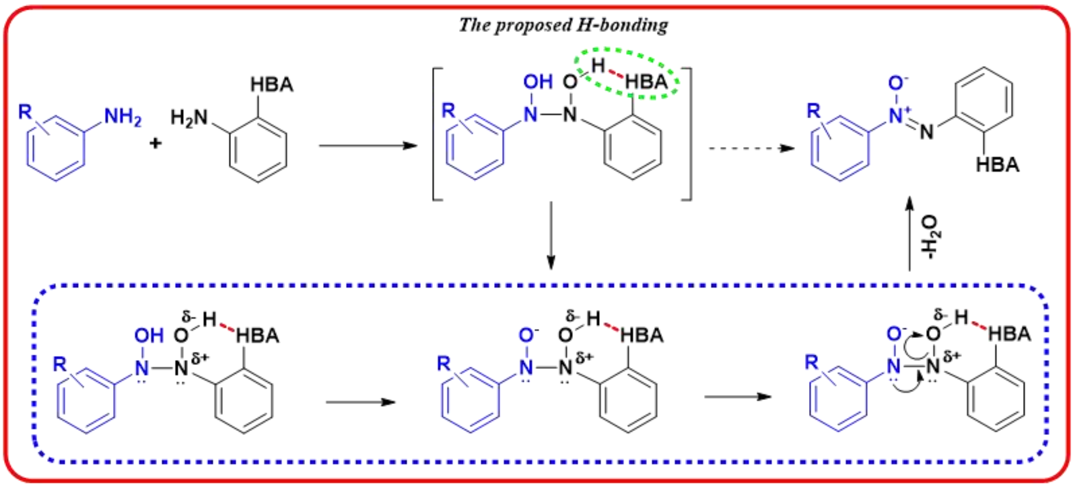

Figure 1. The proposed H-bond acceptor mechanism in regioselective synthesis of unsymmetric azoxy arenes.

Subsequent to the product selectivity achieved by CQD-catalysis, the regioselectivity issue was confronted with an H-bond acceptor mechanism in the cross-coupling of different anilines. In doing so, it was found that an ortho-HBA on one of the coupling anilines could mechanistically establish a six-membered intramolecular hydrogen bonded ring on an N,N′-dihydroxy intermediate. The above-mentioned intramolecular hexagonal ring makes the nearby nitrogen eminently suitable for the slow dehydration step. As a result, the functional oxygen of the azoxy compound is placed far from the HBA. The o-HBA mechanism also controls the regioselectivity ratio in which 1:0 (with an intramolecular H-bonded hexagonal ring), 2:1 (with an intramolecular H-bonded pentagonal ring), and 1:1 (without an ortho-HBA) isomeric mixtures could be achieved.

References:

[1] *J. Org. Chem. 2024, 89, 19, 13836–13846.*

[2] *Org. Lett. 2017, 19, 11, 2777–2780.*

[3] *ACS Catal. 2021, 11, 17, 10778–10788.*

The 30th Iranian Seminar of Organic Chemistry
February 7-9, 2025, Iran University of Science and Technology, Tehran, Iran

Preparation of diazo dyes based on β-naphthol using $SnCl_4$ immobilized on nano kaolin as catalyst under ginding conditions at room temperature

Authors:Ahmed Ayad Abdulbaqi , Abdolhamid Bamoniri* Corresponding author Email: bamoniri@kashanu.ac.ir

Department of Organic Chemistry, Faculty of Chemistry, University of Kashan, Kashan, Iran

Keyword: β-naphthol, Azo dye, SnCl4, Nano Kaolin, Grinding.

Abstract

In recent years, using nano-size solid acids in chemical reactions and synthesis of organic compounds under solvent-free condition have been known as two fundamental principles in the development of green chemistry[1].On the other side, azo compounds as an important class of organic componuds have received much attention for their applications in analytical chemistry, biological applications as dyestuffs[2,3]. So, the widespread application of solid acids, structural and practical diversity of azo compounds, have prompted us to employ the novel and ecofriendly methods for the synthesis of azo dyes based on 2-naphthol in the presence of SnCl4/nano Kaolin using primary aromatic amines, 2-naphthol and sodium nitrite in grinding and solvent free conditions at room temperature. The properties of the catalyst was characterized by fourier transform infrared spectroscopy(FT-IR), field emission scanning electron microscopy (FESEM), transmission electron microscopy (TEM), X-ray diffraction (XRD), energy dispersive X-ray spectroscopy (EDS) and thermal gravimetric analysis (TGA). All derivatives were distinguished by FT-IR and 1H NMR spectroscopy

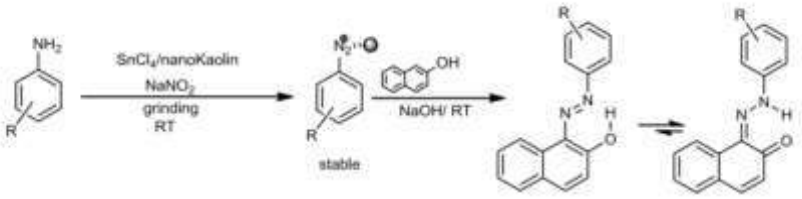

Scheme1

References:

[1] F. Shi, W. Tan, R.Y. Zhu, G. J. Xing, S. J. Tu. Catalytic asymmetric five component tandem reaction: diastereo and enantioselective synthesis of densely functionalized Tetrahydropyridines with biological importance, Adv. Synth. Catal., 2013, 355(8), 1605- 1627.

[2] B.F. Mirjalili, A. Bamoniri, N. Mohaghegh. One-pot synthesis of 2, 4, 5-tri-substitute d1Himidazoles promoted by trichloromelamine. Curr. Chem. Lett., 2013, 2(1), 35-42.

[3] K.T. Chung., Occurrence, uses and carcinogenicity of arylamines, Ind. J. Chem., 2015 , 7(7), 322-367

The 30th Iranian Seminar of Organic Chemistry
February 7-9, 2025, Iran University of Science and Technology, Tehran, Iran

A new nanocomposite based on Multi Wall CNT (MWCNT) and imidazolium-based ionic liquids as novel electrolyte assistant for improving performance of Dye-Sensitized Solar Cells (DSSCs)

Mehrnaz Davoudabdollah[a], Elaheh Kowsari[a,*]
[a] *Department of Chemistry, Amirkabir University of Technology, No. 424, Hafez Avenue, 1591634311, Tehran, Iran*

Keyword: Dye-sensitized solar cell, Ionic liquids, Nanocomposite electrolyte

In recent years, the dye-sensitized solar cell (DSSC) has drawn significant attention due to its relatively high energy conversion efficiency and great nontoxicity compared to conventional silicon-based cells. Researchers typically utilize diverse approaches or chemicals to augment the performance of these cells. The electrolyte plays a crucial role in DSSCs as its properties profoundly influence their performance, including conversion efficiency, by controlling electron transfers. Various types of electrolytes have been developed for DSSC applications,

---

[*] Corresponding author.
E-mail address: Kowsarie@aut.ac.ir (E. Kowsari)

including liquid electrolytes with organic solvents and ionic liquids. Ionic liquids (ILs) are advantageous alternatives to organic solvents in electrochemical devices due to their non-volatility and exceptional chemical stability. Also, carbonaceous materials are acknowledged as remarkable nanofillers (NFs) for DSSC electrolytes because they establish uninterrupted ion-conduction channels. The optimal choice for carbonaceous nanoparticles as an addition in ionic liquid-based electrolytes is the Multi Wall Carbon Nanotube (MWCNT) which can improve the cells' performance owing to its unique topologies. In this work, Imidazolium-based ionic liquids with iodide anions and modified MWCNTs with substances consisting of amine groups have been produced and employed as electrolyte assistant in DSSCs. The findings indicated that incorporating the novel nanocomposite into the electrolyte enhanced the open-circuit voltage (VOC), short-circuit current density (JSC), and the efficiency (η) of the DSSCs from 4.3% (the standard cells based on graphene-free electrolyte) to 7.1%. Furthermore, the results of electrochemical impedance spectroscopy (EIS) can show that adding this additive to the electrolyte causes a drop in the electron resistance (R) compared to the standard electrolyte. In scheme 1, the figures of used materials to produce new nanocomposite is shown.

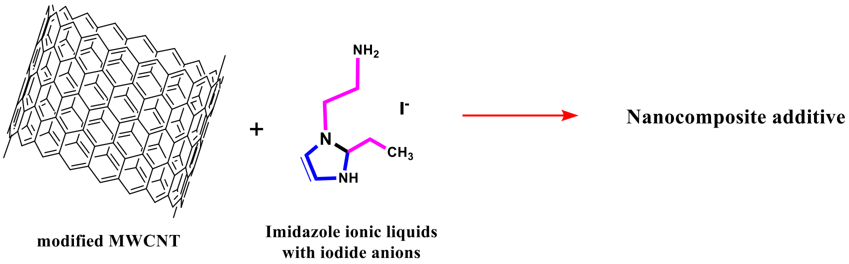

Scheme 1: Synthesis of new nanocomposite as a novel electrolyte additive in DSSC.

References

(1) Rafieepoor Chirani, M.; Kowsari, E.; Ramakrishna, S.; Salar Amoli, H.; Yousefzadeh, M.; Chinnappan, A. *J. Mol. Liq.* **2022**, *364*, 119999.

(2) Najafi, M.D.; Kowsari, E.; Naderi, H.R.; Chinnappan, A.; Ramakrishna, S.; Ehsani, A.; Shokravi, A. *Compos. Sci. Technol.* **2021**, *211*, 108844, doi:10.1016/j.compscitech.2021.108844.

(3) Bigdeloo, M.; Kowsari, E.; Ehsani, A.; Chinnappan, A.; Ramakrishna, S.; AliAkbari, R. *J. Energy Storage* **2021**, *37*, 102474, doi:10.1016/j.est.2021.102474.

The 30th Iranian Seminar of Organic Chemistry
February 7-9, 2025, Iran University of Science and Technology, Tehran, Iran

A Green Ionic Liquid Derived from Amino Acid: Superior Corrosion Inhibition Performance for Mild Steel in Acidic Media

Hossein Malekraisi[a], Elaheh Kowsari[a*], M HosseinpourRokni[b]

[a] *Department of Chemistry, Amirkabir University of Technology, No. 424, Hafez Avenue, 1591634311, Tehran, Iran.*

[b] *Department of Materials and Metallurgical Engineering, Amirkabir University of Technology, No. 424, Hafez Avenue, 1591634311, Tehran, Iran.*

Keyword: Corrosion, green inhibitor, Ionic Liquid, Amino Acid

Corrosion protection in industrial environments is of great importance. The significant economic losses associated with corrosion could be controlled through different methods. The use of organic corrosion inhibitors is one of the most cost-effective methods in this regard. However, inhibitor selection criteria should not be solely limited to their chemistry. The harmful effects of synthetic organic inhibitors increasingly encouraged the need for either environmentally-friendly inhibitors with inexpensive manufacturing processes or finding inhibitors with natural origins. Ionic liquids, a class of organic salts with low melting points, recently attracted significant attention to be applied as corrosion inhibitors. These compounds, with their specific properties—high thermal stability, negligible vapor pressure, low toxicity, good electrical conductivity, and tunable structure—have found widespread applications in various scientific and industrial fields. Amino acid-based ionic liquids are a modern class of ionic liquids being investigated in recent years. Interestingly, amino acid could be green functional groups with acceptable toxicity. In addition, the diversity of amino acids allows to design and synthesis various structures with desirable anti-corrosion properties. In this research, it was aimed to significantly reduce the cost and environmental hazards associated with complex multi-step synthesis methods. An ionic liquid based on amino acid as well as imidazolium groups in a single-step process was synthesized. Different techniques were employed to confirm the quality of the synthesized inhibitor and to compare the inhibition efficiency of the primary amino acid and the synthesized amino acid-based ionic liquid. The results demonstrated that the synthesized chemical present high efficiency in inhibiting metal corrosion in acidic corrosive environments with the help of synergistic effects of imidazolium and amino acid substituents. The synthesized inhibitor exhibited excellent corrosion inhibition efficiency, reducing the corrosion rate of mild steel in acidic media by more than 90%.

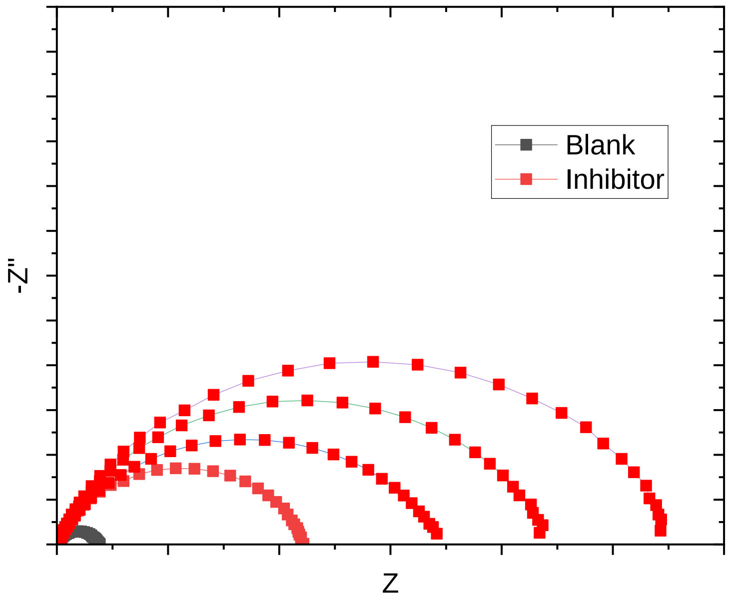

Figure 39: Electrochemical impedance results in blank solution and new synthesized ionic liquid at different concentrations in acidic environments on mild steel.

References

(1) Velusamy S, Sakthivel S, Neelakantan L, Sangwai JS. Imidazolium-based ionic liquids as an anticorrosive agent for completion fluid design. Journal of Earth Science. 2017 Oct;28:949-61.
(2) Ardakani EK, Kowsari E, Ehsani A, Ramakrishna S. Performance of all ionic liquids as the eco-friendly and sustainable compounds in inhibiting corrosion in various media: A comprehensive review. Microchemical Journal. 2021 Jun 1;165:106049.
(3) Kowsari E, Payami M, Amini R, Ramezanzadeh B, Javanbakht M. Task-specific ionic liquid as a new green inhibitor of mild steel corrosion. Applied Surface Science. 2014 Jan 15;289:478-86.

The 30th Iranian Seminar of Organic Chemistry
February 7-9, 2025, Iran University of Science and Technology, Tehran, Iran

Investigating green chemicals as corrosion inhibitors: experimental and theoretical approaches

Mohammad Arif Faramarz[a], Elaheh Kowsari[a,] M HosseinpourRokni[b*], Hossein Malekraisi[a]
[a] *Department of Chemistry, Amirkabir University of Technology, No. 424, Hafez Avenue, 1591634311, Tehran, Iran.*

---

[*] Corresponding author.
E-mail address: Kowsarie@aut.ac.ir (E. Kowsari)

[b] *Department of Materials and Metallurgical Engineering, Amirkabir University of Technology, No. 424, Hafez Avenue, 1591634311, Tehran, Iran.*

Keywords: Corrosion, Ionic Liquid, Steel, DFT

Corrosion is an electrochemical phenomenon that spontaneously occurs on solid materials especially metals, which leaves huge costs. To control and mitigate corrosion, various approaches such as painting, coating, special design of equipment with corrosion-resistant alloys, cathodic and anodic protection, and corrosion inhibitors have been utilized. Corrosion inhibitors due to their versatile use and abundant resources have gained many researchers' attention. Various chemicals have been studied in corrosion inhibition and showed considerable performance, some of which are hazardous and toxic to human beings and the environment. Out of chemicals used as corrosion inhibitors, ionic liquids with great properties high solubility, low vapor pressure and ecofriendly—have been regarded as green candidates instead of conventional corrosion inhibitors. Moreover, the synergyism between anions and cations existing in ionic liquids structures can enhance inhibitive adsorption on the metal surface to construct protecting layers. In this study, we synthesized new functionalized imidazole-based ionic liquids, and comparatively investigated their inhibition efficiencies in an stagnant aggressive acidic solution. The electrochemical tests, including OCP, EIS, and polarization studies, demonstrated considerable inhibition efficiencies for both examined ionic liquids, and the theoretical investigations using adsorption isotherms and first principle technique shed light on probable inhibition mechanisms, on how adsorption of species led to corrosion protection. The results of this study could pave the way to have more efficient corrosion inhibitors in the futuer.

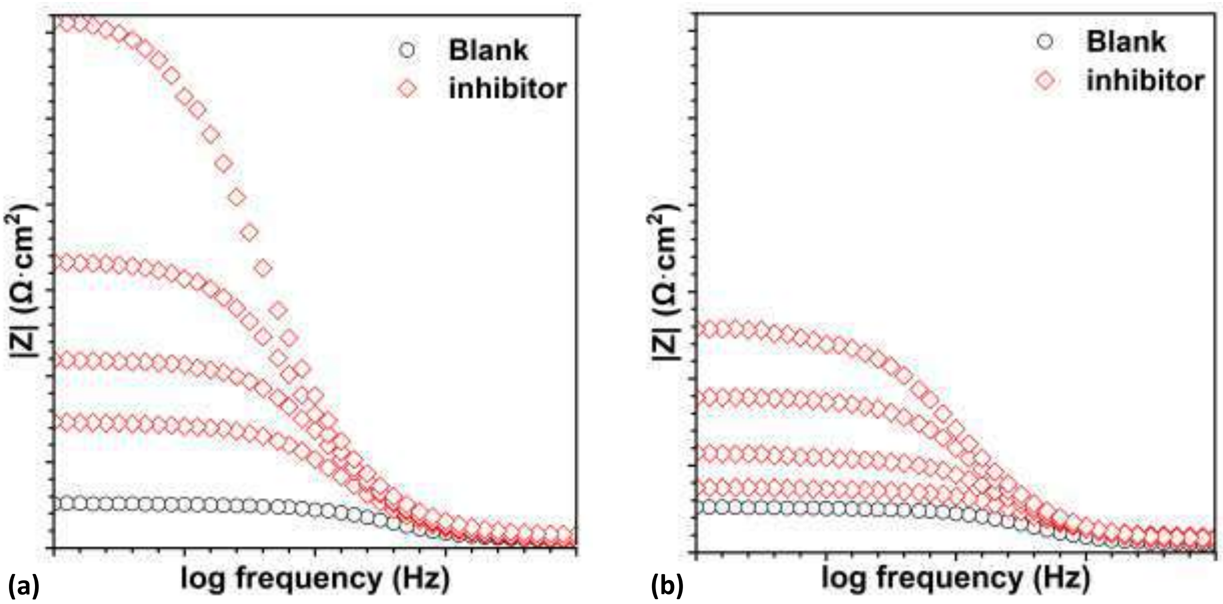

Figure 40: bode graphes resulted from IL1 (a) and IL2 (b) EIS tests on steel subtrate

References

[1] S. M. Taw, "Ionic liquids based gemini cationic surfactants as corrosion inhibitors for carbon steel in hydrochloric acid solution," vol. 216, pp. 624–635, 2016, doi: 10.1016/j.molliq.2016.01.066.

[2] A. Yousefi, S. Javadian, N. Dalir, J. Kakemam, and J. Akbari, "Imidazolium-based ionic liquids as modulators of corrosion inhibition of SDS on mild steel in hydrochloric acid solutions: Experimental and theoretical studies," *RSC Adv.*, vol. 5, no. 16, pp. 11697–11713, 2015, doi: 10.1039/c4ra10995c.

[3] C. Verma, I. B. Obot, I. Bahadur, E. M. Sherif, and E. E. Ebenso, "Choline based ionic liquids as sustainable corrosion inhibitors on mild steel surface in acidic medium: Gravimetric, electrochemical, surface morphology, DFT and Monte Carlo Simulation studies," *Appl. Surf. Sci.*, 2018, doi: 10.1016/j.apsusc.2018.06.035.

[4] G. Gómez-Sánchez *et al.*, "Temperature Effect on the Corrosion Inhibition of Carbon Steel by Polymeric Ionic Liquids in Acid Medium," *Int. J. Mol. Sci.*, vol. 24, no. 7, 2023, doi: 10.3390/ijms24076291.

The 30th Iranian Seminar of Organic Chemistry
February 7-9, 2025, Iran University of Science and Technology, Tehran, Iran

Effect of oxygen-containing groups on inhibitory effects of ionic liquid upon mild steel acidic corrosion

Niloofar Zeighami[a], Mohsen HosseinpourRokni[a], Elaheh Kowsari[a]

[a] *Department of Chemistry, Amirkabir University of Technology, P. O. Box 1591634311, Tehran, Iran*

Keywords: Ionic liquid, Steel, Corrosion, Green inhibitor

Metals and alloys have been generally known as corrosion-prone structural materials, particularly in acidic media. A wide variety of practical considerations and methods can be implemented to protect metallic structures against electrochemical degradation. Application of organic inhibitors in closed corrosive environments as an effective low-cost corrosion protection practice has been investigated widely in the existing publications. Ionic liquids (ILs) are less-toxic organic compounds with specific physicochemical features [2,3]. Several studies have investigated imidazolium-based ILs as corrosion inhibitors for different substrates [4]. In addition, it is generally accepted that the functional groups involving oxygen in their structures can enhance inhibition efficiency [1]. In this study, two imidazolium-base ILs functionalized with oxygen-containing substituents were synthesized and used as corrosion inhibitors for steel. The structural features of the synthesized compounds were verified using NMR and FT-IR spectroscopy. Different measurements—Open circuit potential (OCP), electrochemical impedance spectroscopy (EIS), and potentiodynamic polarization—determined inhibition performance, and adsorptive behavior on the metal surface was studied by X-ray photoelectron spectroscopy (XPS). It was concluded that incorporating oxygen in an inhibitor chemistry may not directly affect inhibition.

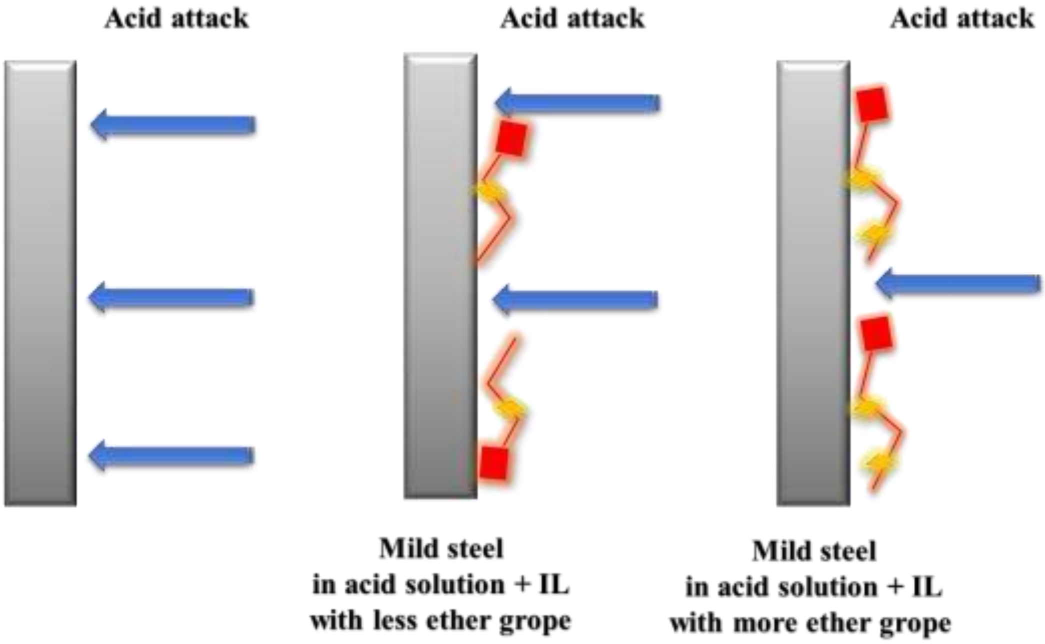

Scheme. 1: Adsorbate-adsorbent interaction in corrosion and inhibition

References

1. Verma, C. *et al.* Experimental, density functional theory and molecular dynamics supported adsorption behavior of environmental benign imidazolium based ionic liquids on mild steel surface in acidic medium. *J Mol Liq* 273, 1–15 (2019).

2. Kamali Ardakani, E., Kowsari, E. & Ehsani, A. Imidazolium-derived polymeric ionic liquid as a green inhibitor for corrosion inhibition of mild steel in 1.0 M HCl: Experimental and computational study. *Colloids Surf A Physicochem Eng Asp* 586, 124195 (2020).

3. Kobzar, Y. L. & Fatyeyeva, K. Ionic liquids as green and sustainable steel corrosion inhibitors: Recent developments. *Chemical Engineering Journal* 425, 131480 (2021).

4. Ardakani, E. K., Kowsari, E., Ehsani, A. & Ramakrishna, S. Performance of all ionic liquids as the eco-friendly and sustainable compounds in inhibiting corrosion in various media: A comprehensive review. *Microchemical Journal* 165, (2021).

The 30th Iranian Seminar of Organic Chemistry
February 7-9, 2025, Iran University of Science and Technology, Tehran, Iran

chiral Imidazolium-based ionic liquid as an effective and sustainable corrosion inhibitor for copper in acidic media

Mohammad Shirzadi [a], Elaheh Kowsari [a*], Mohsen HosseinpourRokni [b]

[a] *Department of Chemistry, Amirkabir University of Technology, No. 424, Hafez Avenue, 1591634311, Tehran, Iran*

Keyword: corrosion inhibitor, chiral Ionic liquids, Imidazole-based ionic liquid

The growing interest in sustainable development has led to the exploration of green corrosion inhibitors derived from natural sources, including plant extracts and other biomass wastes[1]. Imidazole-based ionic liquids fit within this framework by offering an environmentally friendly alternative to more conventional and potentially harmful chemical inhibitors. Imidazole-based ionic liquids (ILs) have gained significant recognition as effective corrosion inhibitors, particularly for metals like copper, owing to their unique chemical properties and environmentally friendly profiles[2]. Characterized by imidazolium cations, these ionic liquids exhibit low volatility, high thermal stability, and non-flammability, making them preferable alternatives to traditional organic inhibitors, which often pose environmental risks[3]. Their ability to form protective layers on metal surfaces has made them a focal point of research in the field of materials science, particularly in enhancing the longevity of copper in various applications. The synthesis of imidazole-based ionic liquids involves creating imidazolium salts through reactions with different halides and anionic species, allowing for the customization of their physical and chemical properties[4]. Their efficacy as corrosion inhibitors is linked to their adsorption capabilities, which form stable protective barriers that reduce corrosion rates by limiting access to aggressive corrosive agents[5]. In this study, a chiral Imidazolium-based ionic liquid with chloride anion and ester functional group have been produced and employed as corrosion inhibitor for copper. The results from electrochemical impedance spectroscopy (EIS) and potentiodynamic polarization (PDP) tests on copper samples in hydrochloric acid (HCl) solution demonstrated that the chiral imidazolium-based ionic liquid has been produced from L-Alanine amino acid shows significant potential as an effective corrosion inhibitor for copper in acidic environments.

---

* Corresponding author.
E-mail address: Kowsarie@aut.ac.ir (E. Kowsari)

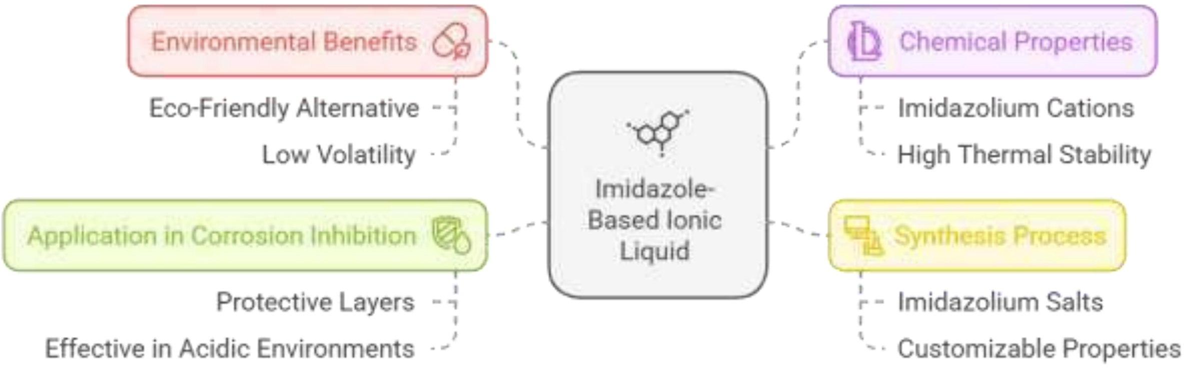

References

1. Thakur, A., Sharma, S., Ganjoo, R., Assad, H. & Kumar, A. Anti-Corrosive Potential of the Sustainable Corrosion Inhibitors Based on Biomass Waste: A Review on Preceding and Perspective Research. *J Phys Conf Ser* **2267**, 012079 (2022).

2. Ganjoo, R. *et al.* Imidazolium based ionic liquids as green corrosion inhibitors against corrosion of mild steel in acidic media. *J Phys Conf Ser* **2267**, 012023 (2022).

3. Green, M. D. & Long, T. E. Designing Imidazole-Based Ionic Liquids and Ionic Liquid Monomers for Emerging Technologies. *Polymer Reviews* **49**, 291–314 (2009).

4. Ha Quoc, B., Nguyen Huu, V. & Nguyen, D. A. Research on synthesis of imidazole-based ionic liquids as metal corrosion inhibitors. *Journal of Military Science and Technology* 102–108 (2024) doi:10.54939/1859-1043.j.mst.94.2024.102-108.

5. Ibrahim, M. A. M. *et al.* Corrosion Inhibition of Carbon Steel by Imidazolium and Pyridinium Cations Ionic Liquids in Acidic Environment. *Portugaliae Electrochimica Acta* **29**, 375–389 (2011).

Activated carbon derived from protein biomass, functionalized graphene oxide, and green ionic liquid for high-performance supercapacitor application

Zahra Seyedhosseini [a], Elaheh Kowsari *[a], Mohammad Mehdi Kamarbeigi [a]

[a] *Department of Chemistry, AmirKabir University of Technology, No. 424, Hafez Avenue, 159163431 Tehran, Iran*

Keywords: Supercapacitor, Protein biomass, Functionalized graphene oxide, Ionic liquid

As human civilization progresses across industrial, urban, and transportation sectors, the demand for energy consumption continues to rise. Researchers strive to reduce reliance on oil and fossil fuels by developing clean and renewable energy sources [1,2]. This commitment to environmentally friendly approaches has led to a burgeoning demand for energy storage solutions. Consequently, the advancement of high-performance energy storage devices has become essential. Supercapacitors have emerged as a promising option due to their unique and remarkable properties, such as rapid charge-discharge rates, long cycling stability, and environmental benefits. This study innovatively explores the repurposing of waste materials to develop supercapacitor electrodes [3,4]. Among the various electrode materials, carbon-based electrode materials play a crucial role in enhancing supercapacitor performance; activated carbon remains a preferred choice due to its high surface area, tunable porosity, and compatibility with diverse electrolytes [5]. This study explores the valorization of protein biomass as a carbon precursor, functionalized graphene oxide, and an ionic liquid as a green solvent to synthesize a high-performance composite. A meticulously designed approach transforms protein biomass into activated carbon via pyrolysis. This carbon is then integrated with functionalized graphene oxide and an ionic liquid, resulting in a composite material. Employing a green solvent in the synthesis process underscores the study's commitment to minimizing environmental impact. The resultant composite material is systematically evaluated for its structural integrity and electrochemical properties. It demonstrates enhanced conductivity, effective ion transport, and superior charge storage capabilities. The synergistic interplay of its components contributes to improved electrochemical behavior by mitigating resistance and optimizing diffusion pathways. This work emphasizes the role of waste recycling and resource efficiency and the potential of integrating green chemistry into energy storage technology. The composite’s alignment with sustainability principles highlights its viability as an alternative to conventional electrode materials. This research advances the feasibility of high-performance, low-impact energy storage solutions for future applications by fostering a shift toward environmentally conscious supercapacitor design. Also, it supports the global effort to address energy challenges with a minimal environmental footprint.

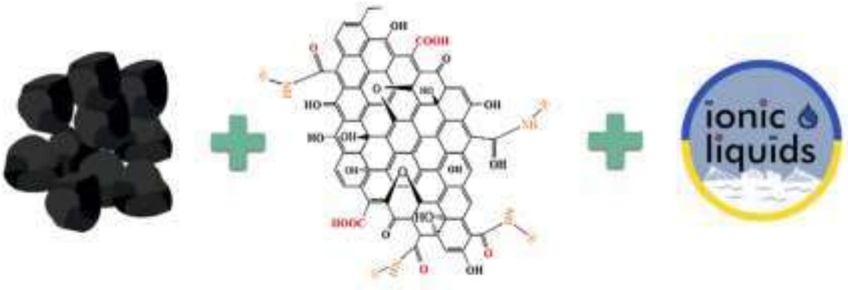

References

[1] C. Drawer, J. Lange, M. Kaltschmitt, Metal hydrides for hydrogen storage – Identification and evaluation of stationary and transportation applications, *J. Energy Storage.* 77 (2024) 109988. https://doi.org/10.1016/j.est.2023.109988.

[2] M.Y. Bhat, S.A. Hashmi, M. Khan, D. Choi, A. Qurashi, Frontiers and recent developments on supercapacitor’s materials, design, and applications: Transport and power system applications, *J. Energy Storage*. 58 (2023) 106104. https://doi.org/10.1016/j.est.2022.106104.

[3] Y. Marfavi, R. AliAkbari, E. Kowsari, B. Sadeghi, S. Ramakrishna, Application of ionic liquids in green energy-storage materials, in: *Ion. Liq. Technol. Environ. Sustain., Elsevier*, 2022: pp. 155–166.

[4] R. Aliakbari, E. Kowsari, Y. Marfavi, S. Ramakrishna, A. Chinnappan, Z.A. Cheshmeh, Comprehensive study on poly ortho-aminophenol composite electrodes and their utilization for supercapacitor applications and green energy storage: A review, *J. Energy Storage*. 44 (2021) 103365.

[5] N.P.D. Ngidi, A.F. Koekemoer, S.S. Ndlela, Recent advancement in the electrochemical performance of electrochemical capacitors based on biomass-derived porous carbon: A review, *J. Energy Storage*. 89 (2024) 111638.

Preparation of a novel ZIF-67@Zn-CMC hydrogel nanocomposite with strong antibacterial potential

Adibeh Mohammadi, Maryam sadat Hashemian, Ali Maleki*

Faculty of Chemistry, Iran University of science and technology, Tehran, Iran. *maleki@iust.ac.ir*

Abstract

Given the increase in bacterial resistance and the global warning to reduce the use of antibiotics, the preparation and development of materials with high antibacterial properties is of great importance. In this study, a new composite of ZIF-67 metal-organic framework encapsulated in Zn-CMC hydrogel network is presented. ZIF-67, a cobalt-based metal-organic framework (MOF), was selected due to its intrinsic antibacterial properties. Encapsulation of ZIF-67 nanoparticles in the hydrogel network improves biocompatibility and sustained release of antibacterial ions. In addition, the antibacterial properties of the hydrogel allow the system to benefit from the synergistic effect of both components. The nanocomposite was characterized using FTIR, XRD, EDX, TGA, and DET analyses, which well confirmed the successful incorporation of ZIF-67 into the Zn-CMC hydrogel matrix. The enhanced antibacterial properties due to synergistic effects as well as the ability of the hydrogel matrix to improve interaction with microbial surfaces and prevent bacterial aggregation can make the prepared nanocomposite a powerful system for biological applications including drug delivery, implant coatings, tissue engineering, and wound healing. These findings demonstrate its ability to combat microbial infections and contribute to responses to antibiotic resistance.

Keywords: Antibacterial nanocomposite, Metal organic frameworks, Antibacterial hydrogel.

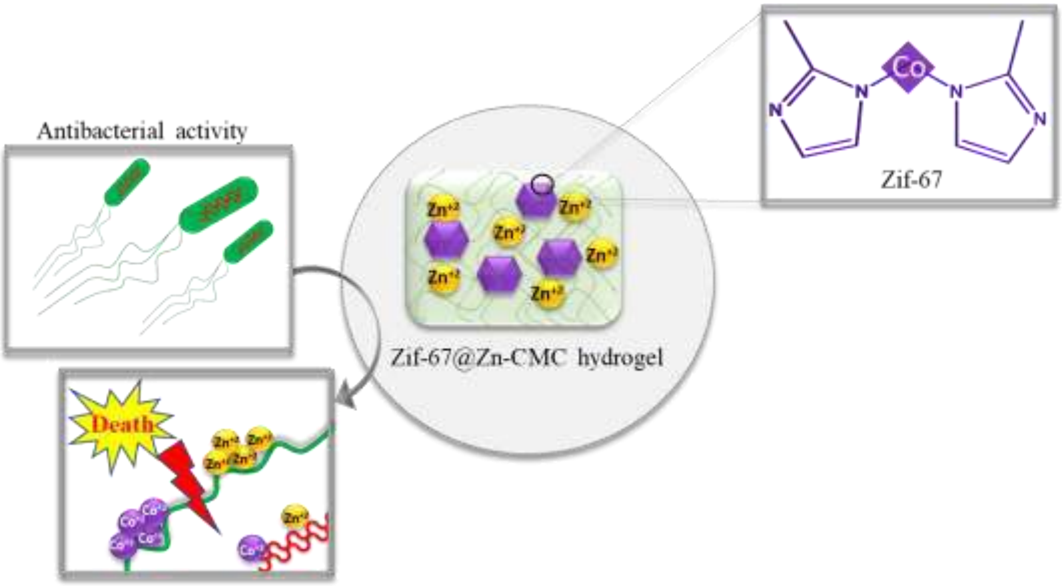

Scheme 1. A schematic diagram of the prepared ZIF-67@ Zn-CMC hydrogel nanocomposite with antibacterial properties.

1. Introduction

The rise of antibiotic-resistant bacterial strains and the dwindling discovery of novel antibiotics [1] have made advanced antibacterial composites increasingly preferred over antibiotic drugs due to their ability to inhibit bacteria without promoting resistance[2]. Due to the growth of antibiotic resistance, the use of antibacterial nanocomposites that do not cause antibiotic resistance has received attention in recent years[3]. nanomaterials offer unique properties, such as improved biocompatibility, sustained release of metal ions with antibacterial activities [4]. MOFs are a nanocomposites resulting in great antibacterial activities against gram-positive and gram-negative bacteria.[5]

MOFs, metal-organic frameworks, are porous crystalline compounds with intrinsic antimicrobial activity [5]. Their large surface area and ability to host active molecules make them attractive for delivering antimicrobial compounds and inhibiting biofilms [6]. MOFs' properties can be tailored by altering their composition, including the metal ions or clusters and organic linkers [7]. Recent advancements include the use of many MOFs such as ZIF-67 for self-disinfecting surfaces and composites with biodegradable polymers for better biocompatibility and controlled antimicrobial drug delivery[8]. ZIF-67 is a metal-organic framework consisting of Cobalt ions and 2-methylimidazole ligands [9]. It is suitable for antibacterial applications due to its high drug-loading efficiency and controlled release properties [9]. In comparison to antibiotics, ZIF-67 with Disinfectant properties offers advantages such as reduced development of drug-resistant bacteria [10] and enhanced therapeutic efficacy through controlled release and increased bioavailability [11]. Additionally, ZIF-67 can be composite with natural biodegradable polymer to increase the biocompatibility.

Carboxymethyl cellulose (CMC) is commonly used as a natural coating for Metal Organic Frameworks (MOFs) due to its role in enhancing the metal cation concentration at the surface of carbohydrates, leading to the rapid self-assembly of MOFs such as ZIF-8.

2. Experimental

2.1. Materials

Cobalt (II) acetate tetrahydrate ($Co(OAc)_2.4H_2O$, ≥99.5%, Sigma Aldrich), 2-Methylimidazole (Hmim, ≥99.0%, Sigma Aldrich), Sodium carboxymethyl cellulose (CMC, Sigma Aldrich), Zinc Chloride ($ZnCl_2$, ≥98.0%, Merck) and ethanol

2.2. Synthesis of ZIF-67

ZIF-67 synthesis was carried out under the optimized synthesis conditions previously reported by Literature [12]0.250 g of Co (OAc) 2.4H_2O and 1.642 g of Hmim were dissolved in 10mL of distilled water. The reaction mixture was transferred into a 25 mL Teflon-lined autoclave,which was heated in a constant-temperature drying oven at 120 °C for 40 min. The obtained purple product was collected through centrifugation and washed three times with distilled water and ethanol before being dried at 80 °C in the oven overnight.

2.3. Synthesis of ZIF-67@ Zn-CMC hydrogel nanocomposite

A mixture of 1:1 with the obtained ZIF-67 and CMC was dissolved in 10.0 mL distilled water, and then the $ZnCl_2$ solution was added dropwise to the CMC to be crosslinked. The ratio of $ZnCl_2$ and CMC was 1:2. The obtained composite was freeze-dried overnight.

3. Result and discussion

In this work, our goal was to prepare a potent antibacterial system consisting of ZIF 67 metal frameworks and CMC hydrogel. The use of both organic and inorganic components in the final structure can enable the use of the antibacterial effects of both components and provide the system with synergistic effects. In addition, the hydrogel coating can enable the slow release of metal ions and increase biocompatibility and cell adhesion. In addition, the presence of the metal-organic framework in the hydrogel structure can increase its mechanical strength. All the above-mentioned features make this nanocomposite a powerful system for biological applications. The structure identification was carried out by various quantitative and qualitative analyses such as FTIR, EDX, XRD,TGA, BET, and all of them confirmed its successful synthesis.

References

[1] I. Francolini, A. Piozzi, (2020).
[2] N.K. Ranjith, (2019).
[3] F.N. Oktar, O. GÜNdÜZ, (2014).
[4] M. Shreya, I. Gajendra Kumar, G. Amel, A. Shahabe Saquib, P. Rajendra, Y. Virendra Kumar, S. Rabbani, S.A. Mohammed, Y. Krishna Kumar, I. Saiful, A. Yongtae, J. Byong-Hun, (2022).
[5] C. Pettinari, R. Pettinari, C. Di Nicola, A. Tombesi, S. Scuri, F. Marchetti, (2021).
[6] b. Claes, T. Boudewijns, L. Muchez, G. Hooyberghs, E. Van der Eycken, J. Vanderleyden, H.P. Steenackers, D. De Vos, (2017).
[7] P. Florczak, E. Janiszewska, K. Kędzierska, S. Kowalak, (2011).
[8] R. Gallegos-Monterrosa, R.O. Mendiola, Y. Nuñez, C. Auvynet, K.M. Kumar, B. Tang, L.I. Ruiz-Ortega, V.H. Bustamante, The Journal of Antibiotics 76 (2023) 603-612.
[9] C. Bruno Altran, A. Marina Paiva, B. Thúlio Wliandon Lemos, S. Bruna Lallo da, F. Rafael Bianchini, I. Guilherme, C. Paulo Inácio da, C. Leila Aparecida, (2023).
[10] N. Allam, W.A. Abbas, G.E. Khedr, A.M. Mohamed, (2022).
[11] S. Sadiq, I. Khan, M. Humayun, P. Wu, A. Khan, S. Khan, A. Khan, S. Khan, A.F. Alanazi, M. Bououdina, ACS Omega 8 (2023) 49244-49258.
[12] X. Guo, T. Xing, Y. Lou, J. Chen, Journal of Solid State Chemistry 235 (2016) 107-112.

Three-component one-pot synthesis of poly substituted 2,6 -dicyanoaniline derivatives in the presence of zinc oxide nanoparticles under solvent-free conditions

Seyed Hossein. Banitaba[a], Seyed Mostafa. Mirtezerjani[b,c*], Mohammad. Karimi[c,d]

[a] *Soil and Water Research Department, Isfahan Agricultural and Natural Resources Research and Education Center(AREEO), Isfahan, Iran*

[b] *Payame Noor University of Ardakan, Department of Chemistry, Ardakan, Yazd, Iran*

[c] *Sirang Company, Research and Development Center, Yazd, Iran*

[d] *Yazd University, Department of Textile, Yazd, Iran*

Email: **Sm.mirtezerjani@gmail.com**

***Keywords*:** 2,6-dicyanoaniline - zinc oxide nanoparticles - nanoparticles - zinc oxide - solvent-free conditions - one-pot synthesis**.**

Abstract

Aromatic amines with biological properties in natural compounds are known as the base of chemical dyes. Due to the high application and importance of aromatic amines, it is important to provide efficient methods for the synthesis of these compounds. Among the aromatic amines, aniline and its derivatives are of special importance. According to the above, in this study, polyunsaturated derivatives of 2 and 6-dicyano-aniline were synthesized from the condensation reaction of acetone, malononitrile and benzaldehyde derivatives in the presence of nanoparticles zinc oxide. This reaction was performed under solvent-free conditions at room temperature.

References:

١.Flores-Rojas GG.; López-Saucedo F.; Bucio E. Green synthesized zinc oxide nanomaterial's and its therapeutic applications. Green Sustainable Process for Chemical and Environmental Engineering and Science. 2021 Jan 1:237-61.

٢.Zonouzi A.; Izakian Z.; Abdi K.; Ng SW. Synthesis of Fluorescent 2, 6-Dicyano-3, 5-Disubstituted Anilines Using Cellulose Sulfuric Acid in Aqueous Media. Helvetica Chimica Acta. 2016 May;99(5):355-60.

٣.Reddy VG.; Reddy TS.; Kayak VL.; Prasad B.; Reddy AP.; Ravi Kumar A.; Taj S.; Kamal A.; Design, synthesis and biological evaluation of N-((1-benzyl-1H-1, 2, 3-triazol-4-yl) methyl)-1, 3-diphenyl-1H-pyrazole-4-carboxamides as CDK1/Cdc2 inhibitors. European Journal of Medicinal Chemistry. 2016 Oct 21; 122:164-77.

Synthesis of the hyaluronic acid-pectin polymer hydrogel and its inorganic porous nanocomposite based on clinoptilolite for cancer drug delivery system.

Mahsa Fatollahi, Mahtab Bahmani, Ali-Reza Akbarzadeh*

Corresponding author: a_akbarzadeh@iust.ac.ir

Abstract

A hydrogel system composed of hyaluronic acid and pectin polymers (HA-Pec), along with a composite incorporating zeolite and these biopolymers, was designed for the controlled delivery of doxorubicin and 5-fluorouracil. Characterization of the synthesized hyaluronic acid–pectin hydrogel via Fourier-transform infrared spectroscopy (FTIR) confirmed successful crosslinking and polymerization. The composite, formed by integrating natural zeolite with the polymer matrix, exhibited a significant enhancement in drug-loading capacity compared to the hydrogel alone.

Keywords: hydrogel, hyaluronic acid, pectin, zeolite

1. introduction

Today, the use of the drug delivery system instead of the traditional method has been considered. The clinical importance of targeted drug delivery is that it allows the drug or drug carrier to accumulate in the target area or at a specific location, thus preventing damage to healthy tissues, organs, or cells. The use of polymer-based carriers facilitates prolonged circulation time, controlled drug release, and enhanced bioavailability [1]. Specifically, biocompatible and biodegradable polymers, such as hyaluronic acid and pectin, have been extensively employed to optimize drug carrier efficacy. In this study, hyaluronic acid-pectin hydrogel was synthesized and investigated as 5-fluorouracil drug carrier. Hyaluronic acid is a hydrophilic biopolymer that can actively bind to the CD44 receptor [2]. Through the complexation of hyaluronic acid on a biocompatible surface and the resulting additional active targeting capability, complexed nanoparticles are able to reach tumor sites and therefore have great potential in clinical application [3].

On the other hand, pectin is a polymer of plant origin, which, with its properties, is considered one of the very good polymers for targeted drug delivery in different tissues [4]. Due to its nature, this polysaccharide is resistant to stomach acid and helps to target the intestine, and with the use of several linkers such as acrylamide, it turns into various hydrogels for medicinal activity and shows better performance. Also, a composite based on hyaluronic acid, pectin and natural zeolite was synthesized to carry doxorubicin and 5-fluorouracil. Zeolite was used as a porous material to increase drug loading due to high pore volume and surface area [5].

2.Experimental

2.1.Preparation of hyaluronic acid-pectin hydrogel (HA-Pec)

To prepare the hydrogel, 0.1 g of pectin was dissolved in 4 mL of deionized water and stirred at 60°C for 2 hours. In a separate beaker, 0.125 g of hyaluronic acid was dissolved in 25 mL of distilled water, followed by the addition of 0.4 g of calcium chloride. The resulting solution was stirred for 30 minutes to ensure complete reaction. Subsequently, the pectin gel was injected dropwise into the hyaluronic acid solution using a syringe, forming spherical hydrogel beads. The reaction proceeded at a controlled low stirring speed for 1 hour to facilitate crosslinking. The obtained hydrogels were thoroughly washed with water to remove unreacted components and dried in an oven at 60°C, yielding the final hydrogel product [6].

2.2.Preparation of Zeolite-hyaluronic acid-pectin Composite (Zeolite-HA-Pec)

For the composite synthesis, 0.1 g of pectin and 0.1 g of natural zeolite were dissolved in 4 mL of deionized water and stirred at 60°C for 2 hours to ensure homogeneous dispersion. Separately, 0.125 g of hyaluronic acid was dissolved in 25 mL of distilled water, followed by the addition of 0.4 g of calcium chloride, and the mixture was stirred for 30 minutes. After the initial reaction, the pectin–zeolite gel was injected dropwise into the hyaluronic acid solution using a syringe, forming discrete spherical composite beads. The mixture was stirred at a controlled low speed for 1 hour to promote uniform crosslinking and structural integrity. The resulting composite hydrogels were subsequently washed with water to remove residual reagents and dried in an oven at 60°C, yielding the final zeolite–polymer composite [6].

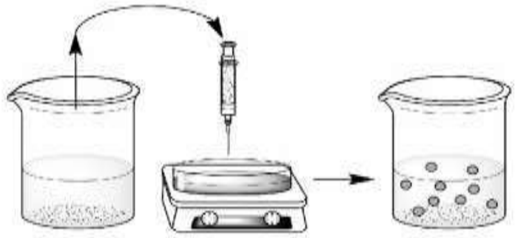

Figure. 1: Preparation of hyaluronic acid-pectin hydrogel [6].

3.Results and discussion

3.1 .FT-IR spectrum

The Fourier-transform infrared (FTIR) spectrum of hyaluronic acid exhibited a strong absorption band at 3436 cm^{-1}, attributed to O–H stretching vibrations. The peak at 2923 cm^{-1} corresponds to C–H stretching vibrations, while the absorption band at 1649 cm^{-1} is associated with asymmetric C=O stretching of carboxyl groups. Additionally, the absorption peak at 1467 cm^{-1} is indicative of amide bond vibrations, and the characteristic peak at 1011 cm^{-1} corresponds to C–O–C stretching in the hyaluronic acid structure [7]. In the FTIR spectrum of pectin, a prominent peak at 3472 cm^{-1} was assigned to O–H stretching vibrations, while the absorption band at 1508 cm^{-1} corresponded to ester carbonyl (C=O) stretching. The peak observed at 926 cm^{-1} was attributed to C–O–C stretching, a characteristic feature of polysaccharides such as pectin. The presence of distinctive absorption bands from both hyaluronic acid and pectin in the final hydrogel spectrum confirmed the successful synthesis and structural integration of the biopolymer-based hydrogel [8].

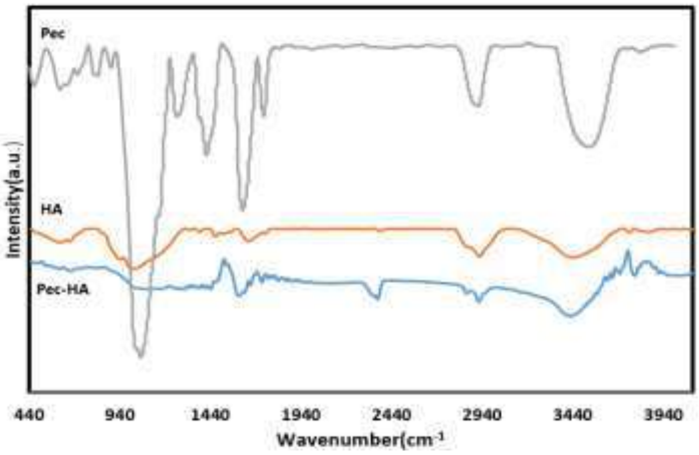

Figure. 2: FT-IR spectrum of HA, Pec, HA-Pec.

3.2. Drug Encapsulation Efficiency

Quantitative analysis of drug encapsulation revealed that the loading efficiency of 5-fluorouracil (5-FU) in the hyaluronic acid–pectin hydrogel was 20%, whereas incorporation into the final zeolite-based composite enhanced drug loading to 29%. Additionally, the doxorubicin loading efficiency in the composite system was measured at approximately 80%, indicating a significant improvement in drug retention within the polymer-zeolite matrix.

Conclusion

This study investigated the application of hyaluronic acid–pectin hydrogel and its zeolite-based composite as potential drug delivery systems. The findings demonstrate that the synthesized hydrogel can effectively serve as a carrier for 5-fluorouracil and doxorubicin. Furthermore, the incorporation of zeolite into the polymeric network significantly enhanced drug loading capacity, highlighting its potential in advanced drug delivery applications.

References:

[1]. Xue, H., Ju, Y., Ye, X., Dai, M., Tang, C., & Liu, L. (2024). Construction of intelligent drug delivery system based on polysaccharide-derived polymer micelles: A review. *International Journal of Biological Macromolecules*, *254*, 128048.

[2]. Pandey, A., Kulkarni, S., Vincent, A. P., Nannuri, S. H., George, S. D., & Mutalik, S. (2020). Hyaluronic acid-drug conjugate modified core-shell MOFs as pH responsive nanoplatform for multimodal therapy of glioblastoma. *International journal of pharmaceutics*, *588*, 119735.

[4]. Bokatyi, A. N., Dubashynskaya, N. V., & Skorik, Y. A. (2024). Chemical modification of hyaluronic acid as a strategy for the development of advanced drug delivery systems. *Carbohydrate Polymers*, 122145.

[5]. Serati-Nouri, H., Jafari, A., Roshangar, L., Dadashpour, M., Pilehvar-Soltanahmadi, Y., & Zarghami, N. (2020). Biomedical applications of zeolite-based materials: A review. *Materials Science and Engineering: C*, *116*, 111225.

[6]. Elena A. Mikhailova1*; Anatoly K. Melekhin1; Vladimir A. Belyy, PhD2; Anatoly A. Shubakov, PhD1. (2017). Stability of Hyaluronan-Pectic Gel Particles in the Conditions of the Artificial Gastrointestinal Environment. International Journal of Biomedicine, 7(4):310-314.

[7]. Bozer, B. M., Özkahraman, B., & Mert, H. (2024). Photocrosslinked methacrylated pectin and methacrylated hyaluronic acıd wound dressing loaded with oleuropein as bioactive agent. *International Journal of Polymeric Materials and Polymeric Biomaterials*, *73*(11), 961-973.

[8]. Kapoor, D. U., Garg, R., Gaur, M., Pareek, A., Prajapati, B. G., Castro, G. R., ... & Sriamornsak, P. (2024). Pectin hydrogels for controlled drug release: Recent developments and future prospects. *Saudi Pharmaceutical Journal*, 102002.

The 30th Iranian Seminar of Organic Chemistry
February 7-9, 2025, Iran University of Science and Technology, Tehran, Iran

Development of Carbon Sphere-Based copper Nanocatalyst for Efficient Synthesis of Imidazo[1,2-a]pyridines derivatives

Saba Rajaeian[a], Hossein Eshghi[b*]
Chemistry Department, Faculty of Science, Ferdowsi University of Mashhad, Mashhad 9177948974, Iran
E-mail*: heshghi@um.ac.ir

Keyword: Heterogeneous nanocatalyst, carbon sphere, imidazo[1,2-*a*]pyridines derivatives

Introduction:

Imidazo[1,2-a]pyridines are an important scaffold in organic and medical chemistry due to their wide biological activity, such as anti-cancer, anti-tumor, antibacterial, anti-inflammatory, antiviral, anti-ulcer, antimicrobial, and sedative effects. They are the core unit of medications such as zolpidem, zolimidine [1], GSK812397 (administered for the treatment of HIV infection) [2], alpidem, saripidem, and olprinone. Also known as drug precursors, these substances are utilized as fluorescent sensors in optoelectronic materials [3]. The demand for green and efficient methods to synthesize imidazo[1,2-a]pyridines has led to the development of numerous synthetic protocols. Transition metal-catalyzed reactions are the most interesting way to synthesize imidazo[1,2-a]pyridines [1]. The use of homogeneous copper requires a large amount to achieve high efficiency. However, its separation and recovery are challenging, and it may form complexes with the final product. Since pharmaceutical compounds must not contain metal residues, the heterogenization of copper is proposed as the best solution to this issue. This approach not only enhances system efficiency but also reduces environmental impacts, is more cost-effective, and is suitable for large-scale applications. Recently, carbon materials have gained interest as supports in heterogeneous catalytic processes. They can be customized for specific needs and offer unique physical and chemical properties. In this study, we stabilized Cu nanoparticles on nitrogen-doped carbon spheres as a highly efficient heterogeneous catalyst. We employed it to synthesize imidazo[1,2-a]pyridine using commercially available substrates through a one-pot three-component procedure.

Method:

The mixture of carbon source, $Cu(NO_3)_2.3H_2O$ and deionized water was prepared and then transferred into a Teflon-lined autoclave for hydrothermal carbonization at a certain temperature. After cooling down to room temperature, the dark brown powder was washed with deionized water and ethanol three times. The final precipitate was dried in air at 80 °C overnight. This catalyst was used for the synthesis of imidazo[1,2-a]pyridine derivatives under mild conditions.

Results and Discussion:

the result Carbon supported copper-based catalysts were characterized using various techniques including SEM, EDX, XRD, TEM, IR, and ICP The performance of the catalyst in this reaction was investigated. To study the scope of the reaction, the effects of electron-donating and electron-withdrawing groups and steric effects were evaluated. The results indicated that these factors had no impact on the course of the reaction. The stability of the catalyst for the reaction after recovery was investigated. After each reaction cycle, the catalyst was separated by filtration and washed. The stability of its morphology and properties was confirmed using SEM, XRD, and IR analyses.

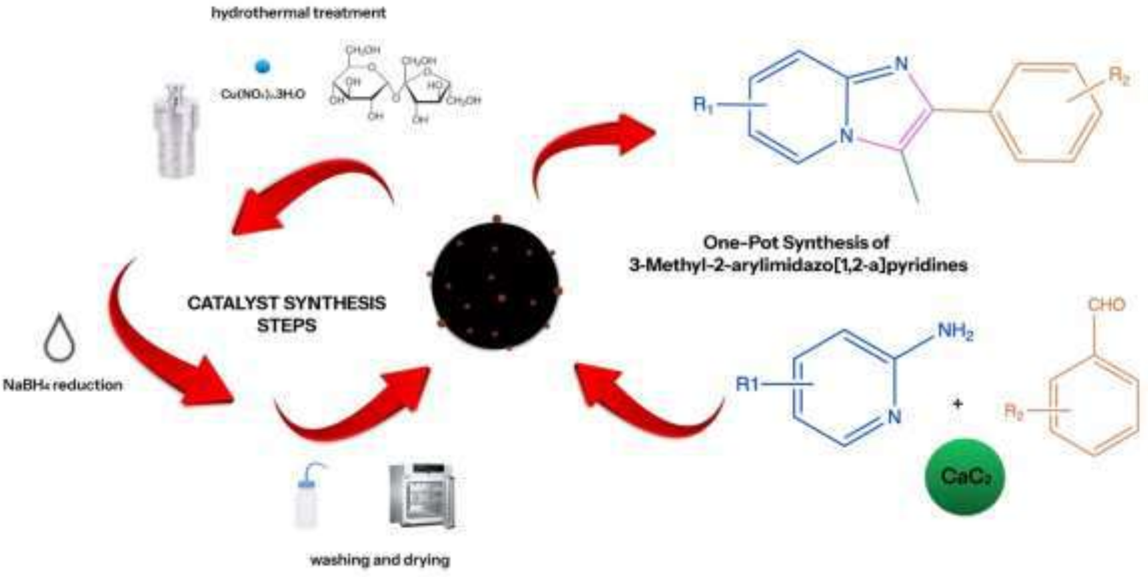

Graphical Abstract

References:

[1] Panda, J., Raiguru, B. P., Mishra, M., Mohapatra, S., & Nayak, S. (**2022**). Recent advances in the synthesis of imidazo [1, 2-a] pyridines: A brief review. *ChemistrySelect*, *7*(3), e202103987.

[2] Azzouzi, M., Ouchaoui, A. A., Azougagh, O., El Hadad, S. E., Abou-Salama, M., Oussaid, A., ... & Rohand, T. (**2024**). Synthesis, crystal structure, and antiviral evaluation of new imidazopyridine-schiff base derivatives: in vitro and in silico anti-HIV studies. *RSC advances*, *14*(50), 36902-36918.

[3] Tran, C., & Hamze, A. (**2022**). Recent developments in the photochemical synthesis of functionalized imidazopyridines. *Molecules*, *27*(11), 3461.

List of Authors

حسین غفوری ....

سامان علوی نیکو...

سیده بهاره عظیمی ....

علی فیوضی ....

فاطمه عزیزی ....

فرانک منطقی ....

محمد حسین محسنی..

مهرداد برون..